Fundamentals in Nuclear Theory

LECTURES PRESENTED AT AN INTERNATIONAL COURSE, TRIESTE, 3 OCTOBER-16 DECEMBER 1966, ORGANIZED BY THE INTERNATIONAL CENTRE FOR THEORETICAL PHYSICS, TRIESTE

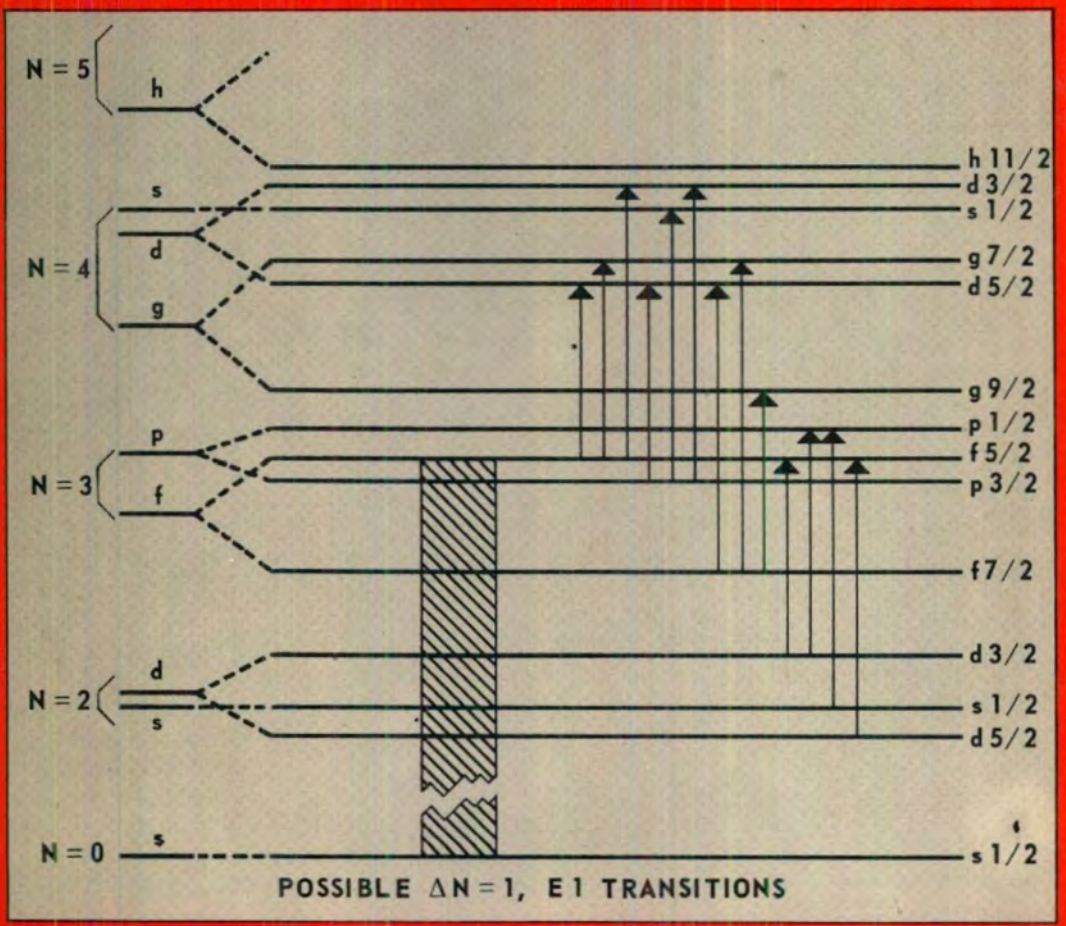

CONTRIBUTIONS BY: V. BENZI, X. CAMPI, K. DIETRICH, L. FONDA, W.E. FRAHN, J. HUMBLET, M. JEAN, R.H. LEMMER, K.W. McVOY, M. MOSHINSKY, E.R. RAE, R. RICCI, G. RIPKA, D.J. ROWE, G.M. TEMMER, F. VILLARS, H. VUCETICH

SCIENTIFIC EDITORS: A. DE-SHALIT, C. VILLI

INTERNATIONAL ATOMIC ENERGY AGENCY, VIENNA, 1967

FUNDAMENTALS IN NUCLEAR THEORY

AUTHORS' CORRECTIONS AND NOTE ADDED IN PROOF

CHAPTER 2

Page 94, line 10

For nuclei read nucleons

Page 96, equation (2.1.1)

Insert minus sign before 2.6

Page 98, equation (2.2.5)

Equation should be:

$$\langle (jm)(j\bar{m}) | v | (j'm')(j'\bar{m}') \rangle = -G_{jj'} \approx -\frac{22}{A} \text{ MeV}$$

Page 100, equation (2.3.8)

Equation should be:

$$\langle (j)^2 J | \hat{G} | (j')^2 J' \rangle = -\delta(J - J') G\Omega$$

Page 101, lines 8 and 9

Replace the lines by the following:

Potential energy for pair coupling $\sim -\frac{N}{2} G\Omega$

Potential energy for aligned coupling $\sim -\frac{N(N-1)}{2} F$ (for $N \ll \Omega$)

Page 102, 9 lines from bottom

For V_ν read u_ν

Page 102, 8 lines from bottom

For U_ν read v_ν

Page 102, 3 lines from bottom

For V_ν read u_ν
For U_ν read v_ν

Page 107, equation (3.3.2)

For $\frac{3}{4\pi}$ read $\frac{3}{2\pi}$

Page 124, equation (6.1.3)

Equation should be:

$$Q(t) = \epsilon \cos \omega t = \tfrac{1}{2} \epsilon \, (e^{-i\omega t} + e^{i\omega t})$$

Page 126, equation (6.3.1)

For $(u_\nu v_{\nu'} + u_{\nu'} v_\nu)$ read $(u_\nu v_{\nu'} + u_{\nu'} v_\nu)^2$

Page 127, equation (6.3.2)

For $(u_\nu v_{\nu'} + u_{\nu'} v_\nu)$ read $(u_\nu v_{\nu'} + u_{\nu'} v_\nu)^2$

Page 131, line 3

For 25 MeV read 50 MeV

CHAPTER 8

Note added in proof

The conclusion reached in Section 4.4, that the two-level approximation to S can be unitary only if the partial width vectors of the two resonances are orthogonal, is based on the assumption that the sum of the partial widths of each resonance equals the corresponding total width. If this condition is relaxed, $t_1^\dagger t_2$ is not necessarily zero, and the conditions (4.37) are replaced by these more general ones:

$$t_1^\dagger t_1 / \Gamma_1 = t_2^\dagger t_2 / \Gamma_2 \equiv \lambda ,$$

$$t_1^\dagger t_2 = \pm (\lambda^2 - 1)^{\frac{1}{2}} (E_2 - E_1^*) ,$$

$$t_1 - B t_1^* = \pm i [(\lambda - 1)/(\lambda + 1)]^{\frac{1}{2}} (t_2 + B t_2^*) ,$$

$$t_2 - B t_2^* = \mp i [(\lambda - 1)/(\lambda + 1)]^{\frac{1}{2}} (t_1 + B t_1^*) ,$$

where λ, the ratio of the sum of the partial widths to the total width, is the same for both states and satisfies the inequalities

$$1 \leq \lambda^2 \leq 1 + \Gamma_1 \Gamma_2 / |E_2 - E_1|^2 .$$

In the two-channel case, $\lambda^2 = 1$ and $t_1^\dagger t_2$ is necessarily zero.

FUNDAMENTALS IN NUCLEAR THEORY

The following States are Members of the International Atomic Energy Agency:

AFGHANISTAN
ALBANIA
ALGERIA
ARGENTINA
AUSTRALIA
AUSTRIA
BELGIUM
BOLIVIA
BRAZIL
BULGARIA
BURMA
BYELORUSSIAN SOVIET SOCIALIST REPUBLIC
CAMBODIA
CAMEROON
CANADA
CEYLON
CHILE
CHINA
COLOMBIA
CONGO, DEMOCRATIC REPUBLIC OF
COSTA RICA
CUBA
CYPRUS
CZECHOSLOVAK SOCIALIST REPUBLIC
DENMARK
DOMINICAN REPUBLIC
ECUADOR
EL SALVADOR
ETHIOPIA
FINLAND
FRANCE
GABON
GERMANY, FEDERAL REPUBLIC OF
GHANA
GREECE
GUATEMALA
HAITI
HOLY SEE
HONDURAS
HUNGARY
ICELAND
INDIA
INDONESIA
IRAN
IRAQ
ISRAEL
ITALY
IVORY COAST
JAMAICA
JAPAN
JORDAN
KENYA
KOREA, REPUBLIC OF
KUWAIT
LEBANON
LIBERIA
LIBYA
LUXEMBOURG
MADAGASCAR
MALI
MEXICO
MONACO
MOROCCO
NETHERLANDS
NEW ZEALAND
NICARAGUA
NIGERIA
NORWAY
PAKISTAN
PANAMA
PARAGUAY
PERU
PHILIPPINES
POLAND
PORTUGAL
ROMANIA
SAUDI ARABIA
SENEGAL
SINGAPORE
SOUTH AFRICA
SPAIN
SUDAN
SWEDEN
SWITZERLAND
SYRIAN ARAB REPUBLIC
THAILAND
TUNISIA
TURKEY
UKRAINIAN SOVIET SOCIALIST REPUBLIC
UNION OF SOVIET SOCIALIST REPUBLICS
UNITED ARAB REPUBLIC
UNITED KINGDOM OF GREAT BRITAIN AND NORTHERN IRELAND
UNITED STATES OF AMERICA
URUGUAY
VENEZUELA
VIET-NAM
YUGOSLAVIA

The Agency's Statute was approved on 26 October 1956 by the Conference on the Statute of the IAEA held at United Nations Headquarters, New York; it entered into force on 29 July 1957. The Headquarters of the Agency are situated in Vienna. Its principal objective is "to accelerate and enlarge the contribution of atomic energy to peace, health and prosperity throughout the world".

Printed by the IAEA in Austria

August 1967

INTERNATIONAL CENTRE FOR THEORETICAL PHYSICS, TRIESTE

FUNDAMENTALS IN NUCLEAR THEORY

LECTURES PRESENTED AT
AN INTERNATIONAL COURSE, TRIESTE
3 OCTOBER - 16 DECEMBER 1966

Scientific Editors: A. DE-SHALIT, C. VILLI

Contributions by:

V. BENZI, X. CAMPI, K. DIETRICH, L. FONDA, W.E. FRAHN,
J. HUMBLET, M. JEAN, R.H. LEMMER, K.W. McVOY,
M. MOSHINSKY, E.R. RAE, R. RICCI, G. RIPKA, D.J. ROWE,
G.M. TEMMER, F. VILLARS, H. VUCETICH

INTERNATIONAL ATOMIC ENERGY AGENCY
VIENNA, 1967

FUNDAMENTALS IN NUCLEAR THEORY
(Proceedings Series)

ABSTRACT. Proceedings of an international course organized by, and held at, the IAEA's International Centre for Theoretical Physics in Trieste, 3 October - 16 December 1966. The course was attended by 139 lecturers and participants representing 26 nationalities and also by the staff and fellows of the Centre.

The publication is divided into three parts containing a total of 14 chapters: Part I - Phenomenological nuclear physics (4 chapters); Part II - Theoretical nuclear physics (9 chapters); Part III - Neutron spectroscopy (1 chapter). Most of the chapters have been compiled from series of lectures given during the course, and each chapter is preceded by a list of its contents.

Contributors are: V. Benzi, X. Campi, K. Dietrich, L. Fonda, W.E. Frahn, J. Humblet, M. Jean, R.H. Lemmer, K.W. McVoy, M. Moshinsky, E.R. Rae, R.A. Ricci, G. Ripka, D.J. Rowe, G.M. Temmer, F. Villars, H. Vucetich.

Entirely in English.

(913 pp., 16 x 24 cm, paper-bound, 278 figs)
(1967) Price: US $16.00; £5.13.0

FUNDAMENTALS IN NUCLEAR THEORY
IAEA, VIENNA, 1967
STI/PUB/145

FOREWORD

One of the principal aims in setting up the International Centre for Theoretical Physics was the development of physics in its various aspects and a quest for a deeper sense of the scope and unified nature of the subject as a whole. In pursuance of this the International Centre has followed a policy of organizing extended research seminars with a comprehensive and synoptic coverage. The first of these - lasting over a month - was held in 1964 on fluids of ionized particles and plasma physics; the second, lasting for two months, concerned itself with physics of elementary particles and high-energy physics. The third, of three months' duration, October-December 1966, covered nuclear theory. The present volume records the proceedings of this research seminar. The long duration of these seminars allows the completeness of presentation of a conference together with the relaxed atmosphere necessary for discussion and review. Since the seminars were attended as far as possible not only by physicists who were working at the Centre but also by participants from other disciplines, the presentation naturally emphasized the inter-relation of differing disciplines, for example of nuclear theory with particle physics, covering both the techniques used, like Regge poles, sum rules and group theory, as well as the basic conceptual framework.

The seminar course was directed by Professors A. de-Shalit and C. Villi. It is the intention of the Centre to continue the tradition of these extended seminars and make them an annual feature of its work.

Abdus Salam

EDITORIAL NOTE

The papers and discussions incorporated in the proceedings published by the International Atomic Energy Agency are edited by the Agency's editorial staff to the extent considered necessary for the reader's assistance. The views expressed and the general style adopted remain, however, the responsibility of the named authors or participants.

For the sake of speed of publication the present Proceedings have been printed by composition typing and photo-offset lithography. Within the limitations imposed by this method, every effort has been made to maintain a high editorial standard; in particular, the units and symbols employed are to the fullest practicable extent those standardized or recommended by the competent international scientific bodies.

The affiliations of authors are those given at the time of nomination.

The use in these Proceedings of particular designations of countries or territories does not imply any judgement by the Agency as to the legal status of such countries or territories, of their authorities and institutions or of the delimitation of their boundaries.

The mention of specific companies or of their products or brand-names does not imply any endorsement or recommendation on the part of the International Atomic Energy Agency.

CONTENTS

PART I

PHENOMENOLOGICAL NUCLEAR PHYSICS

CHAPTER 1

PHENOMENOLOGICAL DESCRIPTION OF NUCLEAR SCATTERING AND DIRECT INTERACTIONS

W.E. FRAHN

A. ELASTIC SCATTERING

1. INTRODUCTION

Phenomenological methods mediate between experimental data and basic theory. With such methods we try to find and correlate the systematic contents of measurements. The systematics is formulated by means of heuristic concepts and simple assumptions within the general framework of quantum mechanics. We hope that basic theory will eventually justify and "explain" this description in terms of more fundamental concepts.

In nuclear interactions, experiment provides us with eigenvalues and transition probabilities in the form of energy levels and their properties, widths and cross-sections. These quantities are determined

The author is at the University of Cape Town, Rondebosch, South Africa.

by the asymptotic behaviour of the wave functions. For scattering processes all physical information is contained in the elements of the scattering (S-) matrix. The S-matrix and quantities related to it will form the general framework for the phenomenological methods to be discussed in this course. We start with a brief survey of its properties and its relation to measurable quantities[1].

1.1. S-matrix

Consider the scattering of two particles with spins $\vec{s}_1$ and $\vec{s}_2$. The total wave function has the asymptotic form

$$\psi^{(+)}_{sm_s}(\vec{k},\vec{r}) \cong e^{i\vec{k}\cdot\vec{r}}\,\chi_{sm_s} + \sum_{s'm'_s} \langle s\, m_s \,|\, F(\vec{k},\vec{r}) \,|\, s'm'_s\rangle \chi_{s'm'_s}\, \frac{e^{ikr}}{r} \tag{1.1}$$

where

$$\chi_{sm_s} = \sum_{m_j} \langle s_1 s_2 m_1 m_2 \,|\, sm_s\rangle\, \chi_{s_1 m_1}\, \chi_{s_2 m_2} \tag{1.2}$$

are eigenfunctions of the channel spin $\vec{s} = \vec{s}_1 + \vec{s}_2$. Equation (1.1) defines the amplitude operator $F(\vec{k},\vec{r})$. The channel spin $\vec{s}$ and the orbital angular momentum $\vec{\ell}$ couple to the total spin $\vec{j} = \vec{\ell} + \vec{s}$ which is conserved in magnitude and direction. Expansion of Eq. (1.1) in eigenfunctions of $\vec{j}$ and $\vec{\ell}$ gives

$$\langle sm_s \,|\, F(\vec{k},\vec{r}) \,|\, s'm'_s\rangle$$

$$= i\,\frac{2\pi}{k} \sum_{\ell\ell' j} \langle \ell sm_s \,|\, \mathcal{S}^j(\hat{\vec{k}},\hat{\vec{r}}) \,|\, \ell' s' m'_s\rangle (\delta_{\ell\ell'}\,\delta_{ss'} - S^j_{\ell s,\ell' s'}) \tag{1.3}$$

where

$$\langle \ell sm_s \,|\, \mathcal{S}^j(\hat{\vec{k}},\hat{\vec{r}}) \,|\, \ell' s' m'_s\rangle$$

$$= \sum_{m'_\ell m_\ell m_j} \langle \ell sm_\ell m_s \,|\, jm_j\rangle \langle \ell' s' m'_\ell m'_s \,|\, jm_j\rangle\, Y_{\ell m_\ell}(\hat{\vec{r}})\, Y^*_{\ell' m'_\ell}(\hat{\vec{k}}) \tag{1.4}$$

The quantities $S^j_{\ell s,\,\ell' s'}$ in the partial-wave expansion (1.3) are the elements of the scattering matrix. General properties of the S-matrix follow from conservation laws. Conservation of angular momentum implies that S is diagonal in j and independent of m_j. If parity is conserved the

---

[1] For a comprehensive treatment of scattering processes I recommend the excellent work of Goldberger and Watson [1].

difference ℓ-ℓ' must be even. From invariance under time reversal it follows that S is symmetric,

$$S^{j}_{\ell s, \ell' s'} = S^{j}_{\ell' s', \ell s} \tag{1.5}$$

Conservation of probability implies that the S-matrix is unitary,

$$\sum_{\ell'' s''} S^{j*}_{\ell s, \ell'' s''} \; S^{j}_{\ell' s', \ell'' s''} = \delta_{\ell\ell'} \, \delta_{ss'} \tag{1.6}$$

It is convenient to introduce the transition operator T which is connected with the amplitude operator F by

$$T = -\frac{2\pi\hbar^2}{M} F \tag{1.7}$$

where M is the reduced mass of the particles in the final state. In the partial-wave representation the T-matrix is related to the S-matrix by

$$T^{j}_{\ell s, \ell' s'} = - i \frac{(2\pi\hbar)^2}{Mk} (\delta_{\ell\ell'} \, \delta_{ss'} - S^{j}_{\ell s, \ell' s'}) \tag{1.8}$$

The differential cross-section for given spin orientations is

$$\frac{d\sigma}{d\Omega} (s m_s , s' m_s') = \left| \langle s m_s \left| F(\vec{k}, \vec{r}) \right| s' m_s' \rangle \right|^2 \tag{1.9}$$

If the incident beam and the target are random mixtures of all possible spin orientations, the measured differential cross-section is an average over all initial states and a sum over all final states:

$$\frac{d\bar{\sigma}}{d\Omega} = \frac{1}{(2s_1 + 1)(2s_2 + 1)} \sum_{s m_s, s' m_s'} \frac{d\sigma}{d\Omega} (s m_s, s' m_s') \tag{1.10}$$

The total cross-section is obtained by integrating over scattering angles

$$\bar{\sigma} = \int \frac{d\bar{\sigma}}{d\Omega} d\Omega$$

$$= \frac{\pi}{k^2} \sum_{\ell\ell' j} \frac{2j + 1}{(2s_1 + 1)(2s_2 + 1)} \left| \delta_{\ell\ell'} \, \delta_{ss'} - S^{j}_{\ell s, \ell' s'} \right|^2 \tag{1.11}$$

1.2. Spin-0 and spin-$\frac{1}{2}$ particles

We shall be interested mainly in the scattering of (non-relativistic) spin-0 and spin-$\frac{1}{2}$ projectiles by spinless targets. For these physically most important cases the scattering formalism simplifies considerably. In the spin-$\frac{1}{2}$ case the amplitude operator $F(\vec{k}, \vec{r}) \equiv f(\theta)$ becomes a 2×2 matrix in spin space

$$f(\theta) = A(\theta)\,\mathbf{1} + B(\theta)\vec{n}\cdot\vec{\sigma} \tag{1.12}$$

where $\vec{n} = \hat{k}\times\hat{k}'$ with $\hat{k}' = \hat{r}$ and $\cos\theta = \hat{k}\cdot\hat{k}'$, and $\vec{\sigma}$ is the Pauli spin operator. The S-matrix reduces to

$$S^j_{\ell\,\frac{1}{2},\ell'\frac{1}{2}} = \delta_{\ell\ell'}\cdot S^j_\ell \tag{1.13}$$

where $j = \ell \pm \frac{1}{2}$. With the shorter notation

$$S^{\ell+\frac{1}{2}}_\ell = \eta^+_\ell = e^{i2\delta^+_\ell},\quad S^{\ell-\frac{1}{2}}_\ell = \eta^-_\ell = e^{i2\delta^-_\ell} \tag{1.14}$$

which defines the real phase shifts $\delta^\pm_\ell$, the "non-spinflip" amplitude $A(\theta)$ and the "spin-flip" amplitude $B(\theta)$ become

$$\begin{aligned} A(\theta) &= \frac{i}{2k}\sum_{\ell=0}^{\infty}\left[(\ell+1)(1-\eta^+_\ell) + \ell(1-\eta^-_\ell)\right] P_\ell(\cos\theta) \\ B(\theta) &= -\frac{1}{2k}\sum_{\ell=0}^{\infty}(\eta^+_\ell - \eta^-_\ell)\frac{d}{d\theta}P_\ell(\cos\theta) \end{aligned} \tag{1.15}$$

It is often convenient to use a special notation for the average and the difference of the S-matrix elements in the two spin states,

$$\bar{\eta}_\ell = \frac{\ell+1}{2\ell+1}\eta^+_\ell + \frac{\ell}{2\ell+1}\eta^-_\ell,\quad \xi_\ell = \eta^+_\ell - \eta^-_\ell \tag{1.16}$$

Scattering in general changes the state of polarization of spin-$\frac{1}{2}$ particles. We confine ourselves to an unpolarized incident beam. The polarization vector is $\vec{P} = P(\theta)\vec{n}$ with the polarization given by

$$P(\theta) = 2\frac{\mathrm{Im}\,A(\theta)\,\mathrm{Im}\,B(\theta) + \mathrm{Re}\,A(\theta)\,\mathrm{Re}\,B(\theta)}{|A(\theta)|^2 + |B(\theta)|^2} \tag{1.17}$$

The differential cross-section for elastic scattering of spin-$\frac{1}{2}$ particles becomes

$$\frac{d\sigma}{d\Omega} = |A(\theta)|^2 + |B(\theta)|^2 \tag{1.18}$$

1.3. The elastic submatrix

The collision of composite particles may lead to channels other than those corresponding to elastic scattering: reaction channels. In this case the S-matrix connecting elastic channels is a submatrix of the complete multi-channel S-matrix. While the full S-matrix is unitary the submatrix is not. For spin-$\frac{1}{2}$ particles this implies

$$|\eta_\ell^\pm| \leq 1 \tag{1.19}$$

This can be described formally by introducing complex phase shifts $\delta_\ell = \delta_\ell^{(1)} + i\delta_\ell^{(2)}$, so that for each spin state

$$\eta_\ell = |\eta_\ell| \, e^{i2\delta_\ell^{(1)}} , \quad |\eta_\ell| = e^{-2\delta_\ell^{(2)}} \tag{1.20}$$

The deviation of the elastic S-matrix from unitarity measures the depletion of the elastic channels due to the presence of reaction channels. This depletion we call absorption.

The total cross-section σ_{tot} is now composed of an elastic scattering cross-section σ_{el} and an absorption cross-section σ_{abs}. In the spin-$\frac{1}{2}$ case we have

$$\sigma_{el} = \frac{\pi}{k^2} \sum_{\ell=0}^{\infty} [(\ell+1)|1-\eta_\ell^+|^2 + \ell|1-\eta_\ell^-|^2]$$

$$= \frac{\pi}{k^2} \sum_{\ell=0}^{\infty} (2\ell+1) \left[|1-\bar{\eta}_\ell|^2 + \frac{\ell(\ell+1)}{(2\ell+1)^2} |\xi_\ell|^2 \right] \tag{1.21}$$

$$\sigma_{abs} = \frac{\pi}{k^2} \sum_{\ell=0}^{\infty} [(\ell+1)(1-|\eta_\ell^+|^2) + \ell(1-|\eta_\ell^-|^2)]$$

$$= \frac{\pi}{k^2} \sum_{\ell=0}^{\infty} (2\ell+1) \left[1 - |\bar{\eta}_\ell|^2 - \frac{\ell(\ell+1)}{(2\ell+1)^2} |\xi_\ell|^2 \right] \tag{1.22}$$

$$\sigma_{tot} = \frac{2\pi}{k^2} \sum_{\ell=0}^{\infty} [(\ell+1)(1-\mathrm{Re}\,\eta_\ell^+) + \ell(1-\mathrm{Re}\,\eta_\ell^-)]$$

$$= \frac{2\pi}{k^2} \sum_{\ell=0}^{\infty} (2\ell+1)(1-\mathrm{Re}\,\bar{\eta}_\ell) \tag{1.23}$$

From Eqs. (1.15) and (1.21) follows an important relation between the total cross-section and the scattering amplitude in the forward direction, the optical theorem,

$$\sigma_{tot} = \frac{4\pi}{k} \mathrm{Im}\, f(0) \tag{1.24}$$

For spin-0 particles the scattering amplitude is a scalar and we have $\eta_\ell^+ = \eta_\ell^-$, or $\bar{\eta}_\ell = \eta_\ell$ and $\xi_\ell = 0$.

1.4. Coulomb effects

In the presence of Coulomb interaction the incoming and outgoing asymptotic waves are distorted and the exponents in Eq. (1.1) are replaced by

$$\begin{aligned} \vec{k}\cdot\vec{r} \to \{\vec{k}\,\vec{r}\} &\equiv \vec{k}\,\vec{r} + n \ln (kr - \vec{k}\cdot\vec{r}) \\ kr \to \{kr\} &\equiv kr - n \ln (2kr) \end{aligned} \tag{1.25}$$

where n is the Coulomb parameter

$$n = \frac{M Z_a Z_A e^2}{\hbar^2 k} \tag{1.26}$$

From the S-matrix elements we separate the point-charge Coulomb effects by replacing

$$S^j_{\ell s, \ell' s'} \to S^j_{\ell s, \ell' s'} e^{i2\sigma_\ell} \tag{1.27}$$

where the Coulomb phase shifts σ_ℓ are given by

$$e^{i2\sigma_\ell} = \frac{\Gamma(\ell + 1 + in)}{\Gamma(\ell + 1 - in)} \tag{1.28}$$

For instance, the scattering amplitude for spin-0 particles becomes

$$\begin{aligned} f(\theta) &= \frac{i}{2k} \sum_{\ell=0}^{\infty} (2\ell + 1)\,(1 - \eta_\ell e^{i2\sigma_\ell})\, P_\ell(\cos\theta) \\ &= f_C(\theta) + \frac{i}{2k} \sum_{\ell=0}^{\infty} (2\ell + 1)\,(1 - \eta_\ell)\, e^{i2\sigma_\ell} P_\ell(\cos\theta) \end{aligned} \tag{1.29}$$

where

$$f_C(\theta) = -\frac{n}{2k(\sin\frac{1}{2}\theta)^2} \exp i[-2n \ln \sin\tfrac{1}{2}\theta + 2\sigma_0] \tag{1.30}$$

is the Coulomb scattering amplitude.

1.5. Phenomenological methods

The measurable quantities in scattering processes are completely determined by the elements of the scattering matrix. For most experiments we need only a submatrix of the complete S-matrix, such as the quantities $\eta_\ell^\pm$ in elastic scattering of spin-$\frac{1}{2}$ particles by spin-0

targets. To determine these quantities one can follow different methods. On the one hand we can try to extract the η_ℓ as uniquely as possible from measured cross-sections. This empirical method is the phase shift analysis. It is practicable only at low energies where the number of relevant partial waves is sufficiently small. On the other hand one can try to determine the structure of the S-matrix elements as completely as possible from basic principles of quantum mechanics, from its general characteristics such as unitarity and symmetry properties, together with dynamical postulates such as analyticity. This is the fundamental approach of dispersion theory. The application of this method to complex nuclei is still at an early stage.

In this situation the description of nuclear processes relies heavily upon phenomenological methods to bridge the gap between experiment and basic theory. The oldest and most popular of these methods is based on specific models of the nuclear interaction. It replaces the many-body interaction by a model Hamiltonian containing an effective two-body potential operator. The S-matrix elements are generated by solving the wave equation and determining the coefficients of the outgoing spherical waves in the asymptotic region. Absorption is described by an imaginary part of the potential operator. This method is the complex potential model (CPM) or optical model.

Another approach has recently been developed which may be regarded as intermediate between phase shift analysis and dispersion theory, the parameterized S-matrix method. The dependence of the S-matrix elements on angular momentum and energy is described by simple functional forms, characterized by a few parameters. Although this method has been largely stimulated by the CPM, it aims at avoiding the potential concept and hopes to find its eventual justification in dispersion theory. It has found its simplest applications so far in processes dominated by strong absorption, and in this form is called strong absorption model (SAM). However there are indications that this approach can be extended to general scattering situations. In these lectures we shall describe how the two phenomenological methods are applied to elastic scattering and direct interactions and how they are related to each other.

2. SCATTERING BY A COMPLEX POTENTIAL

2.1. Spinless particles

First we consider the complex potential model for elastic scattering. Let us start with the simplest case of uncharged spinless particles interacting with a local central potential $U(r) = V(r) + iW(r)$. A solution of the Schrödinger equation

$$(\vec{\nabla}^2 + k^2)\psi = \frac{2M}{\hbar^2} U(r)\psi \qquad (2.1)$$

which behaves asymptotically as

$$\psi^{(+)}(\vec{k}, \vec{r}) \cong e^{i\vec{k}\cdot\vec{r}} + F(\vec{k}, \vec{k}')\frac{e^{ikr}}{r} \qquad (2.2)$$

satisfies the integral equation

$$\psi^{(+)}(\vec{k},\vec{r}) = e^{i\vec{k}\cdot\vec{r}} + \frac{2M}{\hbar^2}\int G_0^{(+)}(\vec{r},\vec{r}')\,U(r')\,\psi^{(+)}(\vec{k},\vec{r}')\,d\vec{r}' \tag{2.3}$$

where $G_0^{(+)}(\vec{r},\vec{r}')$ is the free-space Green's function

$$G_0^{(+)}(\vec{r},\vec{r}') = \frac{1}{4\pi}\frac{e^{ik|\vec{r}-\vec{r}'|}}{|\vec{r}-\vec{r}'|} \tag{2.4}$$

The asymptotic form of Eq. (2.3) is

$$\psi^{(+)}(\vec{k},\vec{r}) \cong e^{i\vec{k}\cdot\vec{r}} - \frac{M}{2\pi\hbar^2}\int e^{-i\vec{k}'\cdot\vec{r}'}\,U(r')\,\psi^{(+)}(\vec{k},\vec{r}')\,d\vec{r}'\,\frac{e^{ikr}}{r} \tag{2.5}$$

and the elastic scattering amplitude becomes

$$\begin{aligned} F(\vec{k},\vec{k}') &= -\frac{M}{2\pi\hbar^2}\int e^{-i\vec{k}'\cdot\vec{r}}\,U(r)\psi^{(+)}(\vec{k},\vec{r})\,d\vec{r} \\ &= -\frac{M}{2\pi\hbar^2}\langle e^{i\vec{k}'\cdot\vec{r}}\,|\,U\,|\psi^{(+)}(\vec{k},\vec{r})\rangle \end{aligned} \tag{2.6}$$

where $\hat{k}' = \hat{r}$. With the definition (1.7) we find for the elastic T-matrix

$$T(\vec{k},\vec{k}') = \langle e^{i\vec{k}'\cdot\vec{r}}\,|\,U\,|\psi^{(+)}(\vec{k},\vec{r})\rangle \tag{2.7}$$

Now we expand both sides of Eq. (2.6) in partial waves. Inserting

$$e^{i\vec{k}\cdot\vec{r}} = 4\pi\sum_{\ell m} i^{\ell} j_{\ell}(kr)\,Y_{\ell m}(\hat{r})\,Y^{*}_{\ell m}(\hat{k}) \tag{2.8}$$

$$\psi^{(+)}(\vec{k},\vec{r}) = \frac{4\pi}{kr}\sum_{\ell m} i^{\ell} f_{\ell}^{(+)}(k,r)\,Y_{\ell m}(\hat{r})\,Y^{*}_{\ell m}(\hat{k}) \tag{2.9}$$

in Eq. (2.6), integrating over angles and comparing with Eq. (1.29) in the form

$$F(\vec{k},\vec{k}') = i\frac{2\pi}{k}\sum_{\ell m}(1-\eta_{\ell})\,Y_{\ell m}(\hat{k}')\,Y^{*}_{\ell m}(\hat{k}) \tag{2.10}$$

gives

$$\eta_{\ell} = 1 - i\frac{4M}{\hbar^2}\int_0^{\infty} j_{\ell}(kr)\,U(r)\,f_{\ell}^{(+)}(k,r)\,r\,dr \tag{2.11}$$

This exact expression for the S-matrix elements in terms of the potential is in itself not very useful for calculating the η_ℓ, except as a starting point for approximation methods. It contains the full radial wave function $f_\ell^{(+)}(k, r)$ which behaves asymptotically as

$$f_\ell^{(+)} \cong \frac{i}{2}\,(H_\ell^* - \eta_\ell H_\ell) \tag{2.12}$$

where

$$H_\ell(kr) = ikr\, h_\ell^{(1)}(kr) \cong \exp i\left(kr - \ell\frac{\pi}{2}\right) \tag{2.13}$$

and $h_\ell^{(1)} = j_\ell + i n_\ell$ is the spherical Hankel function. In practice one calculates the η_ℓ by numerical integration of the radial wave equation

$$\frac{d^2 f_\ell^{(+)}}{dr^2} + \left[k^2 - \frac{\ell(\ell+1)}{r^2}\right] f_\ell^{(+)} = \frac{2M}{\hbar^2}\,U(r)\,f_\ell^{(+)} \tag{2.14}$$

The internal solution is generated from a series expansion in powers of kr by stepwise integration of Eq. (2.14), and matched to the external solution (2.12) at a radius so large that U(r) is negligible. The η_ℓ is determined by the condition of equal logarithmic derivatives of $f_\ell^{(+)}$ at the matching radius.

2.2 Coulomb interaction

For charged particles, the real part of U(r) contains the Coulomb potential $V_C(r)$, usually that of a uniform charge distribution

$$\begin{aligned} V_C(r) &= \frac{Z_a Z_A e^2}{2R_C}\left(3 - \frac{r^2}{R_C^2}\right) \qquad r \le R_C \\ V_C(r) &= \frac{Z_a Z_A e^2}{r} \qquad\qquad\qquad r \ge R_C \end{aligned} \tag{2.15}$$

where R_C is the Coulomb radius. The Coulomb-distorted radial wave function behaves asymptotically as

$$f_\ell^{(+)} \cong \frac{i}{2}\,(H_\ell^{C*} - \eta_\ell H_\ell^C) \tag{2.16}$$

where

$$H_\ell^C = G_\ell + iF_\ell \cong \exp i\left(\{kr\} - \ell\frac{\pi}{2} + \sigma_\ell\right) \tag{2.17}$$

The regular and irregular Coulomb wave functions are denoted by G_ℓ and F_ℓ, respectively, and satisfy the radial equation

$$\frac{d^2 H_\ell^C}{dr^2} + \left[k^2 - \frac{2kn}{r} - \frac{\ell(\ell+1)}{r^2}\right] H_\ell^C = 0 \tag{2.18}$$

The Coulomb phase shifts σ_ℓ are generated from the recursion relation

$$\sigma_\ell = \sigma_{\ell-1} + \operatorname{arctg}(n/\ell) \tag{2.19}$$

Again we obtain η_ℓ from the continuity condition at a suitably chosen matching radius.

2.3. Particles with spin

For particles with spins $\vec{s}_1$ and $\vec{s}_2$ the procedure remains essentially the same though the formalism becomes more involved. The interaction potential in general depends on $\vec{s}_1$, $\vec{s}_2$ and $\vec{\ell}$ as well as on r, and commutes with the total angular momentum $\vec{j}$. The wave function $\psi^{(+)}_{sm_s}(\vec{k},\vec{r})$ satisfies the Schrödinger equation

$$(\vec{\nabla}^2 + k^2)\,\psi^{(+)}_{sm_s} = U\,\psi^{(+)}_{sm_s} \tag{2.20}$$

Expanding $\psi^{(+)}_{sm_s}$ in eigenfunctions of $\vec{j}$ and $\vec{\ell}$,

$$\psi^{(+)}_{sm_s}(\vec{k},\vec{r}) = 4\pi \sum_{\ell\ell' j s' m'_s} \langle \ell s m_s | \mathscr{Y}^j(\hat{\vec{k}},\hat{\vec{r}}) | \ell' s' m'_s \rangle \chi_{s'm'_s} \frac{i^{\ell'} f^{j(+)}_{\ell s,\ell' s'}(k,r)}{kr} \tag{2.21}$$

yields

$$\left[\frac{d^2}{dr^2} + k^2 - \frac{\ell'(\ell'+1)}{r^2}\right] f^{j(+)}_{\ell s,\ell' s'}(k,r) = \frac{2M}{\hbar^2} \sum_{\ell'' s''} U^{j\ell s}_{\ell' s',\ell'' s''}(r)\, f^{j(+)}_{\ell s,\ell'' s''}(k,r) \tag{2.22}$$

where the interaction matrix is given by (see Ref. [1])

$$U^{j\ell s}_{\ell' s',\ell'' s''}(r) = i^{\ell''-\ell'} \frac{2s+1}{2j+1} \cdot \sum_{m'_s m''_s} \left\langle \chi_{s'm'_s} \middle| \iint \langle \ell' s' m'_s | \mathscr{Y}^j(\hat{\vec{k}},\hat{\vec{r}}) | \ell s m_s \rangle^* U \langle \ell'' s'' m''_s | \mathscr{Y}^j(\hat{\vec{k}},\hat{\vec{r}}) | \ell s m_s \rangle d\hat{\vec{r}}\, d\hat{\vec{k}} \middle| \chi_{s''m''_s} \right\rangle \tag{2.23}$$

Equation (2.11) is generalized to

$$S^j_{\ell s,\ell' s'} = \delta_{\ell\ell'}\delta_{ss'} - i\frac{4M}{\hbar^2} \sum_{\ell'' s''} \int_0^\infty j_{\ell'}(kr)\, U^{j\ell s}_{\ell' s',\ell'' s''}(r)\, f^{j(+)}_{\ell'' s',\ell s}(k,r)\, r\, dr \tag{2.24}$$

The radial wave functions $f^{j(+)}_{\ell s, \ell' s'}$ now satisfy a system of $2s+1$ coupled differential equations (2.22). If the interaction is central, we have $U^{j\ell s}_{\ell' s', \ell'' s''} = \delta_{\ell\ell'}\delta_{ss'}U^{j\ell s}$ and the system (2.22) gets uncoupled.

2.4. Spin-$\frac{1}{2}$ and spin-1 particles

Let us now specialize to spin-$\frac{1}{2}$ particles scattered by spinless targets. The interaction will in general contain a spin-orbit term of the form

$$U_s(r)\,\vec{\ell}\cdot\vec{s} \tag{2.25}$$

where $U_s = V_s + iW_s$, in addition to the central potential $U_c(r)$. The eigenvalues of $\vec{\ell}\cdot\vec{s}$ in the two spin states $j = \ell + \frac{1}{2}$ and $j = \ell - \frac{1}{2}$ are $\frac{1}{2}\ell$ and $-\frac{1}{2}(\ell+1)$, respectively. For the radial wave functions we write $f^{\ell\pm\frac{1}{2}(+)}_{\ell\frac{1}{2},\ell'\frac{1}{2}} \equiv \delta_{\ell\ell'} f^{(+)}_{\ell,\pm}$, and Eq. (2.22) becomes

$$\begin{aligned}\left[\frac{d^2}{dr^2} + k^2 - \frac{\ell(\ell+1)}{r^2}\right] f^{(+)}_{\ell,+}(k,r) &= \left[U_c(r) + \tfrac{1}{2}\ell U_s(r)\right] f^{(+)}_{\ell,+}(k,r)\\ \left[\frac{d^2}{dr^2} + k^2 - \frac{\ell(\ell+1)}{r^2}\right] f^{(+)}_{\ell,-}(k,r) &= \left[U_c(r) - \tfrac{1}{2}(\ell+1)U_s(r)\right] f^{(+)}_{\ell,-}(k,r)\end{aligned} \tag{2.26}$$

For spin-1 particles there are three states $j = \ell+1,\ \ell,\ \ell-1$, in which the spin-orbit operator $\vec{\ell}\cdot\vec{s}$ has the eigenvalues $\ell,\ -1,\ -(\ell+1)$, respectively. Under the spin-orbit interaction (2.25) the corresponding radial wave functions $f^{\ell+1,\ell,\ell-1}_{\ell 1,\ell' 1} \equiv \delta_{\ell\ell'}(f_{\ell,+},\ f_{\ell,0},\ f_{\ell,-})$ satisfy three uncoupled differential equations. However, in addition to the vector spin-orbit interaction there may be tensor couplings of the form (see Ref. [2])

$$(\hat{r}\vec{s})^2 - \tfrac{2}{3},\ (\vec{p}\,\vec{s})^2 - \tfrac{2}{3}\vec{p}^{\,2},\ (\vec{\ell}\,\vec{s})^2 + \tfrac{1}{2}\vec{\ell}\,\vec{s} - \tfrac{2}{3}\vec{\ell}^{\,2} \tag{2.27}$$

which in general give a set of coupled radial equations. In this Course we shall confine ourselves to spin-0 and spin-$\frac{1}{2}$ projectiles.

2.5. Isobaric spin coupling

A formalism similar to that for ordinary spin applies to the isobaric spins $\vec{t}_1$ and $\vec{t}_2$ of the particles. Lane [3,4] has suggested an extension of the real potential by an isobaric spin coupling of the form

$$V_t(r)\,\vec{t}\cdot\vec{T} \tag{2.28}$$

which arises from the Heisenberg force in the nucleon-nucleon interaction and is analogous to the spin-orbit interaction (2.25). We shall find it convenient to include a factor $4/A$ in Eq. (2.28), so the real

potential becomes

$$V = V_0 + \frac{4}{A} V_t \vec{t} \cdot \vec{T} \tag{2.29}$$

For nucleons the total isobaric spin can have the values $T' = T + \frac{1}{2}$ and $T' = T - \frac{1}{2}$, where $T = \frac{1}{2}(N - Z)$. In these states the operator $\vec{t} \cdot \vec{T}$ has the eigenvalues $\frac{1}{2}T$ and $-\frac{1}{2}(T + 1)$, respectively. Incident neutrons ($t_3 = +\frac{1}{2}$) can only have $T + \frac{1}{2}$, while protons can have both $T + \frac{1}{2}$ and $T - \frac{1}{2}$. The neutron potential is

$$V_n = V_0 + \frac{2}{A} V_t T = V_0 + V_t \frac{N - Z}{A} \tag{2.30}$$

We obtain the mean proton potential as an average of

$$V_p^{(+)} = V_0 + \frac{2}{A} V_t T \quad \text{and} \quad V_p^{(-)} = V_0 - \frac{2}{A} V_t (T + 1) \tag{2.31}$$

weighted with $(2T + 1)^{-1}$ and $2T(2T + 1)^{-1}$ respectively,

$$V_p = \frac{1}{2T + 1} (V_p^{(+)} + 2T V_p^{(-)}) = V_0 - \frac{2}{A} V_t T = V_0 - V_t \frac{N - Z}{A} \tag{2.32}$$

That part of the optical potential which is proportional to $(N-Z)/A$ is called the symmetry term.

The scattering amplitude has two components, $f^{(+)}(\theta)$ and $f^{(-)}(\theta)$, and the elastic proton scattering amplitude becomes

$$f_{pp}(\theta) = \frac{1}{2T + 1} [f^{(+)}(\theta) + 2T f^{(-)}(\theta)] \tag{2.33}$$

To the spin-flip amplitude in spin-orbit interaction corresponds a charge-exchange reaction amplitude for transition to the isobaric analogue state of the target nucleus,

$$f_{pn}(\theta) = \frac{(2T)^{\frac{1}{2}}}{2T + 1} [f^{(+)}(\theta) - f^{(-)}(\theta)] \tag{2.34}$$

The differential cross-sections for p-p scattering and p-n reaction become

$$\frac{d\sigma}{d\Omega}(pp) = |f_{pp}(\theta)|^2 = \frac{1}{(2T + 1)^2} |f^{(+)}(\theta) + 2T f^{(-)}(\theta)|^2 \tag{2.35}$$

$$\frac{d\sigma}{d\Omega}(pn) = |f_{pn}(\theta)|^2 = \frac{2T}{(2T + 1)^2} |f^{(+)}(\theta) - f^{(-)}(\theta)|^2 \tag{2.36}$$

respectively.

These formulae are valid only if Coulomb forces may be neglected. As the Coulomb interaction is non-central in isobaric spin space, it couples together the equations for the proton and neutron wave functions, the space parts of which behave asymptotically as

$$\psi_p^{(+)}(\vec{k}_p, \vec{r}_p) \cong e^{i\{\vec{k}_p\vec{r}_p\}} + f_{pp}(\theta)\frac{e^{i\{k_p r_p\}}}{r_p} \tag{2.37}$$

$$\psi_n^{(+)}(\vec{k}_n, \vec{r}_n) \cong f_{pn}(\theta)\frac{e^{ik_n r_n}}{r_n} \tag{2.38}$$

In the isobaric spin coupling we have encountered an "extended" potential which can cause transitions to non-elastic channels. We shall discuss other interactions of this kind in later lectures.

3. THE OPTICAL MODEL

3.1. Non-local interaction

Basically, the interaction between complex nuclei is a many-body problem and complex potentials can be calculated, at least in principle, from given nucleon-nucleon forces. This fundamental approach has been developed particularly by Brueckner and his co-workers and has gone a long way in justifying the phenomenological potential treatment of nucleon-nucleus interaction. Though the theory itself is outside the scope of the Course, its result has certain features which should be incorporated in the phenomenological model. It turns out that the nucleon-nucleus interaction operator for finite nuclei [5] is non-local in coordinate space. The interaction is described by a matrix $\langle \vec{r} | V | \vec{r}' \rangle = K(\vec{r}, \vec{r}')$, and the single-particle Schrödinger equation has the form

$$(\vec{\nabla}^2 + k^2)\psi(\vec{r}) = \frac{2M}{\hbar^2}\int K(\vec{r}, \vec{r}')\psi(\vec{r}')\,d\vec{r}' \tag{3.1}$$

In a phenomenological treatment one can describe the effects of the non-locality without knowing the detailed structure of the interaction matrix, by introducing the range of non-locality, b, as a phenomenological parameter. A general form of $K(\vec{r}, \vec{r}')$ can be given by the requirements of (i) symmetry, $K(\vec{r}, \vec{r}') = K(\vec{r}', \vec{r})$, (ii) reduction to a local potential $K(\vec{r}, \vec{r}') \to V(\vec{r})\delta(\vec{r} - \vec{r}')$ in the limit $b \to 0$, and (iii) translation invariance in infinite nuclear matter, $K(\vec{r}, \vec{r}') \to V_0 \delta_b(\vec{r} - \vec{r}')$, where the interaction is equivalent to an effective nucleon mass. From these conditions, Frahn and Lemmer [6, 7] have suggested the form

$$K(\vec{r}, \vec{r}') = V^{(N)}\left(\frac{\vec{r} + \vec{r}'}{2}\right)\delta_b(\vec{r} - \vec{r}') \tag{3.2}$$

with, for instance, $\delta_b(\vec{\rho}) = \pi^{-3/2} b^{-3} \exp(-\rho^2/b^2)$, and investigated Eq. (3.1) in effective mass approximation. The radial wave equation becomes

$$\left[\frac{d^2}{dr^2} + k^2 - \frac{\ell(\ell+1)}{r^2}\right] f_\ell(k,r) = \frac{2M}{\hbar^2} \int_0^\infty K_\ell(r,r') f_\ell(k,r')\, dr' \tag{3.3}$$

where

$$K_\ell(r,r') = 2\pi rr' \int_{-1}^{+1} K(\vec{r},\vec{r}')\, P_\ell(\zeta)\, d\zeta \tag{3.4}$$

This shows that non-local interactions are essentially ℓ-dependent.

Ansatz (3.2) has been used by Perey and Buck [8] as a non-local extension of the complex potential,

$$K(\vec{r},\vec{r}') = \left[V^{(N)}\left(\frac{\vec{r}+\vec{r}'}{2}\right) + i\, W^{(N)}\left(\frac{\vec{r}+\vec{r}'}{2}\right)\right] \delta_b(\vec{r} - \vec{r}') \tag{3.5}$$

It is assumed that the non-local form factor $\delta_b(\rho)$ has the same functional form for both real and imaginary parts of the interaction. From their comprehensive analysis of neutron-nucleus scattering in the energy range 1-25 MeV, Perey and Buck conclude that the energy-dependent local potential is largely equivalent to an energy-independent non-local potential. Furthermore, these authors found that the non-local interaction is well approximated by an energy-dependent "equivalent local potential" $U^{(L)}(\vec{r})$, implicitly defined by

$$U^{(N)}(\vec{r}) = U^{(L)}(\vec{r}) \exp\left[\frac{Mb^2}{2\hbar^2}\,(E - U^{(L)}(\vec{r}))\right] \tag{3.6}$$

where the non-locality for neutrons has a range $b \approx 0.9$ fm. It can be shown [9] that this relation follows from the Perey-Saxon approximation [10] if the Fourier transform of $\delta_b(\rho)$ is expanded about the local wave number associated with the potential $U^{(L)}(\vec{r})$.

An alternative way of defining an equivalent local potential is to require that both interactions give the same scattering, i.e. generate the same S-matrix elements [11]. This requirement has been studied in the three-dimensional case by Fiedeldey [12]. He finds that the equivalent local potential is very close to $U^{(L)}(\vec{r})$ as defined by Eq. (3.6). Perey has shown [13] that the non-local wave function in the nuclear interior is reduced compared with the equivalent local wave function. For this "Perey effect", Fiedeldey obtains the explicit expression

$$\psi_N(\vec{r}) = \psi_L(\vec{r}) \exp\left[\frac{1}{8} b^2 U^{(L)}(\vec{r})\right] \tag{3.7}$$

He also shows that the equivalent local spin-orbit potential $U_s^{(L)}(\vec{r})$ is strongly reduced relative to the non-local spin-orbit potential $U_s^{(N)}(\vec{r})$,

$$U_s^{(L)}(\vec{r}) = \frac{U_s^{(N)}(\vec{r})}{1 - \frac{Mb^2}{2\hbar^2} U^{(L)}(\vec{r})} = \frac{M(\vec{r})}{M} U_s^{(N)}(\vec{r}) \qquad (3.8)$$

where $M(\vec{r})$ is the energy-dependent effective mass function [9].

The non-locality of the nucleon-nucleus interaction resulting from the Brueckner theory explains most of the observed energy-dependence of the real part of the phenomenological potential. However, the energy dependence of the imaginary part has a different physical origin. Absorptive potentials have been calculated in a many-body approach by various authors [14-22]. A general result is that $W^{(L)}(r)$ increases with energy up to about 100 MeV, mainly because nucleon-nucleon scattering is less inhibited by the Pauli principle at higher energies. For this reason it is difficult to justify Perey and Buck's assumption of equal non-local form factors for the real and imaginary parts of $K(\vec{r}, \vec{r}')$. In fact it is not at all clear that the energy dependence of $W^{(L)}(r)$ can be completely replaced by a non-locality [23, 24]. We may, nevertheless, try to describe this dependence phenomenologically by assuming [25]

$$K(\vec{r}, \vec{r}') = V^{(N)}\left(\frac{\vec{r}+\vec{r}'}{2}\right) \delta_{b_R}(\vec{r} - \vec{r}') + i W^{(N)}\left(\frac{\vec{r}+\vec{r}'}{2}\right) \vec{\nabla}^2 \delta_{b_I}(\vec{r}-\vec{r}') \qquad (3.9)$$

A recent investigation [26] shows that this and similar forms of non-locality of the imaginary potential give good agreement with neutron data over a wide range of energies.

In general it appears possible to approximately replace non-local effects in nuclear scattering by a suitably defined local potential, which is easier to handle in numerical calculations. The equivalence would be exact if it could be proved that for a given non-local interaction there always exists a local potential which generates the same S-matrix. To my knowledge this is still an open question. In what follows let us be satisfied with an approximate equivalence.

3.2. Scattering of nucleons

We now turn to applications of the complex potential model to elastic nuclear scattering, where it is usually called the "optical model". You will find a comprehensive account in Hodgson's book [27]. Collecting the various components considered so far, the optical potential becomes

$$U(r) = V_c(r) + i W_c(r) + [V_s(r) + i W_s(r)] \vec{\ell} \cdot \vec{s} + V_C(r) + \frac{4}{A} V_t(r) \vec{t} \cdot \vec{T} \qquad (3.10)$$

Each term (except V_C) may be a function of energy E and is written in the form $U_i = -[V_{0,i} g_{iR}(r) + i W_{0,i} g_{iI}(r)]$, where $V_{0,i}$, $W_{0,i}$ are the "depths" and $g_{iR}(r)$, $g_{iI}(r)$ the radial shapes of the component i. The radial shapes

are usually characterized by two parameters, a radius $R = r_0 A^{\frac{1}{3}}$ and a diffuseness d. In general, each component will have a different shape and different values of r_0 and d. The specific functional forms of $g_i(r)$ are not determined by basic theory and are chosen for mathematical convenience. In most analyses the real central potential $V_c(r)$ is assumed to be of Saxon-Woods (SW) shape

$$g_{cR}(r) = \left[1 + \exp\left(\frac{r - R}{d}\right)\right]^{-1} \tag{3.11}$$

The shape of the absorptive central potential is in general different from that of the real part. At low energies, nucleon-nucleon scattering is less inhibited by the exclusion principle in the nuclear surface than in the nuclear interior and we expect that $g_{cI}(r)$ is surface-peaked. This simple picture is supported by low-energy neutron scattering data [28-32] and confirmed by many-body calculations [18-21]. Possible forms describing surface-peaked absorption are of Gaussian or derivative-SW shape

$$g_{cI}(r) = \exp\left[-\left(\frac{r - R}{d}\right)^2\right] \text{ or } g_{cI} = -4d\,\frac{dg_{cR}(r)}{dr} \tag{3.12}$$

and the imaginary central potential should be a combination of a surface and a volume absorption term. The relative strength of volume absorption increases with energy and at high energies the shape of $W_c(r)$ becomes approximately proportional to the nucleon density distribution.

For the spin-orbit potential one nearly always choses the Thomas form

$$g_s(r) = -\frac{1}{r}\,\frac{dg_{cR}(r)}{dr} \tag{3.13}$$

In the next section we shall see that this assumption can be justified in high-energy approximation if $g_{cR}(r)$ represents the nucleon density distribution. The isobaric spin potential is usually assumed to have SW shape [33], but it has been suggested [34] that $V_t(r)$ should be peaked in the nuclear surface because the proton and neutron density distributions have different radii.

Extensive optical model analyses of nucleon-nucleus scattering data at low and medium energies have been made in recent years. A complete analysis should give simultaneous fits of the differential cross-sections $d\sigma/d\Omega$, the integrated cross-sections σ_{tot} and σ_{abs}, and the polarization $P(\theta)$. Comprehensive investigations have been made of neutron scattering in the range 1-25 MeV by Perey and Buck [8] and by Wilmore and Hodgson [35], of proton scattering in the range 9-22 MeV by Perey [36] and at 30 MeV by Barrett et al. [37]. The most recent and complete analysis has been presented by Rosen et al. [38]. These studies show that it is possible to give a consistent overall description of nucleon-nucleus entrance channel phenomena in the low and medium energy range for not too light target nuclei. However, the

number of phenomenological parameters necessary to obtain satisfactory fits is considerable, and usually one cannot determine their values without ambiguity. The ambiguities in the nucleon-nucleus potential become more serious at higher energies where the absorption is stronger. Consider, for instance, the extensive proton scattering data of Johansson et al. [39] at 180 MeV. With the usual optical potentials it is difficult to reconcile the smooth variation of the differential cross-sections at larger angles with the pronounced oscillatory behaviour of the polarization. One possible solution is to assume [40] that the radius of $W_c(r)$ is about 30% larger than that of $V_c(r)$. Similar features are observed at 150 MeV [41] and 160 MeV [42]. A re-analysis of the 180-MeV data by Haybron and Satchler [43] with a 9-parameter optical potential gives improved fits of $d\sigma/d\Omega$ but the polarization fits still appear to be unsatisfactory. Recently, Elton [44] has shown that an adequate description can be obtained with an entirely different shape of $V_c(r)$, consisting of an attractive peak in the nuclear surface and a repulsive interior part. Potentials of this shape are suggested by the strong absorption model. Analyses with this model show that at very high energies the real central potential differs in both shape and sign from those found in the region below 100 MeV [45, 46].

3.3. Scattering of composite particles

The scattering of composite particles (deuterons, tritons, helium-3, alpha particles and heavy ions) is dominated by strong absorption at all energies above the Coulomb barrier. If we want to describe the interaction by means of a complex potential we would expect that the interior is largely shielded by the absorption in the nuclear surface. Igo [47, 48] was the first to point out that the scattering of alpha particles is largely insensitive to the potential in the nuclear interior. For deuteron scattering the extensive analyses by Perey and Perey [49] and by Halbert [50] revealed certain ambiguities in the depth of the real central potential [51]. These have been investigated by Drisko, Satchler and Bassel [52] who found that the different V(r) that fit the data generate essentially the same values of η_ℓ. The potentials V(r) in the nuclear interior have discrete values such that consecutive well depths differ by one half-wave length of each partial wave that contributes to the scattering. This is easily understood in terms of Austern's WKB calculations (see section 8.2). Similar ambiguities are found for helium-3 and alpha particles (see Ref. [53]).

Can we resolve this ambiguity, is there a criterion by which we can select the "right" optical potential? One might think that combined analyses of direct reactions in distorted-wave Born approximation (DWBA) and of elastic scattering would lead to a unique potential. The radial integrals in DWBA extend mainly over the nuclear interior where the distorted radial waves differ for the different potentials. But so do the radial integrals for elastic scattering, yet they yield the same values of η_ℓ. We shall see later that at least for inelastic scattering, and probably for all surface reactions of strongly absorbed particles, the radial integrals can be expressed in terms of the elastic η_ℓ. It is therefore very unlikely that combined elastic and reaction analyses will determine a unique potential. A more promising possibility is

to calculate V(r) for composite projectiles from given nucleon-nucleus potentials. This has been investigated by Rook [54]. He starts from Watanabe's expression [55] for the deuteron potential

$$V_d(\vec{r}) = \int [V_n(\vec{r}+\tfrac{1}{2}\vec{x}) + V_p(\vec{r}-\tfrac{1}{2}\vec{x})]\ [\varphi_d(\vec{x})]^2\, d\vec{x} \tag{3.14}$$

where V_p and V_n are the proton-nucleus and neutron-nucleus potentials, and $\varphi_d(\vec{x})$ is the deuteron wave function. If V_n and V_p are assumed constant in the nuclear interior we have $V_{0,d} \approx V_{0,n} + V_{0,p} = 2V_{0,N}$, where $V_{0,N}$ is the mean nucleon-nucleus potential well depth $V_{0,N} \approx 50$ MeV. Rook extends this relation to heavier projectiles and conjectures

$$V_{0,P} \approx A_P V_{0,N} \tag{3.15}$$

where A_P is the mass number of projectile P. This selects the "deep" potentials $V_{0,p} \approx 100$ MeV, 150 MeV and 200 MeV for deuterons, tritons and ^{3}He, and alpha particles, respectively. One would expect a similar relation for the depth of the absorptive potential. The ambiguities of W(r) for composite particles have not received as much attention as those of V(r) and deserve further study.

The phenomenological optical model considered so far does not explicitly take into account the contributions to elastic scattering which arise from coupling to inelastic channels. A generalization of the optical potential and the calculation of these effects by means of the coupled-channels theory will be briefly discussed later (see section 11).

4. APPROXIMATION METHODS

The wave equation (2.1) or (3.1) cannot be solved in closed form except in very few special cases, and solutions have to be obtained by numerical integration. It is however often useful and desirable to study the behaviour of wave functions, scattering amplitudes and S-matrix elements in terms of explicit expressions which can be derived by means of approximation methods. We shall now discuss several of these methods.

4.1. Born approximation

Starting from Eq. (2.6) for the elastic scattering amplitude, we obtain the first-order term of the Born series expansion by putting

$$\psi^{(+)}(\vec{k},\vec{r}) \approx e^{i\vec{k}\cdot\vec{r}} \tag{4.1}$$

This yields

$$F^{(B)}(\vec{k},\vec{k}') = -\frac{M}{2\pi\hbar^2}\int e^{i(\vec{k}-\vec{k}')\vec{r}}\ U(\vec{r})\, d\vec{r} = -\frac{M}{2\pi\hbar^2}\,\tilde{U}(\vec{q}) \tag{4.2}$$

where $\tilde{U}(\vec{q})$ is the Fourier transform of the complex potential and $\vec{q} = \vec{k} - \vec{k}'$ the momentum transfer. This approximation is valid roughly if

$$\frac{|U|}{E} kd \ll 1 \tag{4.3}$$

where d is the range over which the potential changes significantly. This condition is however seldom satisfied in nuclear scattering. Much more useful is the WKB approximation.

4.2. WKB approximation

This method starts from the classical limit of the wave equation by means of an expansion in powers of $\hbar$. Since it describes several important non-classical features we may call it a semi-classical approximation. The wave function is written in the form

$$\psi^{(+)}(\vec{k}, \vec{r}) = e^{iS(\vec{k}, \vec{r})} \tag{4.4}$$

where $S(\vec{k}, \vec{r})$ is a complex phase function. Now we write

$$S(\vec{k}, \vec{r}) = S_0(\vec{k}, \vec{r}) - i\hbar S_1(\vec{k}, \vec{r}) \tag{4.5}$$

insert (4.4) in the Schrödinger equation and compare powers of $\hbar$. This yields two equations,

$$(\vec{\nabla} S_0)^2 = k^2(\vec{r}) \tag{4.6}$$

and

$$\vec{\nabla} S_0 \vec{\nabla} S_1 + \vec{\nabla}^2 S_0 = 0 \tag{4.7}$$

where

$$k^2(\vec{r}) = k^2 - \frac{2M}{\hbar^2} U(\vec{r}) \tag{4.8}$$

is the square of the local wave number. Equation (4.7) reduces to the continuity equation for the velocity field $\vec{v}(\vec{r}) = (\hbar/M)\vec{k}(\vec{r})$ and the particle density $|\psi|^2$. Equation (4.6) is equivalent to the Hamilton-Jacobi equation for the characteristic function $S_0(\vec{k}, \vec{r})$ and means that the motion proceeds along trajectories normal to the surfaces $S_0 = \text{const.}$ (geometrical optics approximation). The solution of (4.6) is therefore

$$S_0(\vec{k}, \vec{r}) = \int_{\substack{\text{class.} \\ \text{traject.}}}^{\vec{r}} k(\vec{r}')\, d\vec{r}' = \int_{\substack{\text{class.} \\ \text{traject.}}}^{\vec{r}} \left[k^2 - \frac{2M}{\hbar^2} U(r')\right]^{\frac{1}{2}} d\vec{r}' \tag{4.9}$$

4.3. High-energy approximation [56]

If $E \gg |U|$, we may expand the integrand in (4.9)

$$S(\vec{k},\vec{r}) = \vec{k}\cdot\vec{r} - \frac{M}{\hbar^2 k}\int^{\vec{r}} U(\vec{r}')\,d\vec{r}' \tag{4.10}$$

(where we have dropped the subscript 0). Under the condition $kd \gg 1$ the deviation of the trajectory by the potential will be small and we may replace it by a straight line in the direction of incidence $\hat{k}$ which defines our z-axis. Thus $\vec{r} = \vec{b} + \hat{k}z$, where $|\vec{b}| = b$ is the impact parameter, and (4.10) becomes

$$S(\vec{k},\vec{r}) = \vec{k}\cdot\vec{r} - \frac{M}{\hbar^2 k}\int_{-\infty}^{z} U(\vec{b}+\hat{k}z')\,dz' \tag{4.11}$$

In the relativistic case the same formula holds, but with M replaced by E/c^2 [57]. By inserting (4.11) in Eq. (2.6) we obtain for the scattering amplitude

$$F(\vec{k},\vec{k}') = -\frac{M}{2\pi\hbar^2}\int e^{i(\vec{k}-\vec{k}')\cdot\vec{r}}\; U(\vec{r})\exp\left[-i\frac{M}{\hbar^2 k}\int_{-\infty}^{z} U(\vec{b}+\hat{k}z')dz'\right] d\vec{r} \tag{4.12}$$

At small scattering angles such that $\theta^2 kd \ll 1$ we have $(\vec{k}-\vec{k}')\cdot\vec{r} \approx (\vec{k}-\vec{k}')\cdot\vec{b}$. Hence

$$F(\vec{k},\vec{k}') = -\frac{M}{2\pi\hbar^2}\int e^{i(\vec{k}-\vec{k}')\cdot\vec{b}}\, I(\vec{b})\, d^{(2)}b \tag{4.13}$$

where

$$I(\vec{b}) = \int_{-\infty}^{\infty} U(\vec{b}+\hat{k}z)\exp\left[-i\frac{M}{\hbar^2 k}\int_{-\infty}^{z} U(\vec{b}+\hat{k}z')\,dz'\right] dz \tag{4.14}$$

Now

$$\begin{aligned} I(\vec{b}) &= i\frac{\hbar^2 k}{M}\int_{-\infty}^{\infty}\frac{d}{dz}\exp\left[-i\frac{M}{\hbar^2 k}\int_{-\infty}^{z} U(\vec{b}+\hat{k}z')\,dz'\right] dz \\ &= i\frac{\hbar^2 k}{M}\left\{\exp\left[-i\frac{M}{\hbar^2 k}\int_{-\infty}^{\infty} U(\vec{b}+\hat{k}z')\,dz'\right] - 1\right\} \end{aligned} \tag{4.15}$$

and we obtain

$$F(\vec{k},\vec{k}') = \frac{ik}{2\pi}\int e^{i(\vec{k}-\vec{k}')\cdot\vec{b}}\;\left[1 - e^{i2\delta(\vec{b})}\right] d^{(2)}b \tag{4.16}$$

where

$$\delta(\vec{b}) = -\frac{M}{2\hbar^2 k}\int_{-\infty}^{\infty} U(\vec{b} + \hat{\vec{k}}z)\,dz \tag{4.17}$$

If the potential is symmetrical about the $\hat{\vec{k}}$-axis, $\delta(\vec{b}) = \delta(b)$. Then for small angles $(\vec{k} - \vec{k}')\cdot\vec{b} \approx kb\theta\cos\phi$, and using the integral representation of the Bessel function

$$\int_0^{2\pi} e^{ikb\theta\cos\phi}\,d\phi = 2\pi J_0(kb\theta) \tag{4.18}$$

we have

$$F(\vec{k}, \vec{k}') = ik\int_0^{\infty}[1 - e^{i2\delta(b)}]\,J_0(kb\theta)\,b\,db \tag{4.19}$$

Now we consider scattering of spin-$\frac{1}{2}$ particles and assume that the potential consists of a central and a spin-orbit part, $U(r) = U_c(r) + U_s(r)\vec{\ell}\cdot\vec{s}$. Since $\vec{\ell} = \vec{r}\times\vec{k}$ and $\vec{s} = \frac{1}{2}\vec{\sigma}$, we may write

$$F(\vec{k}, \vec{k}') = \frac{ik}{2\pi}\int e^{i(\vec{k}-\vec{k}')\cdot\vec{b}}\,[1 - e^{i2\delta_c(b)}e^{i2\delta_s(b)(\vec{b}\times\vec{k})\cdot\vec{\sigma}}]\,d^{(2)}b \tag{4.20}$$

where $\delta_c(b)$ is given by (4.17) with $U = U_c$ and

$$\delta_s(b) = -\frac{M}{4\hbar^2 k}\int_{-\infty}^{\infty} U_s(\vec{b} + \hat{\vec{k}}z)\,dz \tag{4.21}$$

By expanding the exponential in the integrand of (4.20) and using the anticommutation properties of the Pauli spin operator we obtain [56]

$F(\vec{k}, \vec{k}') =$

$$\frac{ik}{2\pi}\int e^{i(\vec{k}-\vec{k}')\cdot\vec{b}}\left\{1 - e^{i2\delta_c(b)}\cos[2kb\delta_s(b)] - i\,e^{i2\delta_c(b)}\sin[2kb\delta_s(b)]\,(\hat{\vec{b}}\times\hat{\vec{k}})\vec{\sigma}\right\}d^{(2)}b \tag{4.22}$$

With $\hat{\vec{b}}\times\hat{\vec{k}} = (\hat{\vec{k}}\times\hat{\vec{k}}')\cos\phi$, Eq. (4.18) and

$$\int_0^{2\pi} e^{ikb\theta\cos\phi}\cos\phi\,d\phi = i\,2\pi\,J_1(kb\theta) \tag{4.23}$$

the amplitude can be written in the form (1.12)

$$F(\vec{k},\vec{k}') = f(\theta) = A(\theta) + B(\theta)\vec{n}\vec{\sigma} \tag{4.24}$$

where

$$\begin{aligned} A(\theta) &= ik\int_0^\infty \{1 - e^{i2\delta_c(b)} \cos\,[2kb\delta_s(b)]\}\, J_0(kb\theta)\, bdb \\ B(\theta) &= ik\int_0^\infty \{e^{i2\delta_c(b)} \sin\,[2kb\delta_s(b)]\}\, J_1(kb\theta)\, bdb \end{aligned} \tag{4.25}$$

4.4. Impact parameter approximation

Here we start from the partial-wave expansion (1.15) of $A(\theta)$ and $B(\theta)$,

$$\begin{aligned} A(\theta) &= \frac{i}{2k}\sum_{\ell=0}^{\infty}(2\ell+1)\,(1-\bar{\eta}_\ell)\,P_\ell(\cos\theta) \\ B(\theta) &= -\frac{1}{2k}\sum_{\ell=0}^{\infty}\xi_\ell\,\frac{d}{d\theta}\,P_\ell(\cos\theta) \end{aligned} \tag{4.26}$$

introduce the semi-classical correspondence $\ell+\frac{1}{2}\approx kb$, and replace the summation over ℓ by an integration over impact parameters b. Using Szegö's asymptotic expression for the Legendre polynomials,

$$P_\ell(\cos\theta) \cong \left(\frac{\theta}{\sin\theta}\right)^{\frac{1}{2}} J_0[\,(\ell+\tfrac{1}{2})\theta] \tag{4.27}$$

we obtain for small angles

$$\begin{aligned} A(\theta) &= ik\int_0^\infty [1-\bar{\eta}(b)]\, J_0(kb\theta)\, bdb \\ B(\theta) &= \tfrac{1}{2}k\int_0^\infty \xi(b)\, J_1(kb\theta)\, bdb \end{aligned} \tag{4.28}$$

Comparison with (4.25) gives

$$\bar{\eta}(b) = e^{i2\delta_c(b)} \cos[2kb\delta_s(b)] \tag{4.29}$$

$$\xi(b) = i\,2\,e^{i2\delta_c(b)} \sin[2kb\delta_s(b)] \tag{4.30}$$

This shows that the functions $\delta_c(b)$, $\delta_s(b)$ are the phase shifts for the central and spin-orbit potentials, respectively. For spherically-symmetrical potentials we may rewrite Eqs. (4.17), (4.21) in the form

$$\delta_c(b) = -\frac{M}{\hbar^2 k}\int_b^\infty \frac{U_c(r)\,r\,dr}{(r^2-b^2)^{\frac{1}{2}}} \tag{4.31}$$

$$\delta_s(b) = -\frac{M}{2\hbar^2 k}\int_b^\infty \frac{U_s(r)\,r\,dr}{(r^2-b^2)^{\frac{1}{2}}} \tag{4.32}$$

For the S-matrix elements

$$\eta_\ell^+ = \bar{\eta}_\ell + \frac{\ell}{2\ell+1}\,\xi_\ell, \qquad \eta_\ell^- = \bar{\eta}_\ell - \frac{\ell+1}{2\ell+1}\,\xi_\ell \tag{4.33}$$

we obtain in impact parameter approximation

$$\begin{aligned} \eta^+(b) &\approx \bar{\eta}(b) + \tfrac{1}{2}\xi(b) = \exp\{i\,2[\delta_c(b) + kb\delta_s(b)]\} \\ \eta^-(b) &\approx \bar{\eta}(b) - \tfrac{1}{2}\xi(b) = \exp\{i\,2[\delta_c(b) - kb\delta_s(b)]\} \end{aligned} \tag{4.34}$$

For an independent-particle model of the nucleus, Glauber [56] has shown that the complex nucleon-nucleus potential can be expressed in terms of the nucleon-nucleon scattering amplitude as

$$U(r) = -A\,\frac{2\pi\hbar^2}{M}\left[a_n(0)\rho(r) + i\,b_n'(0)\,\frac{1}{r}\,\frac{d\rho(r)}{dr}\,\vec{l}\cdot\vec{\sigma}\right] \tag{4.35}$$

where A is the target mass number, $\rho(r)$ the nuclear density normalized to unity, and

$$f_n(\theta) = a_n(\theta) + b_n(\theta)\,\vec{n}\cdot\vec{\sigma} \tag{4.36}$$

the nucleon-nucleon scattering amplitude (b_n' denoting the derivative of b_n with respect to angle). Hence we have

$$U_c(r) = -A\,\frac{2\pi\hbar^2}{M}\,a_n(0)\rho(r) \tag{4.37}$$

$$U_s(r) = -A\,\frac{4\pi\hbar^2}{M}\,b_n'(0)\,\frac{1}{r}\,\frac{d\rho(r)}{dr} \tag{4.38}$$

Equation (4.38) justifies assumption (3.13) for the form of the spin-orbit potential. From Eq. (4.37) we obtain, using the optical theorem,

$$W(r) = -A\,\frac{2\pi\hbar^2}{M}\,\mathrm{Im}\,a_n(0)\rho(r) = -A\,\frac{\hbar^2 k}{2M}\,\sigma_n\rho(r) \tag{4.39}$$

where σ_n is the total nucleon-nucleon cross-section. In the nuclear interior, assuming constant nucleon density $\rho_0 = A\rho(0)$, we have

$$W_0 = \frac{\hbar^2 k}{2M}\,\sigma_n\rho_0 = \frac{\hbar^2 k}{2M}\,\frac{1}{L} \tag{4.40}$$

where $L = (\sigma_n\rho_0)^{-1}$ is the classical expression for the nucleon mean free path. From Eqs. (4.29) and (4.31) we can derive an approximate expression for the transparency of the nucleus to low-ℓ partial waves

$$\epsilon \equiv \left|\bar{\eta}(0)\right| = e^{-2\,\mathrm{Im}\delta_c(0)} = \exp\left[\frac{2M}{\hbar^2 k}\int_0^\infty W(r)\,dr\right] \approx \exp\left(-\frac{2M}{\hbar^2 k}\,W_0 R\right)$$

or

$$\epsilon \approx e^{-R/L} \tag{4.41}$$

4.5. Rainbow scattering approximation

Another semiclassical method based on the WKB approximation has been developed by Ford and Wheeler [58]. It is assumed that the nucleus is "semitransparent" and that the interaction can be described by a smoothly varying potential with weak absorption in the nuclear surface. The classical deflection function $\Theta(\ell) = 2d\sigma_\ell/d\ell$ for the nuclear plus Coulomb potential has a maximum θ_r, the "rainbow angle", at a certain angular momentum ℓ_r. By means of suitable approximations of $\Theta(\ell)$ in the vicinity of the rainbow angle one can derive closed expressions for the elastic scattering amplitude. This model has been applied to alpha particle [58, 59] and heavy-ion scattering [60, 61]. Approximate fits can be obtained at large angles where the angular distributions are smooth because of strong Coulomb interference, but owing to the weak-absorption assumption the rainbow model has considerable difficulties in describing other features of heavy particle scattering. However, a recent extension of the Ford-Wheeler method by Sabatier [62] appears to be capable of more general applications.

5. DIFFRACTION MODELS

5.1. Strong absorption in nuclear scattering

Far-reaching approximation methods have been developed which can be applied when strong absorption dominates the scattering. Strong-

absorption situations are encountered quite frequently in nuclear reactions at medium and high energy, in particular for

(i) nucleons, mesons and hyperons of energy $E \gtrsim 100$ MeV,
(ii) composite particles (deuterons, tritons, helium-3, alpha particles and heavy ions) above the Coulomb barrier.

In terms of the complex potential model we may roughly define a strong absorption situation by $I(W) \gtrsim |I(V)|$, where $I(U) \equiv \int U(\vec{r})\, d\vec{r}$ is the volume integral of the potential. An alternative definition is that the transparency should be small, $\epsilon \ll 1$, which by relation (4.41) means that the mean free path be small compared with the nuclear radius

$$L \ll R \tag{5.1}$$

However, a more appropriate characterization of strong absorption is given in terms of the elastic S-matrix elements. In section 1 we have defined absorption as the depletion of the elastic channels due to the presence of open reaction channels, measured by the deviation from unitarity of the elastic S-submatrix. Those partial waves are called strongly absorbed for which

$$|S_\ell^j| \ll 1 \tag{5.2}$$

In situations (i) and (ii) this condition is satisfied for a range of orbital angular momenta below a critical value ℓ_0. In these cases the scattering is closely similar to diffraction by an opaque obstacle, and approximation methods pertaining to such situations are called diffraction models. In the time-independent description of scattering processes there are two different ways of formulating the strong absorption condition, either in configuration space or in angular momentum space. These lead to two different diffraction models which are equivalent only in the semi-classical limit under the correspondence $\ell + \frac{1}{2} \approx kb$. Let us first consider the configuration space description.

5.2. Diffraction model in configuration space

In the formulation developed by Akhiezer and Pomeranchuk [63, 64] we start from the impact parameter formula (4.28), neglecting for simplicity spin-orbit coupling and Coulomb interaction,

$$f(\theta) = ik \int_0^\infty [1 - \eta(b)]\; J_0(kb\theta)\, b\, db \tag{5.3}$$

where $\eta(b)$ is given in terms of the complex potential $U(r)$ by

$$\eta(b) = e^{i2\delta(b)}\,, \quad \delta(b) = -\frac{M}{\hbar^2 k} \int_b^\infty \frac{U(r)\, r\, dr}{[r^2 - b^2]^{\frac{1}{2}}} \tag{5.4}$$

Assuming a square-well potential (sharp-edged nucleus) of radius R,

$$\begin{aligned} U(r) &= -(V_0 + iW_0), \quad r<R \\ U(r) &= 0, \qquad\qquad r>R \end{aligned} \tag{5.5}$$

the phase function becomes

$$\delta(b) = \frac{M}{\hbar^2 k}(V_0 + iW_0)(R^2 - b^2)^{\frac{1}{2}} = \left[k(n-1) + \frac{i}{2L}\right](R^2 - b^2)^{\frac{1}{2}}, \text{for } r<R, \tag{5.6}$$

$$\delta(b) = 0 \text{ for } r > R$$

where $n = 1 + V_0/2E$ is defined as the nuclear refractive index. From this expression follow the cross-section formulae of Fernbach, Serber and Taylor [65]. In the limit of complete absorption $L/R \to 0$, we obtain

$$\begin{aligned} \eta(b) &= 0 \quad \text{for } b < R \\ \eta(b) &= 1 \quad \text{for } b > R \end{aligned} \tag{5.7}$$

Insertion in (5.3) gives

$$f(\theta) = ik\int_0^R J_0(kb\theta)\, b\, db = iR\frac{J_1(kR\theta)}{\theta} \tag{5.8}$$

which is the Airy formula for the amplitude in small-angle Fraunhofer diffraction by a black obstacle of radius R.

Generalizations for incomplete absorption, rounded potentials (diffuse-edged nuclei), Coulomb and spin-orbit effects are straightforward, but the integration over impact parameters can no longer be carried out in closed form and must be done either numerically or by means of approximations. Mathematical methods in the generalized impact parameter formalism, mainly intended for application to high-energy processes, have been developed in recent papers by Predazzi [66] and by Adachi and Kotani [67, 68]. Let us here consider only the effect of Coulomb interaction in the limit of complete absorption. Thus

$$\begin{aligned} f(\theta) &= ik\int_0^\infty [1 - \eta(b)e^{i2\sigma(b)}]\, J_0(kb\theta)\, b\, db \\ &= iR\frac{J_1(kR\theta)}{\theta} - ik\int_R^\infty [e^{i2\sigma(b)} - 1]\, J_0(kb\theta)\, b\, db \end{aligned} \tag{5.9}$$

where $\exp[i2\sigma(b)]$ is the continuation of Eq. (1.28) to continuous $\ell = kb$. In the limit of small Coulomb parameters the expansion of the integrand in (5.9) yields [64]

$$f(\theta) = iR\,\frac{J_1(kR\theta)}{\theta} - \frac{2n}{k}\,\frac{J_0(kR\theta)}{\theta^2} \tag{5.10}$$

A more direct derivation of the diffraction formula starts from Eq. (2.6) for the scattering amplitude

$$F(\vec{k},\vec{k}') = -\frac{M}{2\pi\hbar^2}\int e^{-i\vec{k}'\cdot\vec{r}}\,U(r)\psi^{(+)}(\vec{k},\vec{r})\,d\vec{r} \tag{5.11}$$

Using the wave equation (2.1) this can be transformed to

$$F(\vec{k},\vec{k}') = -\frac{1}{4\pi}\int_{\mathscr{V}} e^{-i\vec{k}'\cdot\vec{r}}\,(\vec{\nabla}^2 + k^2)\psi^{(+)}(\vec{k},\vec{r})\,d\vec{r}$$

$$= -\frac{1}{4\pi}\int_{\mathscr{V}} [e^{-i\vec{k}'\cdot\vec{r}}\,(\vec{\nabla}^2\psi^{(+)}) - (\vec{\nabla}^2 e^{-i\vec{k}'\cdot\vec{r}})\psi^{(+)}]\,d\vec{r} \tag{5.12}$$

(since $k'^2 = k^2$), where the integration extends over a volume $\mathscr{V}$ outside of which $U(r)$ is assumed to vanish. By means of Green's theorem we can convert this integral into an integral over the surface $\mathscr{S}$ bounding $\mathscr{V}$,

$$F(\vec{k},\vec{k}') = -\frac{1}{4\pi}\int_{\mathscr{S}} [e^{-i\vec{k}'\cdot\vec{r}}\,(\vec{\nabla}\psi^{(+)}) - (\vec{\nabla}e^{-i\vec{k}'\cdot\vec{r}})\,\psi^{(+)}]\,d\vec{\mathscr{S}} \tag{5.13}$$

This expression corresponds exactly to Kirchhoff's formulation of Huygens' principle. In the high-energy limit $kR \gg 1$ we can divide the surface into an illuminated and a shadow part, $\mathscr{S} = \mathscr{J} + \mathscr{D}$, on which we impose Kirchhoff's boundary conditions for a black screen,

$$\begin{aligned} &\text{on } \mathscr{J}\text{:}\quad \psi^{(+)} = e^{i\vec{k}\cdot\vec{r}} \qquad \nabla_n\psi^{(+)} = \nabla_n e^{i\vec{k}\cdot\vec{r}} \\ &\text{on } \mathscr{D}\text{:}\quad \psi^{(+)} = 0 \qquad\qquad \nabla_n\psi^{(+)} = 0 \end{aligned} \tag{5.14}$$

Thus

$$F(\vec{k},\vec{k}') = \frac{ik}{4\pi}\,(1+\cos\theta)\int_{\mathscr{J}} e^{i(\vec{k}-\vec{k}')\cdot\vec{r}}\,d\mathscr{S}$$

or

$$f(\theta) = \frac{i}{2}\, kR^2\,(1 + \cos\theta)\,\frac{J_1(x)}{x} \tag{5.15}$$

where $x = qR = 2kR \sin\frac{1}{2}\theta$ or $x = kR\sin\theta$ depending on the approximation made in evaluating the integral. For small angles Eq. (5.15) reduces to (5.8). Generalizations of Eq. (5.15) including reflection, incomplete absorption, real phase shifts and Coulomb effects can be obtained by appropriate changes of the boundary conditions [69, 70].

The simple diffraction formula has been applied to elastic scattering of medium energy alpha particles [71], protons, neutrons and deuterons [70] and was found to describe surprisingly well the oscillatory patterns of the angular distributions. These analyses clearly indicate that the oscillations observed in differential scattering cross-sections for strongly absorbed particles arise from a diffraction process. However, diffraction patterns are found under much wider conditions than those for which the configuration space diffraction model has been derived. A more general derivation of diffraction formulas can be given in terms of the partial-wave expansion of the scattering amplitude. We shall see that diffraction effects in nuclear processes are more appropriately described in angular momentum space than in configuration space, because orbital angular momentum and scattering angle form a pair of canonically conjugate variables.

5.3. Diffraction model in angular momentum space

We now formulate strong absorption for partial waves by means of condition (5.2). The simplest case is that of spinless particles in the limit of complete absorption,

$$\begin{aligned} \eta_\ell &= 0 \quad \text{for } \ell < \Lambda \\ \eta_\ell &= 1 \quad \text{for } \ell \geqq \Lambda \end{aligned} \tag{5.16}$$

where Λ is the "cutoff" angular momentum. This is known as the Blair model [72]. For uncharged particles the scattering amplitude becomes

$$f(\theta) = \frac{i}{2k}\sum_{\ell=0}^{\Lambda-1}(2\ell+1)\,P_\ell(\cos\theta) \approx i\,\frac{\Lambda}{k}\,\frac{J_1(\Lambda\theta)}{\theta} = iR\,\frac{J_1(kR\theta)}{\theta} \tag{5.17}$$

and the integrated cross-sections

$$\sigma_{tot} = \frac{2\pi}{k^2}\Lambda^2 = 2\pi R^2, \quad \sigma_{el} = \sigma_{abs} = \frac{\pi}{k^2}\Lambda^2 = \pi R^2 \tag{5.18}$$

if we define the interaction radius R by

$$\Lambda = kR \tag{5.19}$$

For charged particles the Blair amplitude is

$$f(\theta) = f_C(\theta) + \frac{i}{2k} \sum_{\ell=0}^{\Lambda-1} (2\ell + 1)\, e^{i2\sigma_\ell} P_\ell(\cos\theta) \tag{5.20}$$

Differential scattering cross-sections obtained by numerical evaluation of (5.20) have been compared with experimental data for medium-energy alpha particles [72-74]. The calculated cross-sections show strong diffraction oscillations at larger angles which are not seen in the observed angular distribution. After averaging over these oscillations, which arise from the unrealistic sharp-cutoff assumption (5.16), the Blair model fits the data sufficiently well to determine interaction radii by means of the semiclassical relation

$$\Lambda = kR[1 - (2n/kR)]^{\frac{1}{2}} \tag{5.21}$$

although it fails to reproduce the sharp decrease of the observed angular distributions at large angles.

In view of its simplicity it is surprising that the Blair model is capable of describing the main features in the scattering of heavy charged particles in terms of the single parameter Λ. One expects that its shortcomings can easily be removed by modifying the idealized assumption (5.16). It is instructive to consider in a little more detail the implications of this assumption. The amplitude (5.20) can be evaluated in closed form by means of an approximation method which I shall briefly discuss later on. Under the conditions $\Lambda \gg (2\pi)^{-1}$ and $n \gg (2\pi)^{-1}$, the Blair amplitude (5.20) is in good approximation represented by [75]

$$\begin{aligned} f(\theta) &= f_C(\theta) + f_n^{(-)}(\theta) \quad \text{for } \theta \leqq \theta_c \\ f(\theta) &= f_n^{(+)}(\theta) \qquad\quad \text{for } \theta \geqq \theta_c \end{aligned} \tag{5.22}$$

where

$$\theta_c = 2 \operatorname{arctg}(n/\Lambda) \tag{5.23}$$

is the critical angle (the Coulomb scattering angle corresponding to angular momentum Λ) and

$$f_n^{(\pm)}(\theta) = \frac{i}{k}\left(\frac{\Lambda}{2\pi \sin\theta}\right)^{\frac{1}{2}} e^{i\chi}$$

$$\cdot\left\{\pm G(\pm u)\left(\frac{\Lambda}{2\sin\theta}\right)^{\frac{1}{2}} \frac{\theta-\theta_c}{2\sin\frac{1}{2}(\theta-\theta_c)} e^{-i(\Lambda\theta-\frac{\pi}{4})} - \frac{1}{2\sin\frac{1}{2}(\theta+\theta_c)} e^{i(\Lambda\theta-\frac{\pi}{4})}\right\} \tag{5.24}$$

with

$$\chi = \Lambda\theta_c - 2n\ln\sin\tfrac{1}{2}\theta_c + 2\sigma_0 \tag{5.25}$$

The function G(u) has the form

$$G(u) = \pi^{\frac{1}{2}} e^{i(u^2+\frac{\pi}{4})} \operatorname{erfc}(e^{i\frac{\pi}{4}}u)$$

$$\cdot\left\{1 - u\left(\frac{\sin\theta_c}{2\Lambda}\right)^{\frac{1}{2}}\left[\frac{1}{\sin\theta_c} + (1+i\tfrac{2}{3}u^2)\operatorname{ctg}\tfrac{1}{2}\theta_c\right]\right\}$$

$$+\left(\frac{\sin\theta_c}{2\Lambda}\right)^{\frac{1}{2}}\left[\frac{1}{\sin\theta_c} + (1+iu^2)^{\frac{2}{3}}\operatorname{ctg}\tfrac{1}{2}\theta_c\right] \tag{5.26}$$

with $u \equiv (\Lambda/2\sin\theta_c)^{\frac{1}{2}}(\theta-\theta_c)$, and the complementary error function is defined by

$$\operatorname{erfc}(z) = \frac{2}{\pi^{\frac{1}{2}}}\int_z^\infty e^{-\tau^2}d\tau \tag{5.27}$$

The main feature of the Blair model for charged particles is the critical angle which divides the angular distribution into two regions: $\theta < \theta_c$ where Coulomb scattering is dominant, and $\theta > \theta_c$ where nuclear diffraction scattering (shadow scattering) prevails. In the classical limit, θ_c is the scattering angle of particles moving along a trajectory whose apsidal distance equals the interaction radius R. The differential cross-section divided by the Rutherford cross-section would then be

$$\frac{d\sigma(\theta)}{d\sigma_c(\theta)} = \begin{cases} 1 & \text{for } \theta < \theta_c \\ 0 & \text{for } \theta > \theta_c \end{cases} \tag{5.28}$$

In wave mechanics this discontinuous limit is approached non-uniformly. For $\Lambda \to \infty$ at fixed θ_c, Eq. (5.22) reduces in the vicinity of θ_c to [76]

$$f(\theta) = \tfrac{1}{2} \operatorname{erfc} (e^{i\frac{\pi}{4}} u)\, f_C(\theta) \tag{5.29}$$

and the differential cross-section ratio becomes

$$\frac{d\sigma(\theta)}{d\sigma_c(\theta)} = \tfrac{1}{4} \left| \operatorname{erfc} (e^{i\frac{\pi}{4}} u) \right|^2 = \tfrac{1}{2} \{ [\tfrac{1}{2} - C(w)]^2 + [\tfrac{1}{2} - S(w)]^2 \} \tag{5.30}$$

where C(w) and S(w) are the Fresnel integrals of argument $w = (2/\pi)^{\frac{1}{2}} u = (\Lambda/\pi \sin\theta_c)^{\frac{1}{2}} (\theta - \theta_c)$. This expression is formally identical with the familiar formula for Fresnel diffraction of a wave with incidence angle θ_c by a black obstacle. The scattering of strongly absorbed uncharged particles, Eq. (5.17), and of strongly absorbed charged particles, Eq. (5.29), corresponds in the classical limit $\Lambda \to \infty$, θ_c = const. to Fraunhofer and Fresnel diffraction, respectively. Fresnel patterns can be seen in all angular distributions of heavy charged particles and are particularly striking in the scattering of heavy ions [76].

6. STRONG ABSORPTION MODEL FOR SPIN-0 PARTICLES

6.1. Parameterized phase shift models

For a realistic description of strong absorption scattering we must modify the Blair sharp-cutoff assumption (5.16). The transition of η_ℓ from zero to unity is a gradual one, extending over a range of ℓ-values of width Δ in the vicinity of Λ. This follows semiclassically from the diffuseness of the nuclear interaction region. Particles moving along classical orbits penetrating the diffuse surface region will be only partially absorbed. If Δ is the range of orbital angular momentum that corresponds to the diffuseness d, we obtain by differentiating Eq. (5.19) for neutral particles

$$\Delta = kd \tag{6.1}$$

or Eq. (5.21) for charged particles

$$\Delta = kd \frac{1 - (n/kR)}{[1 - (2n/kR)]^{\frac{1}{2}}} \tag{6.2}$$

We describe the gradual transition of η_ℓ in ℓ-space by means of a continuous function $g(\lambda)$ which depends on $(\Lambda - \lambda)/\Delta$, where $\lambda = \ell + \frac{1}{2}$ and

the "cutoff" Λ is no longer necessarily integer. Furthermore, the nuclear interaction will in general cause real phase shifts δ_ℓ of each partial wave and η_ℓ has an imaginary part. Finally, the low-ℓ partial waves are usually not completely absorbed. This can be described in a first approximation by assuming that η_ℓ is constant for all ℓ-values up to the vicinity of Λ. These three modifications are normally sufficient to describe the average, non-resonant effects of strong absorption scattering on the η_ℓ. Simple functional forms of η_ℓ which incorporate these modifications have been considered by Greider and Glassgold [77] and Elton [78] for uncharged particles, and by McIntyre, Wang and Becker [79] for charged particles. Greider and Glassgold have shown that it is possible to derive closed expressions for the scattering amplitude for neutron scattering, if the smoothing function $g(\lambda)$ has certain simple forms. The summation over partial waves is replaced by an integration over a continuous distribution of ℓ-values, which is a good approximation at high energies where many partial waves are affected by the interaction. In the formulation of McIntyre et al., the modulus and phase of $\eta_\ell = |\eta_\ell| \exp(i\,2\delta_\ell)$ are assumed to have the form

$$|\eta_\ell| = \left[1 + \exp\left(\frac{\Lambda - \lambda}{\Delta}\right)\right]^{-1}, \quad \delta_\ell = \delta\left[1 + \exp\left(\frac{\lambda - \Lambda}{\Delta_\delta}\right)\right]^{-1} \tag{6.3}$$

which describes η_ℓ by means of four parameters Λ, Δ, δ and Δ_δ. Coulomb interaction is included, so the S-matrix elements are given by $\eta_\ell \exp(i\,2\sigma_\ell)$ where σ_ℓ are the Coulomb phases. No analytical formulation has been given in this case and the scattering amplitude is calculated by numerical summation of the partial-wave expansion. This model has been successfully applied to analyse alpha-particle and heavy ion angular distributions [79-81]. The analyses show that the modifications of η_ℓ remove most of the shortcomings of the sharp-cutoff assumption, and the calculated cross-sections describe all essential features of the observed angular distributions at not too large angles. In particular, the smoothing of η_ℓ strongly steepens the average slope of $d\sigma/d\Omega$ and dampens the large oscillations in the diffraction region.

6.2. Analytical formulation of the strong absorption model (SAM)

It is possible to give a completely analytical formulation of the parameterized S-matrix model for very general forms of η_ℓ, with or without Coulomb interaction [75, 82]. The real and imaginary parts of η_ℓ are represented by

$$\begin{aligned} \mathrm{Re}\ \eta_\ell &= g_R + \sum_n \rho_n \frac{d^n g_R}{d\lambda^n} + \epsilon_R (1 - g_R) \\ \mathrm{Im}\ \eta_\ell &= \sum_n \mu_n \frac{d^n g_I}{d\lambda^n} + \epsilon_I\ (1 - g_I) \end{aligned} \tag{6.4}$$

The g are continuously differentiable functions of $(\Lambda - \lambda)/\Delta$ whose first derivatives are symmetrical and peaked at Λ, but otherwise arbitrary. The terms in ϵ describe constant transparency for low-ℓ partial waves. Ansatz (6.4) covers a large variety of structures of η_ℓ in strong absorption situations: the real part changes from finite values at small ℓ to unity at high ℓ through some rapid transition in the vicinity of Λ; the form of the imaginary part is such that real nuclear phase shifts are relevant only for partial waves in some vicinity of Λ, except for transparency contributions at lower ℓ-values. The main term in $\mathrm{Im}\,\eta_\ell$ is the first derivative of g. Higher derivatives in $\mathrm{Im}\,\eta_\ell$ and in $\mathrm{Re}\,\eta_\ell$ describe possible asymmetries and more complicated variations in the transition region. The functional forms of g_R and g_I may be different, and each of the parameters Λ, Δ and ϵ may have different values in $\mathrm{Re}\,\eta_\ell$ and $\mathrm{Im}\,\eta_\ell$. The Greider-Glassgold and McIntyre forms of η_ℓ are special cases of (6.4).

We shall consider a simplified version of (6.4) which is sufficient for most practical purposes,

$$\begin{aligned} \mathrm{Re}\,\eta_\ell &= g + \rho\,\frac{dg}{d\lambda} + \epsilon\,(1 - g) \\ \mathrm{Im}\,\eta_\ell &= \mu_1\,\frac{dg}{d\lambda} + \mu_2\,\frac{d^2g}{d\lambda^2} \end{aligned} \tag{6.5}$$

When we insert this in the partial-wave expansion of $f(\theta)$, the sum over ℓ can be evaluated by means of a consistent approximation method. Under the conditions

$$\Lambda \gg (2\pi)^{-1}, \Delta \ll \Lambda \tag{6.6}$$

and because of the properties of $g(\lambda)$, the main contribution to the sum over partial waves comes from the vicinity of Λ, and $P_\ell(\cos\theta)$ can be replaced by the leading term in its asymptotic expansion. In the neutral case we use Szegö's expression (4.27), in the charged case the somewhat simpler form

$$P_\ell(\cos\theta) \cong \left(\frac{2}{\pi\lambda\sin\theta}\right)^{\frac{1}{2}} \cos\left(\lambda\theta - \frac{\pi}{4}\right) \tag{6.7}$$

The sum over ℓ is converted into an integral by means of the Poisson sum formula. This method has been worked out in detail by Venter [82]. I shall now give a generalization of earlier results [75]. We distinguish two regions of the Coulomb parameter, $n \ll 1$ and $n \gg (2\pi)^{-1}$.

For $n \ll 1$, the scattering amplitude becomes

$$f(\theta) = \epsilon\, f_C(\theta) + f_n(\theta) \tag{6.8}$$

where

$$f_n(\theta) = \frac{\Lambda}{k}\left(\frac{\theta}{\sin\theta}\right)^{\frac{1}{2}} F(\Delta\theta)$$

$$\left\{[i(1-\epsilon)+\mu_2\theta^2]\ \frac{J_1(\Lambda\theta)}{\theta} - \left(\frac{2n}{\Lambda\theta^2} - \mu_1 + i\rho\right)J_0(\Lambda\theta)\right\} \tag{6.9}$$

with the "form factor" $F(\Delta\theta)$ defined as the Fourier transform of $dg/d\lambda$,

$$F(\Delta\theta) = \int \frac{dg}{d\lambda}\ e^{-i\lambda\theta}\, d\lambda \tag{6.10}$$

For $n \gg (2\pi)^{-1}$ we obtain

$$\begin{aligned} f(\theta) &= f_C(\theta) + f_n^{(-)}(\theta) \qquad \text{for } \theta \leqq \theta_c \\ f(\theta) &= \epsilon\, f_C(\theta) + f_n^{(+)}(\theta) \qquad \text{for } \theta \geqq \theta_c \end{aligned} \tag{6.11}$$

where

$$f_n^{(\pm)}(\theta) = \frac{i}{k}\left(\frac{\Lambda}{2\pi\sin\theta}\right)^{\frac{1}{2}}\ e^{i\chi}$$

$$\cdot\ \{A^{(\pm)}\, F[\Delta(\theta-\theta_c)]\ e^{-i(\Lambda\theta-\frac{\pi}{4})} - B\, F[\Delta(\theta+\theta_c)]\ e^{i(\Lambda\theta-\frac{\pi}{4})}\} \tag{6.12}$$

with

$$\begin{aligned} A^{(\pm)} &= \pm G(\pm u)\ (1-\epsilon)\left(\frac{\Lambda}{2\sin\theta_c}\right)^{\frac{1}{2}} - \mu_1 + i[\rho - \mu_2(\theta-\theta_c)] \\ B &= (1-\epsilon)\ (\theta+\theta_c)^{-1} + \mu_1 - i[\rho + \mu_2(\theta+\theta_c)] \end{aligned} \tag{6.13}$$

The functions χ and $G(u)$ are defined by Eqs. (5.25) and (5.26) respectively.

Formulae (6.8), (6.9) and (6.11)-(6.13) cover practically the entire range of Coulomb parameters. They are valid for all angles such that $\pi-\theta \gg (4\Lambda)^{-1}$, which excludes only extreme backward angles. However,

similar formulae can be derived which are valid from 180° downwards.

If we compare these expressions with the sharp-cutoff formulae we see that the effect of the gradual transition in ℓ-space is entirely contained in the form factors. We can easily understand this in a qualitative fashion. In the sharp-cutoff case the only contribution to the scattering amplitude comes from the cutoff angular momentum Λ and gives a term proportional to $J_1(\Lambda\theta)/\theta$. Modification of η_ℓ at neighbouring ℓ-values add similar terms which oscillate in θ with slightly smaller and larger frequencies. All these contributions reinforce the original term at forward angles but cause destructive interference at larger angles. The net result is that the sharp-cutoff oscillation is multiplied by an amplitude factor $F(\Delta\theta)$ which decreases with angle the more strongly the wider the band of ℓ-values in which η_ℓ is modified. This is a consequence of the uncertainty relation between angular momentum and scattering angle, expressed by the Fourier transformation (6.10). As a specific form of $g(\lambda)$ it is convenient to choose a Saxon shape, thus

$$g(\lambda) = \left[1 + \exp\left(\frac{\Lambda - \lambda}{\Delta}\right)\right]^{-1}, \quad F(\Delta\theta) = \frac{\pi\Delta\theta}{\sinh(\pi\Delta\theta)} \tag{6.14}$$

The derivatives of $g(\lambda)$ in (6.4) or (6.5) give contributions to the scattering amplitude whose diffraction oscillations are in phase or out of phase with that of the cutoff contribution if their order is even or odd, respectively, and therefore enhance or dampen the primary oscillation. Coulomb interference with these terms can cause phase reversals at certain angles within the angular distribution.

A large number of scattering data for alpha particles, helium-3, deuterons and heavy ions have been analysed [83, 84] with a simple 3-parameter version of (6.5),

$$\eta_\ell = g + i\mu_1 \frac{dg}{d\lambda} \tag{6.15}$$

The additional derivative terms in (6.5) were first used by Springer and Harvey [85] in their analysis of alpha particle scattering. It was found that the strong absorption model gives a very satisfactory description of heavy charged particle scattering above the Coulomb barrier.

6.3. "Regge pole" approach

We now turn to an alternative method of evaluating the partial-wave expansion

$$f(\theta) = \frac{i}{2k} \sum_{\ell=0}^{\infty} (2\ell + 1)\,(1 - \eta_\ell)\,P_\ell(\cos\theta) \tag{6.16}$$

which has recently been studied by Ericson [86] and Inopin [87]. Here we assume η_ℓ to be an analytic function of complex ℓ. Let us first take the simplest version of (6.5)

$$\eta_\ell = g(\ell) = \left[1 + \exp\left(\frac{\ell_0 - \ell}{\Delta}\right)\right]^{-1} = 1 - \left[1 + \exp\left(\frac{\ell - \ell_0}{\Delta}\right)\right]^{-1} \tag{6.17}$$

where $\ell_0 = \Lambda - \frac{1}{2}$. This has simple poles at

$$\ell_m = \ell_0 \pm i\pi m\Delta \qquad (m = 1, 3, 5, \ldots) \tag{6.18}$$

(see Fig. 1) with residues

$$a_m = \text{Res}\,[1 - \eta_\ell, \ell_m] = \Delta \tag{6.19}$$

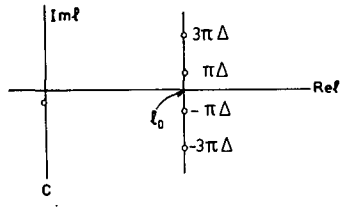

FIG. 1. Poles of $G(\ell)$ in complex ℓ-plane

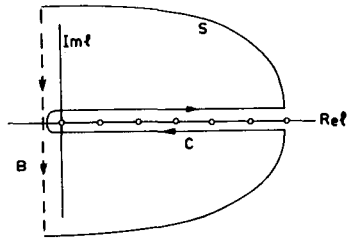

FIG. 2. Integration contours

Now we make a Watson-Sommerfeld transformation of (6.16),

$$f(\theta) = -\frac{1}{2k}\int_C (\ell + \tfrac{1}{2})\,\frac{1 - g(\ell)}{\sin \pi\ell}\,P_\ell\,(-\cos\theta)\,d\ell \tag{6.20}$$

where C is the contour shown in Fig. 2. If we complete C to the closed contour C' = C + S + B, the integral along C' is equal to $(-2\pi i)$ times the sum of the residues at the poles of the integrand,

$$\int_{C'} = i\frac{\pi}{k}\sum_{m}(\ell_m+\tfrac{1}{2})\,\frac{a_m}{\sin\pi\ell_m}\,P_{\ell_m}(-\cos\theta) \tag{6.21}$$

The integral along the semicircle S vanishes, hence

$$\int_{C} = -\int_{B} + \int_{C'}$$

The background integral

$$-\int_{B} = \int_{-\frac{1}{2}-i\infty}^{-\frac{1}{2}+i\infty}$$

extends over values y in $g(-\frac{1}{2}+iy) = \left[1+\exp\left(\frac{\Lambda}{\Delta} - i\frac{y}{\Delta}\right)\right]^{-1}$, which is very small under the strong absorption condition $\Lambda \gg \Delta$, and we shall neglect this contribution. Thus

$$f(\theta) = i\frac{\pi}{k}\sum_{m}(\ell_m+\tfrac{1}{2})\,\frac{a_m}{\sin\pi\ell_m}\,P_{\ell_m}(-\cos\theta)$$

$$= i\frac{\pi\Delta}{k}\sum_{|m|}(\ell_0 \pm i\pi m\Delta)\,\frac{P_{\ell_0 \pm i\pi m\Delta}(-\cos\theta)}{\sin(\pi\ell_0)\cosh(\pi^2 m\Delta) \pm i\cos(\pi\ell_0)\sinh(\pi^2 m\Delta)} \tag{6.22}$$

Closer investigation of the terms in this sum show that at sufficiently large angles the contribution from the nearest poles $|m| = 1$ dominate. Using the asymptotic expression (6.7) with θ replaced by $\pi-\theta$, and imposing the conditions

$$\frac{\pi\Delta}{\ell_0} \ll 1 \quad \text{and} \quad e^{-2\pi^2\Delta} \ll 1 \tag{6.23}$$

we obtain

$$f(\theta) \cong \frac{\Lambda}{k} \frac{2\pi\Delta}{e^{\pi\Delta\theta}} \frac{1}{(2\pi\Lambda \sin\theta)^{\frac{1}{2}}} \left[e^{i(\Lambda\theta - \frac{\pi}{4})} - e^{-i(\Lambda\theta - \frac{\pi}{4})} \right] \tag{6.24}$$

If we recall that

$$J_1(\Lambda\theta) \cong \left(\frac{2}{\pi\Lambda\theta}\right)^{\frac{1}{2}} \sin\left(\Lambda\theta - \frac{\pi}{4}\right) \tag{6.25}$$

and that under our conditions $\frac{1}{2} e^{\pi\Delta\theta} \approx \sinh(\pi\Delta\theta)$, we find that Eq. (6.24) is asymptotically equal to the SAM expression (see Eq. (6.9))

$$f(\theta) = i \frac{\Lambda}{k} \left(\frac{\theta}{\sin\theta}\right)^{\frac{1}{2}} F(\Delta\theta) \frac{J_1(\Lambda\theta)}{\theta} \tag{6.26}$$

with the form factor $F(\Delta\theta)$ given by Eq. (6.14). Ericson [86] has shown that inclusion of the Coulomb phases replaces θ by $\theta - \theta_c$. It appears therefore that at large angles the complex pole method is essentially equivalent to the SAM formalism. However, it has not yet been developed to the same degree of generality. In particular, the nearest-poles-approximation fails at small angles [88].

One way of introducing an imaginary part of η_ℓ has been suggested by Ericson: making the cutoff complex, $\ell_0 \to \ell_0 - i\mu_1$, displaces the string of poles parallel to the imaginary axis by the amount μ_1

$$\eta_\ell = \left[1 + \exp\left(\frac{\ell_0 - \ell}{\Delta} - i\frac{\mu_1}{\Delta}\right)\right]^{-1} \tag{6.27}$$

Now if $\mu_1/\Delta \ll 1$, this leads to the simplified SAM assumption

$$\eta_\ell = g + i\mu_1 \frac{dg}{d\ell}$$

Clearly this works for any form of the g-function

$$\eta_\ell = g(\ell - \ell_0 + i\mu_1) = g(\ell - \ell_0) + i\mu_1 \frac{dg(\ell - \ell_0)}{d\ell} + \ldots, \tag{6.28}$$

and we can derive more general forms of η_ℓ such as (6.5) by introducing a generalized "cutoff" $\Lambda \to \Lambda - (\rho + i\mu_1)$.

7. STRONG ABSORPTION MODEL FOR SPIN-$\frac{1}{2}$ PARTICLES

7.1. Spin-orbit coupling and polarization

The strong absorption model is easily extended to spin-$\frac{1}{2}$ particles by different parameterization of η_ℓ^+ and η_ℓ^-. This was first considered by Greider and Glassgold [77] for high-energy neutrons. The SAM formalism for neutral and charged spin-$\frac{1}{2}$ particles has been developed by Frahn and Venter [89] and applied in analyses of elastic scattering and polarization of 180-MeV protons [90] and of 29-MeV ^{3}He particles by nuclei [91]. Closely similar formulations were given by Hüfner and de-Shalit [92] for medium-energy protons and deuterons, and by Dar et al. [93, 94] for high-energy pion-proton scattering.

In general, each of the parameters in ansatz (6.4) will have a different value in the states $j = \ell + \frac{1}{2}$ and $j = \ell - \frac{1}{2}$, which we distinguish by superscripts + and -, and even the g-functions may have different forms. However, in the optical model, spin-orbit interaction is adequately described by a Thomas-type potential which is predominantly real. Looking at expression (4.30) for $\xi_\ell = \eta_\ell^+ - \eta_\ell^-$ in impact parameter approximation, we see that for real δ_s the spin-orbit interaction affects mainly the imaginary parts of the $\eta_\ell^\pm$. This follows from the potential picture: the potentials $\frac{1}{2}\ell V_s(r)$ and $-\frac{1}{2}(\ell+1)V_s(r)$ in the states $j = \ell + \frac{1}{2}$ and $j = \ell - \frac{1}{2}$ cause different real phase shifts, and since $V_s(r)$ is concentrated in the nuclear surface this will affect only the partial waves in the vicinity of the cutoff Λ. We now make the simplifying assumption that only the magnitudes and not the shapes of Im $\eta_\ell^\pm$ are different. From (6.5) we then have

$$\begin{aligned} \mathrm{Re}\,\bar\eta_\ell &= g + \bar\rho\,\frac{dg}{d\lambda} + \bar\epsilon(1-g), \quad \mathrm{Re}\,\xi_\ell = 0 \\ \mathrm{Im}\,\bar\eta_\ell &= \bar\mu_1\frac{dg}{d\lambda} + \bar\mu_2\frac{d^2g}{d\lambda^2}, \quad \mathrm{Im}\,\xi_\ell = \nu_1\frac{dg}{d\lambda} + \nu_2\frac{d^2g}{d\lambda^2} \end{aligned} \tag{7.1}$$

where $\bar\mu_n = \frac{1}{2}(\mu_n^+ + \mu_n^-)$ etc, and $\nu_n = \mu_n^+ - \mu_n^-$. To simplify matters we neglect Coulomb interaction. The SAM formalism then yields for the amplitudes $A(\theta)$ and $B(\theta)$,

$$\begin{aligned} A(\theta) &= C\left\{\left[i(1-\bar\epsilon) + \bar\mu_2\theta^2\right]\frac{J_1(\Lambda\theta)}{\theta} + (\bar\mu_1 - i\bar\rho)\,J_0(\Lambda\theta)\right\} \\ B(\theta) &= i\frac{C}{2}\left[\nu_1 J_1(\Lambda\theta) - \nu_2\theta\, J_0(\Lambda\theta)\right] \end{aligned} \tag{7.2}$$

where

$$C = \frac{\Lambda}{k}\left(\frac{\theta}{\sin\theta}\right)^{\frac{1}{2}} F(\Delta\theta) \tag{7.3}$$

When we calculate the differential scattering cross-section and the polarization for the general form (6.4) of the η_ℓ, it turns out [95] that

the angular dependence of $P(\theta)$ and its relation to $d\sigma/d\Omega$ depends essentially upon whether $\mathrm{Im}\,\eta_\ell$ is a symmetrical or antisymmetrical function of $\lambda - \Lambda$. We confine ourselves to the simplest forms, and it will be instructive to consider separately the two cases

$$\text{(I)}: \quad \bar{\eta}_\ell = g + \bar{\epsilon}\,(1-g) + i\bar{\mu}_1 \frac{dg}{d\lambda}, \qquad \xi_\ell = i\nu_1 \frac{dg}{d\lambda} \tag{7.4}$$

and

$$\text{(II)}: \quad \bar{\eta}'_\ell = g + \bar{\epsilon}\,(1-g) + i\bar{\mu}_2 \frac{d^2g}{d\lambda^2}, \qquad \xi_\ell = i\nu_2 \frac{d^2g}{d\lambda^2} \tag{7.5}$$

In case (I) we obtain

$$\frac{d\sigma}{d\Omega} = C^2\left\{[(1-\bar{\epsilon})^2 + (\tfrac{1}{2}\nu_1\theta)^2]\left[\frac{J_1(\Lambda\theta)}{\theta}\right]^2 + \bar{\mu}_1^2[J_0(\Lambda\theta)]^2\right\} \tag{7.6}$$

$$P(\theta)\frac{d\sigma}{d\Omega} = \nu_1\theta(1-\bar{\epsilon})\,C^2\left[\frac{J_1(\Lambda\theta)}{\theta}\right]^2 \tag{7.7}$$

while in case (II) we have

$$\frac{d\sigma}{d\Omega} = C^2\left\{[(1-\bar{\epsilon})^2 + (\bar{\mu}_2\theta^2)^2]\left[\frac{J_1(\Lambda\theta)}{\theta}\right]^2 + (\tfrac{1}{2}\nu_2\theta)^2\,[J_0(\Lambda\theta)]^2\right\} \tag{7.8}$$

$$P(\theta)\frac{d\sigma}{d\Omega} = -\nu_2(1-\bar{\epsilon})\,C^2\,J_1(\Lambda\theta)\,J_0(\Lambda\theta) \tag{7.9}$$

The angular dependence of $d\sigma/d\Omega$ and $P(\theta)$ is quite different in the two cases. In case (I) the polarization oscillates only in the range of non-negative values (if $\nu_1 > 0$), and in the differential cross-section the diffraction oscillations are strongly damped because the refractive contribution $\bar{\mu}_1^2\,[J_0(\Lambda\theta)]^2$ is out of phase with the shadow scattering term $[J_1(\Lambda\theta)/\theta]^2$. The remaining weak oscillations in $d\sigma/d\Omega$ are approximately in phase with the strong oscillations of $P(\theta)$. This behaviour is characteristic of proton-nucleus scattering for energies above ~ 100 MeV. In fact, the simple formulae (7.6), (7.7) are found to give a quite satisfactory description of the extensive proton scattering data [39] at 180 MeV [90].

On the other hand, in case (II) the polarization oscillates between positive and negative values with about equal amplitudes. The differential cross-section too is strongly oscillatory, because the refractive contribution is now in phase with the shadow scattering, and the only damping comes from the spin-orbit term $(\tfrac{1}{2}\nu_2\theta^2)^2\,[J_0(\Lambda\theta)]^2$. The polarization oscillates approximately like the derivative of $d\sigma/d\Omega$. This behaviour is found for proton and neutron scattering in the tens-of-MeV region. Hüfner and de-Shalit [92] have recently described polarization

data in this energy region by assuming

$$\mathrm{Im}\,\xi_\ell = \begin{cases} \nu_2 & \text{for } \ell = \Lambda - \tfrac{1}{2} \\ -\nu_2 & \text{for } \ell = \Lambda + \tfrac{1}{2} \\ 0 & \text{otherwise} \end{cases} \tag{7.10}$$

The second-derivative form (7.5) of ξ_ℓ is a "smoothed" version of this assumption, and Eq. (7.9) is the corresponding generalization of the expression derived by Hüfner and de-Shalit.

It appears, therefore, that assumptions (I) and (II) describe simple limiting cases of nucleon-nucleus scattering in the medium and high energy regions, respectively.

7.2. Relations between differential cross-section and polarization

Rodberg [96] first pointed out that there exists a relation between $P(\theta)$ and $d\sigma/d\Omega$ of the form

$$P(\theta)\frac{d\sigma}{d\Omega} = \beta\,\frac{d}{d\theta}\left(\frac{d\sigma}{d\Omega}\right) \approx \beta\frac{d}{d\theta}\,[\mathrm{Im}\,A(\theta)]^2 \tag{7.11}$$

where β is a constant. This follows immediately from the partial-wave expressions (4.26) if ξ_ℓ were proportional to $(2\ell+1)(1-\bar{\eta}_\ell)$. This is usually not the case. However, the medium energy proton data on which Rodberg's conjecture is mainly based are consistent with a relation of the type (7.11) where β is a function of θ which varies slowly compared with the diffraction oscillations. Such relations can be derived under more general conditions. Writing Eqs. (7.7) and (7.9) in the form

$$\text{(I):}\quad P(\theta)\frac{d\sigma}{d\Omega} = \frac{\nu_1\theta}{1-\bar{\epsilon}}\,[\mathrm{Im}\,A(\theta)]^2 \tag{7.12}$$

$$\text{(II):}\quad P(\theta)\frac{d\sigma}{d\Omega} \approx -\frac{\nu_2\,\theta^2}{2(1-\bar{\epsilon})\Lambda}\,\frac{d}{d\theta}\,[\mathrm{Im}\,A(\theta)]^2 \tag{7.13}$$

we see that only in case (II) we have a Rodberg-type relation with $\beta \propto \theta^2$. In general, if

$$\bar{\eta}_\ell = g(\lambda) + \bar{\epsilon}[1-g(\lambda)] + i\bar{h}(\lambda), \quad \xi_\ell = i\,h(\lambda) \tag{7.14}$$

where $\bar{h}$ and h are smooth functions of arbitrary shape confined to the vicinity of Λ, it can be shown [95] that in the diffraction region $\Lambda\theta \gg 1$,

$$P(\theta)\frac{d\sigma}{d\Omega} \cong \alpha(\theta)[\mathrm{Im}\,A(\theta)]^2 + \beta(\theta)\frac{d}{d\theta}[\mathrm{Im}\,A(\theta)]^2 \tag{7.15}$$

The (slowly varying) functions $\alpha(\theta)$ and $\beta(\theta)$ are defined in terms of the Fourier transform $\tilde{h}(\theta)$ of $h(\Lambda)$ by

$$\tilde{h}(\theta) = -(1-\bar{\epsilon})\frac{F(\Delta\theta)}{\theta}\,[\alpha(\theta) + i\,2\Lambda\beta(\theta)] \tag{7.16}$$

such that $\alpha(\theta)$ is determined by the symmetrical part and $\beta(\theta)$ by the antisymmetrical part of $h(\Lambda)$ with respect to Λ.

7.3. Relations between spin-orbit interaction parameters

We can derive approximate relations between the parameters ν_n and the strength of the real spin-orbit potential $V_{s,o}$ defined by

$$V_s(r) = -V_{s,o}\frac{1}{r}\frac{dg_c(r)}{dr} \tag{7.17}$$

by comparing the small-angle limit of $P(\theta)$ from (7.7) or (7.9),

$$\text{(I):}\quad P(\theta) \approx \frac{\nu_1/(1-\bar{\epsilon})}{1+[2\bar{\mu}_1/(1-\bar{\epsilon})\Lambda]^2}\,\theta \tag{7.18}$$

or

$$\text{(II):}\quad P(\theta) \approx -\frac{2\nu_2/(1-\bar{\epsilon})\Lambda}{1+[\bar{\mu}_2\theta^2/(1-\bar{\epsilon})]^2}\,\theta \tag{7.19}$$

with the Born approximation expression $P_B(\theta)$. According to Köhler [97] and Levintov [98] the latter is exact in the small-angle limit, which is independently of the shape of $g_c(r)$ given by

$$P_B(\theta) \approx \frac{k^2(V_{s,o}/W_{c,o})}{1+(V_{c,o}/W_{c,o})^2}\,\theta \tag{7.20}$$

where $V_{c,o}$ and $W_{c,o}$ are the strengths of the real and imaginary central potentials. Thus

$$\frac{\nu_1}{1-\bar{\epsilon}} = -\frac{2}{\Lambda}\frac{\nu_2}{1-\bar{\epsilon}} = k^2\frac{V_{s,o}}{W_{c,o}} \tag{7.21}$$

and in particular the signs of ν_1 and of $-\nu_2$ are the same as that of $V_{s,o}$.

7.4. Isobaric spin coupling

The isobaric spin interaction which we have described in section 2.5 by means of a potential $V_t(r)\vec{t}\cdot\vec{T}$, can be treated in the SAM formalism in close analogy to ordinary spin-orbit coupling. Again the η_ℓ have different parameters in the states $T' = T \pm \frac{1}{2}$ which we distinguish by

superscripts (±). Since $V_t(r)$ is real and probably confined to the nuclear surface [34], the isobaric spin interaction will mainly affect the imaginary parts of $\eta_\ell^{(\pm)}$. For simplicity we again assume that only the magnitudes $\mu_1^{(\pm)}$ of $\mathrm{Im}\,\eta_\ell^{(\pm)}$ are different. With the parameterization

$$\eta_\ell^{(\pm)} = g + \bar{\epsilon}\,(1 - g) + i\mu_1^{(\pm)}\,\frac{dg}{d\lambda} \tag{7.22}$$

and neglecting Coulomb distortion, the amplitudes $f^{(\pm)}(\theta)$ become

$$f^{(\pm)}(\theta) = C\left[i(1-\bar{\epsilon})\,\frac{J_1(\Lambda\theta)}{\theta} + \mu_1^{(\pm)}\,J_0(\Lambda\theta)\right] \tag{7.23}$$

where C is defined by Eq. (7.3). Hence follow the differential cross-sections for p-p scattering, Eq. (2.35), and for the p-n reaction, Eq. (2.36),

$$\frac{d\sigma}{d\Omega}\,(pp) = C^2\left\{(1-\bar{\epsilon})^2\left[\frac{J_1(\Lambda\theta)}{\theta}\right]^2 + \left(\frac{\mu_1^{(+)} + 2T\mu_1^{(-)}}{1+2T}\right)^2 [J_0(\Lambda\theta)]^2\right\} \tag{7.24}$$

$$\frac{d\sigma}{d\Omega}\,(pn) = \nu_T^2\,C^2\,\frac{2T}{(2T+1)^2}\,[J_0(\Lambda\theta)]^2 \tag{7.25}$$

The strength of the p-n transition is measured by the quantity

$$\nu_T = \mu_1^{(+)} - \mu_1^{(-)} \tag{7.26}$$

and an argument analogous to that leading to (7.21) shows that ν_T is proportional to the strength $V_{t,0}$ of the isobaric spin coupling potential. According to (7.25), the oscillations of the (p, n) differential cross-section are out of phase with the diffraction oscillations of the elastic cross-section (7.24). This is in accordance with the phase rules derived by Blair from the Fraunhofer diffraction model [99]. Experimental evidence is provided for instance by the reaction ^{56}Fe (^{3}He, ^{3}H)^{56}Co at 25 MeV. Although the Q-value for this reaction is considerable (Q = -8 MeV) and Coulomb effects by no means negligible, the simple formula (7.25) describes fairly well the diffraction oscillations and the slope of the observed angular distribution [100]. An optical model analysis of these data has been given by Drisko et al. [101].

7.5. Coulomb effects

The effects of Coulomb interaction on the scattering and polarization of spin-$\frac{1}{2}$ particles have been worked out in detail [89]. As the formalism is not essentially different from that in the spin-0 case we shall only mention the qualitative effects on the polarization. The critical angle θ_c again divides the angular distribution into two regions in which $P(\theta)$ behaves qualitatively different. For $\theta < \theta_c$ the destructive Coulomb

interference strongly reduces the magnitude of the polarization, and $P(\theta)$ oscillates about zero with small but slowly increasing amplitude. In the vicinity of θ_c the average polarization rises to positive values (in case (I) for $\nu_1 > 0$), and the diffraction minima in the region $\theta > \theta_c$ are filled in. This damping of the diffraction oscillations is a general effect of Coulomb interaction in strong absorption scattering. It arises from the interference between the terms in $\theta - \theta_c$ and $\theta + \theta_c$ in Eqs. (6.12) or (5.25). In the diffraction region, the Coulomb damping factor for both $d\sigma/d\Omega$ and $P(\theta)$ is quantitatively given by the ratio

$$\frac{F[\Delta(\theta+\theta_c)]}{\theta+\theta_c} \Big/ \frac{F[\Delta(\theta-\theta_c)]}{\theta-\theta_c} = \frac{\sinh[\pi\Delta(\theta-\theta_c)]}{\sinh[\pi\Delta(\theta+\theta_c)]} \cong e^{-2\pi\Delta\theta_c} \tag{7.27}$$

which decreases nearly exponentially with increasing Coulomb parameter n.

Preliminary measurements of the polarization in elastic scattering of 29-MeV ^{3}He particles by nuclei [102] have been analysed in terms of the optical model [53] and the strong absorption model [91]. Estimates by means of Eq. (7.21) indicate that the spin-orbit couplings for ^{3}He and for medium-energy protons are of comparable magnitude.

7.6. Total cross-sections

The integrated cross-sections σ_{el}, σ_{abs} and σ_{tot} in SAM depend only weakly upon the imaginary parts of the η_ℓ and are therefore not very sensitive to the spin-orbit interaction. For instance in case I, Eq. (7.4), we obtain [89]

$$\sigma_{el} = \pi\left(\frac{\Lambda}{k}\right)^2 (1-\bar{\epsilon})^2 \left[1 - \frac{2\Delta}{\Lambda} + \frac{\pi^2}{3}\left(\frac{\Delta}{\Lambda}\right)^2\right] + \sigma_I \tag{7.28}$$

$$\sigma_{abs} = \pi\left(\frac{\Lambda}{k}\right)^2 \left\{(1-\bar{\epsilon}^2)\left[1 + \frac{\pi^2}{3}\left(\frac{\Delta}{\Lambda}\right)^2\right] + (1-\bar{\epsilon})^2 \frac{2\Delta}{\Lambda}\right\} - \sigma_I \tag{7.29}$$

$$\sigma_{tot} = 2\pi\left(\frac{\Lambda}{k}\right)^2 (1-\bar{\epsilon})\left[1 + \frac{\pi^2}{3}\left(\frac{\Delta}{\Lambda}\right)^2\right] \tag{7.30}$$

where σ_I is the contribution from Im $\eta_\ell^\pm$,

$$\sigma_I = \frac{\pi}{3k^2}\frac{\Lambda}{\Delta}\left(\bar{\mu}_1^2 + \frac{1}{4}\nu_1^2 + \frac{1}{2\Lambda}\nu_1\bar{\mu}_1\right) \tag{7.31}$$

and

$$\sigma_I \lesssim \frac{\Delta}{\Lambda}\sigma_{tot} \tag{7.32}$$

8. RELATIONS BETWEEN SCATTERING MATRIX AND COMPLEX POTENTIAL

We now turn to the difficult question of how the elastic S-matrix is connected with the interaction in configuration space. We shall be mainly concerned with the ℓ-dependence of the η_ℓ in relation to the complex potential and shall not consider the much more complicated problem of energy dependence. The simplest connection obtains at high energies where in the semiclassical limit there is a one-to-one correspondence $\ell + \frac{1}{2} \leftrightarrow kb$ between orbital angular momentum and impact parameter. Another limiting situation where the relation between η_ℓ and the complex potential has been clarified is that of strong absorption. Let us start with the semiclassical limit.

8.1. High-energy approximation

The impact parameter approximation led us to relations (4.29)-(4.34) which represent the η_ℓ in terms of integrals over the complex potential. We split the phase shifts in real and imaginary parts, $\delta_c = \delta_c^{(1)} + i\delta_c^{(2)}$, $\delta_s = \delta_s^{(1)} + i\delta_s^{(2)}$, and first disregard spin-orbit coupling, $\delta_s = 0$. Writing $kb = \lambda$, we have

$$\begin{aligned} \mathrm{Re}\,\eta^{(0)}(\lambda) &= e^{-2\delta_c^{(2)}} \cos 2\delta_c^{(1)} \\ \mathrm{Im}\,\eta^{(0)}(\lambda) &= e^{-2\delta_c^{(2)}} \sin 2\delta_c^{(1)} \end{aligned} \tag{8.1}$$

hence

$$\mathrm{Im}\,\eta^{(0)}(\lambda) = \mathrm{tg}\,(2\delta_c^{(1)})\,\mathrm{Re}\,\eta^{(0)}(\lambda) \tag{8.2}$$

Therefore, under conditions of strong absorption, $\mathrm{Im}\,\eta^{(0)}(\lambda)$ is confined to the vicinity of $\Lambda = kR$.

With spin-orbit coupling included we have

$$\begin{aligned} \mathrm{Re}\,\eta^{(+)}(\lambda) &= \exp(-2\delta_c^{(2)} - 2\lambda\delta_s^{(2)}) \cos(2\delta_c^{(1)} + 2\lambda\delta_s^{(1)}) \\ \mathrm{Im}\,\eta^{(+)}(\lambda) &= \exp(-2\delta_c^{(2)} - 2\lambda\delta_s^{(2)}) \sin(2\delta_c^{(1)} + 2\lambda\delta_s^{(1)}) \\ \mathrm{Re}\,\eta^{(-)}(\lambda) &= \exp(-2\delta_c^{(2)} + 2\lambda\delta_s^{(2)}) \cos(2\delta_c^{(1)} - 2\lambda\delta_s^{(1)}) \\ \mathrm{Im}\,\eta^{(-)}(\lambda) &= \exp(-2\delta_c^{(2)} + 2\lambda\delta_s^{(2)}) \sin(2\delta_c^{(1)} - 2\lambda\delta_s^{(1)}) \end{aligned} \tag{8.3}$$

Let us assume U_s = real. Then $\delta_s^{(2)} = 0$, and we obtain

$$\begin{aligned} \bar{\eta}(\lambda) &= \cos(2\lambda\delta_s^{(1)})\,\eta^{(0)}(\lambda) \\ \xi(\lambda) &= i\,2\sin(2\lambda\delta_s^{(1)})\,\eta^{(0)}(\lambda) \end{aligned} \tag{8.4}$$

or

$$\xi(\lambda) = i\,2\mathrm{tg}\,(2\lambda\delta_s^{(1)})\bar{\eta}(\lambda) \tag{8.5}$$

If $2\lambda\delta_s^{(1)} \ll 1$ over the relevant region of λ, then $\bar{\eta}(\lambda) \approx \eta^{(0)}(\lambda)$, and

$$\xi(\lambda) \approx i\,4\lambda\delta_s^{(1)}(\lambda)\eta^{(0)}(\lambda) \tag{8.6}$$

is proportional to $V_{s,o}$, the strength of the spin-orbit potential. Also, $\xi(\lambda)$ is confined to the vicinity of Λ. From these formulae we can easily derive the features of $\eta^+(\lambda)$, $\eta^-(\lambda)$, or $\bar{\eta}(\lambda)$, $\xi(\lambda)$ for given potentials.

We can follow the converse procedure and derive potentials from given phase functions. Inversion of Eqs. (4.31) and (4.32) yields

$$U_c(r) = \frac{2}{\pi}\frac{\hbar^2 k^2}{M}\int_{kr}^{\infty}\frac{\delta_c'(\lambda)\,d\lambda}{[\lambda^2 - (kr)^2]^{\frac{1}{2}}} \tag{8.7}$$

$$U_s(r) = \frac{2}{\pi}\frac{\hbar^2 k^2}{M}\int_{kr}^{\infty}\frac{\delta_s'(\lambda)\,d\lambda}{[\lambda^2 - (kr)^2]^{\frac{1}{2}}} \tag{8.8}$$

where $\delta' = d\delta/d\lambda$. The same formulae are valid in the relativistic case with M replaced by E/c^2.

It is of interest to study the form of the potentials derived from the SAM form (7.22) for η_ℓ. We confine ourselves to the central potential and obtain

$$\delta_c^{(1)}(\lambda) = \tfrac{1}{2}\,\mathrm{arctg}\,\frac{\mathrm{Im}\,\eta_\ell}{\mathrm{Re}\,\eta_\ell},\quad \frac{d\delta_c^{(1)}(\lambda)}{d\lambda} = \tfrac{1}{2}\mu_1\frac{(1-\epsilon)[gg'' - (g')^2] + \epsilon\, g''}{\epsilon^2 + 2\epsilon(1-\epsilon)g + (1-\epsilon)^2 g^2 + \mu_1^2 (g')^2} \tag{8.9}$$

$$\delta_c^{(2)}(\lambda) = -\tfrac{1}{2}\ln|\eta_\ell|,\quad \frac{d\delta_c^{(2)}(\lambda)}{d\lambda} = -\frac{[\epsilon(1-\epsilon) + (1-\epsilon)^2 g + \mu_1^2 g'']\,g'}{\epsilon^2 + 2\epsilon(1-\epsilon)g + (1-\epsilon)^2 g^2 + \mu_1^2 (g')^2} \tag{8.10}$$

With $g(\lambda)$ of the Saxon shape (6.14), the integrals (8.7) cannot be evaluated in closed form, but the qualitative behaviour of the potentials can be seen by inspection of Eqs. (8.9) and (8.10). Thus W(r) is negative-definite, while the sign of V(r) is determined by μ_1. The real potential is surface-peaked and attractive for $\mu_1 > 0$, repulsive for $\mu_1 < 0$. For finite transparency ϵ, the sign of V(r) changes at a certain point in the nuclear interior. Elton [44] has recently pointed out that real potentials of this shape may be more appropriate for proton-nucleus scattering at higher energies than the conventional monotonic forms of V(r).

It is possible to derive an analytic expression for the asymptotic form of the potential, *i.e. for* $r \gg R$. *In this limit*

$$\delta_c'(\lambda) \cong -\frac{1}{2\Delta}\left[\frac{\mu_1}{\Delta} + i(1-\epsilon)\right]\exp\left(\frac{\Lambda-\lambda}{\Delta}\right) \tag{8.11}$$

hence

$$U_c(r) \cong -U_0 e^{\frac{\Lambda}{\Delta}} \int_{kr}^{\infty} \frac{e^{-\frac{\lambda}{\Delta}} d\lambda}{[\lambda^2 - (kr)^2]^{\frac{1}{2}}} = -U_0 e^{\frac{\Lambda}{\Delta}} \int_0^{\infty} e^{-\frac{kr}{\Delta}\cosh\tau} d\tau$$

$$= -U_0 e^{\frac{\Lambda}{\Delta}} K_0\left(\frac{kr}{\Delta}\right) \cong -U_0 \left(\frac{\pi}{2}\frac{d}{r}\right)^{\frac{1}{2}} \exp\left(\frac{R-r}{d}\right) \tag{8.12}$$

where $K_0(x)$ is the modified Hankel function of index zero, and

$$U_0 \equiv -\frac{1}{\pi\Delta}\left[\frac{\mu_1}{\Delta} + i(1-\epsilon)\right]\frac{\hbar^2 k^2}{M} \tag{8.13}$$

This shows that for the Saxon shape of $g(\lambda)$ the central potential $U_c(r)$ has approximately the same tail as the Saxon shape of $g_c(r)$, so that the width parameter d defined by $\Delta = kd$ may be directly compared with the diffuseness d defined by Eq. (3.11).

8.2. WKB approximation

At lower energies the relation between η_ℓ and the complex potential is much more involved, and no longer unique. However, Austern [103] has pointed out that in the case of strong absorption the WKB method is a good approximation and leads to simple expressions for the η_ℓ. With these expressions Austern has given a lucid description of how the ℓ-dependence of η_ℓ for strongly absorbed particles is determined by the conditions in the interaction region.

We start with the radial wave equation (2.14) (for neutral spinless particles) which we write in the form

$$\frac{d^2}{dr^2} f_\ell(k,r) + [k_\ell(r)]^2 f_\ell(k,r) = 0 \tag{8.14}$$

where

$$k_\ell(r) = \left[k^2 - \frac{\ell(\ell+1)}{r^2} - \frac{2M}{\hbar^2}U(r)\right]^{\frac{1}{2}} \tag{8.15}$$

is the local wave number of the ℓ-th partial wave. In lowest-order WKB approximation the radial wave function is

$$f_\ell^{(0)}(k,r) = e^{-i s_\ell(r)} \tag{8.16}$$

where

$$s_\ell(r) = kr + \int_{\infty}^{r} [k_\ell(r') - k]\, dr' \tag{8.17}$$

This is a purely ingoing wave which decreases in amplitude as we go to smaller r because of the damping by the imaginary part of U.

In the lowest-order approximation all reflections are neglected. Actually, reflections will occur at the nuclear surface where U(r) changes appreciably, and at the centrifugal barrier in the nuclear interior. Austern has shown how higher-order WKB corrections can be obtained which take this reflection into account. Let us first consider the centrifugal barrier and define an approximate turning point r_ℓ by

$$k^2 + \frac{2M}{\hbar^2} V_0 = \frac{\ell(\ell+1)}{r_\ell^2} \tag{8.18}$$

where V_0 is the depth of Re U. For $r < r_\ell$ the wave function will be very small, and we can replace the turning point approximately by the requirement that $f_\ell^{(0)} = 0$ at $r = r_\ell$. The wave then consists of an ingoing and a reflected part,

$$f_\ell^{(0)}(k, r) = e^{-is_\ell(r)} - e^{-i2s_\ell(r_\ell)}\ e^{is_\ell(r)} \tag{8.19}$$

so the reflection coefficient is in zero order given by

$$\eta_\ell^{(0)} = -e^{-i2s_\ell(r_\ell)} \tag{8.20}$$

To obtain the higher-order reflection corrections, Austern derives an integral equation for $f_\ell(k, r)$ which can be solved by iteration starting with $f_\ell^{(0)}(k, r)$. The once-iterated solution yields the reflection coefficient

$$\begin{aligned}\eta_\ell^{(1)} &= -e^{-i2s_\ell(r_\ell)} + \tfrac{1}{2}\int_{r_\ell}^{\infty}\left[e^{-i2s_\ell(r')} - e^{-i4s_\ell(r_\ell)}e^{i2s_\ell(r')}\right]\frac{k_\ell'(r')}{k_\ell(r')}\,dr' \\ &= \eta_\ell^{(\mathrm{barr})} + \eta_\ell^{(\mathrm{surf})}\end{aligned} \tag{8.21}$$

The second term describes the reflection by U(r) in the nuclear surface where the logarithmic derivative of $k_\ell(r)$ is appreciable.

From this expression we can see the main features of η_ℓ.

(i) Strong absorption

At low ℓ, $\eta_\ell^{(\mathrm{barr})}$ is small because the barrier is deep inside the nucleus and the wave that reappears at the surface is nearly extinguished by absorption; $\eta_\ell^{(\mathrm{surf})}$ is small because $\exp[-i2s_\ell(r')]$ is nearly sinusoidal in the surface and phase averaging takes place.

At higher ℓ, $\eta_\ell^{(\mathrm{barr})}$ becomes large because r_ℓ moves into the surface region and absorption is no longer effective; $\eta_\ell^{(\mathrm{surf})}$ becomes more appreciable because the barrier in the surface distorts the sinusoidal behaviour of the integrand and phase averaging is upset. Hence η_ℓ gradually increases from 0 to 1.

(ii) Weak absorption

At low ℓ, $\eta_\ell^{(barr)}$ becomes larger because the ingoing and reflected waves are less attenuated; $\eta_\ell^{(surf)}$ is less appreciable because phase averaging is still effective. Thus, for low-ℓ partial waves, the details of the surface are never very important. However, interference between the two contributions causes fluctuations in η_ℓ in the lower-ℓ region.

At higher ℓ, $\eta_\ell^{(barr)}$ increases still further; $\eta_\ell^{(surf)}$ now also becomes appreciable because phase averaging is again upset by distortion in the surface.

In general, for both strong and weak absorption, the reflection at the surface is important only at low energies, such that $\lambda\!\!\!^{-} \gtrsim d$, where d is the surface thickness. However, in most cases $\lambda\!\!\!^{-} \lesssim d$, so the relatively smooth change of U(r) in the surface gives good "impedance matching". The surface reflection is relatively small and it depends on the potential in the interior whether the barrier reflection makes η_ℓ small or large.

In terms of Austern's WKB formalism, Drisko et al. [52] have given a simple explanation of the ambiguities of the optical potential for composite particles. If we neglect surface reflection under conditions of good impedance matching we have for low ℓ-values

$$\eta_\ell \approx \eta_\ell^{(barr)} = -e^{-i2s_\ell(r_\ell)} \tag{8.22}$$

and two potentials V and V' will give the same η_ℓ if the corresponding turning points r_ℓ, r_ℓ' are such that

$$s_\ell(r_\ell') = s_\ell(r_\ell) \pm m\pi \qquad (m = 1, 2, 3, \ldots) \tag{8.23}$$

This condition is satisfied only for certain discrete sets of potential depths which can accommodate partial waves that differ by one half-wave in the nuclear interior.

8.3. "Model of the optical model"

Austern, Prakash and Drisko [104] have recently investigated the structure of η_ℓ in greater detail, with the aim of providing a general framework for parameterized models of η_ℓ which is independent of the potential description and applies to situations in which absorption is not necessarily strong.

The region of nuclear interaction is divided into two parts, an interior region of uniform properties and a diffuse surface region which modifies the effects produced on the wave function by the interior. First, an exact expression for η_ℓ is derived in which the contributions from the interior and surface regions are separated. Thereafter, successive approximations are introduced which lead to parameterized forms of η_ℓ.

The radial wave function $f_\ell^{(+)}$ is written in the form

$$f_\ell^{(+)} = \frac{i}{2}(I_\ell - \eta_\ell O_\ell) \tag{8.24}$$

where I_ℓ and O_ℓ are exact solutions of the radial equation (Jost functions) with asymptotic behaviour $I_\ell \cong H_\ell^*$, $O_\ell \cong H_\ell$. If we now choose a radius $r = b$ which separates the interior and surface regions of the potential $U(r)$, the η_ℓ can be expressed in terms of the logarithmic derivatives of $f_\ell^{(+)}$, O_ℓ and I_ℓ at $r = b$, denoted by $R_\ell^{-1}(b)$, $L_\ell(b)$ and $\bar{L}_\ell(b)$, respectively,

$$\eta_\ell = \frac{I_\ell(b)}{O_\ell(b)} \frac{R_\ell^{-1}(b) - \bar{L}_\ell(b)}{R_\ell^{-1}(b) - L_\ell(b)} \tag{8.25}$$

The interior region $r < b$ determines the R_ℓ^{-1}, the exterior $r > b$ determines the L_ℓ, $\bar{L}_\ell$, I_ℓ and O_ℓ. The latter quantities can be expressed exactly, by means of Green's theorem for the interval $b \leqq r < \infty$, in terms of the asymptotic functions H_ℓ, H_ℓ^*, their logarithmic derivatives $\overset{\circ}{L}_\ell$, $\overset{\circ}{L}_\ell^*$, and the functions I_ℓ, O_ℓ themselves. In this expression a "Born approximation" is introduced by replacing O_ℓ, I_ℓ by their asymptotic forms H_ℓ, H_ℓ^*. After another approximation which is good if b is sufficiently large, η_ℓ becomes

$$\eta_\ell \approx \left(\frac{H_\ell^*}{H_\ell}\right)\left(\frac{R_\ell^{-1} - \overset{\circ}{L}_\ell^* + J_\ell^* + i J_\ell'^*}{R_\ell^{-1} - \overset{\circ}{L}_\ell + J_\ell + i J_\ell'}\right) \tag{8.26}$$

where the quantities

$$J_\ell + i J_\ell' = \frac{2Mb}{\hbar^2}\int_b^\infty [V(r) + iW(r)]\left[\frac{H_\ell(r)}{H_\ell(b)}\right]^2 dr \tag{8.27}$$

contain the surface effects of the potential, while the other terms in η_ℓ contain the volume effects. An important property of the J_ℓ and J_ℓ' is that they vary smoothly with ℓ and that their imaginary parts decrease strongly with increasing ℓ.

At the next stage a specific model is introduced (i) by assuming a complex square well in the nuclear interior, and (ii) by assuming simple analytic forms for the ℓ-dependence of J_ℓ and J_ℓ'. In this way many different cases can be studied and it can be seen how various features of the potential reflect in properties of η_ℓ. The final parameterized expression for η_ℓ depends on nine adjustable parameters, but simplifies in certain limiting cases. In particular, in the limit of strong absorption it reproduces the familiar smooth form of the scattering function in ℓ-space.

B. DIRECT INTERACTIONS

9. INTRODUCTION

9.1. Direct interaction and compound nucleus reaction modes

In the description of nuclear reactions it is convenient to distinguish between transitions involving only a few degrees of freedom and those with excitations of many degrees of freedom. The former are said to proceed via the direct interaction (DI) mode, the latter via the compound nucleus (CN) mode. The distinction is not a sharp one and in any reaction both modes are present. Under certain conditions, however, the DI mode is dominant and in these cases the description of the reaction is particularly simple. For a discussion of the conditions under which the DI mode is favoured I refer to the comprehensive reviews by Austern [69, 105]. Direct interactions feed certain exit channels which have strong overlap with the entrance channel. Such reactions are closely related to elastic scattering and can be described by simple generalizations of the elastic scattering formalism. Each of the phenomenological methods of Part A can be extended to direct reactions. The most successful of these methods is an extension of the optical model. Here the interaction is described by a generalized potential which depends, aside from the relative coordinate and the spins of the reaction partners, on certain internal variables. More recently it has been shown that the parameterized S-matrix method can be extended to certain direct reactions because of approximate relations between the transition matrix elements for these processes and the S-matrix elements for elastic scattering.

The main types of direct processes are inelastic scattering, stripping and knock-out reactions. As the methods of description are basically the same for all three types, which differ mainly in the reaction kinematics, we shall give most attention to inelastic scattering. For a detailed treatment of other processes I refer to Tobocman's book [106].

We start by deriving some general expressions for the transition matrix.

9.2. T-matrix

We use symbols $\underline{a}$, $\underline{b}$, $\underline{c}$, ... to represent the sets of quantum numbers which specify the various channels; the entrance channel is usually denoted by $\underline{a}$. The system is described by a Hamiltonian (in channel $\underline{a}$)

$$H = h_a + K_a + \mathscr{U}_a \tag{9.1}$$

consisting of the internal Hamiltonian h_a of the reaction partners, the kinetic energy K_a of their relative motion, and the interaction operator $\mathscr{U}_a$. We are looking for a solution $\Psi^{(+)}$ of the wave equation

$$(H - E)\,\Psi^{(+)} = 0 \tag{9.2}$$

which consists asymptotically of an incoming free-particle wave (in channel a) and outgoing spherical waves in all channels b (including a),

$$\Psi^{(+)} \cong \phi_a e^{i\vec{k}_a \cdot \vec{r}_a} + \sum_b F_{ab}(\vec{k}_a, \vec{k}_b)\, \phi_b \frac{e^{ik_b r_b}}{r_b} \tag{9.3}$$

This defines the reaction amplitudes $F_{ab}(\vec{k}_a, \vec{k}_b)$ for the transition a → b. The internal wave functions ϕ_a are eigenfunctions of h_a,

$$(h_a - \epsilon_a)\, \phi_a = 0 \tag{9.4}$$

where

$$E - \epsilon_a = E_a = \frac{\hbar^2}{2M_a} k_a^2 \tag{9.5}$$

defines the channel wave number k_a and the reduced mass M_a in channel a.

The differential cross-section for the transition a → b is determined by the reaction amplitude F_{ab},

$$\frac{d\sigma}{d\Omega}(a \to b) = \frac{v_b}{v_a} |F_{ab}|^2 \tag{9.6}$$

where v_a is the relative velocity in channel a.

We expand the total wave function $\Psi^{(+)}$ in a complete set of internal eigenstates ϕ_c,

$$\Psi^{(+)} = \sum_c \psi_c^{(+)} \phi_c \tag{9.7}$$

The expansion coefficients are obtained by scalar multiplication with $\phi_b = \phi_b(\xi_b)$, integrating over the internal variables,

$$\psi_b^{(+)} = \langle \phi_b | \Psi^{(+)} \rangle \tag{9.8}$$

and are functions of the relative coordinate $\vec{r}_b$. By inserting (9.7) in (9.2) and on scalar multiplication with ϕ_b we get

$$\sum_c \langle \phi_b | H - E | \phi_c \rangle \psi_c^{(+)} = 0 \tag{9.9}$$

Using Eqs. (9.1), (9.4) and (9.5) we obtain

$$(E_b - K_b)\psi_b^{(+)} = \sum_c \langle \phi_b | \mathcal{U}_b | \phi_c \rangle \psi_c^{(+)} \tag{9.10}$$

a system of coupled equations for the expansion coefficients $\psi^{(+)}$.

We convert (9.10) to the integral form by means of the free-space Green's function $G_0^{(+)}(\vec{r},\vec{r}')$,

$$\psi_b^{(+)} = e^{i\vec{k}_a\cdot\vec{r}_a}\,\delta_{ab} + \frac{2M_b}{\hbar^2}\int d\vec{r}_b'\, G_0^{(+)}(\vec{r}_b,\vec{r}_b')\sum_c \langle \phi_b|\mathscr{U}_b|\phi_c\rangle\,\psi_c^{(+)} \tag{9.11}$$

Since

$$G_0^{(+)}(\vec{r}_b,\vec{r}_b') \cong -\frac{1}{4\pi}\, e^{-i\vec{k}_b'\cdot\vec{r}_b'}\,\frac{e^{ik_b r_b}}{r_b} \tag{9.12}$$

the asymptotic form of $\Psi^{(+)}$ becomes

$$\Psi^{(+)} = \sum_b \psi_b^{(+)}\phi_b$$

$$\cong \phi_a e^{i\vec{k}_a\cdot\vec{r}_a} - \sum_b \frac{M_b}{2\pi\hbar^2}\int d\vec{r}_b'\, e^{-i\vec{k}_b'\cdot\vec{r}_b'}\langle\phi_b|\mathscr{U}_b|\Psi_b^{(+)}\rangle\phi_b\,\frac{e^{ik_b r_b}}{r_b} \tag{9.13}$$

Comparison with Eq. (9.3) yields for the reaction amplitude

$$F_{ab}(\vec{k}_a,\vec{k}_b) = -\frac{M_b}{2\pi\hbar^2}\langle e^{i\vec{k}_b'\cdot\vec{r}_b}\,\phi_b|\mathscr{U}_b|\Psi^{(+)}\rangle \tag{9.14}$$

For the transition matrix element (see Eq. (1.7))

$$T_{ab} = -\frac{2\pi\hbar^2}{M_b}F_{ab} \tag{9.15}$$

we have

$$T_{ab} = \langle e^{i\vec{k}_b'\cdot\vec{r}_b}\,\phi_b|\mathscr{U}_b|\Psi^{(+)}\rangle \tag{9.16}$$

The differential cross-section in terms of T_{ab} becomes

$$\frac{d\sigma}{d\Omega}(a\to b) = \frac{M_a M_b}{(2\pi\hbar^2)^2}\,\frac{k_b}{k_a}\,|T_{ab}|^2 \tag{9.17}$$

9.3. Gell-Mann-Goldberger transformation

For the description of direct reactions it is often convenient to use a different representation of the T-matrix. We split the full interaction operator $\mathscr{U}_b$, which depends upon all internal variables ξ_b and the relative

coordinate $\vec{r}_b$, into two parts

$$\mathscr{U}_b = U_b + \mathscr{u}_b \tag{9.18}$$

Although the following transformations are formally valid for arbitrary divisions of $\mathscr{U}_b$, we shall have in mind special forms of U_b and $\mathscr{u}_b$ which are appropriate for describing direct interactions. We assume that U_b represents an average interaction potential which is independent of the internal variables, and that $\mathscr{u}_b$ is an operator which aside from $\vec{r}_b$ depends on only a few of the internal variables ξ_b. Then U_b will be an "optical" potential which depends on $\vec{r}_b$ (and possibly the channel spin $\vec{s}_b$, etc.) and causes elastic scattering, while $\mathscr{u}_b$ is the residual interaction which causes transitions to certain exit channels via the DI mode. Transitions to CN states are summarily described by absorption from the entrance channel and represented by an imaginary part of U_b. For charged particles, U_b includes the Coulomb potential.

With these assumptions, the system (9.10) becomes

$$(E_b - K_b - U_b)\,\psi_b^{(+)} = \sum_c \langle \phi_b | \mathscr{u}_b | \phi_c \rangle\, \psi_c^{(+)} \tag{9.19}$$

We convert this to the integral form by means of the Green's function $G^{(+)}(\vec{r}_b, \vec{r}_b')$ of the left-hand side of (9.19),

$$\psi_b^{(+)} = \chi_a^{(+)}\delta_{ab} + \frac{2M_b}{\hbar^2}\int d\vec{r}_b'\, G^{(+)}(\vec{r}_b, \vec{r}_b') \sum_c \langle \phi_b | \mathscr{u}_b | \phi_c \rangle\, \psi_c^{(+)} \tag{9.20}$$

Here, $\chi_a^{(+)}$ is the wave function for elastic scattering by the optical potential U_a, i.e. a solution of

$$(E_a - K_a - U_a)\,\chi_a^{(+)} = 0 \tag{9.21}$$

which behaves asymptotically as

$$\chi_a^{(+)}(\vec{k}_a, \vec{r}_a) \cong e^{i\{\vec{k}_a\vec{r}_a\}} + F_{el}(\vec{k}_a, \vec{k}_a')\frac{e^{i\{k_a r_a\}}}{r_a} \tag{9.22}$$

where F_{el} is the elastic scattering amplitude. The notation $\{\}$ is defined by Eq. (1.25) and denotes Coulomb distortion. The Green's function $G^{(+)}$ has the asymptotic form

$$G^{(+)}(\vec{r}_b, \vec{r}_b') \cong -\frac{1}{4\pi}\,\chi_b^{(-)*}(\vec{k}_b, \vec{r}_b')\,\frac{e^{i\{k_b r_b\}}}{r_b} \tag{9.23}$$

where $\chi^{(-)}$ is the time-reversed scattering wave function and is related to $\chi^{(+)}$ by the Wigner relation

$$\chi^{(-)*}(\vec{k}, \vec{r}) = \chi^{(+)}(-\vec{k}, \vec{r}) \tag{9.24}$$

For $\psi_b^{(+)}$ we now obtain asymptotically

$$\psi_b^{(+)} \cong e^{i\{\vec{k}_a\vec{r}_a\}}\delta_{ab} + F_{el}(\vec{k}_a, \vec{k}_a')\delta_{ab}\frac{e^{i\{k_a r_a\}}}{r_a}$$

$$- \frac{M_b}{2\pi\hbar^2}\int d\vec{r}_b' \chi_b^{(-)*}(\vec{k}_b, \vec{r}_b')\sum_c \langle \phi_b | \mathscr{u}_b | \phi_c \rangle \psi_c^{(+)} \frac{e^{i\{k_b r_b\}}}{r_b} \qquad (9.25)$$

and for $\Psi^{(+)} = \sum_b \psi_b^{(+)}\phi_b$,

$$\Psi^{(+)} \cong \phi_a e^{i\{\vec{k}_a\vec{r}_a\}} + \sum_b \left[F_{el}\,\delta_{ab} - \frac{M_b}{2\pi\hbar^2}\langle \chi_b^{(-)}\phi_b | \mathscr{u}_b | \Psi^{(+)} \rangle \right] \phi_b \frac{e^{i\{k_b r_b\}}}{r_b} \qquad (9.26)$$

Thus,

$$F_{ab}(\vec{k}_a, \vec{k}_b) = F_{el}(\vec{k}_a, \vec{k}_a')\delta_{ab} - \frac{M_b}{2\pi\hbar^2}\langle \chi_b^{(-)}\phi_b | \mathscr{u}_b | \Psi^{(+)} \rangle \qquad (9.27)$$

Recalling that the elastic T-matrix was given by (see Eq. (2.7))

$$T_{el}(\vec{k}_b, \vec{k}_b') = \langle e^{i\vec{k}_b'\cdot\vec{r}_b} | U_b | \chi_b^{(+)} \rangle \qquad (9.28)$$

we may write Eq. (9.27) in the form

$$T_{ab} = \langle e^{i\vec{k}_b'\cdot\vec{r}_b}\phi_b | U_b | \chi_a^{(+)}\phi_a \rangle + \langle \chi_b^{(-)}\phi_b | \mathscr{u}_b | \Psi^{(+)} \rangle \qquad (9.29)$$

The equivalence of Eqs. (9.29) and (9.16) for the general separation $\mathscr{U}_b = U_b + \mathscr{u}_b$ is called the Gell-Mann-Goldberger (GM-G) relation [107].

These expressions are the starting point for different approximation methods. Equation (9.29) is appropriate if the residual interaction $\mathscr{u}_b$ can be considered as a perturbation of the average interaction U_b, that is for Born-type approximations. Equation (9.16) is formally a direct generalization of the elastic T-matrix and will be a suitable basis of approximation for direct reactions which can be considered as generalized scattering processes. This is the case if the internal motions can be treated as adiabatic, and Eq. (9.16) is the appropriate starting point for adiabatic approximations.

10. DISTORTED-WAVE BORN APPROXIMATION [69]

10.1. Plane waves and distorted waves

We consider the non-elastic part of Eq. (9.29),

$$T_{ab} = \langle \chi_b^{(-)}\phi_b | \mathscr{u}_b | \Psi^{(+)} \rangle \qquad (10.1)$$

The simplest approximation is to replace $\Psi^{(+)}$ by

$$\Psi^{(+)} \approx \phi_a e^{i\vec{k}_a \cdot \vec{r}_a} \tag{10.2}$$

This plane-wave Born approximation has the virtue of simplicity and describes a number of qualitative features of observed angular distributions, particularly in stripping reactions. However, for quantitative work it is nearly always essential to take into account the strong distortion of the wave functions by the average interaction U_b. To first order this is achieved by representing $\Psi^{(+)}$ as

$$\Psi^{(+)} \approx \phi_a \chi_a^{(+)} \tag{10.3}$$

and the distorted-wave Born approximation (DWBA) expression of T_{ab} becomes

$$T_{ab} = \langle \chi_b^{(-)}(\vec{k}_b, \vec{r}_b)\phi_b(\xi_b) \left| \omega_b(\vec{r}_b, \xi_b) \right| \phi_a(\xi_a) \chi_a^{(+)}(\vec{k}_a, \vec{r}_a) \rangle \tag{10.4}$$

The functions $\chi^{(+)}$ are obtained by solving the elastic scattering problem (9.21) for given potentials U(r). This, and the evaluation of (10.4), can only be done by numerical computation. Such calculations give an accurate description of a large variety of direct processes and have almost completely superseded the plane-wave treatments.

10.2. *Zero-range approximation*

Despite the complicated structure of the DWBA matrix elements (10.4), the main features of the resulting angular distributions can be fairly simply displayed if we make the further approximation

$$\vec{r}_b \approx \vec{r}_a = \vec{r} \tag{10.5}$$

It means that the "initial" interaction takes place at the same point as the "final" interaction. This is correct for inelastic scattering and is expected to be good in other processes if the range of ω_b is small compared with the local wave lengths of the distorted waves. In zero-range approximation the six-dimensional integration over $\vec{r}_a$ and $\vec{r}_b$ in (10.4) is reduced to a three-dimensional one,

$$T_{ab} = \int \chi_b^{(-)*}(\vec{k}_b, \vec{r}) \langle \phi_b(\xi_b) \left| \omega_b(\vec{r}, \xi_b) \right| \phi_a(\xi_a) \rangle \chi_a^{(+)}(\vec{k}_a, \vec{r})\, d\vec{r} \tag{10.6}$$

This expression can be simplified considerably by introducing the partial-wave expansion of the distorted waves and a multipole expansion of the interaction operator.

We first expand $\omega_b(\vec{r}, \xi_b)$ in multipoles,

$$\omega_b(\vec{r}, \xi_b) = \sum_{LM} u_{LM}(r, \xi_b) Y_{LM}^*(\hat{\vec{r}}) \tag{10.7}$$

so that

$$\langle \phi_b | u_b | \phi_a \rangle = \sum_{LM} \langle \phi_b | u_{LM} | \phi_a \rangle \, Y^*_{LM}(\hat{r}) \tag{10.8}$$

The internal wave functions ϕ_a and ϕ_b are eigenfunctions of the initial and final spins, respectively, and (I_a, M_a) couples with (L, M) to give (I_b, M_b). Using the Wigner-Eckart theorem,

$$\langle \phi_b | u_{LM} | \phi_a \rangle \equiv \langle I_b M_b | u_{LM} | I_a M_a \rangle$$

$$= \langle I_a L M_a M | I_b M_b \rangle \langle I_b || u_L || I_a \rangle \tag{10.9}$$

we obtain

$$T_{ab} = \sum_{LM} \langle I_a L M_a M | I_b M_b \rangle \, T_{LM} \tag{10.10}$$

where

$$T_{LM} = c_L \int \chi_b^{(-)*}(\vec{k}_b, \vec{r}) \omega_L(r) \, Y^*_{LM}(\hat{r}) \chi_a^{(+)}(\vec{k}_a, \vec{r}) d\vec{r} \tag{10.11}$$

and the reduced matrix element is written in the form

$$\langle I_b || u_L || I_a \rangle = c_L \omega_L(r) \tag{10.12}$$

Now we expand $\chi_a^{(+)}$ and $\chi_b^{(-)*}$ in partial waves, choosing our coordinate system such that $\hat{k}_a$ defines the z-axis and $\hat{k}_a \times \hat{k}_b$ the y-axis. Thus

$$\chi_a^{(+)}(\vec{k}_a, \vec{r}) = \frac{(4\pi)^{\frac{1}{2}}}{k_a r} \sum_{\ell} i^{\ell} (2\ell + 1)^{\frac{1}{2}} \, e^{i\sigma_\ell^{(a)}} f_\ell^{(a)}(k_a, r) \, Y_{\ell 0}(\hat{r}) \tag{10.13}$$

$$\chi_b^{(-)*}(\vec{k}_b, \vec{r}) = \frac{4\pi}{k_b r} \sum_{\ell' m'} i^{-\ell'} e^{i\sigma_{\ell'}^{(b)}} f_{\ell'}^{(b)}(k_b, r) \, Y_{\ell' m'}(\theta, 0) \, Y^*_{\ell' m'}(\hat{r}) \tag{10.14}$$

where the radial wave functions have the asymptotic form (2.16). Integration over $\hat{r}$ yields

$$T_{LM} = \frac{4\pi}{k_a k_b} (2L+1)^{\frac{1}{2}} \, c_L \sum_{\ell, \ell'} i^{\ell - \ell'} (2\ell' + 1) \, e^{i(\sigma_\ell^{(a)} + \sigma_{\ell'}^{(b)})} \, R^L_{\ell \ell'}$$

$$\cdot \langle \ell' L \, 00 | \ell 0 \rangle \langle \ell' L, -M M | \ell 0 \rangle \, Y_{\ell', -M}(\theta, 0) \tag{10.15}$$

with the radial integrals defined by

$$R^{L}_{\ell\ell'} = \int_0^\infty f^{(b)}_{\ell'}(k_b, r)\,\omega_L(r)\,f^{(a)}_{\ell}(k_a, r)\,dr \qquad (10.16)$$

The differential cross-section (9.17) implies an average over M_a and a summation over M_b. This yields[2]

$$\frac{d\sigma}{d\Omega}(a\to b) = \frac{M_a M_b}{(2\pi\hbar^2)^2}\,\frac{k_b}{k_a}\sum_{L}\sum_{M=-L}^{L}\frac{2I_b+1}{(2I_a+1)\,(2L+1)}\,|T_{LM}|^2 \qquad (10.17)$$

10.3. Finite-range and non-local effects

The transition elements (10.15) have a fairly simple structure, and we shall see later that in certain cases, such as inelastic scattering of strongly absorbed particles, they can be evaluated in closed form. Since this simplicity is due to the zero-range assumption one must investigate the quality of this approximation. Finite-range calculations have been carried out, mainly for stripping reactions, by Austern et al. [108], Dar et al. [109], Buttle and Goldfarb [110], Bencze and Zimani [111]. It appears that finite-range effects tend to suppress the contributions from the nuclear interior. This changes the magnitude rather than the shape of the angular distributions. As one might expect, there is some resemblance between the effects of finite range and of non-locality of the interaction. A non-local interaction changes the wave functions in the nuclear interior; this is the "Perey effect" which we have discussed in section 3.1. Finite-range and non-local effects both become more appreciable for processes with large momentum transfer than for low-Q reactions.

10.4. Extended optical potential

Let us now consider a special form of the interaction operator $\mathcal{U}_b$. An important class of direct reactions is inelastic scattering via excitation of collective surface modes. One way of describing the interaction in these cases is to assume that the complex potential "follows" the deformation of the nuclear surface and so becomes a function of the collective variables [112-114]. The spherical optical potential U(R, r) is thus extended to

$$\mathcal{U}(\vec{r}, \xi) = U(R + \alpha(\hat{\vec{r}}), r) \qquad (10.18)$$

where $\alpha(\hat{\vec{r}})$ is the displacement in direction $\hat{\vec{r}}$ of the nuclear surface from the spherical shape of radius R. Now we may write

$$\mathcal{U} = U(R, r) + \mathcal{U}(R, r, \alpha(\hat{\vec{r}})) \qquad (10.19)$$

---

[2] No one will confuse the reduced masses in (10.17) with the projection quantum numbers M_a, M_b.

and expand $\mathcal{U}$ in powers of the displacement

$$\mathcal{U} = \alpha(\hat{\vec{r}}) \frac{\partial U}{\partial R} + \tfrac{1}{2} \alpha^2(\hat{\vec{r}}) \frac{\partial^2 U}{\partial R^2} + \ldots \tag{10.20}$$

The dynamical collective variables are defined by the multipole expansion

$$\alpha(\hat{\vec{r}}) = \sum_{LM} \xi_{LM} Y^*_{LM}(\hat{\vec{r}}) \tag{10.21}$$

To first order, we have from (10.7)

$$u_{LM}(r, \xi_{LM}) = \xi_{LM} \frac{\partial U}{\partial R} \tag{10.22}$$

and T_{LM} of Eq. (10.15) is the transition matrix element for single excitation of multipolarity (L, M). The coefficients c_L are the reduced matrix elements of the displacement operators ξ_{LM}, and the form factor is given by $\omega_L(r) = \partial U/\partial R$. It is not reasonable to calculate higher-order excitations, that is contributions from higher orders in the expansion (10.20), from the first-order DWBA term (10.4) of the transition amplitude. Second-order excitations in second-order DWBA have been studied by Austern et al. [115].

The well-known work of Bassel et al. [116] and Rost [117] on inelastic scattering of medium-energy alpha particles is a good example of how DWBA is applied. One first determines the parameters of the central potential by fitting the elastic scattering cross-sections. According to (10.15) the form of the inelastic angular distributions is then fixed, and the only parameters are the reduced matrix elements c_L which are determined by normalization. This method of analysis has been very successful.

However, the procedure of determining the elastic parameters independently of inelastic scattering may not always be applied. In general the elastic and inelastic channels are coupled, and inelastic scattering has an effect on the elastic scattering cross-section. In cases where this coupling is appreciable the DWBA is insufficient and one has to perform a coupled channels calculation.

11. COUPLED CHANNELS

Basically, we go back to the system (9.19) of coupled equations for the expansion coefficients ψ. This infinite system cannot be solved exactly, so we make a Tamm-Dancoff type approximation and assume that only a finite number of channels are coupled together. The contributions of all other channels are disregarded or described summarily by an imaginary part of the average interaction.

Coupled-channels calculations for collective excitations were first suggested by Bohr and Mottelson [118], and applied to scattering of low-energy neutrons from deformed nuclei by Margolis and Troubetzkoy [119] and by Chase, Wilets and Edmonds [113]. The elastic and inelastic scattering of protons and alpha particles by even-A nuclei has been treated by Buck [120-122]. This work was extended to odd-A nuclei and very general interaction potentials by Tamura [123]. Let us briefly describe the principles of the coupled-channels method for inelastic scattering in the general formulation of Tamura.

We consider the interaction of a projectile of spin $\vec{s}$ with a target nucleus, whose levels are labelled by $n = 1, 2, 3 \ldots$ and which are characterized by their spin I_n, parity π_n and ϵ_n. The internal wave functions $\phi_{I_n M_n}$ are eigensolutions of

$$(h - \epsilon_n)\phi_{I_n M_n} = 0 \tag{11.1}$$

For a given channel we first couple the spin of the projectile with the orbital angular momentum $\vec{\ell}_n$ to a total spin of the projectile,

$$\vec{j}_n = \vec{s} + \vec{\ell}_n \tag{11.2}$$

and this we couple with the target spin $\vec{I}_n$ to the total angular momentum of the system

$$\vec{J} = \vec{j}_n + \vec{I}_n \tag{11.3}$$

This, as well as the total parity

$$\Pi = (-)^{\ell_n}\pi_n \tag{11.4}$$

are conserved quantities. If χ_{sm_s} is the projectile spin function, we define

$$\mathcal{Y}_{\ell_n j_n m_j}(\hat{\vec{r}}) = \sum_{m_\ell m_s} \langle \ell_n s\, m_\ell\, m_s \,|\, j_n m_j \rangle\, i^\ell Y_{\ell_n m_\ell}(\hat{\vec{r}})\, \chi_{sm_s} \tag{11.5}$$

and

$$\Phi^{JM}_{I_n j_n \ell_n}(\hat{\vec{r}}, \xi) = \sum_{m_j M_n} \langle j_n I_n\, m_j M_n \,|\, JM \rangle\, \mathcal{Y}_{\ell_n j_n m_j}(\hat{\vec{r}})\, \phi_{I_n M_n}(\xi) \tag{11.6}$$

Now we expand the total wave function Ψ in eigenfunctions of total angular momentum,

$$\Psi(\vec{r}, \xi) = \sum_{JMn\ell_n j_n} \frac{f^J_{n\ell_n j_n}(r)}{r}\, \Phi^{JM}_{I_n j_n \ell_n}(\hat{\vec{r}}, \xi) \tag{11.7}$$

and insert this in

$$(H - E)\Psi = 0 \tag{11.8}$$

with

$$H = h + K + U(r) + \mathcal{U}(r, \xi) \tag{11.9}$$

Scalar multiplication by Φ and integration over the ξ and the angles $\hat{r}$ gives an infinite system of coupled equations for the radial wave functions

$$\left[\frac{\hbar^2}{2M}\left(\frac{d^2}{dr^2} - \frac{\ell_n(\ell_n+1)}{r^2}\right) + E_n - U(r)\right] f^J_{n\ell_n j_n}(r)$$

$$= \sum_{n'\ell'_n j'_n} \langle \Phi^{JM}_{I_n j_n \ell_n} | \mathcal{U} | \Phi^{JM}_{I'_n j'_n \ell'_n} \rangle \, f^J_{n'\ell'_n j'_n}(r) \tag{11.10}$$

where $E_n = E - \epsilon_n$.

If we assume that only a finite number of states in the target nucleus are strongly coupled to the ground state through the interaction $\mathcal{U}$, the system (11.10) can be solved by numerical integration. For the total interaction $\mathcal{U} = U + \mathcal{U}$ one assumes an extended optical potential of the form (10.18), whose diagonal part is a complex spherical potential plus Coulomb term, spin-orbit term, etc. The important point here is that the wave functions for both elastic and inelastic scattering are calculated at the same time. It is therefore not necessary first to fit elastic scattering in order to determine a phenomenological optical potential which is then used to calculate inelastic scattering. The agreement of coupled-channels calculations with scattering data for nucleons, alpha particles, deuterons and heavy ions is very satisfactory. However, the amount of computation is extensive and increases strongly with the number of levels that are taken into account. Fortunately, it is only at relatively low energies that the DWBA fails and coupled-channels calculations become necessary. For energies above the tens-of-MeV region the results of the two methods are found to be in good agreement with each other [69].

12. WKB APPROXIMATION AND ADIABATIC METHOD

12.1. WKB approximation

At sufficiently high energies the DWBA can be simplified by using WKB approximation for the distorted waves. In the DWBA form of the transition matrix in zero-range approximation,

$$T_{ab} = \langle \chi_b^{(-)} \phi_b | \mathcal{U}_b | \phi_a \chi_a^{(+)} \rangle$$

$$= \int \chi_b^{(-)*}(\vec{k}_b, \vec{r}) \langle \phi_b | \mathcal{U}_b | \phi_a \rangle \chi_a^{(+)}(\vec{k}_a, \vec{r})\, d\vec{r} \qquad (12.1)$$

we replace $\chi_a^{(+)}$ by (see Eq. (4.11))

$$\chi_a^{(+)}(\vec{k}_a, \vec{r}) = \exp i \left[\vec{k}_a \cdot \vec{r} - \frac{M_a}{\hbar^2 k_a} \int_{-\infty}^{z} U(\vec{b} + \hat{k}_a z')\, dz' \right] \qquad (12.2)$$

and the time-reversed wave by (see Eq. (9.24))

$$\chi_b^{(-)*}(\vec{k}_b, \vec{r}) = \exp i \left[-\vec{k}_b \cdot \vec{r} - \frac{M_b}{\hbar^2 k_b} \int_{z}^{\infty} U(\vec{b} + \hat{k}_b z')\, dz' \right] \qquad (12.3)$$

If we consider quasi-elastic processes and small-angle scattering: $v_b \approx v_a = v$, $\vec{k}_b \approx \vec{k}_a = \vec{k}$, the two integrals in (12.2) and (12.3) can be combined into a single integral. This yields

$$T_{ab} = \int e^{i\vec{q}\cdot\vec{r}}\, e^{i2\delta(b)} \langle \phi_b | \mathcal{U}_b | \phi_a \rangle d\vec{r} \qquad (12.4)$$

where $\vec{q} = \vec{k}_a - \vec{k}_b$ is the momentum transfer and

$$\delta(b) = -\frac{M}{2\hbar^2 k} \int_{-\infty}^{\infty} U(\vec{b} + \hat{k}z)\, dz \qquad (12.5)$$

the phase shift caused by the distorting potential (see Eq. (4.17)).

Expression (12.4) has been used extensively, with a number of further approximations. If $\mathcal{U}_b$ is axial-symmetrical, we can carry out the azimuthal integration as in section 4.3., and Eq. (12.4) becomes

$$T_{ab} = 2\pi \int_0^{\infty} e^{i2\delta(b)} \mathcal{U}_{ab}(b)\, J_0(qb)\, b\, db \qquad (12.6)$$

with the definition

$$\mathcal{U}_{ab}(b) = \langle \phi_b | \int_{-\infty}^{\infty} \mathcal{U}_b(\vec{b} + \hat{k}z, \xi)\, dz | \phi_a \rangle \qquad (12.7)$$

Equation (12.6) is the generalization to direct reactions of the elastic

formula (4.19) in the high-energy approximation. It has been applied to high-energy processes, for instance by Sopkovich [124], and by Gottfried and Jackson [125].

The case of inelastic scattering via collective excitation, with

$$\mathscr{U} = \alpha(\hat{\vec{r}}) \frac{\partial U}{\partial R} = \sum_{LM} \xi_{LM} Y^*_{LM}(\hat{\vec{r}}) \frac{\partial U}{\partial R} \tag{12.8}$$

has been treated by Bassichis and Dar [126]. They have shown that, under conditions of strong absorption, Eq. (12.4) can be reduced to

$$T_{ab} = -i \frac{2\pi\hbar^2 k}{M_a} \sum_{LM} \langle \phi_b | \xi_{LM} | \phi_a \rangle \, Y_{LM}\left(\frac{\pi}{2}, 0\right)$$

$$\cdot \int_0^\infty J_M(qb) \frac{\partial}{\partial b} \left[e^{i2\delta(b)}\right] b \, db \tag{12.9}$$

This leads to a relation between inelastic and elastic scattering which we shall discuss in more detail later on. Bassichis and Dar include Coulomb interaction and use the SAM form (6.15) for $\eta_l = \exp[i\,2\delta(b)]$. Equation (12.9) then yields simple explicit formulae for the inelastic scattering cross-sections. These are special cases of closed expressions which we shall derive in section 14.

12.2. Adiabatic method

Under certain conditions we may consider direct processes, in particular inelastic scattering, as a generalization of elastic scattering. Compare the T-matrix in the form (9.16)

$$T_{ab} = \langle e^{i\vec{k}'_b \cdot \vec{r}_b} \phi_b | \mathscr{U}_b | \Psi^{(+)} \rangle \tag{12.10}$$

with the elastic T-matrix (9.28)

$$T_{el} = \langle e^{i\vec{k}'_b \cdot \vec{r}_b} | U_b | \chi_b^{(+)} \rangle \tag{12.11}$$

Clearly, the calculation of T_{ab} would be completely analogous to that of T_{el} if we could regard the internal coordinates ξ as fixed parameters rather than as dynamical variables, that is as c-numbers rather than as operators. This is possible if the internal motions are slow compared with the relative motion, in other words under adiabatic conditions. Therefore, the natural starting point for the adiabatic approximation is Eq. (12.10) with $\Psi^{(+)}$ replaced by

$$\Psi^{(+)} \approx \phi_a(\xi_a) \psi_a^{(+)}(\vec{k}_a, \vec{r}_a, \xi_a) \tag{12.12}$$

where $\psi_a^{(+)}$ is defined as a solution of

$$(K_a + \mathcal{U}_a - E_a)\,\psi_a^{(+)} = 0 \tag{12.13}$$

This equation does not contain the internal Hamiltonian h_a, so it describes elastic scattering by a generalized potential $\mathcal{U}_a(\vec{r}_a, \xi_a)$ which depends upon the ξ_a as parameters. Thus in adiabatic approximation the T-matrix becomes

$$T_{ab} = \langle e^{i\vec{k}_b' \cdot \vec{r}}\, \phi_b \,|\mathcal{U}_b|\, \phi_a \psi_a^{(+)} \rangle \tag{12.14}$$

which we now may write in the form

$$T_{ab} = \langle \phi_b |\, t_{ab} |\, \phi_a \rangle \tag{12.15}$$

where

$$t_{ab} = \langle e^{i\vec{k}_b' \cdot \vec{r}} \,|\mathcal{U}_b|\psi_a^{(+)}\rangle \tag{12.16}$$

The adiabatic conditions are most closely approximated in transitions to low-lying excited states which are of a collective nature. If we now consider inelastic scattering, where $\vec{r}_a = \vec{r}_b = \vec{r}$, $\xi_a = \xi_b = \xi$, and make the further approximation $\vec{k}_a = \vec{k}$, $\vec{k}_b' = \vec{k}'$ with $|\vec{k}| = |\vec{k}'|$, then

$$t = \langle e^{i\vec{k}' \cdot \vec{r}} \,|\mathcal{U}|\psi^{(+)}\rangle \tag{12.17}$$

is precisely the T-matrix for elastic scattering by the extended optical potential $\mathcal{U}(\vec{r}, \xi)$ for fixed values of ξ. After having solved this elastic scattering problem we obtain the adiabatic T-matrix by forming the matrix elements (12.15).

For calculating t we can in principle use any of the methods described in Part A. The simplest of these is the diffraction approximation discussed in 5.2, which is appropriate for strongly absorbed particles at high energies. This approach was developed by Drozdov [127], Inopin [128] and Blair [129].

We introduce instead of t the generalized elastic scattering amplitude $F(\vec{k}, \vec{k}', \xi) = -(M/2\pi\hbar^2)t$, and follow the same procedure as with Eq. (5.11) for

$$F(\vec{k}, \vec{k}', \xi) = -\frac{M}{2\pi\hbar^2}\int e^{-i\vec{k}' \cdot \vec{r}}\, \mathcal{U}(\vec{r}, \xi)\, \psi^{(+)}(\vec{k}, \vec{r}, \xi)\, d\vec{r} \tag{12.18}$$

Using the wave equation (12.13) and imposing Kirchhoff's boundary conditions (5.14) for a black screen, we obtain again

$$F(\vec{k}, \vec{k}', \xi) = \frac{ik}{4\pi}\,(1 + \cos\theta) \int_{\mathcal{S}} e^{i(\vec{k} - \vec{k}') \cdot \vec{r}}\, d\vec{\mathcal{S}} \tag{12.19}$$

where the integration extends over the illuminated part $\mathscr{J}$. In high-energy approximation, $\mathscr{J}$ is the projection of the nuclear surface on the plane perpendicular to the incident direction $\hat{\vec{k}}$. If $\mathscr{U}$ has the form (10.18), this projection is bounded by

$$\rho(\phi) = R + \alpha\left(\frac{\pi}{2}, \phi\right) \tag{12.20}$$

For small angles θ, $F(\vec{k}, \vec{k}', \xi) \equiv f(\theta, \xi)$ becomes

$$f(\theta,\xi) = \frac{ik}{2\pi}\int_0^{2\pi} d\phi \int_0^{\rho(\varphi)} e^{-ik\rho\theta\cos\varphi}\rho\, d\rho \tag{12.21}$$

To first order in α we write

$$I(R+\alpha) = \int_0^{R+\alpha} e^{-ik\rho\theta\cos\varphi}\rho\, d\rho \approx I(R) + \alpha\frac{\partial I}{\partial R} \tag{12.22}$$

and use the properties

$$\begin{aligned} Y_{LM}\left(\frac{\pi}{2}, \phi\right) &= i^M\left(\frac{2L+1}{4\pi}\right)^{\frac{1}{2}} [L:M]\, e^{iM\varphi} \qquad \text{for } L+M \text{ even} \\ Y_{LM}\left(\frac{\pi}{2}, \phi\right) &= 0 \qquad\qquad\qquad\qquad\quad \text{for } L+M \text{ odd} \end{aligned} \tag{12.23}$$

with

$$[L:M] \equiv i^L \frac{[(L-M)!\,(L+M)!\,]^{\frac{1}{2}}}{(L-M)!!\,(L+M)!!}, \quad (L+M = \text{even})$$

and

$$\int_0^{2\pi} e^{-ik\rho\theta\cos\varphi} e^{-iM\phi} d\phi = (-i)^{|M|}\, 2\pi J_{|M|}(k\rho\theta) \tag{12.24}$$

This yields

$$f(\theta,\xi) = iR\frac{J_1(kR\theta)}{\theta}$$

$$+ ikR \sum_{\substack{LM \\ (L+M \text{ even})}} \xi_{LM}\left(\frac{2L+1}{4\pi}\right)^{\frac{1}{2}}\left(\frac{M}{|M|}\right)^L [L:M]\, J_{|M|}(kR\theta) \tag{12.25}$$

The first term is the elastic diffraction amplitude which is of course part of the full adiabatic amplitude. For spinless particles exciting a state of multipolarity L, the inelastic scattering cross-section becomes

$$\frac{d\sigma}{d\Omega}(0 \to L) = |c_L|^2 (kR)^2 \frac{2L+1}{4\pi} \cdot \sum_{M=-L,-L+2}^{L} [L:M]^2 [J_{|M|}(kR\theta)]^2 \qquad (12.26)$$

where c_L is the reduced matrix element

$$c_L = \langle \phi_L \| \xi_L \| \phi_0 \rangle \qquad (12.27)$$

Despite its simplicity, Eq. (12.26) describes the main features of the inelastic scattering of alpha particles from low-lying collective states. In particular it expresses the Blair phase rule: In the asymptotic region, the diffraction oscillations in the inelastic angular distributions for L = even are out of phase with those for L = odd and with those for elastic scattering. This rule enables us to determine the parity of a collective level by comparing the phase of oscillation in an inelastic angular distribution with that in the corresponding elastic cross-section.

Another qualitative feature is the behaviour at forward angles, where Eq. (12.26) predicts that $d\sigma/d\Omega\,(0 \to L)$ at $\theta = 0$ vanishes for L = odd and is finite for L = even, and so expresses the Glendenning-Kromminga-McCarthy rules [130, 131]. The structure of (12.26) at small angles is characteristically different for different L-values. Thus, if inelastic cross-section measurements are sufficiently accurate at small angles it is possible to determine not only the parity but also the multipolarity of the excitation, and (12.26) can be a useful tool in nuclear spectroscopy.

Formula (12.26) is derived with a number of simplifying assumptions. It neglects the diffuseness of the nuclear surface, Coulomb effects, contributions from ReU, and its validity is restricted to single excitation and to small scattering angles θ. All these restrictions can be removed by suitably generalizing the derivation [70, 99, 132].

Dar has suggested [70] that Eq. (12.26) applies not only to inelastic scattering but is a good approximation for all "surface" processes of strongly absorbed particles, such as (d, p) stripping, (α, p) knock-out and (d, t) pick-up reactions. He argues that under these conditions the outgoing particles emerge only from an annular region of width ΔR around the surface, and he derives an expression which is the same as (12.26) but with $k|c_L|$ replaced by $[1 + (k_b/k_a)\cos\theta]\, 2\pi\Delta R$. Further, to preserve time reversal invariance, he replaces the argument $kR\theta$ by qR where $\vec{q} = |\vec{k}_a - \vec{k}_b|$. A more detailed diffraction model for surface reactions has been worked out by Henley and Yu [134, 135]. In this model the reaction kinematics and the correct shadow geometry

in configuration space is taken into account. Unfortunately, the resulting expressions for the angular distributions become rather complicated.

13. AUSTERN-BLAIR THEORY

13.1. Relation between inelastic and elastic scattering

It was pointed out by Rost and Austern [136] that there is a close relation between the DWBA and the adiabatic method for inelastic scattering. A general discussion of this relation has been given in a brilliant paper by Austern and Blair [133]. These authors show that under rather general conditions the T-matrix for inelastic scattering can be expressed in terms of the S-matrix elements for elastic scattering. That there exists a close relation between inelastic and elastic scattering is already apparent from the diffraction model and manifests itself most clearly in the Blair phase rules. However, the description of this relation by means of the diffraction model in configuration space is both incomplete and physically unsatisfactory. It is incomplete because the diffraction approximation is limited to high energies and restricted by rather unrealistic conditions which cannot be lifted without making somewhat artificial assumptions about the "geometry" of the interaction. It is physically unsatisfactory because diffraction effects in inelastic scattering, as well as in elastic scattering, originate from the structure of the interaction matrix elements in angular momentum space (see Ref. [76].

A first attempt to put the diffraction description of inelastic scattering on a more satisfactory basis was made by Blair, Sharp and Wilets [137], who expressed the amplitudes for monopole and quadrupole excitations in terms of smoothed parameterized forms of the elastic scattering coefficients η_ℓ. However, as their formulation is still based on "geometrical" conditions, it is difficult to generalize to excitations of higher multipolarity and to include Coulomb interaction.

The decisive steps in the work of Austern and Blair are (i) to clarify the relation between the complete DWBA series and the expansion of the adiabatic amplitude in powers of the nuclear interaction, and (ii) to evaluate the terms of these series by means of approximate relations between the DWBA radial integrals and the elastic η_ℓ. Thereby one combines the virtues of the two approaches: the "physics" of the DWBA, contained in the radial integrals, with the simplicity of the expansion of the adiabatic amplitude.

13.2. Distorted waves in elastic scattering

The T-matrix for elastic scattering by a potential $\mathscr{U}$ has the form

$$T(\vec{k}, \vec{k}') = \langle e^{i\vec{k}'\cdot\vec{r}} \,|\, \mathscr{T} \,|\, e^{i\vec{k}\cdot\vec{r}} \rangle \tag{13.1}$$

where

$$\mathscr{T} = \mathscr{U} + \mathscr{U}\,\mathscr{G}^{(+)}\mathscr{U} \tag{13.2}$$

and

$$\mathcal{G}^{(+)}(\vec{r}, \vec{r}') = (E - K - \mathcal{U} + i\epsilon)^{-1} \tag{13.3}$$

is the Green's function for the potential $\mathcal{U}$. Now suppose that $\mathcal{U}$ is spherically symmetrical and depends on a parameter h, such as the radius or the depth of the potential well. If we make a spherically symmetrical change of h to $h + \alpha$, we may write

$$\mathcal{U}(h + \alpha, r) = U(h, r) + u(h, \alpha, r) \tag{13.4}$$

The change in T caused by the perturbing potential u can be separated from the unperturbed contribution by means of a GM-G transformation. This yields

$$T(\vec{k}, \vec{k}') = T_0(\vec{k}, \vec{k}') + \Delta T(\vec{k}, \vec{k}') \tag{13.5}$$

where

$$T_0(\vec{k}, \vec{k}') = \langle e^{i\vec{k}'\cdot\vec{r}} \,|\, U \,|\, \chi^{(+)}(\vec{k}, \vec{r}) \rangle \tag{13.6}$$

and

$$\Delta T(\vec{k}, \vec{k}') = \langle \chi^{(-)}(\vec{k}', \vec{r}') \,|\, \omega(\vec{r}, \vec{r}') \,|\, \chi^{(+)}(\vec{k}, \vec{r}) \rangle \tag{13.7}$$

with

$$\omega(\vec{r}, \vec{r}') = u + u\mathcal{G}^{(+)}u \tag{13.8}$$

The wave functions $\chi^{(\pm)}$ are the exact scattering solutions for the potential U, for outgoing and ingoing boundary conditions.

We want to express the scattering by the full potential $\mathcal{U}$ in terms of the scattering by the unperturbed potential U. To this purpose we first expand the operator ω in powers of u by iteration,

$$\omega(\vec{r}, \vec{r}') = u + uG^{(+)}u + uG^{(+)}uG^{(+)}u + \ldots, \tag{13.9}$$

where

$$G^{(+)}(\vec{r}, \vec{r}') = (E - K - U + i\epsilon)^{-1} \tag{13.10}$$

is Green's function for the potential U.

Next we expand the perturbation potential u in a Taylor series with respect to the parameter change α,

$$u(h, \alpha, r) = \sum_{n=1}^{\infty} \frac{\alpha^n}{n!} \frac{\partial^n}{\partial h^n} U(h, r) \tag{13.11}$$

By inserting this in (13.9) we obtain

$$\omega(\vec{r},\vec{r}') = \sum_{n=1}^{\infty} \alpha^n \omega_n(\vec{r},\vec{r}') \tag{13.12}$$

where

$$\omega_1 = \frac{\partial U}{\partial h}\ , \quad \omega_2 = \tfrac{1}{2}\frac{\partial^2 U}{\partial h^2} + \frac{\partial U}{\partial h}\, G^{(+)}\, \frac{\partial U}{\partial h}, \text{ etc.} \tag{13.13}$$

Finally we expand everything in partial waves. The expansions of $\chi^{(+)}$ and $\chi^{(-)*}$ are given by Eqs. (10.13) and (10.14), and for ω_n we define

$$\omega_n(\vec{r},\vec{r}') = \sum_{\ell m} \frac{\omega_{n\ell}(r,r')}{rr'}\, Y_{\ell m}(\hat{\vec{r}})\, Y^*_{\ell m}(\hat{\vec{r}}') \tag{13.14}$$

The evaluation of $\Delta T(\vec{k},\vec{k}')$ is quite similar to that of T_{LM} in 10.2 and yields

$$\Delta T(\vec{k},\vec{k}') = \frac{(4\pi)^{\frac{3}{2}}}{k^2} \sum_{\ell} (2\ell+1)^{\frac{1}{2}}\, e^{i2\sigma_\ell} Y_{\ell 0}(\theta,0) \sum_{n=1}^{\infty} \alpha_n R^{(n)}_{\ell\ell} \tag{13.15}$$

where

$$R^{(n)}_{\ell\ell} = \int_0^\infty \int_0^\infty f_\ell(k,r)\,\omega_{n\ell}(r,r')\, f_\ell(k,r')\, dr\, dr' \tag{13.16}$$

On the other hand, the partial-wave expansion of $T(\vec{k},\vec{k}')$ defines the scattering coefficients $\eta_\ell(h,\alpha)$ for the full potential $\mathscr{U}$,

$$T(\vec{k},\vec{k}') = -\frac{2\pi\hbar^2}{M}\,\frac{i}{2k}\,(4\pi)^{\frac{1}{2}} \sum_{\ell} (2\ell+1)^{\frac{1}{2}}\,[1-\eta_\ell(h,\alpha)e^{i2\sigma_\ell}]\, Y_{\ell 0}(\theta,0) \tag{13.17}$$

so that

$$\Delta T(\vec{k},\vec{k}') = i\,\frac{E}{2k^3}\,(4\pi)^{\frac{3}{2}} \sum_{\ell} (2\ell+1)^{\frac{1}{2}}\, e^{i2\sigma_\ell}[\eta_\ell(h,\alpha)-\eta_\ell(h,0)]\, Y_{\ell 0}(\theta,0) \tag{13.18}$$

Taylor expansion of $\eta_\ell(h,\alpha)$ with respect to α and comparison with (13.15)

yields a relation between the radial integrals (13.16) and the derivatives of the elastic scattering coefficients

$$R^{(n)}_{\ell\ell} = i \frac{E}{2k} \frac{1}{n!} \frac{\partial^n \eta_\ell}{\partial h^n} \tag{13.19}$$

In particular, for n = 1 we have

$$R^{(1)}_{\ell\ell} = \int_0^\infty f_\ell(k, r) \frac{\partial U(h, r)}{\partial h} f_\ell(k, r)\, dr = i \frac{E}{2k} \frac{\partial \eta_\ell}{\partial h} \tag{13.20}$$

because $\mathscr{U}$ is a local operator, $\mathscr{U}\delta(r-r')$, and $\omega_{1\ell}$ has the explicit form $\omega_{1\ell}(r, r') = (\partial U/\partial h)\delta(r-r')$.

13.3. Extension to inelastic scattering

Now we regard $\mathscr{U}$ as an extended optical potential, precisely as in (10.19). The unperturbed potential U is a spherical optical potential, for the parameter h we choose the nuclear radius R, and $\alpha = \alpha(\hat{r})$ becomes the displacement operator which depends upon the collective variables through the multipole expansion (10.21). The essential difference from the elastic case is that $\mathscr{U}$ and $\boldsymbol{u}$ are now operators with respect to the internal as well as the external variables.

The full T-matrix becomes

$$T_{ab} = \langle e^{i\vec{k}_b' \cdot \vec{r}'}\, \phi_b | \mathscr{T}_\xi | \phi_a e^{i\vec{k}_a \cdot \vec{r}} \rangle \tag{13.21}$$

where

$$\mathscr{T}_\xi = \mathscr{U} + \mathscr{U}[E - K - \mathscr{U} - h(\xi) + i\epsilon]^{-1}\mathscr{U} \tag{13.22}$$

contains the internal Hamiltonian $h(\xi)$ in Green's function.

The adiabatic approximation as discussed in section 12.2 consists in omitting $h(\xi)$ from (13.22) and treating the internal variables ξ in $\boldsymbol{u}$ as c-numbers. This enables us again to define a generalized elastic T-matrix t_{ab} by

$$T_{ab} = \langle \phi_b | t_{ab} | \phi_a \rangle \tag{13.23}$$

where

$$t_{ab} = \langle e^{i\vec{k}_b' \cdot \vec{r}'} | \mathscr{T} | e^{i\vec{k}_a \cdot \vec{r}} \rangle \tag{13.24}$$

and $\mathscr{T}$ is formally the same as in (13.2) with Green's function (13.3).

Now we split off the proper elastic scattering by making a GM-G transformation

$$t_{ab} = t_{el} + t_{inel} \tag{13.25}$$

We consider only the inelastic part and write t in place of t_{inel}. As in section 12.2 we make the further approximation $\vec{k}_a = \vec{k}$, $\vec{k}'_b = \vec{k}'$ with $|\vec{k}| = |\vec{k}'|$. Thus

$$t(\vec{k}, \vec{k}') = \langle \chi^{(-)}(\vec{k}', \vec{r}') | \tau(\vec{r}, \vec{r}') | \chi^{(+)}(\vec{k}, \vec{r}) \rangle \tag{13.26}$$

where

$$\tau(\vec{r}, \vec{r}') = \mathcal{u} + \mathcal{u} \mathcal{G}^{(+)} \mathcal{u} \tag{13.27}$$

If we now expand τ in powers of $\mathcal{u}$, and $\mathcal{u}$ is of the form (10.20), we obtain

$$\tau(\vec{r}, \vec{r}') = \sum_{n=1}^{\infty} \tau_n(\vec{r}, \vec{r}') \tag{13.28}$$

with

$$\tau_1 = \alpha \frac{\partial U}{\partial h}, \quad \tau_2 = \tfrac{1}{2} \alpha^2 \frac{\partial^2 U}{\partial h^2} + \left(\alpha \frac{\partial U}{\partial h} \right) G^{(+)} \left(\alpha \frac{\partial U}{\partial h} \right), \text{ etc.} \tag{13.29}$$

This is an expansion in powers of the displacement operator α which means, physically, an expansion in orders of excitations. The term linear in α describes single excitation; the quadratic term describes double excitation and consists of a "one step" (or "direct") and a "two-step" contribution. As Austern and Blair emphasize, the expansion (13.28) in α of the adiabatic amplitude corresponds, term by term, to the full DWBA series in the limit Q = 0. It would be nice if we could evaluate the terms of this series in a fashion analogous to the elastic case. This would entail relations, similar to (13.19), between the radial integrals of the DWBA series and the elastic scattering coefficients. We can enforce the analogy by means of some approximations which turn out to be good in cases of special physical interest.

13.4. Approximations

Our first difficulty is that we cannot write τ in the form $\sum_n \alpha^n \omega_n$, because α depends on $\hat{\vec{r}}$ and therefore does not commute with $G^{(+)}(\vec{r}, \vec{r}')$. Let's pretend α does commute with $G^{(+)}$ and write

$$\tau(\vec{r}, \vec{r}') \approx \tfrac{1}{2} \sum_{n=1}^{\infty} [\alpha^n(\vec{r}) \omega_n(\vec{r}, \vec{r}') + \omega_n(\vec{r}, \vec{r}') \alpha^n(\vec{r}')] \tag{13.30}$$

in a symmetrical form to leave τ hermitean. Clearly, this is an approximation only for $n \geq 2$, not for single excitation. Austern and Blair have discussed their assumption (13.30) in detail and find it reasonably good at least for $n = 2$ in the case of strongly absorbed particles. If we now insert τ in (13.26) and (13.23), T_{ab} contains matrix elements of the form $\langle \phi_b | \alpha^n | \phi_a \rangle$. For the moment we confine ourselves to excitations of multipolarity (L, M) in even-A nuclei. In this case we can write

$$\langle \phi_b | \alpha^n | \phi_a \rangle \equiv \langle LM | \alpha^n | 00 \rangle = c_n(L)\, Y^*_{LM}(\hat{\vec{r}}) \tag{13.31}$$

where $c_n(L)$ is the reduced matrix element for n-th order excitation, and the transition element becomes

$$T_{ab} = \tfrac{1}{2} \sum_n c_n(L) \langle \chi^{(-)}(\vec{k}', \vec{r}') | Y^*_{LM}(\hat{\vec{r}}) \omega_n(\vec{r}, \vec{r}') + \omega_n(\vec{r}, \vec{r}')\, Y^*_{LM}(\hat{\vec{r}}') | \chi^{(+)}(\vec{k}, \vec{r}) \rangle \tag{13.32}$$

Again we expand everything in partial waves and obtain, in analogy to (10.15),

$$T_{ab} = \frac{4\pi}{k^2} (2L+1)^{\frac{1}{2}} \cdot \sum_{\ell, \ell'} i^{\ell - \ell'} (2\ell'+1)^{\frac{1}{2}} e^{i(\sigma_\ell + \sigma_{\ell'})} \langle \ell' L\, 00 | \ell 0 \rangle \langle \ell' L, -M\, M | \ell 0 \rangle \cdot Y_{\ell', -M}(\theta, 0) \cdot \sum_n c_n(L)\, R^{(n)}_{\ell' \ell} \tag{13.33}$$

where

$$R^{(n)}_{\ell' \ell} = \int_0^\infty \int_0^\infty f_{\ell'}(k, r)\, \tfrac{1}{2} [\omega_{n\ell'}(r, r') + \omega_{n\ell}(r, r')]\, f_\ell(k, r')\, dr\, dr' \tag{13.34}$$

are the radial integrals for n-th order excitation.

For $\ell = \ell'$ these radial integrals are identical with those defined in (13.16) and can be expressed in terms of η_ℓ through the relation (13.19). The second approximation of Austern and Blair is to extend this relation to $\ell \neq \ell'$ and to replace $R^{(n)}_{\ell' \ell}$ by $R^{(n)}_{\bar{\ell}\bar{\ell}}$ where $\bar{\ell} = \frac{1}{2}(\ell + \ell')$,

$$R^{(n)}_{\ell' \ell} \approx R^{(n)}_{\bar{\ell}\bar{\ell}} = i \frac{E}{2k} \frac{1}{n!} \frac{\partial^n \eta_{\bar{\ell}}}{\partial h^n} \tag{13.35}$$

This approximation is quite accurate for strongly absorbed particles

at medium and high energies, if $|\ell - \ell'|$ is not too large. It is surprisingly good for $|\ell - \ell'| = 1$ at all values of $\bar{\ell}$. The main basis for its validity is the fact that in strong absorption situations the DWBA radial integrals are sharply localized in angular momentum space in the vicinity of the cutoff value $\bar{\ell} \approx \ell_0$ [116, 117].

For strongly absorbed particles and sufficiently high energies we can make two further simplifying assumptions. Firstly, $\eta_{\bar{\ell}}$ depends only on the difference $\bar{\ell} - \ell_0$. This is a basic property of η_ℓ in all strong absorption models. Secondly, if we interpret h as the nuclear radius R, it is connected with the cutoff angular momentum by the semi-classical relation $\ell_0 + \frac{1}{2} \approx kR$ for energies well above the Coulomb barrier. Thus

$$\frac{\partial^n \eta_{\bar{\ell}}}{\partial h^n} = \frac{\partial^n \eta(\bar{\ell} - \ell_0)}{\partial \bar{\ell}^n} \left(-\frac{d\ell_0}{dR}\right)^n \approx (-k)^n \frac{\partial^n \eta_{\bar{\ell}}}{\partial \bar{\ell}^n} \tag{13.36}$$

and finally

$$R^{(n)}_{\ell'\ell} \approx i \frac{E}{2k} \frac{(-k)^n}{n!} \frac{\partial^n \eta_{\bar{\ell}}}{\partial \bar{\ell}^n} \tag{13.37}$$

Eqs. (13.33) and (13.37) are the main result of the Austern-Blair theory of inelastic scattering.

14. STRONG ABSORPTION MODEL FOR INELASTIC SCATTERING

Now we go one step further and introduce the SAM form (6.5) of $\eta_{\bar{\ell}}$ in the Austern-Blair expression (13.37). By means of techniques similar to those developed for elastic scattering, we can evaluate the sums over ℓ, ℓ' in (13.33) and derive simple closed formulae for the inelastic scattering amplitudes [138].

14.1. Single excitation

For the present we confine ourselves to even-A target nuclei and first consider single excitation (n = 1). In this case the differential cross-section is given by

$$\frac{d\sigma}{d\Omega}(0 \to L) = \sum_{M=-L}^{L} \left| f^{(1)}_{LM}(\theta) \right|^2 \tag{14.1}$$

where

$$f^{(1)}_{LM}(\theta) \equiv -\frac{M_b}{2\pi\hbar^2} T^{(1)}_{ab}$$

$$= \frac{i}{2} c_1(L) (2L+1)^{\frac{1}{2}} \sum_{\ell,\ell'} i^{\ell-\ell'} (2\ell'+1)^{\frac{1}{2}} e^{i(\sigma_\ell + \sigma_{\ell'})} \frac{\partial \eta_{\bar{\ell}}}{\partial \bar{\ell}}$$

$$\cdot \langle \ell' L\, 00 | \ell 0 \rangle \langle \ell' L, -MM | \ell 0 \rangle Y_{\ell', -M}(\theta, 0) \tag{14.2}$$

Under the SAM conditions (6.6), $\partial\eta_{\bar{\ell}}/\partial\bar{\ell}$ is confined to a narrow range of $\bar{\ell}$-values in the vicinity of the cutoff ℓ_0. Since the summations in (14.2) extend only over values of ℓ, ℓ' for which $|\ell-\ell'|$ is small, we may approximate the Coulomb phases by

$$\sigma_\ell + \sigma_{\ell'} \approx 2\sigma_{\bar{\ell}} \approx 2\sigma_\Lambda + (\lambda - \Lambda)\,\theta_c \tag{14.3}$$

where

$$\Lambda = \ell_0 + \tfrac{1}{2}$$

$$2\sigma_\Lambda = \Lambda\theta_c - 2n \ln \sin \tfrac{1}{2}\theta_c + 2\sigma_0 - \frac{\pi}{2} \tag{14.4}$$

Hence

$$f^{(1)}_{LM}(\theta) = \frac{i}{2}\, c_1(L)\,(2L+1)^{\frac{1}{2}}\, e^{i2\sigma_\Lambda} \sum_{\ell,\ell'} i^{\ell-\ell'}\,(2\ell'+1)^{\frac{1}{2}}\, P(\bar{\ell})$$

$$\cdot \langle \ell' L\, 00 | \ell 0 \rangle \langle \ell' L, -MM | \ell_0 \rangle\, Y_{\ell', -M}(\theta, 0) \tag{14.5}$$

where

$$P(\bar{\ell}) = e^{i(\lambda-\Lambda)\,\theta_c}\, \frac{\partial \eta_{\bar{\ell}}}{\partial \bar{\ell}} \tag{14.6}$$

Now we expand $P(\bar{\ell})$ in a Taylor series about ℓ' and obtain

$$f^{(1)}_{LM}(\theta) = \tfrac{1}{2} i^{L+1}\, c_1(L)\,(2L+1)^{\frac{1}{2}}\, e^{i2\sigma_\Lambda}$$

$$\cdot \sum_{r=0}^{\infty} \sum_{\ell'} (2\ell'+1)^{\frac{1}{2}}\, P^{(r)}(\ell')\, C^{(r)}_{LM}(\ell')\, Y_{\ell', -M}(\theta, 0) \tag{14.7}$$

where

$$C^{(r)}_{LM}(\ell') = \sum_{\ell} i^{\ell-\ell'-L} \frac{1}{r!} \left(\frac{\ell - \ell'}{2}\right)^r \langle \ell' L\, 00 | \ell 0 \rangle \langle \ell' L, -MM | \ell 0 \rangle \tag{14.8}$$

and $P^{(r)}(\ell')$ denotes the r-th derivative of $P(\bar{\ell})$ at ℓ'.

Next we assume that the angular momentum transfer is small compared with the cutoff angular momentum,

$$L \ll \ell_0 \tag{14.9}$$

Because $P^{(r)}(\ell')$ is localized near ℓ_0 we may disregard the contributions to (14.8) coming from $\ell' \leq L$ and extend the ℓ-summation from $\ell' - L$ to $\ell' + L$. Under assumption (14.9) and the condition $\Lambda \gg (2\pi)^{-1}$, the Clebsch-Gordan coefficient $\langle \ell' L, -M M \,|\, \ell 0 \rangle$ is a slowly varying function of ℓ' for given $\ell - \ell'$, L and M. Using again the localization of $P^{(r)}(\ell')$ near ℓ_0, we may in (14.7) replace the $C^{(r)}_{LM}(\ell')$ by their values at ℓ_0, which we denote by $C^{(r)}_{LM}$. Thus

$$f^{(1)}_{LM}(\theta) = \tfrac{1}{2}\, i^{L+1} c_1(L)\,(2L+1)^{\frac{1}{2}}\, e^{i2\sigma_\Lambda} \sum_{r=0}^{\infty} C^{(r)}_{LM} S^{(r)}_{M} \tag{14.10}$$

where

$$C^{(r)}_{LM} = \sum_{\kappa=-L}^{L} i^{\kappa - L}\, \frac{1}{r!}\, (\tfrac{1}{2}\kappa)^r\, \langle \ell_0 L\, 00 \,|\, (\ell_0+\kappa), 0 \rangle \langle \ell_0 L, -M M \,|\, (\ell_0+\kappa), 0 \rangle \tag{14.11}$$

are real coefficients, and

$$S^{(r)}_{M} = \sum_{\ell'=0}^{\infty} (2\ell'+1)^{\frac{1}{2}}\, P^{(r)}(\ell')\, Y_{\ell', -M}(\theta, 0) \tag{14.12}$$

The sum (14.12) can be evaluated in closed form by means of SAM techniques. If $\eta_{\bar{\ell}}$ has the form (6.5), the result is [138, 139]

$$S^{(r)}_{M} = (-)^{\frac{1}{2}(M - |M|)} \pi^{-\frac{1}{2}} (-i\theta)^{r+1}\, \frac{\Lambda}{2\theta} \left(\frac{\theta}{\sin\theta} \right)^{\frac{1}{2}}$$

$$\cdot \{ [H^{(1)}_{+} + (-)^{r+1} H^{(1)}_{-}]\, J_{|M|-1}(\Lambda\theta) + i\, [H^{(1)}_{+} - (-)^{r+1} H^{(1)}_{-}]\, J_{|M|}(\Lambda\theta) \} \tag{14.13}$$

where

$$H^{(1)}_{\pm} = [(1 + \mu_1 \phi_{\pm}) - i\phi_{\pm}(\rho + \mu_2 \phi_{\pm})]\, F(\Delta\phi_{\pm}) \tag{14.14}$$

with the form factors F defined by (6.10) and $\phi_{\pm} = \theta_c \pm \theta$.

Finally, after summing over r, Eq. (14.10) becomes

$$f^{(1)}_{LM}(\theta) = c_1(L)\,(-)^{\frac{1}{2}(M - |M|)}\, i^{L+1} (2L+1)^{\frac{1}{2}}\, e^{i2\sigma_\Lambda}\, \frac{\Lambda}{4\pi^{\frac{1}{2}}} \left(\frac{\theta}{\sin\theta} \right)^{\frac{1}{2}}$$

$$\cdot \{ (H^{(1)}_{-} + H^{(1)}_{+})\, [\alpha_{LM}(\theta)\, J_{|M|}(\Lambda\theta) - \beta_{LM}(\theta)\, J_{|M|-1}(\Lambda\theta)]$$

$$+ i\, (H^{(1)}_{-} - H^{(1)}_{+})\, [\alpha_{LM}(\theta)\, J_{|M|-1}(\Lambda\theta) + \beta_{LM}(\theta)\, J_{|M|}(\Lambda\theta)] \} \tag{14.15}$$

where

$$\alpha_{LM}(\theta) + i\beta_{LM}(\theta)$$

$$= \sum_{\kappa=-L}^{L} i^{\kappa-L} e^{i\frac{\kappa}{2}\theta} \langle \ell_0 L\, 00 \,|\, (\ell_0+\kappa),\, 0\rangle \langle \ell_0 L,\, -MM \,|\, (\ell_0+\kappa), 0\rangle \tag{14.16}$$

Let us discuss the structure of Eq. (14.15) by considering a few special cases. For this discussion it is convenient to make one further simplification which is consistent with the approximations made so far. Under conditions (14.9) and for $|\kappa| \ll \ell_0$ we may replace the Clebsch-Gordan coefficients in (14.16) by their asymptotic expressions

$$\langle \ell_0 L,\, -MM \,|\, (\ell_0+\kappa), 0\rangle \cong d^{(L)}_{\kappa M}\left(\frac{\pi}{2}\right) \tag{14.17}$$

where $d^{(L)}_{\kappa M}$ is an element of the rotation matrix. Thus

$$\alpha_{LM}(\theta) + i\beta_{LM}(\theta) = \sum_{\kappa=-L}^{L} i^{\kappa-L} d^{(L)}_{\kappa 0}\left(\frac{\pi}{2}\right) d^{(L)}_{\kappa M}\left(\frac{\pi}{2}\right) e^{i\frac{\kappa}{2}\theta} \tag{14.18}$$

and with the symmetry relation

$$d^{(L)}_{\kappa M}\left(\frac{\pi}{2}\right) = (-)^{L+M} d^{(L)}_{-\kappa,M}\left(\frac{\pi}{2}\right) \tag{14.19}$$

we have

$$\begin{aligned} \alpha_{LM}(\theta) &= 0 \qquad \text{for } L+M \text{ odd} \\ \beta_{LM}(\theta) &= 0 \qquad \text{for } L+M \text{ even} \end{aligned} \tag{14.20}$$

First we assume vanishing Coulomb interaction: $\sigma_\Lambda = 0$, $\theta_c = 0$. Then

$$H^{(1)}_{\pm} = [(1 \pm \mu_1\theta) \mp i\theta\,(\rho \pm \mu_2\theta)]\, F(\Delta\theta) \tag{14.21}$$

In the sharp-cutoff limit $H^{(1)}_{\pm} = 1$, and at small angles such that $(\frac{1}{2}L\theta)^2 \ll 1$ we have from (14.18)

$$\alpha_{LM}(\theta) \approx \alpha_{LM}(0), \qquad \beta_{LM}(\theta) \approx 0 \tag{14.22}$$

where

$$\alpha_{LM}(0) = \sum_{\kappa=-L}^{L} i^{\kappa-L} d^{(L)}_{\kappa 0}\left(\frac{\pi}{2}\right) d^{(L)}_{\kappa M}\left(\frac{\pi}{2}\right) = i^{-L}[L : M] \tag{14.23}$$

In this limit we recover the Blair-Fraunhofer formula (see Eq. (12.25)) with $\Lambda = kR$,

$$f^{(1)}_{LM}(\theta) \approx i\, c_1(L)\, (-)^{\frac{1}{2}(M-|M|)} (2L+1)^{\frac{1}{2}} \frac{\Lambda}{2\pi^{\frac{1}{2}}} [L : M]\, J_{|M|}(\Lambda\theta) \tag{14.24}$$

Equation (14.15) generalizes this result in several respects. As usual, smoothing of the cutoff results in a form factor $F(\Delta\theta)$, which steepens the slope of the differential cross-sections with increasing angle. At larger angles the amplitude contains additional terms proportional to $\beta_{LM}(\theta)$ which are in phase with the "Blair terms" proportional to $\alpha_{LM}(\theta)$. Whereas the contributions from the second derivative in $\eta_{\bar{\ell}}$ (proportional to μ_2) are also in phase, those from the first derivatives (proportional to μ_1 and ρ) are out of phase with the Blair terms and therefore cause damping of the Fraunhofer diffraction oscillations.

From Eqs. (14.14) and (14.15) we see that Coulomb interaction affects the differential cross-sections through the form factors $H^{(1)}_{-}$ and $H^{(1)}_{+}$. In particular, the phase rules remain intact, although phase reversals may occur at certain angles within a given angular distribution. For a more detailed discussion of these features I refer to the papers by Potgieter and Frahn [138], Hahne [140], and Bassichis and Dar [126]. As in elastic scattering, the main effect is the "Coulomb damping" of the diffraction oscillations described by Eq. (7.27). For strong Coulomb fields, such as in inelastic scattering of heavy ions by heavy target nuclei, the angular distributions become smooth and peaked in the vicinity of the critical angle θ_c [142].

14.2. Double and mutual excitation

The amplitude for double excitation in the Austern-Blair theory is given by the term with $n = 2$ in Eq. (13.33),

$$f^{(2)}_{LM}(\theta) \equiv -\frac{M_b}{2\pi\hbar^2}\, T^{(2)}_{ab}$$

$$= -\frac{i}{4}\, c_2(L)\, k\, (2L+1)^{\frac{1}{2}} \sum_{\ell,\ell'} i^{\ell-\ell'}\, (2\ell'+1)^{\frac{1}{2}}\, e^{i(\sigma_\ell + \sigma_{\ell'})}\, \frac{\partial^2 \eta_{\bar{\ell}}}{\partial \bar{\ell}^2}$$

$$\cdot \langle \ell' L\, 00 \,|\, \ell 0 \rangle \langle \ell' L, -MM \,|\, \ell 0 \rangle\, Y_{\ell', -M}(\theta, 0) \tag{14.25}$$

With the same procedure as for single excitation we find [139]

$$f^{(2)}_{LM}(\theta) = c_2(L)\,(-)^{\frac{1}{2}(M-|M|)}\,i^{L+1}\,\tfrac{1}{2}k\,(2L+1)^{\frac{1}{2}}\,e^{i2\sigma_\Lambda}\,\frac{\Lambda}{4\pi^{\frac{1}{2}}}\left(\frac{\theta}{\sin\theta}\right)^{\frac{1}{2}}$$

$$\cdot\{(H^{(2)}_{-}+H^{(2)}_{+})\,[\alpha_{LM}(\theta)\,J_{|M|}(\Lambda\theta)-\beta_{LM}(\theta)\,J_{|M|-1}(\Lambda\theta)]$$

$$+\,i\,(H^{(2)}_{-}-H^{(2)}_{+})\,[\alpha_{LM}(\theta)\,J_{|M|-1}(\Lambda\theta)+\beta_{LM}(\theta)\,J_{|M|}(\Lambda\theta)]\} \qquad (14.26)$$

where

$$H^{(2)}_{\pm} = i\phi_{\pm}H^{(1)}_{\pm} \qquad (14.27)$$

Thus, the essential change from single excitation is contained in the form factors. The factors $\phi_{\pm} = \theta_c \pm \theta$ in Eq. (14.27) show (i) that the phase of the diffraction oscillations for double excitation is reversed with respect to that for single excitation, and (ii) that the slope of the angular distribution is less steep. This can be seen most clearly in the neutral case where for single excitation

$$H^{(1)}_{-}+H^{(1)}_{+} = 2(1-i\mu_2\theta^2)\,F(\Delta\theta)$$

$$H^{(1)}_{-}-H^{(1)}_{+} = -2(\mu_1-i\rho)\,\theta\,F(\Delta\theta) \qquad (14.28)$$

and the terms $\alpha_{LM}J_{|M|}$ dominate over the terms $\alpha_{LM}\,J_{|M|-1}$, whereas for double excitation,

$$H^{(2)}_{-}+H^{(2)}_{+} = 2i\,(\mu_1-i\rho)\,\theta^2F(\Delta\theta)$$

$$H^{(2)}_{-}-H^{(2)}_{+} = -2i\,(1-i\mu_2\theta^2)\,\theta F(\Delta\theta) \qquad (14.29)$$

and the terms $\alpha_{LM}\,J_{|M|-1}$ are the dominant ones. These features are well known from DWBA calculations [115].

In inelastic scattering of composite particles both reaction partners may be excited to levels of multipolarity L_1 and L_2, respectively. This mutual excitation, too, is a second-order process and is described by the same amplitude as for double excitation, except for a factor,

$$f^{(L_1L_2)}_{LM}(\theta) = \frac{1}{\pi^{\frac{1}{2}}}\,\langle L_1L_2\,00\,|\,L\,0\rangle\,\frac{c_1(L_1)c_1(L_2)}{c_2(L)}\left[\frac{(2L_1+1)\,(2L_2+1)}{2L+1}\right]^{\frac{1}{2}}f^{(2)}_{LM}(\theta) \qquad (14.30)$$

The differential cross-section for mutual excitation is given by

$$\frac{d\sigma}{d\Omega}\begin{pmatrix}0\to L_1\\0\to L_2\end{pmatrix} = \sum_{L}\sum_{M=-L}^{L}\left|f^{(L_1L_2)}_{LM}(\theta)\right|^2 \qquad (14.31)$$

For a permanently deformed axially-symmetric nucleus the reduced matrix element $c_2(L)$ for double excitation is related to that for single excitation by [133].

$$c_2(L) = \frac{1}{(4\pi)^{\frac{1}{2}}} \langle L'L\,00 \,|\, L'0 \rangle^2 \,(2L'+1)[c_1(L')]^2 \qquad (14.32)$$

14.3. Applications

The adiabatic strong absorption theory has been extensively applied to inelastic scattering of alpha particles and heavy ions and it has proved to be a powerful tool in nuclear spectroscopy. Springer and Harvey [85, 143] have used the "open" Austern-Blair expression (13.33) with $\eta_{\bar{\ell}}$ in the form (6.5)(but $\epsilon = 0$) in analysing the scattering of 50.9-MeV alpha particles by ^{40}Ca and ^{20}Ne. Similar analyses for 42-MeV alpha particles have been made by Peterson for ^{48}Ca [144] and Alster et al. for the lead isotopes [145] and ^{88}Sr [146]. The closed SAM expression (14.15) for single excitation has been applied with a three-parameter $\eta_{\bar{\ell}}$ to 64.3 MeV alphas scattered by ^{58}Ni [138], and with a five-parameter $\eta_{\bar{\ell}}$ to 50.9-MeV alphas scattered by ^{40}Ca [139]. The latter analysis tests the accuracy of the closed formula (14.15) by comparison with the Springer-Harvey analysis [85] in which the open expression (13.33) had been used. General agreement was found within a few per cent over the entire angular distribution so that the explicit expressions are quite reliable for quantitative analyses. The advantages of having accurate closed formulae are obvious. Not only the physical structure of the inelastic amplitudes and their relation to the elastic amplitude becomes transparent, also the practical numerical computation of the cross-sections and the search for best fits are greatly simplified. This is true particularly for heavier projectiles (as in heavy ion scattering) and at higher energies where direct summations over the large number of partial waves become increasingly time-consuming, while the accuracy of the explicit formulae improves.

In these analyses, the elastic and inelastic cross-sections are fitted simultaneously. The $\eta_{\bar{\ell}}$-parameters are determined by a best fit to the elastic cross-section using the closed SAM formulae (6.11)-(6.13). All inelastic cross-sections are then calculated with the same parameters and the reduced matrix elements $c_1(L)$ are obtained by normalization. It is customary to express the results in terms of deformation distances δ_L defined by

$$\alpha(\hat{\mathbf{r}}) = \sum_L \delta_L Y_{L0}(\hat{\theta}, 0) \qquad (14.33)$$

where $\hat{\theta}$ is the polar angle between the nuclear symmetry axis and the field point $\hat{\mathbf{r}}$. The δ_L are related to the $c_1(L)$ by

$$\delta_L = (2L+1)^{\frac{1}{2}} c_1(L) \qquad (14.34)$$

and can be compared with the usual spectroscopic deformation parameters β_L by

$$\delta_L = (\Lambda/k)\,\beta_L \approx R\beta_L \tag{14.35}$$

Similar analyses have been made by Bassichis and Dar [126] for 44-MeV alphas scattered by ^{62}Ni. These authors have shown that the Austern-Blair relations can also be obtained in WKB approximation (see 12.1, Eq. (12.9)), and have derived closed formulae for the inelastic amplitudes for single, double and mutual excitation which are special cases of the SAM expressions (14.15), (14.26) and (14.30).

The inelastic scattering of heavy ions is of special interest for applications of the SAM formalism. The strong absorption conditions are particularly well satisfied, different types of excitation (mutual excitation) can occur, and the Coulomb parameters vary over a wide range. Earlier analyses of inelastic heavy ion scattering have been made in DWBA [147, 148], and by Dar and coworkers [126, 141, 149] using their WKB formalism. A recent investigation [142] of elastic and inelastic scattering in the systems $^{16}O + {}^{12}C$ at 168 MeV, $^{12}C + {}^{12}C$ at 127 MeV, and $^{12}C + {}^{208}Pb$ at 125.6 MeV, has shown that the closed SAM formulae give a satisfactory description of the heavy ion data with a consistent set of parameters. In the $^{12}C + {}^{12}C$ system the reaction partners are identical bosons and the amplitudes have to be properly symmetrized. The elastic scattering amplitude $f_{el}(\theta)$ must be replaced by

$$f_{el}^{(s)}(\theta) = f_{el}(\theta) + f_{el}(\pi - \theta) \tag{14.36}$$

and the inelastic amplitudes $f_{LM}(\theta)$ for single, double and mutual excitation by

$$f_{LM}^{(s)}(\theta) = f_{LM}(\theta) + (-)^{L+M} f_{LM}(\pi - \theta) \tag{14.37}$$

14.4. Odd-A nuclei; core excitation

Odd-A nuclei can be regarded as consisting of an even-A core to which the odd nucleon (particle or hole) is coupled. If we assume a model for this coupling we can relate the cross-sections for collective excitation of the odd-A nucleus to those for collective excitation of the even core. If the nucleon-core coupling is weak, this relation is given by [150]

$$\frac{d\sigma}{d\Omega}(L; I \to I') = \frac{2I'+1}{(2L+1)\,(2I+1)} \frac{d\sigma}{d\Omega}(0 \to L) \tag{14.38}$$

where I, I' are the spins of the ground state and excited state, respectively, and L is the multipolarity of the transition. In this model the odd

nucleon is a spectator which does not affect the collective excitation of the even-A core. It only produces a splitting of the excited levels which is reflected in the statistical factor in Eq. (14.38). The ground state spin I is given by the shell model angular momentum j of the odd particle (hole). One would expect that this model works in good approximation for nuclei in the vicinity of closed shells. It has been tested by inelastic scattering of alpha particles from ^{63}Cu, ^{65}Cu (cores ^{62}Ni, ^{64}Ni)[151]; ^{15}N(^{16}O) [152]; ^{27}Al(^{28}Si) [153]; ^{207}Pb, ^{209}Bi (^{208}Pb) [145]; ^{89}Y(^{88}Sr) [146]. These investigations show that core excitation does occur in many cases and accounts for the phase relations between inelastic angular distributions of neighbouring nuclei. However, the detailed predictions of the weak coupling model are often not confirmed, and there are odd-A nuclei such as ^{89}Y whose excited states cannot be described by pure collective core excitation [146].

For nuclei with a permanently deformed core we expect strong nucleon-core coupling. In the adiabatic approximation, the inelastic cross-section for transitions within the ground-state band is then given by [154]

$$\frac{d\sigma}{d\Omega}(L;I,K\to I',K) = \langle IL\,K0\,|\,I'K\rangle^2 \frac{d\sigma}{d\Omega}(0\to L) \qquad (14.39)$$

where K is the projection of the total angular momentum on the nuclear symmetry axis. This model was found to describe satisfactorily the inelastic alpha scattering from ^{25}Mg (^{24}Mg), but it is not successful for ^{27}Al(^{28}Si) [155].

At present, then, the excitations of odd-A nuclei are not as well understood as those of even-A nuclei for which the adiabatic strong absorption theory and the DWBA have been completely satisfactory.

15. CONCLUSION

15.1. "Surface" reactions

In our discussion of direct reactions we have been mainly concerned with inelastic scattering of strongly absorbed particles. This is the simplest case of so-called surface reactions and it is likely that the theory developed for inelastic scattering is the prototype and forerunner of a more general description for all "surface" interactions. The latter are characterized by the circumstance that the elements of the transition matrix are confined to a narrow band of orbital angular momenta around a critical value ℓ_0. As this is the basic property which made it possible to evaluate the inelastic amplitudes in explicit and closed forms, we would expect that similar methods can be applied to other reactions of this type. That this expectation is reasonable is indicated by the success with which configuration space diffraction and WKB models have been extended to describe stripping, knock-out and pick-up reactions of deuterons, ^{3}He, alpha particles and other strongly absorbed projectiles [70, 134, 135, 156-158]. The angular distributions for these reactions often show the marked oscillatory structure that is characteristic of diffraction processes. Here again the diffraction would be more appropriately described in angular momentum space than in configuration space. From the form of the T-matrix elements (10.15) in zero-range DWBA

we see that such a description is possible if the radial integrals $R^L_{\ell\ell'}$ (Eq. (10.16)) are localized in angular momentum space. This is, by definition, the case for all "surface" interactions and we expect that the amplitudes for these reactions have a structure which is very similar to those given by the Austern-Blair theory for inelastic scattering. In particular, for reactions which are "quasi-elastic" in the sense that $|Q| \ll E$, we can make the adiabatic approximation and directly apply the Austern-Blair formulae. The angular distributions would then be the same as those for inelastic scattering and only the reduced matrix elements c_L would have different values. Good examples of reactions for which these conditions are well satisfied are the single-nucleon transfer reactions between heavy ions.

15.2. Nucleon transfer reactions

The various theories of nucleon transfer reactions between heavy ions have been reviewed by Greider [159]. Here I shall confine myself to the "adiabatic" approach indicated just now and apply it to single-nucleon transfer above the Coulomb barrier [160]. We neglect the difference between the incoming and outgoing wave numbers in Eq. (10.15), $k_a \approx k_b = k$, and assume that the radial integrals (10.16) can be approximated by

$$R^L_{\ell\ell'} \approx -\frac{i}{2} E \frac{\partial \eta_{\bar{\ell}}}{\partial \bar{\ell}}, \quad \bar{\ell} = \tfrac{1}{2}(\ell + \ell') \tag{15.1}$$

where $\eta_{\bar{\ell}}$ are the S-matrix elements for elastic scattering. The localization of the radial integrals described by (15.1) can be understood qualitatively as follows. Partial waves with large $\bar{\ell}$-values will undergo pure Coulomb scattering, while low-$\bar{\ell}$ partial waves will be absorbed owing to compound nucleus formation or direct processes other than transfer. Thus the only contributions to the radial integrals for transfer come from a narrow range of $\bar{\ell}$-values in the neighbourhood of the cutoff angular momentum ℓ_0. If we confine ourselves to spinless particles and use Eq. (15.1), the transfer amplitude (10.15) becomes formally identical with the Austern-Blair amplitude (14.2) for inelastic scattering via single excitation. For heavy ions the SAM conditions are well satisfied and the closed form (14.15) of this amplitude will be a good approximation.

If we use the simplified form (6.15) for $\eta_{\bar{\ell}}$, the differential cross-section for transfer with multipolarity L becomes

$$\left(\frac{d\sigma}{d\Omega}\right)_L = |c_L|^2 (2L+1) \frac{\Lambda}{16\pi} \frac{\theta}{\sin\theta}$$

$$\cdot \left\{ (H_-^2 + H_+^2) \sum_{M=-L}^{L} [\alpha^2_{LM}(\theta) + \beta^2_{LM}(\theta)] \, [J^2_{|M|}(\Lambda\theta) + J^2_{|M|-1}(\Lambda\theta)] \right.$$

$$\left. + 2 H_- H_+ \sum_{M=-L}^{L} [\alpha^2_{LM}(\theta) - \beta^2_{LM}(\theta)] \, [J^2_{|M|}(\Lambda\theta) - J^2_{|M|-1}(\Lambda\theta)] \right\} \tag{15.2}$$

where

$$H_{\pm} = [1+\mu_1(\theta_c \pm \theta)]\, F[\Delta(\theta_c \pm \theta)] \tag{15.3}$$

To simplify this expression we consider the asymptotic region $\theta \gg |M|/\Lambda$. Using

$$\begin{aligned} J^2_{|M|}(\Lambda\theta) + J^2_{|M|-1}(\Lambda\theta) &\cong \frac{2}{\pi\Lambda\theta} \\ J^2_{|M|}(\Lambda\theta) - J^2_{|M|-1}(\Lambda\theta) &\cong (-)^M \frac{2}{\pi\Lambda\theta}\sin(2\Lambda\theta) \end{aligned} \tag{15.4}$$

Eq. (15.2) reduces to

$$\begin{aligned} \left(\frac{d\sigma}{d\Omega}\right)_L &\cong |c_L|^2 (2L+1)\frac{\Lambda}{8\pi^2\sin\theta} \\ &\cdot \left\{(H_-^2 + H_+^2)\sum_{M=-L}^{L}[\alpha^2_{LM}(\theta) + \beta^2_{LM}(\theta)]\right. \\ &\left. + 2H_+H_-\sin(2\Lambda\theta)\sum_{M=-L}^{L}(-)^M[\alpha^2_{LM}(\theta) - \beta^2_{LM}(\theta)]\right\} \end{aligned} \tag{15.5}$$

With α_{LM}, β_{LM} in the form (14.18), and using the orthogonality relation

$$\sum_{M=-L}^{L} d^{(L)}_{\kappa M}\left(\frac{\pi}{2}\right) d^{(L)}_{\kappa' M}\left(\frac{\pi}{2}\right) = \delta_{\kappa\kappa'}, \tag{15.6}$$

and the symmetry relation (14.19), we have

$$\begin{aligned} \sum_{M=-L}^{L}[\alpha^2_{LM}(\theta) + \beta^2_{LM}(\theta)] &= 1 \\ \sum_{M=-L}^{L}(-)^M[\alpha^2_{LM}(\theta) - \beta^2_{LM}(\theta)] &= (-)^L \end{aligned} \tag{15.7}$$

Equation (15.5) simplifies to

$$\left(\frac{d\sigma}{d\Omega}\right)_L \cong |c_L|^2 (2L+1)\frac{\Lambda}{8\pi^2\sin\theta}[H_-^2 + H_+^2 + (-)^L 2H_-H_+\sin(2\Lambda\theta)] \tag{15.8}$$

The angular distribution described by this expression is oscillatory and exhibits the Blair phase factor $(-)^L$ associated with the multipolarity L. However, reactions between heavy ions are often dominated by strong Coulomb interaction. In these cases $H_+ \ll H_-$, and in the limit of complete Coulomb damping we obtain

$$\left(\frac{d\sigma}{d\Omega}\right)_L \cong |c_L|^2 (2L+1) \frac{\Lambda}{8\pi^2 \sin\theta} (H_-)^2 \qquad (15.9)$$

In collisions of heavy particles it is convenient to extract the $1/\sin\theta$ dependence which arises from the restriction of the reaction products to the scattering plane in the classical limit of scattering. We therefore define

$$\left(\frac{d\sigma}{d\theta}\right)_L = 2\pi \sin\theta \left(\frac{d\sigma}{d\Omega}\right)_L$$

$$\cong |c_L|^2 (2L+1) \frac{\Lambda}{4\pi} \{[1 - \mu_1 (\theta - \theta_c)] F[\Delta(\theta - \theta_c)]\}^2 \qquad (15.10)$$

With the form factor

$$F[\Delta(\theta - \theta_c)] = \frac{\pi\Delta(\theta - \theta_c)}{\sinh[\pi\Delta(\theta - \theta_c)]} \qquad (15.11)$$

this describes a smooth angular distribution which is peaked at $\theta_0 \approx \theta_c - (3\mu_1/\pi\Delta)$. Equation (15.8) with $\mu_1 = 0$ and $L = 0$ has been used [160] to analyse various single-nucleon transfer cross-sections and the agreement was found to be quite satisfactory.

A closely related treatment of transfer reactions has been presented by Dar [161], who uses a configuration-space diffraction model and the WKB approximation to evaluate the radial integrals. For energies above the Coulomb barrier, Dar's result has the same form as (15.8) for $\mu_1 = 0$ and $L = 0$, but he finds a different form factor

$$(F_-)^2 = \left\{\cosh^2[\pi\Delta(\theta - \theta_c)] - \cos^2\left(\pi \frac{\Delta}{\Delta'}\right)\right\}^{-1} \qquad (15.12)$$

where $\Delta' = kr_0$ and r_0 is the range of the bound-state wave function of the captured nucleon. The detailed structure of the form factors clearly depends on assumptions about the reaction mechanism and on how the radial integrals are evaluated. Relevant are the general properties of the form factors which are determined by the localization in ℓ-space of the radial integrals, of which they are essentially the Fourier transforms.

Dar's treatment applies also to energies below the Coulomb barrier where his results are in agreement with the tunneling model of Breit. An extension of Dar's theory to non-zero angular momentum transfer

has been given by Dar and Kozlowsky [162]. Again their expressions are of the same form as (15.2) or (15.8), except for different form factors.

In some cases where from Eq. (15.8) one would expect to see diffraction oscillations in the transfer cross-sections, smooth angular distributions are observed [163]. The unexpected absence of an oscillatory structure has been attributed to recoil and finite range effects [164]. However, as Dar and Kozlowsky have pointed out, a more likely explanation is an approximate cancellation of the oscillatory terms in (15.8) from odd and even L-values if transfer occurs with different multipolarities.

We have mentioned earlier the investigation of Dar [70] which shows that even the simple Fraunhofer limit of Eq. (15.2) gives good fits to the angular distributions of a wide variety of direct reactions. This, too, supports the conclusion that Eq. (15.2) with suitable form factors is an adequate description of low-Q surface interactions in general (see also Ref. [157]). It is significant that the form of this expression is "model-independent" and that its general structure depends only upon the asymptotic wave functions.

15.3. Concluding remarks

The final step towards a model-independent description of nuclear processes would be a formulation which is based entirely upon the properties of the scattering matrix. Such methods have been developed in high-energy physics and are known as dispersion theories. Only recently attempts have been made to apply these methods to nuclear reactions at lower energies. These are reviewed by Shapiro [165] and Schnitzer [166]. The simplest applications so far have been made to exchange processes in which the reaction A(a, b)B can be described by a diagram of the form shown in Fig. 3 where x denotes the exchanged

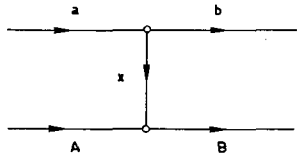

FIG. 3. Reaction A(a, b)B

particle. Most direct reactions are basically of this type. Processes which we have called "surface reactions" at medium energies are known as peripheral reactions in high-energy physics. There is a close relation between the descriptions of direct reactions at medium and at high energies, as Henley has emphasized [158], and the phenomenological methods which we have discussed in this Course can be applied in both energy regions. It is with such a unifying description in mind that we have given special attention to those phenomenological methods which aim at avoiding the potential concept and are formulated directly in terms of scattering matrix elements. For direct nuclear interactions, perhaps the most significant step in the direction of a potential-free formulation is the theory of Austern and Blair and it is appropriate to repeat here the question which concludes their paper [133]: "Is it likely that these relations and generalizations thereof do not presuppose the validity

of the optical model but rather that the optical model has been a 'crutch' used in their derivation, much as potential models are employed to suggest the dispersion relations of high energy physics?" It is not unlikely that the phenomenological S-matrix methods will eventually find their foundation in dispersion theory. A promising start in this direction was recently made by several authors [167, 168]. However, nuclei (and their constituents) are complex things, and it is possible that their interactions are not completely determined by asymptotic states. Who knows?

REFERENCES

[1] GOLDBERGER, M. L., WATSON, K. M., Collision Theory, John Wiley, New York (1964).
[2] SATCHLER, G. R., Nucl. Phys. 21 (1961) 116.
[3] LANE, A. M., Phys. Rev. Lett. 8 (1962) 171.
[4] LANE, A. M., Nucl. Phys. 35 (1962) 676.
[5] BRUECKNER, K. A., LOCKETT, A. M., ROTENBERG, M., Phys. Rev. 121 (1961) 255.
[6] FRAHN, W. E., LEMMER, R. H., Nuovo Cim. 5 (1957) 1564, ibid. 6 (1957) 1221.
[7] FRAHN, W. E., LEMMER, R. H., Nuovo Cim. 6 (1957) 664.
[8] PEREY, F., BUCK, B., Nucl. Phys. 32 (1962) 353.
[9] FRAHN, W. E., Nucl. Phys. 66 (1965) 358.
[10] PEREY, F. G., SAXON, D. S., Phys. Lett. 10 (1964) 107.
[11] AUSTERN, N., Phys. Rev. 137 (1965) B752.
[12] FIEDELDEY, H., Nucl. Phys. 77 (1966) 149.
[13] PEREY, F. G., Proc. Conf. Direct Interactions and Nuclear Reaction Mechanisms, Padua, Italy, September 3-8, 1962 (CLEMENTEL, E., VILLI, C., Eds.), Gordon and Breach, Science Publishers, New York (1963) 125.
[14] LANE, A. M., WANDEL, C. F., Phys. Rev. 98 (1955) 1524.
[15] CLEMENTEL, E., VILLI, C., Nuovo Cim. 2 (1955) 176.
[16] RIESENFELD, W. B., WATSON, K. M., Phys. Rev. 102 (1956) 1157.
[17] HARADA, K., ODA, N., Prog. theor. Phys. 21 (1959) 260.
[18] KIKUCHI, K., Nucl. Phys. 12 (1959) 305.
[19] LEMMER, R. H., MARIS, T. A. J., TANG, Y. C., Nucl. Phys. 12 (1959) 619.
[20] GOMES, L. C., Phys. Rev. 116 (1959) 1226.
[21] SHAW, G. L., Ann. Phys. (N. Y.) 8 (1959) 509.
[22] SAWICKI, J., MOSZKOWSKI, S. A., Nucl. Phys. 21 (1960) 456.
[23] FESHBACH, H., Ann. Rev. nucl. Sci. 8 (1958) 49.
[24] FESHBACH, H., Ann. Phys. (N. Y.) 5 (1958) 357.
[25] FRAHN, W. E., 1962, unpublished.
[26] ENGELBRECHT, C. A., FIEDELDEY, H., Ann. Phys. (N. Y.), to be published.
[27] HODGSON, P. E., The Optical Model of Elastic Scattering, Oxford University Press, Oxford (1963).
[28] LANE, A. M., LYNN, J. E., MELKANOFF, M. A., RAE, E. R., Phys. Rev. Lett. 2 (1959) 424.
[29] KHANNA, F. C., TANG, Y. C., Nucl. Phys. 15 (1959) 337.
[30] KRUEGER, T. K., MARGOLIS, B., Nucl. Phys. 28 (1961) 578.
[31] FIEDELDEY, H., FRAHN, W. E., Ann. Phys. (N. Y.) 16 (1961) 387.
[32] FIEDELDEY, H., FRAHN, W. E., Nucl. Phys. 38 (1962) 686.
[33] HODGSON, P. E., ROOK, J. R., Nucl. Phys. 37 (1962) 632.
[34] TERASAWA, T., SATCHLER, G. R., Phys. Lett. 7 (1963) 265.
[35] WILMORE, D., HODGSON, P. E., Nucl. Phys. 55 (1964) 673.
[36] PEREY, F. G., Phys. Rev. 131 (1963) 745.
[37] BARRETT, R. C., HILL, A. D., HODGSON, P. E., Nucl. Phys. 62 (1964) 133.
[38] ROSEN, L., BEERY, J. G., GOLDHABER, A. S., AUERBACH, E. H., Ann. Phys. (N. Y.) 34 (1965) 96.
[39] JOHANSSON, A., SVANBERG, U., HODGSON, P. E., Ark. Fys. 19 (1961) 541.
[40] HODGSON, P. E., Phys. Rev. Lett. 6 (1961) 358.
[41] ROLLAND, C., GEOFFRIOU, B., MARTY, N., MORLET, M., TATISCHEFF, B., WILLIS, A., Nucl. Phys. 80 (1966) 625.
[42] ROOS, P. G., WALL, N. S., Phys. Rev. 140 (1965) B1237.

[43] HAYBRON, R. M., SATCHLER, G. R., Phys. Lett. 11 (1964) 313.
[44] ELTON, L. R. B., Nucl. Phys. 89 (1966) 69.
[45] FRAHN, W. E., WIECHERS, G., Phys. Rev. Lett. 16 (1966) 810.
[46] FRAHN, W. E., WIECHERS, G., Ann. Phys. (N. Y.), 41, 3 (1967) 442.
[47] IGO, G., Phys. Rev. Lett. 1 (1958) 72.
[48] IGO, G., Phys. Rev. 115 (1959) 1665.
[49] PEREY, C. M., PEREY, F. G., Phys. Rev. 132 (1963) 755.
[50] HALBERT, E. C., Nucl. Phys. 50 (1964) 353.
[51] HODGSON, P. E., Adv. Phys. 15 (1966) 329.
[52] DRISKO, R. M., SATCHLER, G. R., BASSEL, R. H., Phys. Lett. 5 (1963) 347.
[53] HODGSON, P. E., C. r. Congr. International de Physique Nucléaire I (GUGENBERGER, P., Ed.), Paris (1964) 257.
[54] ROOK, J. R., Nucl. Phys. 61 (1065) 219.
[55] WATANABE, S., Nucl. Phys 8 (1958) 484.
[56] GLAUBER, R. J., in Lectures in Theoretical Physics I, Univ. of Colorado (1958) 374.
[57] McCAULEY, G. P., BROWN, G. E., Proc. Phys. Soc. 71 (1958) 893.
[58] FORD, K. W., WHEELER, J. A., Ann. Phys. (N. Y.) 7 (1959) 287.
[59] EISBERG, R. M., PORTER, C. E., Rev. mod. Phys. 33 (1961) 190.
[60] HALBERT, M. L., ZUCKER, A., Nucl. Phys. 16 (1960) 158.
[61] KALINKIN, B. N., GRABOWSKI, J., Proc. Third Conf. Reactions between Complex Nuclei, Asilomar, Calif., 1963 (GHIORSO, A., DIAMOND, R. M., CONZETT, H. E., Eds.), University of California Press, Berkeley (1963) 129.
[62] SABATIER, P. C., Nuovo Cim. 37 (1965) 1180.
[63] AKHIEZER, A. I., POMERANCHUK, I. J., J. Phys. (USSR) 9 (1945) 471.
[64] AKHIEZER, A. I., POMERANCHUK, I. J., Usp. fiz. Nauk 65 (1958) 593.
[65] FERNBACH, S., SERBER, R., TAYLOR, T., Phys. Rev. 75 (1949) 1352.
[66] PREDAZZI, E., Ann. Phys. (N. Y.) 36 (1966) 228, 250.
[67] ADACHI, T., KOTANI, T., Prog. theor. Phys. Suppl. (1965) 316.
[68] ADACHI, T., Prog. theor. Phys. 35 (1966) 463.
[69] AUSTERN, N., "Direct reactions", Selected Topics in Nuclear Theory, IAEA, Vienna (1963) 17.
[70] DAR, A., Nucl. Phys. 55 (1964) 305.
[71] YAVIN, A., FARWELL, G. W., Nucl. Phys. 12 (1959) 1.
[72] BLAIR, J. S., Phys. Rev. 95 (1954) 1218.
[73] KERLEE, D. D., BLAIR, J. S., FARWELL, G. W., Phys. Rev. 107 (1957) 1343.
[74] BLAIR, J. S., Phys. Rev. 108 (1957) 827.
[75] FRAHN, W. E., VENTER, R. H., Ann. Phys. (N. Y.) 24 (1963) 243.
[76] FRAHN, W. E., Nucl. Phys. 75 (1966) 577.
[77] GREIDER, K. R., GLASSGOLD, A. E., Ann. Phys. (N. Y.) 10 (1960) 100.
[78] ELTON, L. R. B., Nucl. Phys. 23 (1961) 681.
[79] McINTYRE, J. A., WANG, K. H., BECKER, L. C., Phys. Rev. 117 (1960) 1337.
[80] McINTYRE, J. A., BAKER, S. D., WANG, K. H., Phys. Rev. 125 (1962) 584.
[81] ALSTER, J., CONZETT, H. E., Phys. Rev. 139 (1965) B 50.
[82] VENTER, R. H., Ann. Phys (N. Y.) 25 (1963) 405.
[83] VENTER, R. H., FRAHN, W. E., Ann. Phys. (N. Y.) 27 (1964) 401.
[84] FRAHN, W. E., JANSEN, L. P. C., Nucl. Phys. 59 (1964) 641.
[85] SPRINGER, A., HARVEY, B. G., Phys. Lett. 14 (1965) 116.
[86] ERICSON, T. E. O., in Preludes in Theoretical Physics (de-SHALIT, A., FESHBACH, H., van HOVE, L., Eds.), North-Holland Publishing Co., Amsterdam (1965) 321.
[87] INOPIN, E. V., JETP 48 (1965) 1620 (engl. transl. Soviet Physics JETP 21 (1965) 1090).
[88] HÖGAASEN, J., CERN preprint 1966.
[89] FRAHN, W. E., VENTER, R. H., Ann. Phys. (N. Y.) 27 (1964) 135.
[90] VENTER, R. H., FRAHN, W. E., Ann. Phys. (N. Y.) 27 (1964) 385.
[91] FRAHN, W. E., WIECHERS, G., Nucl. Phys. 74 (1965) 65.
[92] HÜFNER, J., de-SHALIT, A., Phys. Lett. 15 (1965) 52.
[93] DAR, A., KOZLOWSKY, B., Phys. Lett. 20 (1966) 311, 314.
[94] ALEXANDER, G., DAR, A., KARSHON, U., Phys. Rev. Lett. 14 (1965) 918.
[95] FRAHN, W. E., Proc. 2nd International Symposium on Polarization Phenomena of Nucleons (HUBER, P., SCHOPPER, H., Eds.), Birkhäuser Verlag, Basel (1966).
[96] RODBERG, L. S., Nucl. Phys. 15 (1959) 72.

[97] KÖHLER, H. S., Nucl. Phys. 6 (1958) 161.
[98] LEVINTOV, I. I., Dokl. Akad. Nauk SSSR 107 (1956) 240.
[99] BLAIR, J. S., Proc. Conf. Direct Interactions and Nuclear Reaction Mechanisms, Padua, Italy, September 3-8, 1962 (CLEMENTEL, E., VILLI, C., Eds.), Gordon and Breach, Science Publishers, New York (1963) 669.
[100] FRAHN, W. E., VENTER, R. H., 1963, unpublished.
[101] DRISKO, R. M., BASSEL, R. H., SATCHLER, G. R., Phys. Lett. 2 (1962) 318.
[102] BURCHAM, W. E., ENGLAND, J. B. A., EVANS, J. E., GARCIA, A., HARRIS, R. G., WILNE, C., C. r. Congr. International de Physique Nucléaire II (GUGENBERGER, P., Ed.), Paris (1964) 877.
[103] AUSTERN, N., Ann. Phys. (N. Y.) 15 (1961) 299.
[104] AUSTERN, N., PRAKASH, A., DRISKO, R. M., Ann. Phys. (N. Y.) 39 (1966) 253.
[105] AUSTERN, N., Nuclear Spectroscopy with Direct Reactions. II. Proceedings, Argonne National Laboratory Report ANL-6848, March 1964, p. 1.
[106] TOBOCMAN, W., Theory of Direct Nuclear Reactions, Oxford University Press (1961).
[107] GELL-MANN, M., GOLDBERGER, M. L., Phys. Rev. 91 (1953) 398.
[108] AUSTERN, N., DRISKO, R. M., HALBERT, E. C., SATCHLER, G. R., Phys. Rev. 133 (1964) B3.
[109] DAR, A., de-SHALIT, A., REINER, A. S., Phys. Rev. 131 (1963) 1732.
[110] BUTTLE, P. J. A., GOLDFARB, L. J. B., C. r. Congr. International de Physique Nucléaire II (GUGENBERGER, P., Ed.), Paris (1964) 969.
[111] BENCZE, G., ZIMANI, J., Phys. Lett. 9 (1964) 246.
[112] HAYAKAWA, S., YOSHIDA, S., Prog. theor. Phys. 14 (1955) 1.
[113] CHASE, D. M., WILETS, L., EDMONDS, A. R., Phys. Rev. 110 (1958) 1080.
[114] SANO, M., YOSHIDA, S., TERASAWA, T., Nucl. Phys. 6 (1958) 20.
[115] AUSTERN, N., DRISKO, R. M., ROST, E., SATCHLER, G. R., Phys. Rev. 128 (1962) 733.
[116] BASSEL, R. H., SATCHLER, G. R., DRISKO, R. M., ROST, E., Phys. Rev. 128 (1962) 2693.
[117] ROST, E., Phys. Rev. 128 (1962) 2708.
[118] BOHR, A., MOTTELSON, B. R., Mat.-fys. Meddr 27 16 (1953).
[119] MARGOLIS, H., TROUBETZKOY, E. S., Phys. Rev. 106 (1957) 105.
[120] BUCK, B., Phys. Rev. 127 (1962) 940.
[121] BUCK, B., Phys. Rev. 130 (1963) 712.
[122] BUCK, B., STAMP, A. P., HODGSON, P. E., Phil. Mag. 8 (1963) 1805.
[123] TAMURA, T., Rev. mod. Phys. 37 (1965) 679.
[124] SOPKOVICH, N. J., Nuovo Cim. 26 (1962) 186.
[125] GOTTFRIED, K., JACKSON, J. D., Nuovo Cim. 34 (1964) 735.
[126] BASSICHIS, W. H., DAR, A., Ann. Phys. (N. Y.) 36 (1966) 130.
[127] DROZDOV, S. I., JETP (USSR) 28 (1955) 734, 736.
[128] INOPIN, E. V., JETP (USSR) 31 (1956) 901.
[129] BLAIR, J. S., Phys. Rev. 115 (1959) 928.
[130] GLENDENNING, N. K., Phys. Rev. 114 (1959) 1297.
[131] KROMMINGA, A. J., McCARTHY, I. E., Phys. Rev. Lett. 6 (1961) 62.
[132] DROZDOV, S. I., JETP (USSR) 38 (1960) 499.
[133] AUSTERN, N., BLAIR, J. S., Ann. Phys. (N. Y.) 33 (1965) 15.
[134] HENLEY, E. M., YU, D. U. L., Phys. Rev. 133 (1964) B1445.
[135] HENLEY, E. M., YU, D. U. L., Phys. Rev. 135 (1964) B1152.
[136] ROST, E., AUSTERN, N., Phys. Rev. 120 (1960) 1375.
[137] BLAIR, J. S., SHARP, D., WILETS, L., Phys. Rev. 125 (1962) 1625.
[138] POTGIETER, J. M., FRAHN, W. E., Nucl. Phys. 80 (1966) 434.
[139] POTGIETER, J. M., FRAHN, W. E., Phys. Lett. 21 (1966) 211.
[140] HAHNE, F. J. W., Nucl. Phys. 80 (1966) 113.
[141] BASSICHIS, W. H., DAR, A., Phys. Rev. Lett. 14 (1965) 648.
[142] POTGIETER, J. M., FRAHN, W. E., Nucl. Phys. A 92 (1967) 84.
[143] SPRINGER, A., HARVEY, B. G., Phys. Rev. Lett. 14 (1965) 316.
[144] PETERSON, R. J., Phys. Rev. 140 (1965) B1479.
[145] ALSTER, J., Phys. Rev. 141 (1966) 1138.
[146] ALSTER, J., SHREVE, D. C., PETERSON, R. J., Phys. Rev. 144 (1966) 999.
[147] BASSEL, R. H., SATCHLER, G. R., DRISKO, R. M., Proc. Third Conf. Reactions between Complex Nuclei, Asilomar, Calif., 1963 (GHIORSO, A., DIAMOND, R. M., CONZETT, H. E., Eds.), University of California Press, Berkeley (1963) 45.
[148] HIEBERT, J. H., GARVEY, G. T., Phys. Rev. 135 (1964) B346.

[149] VARMA, S., DAR, A., Ann. Phys. (N.Y.) 39 (1966) 435.
[150] De-SHALIT, A., Phys. Rev. 122 (1961) 1530.
[151] BRUGE, G., FAIVRE, J.C., BARLOUTAUD, M., FARAGGI, H., SAUDINOS, J., Phys. Lett. 7 (1963) 203.
[152] BUSSIERE, A., GLENDENNING, N.K., HARVEY, B.G., MAHONEY, J., MERIWETHER, J.R., Phys. Lett. 16 (1965) 296.
[153] KOKAME, J., FUKUNAGA, K., NAKAMURA, H., Phys. Lett. 14 (1965) 234.
[154] BLAIR, J.S., Nuclear Spectroscopy with Direct Reactions. II. Proceedings Argonne National Laboratory Report ANL-6848, March 1964, 143.
[155] NAQIB, I.M., FARWELL, G.W., (quoted in [154]).
[156] DAR, A., KUGLER, M., DOTHAN, Y., NUSSINOV, S., Phys. Rev. Lett. 12 (1964) 82.
[157] DAR, A., Nucl. Phys. 82 (1966) 354.
[158] HENLEY, E.M., in Preludes in Theoretical Physics (de-SHALIT, A., FESHBACH, H., van HOVE, L., Eds.), North-Holland Publishing Co., Amsterdam (1965) 89.
[159] GREIDER, K.R., Adv. theor. Phys. 1 (1965) 245; Ann. Rev. nucl. Sci. 15 (1965) 291.
[160] FRAHN, W.E., VENTER, R.H., Nucl. Phys. 59 (1964) 651.
[161] DAR, A., Phys. Rev. 159 (1965) B1193.
[162] DAR, A., KOZLOWSKY, B., Phys. Rev. Lett. 15 (1965) 1036.
[163] BIRNBAUM, J., Thesis, Yale University, 1965.
[164] DODD, L.R., GREIDER, K.R., Phys. Rev. Lett. 14 (1965) 959.
[165] SHAPIRO, I.S., "Dispersion theory of direct nuclear reactions", Selected Topics in Nuclear Theory, IAEA, Vienna (1963) 85.
[166] SCHNITZER, H.J., Rev. mod. Phys. 37 (1965) 666.
[167] OMNES, R., Phys. Rev. 137 (1965) B649.
[168] BALL, J.S., FRAZER, W.R., Phys. Rev. Lett. 14 (1965) 746.

CHAPTER 2

PHENOMENOLOGICAL COLLECTIVE MODELS

D. J. ROWE

I. INDEPENDENT PARTICLES AND COLLECTIVE MOTION

1. INTRODUCTION

The nucleus is a system with many aspects and we tend to view it differently according to which of its properties for the moment concerns us. In this way several models of the nucleus have developed, each of which one hopes will one day appear as a special case of some much more general and complex treatment.

It is interesting that the two major models of nuclear structure, in current use, already existed in crude form as long ago as the thirties, although no one then had much faith in either. One was the independent particle model (IPM), which found its fulfilment in the shell model. The other was the liquid drop model, the forerunner of the collective model. Both models were eventually forced into respectability by their overwhelming successes. Instead of discrediting them one was therefore obliged to try and understand them.

The author, previously at the Atomic Energy Research Establishment, UKAEA, Harwell, Berks, United Kingdom, is now in the Department of Physics and Astronomy, The University of Rochester, Rochester, N.Y., United States of America.

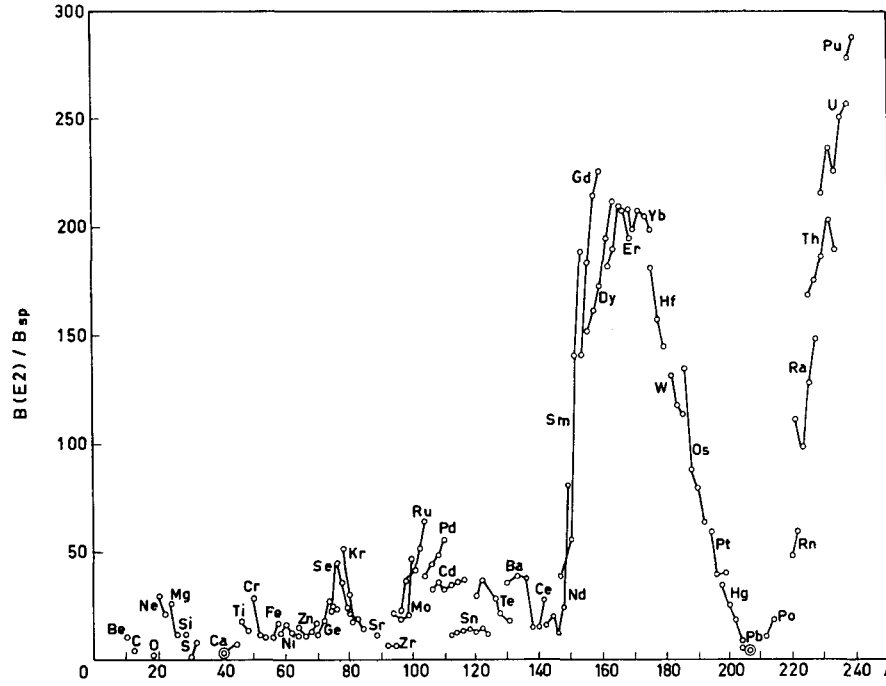

FIG.1. The reduced transition probability B(E2) for the excitation of the first 2^+ state in even-even nuclei versus masses in units of the single-proton estimate $B(E2; 0 \rightarrow 2) = 0.3A^{4/3}$ e^2 fm^4 (Taken from Ref. [4], courtesy of North-Holland Publishing Co.)

The problem of the IPM was that the nucleon-nucleon interaction, although predominately attractive, has a repulsive hard core. All attempts to calculate the effects of such a hard core led to the conclusion that the IPM itself must be destroyed. It was not until the advent of Brueckner's theory [1] in 1953 that one began to appreciate the healing powers of the Pauli principle and its ability to restrain the nuclear particles from scattering far and wide out of their shell-model orbitals.

Suspicion of the liquid drop model was founded largely on the unliquid-like nature of nuclear matter. Molecules in liquids[1] have long-range interactions and are essentially localized, whereas nuclei have short-range interactions and are not in the least localized. Since it is just these properties which characterize a liquid one was naturally not too happy about the analogy. The model was nevertheless very successful in a few important respects, in particular in determining the stability of nuclei against β-decay and fission. It was not very successful though in predicting vibrational states which come out much too high in energy.

Nevertheless we nowadays believe that such liquid drop like collective motion plays a very important part in nuclear spectroscopy. Its existence

[1] Molecules in liquids have kinetic energies ~ 0.1 eV corresponding to a de Broglie wavelength $\lambda\!\!\!^{-} \sim 5 \times 10^{-9}$ cm which is very much less than the intermolecular spacing. Nucleons in the nucleus have kinetic energies ~ 10 MeV corresponding to $\lambda\!\!\!^{-} \sim 10^{-13}$ cm which is comparable with inter-nucleon distances (see Blatt and Weisskopf [2]).

is demonstrated most forcefully by the systematic appearance, throughout the periodic table, of low-lying 2^+ excited states of even-even nuclei. These states have ground-state transition strengths of very many single-particle magnitudes, as shown in Fig. 1. Such large strengths can only be envisaged as the co-operative effect of many particles, i.e. collective motion. For the rare-earth and actinide nuclei, these strengths are especially large. The excited states also have large quadrupole moments. The interpretation is that these nuclei have highly deformed equilibrium shapes and should consequently exhibit rotational spectra. Indeed numerous examples of spectra in which the energies are accurately proportional to the rotational $I(I+1)$ law are observed throughout the deformed regions. Other nuclei have little or no static quadrupole moment. The transition strength then comes from a collective vibration of the nucleus about its spherical equilibrium shape.

In spite of the problems of the liquid drop model, it was later revived in the now classic papers of Bohr and Mottelson [3] and unified with the shell model in order to explain simultaneously collective and particle-like phenomena. The obstacles of the liquid drop model were side-stepped by treating the collective parameters empirically.

A microscopic understanding of why the collective model works as well as it does is even nowadays far from complete, although a lot of progress has been made in this direction. To a large extent the microscopic collective theories, in terms of the extended shell models, have progressed independently of the phenomenological models so that it is possible to make some sort of division between the two. In this chapter I plan to review some of the phenomenological models. Some models are of course partly phenomenological and partly microscopic and these will also be included. In Chapter 10 I will talk about the microscopic theories and also say something about the relationship between the two.

2. NUCLEAR SYSTEMATICS - COUPLING SCHEMES

Why is it that some nuclei are spherical and vibrate while others are deformed and rotate? Some light is thrown on this question by considering the possible ways in which the particles can couple and the resulting equilibrium shapes that are favoured by the different coupling schemes.

2.1. Field producing forces (aligned coupling)

The shell-model concept, of particles moving independently in the self-consistent field that they generate, has proved itself a good basis for a study of nuclear spectroscopy. It is worth while therefore to consider the coupling scheme for particles which interact via their fields.

First of all, for a closed shell there is no ambiguity in coupling and the density distribution is completely spherical.

Now add one particle, e.g. ^{17}O. In zero order ^{17}O is a ^{16}O core plus a $d_{5/2}$ neutron. The 'closed shell plus one' nucleus is now no longer spherical, as illustrated classically in Fig. 2. ^{17}O should therefore have a finite mass quadrupole moment but, since the odd particle is a neutron, it has a zero charge quadrupole moment. Experimentally, however, it is

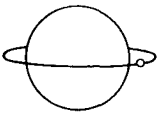

FIG. 2. The classical orbit of an odd particle about a spherical core

observed to have a charge quadrupole moment

$$\langle Q \rangle = 2.6 \times 10^{-26} \text{ cm}^2 \tag{2.1.1}$$

which is almost as large as would be expected for an odd proton (i.e. -3.0×10^{-26} cm^2).

This problem is usually patched up in the shell model by using effective charges $e^{(2)}_{\text{eff}}(n) \approx e_p$ and $e^{(2)}_{\text{eff}}(p) \approx 2e_p$. But what is the physics behind this result? It must be that the odd particle is polarizing the core. In other words, the core particles are attempting to align their orbits with the deformed field of the odd neutron. Given the potential well, one can calculate the amount of polarization expected, for example one finds $e^{(2)}_{\text{eff}} = e + (Z/A)e_p$ for a harmonic oscillator potential, and $e^{(2)}_{\text{eff}} = e + (3-5)(Z/A)e_p$ for a square well potential. The factor $(3-5)$ for the square well depends on the particular orbit of the odd particle.

Now consider a closed shell plus two particles. The second particle is going to align itself with the deformed field of the first, making the overall shape even more deformed (Fig. 3). Thus the two-particle wave function would be

$$\psi = \mathscr{A}\, \varphi^j_j(1)\, \varphi^j_{-j}(2) \tag{2.1.2}$$

where $\mathscr{A}$ is an antisymmetrization operator.

Further extra-core particles will also want to align their orbits as near to the equatorial plane as the Pauli principle will allow, i.e.

$$\psi = \mathscr{A}\, \varphi^j_j(1)\, \varphi^j_{-j}(2)\, \varphi^j_{j-1}(3)\, \varphi^j_{-j+1}(4) \ldots \tag{2.1.3}$$

For large j, a large oblate deformation can be built up in this way.

This is not the only possibility, however. It may actually be more favourable for the particles to concentrate their densities along the polar axis, i.e.

$$\psi = \mathscr{A}\, \varphi^j_{1/2}(1)\, \varphi^j_{-1/2}(2)\, \varphi^j_{3/2}(3)\, \varphi^j_{-3/2}(4) \ldots \tag{2.1.4}$$

producing a prolate shape. Which is the more favourable shape we can only tell by calculation. But qualitatively we can say that, for field-

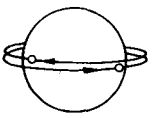

FIG. 3. The classical orbits for two particles about a spherical core

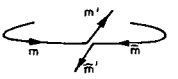

FIG. 4. Trajectories of two particles when a strong short-range interaction occurs

producing forces, it is energetically favourable for the particles to align one way or another and that this alignment will tend to produce non-spherical nuclear shapes. It turns out that towards the beginning of a j-shell the nucleus is prolate and towards the end it becomes oblate.

Of course once the field is deformed the single-particle wave functions themselves are modified, ceasing to have good j. Provided the deformation is axially symmetric, however, they retain good m and the above coupling scheme persists. One consequence is that, as the deformed field is turned on, different unperturbed j-shells tend to intermingle, allowing for even better alignment. This happens for example in the rare-earth region where very large deformations are stabilized.

Again it should be pointed out that the energetically most favourable shape need not necessarily be axially symmetric. Neither need it be reflection-symmetric. It might for example be pear-shaped. There is some evidence for the existence of these more exotic shapes, but it appears that the bulk of the experimental data can be understood in terms of prolate or oblate spheroids and so we shall consider principally these.

2.2. Short-range forces (pair coupling)

If we believed that the aligned coupling scheme was the whole story, we would have to accept that all nuclei other than those with doubly closed shells should be deformed. But we know that in fact the spherical shape is very much more stable. A simple explanation for this can be given in terms of the short-range interactions. Consider the situation classically. If two particles are moving in time-reversed orbits they come close to each other twice in every orbit. If there is a strong short-range interaction between them, they frequently scatter into new but still time-reversed orbits (see Fig. 4). In this way they rapidly spread over all angular space, making for a spherical density distribution.

We can express this phenomenon more precisely in quantal language by looking at the spectrum of energy levels for two particles in a j^2 con-

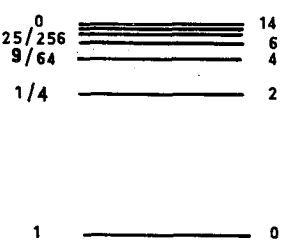

FIG. 5. Spectrum for two particles in a $j^2 = (15/2)^2$ configuration with a δ-interaction. (After Mottelson [5])

figuration, with a δ-interaction. The appropriate matrix element is

$$\langle j^2 J | \delta(\vec{r}_1 - \vec{r}_2) | J^2 j \rangle = \frac{R}{4\pi} (j+\tfrac{1}{2})(J\, j\, 0\, \tfrac{1}{2} | j\, \tfrac{1}{2})^2 \qquad (2.2.1)$$

where R is the radial integral

$$R = \int [R_{n\ell}(r)]^4 r^2 dr \qquad (2.2.2)$$

The result is shown in Fig. 5. We find that the J = 0 state is much more strongly bound than the others. This is because in a J = 0 state the particles come most closely together.

This pairwise coupling of particles to stable J = 0 configurations has been recognized for a long time, and has been expressed in terms of Racah's seniority coupling scheme. The seniority v = 0 (no unpaired particles) ground state for a j^n configuration of an even number n of particles is

$$\psi_0 = \mathscr{A} \varphi_0(1\ 2)\, \varphi_0(3\ 4) \ldots \qquad (2.2.3)$$

A seniority v = 2 (2 unpaired particles) excited state might be

$$\psi_{2J} = \mathscr{A} \varphi_J(1\ 2)\, \varphi_0(3\ 4) \ldots \qquad (2.2.4)$$

The importance of the short-range pairing forces in nuclear spectroscopy was recognized for the following reasons:

(a) Even-even nuclei invariably have spin J = 0 ground states.
(b) The low-lying spectrum for even-even nuclei is particularly simple. There is an energy gap, corresponding to the energy required to break a J = 0 pair, below which only collective states appear. Figure 6 contrasts the energy spectra for neighbouring even-even, even-odd, and odd-odd nuclei.
(c) The last nucleon is less strongly bound in an odd nucleus than in the neighbouring even-even nucleus, where it can form a pair.

The short-range interaction, which has a strength defined by

$$\langle (jm)(j\bar{m}) | v | (jm')(j\bar{m}') \rangle = G_{jj'} \approx \frac{22}{A} \text{ MeV} \qquad (2.2.5)$$

generally overlaps different j-subshells. Fortunately for the shell model it does not usually overlap major shells (~ 10 MeV). We must therefore go beyond the seniority coupling scheme and express the paired wave function

$$\varphi_0(1\ 2) = \sum_j c_j\, \varphi_0^{(j)}(1\ 2) \qquad (2.2.6)$$

The angular momentum is still J = 0 however, and the density distribution spherical.

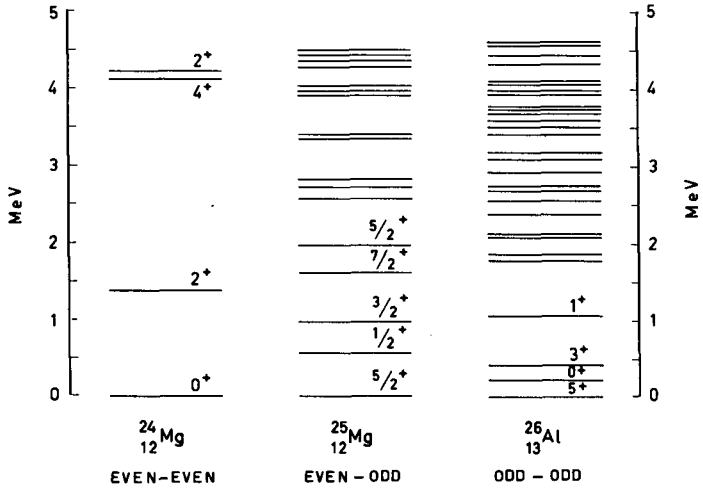

FIG. 6. Energy spectra for neighbouring even-even, even-odd and odd-odd nuclei

2.3. Schematic forces

To what part of the two-body interaction do the field forces correspond? Neglecting exchange, the field is

$$u(\vec{r}) = \int d\vec{r}' \, V(\vec{r} - \vec{r}')\rho(\vec{r}') \tag{2.3.1}$$

If we now make a multipole expansion of the interaction

$$V(\vec{r}_{ij}) = \sum_{\lambda} f_\lambda(r_i, r_j) P_\lambda(\cos\theta_{ij})$$

$$= \sum_{\lambda\mu} f_\lambda(r_i, r_j) \frac{4\pi}{2\lambda+1} Y_{\lambda\mu}(\theta_i) Y^*_{\lambda\mu}(\theta_j) \tag{2.3.2}$$

we obtain for the field

$$u(\vec{r}) = \sum_{\lambda\mu} u_{\lambda\mu}(\vec{r}) = \sum_{\lambda\mu} Y_{\lambda\mu}(\theta) \frac{4\pi}{2\lambda+1} \int d\vec{r}' \, f_\lambda(r, r') Y^*_{\lambda\mu}(\theta') \rho(\vec{r}') \tag{2.3.3}$$

The different multipoles in the field thus arise from the corresponding multipoles in the two-body interaction. Thus

- $\lambda = 0$ contributes to the spherical field,
- $\lambda = 1$ corresponds to a centre of mass displacement (or, if τ-dependent, to a dipole displacement of protons against neutrons),
- $\lambda = 2$ corresponds to a quadrupole deformation,
- $\lambda = 3$ corresponds to an octupole deformation, etc.

The field-producing forces, expressible in terms of a deformed field, are therefore the low multipoles of the interaction.

What about the short-range forces? A δ-force can similarly be expanded

$$\delta(\vec{r}_{ij}) = \sum_{\lambda} \delta(r_i - r_j) \frac{2\lambda+1}{2\pi r_i^2} P_\lambda(\cos\theta_{ij}) \qquad (2.3.4)$$

Thus a δ-force involves all the multipole components, with emphasis on the high multipoles.

We ought of course to work with the proper two-body interaction (assuming that we know it), but it is reasonable to suppose that a schematic force, composed of an appropriate low multipole plus a δ-force, would be a good caricature. If there is to be any point in using a schematic force it must of course be simple. For this reason we usually suppose $f_\lambda(r_i, r_j)$ to be separable, and approximate

$$V_\lambda = -\chi_\lambda \sum_{\lambda} r_i^\lambda r_j^\lambda Y_{\lambda\mu}(\theta_i) Y^*_{\lambda\mu}(\theta_j) \qquad (2.3.5)$$

and the field

$$u_\lambda(\vec{r}) = -\chi_\lambda \sum_{\mu} r^\lambda Y_{\lambda\mu}(\theta) \langle r^\lambda Y^*_{\lambda\mu} \rangle \qquad (2.3.6)$$

This particular radial dependence has very little justification. It just happens to be mathematically convenient, particularly in relating matrix elements of the field to those of the M(Eλ) operators. We believe that, for most purposes, the results are not very sensitive to the particular radial dependence.

It is also customary to replace the δ-force by a computationally simpler schematic force, namely the 'pairing force'. We have seen that

$$\langle (j)^2 J=0 \,|\, \delta(\vec{r}) \,|\, (j')^2 J=0 \rangle \gg \langle (j)^2 J\neq 0 \,|\, \delta(\vec{r}) \,|\, (j')^2 J\neq 0 \rangle \qquad (2.3.7)$$

The pairing force $\hat{G}$ is defined by

$$\langle (j)^2 J \,|\, \hat{G} \,|\, (j')^2 J' \rangle = \delta(J=J'=0) G\Omega \qquad (2.3.8)$$

This force leads to a two-particle spectrum in a $(j)^2$ configuration (Fig. 7).

The schematic force therefore becomes a sum of a pairing force plus the appropriate multipole force. For example, if we are interested in quadrupole deformations or vibrations, we use the 'pairing + P_2' force

$$V_2 = \hat{G} - \tfrac{1}{2}\chi_2 \sum_{ij}^{A} \sum_{\mu} r_i^2 r_j^2 Y_{2\mu}(\theta_i) Y^*_{2\mu}(\theta_j) \qquad (2.3.9)$$

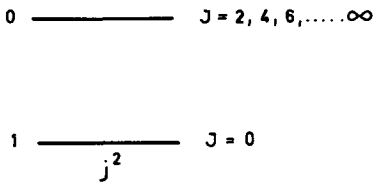

FIG. 7. Spectrum for two particles in a j^2 configuration interacting with a pairing force

2.4. Competition between the aligned and pair-coupling schemes

The equilibrium shape of the nucleus depends on which of these principle ingredients wins out. The field forces tend to align the particle orbits and create a deformed nucleus, while the short-range pairing forces scatter the particles isotropically and tend to stabilize the spherical shape.

Consider N particles in 2Ω more or less degenerate magnetic substates.

$$\text{Energy for pair coupling} \quad \sim NG\Omega/2 \qquad (G \approx 200 \text{ keV})$$

$$\text{Energy for aligned coupling} \quad \sim N(N-1)F/2$$

Since shell structure exists, which it would not do if G were of the order of the shell spacing, one finds that

$$G < F.$$

It follows therefore that the pair coupling will win out near the beginning of the shell when $N \ll \Omega$, but that when $N \gtrsim G\Omega/F$ the aligned scheme will dominate and the nucleus become deformed. According to our simple arguments this should happen before the middle of the shell when $N = \Omega$. The situation in the second half of the shell is rather similar except that

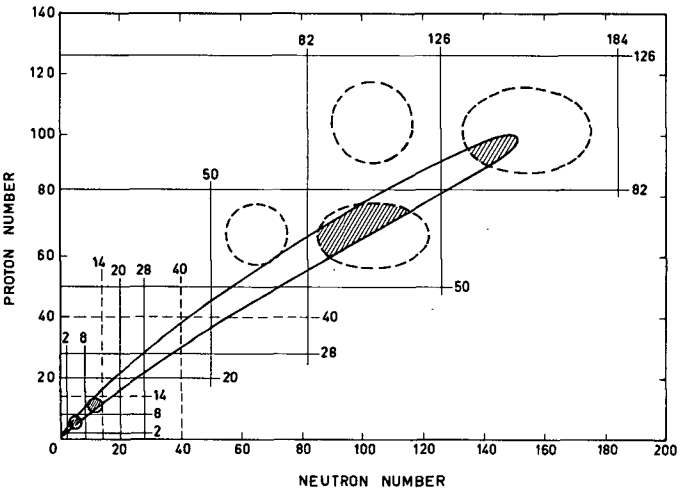

FIG. 8. Regions of the periodic table where nuclei are expected and observed to have stable equilibrium deformations. (Taken from Ref. [6], courtesy of American Institute of Physics)

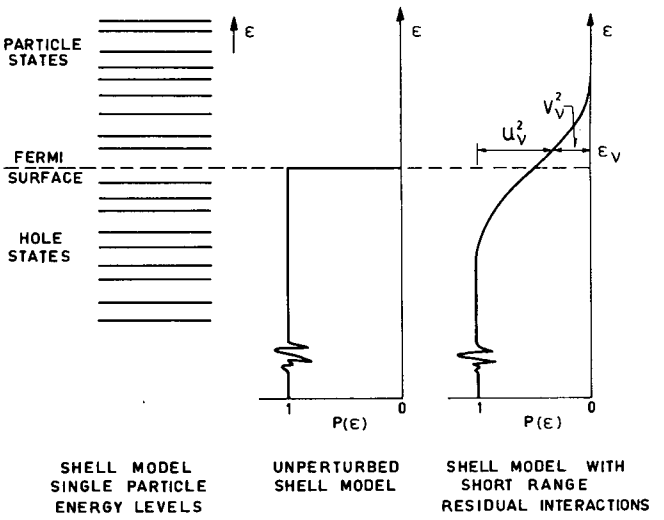

FIG. 9. Influence of the pairing force on Fermi surface

we talk of holes rather than particles. Near the middle of the shell there is a sudden flip over from the prolate to the oblate shape (i.e. the holes align their orbits along the polar axis), which diminishes until, near the end of the shell, the pairing of holes restores again the spherical shape.

In terms of the above arguments we can make a good guess as to where nuclei of large deformation should be found in the periodic table. The regions are shown in Fig. 8 and correspond well to observation.

2.5. Quasi-particles

We have found that the inclusion of the pairing force is essential for determining equilibrium shapes. It also profoundly affects the rigidity parameter for vibrations, the rotational moment of inertia, transition strengths and other observable quantities.

Unfortunately it destroys the independent particle structure which is a feature of field forces, and causes a diffuseness of the Fermi surface, as illustrated in Fig. 9. The difficulty is overcome by introducing 'independent quasi-particles', which are partly particles (with amplitude V_ν) and partly holes (with amplitude U_ν). This is a mathematical device which I shall reserve for Chapter 10. Fortunately it alters none of our development or any of the physical ideas of collective motion. I shall therefore leave out pairing in the following and just show how it modifies the results. Essentially it means going back and replacing the words 'particle' and 'hole' by 'quasi-particle', and inserting a factor V_ν or U_ν with every single-particle wave function as it appears in the role of a particle or a hole state, respectively.

II. SPHERICAL NUCLEI

3. THE COLLECTIVE VIBRATIONAL MODEL

Before embarking on a discussion of collective vibrational models, it is worthwhile to pause and ask the question: "Do we know that nuclear vibrations actually exist?" Well, what is a vibration but a periodic time-dependent oscillation of the density?

Consider the time-dependent wave function

$$\psi(t) = e^{-iE_0 t}\psi_0 + \epsilon e^{-iE_i\theta}\psi_i , \qquad (\hbar = 1)$$

for infinitesimal ϵ, where ψ_0 is the ground state and ψ_i an excited state eigenfunction of the nucleus. The density for this time-dependent wave function, unlike that for a stationary state, oscillates about the ground-state density distribution:

$$\rho(t) = \rho_0 + \epsilon\left\{\rho_{0i}\, e^{-i(E_i - E_0)t} + \text{c.c.}\right\} + O(\epsilon^2)$$

Such a density oscillation can meaningfully be described as a normal mode, since it cannot lose its energy to any other mode (i.e. $\psi(t)$ is a good time-dependent wave function for the Hamiltonian). What we have described is actually the small amplitude limit of the classical correspondence for harmonic vibrations, which we shall consider in more detail in Chapter 10.

Thus density oscillations most certainly do exist inasmuch as excited states exist. Furthermore, since the particles are indistinguishable, any mode corresponds to the summed effect of all the particles and could meaningfully be described as 'collective'. The term 'collective' is usually reserved, however, to describe a mode in which many particles contribute coherently to give a large amplitude oscillation of, for example, an electromagnetic multipole moment. The mere existence of B(E2) values of many times single-particle strength signifies unambiguously that such coherent collective motion does occur, but it need not be 100% coherent.

The question we should ask therefore is not whether collective vibrations exist, but: "What are the normal modes of oscillation of the nucleus?" This question is not so easy to answer and so we must make a guess and see how well it works.

3.1. Shape oscillations

By analogy with a liquid we suppose that the nucleus can support shape oscillations. The shape of a liquid drop, being of constant density throughout, can be defined by specifying its radius R_θ at all angles θ. By expanding R_θ in multipoles

$$R_\theta = R_0\left\{1 + \sum_{\lambda\mu} \alpha^*_{\lambda\mu} Y_{\lambda\mu}(\theta)\right\} + O(\alpha^2) \qquad (3.1.1)$$

we can specify the shape at any instant by the set of parameters $\alpha_{\lambda\mu}$.

Now nuclear density is not constant throughout (see Fig. 10). However, if we suppose that nuclear density oscillations are volume-conserving,

the above expression for R_θ can be applied to each equidensity surface. Otherwise we must parameterize in another manner.

For small amplitude oscillations we postulate a surface Hamiltonian[2]

$$H_S = \frac{1}{2}\sum_{\lambda\mu} B_\lambda |\dot{\alpha}_{\lambda\mu}|^2 + \frac{1}{2}\sum_{\lambda\mu} C_\lambda |\alpha_{\lambda\mu}|^2 \qquad (3.1.2)$$

(This is the only possible quadratic which is a scalar and invariant under time reversal.) This harmonic oscillator has the well-known classical solutions:

$$\omega_\lambda = \sqrt{\frac{C_\lambda}{B_\lambda}}, \qquad \alpha_{\lambda\mu} = \epsilon_{\lambda\mu}\cos\omega t, \qquad E = \sum_{\lambda\mu} \tfrac{1}{2}\epsilon_{\lambda\mu}^2\omega_\lambda^2 B_\lambda$$

To quantize the motion, introduce the momentum co-ordinates

$$\pi_{\lambda\mu} = \frac{\partial T}{\partial \dot{\alpha}_{\lambda\mu}} = B_\lambda \dot{\alpha}^*_{\lambda\mu} \qquad (3.1.3)$$

and the commutators

$$[\alpha_{\lambda\mu}, \pi_{\lambda\mu}] = i\hbar \qquad (3.1.4)$$

with solution

$$\pi_{\lambda\mu} = -i\hbar \frac{\partial}{\partial \alpha_{\lambda\mu}} \qquad (\text{or} \quad \alpha_{\lambda\mu} = i\hbar \frac{\partial}{\partial \pi_{\lambda\mu}}) \qquad (3.1.5)$$

---

[2] The $\alpha_{\lambda\mu}$ are complex, like the $Y_{\lambda\mu}$, but if the nuclear radius is to be real they are not independent and

$$\alpha_{\lambda-\mu} = (-1)^\mu \alpha^*_{\lambda\mu}$$

If we wish to consider independent oscillators, we must make the transformation

$$\left.\begin{aligned} \sigma_{\lambda\mu} &= \frac{1}{\sqrt{2}}(\alpha_{\lambda\mu} + \alpha^*_{\lambda\mu}) & X_{\lambda\mu} &= \frac{1}{\sqrt{2}}(Y_{\lambda\mu} + Y^*_{\lambda\mu}) \\ \sigma_{\lambda-\mu} &= \frac{i}{\sqrt{2}}(\alpha_{\lambda\mu} - \alpha^*_{\lambda\mu}) & X_{\lambda-\mu} &= \frac{i}{\sqrt{2}}(Y_{\lambda\mu} - Y^*_{\lambda\mu}) \end{aligned}\right\} \mu > 0$$

$$\sigma_{\lambda 0} = \alpha_{\lambda 0} \qquad X_{\lambda 0} = Y_{\lambda 0} \qquad \mu = 0$$

whence R_θ is given by

$$R_\theta = R_0\left\{1 + \sum_{\lambda\mu} \sigma_{\lambda\mu} X_{\lambda\mu}(\theta)\right\}$$

and the surface Hamiltonian

$$H_S = \frac{1}{2}\sum_{\lambda\mu} B_\lambda \dot{\sigma}^2_{\lambda\mu} + \frac{1}{2}\sum_{\lambda\mu} C_\lambda \sigma^2_{\lambda\mu}$$

The $\sigma_{\lambda\mu}$ are all real and independent.

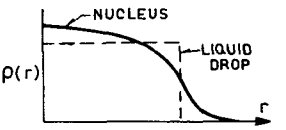

FIG.10. Nuclear density as a function of radius

Following the usual method for harmonic oscillators, we make a transformation to boson creation and destruction operators,

$$O^{\dagger}_{\lambda\mu} = \sqrt{\frac{\omega B}{2\hbar}}\left(\alpha_{\lambda\mu} - \frac{i}{\omega B}(-1)^{\mu}\pi_{\lambda-\mu}\right) \qquad \alpha_{\lambda\mu} = \sqrt{\frac{\hbar}{2\omega B}}\,(O^{\dagger}_{\lambda\mu} + (-1)^{\mu}O_{\lambda-\mu})$$

$$O_{\lambda\mu} = \sqrt{\frac{\omega B}{2\hbar}}\left((-1)^{\mu}\alpha_{\lambda-\mu} + \frac{i}{\omega B}\pi_{\lambda\mu}\right) \qquad \pi_{\lambda\mu} = i\sqrt{\frac{\hbar\omega B}{2}}\,((-1)^{\mu}O^{\dagger}_{\lambda-\mu} - O_{\lambda\mu}) \tag{3.1.6}$$

which obey the commutation relations

$$[O_{\lambda\mu}, O^{\dagger}_{\lambda\mu}] = 1 \tag{3.1.7}$$

In terms of these boson operators, the Hamiltonian becomes

$$H_S = \sum_{\lambda\mu} \hbar\omega_{\lambda}(O^{\dagger}_{\lambda\mu}O_{\lambda\mu} + \tfrac{1}{2}) \tag{3.1.8}$$

The ground-state wave function is defined by

$$O_{\lambda\mu}\,\varphi_0(\alpha) \equiv 0 \quad \text{all } \lambda\mu \tag{3.1.9}$$

and we obtain a harmonic spectrum of energy levels (Fig. 11) for each multipole mode λ, from the equation of motion

$$[H, O^{\dagger}_{\lambda\mu}] = \omega_{\lambda} O^{\dagger}_{\lambda\mu} \quad \text{all } \lambda\mu \tag{3.1.10}$$

(See Ref. [7] for a discussion of the possible spins obtainable by coupling of phonons.)

3.2. Electromagnetic transitions

Associated with these density oscillations are strong electric multipole moments. If

$$\text{charge density} \sim \text{mass density}$$

as for a uniformly charged oscillating nucleus, electric multipole moments are given by[3]

$$\mathcal{M}(E\lambda,\mu) = \frac{Ze}{A}\int r^{\lambda}Y^{*}_{\lambda\mu}(\theta)\rho_{\alpha}(\vec{r})d\vec{r}$$

$$= \frac{\lambda+3}{4\pi}\,Ze\,\langle r^{\lambda}\rangle_0\,\alpha^{*}_{\lambda\mu} + O(\alpha^2) \tag{3.2.1}$$

[3] In this equation $\rho_{\alpha}(\vec{r})$ corresponds to a wave function with a definite deformation, i.e. an eigenstate of $\alpha_{\lambda\mu}$ and not of the Hamiltonian which has a distribution in $\alpha_{\lambda\mu}$.

where $\langle r^\lambda \rangle_0$ is evaluated at zero deformation. Thus we obtain the matrix elements

$$\langle m_{\lambda\mu} | \mathcal{M}(E\lambda,\mu) | n_{\lambda\mu} \rangle = \frac{\lambda+3}{4\pi} Ze \langle r^\lambda \rangle_0 \left\{ \sqrt{\frac{\hbar n_{\lambda\mu}}{2\omega_\lambda B_\lambda}} \delta_{m,n-1} + \sqrt{\frac{\hbar(n_{\lambda\mu}+1)}{2\omega_\lambda B_\lambda}} \delta_{m,n+1} \right\} \qquad (3.2.2)$$

To leading order in α, we find the selection rule

$$\Delta n = \pm 1$$

so that cross-over transitions are forbidden. A particular transition of interest is the decay of the one-phonon state, for which[4]

$$B(E\lambda; \lambda_1 \to 0) = \left(\frac{\lambda+3}{4\pi} Ze \langle r^\lambda \rangle_0 \right)^2 \frac{\hbar}{2\omega_\lambda B_\lambda} \qquad (3.2.3)$$

A consequence of the vibrational model is that all $B(E\lambda)$'s within a band should be simple multipoles of $B(E\lambda; \lambda_1 \to 0)$ e.g.

$$B(E2; O_2, 2_2, 4_1 \to 2_1) = 2B(E2; 2_1 \to 0) \qquad (3.2.4)$$

For comparison, transition strengths can be expressed in terms of the single-particle estimate

$$B_{sp}(E2; 2_1 \to 0) = \frac{e^2}{4\pi} \langle r^2 \rangle_0$$
$$B(E2; 2_1 \to 0) = \frac{25}{4\pi} Z^2 \frac{\hbar}{2\omega_2 B_2} B_{sp}(E2; 2_1 \to 0) \qquad (3.2.5)$$

The collective enhancement factor, as shown in Fig. 1, can be anything from 10 to 50.

All other electric multipole transitions involve higher powers of α and are expected to be an order of magnitude smaller. The deformation of a uniformly charged fluid induces no magnetic moment and so the model predicts zero magnetic transitions. In fact, M1 transitions are inhibited by factors ~ 100.

3.3. The hydrodynamic collective parameters

Assuming constant nuclear density and irrotational flow, Bohr [3] has derived the mass parameter

$$B_\lambda = \frac{1}{\lambda} \cdot \frac{3}{4\pi} AMR_0^2 \qquad (3.3.1)$$

---

[4] An estimate of $\langle r^\lambda \rangle_0$ is obtained by approximating the nucleus to be of constant density and radius R_0, whence $\langle r^\lambda \rangle_0 = 3R_0^\lambda/(\lambda+3)$ and $B(E\lambda; \lambda_1 \to 0) = ((3/4\pi) ZeR_0^\lambda)^2 \hbar/2\omega_\lambda B_\lambda$

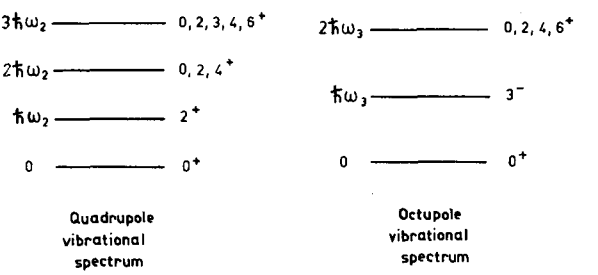

FIG. 11. Harmonic spectrum of energy levels

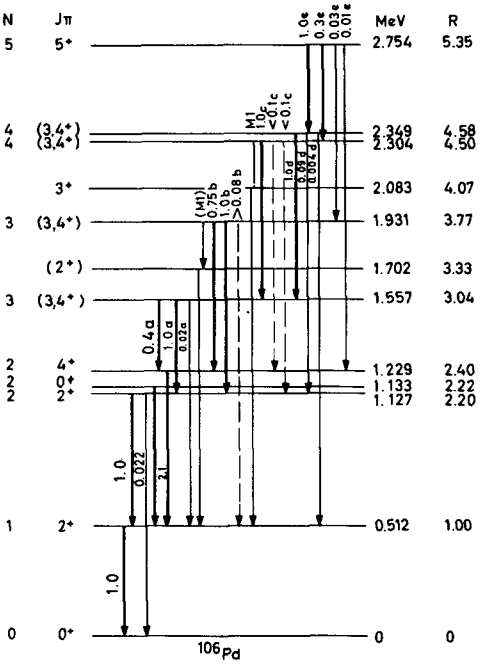

FIG. 12. Harmonic vibrational spectrum of ^{106}Pd (Taken from Ref. [4], courtesy of North-Holland Publishing Co.)

In the hydrodynamic model, the restoring force is due to surface tension opposed by the electrostatic repulsion. The restoring force parameter is:

$$C_\lambda = (\lambda-1)(\lambda+2)R_0^2 S - \frac{3}{4\pi}\,\frac{\lambda-1}{2\lambda+1}\,\frac{Z^2e^2}{R_0} \qquad (3.3.2)$$

The surface tension S is obtainable from the Weizsäcker mass formula.

3.4. Comparison with experiment

Good examples of harmonic vibrational spectra are not very numerous. One of the best examples, ^{106}Pd, is shown in Fig. 12. There are few cases

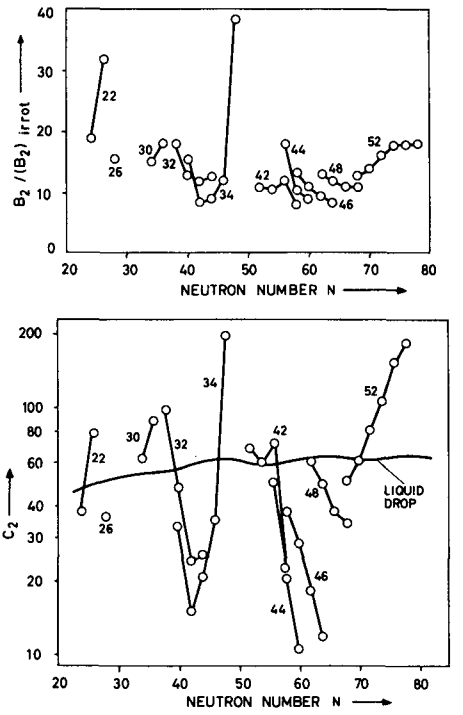

FIG. 13. Comparison of B_2 and C_2 with their hydrodynamic estimates (Taken from Ref. [8], courtesy of North-Holland Publishing Co.)

where all three members of the quadrupole triplet are observable, although there are several with two. The two-phonon states are just about in the region of the non-collective particle excitations and it would be surprising if some dilution did not take place. Even so the absence of even one state does mean a break-down, already at the two-phonon level, of at least the harmonic vibrational model.

The strongest support for the collective model is the very large strength of the systematic quadrupole and octupole states. At the same time, selection rules are frequently obeyed rather well. For instance the cross-over $2_2 \rightarrow 0$ transitions are typically a factor 1/100 down on the allowed transitions.

The ratios of transitions are just about what they should be, e.g.

$$\frac{B(E2;\ 2_2 \rightarrow 2_1)}{B(E2;\ 2_1 \rightarrow 0)} \approx 0.7 - 1.6 \qquad \frac{B(E2;\ 4_1 \rightarrow 2_1)}{B(E2;\ 2_1 \rightarrow 0)} \approx 2 \qquad (3.4.1)$$

Data for octupole spectra are rather more scarce. Generally only the first excited states are observed. This is not surprising since the two phonon states generally lie well up among a large number of non-collective states.

A comparison of B_2 and C_2, with their hydrodynamic estimates, is shown in Fig. 13. The nucleus appears to be much more 'heavy' than the hydrodynamic model would predict. Its rigidity fluctuates wildly as compared to the smoothly varying liquid drop value. This is attributable to

the local shell structure, which, as we have already shown in section 2, has a large influence on the stability of the spherical shape.

The failure of the liquid drop model to give the vibrational parameters fortunately does not destroy the collective model. It does mean, however, that the nuclear vibrations are almost certainly not irrotational flow oscillations. This interpretation is revealed clearly by a study of sum rules which we now discuss. We must therefore look for better ways of determining the vibrational parameters in terms of the particle structure.

3.5. Sum rules

Sum rules provide useful yardsticks for measuring quantitatively the degree of collectiveness of a given excited state. There are two sum rules in use, the non-energy-weighted S_{NEW} and the energy-weighted S_{EW}. S_{NEW} is defined by

$$S_{NEW}^{E\lambda} = \sum_f B(E\lambda;\ 0 \to f)$$

$$= \sum_\mu \langle 0 | \mathcal{M}^*(E\lambda;\ \mu)\, \mathcal{M}(E\lambda;\ \mu) | 0 \rangle \qquad (3.5.1)$$

The magnitude of this sum can be estimated from the shell model. Taking antisymmetry of the wave function into account via a correction factor z, we deduce

$$S_{NEW}^{E\lambda} = \sum_\mu \frac{Ze^2}{4\pi} \langle r^{2\lambda} \rangle z \qquad (3.5.2)$$

where z is expected to lie between $\frac{1}{2}$ and 1.

This sum rule includes both $\Delta T = 0$ and $\Delta T = 1$ excitations. If isobaric spin is good, it splits between the two in the ratio $Z/A : n/A$ respectively.

A typical $\Delta T = 0$ 'collective' state exhausts something like 50% of the sum, while in a few cases it more than exhausts it. The fact that this can happen reflects the model-dependence of the non-energy-weighted sum rule.

For this reason the energy-weighted sum rule is usually preferred. It is almost model-independent and therefore more reliable. It is defined by

$$S_{EW}^{E\lambda} = \sum_f (E_f - E_0)\, B(E\lambda;\ 0 \to f)$$

$$= \frac{1}{2} \sum_\mu \left\{ \langle 0 | [\mathcal{M}(E\lambda;\ \mu),\ H] \mathcal{M}^*(E\lambda;\ \mu) | 0 \rangle + \langle 0 | \mathcal{M}^*(E\lambda;\mu)\, [H,\ \mathcal{M}(E\lambda;\mu)] | 0 \rangle \right\}$$

$$= \frac{1}{2} \sum_\mu \langle 0 | [[\mathcal{M}(E\lambda;\ \mu),\ H],\ \mathcal{M}^*(E\lambda;\ \mu)] | 0 \rangle \qquad (3.5.3)$$

If the two-body interaction term in the Hamiltonian H is local, it commutes with $\mathscr{M}(E\lambda)$. Then, neglecting velocity-dependent and exchange forces, the only contribution comes from the momentum term $-(\hbar^2/2M)\sum_i \nabla_i^2$. We find

$$S_{EW}^{E\lambda} = \frac{Ze^2\hbar^2}{2M}\sum_{\mu}\langle 0|\vec{\nabla}(r^\lambda Y_{\lambda\mu}(\theta))\cdot\vec{\nabla}(r^\lambda Y_{\lambda\mu}^*(\theta))|0\rangle$$

$$= \frac{Ze^2\hbar^2}{2M}\,\frac{\lambda(2\lambda+1)^2}{4\pi}\langle r^{2\lambda-2}\rangle \qquad (3.5.4)$$

Experimentally about 10% of the $\Delta T = 0$ part of this sum is exhausted by a single low-lying collective state.

Now let us see what fraction of the energy-weighted sum rule is attributed to the vibrational state in the hydrodynamic model. For a constant density nucleus of radius R, the sum rule bcomes

$$S_{EW}^{E\lambda}(T=0) = \frac{3}{4\pi}\,\lambda(2\lambda+1)\,\frac{Z^2e^2\hbar^2}{2AM}\,R^{2\lambda-2} \qquad (3.5.5)$$

For the hydrodynamic collective state

$$\hbar\omega\, B(E\lambda;\, 0\to\lambda) = \left(\frac{3}{4\pi}\right)^2 Z^2e^2R^{2\lambda}\,\frac{\hbar^2}{2B_\lambda}(2\lambda+1)$$

$$= \frac{3}{4\pi}\,\lambda(2\lambda+1)\,\frac{Z^2e^2\hbar^2}{2AM}\,R^{2\lambda-2} \qquad (3.5.6)$$

which just exhausts the sum rule. Thus, for irrotational flow, the whole multipole strength is vested in a single normal mode, which, as experiment shows, is not the case for nuclei.

4. THE UNIFIED MODEL

Throughout the periodic table we observe many phenomena, such as ground-state spins, magnetic moments, excited states, magic numbers, etc., all of which are characteristic of independent particles and have a natural explanation in terms of the shell model. At the same time we find, among the particle-like spectra, states of undeniable collective character. These have a natural explanation in terms of the collective model.

The many-body Hamiltonian, of course, is potentially capable of describing all states but since we cannot solve it we must be content with making more and more sophisticated models to incorporate as many aspects of nuclear structure as possible. The unified model is such an attempt to bring together the shell model and the collective model into a single unified description.

The unified model was conceived in the early fifties [3] and its essential content still stands today. Furthermore, it laid the foundation for all the important advances in phenomenological vibration theory. However, present-day understanding requires us to regard it in a somewhat different light to that in which it was originally formulated.

We first of all describe its application to nuclei with zero intrinsic spin, namely the even-even nuclei, and then show how particles with spin can be coupled to a vibrational core.

4.1. Even-even nuclei

The shell-model concept is of independent particle motion in a static field. This field has a shape closely related to the nuclear density shape, so it is natural to expect it to reflect the same shape fluctuations.

Consider the shell-model Hamiltonian $H(\alpha)$, for a fixed field of deformation α. For a volume-conserving vibration of the nucleus, α is an oscillating function of time $\alpha(t)$. Now from the time-dependent wave functions $\varphi(t)$ of $H(\alpha(t))$, which obey the self-consistency requirement that their density deformations oscillate in phase with the field, we obtain the energy expectation

$$E(\alpha, \dot{\alpha}) = E_0 + \tfrac{1}{2}B\dot{\alpha}^2 + \tfrac{1}{2}C\alpha^2 + \ldots . \tag{4.1.1}$$

Thus it is apparent that the equation for free small-amplitude oscillation is

$$\alpha = \epsilon \cos \omega t, \quad \text{where} \quad \omega = \sqrt{C/B} \tag{4.1.2}$$

What we are really interested in of course is not so much the classical equation of motion as the low-energy eigenstates. Somehow then we have to quantize the motion. This is done in the Unified Model, exactly as in the collective model; that is by taking α and $\pi = B\dot{\alpha}^*$ as dynamic variables and by postulating the commutator

$$[\alpha, \pi] = i\hbar \tag{4.1.3}$$

with solution

$$\pi = -i\hbar \frac{\partial}{\partial \alpha} \tag{4.1.4}$$

$E(\alpha, \dot{\alpha})$ is then interpreted as a surface Hamiltonian and, from there on, all the results of the collective model follow.

While this quantization procedure was alright in the collective model, it is strictly incorrect in the present case. This is because α and $\dot{\alpha}$ are now really nothing more than parameters and c-numbers, detailing the shape and motion of the shell-model field. As such they are not subject to the uncertainty principle, and

$$[\alpha, \pi] = 0 \neq i\hbar \tag{4.1.5}$$

However, the approximation must clearly lead to the correct results in the classical limit when, effectively, $\hbar \to 0$. The unified model assumption is that the results remain valid generally. This is known as a semi-classical approximation. It turns out, as we shall show in Chapter 10, that, as far as the results are concerned, this approximation is justified by the classical correspondence principle.

What other approximations are implied in the model? It was originally assumed that one essential ingredient is the adiabatic approximation. It

FIG. 14. Spectrum for a coupled, but non-interacting, particle and vibrational core

was thought that the shape oscillation, to be a good approximation to a normal mode, must be slow enough to allow the particles time to adjust their orbits to the motion of the field without being excited. This picture is not correct and actually misses the secret of the model's success. Its success is due to the fact that it does not guess the normal mode of the nucleus but only the corresponding mode of the field, which is a much less stringent assumption. Thus coupling of the pure shape oscillation to the other intrinsic modes is permitted and for this very reason the unified model is superior to the irrotational flow model. The recognition of this point enables us to relax the adiabatic restriction. In fact another approximation of the unified model, namely that the oscillating nucleus has at each instant an independent particle wave function, actually breaks down in the adiabatic limit.

So far we have discussed a basis for extracting the collective parameters from the shell model, but we have not discussed the ultimate marriage of the collective and shell models in terms of a unified wave function. This we shall not do since the old unified model wave function is basically incorrect, for the following reasons:

(a) It employs the adiabatic approximation, which does not do justice to the more general applicability of the model;
(b) It makes a distinction between the collective and the particle degrees of freedom by employing redundant collective co-ordinates, which is unnecessary;
(c) The extra collective co-ordinate is a classical variable and its use in the unified model wave function is not justified by the correspondence principle.

Fortunately, since the unified model provides us directly with energy levels and transition probabilities, the derivation of the wave function is something of a luxury that we can manage without. As we shall see in Chapter 10, the wave function does not readily emerge even in a microscopic treatment.

4.2. Odd nuclei

If the nucleus has non-zero intrinsic spin, as in odd or odd-odd nuclei (or even excited states of even-even), then we have to couple this intrinsic spin j to the vibrational angular momentum λ to give total spin J.

$$\vec{J} = \vec{\lambda} + \vec{j} \tag{4.2.1}$$

In the absence of interactions we get the vibrational spectrum of Fig. 14. The only effect on transition strengths is through geometric factors. Thus for transitions involving a change in the vibrational phonon number $\Delta n_\lambda = 1$,

$$\begin{aligned} B(E\lambda;\ J_1 \to J_0) &= B(E\lambda;\ \lambda_1 \to 0_0) \\ B(E\lambda;\ J_0 \to J_1) &= \frac{(2J_1+1)}{(2J_0+1)(2\lambda+1)}\, B(E\lambda;\ 0_0 \to \lambda_1) \end{aligned} \tag{4.2.2}$$

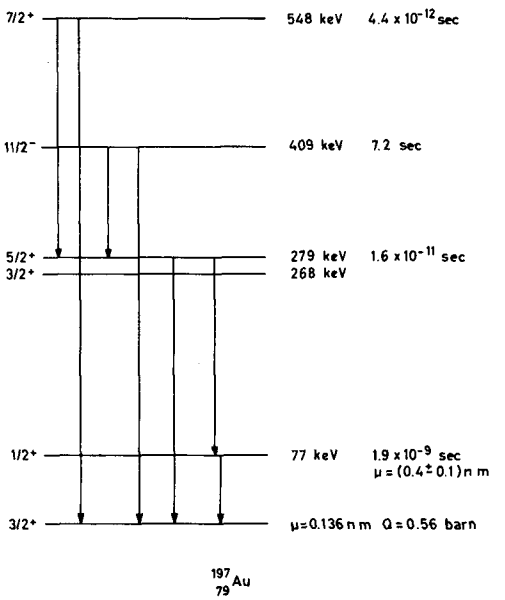

FIG. 15. Weak coupling of a $d_{3/2}$ proton to a $^{196}_{78}Pt$ core. All electromagnetic data are fitted well with wave functions which are $\gtrsim$ 96% particle x core (Taken from Ref. [9], courtesy of North-Holland Publishing Co.)

Note that transitions involving a change in the vibrational part of the wave function $\Delta n = 1$ simultaneously with a change in the intrinsic spin $j \to j'$, are forbidden.

Generally there will be interactions which split the degeneracies. Let us consider for example an odd particle coupled to a vibrational core (Fig. 15). The particle-vibration coupling arises from the vibrational shape fluctuations of the potential well in which the odd particle is moving.

For small deformations, equipotential surfaces of the potential $u_\alpha(\vec{r})$ are given by

$$r_\theta = r\left[1 + \sum_{\lambda\mu} \alpha^*_{\lambda\mu} Y_{\lambda\mu}(\theta)\right] \tag{4.2.3}$$

for constant r. In other words,

$$u_\alpha(r_\theta, \theta) = u_0(r) \quad \text{(see Fig. 16)} \tag{4.2.4}$$

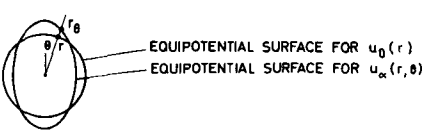

FIG. 16. Equipotential surfaces for $u_0(r)$ and $u_\alpha(r, \theta)$

Conversely

$$u_\alpha(r,\theta) = u_0\left(\frac{r}{1+\sum_{\lambda\mu}\alpha^*_{\lambda\mu}Y_{\lambda\mu}(\theta)}\right) \tag{4.2.5}$$

Expanding

$$u_\alpha(r,\theta) = u_0(r) - r\,\frac{du_0(r)}{dr}\sum\alpha^*_{\lambda\mu}Y_{\lambda\mu}(\theta) + O(\alpha^2) \tag{4.2.6}$$

Thus the particle-vibration interaction H_{int} is

$$H_{int} = -k(r)\sum\alpha^*_{\lambda\mu}Y_{\lambda\mu}(\theta) \tag{4.2.7}$$

where

$$k(r) = r\,\frac{du_0(r)}{dr} \tag{4.2.8}$$

Consider first the weak coupling limit, when we can use perturbation theory. The unperturbed ground-state wave function is

$$|(n_\lambda = 0, j)jm\rangle = \Psi_0(n_\lambda = 0)\varphi_{jm} \tag{4.2.9}$$

In first order, this couples to configurations

$$|(n_\lambda = 1, j')jm\rangle = \sum_{m'(\mu)}(j'\lambda m'\mu|jm)\Psi_{\lambda\mu}(n_\lambda = 1)\varphi_{j'm'} \tag{4.2.10}$$

The matrix element for H_{int} between these states, $\beta(n_\lambda = 1, j')$, is given by

$$\begin{aligned}\beta(n_\lambda = 1, j') &= \langle(n_\lambda = 1, j')jm|H_{int}|(n_\lambda = 0, j)jm\rangle \\ &= -(-1)^{j'-j}\sqrt{\frac{2j'+1}{2j+1}}\,(j'||k(r)Y_\lambda||j)\sqrt{\frac{\hbar}{2\omega_\lambda B_\lambda}}\end{aligned} \tag{4.2.11}$$

Using first-order perturbation theory, the perturbed wave function becomes

$$|jm\rangle = |(n_\lambda = 0, j)jm\rangle - \sum_{j'}\frac{\beta(n_\lambda = 1, j')}{\hbar\omega_\lambda + \epsilon_{j'} - \epsilon_j}|(n_\lambda = 1, j')jm\rangle \tag{4.2.12}$$

where ϵ_j is the unperturbed single-particle energy.

As an example of the effect this mixing has on the properties of the single-particle spectrum, let us consider the ground state quadrupole

moment

$$Q = \sqrt{\frac{16\pi}{5}} \langle jj | \mathcal{M}(E2,0) | jj \rangle \qquad (4.2.13)$$

The quadrupole operator $\mathcal{M}(E2,0)$ can be expressed (see section 3.2)

$$\mathcal{M}(E2,0) = \frac{5}{4\pi} Ze \langle r^2 \rangle_0 \alpha_{20} + e_p r^2 Y_{20}(\theta) \qquad (4.2.14)$$

and has a contribution from the core and from the odd particle.

Taking them separately, the particle contribution is

$$Q_p = e_p \sqrt{\frac{16\pi}{5}} (j\,2\,j\,0|jj) \langle j||r^2 Y_2||j\rangle \qquad \Delta n = 0 \qquad (4.2.15)$$

and the core contribution

$$Q_{\text{core}} = e \sqrt{\frac{16\pi}{5}} \frac{5}{4\pi} Z \langle r^2 \rangle_0 \frac{1}{C_2} (j\,2\,j\,0|jj) \langle j||k(r) Y_2||j\rangle \qquad \Delta n = 1 \qquad (4.2.16)$$

If the $\Delta n = 1$ contribution of the core is incorporated into the quadrupole moment of the odd particle by the use of an effective change, as is common in shell-model calculations, then the unified model prediction for this effective charge is

$$e_{\text{eff}}^{(2)} = e_p + e \frac{5}{4\pi} Z \langle r^2 \rangle_0 \frac{1}{C_2} \frac{(j||k(r) Y_2||j)}{(j||r^2 Y_2||j)} \qquad (4.2.17)$$

The contribution of the core to the static quadrupole moment implies that it is polarized by the odd particle. If this polarization becomes large the above weak coupling perturbation treatment is no longer valid. This will depend essentially on the magnitude of the parameter

$$\kappa = \frac{k}{\omega \sqrt{\omega B}} = \frac{k}{\sqrt{\omega C}} \qquad (4.2.18)$$

where k is an average value of k(r) over the nuclear volume. Physically one can see what happens as this parameter increases. It becomes large because the vibrational state, in the neighbouring even-even nucleus, is falling and because the rigidity of the nucleus against deformation is decreasing. It is apparent that this situation occurs in the transition region when the nucleus is about to acquire a large permanent deformation.

In the strong coupling limit, when the nucleus acquires a large permanent deformation, the problem again simplifies. One can then consider first the relatively fast motion of the odd nucleon in a deformed field and subsequently the slower vibrations and rotations of the entire system. We shall discuss this limit in connection with rotations.

In the intermediate region one has either to diagonalize the particle-vibration interaction in the product configuration space of unperturbed particle and core wave functions, or give up the collective model description, which is probably more realistic.

5. THE ADIABATIC MODEL

This is not really a new model in its own right but merely an approximate execution of the unified model prescription for determining the collective vibrational parameters. The method is to determine the energy increments, associated with small shape deformation and slow oscillation of the nucleus, in adiabatic perturbation theory.

5.1. The restoring force parameter

According to the Unified Model, we must seek the self-consistent solutions for the nuclear wave function in a deformed shell-model field. For a general small deformation, the deformed shell-model Hamiltonian is, to leading order,

$$H(\alpha) = H_0 - k(r) \sum \alpha^*_{\lambda\mu} Y_{\lambda\mu}(\theta) \qquad (5.1.1)$$

Let us restrict consideration to a single independent mode of deformation so that (see section 3.1)

$$H(\alpha) = H_0 - \frac{\alpha_{\lambda\mu} + \alpha^*_{\lambda\mu}}{\sqrt{2}} k(r) \frac{Y_{\lambda\mu}(\theta) + Y^*_{\lambda\mu}(\theta)}{\sqrt{2}} \quad (\mu > 0) \qquad (5.1.2)$$

The deformation field has therefore a form proportional to $\hat{Q}(\vec{r})$ where

$$\hat{Q}(\vec{r}) \propto k(r)\,(Y_{\lambda\mu}(\theta) + Y^*_{\lambda\mu}(\theta)) \qquad (5.1.3)$$

and a magnitude proportional to

$$(\alpha_{\lambda\mu} + \alpha^*_{\lambda\mu}) \propto \langle \psi(Q) | \hat{Q}(\vec{r}) | \psi(Q) \rangle \equiv Q \qquad (5.1.4)$$

where $\psi(Q)$ is a self-consistent solution of $H(\alpha)$. The Hamiltonian $H(\alpha)$ can therefore be written in the form

$$H(Q) = H_0 - \chi Q \hat{Q}(\vec{r}) \qquad (5.1.5)$$

which more readily expresses its self-consistent nature. χ is a coupling constant depending on the relative normalization of $\hat{Q}(\vec{r})$ and $k(r)$. Given this it is readily calculable[5].

The self-consistent solution $\psi(Q)$ of $H(Q)$, for a specified value of the field deformation, is that solution for which the density deformation

---

[5] This expression for H(Q) also follows directly from considering the single-particle field associated with the schematic residual two-body interaction.

$$V_{res} = -\frac{1}{2} \chi \sum_{ij}{}' \hat{Q}(\vec{r}_i)\, \hat{Q}(\vec{r}_j)$$

(cf. section 2.3), and neglecting exchange terms. But then the coupling constant χ does not appear naturally with any particular value.

is also Q. It is thus subject to the constraint

$$Q = \langle \psi(Q) | \hat{Q} | \psi(Q) \rangle \tag{5.1.6}$$

and is consequently an eigenstate of H'(Q), where

$$H'(Q) = H(Q) - \mu \hat{Q}(\vec{r}) = H_0 - (\mu + \chi Q)\hat{Q}(\vec{r}) \tag{5.1.7}$$

and μ is a Lagrangian multiplier. Physically, the extra term is the force that must be applied to maintain the nuclear deformation.

For small deformations we can write

$$\psi(Q) = |\rangle + \sum_i c_i |i\rangle \tag{5.1.8}$$

where $|\rangle$ is the ground state and $|i\rangle$ excited eigenstates of H_0. Using first-order perturbation theory,

$$c_i = (\mu + \chi Q)\frac{\langle i|\hat{Q}|\rangle}{E_i - E_0} \tag{5.1.9}$$

The self-consistency equation for μ is now

$$\langle \psi(Q)|\hat{Q}|\psi(Q)\rangle = 2(\mu + \chi Q)\sum \frac{|\langle i|\hat{Q}|\rangle|^2}{E_i - E_0} = Q \tag{5.1.10}$$

To determine the restoring force parameter C, we evaluate the energy increment

$$E(Q) = \langle H_0 \rangle - \tfrac{1}{2}\chi Q^2 \tag{5.1.11}$$

(the factor $\frac{1}{2}$ is to avoid counting two-body interactions twice), and equate

$$E(Q) = E_0 + \tfrac{1}{2} C Q^2 \tag{5.1.12}$$

We get

$$E(Q) = E_0 + \sum_i |C_i|^2 (E_i - E_0) - \tfrac{1}{2}\chi Q^2$$

$$= E_0 + (\mu + \chi Q)^2 \sum_i \frac{|\langle i|\hat{Q}|\rangle|^2}{E_i - E_0} - \tfrac{1}{2}\chi Q^2$$

$$= E_0 + \frac{1}{4}\left\{\sum_i \frac{|\langle i|\hat{Q}|\rangle|^2}{E_i - E_0}\right\}^{-1} Q^2 - \tfrac{1}{2}\chi Q^2 \tag{5.1.13}$$

and hence

$$C = \frac{1}{2}\left\{\sum_i \frac{|\langle i|\hat{Q}|\rangle|^2}{E_i - E_0}\right\}^{-1} - \chi \tag{5.1.14}$$

The first term is the unperturbed shell-model contribution and the second is the reduction due to the residual field interactions.

5.2. The mass parameter

To determine the mass parameter, we must consider the time-dependent wave function for the Hamiltonian

$$H(Q(t)) = H_0 - (\mu(t) + \chi Q(t))\,\hat{Q}(\vec{r}) \tag{5.2.1}$$

For small $Q(t)$ and $\dot{Q}(t)$ we can write

$$\psi(Q(t)) = e^{-iE_0 t/\hbar}\left\{|\,\rangle + \sum C_i(t)\,|i\,\rangle\right\} \tag{5.2.2}$$

where the $C_i(t)$ are given by first-order time-dependent perturbation theory:

$$C_i(t) = \frac{1}{E_i - E_0 - i\hbar\frac{\partial}{\partial t}}\,(\mu(t) + \chi Q(t))\langle i|\hat{Q}|\,\rangle \tag{5.2.3}$$

In the adiabatic limit

$$C_i(t) = (\mu(t) + \chi Q(t))\frac{\langle i|\hat{Q}|\,\rangle}{E_i - E_0} + i\hbar(\dot{\mu}(t) + \chi\dot{Q}(t))\frac{\langle i|\hat{Q}|\,\rangle}{(E_i - E_0)^2} \tag{5.2.4}$$

The self-consistency equation for $\mu(t)$ is

$$\begin{aligned} Q(t) &= \langle \psi(Q(t))\,|\hat{Q}|\,\psi(Q(t))\,\rangle \\ &= (\mu(t) + \chi Q(t))\sum_i \frac{|\langle i|\hat{Q}|\,\rangle|^2}{E_i - E_0} + i\hbar(\dot{\mu}(t) + \chi\dot{Q}(t))\sum_i \frac{|\langle i|\hat{Q}|\,\rangle|^2}{(E_i - E_0)^2} + \text{c.c.} \end{aligned} \tag{5.2.5}$$

For real density oscillations ($\hat{Q}$ is already real), the last term is purely imaginary and hence vanishes, so that as before

$$2(\mu(t) + \chi Q(t)\sum_i \frac{|\langle i|\hat{Q}|\,\rangle|^2}{E_i - E_0} = Q(t) \tag{5.2.6}$$

Consider the expectation of the energy at $\mu(t) = Q(t) = 0$

$$\begin{aligned} E(\dot{Q}) &= E_0 + \sum_i |C_i|^2 (E_i - E_0) \\ &= E_0 + \hbar^2(\dot{\mu}(t) + \chi\dot{Q}(t))^2 \sum_i \frac{|\langle i|\hat{Q}|\,\rangle|^2}{(E_i - E_0)^3} \end{aligned} \tag{5.2.7}$$

Equating

$$E(\dot{Q}) = E_0 + \tfrac{1}{2}B\dot{Q}^2 \tag{5.2.8}$$

we obtain[6]

$$B = \frac{\hbar^2}{2}\left\{\sum_i \frac{|\langle i|\hat{Q}|\rangle|^2}{E_i - E_0}\right\}^{-2} \sum_i \frac{|\langle i|\hat{Q}|\rangle|^2}{(E_i - E_0)^3} \tag{5.2.9}$$

5.3. The vibrational spectrum and transition probabilities

The vibrational spectrum is obtained by treating Q and $\dot{Q}$ as vibrational co-ordinates in a collective Hamiltonian

$$H_{vib} = \tfrac{1}{2}B\dot{Q}^2 + \tfrac{1}{2}CQ^2 \tag{5.3.1}$$

according to the Unified Model. This gives a harmonic spectrum of energy levels of spacing $\hbar\omega$, where

$$\omega = \sqrt{C/B} \tag{5.3.2}$$

Transition probabilities are deduced by relating the Eλ-multipole operator to Q, as we did in section 3.2 for the deformation parameters

---

[6] This method is equivalent to the Inglis cranking model and the results are identical. The cranking model expression is

$$B = 2\hbar^2 \sum_i \frac{|\langle i|\partial/\partial Q|\rangle|^2}{E_i - E_0}$$

where

$$\frac{\partial}{\partial Q}|\rangle \equiv \frac{\partial \psi(Q)}{\partial Q}\bigg|_{Q=0}$$

Consider

$$\langle i|\frac{\partial H'}{\partial Q}|\rangle = \langle i|\frac{\partial}{\partial Q}H'|\rangle - \langle i|H'\frac{\partial}{\partial Q}|\rangle$$

$$= -(E_i - E_0)\langle i|\frac{\partial}{\partial Q}|\rangle$$

Therefore

$$\langle i|\frac{\partial}{\partial Q}|\rangle = \left(\frac{\partial \mu}{\partial Q} + \chi\right)\frac{\langle i|\hat{Q}|\rangle}{E_i - E_0}$$

and

$$\frac{1}{2}B\dot{Q}^2 = \hbar^2\dot{Q}^2\sum_i \frac{|\langle i|\partial/\partial Q|\rangle|^2}{E_i - E_0} = \hbar^2(\dot{\mu} + \chi\dot{Q})^2 \sum \frac{|\langle i|\hat{Q}|\rangle|^2}{(E_i - E_0)^3}$$

which is identical to our expression.

$\alpha_{\lambda\mu}$, and using the formula

$$\langle 0|Q|1\rangle = \sqrt{\frac{\hbar}{2\omega B}} \tag{5.3.3}$$

where $|0\rangle$ is the vibrational ground state and $|1\rangle$ the one phonon state. To do this we need to know the radial dependence of $\hat{Q}(\vec{r})$. Now it is usually considered that the radial form of $\hat{Q}(\vec{r})$ is not very important, provided it has no nodes and gives most weight to the surface region. For convenience in calculating transition probabilities one therefore frequently puts it equal to r^λ, i.e.

$$\hat{Q}(\vec{r}) \to r^\lambda . \frac{Y_{\lambda\mu}(\theta) + Y^*_{\lambda\mu}(\theta)}{\sqrt{2}} \tag{5.3.4}$$

in which case

$$B(E\lambda;\ \lambda_1 \to 0_0) = \frac{\hbar}{2\omega B}\ e^2_{eff} \tag{5.3.5}$$

This approximation is equivalent to using a schematic P_λ two-body interaction (see section 2.3).

e_{eff} is the average effective charge of the contributing particles. In practice this effective charge will differ from the real charge for the following reason. To make a calculation feasible it is customary to treat the closed shell core as inert and consider only a limited number of unperturbed configurations $|i\rangle$ for the extra-core particles. The effect of core polarization and of neglected configurations on the transitions are then taken into account by the use of an effective charge, as discussed in section 4.2 for a single odd particle.

Similarly we can expect more realistic results by using an effective two-body interaction. For this reason the coupling constant χ is often treated as a fitting parameter rather than given its theoretical value.

5.4. Effect of short-range pairing forces

In the above treatment we have suggested that H_0 should be the unperturbed shell-model Hamiltonian. This means a ground-state wave function with a sharp Fermi surface, corresponding to single-particle states being either fully occupied or completely empty. An excited state $|i\rangle$ is correspondingly a pure 'particle-hole' state, of the form

$$|i\rangle = |(\nu'_h)^{-1}\nu_p\rangle$$

or as shown diagrammatically in Fig. 17.
The matrix elements that occur have the simple expression

$$\langle i|\hat{Q}|\rangle = \langle \nu_p|\hat{Q}|\nu'_h\rangle \tag{5.4.1}$$

If the short-range residual interactions are taken into account, the Fermi surface becomes smeared out (cf. section 2.5) and a given single-particle state ν becomes occupied with probability amplitude v_ν and un-

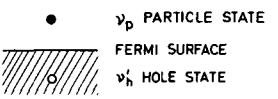

FIG.17. A particle-hole state shown diagrammatically

occupied with amplitude u_ν. It is natural to suppose therefore that, in generalizing matrix elements to include short-range interactions, one should associate with every single-particle state ν the factor u_ν or v_ν as it appears in the role of a particle or a hole state, respectively. Thus

$$\langle i|\hat{Q}|\rangle \rightarrow \langle \nu|\hat{Q}|\nu'\rangle u_\nu v_{\nu'} + \langle \bar{\nu}'|\hat{Q}|\bar{\nu}\rangle u_{\nu'} v_\nu$$

$$= \langle \nu|\hat{Q}|\nu'\rangle (u_\nu v_{\nu'} \pm u_{\nu'} v_\nu) \qquad (5.4.2)$$

with the $\pm$ sign depending on whether $\hat{Q}$ is +ve or −ve under time reversal, respectively. In the present case, for real density oscillations, we always define $\hat{Q}$ to be +ve under time reversal.

Similarly it is natural to make the generalization

$$E_i - E_0 = \epsilon_\nu - \epsilon_{\nu'} \quad \text{(unperturbed shell model)}$$

$$\rightarrow E_\nu + E_{\nu'} \quad \text{(shell model + residual interactions)} \qquad (5.4.3)$$

where the E_ν are particle-binding energies measured with respect to the chemical potential.

Thus we obtain the formulae

$$C = \frac{1}{2}\left\{\sum_{\nu\nu'} \frac{|\langle \nu|\hat{Q}|\nu'\rangle|^2 (u_\nu v_{\nu'} + u_{\nu'} v_\nu)^2}{E_\nu + E_{\nu'}}\right\}^{-1} - \chi \qquad (5.4.4)$$

$$B = \frac{\hbar^2}{2}\left\{\sum_{\nu\nu'} \frac{|\langle \nu|\hat{Q}|\nu'\rangle|^2 (u_\nu v_{\nu'} + u_{\nu'} v_\nu)^2}{E_\nu + E_{\nu'}}\right\}^{-2} \sum_{\nu\nu'} \frac{|\langle \nu|\hat{Q}|\nu'\rangle|^2 (u_\nu v_{\nu'} + u_{\nu'} v_\nu)^2}{(E_\nu + E_{\nu'})^3}$$

The above results are in fact just what one derives from BCS theory, when the states ν are described as quasi-particle states due to their dual role of being partly particle and partly hole states.

5.5. Comparison with experiment

A number of calculations based on the above adiabatic model have been carried out; notably by Kisslinger and Sørensen [10] for spherical nuclei, and by Bès [11] and Bès and Szymanski [12] for deformed nuclei. By way of illustration a small sample of some of Kisslinger and Sørensen's results are shown in Fig. 18, namely their fits to the quadrupole vibrational 2^+ states of the Sn and Pb isotopes. Their fits to the B(E2) values for excitation of the same states are given in Table I.

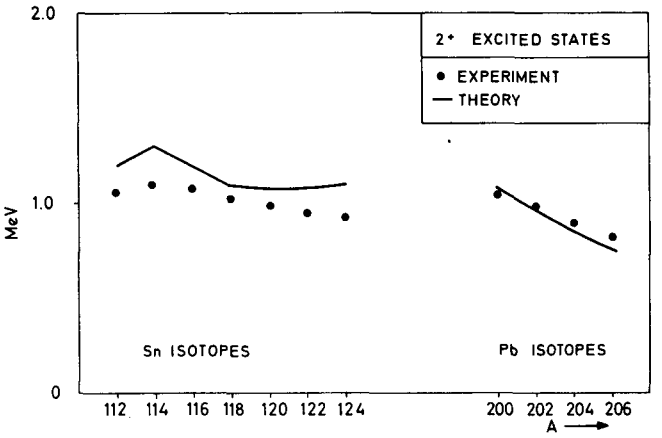

FIG. 18. A sample of Kisslinger and Sørensen's results (Taken from Ref. [10], courtesy of Matematisk-fisiske Meddelelser)

TABLE I. FITS TO THE B(E2) VALUES FOR THE EXCITATION OF 2^+ STATES

Isotope	$B(E2)_{theor.}$ $e^2 \times 10^{-48}$ cm^4	$B(E2)_{exp.}$ $e^2 \times 10^{-48}$ cm^4	$\frac{B(E2)_{exp.}}{B(E2)_{s.p.}}$
^{112}Sn	0.25	0.18	11
^{114}Sn	0.20	0.20	11
^{116}Sn	0.26	0.21	12
^{118}Sn	0.29	0.23	13
^{120}Sn	0.28	0.22	13
^{122}Sn	0.25	0.25	14
^{124}Sn	0.20	0.21	12
^{200}Pb	0.33	-	-
^{202}Pb	0.29	-	-
^{204}Pb	0.22	0.17	5
^{206}Pb	0.13	0.13	4

5.6. The possibility of going to higher order

The possibility of going beyond first-order perturbation theory, to derive higher-order anharmonic correction terms to the vibrational Hamiltonian, is an attractive one. But it is not without danger.

The principle of the model (and of the Unified Model on which it is based) is to feel out the shape of the energy surface as a function of α

and $\dot{\alpha}$ (or Q and $\dot{Q}$ or whatever parameters one chooses to define the nuclear shape). Ideally one would like to probe the energy surface out to regions of α and $\dot{\alpha}$ comparable with their zero point amplitudes in the vibrational ground state[7]. Now to probe out the energy surface one really needs a δ-function in both α and in its conjugate co-ordinate $\pi = \dot{\alpha}/B$ or at least something with a spread in α and π which is small, compared with the zero point amplitude of these co-ordinates, in the vibrational ground state. The zero point amplitudes are in fact given by

$$\langle 0|\alpha^2|0\rangle = \frac{\hbar}{2\omega B}, \qquad \langle 0|\pi^2|0\rangle = \frac{\hbar\omega B}{2} \tag{5.6.1}$$

The best probe that quantum mechanics allows us is therefore the state for which

$$\frac{\alpha^2}{\langle 0|\alpha^2|0\rangle} + \frac{\pi^2}{\langle 0|\pi^2|0\rangle} = \frac{4}{\hbar\omega}\left\{\frac{1}{2B}\pi^2 + \frac{C}{2}\alpha^2\right\} \tag{5.6.2}$$

is a minimum. This is clearly the vibrational ground state itself, which does not fulfil the requirement of being a sharp probe.

What then do we actually measure when we use a blunt probe with a probability distribution $\rho(\alpha)$? Consider just the potential energy surface ($\dot{\alpha} = 0$). We want to find the various derivatives of $H(\alpha)$ at the origin

$$H(\alpha) = H(0) + \alpha\frac{\partial H}{\partial\alpha}\bigg|_{\alpha=0} + \tfrac{1}{2}\alpha^2\frac{\partial^2 H}{\partial\alpha^2}\bigg|_{\alpha=0} + \ldots \tag{5.6.3}$$

What we measure when we take an energy expectation of the nucleus, displaced a distance x in α, is

$$\int \rho(\alpha - x)H(\alpha)d\alpha = \int \rho(\alpha)H(\alpha + x)d\alpha$$

$$= \int \rho(\alpha)H(\alpha)d\alpha + x\int \rho(\alpha)\frac{\partial H(\alpha)}{\partial\alpha}\,d\alpha + \tfrac{1}{2}x^2\int \rho(\alpha)\frac{\partial^2 H(\alpha)}{d\alpha^2}\,d\alpha + \ldots \tag{5.6.4}$$

The coefficients of the different powers of x that we determine are thus not the derivatives at the origin but their mean values taken over $\rho(\alpha)$. If these derivatives are constant over the range, as for example if the potential energy surface is purely harmonic, we get the correct answer. If we are looking for anharmonic terms, however, we will not get quite what we expect.

It might nevertheless be possible to make the necessary corrections, provided the energy surface is reasonably smooth. We could determine

$$\langle H(\alpha + x)\rangle = H(x) + \frac{\partial H(x)}{\partial x}\langle\alpha\rangle + \frac{1}{2}\frac{\partial^2 H(x)}{dx^2}\langle\alpha^2\rangle + \ldots \tag{5.6.5}$$

and hence its derivatives

$$\frac{\partial}{\partial x}\langle H(\alpha + x)\rangle = \frac{\partial H(x)}{\partial x} + \frac{\partial^2 H(x)}{\partial x^2}\langle\alpha\rangle + \frac{1}{2}\frac{\partial^2 H(x)}{\partial x^3}\langle\alpha^2\rangle + \ldots \tag{5.6.6}$$

[7] For such large amplitudes, perturbation theory diverges but one could use other methods.

Then, if we know $\rho(\alpha)$ and can calculate $\langle \alpha \rangle$, $\langle \alpha^2 \rangle$ etc., it is possible that the above equations could be inverted to give H(x) and its derivatives.

6. THE VIBRATING POTENTIAL MODEL

Besides trying to extend the treatment beyond first-order perturbation theory, we might try to remove the adiabatic approximation. In the adiabatic model terms of order $\hbar\omega/(E_i - E_0)$ are neglected, which may well be as large as 0.5 or even larger. In the VPM no such terms are neglected.

6.1. A dispersion equation for the frequency

We now look for free oscillations of the nucleus as opposed to forced adiabatic oscillations. Consequently we can dispense with the Lagrangian multipliers. The self-consistency condition, that the field and the density should oscillate in phase, determines the natural frequencies of the motion.

The oscillating shell-model Hamiltonian is

$$H(t) = H_0 - \chi Q(t)\hat{Q} \tag{6.1.1}$$

Again we write

$$\psi(t) = e^{-iE_0 t}\left\{|\,\rangle + \sum_{i\neq 0} C_i(t)|\,i\rangle\right\} \tag{6.1.2}$$

Expanding

$$Q(t) = \delta \cos\omega t = \tfrac{1}{2}(e^{-i\omega t} + e^{i\omega t}) \tag{6.1.3}$$

and using first-order time-dependent perturbation theory, but without the adiabatic approximation, we get

$$C_i(t) = \tfrac{1}{2}\chi\epsilon \langle i|\hat{Q}|\,\rangle \left\{\frac{e^{-i\omega t}}{E_i - E_0 - \hbar\omega} + \frac{e^{i\omega t}}{E_i - E_0 + \hbar\omega}\right\}$$

$$= \chi e \langle i|\hat{Q}|\,\rangle \frac{(E_i - E_0)\cos\omega t - i\hbar\omega \sin\omega t}{(E_i - E_0)^2 - (\hbar\omega)^2} \tag{6.1.4}$$

The self-consistency condition

$$\langle \hat{Q} \rangle = Q(t) \tag{6.1.5}$$

gives the eigenfrequency equation

$$2\chi\epsilon \sum_i \frac{|\langle i|\hat{Q}|\,\rangle|^2 (E_i - E_0)\cos\omega t}{(E_i - E_0)^2 - (\hbar\omega)^2} = Q(t) \tag{6.1.6}$$

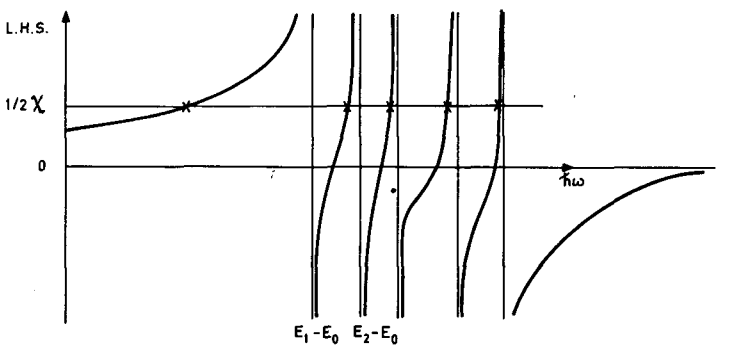

FIG. 19. Graphical solution of the VPM dispersion equation

or

$$\sum_i \frac{|\langle i|\hat{Q}|\rangle|^2(E_i - E_0)}{(E_i - E_0)^2 - (\hbar\omega)^2} = \frac{1}{2\chi} \qquad (6.1.7)$$

The solutions of this dispersion equation for ω are the possible frequencies at which the nucleus can oscillate self-consistently.

This equation is readily solved graphically, as illustrated in Fig. 19. For zero coupling, $\chi = 0$, we get the unperturbed shell-model excitations as we ought to. As the coupling is turned on one state drops a long way below the rest and may be identified with the so-called vibrational state. It is this solution which is given less accurately in the adiabatic model.

6.2. The vibrational parameters

The mass parameter and restoring force parameter, associated with a shape oscillation, are again derived by considering the expectation of the energy.

$$\langle H\rangle = E_0 + \sum |C_i(t)|^2(E_i - E_0) - \tfrac{1}{2}\chi Q^2(t)$$

$$= E_0 + \chi^2\epsilon^2 \sum_i \frac{|\langle i|\hat{Q}|\rangle|^2\{(E_i - E_0)^2\cos^2\omega t\, t(\hbar\omega)^2\sin^2\omega t\}(E_i - E_0)}{[(E_i - E_0)^2 - (\hbar\omega)^2]^2} - \tfrac{1}{2}\chi Q^2(t)$$

$$= E_0 + \chi^2\epsilon^2(\hbar\omega)^2 \sum_i \frac{|\langle i|\hat{Q}|\rangle|^2(E_i - E_0)}{[(E_i - E_0)^2 - (\hbar\omega)^2]^2} \qquad (6.2.1)$$

Thus equating

$$\langle H\rangle = E_0 + \tfrac{1}{2}\epsilon^2\omega^2 B(\omega) \qquad (6.2.2)$$

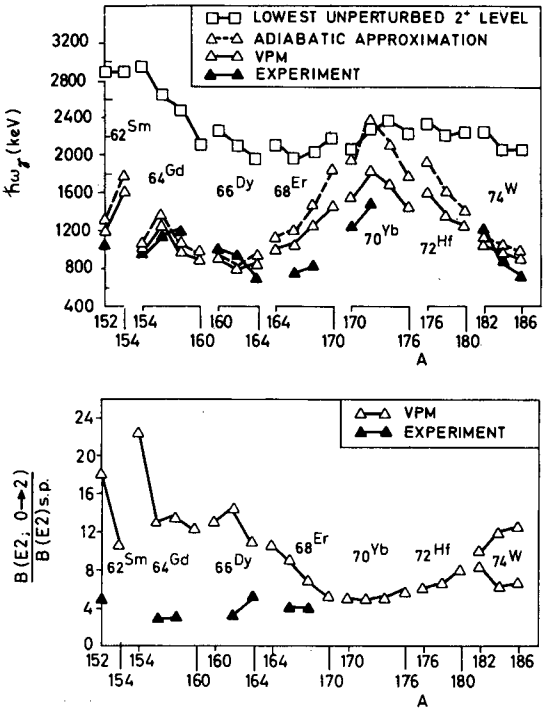

FIG. 20. Results of some VPM calculations by Marshalek and Rasmussen (Taken from Ref. [13], courtesy of North-Holland Publishing Co.)

we obtain

$$B(\omega) = 2\hbar^2\chi^2 \sum_i \frac{|\langle i|\hat{Q}|\rangle|^2 (E_i - E_0)}{[(E_i - E_0)^2 - (\hbar\omega)^2]^2} \tag{6.2.3}$$

and

$$C(\omega) = \omega^2 B(\omega) \tag{6.2.4}$$

These expressions reduce to those of the adiabatic model if we neglect terms of order $\hbar\omega/(E_i - E_0)$.

Transition probabilities are given in terms of ω and $B(\omega)$ exactly as before.

6.3. Inclusion of short-range forces

The generalization of the above formulae to include the effects of short-range forces can be made just as in the adiabatic model. The dispersion equation becomes

$$\sum_{\nu\nu'} \frac{|\langle \nu|\hat{Q}|\ \nu'\rangle|^2 (u_\nu v_{\nu'} + u_{\nu'} v_\nu)(E_\nu + E_{\nu'})}{(E_\nu + E_{\nu'})^2 - (\hbar\omega)^2} = \frac{1}{2\chi} \tag{6.3.1}$$

and the mass parameter

$$B(\omega) = 2\hbar^2\chi^2 \sum_{\nu\nu'} \frac{|\langle \nu|\hat{Q}|\nu'\rangle|^2 (u_\nu v_{\nu'} + u_{\nu'} v_\nu)(E_\nu + E_{\nu'})}{[(E_\nu + E_{\nu'})^2 - (\hbar\omega)^2]^2} \qquad (6.3.2)$$

6.4. Comparison with experiment

In Fig. 20 the results of some VPM calculations of Marshalek and Rasmussen [13] are shown. They are actually for the ν-vibrations of the deformed rare-earth nuclei, but the formalism is exactly the same. For comparison with experiment, allowance has been made for the rotational motion which introduces some uncertainties and agreement cannot be expected to be so good as it might have been for spherical nuclei. For instance, no account is taken of the possible coupling of the vibrational to the rotational motion. For comparison, excitation energies in the adiabatic approximation are also shown. In every case the VPM is better.

Agreement with experiment for the B(E2) values is not very good but this is almost certainly due to computational uncertainties rather than the inadequacy of the model.

It is to be noted that the Marshalek and Rasmussen calculation contains no adjustable parameter, since the coupling constant χ is given its theoretical value and is not treated as a fitting parameter.

6.5. Discussion

By removing the adiabatic approximation we obtain not just one but a complete set of solutions. For zero coupling to the deformation field these are just the unperturbed shell-model states. As the coupling is turned on, one state falls a long way below the rest and acquires collective properties, a low excitation energy and large transition strength. The other states are modified only a little and retain the appearance of particle excitations. It is a very attractive feature of the model that the collective and particle excitations should appear on an equal footing and that there should be just the correct number of states and no spurious state, due to the introduction of redundant collective variables. It can also be shown that the VPM excitations form a complete orthogonal set.

The consequences of removing the adiabatic approximation are thus seen to be much more widespread than merely going to a higher order of approximation. The adiabatic model gives a single solution, which approximates to the lowest frequency VPM solution, and provides a reasonable description of the so-called 'collective state'. To obtain the other states one is obliged to return to the IPM, consequently ending up with an overcomplete set. The VPM, rather than the adiabatic model, appears therefore as the real fulfilment of the unified model, providing a common description of both the collective and the particle-like excitations. In fact, in the VPM there no longer remains any distinction between the different modes. One merely observes that the lowest frequency solution is more collective than the rest, and this is how it ought to be.

There are, however, several things which need explaining. For instance:

(a) Why, when we have apparently introduced extra degrees of freedom

into the already complete IP Hamiltonian, do we not get spurious states?

(b) The same semi-classical co-ordinates Q and $\dot{Q}$ serve as normal co-ordinates for all the modes, including collective-like and particle-like, which if they have any significance must be orthogonal.

(c) We get a different mass parameter $B(\omega)$ for each solution, which implies that there is not a single energy surface for shape deformation but many, depending on the frequency.

A proper understanding of what is going on and the true nature of the approximations involved will be obtained when we derived the model microscopically. Briefly, the essential point is that neither Q (nor α) is actually a collective co-ordinate at all. They are merely parameters and c-numbers, denoting the instantaneous shape of the nuclear field, associated with an oscillation in one of its various normal modes. All of the true normal modes exhibit to some extent motion of the nuclear shape. The shape oscillation is not itself a normal mode. It is for this reason that the hydrodynamic model, which puts all the collective strength into a single excited state, fails. The present approximation is good because only the overall shape of the field is really important and not the details associated with the other shorter-range components of the density oscillations.

7. ANHARMONIC VIBRATIONS

The only experimental data available of vibrational states, above the one-phonon states, are for the quadrupole vibrations. For these we expect a degenerate two-phonon triplet, of spin $0, 2, 4^+$, at twice the energy of the first 2^+ state. Sometimes all members of the triplet are observed,

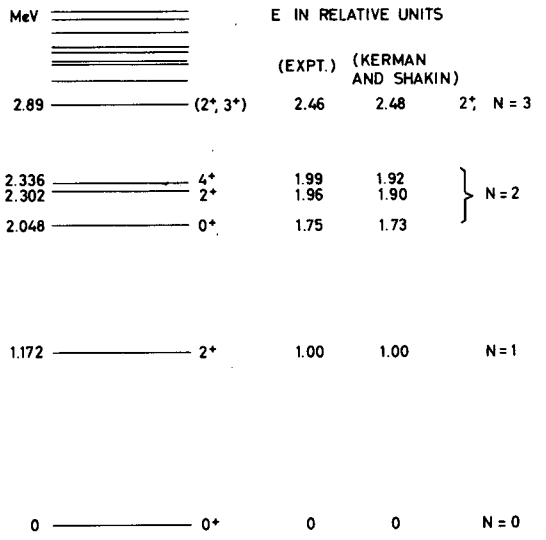

FIG. 21. Energy spectrum of ^{62}Ni. Results of Kerman and Shakin (Taken from Ref. [7], courtesy of North-Holland Publishing Co.)

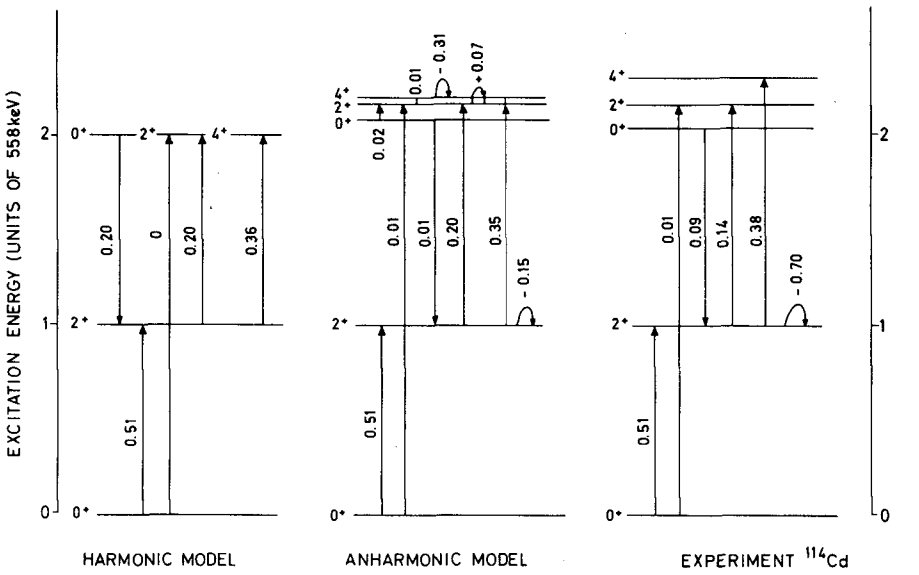

FIG. 22. Comparison of the ^{114}Cd spectrum with the harmonic and the anharmonic model (Taken from Ref. [16], courtesy of North-Holland Publishing Co.)

sometimes one is conspicuously absent. Invariably their degeneracy is substantially split.

In terms of the vibrational model, such effects reflect the anharmonic nature of the collective Hamiltonian. A general collective Hamiltonian has the form

$$H = W^{21}\{O^\dagger O\}_0 + W^{30}\{O^\dagger O^\dagger O^\dagger\}_0 + W^{31}\{O^\dagger O^\dagger O\}_0 + \text{h.c.}$$

$$+ \text{higher order terms}$$

where the phonon operators are coupled within the brackets to form scalars.

To see if such a Hamiltonian can explain the two-phonon splitting, Kerman and Shakin [14] attempted to fit the ^{62}Ni spectrum with just cubic anharmonic terms, using second-order perturbation theory. Their results are shown in Fig. 21, and are reasonably successful. For other nuclei, however, they were not so successful and this they attribute to the necessity of including quartic terms[8]. The data is insufficient, however, to permit the introduction of any more adjustable parameters. A meaningful test of the anharmonic model therefore requires the determination of the extra parameters theoretically from the energy surface or from a microscopic theory.

Just recently, nuclear orientation experiments have brought to light some very serious departures from harmonicity, and that in nuclei which

[8] Quartic terms contribute to the energy in first order whereas cubic terms contribute first in second order. Thus to be consistent both should be introduced on an equal footing, even though the quartic terms may be of an order of magnitude smaller.

were hitherto considered amongst the best examples for harmonic vibrations. ^{114}Cd for example, has a spectrum which is very close to harmonic (see Fig. 22). Its transition strengths are about right and it nicely demonstrates the selection rule inhibiting the $2_2 \rightarrow 0_1$ cross-over transition. Then de Boer et al. [15] do an experiment and find a static quadrupole moment for the first 2^+ state of about five single-particle magnitudes. This result is completely at variance with the purely harmonic vibrations of a spherical nucleus, which are all centred about zero deformation. Maybe then ^{114}Cd is not spherical but has a deformed equilibrium shape. This hypothesis has some support from the fact that the experimentally observed ratio of quadrupole matrix elements

$$\frac{\langle 2_1 || \mathscr{M}(E2) || 2_1 \rangle}{\langle 0_1 || \mathscr{M}(E2) || 2_1 \rangle} = -1.30 \pm 0.39$$

is consistent with the value -1.20, for the pure rotational motion of a stable deformed nucleus. The remaining data is, however, more consistent with the vibrational picture, but a strongly interacting vibrational-rotational motion is not out of the question.

The possibility of fitting the data with an anharmonic vibrational model has been investigated by Sørensen [16], again using only cubic terms. The anharmonic components needed were far too large for perturbation theory and he diagonalizes in the subspace of up to seven-phonon vibrational configurations. His results are shown in Fig. 22. He too concludes that a completely satisfactory fit is not possible without quartic terms.

8. THE E1 PHOTORESONANCE

Measurements of γ-absorption cross-sections reveal a giant dipole resonance centred at about 80 $A^{-1/3}$ MeV for heavy nuclei, which settles down to about 20 MeV for nuclei $A \lesssim 40$. Its width varies around 5 MeV.

Early attempts to understand the phenomenon followed either the collective or the independent particle approach and there was considerable debate as to which, if either, was correct. We now know that the two approaches are not orthogonal but different ways of looking at the same thing. Since the equivalence of these viewpoints underlies our present understanding of collective vibrations, we shall briefly review the two methods and their eventual reconciliation.

8.1. The collective model

The collective model interpretation was proposed by Goldhaber and Teller [17]. They regarded the dipole resonance as a quantized oscillation of proton and neutron densities in antiphase, the centre of mass remaining fixed.

Two major possibilities were envisaged: (a) The proton and neutron densities oscillate through each other as hard spheres. (b) The densities oscillate such that the sum density, at any point, remains constant. The second possibility appears to give better agreement with experiment, although the first is more readily understood in terms of the shell model.

Consider the second (sometimes described as second sound). The energy increment, associated with a local density fluctuation $\delta\rho_N = -\delta\rho_p$,

can be deduced from the symmetry energy in the Weizsäcker mass formula

$$\tfrac{1}{2}\,\epsilon_{sym}\,\frac{(N-Z)^2}{A} \qquad (8.1.1)$$

where $\epsilon_{sym} \approx 25$ MeV. Knowing the density and the energy increment for a density fluctuation, the velocity of sound in the medium can be calculated. The dipole oscillation frequency is then determined by the boundary conditions for a standing wave in the nucleus. This problem was essentially solved by Lord Rayleigh [18]. The result is

$$\hbar\omega_{dip} = 78\ A^{-1/3}\text{MeV} \qquad (8.1.2)$$

which is a great success for the model.

This treatment gives a single state of zero width, rather than the 5 MeV or so observed. However, a width is easily fed into the model by supposing that the collective oscillation is damped. In view of the large number of background states at this energy, it would be very surprising if it were not damped by a small coupling to some of them.

The cross-section for exciting the dipole state can be deduced from the energy-weighted sum rule, since the collective model puts all the strength into a single mode. The dipole sum is

$$S^{EI}_{Ew}(T=1) = \frac{9}{4\pi}\,\frac{\hbar^2 e^2}{2M}\,\frac{NZ}{A} = \hbar\omega\, B(E1;0 \to 1) \qquad (8.1.3)$$

Experimentally, the integrated strength in the resonance region just about equals this sum, again a success for the model.[9]

8.2. The shell model

The protagonists of the shell-model approach (Wilkinson [20], Rand and others) took the attitude that the dipole resonance is not a single broad collective state, but an aggregate of single-particle shell-model excitations.

For a harmonic oscillator potential, all such excited states would be degenerate at an energy $\hbar\omega$, where ω is the oscillator frequency. When the spin-orbit interaction is included and a more realistic potential well taken, the degeneracy is split. Nevertheless excited states still tend to cluster within a comparatively narrow energy region (see, for example, Figure 23, where the sort of configurations excitable by a dipole operator are illustrated for a hypothetical nucleus with a partially filled $1f_{5/2}$ subshell).

If an imaginary component is included in the potential well, as in the optical model, these unperturbed configurations acquire a width and may overlap. The photoresonance is then the envelope of all such states.

Again all the dipole strength must lie within the resonance region, but not now in a single broad collective state.

The major problem with the independent-particle shell model is that the energy comes out about half the experimental value. It can be increased

[9] Bethe and Levinger [19] point out that the neglected exchange terms can add something like 40% to the sum rule. The extra strength probably lies at high energies and is associated with the high momentum two-particle correlations for which the short-range repulsive core is responsible.

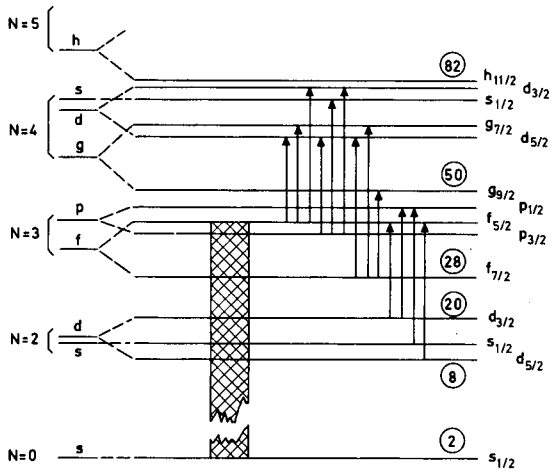

FIG. 23. Possible $\Delta N = 1$, E1 transitions

by taking into account pairing, but to get it up to value needs an effective mass $m^* \approx m/2$, which is unreasonably small. It also tends to overestimate the width of the photopeak.

8.3. Equivalence of the two approaches

At first sight the two descriptions are diametrically opposed and it is not surprising that there was controversy. The energy of the resonance is given more accurately in the collective model, while the shell model explains more readily its willingness to decay by particle emission. The shell model tends to overestimate the width, but at the same time allows for the possibility of structure, whereas the collective model predicts a completely smooth cross-section. Later of course, with better resolution, structure was observed, although it proved to have a different complexity to that envisaged by the shell model (see, for example, the photonuclear cross-section for ^{28}Si in Fig. 24, measured for different reactions with different resolutions).

The compatibility of the two approaches was first elucidated by Brink [22]. Consider the dipole operator. Allowing for centre-of-mass recoil, it is

$$\vec{\mathcal{M}}(E1) = e \sum_{i}^{Z} (\vec{r}_i - \vec{R}) \qquad (8.3.1)$$

where $\vec{R}$ is the centre-of-mass co-ordinate

$$\vec{R} = \frac{1}{A}\left[\sum_{i}^{Z} \vec{r}_i + \sum_{j}^{N} \vec{r}_j \right] \qquad (8.3.2)$$

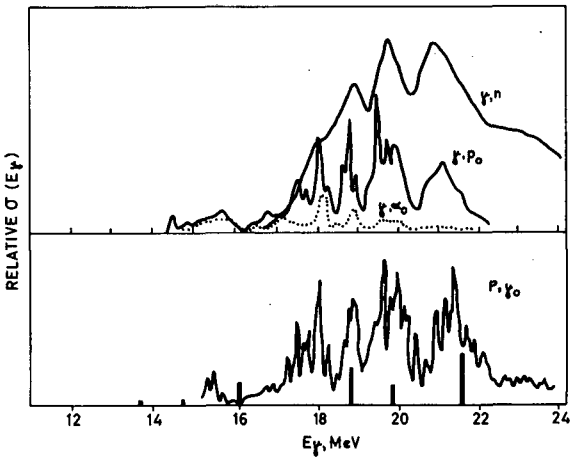

FIG. 24. Photonuclear cross-sections for ^{28}Si (Taken from Ref. [21], courtesy of Annual Reviews Inc.)

Substituting, we obtain

$$\vec{\mathcal{M}}(E1) = e\frac{N}{A}\sum_{i}^{Z}\vec{r}_i - e\frac{Z}{A}\sum_{j}^{N}\vec{r}_j$$

$$= e\frac{NZ}{A}(\vec{R}_Z - \vec{R}_N) \equiv e\frac{NZ}{A}\vec{r} \qquad (8.3.3)$$

where $\vec{r}$ is the relative co-ordinate of the proton and neutron centre of masses.

Thus the dipole operator, acting on the ground state, creates a state of relative neutron-proton motion. At the same time, being a single-particle operator, it can only change the state of, at most, one particle in a single operation. The dipole state can therefore be simultaneously a collective and a superposition of single-particle excitations.

If this is not convincing, recall the question that was asked in the early days of quantum mechanics. Can electrons, passing singly through a diffraction grating, produce an interference pattern? The anwer is that they can, because one does not know through which slit a given electron passes. The slits in the grating correspond to single-particle excitations; the grating is a superposition of them. The electron corresponds to the photon absorption process. It can only excite a single configuration at a time, but if, as in the collective state, the amplitudes for each possibility add coherently, the total excitation probability will be very large.

The two models are therefore not opposed but, at the same time, they are not equivalent. In the collective model, the 'collective dipole state' appears as a damped eigenstate, whereas in the shell model it is split among many damped single-particle excitations. In fact both are inadequate.

The collective model fails because the broadening is treated too classically. If the coupling to other excited states of the nucleus were treated explicitly, it must necessarily produce a splitting of the collective state

into a large number of discrete energy states, each of which is then broadened by its particle emission width. The collective model can therefore only be expected to give the average properties of the resonance and not the details, which must reflect the local shell structure of the particular nucleus.

The independent particle shell model fails because it neglects residual interactions. The calculations of Elliott and Flowers [23] showed that residual interactions effect a concentration of the collective strength into just a few excited states, which results in a considerable reduction of the overall width. These states are also pushed up in energy, eliminating the necessity for an unrealistic effective mass.

Let us look again at the experimental results for ^{28}Si. With good resolution, all sorts of fine structure appear, although not for all nuclei. In terms of the shell model, this fine structure may be attributed to the coupling of the one particle-hole (1 ph) configurations to the 2 ph, the 3 ph, etc. Whether fine structure exists, in a particular nucleus, depends on the relative widths and spacing of the component states.

Pictorially, the energy of the dipole oscillation can be given up in one of two competing processes. It can decay directly by particle emission, or, if this takes too long because of the height of the Coulomb and angular momentum barriers, it can first thermalize its energy among the more complicated degrees of freedom of the nucleus and eventually emit low angular momentum evaporation neutrons. In light nuclei the direct process tends to dominate, although not always. In heavy nuclei thermalization more frequently occurs and fine structure is observable.

III. DEFORMED NUCLEI

9. THE COLLECTIVE ROTATIONAL MODEL

9.1. The existence of rotations

In section 3 we were able to give a precise quantal meaning to the classical concept of a vibrating nucleus, and to show in what sense 'collective vibrations' can meaningfully be said to exist. Can we now do the same for rotations?

Consider first just two interacting nucleons, with a Hamiltonian

$$H = -\frac{\hbar^2}{2M}(\nabla_1^2+\nabla_2^2)+V(r) \qquad (9.1.1)$$

This Hamiltonian can be separated into relative and centre-of-mass parts:

$$H = \underbrace{-\frac{\hbar^2}{M}\nabla^2+V(r)}_{\text{(relative)}} \underbrace{-\frac{\hbar^2}{4M}\nabla_R^2}_{\text{(centre-of-mass)}} \qquad (9.1.2)$$

The Schrödinger equation for the relative motion is

$$\nabla^2\psi+\frac{M}{\hbar^2}[E-V(r)]\psi = 0 \qquad (9.1.3)$$

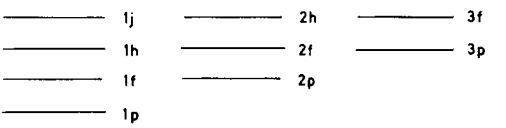

FIG. 25. Rotational bands for a two-particle nucleus (identical particles can only exist in relative odd parity states)

which, written in spherical co-ordinates, becomes

$$\frac{1}{r^2}\frac{\partial}{\partial r}\left(r^2\frac{\partial\psi}{\partial r}\right) + \frac{1}{r^2}\underbrace{\left[\frac{1}{\sin\theta}\frac{\partial}{\partial\theta}\left(\sin\theta\frac{\partial\psi}{\partial\theta}\right)+\frac{1}{\sin^2\theta}\frac{\partial^2\psi}{\partial\varphi^2}\right]}_{\Lambda\psi} + \frac{M}{\hbar^2}[E-V(r)]\psi = 0 \qquad (9.1.4)$$

It is clear that ψ is separable into radial and angular parts

$$\psi = R(r)\,Y_{\ell m}(\theta) \qquad (9.1.5)$$

where $Y_{\ell m}(\theta)$ is a spherical harmonic and a solution of the well-known equation

$$\Lambda Y_{\ell m} + \ell(\ell+1)Y_{\ell m} = 0 \qquad (9.1.6)$$

and R(r) is a solution of the equation

$$\left\{\frac{1}{r^2}\frac{d}{dr}\left(r^2\frac{d}{dr}\right) - \frac{\ell(\ell+1)}{r^2} + \frac{M}{\hbar^2}[E - V(r)]\right\} R(r) = 0 \qquad (9.1.7)$$

For the two-particle system, R(r) can also be regarded as the intrinsic wave function and $Y_{\ell m}(\theta)$ a rotational wave function. Consider the energy spectrum for a harmonic interaction

$$V(r) = kr^2 \qquad (9.1.3)$$

The energy levels can be arranged in bands, each band characterized by an intrinsic or radial quantum number (Fig. 25).

Thus rotational motion undeniably exists for the two-particle system, although the spectrum does not follow the I(I+1) energy rule expected for a rotor. This is for the obvious reason that the rotational energy $\hbar^2\ell(\ell+1)/Mr^2$ is of the same order of magnitude as the intrinsic excitation energies, and the two are strongly coupled. In other words, the centrifugal force distorts the intrinsic structure.

For many particles, an orientation angle can be defined in terms of the inertia tensor, and a change of co-ordinates, in principle, made. The intrinsic system can now have many degrees of freedom, including angular motions, provided that such motions do not involve the orientation of the principal axes of the inertia tensor. Extra coupling terms are thereby possible, in particular the Coriolis coupling.

Now if the mean moment of inertia is very large, the rotational angular velocity for a given angular momentum is small, compared with characteristic intrinsic frequencies. In this adiabatic limit the coupling

should be small and a pure rotational spectrum observable. Thus we define a pure rotation as one which leaves the intrinsic structure unaltered. To the question "do pure rotations exist?", the answer is almost certainly "no". (It is my guess that if they did we would get the rigid body moment of inertia, although I do not think that this has been demonstrated.) However, it is reasonable to suppose that we get near enough to the limit, that a pure adiabatic rotational model makes a good first approximation. Coupling of rotational and intrinsic motion can then be treated as a perturbation and perhaps by a renormalization of the effective moment of inertia.

9.2. The rotational Hamiltonian

Assuming that an appropriate transformation to rotational and intrinsic co-ordinates has been made, the Hamiltonian has the form

$$H = H_{rot} + H_{intr} \tag{9.2.1}$$

where

$$H_{rot} = \sum_k \frac{\hbar^2}{2\mathcal{I}_k} (I_k - J_k)^2 \tag{9.2.2}$$

with k labelling the principal axes of the inertia tensor. The total angular momentum $\vec{I}$ is given by

$$\vec{I} = \vec{R} + \vec{J} \tag{9.2.3}$$

where $\vec{J}$ is the intrinsic angular momentum and $\vec{R}$ is the angular momentum associated with the rotating intrinsic co-ordinate axes. H_{intr} is left undefined in this purely phenomenological model.

From the theory of the rotating top, we know that I and $M = I_z$ are constants of the motion, but that I_3, the projection of the angular momentum along the intrinsic z-axis, is not, unless the body happens to be symmetric about this axis. Since it appears to be possible to explain nuclear data in terms of axial symmetry (together with vibrations about axial symmetry) we shall make this assumption and benefit from the considerable simplification that results. Thus we put

$$\mathcal{I}_1 = \mathcal{I}_2 = \mathcal{I} \tag{9.2.4}$$

H_{rot} can now be expanded

$$H_{rot} = \frac{\hbar^2}{2\mathcal{I}}(\vec{I}^2 - I_3^2 - J_3^2) + \frac{\hbar^2}{2\mathcal{I}_3}(I_3 - J_3)^2 - \underbrace{\frac{\hbar^2}{2\mathcal{I}}(I_+J_- + I_-J_+)}_{\text{RPC}} + \underbrace{\frac{\hbar^2}{2\mathcal{I}}\vec{J}^2}_{\text{intrinsic}} \tag{9.2.5}$$

The last term operates only on the intrinsic variables and is naturally incorporated into H_{intr}. The term labelled RPC (rotation-particle coupling) is the Coriolis interaction, coupling the intrinsic motion to the rotation,

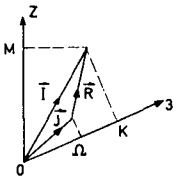

FIG. 26. Quantum numbers characterizing the rotational eigenstates

and is neglected in the adiabatic approximation. The moment of inertia $\mathscr{I}$, although written as a constant, is really a function of the intrinsic variables. Again, in the adiabatic approximation, it is taken to be a constant, and in this way the centrifugal interaction is neglected.

With neglect of these interaction terms, one is left with four good quantum numbers to characterize the rotational eigenstates, namely I, $M = I_z$, $K = I_3$ and $\Omega = J_3$ (see Fig. 26). An eigenstate of these quantum numbers is the wave function (see Appendix)

$$\psi^{I}_{\Omega KM} = \sqrt{\frac{2I+1}{8\pi^2}}\, \mathscr{D}^{I}_{MK}(\theta)\, \varphi^{(\theta)}_{\Omega} \tag{9.2.6}$$

For a given intrinsic wave function φ_Ω, we therefore expect the rotational energy spectrum

$$E_{rot} = \frac{\hbar^2}{2\mathscr{I}}[I(I+1) - K^2 - \Omega^2] + \frac{\hbar^2}{2\mathscr{I}_3}(K-\Omega)^2 \tag{9.2.7}$$

9.3. Symmetry properties

For an axially symmetric nucleus, the choice of intrinsic axes is not unique. Consequently there follow certain restraints on the symmetry of the wave function. In particular, the wave function must be invariant under the following two transformations:

(a) Rotating the intrinsic co-ordinate axes through an angle δ about the symmetry axis, but leaving the nuclear wave function fixed in space, should alter nothing, not even a phase factor. Rotating the function of angle $\mathscr{D}^{I}_{MK}(\alpha\beta\gamma)$ we get

$$\mathscr{D}^{I}_{MK}(\alpha\beta\gamma) \rightarrow \mathscr{D}^{I}_{MK}(\alpha\beta\gamma-\delta) = e^{-iK\delta}\mathscr{D}^{I}_{MK}(\alpha\beta\gamma) \tag{9.3.1}$$

Rotating the axes of the function $\varphi^{(\theta)}_{\Omega}$ we get

$$\varphi^{(\theta)}_{\Omega} \rightarrow e^{i\delta J_3}\, \varphi^{(\theta)}_{\Omega} = e^{i\Omega\delta}\varphi^{(\theta)}_{\Omega} \tag{9.3.2}$$

Thus, in order that the product function should be invariant under this transformation, we must require that

$$K = \Omega \tag{9.3.3}$$

(b) Rotating the intrinsic axes an angle π about the 2-axis, but again leaving the wave function fixed in space, should change nothing. We

obtain

$$\mathscr{D}^{I}_{MK}(\alpha\beta\gamma) \rightarrow \mathscr{D}^{I}_{MK}(\alpha, \beta-\pi, -\gamma) = (-1)^{I+K} \mathscr{D}^{I}_{M-K}(\alpha\beta\gamma) \qquad (9.3.4)$$

and

$$\varphi^{(\theta)}_{K} \rightarrow e^{i\pi J_2} \varphi^{(\theta)}_{K} \equiv \varphi^{(\theta)}_{\bar{K}} \qquad (9.3.5)$$

where $\varphi_{\bar{K}}$ is defined by this equation.[10] Thus the symmetrized wave function becomes

$$\psi^{I}_{KM} = \sqrt{\frac{2I+1}{16\pi^2}} \left\{ \mathscr{D}^{I}_{MK}(\theta)\, \varphi^{(\theta)}_{K} + (-1)^{I+K} \mathscr{D}^{I}_{M-K}(\theta) \varphi^{(\theta)}_{\bar{K}} \right\} \qquad (9.3.6)$$

for $K \neq 0$; $K = 0$ is an exception since $\varphi_{\bar{0}}$ is not distinct from φ_0.

The energy spectrum is now given by

$$E_{rot} = \frac{\hbar^2}{2\mathscr{I}}[I(I+1) - 2K^2] \qquad (9.3.7)$$

for $K \neq \frac{1}{2}$; $K = \frac{1}{2}$ is an exception because, after symmetrization, the RPC gives diagonal contributions to the energy and cannot reasonably be neglected. In the following discussion the K^2 term in the energy will be dropped and assumed to be incorporated into the intrinsic energy.

9.4. K = 0 bands

For $K = 0$ the intrinsic wave function $\varphi_{\bar{0}}$ is not distinct from φ_0 but neither is it necessarily identical. In fact

$$\varphi_{\bar{0}} = (-1)^{J} \varphi_0 = r\varphi_0 \qquad (9.4.1)$$

so that $r = \pm 1$. J is an integer for all components φ^{I}_{0} of φ_0. Thus the symmetrized wave function vanishes unless

$$I = 0, 2, 4 \ldots \quad \text{for } r = +1$$

$$= 1, 3, 5 \ldots \quad \text{for } r = -1$$

For even-even nuclei, particles are coupled pairwise in time reversal conjugates and consequently $r = +1$. Thus $K = 0$ bands contain only even

---

[10] If φ_K is expanded in eigenstates of J

$$\varphi_K = \sum_J c_J \varphi^{J}_{K}$$

then

$$\varphi_{\bar{K}} = \sum_J (-1)^{J+K} \varphi^{J}_{-K} = (-1)^{J+K} \varphi_{-K}$$

With a suitable choice of phases for combining space and spin wave functions, $\varphi_{\bar{K}}$ is just the time reverse of φ_K.

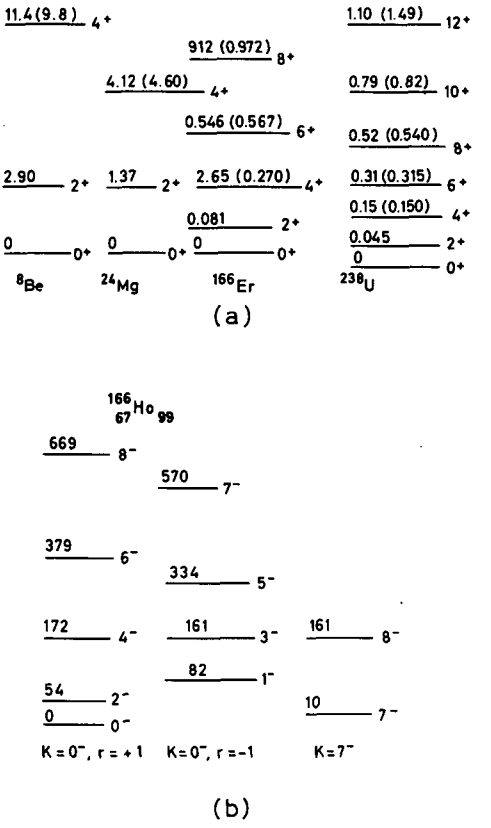

FIG. 27. (a) Some typical examples of rotational bands in even-even nuclei, (b) the low-energy level structure of ^{166}Ho (Taken from Ref. [24], courtesy of Annual Reviews Inc.)

spins (Fig. 27a). For odd-odd nuclei, however, $r = -1$ is also a possibility (Fig. 27b).

Note that r has nothing to do with parity. If the nucleus is reflection-symmetric, φ_K has good parity, which is also the parity of each member of the band. If the nucleus is not reflection-symmetric, e.g. pear-shaped, it may not have good parity, but it must always be possible to take linear combinations which do have good parity

$$\varphi_{K\pm} = \frac{1}{\sqrt{2}}(1 \pm \pi)\varphi_K \tag{9.4.2}$$

9.5. $K = \frac{1}{2}$ bands

$K = \frac{1}{2}$ bands are also special, because for these

$$-\frac{\hbar^2}{2\mathcal{I}}(I_+ J_- + I_- J_+) \tag{9.5.1}$$

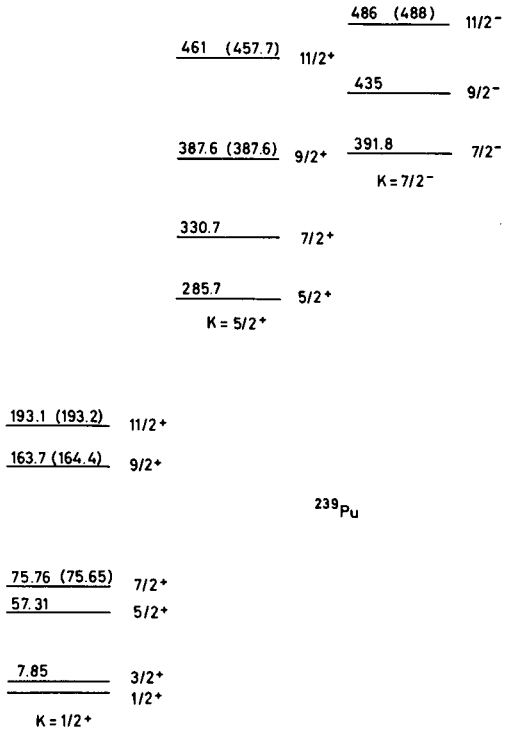

FIG. 28. Spectrum for ^{239}Pu. Energy levels are given in keV. Theoretical values are enclosed in brackets.

has a diagonal component which cannot reasonably be neglected. Its diagonal contribution to the energy spectrum is readily calculated in terms of the decoupling parameter a, defined by

$$a = - \langle \varphi_{\frac{1}{2}} | J_+ | \varphi_{\bar{\frac{1}{2}}} \rangle \tag{9.5.2}$$

The rotational part of the matrix element is

$$\int \mathcal{D}^{*I}_{M\frac{1}{2}}(\theta)\, I_-\, \mathcal{D}^{I}_{M-\frac{1}{2}}(\theta)\, d\theta = \frac{8\pi^2}{2I+1}(I+\tfrac{1}{2}) \tag{9.5.3}$$

Hence we obtain the energy spectrum

$$E_{rot} = \frac{\hbar^2}{2\mathcal{I}}[I(I+1) + \delta_{K\frac{1}{2}}\, a(-1)^{I+\frac{1}{2}}(I+\tfrac{1}{2})] \tag{9.5.4}$$

The decoupling parameter is so called because it implies a breakdown of the strong coupling of the particle to the deformed nuclear shape. The pure adiabatic model is sometimes called the strong coupling model for the reason that, in this limit, the particles are strongly coupled to a deformed shape which is not significantly perturbed by the rotation.

Figure 28 shows the spectrum for ^{239}Pu fitted with the above rotational formula. Included is a $K = \frac{1}{2}$ band strongly modified by decoupling. In

some cases, particularly in light nuclei, e.g. B", C", the decoupling parameter can be so large as to bring about a re-ordering of $K = \frac{1}{2}$ levels.

9.6. Electromagnetic moments and transitions

(a) The general structure of matrix elements

Since members of a band differ only by their rotational wave function, which has well-known properties, many matrix elements are simply related by geometric factors.

Matrix elements are best evaluated by transforming the operator into the intrinsic frame. The electromagnetic multipole operator transforms

$$\mathscr{M}(\lambda\mu) = \sum_{\nu} \mathscr{D}^{\lambda}_{\mu\nu}(\theta)\, \mathscr{M}^{(\theta)}(\lambda\nu) \tag{9.6.1}$$

For K_i, $K_f \neq 0$, therefore,

$$\langle I_f M_f K_f | \mathscr{M}(\lambda\mu) | I_i M_i K_i \rangle = \sum_{\nu} \frac{\sqrt{(2I_i+1)(2I_f+1)}}{8\pi^2} \times \left\{ \int \mathscr{D}^{*\,I_f}_{M_f K_f} \mathscr{D}^{\lambda}_{\mu\nu}\, \mathscr{D}^{I_i}_{M_i K_i} \langle K_f | \mathscr{M}(\lambda\nu) | K_i \rangle + (-1)^{I_i + K_i} \int \mathscr{D}^{*\,I_f}_{M_f K_f} \mathscr{D}^{\lambda}_{\mu\nu}\, \mathscr{D}^{I_i}_{M_i - K_i} \langle K_f | \mathscr{M}(\lambda\nu) | \bar{K}_i \rangle \right\} \tag{9.6.2}$$

Note that $\mathscr{M}(\lambda\mu)$, being independent of θ, is invariant under the transformation which rotates the intrinsic axes through π, and hence the two halves of the matrix element are identical. Evaluating the integrals, according to the formulae in Appendix A.2, we deduce the reduced matrix element

$$\langle I_f K_f \| \mathscr{M}(\lambda) \| I_i K_i \rangle = \sqrt{(2I_i+1)}\, \{ (I_i \lambda K_i, K_f - K_i | I_f K_f) \langle K_f | \mathscr{M}(\lambda, K_f - K_i) | K_i \rangle + (-1)^{I_i + K_i} (I_i \lambda - K_i, K_f + K_i | I_f K_f) \langle K_f | \mathscr{M}(\lambda, K_f + K_i) | \bar{K}_i \rangle \} \tag{9.6.3}$$

for K_i, $K_f \neq 0$

For $K_i = 0$

$$\langle I_f K_f \| \mathscr{M}(\lambda) \| I_i K_i = 0 \rangle = \sqrt{(2I_i+1)} (I_i \lambda\, 0\, K_f | I_f K_f) \langle K_f | \mathscr{M}(\lambda, K_f | K_i = 0 \rangle \times \begin{cases} \sqrt{2} & \text{if } K_f \neq 0 \\ 1 & \text{if } K_f = 0 \end{cases} \tag{9.6.4}$$

The reduced transition probability, defined by

$$B(\lambda; I_i \to I_f) = \frac{|\langle I_f \| \mathscr{M}(\lambda) \| I_i \rangle|^2}{2I_i + 1} \tag{9.6.5}$$

follows from the above. For K_i, $K_f \neq 0$

$$B(\lambda; I_i K_i \to I_f K_f) = |(I_i \lambda K_i,\ K_f - K_i | I_f K_f) \langle K_f | \mathscr{M}(\lambda,\ K_f - K_i)) | K_i \rangle + (-1)^{I_i + K_i} (I_i \lambda - K_i,\ K_f + K_i | I_f K_f) \langle K_f | \mathscr{M}(\lambda,\ K_f + K_i) | \overline{K}_i \rangle|^2 \tag{9.6.6}$$

For $K_i = 0$

$$B(\lambda; I_i K_i = 0 \to I_f K_f) = (I_i \lambda 0\, K_f | I_f K_f)^2 |\langle K_f | \mathscr{M}(\lambda,\ K_f) | K_i = 0 \rangle|^2 \times \begin{cases} 2 & \text{if } K_f \neq 0 \\ 1 & \text{if } K_f = 0 \end{cases} \tag{9.6.7}$$

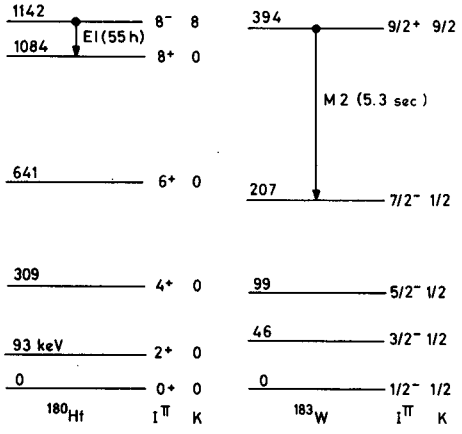

FIG. 29. K-forbidden transitions

Thus it is clear that the rotational model predicts a K-selection rule, forbidding transitions for which the vector coupling coefficients vanish. In particular the transition is forbidden if

$$\lambda < |K_i - K_f| \tag{9.6.8}$$

Some examples of K-forbidden transitions, which are otherwise allowed, are given in Fig. 29.

(b) Electric quadrupole moments

The electric quadrupole moment Q, of a nucleus in the state $|IKM\rangle$, is defined as

$$Q = \sqrt{\frac{16\pi}{5}} \langle IKM = I | \mathscr{M}(E2, 0) | IKM = I \rangle \tag{9.6.9}$$

If the intrinsic quadrupole moment Q_0^K is defined as

$$Q_0^K = \sqrt{\frac{16\pi}{5}} \langle K | \mathcal{M}(E2,0) | K \rangle \tag{9.6.10}$$

then

$$Q = (I\,2\,I\,0 \,|\, I\,I)(I\,2\,K\,0 \,|\, I\,K)\, Q_0^K \tag{9.6.11}$$

For $K = \frac{1}{2}, 1$ there are also cross-terms, but these are associated with fluctuations of the deformation and are much smaller and of single-particle magnitude. In contrast the direct terms, because of the collective deformation of the nucleus, are strongly enhanced.

Expanding the coupling coefficients we get

$$Q = \frac{\{3r^2 - I(I+1)\}\{3K^2 - I(I+1)\}}{(2I-1)I(I+1)(2I+3)} Q_0^K$$

$$= \frac{3K^2 - I(I+1)}{(I+1)(2I+3)} Q_0^K \tag{9.6.12}$$

which enables one to measure experimentally the intrinsic quadrupole moment.

Similarly E2 transitions within a band are collectively enhanced, since the intrinsic matrix element is diagonal and large. Thus

$$B(E2; I_i K \to I_f K) = \frac{5}{16\pi} (I_i\,2\,K\,0 \,|\, I_f K)^2 (Q_0^K)^2 \tag{9.6.13}$$

again neglecting the cross-term as being of an order of magnitude smaller. Immediately one observes that all the E2 transitions within a band are given by the single parameter Q_0^K, proving a good means of testing the model. Some comparisons with experiment are given in Table II (after Mottelson [5]) and are generally pretty convincing.

Interband E2 transitions are of an order of magnitude smaller since they involve an excitation of the intrinsic state. Generally such transitions are of single-particle magnitude and may be neglected since they are invariably swamped by the diagonal transitions permitted by the small amount of band mixing that inevitably occurs.

(c) Magnetic dipole moments

The magnetic dipole operator is

$$\vec{\mu} = \sum_k^A \{g_\ell^k \vec{\ell}_k + g_s^k \vec{s}_k\} \tag{9.6.14}$$

where $g_\ell = 0$, $g_s = -3.83$ for neutrons

and $g_\ell = 1$, $g_s = 5.59$ for protons.

TABLE II. SOME COMPARISONS WITH EXPERIMENT

Nucleus	$I_0 = K$	$\frac{E(K+2)}{E(K+1)}$	$\frac{B(E2;\ K \to K+2)}{B(E2;\ K \to K+1)}$	$\frac{B(E2;\ K+2 \to K+1)}{B(E2;\ K+2 \to K)}$
^{153}Eu	5/2	2.33 (2.29)	0.31 (0.35)	2.6 (3.0)
^{155}Gd	3/2	2.42 (2.40)	0.52 (0.56)	2.5 (1.5)
^{157}Gd	3/2	2.43 (2.40)	0.55 (0.56)	1.6 (1.5)
^{159}Tb	3/2	2.37 (2.40)	0.51 (0.56)	1.6 (1.5)
^{161}Dy	5/2	2.33 (2.29)	0.27 (0.35)	-
^{163}Dy	5/2	2.32 (2.29)	0.27 (0.35)	3.0 (3.0)
^{165}Ho	7/2	2.21 (2.22)	0.26 (0.26)	4.9 (4.7)
^{167}Er	7/2	2.25 (2.22)	0.23 (0.26)	3.8 (4.7)
^{171}Yb	1/2	1.14 -	1.5 (1.5)	-
^{173}Yb	5/2	2.23 (2.29)	0.31 (0.35)	2.6 (3.0)
^{175}Lu	7/2	2.21 (2.22)	0.24 (0.26)	5.0 (4.7)
^{177}Hf	7/2	2.22 (2.22)	0.31 (0.26)	5.5 (4.7)
^{179}Hf	9/2	-	0.25 (0.20)	5.0 (6.5)
^{181}Ta	7/2	2.21 (2.22)	0.29 (0.26)	6.0 (4.7)

It is more convenient to separate off the part concerned with rotational motion and so we write

$$\vec{\mu} = g_R \vec{R} + \sum_k^A \{g_\ell^k \vec{\ell}_k + g_s^k \vec{s}_k\} \tag{9.6.15}$$

where $\vec{\ell}$ and $\vec{s}$ now refer only to the intrinsic angular momentum. We get

$$\vec{\mu} = g_R \vec{I} + \sum_k \{(g_\ell^k - g_R)\vec{\ell}_k + (g_s^k - g_R)\vec{s}_k\}$$

$$\equiv g_R \vec{I} + \vec{\mu}' \tag{9.6.16}$$

The first term is most readily evaluated in the laboratory frame, the second in the intrinsic frame. Thus

$$\mu = \langle IKM = I | \mu_0 | IKM = I \rangle$$

$$= g_R I + (I\,1\,I\,0 | I\,I) \left\{ (I\,1\,K\,0 | I\,K) \langle K | \mu'_0 | K \rangle \right.$$

$$\left. + \delta_{K\frac{1}{2}} (-1)^{I+\frac{1}{2}} (I\,1\,-\tfrac{1}{2}\,1 | I\,\tfrac{1}{2}) \frac{(-1)}{\sqrt{2}} \langle \tfrac{1}{2} | \mu'_+ | \bar{\tfrac{1}{2}} \rangle \right\} \tag{9.6.17}$$

This expression is simplified by introducing the gyromagnetic ratio g_K, defined by

$$\langle K|\mu_0'|K\rangle = \langle K|\sum_k \{(g_\ell^k - g_R)\ell_{k0} + (g_s^k - g_R)s_{k0}\}|K\rangle \equiv (g_K - g_R)K \tag{9.6.18}$$

and the matrix element b_0, defined by

$$\langle \tfrac{1}{2}|\mu_+'|\tfrac{\bar{1}}{2}\rangle = \langle \tfrac{1}{2}|\sum_k \{(g_\ell^k - g_R)\ell_{k+} + (g_s^k - g_R)s_{k+}\}|\tfrac{\bar{1}}{2}\rangle \equiv (g_K - g_R)b_0 \tag{9.6.19}$$

whence

$$\mu = g_R I + (g_K - g_R)\frac{K^2}{I+1}\{1 + \delta_{K\frac{1}{2}}(-1)^{I+\frac{1}{2}}(2I+1)b_0\} \tag{9.6.20}$$

The M1 multipole operator is

$$\mathcal{M}(M1) = \sqrt{\frac{3}{4\pi}}\frac{e\hbar}{2Mc}\vec{\mu} \tag{9.6.21}$$

but $g_R\vec{I}$ does not contribute to transitions, since I is diagonal. We obtain

$$\begin{aligned} B(M1; I_iK - I_fK) &= \frac{3}{4\pi}\left(\frac{e\hbar}{2Mc}\right)^2 \Big| (I_i|K\,0|I_fK)\langle K|\mu_0'|K\rangle \\ &\quad + \delta_{K\frac{1}{2}}(-1)^{I_i+\frac{1}{2}}(I_i\,1\,-\tfrac{1}{2}\,1|I_f\,\tfrac{1}{2})\frac{(-1)}{\sqrt{2}}\langle \tfrac{1}{2}|\mu_+'|\tfrac{\bar{1}}{2}\rangle\Big|^2 \\ &= \frac{3}{4\pi}\left(\frac{e\hbar}{2Mc}\right)^2 (I_i|K\,0|I_fK)^2K^2(g_K - g_R)^2\{1 + \delta_{K\frac{1}{2}}(-1)^{I>+\frac{1}{2}}b_0\}^2 \end{aligned} \tag{9.6.22}$$

where use is made of the identity

$$\frac{(I_i\ 1\ -\frac{1}{2}\ 1|I_f\ \frac{1}{2})}{(I_i\ 1\ \frac{1}{2}\ 0|I_f\ \frac{1}{2})} = \pm\frac{1}{\sqrt{2}} \qquad \text{for } I_f = I_i \pm 1 \tag{9.6.23}$$

9.7. Band mixing

Although the adiabatic model is very successful, it is not perfect. K-forbidden transitions do occur and departures from the $I(I+1)$ law are frequently observed. A break-down of the adiabatic approximation will manifest itself in terms of band mixing.

(a) $\Delta K = \pm 1$ mixing

The most obvious source of band mixing is the Coriolis interaction

$$V = -\frac{\hbar^2}{2\mathcal{I}}(I_+J_- + I_-J_+) \tag{9.7.1}$$

which can mix bands for which $\Delta K = \pm 1$.

Let us consider the effect of coupling two bands K and K+1. The perturbed energy levels are given (exactly) by the leading term in the Brillouin-Wigner expansion

$$E = E_0 + V_{00} + \frac{|V_{n0}|^2}{E - E_n} \tag{9.7.2}$$

where

$$V_{n0} = -\frac{\hbar^2}{2\mathcal{I}} \langle IK+1M | I_- J_+ | IKM \rangle \tag{9.7.3}$$

If we define the intrinsic matrix element

$$A_K = \frac{\hbar^2}{2\mathcal{I}} \langle K+1 | J_+ | K \rangle \tag{9.7.4}$$

we get

$$V_{n0} = -A_K \sqrt{(I-K)(I+K+1)} = -A_K \sqrt{\{I(I+1) - K(K+1)\}} \tag{9.7.5}$$

and

$$E(I) = \frac{\hbar^2}{2\mathcal{I}} [I(I+1) + \delta_{K\frac{1}{2}} (-1)^{I+\frac{1}{2}} (I+\tfrac{1}{2})a] + \frac{|A_K|^2}{E(I) - E_{K+1}(I)} [I(I+1) - K(K+1)] \tag{9.7.6}$$

where $E_{K+1}(I)$ is the unperturbed energy of level I in the K+1 band. In first order the denominator is replaced by $E_K(I) - E_{K+1}(I)$ which, provided the moments of inertia are the same for both bands, is independent of I. Thus the first-order effect of the band mixing on the energy spectrum is merely a renormalization of the effective moment of inertia. The lower band gets compressed ($\hbar^2/2\mathcal{I}_{eff}$ decreased) while the upper band gets expanded ($\hbar^2/2\mathcal{I}_{eff}$ increased).

Thus we conclude that this sort of band mixing has to be quite strong before it produces an observable effect on the energy spectrum. For example, consider the results for ^{183}W calculated with and without taking band mixing into account explicitly (Fig. 30). Without band mixing the fit is already pretty good and, of course, with one less free parameter. But note the change in $\hbar^2/2\mathcal{I}$ (Table III), when mixing is explicitly included.

The mixing will, however, produce a large first-order effect on transitions, especially those which are otherwise inhibited by a K-selection rule. The perturbed wave function is given by

$$\psi \propto \psi_0 + \frac{V_{n0}}{E - E_n} \psi_n \tag{9.7.7}$$

or

$$\psi(I) \propto \psi_K(I) + \frac{A_K \sqrt{\{I(I+1) - K(K+1)\}}}{E(I) - E_K(I)} \psi_{K+1}(I) \tag{9.7.8}$$

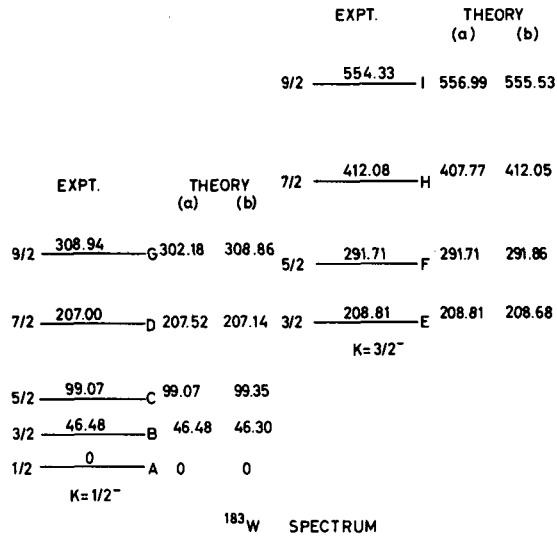

FIG. 30. Comparison of the rotational model with experiment (a) without band mixing (the parameters are fitted to the lowest levels of each band), (b) with band mixing [25] (least square fit)

TABLE III. CHANGE IN $\hbar^2/2\mathcal{I}$

Band	$\hbar^2/2\mathcal{I}_{eff}$	
	Without band mixing	With band mixing
$K = \frac{1}{2}$	13.006 keV	15.852 keV
$K = \frac{3}{2}$	16.580 keV	14.055 keV

where the proportionality constant is determined by the normalization.

Now E2 transitions are collectively enhanced for $\Delta K = 0$, but remain an order of magnitude smaller for $\Delta K = 1$. Thus interband E2 transitions should be very much increased by the mixing. As an example, look at the B(E2) values for exciting states, calculated first in the adiabatic model and then for the mixing determined by fitting the energy spectrum (Table IV).

B(E2, A → B) is fitted in both cases, otherwise there is no adjustable parameter. Impressive agreement is also obtained for the branching ratios for M1 and E2 decay of all the members of these bands.

(b) Higher order couplings

Higher order coupling terms are introduced when we admit that the moment of inertia is not really a constant but a function of the intrinsic

TABLE IV. B(E2) VALUES FOR EXCITING STATES IN THE ADIABATIC MODEL AND FOR MIXING

	Expt.	Without band mixing	With band mixing
B(E2, A → B)	1.52 ± 0.07	1.52	1.52
B(E2, A → C)	2.04 ± 0.08	2.28	2.14
B(E2, A → E)	0.08 ± 0.02	~ 0	0.09
B(E2, A → F)	0.30 ± 0.05	~ 0	0.28

variables. To show what the interactions are would require a model for the intrinsic structure, but we can say a few things on general grounds.

If $\mathcal{I}$ is made a function of intrinsic co-ordinates, the term $\hbar^2\mathbf{I}^2/2\mathcal{I}$ can couple bands for which $\Delta K = 0$. Such a coupling introduces terms proportional to $I^2(I+1)^2$ into the energy spectrum, in leading order. The rotational form of the wave function is maintained except that the intrinsic wave function becomes a function of the total angular momentum, i.e. $\varphi_K \rightarrow \varphi_K(I)$ (cf. two-particle rotations).

Another coupling arises from the neglected term

$$-\frac{\hbar^2}{8}\left(\frac{1}{\mathcal{I}_1}-\frac{1}{\mathcal{I}_2}\right)(I_+^2+I_-^2+J_+^2+J_-^2-2I_+J_+-2I_-J_-) \qquad (9.7.9)$$

Although $(1/\mathcal{I}_1 - 1/\mathcal{I}_2)$ has mean value zero for an axially symmetric nucleus, there may be fluctuations about this mean, which leads to a coupling of bands for which $\Delta K = \pm 2$. For example the schematic interaction

$$V = h_{+2}I_-^2 + h_{-2}I_+^2 \qquad (9.7.10)$$

contributes a term in the energy spectrum proportional to

$$|\langle IK+2, M|h_{+2}I_-^2|IKM\rangle|^2 = |H_K|^2[I(I+1)-K(K+1)]\,[I(I+1)-(K+1)(K+2)]$$
$$\rightarrow |H_0|^2[I^2(I+1)^2 - 2I(I+1)] \quad \text{if } K=0 \qquad (9.7.11)$$

where H_K is an intrinsic matrix element.

Nielsen [26] and collaborators have measured the K = 0 and K = 2 band mixing from observation of the E2 transitions between these bands, for a number of even nuclei. Their results generally agree quite well with the mixing expected if the K = 2 intrinsic state is a γ-vibration. They also observe, however, that this $\Delta K = 2$ mixing accounts for only about 10% of the $I^2(I+1)^2$ terms in the energy spectrum. There must therefore be other perturbing terms in the 'true' Hamiltonian.

10. THE UNIFIED MODEL FOR ROTATIONS

As we saw in section 2 the field forces, acting between particles in shell-model orbitals, cause them to line up to produce a total wave function of spheroidal density distribution. This aligned wave function does not have good angular momentum and consequently cannot describe the total state of the system. The idea of the Unified Model is to interpret it as the intrinsic wave function of the rotational model. One can then go on to calculate intrinsic excitation energies, moments of inertia, etc.

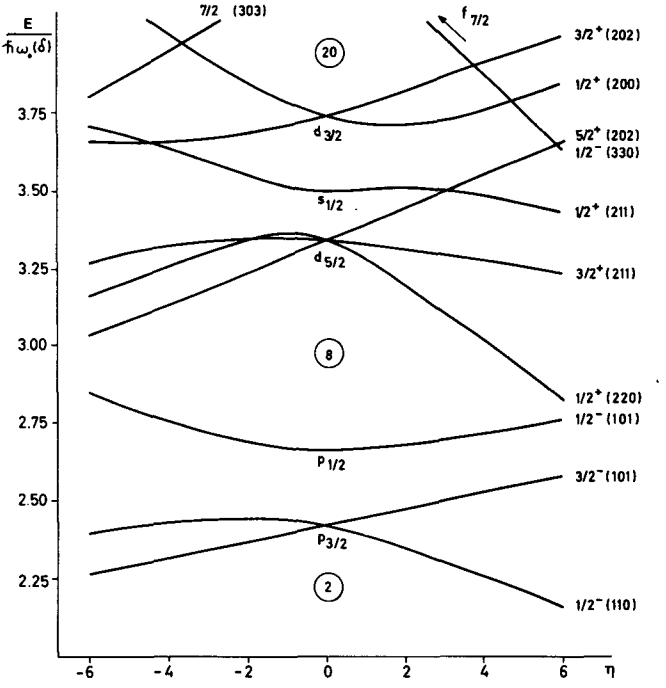

FIG. 31. Single-particle energy levels in a Nilsson potential as a function of the deformation parameter $\eta = -o\frac{2\hbar\omega_0(o)}{c}$ (Taken from Ref. [27], courtesy of Matematisk-fisiske Meddelelser)

What approximation does such a model imply? The essential approximation is one of redundant co-ordinates. The 'intrinsic' wave function $\varphi_K^{(\theta)}(\vec{r})$ already contains a complete set of co-ordinates without the extra orientation variables. It would be a true intrinsic function if the index θ provided a constraint on the particle co-ordinates $\vec{r}$, i.e. if, for a specified θ, $\varphi_K^{(\theta)}(\vec{r})$ were only a function of N-3 independent variables. In fact θ is only a constraint on the mean orientation of the nucleus. The approximation should nevertheless be good provided the rotational wave function $\mathscr{D}^I_{MK}(\theta)$ varies little over the range of orientation fluctuations of the intrinsic wave function about its mean. To be more specific, let us consider the fluctuations in angle about the z-axis, of a system specified by a wave function ψ_{jm}. A rotation of ψ_{jm} through any angle can always be expressed in terms of the $2j+1$ magnetic projections of this wave function. Thus ψ_{jm} can be said to span, on average, a solid angle

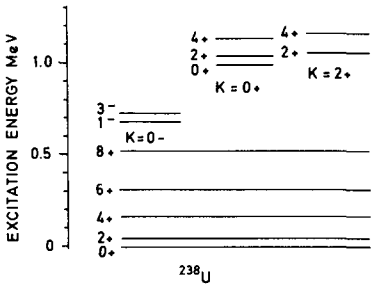

FIG.32. Spectrum of ^{238}U (Taken from Ref. [24], courtesy of Annual Reviews Inc.)

$\sim 4\pi/(2j+1)$. The use of redundant rotational co-ordinates should therefore be a good approximation, provided the intrinsic wave function is composed of high angular momentum components as compared with I. This criterion is best satisfied in the limit of large deformations.

We consider then the single-particle orbitals in a deformed shell-model potential. Extensive calculations of this sort were carried out by Nilsson [27]. They are briefly described below.

10.1. The Nilsson model

The single-particle potential is taken as

$$H = H_0 - \frac{2}{3}\delta M\omega^2 r^2 P_2(\cos\theta) + C\vec{\ell}\cdot\vec{s} + D\vec{\ell}^2$$

where H_0 is, for simplicity, a harmonic oscillator Hamiltonian of frequency ω, and $D\vec{\ell}^2$ a correction term, which simulates the squarer shape of a more realistic potential well. C and D are adjusted to reproduce the shell-model level sequence at zero deformation.

The Hamiltonian can be solved for small δ using perturbation theory on the ordinary shell-model solutions. For large deformation the $\vec{\ell}\cdot\vec{s}$ and $\vec{\ell}^2$ terms become relatively unimportant and one has independent oscillator equations for each of the three Cartesian axes. Thus we get the asymptotic wave function $|Nn_z\Lambda\Omega\rangle$, where N is the total number of oscillator quanta, n_z the number along the z-axis and $\Lambda = N - n_z, N - n_z - 2, \ldots,$ 0 or 1.

In the intermediate region, Nilsson diagonalizes among the basis configurations $|N\ell\Lambda\Sigma\rangle$, where Σ is the z-projection of the intrinsic spin. We must of course have

$$\Lambda + \Sigma = \Omega \qquad (10.1.1)$$

His results for the region $0 < A < 40$ are shown in Fig. 31.

10.2. Intrinsic structure

The problem is very similar to that for spherical nuclei if we replace shell-model orbitals by Nilsson orbitals. There are two major differences: (i) The deformation lifts the degeneracy associated with the j subshells of the spherical shell model. The orbitals become just pairwise degenerate. Due to the splitting, the single-particle level density becomes almost

uniform for large deformation, so that the shell structure is largely lost and large deformations can become energetically favourable. (ii) The coupling scheme becomes trivial since we do not have to worry about good total angular momentum. We simply construct an antisymmetrized product of Nilsson orbitals up to the Fermi surface (i.e. aligned coupling scheme). In principle we should check for self-consistency between the deformation of the particle density and the potential well used to calculate it. In practice we usually deduce the deformation from the measured quadrupole moment.

(a) Even-even nuclei

Intrinsic excited particle-hole states may be expected just as in spherical nuclei. Because of pairing, which is also of some importance for deformed nuclei, these generally lie quite high in energy (a few MeV). But, among these particle-hole states, intrinsic vibrational states exist and fall low in energy. Of particular interest are the quadrupole vibrations since they are frequently observed. Not surprisingly, they differ from the quadrupole vibrations of spherical nuclei in that the deformation has split their degeneracy. Thus we distinguish β-vibrations which conserve axial symmetry, and γ-vibrations which are vibrations of the nuclear shape about axial symmetry. For the former $K = 0$, and the latter $K = \pm 2$. It can be shown that the $K = \pm 1$ modes correspond to vibrations in the nuclear orientation angle for which there is no restoring force, in other words to rotations. The spectrum of ^{238}U, shown in Fig. 32, is a good example of low-lying vibrational bands.

The parameters for the intrinsic vibrations, i.e. mass and restoring force parameters, can be calculated by any of the methods used for spherical nuclei.

(b) Odd nuclei

The first approximation is to couple a Nilsson single-particle wave function onto an even-even deformed core. With this wave function we can calculate intrinsic matrix elements, gyromagnetic ratios, etc. For example, the decoupling parameter 'a', for a $K = \frac{1}{2}$ band, is easily found: Expand

$$\varphi_{\frac{1}{2}} = \sum_j c_j \varphi^j_{\frac{1}{2}} \qquad (10.2.1)$$

then

$$\begin{aligned} a &= -\langle \varphi_{\frac{1}{2}} | J_+ | \varphi_{\frac{1}{2}}^- \rangle \\ &= -\sum_j (-1)^{j+\frac{1}{2}} |c_j|^2 \langle \varphi^j_{\frac{1}{2}} | J_+ | \varphi^j_{-\frac{1}{2}} \rangle \\ &= \sum_j (-1)^{j-\frac{1}{2}} |c_j|^2 (j+\tfrac{1}{2}) \end{aligned} \qquad (10.2.2)$$

This result is in good agreement with experiment.

Peculiar to deformed nuclei is the appearance of an asymptotic selection rule in $\Delta\Lambda$. For example, the β-decay operator is τ_+ for Fermi transitions and $\vec{\sigma}\tau_+$ for Gamow-Teller, so that all β-decay is forbidden unless $\Delta\Lambda = 0$. Even for finite deformation when Λ is not a good quantum number there still remains a large hindrance factor.

In common with spherical nuclei electromagnetic multipole matrix elements, calculated with the above wave function, will be inaccurate for the following two major reasons.

The first effect is due to pairing. We should have

$$\langle \varphi_{\nu_2} | F | \varphi_{\nu_1} \rangle = u_{\nu_2} u_{\nu_1} \langle \nu_2 | F | \nu_1 \rangle - v_{\nu_2} v_{\nu_1} \langle \bar{\nu}_1 | F | \bar{\nu}_2 \rangle$$

$$= (u_{\nu_2} u_{\nu_1} - \tau v_{\nu_2} v_{\nu_1}) \langle \nu_2 | F | \nu_1 \rangle \qquad (10.2.3)$$

where $\tau = \pm 1$ according as F is $\pm$ve under time reversal. Now electric operators are +ve and magnetic are −ve, so that the former are hindered by pairing while the latter are not significantly affected.

Secondly, the odd particle can polarize the core or, in other words, couple to core vibrations. One can calculate this effect explicitly or take it into account implicitly by the use of an effective charge.

11. THE MOMENT OF INERTIA

11.1. The rigid-body estimate

The simplest estimate of the nuclear moment of inertia is obtained by treating it as a rigid body:

$$\mathcal{I}_{\text{rig}} = M \sum_k^A \langle y_k^2 + z_k^2 \rangle \approx \frac{2}{5} AMR_0^2 (1 + 0.33\beta) \qquad (11.1.1)$$

where, for an axially symmetric nucleus,

$$\beta = a_{20} \quad \text{(see below)},$$

and measures the deformation in the intrinsic co-ordinate frame.

A comparison with experiment, Fig. 33 shows that $\mathcal{I}_{\text{rig}}$ is something like a factor 2 too large.

11.2. The irrotational flow model

The fact that $\mathcal{I}_{\text{rig}}$ is too large comes as no great surprise. The nucleons are not frozen inside the nucleus and we might expect the nucleus to behave more like a liquid drop.

If the kinetic energy term $\frac{1}{2}B \sum |\dot{\alpha}_{2\mu}|^2$ of the liquid drop Hamiltonian is transformed into intrinsic and rotational co-ordinates

$$\text{i.e. } \alpha_{2\mu} = \sum \mathcal{D}^2_{\mu\nu}(\theta) a_{2\nu} \qquad (11.2.1)$$

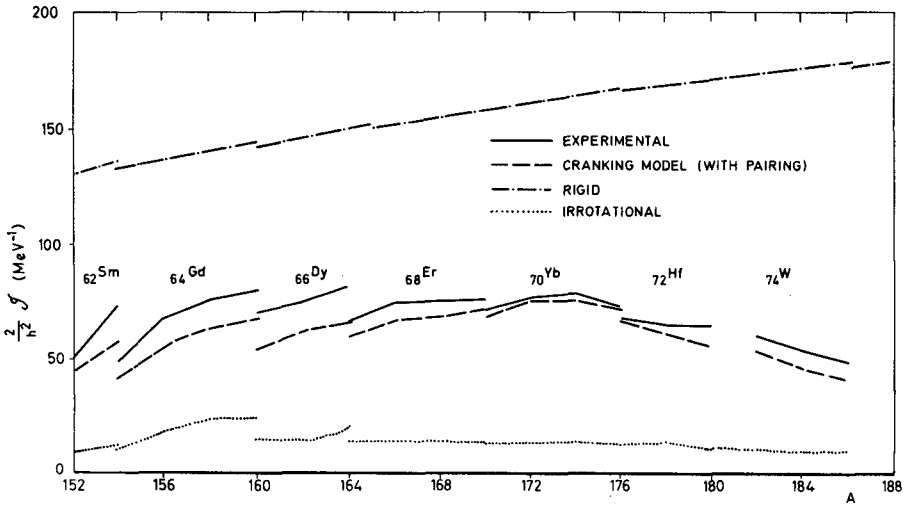

FIG.33. Comparison of estimated $\mathcal{J}$ with its experimental value

such that

$$a_{20} = \beta \cos\gamma, \quad a_{22} = a_{2-2} = \frac{1}{\sqrt{2}}\beta \sin\gamma$$
$$a_{21} = a_{2-1} = 0 \tag{11.2.2}$$

then it splits up into a vibrational and a rotational part

$$\frac{1}{2} B \sum_{\mu} |\dot{\alpha}_{2\mu}|^2 = \frac{1}{2} B(\dot{\beta}^2 + \beta^2 \dot{\gamma}^2) + \sum_{k=1}^{3} \frac{\hbar^2 R_k^2}{8B\beta^2 \sin^2\left(\gamma - k\frac{2\pi}{3}\right)} \tag{11.2.3}$$

Thus we have the moment of inertia

$$\mathcal{J}_k = 4B\beta^2 \sin^2\left(\gamma - k\frac{2\pi}{3}\right), \qquad k = 1, 2, 3 \tag{11.2.4}$$

so that, for an axially symmetric nucleus ($\gamma = 0$), we have

$$\mathcal{J}_3 = 0 \qquad \mathcal{J}_1 = \mathcal{J}_2 = 3B\beta^2 \tag{11.2.5}$$

Taking the irrotational flow value for B

$$B = \frac{3}{8\pi} AMR_0^2 \tag{11.2.6}$$

$$\mathcal{J}_1 = \mathcal{J}_2 = \frac{9}{8\pi} AMR_0^2\beta^2 \approx 0.9\beta^2 \frac{2}{5} AMR_0^2 \tag{11.2.7}$$

A comparison with experiment shows that $\mathcal{I}_{in}$ is generally about a factor of 5 too small.

This is similar to the result found for B itself for vibrations. It appears that if we use the measured rather than the hydrodynamic estimate for B, in the expression for the moment of inertia, we get something approaching the correct answer.

11.3. The cranking model

Using the Nilsson model for the intrinsic structure, we can hope to derive the moment of inertia on a more microscopic basis.

The idea of the cranking model is to look for an intrinsic wave function which is stationary in a rotating co-ordinate frame. Let this frame be rotating about the x-axis with angular velocity ω. Let the rotating and space-fixed axes coincide at time t. Then the rotating wave function $\varphi(\vec{r}, t)$ is a solution of

$$H\varphi(\vec{r}, t) = i\hbar \frac{\partial}{\partial t} \varphi(\vec{r}, t) \tag{11.3.1}$$

expressed in the co-ordinates of the space-fixed frame. Related to this wave function we can define $\hat{\varphi}(\vec{r}, t)$

$$\hat{\varphi}(\vec{r}, t) = e^{i\omega t J_x} \varphi(\vec{r}, t) \tag{11.3.2}$$

which is stationary in the stationary frame. The wave equation for $\hat{\varphi}$ is

$$H\hat{\varphi}(\vec{r}, t) = i\hbar \frac{\partial}{\partial t} \hat{\varphi}(\vec{r}, t) + \omega J_x \hat{\varphi}(\vec{r}, t) \tag{11.3.3}$$

Since we now require $\hat{\varphi}$ to be stationary in the stationary frame it must obey the eigenfunction equation

$$(H - \omega J_x)\hat{\varphi}(\omega) = E(\omega)\hat{\varphi}(\omega) \tag{11.3.4}$$

where

$$\hat{\varphi}(\vec{r}, t) = \hat{\varphi}(\omega) e^{-\frac{i}{\hbar} E(\omega) t} \tag{11.3.5}$$

If we find $\hat{\varphi}(\omega)$ we can determine the moment of inertia from

$$\langle \varphi(\vec{r}, t) | J_x | \varphi(\vec{r}, t) \rangle = \langle \hat{\varphi}(\omega) | J_x | \hat{\varphi}(\omega) \rangle \equiv \mathcal{I}_x \omega \tag{11.3.6}$$

or from

$$\langle \varphi(\vec{r}, t) | H | \varphi(\vec{r}, t) \rangle = \langle \hat{\varphi}(\omega) | H | \hat{\varphi}(\omega) \rangle$$
$$\equiv \langle 0 | H | 0 \rangle + \tfrac{1}{2} \mathcal{I}_x \omega^2 \tag{11.3.7}$$

where

$$|0\rangle = \hat{\varphi}(0) \tag{11.3.8}$$

To determine $\hat{\varphi}(\omega)$ for small ω, we use perturbation theory for the extra term ωJ_x in the Hamiltonian. Thus

$$\hat{\varphi}(\omega) = |0\rangle + \omega \sum_{i \neq 0} \frac{\langle i|J_x|0\rangle}{E_i - E_0} |i\rangle \tag{11.3.9}$$

and

$$\langle \hat{\varphi}(\omega)|J_x|\hat{\varphi}(\omega)\rangle = 2\omega \sum_{i \neq 0} \frac{|\langle i|J_x|0\rangle|^2}{E_i - E_0} \tag{11.3.10}$$

Hence we get the moment of inertia

$$\mathcal{I}_x = 2 \sum_{i \neq 0} \frac{|\langle i|J_x|0\rangle|^2}{E_i - E_0} \tag{11.3.11}$$

To check that the energy comes out correctly, evaluate

$$\langle \hat{\varphi}(\omega)|H|\hat{\varphi}(\omega)\rangle = E_0 + \sum_{i \neq 0} |c_i|^2 (E_i - E_0)$$

$$= E_0 + \omega^2 \sum_{i \neq 0} \frac{|\langle i|J_x|0\rangle|^2}{E_i - E_0}$$

$$= E_0 + \tfrac{1}{2}\mathcal{I}_x\omega^2 \neq E(\omega) = E_0 - \tfrac{1}{2}\mathcal{I}_x\omega^2$$

To evaluate $\mathcal{I}_x$ we must feed in the wave functions $|i\rangle$ from our model for the intrinsic structure. For independent particles in a deformed potential (e.g. Nilsson model), the ground state $|0\rangle$ for an even-even nucleus has $K = 0$ and $|i\rangle$ is a particle-hole state $|\nu_p(\nu'_h)^{-1}\rangle$ so that

$$\langle i|J_x|0\rangle = \langle \nu_p|J_x|\nu'_h\rangle \tag{11.3.12}$$

Inserting in the expression for $\mathcal{I}_x$, we get

$$\mathcal{I}_x = 2 \sum_{\nu_p \nu'_h} \frac{|\langle \nu_p|J_x|\nu'_h\rangle|^2}{E_{\nu_p} + E_{\nu_h}} \tag{11.3.13}$$

This expression can be evaluated analytically in the special case of the pure deformed harmonic oscillator potential, without a spin orbit force or residual interactions. It leads to some interesting results. For spherical nuclei it vanishes identically, regardless of model, as is obvious if $J_x|0\rangle \equiv 0$. For deformed nuclei, the core contributes an amount equal to the irrotational flow value, while the extra core particles bring the

moment of inertia up to the rigid body value. (For a discussion of this phenomenon see Inglis [28] and Villars [29].)

This model for the intrinsic structure is of course unrealistic. To obtain results in agreement with experiment, it is necessary to put in the spin-orbit force and short-range interactions. The extension of the above formula to include 'pairing' is straightforward

$$\langle i|J_x|0\rangle - \langle \nu|J_x|\nu'\rangle u_\nu v_{\nu'} + \langle \bar{\nu}'|J_x|\bar{\nu}\rangle v_\nu u_{\nu'}$$

$$= \langle \nu|J_x|\nu'\rangle (u_\nu v_{\nu'} - v_\nu u_{\nu'}) \qquad (11.3.14)$$

and we get

$$\mathcal{I}_x = 2 \sum_{\nu\nu'} \frac{|\langle \nu|J_x|\nu'\rangle|^2 (u_\nu v_{\nu'} - v_\nu u_{\nu'})^2}{E_\nu + E_{\nu'}} \qquad (11.3.15)$$

A comparison of this result with experiment (Fig. 33) is seen to be very good. There is, however, one disturbing feature of the cranking model expression. It was derived in its general form, e.g. section 11.1, without reference to any model of the nuclear structure. One might suppose therefore that it should be exact if one knew the eigenfunctions of the exact Hamiltonian. But the true Hamiltonian is invariant under rotations. Its eigenstates are therefore also eigenstates of angular momentum, and $\mathcal{I}_x$ vanishes identically. The cranking model's success therefore appears to depend on the approximate nature of the deformed shell-model Hamiltonian, and in particular on the fact that it is not rotationally invariant. At first sight this casts some doubt on the model's general validity. To see what is happening, let us look at the 'pushing model' for translational motion, where we already know the answer.

11.4. The pushing model

The pushing model can be derived in a completely analogous manner. For the nuclear mass we find

$$\mathcal{M} = 2 \sum_{i \neq 0} \frac{|\langle i|P_x|0\rangle|^2}{E_i - E_0} \qquad (11.4.1)$$

Again we see that if the states $|0\rangle$ and $|i\rangle$ are eigenstates of the exact Hamiltonian, they are also eigenstates of the momentum and $\mathcal{M}$ vanishes.

What happens if we use eigenstates of the approximate shell-model Hamiltonian, H_{SM}? Since the kinetic energy term of the shell model is still exact, we have

$$[H_{SM}, X] = -\frac{i\hbar}{AM} P_x \qquad \text{(Galilean invariance)} \qquad (11.4.2)$$

and so

$$\langle i|P_x|0\rangle = \frac{i}{\hbar} AM \langle i|[H_{SM}, X]|0\rangle$$

$$= \frac{i}{\hbar} AM (E_i - E_0)\langle i|X|0\rangle \qquad (11.4.3)$$

Inserting this expression into the pushing model formula, we get

$$\mathcal{M} = \frac{i}{\hbar} AM \sum_{i \neq 0} \{\langle 0|P_x|i\rangle\langle i|X|0\rangle - \langle 0|X|i\rangle\langle i|P_x|0\rangle\}$$

$$= \frac{i}{\hbar} AM \langle 0|[P_x, X]|0\rangle$$

$$= AM \qquad (11.4.4)$$

Thus the shell-model Hamiltonian gives the exact mass, whereas the exact Hamiltonian does not. At first sight it might appear that the derivation $\mathcal{M} = AM$ for the shell model also applies in the exact case. In fact it breaks down if the wave functions $|0\rangle$ and $|i\rangle$ are unbounded, as are plane waves. This is because $X|0\rangle$ is not expandable in terms of a complete set of plane waves, being divergent at infinity.

The derivation of the pushing model formula oddly enough breaks down if the Hamiltonian is translationally invariant, i.e. if

$$[H, P] = 0 \qquad (11.4.5)$$

because the perturbed state, i.e. the ground state in the moving frame, is actually orthogonal to the unperturbed state. In other words, momentum is an adiabatic invariant. A perturbation method is therefore inappropriate and not surprisingly gives the wrong answer.

Similarly the cranking model will give a vanishing moment of inertia if used in conjunction with eigenstates of a rotational invariant Hamiltonian. This result must therefore be regarded as spurious. In practice this is no restriction since one would never apply the rotational model to a spherical nucleus.

REFERENCES

[1] EDEN, R.J., Nuclear Reactions I (Endt, P.M., Demeur, M., Eds.) North-Holland Publishing Co., Amsterdam (1959) 22.

[2] BLATT, J.M., WEISSKOPF, V.F., Theoretical Nuclear Physics, 4th ed., John Wiley & Sons, New York (1952) 300.

[3] BOHR, A., Mat.-fys. Meddr 26 14 (1952); BOHR, A., MOTTELSON, B.R., Mat.-fys. Meddr 27 16 (1953).

[4] NATHAN, O., NILSSON, S.G., "Collective nuclear motion and the unified model", Alpha-, Beta-, and Gamma-ray Spectroscopy (Siegbahn, K., Ed.) North-Holland Publishing Co., Amsterdam (1965) 601.

[5] MOTTELSON, B.R., Selected Topics in the Theory of Collective Phenomena in Nuclei, Varenna Summer School XV (1960).

[6] MARSHALEK, E., PERSON, L.W., SHELINE, R.K., Rev. mod. Phys. 35 (1963) 108.

[7] HECHT, K.T., "Collective models", Selected Topics in Nuclear Spectroscopy (Verhaar, B.J., Ed.) North-Holland Publishing Co., Amsterdam (1964).

[8] ARAÚJO, J.M., Nuclear Reactions II (Endt, P.M., Demeur, M., Eds.) North-Holland Publishing Co., Amsterdam (1962) 195.

[9] BRAUNSTEIN, A., de SHALIT, A., Phys. Lett. 1 (1962) 264.

[10] KISSLINGER, L.S., SØRENSEN, R.A., Mat.-fys. Meddr 32 9 (1960).

[11] BÈS, D.R., Mat.-fys. Meddr 33 2 (1961).

[12] BÈS, D.R., SZYMANSKI, Z., Nucl. Phys. 28 (1961) 42.

[13] MARSHALEK, E.R., RASMUSSEN, J.O., Nucl. Phys. 43 (1961) 438.
[14] KERMAN, A.K., SHAKIN, C.M., Phys. Lett. 1 (1962) 151.
[15] de BOER, J., et al., Phys. Rev. Lett. 14 (1965) 564.
[16] SØRENSEN, B., Phys. Lett. 21 (1966) 683.
[17] GOLDHABER, M., TELLER, E., Phys. Rev. 74 (1948) 1046.
[18] RAYLEIGH, (Lord) J.W.S., The Theory of Sound, MacMillan, London (1896).
[19] BETHE, H.A., LEVINGER, J.S., Phys. Rev. 78 (1950) 115.
[20] WILKINSON, D.H., Physica 22 (1956) 1039; RAND, S., Phys. Rev. 107 (1957) 208; WILKINSON, D.H., A. Rev. nucl. Sci. 9 (1959) 1.
[21] DANOS, M., FULLER, E.G., A. Rev. nucl. Sci. 15 (1962) 29.
[22] BRINK, D.M., Nucl. Phys. 4 (1957) 215.
[23] ELLIOTT, J.P., FLOWERS, B.H., Proc. R. Soc. 24, 2A (1957) 57.
[24] ROGERS, J.D., A. Rev. nucl. Sci. 15 (1965) 241.
[25] ROWE, D.J., Nucl. Phys. 61 (1965) 1.
[26] NIELSEN, O.B., Proc. Rutherford Jubilee Int. Conf. (1962) 317.
[27] NILSSON, S.G., Mat.-fys. Meddr 29 16 (1955); MOTTELSON, B.R., NILSSON, S.G., Mat.-fys. Meddr 1 8 (1959).
[28] INGLIS, D.R., Phys. Rev. 96 (1954) 1059; INGLIS, D.R., Phys. Rev. 103 (1956) 1786.
[29] VILLARS, F., A. Rev. nucl. Sci. 7 (1957) 185.

APPENDIX A. THE ROTATION MATRIX

A.1. DEFINITION

The rotation matrix enables us to express a function in terms of another reference frame, at an angle to the original frame.

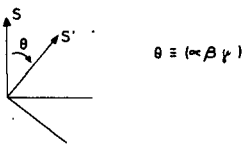

FIG. 34. Euler angles for the change of reference from frame S to S'

Suppose the Euler angles $(\alpha\beta\gamma)$ take the reference frame S into S' (Fig. 34) and that we have a function $\varphi(\vec{r}')$ in the S' frame, which we wish to express in terms of the S co-ordinates, $\varphi^{(\theta)}(\vec{r})$. Let the S and S' frames be initially coincident in the S' position, so that the function is initially $\varphi(\vec{r})$. We then rotate the axes from the initial S' to the final S orientation. This rotation can be performed by the operator $R(\alpha\beta\gamma)$ defined by

$$\varphi^{(\theta)}(\vec{r}) = R(\alpha\beta\gamma)\varphi(\vec{r}) = e^{-i\alpha J_z} e^{-i\beta J_y} e^{-i\gamma J_z} \varphi(\vec{r}) \qquad (A.1.1)$$

The rotation matrix is now defined by

$$\varphi^{(\theta)}_{jm}(\vec{r}) = R(\alpha\beta\gamma)\varphi_{jm}(\vec{r}) = \sum_{m'} \mathcal{D}^{*j}_{m'm}(\alpha\beta\gamma)\varphi_{jm'}(\vec{r}) \qquad (A.1.2)$$

If $\varphi_{jm}(\vec{r})$ transforms like a spherical harmonic $Y_{jm}(\theta)$

$$\mathscr{D}^{*j}_{m'm}(\alpha\beta\gamma) = \langle jm' | e^{-i\alpha I_z} e^{-i\beta I_y} e^{-i\gamma I_z} | jm \rangle$$

$$= e^{-im'\alpha} d^{*j}_{m'm}(\beta) e^{-im\gamma} \qquad (A.1.3)$$

A.2. PROPERTIES OF THE ROTATION MATRIX

(a) Symmetry:

$$\mathscr{D}^{*j}_{m'm}(\theta) = \mathscr{D}^{j}_{mm'}(-\theta) \qquad (A.2.1)$$

(b) Closure:

$$\sum_m \mathscr{D}^{*j}_{\mu m}(\theta)\, \mathscr{D}^{j}_{\nu m}(\theta) = \delta_{\mu\nu} = \sum_m \mathscr{D}^{*j}_{m\mu}(\theta)\, \mathscr{D}^{j}_{m\nu}(\theta) \qquad (A.2.2)$$

follows from the inverse rotation

$$\varphi_{jm'} = \sum_m \mathscr{D}^{*j}_{mm'}(-\theta)\varphi^{(\theta)}_{jm} = \sum \mathscr{D}^{j}_{m'm}(\theta)\varphi^{(\theta)}_{jm} \qquad (A.2.3)$$

(c) Combination:

$$\mathscr{D}^{j_1}_{\mu_1 m_1}(\theta)\, \mathscr{D}^{j_2}_{\mu_2 m_2}(\theta) = \sum_j (j_1 j_2 \mu_1 \mu_2 | j\mu)(j_1 j_2 m_1 m_2 | jm)\, \mathscr{D}^{j}_{\mu m}(\theta)$$

follows from rotating the coupled function

$$\chi_{jm}(12) = \sum_{m_1(m_2)} (j_1 j_2 m_1 m_2 | jm)\varphi_{j_1 m_1}(1)\varphi_{j_2 m_2}(2) \qquad (A.2.4)$$

(d) Orthogonality:

$$\int \mathscr{D}^{j}_{\mu m}(\theta) d\vec{\theta} = 8\pi^2 \delta(j0)\, \delta(\mu 0)\, \delta(m0)$$

$$\int \mathscr{D}^{*j_1}_{\mu_1 m_1}(\theta)\, \mathscr{D}^{j_2}_{\mu_2 m_2}(\theta) d\vec{\theta} = \frac{8\pi^2}{2j_1+1} \delta_{j_1 j_2} \delta_{\mu_1 \mu_2} \delta_{m_1 m_2} \qquad (A.2.5)$$

$$\int \mathscr{D}^{*j_3}_{\mu_3 m_3}(\theta)\, \mathscr{D}^{j_2}_{\mu_2 m_2}(\theta)\, \mathscr{D}^{j_1}_{\mu_1 m_1}(\theta) d\vec{\theta} = \frac{8\pi^2}{2j_3+1} (j_1 j_2 \mu_1 \mu_2 | j_3 \mu_3)(j_1 j_2 m_1 m_2 | j_3 m_3)$$

A.3. ROTATING CO-ORDINATES

Suppose S is the laboratory-fixed co-ordinate frame and S' can rotate with respect to S. Thus θ becomes a dynamic variable, and can have associated with it an angular momentum $\vec{R}$. The total angular momentum of the system $\vec{I}$ is then

$$\vec{I} = \vec{R} + \vec{J} \tag{A.3.1}$$

where $\vec{J}$ acts on $\vec{r}$ and leaves θ alone, while $\vec{R}$ acts on θ and leaves $\vec{r}$ alone. Now[11]

$$\vec{I}\,\varphi^{(\theta)} \equiv (\vec{R} + \vec{J})\,\varphi^{(\theta)} = 0 \tag{A.3.2}$$

and

$$\varphi_{jm}(\vec{r}) = \sum_{m'} \mathscr{D}^{j}_{mm'}(\theta)\,\varphi^{(\theta)}_{jm'} \tag{A.3.3}$$

so that

$$\vec{I}\,\varphi_{jm} = \sum_{m'} (\vec{I}\,\mathscr{D}^{j}_{mm'}(\theta))\,\varphi^{(\theta)}_{jm'} \tag{A.3.4}$$

Thus we obtain the important relations

$$\begin{aligned} I^2\,\mathscr{D}^{I}_{MK}(\theta) &= I(I+1)\,\mathscr{D}^{I}_{MK}(\theta) \\ I_z\,\mathscr{D}^{I}_{MK}(\theta) &= M\,\mathscr{D}^{I}_{MK}(\theta) \\ I_\pm\,\mathscr{D}^{I}_{MK}(\theta) &= \sqrt{(I \mp M)(I \pm M + 1)}\;\mathscr{D}^{I}_{M\pm1,K}(\theta) \end{aligned} \tag{A.3.5}$$

where

$$I_\pm = I_x \pm i I_y \tag{A.3.6}$$

We also have the identity

$$\begin{aligned} 0 &= \vec{R}\,\varphi_{jm}(\vec{r}) \\ &= \sum \left\{ (\vec{R}\,\mathscr{D}^{j}_{mm'}(\theta))\varphi^{(\theta)}_{jm'} - \mathscr{D}^{j}_{mm'}(\theta)(\vec{J}\,\varphi^{(\theta)}_{jm'}) \right\} \end{aligned} \tag{A.3.7}$$

---

[11] This is because $\vec{J}$ rotates the system, $\vec{R}$ rotates the axes it is measured with respect to, so that there is no observable effect. Mathematically:

$$e^{-i\alpha\vec{J}}\,\varphi^{(\theta)}(\vec{r}) = R(\theta)\,R(\alpha)\,\varphi(\vec{r}) = R(\theta)\,\varphi^{(\alpha)}(\vec{r}) = \varphi^{(\theta+\alpha)}(\vec{r})$$

$$e^{-i\alpha\vec{R}}\,\varphi^{(\theta)}(\vec{r}) = \varphi^{(\theta-\alpha)}(\vec{r})$$

whence

$$I'_{\pm}\,\mathscr{D}^{I}_{MK}(\theta) = \sqrt{(I \pm K)(I \mp K + 1)}\;\mathscr{D}^{I}_{M\,K\mp1}(\theta)$$
$$I_3\,\mathscr{D}^{I}_{MK}(\theta) = K\,\mathscr{D}^{I}_{MK}(\theta) \qquad \text{(A.3.8)}$$

where

$$I'_{\pm} = I_1 \pm i I_2 \qquad \text{(A.3.9)}$$

and 1, 2, 3 are the xyz axes of the S' frame.

CHAPTER 3

ISOSPIN AND ITS CONSEQUENCES IN NUCLEAR PHYSICS

G.M. TEMMER

1. Introduction and definition of isospin. Its formalism. 1.1. Historical development. 1.2. Equality of nuclear faces. 1.3. Net nuclear binding energy. 1.4. Definition of isospin. 1.5. Connection between charge exchange operator and isospin operator. 1.6. The concept of charge parity. 1.7. Sources of possible isospin impurities. 1.8. Generalized Pauli principle. 1.9. Role of charge independence. 1.10. Isospin impurities. 2. Isospin selection rules. 2.1. General. 2.2. Beta decay. 2.3. Radiative selection rules. (a) E1 transitions. (b) M1 transitions. (c) Applications to photonuclear reactions. 2.4. Selection rules for particle reactions. (a) Direct reaction mechanism. (b) Resonance reactions. 3. Special consequences of isospin conservation in nuclear reactions. 3.1. An intensity prediction. (a) Compound nucleus formation. (b) Direct reaction picture. 3.2. Compound resonance isospin inferred. 4. Isospin forbidden reactions. 4.1. Example. 4.2. Overriding angular momentum and parity selection rules which simulate isospin conservation. 4.3. Isospin-forbidden compound nucleus reactions. 5. A symmetry theorem based on isospin. 5.1. Theorem and example. 5.2. More examples. 5.3. Special symmetry selection rules. 5.4. An addendum to the Barshay-Temmer theorem. 6. Charge exchange reactions. 6.1. Experiments. 6.2. Shell-model view of analogue states. 6.3. Theoretical description of charge-exchange reactions. 6.4. Quasi-inelastic scattering. 6.5. Anderson's experiments. 7. T-splitting. 7.1. General. 7.2. Expansions of states in terms of states with good T. 7.3. Isospin doublet splitting in $^{89}_{40}Zr_{49}$. 7.4. Effective nucleon-nucleon interaction. 8. A look at $d_{3/2}$ hole states in the $f_{7/2}$ shell. 8.1. Low-lying hole states in the $f_{7/2}$ region. 8.2. Nucleon holes. 8.3. Other hole states. 9. Isospin in pick-up and stripping reactions. 9.1. General remarks. 9.2. Example: ^{60}Ni(p, d) ^{59}Ni. 9.3. General remarks concerning direct (p, d) (d, p) reactions. 9.4. Centre of gravity displacement between $T_<$ and $T_>$ states. 9.5. Determination of U_1. 9.6. Nucleon transfers. 9.7. Coulomb energy difference for (p, d) reactions. 9.8. Second Coulomb energy difference. 10. Isobaric analogue resonance. 10.1. Introduction. 10.2. Energetics of analogue resonance reactions. 10.3. Elastic analogue resonances and isospin impurities. 10.4. Resonances in the medium to heavy region. 10.5. The reaction ^{89}Y + p. 10.6. Comparison of stripping and elastic scattering reduced widths. 10.7. Fine structure in isobaric analogue states. 10.8. Spreading width. 10.9. Comparison of reduced widths for proton and neutron addition (or removal). 10.10. Analogue resonance in inelastic proton scattering. 10.11. The window effect in inelastic scattering. 10.12. Remark. 10.13. Summary. 10.14. Polarization measurements on analogue resonances. 11. Other ways of forming analogue states. 11.1. Yavin method. 11.2. Photoprotons from $T_>$ states. 11.3. Coupling of the analogue channels in (d, p) and (d, n) reactions. 12. How good is isospin in heavy nuclei? 13. Coulomb displacement energies and isotope shifts.

1. INTRODUCTION AND DEFINITION OF ISOSPIN. ITS FORMALISM

1.1. Historical development

We shall start with a short historical development of the concept of isospin from its initial formulation in 1932 until the present (1966). Heisenberg's first paper [1] introducing the idea of an analogy between

The author is in the Department of Physics, Rutgers, The State University, New Brunswick, NJ, United States of America.

[1] W. Heisenberg, Z. Phys. 77 (1932) 1-11.

TABLE I. A COMPARISON OF THE TOTAL BINDING ENERGIES FOR ISOBARS OF MASS 200

Isobars	$^{200}_{79}Au$	$^{200}_{80}Hg$	$^{200}_{81}Tl$	$^{200}_{82}Pb$	$^{200}_{83}Bi$	$^{200}_{84}Po$
Total binding energy (MeV)	1579.7	1581.4	1578.8	1576.9	1533.5	1566.2

TABLE II. TABLE FOR MIRROR NUCLEI (ISO-DOUBLETS, $T = \frac{1}{2}$)

A	Nucleus	Total binding energy (MeV)	Coulomb energy (MeV)	Net nuclear binding energy (MeV)
3	^{3}H	- 8.486	0	- 8.486
	^{3}He	- 7.723	+ 0.829	- 8.552
13	^{13}C	- 97.10	+ 7.631	-104.734
	^{13}N	- 94.10	+10.683	-104.770
23	^{23}Na	-186.54	+23.13	-209.67
	^{23}Ne	-181.67	+27.75	-209.42
41	^{41}Ca	-350.53	+65.91	-416.44
	^{41}Sc	-343.79	+72.84	-416.63

TABLE III. TABLE FOR ISOBARIC TRIPLETS (T = 1)

A	Nucleus	Total binding energy (MeV)	Coulomb energy (MeV)	Net nuclear binding energy (MeV)
10	^{10}Be	- 64.97	+ 3.33	- 68.30
	$^{10}B^{*}(1.74)$	- 63.01	+ 5.52	- 68.52
	^{10}C	- 60.04	+ 8.33	- 68.37
14	^{14}C	-105.27	+ 7.44	-112.71
	$^{14}N^{*}(2.31)$	-102.73	+10.42	-112.76
	^{14}O	- 98.73	+13.90	-112.63

the spin up-spin down duality for 1/2 particles (fermions), and the two states of a nucleon, proton and neutron, was truly a masterpiece of intuition. Information on n-p and p-p forces did not become available for several more years. Yet, only three months after the publication of Chadwick's paper on the discovery of the neutron, Heisenberg concluded that the neutron and proton could be treated as two states of the same particle – the nucleon. (Note: However, Heisenberg made a wrong guess concerning the actual relative strengths of p-p and n-p forces; in fact, he assumed that only the Coulomb force was acting between two protons.)

As an example of the type of evidence pointing to charge independence, let us compare the total binding energies for isobars of mass 200 (see Table I). These numbers indicate, at least to first order, that neutrons and protons must play rather similar roles in the nucleus.

1.2. Equality of nuclear forces

Experimental evidence began to accumulate around 1935 indicating that the nuclear n-n, p-p, and n-p forces were all equal. It came from various sources:

(a) Semi-empirical mass formulas did not distinguish much between neutrons and protons, but depended mainly on A. (Volume increases as $A^{1/3}$ and surface energy goes as $A^{2/3}$.)

(b) Nucleon-nucleon scattering: n-p and p-p scattering, when properly compared in the states allowed by the Pauli principle, seemed to be equal. Neutron-neutron scattering has never been directly studied, because of the difficulties in preparing a neutron target, and conclusions have been inferred only indirectly from such reactions as $\pi^- + d \rightarrow n + n + \gamma$ etc.

(c) Equivalence of the spectra of mirror nuclei: By equivalence of states we mean in all nuclear properties – energy, spin, parity, reduced widths, etc. This result assumed only charge symmetry (n - n = p-p) and not charge independence (n-n = p-p = n-p), since for mirror nuclei the number of n-p bonds are the same (see Tables II and III).

(d) Second order mirrors have equivalent states. (Example: ^{10}Be, ^{10}C; 2 protons changed into 2 neutrons.) The fact that these levels correspond to some of the levels of the middle member, e.g. ^{10}B, implies charge independence. We should realize, however, that even a rather large difference between the n-p force and the (n-n, p-p) forces would not substantially change the level structure since the n-p forces enter quite weakly here, producing only a small effect, so that this is not really a strong argument for charge independence.

There are obvious differences between neutrons and protons and their reactions: (a) Neutron-proton mass difference. (b) $\pi^+ - \pi^0$ mass difference, these mesons being presumably the "mediators" of the nuclear forces. (c) Different magnetic moments for the proton and neutron.

1.3. Net nuclear binding energies

The net nuclear binding energies of equivalent levels should be equal. To illustrate this point we subtract the Coulomb energy from the measured binding energies for several nuclei to compare the net nuclear binding energies.

The total Coulomb energy for discrete point protons uniformly distributed in a nucleus is conveniently expressed as:

$$E_c \cong 0.6 \frac{Z(Z-1)}{A^{1/3}} \text{MeV} \qquad (1.3.1)$$

using $r_0 = 1.41 \times 10^{-13}$ cm.

1.4. Definition of isospin

(a) The third component of the isospin vector $\vec{t}_z$ has a precise definition:

$$t_z = + \tfrac{1}{2} \text{ for the neutron} \qquad (1.4.1)$$

$$t_z = - \tfrac{1}{2} \text{ for the proton} \qquad (1.4.2)$$

and is a good quantum number as long as charge is conserved.

For a system of nucleons

$$T_z = \sum_{i=1}^{A} t_z^{(i)} = \frac{N-Z}{2} \qquad (1.4.3)$$

$$T_{max} = \frac{A}{2} \qquad (1.4.4)$$

(b) T itself can be regarded as a bookkeeping parameter which shows how many neutrons may be changed into protons (and vice versa) with impunity, consistent with the Pauli exclusion principle.

Possible T values are: $0 \rightarrow \frac{A}{2}$ (Even nuclei)

$$\tfrac{1}{2} \rightarrow \frac{A}{2} \text{ (Odd nuclei)}$$

$(2T+1)$ isobars belong to a family.

Figure 1 shows the example of four nucleons distributed among two energy levels (assumed to be both s-states) consistent with the Pauli principle. All possible configurations of two kinds of particles (white and black) with spin up or spin down, distributed among two states, are shown and classified into spin I and isospin T. One sees that the most symmetric configuration involves equal numbers of black and white particles with their spins paired off to zero, all lying in the lowest state ($T = 0$). This is presumably the alpha particle. Similar diagrams can be constructed for any given nuclear configuration.

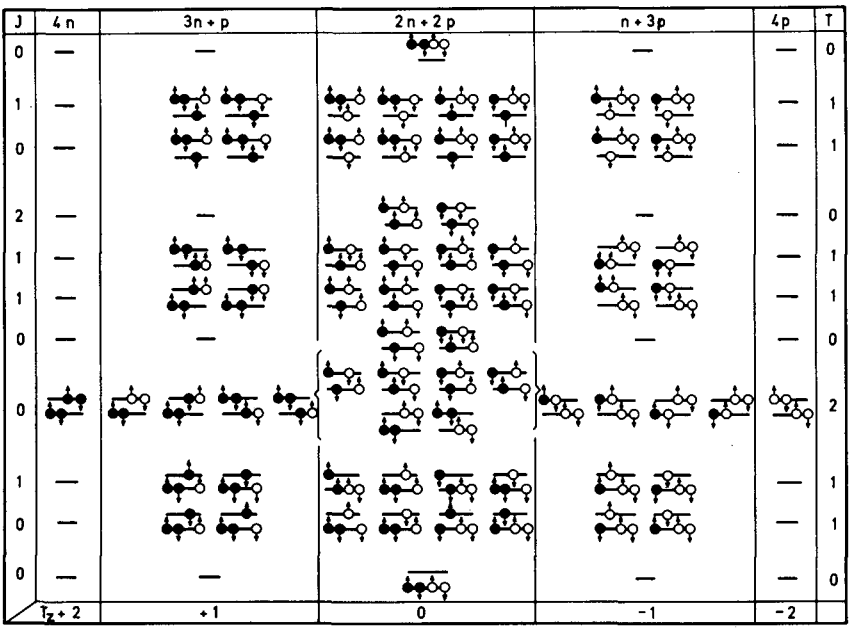

FIG. 1. An example of four nucleons distributed among two ($\ell = 0$) energy levels (consistent with the Pauli principle)

(c) The formalism developed for spin carries over intact to isospin

$$\tau_x = \begin{pmatrix} 0 & 1 \\ 1 & 0 \end{pmatrix}, \quad \tau_y = \begin{pmatrix} 0 & -i \\ i & 0 \end{pmatrix}, \quad \tau_z = \begin{pmatrix} 1 & 0 \\ 0 & -1 \end{pmatrix} \tag{1.4.5}$$

These isospin operators are equivalent, mathematically, to the ordinary Pauli spin operators, $\vec{\sigma}$.

(d) Experimentally, it is found that nuclei have $T = T_z$ in their ground states. There are exceptions such as ${}^{34}_{17}Cl_{17}$ ($T_z = 0$, $T = 1$ for the ground state; the first $T = 0$ level occurs at 143 keV excitation) and also ${}^{48}_{21}Sc$ seems to have $T = 1$ ground state ($I = 0^+$, of course).

(e) Differences between isospin and spin.

(1) The isospin vector does not point in real space.

(2) All particles are automatically polarized in isospin space.

(3) There is no isospin analogue to orbital angular momentum.

(f) We define $t_i \equiv \frac{1}{2}\tau_i$ as in the case of $\vec{s} = \frac{1}{2}\vec{\sigma}$

$$\tau^{\pm} = \tfrac{1}{2}(\tau_x \pm i\tau_y) \tag{1.4.6}$$

where τ^+ is called the raising operator and

τ^- is called the lowering operator.

$$\tau^+ = \begin{pmatrix} 0 & 1 \\ 0 & 0 \end{pmatrix} \tag{1.4.7}$$

transforms a proton state into a neutron state, and annihilates a neutron state.

$$\tau^- = \begin{pmatrix} 0 & 0 \\ 1 & 0 \end{pmatrix} \tag{1.4.8}$$

transforms a neutron state into a proton state, and annihilates a proton state.

A neutron state is represented by $\begin{pmatrix} 1 \\ 0 \end{pmatrix}$

and a proton state by $\begin{pmatrix} 0 \\ 1 \end{pmatrix}$

(g) We define $q^{\pm}$

$$q^+ = \tfrac{1}{2}(1+\tau_z) = \begin{pmatrix} 1 & 0 \\ 0 & 0 \end{pmatrix} \tag{1.4.9}$$

q^+ annihilates protons and maintains neutrons.

$$q^- = \tfrac{1}{2}(1-\tau_z) = \begin{pmatrix} 0 & 0 \\ 0 & 1 \end{pmatrix} \tag{1.4.10}$$

q^- annihilates neutrons and maintains protons

e.g.

$$q^+ n = \begin{pmatrix} 1 & 0 \\ 0 & 0 \end{pmatrix} \begin{pmatrix} 1 \\ 0 \end{pmatrix} = \begin{pmatrix} 1 \\ 0 \end{pmatrix}$$

$$q^+ p = \begin{pmatrix} 1 & 0 \\ 0 & 0 \end{pmatrix} \begin{pmatrix} 0 \\ 1 \end{pmatrix} = \begin{pmatrix} 0 \\ 0 \end{pmatrix} = 0 \text{ etc.} \tag{1.4.11}$$

1.5. Connection between charge exchange operator and isospin operator

(a) The charge exchange operator P^{τ}_{ik} changes neutrons into protons and vice versa.

$$P^{\tau}_{ik} = \tau^{(i)^-}\tau^{(k)^+} + \tau^{(i)^+}\tau^{(k)^-} + q^{(i)^-}q^{(k)^-} + q^{(i)^+}q^{(k)^-}$$

$$= \frac{1 + \vec{\tau}^{(i)} \cdot \vec{\tau}^{(k)}}{2} \tag{1.5.1}$$

as can be easily seen from the above definitions.

(b) In a nucleus

$$\vec{T} = \sum_{i=1}^{A} \vec{t}^{(i)} \tag{1.5.2}$$

where the eigenvalue of $t^2 = t(t+1)$ in analogy to $s^2 = s(s+1)$.

The eigenvalues of $\vec{T}^2$ are $T(T+1)$ from $\sum_{i=1}^{A} t^{(i)} = T$:

$$\vec{T}^2 = \frac{1}{4}\left[\sum_{i=1}^{A} \vec{\tau}^{(i)} \cdot \sum_{k=1}^{A} \vec{\tau}^{(k)}\right]$$

$$= \frac{1}{4}\left[\sum_{i=1}^{A} \left|\vec{\tau}^{(i)}\right|^2 + 2\sum_{i<k}^{A} \vec{\tau}^{(i)} \cdot \vec{\tau}^{(k)}\right]$$

$$= \frac{3}{4} A + \sum_{i<k}^{A} \frac{1}{2} (2 P_{ik}^{\tau} - 1)$$

since $$\left|\vec{\tau}^{(i)}\right|^2 = 3$$

$$\vec{T}^2 = \frac{3}{4} A + \sum_{i<k}^{A} (P_{ik}^{\tau} - \tfrac{1}{2})$$

but $$\sum_{i<k}^{A} (\tfrac{1}{2}) = \frac{A(A-1)}{2} (\tfrac{1}{2})$$

Consequently

$$\vec{T}^2 = \frac{3}{4} - \frac{A(A-1)}{4} + \sum_{i<k}^{A} P_{ik}^{\tau}$$

$$= A - \frac{A^2}{4} + \sum_{i<k}^{A} P_{ik}^{\tau} \qquad (1.5.3)$$

Consider two limiting cases:

(1) If isospin part is fully symmetric, then $P_{ik}^{(\tau)}$ always gives + 1.

Therefore $$\vec{T}^2 = A - \frac{A^2}{4} + \frac{A(A-1)}{2} = \frac{A}{2}\left(\frac{A}{2} + 1\right)$$

$$= T(T+1) \qquad (1.5.4)$$

where $T = A/2$, the maximum possible value of T for A nucleons of one kind.

(2) For two particles

$$T^2 = 1 + P_{12} \qquad (1.5.5)$$

Symmetric case: $P_{12} = +1$ therefore $T^2 = 2$ as given also by $T(T+1)$ for $T = 1$
Anti-symmetric case: $P_{12} = -1$ therefore $T^2 = 0$ as given also by $T(T+1)$ for $T = 0$.

Summary:

I-spin formalism is a way of properly keeping track of neutrons and protons as nucleons. It never leads to new results not also obtainable in the n-p scheme, but is a convenient framework for maintaining appropriate symmetries and classifying states according to their n-p exchange properties.

Consider a nucleus in a state $|T, T_z\rangle$, not considering any other quantum numbers.

$$T^{\pm}|T, T_z\rangle = \sqrt{(T \mp T_z)(T \pm T_z + 1)}\ |T, T_z \pm 1\rangle \qquad (1.5.6)$$

($T^{\pm}$: operator; $|T, T_z\rangle$: initial state; $|T, T_z \pm 1\rangle$: final state)

where $T^{\pm}$ is a raising (+) or lowering (-) operator of the T_z component only (cf. orbital angular momentum operators $L^{\pm}$).

e.g. if $T_z = T$ then

$$T^{+}|T, T\rangle = 0 \qquad (1.5.7)$$

since T_z cannot be greater than T

$$T^{-}|T, T\rangle = \sqrt{2T}\ |T, T-1\rangle \qquad (1.5.8)$$

1.6. The concept of charge parity (Ref. Kroll and Foldy)

Charge parity is another quantum number. Most of the tests on isospin purity, until recently, were done on self conjugate nuclei ($N = Z = A/2$), usually light nuclei. In order to explain the results one only required the conservation of charge parity and not of isospin.

(a) Consider the reaction

$$^{16}O(d, \alpha)^{14}N$$

$$T \quad 0 \quad 0 \quad 0 \qquad (1.6.1)$$

0 - ground state
1 - first excited state (2.31 MeV)

Charge parity says that one has either charge even or charge odd states. Once the charge state is even (or odd) it must remain so forever. In the case of $^{16}O(d, \alpha)^{14}N$ the initial state of $^{16}O + d$ is charge (T) even and therefore the reaction in which ^{14}N is left in the first excited charge-odd state is forbidden. However, charge parity conservation does not forbid $T = 2$ (charge even) in the final state. Therefore it is weaker than isospin conservation.

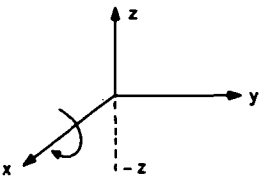

FIG. 2. Charge parity operation in isospin space

If one does not see T= 2 states being formed (and they are being identified at a rapid rate these days in $T_z = 0$ nuclei) then one can no longer use charge parity selection rules, but rather must invoke isospin conservation.

(b) For self-conjugate nuclei, the Hamiltonian is invariant under interchange of neutrons and protons, i.e. invariant under rotation of the isospin vector by 180° around the x-axis (Fig. 2)

$$P_T \equiv \text{charge parity operator} = \exp \frac{i}{\pi} T_x$$

$$= \exp i \frac{\pi}{2} \sum_{i=1}^{A} t_{(x)}^{(i)} \qquad (1.6.2)$$

Therefore

$$P_T = i^A \prod_{i=1}^{A} t_x^{(i)} \qquad (1.6.3)$$

H is invariant under this operation if $[P_T, H] = 0$. One has the same eigenfunctions for P_T and H but it can be shown that $[P_T, T_z] = 2 P_T T_z$ which is $\neq 0$ unless $T_z = 0$.

Therefore the eigenfunctions of T_z are not eigenfunctions of P_T except when $T_z = 0$; then P_T is a good quantum number. This is the case for self-conjugate nuclei, where one only needs to invoke charge symmetry (n- n = p - p) and not charge independence (n - n = p - p = n - p) of nuclear forces.

(c) As a charge parity consequence consider the following:

$$^{16}O\,(d, p)^{17}O$$

P_T (charge parity conservation) tells us that one must get the same amount of $^{16}O(d, n)^{17}F$. Since $^{16}O + d \rightarrow {}^{18}F^*$ (compound resonance) must be charge even, then only certain $^{17}O + p$ states are allowed.

1.7. Sources of possible isospin impurities

(a) First, let us consider the effect of the neutron-proton mass difference alone (δ = 782 keV). The rest energy and kinetic energy parts of the

Hamiltonian are written as

$$H = \sum_{i=1}^{A} \left[m_n c^2 \frac{(1+\tau_z^{(i)})}{2} + m_p c^2 \frac{(1-\tau_z^{(i)})}{2} \right]$$

$$- \sum_{i=1}^{A} \left[\frac{\hbar^2}{2m_n} \frac{(1+\tau_z^{(i)})}{2} + \frac{\hbar^2}{2m_p} \frac{(1-\tau_z^{(i)})}{2} \right] \Delta_i \qquad (1.7.1)$$

$$H = \underset{①}{A \frac{(m_n + m_p)c^2}{2}} + \underset{②}{(m_n - m_p)c^2 T_z} - \underset{③}{\frac{\hbar^2}{2m} \sum_{i=1}^{A} \Delta_i} + \underset{④}{\frac{\hbar^2 (m_n - m_p)}{4 m_n m_p} \sum_{i=1}^{A} \tau_z^{(i)} \Delta_i} \qquad (1.7.2)$$

where

$$m = \frac{2 m_n m_p}{(m_n + m_p)}$$

The first, second and third terms do not mix isospin; the second, however, produces an energy shift proportional to T_z; the fourth appears to violate isospin, i.e. mixes states with different T_z. It is probably small and usually neglected. However, in the case of the triton, since there is no Coulomb term, the presence of this fourth term might be felt in the Hamiltonian.

(b) Introducing the Coulomb energy term

$$\sum_{i<k}^{A} e^2 \frac{(1-\tau_z^{(i)})(1-\tau_z^{(k)})}{4 r_{ik}} \qquad (1.7.3)$$

We can write this as

$$\sum_{i<k}^{A} \frac{e^2}{4 r_{ik}} \{ (1 + \tfrac{1}{3} \vec{\tau}^{(i)} \cdot \vec{\tau}^{(k)}) - (\tau_z^{(i)} + \tau_z^{(k)}) + (\tau_z^{(i)} \tau_z^{(k)} - \tfrac{1}{3} \vec{\tau}^{(i)} \cdot \vec{\tau}^{(k)}) \} \qquad (1.7.4)$$

Scalar Vector Tensor

(1) The scalar terms can be lumped with the nuclear interaction. They introduce no T violation and no energy shifts between members of an isospin multiplet, just a general decrease of the effective nucleon-nucleon force.
(2) The vector term tilts the multiplet, i.e. it causes energy shifts proportional to T_z (due to charge effect). In first approximation the vector term produces a relative energy shift in second approximation it can produce admixtures of $T' = T \pm 1$.
(3) The tensor term introduces quadratic energy shifts. It introduces a

$$\Delta E \propto T_z^2 - \tfrac{1}{3} T(T+1) \qquad (1.7.5)$$

in second approximation it can produce isospin impurities $T' = T \pm 2$ (as well as $T' = T \pm 1$).
(4) Consider the isobaric multiplet mass formula $M = a + bT_z + cT_z^2$, where a, b, and c are functions of A and T, but not of T_z. One needs at least four members or more in the multiplet to make meaningful predictions since three terms are needed to determine, a, b, and c. Hence, $T = 3/2$ is the minimum value for useful comparisons.

(c) Scalar, vector, and tensor Coulomb energy terms
(Ref.: J. Jahnecke, Nuclear Physics 1966)

We obtain from first order perturbation theory the following expression for the energy of each member of an isobaric multiplet:

$$E_c(A,T,T_z) = E_c^{(0)}(A,T) - T_z E_c^{(1)}(A,T) + [(3T_z^2 - T(T+1))]\, E_c^{(2)}(A,T) \qquad (1.7.6)$$

where the scalar, vector and tensor Coulomb energies $E_c^{(0)}$, $E_c^{(1)}$, $E_c^{(2)}$ are coefficients independent of T_z. Inverting the above equation yields the following results for the coefficients

$$E_c^{(0)}(A,T) = \frac{1}{2T+1} \sum_{T_z=-T}^{+T} E_c(A,T,T_z) \qquad (1.7.7)$$

$$E_c^{(1)}(A,T) = \frac{3}{T(T+1)(2T+1)} \sum_{T_z=-T}^{+T} (-T_z) E_c(A,T,T_z) \qquad (1.7.8)$$

$$E_c^{(2)}(A,T) = \frac{5}{T(T+1)(2T-1)(2T+1)(2T+3)} \sum_{T_z=-T}^{+T} (3T_z^2 - T(TH)) E_c(A,T,T_z) \qquad (1.7.9)$$

These equations are overdetermined for $T > 1$. Any combination of three members of an isobaric multiplet can be used to extract $E_c^{(0)}$, $E_c^{(1)}$, $E_c^{(2)}$ and predict the energies of the other members of the multiplet. For $T = \frac{1}{2}$ we have

$$E_c^{(0)}(A,1/2) = \tfrac{1}{2}(E_c(A,1/2,-1/2) + E_c(A,1/2,+1/2)) \qquad (1.7.10)$$

$$E_c^{(1)}(A,1/2) = E_c(A,1/2,-1/2) - E_c(A,1/2,+1/2) \qquad (1.7.11)$$

and for $T = 1$

$$E_c^{(0)}(A,1) = \tfrac{1}{3}(E_c(A,1,-1) + E_c(A,1,0) + E_c(A,1,+1)) \qquad (1.7.12)$$

$$E_c^{(1)}(A,1) = \tfrac{1}{2}(E_c(A,1,-1) - E_c(A,1,+1)) \qquad (1.7.13)$$

$$E_c^{(2)}(A,1) = \tfrac{1}{6}(E_c(A,1,-1) - 2E_c(A,1,0) + E_c(A,1,+1)) \qquad (1.7.14)$$

The Coulomb energy difference between neighbouring members of a multiplet is given by

$$\Delta E_c(A, T, T_z \,|\, T_z + 1) = E_c(A, T, T_z) - E_c(A, T, T_z + 1) \tag{1.7.15}$$

in terms of which the above equations become

$$E_c^{(1)}(A, 1/2) = \Delta E_c(A, 1/2 - 1/2\,|\, + 1/2) \tag{1.7.16}$$

$$E_c^{(1)}(A, 1) = \tfrac{1}{2}(\Delta E_c(A, 1, -1\,|\,0) + \Delta E_c(A, 1, 0\,|\, + 1) \tag{1.7.17}$$

$$E_c^{(2)}(A, 1) = \tfrac{1}{6}(\Delta E_c(A, 1, -1\,|\,0) - \Delta E_c(A, 1, 0\,|\, + 1) \tag{1.7.18}$$

The masses of the members of an isobaric multiplet are given by $M(A, T, T_z) = M_0(A, T) + E_c(A, T, T_z) + T_z\delta$ where $\delta = 0.782$ MeV is the n-hydrogen mass difference.

The isobaric mass formula

$$M(A, T, T_z) = \alpha(A, T) + \beta(A, T)T_z + \gamma(A, T)T_z^2 \tag{1.7.19}$$

is obtained from the above expression for the masses of isobaric multiplet members by substituting for $E_c(A, T, T_z)$.

The relation between coefficients is then given by

$$\alpha(A, T) = M_0(A, T) + E_c^{(0)}(A, T) - T(T + 1)\, E_c^{(2)}(A, T) \tag{1.7.20}$$

$$\beta(A, T) = \Delta M - E_c^{(1)}(A, T) \tag{1.7.21}$$

$$\gamma(A, T) = 3E_c^{(2)}(A, T) \tag{1.7.22}$$

Let us consider first a uniformly charged sphere as a nuclear model with a radius $R = r_0 A^{1/3}$.

We then obtain

$$E_c = \tfrac{3}{5}\frac{e^2}{r_0}\frac{Z^2}{A^{1/3}} \tag{1.7.23}$$

and

$$\Delta E_c = \tfrac{6}{5}\frac{e^2}{r_0}\frac{Z}{A^{1/3}}, \quad Z = \frac{Z_1 + Z_2}{2} \tag{1.7.24}$$

then

$$E_c^{(1)} = \tfrac{3}{5}\frac{e^2}{r_0} A^{2/3} \tag{1.7.25}$$

and

$$E_c^{(2)} = \tfrac{1}{5}\frac{e^2}{r_0}\frac{1}{A^{1/3}} \tag{1.7.26}$$

Therefore

$$\frac{E_c^{(2)}}{E_c^{(1)}} = \frac{1}{3A} \tag{1.7.27}$$

so that

$$\frac{E_c^{(2)}}{E_c^{(1)}} \times A \cong 1/3 \tag{1.7.28}$$

and this is approximately found empirically.

1.8. The generalized Pauli principle (cf. MacDonald, 1960)

Consider a system of two nucleons. The wave functions can be factored into a product of space, spin and isospin parts. The eigenfunctions of (T, T_z) are given by

$$T = 1 \begin{cases} T_z = 1 \quad X(1,1) = X_+(1)X_+(2) \\ T_z = 0 \quad X(1,0) = \frac{1}{\sqrt{2}}\left(X_+(1)X_-(2) + X_+(2)X_-(1)\right) \\ T_z = -1 \quad X(1,-1) = X_-(1)X_-(2) \end{cases} \tag{1.8.1}$$

$$T = 0 \quad T_z = 0 \quad X(0,0) = \frac{1}{\sqrt{2}}\left(X_+(1)X_-(2) - X_+(2)X_-(1)\right) \tag{1.8.2}$$

These isospin functions are either symmetric or antisymmetric. The total wave function must also possess certain symmetry properties. The isospin functions $X(1,1)$, $X(1,-1)$ represent states of two neutrons and two protons, respectively. If $\phi_a(\alpha J)$ denotes the space and spin state of two neutrons or two protons with angular momentum J and other quantum numbers α, then $\phi_a(\alpha J)$ must be anti-symmetric under the interchange of two nucleons because of the ordinary Pauli principle. The total wave function for these states can then be written as

$$\psi(\alpha, J, T, T_3) = \phi_a(\alpha J)X(T, T_3) \quad (T, T_3) = (1,1);\ (1,-1) \tag{1.8.3}$$

For the neutron-proton system the spin and space wave function can be a linear combination of an anti-symmetric $\phi_a(\alpha, J)$ and a symmetric $\phi_s(\alpha, J)$. Since both symmetric and anti-symmetric isospin functions are available, $X(1,0)$ and $X(0,0)$, a totally anti-symmetric ψ can be constructed with either ϕ_s or ϕ_a.

$$\psi(\alpha J00) = \phi_s(\alpha J)\, X(0,0) \tag{1.8.4}$$

$$\psi(\alpha J10) = \phi_a(\alpha J)\, X(1,0) \tag{1.8.5}$$

It follows that any state of nucleons compatible with the Pauli principle can be described by linear combinations of wave functions which are anti-symmetric under the interchange of the space, spin and isospin co-ordinates of the nucleons. It turns out that the additional restrictions imposed by this condition are just offset by the additional freedom in forming symmetrized wave functions for mixed neutron-proton systems. The reason for using totally anti-symmetric wave functions rather than a set of independent unsymmetrized states is that the operation of symmetric nucleon operators, e.g. $T^{\pm}$, on totally anti-symmetric states will never yield wave functions which violate the Pauli principle.

For the two particle system the requirement of having an overall anti-symmetric wave function can be represented by

$$(-1)^{L} \times (-1)^{(S+1)} \times (-1)^{T+1} = -1 \tag{1.8.6}$$

or

$$(-1)^{S} (-1)^{T} (-1)^{L} = -1 \tag{1.8.7}$$

$$(-1)^{S+T+L} = -1 \tag{1.8.8}$$

General proofs have been given for many nucleon systems which show that it is sufficient (not necessary) to consider only those wave functions which are anti-symmetric under the exchange of co-ordinates of any two nucleons. This result is called the generalized Pauli principle.

1.9. Role of charge independence

The assumption of the charge independence of two-body nuclear forces ($[H, T^2] = 0$) and charge conservation imply a nuclear interaction with the following most general isospin dependence:

$$V(r_{ij}) = V^0(r_i r_j \sigma_i \sigma_j) + V^1(r_i r_j \sigma_i \sigma_j)\,(\vec{t}_i \cdot \vec{t}_j) \tag{1.9.1}$$

This interaction is explicitly charge independent (invariant under rotation in isospace). The experimental evidence available from a variety of two-nucleon scattering experiments supports charge independence, it does not however presently rule out a charge-dependent interaction amounting to a few per cent of the charge-independent interaction.

1.10. Isospin impurities (Refs. M. MacDonald, 1960, and Wilkinson, 1957)

Since isospin is approximately conserved, we shall use a set of basis states ψ_μ of good T, and calculate admixtures of other T' by perturbation theory. The Coulomb interaction will mix into a state of isospin T varying amplitudes of states with the same spin and parity but different ($T' \neq T$). In general, we can also have mixing of states of the same spin, parity, and T into a given state $\psi_0(T)$. The resultant

wave function for a state is then

$$\psi_0 = \Psi_0\ (T) + \sum_{\mu \neq 0} b_\mu(T)\psi_\mu\ (T) + \sum_{\nu\, T \neq T'} a_\nu^T(T')\psi_\nu(T') \qquad (1.10.1)$$

We will ignore the second term and consider only mixing with $T' \neq T$ states. The amplitude

$$a_\nu^T(T') = \frac{\langle \psi_\nu\ (T') | V_c | \psi_0(T) \rangle}{E_\nu - E_0} \qquad (1.10.2)$$

where V_c is the Coulomb interaction.

We shall define the impurity with T' in state T as

$$\sum_\nu \left| a_\nu^T\ (T') \right|^2 \qquad (1.10.3)$$

In light nuclei the impurity in the ground state is

$$10^{-3} > \sum_\nu \left| a_\nu^T(T') \right|^2 \geq 10^{-5} \qquad (1.10.4)$$

Sliv (Leningrad) has calculated the amount of T impurity in the ground states of nuclei. This starts at low values for light nuclei, peaks at

$$^{40}_{20}Ca_{20}\ (\sim 7\%),$$ and falls to about 2% at Pb!

There are a number of methods for determining these impurities from experiment:

(a) From E1 selection rule violations (cf. next section).
(b) From particle T-selection rule violations (see below).

Both of these yield the intensity of the impurity, namely

$$\left| \alpha^T(T) \right|^2$$

(c) From neutron-proton branching ratio in the emission reduced widths to members of an isospin multiplet. The predicted ratio is given by the vector coupling coefficients, and departures therefrom reflect isospin impurities, but as amplitudes $\alpha^T(T')$ if both the T and T' components can emit neutrons and protons and hence can interfere. An example is shown in Fig. 3 which may arise from (γ, p) and (γ, n)

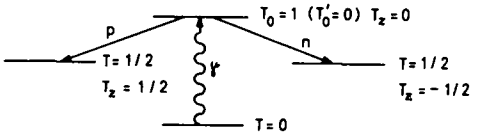

FIG. 3. Emission scheme for (γ, p) and (γ, n) reactions through the giant resonance $(T = 1)$

reactions through the giant resonance $(T = 1)$.

$$R = \frac{\gamma_p^2}{\gamma_n^2} = \frac{[(\frac{1}{2}\,\frac{1}{2}\,\frac{1}{2} - \frac{1}{2} \,|\, 10) + \alpha'(0)(\frac{1}{2}\,\frac{1}{2}\,\frac{1}{2} - \frac{1}{2} \,|\, 00)]^2}{[(\frac{1}{2} - \frac{1}{2}\,\frac{1}{2}\,\frac{1}{2} \,|\, 10) - \alpha'(0)(\frac{1}{2} - \frac{1}{2}\,\frac{1}{2}\,\frac{1}{2} \,|\, 00)]^2} = \left(\frac{1+\alpha'(0)}{1-\alpha'(0)}\right)^2 \qquad T_0 = 1 \qquad T_0' = 0$$

This radio is, in principle, very sensitive to impurities; e.g. an α^2 of 0.04 $(\alpha = 0.2)$ produces R = 2.25. There are however difficulties in evaluating the reduced widths and correcting properly for penetration effects.

2. ISOSPIN SELECTION RULES

2.1. General

Consider the matrix element

$$M = \langle TT_z \,|\, F \,|\, T'T_z' \rangle \qquad (2.1.1)$$

where only the isospin quantum numbers are shown explicitly. For a transition to occur between initial state $|T'T_z'\rangle$ and final state $|TT_z\rangle$ we must have $M \neq 0$. This imposes different conditions on the isospin quantum numbers involved, depending on the form of the operator F.

We consider several cases:

(a) F is invariant under rotation in isospace

$M = \delta_{TT'}\delta_{T_zT_z'} \neq 0$ only if $T = T'$, $T_z = T_z'$.

(b) $F = P_z$ (transforms like the third component of a vector)

$M \neq 0$ only if $T - T' = \pm 1$, $T_z = T_z'$ or $T = T'$ as long as $T_z = T_z' \neq 0$.

(c) $F = P^+$ (transforms like $T_x + iT_y$)

$M \neq 0$ only if $\begin{cases} T - T' = 0, \pm 1, \\ T_z = T_z' + 1. \end{cases}$

(d) $F = P^-$ (transforms like $T_x - iT_y$)

$M \neq 0$ only if $\begin{cases} T - T' = 0, \pm 1, \\ T_z = T_z' - 1. \end{cases}$

2.2. Beta decay. (Ref. S.D. Bloom, 1964)

The matrix element for β-decay can be written

$$H = \langle \psi_f | H_{\pm}^{\beta} | \psi_i \rangle; \quad H_{\pm}^{\beta} = \sum_k t_{\pm}^{(k)} O_k \tag{2.2.1}$$

where $\sum_k$ extends over all nucleons, and O_k is an operator depending on spin and space only. This implies that for allowed β-decay

$$\Delta T = 0, \pm 1 \quad \Delta T_z = \pm 1 \tag{2.2.2}$$

(a) For Fermi decay ($0^+ \to 0^+$), there is no nuclear structural change and O_k does not change with k;

$$H_{\pm}^{\beta} = O \sum_k t_{\pm}^{(k)} = O T^{\pm} \tag{2.2.3}$$

and we obtain $\Delta T = 0$, $\Delta T_z = \pm 1$ since $T^{\pm}$ conserves T and raises or lowers T_z.

(b) For Gamow-Teller decay, we have

$$\Delta T = 0, \pm 1, \quad \Delta T_z = \pm 1 \tag{2.2.4}$$

For a $\Delta T = 0$ transition with $\Delta I = 0$ ($I \neq 0$) both Fermi and G-T matrix elements contribute; however, only Fermi is allowed for $0^+ \to 0^+$ ($\Delta T = 0$) transitions.

(c) Example: (Ref.: Alford and French) (see Fig. 4)

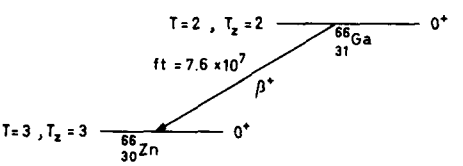

FIG. 4. $^{66}_{31}Gd \xrightarrow{\beta^+} {}^{66}_{30}Zn$ Fermi transition

Here we have $\Delta T = 1$, $0^+ \to 0^+$ which violates Fermi selection rule. This transition would go very fast (superallowed) if it were $\Delta T = 0$; here it decays only via the $T' = 3$ impurity in the $T = 2$ ground state of ^{66}Ga ($T' = 2$ impurity in $T = 3$ ground state of ^{66}Zn is impossible because $T \nless T_z$). Hence we can deduce the impurity as follows: For

a superallowed $0^+ \rightarrow 0^+$, $\Delta T = 0$ Fermi transition $(T, T_z) \rightarrow (T, T_z + 1)$

$$|M_F|^2 = (T - T_z)(T + T_z + 1) = 6 \text{ for } {}^{66}\text{Ga } \beta^+ \qquad (2.2.5)$$

Using the latest value for superallowed transitions

$$|M_F|^2_{SA} = \frac{6090}{(ft)_{SA}} \qquad (2.2.6)$$

we get for ^{66}Ga,

$$\text{impurity } |\alpha|^2 = \frac{|M_F|^2_{Ga}}{|M_F|^2_{SA}} = \frac{(ft)_{SA}}{(ft)_{Ga} \times 6} = \frac{6090}{7.6 \times 10^7 \times 6} = 1.3 \times 10^{-5} \qquad (2.2.7)$$

If the transition were superallowed, its half-life would be ~1 s instead of the observed 9.4 h.

2.3. Radiative transitions

The Hamiltonian for a system of nucleons interacting with an electromagentic field is given by

$$H^I = \sum_{i=1}^{A} \left\{ \frac{e}{Mc} \vec{p}_i \cdot \vec{A}(\vec{r}) \frac{1 - \tau_z^{(i)}}{2} + \left[\mu_n \frac{1 + \tau_z^{(i)}}{2} + \mu_p \frac{1 - \tau_z^{(i)}}{2} \right] \vec{\sigma} \cdot \nabla \times \vec{A} \right\} \qquad (2.3.1)$$

Orbital current contribution — Intrinsic nucleon moment contribution

This can be separated by

$$H^I = H^I_0 + H^I_1 = H^I_0 + \sum_{i=1}^{A} f_i \tau_z^{(i)} \qquad (2.3.1^*)$$

The first term is an isoscalar term and the second transforms as the third component of a vector in isospace.

The scalar term will allow transitions between states such that $\Delta T = 0$, $\Delta T_z = 0$.

The vector term will allow transition for which

$\Delta T = 0, \pm 1$, with $\Delta T = 0$ forbidden for $T_z = 0$ nuclei.

(a) E1 transitions

For the special (but important) case of E1 transitions, there is no contribution from the scalar term for $T_z = 0$, since this term is $(e/2Mc)\vec{p} \cdot \vec{A}$, i.e. the current produced by a system of equal charges, each having the value $e/2$.

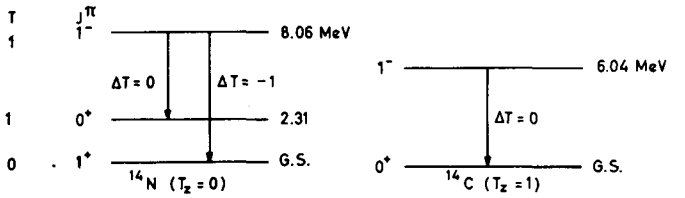

FIG. 5. Isospin-allowed and forbidden E1 transitions in $^{14}N(T_z = 0)$ and $^{14}C(T_z = 1)$

The selection rule on the vector part is

$$\begin{aligned} \Delta T &= 0, \pm 1 \qquad T_z \neq 0 \\ \Delta T &= \pm 1 \qquad\quad T_z = 0 \end{aligned} \tag{2.3.2}$$

Hence ΔT must algebraically change by one unit for $T_z = 0$ nuclei. Therefore E1 transitions can proceed in $T_z = 0$ nuclei between $T_i = T_f$ states only via (1) isospin impurities in initial and final states; (2) retardation terms of order $(kR)^2$ in the E1 matrix element; (3) the (n-p) mass difference which displaces center of mass from the center of charge; (4) recoil effects caused by emission or absorption of virtual mesons.

For example, consider the two E1 transitions in ^{14}N ($T_z = 0$) shown in Fig. 5. The $1^- \rightarrow 1^+$ transition is found to have normal strength ($\Delta T = 1$) while the 1^- to 0^+ transition has only 2% of normal strength ($\Delta T = 0$).

But, for $T_z \neq 0$, as in ^{14}C ($T_z = 1$), the analogue $\Delta T = 0$ transition is found to have normal strength.

For a thorough experimental investigation of the effect of the E1 selection rule, see the series of references by Wilkinson et al. (1953-1957).

(b) M1 Transitions (Ref. Morpurgo, 1958)

In the special case of $\Delta T = 0$ transitions, the matrix element for M1 transitions is, in general:

$$M(M1) \sim \left\langle f \left| \sum_{\text{protons}} \vec{L}^{(i)} + \mu_p \sum_{\text{protons}} \vec{\sigma}^{(i)} + \mu_n \sum_{\text{neutrons}} \vec{\sigma}^{(i)} \right| i \right\rangle$$

$$= \left\langle f \left| \sum_{i=1}^{A} \left[\vec{L}^{(i)} \left(\frac{1 - \tau_z^{(i)}}{2} \right) + \mu_p \vec{\sigma}^{(i)} \left(\frac{1 - \tau_z^{(i)}}{2} \right) + \mu_n \vec{\sigma}^{(i)} \left(\frac{1 + \tau_z^{(i)}}{2} \right) \right] \right| i \right\rangle \tag{2.3.3}$$

For self-conjugate nuclei ($T_z = 0$), the terms in $\tau_z^{(i)}$ cannot contribute for $\Delta T = 0$ transitions (see above); we are left with

$$M(M1)_{\substack{\Delta T = 0 \\ T_z = 0}} \sim \tfrac{1}{2} \left\langle f \left| \sum_{i=1}^{A} [\vec{L}^{(i)} + (\mu_p + \mu_n)\vec{\sigma}^{(i)}] \right| i \right\rangle \tag{2.3.4}$$

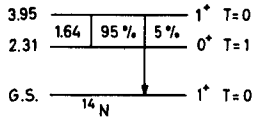

FIG. 6. Normal ($\Delta T = 1$) and inhibited ($\Delta T = 0$) M1 transitions in $^{14}N(T_z = 0)$

Adding and subtracting $\frac{1}{2}\vec{\sigma}^{(i)}$, we have

$$\frac{1}{2}\left\langle f\left|\sum_{i=1}^{A}\left[(\vec{L}^{(i)} + \frac{1}{2}\vec{\sigma}^{i}) + (\mu_p + \mu_n - \tfrac{1}{2})\vec{\sigma}^{(i)}\right]\right|i\right\rangle \qquad (2.3.5)$$

$\vec{J}$

The term $\langle f|\vec{J}|i\rangle = 0$ since $|i\rangle$ and $\langle f|$ are orthogonal and $\vec{J}$ is a constant of the motion.

There remains only

$$\tfrac{1}{2}(\mu_p + \mu_n - \tfrac{1}{2})\left\langle f\left|\sum_{i=1}^{A}\vec{\sigma}^{(i)}\right|i\right\rangle = 0.19\left\langle f\left|\sum_{i=1}^{A}\vec{\sigma}^{(i)}\right|i\right\rangle \qquad (2.3.6)$$

This is a small quantity, equivalent to all nucleons having no orbital contributions and intrinsic moments of ~ 0.19 nuclear magnetons.

For 'normal' M1 transitions, the dominant term multiplying $T_z^{(i)}$ is

$$\frac{1}{2}\left\langle f\left|\sum_{i=1}^{A}\tau_z^{(i)}\left[\vec{L}^{(i)} + (\mu_p - \mu_n)\vec{\sigma}^{(i)}\right]\right|i\right\rangle \qquad (2.3.7)$$

There the coefficient of $\vec{\sigma}^{(i)}$ is $(\mu_p - \mu_n)/2 = 2.35$. Hence the relative inhibition of the $\Delta T = 0$, $T_z = 0$ M1 matrix element is $(0.19/2.35)^2 \sim 6.5 \times 10^{-3}$; in other words, a smaller Weisskopf unit is appropriate for these transitions.

Example: (Fig. 6)

The observed branching ratio from the 3.95 MeV-state favours the $\Delta T = 1$ branch by 20 to 1, whereas the ground-state transition should a priori be 14 times stronger; hence the $\Delta T = 0$ branch is suppressed by a factor of 280. There is, in addition, a statistical favouring of the ground state in view of its spin of 1 compared to I = 0.

(c) Applications to Photonuclear Reactions

Examples: (γ, p), (γ, n), (γ, d), (γ, α).

These reactions combine radiative selection rules in the incoming channel and particle selection rules in the outgoing channel.

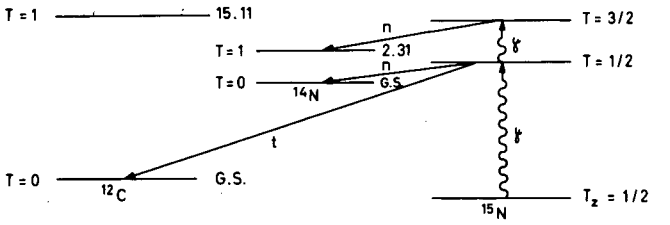

FIG. 7. Comparison of $^{15}N(\gamma,n)^{14}N$ with $^{15}N(\gamma,t)^{12}C$, between states of various isospins

(1) 4n target nuclei (n = integer): A giant dipole resonance will not be observed in a photonuclear reaction on a $T_z = 0$ target until we have enough energy in the incident gamma ray to excite the first T = 1 state in the target having spin 1^-. (Remember, for E1 transitions to occur in $T_z = 0$ nuclei, $\Delta T = \pm 1$). Once formed, the excited nucleus must decay subject to the condition that the vector sum of the isospins of the final particles T_1, T_2 be 1, i.e.

$$|T_1 - T_2| \leq |\leq T_1 + T_2 \qquad (2.3.8)$$

Thus for outgoing alpha particles in (γ, α) reactions, since T = 0 for alphas, one can only populate T = 1 states in the residual nucleus whereas an outgoing proton or neutron in (γ, p) or (γ, n) reactions can populate either $T = \frac{1}{2}$ or $T = \frac{3}{2}$ states in the residual nucleus. This selection rule accounts for the observed displacement of the (γ, α) yield peak toward higher energies compared to the (γ, p) and (γ, n) peak.

(2) 4n + 3 target nuclei: We can derive a selection rule for comparing (γ, n) with (γ, t) reactions on the same nucleus. The selection rule on gamma absorption ($T_z = \frac{1}{2} \neq 0$) shows that both $T = \frac{1}{2}$ and $\frac{3}{2}$ states can be reached in the target nucleus. The $T = \frac{1}{2}$ states can decay by neutron or triton emission to T = 0 states.

The $T = \frac{3}{2}$ states can decay only to T = 1 states. The final nucleus is A = 4n + 2 for the (γ, n) reaction, and A = 4n for the (γ, t) reaction. The T = 1 states in A = 4n + 2 nuclei begin at low energies, e.g. ^{6}Li(3.56), ^{10}B(1.74), ^{14}N(2.31), while in A = 4n light nuclei these states first occur at high excitation energies, e.g. ^{8}Be(16.62), ^{12}C(15.11), ^{16}O(12.79). Consequently, the (γ, t) reactions through $T = \frac{3}{2}$ states have a higher threshold, and the lowest such states can be observed in the (γ, n) cross-section but not in the (γ, t) cross-section. As an example, compare $^{15}N(\gamma, n)^{14}N$ with $^{15}N(\gamma, t)^{12}C$ (Fig. 7).

(3) Special case

^{6}Li(γ, α)d can never go through a giant resonance (E1) since the

$T\ 0\quad 0\ 0$

T = 1 compound states would be forced to decay through a T = 0 channel. The reaction will go by E2, M1, or by T impurity, but should be weak. At E_γ = 17 MeV, the cross-section is 5 μ barns. By comparison, ^{7}Li$(\gamma, t)^4$He has a cross-section of 120 μ barns.

(4) Giant dipole splitting (Fig. 8)

The relative probability of gamma exciting a T + 1 state relative to a T state (aside from all other possible factors not involving T) is shown in Fig. 8. The dipole photon can be described by $(\tau, 0)$ with $\tau = 1$

$$(E1)\alpha\, c^2 = (TT_z\, \tau 0 \,|\, TT_z)^2 = (TT\,|\,0\,|\,TT)^2 = \frac{T}{T+1} \qquad (2.3.9)$$

$$(E1)'\, \alpha c'^2 = (TT\tau 0 \,|\, T+1, T)^2 = \frac{1}{T+1} \qquad (2.3.10)$$

$$\frac{(E1)'}{(E1)} = \frac{1}{T}$$

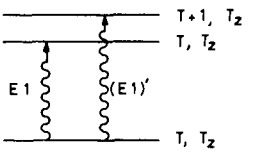

FIG. 8. E1-excitation to states of $T = T_z$ and $T' = T_z + 1$

2.4. Selection rules for particle reactions

(a) Direct reaction mechanism

(1) Coulomb excitation: As we have seen, we may violate isospin between initial and final states through the Coulomb field. (Most transitions are E2.)

$\Delta T = 0, \pm 1$ (as for general radiative transition)

Multiple Coulomb excitation: $\Delta T = n, n-1, \ldots, -n$, where n = order of multiple excitation.

(2) Direct, nuclear inelastic excitation (t = isospin projectile)

$\Delta T = 2t, 2t-1, \ldots, -2t$ (provided $T \geq T_z$).

(i) Direct collisions (see Fig. 9):

Here with no charge exchange $\Delta T = 0$; with charge exchange $\Delta T = 0, \pm 1$.

(ii) Exchange collisions (see Fig. 10):

Here with no charge exchange $\Delta T = 0, \pm 1$; with charge exchange $\Delta T = 0$. (Through an interaction $\frac{1}{2} + 2\vec{t}^{(i)} \cdot \vec{t}^{(i)}$ between incident nucleon (i) and target nucleon (j).)

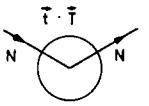

FIG. 9. Direct collision (N stands for nucleon)

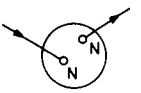

FIG. 10. Exchange collision (N stands for nucleon)

(3) Direct transfer reactions

Apply vector inequality for isospin

$$|T_r - T_t| = (t + t'), \ldots, -(t + t') \qquad (2.3.11)$$

Residual nucleus — Target — Projectile — Detected particle

For example, through the $^{26}_{T}\mathrm{Mg}\,(p,t)^{24}_{1}\mathrm{Mg}$ reaction we can excite $T = 2$ states in $^{24}\mathrm{Mg}$. If only neutrons are transferred, no Coulomb forces are directly involved; the same is true for neutron-induced reactions.

(b) Resonance reactions

The vector inequality still applies along with the additional condition that we must include the isospin of the compound nucleus.

$$A + a \rightarrow C^* \rightarrow B + b \qquad (2.3.12)$$

$$\vec{T}_A + \vec{T}_a = \vec{T}_C = \vec{T}_B + \vec{T}_b \qquad (2.3.13)$$

Isospin conservation for resonance reactions:

(1) Isolated resonances, see relation (2.3.13).
(2) Overlapping resonances.

I. If they have the same T, the isospin selection rule (2.3.13) holds for each resonance separately.
II. If we have different T's and

(i) different J^π, (2.3.13) still holds for each resonance separately
(ii) the same J^π, mixing occurs because of the Coulomb force.

(c) At very high excitation energies, with many broad overlapping resonances, T becomes good again. We must take the mixing time, $\tau_{\text{mixing}} = \hbar/H_{cc'}$, into account. $H_{cc'}$, the Coulomb matrix element, typically runs between 0.05 to 0.5 MeV. If $\tau_{\text{decay}} = \hbar/\Pi \ll \tau_{\text{mixing}}$, then

the system has no time to introduce isospin impurities and isospin is conserved. (Wilkinson, 1957). This happens for $\Gamma \gg H_{cc'}$.

3. SPECIAL CONSEQUENCES OF ISOSPIN CONSERVATION IN NUCLEAR REACTIONS

3.1. An intensity prediction

Let us consider the following example of the analogue reactions $^{9}Be(d,p)^{10}Be$ and $^{9}Be(d,n)^{10}B*$ (1.72 MeV, 0^+) and calculate the branching ratio (d, p)/(d, n) from isospin considerations alone. Furthermore, let us consider two extreme mechanisms.

(a) Compound nucleus formation

$$^{9}Be + d \rightarrow {}^{11}B* \begin{cases} \rightarrow p + {}^{10}Be \\ \rightarrow n + {}^{10}Be* \ (T = 1, 0^+) \end{cases} \qquad (3.1.1)$$

Using the notation $\Phi(T, T_z)$, the isospin triplet ^{10}Be, $^{10}B*$ and ^{10}C wave functions can be written as $\Phi(1,1)$, $\Phi(1,0)$, and $\Phi(1,-1)$. Writing the ^{11}B wave function as $\psi(1/2, 1/2)$ and the neutron and proton wave functions as $\varphi\ (1/2, t_z)$, we can expand $\psi(1/2, 1/2)$ into the following product sum:

$$\psi\ (1/2, 1/2) = \sum_{T_z t_z} C\ \Phi(1, T_z)\ \varphi(1/2\, t_z) \qquad (3.1.2)$$

where $C = (1, T_z,\ 1/2, t_z \mid 1/2, 1/2)$ are the Clebsch-Gordan coefficients, connecting (T, t) to (1/2, 1/2). Expanding the summation, the following terms survive:

$$\psi(1/2, 1/2) = (1, 1, 1/2, -1/2 \mid 1/2, 1/2)\ \Phi(1,1)\varphi(1/2, -1/2)$$

$$+ (1, 0, 1/2, 1/2 \mid 1/2, 1/2)\Phi(1,0)\varphi(1/2, 1/2)$$

$$= \sqrt{2/3}\ \Phi(1,1)\varphi(1/2, -1, 2) - \sqrt{1/3}\ \Phi(1,0)\varphi(1/2, 1/2) \qquad (3.1.3)$$

or

$$^{11}B = \sqrt{2/3}\ (^{10}Be + p) - \sqrt{1/3}\ (^{10}B + n) \qquad (3.1.4)$$

Therefore the intensity ratio is

$$\frac{(d,p)}{(d,n)} = \left|\sqrt{2/3} \Big/ -\sqrt{1/3}\right|^2 = 2 \qquad (3.1.4^*)$$

i.e. from isospin considerations the proton decay intensity should be twice that of the neutron decay channel.

(b) Direct reaction picture

$^{11}B^*$ does not enter here. One builds ^{10}Be from $^9Be + n$: $\Phi(1,1) = \psi(1/2,1/2)\varphi(1/2,1/2)$ while $^{10}B^*$ is constructed from

$$\Phi(1,0) = (1/2,1/2,1/2,-1/2\,|\,1,0)\psi(1/2,1/2)\varphi(1/2,-1/2) + (1/2,-1/2,1/2,1/2\,|\,1,0)\psi(1/2,-1/2)\varphi(1/2,1/2) \quad (3.1.5)$$

$$\Phi(1,0) = \frac{1}{\sqrt{2}}\psi(1/2;1/2)\varphi(1/2,-1/2) + \frac{1}{\sqrt{2}}\psi(1/2,-1/2)\varphi(1/2,1/2) \quad (3.1.6)$$

or

$$^{10}B^* = \frac{1}{\sqrt{2}}(^9Be + p) + \frac{1}{\sqrt{2}}(^9B + n).$$

Therefore the intensity ratio

$$\frac{^9Be + n}{^9Be + p} = \left|\frac{1}{1/\sqrt{2}}\right|^2 = 2$$

as before.

This ratio therefore seems to cover all eventualities.

3.2. Compound resonance isospin inferred (see Fig. 11)

Example: $^9Be + p \rightarrow {}^{10}B^* \rightarrow {}^6Li^* + \alpha$

Alpha particles are observed only to the 0^+, T = 1 state in ^6Li when forming the proton resonance at 8.89 MeV in $^{10}B^*$; we infer that the 8.89 MeV state in ^{10}B has T = 1. Note that the incoming proton channel can form either T = 0 or T = 1.

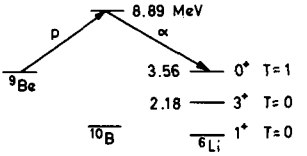

FIG. 11. $^9Be(p,\alpha)^6Li$ through resonance in ^{10}B

4. ISOSPIN FORBIDDEN REACTIONS

4.1. General

Intrinsic $\Delta T = 0$ reactions cannot connect states that differ in T. Using $\Delta T = 0$ reactions such as (d,α), (α,d), (d,d') etc., one can study

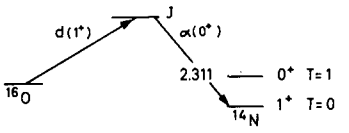

FIG. 12. $^{16}O(d,\alpha)^{14}N$

isospin impurities by bombarding $T = T_0$ nuclei and looking for excitation of $T = T_0 + 1$ states.

T impurities may arise from 3 sources: (1) projectiles carry isospin impurities; (2) targets have isospin impurities; (3) intermediate stages bring in impurities, either during compound nucleus formation, or through dynamic distortions.

Example:

Let us consider the isospin-forbidden reaction $^{16}O(d,\alpha)^{14}N^*$ ($T = 1$) which is found to excite $T = 1$ levels in ^{14}N weakly. The question here is: 'Where does the isospin impurity come from?' One possibility is the intermediate state in ^{18}F. To determine compound nucleus effects, one can examine other reactions such as $^{14}N(\alpha,\alpha')^{14}N^*$, $^{14}N(d,d')^{14}N^*$ and try to locate the sources of impurities.

4.2. Overriding angular momentum and parity selection rules which simulate isospin conservation

(a) Compound nucleus. Let us look at the foregoing reaction more closely. Since the deuteron has unnatural parity (1^+), angular momentum and parity conservation alone will restrict the L values of the reaction shown in Fig. 12.

Since the compound state can be formed with $J = \ell$, $\ell \pm 1$ and parity $(-1)^\ell$ is conserved, we can only reach states with $J = \ell$ i.e. only natural parity states, because otherwise alpha particles could not be emitted to the 0^+ state in ^{14}N. Thus angular momentum and parity restricts us to only one out of three J values in the compound nucleus, compared to ^{14}N states having $I \neq 0^+$ (such as the ground state). Moreover, there is a statistical factor of 3 against the 0^+ state.

(b) Direct reaction process. If the (d,α) reaction occurs by direct deuteron pick-up, then the $0^+ \rightarrow 0^+$ transition is completely forbidden, because of the unnatural parity of the deuteron. (The same would apply for ^6Li, ^{10}B and ^{14}N-induced reactions.)

(c) Example of an apparently isospin-forbidden compound resonance (Fig. 13): consider $\alpha + d \rightarrow {}^6Li^*$ ($T = 1$).

This is another example where spin and parity restrict reaction. One cannot excite the 0^+, $T = 1$ level in ^6Li because one cannot couple 1^+ (deuteron) and 0^+ (alpha) to form a 0^+ state and conserve parity. This is a bad case in which to look for isospin impurities, since the $T = 1$ state is 0^+. Hence a reduced reaction yield to an isospin forbidden state must be carefully examined before drawing conclusions as to isospin impurities.

The examination of (α,α') or (d,d') reactions for target nuclei with $T \neq 0$ will usually not suffer from the above difficulties and should reveal T impurities rather directly in nuclei with neutron excess.

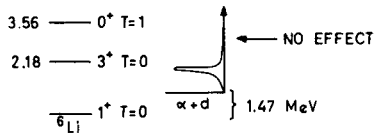

FIG. 13. $\alpha + d \rightarrow {}^{6}Li$ compound resonances

4.3. Isospin-forbidden compound nucleus reactions

The isospin selection rule for a compound nucleus reaction $A + a \rightarrow C^* \rightarrow B + b$ was given in section 2 as $\vec{T}_A + \vec{T}_a = \vec{T}_c = \vec{T}_B + \vec{T}_b$. In the light nuclei most targets have T = 0, 1/2 or 1 in their ground state, while projectiles have t = 0, 1/2. This would seem to limit us to studies of $T \leq 3/2$ compound states. Consider the example $^{16}O + p \rightarrow {}^{17}F^*$; here we would only expect to be able to excite T = 1/2 states in ^{17}F, while we would really like to look for the $(T, T_z) = (3/2, -1/2)$ member of the T = 3/2 quartet ^{17}N, ^{17}O, ^{17}F, and ^{17}Ne. Using a reaction such as $^{15}N + p \rightarrow {}^{16}O^*$ we can excite T = 0, 1 states and not the T = 2 states, which are of much current interest.

To excite compound states of T = 3/2, such as in ^{17}F, with the reaction $^{16}O + p$, we have to 'violate' isospin by one unit. Furthermore, if only the elastic and low-lying inelastic, as well as reaction channels are considered, we have to violate isospin twice, since the exit channel has the same T as the incoming channel. If excited $T = T_0 + 1$ levels in the target nucleus were energetically accessible, inelastic scattering to these states would only violate isospin once. Such might be the case when examining the 2nd T = 3/2 state in ^{13}N via the $^{12}C + p$ channel. Since the 15.11 eV (T = 1) state in ^{12}C is available, inelastic protons to this level would lead to isospin violation in the incoming channel only.

Since the Coulomb field can mix T_0 and $T_0 \pm 1$ states, T = 3/2 states might be excited in ^{17}F via T = 1 admixtures in the ^{16}O ground state, or T = 1/2 admixture in the T = 3/2 state in ^{17}F. By excitation of states such as these, several important facts can be learned: An estimate of $T = T_0 + 1$ impurities in the target nucleus ground state and $T = T_0'$ impurities in the compound state, the excitation energy of the compound states and their width. Since impurities arise from the $T = T_0 + 1$ part of the ground state wave function, the coefficient A_ν in the sum $\sum A_\nu \psi_\nu (T = T_0 + 1)$ can be estimated, which in turn allows estimates of the Coulomb matrix elements which mix these states.

Thus, in the reaction $^{16}O + p \rightarrow {}^{17}F^* (T = 3/2) \rightarrow {}^{16}O + p$, the T = 1 part of the ^{16}O wave function and the T = 1/2 part of the $^{17}F^*$ wave function are not zero if the T = 3/2 states are seen as resonances. In experiments such as these, done at Rutgers (Bredin et al., 1966), T = 3/2 states have been observed in the compound nucleus ^{17}F. The lowest T = 3/2 state in ^{13}N was seen as a compound nucleus resonance in elastic scattering of protons on ^{12}C, at an excitation energy of 15.068 ± 0.008 MeV, having a width of $\Gamma \sim 1.9$ keV. We must emphasize that these resonances are very sharp, having proton widths $\lesssim 1$ keV, due to the slight violation of the isospin selection rule. Since the interest has been generated in $T = T_0 + 1$ states in ^{13}N, ^{13}C, ^{29}P, etc., they also have been studied by reactions such as (p, γ), (α, n) and (α, γ).

Note that such reactions with gamma-rays in the outgoing channel are only "once" forbidden, since electromagnetic transitions can connect states whose T differ by unity.

5. A SYMMETRY THEOREM BASED ON ISOSPIN (Ref. Barshay and Temmer, 1964)

5.1. Theorem and example

Consider the reaction

$$A + B \leftrightarrows C + C' \tag{5.1.1}$$

where C and C' are members of an isospin multiplet, i.e. C and C' are related by a rotation in isospin space; they have the same t, the same spin and parity, but different values for t_z. The theorem states that if either A or B has T = 0, isospin considerations show that the differential cross-section must be symmetric about 90° (c.m.)

Since either A or B has T = 0, the left-hand side of the reaction couples to only one T value. If isospin is conserved, one must also have the same value of T on the right-hand side. Therefore let us couple the wave functions of C and C', in the above reaction, to the isospin value T.

$$[C + C']_T \Rightarrow [\phi(t, t_z)\,\phi(t, t_z')]_T \tag{5.1.2}$$

Example:

Consider the formation of the fermion doublets, ^{3}He-t, ^{13}C-^{13}N, etc. with t = 1/2. The generalized Pauli principle states that ψ_{total} must be anti-symmetric. Let us examine the reaction

$$^{16}O + {}^{10}B \rightarrow {}^{13}C + {}^{13}N \tag{5.1.3}$$

Since the T of both ^{16}O and ^{10}B is zero, T must equal zero for the final state. (The spin of ^{13}C and ^{13}N is 1/2$^-$).
Therefore

$$\psi_{total} = \psi^{anti\text{-}sym.}_{T=0} \times \phi_{space} \times \chi_{spin} \tag{5.1.4}$$

$$\text{or} \quad {}^{sym.}_{anti\text{-}sym.} \times {}^{sym.}_{anti\text{-}sym.}$$

The most general total wave function for a T = 0 state is

$$\psi_{total} = \psi^{anti\text{-}sym.}_{T=0}[a\,\chi^{sym.}_{spin} Y_\ell\,(even) + b\,\chi^{anti\text{-}sym.}_{spin} Y_\ell(odd)] \tag{5.1.5}$$

From the observable $|\psi_{total}|^2$, we see that there can be no cross terms since

$$\chi^{sym.}_{spin} \times \chi^{anti\text{-}sym.}_{spin} = 0 \tag{5.1.6}$$

i.e. they are orthogonal.

Hence there will only remain even powers of $\cos\theta$, and we will always have symmetry of $d\sigma/d\Omega(\theta)$ about 90°. Another way of seeing this is to realize that the forcing of the reaction into a unique T channel essentially treats the mirror nuclei as truly identical particles in space and spin, hence fore-and-aft symmetry.

One must ensure that there are no other overriding reasons for this symmetry, such as

(a) identical particles on one side of the reaction
e.g.,

$$\begin{array}{lcccc} & {}^{14}\mathrm{N} + {}^{14}\mathrm{N} & \rightarrow & {}^{14}\mathrm{C} + {}^{14}\mathrm{O} \\ T & 0 \quad 0 & & 1 \quad 1 & \\ T_z & & & +1 \quad -1 & \end{array}$$

(b) only one ℓ value participates, such as
(1) S wave only,
(2) L (characteristic ℓ value, especially for heavy-ion surface interaction, where L corresponds to kR);

(c) A definite spin and parity in an isolated intermediate-state resonance;

(d) Many overlapping resonances in the compound system (statistical, or Hauser-Feshbach régime).

5.2. More examples

(a) Consider the isospin triplet of mass 14. It can be formed, two members at a time, by various incident channels:

$$\begin{array}{lcccc} & {}^{24}\mathrm{Mg} + \alpha & \rightarrow & {}^{14}\mathrm{C} + {}^{14}\mathrm{O} \\ T & 0 \quad 0 & & 1 \quad 1 & \\ T_z & & & +1 \quad -1 & \end{array} \qquad (5.2.1)$$

$$\begin{array}{lcccc} & {}^{16}\mathrm{O} + {}^{12}\mathrm{C} & \rightarrow & {}^{14}\mathrm{C} + {}^{14}\mathrm{O} \\ T & 0 \quad 0 & & 1 \quad 1 & \\ T_z & & & +1 \quad -1 & \end{array}$$

(These are the extreme members of the multiplet.)

$$\begin{array}{lcccc} & {}^{26}\mathrm{Mg} + \mathrm{d} & \rightarrow & {}^{14}\mathrm{C} + {}^{14}\mathrm{N}^* \ (2.31\ \mathrm{MeV}) \\ T & 1 \quad 0 & & 1 \quad 1 & \\ T_z & & & 1 \quad 0 & \end{array}$$

$$\begin{array}{lcccc} & {}^{22}\mathrm{Ne} + {}^{6}\mathrm{Li} & \rightarrow & {}^{14}\mathrm{C} + {}^{14}\mathrm{N}^* & \text{"} \\ & {}^{18}\mathrm{O} + {}^{10}\mathrm{B} & \rightarrow & {}^{14}\mathrm{C} + {}^{14}\mathrm{N}^* & \text{"} \\ & {}^{14}\mathrm{C} + {}^{14}\mathrm{N} & \rightarrow & {}^{14}\mathrm{C} + {}^{14}\mathrm{N}^* & \text{"} \end{array} \qquad (5.2.2)$$

(Middle member and one side member of triplet.)

On the other hand, for example,

$^{26}Mg + d \rightarrow {}^{14}C + {}^{14}N$ (in the ground state)

can also go to: ^{14}C ($T = 1$), ^{14}N ($T = 0$) → can also have different spins from ^{14}C.

Here one cannot make any definite statement about the symmetry of $d\sigma/d\Omega(\theta)$ about 90°, unless the compound nucleus, ^{28}Al, is in a definite spin and parity state. Since $^{26}Mg + d$ can form both the $^{14}N(T = 0)$ and $^{14}N^*$ $(T = 1)$ states, one should search for an angular distribution as anisotropic as possible in the $^{14}N(T = 0)$ channel, and then look for the $^{14}N^*$ $(T = 1)$ symmetry effect. The degree of symmetry will be a measure of the goodness of isospin when compared to the anisotropy in the former channel. Note that departures from symmetry are sensitive to the T-impurities in the amplitude.

(b) In the isospin formalism, $^{14}C + {}^{14}N^*$ coupled to $T = 1$, $T_z = 1$ yields

$$\Psi^{T_z=1}_{T=1} = \sum_{m_1,m_2=-1}^{1} (1\, m_1\, 1 m_2 \,|\, 11)\, \chi_1^{m_1}(1)\, \chi_1^{m_2}(2) \qquad (\chi_1^{m_1}(1) \rightarrow C,\ \chi_1^{m_2}(2) \rightarrow C')$$

$$= (1110\,|\,11)\,\chi_1^1(1)\,\chi_1^0(2) + (1011\,|\,11)\,\chi_1^0(1)\,\chi_1^1(2) \qquad (5.2.3)$$

$$\Psi^{T_z=1}_{T=1} = \frac{1}{\sqrt{2}}\left[\chi_1^1(1)\,\chi_1^0(2) - \chi_1^0(1)\,\chi_1^1(2)\right] \qquad (5.2.4)$$

where $(1110\,|\,11) = 1/\sqrt{2}$
$(1011\,|\,11) = -1/\sqrt{2}$

Ψ_1^1 is clearly anti-symmetric.

The ground state of ^{14}C and hence the $^{14}N^*$ (2.31 MeV) state have spin 0^+ (they are analogues). Therefore, since $S = 0$ is symmetric,

$$\psi_{\text{total}} = \psi^1_{T=1}\,[\text{anti-sym.}]\ Y^m_\ell\, \chi^0_{S=0}\,[\text{sym.}] \text{ and } Y^m_\ell,$$

depending on the relative ℓ value between these two nuclei, must be odd, for we are dealing with two bosons and ψ_{total} must be symmetric. This means that the compound system $^{28}Al^*$ must have odd spin and parity for this reaction.

For a multiplet such as ^{12}B, $^{12}C^*$, $^{12}N(1^+$ multiplet), however, the spin wave function would be anti-symmetric and hence compound resonances having only even spin and parity can contribute.

(c) Consider $^{14}C + ^{14}O$:

$$\Psi^0_{T=0} = \sum_{m_1, m_2=-1}^{1} (1m_1 1m_2 | 00) \chi_1^{m_1}(1) \chi_1^{m_2}(2)$$

$$= (111-1|00)\chi_1^1(1)\chi_1^{-1}(2) + (1-111|00)\chi_1^{-1}(1)\chi_1^1(2)$$

$$+ (1010|00)\chi_1^0(1)\chi_1^0(2) \qquad (5.2.5)$$

$$\Psi^0_{T=0} = \frac{1}{\sqrt{3}}[\underbrace{\chi_1^1(1)\chi_1^{-1}(2)}_{^{14}C} + \underbrace{\chi_1^{-1}(1)\chi_1^1(2)}_{^{14}O}] - \frac{1}{\sqrt{3}} \underbrace{\chi_1^0(1)\chi_1^0(2)}_{^{14}N^* + ^{14}N^*} \qquad (5.2.6)$$

where $\psi^0_{T=0}$ is symmetric upon interchange of (1) and (2). We see that $^{14}O + ^{14}C$ do not form a pure T state, i.e.

$$\chi_1^1(1)\chi_1^{-1}(2) = \sum_{T=0}^{2} (111-1|T0)\psi^0_T$$

$$= (111-1|00)\psi^0_0 + (111-1|10)\psi^0_1 + (111-1|20)\psi^0_2 \qquad (5.2.7)$$

$$\chi_1^1(1)\chi_1^{-1}(2) = \frac{1}{\sqrt{3}}\psi^0_0 + \frac{1}{\sqrt{2}}\psi^0_1 + \frac{1}{\sqrt{6}}\psi^0_2 \qquad (5.2.8)$$

In words: the formation of a T = 0 state implies the appearance of $^{14}N^* + ^{14}N^*$ to a prescribed extent, or conversely, $^{14}O + ^{14}C$ involves states with isospin 0, 1, and 2 (and $T_z = 0$, of course).

(d) The reaction $^4He + d \rightleftarrows ^3He + t$: This is probably the most interesting reaction to which the Barshay-Temmer theorem applies, because it bears on the three-nucleon system and its isospin purity. Experiments at both low (1-2 MeV) and high energies (23 MeV) (for the inverse $^3He + t \rightarrow d + ^4He$ reaction) show striking symmetry about 90°.

5.3. Special symmetry selection rules

We can easily see that there exist special symmetry selection rules in nuclear reactions involving isospin multiplets, in addition to the usual angular momentum and parity selection rules.

Example:

Consider the reaction

$$^{24}Mg + d \xrightarrow{S=1^+} {}^{13}C + {}^{13}N \text{ [fermion doublet, mirror nuclei]}.$$
$$T=0$$

TABLE IV. COMPOUND STATES WHICH ARE ELIGIBLE TO CONTRIBUTE TO $^{24}Mg + d \rightarrow {}^{13}C + {}^{13}N$

Compound state	ℓ_{final}	S_{final}	$T_{allowed}$	Reaction
0^-	1	1	0(anti-sym.)	Symmetry forbidden
0^+	0	0	0	Parity forbidden (see note below)
1^+	0,2	1	0	O.K.
1^-	1	0.1	0	O.K. for $S_{final} = 0$
2^+	2	0.1	0	O.K. for $S_{final} = 1$
2^-	1.3	1	0	Symmetry forbidden
3^+	2.4	1	0	O.K.
3^-	3	0.1	0	O.K. for $S_{final} = 0$
4^+	4	0.1	0	O.K. for $S_{final} = 1$
4^-	3.5	1	0	Symmetry forbidden

Note: $^{24}Mg + d \neq 0^+$ state in entrance channel since $S_{initial} = 1^+$. To get 0 spin, $\ell_{incident}$ must be 1, therefore the initial parity would be $(-1)^{\ell} = -1$, q.e.d.

^{13}C and ^{13}N of course have the same spin (1/2). The compound nucleus is ^{26}Al and we wish to discover which compound resonances are eligible to contribute to the above reaction. Since ^{13}C and ^{13}N are fermions, ψ_{total} must be anti-symmetric.

5.4. An addendum to the Barshay-Temmer theorem

The reaction

$$\begin{array}{lcccc} & p + p \rightarrow & \pi^+ + & d & \\ T_z & -\frac{1}{2} \quad -\frac{1}{2} & -1 & 0 & \\ T & \frac{1}{2} \quad \frac{1}{2} & 1 & 0 & \end{array} \qquad (5.4.1)$$

has been widely studied (first to determine the spin of the pion from detailed balancing arguments) and may be compared with

$$\begin{array}{lcccc} & n + p \rightarrow & \pi^0 + & d & \\ T_z & \frac{1}{2} \quad -\frac{1}{2} & 0 & 0 & \\ T & \frac{1}{2} \quad \frac{1}{2} & 1 & 0 & \end{array} \qquad (5.4.2)$$

It was long ago realized[2] that charge independence has as a consequence that

$$\sigma_{(2)}(\theta) = 1/2\, \sigma_{(1)}(\theta) \qquad (5.4.3)$$

[2] C.N. Yang, 1952 (unpublished).

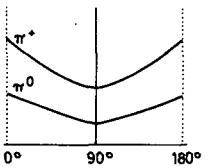

FIG. 14. Angular distributions for $p + p \rightarrow \pi^+ + d$ and $n + p \rightarrow \pi^0 + d$

The experimental results are that

$$\sigma_{total}\,(2) = 1.5 \pm 0.3\ (\text{Mb}) \tag{5.4.4}$$

$$\sigma_{total}\,(1) = 3.10 \pm 0.24\ (\text{Mb}) \tag{5.4.5}$$

and the angular distributions are of course symmetric around 90° (Fig. 14). The best fit to the π^0 angular distribution is obtained by assuming a functional dependence of the form

$$f(\theta) = 0.22 + \cos^2\theta \tag{5.4.6}$$

The symmetry around 90° for the reaction (5.4.2) can be considered a special case of the Barshay-Temmer theorem; it follows also from its relation to reaction (5.4.1) where symmetry about 90° is trivial. Conversely, the following types of pairs of reactions can also be examined from the point of view of relation (5.4.3).

$$^7\text{Li} + {}^7\text{Li} \rightarrow {}^{10}\text{Be} + \alpha \tag{5.4.7}$$

$$^7\text{Li} + {}^7\text{Be} \rightarrow {}^{10}\text{Be}^*(T = 1) + \alpha \tag{5.4.8}$$

$$^7\text{Li} + {}^7\text{Li} \rightarrow {}^{12}\text{B} + d \tag{5.4.9}$$

$$^7\text{Li} + {}^7\text{Be} \rightarrow {}^{12}\text{C}^*(T = 1) + d \tag{5.4.10}$$

In exact analogy to the meson reactions discussed above, the ratio of the cross-sections $\sigma(5.4.7)/\sigma(5.4.8)$ and $\sigma(5.4.9)/\sigma(5.4.10)$ should be 2 and the angular distributions should, of course, be symmetric about 90°. Other test reactions are

$$^3\text{He} + {}^3\text{He} \rightarrow \alpha + 2p \quad \text{(di-proton)} \tag{5.4.11}$$

$$^3\text{He} + T \rightarrow \alpha + d \quad \text{(singlet state)} \tag{5.4.12}$$

$$T + T \rightarrow \alpha + 2n \quad \text{(di-neutron)} \tag{5.4.13}$$

with cross-section magnitudes in the ratio 2 to 1 to 2, and identical shapes. To sum up, in these special reactions, not only is symmetry around 90° required by the Barshay-Temmer theorem but the precise shape of the differential cross-section can be predicted by measuring it in the identical-particle case and dividing by 2. This has not been tested so far.

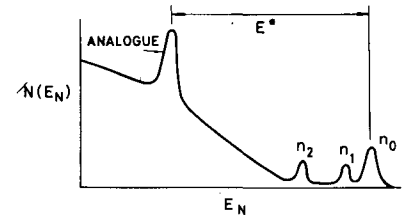

FIG. 15. Neutron spectrum for $^{90}_{40}Zr_{50}(p,n)^{90}_{41}Nb^{*}_{49}$

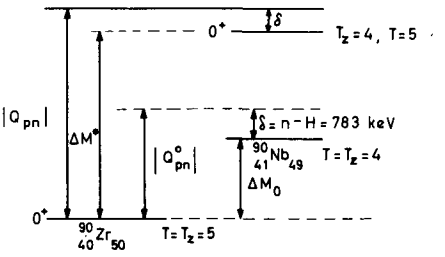

FIG. 16. Energetics for $^{90}_{40}Zr_{50}(p,n)^{90}_{41}Nb^{*}_{49}$

6. CHARGE-EXCHANGE REACTIONS (Ref. Bloom et al., March 1961)

6.1. Experimental

Anderson, Wong, and McClure (1961) performed A(p, n)B experiments using a cyclotron and neutron time-of-flight techniques; they first studied reactions involving mirror nuclei such as $^{13}C(p,n)^{13}N$ and $^{7}Li(p,n)^{7}Be$ where strong transitions take place to the ground (analogue) states; and then moving up to nuclei having larger neutron excesses.

We shall concern ourselves with the specific example

$$^{90}_{40}Zr_{50}(p,n)^{90}_{41}Nb^{*}_{49} \qquad (6.1.1)$$

The neutron spectrum for this reaction is shown schematically in Fig. 15. The higher energy neutron groups correspond to leaving ^{90}Nb in its ground and first few excited states. The prominent low-energy neutron group corresponds to leaving ^{90}Nb in its first T = 5 state. Here $T_z = 4$, of course. This sort of group was found in every case investigated.

The energy level diagram for this reaction is shown in Fig. 16 where

ΔM_0 = mass difference between ground states of ^{90}Zr and ^{90}Nb

ΔM^* = mass difference between the ground state of ^{90}Zr and its analogue in ^{90}Nb

$|Q^0_{pn}|$ is the Q value for the (p, n) reaction leading to the ground state of ^{90}Nb

$|Q_{pn}|$ is the Q value for the (p, n) reaction connecting the ground state of ^{90}Zr and its analogue in ^{90}Nb

δ = neutron-neutral hydrogen mass difference

Clearly $\Delta M^* = |Q_{pn}| - \delta$, but the analogue relationship between the two states means that $\Delta M^* = E_c - \delta$; that is, ΔM^* equals the Coulomb

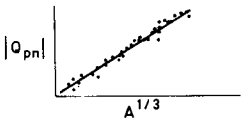

FIG. 17. A plot of $|Q_{pn}|$ versus $A^{1/3}$ (Anderson & Wong)

energy of the additional proton corrected by the neutron-hydrogen mass difference. Hence $|Q_{pn}| = E_c$ and a determination of the $|Q_{pn}|$ from experiment provides a direct measurement of E_c.

Indeed, a plot of $|Q_{pn}|$ vs. $A^{1/3}$ for various (p, n) reactions generally bears out the linear relationship expected for E_c vs. $A^{1/3}$ on the basis of a uniform charge distribution in the nucleus (see Fig. 17).

6.2. Shell model view of analogue states

It is possible via (p, n) reactions to have $\Delta T = \pm 1, 0$; that is to say, to form isospin states in the residual nucleus having the same isospin as the target or differing by one unit. $\Delta T = 0$ reactions proceeding via an isoscalar term of an isospin-dependent interaction, thus form $T = 5$ states in ^{90}Nb (in this example); $\Delta T = 1$ reactions can go via an isovector T-dependent interaction allowing one to reach $T = 6$ states in ^{90}Nb($T_z = 4$) as well as the low-lying $T = 4$ states. It should be noted that the (^{3}He, t)

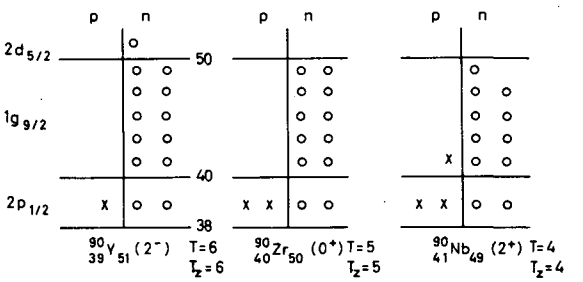

FIG. 18. Shell-model descriptions of the ground states of three neighbouring nuclei with A = 90

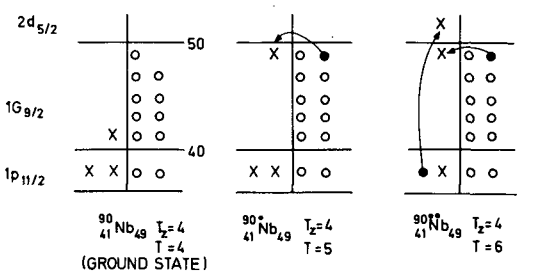

FIG. 19. Lowest-lying T = 4, T = 5 and T = 6 states of ^{90}Nb($T_z = 4$)

reaction also can be used for studying the charge-exchange process (Blair and Armstrong, 1965). The cross-section is found to be much weaker than for the (p, n) reaction, but there is the experimental advantage of outgoing charged particles.

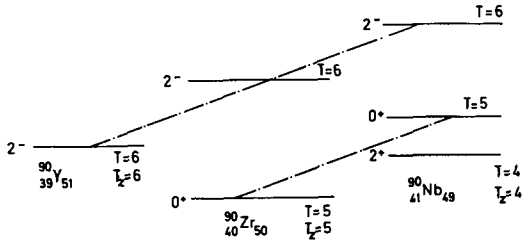

FIG. 20. Level scheme for the T-multiplets

Consider the following three members of the A = 90 isobar and a shell-model description of their ground states (Fig. 18). Since we are showing the ground states of these nuclei, $T = T_z$. Now consider the description (Fig. 19) of the lowest lying T = 5, and T = 6 states of $^{90}Nb(T_z = 4)$. Clearly the T = 5 state can easily be obtained from the ground state configuration of ^{90}Zr by a (p, n) reaction which charge exchanges a $1g_{9/2}$ proton for a neutron. The T = 6 state can also be reached, in an isospin sense, but requires not only the charge exchange of a $1g_{9/2}$ neutron, but also exciting a $2p_{1/2}$ proton to a $2d_{5/2}$ level. This is obviously more complicated, and costly in energy, but has been observed with 50-MeV protons (Stafford et al., 1966). These may be termed 'double-analogue' states since they are obtained by the operation $(T^-)^2$ on the parent ^{90}Y. The level scheme for the associated T-bands is shown in Fig. 20.

6.3. Theoretical description of charge-exchange reactions

These reactions have been described by Lane and Soper (1962) by assuming that the optical potential has an isospin-dependent part. That is, the optical potential may be written as $U = U_0 + U_1(\vec{t} \cdot \vec{T})$, $(\vec{t} \cdot \vec{T})$ transforming as a scalar in isospin space.

Following Robson's treatment (1965) the (p, n) reaction can be written as

$$p + C \rightarrow n + A + Q_{pn} \qquad (6.3.1)$$

where $M_A - M_C = |Q_{pn}| - \delta$, C stands for the target state and A for its analogue. Now we write the proton-target isospin wave function as $|pC\rangle$ and the neutron-analogue wave function as $|nA\rangle$.

The general relationship for the T-lowering operator

$$|T, T_3 - 1\rangle = \frac{T^-}{\sqrt{(T + T_3)(T - T_3 + 1)}} |T, T_3\rangle \qquad (6.3.2)$$

yields for $T = T_z$

$$|T, T - 1\rangle = \frac{T^-}{\sqrt{2T}} |T, T\rangle \qquad (6.3.3)$$

FIG. 21. Vector model description of the T coupling

We may write the operator $(\vec{t}\cdot\vec{T})$ as

$$(\vec{t}\cdot\vec{T}) \equiv \tfrac{1}{2}(t^+T^- + t^-T^+) + t_zT_z \qquad (6.3.4)$$

and with our usual convention the following relationships follow:

$$t^+(p) = n \qquad t^+(n) = 0 \qquad T^+(A) = \sqrt{2T}\,C$$

$$t^-(n) = p \qquad t^-(p) = 0 \qquad T^-(C) = \sqrt{2T}\,A$$

$$t_z(n) = \tfrac{1}{2}n \qquad t_z(p) = -\tfrac{1}{2}P \qquad T_z(A) = (T-1)A$$

$$T_z(C) = TC \qquad (6.3.5)$$

As a brief aside: consider the vector model description (Fig. 21) of the T coupling

$$T_R^2 = T^2 + t^2 + 2(\vec{t}\cdot\vec{T}) \qquad (6.3.6)$$

then

$$(\vec{t}\cdot\vec{T}) = \tfrac{1}{2}(T_R^2 - T^2 - t^2) \qquad (6.3.7)$$

where the eigenvalues of T_R^2, T^2, t^2 may be substituted for the operators, yielding

$$(\vec{t}\cdot\vec{T}) = \tfrac{1}{2}\{T_R(T_R+1) - T(T+1) - t(t+1)\} \qquad (6.3.8)$$

(Landé formula)

Since $T_R = T \pm \frac{1}{2}$ we have for $T_R = T + \frac{1}{2}$

$$(\vec{t}\cdot\vec{T}) = T/2 \qquad (6.3.9)$$

and for $T_R = T - \frac{1}{2}$

$$(\vec{t}\cdot\vec{T}) = -\frac{(T+1)}{2} \qquad (6.3.10)$$

and the energy splitting between these $(E\uparrow - E\downarrow)$ is $\propto \frac{1}{2}(2T+1)$. As a working rule of thumb, this yields a splitting of ~ 1 MeV/excess neutron.

In preparation for writing down the Schrödinger equation for the $|pC\rangle$ channels, we evaluate

$$(\vec{t}\cdot\vec{T})|pC\rangle = \tfrac{1}{2}|(t^+p)(T^-C)\rangle - \frac{T}{2}|pC\rangle \qquad (6.3.11)$$

$$(\vec{t}\cdot\vec{T})|nA\rangle = \sqrt{\frac{T}{2}}\,|pC\rangle + \frac{T-1}{2}|nA\rangle \qquad (6.3.12)$$

using the identity (6.3.4) above.

The net result is that the $\vec{t}\cdot\vec{T}$ operator is a coupling operator in the sense that operating $\vec{t}\cdot\vec{T}$ on $|pC\rangle$ or $|nA\rangle$ introduces components of the other channel.

With $V = U_0 + \vec{t}\cdot\vec{T}\,U_1$ being used for the potential energy term, the Schrödinger equation for the $|pC\rangle$ channel becomes

$$\left(-\frac{\hbar^2}{2m}\nabla^2 + U_0 - \frac{T}{2}U_1 + V_c - E\right)|pC\rangle = -\sqrt{\frac{T}{2}}U_1|nA\rangle \qquad (6.3.13)$$

$$H_C|pC\rangle = -\sqrt{\frac{T}{2}}U_1|nA\rangle \qquad (6.3.14)$$

where V_c is the Coulomb potential for the proton in the field of C; and for the $|nA\rangle$ channel:

$$\left(-\frac{\hbar^2}{2m}\nabla^2 + U_0 + \frac{T-1}{2}U_1 - E + |Q_{pn}|\right)|nA\rangle = -\sqrt{\frac{T}{2}}U_1|pC\rangle \qquad (6.3.15)$$

$$H_A|nA\rangle = -\sqrt{\frac{T}{2}}U_1|pC\rangle \qquad (6.3.16)$$

where the eigenvalue is $E - |Q_{pn}|$ because of the Coulomb energy shift, and $V_c = 0$.

Re-writing the wave functions as $|\uparrow\rangle$ or $|\downarrow\rangle$ corresponding to good isospin wave functions with $T + 1/2$ or $T - 1/2$, we have:

$$|\uparrow\rangle = a|pC\rangle + b|nA\rangle \qquad (6.3.17)$$

$$|\downarrow\rangle = c|pC\rangle + d|nA\rangle \qquad (6.3.18)$$

where

$$a = (TT\tfrac{1}{2} - \tfrac{1}{2}|T + \tfrac{1}{2}\ T - \tfrac{1}{2}) = \frac{1}{\sqrt{2T+1}} \qquad (6.3.19)$$

$$b = (T\,T - 1\ \tfrac{1}{2}\tfrac{1}{2}|T + \tfrac{1}{2}\ T - \tfrac{1}{2}) = \sqrt{\frac{2T}{2T+1}} \qquad (6.3.20)$$

$$c = (T\,T\tfrac{1}{2} - \tfrac{1}{2}|T - \tfrac{1}{2}\ T - \tfrac{1}{2}) = \sqrt{\frac{2T}{2T+1}} \qquad (6.3.21)$$

$$d = (T\,T - 1\ \tfrac{1}{2}\tfrac{1}{2}|T - \tfrac{1}{2}\ T - \tfrac{1}{2}) = -\frac{1}{\sqrt{2T+1}} \qquad (6.3.22)$$

therefore:

$$|\uparrow\rangle = \frac{1}{\sqrt{2T+1}}\ |pC\rangle + \sqrt{\frac{2T}{2T+1}} \qquad (6.3.23)$$

$$|\downarrow\rangle = \sqrt{\frac{2T}{2T+1}}|pC\rangle - \frac{1}{\sqrt{2T+1}}|nA\rangle \qquad (6.3.24)$$

Upon inverting these relations

$$|pC\rangle = \frac{1}{\sqrt{2T+1}}\left(|\uparrow\rangle + \sqrt{2T}\,|\downarrow\rangle\right) \tag{6.3.25}$$

$$|nA\rangle = \frac{1}{\sqrt{2T+1}}\left(\sqrt{2T}\,|\uparrow\rangle - |\downarrow\rangle\right) \tag{6.3.26}$$

Using the I-spin scheme, we can write

$$H\uparrow|\uparrow\rangle \equiv \left(-\frac{\hbar^2}{2m}\nabla^2 - E + U_0 + |Q_{pn}| + \frac{T}{2}U_1\right)|\uparrow\rangle = \frac{1}{\sqrt{2T+1}}\left(|Q_{pn}| - V_c\right)|pC\rangle \tag{6.3.27}$$

$$H\downarrow|\downarrow\rangle \equiv \left(-\frac{\hbar^2}{2m}\nabla^2 - E + U_0 + V_c - \left(\frac{T+1}{2}\right)\right)|\downarrow\rangle = \frac{1}{\sqrt{2T+1}}\left(|Q_{pn}| - V_c\right)|nA\rangle \tag{6.3.28}$$

where

$$H\uparrow = H_A + \tfrac{1}{2}U_1 \text{ and } H\downarrow = H_c - \tfrac{1}{2}U_1 \tag{6.3.29}$$

One notes that if $|Q_{pn}|$ were equal to V_c then these equations would no longer be coupled.

Robson's approach consists in choosing a radius R such that the effective cancellation of $|Q_{pn}|$ and V_c is optimized inside the radius R (see Fig. 22). In this way the internal equations are uncoupled, and

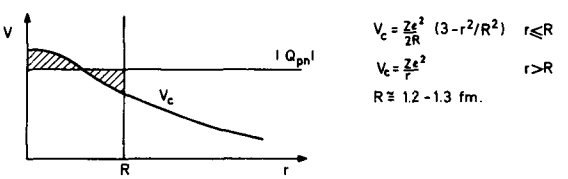

FIG. 22. Minimization of $|Q_{pn}| - V_c$ in the "inside" region ($r < R$)

if it is assumed that T is a good quantum number inside, there will be no internal T mixing.

Outside $|Q_{pn}|$ cannot equal V_c. It would appear at first sight that these equations are coupled in the external region. However, U, the nuclear interaction potential, is zero outside, i.e.

$$U = U_0 + U_1\vec{t}\cdot\vec{T} = 0 \qquad \left.\begin{matrix} U_0 = 0 \\ U_1 = 0 \end{matrix}\right\} \; r > R \tag{6.3.30}$$

Therefore the equations are uncoupled outside, as well.

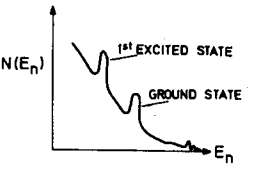

FIG. 23. Neutron spectrum resulting from (p,n) quasi-elastic and (p,n_1) quasi-inelastic scattering reaction

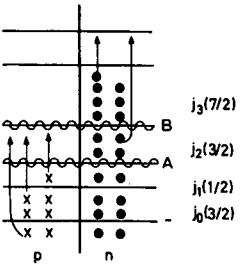

FIG. 24. T-preserving rearrangements in a fictitious nucleus

6.4. Quasi-inelastic scattering

Using the potential $(U_0 + U_1 \vec{t} \cdot \vec{T})$, one can describe ordinary inelastic scattering by deforming the nuclear potential, U_0; that is, by taking the nuclear radius as $R = R_0\ (1 + \Sigma\ \beta_\ell Y_\ell^m)$. One then gets coupled equations for the ground and first excited states linking elastic (p, p_0) and (p, p') scattering.

Similarly, the $U_1(\vec{t} \cdot \vec{T})$ term in the optical potential introduces quasi-elastic or (p, n_0) reactions; if we deform the form factor U_1, we analogously obtain coupling to (p, n') quasi-inelastic scattering to excited analogue states, normally analogues of states seen in (p, p') inelastic scattering. (Satchler, Drisko and Bassel, 1964). To fit the data, however, the deformations needed for U_1 are 3-5 times larger than those required for (p, p') experiments (see Fig. 23).

6.5. Anderson's experiments

Anderson's report at the Tallahassee Conference (1966) states that one seems to observe a $(\vec{t}^{(i)} \cdot \vec{t}^{(j)})\ (\vec{\tau}^{(i)} \cdot \vec{\tau}^{(j)})$ interaction, in addition to the $(\vec{t}^{(i)} \cdot \vec{t}^{(j)})$ (Heisenberg) interaction.

(a) He uses the test reaction

$$^{26}\mathrm{Mg}\ (p, n),\ ^{26}\mathrm{Mg}\ (0^+) \qquad (6.5.1)$$

$$^{25}\mathrm{Mg}\ (p, n),\ ^{25}\mathrm{Mg}\ (5/2^+) \qquad (6.5.2)$$

and explains the significant difference between the cross-sections and angular distributions of these two reactions by using the term above, with about equal strength as the $\vec{t}^{(i)} \cdot \vec{t}^{(j)}$ term.

(b) When $(\vec{t}^{(i)} \cdot \vec{t}^{(j)})$ $(\vec{\tau}^{(i)} \cdot \vec{\tau}^{(j)})$ is used, the $(T^-)^2$ isospin flip operator can also be carried by a (p,n) reaction, i.e. previously one only used $\{\vec{t}^{(i)} \cdot \vec{t}^{(j)}\}$ $\Delta T = 0$ in (p,n) reactions, but now one can have $\Delta T = 1$, i.e. isospin flip (see above). One should also excite spin flip (magnetic dipole) transitions in the analogue nucleus via this term. Little is known about this form of quasi-elastic spin flip scattering.

7. T-SPLITTING (Ref. J.B. French, Proc. of Argonne Conf. on Direct Reactions (1964))

7.1. General

T-splitting can occur only when the nucleus has a neutron excess; all excess neutrons are 'polarized' in I-space. Adding a nucleon or nucleon hole to the nucleus, there will be an interaction energy whose sign will depend on the alignment of the $t = \frac{1}{2}$ addition with the original T, being positive for the parallel and negative for the anti-parallel case. This gives rise to isobaric spin splitting for single nucleon and single-hole states. (French and MacFarlane, 1960, 1961.)

Consider T-preserving manipulations among protons and neutrons, or T-preserving excitations.

Consider a fictitious nucleus (Fig. 24) where

A ≡ boundary above which no proton states are filled, and
B ≡ boundary above which there are no filled neutron shells.

Moving protons up to B from any lower levels leaves the nucleus in the same T state. Moving neutrons up from anywhere above A (arrows) preserves T as well. This is because one cannot exchange a proton with a neutron below A, since the protons have no place to go. (Pauli principle). Any other excitations will not produce states of good isospin.

7.2. Expansion of states in terms of states with good T

Shell model states which do not have good isospin may be expanded in terms of states with good T. This expansion can be written in two different formalisms.

For example, consider the addition of a $2p_{3/2}$ proton to a ^{48}Ca core to form a $3/2^-$ state in ^{49}Sc.

(a) n-p formalism, taking into account the Pauli principle and charge independence (see Fig. 25).

The second term in each bracket corresponds to a $2p_{3/2}$ neutron 'revolving' around a $^{48}_{21}$Sc core.

(b) T formalism

$$\Psi = \sqrt{\frac{1}{9}} \underset{T=9/2}{\overset{T_0=4}{\triangle}}{}^{\frac{1}{2}} + \sqrt{\frac{8}{9}} \underset{T=7/2}{\overset{T_0=4}{\triangle}}{}^{\frac{1}{2}} \qquad (7.2.1)$$

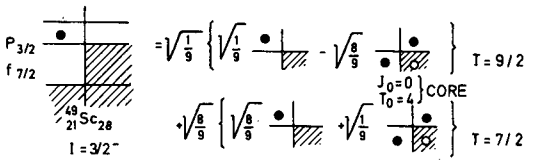

FIG. 25. Pictorial representation of $^{49}Sc(p_{3/2})$ in terms of states of good T

This is the notation in the isospin scheme which often has advantages, for instance, when we are trying to see the connection with the isobaric analogue state in $^{49}_{20}Ca$. The numbers which appear in these expressions are the appropriate isospin Clebsch-Gordan coefficients,

$$(4\,4\ 1/2\ -1/2\,|\,9/2\ \ 7/2) \text{ and } (4\,4\ 1/2\ -1/2\,|\,7/2\ 7/2) \qquad (7.2.2)$$

The n-p hole-particle pair in the $f_{7/2}$ - shell needed in the above example must be coupled to the 'core' angular momentum $J_0 = 0$ to allow free exchange without angular momentum change, and must have $T_0 = 4$ (from group theory).

TABLE V. $T_0 = 3$ STATES RESULTING FROM COUPLING A $J_0 = 1$-7 CORE TO A $p_{3/2}$ PROTON

No. of states \ J_0	1	2	3	4	5	6	7
2	1/2	1/2					
(3)	3/2	3/2	3/2				
4	5/2	5/2	5/2	5/2			
4		7/2	7/2	7/2	7/2		
4			9/2	9/2	9/2	9/2	
4				11/2	11/2	11/2	11/2
3					13/2	13/2	13/2
2						15/2	15/2
1							17/2

There is however, another set of states in which the hole-particle pair is coupled to $J_0 \neq 0$ (and hence $T_0 = 3$, from group theory). Table V shows those $T_0 = 3$ states resulting from coupling a $J_0 = 1$-7 core to a $p_{3/2}$ proton.

Three of these states, with $J_0 = 1, 2, 3$, have $J = 3/2^-$, $T = 7/2$. If the $3/2^-$ states are being formed by the process ^{48}Ca + proton, these 'core-polarization' states carry none of the strength, since ^{48}Ca in its ground state looks mainly as shown in Fig. 26.

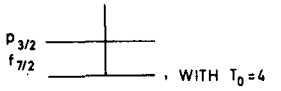

FIG. 26. ^{48}Ca ground state

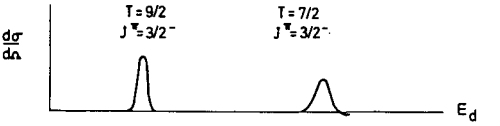

FIG. 27. (p, d) spectrum expected without core polarization splitting

FIG. 28. (p, d) spectrum with core polarization splitting

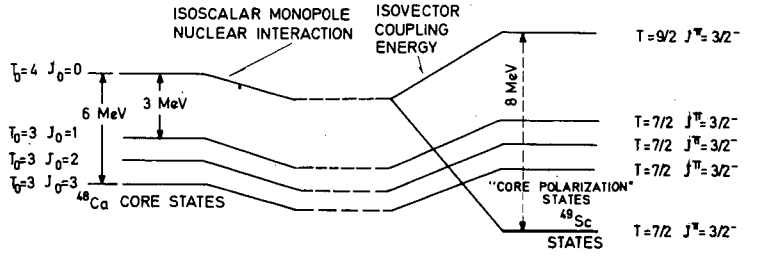

FIG. 29. "Core polarization" states and their effect on ^{49}Sc

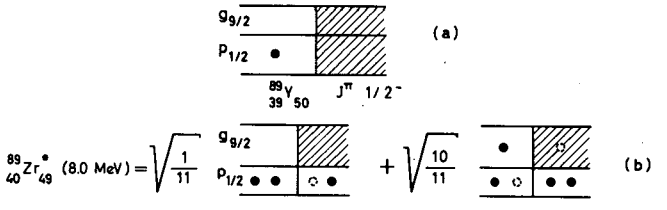

FIG. 30. (a) ^{89}Y ground state configuration ($T_>$ = 11/2)
(b) ^{89}Zr* analogue state configuration ($T_>$ = 9/2)

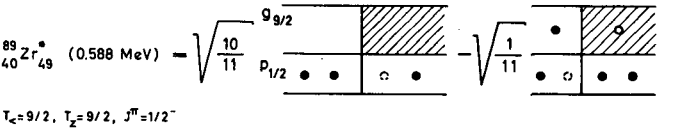

FIG. 31. ^{89}Zr* analogue state configuration ($T_<$ = 9/2)

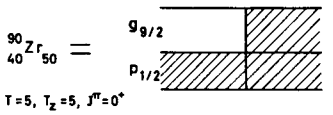

FIG. 32. ^{90}Zr ground state configuration

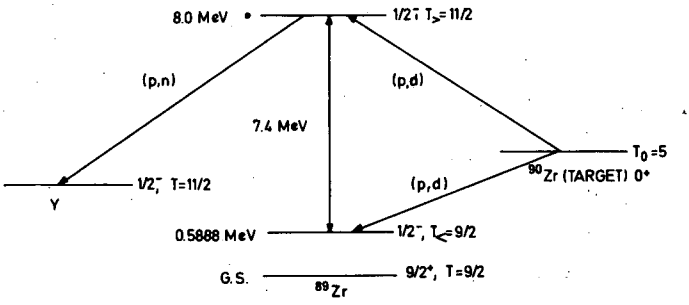

FIG. 33. Energetics for $T_<$ and $T_>$ states in ^{89}Y and ^{89}Zr

These states may, however, admix with the T = 7/2 single-nucleon state, thereby fragmenting the (T_0 - 1/2) strength and producing a fine structure in this $T_<$ member of the doublet. This is merely an example of the Lane-Thomas-Wigner giant-resonance phenomenon[3], as illustrated below:

(1) Without coupling two bumps (Fig. 27) in the ^{48}Ca + 'p' reaction are observed (say via (^{3}He, d) or (d, n)):

(2) With coupling, the T = 7/2 'state' is observed (Fig. 28) to consist of 4 members.

The core states involved in this splitting are shown in Fig. 29. Hence there is a competition as to the sharing of the $T_<$ strength, which depends sensitively on the relative strengths of the isoscalar (depressing) and the isovector (splitting) contributions.

7.3. Isospin doublet splitting in $^{89}_{40}Zr_{49}$

The $T_>$ = 11/2 state in ^{89}Zr is located at 8.0 MeV and is simply the analogue of the ground state of $^{89}_{39}Y_{50}$, which is shown in Fig. 30.

The $T_<$ = 9/2 state in ^{89}Zr is located at 0.588 MeV and is simply a $2p_{1/2}$ hole weakly coupled to a $^{90}_{40}Zr_{50}$ ground-state core (T_0 = 5) (see Fig. 31).

The isospin doublet splitting is therefore about 7.4 MeV. The $T_>$ state is populated by a (p, n) reaction on ^{89}Y; the $T_<$ state is favored in a (p, d) reaction by a factor of 10 on ^{90}Zr, but the $T_>$ can also be formed, as can be seen by considering the snatching of a neutron from $^{90}_{40}Zr_{50}$ (see Figs. 32 and 33).

7.4. Effective nucleon-nucleon interaction

We shall try to calculate the magnitude of the isospin doublet splitting and thereby obtain information about the effective nucleon-

[3] A.M. Lane, R.G. Thomas, E.P. Wigner, Phys. Rev. 98 (1955) 693.

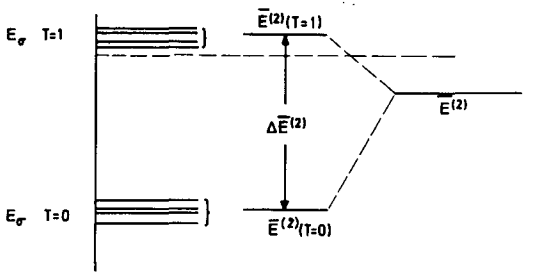

FIG. 34. T = 1 and T = 0 centres of gravity for a two-nucleon system, their weighted centre of gravity and isospin splitting

nucleon interaction in nuclei. Consider the energies for two particles in different orbits, j_1 and j_2. Let $\bar{E}^{(2)}$ be the center of gravity of the states (which a $(2J+1)(2T+1)$ weighting), and $\Delta\bar{E}^{(2)}$ the difference between the separate T = 1 and T = 0 centers of gravity for the two-nucleon system (Fig. 34). If we now consider only the monopole parts of the interaction of a j_2 particle with a $(j_1^n)J_0T_0$ group in a complex nucleus, then for the interaction energy we have for the

Hamiltonian

$$H_{\text{int.}}^{(\text{Monopole})} \equiv n\bar{E}^{(2)} + \Delta\bar{E}^{(2)}(\vec{T}_0 \cdot \vec{t}) \tag{7.4.1}$$

whose eigenvalue is

$$E^{(n+1)} = n\bar{E}^{(2)} + \frac{\Delta\bar{E}^{(2)}}{2}\left[T(T+1) - T_0(T_0+1) - \tfrac{3}{4}\right] \tag{7.4.2}$$

It follows that

$$\bar{E}^{(n+1)} = n\bar{E}^{(2)} \tag{7.4.3}$$

For $T = T_0 + \frac{1}{2}$

$$E_{T_>}^{(n+1)} = n\bar{E}^{(2)} + \frac{T_0}{2}\Delta\bar{E}^{(2)} \tag{7.4.4}$$

For $T = T_0 - \frac{1}{2}$

$$E_{T_<}^{(n+1)} = n\bar{E}^{(2)} - \frac{(T_0+1)}{2}\Delta\bar{E}^{(2)} \tag{7.4.5}$$

Consequently

$$E_{T_>}^{(n+1)} - E_{T_<}^{(n+1)} = \frac{2T_0+1}{2}\Delta\bar{E}^{(2)} \tag{7.4.6}$$

If we think of the $(n+1)^{st}$ particle scattering from the nucleus containing n particles, the optical model potential will, of course, contain the same Lane term $\Delta\bar{E}^{(2)}(\vec{T}_0 \cdot \vec{t})$. For hole states one must replace $\bar{E}^{(2)}$ by $-\bar{E}^{(2)}$. From available data for isospin-doublet splittings in

complex nuclei, we deduce the two-nucleon effective parameters $\Delta\bar{E}^{(2)} \approx 1.5\text{-}3.0$ MeV $E^{(2)} \lesssim 0.25$ MeV. From the binding energy of the deuteron we see that $\Delta\bar{E}^{(2)}$ for free nucleons ≈ 2.28 MeV.

8. A LOOK AT $d_{3/2}$ HOLE STATES IN THE $f_{7/2}$ SHELL (Ref.: Bansal and French, 1965)

8.1. Low-lying hole states in the $f_{7/2}$ regions

Consider the low-lying hole states in the $f_{7/2}$ region. As we saw earlier, talking about a hole, we must set $\bar{E}^{(2)} = -\bar{E}^{(2)}$. Specifically, let us consider those hole states found via (p, d) and (d, ^{3}He) reactions on the Ti isotopes. We consider the Ti isotopes to be built on a ^{40}Ca core. These hole states then refer to the coupling of a $d_{3/2}$ or $s_{1/2}$ hole to the ground states of the various Ti isotopes. The low-lying states found via (d, ^{3}He) in the Sc isotopes are those with $T = T_> = T_0 + \frac{1}{2}$ and those found via (p, d) have $T = T_< = T_0 - \frac{1}{2}$. The energy of a $d_{3/2}$ hole state can be calculated, in a semi-empirical way, in terms of known binding energies and the two monopole parameters $\bar{E}^{(2)}$ and $\Delta\bar{E}^{(2)}$ of the $d_{3/2} - f_{7/2}$ interaction. The excitation energy E^* of a hole state in the nucleus $(f_{7/2})^N \otimes {}^{40}$Ca is given by

$$E^* = E\{j^{-1} \otimes (f_{7/2}^{N+1} \times {}^{40}\mathrm{Ca})_{X_0 J_0 T_0}\}_{JT} - E\{f_{7/2}^{N} \otimes {}^{40}\mathrm{Ca}\}_{g.s.} \qquad (8.1.1)$$

where X_0 refers to all other quantum numbers; we rewrite this as

$$E^* = \overset{C}{E\{j^{-1} \otimes {}^{40}\mathrm{Ca}\}} - \overset{D}{E\{{}^{40}\mathrm{Ca}\}} - \overset{B}{E\{f_{7/2}^{n} \otimes {}^{40}\mathrm{Ca}\}}_{g.s.}$$

$$+ \overset{A}{E\{f_{7/2}^{N+1} \otimes {}^{40}\mathrm{Ca}\}} + E_{int.}\{j^{-1} \otimes f_{7/2}^{N+1})_{X_0 J_0 T_0}\}_{JT} + \epsilon_c(f^{-1} f_{7/2}) \qquad (8.1.2)$$

where $E\{{}^{40}\mathrm{Ca}\}$ corresponds to a 'vacuum' renormalization term. $\epsilon_c \sim -400$ keV for the specific Coulomb interaction of each $f_{7/2}$ proton with the proton hole. The hole states are defined by the quantum numbers $(X_0 J_0 T_0)$ of the core, the ℓ and j of the hole orbit, and the resultant values J, T.

As an example we calculate the energy of the $d_{3/2}$ hole state produced by the (d, ^{3}He) reaction on ^{46}Ti.

We have

$$E^* = \overset{A}{E(^{46}\mathrm{Ta})} - \overset{B}{E(^{45}_{21}\mathrm{Sc}_{24})} + \overset{C}{E(^{39}_{19}\mathrm{K}_{20})} - \overset{D}{E(^{40}_{20}\mathrm{Ca}_{20})} + E_{int.} + 2\epsilon_c \qquad (8.1.3)$$

where the letters above the equation identify the terms they are related to in the previous equation.

Now

$$2\epsilon_c + E_{int.} = -6\bar{E}^{(2)} + \tfrac{1}{2}\,\Delta\bar{E}^{(2)} - Z \times (0.4)\,\mathrm{MeV} \qquad (8.1.4)$$

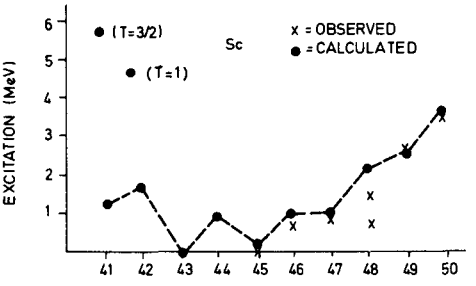

FIG. 35. Calculated and observed $d_{3/2}$ hole states in the Sc isotopes

where we have $T_0 = 1$ and the hole interacts with two protons in ^{46}Ti. From the mass values, terms (A), (B), (C) and (D) yield -2.0 MeV, so that finally:

$$E^* = -6\bar{E}^{(2)} + \tfrac{1}{2}\Delta\bar{E}^{(2)} - 2.8 \text{ MeV} \qquad (8.1.5)$$

Therefore, if we see two or more hole states experimentally we can again determine the two-nucleon parameters $\bar{E}^{(2)}$ and $\Delta\bar{E}^{(2)}$.

8.2. Nucleon holes

It should be remembered that when $T_z = T_0 = 1/2$, the hole is not a pure neutron hole, but rather partially a neutron and partially a proton hole; one should only talk about a nucleon hole. The calculated and observed $d_{3/2}$ hole states in the Sc isotopes are shown in Fig. 35 (French, Proceedings of the Argonne Conference on Direct Interactions, 1964). The fit is calculated by using $\bar{E}^{(2)} = -0.25$ MeV and $\Delta\bar{E}^{(2)} = 2.9$ MeV. For the even scandium isotopes, the core is odd and is easily excited. The strength can then be distributed, since the core can be coupled to various angular momenta. The two T values shown for ^{41}Sc and ^{42} Sc

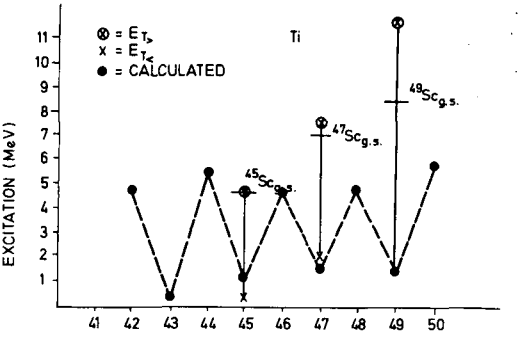

FIG. 36. Calculated and observed $d_{3/2}$ hole states in the Ti isotopes

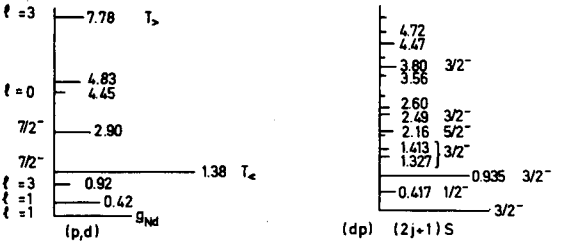

FIG. 37. Experimental results for $^{56}Fe(p,d)$ and $^{54}Fe(d,p)^{55}Fe$

arise because proton-removal reactions here allow us to form both $T_>$ states as well as $T_<$ states, since they are proton-excess nuclei.

Similar results arise for neutron pick-up and are shown in Fig. 36. By applying a Coulomb correction to the Sc results we can locate the $T_>$ states and show explicitly how the isobaric spin splitting increases with increasing neutron excess (increasing T) (see Fig. 36). The large even-odd alternations in the excitation energy of the $T_<$ states is due to the $(f_{7/2})^N$ identical-particle pairing effect. An extra particle outside an odd core is attracted, whereas an extra particle outside an even core is repelled, or only weakly attracted by an even N group.

8.3. Other hole states

For example the $2s_{1/2}$ hole state in A = 40 occurs at an excitation of 2.6 MeV above the $d_{3/2}$ hole state. The separation in other $f_{7/2}$ nuclei is about the same except for the difference between the $(d_{3/2}^{-1})$ $-f_{7/2}$ and $(S_{1/2}^{-1})$ $-f_{7/2}$ interaction. These states have been fitted using $\bar{E}^{(2)} \simeq 0$ and $\Delta\bar{E}^{(2)} \cong 2.5$ MeV.

9. ISOSPIN IN PICK-UP AND STRIPPING REACTIONS

9.1. General remarks

Note that one essentially studies different states using reactions such as $^{54}Fe(d,p)^{55}Fe$ and $^{56}Fe(p,d)^{55}Fe$. Also, the (p, d) reaction can excite both $T_0 + 1/2$ states, while (d, p) or (p, p) reactions excite only one of these, so that is a more powerful tool for studying the shell model and analogue states.

Let us recall that, in addition to using a shell-model potential well, one takes account of the nucleon-nucleon interaction by using an effective residual interaction having matrix elements of the form $\langle \psi_{\ell jm} | H_{int} | \psi_{\ell' j' m'} \rangle$ where the $\psi_{\ell jm}$'s are pure shell-model basis wave functions. Using this description one finds for instance that (d, p) reactions on the isotope ^{48}Ca can lead to (weak) $f_{7/2}$ neutron states even though the $f_{7/2}$ shell is supposedly filled. In other words, the (d, p) reactions measure neutron vacancies, while the (p, d) reaction locates (partially) occupied neutron states.

$^{54}Fe(d,p)$: adds neutrons to $2p_{3/2}$, $2p_{1/2}$, $1f_{5/2}$, $1g_{9/2}$, $2d_{5/2}$, and higher

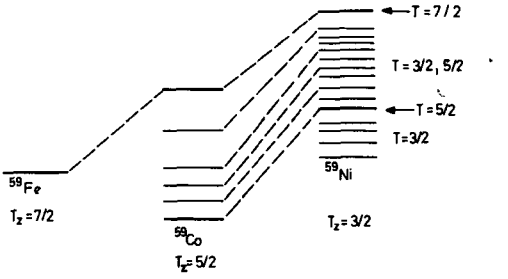

FIG. 38. Level schemes for $^{59}Fe(T_z = 7/2)$, $^{59}Co(T_z = 5/2)$ and $^{59}Ni(T_z = 3/2)$

while

$^{56}Fe(p, d)$: removes neutron from 2p, $1f_{7/2}$, $1d_{5/2}$, and deeper.

Experimental results[4] for $^{56}Fe(p, d)$, $\theta = 35°$, $E_p = 28$ MeV are shown in Fig. 37.

$^{56}_{26}Fe_{30}$ has T = 2; removing a neutron can lead to T = 5/2, 3/2; $T_z = 3/2$. The $T_>$ state is the isobaric analogue of $^{55}_{25}Mn_{30}$, which is the parent nucleus, having $T = T_z = 5/2$. Note that the $T_>$ state cannot be excited using $^{54}Fe(d, p)^{55}Fe$ since we can couple at most to T = 3/2 by neutron addition to ^{54}Fe (T = 1).

9.2. Example: $^{60}Ni(p, d)^{59}Ni$

For ^{60}Ni, $T_0 = 2$ and the (p, d) reaction can lead to $T_>$ and $T_<$ states; in this case $T_> = 5/2$, $T_< = 3/2$; $T_z = 3/2$. The T = 7/2 levels cannot be reached (Fig. 38). The T = 5/2 state indicated in ^{59}Ni is the isobaric analogue of the ground state of ^{59}Co. We can describe the ground states as shown in Fig. 39. We can reach the ^{59}Ni ground state by a $p_{3/2}$ neutron pick-up from ^{60}Ni, but to reach the isobaric analogue state in ^{59}Ni we must remove an $f_{7/2}$ neutron.

$$^{59}Ni^* = \frac{1}{\sqrt{2T}} T^- \left(\frac{0}{7}\middle|\frac{4}{8}\right) = \left[\sqrt{\frac{1}{5}}\left(\frac{0}{8}\middle|\frac{4}{7}\right) + \sqrt{\frac{4}{5}}\left(\frac{1}{7}\middle|\frac{3}{8}\right)\right]_{T_> = 5/2} \quad (9.2.1)$$

The second term here would be weakly excited in a (p, d) reaction since we not only have to pick up a $p_{3/2}$ neutron, but a proton would have to be promoted from $1f_{7/2}$ to $2p_{3/2}$. A pick-up of an $f_{7/2}$ neutron also leads to the $T_<$ state ('ortho-analogue') in fact with four times the intrinsic probability:

$$\left[\sqrt{\frac{4}{5}}\left(\frac{0}{8}\middle|\frac{4}{7}\right) - \sqrt{\frac{1}{5}}\left(\frac{1}{8}\middle|\frac{3}{8}\right)\right]_{T_< = 7/2^-} \quad (9.2.2)$$

which is orthogonal to the isobaric analogue state $T_>$.

[4] R. Sherr, Summer Inst. Theoretical Physics, Colorado, 1965.

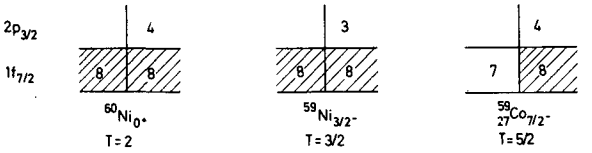

FIG. 39. Ground states of $^{60}Ni_{0^+}$ (T = 2), $^{59}Ni_{(3/2)^-}$ (T = 3/2) and $^{59}_{27}Co_{(7/2)^-}$ (T = 5/2)

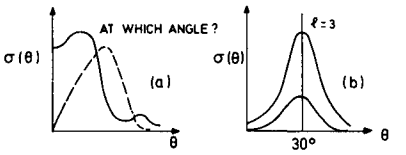

FIG. 40. (a) Angular distribution for different ℓ, (b) $\sigma(\theta)$ for $\ell = 3$ states

9.3. General remarks concerning direct (p, d), (d, p) reactions

The differential cross-section $\sigma(\theta) = S\sigma^{\ell}_{DW}(\theta)$ where S ≡ spectroscopic factor; it contains the nuclear information. $\sigma^{\ell}_{DW}(\theta)$ gives the shape of the angular distribution, usually calculated by distorted wave methods;

$$\sigma^{\ell}_{DW}(\theta) = f(\vec{k}_p, \vec{k}_d, \ell_n, V_{(p,d)}, W_{(p,d)}) \qquad (9.3.1)$$

A particle spectrum at a specific angle is indicative but not conclusive about the value of S, since this angle may be where the Bessel functions are small for some states, large for others. For example: $^{60}Ni(p,d)^{59}Ni$. The $7/2^-$ states of ^{59}Ni need $\ell_n = 3$; therefore, since the Bessel function has a maximum at 30° for $\ell = 3$, this is the angle at which one gets a fair picture of the $7/2^-$ states. In other words, at ($\ell = 3$)30°, the spectrum looks more like S (see Fig. 40).

(a) Spectroscopic factor

$$S = S\{\psi\}$$

↳ nuclear wave functions

S always refers to a reaction connecting 2 states.

(b) Fractional parentage expansion gives

$$\Psi\left(^{60}_{28}Ni_{32}\right)^{\left.\begin{matrix} I_0 = 0 \\ T_0 = 2 \end{matrix}\right\}\ \text{target}} = \sum_{j,T} C_{j,T} \underbrace{\left[\Psi^{j,T}(^{59}Ni)\,\varphi^{j,\frac{1}{2}}\ (\text{neutron})\right]^{\substack{I_0 = 0 \\ T_0 = 2}}}_{(T = 3/2 \text{ or } 5/2)} \qquad (9.3.2)$$

fractional parentage coefficients

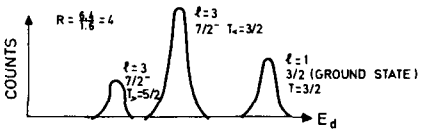

FIG. 41. Stylized spectrum for ^{60}Ni(p, d)^{59}Ni

(c) By definition,

$$S(J_0 = 0,\ T_0 = 2 \rightarrow j, T) \equiv N_j [C_{j,T}]^2 \tag{9.3.3}$$

where N_j is the number of neutrons present in the j^{th} shell, or the number of neutrons in the j^{th} shell which can participate, indistinguishably, in the pick-up reaction.

m

The ^{60}Ni(p, d)^{59}Ni reaction:

(1) Consider $S(0^+ \rightarrow 3/2^-,\ T = 3/2) = 4$ ($\ell = 1$ neutrons)$\times [C_{j,T}]^2$ since $C_{j,T} = 1$ here, $S(0^+ \rightarrow 3/2^-,\ 3/2) = 4$.

(2) Consider $S(0^+ \rightarrow 7/2^-,\ T = 5/2) = 8/5 = 1.6$; for the isobaric analogue state of ^{59}Co in ^{59}Ni. ($E = 7.28$ MeV for $T_>$ case.)

The wave function of ^{59}Ni I. A. S.

$$= \frac{1}{\sqrt{5}} \left|\begin{matrix}4\\8\end{matrix}\right| \left|\begin{matrix}\\7\end{matrix}\right| + \sqrt{\frac{4}{5}} \left|\begin{matrix}1\\7\end{matrix}\right| \left|\begin{matrix}3\\8\end{matrix}\right| \tag{9.3.4}$$

↓ { This term contributes to the reaction ^{60}Ni(p, d)^{59}Ni. }

↓ is a second order process

$$\therefore\ C_{j,T} = \frac{1}{\sqrt{5}}$$

(3) For $T_<$ wave function,

$$^{59}\text{Ni} = \sqrt{\frac{4}{5}} \left|\begin{matrix}4\\8\end{matrix}\right| \left|\begin{matrix}\\7\end{matrix}\right| - \sqrt{\frac{1}{5}} \left|\begin{matrix}1\\7\end{matrix}\right| \left|\begin{matrix}3\\8\end{matrix}\right| \tag{9.3.5}$$

$$\therefore\ C_{j,T_<} = \sqrt{\frac{4}{5}} \tag{9.3.6}$$

$$S(0^+ \rightarrow 7/2^-,\ T_< = 3/2) = 8(4/5) = 6.4 \tag{9.3.7}$$

In view of the above results, one would expect the spectrum for this reaction to be similar to that in Fig. 41. Experimentally, however, one finds the ratio to be 8/1 instead of 6.4/1.6 = 4/1. This implies that either the DWBA calculation is still not in good shape, or that the nuclear state wave functions are not as simple as we wrote them down.

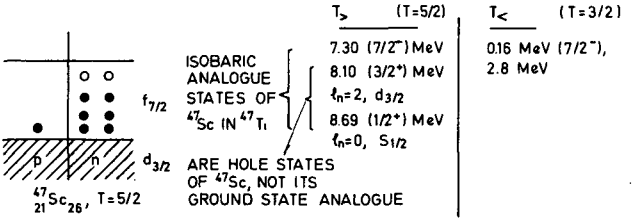

FIG. 42. Parent states of ^{47}Sc in shell-model description

(d) Consider $^{58}_{28}Ni_{30}(p,d)^{57}Ni$:

$$^{57}Ni = A\left\{\frac{1}{\sqrt{3}}\ \frac{|2}{8|7} + \sqrt{\frac{2}{3}}\ \frac{1|1}{7|8}\right\}_{T_>} + B\left\{-\sqrt{\frac{2}{3}}\ \frac{|2}{8|7} + \sqrt{\frac{1}{3}}\ \frac{1|1}{7|8}\right\}_{T_<} \qquad (9.3.8)$$

$N_j = 2$; 2 neutrons in the $p_{3/2}$ shell of ^{58}Ni.

$S(0^+ \rightarrow 3/2^-) = 2$ since $C_{j,T} = 1$, $N_j = 2$.

$S_>(0^+ \rightarrow 7/2^-,\ T = 3/2) = (8)\left(\sqrt{\frac{1}{3}}\right)^2 = 2.66$ we are now in the $f_{7/2}$ shell

$S_<(0^+ \rightarrow 7/2^-,\ T = 1/2) = (8)\left(\sqrt{\frac{2}{3}}\right)^2 = 4.33$

One does not as yet know how to calculate exactly how the strength is shared among the $T_<$ states, or how $S_<$ is fragmented.

9.4. Centre of gravity displacement between $T_<$ and $T_>$ states

$T_>$	$T_<$
^{57}Ni(^{57}Co) 5.22 MeV	2.59, 3.23, 4.20 MeV
^{59}Ni(^{59}Co) 7.28 MeV	2.63, 3.04, 4.17 MeV
^{61}Ni(^{61}Co) 9.55 MeV	1.46, 2.90, 3.28 MeV

We see that the centre of gravity of the $T_<$ states does not change much with A; therefore, the splitting between the $T_<$ and $T_>$ states does increase with neutron excess, i.e. with $T = T_z$. (^{3}He, d) and (d, n) can reveal both $T_>$ and $T_<$ states, but (p, p) resonances cannot.

e.g. $^{48}_{22}Ti_{26}$ in $1f_{7/2}$ shell

^{48}Ti(p, d)^{47}Ti. (One finds 3 peaks in the analogue region; i.e. several isobaric analogues! (Fig. 42)).

9.5. Determination of U_1

From (p, d) (^{3}He, d), (^{3}He, α), etc. reactions one can determine the centre of gravity of the $T_>$ and $T_<$ states

$$E\uparrow = \sum_i \frac{S_{\uparrow i} E_i}{\sum_i S_{\uparrow i}} \text{ for } T + \tfrac{1}{2}$$

and

$$E\downarrow = \sum_i \frac{S_{\downarrow i} E_i}{\sum_i S_{\downarrow i}} \text{ for } T - \tfrac{1}{2}$$

We now might compare the T splitting, $E\uparrow - E\downarrow$, to the Lane term in the optical model potential.

$$E\uparrow - E\downarrow = \frac{U_1}{2A}(2T_t + 1) \text{ where } U = U_0 + U_1(\vec{t}\cdot\vec{T})$$

Therefore, from the above equation we can determine U_1;

$$U_1 \sim 90\text{-}130 \text{ MeV}$$

Other sources of U_1 are:

(1) Semi-empirical mass formula - symmetry term.
(2) Elastic scattering - optical model fit of V, W; then look at the variation of these parameters for various isotopes of the same element (increasing T).

9.6. Nucleon transfers

Two or more nucleon transfers to locate higher analogue states:

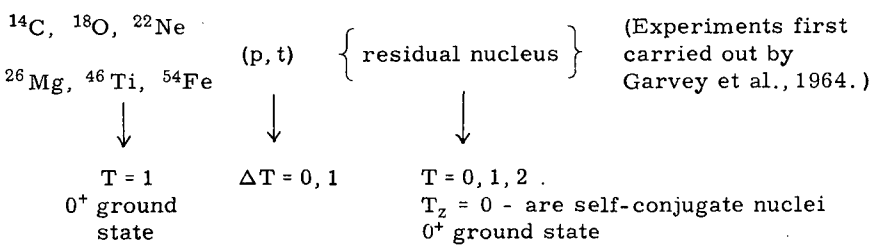

The transfer of two neutrons coupled to spin 0, is L = 0. (p, ^{3}He) reactions form odd-odd neighbours where $T_z = 1$ consequently $T = 1, 2$. The addition of two protons (^{3}He, n) also can lead to $T = T_z + 2$ states.

More than 2 nucleon pick-up:

$(^3He, ^6He)$	$(^4He, ^8He)$
$\Delta T = 3/2, 1/2$	$\Delta T = 2$

The exotic reaction $(^7_4Be_3, t)$ can give T = 2 states in odd-odd nuclei, e.g., first T = 2 state in ^{14}N.

$\downarrow \Delta T = 1$

$T_z = -1/2$

9.7. Coulomb energy differences for (p, d) reactions (Fig. 43)

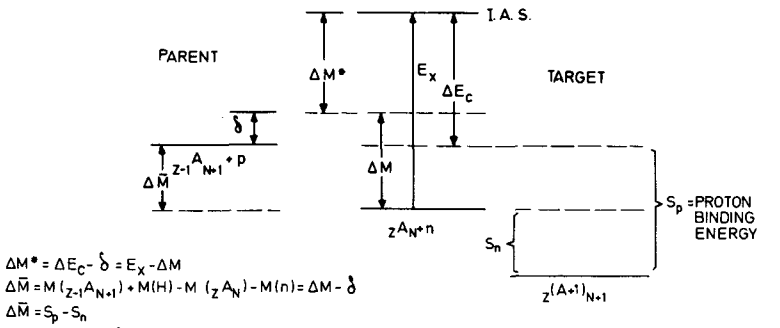

FIG. 43. Energetics for (p, d) reactions

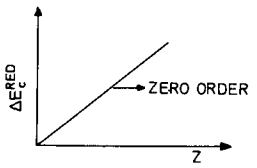

FIG. 44. Reduced Coulomb energy differences versus Z

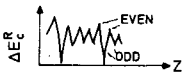

FIG. 45. Odd-even staggering of Coulomb energy differences

We will speak of the reduced Coulomb energy difference, i.e. we have removed the $A^{1/3}$ dependence by calculating

$$\Delta E_c^{red} = \Delta E_c \left(\frac{A}{2Z}\right)^{1/3} \qquad (9.7.1)$$

It is normalized to the isotope which lies on the 45° line (Fig. 44), i.e. ΔE_c^{red} should be the same for all isotopes of an element if the proton distribution were uniform, and $R \propto A^{1/3}$. First order effects:

(Z = 4-30)-the interval where the odd-even effect is pronounced (Fig. 45). Two protons coupled to S = 0 (anti-symmetric) must have symmetric space wave function. They can then get closer together and thereby feel a greater Coulomb effect and so are repelled more. Carlson and Talmi also state that this effect washes out as we add more and more neutrons. The analogue states look less and less like proton states; at higher neutron numbers, an even proton nucleus behaves more and more like an odd proton nucleus, e.g. (^{57}Ni, ^{57}Co). The extra low points on the graph are F(Z = 9) and Sc(Z = 21); they reflect the fact that a single proton outside a closed shell is weakly bound, hence its Coulomb energy is less.

9.8. Second Coulomb energy difference

Let us investigate the difference of the Coulomb energy displacement between successive elements (same A, different Z). Define

$$\Delta_2(Z) \equiv \Delta E_c^{red}(Z) - \Delta E_c^{red}(Z-1)$$

(a) Consider 2 protons:

If $\uparrow\downarrow$ = 0 let the extra Coulomb energy be ϵ_s. If the proton is unpaired, $\bar{\epsilon} = 3/4\ \epsilon_a + 1/4\ \epsilon_s$, where ϵ_a refers to $\uparrow\uparrow$ coupling of the two protons
(S = 1) (S = 0)
(considering its bonds statistically with the rest of the nucleus).

For an odd-Z nucleus (one unpaired proton):

$$\Delta E_c(Z) = E_c(Z) - E_c(Z-1) = (Z-1)\bar{\epsilon} \qquad (9.8.1)$$

($\bar{\epsilon}$: bonds)

For an even Z nucleus:

$$\Delta E_c(Z) = (Z-2)\,\bar{\epsilon} + \epsilon_s \qquad (9.8.2)$$

($\bar{\epsilon}$: with 'core'; ϵ_s: with other proton)

Therefore

$$\Delta_Z(Z \text{ even}) = (Z-2)\bar{\epsilon} + \epsilon_s - ((Z-2)\bar{\epsilon}) = \epsilon_s \qquad (9.8.3)$$

$$\Delta_Z(Z \text{ odd}) = (Z-1)\bar{\epsilon} - [(Z-3)\bar{\epsilon} + \epsilon_s] = 2\bar{\epsilon} - \epsilon_s \qquad (9.8.4)$$

From experiment, we find that

$$\epsilon_s \sim 0.44 \text{ MeV}, \qquad \Delta_2(\text{even}) = 0.44 \text{ MeV}$$

$$\bar{\epsilon} \sim 0.30 \text{ MeV}, \qquad \Delta_2(\text{odd}) = 0.16 \text{ MeV}$$

As an example, let us calculate the Coulomb energy differences for states in ^{57}Ni and ^{57}Co which are analogues of each other. The wave

function for $^{57}_{28}Ni^{*}_{29}$ looks like

$$\psi = \sqrt{\frac{1}{3}}\left(\frac{0|2\ p_{3/2}}{8|7\ f_{1/2}}\right) + \sqrt{\frac{2}{3}}\left(\frac{1|1}{7|8}\right) \qquad (9.8.5)$$

The first term has even Z while the second term has odd Z, so that the Coulomb energy for ^{57}Ni will look more like that for an odd Z nucleus. Taking this into account, we find the Coulomb energy difference between $^{57}_{28}$Ni and $^{57}_{27}$Co to be

$$\Delta E_c = \underset{\text{Even Z}}{\frac{1}{3}\left[(Z-2)\bar{\epsilon} + \epsilon_S\right]} + \underset{\text{Odd Z}}{\frac{2}{3}\left[(Z-1)\bar{\epsilon}\right]} \qquad (9.8.6)$$

$$= \left(Z - \frac{4}{3}\right)\bar{\epsilon} + \frac{1}{3}\epsilon_S$$

For states in ^{59}Ni which are analogues of states in ^{59}Co

$$\Delta E_c = \underset{\text{Even Z}}{\frac{1}{5}\left[(Z-2)\bar{\epsilon} + \epsilon_S\right]} + \underset{\text{Odd Z}}{\frac{4}{5}\left[(Z-1)\bar{\epsilon}\right]} \qquad (9.8.7)$$

$$= \left(Z - \frac{2}{5}\right)\bar{\epsilon} + \frac{1}{5}\epsilon_S$$

This nucleus looks even more 'odd'.

We see that the odd-even effect decreases with increasing neutron number.

We should really take account of the difference in $\bar{\epsilon}$ for a $2p_{3/2}$ proton interacting with a $1f_{7/2}$ proton and two interacting $1f_{7/2}$ protons.

Presumably

$$\bar{\epsilon}_{2p\ 2/3 - 1f_{7/2}} < \bar{\epsilon}_{1f_{1/2} - 1f_{7/2}} \qquad (9.8.8)$$

In general the observed odd-even effect is larger than the odd-even effect predicted by Carlson and Talmi (Phys. Rev. 96 (1964) 436).

10. ISOBARIC ANALOGUE RESONANCES

10.1. Introduction

Isobaric analogue states may also be observed as resonances in the compound nucleus system. The first analogue resonances were accidentally observed by Fox et al. at Florida State University in late 1962 when doing a (p, n) reaction on $^{89}_{39}Y_{50}$. They observed two strong peaks in the excitation curve at a proton energy of about 5 MeV (see Fig. 46).

At first these two bumps presented a real puzzle, since they occurred at an excitation energy in the compound nucleus, $^{90}_{40}Zr_{40}$,

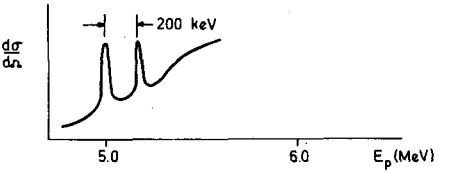

FIG. 46. Excitation curve for (p,n) reaction on ^{89}Y, in region of 2^-, 3^- resonances of ^{90}Zr

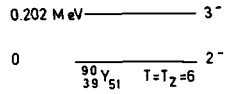

FIG. 47. 2^-, 3^- parent states of $^{90}_{39}Y_{51}$

(about 10 MeV) at which the level density is known to be very high and no single state would be expected to produce an isolated resonance. The suggestion was then advanced by Robson that these states in ^{90}Zr are analogues of low-lying (simple) states in $^{90}_{39}Y_{51}$. Analysis of standard elastic proton scattering experiments then revealed the spins and parities of these two states to be 2^- and 3^-, in agreement with the spins and parities of the ground state and first-excited state of ^{90}Y (Fig. 47). Their energy separation was almost identical. The surprising fact is that the reaction which discovered analogue resonances was forbidden by isospin selection rules.

$$^{89}_{39}Y_{50} + p \rightarrow {}^{90}_{40}Zr^*_{50} \rightarrow {}^{89}_{40}Zr_{49} + n \qquad (10.1.1)$$

T	$\frac{11}{2}$	$\frac{1}{2}$	6	$\frac{9}{2}$	$\frac{1}{2}$

$\vec{11}/2 + \vec{1}/2$ may couple to $\vec{6}$, but $\vec{9}/2 + \vec{1}/2$ can, at most, couple to $\vec{5}$. The reaction occurs, however, because of T = 5 impurities in the $^{90}Zr^*$ wave function and/or a T = 11/2 impurity in ^{89}Zr (G.S.), introduced by Coulomb mixing.

10.2. Energetics of analogue resonance reactions

We may relate the Coulomb energies of ^{90}Y (G.S.) and its analogue in ^{90}Zr by considering a (p,n) reaction on ^{90}Y leaving ^{90}Zr in the analogue state (denoted by a * in Fig. 48).

$$\begin{aligned} Q_{pn} &\equiv M_{\text{target}} + p - M_{\text{residual nucleus}} - n \\ &= {}^{90}Y + p - {}^{90}Zr^* - n \end{aligned} \qquad (10.2.1)$$

But, from the diagram

$$^{90}Zr^* = {}^{89}Y + p + E_p^{cm} \qquad (10.2.2)$$

Therefore

$$\begin{aligned} Q_{pn} &= {}^{90}Y + p - {}^{89}Y - p - E_p^{cm} - n \\ &= {}^{90}Y - {}^{89}Y - n - E_p^{cm} \end{aligned} \qquad (10.2.3)$$

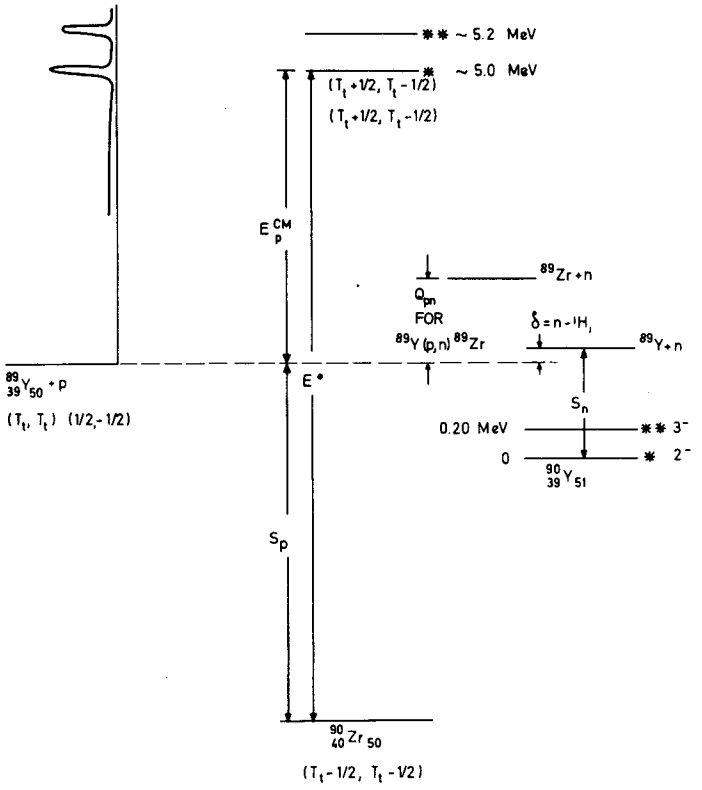

FIG. 48. Energetics for analogue resonances in $^{90}_{40}Zr$

But the separation energy for a neutron from ^{90}Y is given by

$$S_n = {}^{89}Y + n - {}^{90}Y \qquad (10.2.4)$$

Thus

$$Q_{pn} = - S_n - E_p^{cm} \qquad (10.2.5)$$

Now, analogue states, by definition, have the same nuclear interaction energy, and differ only by their Coulomb energies and the difference in mass between a neutron and a hydrogen atom, i.e.

$$^{90}Zr^* - {}^{90}Y = \Delta E_c - n + H \qquad (10.2.6)$$

therefore

$$\Delta E_c = {}^{90}Zr^* + n - {}^{90}Y - H = - Q_{pn} \qquad (10.2.7)$$

Substituting our previous equation for Q_{pn}, we find the difference in Coulomb energies for the two analogue states to be simply

$$\Delta E_c = S_n + E_p^{cm} \qquad (10.2.8)$$

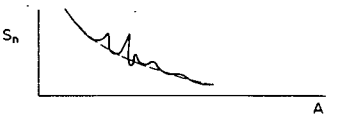

FIG. 49. Variation of S_n (neutron binding energy) as a function of A

In the Anderson-Wong (p, n) experiments Q_{pn} is measured directly from the neutron spectrum and no further calculation is necessary to obtain ΔE_c. Another form for the equation for ΔE_c in terms of the excitation energy E^* and the proton separation energy S_p is immediately available from the diagram

$$E^* = E_p^{cm} + S_p \tag{10.2.9}$$

therefore

$$\Delta E_c = - Q_{pn} = E^* + (S_n - S_p) \tag{10.2.10}$$

which is the same expression as that of Fig. 43.

We may invert the above equations, solving for E_p^{cm}, to see in which regions of the periodic table analogue resonance experiments are possible.

$$E_p^{cm} = \Delta E_c - S_n \tag{10.2.11}$$

Now

$$\Delta E_c = \text{constant} \times Z/A^{1/3} \tag{10.2.12}$$

S_n varies over the periodic table, but the general trend is to decrease with increasing A (see Fig. 49).

The requirement for a possible experiment is that E_p^{cm} be positive. For light elements, the Coulomb barrier is low and $\Delta E_c < S_n$, so that we cannot excite analogues of low-lying states via resonance reactions. Beginning around ^{40}Ca, $\Delta E_c > S_n$ and resonance experiments become energetically possible. Since ΔE_c increases with Z and S_n decreases slowly with increasing A, the required proton bombarding energy increases more rapidly than Z, and in fact we land higher and higher on the Coulomb barrier for increasing atomic number. Hence penetration effects become more important for the heavy elements.

10.3. Elastic analogue resonances and isospin impurities

Historically the first analogue resonance experiment was performed and analysed at Chalk River[5], although it was not labelled as such. The reaction involved was

$$^{14}\text{C}\,(\text{p, n})\,^{14}\text{N}^*$$
$$T = 1 \quad \tfrac{1}{2} \quad \tfrac{1}{2} \quad 0 \tag{10.3.1}$$

[5] G.A. Bartholomew, A.E. Litherland, E.B. Paul, H.E. Gove, Can. J. Phys. 34 (1956) 147; J.B. French, E. Vogt, S. Iwao, Phys. Rev. 122 (1961) 1248.

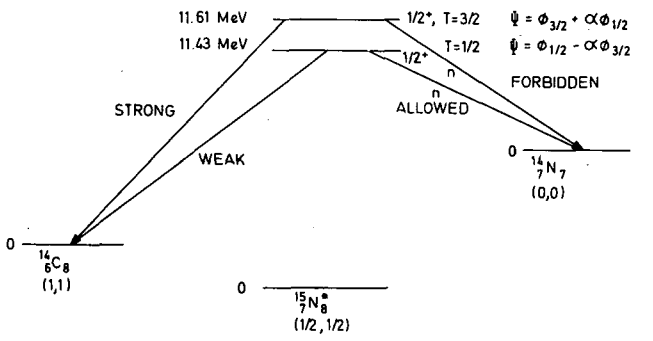

FIG. 50. Level scheme for T = 3/2 resonance in $^{14}C + p \rightarrow {}^{15}N^*$

Two closely spaced resonances, both with $J^\pi = \frac{1}{2}^+$, were observed in the excitation curve; the lower at 11.43 MeV decayed strongly to the ground state of ^{14}N, while the upper at 11.61 decayed weakly. This, along with other evidence, led to the conclusion that the upper state had an isospin one unit larger (= 3/2) than the lower state (T = 1/2) and the upper neutron decay was isospin forbidden. By assuming that the two states mixed their isospins and represented impurities in each other's wave functions, they were able to arrive at a value for the mixing parameter α

$$|\alpha|^2 = \frac{\gamma_n^2(11.61)}{\gamma_n^2(11.43)} \sim 4\% \qquad (10.3.2)$$

The energetics for the reaction are shown in Fig. 50.

What these workers failed to advertise is that the T = 3/2 state in ^{15}N at 11.61 MeV is the analogue of the ground state of $^{19}_{6}C_9$ ($T = T_z = 3/2$; $J^\pi = 1/2^+$). The T = 1/2 state at 11.43 MeV in ^{15}N is not the main companion $T_<$ state, however, since its proton decay to the ^{14}C ground state is weak.

The following points are worth noting when looking for analogue resonances:

(1) We cannot easily discover analogue resonances much above the (p, n) threshold, since the widths become too large and the strength is spread over too large an energy region.

(2) Weak transitions in (d, p) reactions on a given target will not show up as analogue resonances in the analogue, since they do not have large single-particle widths, and moreover will land on the large elastic scattering yield where a small, incremental yield will be much more difficult to detect.

Many analogue states have been observed as elastic scattering anomalies by now. However, not all the states which one might a priori expect to excite are observable. Specifically, no one has yet observed elastic analogue resonances of collective states or of states which have a complex mixture of configurations. Those states which are strongly excited via (p, p) reactions can be described as being good single-particle states, almost by definition.

The relationship between (d, p) and (p, p) studies on the same target is very essential and deserves further clarification. The (d, p) reaction

can be used to form the parent states of an isobaric analogue pair. These reactions add neutrons into bound, low-lying states. The only way to do this is via either (d, p) or (t, d) reactions. The (n, γ) reaction, on the other hand, puts neutrons into unbound states. The (p, p) reaction is a proton deposition reaction which puts protons into unbound, compound-resonant states and, like (n, γ) reactions, can only excite higher states in the daughter nucleus. These states can have $T = T_{target} \pm 1/2$.

Denoting the target (core) nucleus by C, let us consider

$$\begin{array}{llll} & C + p \rightarrow & (C + p)^* \rightarrow & C + p \\ T_z & T_z - 1/2 & T_z - 1/2 & \\ T & T_z \quad 1/2 & T_z + 1/2 & \end{array} \qquad (10.3.3)$$

where the analogue state (*) is a state in the compound system.

As a specific example consider the case of

$$\begin{array}{llll} & {}^{89}_{39}Y_{50} + p \rightarrow & ({}^{90}_{40}Zr_{50})^* \ (J = 2^-) & \\ T_z & 11/2 \quad -1/2 & T_z = 5 & \\ T & 11/2 \quad 1/2 & T = 6 & \end{array} \qquad (10.3.4)$$

(The $T = 6$, $T_z = 5$ state is an analogue of the ground state of ${}^{90}_{39}Y_{51}$ ($T = T_z = 6$).

The agreement between the two level schemes, that is to say between the known states of ${}^{90}Y$ and those excited in ${}^{90}Zr^*$ as compound-nucleus resonances is probably the most spectacular seen to date. (These results are reported in the Heidelberg Conference, 1966, by J.D. Fox.) The level schemes are shown in Fig. 51. The analysis of these reactions is more or less straight-forward and allows one to extract the pertinent resonance parameters.

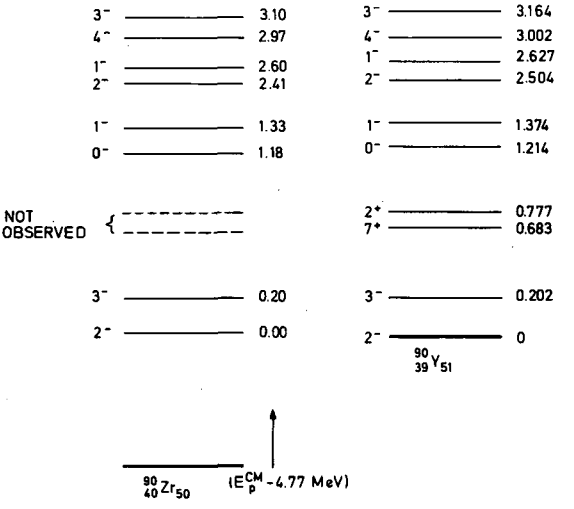

FIG. 51. Level schemes for ${}^{90}_{40}Zr_{50}$ (analogues) and ${}^{90}_{39}Y_{51}$ (parent states)

10.4. Resonances in the medium-to-heavy region

The analysis of the resonances occurring in the medium-to-heavy region has been carried out usually assuming only a contribution from Coulomb scattering, and a single isolated resonance. Three terms then contribute to the elastic scattering: a Coulomb term, a resonance term and an interference term.

$$\left(\frac{d\sigma}{d\Omega}\right)_{\text{Elastic}} = \left(\frac{d\sigma}{d\Omega}\right)_{\text{Coulomb}} + \left(\frac{d\sigma}{d\Omega}\right)_{\text{Resonance}} + \left(\frac{d\sigma}{d\Omega}\right)_{\text{Interference}} \tag{10.4.1}$$

where

$$\left(\frac{d\sigma}{d\Omega}\right)_{\text{Coulomb}} = \frac{\pi}{k^2}\left|C(\theta)\right|^2 \tag{10.4.2a}$$

and

$$C(\theta) = \frac{1}{\sqrt{\pi}}\eta\left(\frac{\theta}{2}\right)\exp\left[-2i\eta\ln\left(\sin\left(\frac{\theta}{2}\right)\right)\right] \tag{10.4.2b}$$

where

$$\eta = \frac{Z_1 Z_2 e^2}{\hbar v_{\text{Relative}}} \simeq \left\{\frac{\text{distance of closest approach}}{\lambda\!\!\!^{-}}\right\} \tag{10.4.3}$$

or numerically

$$\eta = 0.15748\, Z_1 Z_2 \sqrt{\frac{M}{E}}$$

where E is measured in MeV and M is the reduced mass in atomic mass units. The resonant term is given by

$$\left(\frac{d\sigma}{d\Omega}\right)_{\text{Resonance}} = \frac{1}{(2i+1)(2I+1)} \times \frac{1}{k^2} \sum_{ss'L} B_L(s,s')P_L(\cos\theta) \tag{10.4.4}$$

where

$$B_L(s,s') = \frac{1}{4} \sum_{\substack{J_M J_N \\ \ell_M \ell_N \\ \ell'_M \ell'_N}} (-1)^{s-s'} \times Z(\ell_M J_M \ell_N J_N | sL) \times Z(\ell'_M J'_M \ell'_N J'_N | sL) \times T^{J_M}_{s\ell_M s'\ell'_M} \times T^{J_N *}_{s\ell_N s'\ell'_N} \tag{10.4.5}$$

and

$$T_{s\ell s'\ell'} = e^{2i\omega_\ell}\,\delta_{\ell\ell'}\delta_{ss'} - e^{i(\omega_\ell - \phi_\ell)}\, e^{i(\omega'_{\ell'} - \phi'_{\ell'})}\left\{\delta_{ss'}\,\delta_{\ell\ell'} + \frac{i\sqrt{\Gamma_{J_{s\ell}}}\,\sqrt{\Gamma_J}}{(E_J - E) + \frac{i\Gamma_J}{2}}\right\} \quad (10.4.6)$$

$$\omega_\ell = \sum_{m=1}^{\ell} \mathrm{tau}^{-1}\,\frac{\eta}{m} \quad (10.4.7)$$

$\omega_0 = 0$ is the Coulomb phase shift and i and I refer to the spin of the projectile and target, respectively. The purely resonant term is usually small, the observed elastic scattering anomaly being caused principally by the interference term

$$\left(\frac{d\sigma}{d\Omega}\right)_{\text{Interference}} = \frac{1}{(2i+1)(2I+1)}\,\frac{\sqrt{\pi}}{k^2}\sum_{SLJ}(2J+1)\,\mathrm{Re}\left[i\,T^J_{s,\ell,s\ell}\,C(\theta)\right]P_L(\cos\theta) \quad (10.4.8)$$

where P_L = the nuclear phase shift for the ℓ'th partial wave.

Summations are subject to the following restrictions:

$$|i - I| \le s \le I + i; \quad |J - s| \le \ell \le J + s$$

$$|\ell_N - \ell_M| \le L \le \ell_N + \ell_M \quad (10.4.9)$$

$$L \le 2\ell_{Max};\ 2\ell'_{Max} \text{ or } 2J \qquad \text{whichever is smallest.}$$

It should be noted that the analyses of analogue states in the heavy nuclei A ~200 have included the effects of nuclear potential scattering by assuming that the underlying background, in addition to Coulomb scattering, can be described by an optical model, and then superimposing a resonance term on this background and extracting the important resonance parameters. Clearly this method breaks down when the resonance under study exhausts a large portion of the single-particle limit, since the optical model generates such a single-particle resonance by itself, and we would have a redundancy.

This expression is somewhat simplified for spin 1/2 on spin 0 (Coulomb amplitude plus one partial wave).

$$\left.\frac{d\sigma}{d\Omega}\right|_{\text{Coulomb}} = |f(\theta)|^2 \quad (10.4.10)$$

$$\left.\frac{d\sigma}{d\Omega}\right|_{\text{Resonance}} = \sum_{ss'L}(-1)^{s-s'}\,\frac{\bar{Z}(\ell j \ell j s L)\,\bar{Z}(\ell j \ell j s' L)\,\Gamma^p_{\ell s j}\,\Gamma^{p_0}_{\ell s j}\,P_L(\cos\theta)}{8k^2\left\{(E^{J^\pi} - E)^2 + 1/4\,\Gamma^{J^{\pi 2}}\right\}} \quad (10.4.11)$$

$$\left.\frac{d\sigma}{d\Omega}\right|_{\text{Interference}} = -\frac{1}{2k}\,(2J+1)\,\Gamma^p_{\ell j s}\,\mathrm{Re}\left\{\frac{f(\theta)\,\ell^{-2i\omega_\ell}\,P_\ell(\cos\theta)}{\left(E_{J^\pi} - E - \frac{i\Gamma_{J^\pi}}{2}\right)}\right\} \quad (10.4.12)$$

where $L_{Max} = 2\ell, 2J$, whichever is smaller.

In general a measure of the size of the resonant 'effect' is given by

$$\sim \frac{(2J+1)}{(2I+1)\,(2i+1)} \frac{\Gamma^{p}}{\Gamma_{\text{Total}}} P_{\ell}(\cos\theta) \qquad (10.4.13)$$

so that spin 0 (even-even) targets will naturally show larger effects. Also, to locate resonances, the larger the θ the better. Some standard 'signatures' for different ℓ-values can be seen, for example, in Vourvopoulos et al. (1966).

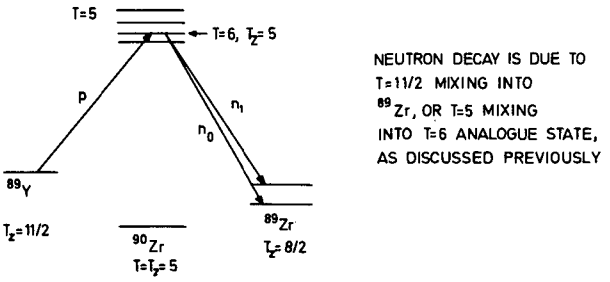

FIG. 52. Neutron and proton channels for the reaction $^{89}Y(p,n)^{89}Zr$

10.5. The reaction $^{89}Y + p$

Let us look at the reaction $^{89}Y + p$ and examine the neutron and proton channels (Fig. 52).

In ^{89}Zr, $T = 11/2$ states (of same spin and parity) mix with the ground state, owing to the Coulomb field; thus we can couple T in an allowed way in the exit channel. What one observes is a proton width comparable to the neutron width; this may be understood when we consider the strength of these two channels in terms of the square of the Clebsch-Gordan coefficients coupling the neutron and proton channels:

(1) for the proton channel:

$$(T_t T_t \tfrac{1}{2} \; -\tfrac{1}{2} \,|\, T_t \; +\tfrac{1}{2}\, T_t \; -\tfrac{1}{2})^2 = \frac{1}{2T_t + 1}$$

(2) (a) for the neutron channel (the $T = 5$ impurity in the $T = 6$ state)

$$(T_t \; -1 \; T_t \; -1 \; \tfrac{1}{2}\,\tfrac{1}{2} \,|\, T_t \; -\tfrac{1}{2}\; T \; -\tfrac{1}{2})^2 = 1$$

in other words, the proton is handicapped by a $(2T_t + 1)$ factor due to geometry alone.

(b) for the neutron channel impurity due to $T = 11/2$ in ^{89}Zr

$$(T_t\, T_t \; -1 \; \tfrac{1}{2}\,\tfrac{1}{2} \,|\, T_t + \tfrac{1}{2}\; T_t \; -\tfrac{1}{2})^2 = \frac{2T_t}{2T_t + 1} \cong 1 \text{ also.}$$

When the reduced widths for neutron decay and proton decay are compared one must put them on an equal footing. The quantities to be compared are $(2T_t + 1)\theta_p^2$ and θ_n^2, and not θ_p^2 and θ_n^2. With the R-matrix approach and a square-well potential model, the reduced widths are derived from the experimentally observed width

$$\Gamma_{\ell js}^{obs} = 2 P_\ell \gamma_{\ell s}^2$$

where P_ℓ is the penetration factor for ℓ - wave protons. Using the Wigner limit $\gamma_\omega^2 = 3/2\ \hbar^2/\mu a^2$ we define $\theta^2 = \gamma_{\ell s}^2/\gamma_\omega^2$.

Boosting the proton width by the $(2T_t + 1)$ factor and including barrier penetration, we find $(2T+1)\theta_p^2/\theta_n^2 \simeq 10^2 - 10^3$ for the special case of $^{90}Zr^*$ where $\Gamma_p \simeq \Gamma_n \simeq 5$ keV. In other words, the intrinsic probability for neutron emission is highly suppressed.

10.6. Comparison of stripping and elastic scattering reduced widths

One can also obtain reduced widths from (d, p) experiments:
Compound nucleus resonance: $C + p \rightarrow A \rightarrow C + p$ leads to γ_p^2, the reduced width for proton capture into analogue states.
Stripping: $C + d \rightarrow C + n + p$ leads to γ_n^2, the reduced width for neutron capture into a bound parent state.

By expressing the $|T, T-1\rangle$ wave function with fractional parentage coefficients

$$\Psi_{T,T-1} = \sum_{\alpha T_f} a_{\alpha T_f} \sum_m (T\, M_f\, \tfrac{1}{2}\, m \,|\, T\, T-1)\psi_{\alpha T_f M_f}\varphi_{1/2\, m} \qquad (10.6.1)$$

the reduced width is expressed as

$$\gamma^2_{\alpha T_f M_f m} = [a_{\alpha T_f}(T_f\, M_f\, \tfrac{1}{2}\, m \,|\, T\, T-1)]^2 \qquad (10.6.2)$$

The reduced width expresses the probability that $\Psi_{T,T-1}$ can be written as $\psi_{\alpha T_f M_f}$ multiplied by a nucleon $\varphi_{1/2m}$, where $a_{\alpha T_f}$ is the fractional parentage coefficient.

Also note that

$$\frac{\gamma_p^2}{\gamma_n^2} = \frac{(T_t\, T_t\, \tfrac{1}{2} - \tfrac{1}{2} \,|\, T_t + \tfrac{1}{2}\ \ T_t - \tfrac{1}{2})^2}{(T_t\, T_t\, \tfrac{1}{2}\, \tfrac{1}{2} \,|\, T_t + \tfrac{1}{2}\ \ T_t + \tfrac{1}{2})^2} = \frac{1}{2T_t + 1} \qquad (10.6.3)$$

10.7. Fine structure in isobaric analogue states

Not so long ago several reactions were studied in which it was expected that the total width Γ of a compound nucleus resonance should be equal to Γ_p, the partial proton width. Such cases would exist if none, or few channels were open, other than the incident (elastic) channel. An example is $^{92}Mo(p,p)^{92}Mo$, where an isobaric analogue resonance exists such that $|Q_{pn}| > E_p^{cm}$; i.e. the (p, n) channel is closed; with poor resolution, we see something like Fig. 53(a).

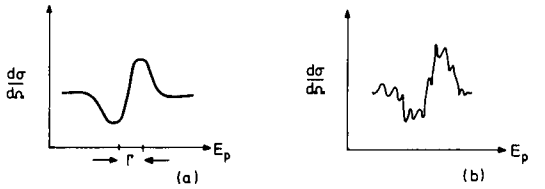

FIG. 53. (a) Elastic scattering (poor resolution)
(b) Elastic scattering (high resolution)

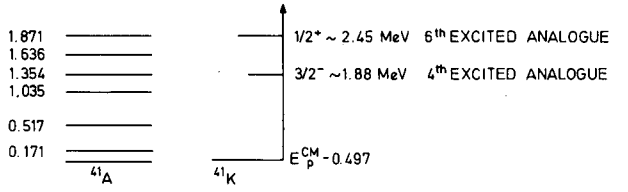

FIG. 54. Isobaric analogues in the Duke experiment

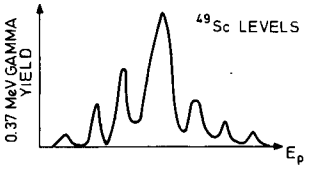

FIG. 55. Fine structure of ^{49}Ca ground-state analogue in ^{49}Sc (Ricci et al.)

However, the best fit to the experimental cross-section yields $\Gamma_p \sim 1/3\ \Gamma$, (the resonance was 30 keV wide) i.e. Γ_p could account for only 10 keV. Thus we are not dealing with a simple resonance, but with many closely-spaced resonances of the same spin and parity, and lower T, which are seen when the experiment is redone with higher resolution (Fig. 53(b)).

In the ^{40}Ar+p 'Duke experiment' (Keyworth et al., 1966), a rather light analogue experiment, the level density of $T_<$ states is low enough so that the best resolution experiments could just resolve them and analyse them individually over the entire 'analogue state' region.

At 1.88 MeV levels, the excitation function was found with an energy resolution of the order of 250 volts (and sophisticated equipment). What was seen was not one $3/2^-$ resonance (see Fig. 54) but 17 of them, all $3/2^-$ having total widths varying from 70 volts to 800 volts. Every one of these resonances had the signature of $3/2^-$. When looked at with poor energy resolution (5 keV), the signature was also $3/2^-$, but just one resonance was seen. All 17 levels add coherently to give an overall $3/2^-$ shape when the beam energy spread becomes large enough.

With the ^{48}Ca(p, nγ)^{48}Sc reaction, what was observed was the yield of 0.37 MeV gamma radiation, which reflects more or less the total

neutron yield to several low-lying states of ^{48}Sc. Seven components were resolved whose widths varied between 1.2 and 3.4 keV,[6] presumably corresponding to the ground state of ^{49}Ca (see Fig. 55).

10.8. Spreading width

As we have seen, when many levels participate in a resonance, the partial proton width may be less than the total width, even when we know that no other channels having appreciable width are open; i.e.

$$\Gamma_{\text{Total}} \neq \sum_{c'} \Gamma_c$$

Thus we define a 'spreading width' as the remaining width

$$W = \Gamma_{\text{Total}} - \sum_{c} \Gamma_c \qquad (10.8.1)$$

A better definition extends the sum $\sum_{c'} \Gamma_c$, only over channels which enjoy T-allowed decay, before the mixing with $T_<$ is turned on.

The theory dealing with the fine structure near analogue resonances is due to Robson (1965), and will not be discussed here. The origin of the spreading width is presumably the Coulomb field but details are not fully understood at present, both theory and experiment are actively being pursued at this time.

The Duke data (Kayworth et al., 1966) for elastic proton scattering from ^{40}A, with extremely high energy resolution being used, found all of the individual members of two Lane-Wigner-Thomas giant resonances in ^{41}K. Standard elastic scattering analysis showed that each individual resonance had $J^\pi = 3/2^-$ (or $1/2^+$) and $\Gamma_p/\Gamma \cong 1$. Thus a simple $3/2^-$ ($1/2^+$) shell-model configuration for the 1.88 MeV (2.43 MeV) state in ^{41}K had been fragmented through the residual interactions into many components. Earlier data taken at Iowa with cruder resolution showed only a single $3/2^-$ ($1/2^+$) resonance (see Figs. 56 and 57). Upon analysis, the experimenters found $\Gamma_p/\Gamma < 1$. The question here is what happened to the missing width, i.e. why isn't $\Gamma_p = \Gamma$? The answer is that Γ_{observed} was larger than $\Sigma\Gamma_{\text{Duke resonances}}$, since the tails of individual resonances added coherently to produce one large resonance, with much non-resonant range in between. The surplus width is known as the spreading width

$$W = \Gamma - \sum_{c} \Gamma_c \qquad (10.8.2)$$

10.9. Comparison of reduced widths for proton and neutron addition (or removal)

$$\gamma_p^{\text{obs.}} = \gamma_p + \gamma_p^{\text{mixing}} \qquad (10.9.1)$$

[6] Chilosi, Ricci and Vingiani, Heidelberg Conference, 1966, and private communication.

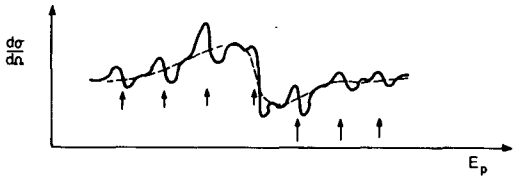

FIG. 56. Fragmentation of a simple $3/2^-$ $(1/2^+)$ shell-model configuration state into many components through the residual interaction (stylized)

The true proton reduced width amplitude γ_p depends on the assumption of a sharp nuclear radius R, i.e. the possibility of factoring the penetrability.

$$\text{Limit}_{R \to \infty} \gamma_p = 0 \qquad (10.9.2)$$

since the analogue state is a 'bound' state and hence vanishes exponentially at infinity. According to Robson, $\gamma_p^{\text{mixing}} = 0$ in the interior region, since, as we saw earlier, the Schrödinger equation becomes uncoupled in the interior region because, on the average, we have a cancellation between $|Q_{pn}|$ and V_c.

A more recent approach to the mixing problem has been carried out by Schiffer (1966) and Bondorf (1966). By means of a computer calculation, they consider protons scattering from an optical model potential, (having no imaginary part which would correspond to the absorption of particles - or a reaction) where the well depth is adjusted so that the neutron binding energy, S_n, agrees with experiment. Then, adding a uniform single-particle Coulomb potential for proton scattering, the calculation should yield a resonance in the cross-section whose width Γ is the maximum single-particle width for protons scattering from a given target nucleus. This Γ serves as a 'Wigner limit' for the problem. The ratio of the observed width $\Gamma_{obs.}$ to Γ is defined as the spectroscopic factor

$$S_{p,p} = \frac{\Gamma_{obs.}}{\Gamma} \qquad (10.9.3)$$

To provide a fair comparison with neutron reduced widths our $\Gamma_{obs.}$ should be multiplied by $2T + 1$ (since we cannot see all of the single-particle state in scattering).

$$S_{p,p} = \frac{(2T+1)\Gamma^{obs.}_{pI_jJ}}{\Gamma^{\text{Single Particle}}_{pI_jJ}} \qquad (10.9.4)$$

The neutron spectroscopic factor, usually obtained from (d, p) reactions via DWBA analysis, is defined by

$$S_{d,p} = \frac{\gamma^2_{nI_jJ}}{\gamma^{2\ \text{Single Particle}}_{nI_jJ}} \qquad (10.9.5)$$

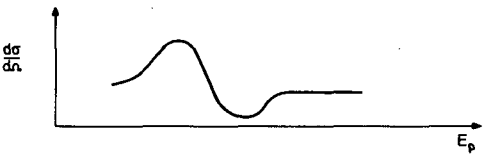

FIG. 57. Same as Fig. 56, with low resolution

TABLE VI. A COMPARISON OF NEUTRON AND PROTON SPECTROSCOPIC FACTORS FOR ^{49}Ca-^{49}Sc

J	Γ_t (keV)	Γ_p (keV)	$S_{p,p}$	$S_{d,p}$
$3/2^-$	8.2	2	0.64 ± 0.07	1.03
$1/2^-$	200	136	1.24 ± 0.27	1.33
$5/2^-$	40	24	0.91 ± 0.2	0.72
$9/2^+$	25	2.7	0.31 ± 0.1	0.31

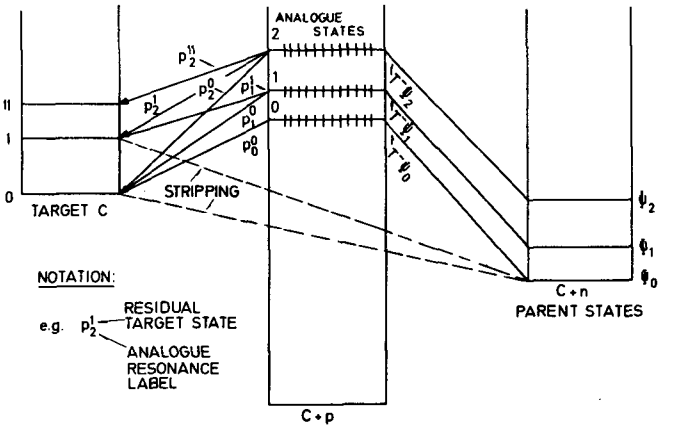

FIG. 58. Relation of the compound nucleus (C + p) and corresponding parent states in the nucleus (C + n), to the target nucleus C

A comparison of proton and neutron spectroscopic factors for ^{49}Ca-^{49}Sc is in Table VI, based on data from Schiffer et al. (1966) at Argonne National Laboratory.

10.10. Analogue resonances in inelastic proton scattering

Analogue states in the compound nucleus (C + p) may decay to the ground state or the low-lying excited states of the target nucleus C;

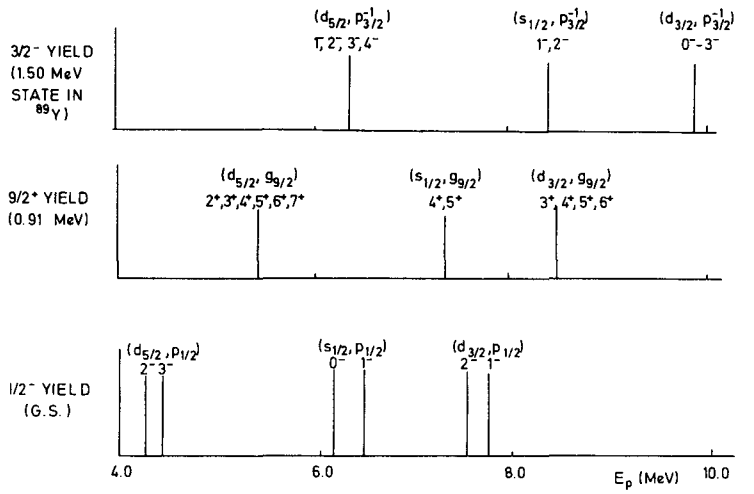

FIG. 59. Proton energies at which resonances should be observed in $^{89}Y + p$, elastic and inelastic scattering and probable particle-hole configurations for coupling the target nucleus ^{89}Y weakly to a proton

therefore, resonances are expected in both elastic and inelastic scattering at the appropriate incident proton energies. Possible decays of the compound nucleus are illustrated in Fig. 58, as well as the corresponding parent states in the nucleus (C + n).

The question of how a compound-nuclear analogue state distributes its strength among the target levels in inelastic scattering depends upon how well the target and compound levels can be described by various configurations.

Example: This point is well illustrated in data on proton scattering from doubly-magic $^{208}_{82}Pb_{126}$ (Moore et al., Phys. Lett. 22 (1966) 616). ^{208}Pb has three low-lying levels at energies of 2.61 MeV, 3.19 MeV, and 3.48 MeV with $J^\pi = 3^-$, 5^-, and 4^-, respectively. The 5^- and 4^- states can be described simply as the coupling of a $g_{9/2}$ particle to a $p_{1/2}$ hole, i.e. $(g_{9/2}, p_{1/2}^{-1})_{4^-,5^-}$, while the 3^- state consists of mixing about 30 single-particle configurations. Thus when we excite the $9/2^+$ analogue state in ^{209}Bi of the ground state of ^{209}Pb, we observe a strong yield only on resonance to the 5^- and 4^- states in ^{208}Pb, with yield to the 3^- state coming from a wide region of excitation in ^{209}Bi. Furthermore, we find that the angular distribution of inelastically-scattered protons to the 5^- and 4^- states is isotropic. The explanation for this fact is that in order to create a $p_{1/2}$ hole to form a $(g_{9/2}, p_{1/2}^{-1})_{5^-,4^-}$ configuration we must emit a $p_{1/2}$ proton and, since one of the restrictions on the complexity of a resonant angular distribution is that $L \leq 2j = 2\frac{1}{2} = 1$ and L must be even, the only Legendre polynomial contributing to the cross-section is $P_0(\cos\theta) = 1$. Similarly, we can form analogues of ^{208}Pb in ^{208}Bi via the reaction

$$^{207}Pb(p_{1/2}^{-1}) + p \rightarrow {}^{208}Bi^* \sim {}^{208}Pb \qquad (10.10.1)$$

and now observe elastic scattering through the 5^- and 4^- states as compound resonances formed by a $g_{9/2}$ proton coupling to the $p_{1/2}$ hole of ^{207}Pb, while seeing no anomaly at the location corresponding to the 3^- state (Bredin et al., 1966).

10.11. The window effect in inelastic scattering (Ref. D.L. Allan, 1965)

The diagrams in Fig. 59 indicate the proton energies at which resonances are observed in the cross-section for scattering to the ground state ($1/2^-$), the 0.91 MeV first-excited state ($9/2^+$), and 1.50 MeV second-excited state ($3/2^-$) of ^{89}Y. Also shown are probable single-particle configurations for coupling the residual nucleus, thought of as a $2p_{1/2}$ particle (G.S.), $1g_{9/2}$ particle (0.91 MeV state) and $2p_{3/2}$ hole (1.50 MeV state), respectively, with a proton first in the $2d_{5/2}$ shell, next in the $3s_{1/2}$ shell, and finally in the $2d_{3/2}$ shell as we increase the incident proton energy.

For the excited-state yields we are using the extreme weak coupling model so that all possible couplings are degenerate in energy, e.g. 2^+, 3^+, 4^+, 5^+, 6^+, 7^+ in the case of ($d_{5/2}$, $g_{9/2}$). What Allan noted from such experiments (actually in Sn isotopes) is that resonances occur in the inelastic yields to states in the target in an energy band ΔE approximately ΔE above the ground state analogue resonant energy; in our example this would be the energy of a $d_{5/2}$, $s_{1/2}$, or $d_{3/2}$ proton plus the excitation energy in ^{89}Y for the residual excited state. This effect has also been observed in many other nuclei.

10.12. Remark

An interesting effect should exist in (p,n) analogue resonance reactions, where the isospin-forbidden neutron groups to the various states of the residual nucleus can be resolved: one should observe the same branching ratios and other characteristic properties for the different neutron groups on and off resonance. The reason is that the only neutron decay strength of these resonances is introduced through isospin mixing with $T_<$ states, an overlapping sea of which (with slowly varying decay properties) surrounds our particular $T_>$

TABLE VII. COMPETING PROCESSES IN ISOBARIC ANALOGUE RESONANCE EXPERIMENTS

Scattering	Resonant	Non-resonant		
		Coulomb	Nuclear	
Elastic	Compound Nucleus: analogue states and $T_<$ states	Rutherford	Optical Model	Channel coupling
Inelastic	Compound Nucleus: analogue states and $T_<$ states	Coulomb excitation	Direct excitation	(Satchler, Tamura, etc.)
	→ Channel coupling (Robson)	Background on which the analogue resonance sits.		

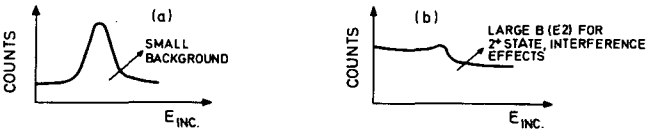

FIG. 60. Inelastic resonant excitation curves:
(a) for small direct excitation
(b) for large Coulomb (or other direct) excitation

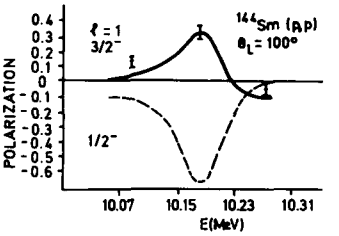

FIG. 61. Proton polarization determines J for analogue state of ^{145}Sm

state; hence the neutron decay of $T_>$ should reflect only the $T_<$ properties.

In a similar manner, for the isospin-forbidden resonance reactions discussed earlier, where the proton decay is isospin forbidden, all proton decay properties should reflect those of the (few?) $T_<$ states (having same spin and parity) which admix into the state in question. We thus have a powerful 'tracer' technique for locating the specific sources of isospin impurity.

10.13. Summary (see Table VII)

Interference can occur between any of the columns of Table VII. If the B(E2) to excited target states is small, then not only is the Coulomb excitation contribution weak, but the direct excitation is likely to be small as well. For the 2^+ first excited states of even-even nuclei which have large B(E2) values, there is a good overlap between ground state and 2^+ states. Since the 2^+ state is mostly a collective state, single particle processes (such as ours) proceed weakly, i.e. not only is there a large non-resonant background (Fig. 60) but there is not much resonant contribution, so that these states show little effect at resonance. The same is true for the 3^- collective states.

10.14. Polarization measurements on analogue resonances
Refs. Moore and Terrell, Fiarman et al., 1966)

These authors determine the J value unequivocally after the ℓ value is known; it requires only a semi-theoretical treatment. Elastic scattering experiments determine the ℓ value, and from this one predicts (theoretically) the polarization curves for $\ell \pm 1/2$. One then performs the polarization experiment (second scattering from a known

polarizer, e.g. carbon) to see which of the vastly different curves is applicable (Fig. 61).

$$\left(\frac{d\sigma}{d\Omega}\right)_{\text{elastic}} = A^* A + B^* B$$

$$P = \text{polarization} = \frac{A^* B + B^* A}{A^* A + B^* B}$$

Therefore

$$\frac{d\sigma}{d\Omega} P = A^* B + B^* A = 2\text{Re}(A^* B)$$

where

$$A = -\frac{\eta}{2k} \text{cosec}^2 \frac{\theta}{2} e^{i\eta \ell n \text{cosec}^2 \theta/2} + \frac{i}{2k} \sum_{L,J} (J + \tfrac{1}{2}) T_{L,J} P_\ell(\cos\theta)$$

and

$$B = \frac{1}{2k} \sum_{L,J} (-1)^{L+J+1/2} T_{L,J} P_\ell^1(\cos\theta)$$

$$T_{L,J} = e^{2i\omega_L} - U_{L,J}, \quad \omega_L = \text{Coulomb phase} \qquad (10.14.1)$$

$$U_{L,J} = e^{2i\omega_L} \left[e^{2i\xi_L} + e^{2i\varphi_L} \frac{i\Gamma}{(E_J - E) - \frac{i\Gamma_L}{2}} \right] \qquad (10.14.2)$$

where ξ_L = optical model phase (complex)
φ_L = background resonant phase (real)
and when $\text{Im}\xi_L = 0$ then $\xi_L = \varphi_L$.

At resonance one sees a large polarization effect, whereas the effect in the elastic cross-section might be small; $d\sigma/d\Omega$ is proportional to $|A|^2 + |B|^2$ and $|A| > |B|$, therefore $|A|^2 \gg |B|^2$ (the first term in A is large and non-resonant). However, P is linear in A^*B and the resonant term modifies the non-resonant term in first order.

11. OTHER WAYS OF FORMING ANALOGUE STATES

11.1. Yavin method (Figs. 62 and 63)

The Yavin method also makes use of the (p,n) reaction, but instead of looking at the outgoing neutrons (Anderson, Wong – time-of-flight measurements), one is interested in the subsequent outgoing protons, specifically, the 'delayed' protons emitted after the (p,n) reaction. (Yavin et al., Phys. Rev. Lett. 16 (1966) 1049).

$$Z^A + p \rightarrow (Z+1)^{A*} + n \qquad (11.1.1)$$
$$\hookrightarrow Z^{A-1}(\text{ground state}) + \bar{p}$$

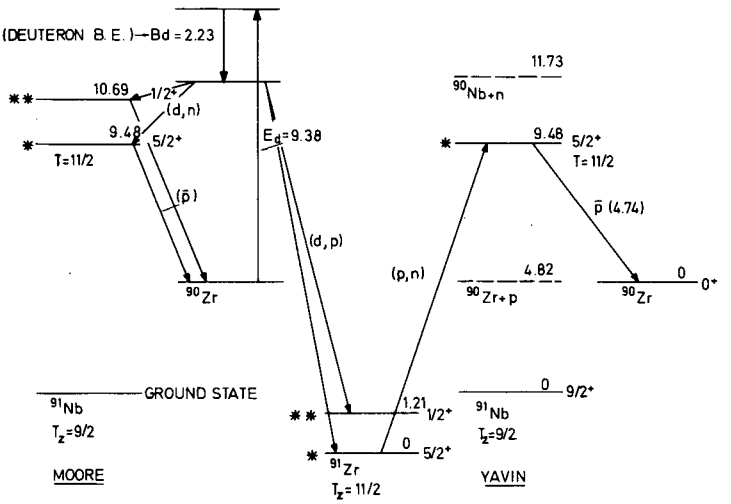

FIG. 62. Energetics for (p, np̄) (Yavin et al.) and (d, np̄) (Moore et al.) experiments

The reaction they investigated was $^{91}Zr\,(p, n\bar{p})^{90}Zr; {}^{91}Nb^{*}$ is proton unstable but neutron stable. This experiment can be done with poor beam resolution. In fact, for the analogue state to be distinct in the proton spectrum, poor beam resolution is preferable. Very good resolution would show the fine structure associated with the $T_<$ states surrounding the analogue state thereby masking the analogue peak. The detector resolution, however, should be as good as the width of the analogue state. Note that

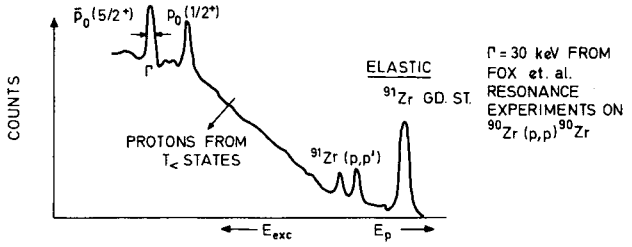

FIG. 63. Proton spectrum for ^{91}Zr + p experiment of Yavin

1. (p, n) reaction picks out $T_>$ states because it is mainly an isoscalar reaction ($\Delta T = 0$).
2. Since $^{91}Nb^{*}$ (9.48 MeV) is an analogue state, it has a simple configuration and therefore a large reduced width for proton emission (analogue states are mostly single particle states.).

The proton spectrum (Fig. 63) shows that, although one has poor beam resolution, the 'delayed' proton-peak widths will be sharp as long as they are not hampered by poor detector resolution. If the incident proton energy is changed, the analogue peaks will not shift (to first order*)

although the proton elastic and inelastic scattering spectrum will shift. For proton energies far above threshold, however, in the $(p, n\bar{p})$ reaction on ^{91}Zr, the analogue levels are broadened due to the large momentum given $^{91}Nb^*$ which then emits a proton; this is a Doppler broadening of the level. Therefore the best results are obtained when E_{inc} is near the $(p, n\bar{p})$ threshold.

11.2. Photoprotons from $T_>$ states (Ref. Temmer, unpublished)

As was mentioned earlier, one can excite $T = T_z$ as well as $T = T_z + 1$ states by electric-dipole photons on neutron-excess nuclei. (Fallieros et al., 1966). Once again, in the spirit of Yavin, one can use a poor resolution photon beam (that is the way they are, usually!) and good resolution proton detector to find the protons from the (γ, p) reaction through the analogue state. Again, the simplicity of the $T_>$ analogue configuration compared to the $T_<$ configurations around it will favour proton emission; moreover, the above-threshold broadening effect mentioned in connection with the $(p, n\bar{p})$ reaction does not occur because of the small momentum of the photon. There is a geometric factor (cf. section 2.3(c)) as well as a structure factor against the $T_>$ state, and it remains to be seen experimentally if the $T_>$ proton groups stand out sufficiently over the background to be identified. If so, this gives a useful handle on the determination of the radiative widths of analogue states.

11.3. Coupling of the analogous channels in (d, p) and (d, p) reactions (Ref. Moore et al., Phys. Rev. Lett. 17 (1966) 926)

The reactions considered were

$$^{90}Zr(d, p)^{91}Zr \qquad (11.3.1)$$

$$^{90}Zr(d, n)^{91}Nb^*(\bar{p})^{90}Zr \qquad (11.3.2)$$

In these reactions one also sees peaks in the proton spectrum which do not move as the bombarding energy is increased, i.e. 'delayed' protons. Moore et al. observed the ground state $(5/2^+)$ and first

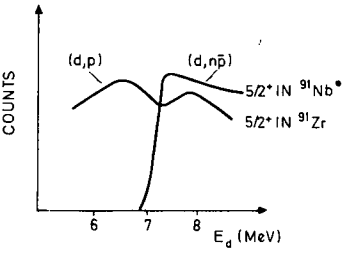

FIG. 64. Analogue channel coupling for $^{90}Zr(d,p)^{91}Zr$ and $^{90}Zr(d,n)^{91}Nb$ experiments by Moore et al.

excited state ($1/2^+$) analogues of ^{91}Zr, in ^{91}Nb, at the same time as observing the parent states in ^{91}Zr resulting from the (d, p) reaction.

They also obtained an excitation function, with good beam resolution, to investigate proton thresholds for the reaction $^{90}Zr(d, n\bar{p})^{90}Zr$ from the 9.48 and 10.69 MeV levels of ^{91}Nb. For the 9.48 MeV level ($5/2^+$) the proton threshold occurs at a deuteron energy of ~ 7 MeV. If we increase the energy by 100 keV the cross-section increases very rapidly, and then begins to level off. The protons emitted from this highly excited state do not have the usual difficulties of Coulomb barrier penetration, hence the rapid onset of yield beyond threshold. They also recorded the protons from (d, p) to the ground state of ^{91}Zr (Fig. 64). This reaction seems to take notice of the onset of the (d, $n\bar{p}$) reaction. This is due to the isospin coupling between the ($^{91}Zr + p$) and ($^{91}Nb^* + n$) channels, related to each other by the coupling operator $T^- t^+$. The anomaly in the (d, p) excitation curve also appears in the $S_{1/2}$ level, the first excited state of ^{91}Zr, at an energy corresponding to the proton threshold energy for this state. Detailed understanding of this coupling is not yet available.

12. HOW GOOD IS ISOSPIN IN HEAVY NUCLEI?

After all the use we have made of the isospin quantum number it is not inappropriate to ask whether it is a good quantum number. At first sight it seems that it must be good in order to lead to the many striking consequences we have discussed in these lectures. However, it turns out that most of these consequences would not have been greatly altered even if considerable isospin impurities existed. Experiments such as beta decay in heavy nuclei between 0^+ states (cf. section 2) where $\Delta T \neq 0$ seem to yield tiny amounts of admixtures of $\Delta T = 0$ component, it is true. On the other hand, this represents only one type among many possible impurities; moreover it deals only with low-lying nuclear states. Similar situations exist in almost every other so-called test for isospin impurity. When the Coulomb interaction is treated as a perturbation, one also usually obtains small admixtures. This body of circumstantial evidence seems very compelling in favour of good isospin, but one should not let down one's guards against possible surprises in this area. A more clear-cut type of impurity test such as

TABLE VIII. VALUES FOR THE γ COEFFICIENTS

Nucleus	% of (T + 1) into T ground state (γ^2)
^{16}O	0.15
^{40}Ca	2.19
^{90}Zr	2.20
^{208}Pb	2.69

(α, α') or (d, α) reactions on heavy nuclei to $T = T_z + 1$ states in $T = T_z$ nuclei was discussed earlier.

A simple picture for the mechanism introducing isospin impurity was given by Soper (unpublished?) and used to obtain numerical estimates for the admixtures in a series of nuclei, shown in Table VIII. The proton single-particle wave functions are allowed to expand owing to the Coulomb repulsion. This necessarily introduces T-impurity since it is a neutron-proton distinguishing deformation of the wave functions. In a simple oscillator-well picture, using the neutron wave functions as basis states, we expand the proton wave functions in this orthonormal set. What this involves is the excitation of protons from below the Fermi level to unfilled states above. As we know, such transitions are only T-mixing if the unfilled states lie above the neutron Fermi level. Moreover, it turns out that only certain protons can contribute to such transitions, namely those going from orbits (n, ℓ) to $(n+1, \ell)$. Writing the wave function as $\psi = \phi_T + \gamma \phi_{T+1}$, Soper finds the values for the coefficients given in Table VIII. We see that there is no significant increase between Ca and Pb. This is due to the opposing effects of the increasing charge on the one hand, and the increasing neutron excess on the other, the latter making it energetically more difficult to excite protons above the neutron Fermi level for large T_z.

We see that, paradoxically, the very Coulomb field which is presumably the sole culprit introducing T-impurities, is also the cause for the neutron excess in heavy nuclei, which in turn seems to contribute to maintaining isospin purity. Another way of stating this is to say that the neutron excess component by itself has of course pure isospin (the basic isospin $T = T_z$, in fact). The impurity arises from the 2Z remaining nucleons filling equivalent (or rather not so equivalent!) orbits. These two tendencies result in an overall more-or-less constant impurity predicted for heavy elements.

One final, more formal way of looking at the problem examines the scalar, vector and tensor portions of the Coulomb interaction. The S part does not contribute to mixing; the T part is presumably very small, and the vector part is the most important. To a good approximation, it is proportional to T_z which produces an energy shift but no mixing. When there is Coulomb mixing, specifically in the region of highly excited states where isobaric analogue resonances occur, we are saved in another way. Namely, the $T_<$ configurations which admix with the simple $T_>$ analogue configuration must also be simple, for large overlap; however, the simple $T_<$ configurations occur at much lower excitation energies, and hence the energy denominator will tend to suppress the mixing markedly.

In summing up we can say that there is either a very clever conspiracy to make us believe that isospin is good in heavy nuclei in all possible situations, or it is, in fact, a good quantum number. The latter hypothesis is operationally much simpler and useful until shown to be inadequate.

13. COULOMB DISPLACEMENT ENERGIES AND ISOTOPE SHIFTS

With the availability of the location of many isobaric analogue states it has become of interest to study some of the systematics of

the Coulomb displacement energies ΔE_c between neighbouring isobars. In an overall way it is known that ΔE_c varies as $Z/A^{1/3}$ over the entire nuclear domain. However, looking at several isotopes of the same element, much more complicated and non-systematic behaviour can be discerned. It should be remembered that when we compare, say, the pairs ^{205}Pb-^{205}Bi, ^{207}Pb-^{207}Bi, ^{209}Pb-^{209}Bi (isotope shift), we are actually comparing the behaviour of one additional proton in lieu of a neutron, in a highly-excited (but simple) state, as we add pairs of neutrons to the core. A microscopic calculation of such effects must take into account the different fractions of time the proton spends in the various orbits involved in the description of the isobaric analogue state. Such calculations are being made by Schiffer (1966) and others, and seem to be able to account for the facts.

One final word is in order to relate such isotope shift measurements to the more conventional sources of this information, namely the hyperfine structure observed in optical spectra and mu-mesic X-ray spectra. In this case the nuclei are immersed statically in an electromagnetic cloud, and the nuclear size and its low moments are explored by this weak interaction by way of the deviations of the Coulomb field from that of a point nucleus. It is clear that there is no a priori reason to expect identical results from the two approaches to the problem, since nuclear forces are indirectly involved in the proton motion of the isobaric analogue states.

For instance, there is a well-known odd-even isotope staggering effect in the HFS measurements, whereas no such effect exists for the heaviest nuclei (although it is present in lighter nuclei). This is believed to be due to the dilution of the pairing effect by the changing role of the extra proton, as we have already alluded to earlier in connection with pick-up reactions in the Ca region.

Much interesting information will be forthcoming in trying to relate these measurements theoretically.

ACKNOWLEDGEMENTS

These notes were prepared during the presentation of this material in a series of eighteen lectures on Advanced Topics in Nuclear Physics at Rutgers University, in the Fall Term of 1966. I wish to express my appreciation to my own graduate students, Messrs. G.H. Lenz, B. Teitelman, and R. Van Bree, and Miss M. Wiesen, for their help in writing up these notes. I do, however, absolve them from any responsibility for the contents, since I had the opportunity to correct, amplify and modify the notes considerably.

Finally, I record my gratitude to Miss Ruth Freeswick, my secretary, for her devotion in typing the manuscript and for co-ordinating the assembly of the notes under great pressure; this made it possible to distribute the notes to the participants in Trieste at the very beginning of my course, a fact which I believe added considerably to its scope and usefulness.

BIBLIOGRAPHY

Historical (Theory)

BREIT, G., CONDON, E., PRESENT, R.D., Phys.Rev. 50 (1936) 825-45.
BREIT, G., FEENBERG, E., Phys.Rev. 50 (1936) 850-56.
CASSEN, B., CONDON, E.U., Phys.Rev. 50 (1936) 846-49.
HEISENBERG, W., Z.Phys. 77 (1932) 1-11.
INGLIS, D.R., Rev.mod.Phys. 25 (1953) 390-450.
KLEIN, P., J.Phys.Radium, Ser. 7, 9 (1938) 1-12.
KROLL, N.M., FOLDY, L.L., Phys.Rev. 88 (1952) 1177.
MACDONALD, W.M., Phys.Rev. 98 (1955) 60-65.
MORPURGO, G., Nuovo Cimento 12 (1954) 60-80.
MORPURGO, G., Phys.Rev. 110 (1958) 721-25.
RADICATI, L.A., Phys.Rev. 87 (1952) 521-27.
ROSENFELD, L., in Nuclear Forces, Chap.IV, Interscience, New York (1948) 43-65.
TRAINOR, L.E.H., Phys.Rev. 85 (1952) 962-72.
WIGNER, E.P., Phys.Rev. 51 (1937) 106-19, 947-58.
WIGNER, E.P., Phys.Rev. 56 (1939) 519-26.

Historical (Experiment)

ADAIR, R.K., Phys.Rev. 87 (1952) 1041-43.
BLOOM, S.D., TOPPEL, B.J., WILKINSON, D.H., Phil.Mag. 2 (1957) 57-60.
BOCKELMAN, C.K., BROWNE, C.P., BUECHNER, W.W., SPERDUTO, A., Phys.Rev. 92 (1953) 664.
JONES, G.A., WILKINSON, D.H., Phil.Mag. 45 (1954) 703-11.
WILKINSON, D.H., JONES, G.A., Phil.Mag. 44 (1953) 542-47.
WILKINSON, D.H., Phil.Mag. 44 (1953) 1019-27.
WILKINSON, D.H., Phys.Rev. 90 (1953) 721-22.
WILKINSON, D.H., CLEGG, A.B., Phil.Mag. 44 (1953) 1269-75, 1322-25.
WILKINSON, D.H., CLEGG, A.B., Phil.Mag. 1 (1956) 291-97.
WILKINSON, D.H., Phil.Mag. 1 (1956) 379-92, 1031-42.
WILKINSON, D.H., BLOOM, S.D., Phil.Mag. 2 (1957) 63-82.

Review Articles

ACADEMIC PRESS, Proc.Conf.on Isobaric Spin, Academic Press, New York (1966).
AKADEMIE-VERLAG, Der Isospin von Atomkernen (Three Russian articles, as translated and edited by J. Schintlmeister). Akademie-Verlag, Berlin (1960).
BLOOM, S.D., Nuovo Cimento 32 (1964) 1023-36.
BURCHAM, W.E., Prog.nucl.Phys. 4 (1955) 171-214.
MACDONALD, W.M., in Nuclear Spectroscopy, Part B. 932-959. (AJZENBERG-SELOVE, F. Ed.) Academic Press, New York and London (1960).
ROBSON, D., A.Rev.nucl. Sci. 16 (1966) 119-52.
WIGNER, E.P., Proc.R. Welch Foundation Conf.on Chemical Research, November 1957, (unpublished).

Recent Experiments

ALLAN, D.L., Phys.Lett. 14 (1965) 311-13.
ANDERSON, J.D., WONG, C., McCLURE, J.W., Phys.Rev. 126 (1962) 2170-73; ibid 129 (1964) 2718-22.
ANDERSON, J.D., WONG, C., McCLURE, J.W., Phys.Rev. 138B (1965) 615-18.
BATTY, C.J., FRIEDMAN, E., ROWE, P.C., HUNT, J.B., Phys.Lett. 19 (1965) 33-35.
BATTY, C.J., GILMORE, R.S., STAFFORD, G.H., Nucl.Phys. 75 (1966) 599-608.
BLAIR, A.G., ARMSTRONG, D.D., Phys.Lett. 16 (1965) 57-59.
BREDIN, D.J., HANSEN, O., LENZ, G.H., TEMMER, G.M., Phys.Lett. 21 (1966) 677-80.
von BRENTANO, D., MARQUARDT, N., WURM, J.P., ZAIDI, S.A.A., Phys.Lett. 17 (1966) 124-26.
CERNY, J., PEHL, R.H., GOULDING, F.S., LANDIS, D.A., Phys.Rev.Lett. 13 (1964) 726-28.

CERNY, J., COSPER, S.W., BUTLER, G.W., PEHL, R.H., GOULDING, F.S., LANDIS, D.A., DETRAZ, C., Phys.Rev.Lett. 16 (1966) 469-73.
CERNY, J., PEHL, R.H., BUTLER, G., FLEMING, D.G., MAPLES, C., DETRAZ, C., Phys.Lett. 20 (1966) 35-37.
FIARMAN, S., LUDWIG, E.J., MICHELMAN, L., ROBBINS, A.B., Phys.Lett. 22 (1966) 175-76.
FLIAGIN, V.B., DZHELEPOV, V.P., DISELEV, V.S., OGANESIAN, K.O., J.exp.theor.Phys. (USSR) 35, (1958) 854-67; Soviet Phys. JETP 8 (1959) 592-600.
FOX, J.D., MOORE, C.F., ROBSON, D., Phys.Rev.Lett. 12 (1964) 198-200.
JONES, G.A., LANE, A.M., MORRISON, G.C., Phys.Lett. 11 (1964) 329-31.
JONES, K.W., SCHIFFER, J.P., LEE, L.L., MARINOV, A., LERNER, J.L., Phys.Rev. 145 (1966) 894.
KEYWORTH, G.A., KYKER, G.C., BILPUCH, E.G., NEWSON, H.W., Phys.Lett. 20 (1966) 281-84.
KÜHN, B., SCHLENK, B., Nucl.Phys. 48 (1963) 353-60.
MOORE, C.F., RICHARD, P., WATSON, C.E., ROBSON, D., FOX, J.D., Phys.Rev. 141 (1966) 1166-79.
MOORE, C.F., TERRELL, G.E., Phys.Rev.Lett. 16 (1966) 804-06.
MOORE, C.F., PARISH, L.J., von BRENTANO, P., ZAIDI, S.A.A., Phys.Lett. 22 (1966) 616-18.
MOORE, C.F., WATSON, C.E., ZAIDI, S.A.A., KENT, J.J., KULLECK, J.G., Phys.Rev.Lett. 17 (1966) 926-28.
RICHARD, P., MOORE, C.F., ROBSON, D., FOX, J.D., Phys.Rev.Lett. 13 (1964) 343-45.
RICHARD, P., MOORE, C.F., BECKER, J.A., FOX, J.D., Phys.Rev. 145 (1966) 971-81.
SHERR, R., BAYMAN, B.F., ROST, E., RICKEY, M.E., HOOT, C.G., Phys.Rev. 139B (1965) 1272-93.
SHERR, R., BLAIR, A.G., ARMSTRONG, D.D., Phys.Lett. 20 (1966) 392.
VOURVOPOULOS, G., FOX, J.D., Phys.Rev. 141 (1966) 1180-84.
YAVIN, A.I., HOFFSWELL, R.A., JONES, C.H., NOWEIR, F.M., Phys.Rev.Lett. 16 (1966) 1049.

For recent results in both theory and experiment, see especially: Proc.Conf.on Isobaric Spin in Nuclear Physics, Academic Press, New York (1966) as well as Proc.Int.Conf. on Nuclear Physics, Gatlinburg (1966); and Recent Progress in Nuclear Physics With Tandem Accelerators, Heidelberg (1966).

Recent Theory

ALFORD, W.P., FRENCH, J.B., Phys.Rev.Lett. 6 (1961) 119.
ANDERSEN, B.L., BONDORF, J.P., MADSEN, B.S., Phys.Lett. 22 (1966) 651-54.
ANDERSON, J.D., WONG, C., McCLURE, J.W., Phys.Rev. 138 (1965) 615.
AUERBACH, E.H., DOVER, C.B., KERMAN, A.K., LEMMER, R.H., SCHWARCZ, E.H., Phys.Rev.Lett. 17 (1966) 1184-86.
BANSAL, R.K., FRENCH, J.B., Phys.Lett. 19 (1965) 223-26.
BARSHAY, S., TEMMER, G.M., Phys.Rev.Lett. 12 (1964) 728.
BONDORF, J.P., LÜTKEN, H., JÄGARE, S., Phys.Lett. 21 (1966) 185-87.
CARLSON, B.C., TALMI, I., Phys.Rev. 96 (1964) 436.
FALLIEROS, S., GOULARD, B., VENTER, R.H., Phys.Lett. 19 (1965) 398-400.
FRENCH, J.B., MACFARLANE, M.H., Nucl.Phys. 26 (1961) 168-76.
FRENCH, J.B., Nuclear Spectroscopy with Direct Reactions II, ANL Rep. 6848 (1964) 181-206.
GARVEY, G.T., CERNY, J., PEHL, R.H., Phys.Rev.Lett. 12 (1964) 726-28.
GARVEY, G.T., KELSON, I., Phys.Rev.Lett. 16 (1966) 197-200.
HARCHOL, M., JAFFE, A.A., MIRON, J., UNNA, I., ZIONI, J., Nucl.Phys. A90 (1967) 459-72.
HASIMOTO, Y., ALFORD, W.P., Phys.Rev. 116 (1959) 981-85.
LANE, A.M., Nucl.Phys. 35 (1962) 676-85.
LANE, A.M., SOPER, J.M., Nucl.Phys. 37 (1962) 663-78.
LONG, D.D., RICHARD, P., MOORE, C.F., FOX, J.D., Phys.Rev. 149 (1966) 906-12.
ROBSON, D., Phys.Rev. 137B (1965) 535-46.
ROBSON, D., FOX, J.D., RICHARD, P., MOORE, C.F., Phys.Lett. 18 (1965) 86-88.
SATCHLER, G.R., DRISKO, R.M., BASSEL, R.H., Phys.Rev. 136B (1964) 637-47.
TAMURA, T., Phys.Lett. 22 (1966) 644-48.
ZAIDI, S.A.A., von BRENTANO, P., Phys.Lett. 23 (1966) 466-67.

CHAPTER 4

Selected topics in phenomenological nuclear physics

CALCULATIONS OF NEUTRON-CAPTURE CROSS-SECTIONS WITH THE STATISTICAL MODEL

V. BENZI

1. INTRODUCTION

It is generally accepted that for not-too-light nuclei the optical model allows an estimate of total and shape elastic neutron cross-sections to be made with an accuracy better than 20% [1].

The meaning of this statement, which should be accepted with some caution, is that, for the most common optical potential adopted, there are systematic procedures to estimate the parameters required for the evaluation of total and shape elastic cross-sections, when no experimental data are available.

Similar methods for estimating radiative capture cross-sections have not been evolved, and no extensive analyses have been carried out to test whether some systematic method can be established to determine values not yet measured in this field.

It would seem of value to analyse a large amount of experimental data in terms of a given model to see whether any useful features can be distinguished.

In this regard, some aspects of numerical evaluation of radiative capture cross-sections using statistical models are treated here.

2. THE MODELS

The first detailed formula for the evaluation of the average radiative capture cross-section was developed by Margolis [2], on the basis of the statistical Hauser-Feshbach theory. The formula is

$$\sigma_{n\gamma}(E) = \frac{\pi \lambda^2}{2(2I+1)} \sum_{\ell=0}^{\infty} T\ (\ell ; E) \sum_{J=0}^{\infty} \frac{\epsilon^J_{j\ell}\,(2J+1)\,T_c\,(J ; E)}{T_\gamma\,(J ; E) + \sum_{\ell', E'} \epsilon^J_{j'\ell'}\,T_n\,(\ell' ; E')} \cdot S(E) \qquad (1)$$

The author is at the Centro di Calcolo del C. N. E. N. -Bologna, Italy.

In Eq. (1), $2\pi\lambda$ is the neutron wavelength of the incident neutron, E is the incident neutron energy and E' the energy of the scattered neutron. I is the spin of the target nucleus, ℓ and ℓ' are the orbital angular momenta of the incident and scattered neutrons, and j is the channel spin, equal to $I \pm \frac{1}{2}$ except when $I = 0$ in which case $j = \frac{1}{2}$. J is the spin of the compound nucleus which can have any value obtained by combining j and ℓ. $\epsilon^J_{j\ell} = 2, 1$, or 0 according to whether $|J - \ell| \leq j \leq |J + \ell|$ is satisfied for both channel spins j, one channel spin, or none. T_n represents the neutron wave-mechanical penetrability of the nuclear surface and is taken to be independent of J and j. T_γ represents the total probability of decay of the compound nucleus by γ emission, and must be carefully distinguished from T_c, which gives the neutron radiative capture probability. The function S(E) takes into account the fact that formula (1) is written as function of the average widths rather than as the average of the functions. The following relations hold

$$T_n(\ell, E) = 2\pi \frac{<\Gamma_n(J ; \ell ; E)>}{<D(J ; E)>} \tag{2}$$

$$T_r(J, E) = 2\pi \frac{<\Gamma_n(J ; E)>}{<D(J ; E)>} \tag{3}$$

where $\Gamma_n(J ; \ell ; E)$ is the width of a level of spin J for the emission of ℓ-wave neutrons of energy E, and $\Gamma_r(J ; E)$ is the partial width of a level of spin J formed by the addition of a neutron of energy E, for decay through the channel r. $D(J ; E)$ is the spacing of levels of spin J and one parity formed by neutrons of energy E.

Following Margolis [2] and Lane and Lynn [3], for dipole γ-ray emissions, one has

$$\Gamma_\gamma(J ; B_n + E) \simeq \frac{\Gamma_\gamma(J ; B_n)}{D(J ; B_n)} \cdot \frac{D(J ; B_n + E) \int_0^{B_n+E} \frac{\epsilon^3 \, d\epsilon}{D(0 ; B_n + E - \epsilon)}}{\int_0^{B_n} \frac{\epsilon^3 \, d\epsilon}{D(0 ; B_n - \epsilon)}} \tag{4}$$

$$\Gamma_c(J ; B_n + E) \simeq \frac{\Gamma_\gamma(J ; B_n)}{D(J ; B_n)} \cdot D(J ; B_n + E) \frac{\int_E^{B_n+E} \frac{\epsilon^3 \, d\epsilon}{D(0 ; B_n + E - \epsilon)}}{\int_0^{B_n} \frac{\epsilon^3 \, d\epsilon}{D(0 ; B_n - \epsilon)}} \tag{5}$$

with neutron binding energy B_n and $(D(0 ; U) = (2J + 1) D(J ; U)$. The expression for Γ_c differs from the expression for Γ_γ by the limits of the integral which appear in the denominator. These limits are changed to omit the cases where the initial γ-ray has an energy less than the incident

neutron energy, because in these cases the initial γ-ray will be almost always followed by neutron emission rather than capture. Putting

$$T_n(\ell\,;E) \equiv T_\ell(E) \tag{6}$$

$$D(J\,;B_n) \equiv D^J(B_n) \tag{7}$$

$$\Gamma_\gamma(J\,;B_n) \equiv \Gamma_\gamma^J(B_n) \tag{8}$$

$$\xi_J = D^J(B_n) / [2\pi\Gamma_\gamma^J(B_n)] \tag{9}$$

$$[D(0\,;U)]^{-1} \equiv \rho_{0c}(U) \tag{10}$$

$$f(E\,;\omega) = \int_{\omega}^{B_n+} \epsilon^3\rho_{0c}(B_n+\omega-\epsilon)d\epsilon \Big/ \int_{0}^{B_n+E} \epsilon^3\rho_{0c}(B_n+E-\epsilon)d\epsilon \tag{11}$$

and assuming $S = 1$, Eq. (1) reduces to

$$\sigma_{n\gamma}(E) = \frac{\pi\lambda^2}{2(2I+1)} \sum_{\ell=0}^{\infty} T_\ell(E) \sum_{J=0}^{\infty} \frac{\epsilon_{j1}^J(2J+1)f(E\,;E)}{1+\xi_J f(E\,;0)\sum_{\ell'}\sum_{k}\epsilon_{j_k\ell'}^J T_{\ell'}(E-E_k)} \tag{1a}$$

where E_k is the energy of the k-th excited level.

The inelastic scattering by target nucleus levels with unknown characteristics can be approximately taken into account putting

$$\sum_{\ell'}\sum_{n}\epsilon_{j_n\ell'}^J T_{\ell'}(E-E_n) \approx \sum_{\ell'}\sum_{n\le p}\epsilon_{j_n\ell'}^J T_{\ell'}(E-E_n) + \sum_{E_p}^{E}(2J+1)\rho_{0t}(E-\epsilon)\sum_{\ell}T_{\ell'}(\epsilon)d\epsilon \tag{1b}$$

where E_p is the energy of the highest known level and $\rho_{0t}(U)$ is the density of states of the target nucleus at excitation energy U. Under the hypothesis of high level density and assuming an equal distribution of levels between the two parities, Eq. (1a) reduces to [4]

$$\sigma_{n\gamma}(E) \approx \frac{\pi^2\hbar^2}{2m}\left(\mu+\frac{\nu}{E}\right)\overline{\Gamma}_\gamma(B_n)\rho_{0c}(B_n)\cdot\frac{g(E)}{\int_0^E(\mu\epsilon+\nu)\rho_{0t}(U-\epsilon)d\epsilon} \tag{12}$$

with m being the neutron mass, $\overline{\Gamma}_\gamma(B_n)$ the average radiation width at neutron binding excitation energy (assumed to be parity and J-independent) and

$$g(E) = \int_{E}^{E+B_n} \epsilon^{2\phi+1}\rho_{0c}(U'-\epsilon)d\epsilon \Big/ \int_{0}^{B_n} \epsilon^{2\phi+1}\rho_{0c}(U''-\epsilon)d\epsilon \tag{13}$$

The quantities μ and ν are empirical A-dependent parameters defined by

$$\sigma_c(E) \approx \sigma_g\left(\frac{\mu+\nu}{E}\right) \tag{14}$$

where $\sigma(E)$ and σ_g are the compound and geometrical cross-sections respectively of a nucleus of mass number A.

The above equations provide a method for estimating neutron radiative capture cross-sections which represent an average over resonances in the low energy region, and which approximate the actual cross-sections in the smoothly varying region if only neutron and γ-ray emission are allowed. It must be noted that in Eq. (1a) the fluctuations of the neutron widths around the average value are neglected. In addition, direct and cascade capture are not taken into account, two processes which can play an important role at energies of several MeV [5, 6]. The direct capture cross-section can be estimated very roughly by means of the following formula [5]

$$\left[\sigma_{n\gamma}(E)\right]_d \approx K\frac{Z^2}{A}\left[\frac{(E+4)}{E^{\frac{1}{2}}}\right]^3 \tag{15}$$

with E in MeV, K = constant and Z atomic number.

3. THE LEVEL-DENSITY FORMULA

To compute $\sigma_{n\gamma}(E)$ by means of the above equations, it is necessary to specify the dependence of the level density $\rho(U)$ on the excitation energy U. It is well known that the number of levels as a function of the excitation energy for neighbouring nuclei depends mainly on the odd-even character of the nucleus considered. If one plots the total number of states N(U) up to an excitation energy U as a function of U for odd, odd mass and even nuclei with about the same mass number A, the odd-even effect manifests itself as a shift on the excitation energy U. The magnitude of this shift is of the same order as the pairing energy of the nuclei considered.

This means that the level density ρ of a nucleus is independent of the odd-even character of the nucleus itself, if an effective excitation energy $\overline{U}$ is defined in a suitable manner.

About the definition of this effective energy, one can consider two possibilities. First, one can assume that this energy has to be evaluated from a reference level which is the fundamental state of odd-odd nuclei [7]. In this case, the effective excitation energy $\overline{U}$ is given by

$$\overline{U} = U + \Delta \tag{16}$$

with

$$\Delta = \begin{cases} 0 \text{ for odd-odd nuclei} \\ \delta \text{ for odd-A nuclei} \\ 2\delta \text{ for even-even nuclei} \end{cases}$$

and where U is the excitation energy evaluated from the ground state and 2δ is a negative quantity of the order of the pairing energy for even-even nuclei.

This assumption is based upon the fact that an amount of energy equal to the pairing energy is required to break the binding of the coupled nucleons in the nucleus, so that such an energy must be added to the excitation energy in order that all the nuclei behave in the same way (i.e. as uncorrelated gas).

On the other hand, one can assume that the effective excitation energy has to be evaluated from the ground state of even-even nuclei, so that the level density of odd-odd or odd-A nuclei starts at a higher value than that of even-even nuclei [8]. In this case, one has

$$\rho_{\text{odd-A}}(U) = \rho_{\text{even-even}}(U + \delta) \tag{17a}$$

$$\rho_{\text{odd-odd}}(U) = \rho_{\text{even-even}}(U + 2\delta) \tag{17b}$$

where U and 2δ are defined as before, but 2δ is assumed to be a positive quantity. With this assumption, one has

$$\overline{U} = U + \Delta \tag{16a}$$

with

$$\Delta = \begin{cases} 0 \text{ for even-even nuclei} \\ \delta \text{ for odd-A nuclei} \\ 2\delta \text{ for odd-odd nuclei} \end{cases}$$

This second definition of $\overline{U}$ has the advantage that there are no gaps in the level density of an even-even nucleus for energies above the ground state smaller than the pairing energy.

For numerical evaluations, this fact simplifies the computations of the integrals over the level density of the residual (target) nucleus.

For the dependence of ρ_0 on $\overline{U}$, there are several formulae available. A very simple one, based on the gas-like model [9], is

$$\rho_0(\overline{U}) = C\left[A(\overline{U} + t)\right]^{-2} \exp\left[2(b\,\overline{U})^{\frac{1}{2}}\right] \tag{18}$$

where C is a constant for all nuclei, A the mass number of the nucleus considered, b is a parameter and t is defined by

$$\overline{U} = bt^2 + t \tag{19}$$

4. SYSTEMATICS

If we want to use formulae (1), (12), (15), (18) for the evaluation of the radiative capture cross-section of a given nucleus, we need to know, in addition to the spin and parity of the excited levels, the following

quantities:

$T_\ell(E)$ – Eq. (1a); $\overline{\Gamma}_\gamma^J$ – Eq. (1a); $\overline{\Gamma}_\gamma$ – Eq. (12); $\overline{D}^J$ – Eq. (1a); E_n – Eq. (1a);

C – Eq. (18); δ_i or Δ_i – Eqs. (1a), (12), (18); δ_f or Δ_f – Eqs. (12), (18);

b_i and b_f – Eqs. (1a), (12), (18); μ and ν – Eq. (12); and

B_n – Eqs. (1a), (12), (18).

Now, our problem in its very general formulation is: "Given the mass and the atomic number of a nucleus, how do we proceed to find the parameters required for a reasonable estimate or fit by means of the statistical model of the capture cross-section of that nucleus in the energy range above the resolved resonances up to several MeV?"

In principle, it is not impossible to try to answer this question starting from a purely theoretical basis. However we will assume that something is known experimentally about the levels scheme, and we will follow an empirical approach for the estimate of the level density parameters and radiation widths.

Now, let us consider in detail all the quantities involved in formulae (1), (12), (15), (18).

4.1. The penetrabilities $T_\ell(E)$

These quantities can be evaluated using the optical model, so that the systematics developed for optical model calculations can be used. However, it must be noted that formula (1a) is not as sensitive to the variation in the values of $T_\ell(E)$. It has been shown [10] that if one increases or decreases all the T_ℓ by a factor of ~ 10, the cross-section does not vary more than by a factor of ~ 2, except at very low energies where $\sigma_{n\gamma}$ depends on T_0 only.

This is due to the fact that the contribution of the ℓ-th partial cross-section to the total cross-section is proportional to the following quantity (assuming no inelastic scattering)

$$\frac{\overline{\Gamma}_{n\ell}^J \overline{\Gamma}_\gamma^J}{(\overline{\Gamma}_{n\ell}^J + \overline{\Gamma}_\gamma^J)\overline{D}^J} \tag{20}$$

Now

$$\overline{\Gamma}_{n\ell}^J(E) = \frac{T_\ell(E)\,\overline{D}^J}{2\pi} \tag{21}$$

so that at low energies, where $\overline{\Gamma}_{n\ell}^J \ll \overline{\Gamma}_\gamma^J$, the ℓ-th contribution strongly depends on T_ℓ, whereas at high energies $\overline{\Gamma}_\gamma^J \ll \overline{\Gamma}_{n\ell}^J$, and the ℓ-th contribution depends only on $\overline{\Gamma}_\gamma^J/\overline{D}^J$.

On these bases and in order to considerably reduce the computer time required for the calculations, it can be assumed as a first approximation that the T_ℓ can be computed in the framework of the "strong

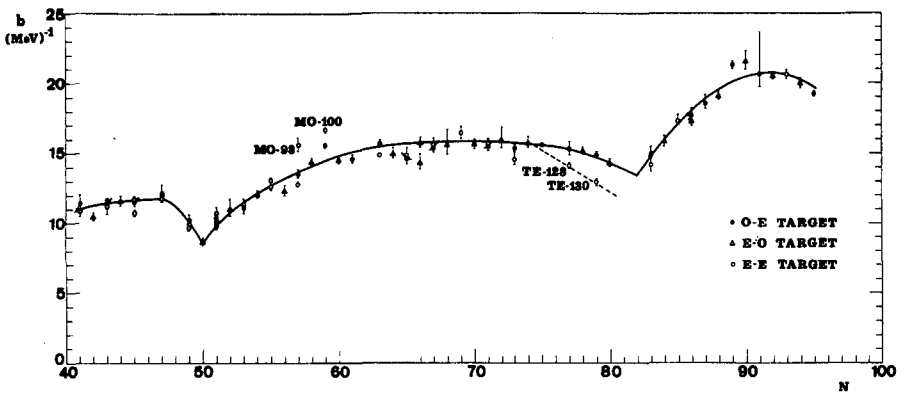

FIG.1. Values of b from the analysis of $\bar{D}_{obs}$ as a function of neutron number N

interaction'' model which gives

$$T_\ell = \frac{4x\chi v_\ell}{\left[\chi^2 + (2x\chi + x^2 v_\ell')v_\ell\right]} \tag{22}$$

where $x = R/\lambda\!\!\!^{-}_0$, $\chi^2 = \chi_0^2 + x^2$, $\chi_0 \simeq 10^{13}$ and R = nuclear radius (cm). The v_ℓ and v_ℓ' are functions defined in terms of spherical Bessel's and Neumann's functions. For the nuclear radius R one can assume, as usual,

$$R = r_0 A^{\frac{1}{3}} \text{ cm} \tag{23}$$

with r_0 = const. $\simeq 1.25 \times 10^{-13}$ cm.

4.2. Nuclear level densities and spacings

Formula (18) contains three parameters, namely C, b and Δ (or δ). This last quantity can be estimated as a function of A by means of an empirical relationship given by Newton [11]

$$2\delta \approx 0.82\ (4 - A/100)\text{MeV};\ A > 40 \tag{24}$$

As far as the parameters b are concerned, they can be obtained from the analysis of the observed low energy resonance spacings. If $\bar{D}_{obs}$ is the observed mean spacing for $\ell = 0$ neutron resonances for a target nucleus of spin I, one has

$$\rho_0(B_n) \approx \left[(2I+1)\bar{D}_{obs}\right]^{-1} \approx \frac{n-1}{(2I+1)(E_H - E_L)} \tag{25}$$

where n is the total number of observed resonances, and E_H and E_L are the energies of the observed higher and lower resonances, respectively. From the values of $\rho_0(B_n)$ obtained in this way the b-values can be

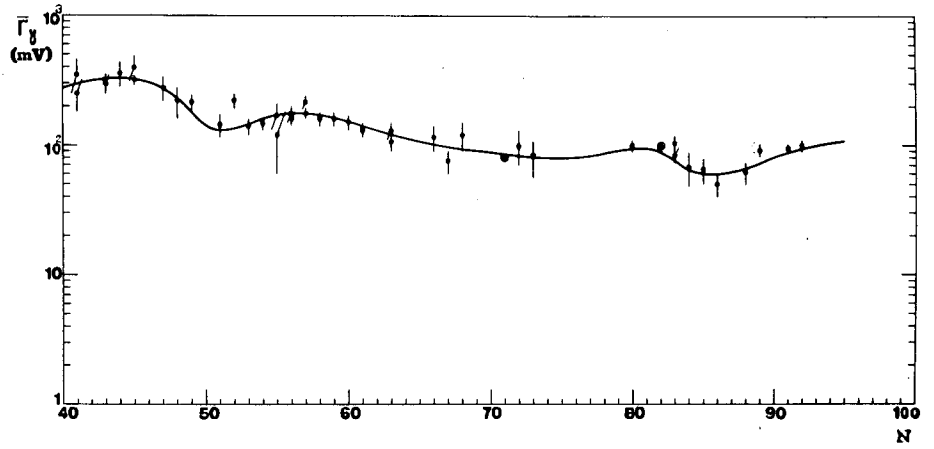

FIG. 2. Values of average radiation widths as a function of the neutron number in the compound nucleus

estimated by means of formula (18) and assuming [4]

$$C = 1 \text{ MeV}$$

when $\bar{U}$ and t are expressed in MeV and ρ_0 in $(\text{MeV})^{-1}$. In Fig. 1 the dependence of b on the neutron number $40 \leq N \leq 100$ of the nucleus is shown. There is a resonably good behaviour of b as a function of N, and it seems that the full line drawn through the points can be used with some confidence for an estimate of b when experimental values of $\bar{D}_{obs}$ are lacking. It has to be noted that a variation of 10% of b corresponds to a variation of $\sim$ 30 to 50% of $\bar{D}_{obs}$.

4.3. The average radiation widths

In the nuclei far from magic numbers, radiative capture proceeds with the neutrons making transitions into a large number of different states, making the number of reaction channels large in this case.

Therefore, the radiation width is the sum of a large number of widths, one for each channel, and thus it does not change much from one level to the next.

The dependence of the radiation width on J can be estimated by using a formula given by Blatt and Weisskopf [12].

$$\bar{\Gamma}_\gamma^J \sim \int_0^U (U - \epsilon)^3 \sum_{J'} \frac{D^J(U)}{D^{J'}(\epsilon)} \, d\epsilon \tag{26}$$

assuming dipole γ-rays only. If one assumes the validity of the formula

$$\bar{D}^J = \frac{\bar{D}_0}{2J+1} = \frac{\rho_0^{-1}}{2J+1} = \rho_J^{-1} \tag{27}$$

it may be seen that the final states combine to give a total statistical weight proportional to $(2J + 1)$ which cancels the $(2J + 1)$ factor in the level spacing for the initial state. The radiation width is therefore expected

to be independent of J. However a more complicated J-dependence of ρ_J can be assumed, as for example

$$\rho_J = (2J + 1) \exp \{ - \sigma (J + 1/2)^2 \} \rho_0 \qquad (28)$$

and in this case $\overline{\Gamma}_\gamma$ is expected to be independent of J only if the exponential factor can be neglected, i.e. for small J. In those cases where radiation widths in a nucleus have been measured for levels with varying J, they have been found, with few exceptions, unchanged within the experimental accuracies. So, it seems that one can assume

$$\overline{\Gamma}_\gamma^J \simeq \overline{\Gamma}_\gamma \qquad (29)$$

independent of J.

Equation (26) gives a tool for a theoretical estimate of $\overline{\Gamma}_\gamma$. However, it seems much better to use experimental values of $\overline{\Gamma}_\gamma$ whenever available. Some of these values are plotted as a function of N in Fig. 2.

As one can see the N-dependence of $\overline{\Gamma}_\gamma$ is rather smooth, so that it seems that a $\overline{\Gamma}_\gamma$-value can be estimated reasonably well from neighbouring nuclei when no experimental data are available. However, it is important to notice that $\overline{\Gamma}_\gamma$ is expected to be higher for odd-A isotopes than for even-even isotopes, due to the $\overline{\Gamma}_\gamma$ dependence on binding energy [cf. Eq. (26)].

4.4. A-dependence of μ and ν

For μ and ν parameters, the following A-dependence can be adopted

$$\mu = 0.76 + 2.2\ A^{-\frac{1}{3}}$$

$$\nu = 2.12\ A^{-\frac{2}{3}} - 0.05$$

Such a dependence was obtained by fitting a large number of σ_c cross-sections calculated by means of the optical model [13].

4.5. K-value

The value of the constant K appearing in Eq. (15) can be estimated assuming that at ~ 14 MeV the radiative capture process is practically due to the direct mechanism only. An analysis based on experimental values of $\sigma_{n\gamma}$ for various nuclei at ~ 14 MeV neutron energy [14] gives for K the following average value

$$\overline{K} \simeq 10^{-3}$$

if in formula (15) $\sigma_{n\gamma}$ is given in mb and E in MeV. Table I gives the method of estimate suggested for the various quantities required in formulae (1), (12), (15), (18).

TABLE I. SUGGESTED METHODS FOR ESTIMATING $T_\ell(E)$, Δ, C, b, $\overline{\Gamma}_\gamma$, μ, ν, $\overline{K}$

Quantity	Method of estimate
$T_\ell(E)$	black nucleus
Δ	from mass differences
C, b	from $\overline{D}_{obs}$
$\overline{\Gamma}_\gamma$	from experiments or by interpolation
μ, ν	from fit of optical model σ_c
$\overline{K}$	from $\sigma_{n\gamma}$ at ~ 14 MeV

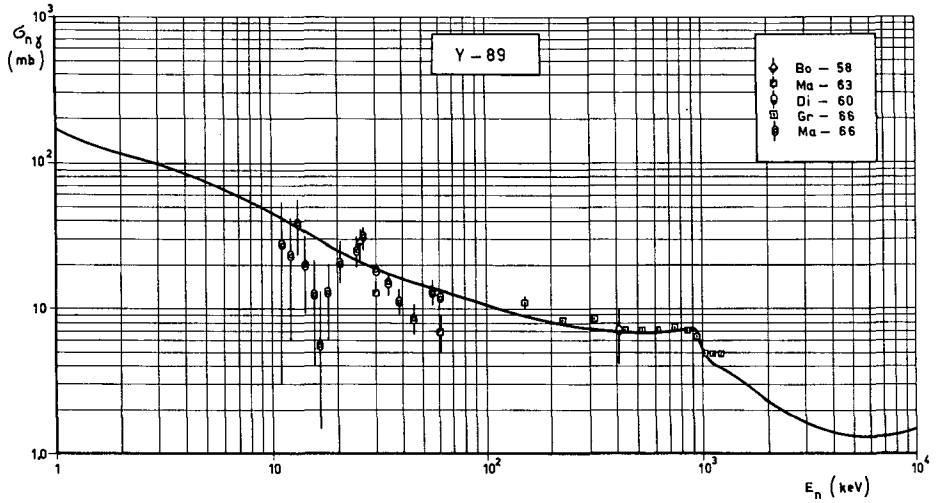

FIG. 3. Results of neutron capture cross-section calculations for ^{89}Y, made using Eqs.(1a), (12), (15) and (18)

5. SOME EXAMPLES

Figures 3, 4 and 5 show the results of some calculations performed using formulae (1a), (12), (15), (18) with black nucleus penetrabilities.

The procedure adopted for these calculations was as follows. First, the experimental data on $\sigma_{n\gamma}$ were renormalized, whenever possible, to the same standard values. In fact, most of the measurements were not absolute ones, so that it was necessary to renormalize all the cross-sections to the same standard values.

Then computations were performed starting, whenever possible, from the average experimental values of $\overline{D}_{obs}$ and $\overline{\Gamma}_\gamma$ obtained from the analysis of low energy resonances.

For the b_i-values, formula (12), the values were taken from the continuous curve given in Fig. 1.

The maximum ℓ-value considered was $\ell = 4$; and the number of inelastically excited levels allowed could reach 10. Equation (12) was

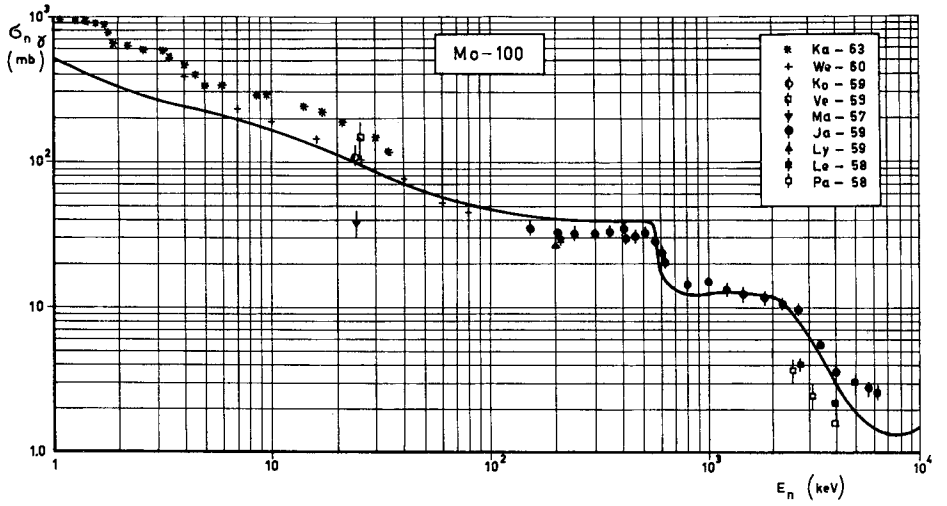

FIG. 4. Results of neutron-capture cross-section calculations for ^{100}Mo

assumed valid above 2 MeV, whenever a detailed level scheme was not available up to or above this energy.

In some cases, and for some energies the intermediate formula (1b) was adopted.

The validity of formula (15) was assumed for $E \gtrsim 4$ MeV.

The results of the computations were then compared with the experimental values and, if necessary, $\overline{\Gamma}_\gamma$ and $\overline{D}_{obs}$ were adjusted until a reasonably good fit was reached. As one can see, the shape of the theoretical capture cross-section agrees reasonably well with the experimental one. In general, in this kind of analyses, the strongest discrepancies occur in the regions of a few keV or a few MeV, where the chosen model is rather inadequate. The situation can be improved at the lower end of

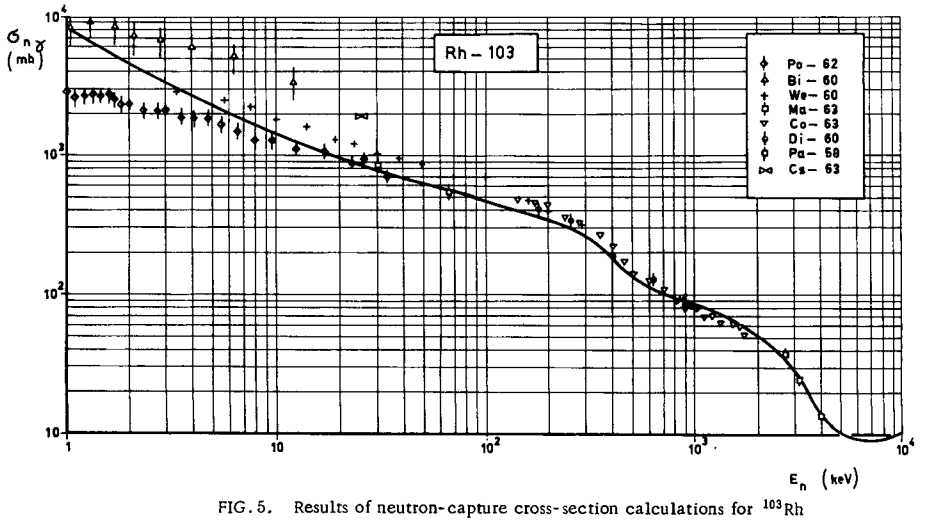

FIG. 5. Results of neutron-capture cross-section calculations for ^{103}Rh

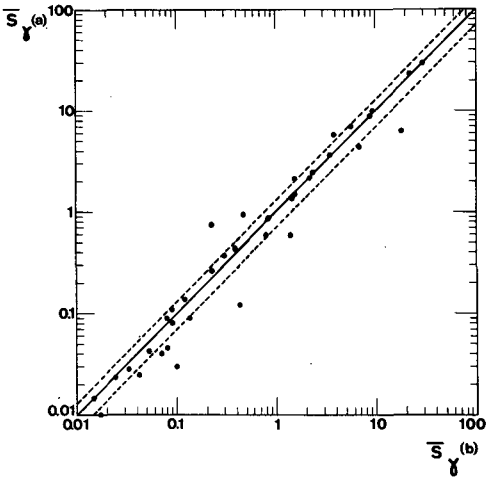

FIG. 6. Values of $\overline{S}_\gamma(a) = \overline{\Gamma}_\gamma/\overline{D}_{obs}$ obtained from fits of $\sigma_{n\gamma}$ versus $S_\gamma(b)$ obtained from the full line curves of Figs 1 and 2

the energy range using optical model T_ℓ and taking into account the fluctuations in the neutron width. Also in the high energy region, more sophisticated models should be used; however in this region the experimental data are very scarce, and it is difficult to draw any convincing conclusions.

As far as the absolute values of $\sigma_{n\gamma}$ are concerned, it is difficult to give a meaningful "goodness of fit" parameter.

It can be noted that for not too low energies one has, very roughly,

$$\frac{|\delta\sigma_{n\gamma}|}{\sigma_{n\gamma}} \sim \frac{|\delta\overline{S}_\gamma|}{\overline{S}_\gamma} \qquad (30)$$

where $\overline{S}_\gamma = \overline{\Gamma}_\gamma/\overline{D}_{obs}$. In Fig. 6 are plotted values of $\overline{S}_\gamma$ obtained from the fit of experimental measurements of $\sigma_{n\gamma}$ in the neutron number region $40 \leq N \leq 100$ versus S_γ-values obtained using the full line curves of Figs. 1 and 2 (quoted as $\overline{S}_\gamma(a)$ and $\overline{S}_\gamma(b)$, respectively).

Points falling in the region bounded by the two broken lines show a difference between corresponding values of less than 30%. As one can see, the agreement is in general rather good, and this seems to confirm that the statistical model is a powerful tool for predicting with reasonable accuracy cross-sections for those nuclei for which no experimental measurements exist.

REFERENCES

[1] FRANCIS, N. C., ANS Trans. 8 1 (1965) 214.
[2] MARGOLIS, B., Phys. Rev. 88 (1952) 327.
[3] LANE, A. M., LYNN, J. E., Proc. phys. Soc. 70 8-A (1957) 38.
[4] BENZI, V., BORTOLANI, M. V., Nuovo Cim. 38 (1965) 216.
[5] LANE, A. M., LYNN, J. E., Nucl. Phys. 11 (1959) 646.
[6] ZAKHAROVA, S. M., MALYSHEV, A. V., Proc. Antwerp Int. Conf. on Study of Nuclear Structure, P/201 (1965).
[7] HURWITZ, H., BETHE, H. A., Phys. Rev. 81 (1951) 898.

[8] VANDENBOSCH, R., HUIZENGA, J.R., MILLER, W.F., KEBERLE, E.M., Nucl. Phys. 25 (1961) 511.
[9] LANG, J.M.B., Le COUTER, K.J., Proc. phys. Soc. 67A (1954) 586.
[10] CAMERON, A.G.W., LAZAR, N.H., SCHMITT, H.W., Fast Neutron Physics, Part II, Ch. V.M., "Fast neutron capture cross-sections" (MARION, J.B., FOWLER, J.L., Eds), Interscience, New York (1963).
[11] NEWTON, T.D., Canad. J. Phys. 34 (1956) 804.
[12] BLATT, J.M., WEISSKOPF, V.F., Theoretical Nuclear Physics, Wiley, New York (1952).
[13] DOSTROVSKY, I., FRAENKEL, Z., Phys. Rev. 116 (1959) 683.
[14] BENZI, V., BORTOLANI, M.V., "Fission-product neutron-capture cross-sections in the energy range 1 keV to 10 MeV", Neutron Data for Reactors 1, IAEA, Vienna (1967) 537.

ISOBARIC ANALOGUE RESONANCES IN THE $f_{7/2}$ REGION BY (p, nγ) REACTIONS

R. A. RICCI

1. INTRODUCTION

It is now well established that isobaric analogue states may be observed as compound nucleus resonances [1, 2]. Since the pioneer work of the Florida State group [3], who found strong anomalous resonances in the excitation curve of the ^{89}Y(p, n) ^{89}Zr reaction, many other experiments have shown that such anomalies occur in the reaction cross-section and in the elastic scattering of protons at excitation energies for which no isolated resonances are expected, owing to the high level density of the compound nucleus.

Since the energy difference between these unexpected resonances in the $_{Z}A_{N}$ compound system and the ground state and/or low-lying levels of the $_{Z-1}A_{N+1}$ parent nucleus fit quite well the Coulomb shift expected by replacing a neutron and a proton in the latter, such resonances are interpreted as the isobaric analogues ($T = (N - Z)/2 + 1$, $T_z = (N - Z)/2$) of the normal levels of the parent system ($T = T_z = [(N + 1) - (Z - 1)]/2 = (N - Z)/2 + 1$). It is clear that resonance experiments leading to such analogue states are energetically possible if the Coulomb displacement energy ΔE_c is greater than the neutron separation energy S_n in the parent nucleus.

Owing to the decreasing trend of S_n with A and the increasing Coulomb barrier, heavy nuclei are more reliable for such experiments, though higher and higher bombarding energies are required [2] (tandem energies).

So far the experimental investigations have been confined to nuclei heavier than Zn and to elastic proton resonances [1], and many peculiar features of the isobaric analogue resonances have been found; of special interest is the "fine structure" revealed by the resonances found in the ^{92}Mo(p, p) experiment performed by the Florida State group [4]. Since we are dealing, in this case, with a typical heavy compound nucleus (^{93}Tc) with high normal level density in the analogue state region, this fine structure is interpreted as being due to the fluctuations of many overlapping levels with the same spin and parity as the analogue one ($T_>$) but with lower isospin ($T_<$).

Resonance experiments on lighter nuclei such as the ^{40}A(p, p) scattering performed at Duke University [5] and a few (p, p), (p, n) and (p, γ) reactions performed in the region of $f_{7/2}$ nuclei [6, 7] have shown

The author is at the Istituto di Fisica dell'Università, Firenze, and the Istituto Nazionale di Fisica Nucleare, Sottosezione di Firenze, Italy.

the possibility of investigating analogue resonances at sub-tandem bombarding energies; here the neutron separation energy may be lowered owing to the vicinity of closed shells and the density of normal states in the compound nucleus may not be very high; so the mixing with analogue states could be of a different nature from that found in heavier nuclei. In fact the 'fine structure' observed in the high resolution experiment at Duke University [5] is related to individual overlapping resonances which add coherently, rather than to statistical fluctuations [2].

We will concern ourselves here with the characterization of isobaric analogue resonances in the $f_{7/2}$ region by means of the spectroscopy of the gamma rays in the residual nucleus associated with the neutron emission, i.e., by (p, nγ) reactions.

2. THE ^{48}Ca (p, nγ) ^{48}Sc REACTION

It is generally assumed that for heavy nuclei, if the analogue resonances have good isobaric spin, the neutron decay is forbidden; its occurrence is taken as an indication of the strong mixing of the analogue state ($T_>$) with the surrounding $T_<$ states [8]. (It is assumed here that the low-lying levels of the residual nucleus, at which neutron emission occurs, are normal $T = T_z$ states, with reasonably pure isobaric spin.)

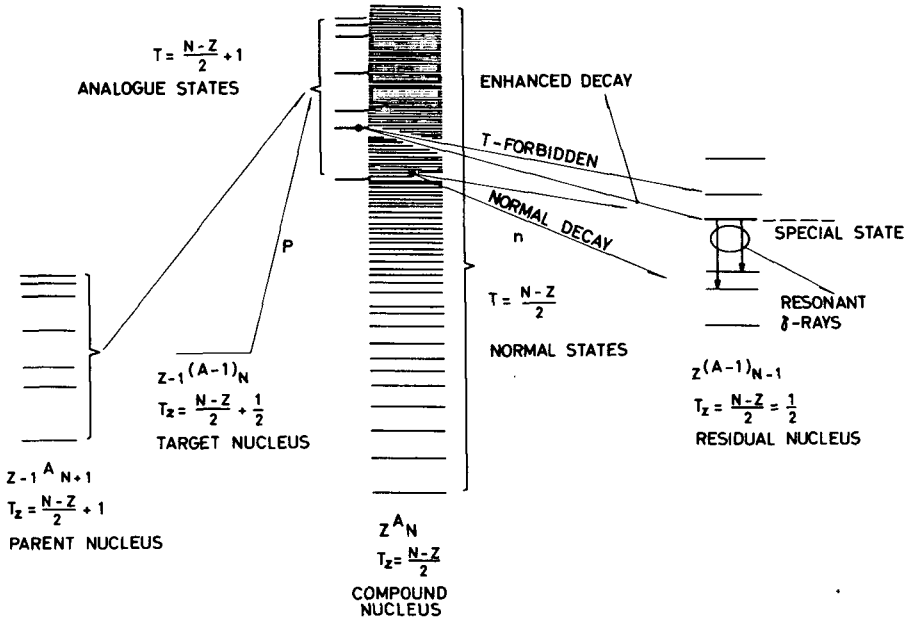

FIG.1. Schematic representation of a (p,nγ) reaction leading to isobaric analogue resonances. The isospin forbidden neutron decay of the analogue states ($T = (N-Z)/2 + 1$, $T_z = (N-Z)/2$) to the normal states of the residual nucleus ($T = T_z = (N-Z)/2 - \frac{1}{2}$) can be favoured by special properties of some final levels. The resonant character of the γ-decay of the latter will then be enhanced

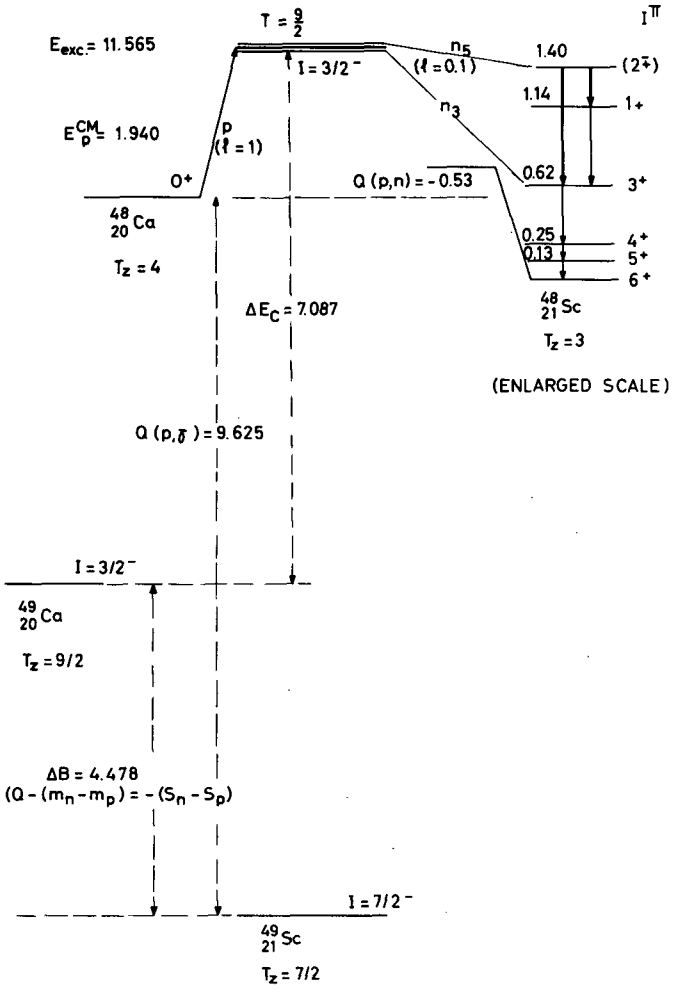

FIG. 2. Schematic diagram of the $^{48}Ca(p,n\gamma)$ reaction leading to the isobaric analogue of the ^{49}Ca ground state, in the ^{49}Sc compound nucleus. The Coulomb energy shift ΔE_C has been computed by the relation: $E_{exc} + (S_n - S_p)$ (see Ref. [2]), where $E_{exc} = Q(p,\gamma) + E_p^{CM}$. For a detailed illustration of the ^{48}Sc level scheme and the neutron decay of the ^{49}Sc resonances, see Fig. 5

Fig. 1 shows a schematic representation of a $(p, n\gamma)$ reaction leading to isobaric analogue resonances in the $_ZA_N$ ($T_z = (N - Z)/2$) nucleus.

The γ-rays associated with the neutron decay to the normal levels of the residual nucleus will follow the resonant character of the (p, n) reaction cross-section in correspondence with the analogue state of the compound nucleus.

However, there may be special states of the residual nucleus which particularly favour the neutron emission of the analogue resonance, owing to a particular configuration or isospin mixing. The yield of the γ-rays which arise from such states is then a good measure of the properties of the analogue resonance.

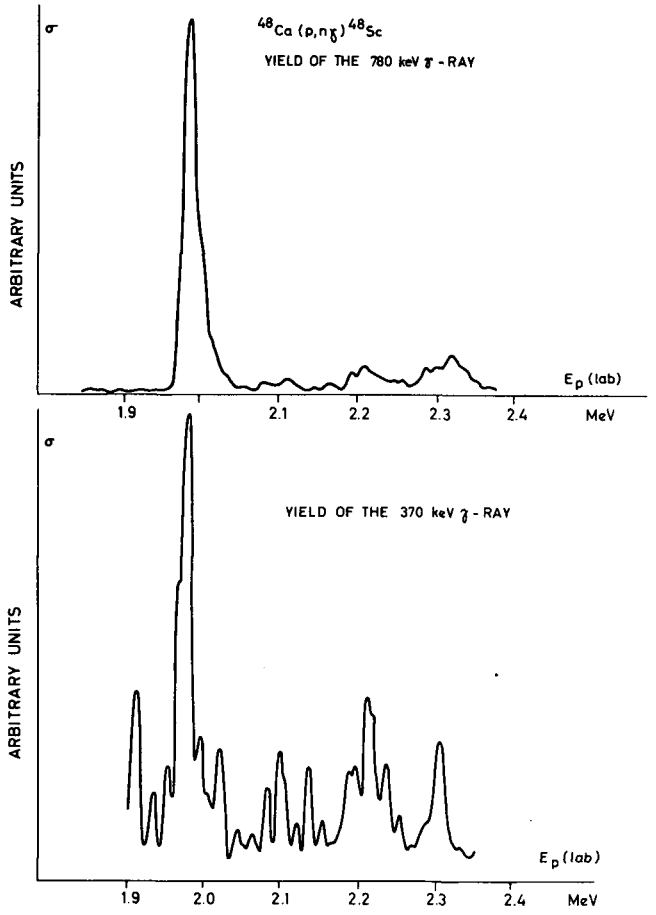

FIG. 3. Yield of the typical ^{48}Sc γ-rays in a thick target (poor resolution) experiment. The resonance behaviour of such γ-rays follows well the neutron decay of the analogue and normal states of ^{49}Sc

A typical example is given by the ^{48}Ca(p, nγ)^{48}Sc reaction investigated by the present author and colleagues at the 5.5 MeV Van de Graaff Laboratory of the University of Padua [9]. The schematic diagram of the reaction is shown in Fig. 2.

The decay modes of the analogue resonance found at E_p^{CM} = 1940 keV are covered by elastic and inelastic protons, neutron emission and capture γ-rays.

The elastic proton scattering experiment has been performed by Jones et al. [7], who found resonances in the excitation curve at E_p^{CM} = 1945 and 1935 keV, corresponding to the isobaric analogue ($T = 9/2$, $T_z = 7/2$) of the ^{49}Ca ground-state ($T = T_z = 9/2$).

In our case we were concerned with the neutron decay to levels in the ^{48}Sc residual nucleus. The interesting part of the level scheme of the latter [10] is also shown in Fig. 2 and Fig. 5 and is in substantial agreement with that proposed by Chasman et al. [11]. (We found, in addition, evidence for a 260 keV gamma ray from the 1403 keV level [10].)

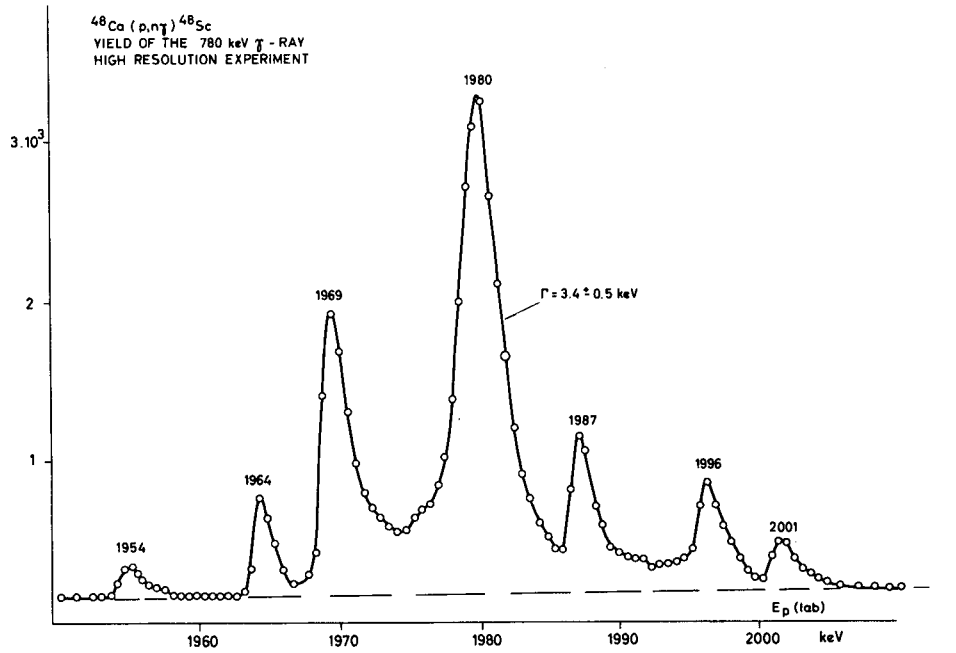

FIG.4. Yields of the 780 keV γ-ray, in the region of the analogue resonance, in a thin target (high resolution) experiment. The 'fine structure' is analysed in, at least, seven components. The proton energy is given in the laboratory system

The experiment was performed with $CaCO_3$ targets enriched to 90% in mass 48 on carbon or tantalum backings, and with NaI(Tl) and Ge(Li-drifted) γ-ray detectors connected with Laben multi-channel analysers.

The γ-ray spectroscopy concerning the decay of the low-lying levels of ^{48}Sc enabled us to establish that at $E_p \cong 1980$ keV (i.e. $E_p^{CM} \cong 1940$ keV) there is in most cases one neutron channel open leading to the 1403 keV state (n5).

In a poor resolution experiment this corresponds to a resonant structure of the 780 keV γ-ray yield peaked at this proton energy, as shown in Fig.3.

This should be compared with the yield of the 370 keV γ-ray, which arises from the 623 keV level in ^{48}Sc; a resonance at the same proton energy is also present in this case together with many other resonances corresponding to neutron emission from single normal states of the compound ^{49}Sc nucleus. This result was already found by El Nadi et al. [12].

It is clear that the yield of the 780 keV γ-ray which is the prominent transition arising from the 1403 keV level in ^{48}Sc, is an excellent measure of the features of the T = 9/2 isobaric analogue resonance in ^{49}Sc.

3. FINE STRUCTURE OF THE ISOBARIC ANALOGUE RESONANCE

A high resolution experiment performed with a target thickness of about 1.2 keV at 1 MeV proton energy enabled us to resolve this resonance

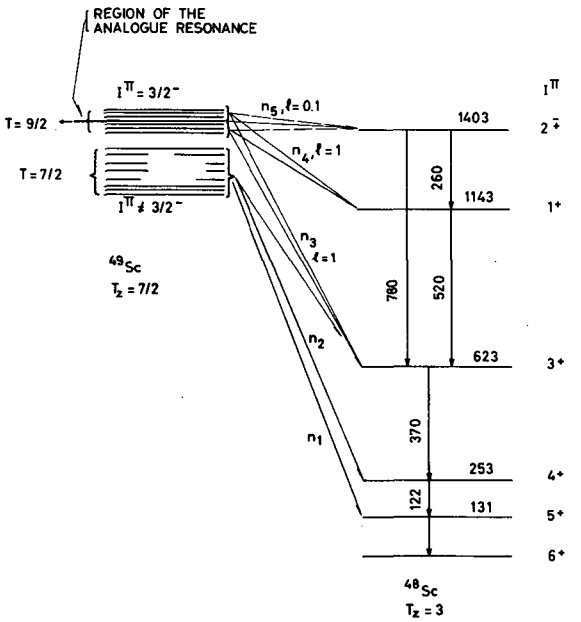

FIG. 5. Detailed illustration of the neutron decay of the ^{49}Sc compound nucleus resonances to the levels of the ^{48}Sc residual nucleus. The n_1 and n_2 branching are available only to the ^{49}Sc normal states ($T = T_z = 7/2$) with $I^\pi \neq 3/2^-$, ($\ell = 3$ protons and $\ell = 1$ neutrons, or vice versa, and/or $\ell = 2$ protons and $\ell = 2$ neutrons). To the $3/2^-$ ($T = 7/2$ mostly) states the n_3, n_4 and n_5 branching are available, whilst only the n_5 branching corresponds to the neutron decay of the $T = 9/2$ ($I^\pi = 3/2^-$) analogue state

in at least seven components. A detailed portion of the 780 keV γ-ray yield over the region of the analogue state production is reported in Fig. 4.

The major resonance found in the proton scattering experiment [7] at $E_p^{CM} = 1945 \pm 3$ keV fits well with the strong peak found in our experiment at $E_p = 1980$ keV (i.e. $E_p^{CM} = 1940 \pm 3$ keV), while the second one reported at $E_p^{CM} = 1935 \pm 3$ keV appears to be a doublet in our work, i.e. the two peaks at $E_p = 1969$ and 1964 keV ($E_p^{CM} = 1930 \pm 3$ and 1924 ± 3 keV, respectively). One important result of this high resolution experiment is that for the major resonance at 1980 keV we found the γ-ray spectroscopy to be such that the only neutron channel open is the one (n_5) leading to the 1403 keV level in ^{48}Sc. For the other components, other neutron channels become available (mostly n_3); so the neutron branching to excited states, other than the 1403 keV level, is quite important. This could be explained assuming that the 1403 keV level is a state of a particular nature, i.e. with a configuration strongly similar to that of the $T = 9/2$ analogue resonance or with important $T = 4$ mixing. On the other hand a large coherent effect due to an $\ell_n = 1$ giant resonance behaviour like that found in heavier nuclei [15] could also be considered; however, it would remain to be explained why the neutron decay on and off resonance is not the same [12]. The neutron decay from the ^{49}Sc resonances is illustrated in Fig. 5, where the spin assignment to the levels of ^{48}Sc is based on the γ-ray spectroscopy [10].

The ^{49}Sc resonances in the region of the analogue states have "signature" $3/2^-$ as the ^{49}Ca ground state. Assuming pure configurations and charge independence of nuclear forces, the ($T = 9/2$, $T_z = 7/2$) analogue resonance cannot decay to the ($T = T_z = 3$) normal states of ^{48}Sc. If such decay is due to the Coulomb mixing with the $T = 7/2$ states of ^{49}Sc, it should have the same neutron branching as the latter.

Among the levels of ^{48}Sc, at least the 623 keV (3^+) and the 1143 keV (1^+) ones are also available for the neutron decay from the $3/2^-$ ^{49}Sc resonances. Experimentally, the neutron decay of the major $T = 9/2$ resonance at $E_p^{CM} = 1940$ keV occurs only to the 1403 keV level of ^{48}Sc, whereas the surrounding resonances have important branching to other levels. Since the corresponding neutron energy is of the order of 10 keV (i.e., $\ell_n = 0$ or 1) the signature of the 1403 keV level is $1^\pm$ or $2^\pm$, taking into account also the corresponding γ-decay.

The assignment 2^+ is what is expected from shell model considerations [12].

4. COMPARISON WITH PROTON SCATTERING DATA AND STRIPPING SPECTROSCOPIC FACTOR

The main features of the ^{49}Sc resonances in the region of the analogue state have been analysed by measuring the corresponding strengths $\omega\gamma$ and widths Γ. The results found for the most prominent peaks of the observed fine structure are reported in Table I, where a comparison is made with the proton scattering data [7]. Here $\omega\gamma = \omega\,\Gamma_p\Gamma_n/\Gamma$; Γ is the total width, Γ_p and Γ_n the corresponding widths for proton scattering and neutron emission ($\Gamma_p + \Gamma_n \simeq \Gamma$ in our case[1]) and $\omega = (2I+1)/(2s+1)(2I_0+1) = 2$ is a statistical factor.

The $\omega\gamma$ values derived in our experiment from the comparison between the N_γ/N_p ratios found for thick and thin targets, with the assumption that N_γ is a good measure of the neutron number N_n, do not agree with the corresponding quantities inferred by proton scattering [7] by a 'puzzling' factor 10.

The Γ_p and Γ_n, which can be derived from our data, have to be chosen between two possible sets of values given by the relations: $\Gamma_p\Gamma_n = \frac{1}{2}\Gamma\cdot\omega\gamma$ and $\Gamma_p + \Gamma_n = \Gamma$.

Since $\Gamma >> \Gamma_p\Gamma_n/\Gamma$ for each resonance reported in Table I, one obtains: $\Gamma_n \simeq \Gamma_p\Gamma_n/\Gamma$ and $\Gamma_p \simeq \Gamma$, or vice versa.

From our data we get $\Gamma_p = 3.32 \pm 0.56$ and $\Gamma_n = 0.08 \pm 0.06$ or vice versa for the major resonance at $E_p^{CM} = 1940$ keV. We evaluate then the spectroscopic factor for proton scattering, i.e. $S_{pp} = (2T+1)\,\Gamma_p/\Gamma_{sp}$ (where Γ_{sp} is the single proton width estimated from optical model calculations adjusted for $2p_{3/2}$ proton resonances [13], and $T = 4$ is the isobaric spin of the target nucleus). If we take $\Gamma_p = 3.32$ keV we get $S_{pp} = 1.06 \pm 0.15$ in excellent agreement with the spectroscopic factor $S_{dp} = 1.03$ inferred from stripping experiments leading to the ^{49}Ca ground state [14].

The above arguments seem then to form a self-consistent way which supports the conclusion that the major resonance found at $E_p^{CM} = 1940 \pm 3$ keV (i.e. at an excitation energy of 11.565 MeV in ^{49}Sc) is

---

[1] A capture γ-ray experiment performed in connection with the (p, nγ) reaction showed that $\Gamma_\gamma < 10^{-2}\,\Gamma_n$.

TABLE I. SUMMARY OF THE RESULTS

Resonance strengths ω_γ and widths Γ found in the present work are compared with the ones derived from Ref. [7], as discussed in the text. The spectroscopic factor S_{pp} for proton scattering, has been derived, in our case, only for the major resonance at E_p^{CM} = 1940 KeV, from the relation $S_{pp} = (2T+1)(\Gamma_p/\Gamma_{sp})$, where T = 4, Γ_p = 3.32 keV (see the text) and Γ_{sp} is the single-particle proton width calculated in Ref. [7]. The S_{pp} value is compared with the S_{dp} spectroscopic factor inferred from stripping data (Ref. [14]). E_p, $\omega_\gamma = \omega\,\Gamma_p\Gamma_n/\Gamma$, and Γ are given in keV.

^{48}Ca(p, nγ) (present work)					^{48}Ca (p, p) (Ref. [7])					Stripping (Ref. [14])
E_p^{CM}	ω_γ	Γ	Γ_p	S_{pp}	E_p^{CM}	ω_γ	Γ	Γ_p	S_{pp}	S_{dp}
1940 ± 3	0.15 ± 0.06	3.4 ± 0.5	3.32 ± 0.5	1.06 ± 0.15	1945 ± 3	1.5 ± 0.4	3.6 ± 0.5	1.10 ± 0.2	0.64 ± 0.07	1.03
1930 ± 3	0.085 ± 0.034	2.2 ± 0.4			1935 ± 3	1.4 ± 0.4	4.6 ± 0.5	0.87 ± 0.2		
1924 ± 3	0.037 ± 0.016	1.2 ± 0.4								

essentially the 'true' isobaric analogue of the ^{49}Ca ground state, corresponding to a 7.087 ± 0.005 MeV Coulomb energy shift.

The surrounding resonances may be interpreted as normal ($T = 7/2$, $T_z = 7/2$) states with some mixing due to the presence of the ($T = 9/2$, $T_z = 7/2$, $I^\pi = 3/2^-$) analogue state.

These states could be complicated shell model states so that the isobaric analogue resonance would be coupled to the outgoing neutron channel only via that configuration which selects the decay to the 1403 keV level of ^{48}Sc.

REFERENCES

[1] Cf. FOX, J. D., Proceedings of the Conference on Recent Progress in Nuclear Physics with Tandems, Heidelberg (1966, July).

[2] TEMMER, G. M., Chapter 3 of this book.

[3] FOX, J. D., MOORE, C. F., ROBSON, D., Phys. Rev. Lett. 12 (1964) 198.

[4] RICHARD, P., MOORE, C. F., FOX, J. D., ROBSON, D., Phys. Rev. Lett. 13 (1964) 343.

[5] KEYWORTH, G. A., KYKER, G. C., Jr., BILPUCH, E. G., NEWSON, H. W., Phys. Lett. 20, (1966) 281.

[6] TERANISHI, E., FURUBAYASHI, B., Proceedings of the Conference on Isobaric Spin in Nuclear Physics, Tallahassee (1966, March).

[7] JONES, K. W., SCHIFFER, J. P., LEE, L. L., Jr., MARINOV, A., LEBNER, J. L., Phys. Rev. 145 (1966) 894.

[8] Cf. VON BRENTANO, P., Proceedings of the Conference on Isobaric Spin in Nuclear Physics, Tallahassee (1966, March).

[9] RICCI, R. A., CHILOSI, G., VINGIANI, G. B., to be published; RICCI, R. A., Proceedings of the Conference on Recent Progress in Nuclear Physics with Tandems, Heidelberg, (1966, July).

[10] VINGIANI, G. B., RICCI, R. A., NOTARRIGO, S., SPERANZA, R., GIACOMICH, R., POIANI, G., to be published.

[11] CHASMAN, C., JONES, K. W., RISTINEN, R. A., Phys. Rev. 140 (1965) B212.

[12] McCULLEN, J. D., BAYMAN, B. F., ZAMICK, L., Phys. Rev. 134 (1964) B515.

[13] SCHIFFER, J. P., Nucl. Phys. 46 (1963) 246.

[14] KASHY, E., SPERDUTO, A., ENGE, H. A., BUECHNER, W. W., Phys. Rev. 135 (1965) B865.

[15] MANI, G. S., DUTT, G. C., Phys. Lett. 16 (1965) 50.

PART II

THEORETICAL NUCLEAR PHYSICS

CHAPTER 5

COLLISION THEORY

F. VILLARS

INTRODUCTORY REMARKS

The purpose of this Chapter is didactical. It is assumed that the reader is familiar with elementary scattering theory: phase-shifts, Born-approximations, for the scattering of a particle by a potential. But the nuclear physicist faces now the problem of describing much more complex collision processes, involving composite target structures (nuclei) as well as possible composite projectiles (deuterons, α-particles). There are exchange effects to be considered, due to the identity of particles in projectile and target, and rearrangement collisions (reactions) to be analysed. It is hoped that this Chapter will provide a basis for the understanding and proper description of these processes.

Section 1 deals with collision of an elementary non-relativistic particle with a fixed potential V. This process is used to develop, in a simple and familiar context, the notions of in- and out-going scattering states, the T-matrix, the S-matrix, the unitarity condition. An attempt is made also to clarify the relation between the time-independent description in terms of wave packets.

The arsenal of tools mobilized may appear excessive, but the aim of this part is not application but to lay a basis from which to generalize. Indeed, it will be seen in section 2 that the generalization to more complex situations is quite straightforward.

In section 2 composite targets are introduced, with a case of minimum complexity as an example. After reading this section, more general cases should offer no difficulty. The very important problem of presenting suitable approximation techniques is not touched upon at all in the section. This is much too vast a field to be included here, and the reader must be content with finding the exact expressions for reaction amplitudes, and

* The author is at the Laboratory for Nuclear Science and Physics Department, Massachusetts Institute of Technology, Cambridge, Massachusetts, United States of America.

possibly equations satisfied by them. Not the least part of the problem is in fact to know what quantity to find an approximation to.

In section 3 the case of identical particles is considered in more detail. The method of second quantization is introduced and it is shown how to formulate a collision problem for identical particles in this language. This opens the way for discussion of nuclear reactions in the framework of Hartree-Fock theory, which is so important for unifying nuclear reaction theory with nuclear spectroscopy.

1. REVIEW OF BASIC CONCEPTS

1.A. Scattering states, scattering amplitude, T-matrix

We discuss here the example of the scattering of a spinless elementary particle by a potential V, in the non-relativistic limit.

The Hamiltonian is thus

$$H = \frac{p^2}{2m} + V \tag{1.1}$$

Before developing the subject, a word about notation must be said. The Dirac notation (with a few occasional modifications) appears to be the most generally useful way of writing probability amplitudes. In the discussion of scattering problems, the co-ordinate and momentum representations play a distinguished role.

Initially both these representations will be used, for the sake of clarity; eventually we shall go over to a representation-independent notation in terms of state vectors.

An unspecified quantum state of the particle will be described by the co-ordinate space amplitude $\langle \vec{r} | \psi \rangle$ or by the momentum space amplitude $\langle \vec{k}' | \psi \rangle$. (If their time dependence is to be emphasized, we write $\langle \vec{r} | \psi(t) \rangle$ and $\langle \vec{k} | \psi(t) \rangle$.)

The co-ordinate and momentum representations are connected through the transformation

$$\langle \vec{r} | \vec{k} \rangle = e^{i\vec{k}\cdot\vec{r}}/(2\pi)^{\frac{3}{2}} :$$
$$\langle \vec{r} | \psi \rangle = \int d^3k \, \langle \vec{r} | \vec{k} \rangle \langle \vec{k} | \psi \rangle = \int \frac{d^3k}{(2\pi)^{\frac{3}{2}}} \, e^{i\vec{k}\cdot\vec{r}} \langle \vec{k} | \psi \rangle \tag{1.2}$$

The inverse relation involves $\langle \vec{k} | \vec{r} \rangle = \langle \vec{r} | \vec{k} \rangle^*$.

The Hamiltonian (1.1) may be written more explicitly, in the $\vec{r}$- and $\vec{k}$-representation, as the matrix

$$\langle \vec{r}' | H | \vec{r} \rangle = \frac{-\hbar^2}{2m} \cdot \nabla^2 \delta(\vec{r}' - \vec{r}) + \langle \vec{r}' | V | \vec{r} \rangle$$

and (1.3a)

$$\langle \vec{k}' | H | \vec{k} \rangle = \int d^3r \int d^3r' \cdot \langle \vec{k}' | \vec{r}' \rangle \langle \vec{r}' | H | \vec{r} \rangle \langle \vec{r} | \vec{k} \rangle$$

$$= \frac{\hbar^2}{2m} k^2 \delta(\vec{k}' - \vec{k}) + \langle \vec{k}' | V | \vec{k} \rangle \tag{1.3b}$$

If V is a local potential, then

$$\langle \vec{r}' | V | \vec{r} \rangle = V(\vec{r})\, \delta(\vec{r}' - \vec{r}) \tag{1.4a}$$

and in this case

$$\langle \vec{k}' | V | \vec{k} \rangle = \int d^3r \, \langle \vec{k}' | \vec{r} \rangle V(\vec{r}) \langle \vec{r} | \vec{k} \rangle = \int \frac{d^3r}{(2\pi)^3} e^{-i(\vec{k}' - \vec{k})\cdot\vec{r}} V(\vec{r}) = V(\vec{k}' - \vec{k}) \tag{1.4b}$$

The time-independent Schrödinger equation for states of energy E may then be written (we consider a local potential) as:

$$\left(\frac{-\hbar^2}{2m} \nabla^2 - E \right) \langle \vec{r} | \psi \rangle + V(r) \langle \vec{r} | \psi \rangle = 0 \tag{1.5a}$$

or equivalently

$$(E_{k'} - E) \langle \vec{k}' | \psi \rangle + \int d^3k'' \, \bar{V}(\vec{k}' - \vec{k}'') \langle \vec{k}'' | \psi \rangle = 0 \tag{1.5b}$$

Here $E_{k'} = \frac{\hbar^2 k^2}{2m}$, the kinetic energy for a particle of momentum $\hbar \vec{k}$.

The solution of Eqs (1.5) fall into the two groups:

a) Bound states ($E < 0$); for these we introduce the amplitude $\langle \vec{r} | n \rangle$, n being a discrete set of quantum number labelling the state.

b) Continuum states. These may be viewed as the limiting case of a wave packet, and must be characterized by a boundary condition.

This boundary condition may be incorporated into the Schrödinger equation by writing it as an integral equation:

$$\langle \vec{r} | \psi \rangle = \langle \vec{r} | \phi \rangle + \int d^3r'' \langle \vec{r} | \frac{1}{E + \frac{\hbar^2}{2m} \nabla^2} | \vec{r}'' \rangle V(\vec{r}'') \langle \vec{r}'' | \psi \rangle \tag{1.6a}$$

or

$$\langle \vec{k}' | \psi \rangle = \langle \vec{k}' | \phi \rangle + \frac{1}{E - E_{k'}} \int d^3k'' \, \bar{V}(k' - k'') \langle k'' | \psi \rangle \tag{1.6b}$$

$\langle \vec{r} | \phi \rangle$ and $\langle \vec{k}' | \phi \rangle$ are solutions of the equation

$$\left(\frac{-\hbar^2}{2m} \nabla^2 - E \right) \langle \vec{r} | \phi \rangle = 0 \quad \text{and} \quad (E_{k'} - E) \langle \vec{k}' | \phi \rangle = 0 \tag{1.7}$$

The Green's function $\langle \vec{r} | \frac{1}{E + (\hbar^2/2m)\nabla^2} | \vec{r}' \rangle$ is defined by

$$\langle \vec{r} | \frac{1}{E + \frac{\hbar^2}{2m} k^2} | \vec{r}' \rangle = \int d^3k' \, \langle \vec{r} | \vec{k}' \rangle \frac{1}{E - \frac{\hbar^2}{2m} k'^2} \langle \vec{k}' | \vec{r}' \rangle$$

$$= \int \frac{d^3k'}{(2\pi)^3} \frac{e^{i\vec{k}'\cdot(\vec{r} - \vec{r}')}}{E - E_{k'}}$$

Define a momentum $k > 0$ by $E = \hbar^2 k^2/2m$; then at $k' = \pm k$, the integrand is singular, and the integral must be defined either as the Cauchy principal value, or by a limiting process, replacing first E by $E \pm i\eta$ ($\eta > 0$), and then taking $\eta \to 0$ in the end. Consider this latter alternative; one has then:

$$\int \frac{d^3k'}{(2\pi)^3} \frac{e^{i\vec{k}'\cdot(\vec{r}-\vec{r}')}}{E-E_{k'}\pm i\eta} = \frac{1}{(2\pi)^2} \left(\frac{2m}{\hbar^2}\right) \int_0^\infty k'^2\, dk' \int_{-1}^{+1} dx\, \frac{e^{ik'(\vec{r}-\vec{r}')x}}{k^2 - k'^2 \pm i\epsilon}$$

$$= \left(\frac{2m}{\hbar^2}\right) \left(\frac{1}{2\pi}\right)^2 \frac{1}{i|\vec{r}-\vec{r}'|} \int_0^\infty dk'\, k' \frac{e^{ik'|\vec{r}-\vec{r}'|} - e^{-ik'|\vec{r}-\vec{r}'|}}{k^2 - k'^2 \pm i\epsilon}$$

$$= \left(\frac{2m}{\hbar^2}\right) \left(\frac{1}{2\pi}\right)^2 \frac{1}{i|\vec{r}-\vec{r}'|} \int_{-\infty}^{+\infty} k'\, dk' \frac{e^{ik'|\vec{r}-\vec{r}'|}}{k^2 - k'^2 \pm i\epsilon}$$

The k'-integral may now be handled by contour integration, and gives: $-i\pi \exp \pm ik|\vec{r}-\vec{r}'|$; so the full answer is

$$\langle \vec{r}| \frac{1}{E_k + \frac{\hbar^2}{2m}\nabla^2 \pm i\eta} |\vec{r}'\rangle = -\left(\frac{2m}{\hbar^2}\right) \frac{e^{\pm ik|\vec{r}-\vec{r}'|}}{4\pi|\vec{r}-\vec{r}'|} \tag{1.8}$$

Notice that the difference between the two solutions (1.8) is proportional to

$$\sin k|\vec{r}-\vec{r}'|/|\vec{r}-\vec{r}'|$$

which, as a function of $\vec{r}$ is a solution of the homogeneous equation (1.7).

We therefore get a complete set of solutions to (1.6) by choosing either the in- or out-going wave Green's function (1.8), and using a complete set of solutions ϕ to the homogeneous equation (1.7).

A complete set of ϕ's is obtained by choosing them to be plane waves:

$$\langle \vec{r}|\phi\rangle \to \langle \vec{r}|\vec{k}\rangle = e^{i\vec{k}\cdot\vec{r}}/(2\pi)^{\frac{3}{2}}$$

so that

$$\langle \vec{k}'|\phi\rangle \to \langle \vec{k}'|\vec{k}\rangle = \int d^3r\, \langle \vec{k}'|\vec{r}\rangle \langle \vec{r}|\vec{k}\rangle = \delta(\vec{k}'-\vec{k})$$

The associated solutions $\langle \vec{r}|\psi\rangle$ and $\langle \vec{k}'|\psi\rangle$ of (1.6) we shall call

$$\langle \vec{r}|k^{(\pm)}\rangle \quad \text{resp.} \quad \langle \vec{k}'|k^{(\pm)}\rangle,$$

depending on the choice of out- or in-going wave boundary conditions. So we have

$$\langle \vec{r}|k^{(\pm)}\rangle = \frac{e^{i\vec{k}\cdot\vec{r}}}{(2\pi)^{\frac{3}{2}}} - \frac{2m}{\hbar^2} \int d^3r'\, \frac{e^{ik|\vec{r}-\vec{r}'|}}{4\pi|\vec{r}-\vec{r}'|} V(\vec{r}') \langle \vec{r}'|k^{(+)}\rangle \tag{1.9a}$$

and

$$\langle \vec{k}' | k^{(+)} \rangle = \delta(\vec{k}' - \vec{k}) + \frac{1}{E_k - E_{k'} + i\eta} \int d^3k'' \, \overline{V}(\vec{k}' - \vec{k}'') \langle \vec{k}'' | k^{(+)} \rangle \qquad (1.9b)$$

In section 1.C we shall use these amplitudes to construct wave packets and discuss their evolution, but before that, we shall develop the subject somewhat further.

In the limit $|r'| \to \infty$, and for a short range potential[1] one may use the asymtotic form

$$\frac{e^{ik|\vec{r}' - \vec{r}''|}}{|\vec{r}' - \vec{r}''|} \to \frac{e^{ikr'}}{r'} e^{-ik\frac{\vec{r}'}{r'} \cdot \vec{r}''} = \frac{e^{ikr'}}{r'} e^{-i\vec{k}' \cdot \vec{r}''}$$

where

$$\vec{k}' \equiv k \frac{\vec{r}'}{r'} \quad \text{(so that } |\vec{k}'| = k\text{)}.$$

Hence

$$\langle \vec{r}' | k^{(+)} \rangle \underset{|\vec{r}'| \to \infty}{\longrightarrow} \frac{e^{i\vec{k} \cdot \vec{r}}}{(2\pi)^{\frac{3}{2}}} - \frac{e^{ikr'}}{4\pi r'} \int d^3r'' \, e^{-i\vec{k}' \cdot \vec{r}''} \frac{2m}{\hbar^2} V(r'') \langle \vec{r}'' | k^{(+)} \rangle \qquad (1.10)$$

This defines a scattering amplitude $f(\theta)$ [$\cos\theta = \vec{k} \cdot \vec{k}'/k^2$] by means of

$$\langle \vec{r}' | k^{(+)} \rangle \to \text{const} \left(e^{i\vec{k} \cdot \vec{r}'} + f(\theta) \frac{e^{ikr'}}{r'} \right) \qquad (1.11)$$

Comparing with (1.10), it follows that

$$f(\theta) = f(\vec{k}'; \vec{k}) = 2\pi^2 \left(-\frac{2m}{\hbar^2} \right) \int d^3r'' \langle \vec{k}' | r'' \rangle V(\vec{r}'') \langle \vec{r}'' | k^{(+)} \rangle \qquad (1.12)$$

A well known argument about the flux associated with $\exp i\vec{k} \cdot \vec{r}$ and $(\exp ikr)/r$ then leads to the interpretation of

$$|f(\theta)|^2 = \sigma(\theta) \qquad (1.13)$$

as the differential cross-section - that is, cross-section per unit solid angle - for scattering by the potential V.

It is customary to define a matrix T by means of (1.12)[2]:

$$\begin{aligned} \langle k' | T | k \rangle &= \int d^3r' \, | k' | r' \rangle \, V(r') \langle r' | k^{(+)} \rangle \\ &= \int d^3r' \int d^3k'' \langle k' | r' \rangle \, V(r') \langle r' | k'' \rangle \langle k'' | k^{(+)} \rangle \\ &= \int d^3k'' \, \langle k' | V | k'' \rangle \langle k'' | k^{(+)} \rangle \end{aligned} \qquad (1.14)$$

[1] This excludes the Coulomb potential.

[2] The arrows on vectors will often be omitted when no confusion is caused thereby.

T is defined by all values of $\vec{k}'$ and $\vec{k}$ by this equation, not only for $|k'| = |k|$, as (1.12) might suggest. The scattering amplitude is then

$$f(\vec{k}', \vec{k}) = -\frac{4\pi^2 m}{\hbar^2} \langle \vec{k}' | T | \vec{k} \rangle |_{|\vec{k}'| = |\vec{k}|} \tag{1.15}$$

We see also that the momentum space amplitude $\langle k' | k^{(+)} \rangle$ can be simply expressed through T; by (1.9b) and (1.14), one has

$$\langle \vec{k}' | \vec{k}^{(+)} \rangle = \delta(\vec{k}' - \vec{k}) + \frac{\langle \vec{k}' | T | \vec{k} \rangle}{E_k - E_{k'} + i\eta} \tag{1.16}$$

Multiplying this equation into V, and using (1.14) again, gives the Lippman-Schwinger integral equation for T:

$$\langle k' | T | k \rangle = \langle k' | V | k \rangle + \int d^3k'' \langle k' | V | k'' \rangle \frac{\langle k'' | T | k \rangle}{E_k - E_{k''} + i\eta} \tag{1.17}$$

A solution by iteration of this equation generates the Born-perturbation series:

$$\langle k' | T | k \rangle = \langle k' | V | k \rangle + \int d^3k'' \langle k' | V | k'' \rangle \langle k'' | V | k \rangle / E_k - E_{k''} + i\eta + \ldots$$

For the convergence of this series, see general bibliography.

1.B. Some properties of scattering states

We shall from here on use the short-hand notation of state vectors $|\psi\rangle$, abstracted from the amplitudes $\langle \vec{r} | \psi \rangle$ or $\langle \vec{k} | \psi \rangle$, as well as the adjoint vector $\langle \psi |$, abstracted from the complex conjugate amplitudes $\langle \psi | \vec{r} \rangle$ and $\langle \psi | \vec{k} \rangle$.

Calling H_0 the kinetic energy operator $p^2/2m$, we write (for 1.5a, b):

$$(H_0 - E) | \psi \rangle + V | \psi \rangle = 0$$

and for the two equations (1.9a, b):

$$k^{(+)} \rangle = |k\rangle + \frac{1}{E_k - H_0 + i\eta} V | k^{(+)} \rangle \tag{1.18}$$

There is a corresponding adjoint relation, abstracted from the complex conjugate of (1.9):

$$\langle k^{(+)} | = \langle k | + \langle k^{(+)} | V \frac{1}{E_k - H_0 - i\eta} \tag{1.18a}$$

Normalizations and orthogonality of states are expressed through the scalar product

$$\langle \psi' | \psi \rangle = \int d^3r \langle \psi' | r \rangle \langle r | \psi \rangle = \int d^3k \langle \psi' | k \rangle \langle k | \psi \rangle$$

in particular

$$\langle\psi|\psi\rangle = \int d^3r\, \langle\psi|r\rangle\langle r|\psi\rangle = \int d^3r\, |\langle r|\psi\rangle|^2$$

The plane wave states $|\vec{k}\rangle$ form an ortho-normal set:

$$\langle\vec{k}'|\vec{k}\rangle = \int d^3r\, \langle\vec{k}'|\vec{r}\rangle\langle\vec{r}|\vec{k}\rangle = \int \frac{d^3r}{(2\pi)^3} e^{-i(\vec{k}'-\vec{k})\cdot\vec{r}} = \delta(\vec{k}'-\vec{k})$$

We now prove that the same relation also holds for the scattering states $|\vec{k}^{(+)}\rangle$:

$$\langle\vec{k}'^{(+)}|\vec{k}^{(+)}\rangle = \langle\vec{k}'|\vec{k}\rangle = \delta(\vec{k}'-\vec{k}) \tag{1.19}$$

First, we find an alternative expression for $|k^{(+)}\rangle$. Writing $H = H_0 + V$ there is a formal identity

$$\frac{1}{E - H_0 + i\eta} = \frac{1}{E - H + i\eta}\left(1 - V\frac{1}{E - H_0 + i\eta}\right)$$

Introducing this into (1.18), one has

$$|k^{(+)}\rangle = |k\rangle + \frac{1}{E_k - H + i\eta} V\left\{|k^{(+)}\rangle - \frac{1}{E_k - H_0 + i\eta} V|k^{(+)}\rangle\right\}$$

$$= |k\rangle + \frac{1}{E_k - H + i\eta} V|k\rangle \tag{1.20}$$

Of course, there is then also the adjoint relation

$$\langle k^{(+)}| = \langle k| + \langle k| V \frac{1}{E_k - H - i\eta} \tag{1.20a}$$

With the help of (1.20a), the scalar product $\langle k'^{(+)}|k^{(+)}\rangle$ may now be written as

$$\langle k'^{(+)}|k^{(+)}\rangle = \langle k'|k^{(+)}\rangle + \langle k'| V \frac{1}{E_{k'} - H - i\eta}|k^{(+)}\rangle$$

$$= \langle k'|k\rangle + \langle k'|\frac{1}{E_k - H_0 + i\eta} V|k^{(+)}\rangle + \langle k'| V \frac{1}{E_{k'} - H - i\eta}|k^{(+)}\rangle$$

Use is now made of the general relation

$$F(H_0)|k\rangle = F(E_k)|k\rangle; \quad F(H)|k^{(+)}\rangle = F(E_k)|k^{(+)}\rangle$$

With this, the scalar product can be written as

$$\langle k'^{(+)}|k^{(+)}\rangle = \langle k'|k\rangle + \frac{\langle k'|V|k^{(+)}\rangle}{E_k - E_{k'} + i\eta} + \frac{\langle k'|V|k^{(+)}\rangle}{E_{k'} - E_k - i\eta} = \langle k'|k\rangle = \delta(\vec{k}'-\vec{k})$$

The scattering states do not form a complete set if V admits bound states. In this case, the completeness relation is

$$\int d^3k \, \langle \vec{r} | k^{(+)} \rangle \langle k^{(+)} | \vec{r}' \rangle + \sum_n \langle \vec{r} | n \rangle \langle n | \vec{r}' \rangle = \delta(\vec{r} - \vec{r}') \tag{1.21}$$

a relation which we abstract into

$$\int d^3k \, | k^{(+)} \rangle \langle k^{(+)} | + \sum_n | n \rangle \langle n | = 1 \tag{1.21a}$$

the "I" standing for the unit matrix in whatever representation we choose to have in mind.

1.C. The S-matrix and the unitarity condition

We now introduce also the ingoing wave states $|k^{(-)}\rangle$, for which we have the equations - in analogy to (1.18) and (1.20):

$$|k^{(-)}\rangle = |k\rangle + \frac{1}{E_k - H_0 - i\eta} V |k^{(-)}\rangle \tag{1.22}$$

$$= |k\rangle + \frac{1}{E_k - H - i\eta} V |k\rangle \tag{1.22a}$$

As will be shown later, wave packets formed by superpositions of such states reduce to free wave packets (without scattered wave) as $t \to +\infty$, in contrast to packets of $|k^{(+)}\rangle$ states, which reduce to free wave packets as $t \to -\infty$.

The $|k^{(-)}\rangle$ states are also an ortho-normal set, and satisfy orthogonality completeness relations analogous to (1.19) and (1.21). They may therefore be expanded in terms of the states $|k'^{(+)}\rangle$:

$$|k^{(-)}\rangle = \int d^3k' \, |k'^{(+)}\rangle \langle k' | S | k \rangle \tag{1.23}$$

The expansion coefficient $\langle k' | S | k \rangle$ is the transformation matrix from one ortho-normal set to another, spanning the same space; it is therefore unitary. We call it the S-matrix; an alternative definition to (1.23) is obviously

$$\langle k' | S | k \rangle = \langle k'^{(-)} | k^{(+)} \rangle \tag{1.23a}$$

The inverse transformation to (1.23) defines the adjoint $(k' | S^+ | k)$, and

$$\langle k' | S^\dagger | k \rangle = \langle k'^{(+)} | k^{(-)} \rangle = \langle k | S | k' \rangle^* \tag{1.24}$$

The unitarity property is then expressed by

$$\int d^3k'' \langle k' | S | k'' \rangle \langle k'' | S^\dagger | k' \rangle = \int d^3k'' \langle k' | S^\dagger | k'' \rangle \langle k'' | S | k' \rangle = \delta(k' - k) \tag{1.25}$$

These relations are seen to follow immediately from (1.21):

$$\int d^3k'' \langle k'|S|k''\rangle\langle k''|S|k\rangle = \int d^3k'' \langle k'^{(-)}|k''^{(+)}\rangle\langle k''^{(+)}|k^{(-)}\rangle$$

$$= \langle k'^{(-)}|k^{(-)}\rangle - \sum_n \langle k'^{(-)}|n\rangle\langle n|k^{(-)}\rangle = \langle k'^{(-)}|k^{(-)}\rangle = \delta(k'-k)$$

Using the equations (1.18, 20 and 1.22), we can give a more explicit expression for S:

$$\langle k'|S|k\rangle = \langle k'^{(-)}|k^{(+)}\rangle = \langle k'|k^{(+)}\rangle + \langle k'|V\frac{1}{E_{k'}-H+i\eta}|k^{(+)}\rangle$$

$$= \langle k'|k\rangle + \langle k'|\frac{1}{E_k-H_0+i\eta}V|k^{(+)}\rangle + \langle k'|V\frac{1}{E_{k'}-H+i\eta}|k^{(+)}\rangle$$

$$= \langle k'|k\rangle + \langle k'|V|k^{(+)}\rangle\left(\frac{1}{E_k-E_{k'}+i\eta} + \frac{1}{E_{k'}-E_k+i\eta}\right)$$

$$= \langle k'|k\rangle + \langle k'|V|k^{(+)}\rangle\frac{-2i\eta}{(E_k-E_{k'})^2+\eta^2}$$

Now,[3]

$$\lim_{\eta\to 0^+}\frac{\eta}{q^2+\eta^2} = \pi\,\delta(q) \tag{1.26}$$

So we have, using (1.14) and (1.26):

$$\langle k'|S|k\rangle = \langle k'|k\rangle - 2\pi i\,\delta(E_{k'}-E_k)\langle k'|T|k\rangle \tag{1.27}$$

We could have used as a first step in this derivation the step:

$$\langle k'|S|k\rangle = \langle k'^{(-)}|k\rangle + \langle k'^{(-)}|\frac{1}{E_k-H+i\eta}V|k\rangle$$

and would have found

$$\langle k'|S|k\rangle = \langle k'|k\rangle - 2\pi i\delta(E_{k'}-E_k)\langle k'^{(-)}|V|k\rangle$$

which shows that on the energy shell ($E_{k'} = E_k$) the two matrices

$$\langle k'|V|k^{(+)}\rangle \text{ and } \langle k'^{(-)}|V|k\rangle$$

are equal and define the scattering amplitude. They are clearly unequal off the energy shell.

---

[3] $\lim_{\eta\to 0^+}\left(\frac{1}{q\pm i\eta}\right) = \lim_{\eta\to 0^+}\left(\frac{q}{q^2+\eta^2} \mp i\pi\frac{\eta/\pi}{q^2+\eta^2}\right) = P(1/q) \mp i\pi\delta(q)$, where P (1/q) is the Cauchy principal value.

The connection between S and T (1.27), and the unitarity property (1.25) of S lead to the unitarity relation for T:

$$\begin{aligned}\langle k'|k\rangle &= \int d^3k'' \langle k'|S^\dagger|k''\rangle\langle k''|S|k\rangle \\ &= \int d^3k'' \{\langle k'|k''\rangle + 2\pi i\,\delta(E'-E'')\langle k'|T^\dagger|k''\rangle\} \\ &\quad \{\langle k''|k\rangle - 2\pi i\,\delta(E''-E)\langle k''|T|k\rangle\} \\ &= \langle k'|k\rangle - 2\pi i\,\delta(E'-E)\,(\langle k'|T|k\rangle - \langle k'|T^\dagger|k\rangle) \\ &\quad + 4\pi^2\,\delta(E'-E)\int d^3k''\,\langle k'|T^\dagger|k''\rangle\,\delta(E''-E)\,\langle k''|T|k\rangle\end{aligned}$$

This gives the relation, valid for $E_{k'} = E_k$:

$$i\,(\langle k'|T|k\rangle - \langle k'|T^\dagger|k\rangle) = 2\pi\int d^3k''\langle k'|T^\dagger|k''\rangle\delta(E''-E)\langle k''|T|k\rangle \tag{1.28}$$

(Notice that on the r.h.s. one may interchange the role of T and $T^\dagger$:) It is conventional to write:

$$\begin{aligned}\int d^3k''\,\delta(E_{k''}-E) &= \int_0^\infty k''^2\,dk''\int d\Omega''\,\delta(E_{k''}-E) \\ &= \int dE''\left(\frac{mk''}{\hbar^2}\right)\delta(E''-E)\int d\Omega'' = \frac{mk}{\hbar^2}\int d\Omega'' \equiv \rho(E)\int d\Omega''\end{aligned}$$

($d\Omega''$ ≡ element of solid angle)

$\rho(E)$ is the "density of states" per unit energy and solid angle.

Applied to (1.28) for the case $\vec{k}' = \vec{k}$, one has

$$\int d\Omega''\,|\langle\vec{k}''|T|\vec{k}\rangle|^2 = -\frac{\hbar^2}{m\pi k}\,\mathrm{Im}\,(\langle\vec{k}|T|\vec{k}\rangle) \tag{1.29}$$

and using (1.12, 14):

$$\sigma_{tot} = \int d\Omega''\,|f(\vec{k}'', \vec{k})|^2 = -\left(\frac{4\pi^2 m}{\hbar^2}\right)\frac{\hbar^2}{m\pi k}\,\mathrm{Im}\,(\langle k|T|k\rangle)$$

or

$$\sigma_{tot} = \frac{4\pi}{k}\,\mathrm{Im}\,(f(k,k)) \tag{1.30}$$

This is the Bohr-Peierls-Placzeck theorem or optical theorem, relating the total cross-section (which in the present case is purely elastic) to the imaginary part of the forward scattering amplitude.

Of course it is not necessary to go through the S-matrix formalism to derive this result. A more direct way is to start with Eq. (1.20), and to construct T according to (1.14). This gives the "Low-equations":

$$\langle k'|V|k^{(+)}\rangle = \langle k'|T|k\rangle = \langle k'|V|k\rangle + \langle k'|V\frac{1}{E_k - H + i\eta}V|k\rangle$$

By means of the completeness relation (1.21) one may now write:

$$\frac{1}{E_k - H + i\eta} = \int d^3k'' \, |k''^{(+)}\rangle \frac{1}{E_k - E_{k''} + i\eta} \langle k''^{(+)}| + \sum_n |n\rangle \frac{1}{E_k - E_n} \langle r|$$

and get:

$$\langle k'|T|k\rangle = \langle k'|V|k\rangle + \sum_n \langle k'|V|n\rangle \frac{1}{E_k - E_n} \langle n|V|k\rangle$$

$$+ \int d^3k'' \langle k'|T|k''\rangle \frac{1}{E_k - E_{k''} + i\eta} \langle k''|T^\dagger|k\rangle \qquad (1.31)$$

Notice that this is a non-linear equation for T, of a structure familiar mostly in a different context, scattering of π-mesons from static nucleons.

In (1.31) the two first terms on the r.h.s. are hermitian, and extraction of the anti-hermitian part of (1.31) immediately gives the desired unitarity relation.

1.D. Transition rates from time-dependent wave-packets

Scattering is a time-dependent process, and its proper description is done in terms of wave packets, which in the limit $t \to -\infty$ (the "remote past") do not overlap with the scatterer (that is, are outside the range of the potential V), but more towards it. We choose $t \approx 0$ as the time of maximum overlap. We shall show that scattering begins as the packet starts to overlap the scatter; only then does an outgoing scattered wave begin to form.

The previous construction of eigenstates $|k^{(+)}\rangle$ of H is most useful for the purpose of this demonstration: we now construct time-dependent states $|\psi(t)\rangle$ by simple superposition; we shall then be able to recognize that almost all information of interest is contained already in the structure of the time-independent eigenstates $|k^{(+)}\rangle$.

We construct - in the momentum representation - the wave packet

$$\langle k'|\psi^{(+)}_{k_0}(t)\rangle = \int d^3k \, \langle k'|k^{(+)}\rangle \, e^{-\frac{i}{\hbar}E_k t} \, C(k, k_0) \qquad (1.32)$$

which of course satisfies the time-dependent Schrödinger equation

$$i\frac{\partial}{\partial t}\langle k'|\psi^{(+)}_{k_0}(t)\rangle = \int d^3k'' \langle k'|H|k''\rangle \langle k''|\psi^{(+)}_{k_0}(t)\rangle .$$

In (1.32), $C(k, k_0)$ is an amplitude distribution of momenta, centred about a value $\vec{K}_0$, for example

$$C(\vec{k}, \vec{k}_0) = \delta(\vec{k}_\perp) \frac{\gamma/\pi}{(k_\parallel - k_0)^2 + \gamma^2} \qquad (1.33)$$

$k_\parallel$ and $\vec{k}_\perp$ are the components of $\vec{k}$ parallel and perpendicular to $\vec{k}_0$, respectively. $C(\vec{k}, \vec{k}_0)$ therefore produces a one-dimensional packet, with

a finite width in the "forward"-direction, parallel to $\vec{k}_0$, only (see Fig. 1). It is assumed that $\gamma > 0$, and $\gamma \ll k_0$.

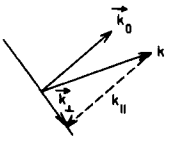

FIG. 1. Decomposition of $\vec{k}$ into $\vec{k}_\perp$ and $\vec{k}_\parallel$

The interpretation of $|\langle k'|\psi^{(+)}(t)\rangle|^2 d^3k'$ is that of the probability for finding the particle within the region d^3k' in momentum space. Hence

$$\frac{d}{dt}\left|\langle k'|\psi^{(+)}_{k_0}(t)\rangle\right|^2 = \frac{d}{dt}\, P(k',\, k_0) \tag{1.34}$$

is the rate of increase of that differential probability, and defines the transition rate of the packet into the momentum state $|k'\rangle$.

Let us calculate this rate. Let us call

$$\mathscr{A}^{(+)}(k',\, k_0;t) \equiv e^{+\frac{i}{\hbar}E_{k'}t}\langle k'|\psi^{(+)}_{k_0}(t)\rangle \tag{1.35}$$

Using Eq. (1.16) for $\langle k'|k^{(+)}\rangle$, one has then

$$\mathscr{A}^{(+)}(k',k_0;t) = C(k',k_0) + \int d^3k''\frac{\langle k'|T|k''\rangle}{E_{k''}-E_{k'}+i\eta}\, C(k'',k_0)\, e^{-\frac{i}{\hbar}(E_{k''}-E_{k'})t}$$

The assumption is now made that the range of values k'' defined by $C(k'', k_0)$ is narrow enough so that one may replace $(k'|T|k'')$ by $(k'|T|k_0)$; this requires the width γ of the distribution $C(k'', k_0)$ to be sufficiently narrow, that is, narrow compared with the width of any resonance in the behaviour of T. (Such resonances will be discussed in the next section.)

We now use $k_\parallel - k_0 \equiv \kappa$, and expand:

$$E_k = E_{k_0} + \hbar\kappa v_0 \qquad v_0 = \hbar k_0/m$$

and also write

$$\frac{1}{E_{k''}-E_{k'}+i\eta} = \frac{1}{i\hbar}\int_{-\infty}^{0} ds\, e^{-\frac{i}{\hbar}(E_{k''}-E_{k'}+i\eta)s}$$

$$\frac{\gamma/\pi}{(k_\parallel - k_0)^2+\gamma^2} = \frac{1}{2\pi}\int_{-\infty}^{+\infty} d\tau'\, e^{i\kappa\tau'-\gamma|\tau'|}$$

$$= \frac{v_0}{2\pi}\int_{-\infty}^{+\infty} d\tau\, e^{i\kappa v_0\tau-\gamma v_0|\tau|}$$

With these preliminaries, one may write

$$\mathscr{A}^{(+)}(k', k_0;t) \cong C(k', k_0) + \langle k'|T|k_0\rangle \frac{v_0}{2\pi i\hbar}\int_{-\infty}^{+\infty} d\tau\, e^{-\gamma v_0|\tau|} \times \int_{-\infty}^{0} ds\, e^{+\frac{\eta}{\hbar}s} e^{-\frac{i}{\hbar}(E_{k_0} - E_{k'})s} \int_{-\infty}^{+\infty} d\kappa\, e^{-iv_0\kappa(s+t-\tau)}$$

The last factor is $(2\pi/v_0)\,\delta(s + t - \tau)$; so, writing σ for $s+t$:

$$\mathscr{A}^{(+)}(k', k_0;t) \cong C(k', k_0) + \langle k'|T|k_0\rangle \frac{e^{-\frac{\eta}{\hbar}t}}{i\hbar}\int_{-\infty}^{t} d\sigma\, e^{-\gamma v_0|\sigma|}\, e^{-\frac{i}{\hbar}(E_0 - E_{k'} + i\eta)\sigma}$$

For $t \leq 0$, integration gives:

$$\mathscr{A}^{(+)}(k', k_0; t) \cong C(k', k_0) + \frac{\langle k'|T|k_0\rangle}{E_0 - E_{k'} + i(\eta + \hbar\gamma v_0)}\, e^{+\gamma v_0 t}\, e^{-\frac{i}{\hbar}(E_0 - E_{k'})t} \qquad (1.36)$$

(η may be neglected compared to $\hbar\gamma v_0$, which is finite) and hence

$$\mathscr{A}^{(+)}(k', k_0; t) \xrightarrow[t \to -\infty]{} C(k', k_0) \qquad (1.36a)$$

In the remote past, $(-t) \gg 1/\gamma v_0$, the wave packet $\langle k'|\psi^{(+)}(t)\rangle$ reduces to the free particle wave packet: $C(k', k_0)e^{-\frac{i}{\hbar}E_{k'}t} = \langle k'|\phi_{k_0}(t)\rangle$.

For $t > 0$, one has

$$\mathscr{A}^{(+)}(k', k_0;t) \cong C(k', k_0) + \langle k'|T|k_0\rangle \left\{\frac{1}{E_{k_0} - E_{k'} + i\hbar\gamma v_0} + \frac{e^{-\frac{i}{\hbar}(E_0 - E_{k'})t} e^{-\gamma v_0 t} - 1}{E_{k_0} - E_{k'} - i\hbar\gamma v_0}\right\}$$

$$= C(k', k_0) + \langle k'|T|k_0\rangle \left\{\frac{-2i\hbar\gamma v_0}{(E_{k_0} - E_{k'})^2 + (\hbar\gamma v_0)^2} + e^{-\gamma v_0 t}\, \frac{e^{-\frac{i}{\hbar}(E_0 - E_{k'})t}}{E_0 - E_{k'} - i\hbar\gamma v_0}\right\} \qquad (1.37)$$

So as $t \to +\infty$, the result is

$$\mathscr{A}^{(+)}(k', k_0; t) \xrightarrow[t \to +\infty]{} C(k', k_0) - \frac{2i\hbar\gamma v_0}{(E_0 - E_{k'})^2 + (\hbar\gamma v_0)^2}\langle k'|T|k_0\rangle$$

which, using again the explicit form for $C(k', k_0)$, may be written as

$$\delta(k'_\perp)\frac{\gamma/\pi}{(k'_\parallel - k_0)^2 + \gamma^2} - \frac{2\pi i m}{\hbar^2 k_0}\langle k'|T|k_0\rangle \frac{\gamma/\pi}{(|k'| - k_0)^2 + \gamma^2} \qquad (1.37a)$$

Notice that the distribution of forward components of momenta in the incident wave packet reappears as a distribution of magnitudes of momenta in the scattered wave packet.

The time of maximum overlap, and hence of maximum rate of change of the wave packet is $t \approx 0$; from (1.36) one has, for every $\vec{k}$ not parallel to $\vec{k}_0$:

$$P(k', k_0; t) \equiv \left|\mathcal{A}^{(+)}(k', k_0; t)\right|^2 = \frac{e^{2\gamma v_0 t}}{(E_0 - E_{k'})^2 + (\hbar\gamma v_0)^2} \left| \langle k' | T | k_0 \rangle \right|^2$$

and therefore

$$\frac{d}{dt} P(k', k_0; t)\Big|_{t=0^-} = \frac{2\pi}{\hbar} \left| \langle k' | T | k_0 \rangle \right|^2 \frac{\hbar\gamma v_0/\pi}{(E_0 - E_{k'})^2 + (\hbar\gamma v_0)^2}$$

$$\to \frac{2\pi}{\hbar} \left| \langle k' | T | k_0 \rangle \right|^2 \delta_\gamma (E_k - E_{k'}) \tag{1.38}$$

The factor on the r.h.s. is in fact a delta function in energy, but of finite, but small, energy width $\Delta E = \hbar\gamma v_0$, reflecting the uncertainty in energy of the incident wave packet.

One may again define the differential transition rate w by

$$\frac{d}{dt} \int d^3k' \, P(k', k_0; t) = \frac{d}{dt} \int d\Omega_{k'} \int dE_{k'} \, \rho(E_{k'}) \, P(k', k_0; t) \equiv \int d\Omega_{k'} \, w(k', k_0)$$

$w(k', k_0)$ is then the transition rate per unit solid angle, and is given by

$$w(k', k_0) = \frac{2\pi}{\hbar} \left| \langle k' | T | k_0 \rangle \right|^2 \rho(E_0) \tag{1.39}$$

From the expression for the differential transition rate, one passes to that of the differential cross-section by dividing through the flux density of the incident wave packet

$$\langle r | \phi(t) \rangle = \int d^3k' \, \langle r | k' \rangle \, e^{-\frac{i}{\hbar} E_{k'} t} \, c(k', k_0)$$

This flux is

$$J(\vec{r}, t) \cong \frac{\hbar k_0}{m} \frac{e^{-\gamma |s - v_0 t|}}{(2\pi)^3} \; ; \; s = \frac{\vec{k}_0}{k_0} \cdot \vec{r}$$

and so the incident flux is $J = v_0/(2\pi)^3$ at $t \approx 0$. This gives, with $\rho(E_0) = mk_0/\hbar^2$:

$$\sigma(k', k_0) = \frac{1}{J} w(k', k_0) = \left(\frac{4\pi^2 m}{\hbar^2}\right)^2 \left| \langle k' | T | k_0 \rangle \right|^2 \tag{1.40}$$

which agrees with (1.13), (1.15).

We terminate this section by a comment on the S-matrix and on the physical meaning of the unitarity condition (1.25).

In (1.32) we had constructed the wave packet $\langle k' | \psi_{k_0}^{(+)}(t) \rangle$ by means of states $\langle k' | k^{(+)} \rangle$, and seen that for $t \to -\infty$, it goes over into a free

particle wave packet

$$\langle k' | \psi^{(+)}_{k_0}(t) \rangle \xrightarrow[t \to -\infty]{} \langle k' | \phi_{k_0}(t) \rangle = e^{-\frac{i}{\hbar} E_{k'} t} C(k', k_0)$$

which simply represents the incident particle.

If, in (1.32), we replace $\langle k' | k^{(+)} \rangle$ by $\langle k' | k^{(-)} \rangle$, we obtain a packet $\langle k' | \psi^{(-)}_{k_0}(t) \rangle$, whose behaviour in the two limits $t \to \pm\infty$ is just the reverse. This is because we now have to use

$$(E_{k''} - E_{k'} - i\eta)^{-1} = \frac{1}{-i\hbar} \int_0^{+\infty} ds\, e^{-\frac{i}{\hbar}(E_{k''} - E_{k'} - i\eta)s}$$

in place of

$$(E_{k''} - E_{k'} + i\eta)^{-1} = \frac{1}{i\hbar} \int_{-\infty}^{0} ds\, e^{-\frac{i}{\hbar}(E_{k''} - E_{k'} + i\eta)s}$$

and this leads to

$$\mathscr{A}^{(-)}(k', k; t) = C(k', k_0) + \frac{\langle k' | T | k_0 \rangle}{E_0 - E_{k'} - i\hbar\gamma v_0} e^{-\gamma v_0 t}\, e^{-\frac{i}{\hbar}(E_0 E_{k'})t} \quad \text{for } t > 0$$

Hence

$$\langle k' | \psi^{(-)}_{k_0}(t) \rangle \xrightarrow[t \to +\infty]{} e^{-\frac{i}{\hbar} E_{k'} t}\, C(k', k_0) = \langle k' | \phi_{k_0}(t) \rangle$$

a free particle wave packet running away from the scattering centre.

Let us now look at the S-matrix. First, consider the scalar product of the two time-dependent wave packets

$$S_{fi} = \langle \psi^{(-)}_{k_f}(t) | \psi^{(+)}_{k_i}(t) \rangle$$

It is easily seen that this scalar product is exactly time-independent (since both $\psi^{(+)}$ and $\psi^{(-)}$ satisfy the same time-dependent Schrödinger equation). To interpret S_{fi} physically, we may use the limit $t \to +\infty$, in which case it becomes

$$S_{fi} = \langle \phi_{kf}(\infty) | \psi^{(+)}_{ki}(\infty) \rangle$$

One sees that S_{fi} essentially samples, by means of the momentum "probe" ϕ_{kf}, the momentum distribution of the packet $\psi^{(+)}_{k_i}(\infty)$. The unitarity condition (1.25) then is just a conservation equation, expressing the fact that the sum of probabilities of finding a momentum k_f in $\psi^{(+)}_{k_i}(\infty)$ must add up to 1 (or to whatever $\psi^{(+)}$ is normalized to).

But the time-independence of S_{fi} is crucial in the following way. We may evaluate S_{fi} also at $t = 0$, which is the time of maximum overlap of the two packets, and what determines the value of S_{fi} is the way the packets are affected by the potential V (see Eqs. (1.14) and (1.27)). It can then not matter very much just how far the packets spread in space, and we may replace them by their limiting case of infinite spread, namely the state amplitudes $\langle \vec{r} | k_i^{(+)} \rangle$ and $\langle k_f^{(-)} | \vec{r} \rangle$, in which case $S_{fi} \to \langle k_f | S | k_i \rangle$.

Notice that this second part of the argument could not be made, had we used the apparently natural definition

$$S'_{fi}(t) = \langle \phi_{k_f}(t) | \psi^{(+)}_{k_i}(t) \rangle$$

Indeed $S'_{fi}(\infty) = S_{fi}(\infty)$ but S'_{fi} is not time-independent, and $\langle \phi_{ki}(0) | \psi^{(+)}_{ki}(0) \rangle$ does not give the scattering amplitude.

1.E. Diagonalization of S-matrix; Phase shifts

In this section, the spherical harmonics $Y_{\ell m}$ are used extensively. We use the standard Condon-Shortley phase convention. The $Y_{\ell m}$ are functions of a point on the unit sphere, which may be fixed by either the two polar angles θ, φ, or by the associated unit vector. Wherever a direction is fixed by some vector, say $\vec{r}$ or $\vec{k}$, we shall write

On the energy shell, T_ℓ depends on one variable only:

$$T_\ell(k';k)\big|_{E_{k'}=E_k} \equiv T_\ell(k)$$

Using the expression (1.27) for S, together with (1.43) and (1.45) one has

$$\langle \vec{k}' | S | \vec{k} \rangle = \frac{\hbar^2}{mk} \delta(E_{k'} - E_k) \sum_{\ell m} Y_{\ell m}(\hat{k}') \left(1 - \frac{2\pi i m k}{\hbar^2} T_\ell(k)\right) Y^*_{\ell m}(\hat{k})$$

This must be of the form (1.44); hence

$$e^{2i\delta_\ell} = 1 - \frac{2\pi i m k}{\hbar^2} T_\ell(k)$$

or

$$\frac{m\pi k}{\hbar^2} T_\ell(k) = -e^{i\delta_\ell} \sin\delta_\ell \qquad (1.46)$$

Compare this with the expression (1.15) for the scattering amplitude $f(\vec{k}',\vec{k})$:

$$f(\vec{k}',\vec{k}) = -\frac{4\pi^2 m}{\hbar^2} \langle \vec{k}' | T | \vec{k} \rangle$$

$$= -\frac{4\pi^2 m}{\hbar^2} \sum_\ell \frac{2\ell+1}{4\pi} T_\ell(k) P_\ell(\hat{k}' \cdot \hat{k})$$

So (1.46) gives

$$f(\vec{k}',\vec{k}) = \frac{1}{k} \sum_\ell (2\ell+1) e^{i\delta_\ell} \sin\delta_\ell P_\ell(\hat{k}' \cdot \hat{k}) \qquad (1.47)$$

So if partial wave scattering amplitudes $f_\ell(k)$ are defined by

$$f(\vec{k}',\vec{k}) = \sum_\ell Y_{\ell m}(\hat{k}') f_\ell(k) Y^*_{\ell m}(\hat{k}) \qquad (1.48)$$

they have the form

$$f_\ell(k) = \frac{4\pi}{k} e^{i\delta_\ell} \sin\delta_\ell \tag{1.49}$$

From (1.48) it is seen that they satisfy separately the partial wave "optical theorem":

$$|f_\ell|(k)|^2 = \frac{4\pi}{k} \mathrm{Im}\,(f_\ell(k)) \tag{1.50}$$

Combining (1.49) with (1.48), the relation (1.30) is recovered:

$$\hat{r} \equiv \frac{\vec{r}}{r} \quad \text{or} \quad \hat{k} \equiv \frac{\vec{k}}{k}$$

for the corresponding unit vector, and also use the notation

$$Y_{\ell m}(\hat{r}) \text{ or } Y_{\ell m}(\hat{k})$$

Direction $\hat{k}$ and magnitude k specify the vector $\vec{k}$. The simplest unitary matrix is the unit matrix:

$$\langle \vec{k}' | 1 | \vec{k} \rangle = \langle \vec{k}' | \vec{k} \rangle = \delta(\vec{k}' - \vec{k}) \tag{1.41}$$

The completeness of the spherical harmonics makes it possible to write this matrix in polar co-ordinates, that is, in terms of the magnitudes k, k' and the direction $\hat{k}$, $\hat{k}'$:

$$\langle \vec{k}' | 1 | \vec{k} \rangle = \sum_{\ell m} Y_{\ell m}(\hat{k}') Y^*_{\ell m}(\hat{k}) \frac{\delta(k' - k)}{k' k} \tag{1.42}$$

The argument of the delta function can be scaled according to $\delta(x) = f'(x)\delta(f(x))$; by means of this we replace k by $E_k = \hbar^2 k^2/2m$:

$$\langle \vec{k}' | 1 | \vec{k} \rangle = \frac{\hbar^2}{mk} \sum_{\ell m} Y_{\ell m}(\hat{k}') Y^*_{\ell m}(\hat{k}) \delta(E_{k'} - E_k) \tag{1.43}$$

The unitarity of the r.h.s. of (1.43) is assured by the ortho-normality properties of the $Y_{\ell m}$:

$$\int d\Omega_k \; Y^*_{\ell m}(\hat{k}) Y_{\ell' m'}(\hat{k}) = \delta_{\ell\ell'}\delta_{mm'}$$

It is therefore easily seen that the unitarity of this expression is unaffected by the insertion of phase factors $\exp 2i\delta_{\ell m}$; that is:

$$\langle \vec{k}' | U | \vec{k} \rangle = \frac{\hbar^2}{mk} \delta(E_{k'} - E_k) \sum_{\ell m} Y_{\ell m}(\hat{k}') e^{2i\delta_\ell} Y^*_{\ell m}(\hat{k}) \tag{1.44}$$

is still a unitary mattix. If we require U to be a scalar function of $\vec{k}$ and $\vec{k}'$ and diagonal in energy, then (1.44) is in fact the most general unitary matrix.

In the case of scattering of a spinless particle by a central (that is, scalar) potential, the S-matrix is a scalar, unitary matrix and is necessarily of the form (1.44). The T-matrix too is a scalar, and we expand it as follows:

$$\langle \vec{k}' | T | \vec{k} \rangle = \sum_{\ell} \frac{2\ell+1}{4\pi} T_{\ell}(k'; k) P_{\ell}(\hat{k}' \cdot \hat{k})$$

$$= \sum_{\ell m} Y_{\ell m}(\hat{k}') T_{\ell}(k'; k) Y^{*}_{\ell m}(\hat{k}) \qquad (1.45)$$

$$\langle s'\vec{k}' | f | s\vec{k} \rangle = -\frac{4\pi^2 m}{\hbar^2} \langle s'\vec{k}' | T | s\vec{k} \rangle$$

$$= -\frac{4\pi^2 m}{\hbar^2} \sum_{\ell} \frac{2\ell+1}{4\pi} \sum_{j} T_{\ell j}(k) \langle s' | P_{\ell j} | s \rangle P_{\ell}(\hat{k}' \cdot \hat{k})$$

$$= \frac{1}{k} \sum_{\ell} \left\{ (\ell+1) e^{i\delta_{\ell^+}} \sin\delta_{\ell^+} + \ell\, e^{i\delta_{\ell^-}} \sin\delta_{\ell^-} \right\} \delta_{s's} P_{\ell}(\hat{k}' \cdot k)$$

$$+ \frac{1}{k} \sum_{\ell} \left\{ e^{i\delta_{\ell^+}} \sin\delta_{\ell^+} - e^{i\delta_{\ell^-}} \sin\delta_{\ell^-} \right\} (s' | \vec{\sigma} | s) \cdot \vec{L}\, P_{\ell}(\hat{k}' \cdot \hat{k}). \qquad (1.54)$$

These steps are given here in some detail as they are representative of further generalizations, like iso-spin dependence of the interaction, etc.

We terminate this section by looking at the radial wave functions, for the spinless case.

There is a well known decomposition of the plane wave

$$\langle \vec{r} | \vec{k} \rangle = \frac{e^{i\vec{k}\cdot\vec{r}}}{(2\pi)^{\frac{3}{2}}} = \frac{1}{(2\pi)^{\frac{3}{2}}} \sum_{\ell} (2\ell+1)\, i^{\ell} j_{\ell}(kr) P_{\ell}(\hat{k} \cdot \hat{r})$$

$$= \frac{4\pi}{(2\pi)^{\frac{3}{2}}} \sum_{\ell} i^{\ell} j_{\ell}(kr) \sum_{m} Y_{\ell m}(\hat{r}) Y^{*}_{\ell m}(\hat{k}) \qquad (1.55)$$

($j_{\ell}(kr)$ being the spherical Bessel functions)

By analogy to this, we write:

$$\langle \vec{r} | k^{(+)} \rangle = \frac{4\pi}{(2\pi)^{\frac{3}{2}}} \sum_{\ell} i^{\ell} u_{\ell k}(r) \sum_{m} Y_{\ell m}(\hat{r}) Y^{*}_{\ell m}(\hat{k})$$

Using the definition (1.14) of $\langle k' | T | k \rangle$ and (1.45) of $T_{\ell}(k)$, one has at once

$$T_{\ell}(k) = \frac{2}{\pi} \int_{0}^{\infty} r^2 dr\, j_{\ell}(kr) V(r) u_{\ell k}(r) \qquad (1.56)$$

$u_{\ell k}(r)$ satisfied the radial Schrödinger equation

$$\frac{-\hbar^2}{2m}\left(r\frac{d^2}{dr^2}r - \frac{\ell(\ell+1)}{r^2}\right)u_{\ell k}(r) + V(r)\,u_{\ell k}(r) = E_k\,u_{\ell k}(r)$$

and is subject to the boundary conditions

$$u_{\ell k}(r) \xrightarrow[r\to\infty]{} \frac{e^{i\delta_\ell}}{kr}\sin\left(kr - \frac{\ell\pi}{2} + \delta_\ell\right)$$

$$r\,u_{\ell k}(r) \xrightarrow[r\to\infty]{} 0$$

Using the relation (1.46) between T_ℓ and the phase-shifts, and defining a real radial function $\bar{u}(r)$ by

$$\sigma_{tot} = \int d\Omega' \left|f(\vec{k}', \vec{k})\right|^2 = \sum_\ell \frac{2\ell+1}{4\pi}\left|f_\ell(k)\right|^2$$

$$= \frac{4\pi}{k}\sum\frac{2\ell+1}{4\pi}\,\mathrm{Im}\,(f_\ell(k)) = \frac{4\pi}{k}\,\mathrm{Im}\,(f(\vec{k}, \vec{k}))$$

We may at this point briefly indicate how this generalizes to the case of a particle with spin, incident on a scalar, but possibly spin-dependent potential. Let $s = \pm\frac{1}{2}$ label the spin-variable. The unit matrix is then

$$\langle \vec{k}'\,s' \left| 1 \right| \vec{k}s \rangle = \delta(\vec{k}' - \vec{k})\,\delta_{s's}$$

$$= \frac{\hbar^2}{mk}\,\delta(E_{k'} - E_k)\,\delta_{s's}\sum_{\ell m} Y_{\ell m}(\hat{k}')\,Y^*_{\ell m}(\hat{k}) \qquad (1.51)$$

$\delta_{s's}$ may now be written, for each value of ℓ, as the sum of the two projection operators on the values $j = \ell \pm \frac{1}{2}$ of the total angular momentum:

$$\delta_{s's} = \sum_{j=\ell\pm\frac{1}{2}} \langle s' \left| P_{\ell j} \right| s \rangle$$

$$P_{\ell,\ell+\frac{1}{2}} = \frac{\ell + 1 + \vec{\sigma}\cdot\vec{L}}{2\ell+1}, \qquad P_{\ell,\ell-\frac{1}{2}} = \frac{\ell - \vec{\sigma}\cdot\vec{L}}{2\ell+1}$$

where

$$\vec{L} = \frac{1}{i}(\vec{k}' \times \vec{\nabla}_{k'})$$

A scalar unitary matrix, generalizing (1.44), is then

$$\langle \vec{k}'s' \left| U \right| \vec{k}s \rangle = \frac{\hbar^2}{mk}\,\delta(E_{k'} - E_k)\sum_{\ell m}\sum_j \langle s' \left| P_{\ell j} \right| s \rangle\, Y_{\ell m}(\hat{k}')\, e^{2i\delta_{\ell j}}\, Y^*_{\ell m}(\hat{k}) \qquad (1.52)$$

The S-matrix, for a scalar, spin-dependent potential, is a scalar, that is, commutes with $\vec{J} = \vec{L}+\vec{S}$, and is of the form (1.52). The T-matrix is a scalar, and may be written as

$$\langle \vec{k}'s' | T | \vec{k}s \rangle = \sum_{\ell m} \sum_{j} \langle s' | P_{\ell j} | s \rangle Y_{\ell m}(\hat{k}') \, T_{\ell j}(k';k) \, Y^{*}_{\ell m}(\hat{k}) \tag{1.53}$$

This gives at once, in analogy to (1.46):

$$-\frac{m\pi k}{\hbar^2} T_{\ell j}(k) = e^{i\delta_{\ell j}} \sin \delta_{\ell j}$$

The scattering amplitude is

$$u_{\ell k}(r) = \frac{e^{i\delta_\ell}}{kr} \bar{u}_{\ell k}(r)$$

$$\bar{u}_{\ell k}(r) \xrightarrow[r\to\infty]{} \sin(kr - \ell\pi/2 + \delta_\ell)$$

$$\bar{u}_{\ell k}(r) \xrightarrow[r\to 0]{} 0$$

one has

$$\sin \delta_\ell (k) = \int_0^\infty r dr \, j_\ell (kr) \left(\frac{-2m}{\hbar^2} V(r) \right) \bar{u}_{\ell k}(r) \tag{1.57}$$

1.F. Scattering by the sum of two potentials

It is a common situation to have two potentials acting simultaneously on one particle. Thus, in proton-proton scattering, the Coulomb is superposed to the nuclear interaction. Often one of the interactions may be treated as a perturbation; it is of interest however, to have exact expressions for the transition amplitude first.

The total potential energy is $V = V_1 + V_2$.

In many situations, as in nucleon nuclear scattering, we may be interested in the scattering amplitude due to say V_1 alone; we may also want to see what scattering is produced by V_2 in the presence of V_1. For instance, we may want to separate the effects of nuclear and Coulomb forces in nucleon scattering.

To this effect we introduce, in addition to $H_0 = p^2/2m$ and $H = H_0 + (V_1 + V_2)$, the intermediate Hamiltonian $H_1 = H_0 + V_1$.

Let $|k^{(+)}\rangle$ stand for the outgoing wave scattering states of H_1, and write $|k^{(+)}\rangle\!\rangle$ for the o.w. scattering states of H.

In analogy with (1.18) and (1.20), we have:

$$|k^{(+)}\rangle = |k\rangle + \frac{1}{E_k - H_0 + i\eta} V_1 |k^{(+)}\rangle \tag{1.58a}$$

$$= |k\rangle + \frac{1}{E_k - H_1 + i\eta} V_1 |k\rangle \tag{1.58b}$$

and

$$|k^{(+)}\rangle\!\rangle = |k\rangle + \frac{1}{E_k - H_0 + i\eta} (V_1 + V_2) |k^{(+)}\rangle\!\rangle \tag{1.59a}$$

(1.59) may be rewritten - using (1.58b) - as

$$|k^{(+)}\rangle\!\rangle = |k^{(+)}\rangle - \frac{1}{E_k - H_1 + i\eta} V_1 |k\rangle + \frac{1}{E_k - H_0 + i\eta} (V_1 + V_2) |k^{(+)}\rangle\!\rangle$$

and by using the identity

$$\frac{1}{E - H_0 + i\eta} = \frac{1}{E - H_1 + i\eta} - \frac{1}{E - H_1 + i\eta} V_1 \frac{1}{E - H_0 + i\eta}$$

$$|k^{(+)}\rangle\!\rangle = |k^{(+)}\rangle - \frac{1}{E - H_1 + i\eta} V_1 \left\{ |k\rangle + \frac{1}{E - H_0 + i\eta} (V_1 + V_2) |k^{(+)}\rangle\!\rangle \right\}$$

$$+ \frac{1}{E - H_1 + i\eta} (V_1 + V_2) |k^{(+)}\rangle\!\rangle$$

which - by using (1.59) again - reduces to

$$|k^{(+)}\rangle\!\rangle = |k^{(+)}\rangle + \frac{1}{E_k - H_1 + i\eta} V_2 |k^{(+)}\rangle\!\rangle \qquad (1.59b)$$

Yet another version of this is obtained by applying to (1.59b) the identity

$$\frac{1}{E - H_1 + i\eta} = \frac{1}{E - H + i\eta} - \frac{1}{E - H + i\eta} V_2 \frac{1}{E - H_1 + i\eta} :$$

$$|k^{(+)}\rangle\!\rangle = |k^{(+)}\rangle + \frac{1}{E_k - H + i\eta} V_2 \left\{ |k^{(+)}\rangle\!\rangle - \frac{1}{E - H_1 + i\eta} V_2 |k^{(+)}\rangle\!\rangle \right\}$$

or (using 1.59b again):

$$|k^{(+)}\rangle\!\rangle = |k^{(+)}\rangle + \frac{1}{E - H + i\eta} V_2 |k^{(+)}\rangle \qquad (1.59c)$$

We are now in a position to write the T-matrix, according to (1.14), this is

$$\langle k' | T | k \rangle = \langle k' | (V_1 + V_2) | k^{(+)}\rangle\!\rangle$$

Using (1.59b), one has

$$\langle k' | T | k \rangle = \langle k' | V_1 | k^{(+)}\rangle + \left(\langle k' | V_1 \frac{1}{E_k - H_1 + i\eta} + \langle k' | \right) V_2 | k^{(+)}\rangle\!\rangle$$

On the energy shell - $E_{k'} = E_k$ - the vector in brackets is

$$\langle k' | V_1 \frac{1}{E_{k'} - H_1 + i\eta} + \langle k' | = \langle k'^{(-)} |$$

according to (1.58b). So one has

$$\langle k' | T | k \rangle \Big|_{E_{k'} = E_k} = \langle k' | V_1 | k^{(+)}\rangle + \langle k'^{(-)} | V_2 | k^{(+)}\rangle\!\rangle \qquad (1.60)$$

The first term in this expression is just $\langle k' | T_1 | k \rangle$, the T-matrix due to V_1 acting alone. The contribution of V_2 to T is then expressed by means of states "distorted by the presence of V_1".

2. COLLISIONS OF A PARTICLE WITH A COMPOSITE SYSTEM

In this section we shall discuss, again by using the simplest possible model, the case of collisions of a particle with a composite system, that is, with a target endowed with internal degrees of freedom. As a result of collision, the target can be lifted into excited discrete quantum states, or "ionized". The simplest non-trivial system having these features is as follows.

Consider a particle "a", of mass m_a, subject to a potential $U_a(r_a)$. We assume that U_a may bind the particle a into several bound states $|n\rangle$. We call this bound system the system A. Of course there will also be continuum states $|k^{(+)}\rangle$ in U_a, as investigated in section 1.

In addition the model has a particle "b", of mass m_b, being free except for an interaction $V_{ab}(\vec{r}_a - \vec{r}_b)$ with particle a. This interaction is capable of producing just one bound state of the two particles, the system (ab) (a "deuteron").

This model describes the following processes:

(1)	$b + A \rightarrow b' + A'$:	Elastic and inelastic scattering of b by the system A
(2)	$b + A \rightarrow b' + a'$:	Ionization of the target system
(3)	$b + A \rightarrow (ab)$:	Pick-up reaction, forming a "deuteron"
(4)	$(ab) \rightarrow (ab)'$:	Scattering of a "deuteron"
(5)	$(ab \rightarrow A' + b'$:	Stripping reaction
(6)	$(ab) \rightarrow a' + b'$:	Break-up reaction

The Hamiltonian of the system is

$$H = \frac{p_a^2}{2m_a} + U_a(r_a) + \frac{p_b^2}{2m_b} + V_{ab}(r_a - r_b) \tag{2.1}$$

It is useful to consider the following Hamiltonians of subsystems:

$$H_a = \frac{p_a^2}{2m_a} \quad \text{with eigenfunctions } \langle r_a | k_a \rangle \tag{2.2}$$

$$H_A = \frac{p_a^2}{2m_a} + U_a(r_a) \text{ with eigenfunctions } \begin{cases} \langle r_a | n \rangle & : \text{bound} \\ \langle r_a | k_a^{(+)} \rangle & : \text{contin.} \end{cases} \tag{2.3}$$

$$H_b = \frac{p_b^2}{2m_b} \quad \text{with eigenfunctions } \langle r_b | k_b \rangle$$

$$H_{(ab)} = \frac{p_a^2}{2m_a} + \frac{p_b^2}{2m_b} + V_{ab}(r_a - r_b)$$

$$= \frac{P^2}{2M} + \frac{p^2}{2m} + V_{ab}(r) \tag{2.4}$$

where

$$P = p_a + p_b, \quad p = (m_b p_a - m_a p_b)/(m_a + m_b)$$

$$R = (m_a r_a + m_b r_b)/(m_a + m_b), \quad r = r_a - r_b$$

$$M = m_a + m_b, \quad m = m_a m_b/(m_a + M_b)$$

$H_{(ab)}$ has eigenfunctions $\langle \vec{r}_a \vec{r}_b | B \vec{K} \rangle = \langle \vec{r} | B \rangle \langle \vec{R} | \vec{K} \rangle$, the bound "deuteron" being represented by $\langle \vec{r} | B \rangle$,

and

$$\langle \vec{k} | \vec{K} \rangle = (2\pi)^{-\frac{3}{2}} e^{iK \cdot R} \tag{2.4a}$$

It has also continuum states $\langle \vec{r}_a \vec{r}_b | \vec{\kappa}^{(+)} \vec{K} \rangle = \langle \vec{r} | \vec{\kappa}^{(+)} \rangle \langle \vec{R} | \vec{K} \rangle$, where $\langle \vec{r} | \vec{\kappa}^{(+)} \rangle$ is an outgoing wave solution for the Hamiltonian

$$p^2/2m + V_{ab}(r) \tag{2.5}$$

We shall now consider one by one some of the possible processes (1) - (6) and investigate their salient features.

2.A. Elastic and inelastic scattering; resonances and Breit-Wigner formula

Here we consider the process $b + A \to b' + A'$; accordingly, we write

$$H = H_A + H_b + V_{ab} \tag{2.6}$$

Choose a representation in which H_A and H_b are diagonal:

$$H_A | n \rangle = E_n | n \rangle$$

$$H_b | k \rangle = \epsilon_k | k \rangle$$

$$\langle n'k' | H | nk \rangle = (E_n + \epsilon_k) \delta_{n'n} \delta(k' - k) + \langle n'k' | V_{ab} | nk \rangle \tag{2.7}$$

where

$$\langle n'k' | V_{ab} | nk \rangle = \int d^3 r_a \int d^3 r_b \langle n'k' | r_a r_b \rangle V_{ab}(r_a - r_b) \langle r_n r_b) nk \rangle$$

Eq. (2.7) is actually a submatrix only of the Hamiltonian, since H_A has also continuum states $| k_a^{(+)} \rangle$, and there are non-vanishing matrix elements $\langle k'^{(+)}_a k'_b | V_{ab} | n k_b \rangle$. We shall not include these explicitly, but in what follows, every $\sum_n$ should be supplemented by an $\int d^3 k'_a$.

In this nk representation, a scattering state $|nk^{(+)}\rangle\!\rangle$ has an amplitude $\langle n'k'|nk^{(+)}\rangle\!\rangle$ satisfying the equation:

$$\langle n'k'|nk^{(+)}\rangle\!\rangle = \delta_{n'n}\,\delta(k'-k) + \frac{1}{E_{nk} - E_{n'k'} + i\eta} \int d^3k'' \sum_{n''} \langle n'k'|V_{ab}|n''k''\rangle \langle n''k''|nk^{(+)}\rangle\!\rangle \tag{2.8}$$

($E_{nk} = E_n + \epsilon_k$). In abstract vector notation, this is again

$$|nk^{(+)}\rangle\!\rangle = |nk\rangle + \frac{1}{E_{nk} - (H_a + H_b) + i\eta} V_{ab}\,|nk^{(+)}\rangle\!\rangle \tag{2.8a}$$

It is transparent that all the previous results about S- and T-matrices apply directly. The T-matrix is

$$\langle n'k'|T|nk\rangle = \langle n'k'|V_{ab}\,|nk^{(+)}\rangle\!\rangle \tag{2.9}$$

and satisfies the equation

$$\langle n'k'|T|nk\rangle = \langle n'k'|V_{ab}\,|nk\rangle + \int d^3k'' \sum_{n''} \langle n'k'|V_{ab}|n''k''\rangle \frac{\langle n''k''|T|nk\rangle}{E_{nk} - E_{n''k''} + i\eta} \tag{2.10}$$

Inelastic collision may take place wherever $\epsilon_k + (E_n + (E_{n'}) > 0$. They enter into the unitarity relation for T, generalized from (1.28, 29). The scattering amplitude f is again given by

$$\langle n'\vec{k}'|f|n\vec{k}\rangle = -\frac{4\pi^2 m_b}{\hbar^2} \langle n'k'|T|nk\rangle$$

and (1.30) is generalized to

$$\sigma_{tot} = \sum_{n''} \int d\Omega_{k''} \left(\frac{k''}{k}\right) |\langle n''k''|f|nk\rangle|^2 \Big|_{E_{n''k''} = E_{nk}} = \frac{4\pi}{k}\,\mathrm{Im}\left(\langle n\vec{k}|f|n\vec{k}\rangle\right) \tag{2.11}$$

Notice that the factor (k''/k) in (2.11) arises from a consideration of the fluxes associated with incoming and scattered particles, respectively. In a derivation based on a generalized equation (1.28), k'' arises from the "density of states" factor $\rho(E) = m_b k''/\hbar^2$, and $1/k$ from the current density $\hbar k/(2\pi)^3 m_b$.

We consider now in more detail collision below the inelastic threshold, assuming system A to be in its ground state, $n = 0$. So we have $E_k < (E_1 - E_0)$. It is useful to decompose the matrix $\langle n'k'|H|nk\rangle$ as follows

$$\left(\begin{array}{c|c} \langle 0k'|H|0k\rangle & \langle 0k'|V_{ab}|nk\rangle \\ \hline \langle n'k'|V_{ab}|0k\rangle & \langle n'k'|H|nk\rangle \end{array}\right) \quad \text{or, in short} \quad \left(\begin{array}{c|c} H^P & V^{PQ} \\ \hline V^{QP} & H^Q \end{array}\right) \tag{2.12}$$

where $n, n' > 0$ is understood.

H^P is the matrix:

$$\langle 0k' | H | 0k \rangle = (E_0 + \epsilon_k)\,\delta(k'-k) + \langle 0k' | V_{ab} | 0k \rangle$$

that is

$$H^P = H_0^P + V^P \tag{2.13a}$$

Similarly, H^Q is the matrix

$$\langle n'k' | H | nk \rangle |_{n',n>0} = (E_n + \epsilon_{k'})\,\delta_{n'n}\,\delta(k'-k) + \langle n'k' | V_{ab} | nk \rangle$$

that is

$$H^Q = H_0^Q + V^Q \tag{2.13b}$$

Let us look at the energy spectra of these various Hamiltonians (Fig. 2).

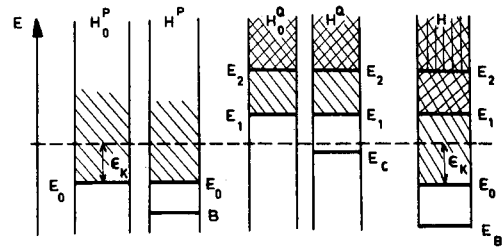

FIG. 2. Energy spectra of some Hamiltonians

The spectra of H^P and H^Q differ from those of H_0^P and H_0^Q by the possible addition of a bound state, in which particle b is bound to the target. Notice that E_c is a discrete state of H^Q, embedded in the continuum of states of H. As we shall see, it is the existence of such levels that gives rise to scattering resonances.

We now establish the following notation:

$|nk\rangle$ are eigenstates of H_0 $(=H_A + H_0)$

The eigenstates of H^P will be written as $|B\rangle$ and $|0, k^{(+)}\rangle \equiv |k^{(+)}\rangle$
those of H^Q as $|c\rangle$ and $|n, k^{(+)}\rangle$,
those of H as $|n, k^{(+)}\rangle\!\rangle$. Actually we are only interested in
$|0, k^{(+)}\rangle\!\rangle \equiv |k^{(+)}\rangle\!\rangle$.

We now write the Schrödinger equation;

$$H|k^{(+)}\rangle\!\rangle = E_k |k^{(+)}\rangle\!\rangle$$

in a representation, in which H^P and H^Q are diagonal. This gives coupled equations for the amplitudes $\langle B|k^{(+)}\rangle\!\rangle$, $\langle k'^{(+)}|k^{(+)}\rangle\!\rangle\langle c|k^{(+)}\rangle\!\rangle$ and $\langle n'k'^{(+)}|k^{(+)}\rangle\!\rangle$.

As we want to study the effect of the level E_c in a case when E_k is near $E_c - E_0$, we omit the components $\langle B|k^{(+)}\rangle\!\rangle$ and $\langle n'k'^{(+)}|k^{(+)}\rangle\!\rangle$ $(n' > 0)$

from the equation; their effect will be small provided the energy difference $(E_0 + E_k) - E_B$ and $E_1 - (E_0 + E_k)$ are sufficiently large (we must therefore not be near inelastic threshold).

This truncated Schrödinger equation now reads (we have chosen $E_0 = 0$ as the zero of energy):

$$(\epsilon_{k'} - \epsilon_k) \langle k'^{(+)} | k^{(+)} \gg + \langle k'^{(+)} | V^{PQ} | c \rangle \langle c | k^{(+)} \gg = 0 \tag{2.14a}$$

$$(E_c - \epsilon_k) \langle c | k^{(+)} \gg + \int d^3k'' \langle c | V^{QP} | k''^{(+)} \rangle \langle k''^{(+)} | k^{(+)} \gg = 0 \tag{2.14b}$$

The boundary condition on $|k^{(+)}\gg$ is incorporated by writing (2.14a) as

$$\langle k'^{(+)} | k^{(+)} \gg = \delta(\vec{k}' - \vec{k}) + \frac{1}{\epsilon_k - \epsilon_{k'} + i\eta} \langle k'^{(+)} | V^{PQ} | c \rangle \langle c | k^{(+)} \gg \tag{2.15}$$

Inserting this into (2.14b), one has:

$$(E_c - \epsilon_k + F_k) \langle c | k^{(+)} \gg + \langle c | V^{QP} | k^{(+)} \rangle = 0 \tag{2.16}$$

where

$$F_k = \int d^3k'' \frac{|\langle c | V^{QP} | k''^{(+)} \rangle|^2}{\epsilon_k - \epsilon_{k''} + i\eta} = A_k - \frac{i}{2} \Gamma_k \tag{2.17}$$

Δ_k and Γ_k are real, and Γ_k is positive

$$\Gamma_k = 2\pi \int d^3k'' \, \delta(\epsilon_k - \epsilon_{k''}) |\langle c | V^{QP} | k''^{(+)} \rangle|^2 \tag{2.18}$$

Equation (16) gives

$$\langle c | k^{(+)} \gg = \frac{\langle c | V^{QP} | k^{(+)} \rangle}{\epsilon_k - E_c - F_k} \tag{2.19}$$

We have now all the pieces to write the expression for the T-matrix (for elastic scattering, remember):

$$\langle k' | T | k \rangle = \langle 0\, k' | V_{ab} | k^{(+)} \gg = \langle 0\, k' | V^P + V^{PQ} | k^{(+)} \gg$$

$$= \int d^3k'' \langle 0\, k' | V^P | k''^{(+)} \rangle \langle k''^{(+)} | k^{(+)} \gg + \langle 0\, k' | V^{PQ} | c \rangle \langle c | k^{(+)} \gg$$

Using (15) and (19), this gives:

$$\langle k' | T | k \rangle = \langle 0\, k' | V^P | k^{(+)} \rangle$$

$$+ \left\{ \int d^3k'' \langle 0\, k' | V^P | k''^{(+)} \rangle \frac{\langle k''^{(+)} | V^{PQ} | c \rangle}{E_k - E_{k''} + i\eta} + \langle 0\, k' | V^{PQ} | c \rangle \right\} \langle c | k^{(+)} \gg \tag{2.20}$$

We now specify T to be on the energy shell, $E_{k'} = E_k$; in addition we use the fact that

$$\int d^3k'' \; F\,(\epsilon_{k''}) \left|k''^{(+)}\right\rangle \left\langle k''^{(+)}\right| = \int d^3k'' \; F\,(\epsilon_{k''}) \left|k''^{(-)}\right\rangle \left\langle k''^{(-)}\right|$$

to write the bracket in (20) as

$$-\int d^3k'' \left\{ \frac{\left\langle 0\,k' \middle| V^P \middle| k''^{(-)} \right\rangle}{\epsilon_{k''} - \epsilon_{k'} - i\eta} - \left\langle 0\,k' \middle| k''^{(-)} \right\rangle \right\} \left\langle k''^{(-)} \middle| V^{PQ} \middle| c \right\rangle$$

$$= \int d^3k'' \; \delta\,(k' - k'') \left\langle k''^{(-)} \middle| V^{PQ} \middle| c \right\rangle = \left\langle k'^{(-)} \middle| V^{PQ} \middle| c \right\rangle$$

This gives the final form for T:

$$\left\langle k' \middle| T \middle| k \right\rangle = \left\langle 0\,k' \middle| V^P \middle| k^{(+)} \right\rangle + \frac{\left\langle k'^{(-)} \middle| V^{PQ} \middle| c \right\rangle \left\langle c \middle| V^{QP} \middle| k^{(+)} \right\rangle}{\epsilon_k - E_c - \Delta_k + \frac{i}{2}\Gamma_k} \tag{2.21}$$

$\left\langle\!\left\langle k' \middle| V^P \middle| k^{(+)} \right\rangle\!\right\rangle$ is the transition amplitude due to V^P alone; it represents the approximation where the target is "frozen" in the quantum state n = 0. The second term represents the effect of the coupling of the continuum state $\left|k^{(+)}\right\rangle$ to the state $\left|c\right\rangle$ of the compound system.

Expression (21) satisfies the unitarity condition, since all the approximations made left us still with a hermitian sub-Hamiltonian.

It is useful to apply an angular momentum consideration to (2.21). If we assume that both $U_a(r_a)$ and $V_{ab}(r_a - r_b)$ are central potentials, angular momentum is conserved. Assume, for definiteness, that the state n = 0 of H_A has zero angular momentum, and that the compound state $\left|c\right\rangle$ has angular momentum L. $\left\langle 0k' \middle| V^P \middle| 0\,k^{(+)} \right\rangle$ is then the T-matrix in the central potential $\left\langle 0\,k' \middle| V^P \middle| 0\,k \right\rangle$, and gives rise to a partial wave scattering amplitude

$$f_L\,(k) = \frac{4\pi}{k}\, e^{i\delta_L} \sin\delta_L$$

In the second term of (2.21), the matrix-element

$$\left\langle c \middle| V^{QP} \middle| k^{(\pm)} \right\rangle$$

has the form

$$\left\langle c_{LM} \middle| V^{QP} \middle| k^{(\pm)} \right\rangle = Y^*_{LM}\,(\hat{k})\, e^{+i\delta_L}\; \gamma_{kL} \tag{2.22}$$

γ_{kL} being real. It follows that Γ_k (2.18) has the value

$$\Gamma_k = 2\pi\, \rho(\epsilon_k)\, \gamma^2_{kL} \qquad \rho\,(\epsilon_k) = \frac{mk}{\hbar^2}$$

and that

$$\sum_M \langle k'^{(-)} | V^{PQ} | c_{LM} \rangle \langle c_{LM} | V^{QP} | k^{(+)} \rangle = \sum_M Y_{LM}(\hat{k}') \, e^{2i\delta_L} \, \gamma_{kL}^2 \, Y_{LM}^*(\hat{k})$$

Using the relation (1.45 - 1.48) between f_L and $\langle k' | T | k \rangle$, it is seen that the resonant term in (2.21) contributes to f_L as

$$-\frac{4\pi^2 m}{\hbar^2} e^{2i\delta_L} \frac{\gamma_{kL}^2}{\epsilon_k - E_c - \Delta_k + \frac{i}{2}\Gamma_k} = -\frac{4\pi}{k} e^{2i\delta_L} \frac{\frac{1}{2}\Gamma_k}{\epsilon_k - E_c - \Delta_k + \frac{i}{2}\Gamma_k}$$

Hence, if the resonance occurs in the L-th partial wave, the partial wave amplitude is given by

$$f_L(k) = \frac{4\pi}{k} \left\{ e^{i\delta_L} \sin\delta_L - e^{2i\delta_L} \frac{\frac{1}{2}\Gamma_k}{\epsilon_k - E_c - \Delta_k + \frac{i}{2}\Gamma_k} \right\} \qquad (2.23)$$

This is the well-known Breit-Wigner formula for a single, isolated resonance. It is easy to verify that this expression satisfies the partial wave unitarity relation (1.50); indeed, f_L can be written in the form:

$$f_L(k) = \frac{4\pi}{k} \frac{1}{2i} \left\{ e^{2i\delta} \frac{\epsilon_k - E_c - \Delta_k - \frac{i}{2}\Gamma_k}{\epsilon_k - E_c - \Delta_k + \frac{i}{2}\Gamma_k} - 1 \right\}$$

$$= \frac{4\pi}{k} e^{i(\delta+\varphi)} \sin(\delta+\varphi) \qquad (2.24)$$

with

$$e^{2i\varphi} = \frac{\epsilon_k - E_c - \Delta_k - \frac{i}{2}\Gamma_k}{\epsilon_k - E_c - \Delta_k + \frac{i}{2}\Gamma_k}$$

As ϵ_k sweeps over the region of resonance - of width Γ -, φ goes rapidly through 90°, and produces a maximum in f_L of width Γ in energy.

With (2.24), the validity of (1.50) is obvious.

2.B. Rearrangement collisions; pick-up and stripping

We now consider states, where the two particles a and b form a bound system, the 'deuteron'. In this case, we will write H (2.1) in the form

$$H = H_{ab} + U_a(r_a) \qquad (2.25)$$

with H_{ab} given by (2.4).

We are now interested in a situation when a 'deuteron' of momentum $\vec{K}$ is incident on the potential U_a, and is either scattered (reaction (4)), or stripped (reaction (5)). Or conversely, we want to consider the case of particle b incident on system A, and picking up particle a to form a 'deuteron' (reaction (3)). For all these, we need the scattering states

$|B, K^{(\pm)}\rangle\!\rangle$, defined by the equation

$$|B, K^{(\pm)}\rangle\!\rangle = |B, K\rangle + \frac{1}{E_B + E_K - H_{ab} \pm i\eta} U_a |B, K^{(\pm)}\rangle\!\rangle \tag{2.26}$$

Notice that the "plane wave parts" in (2.26) and (2.8a) are not orthogonal, being eigenvectors of different Hamiltonians:

$$\langle B, K | n k_b \rangle \neq 0$$

On the other hand, the associated scattering states are orthogonal:

$$\langle\!\langle B, K^{(+)} | n k_b^{(+)} \rangle\!\rangle = 0 \tag{2.27}$$

This fact can be understood as follows. Both states in question are eigenstates of H, and must more precisely be viewed as the limiting cases of wave packets, with a narrow spread in $\vec{K}$ and k_b, respectively. It is now easily seen that these wave packets are orthogonal at $t \to -\infty$, since in this limit, particle a is bound in $U_a(r_a)$ in $|n k_b^{(+)}\rangle\!\rangle$, and localized an infinite distance away from $U_a(r_a)$ in $|B K^{(+)}\rangle\!\rangle$. But both packets, call them $|\psi_B(t)\rangle$ and $|\psi_n(t)\rangle$, satisfy the same time-dependent Schrödinger equations:

$$i\hbar \frac{\partial}{\partial t} |\psi_B(t)\rangle = H |\psi_B(t), \quad i\hbar \frac{\partial}{\partial t} |\psi_n(t)\rangle = H |\psi_n(t)\rangle$$

It then follows that

$$\frac{d}{dt} \langle \psi_B(t) | \psi_n(t) \rangle = 0$$

They are therefore orthogonal at all times. The avoidance of the explicit use of wave packets is just a convenience, and (2.27) must be interpreted properly as holding for every normalized wave packet constructed from $|BK\rangle\!\rangle$ and $|n k_b^{(+)}\rangle\!\rangle$. It is therefore a 'formal' statement, of the same nature as the statement of orthogonality of two plane waves $\langle r | k' \rangle$ and $\langle r | k'' \rangle$.

We shall now 'prove' (2.27) by using Eqs (2.8a) and (2.26) in their equivalent forms

$$|BK^{(+)}\rangle\!\rangle = |BK\rangle + \frac{1}{E_B + E_K - H + i\eta} U_a |BK\rangle$$

$$|n k_b^{(+)}\rangle\!\rangle = |n k_b\rangle + \frac{1}{E_n + \epsilon_k - H + i\eta} V_{ab} |n k_b\rangle$$

Then

$$\langle\!\langle BK^{(+)} | n k_b^{(+)} \rangle\!\rangle = \langle BK | n k_b^{(+)} \rangle\!\rangle + \langle BK | U_a \frac{1}{E_B + E_K - H - i\eta} | n k_b^{(+)} \rangle\!\rangle$$

$$= \langle BK | n k_b \rangle + \langle BK | \frac{1}{E_n + \epsilon_k - H + i\eta} V_{ab} | n k_b \rangle + \frac{\langle BK | U_a | n k_b^{(+)} \rangle\!\rangle}{E_B + E_K - (E_n + \epsilon_k) - i\eta} \tag{2.28}$$

Use the identity, based on $H = H_{ab} + U_a$

$$\frac{1}{E - H + i\eta} = \frac{1}{E - H_{ab} + i\eta} + \frac{1}{E - H_{ab} + i\eta} U_a \frac{1}{E - H + i\eta}$$

to express the middle term on the r.h.s. of (2.28) as

$$\langle BK| \frac{1}{E_n + \epsilon_k - H_{ab} + i\eta} V_{ab} |n k_b\rangle + \langle BK| \frac{1}{E_n + \epsilon_k - H_{ab} + i\eta} U_a \left\{ |n k_b^{(+)}\rangle\!\rangle - |n k_b\rangle \right\}$$

$$= \frac{\langle BK|(V_{ab} - U_a)|n k_b\rangle}{E_n + \epsilon_k - (E_B + E_K) + i\eta} + \frac{\langle BK| U_a |n k_b^{(+)}\rangle\!\rangle}{E_n + \epsilon_k - (E_B + E_K) + i\eta}$$

Now $V_{ab} - U_a = H_{ab} - (H_a + H_b)$, and so

$$\frac{\langle BK|(V_{ab} - U_a)|n k_b\rangle}{(E_n + \epsilon_k) - (E_B + E_K) + i\eta} = - \langle BK|n k_b\rangle$$

Putting this into (2.28), all terms are seen to cancel.

Replacing $\langle\!\langle BK^{(+)}|$ by $\langle\!\langle BK^{(-)}|$, we get the S-matrix-element

$$\langle BK|S|n k_b\rangle = \langle\!\langle BK^{(-)}|n k_b^{(+)}\rangle\!\rangle$$

This differs from (2.27) by the change of sign of $i\eta$ in the third term on the r.h.s. of (2.28). Hence

$$\langle BK|S|n k_b\rangle = - 2\pi i \delta (E_B + E_K - E_n - \epsilon_k) \langle BK|U_a|n k_b^{(+)}\rangle\!\rangle$$

The T-matrix for the pickup reaction $A + b \to (ab)$ is therefore given by

$$\langle BK|T|n k_b\rangle = \langle BK|U_a|n k_b^{(+)}\rangle\!\rangle \tag{2.29}$$

An alternative expression for T is found by starting differently:

$$\langle\!\langle BK^{(-)}|n k_b^{(+)}\rangle\!\rangle = \langle\!\langle BK^{(-)}|n k_b\rangle + \frac{\langle\!\langle BK^{(-)}|V_{ab}|nk\rangle}{E_n + \epsilon_k - (E_B + E_K) + i\eta}$$

and developing this in a similar manner:

$$\langle BK|T|n k_b\rangle = \langle\!\langle BK^{(-)}|V_{ab}|n k_b\rangle \tag{2.30}$$

Notice that (2.29) and (2.30) are equal only on the energy shell. By using the equations for the scattering states again, an integral equation for T can be found. In this equation, the known term is the Born approximation term. Depending on the use of (29) or (30), this Born term is either

$$\langle BK|U_a|n k_b\rangle \quad \text{or} \quad \langle BK|V_{ab}|n k_b\rangle \tag{2.31}$$

U_a is the residual interaction for the Hamiltonian H_{ab} with eigenstates $|BK\rangle$; V_{ab} is the residual interaction for the Hamiltonian (H_A+H_b) with eigenstates $|nk_b\rangle$. Eqs.(2.29) and (2.30) express the well-known ambiguity in the definition of the residual interaction in rearrangement collisions. The T-matrix on the energy shell is, however, unambiguous even in the Born-approximation. Indeed, the two expressions (2.31) are identical, since

$$U_a - V_{ab} = (H_A + H_b) - H_{ab}$$

so that

$$\langle BK|U_a - V_{ab}|nk_b\rangle = (E_n + \epsilon_k - (E_B+E_K))\,\langle BK|nk_b\rangle = 0$$

on the energy shell.

Finally we observe that the T-matrices for the inverse reaction (ab)→ A + b, that is, for stripping, are given by the negative complex conjugates of (2.29) and (2.30).

To get the reaction cross-section, one may use Eq. (1.40). This gives:

(1) For Stripping

$$\sigma_{nk_b\leftarrow BK} = \left(\frac{4\pi^2}{\hbar^2}\right)^2 m_b M \left(\frac{k_b}{K}\right) |\langle BK|T|nk_b\rangle|^2 \qquad (2.32a)$$

(2) For Pickup:

$$\sigma_{BK\leftarrow nk_b} = \left(\frac{4\pi^2}{\hbar^2}\right)^2 m_b M \left(\frac{K}{k_b}\right) |\langle BK|T|nk_b\rangle|^2 \qquad (2.32b)$$

2.C. Scattering with particle exchange; identical particles

The model defined by the Hamiltonian (2.1) may be made more symmetric by adding a potential $U_b(r_b)$, centred about the same origin ($r = 0$), and acting on particle b. If it is strong enough to bind particle b into a bound system B, a new type of reacting in addition to (1) - (6) can occur: (7): $b+A\rightarrow a'+B'$: the ' particle exchange' reaction (plus the similar processes: $a + B \rightarrow a' + B'$, $a + B \rightarrow b' + A'$).

A special case of this occurs if particles a and b are in fact identical (that is, $m_a = m_b$, $U_a = U_b$). In this case (7) is nothing but a contribution to (1), and represents the exchange contribution to elastic or inelastic scattering. But 'direct' and 'exchange' contribution to the scattering amplitude are only formal, not operational concepts. The exclusive use of symmetrized (or anti-symmetrized) wave function in the case of identical particles in fact guarantees that reactions (1) and (7) are fused into one single process.

Writing

$$H = H_A + H_B + V_{ab}$$

$$H_A = \frac{p_a^2}{2m_a} + U_a \qquad H_B = \frac{p_b^2}{2m_b} + U_b \qquad (2.33)$$

and introducing the eigenstates $|n_a k_b^{(+)}\rangle$ and $|n_b k_a^{(+)}\rangle$ of $H_A + H_B$, we can construct the two scattering states:

$$|n_a k_b^{(+)}\gg = |n_a k_b^{(+)}\rangle + \frac{1}{E_{n_a} + \epsilon_{k_b} - (H_A+H_B)+i\eta} V_{ab} |n_a, k_b^{(+)}\gg \quad (2.34a)$$

$$|n_b k_a^{(+)}\gg = |n_b k_a^{(+)}\rangle + \frac{1}{E_{n_b} + \epsilon_{k_a} - (H_A+H_B)+i\eta} V_{ab} |n_b\ k_a^{(+)}\gg \quad (2.34b)$$

For distinguishable particles, they describe distinct processes, and are used to define the S-matrix elements for processes (1) and (7):

$\ll n'_a\ k'^{(-)}_b |n_a k_b^{(+)}\gg$ describes (1): $A + b \to A' + b'$

$\ll n'_b\ k'^{(-)}_a |n_a k_b^{(+)}\gg$ describes (7): $A + b \to B' + a'$

If the two particles are identical, then the operator

$$\frac{1}{E - (H_A+H_B)+i\eta} V_{ab}$$

is symmetric in the variables of the two particles, and (2.34a, b) may be combined into the symmetrized or anti-symmetrized equation

$$|nk^{(+)}\gg = |nk^{(+)}\rangle + \frac{1}{E_n + \epsilon_k - (H_A+H_B)+i\eta} V_{ab} |nk^{(+)}\gg \quad (2.35)$$

where $|nk^{(+)}\rangle$ is a vector with the amplitude

$$\langle r_a r_b |nk^{(+)}\rangle = \frac{1}{\sqrt{2}} \left(\langle r_a|n\rangle\langle r_b|k^{(+)}\rangle \pm \langle r_a|k^{(+)}\rangle\langle r_b|n\rangle\right) \quad (2.36)$$

With (2.35), we now find the single S-matrix element describing processes (1) and (7):

$$\langle n'k'|S|nk\rangle = \ll n'k'^{(-)}|nk^{(+)}\gg$$

which along now familiar lines can be written as

$$\ll n'k'^{(-)}|nk^{(+)}\gg = \langle n'k'^{(-)}|nk^{(+)}\rangle - 2\pi i\delta\ (E_n + \epsilon_k - E_{n'} - \epsilon_{k'})\ \langle n'k'^{(-)}|V_{ab}|nk^{(+)}\gg$$

Using (2.36), the first term of this is

$$\langle n'k'^{(-)}|nk^{(+)}\rangle = \langle n'|n\rangle\langle k'^{(-)}|k^{(+)}\rangle$$

$$= \delta_{n'n}\{\delta\ (k'-k) - 2\pi\, i\,\delta\ (\epsilon_{k'} - \epsilon_k)\ \langle k'|U|k^{(+)}\rangle\}$$

so that

$$\langle n'k'|S|nk\rangle = \delta_{n'n}\,\delta(k'-k)$$
$$-2\pi i\,\delta(E_n+\epsilon_k-E_{n'}-\epsilon_{k'})\,\{\delta_{n'n}\langle k'|U|k^{(+)}\rangle + \langle n'k'^{(-)}|V_{ab}|nk^{(+)}\rangle\!\rangle\} \qquad (2.37)$$

which also gives the T-matrix for the process.

This T-matrix gives directly the transition amplitude for the following process. An incident particle of a certain kind, and momentum k, hits a target and a particle of the same kind appears with momentum k'. The cross-section is therefore given again by the analog of (2.11)

$$\left(\frac{d\sigma}{d\Omega_{k'}}\right)_{(n'k'\leftarrow nk)} = \left(\frac{4\pi^2 m}{\hbar^2}\right)^2 \left|\sigma_{n'n}\langle k'|U|k^{(+)}\rangle + \langle n'k'^{(-)}|V_{ab}|nk^{(+)}\rangle\!\rangle\right|^2 \qquad (2.38)$$

3. IDENTICAL PARTICLES

Atomic nuclei are - to an excellent approximation - systems of identical particles, endowed with two internal degrees of freedom, spin and isospin. The wave function for any system of nucleons is an anti-symmetric function of all its variables. In this section we develop and illustrate the application of the technique of 'second quantization' for dealing with anti-symmetric states.

3.A. The method of 'second quantization'

The set of all anti-symmetrized N particle wave function spans a subspace of the space of all N particle wave functions. We first construct a complete basis in this subspace. To this end, we define first a complete set of orthogonal and normalized one-particle wave functions $\varphi_\alpha(\vec{x}, s)$, s standing for spin and isospin variables:

$$\int d\tau\ \varphi_\alpha^*(\vec{x}, s)\,\varphi_\beta(\vec{x}, s) = \delta_{\alpha\beta} \qquad (3.1a)$$

$$\sum_\alpha \varphi_\alpha(\vec{x}, s)\,\varphi_\alpha^*(\vec{x}', s')\,\delta(\vec{x}-\vec{x}')\,\delta_{s,s'} \qquad (3.1b)$$

In Eq. (3.1a) $\int d\tau$ stands for $\int d^3x \sum_s$

We now assume that the set of all quantum numbers α, labelling the single particle states, be ordered in a linear sequence in some manner. Let $\{\alpha\}$ be an ordered subset $\alpha_1 < \alpha_2 \ldots < \alpha_A$ of A quantum numbers α, and form the wave function:

$$\Phi_{\{\alpha\}}(1, 2, \ldots A) = \frac{1}{\sqrt{A!}} \begin{vmatrix} \varphi_{\alpha_1}(1) & \varphi_{\alpha_2}(1) \ldots & \varphi_{\alpha_A}(1) \\ \varphi_{\alpha_1}(2) & \varphi_{\alpha_2}(2) \ldots & \varphi_{\alpha_A}(2) \\ \ldots & \ldots & \ldots \\ \varphi_{\alpha_1}(A) & \varphi_{\alpha_2}(A) \ldots & \varphi_{\alpha_A}(A) \end{vmatrix}$$

$$= \frac{1}{\sqrt{A!}} \det|\varphi_{\alpha_i}(j)| = \frac{1}{\sqrt{A!}} \sum_p \epsilon_p\,\varphi_{\alpha_1}(p_1)\,\varphi_{\alpha_2}(p_2) \ldots \varphi_{\alpha_A}(p_A) \qquad (3.2)$$

where $p_1 p_2 \ldots p_A$ is a permutation of $12 \ldots A$, and ϵ_p the sign of the permutation.

The set of all possible $\Phi_{\{\alpha\}}$ provides then a complete, ortho-normal basis for anti-symmetric A-particle states. (Clearly, any Φ defined in terms of an unordered set $\{\alpha_1 \beta \ldots \zeta\}$: $\Phi_{\{\text{unordered}\}}$ is just $(-1)^{\epsilon_p}$ $\Phi_{\{\text{ordered}\}}$, ϵ_p being the sign of the permutation needed to order the set.)

In any system of identical particles, all operators are symmetric functions of the particle variables. It is useful to classify operators in the following manner:

(a) One-particle operators $F_1 (1, 2, \ldots A) = \sum_{i=1}^{A} f(i)$ (3.3a)

(b) Two-particle operators $F_2 (1, 2, \ldots A) = \sum_{i<j}^{A} f(i, j)$ (3.3b)

(c) 3- and many-particle operators, by an obvious generalization.

The problem at hand is now to construct matrix elements of symmetric operators F with respect to the anti-symmetric basis states $\Phi_{\{\alpha\}}$: $\int d\tau_1 \ldots d\tau_A \, (\Phi_{\{\beta\}} \; F \; \Phi_{\{\alpha\}})$

One-particle operators: $F_1 = \sum_{i=1}^{A} f(i)$

Let us define

$$(\beta | f | \alpha) = \int d\tau \, (\varphi_\beta^* \, f \, \varphi_\alpha)$$
$$f \varphi_\alpha = \sum_\beta \varphi_\beta \, (\beta) \, f \, (\alpha) \qquad (3.4)$$

One has then

$$F_1 \, \Phi_{\{\alpha\}} = \frac{1}{\sqrt{A!}} \sum_p \epsilon_p \left(\sum_i^A f(p_i) \right) \left(\varphi_{\alpha_1}(p_1) \, \varphi_{\alpha_2}(p_2) \ldots \varphi_{\alpha_A}(p_A) \right)$$

$$= \frac{1}{\sqrt{A!}} \sum_p \epsilon_p \sum_{i=1}^{A} \varphi_{\alpha_1}(p_1) \ldots (f \varphi_{\alpha_i}(p_i)) \ldots \varphi_{\alpha_A}(p_A)$$

$$= \sum_\beta \sum_i \left\{ \frac{1}{\sqrt{A!}} \sum_p \epsilon_p \, \varphi_{\alpha_1}(p_1) \ldots \varphi_{\alpha_{i-1}}(p_{i-1}) \varphi_\beta(p_i) \ldots \varphi_A(p_A) \right\} (\beta | f | \alpha_i)$$

$\sum_\beta$ runs over all one-particle indices. One has 3 cases:

(1) $\beta = \alpha_i$: gives a diagonal element.

(2) $\beta \neq \alpha_i$, but $\beta \in \{\alpha\}$. In this case two identical labels occur, and we get zero.

(3) $\beta \notin \{\alpha\}$: In this case we get a non-zero off-diagonal element.

So we have

$$F_1 \Phi_{\{\alpha\}} = \sum_i (\alpha_i | f | \alpha_i) \Phi_{\{\alpha\}} + \sum_{\beta \notin \{\alpha\}} \sum_{i=1}^{A} (\beta | f | \alpha_i) \Phi_{\{\alpha_1 \ldots \alpha_{i-1} \beta \alpha_{i+1} \ldots \alpha_A\}} \quad (3.5)$$

Notice that the last Φ has generally an unordered label, and that ordering introduces a factor $(-1)^p$. From (3.5), and the orthogonality relations of the $\Phi_{\{\alpha\}}$ one has the matrix-elements of F.

We now consider an abstract vector space, constructed as follows. To each one-particle state α, we associate a pair of operators a_α and $a_\alpha^\dagger$ (its hermitian adjoint) with the properties:

$$a_\alpha a_\beta = -a_\beta a_\alpha \quad (3.6a)$$

$$a_\alpha^\dagger a_\beta^\dagger = -a_\beta^\dagger a_\alpha^\dagger \quad (3.6b)$$

$$a_\alpha a_\beta^\dagger = \delta_{\alpha\beta} - a_\beta^\dagger a_\alpha \quad (3.6c)$$

It follows that the operator $N_\alpha = a_\alpha^\dagger a_\alpha$ satisfies the relation $N_\alpha (1 - N_\alpha) = 0$, and has therefore eigenvalues 0 and 1. These eigenvalues represent the number of particles in state α.

Notice that (3.6a, b) imply that $(a_\alpha)^2 = (a_\alpha^\dagger)^2 \equiv 0$ (3.6d).

We now define a basis vector $|0\rangle$ (the vacuum state) and its adjoint $\langle 0|$ by the properties

$$a_\alpha |0\rangle = 0 \quad \text{(all } \alpha\text{)} \quad (3.7a)$$

$$\langle 0| a_\alpha^\dagger = 0 \quad \text{(all } \alpha\text{)} \quad (3.7b)$$

This vacuum state is normalized to one

$$\langle 0|0\rangle = 1 \quad (3.8)$$

Eq. (6) now enables us to construct an ortho-normal system of vectors as follows:

(1) One-particle state vectors $|\alpha\rangle = a_\alpha^\dagger |0\rangle$, $\langle\alpha| = \langle 0| a_\alpha$ These have the properties (by 3.6, 3.7 and 3.8):

$$\langle\beta|\alpha\rangle = \langle 0| a_\beta a_\alpha^\dagger |0\rangle = \langle 0| \delta_{\alpha\beta} - a_\alpha^\dagger a_\beta |0\rangle = \delta_{\alpha\beta} \langle 0|0\rangle = \delta_{\alpha\beta}$$

(2) Two-particle-state vectors:

$$|\alpha\beta\rangle = a_\alpha^\dagger a_\beta^\dagger |0\rangle$$

$$\langle\alpha\beta| = \langle 0| a_\beta^\dagger a_\alpha \text{ (notice order: } \langle\alpha\beta| = -\langle\beta\alpha|\text{)}$$

$$\langle\gamma\delta|\alpha\beta\rangle = \langle 0| a_\delta a_\gamma a_\alpha^\dagger a_\beta^\dagger |0\rangle = \delta_{\alpha\gamma}\delta_{\beta\delta} - \delta_{\alpha\delta}\delta_{\beta\gamma}$$

All two-particle states are orthogonal to one-particle states and the vacuum.
All one-particle states are orthogonal to the vacuum.

(3) A-particle states: We again invoke the ordered subset $\{\alpha\}$ and may construct a normalized state vector

$$|\{\alpha\}\rangle = a_{\alpha_1}^\dagger a_{\alpha_2}^\dagger \cdots a_{\alpha_A}^\dagger |0\rangle$$

and its adjoint

$$\langle\{\alpha\}| = \langle 0| a_{\alpha_A} a_{\alpha_{A-1}} \cdots a_{\alpha_1}$$

It is now obvious that these vector $|\{\alpha\}\rangle$ are in a one-to-one correspondence with the anti-symmetric particle wave functions $\Phi\{\alpha\}$. Consider now the vector

$$|\{\alpha\}\rangle = |\alpha_1\alpha_2\ldots\alpha_A\rangle = a_{\alpha_1}^\dagger a_{\alpha_2}^\dagger \cdots a_{\alpha_A}^\dagger |0\rangle \tag{3.9}$$

Operate on it with $a_\beta^\dagger a_\gamma$: $a_\beta^\dagger a_\gamma |\{\alpha\}\rangle$.
There are four possible results:

(1) $\beta = \gamma \in \{\alpha\}$, say $\gamma = \alpha_i$; then (3.6) gives $a_{\alpha_i}^\dagger a_{\alpha_i} |\{\alpha\}\rangle = |\{\alpha\}\rangle$

(2) $\gamma = \alpha_i$, $\beta \neq \gamma$, but $\beta \in \{\alpha\}$; then we get zero since the operator $a_\beta^\dagger$ would occur twice.

(3) $\gamma = \alpha_i$, but $\beta \notin \{\alpha\}$; this gives the state

$$a_{\alpha_1}^\dagger \cdots a_{\alpha_{i-1}}^\dagger a_\beta^\dagger \cdots a_{\alpha_A}^\dagger |0\rangle = |\alpha_1 \cdots \alpha_{i-1}\, \alpha_\beta \cdots \alpha_A\rangle$$

(4) $\gamma \notin \{\alpha\}$, then we get zero.

Cases 1, 2, 3 and their results are the exact analogs of cases 1-3 preceding Eq. (3.5). It follows that if instead of $a_\beta^\dagger a_\gamma$ we consider the linear combination

$$\mathrm{IF}_1 = \sum_{\beta\gamma} (\beta|f|\gamma)\, a_\beta^\dagger a_\gamma \tag{3.10}$$

we find the properties:

$$\mathbb{F}_1 \,|\,\{\alpha\}\rangle = \sum_{i=1}^{A} (\alpha_i\,|f|\,\alpha_i)\,|\,\{\alpha\}\rangle$$

$$+ \sum_{\beta \notin \{\alpha\}} \sum_{i} (\beta\,|f|\,\alpha_i)\,|\,\alpha_1 .. \alpha_{i-1}\,\beta\,..\,\alpha_A\rangle \qquad (3.11)$$

which is the exact analog of (3.5).

We conclude from this that the operator $\mathbb{F}$ (3.10), defined in the abstract vector space of states $|\{\alpha\}\rangle$, has the same matrix elements as the operator $F = \Sigma f(i)$, defined in the space of anti-symmetric wave function $\Phi_{\{\alpha\}}(1 \ldots A)$.

'Second quantization' consists of using the abstract space of states $|\{\alpha\}\rangle$, defined by (3.9); to each operator F in configuration space corresponds an operator $\mathbb{F}$ in the abstract space. This correspondence was established for one-particle operators F (Eq. 3.3a) and $\mathbb{F}_1$ (Eq. 3.10).

The correspondence for two-particle operators F_2 and $\mathbb{F}_2$ can be established by using the special two-particle operator

$$F_2 = \tfrac{1}{2}\left(\sum_i f(i)\right)^2 - \tfrac{1}{2}\sum_i f^2(i) = \sum_{i<j} f(i)\, f(j)$$

One has

$$\mathbb{F}_2 = \tfrac{1}{2}\left(\sum_{\alpha\beta} (\beta\,|f|\,\alpha) a_\beta^\dagger a_\alpha\right)^2 - \tfrac{1}{2}\sum_{\alpha\beta} (\beta\,|f^2|\,\alpha)\, a_\beta^\dagger a_\alpha$$

$$= \frac{i}{2}\sum_{\alpha\beta}\sum_{\gamma\delta} (\beta\,|f|\,\alpha)\,(\delta\,|f|\,\gamma)\, a_\beta^\dagger a_\alpha\, a_\delta^\dagger a_\gamma - \tfrac{1}{2}\sum_{\alpha\beta\delta} (\beta\,|f|\,\delta)\,(\delta\,|f|\,\alpha)\, a_\beta^\dagger a_\alpha$$

$$= \tfrac{1}{2}\sum_{\alpha\beta\gamma\delta} (\beta\,|f|\,\alpha)\,(\delta\,|f|\,\gamma)\, a_\beta^\dagger a_\delta^\dagger a_\gamma a_\alpha \qquad \text{by Eq. (3.6).}$$

From this we easily get the general case, where

$$F_2 = \sum_{i<j}^{A} f(i, j)$$

Define

$$(\beta\delta\,|f|\,\alpha\gamma) = \int\int d\tau_1\, d\tau_2\, \varphi_\beta^*(1)\, \varphi_\delta^*(2)\, f(1,2)\, \varphi_\alpha(1)\, \varphi_\gamma(2) \qquad (3.12)$$

and have

$$\mathbb{F}_2 = \tfrac{1}{2}\sum_{\alpha\beta\gamma\delta} (\beta\delta\,|f|\,\alpha\gamma)\, a_\beta^\dagger a_\delta^\dagger a_\gamma\, a_\alpha \qquad (3.13)$$

Notice that the characteristic of a true two-particle operator is the appearance of two a's to the right of the two $a^\dagger$'s. The effect of $\mathbb{F}_2$ is therefore to remove two particles from states α and γ and replace them

by putting two particles into states β and δ. $\mathbb{F}_2$ operating on any state with less than two particles gives identically zero.

The field operators $\psi(\vec{x}, s)$ and $\psi^\dagger(\vec{x}, s)$.

The choice of the basis φ_α (Eq. 3.1) was arbitrary, and yet the expression for operators $\mathbb{F}$ make explicit reference to it. In fact, these operators are independent of the choice of that basis. This is seen as follows, for $\mathbb{F}_1$

$$\mathbb{F}_1 = \sum_{\alpha\beta} a_\beta^\dagger (\beta|f|\alpha)\, a_\alpha$$

$$= \int d\tau \left(\sum_\beta a_\beta \varphi_\beta^* (\vec{x}, s) \right) f \left(\sum_\alpha \varphi_\alpha (\vec{x}, s)\, a_\alpha \right)$$

$$= \int d\tau\, \psi^\dagger(\vec{x}, s)\, f\, \psi(\vec{x}, s) \tag{3.14}$$

So $\mathbb{F}_1$ may be expressed in terms of the field operators $\psi^\dagger$ and ψ, where

$$\psi(\vec{x}, s) = \sum_\alpha a_\alpha \varphi_\alpha(\vec{x}, s) \tag{3.15}$$

The properties of ψ and $\psi^\dagger$ are embodied in the relations derived from (3.6) and (3.1):

$$\psi(\vec{x}, s)\, \psi(\vec{x}', s') = -\psi(\vec{x}', s')\, \psi(\vec{x}, s) \tag{3.16a}$$

(and the corresponding adjoint relation)

and

$$\psi(\vec{x}, s)\, \psi^\dagger(\vec{x}', s') = \delta(\vec{x}-\vec{x}')\, \delta_{s s'} - \psi^\dagger(\vec{x}', s')\, \psi(\vec{x}, s) \tag{3.16b}$$

The expansion of $\psi(\vec{x}, s)$ in a complete orthogonal system $\chi_\lambda(\vec{x}, s)$ of one-particle wave functions defines an alternative set of creation and annihilation operators $b_\lambda^\dagger$ and b_λ:

$$\psi(\vec{x}, s) = \sum_\lambda b_\lambda \chi_\lambda(\vec{x}, s)$$

The b_λ, $b_\lambda^\dagger$ also satisfy Eqs (3.a -d); in fact they are related to the $a_\alpha^\dagger$, a_α by a unitary transformation:

$$b_\lambda = \sum_\alpha u_{\lambda\alpha}\, a_\alpha \qquad u_{\lambda\alpha} = \int d\tau\, \chi_\lambda^*\, \varphi_\alpha$$

where

$$b_\lambda^\dagger = \sum_\alpha a_\alpha^\dagger\, u_{\alpha\lambda}^\dagger \qquad u_{\alpha\lambda}^\dagger = \int d\tau\, \varphi_\alpha^*\, \chi_\lambda$$

3.B. Hamiltonian of identical particle system; Hartree-Fock basis

We assume now a system of nucleons subject to two-body interactions only. Their Hamiltonian is

$$H = \sum_{i=1}^{A} \frac{p^2(i)}{2m} + \frac{1}{2} \sum_{i<j}^{A} V(i,j) \tag{3.17}$$

It is now trivial to write the corresponding operator $\mathbb{H}$, using (3.10, 13):

$$\mathbb{H} = \sum_{\alpha\beta} a_\alpha^\dagger (\alpha | \frac{p^2}{2m} | \beta) a_\beta + \frac{1}{2} \sum_{\alpha\beta\gamma\delta} a_\alpha^\dagger a_\beta^\dagger (\alpha\beta | V | \gamma\delta) a_\delta a_\gamma \tag{3.17a}$$

Notice that, in contrast to H, the operator $\mathbb{H}$ does not tell us that we deal with A-particles; it is the same operator no matter what the number of particles; that number enters only through the nature of the state on which $\mathbb{H}$ acts, and may be ascertained by means of the number operator:

$$\mathbb{N} = \sum_{\alpha} a_\alpha^\dagger a_\alpha = \sum_{\alpha} \mathbb{N}_\alpha \tag{3.18}$$

whose eigenvalues are A, the number of particles. (Notice that $\mathbb{N}_\alpha^2 = \mathbb{N}_\alpha$, so its eigenvalues are 0 or 1).

The most relevant feature of $\mathbb{H}$, however, is that it is no longer expressed in terms of identifiable particles, but only in terms of particle states. It is not possible, to separate from $\mathbb{H}$ a term representing the interaction between a target nucleus and a projectile, since the projectile is not a particular particle distinct from the rest. The proper language to use now is to say that in a scattering state, one particle occupies a continuum state, whereas the others are bound together; the particle in the continuum is not identified, however. One sees that in using this formation, it is just not possible to express a situation in which things are not properly anti-symmetrized. This is the great merit of the method - quite apart from technical advantages.

In formulating scattering processes, this feature produces certain novel problems. One would like to construct states (wave packets), which for instance represent an eigenstate of the target plus a free particle. Such states can be constructed, but it turns out that they are not orthogonal. Orthogonal states can only be obtained if at least part of the interaction between the target particles themselves is also "switched off". These features will be illustrated as we go along.

An important aspect of nuclear reaction studies is to connect its formulation with the independent particle picture of nuclei, so successful in spectroscopy. In this picture, the nuclear ground state is approximately described by $|\{\alpha\}\rangle$, with the provision that the basis φ_α be properly chosen. The best independent particle basis - in a sense to be defined - is the Hartree-Fock basis, which we find as follows.

Let the set $\varphi_\alpha(x, s)$ be the set of eigenfunctions of the one-particle equation

$$\left(\frac{p^2}{2m} + U(r)\right) \varphi_\alpha = \epsilon_\alpha \varphi_\alpha \tag{3.19}$$

where the potential U is yet unspecified. Choose the A states of lowest energy ϵ_α to form the vector

$$|\mathcal{G}\rangle = |\{\alpha\}_0\rangle = a_1^\dagger a_2^\dagger \ldots a_A^\dagger |0\rangle \tag{3.20}$$

In the future, we use the indices λ, μ, ν to indicate all states $\alpha \epsilon \{\alpha\}_0$, that is, occurring in $|\mathcal{G}\rangle$. For all other states, we use the symbols $\sigma, \tau, \ldots$. We continue to use $\alpha\beta\gamma\delta \ldots$ if no distinction is intended. Notice that due to (6b), $|\mathcal{G}\rangle$ has the property that

$$a_\sigma |\mathcal{G}\rangle = 0 \qquad a_\sigma^\dagger |\mathcal{G}\rangle \neq 0$$

but

$$a_\mu^\dagger |\mathcal{G}\rangle = 0 \qquad a_\mu |\mathcal{G}\rangle \neq 0$$

$a_\mu |\mathcal{G}\rangle \neq 0$ because a_μ can 'create' a 'hole' in $|\mathcal{G}\rangle$ by removing a particle: it is a hole creation operator.

Also, since $a_\mu^\dagger |\mathcal{G}\rangle = 0$, $a_\mu^\dagger$ operating on $(a_\mu |\mathcal{G}\rangle)$ gives $|\mathcal{G}\rangle$; that is, $a_\mu^\dagger$ removes the hole created by a_μ : it is a hole annihilation operator.

In (3.18) $\mathbb{H}$ has all its operators a† to the left of all a's. This ensures that $\langle 0|\mathbb{H}|0\rangle$ is zero by virtue of $a_\alpha |0\rangle = \langle 0| a_\alpha^\dagger = 0$.

We now want to consider $|\mathcal{G}\rangle$ rather than $|0\rangle$ as a new 'reference' state. $a_\sigma^\dagger$ and a_μ are then 'creation' operators, and a_σ, $a_\mu^\dagger$ 'annihilation' operators. With respect to this interpretation, the operators as they stand in $\mathbb{H}$ are not ordered. We now proceed to order them.

For this we need a rule of procedure, Wick's theorem. Let $A_1 A_2 \ldots A_n$ be a product of a and a† (nor ordered). Let $A_{p_1} A_{p_2} \ldots A_{p_n}$ be a permutation of the factors of the product which orders the factors (all $a_\sigma^\dagger$, a_μ to the left of all a_σ, $a_\mu^\dagger$). Then we define the ordered product: $A_1 A_2 .. A_n$: by

$$: A_1 A_2 \ldots A_n : = \epsilon_p A_{p_1} A_{p_2} \ldots A_{p_n} \tag{3.21}$$

ϵ_p being the sign of the permutation of factors. The ordered product differs from the original product of operators by certain terms (due to $\delta_{\alpha\beta}$ in Eq. 3.6c); these terms are obtained by 'contractions'. The rule (Wick's theorem) is best stated by the two simplest examples:

$$AB = : AB : + \langle \mathcal{G}|AB|\mathcal{G}\rangle \tag{3.22a}$$

$$\begin{aligned} ABCD = {} & : ABCD : + : AB : \langle CD\rangle - : AC : \langle BD\rangle \\ & + : AD : \langle BC\rangle - : BD : \langle AC\rangle \\ & + \langle AB\rangle\langle CD\rangle - \langle AC\rangle\langle BD\rangle \end{aligned} \tag{3.22b}$$

The only non-vanishing contractions in our case are

$$\langle \mathcal{G}| a_\beta^\dagger a_\alpha |\mathcal{G}\rangle = \sum_{\mu=1}^{A} \delta_{\alpha\mu}\, \delta_{\beta\mu}$$

With this, $\mathbb{H}$ can be written as:

$$\mathbb{H} = \sum_{\mu=1}^{A} (\mu|\frac{p^2}{2m}|\mu) + \frac{1}{2}\sum_{\lambda,\mu}^{A}\Big((\lambda\mu|V|\lambda\mu) - (\lambda\mu|V|\mu\lambda)\Big)$$
$$+ \sum_{\alpha\beta}\Big\{(\alpha|\frac{p^2}{2m}|\beta) + \sum_{\mu=1}^{A}\Big[(\alpha\mu|V|\beta\mu) - (\alpha\mu|V|\mu\beta)\Big]\Big\} : a_\alpha^\dagger a_\beta :$$
$$+ \frac{1}{2}\sum (\alpha\beta|V|\gamma\delta) : a_\alpha^\dagger a_\beta^\dagger a_\delta a_\gamma : \qquad (3.23)$$

$\mathbb{H}$ is the sum of 3 terms; the first, a number, is just $\langle\mathcal{G}|\mathbb{H}|\mathcal{G}\rangle = E_{\mathcal{G}}$ the second is a one-particle operator, and the third a two-body term.

The best representation of one-particle states is then that which will make the one-body operator in (23) diagonal:

$$(\alpha|h|\beta) = (\alpha|\frac{p^2}{2m}|\beta) + (\alpha|U|\beta) = \epsilon_\alpha \delta_{\alpha\beta} \qquad (3.24)$$

where

$$(\alpha|U|\beta) = \sum_{\mu=1}^{A}\Big[(\alpha\mu|V|\beta\mu) - (\alpha\mu|V|\mu\beta)\Big] \qquad (3.25)$$

$(\alpha|U|\beta)$ is the Hartree-Fock potential - which from its defining equation must be constructed by a self-consistency condition.

For more details of this, see General Bibliography. With 3.24, $\mathbb{H}$ takes its final form

$$\mathbb{H} = E_{\mathcal{G}} + \sum_{\alpha} \epsilon_\alpha : a_\alpha^\dagger a_\alpha : + \frac{1}{2}\sum (\alpha\beta|V|\gamma\delta) : a_\alpha^\dagger a_\beta^\dagger a_\delta a_\gamma :$$
$$= E_{\mathcal{G}} + \mathbb{H}_0 + \mathbf{V} \qquad (3.26)$$

A few remarks are in order:

(1) $:a_\alpha^\dagger a_\alpha:$ is the operator for the number of particles, or minus the number of holes. Indeed, for $\alpha = \sigma > A$:
$:a_\alpha^\dagger a_\alpha: = a_\alpha^\dagger a_\alpha = N_\alpha$, $N_\alpha^2 = N_\alpha$, so its eigenvalues are 0 or 1.
But for $\mu \leq A$, $:a_\mu^\dagger a_\mu: = -a_\mu a_\mu^\dagger = -N_\mu$
So the one-particle term in $\mathbb{H}$ is of the form

$$\mathbb{H}_0 = \sum_{\sigma>A} \epsilon_\sigma \mathbb{N}_\sigma - \sum_{\mu\leq A} \epsilon_\mu \mathbb{N}_\mu \qquad (3.27)$$

(2) The Hartree-Fock potential $(\alpha|U|\beta)$ may be transformed into co-ordinate space:

$$(\vec{x}\,s|U|\vec{x}'s') = \sum_{\alpha\beta} \varphi_\alpha(\vec{x}, s)(\alpha|U|\beta)\varphi_\beta^*(\vec{x}', s')$$

and represents there a non-local potential which goes to zero as $|\vec{x}|$ and $|\vec{x}'| \to \infty$. It accomodates a finite number of bound states; not all of them are occupied by the states μ, in general, so that there exist bound excited states of $\mathbb{H}_0$.
It also has continuum states, which represent waves scattered by the potential U.
We shall later use σ to label unoccupied bound states, and use the label $k^{(\pm)}$ to indicate continuum states.

(3) Despite its attractive form $\mathbb{H}$, (3.26) has the problem that it makes it almost impossible to observe the momentum balance. The total momentum operator is

$$\mathbb{P} = \sum_{\alpha\beta} (\alpha|p|\beta)\, a_\alpha^\dagger a_\beta = \sum (\alpha|p|\beta) : a_\alpha^\dagger a_\beta :, \tag{3.28}$$

provided $\langle \mathcal{G}|\mathbb{P}|\mathcal{G}\rangle = 0$, which we assume. But $|\mathcal{G}\rangle$ is not an eigenstate of $\mathbb{P}$, and $\mathbb{H}_0$ does not commute with $\mathbb{P}$. All approximation schemes based on the use of $\mathbb{H}_0$ deal therefore with states of indefinite momentum. (A similar situation may prevail with respect to angular momentum.)

3.C. A simple example: nucleon scattering

This example is intended to illustrate the formulation of a scattering problem based on the Hamiltonian (3.26). We shall, in the next section, develop exact expressions for the scattering amplitude. But first, it will be useful to see a simple application; the simplification is obtained by a drastic reduction of basis vectors used in representing a scattering state; the example will also serve to illustrate the problems which arise if such simplifying assumptions are not made.

As mentioned before, the particle states σ are of two kinds:

(a) Unoccupied bound states in the H.F. potential U. We shall now call those σ.

(b) Continuum states. They have wave functions $\varphi_k^{(+)}(\vec{x}, s)$ or $\varphi_k^{(-)}(\vec{x}, s)$, and describe scattering in a potential U. Then wave functions define a one-nucleon S-matrix:

$$\langle k'|S|k\rangle = \int d\tau\, \varphi_{k'}^{*(-)}\, \varphi_k^{(+)} \tag{3.29}$$

We shall normalize these wave functions as in section 1, and correspondingly define creation and annihilation operators

$$a^\dagger(k^{(+)}) \text{ or } a^\dagger(k^{(-)}) \quad \text{and} \quad a(k^{(+)}) \text{ or } a(k^{(-)}).$$

These satisfy

$$a^\dagger(k^{(\pm)})\, a(k'^{(\pm)}) = \delta(\vec{k}'-\vec{k}) - a(k'^{(\pm)})\, a^\dagger(k^{(\pm)}) \tag{3.30}$$

The states $k^{(+)}$, σ, μ, or $k^{(-)}$, σ, μ form a complete one-particle basis. Eq. (3.29) in conjunction with (3.15) gives the relation

$$a(k^{(-)}) = \int d^3k' \, (k|s|k') \, a(k'^{(+)}) \tag{3.31}$$

We now construct a scattering state, as a superposition of eigenstates of $\mathbb{H}_0$; we shall however construct only an approximate eigenstate of $\mathbb{H}$ here, by restricting the number and type of components:

$$|k^{(+)}\gg \cong \int d^3k' \, A(k') \, a^\dagger(k'^{(+)})|\mathscr{G}\rangle + \sum_{\sigma\tau\mu} B(\sigma\tau\mu) \, a_\sigma^\dagger a_\tau^\dagger a_\mu |G\rangle \tag{3.32}$$

$|k^{(+)}\rangle = a^\dagger(k^{(+)})|\mathscr{G}\rangle$ represents a particle scattered by a target, approximated by the ground state of $\mathbb{H}_0$, $|n\rangle = a_\sigma^\dagger a_\tau^\dagger a_\mu |\mathscr{G}\rangle$ a component, where the previously free particle is captured into a bound state σ (or τ), and has excited a particle-hole pair (τ,μ) or (σ,μ) in addition. These states $|k^{(+)}\rangle$ and $|n\rangle$ satisfy $\mathbb{H}_0|k^{(+)}\rangle = \epsilon_k|k^{(+)}\rangle$, $\mathbb{H}_0|n\rangle = \epsilon_n|n\rangle$. (We drop $E_{\mathscr{G}}$ as an irrelevant constant.)

The non-vanishing matrix-elements of $\mathbf{V}$ are:

$$\langle k'^{(+)}|\mathbf{V}|n\rangle = \langle n|\mathbf{V}|k'^{(+)}\rangle^* = (k'^{(+)}\mu|V|\sigma\tau)$$

and $\langle n'|\mathbf{V}|n\rangle$. Notice that $\langle k'^{(+)}|\mathbf{V}|k^{(+)}\rangle = 0$.

The approximate Schrödinger equation is then

$$\langle k^{(+)}|\mathbb{H} - E|\gg = 0, \quad \langle n|\mathbb{H} - E|\gg = 0$$

which gives

$$(\epsilon_k - E) \, A(k) + \sum_n \langle k^{(+)}|\mathbf{V}|n\rangle \, B(n) = 0 \tag{3.33a}$$

$$(\epsilon_n - E) \, B(n) + \sum_{n'} \langle n'|\mathbf{V}|n\rangle \, B(n') + \int d^3k' \, \langle n|\mathbf{V}|k'^{(+)}\rangle A(k') = 0 \tag{3.33b}$$

Introduce the normalized eigenvector $\langle n|c\rangle$ of

$$(\epsilon_n - E_c)\langle n|c\rangle + \sum_{n'} \langle n|\mathbf{V}|n'\rangle\langle n'|c\rangle = 0$$

and the notation

$$|c\rangle = \sum_n |n\rangle\langle n|c\rangle, \qquad |n\rangle = \sum_c |c\rangle\langle c|n\rangle$$

$$B(c) = \sum_n \langle c|n\rangle \, B(n), \qquad B(n) = \sum_c \langle n|c\rangle \, B(c) \text{ etc.}$$

and get:

$$(\epsilon_k - E)\, A(k) + \sum_c \langle k^{(+)} | V | c \rangle\, B(c) = 0 \tag{3.34a}$$

$$(\epsilon_c - E)\, B(c) + \int d^3k' \, \langle c | V | k'^{(+)} \rangle\, A(k') = 0 \tag{3.34b}$$

We see now that this is exactly the system of equations discussed previously, Eqs (2.14a, b), based on a quite different model. This system is then handled in exactly the same manner; the T-matrix is the same as (2.21):

$$\langle k' | T | k \rangle = \langle k' | t | k \rangle + \frac{\langle k'^{(-)} | V | c \rangle \langle c | V | k^{(+)} \rangle}{\epsilon_k - E_c - \Delta_k + \frac{1}{2} \Gamma_k} \tag{3.35}$$

where the matrix $\langle k | t | k \rangle$ is due to the Hartree-Fock potential U, and derived from (3.29):

$$\langle k' | t | k \rangle = \langle k' | U | k^{(+)} \rangle = \int d\tau \, d\tau' \, \frac{e^{-ik' \cdot x'}}{(2\pi)^{\frac{3}{2}}} \, (x's' | U(xs) \, \varphi_k^{(+)}(x, s)$$

It will be useful at this point to indicate the complications that arise if the simple structure (3.32) of the approximate scattering state $|k^{(+)}\rangle\!\rangle$ is abandoned:

First: The target should be an eigenstate of $\mathbb{H}$, not of $\mathbb{H}_0$ as in our approximation. If, therefore, one constructs a more general expansion of $|k^{(+)}\rangle\!\rangle$ in eigenstates of $\mathbb{H}_0$ one will inextricably mix the eigenvalue problem for the target ($\mathbb{H} |\mathcal{G}\rangle\!\rangle = E_G |\mathcal{G}\rangle\!\rangle$) with the scattering problem.

Second: One may try to avoid this first problem by making an expansion like (3.32), but using $|\mathcal{G}\rangle\!\rangle$ instead of $|\mathcal{G}\rangle$. This has the disadvantage that now the states $a^\dagger(k^{(+)}) |\mathcal{G}\rangle\!\rangle$ $a_\sigma^\dagger \, a_\tau^\dagger \, a_\mu^- |\mathcal{G}\rangle\!\rangle$ do not form an orthogonal basis. For instance (using 3.30):

$$\langle\!\langle \mathcal{G} | a(k') \, a^\dagger(k) | \mathcal{G} \rangle\!\rangle = \langle\!\langle \mathcal{G} | \delta(k'-k) - a^\dagger(k) \, a(k') | \mathcal{G} \rangle\!\rangle$$

$$= \delta(k'-k) - \langle\!\langle \mathcal{G} | a^\dagger(k) \, a(k') | \mathcal{G} \rangle\!\rangle$$

Now $a(k^{(+)}) |\mathcal{G}\rangle$ is zero, but $a(k^{(+)}) |\mathcal{G}\rangle\!\rangle$ is not, since $|\mathcal{G}\rangle\!\rangle$ will contain many continuum components.

3.D. Amplitudes for elastic and inelastic nucleon scattering, deuteron stripping and pickup, etc.

In this section we shall derive expressions for scattering states describing a variety of collision processes, and - by means of the S-matrix - give expression for the corresponding transition amplitudes. First nucleon scattering will be described and discussed, and then deuteron

scattering and stripping, the latter as an example of a rearrangement collision. It will be easily seen that the method generalizes to any kind of two-body collision. For the purpose of deriving general formulae, it will be useful to choose freely any representation of single particle states we want. Plane wave states are particularly convenient; they correspond to the decomposition

$$\psi(\vec{x}, s) = \int d^3k \, \langle \vec{x} | \vec{k} \rangle \, a(\vec{k}, s) \qquad \langle x | k \rangle = \frac{e^{ik \cdot x}}{(2\pi)^{\frac{3}{2}}}$$

which gives the operator $a(k, s)$, $a^\dagger(k, s)$ the property

$$\{a(k, s), \; a^\dagger(k', s')\} = \delta(k - k') \, \delta_{ss'}$$

Of course the Hartree-Fock representation will be used too; in this case the single-particle continuum states are not momentum eigenstates but scattering states themselves, and the T-matrices for elastic scattering will have an extra term.

The Hamiltonian will be written as

$$\mathbb{H} = H_0 + \mathbb{V}$$

with $\mathbb{H}_0$ either the kinetic energy or, as in (3.26), the Hartree-Fock one-particle energy. We shall first assume that $\mathbb{H}_0$ is just the kinetic energy:

$$\mathbb{H}_0 = \int d\tau_k \; \epsilon_k \, a^\dagger(k) \, a(k), \qquad \epsilon_k = \hbar^2 k^2 / 2m$$

Bound states of $\mathbb{H}$ composed of A nucleons, will be called $|n_A\rangle\!\rangle$, and have energy E_{n_A}: $\mathbb{H} |n_A\rangle\!\rangle = E_{n_A} |n_A\rangle\!\rangle$. n_A is a set of suitable quantum numbers. We assume them orthogonal according to $\langle\!\langle n' | n \rangle\!\rangle = \delta_{n'n}$. These states represent targets in collision processes.

The state $a^\dagger(k_i) |n_A\rangle\!\rangle$ - more precisely: the wave packet

$$a^\dagger(i, \epsilon) n_A\rangle\!\rangle = \int d\tau_k \; f_i(k) \, e^{-i\epsilon_k t} \, a^\dagger(k) |n_A\rangle\!\rangle$$

represents a free nucleon of (mean) momentum k_i incident on a target. It is good to notice that these states are neither stationary nor orthogonal; in fact, by (3.6)

$$\begin{aligned} \langle\!\langle n'_A | a(k') \, a^\dagger(k) | n_A \rangle\!\rangle &= \langle\!\langle n'_A | \delta(k'-k) - a^\dagger(k) \, a(k') | n_A \rangle\!\rangle \\ &= \delta(k'-k) \, \delta_{n'n} - \langle\!\langle n'_A | a^\dagger(k) \, a(k') | n_A \rangle \\ &= \delta(k'-k) \, \delta_{n'n} - \langle n'k' | K | nk \rangle \end{aligned} \tag{3.36}$$

K is non-zero; for $n' = n$ it is just the density matrix of the state $|n\rangle\!\rangle$, and

$$\int d\tau_k \, \langle nk | K | nk \rangle = A$$

Nucleon scattering states will be written as $|n_A, k^{(+)}\gg$; they contain, in addition to the term $a^\dagger(k)|n_A\gg$, an outgoing wave of scattering and reaction products. They are eigenstates of $\mathbb{H}$

$$(\mathbb{H} - (E_{n_A} + \epsilon_k))|n_A, k^{(+)}\gg = 0 \tag{3.37}$$

Our aim is to express these states in terms of the target state; to this end, define operators $J(k)$ and $J^\dagger(k)$ by

$$[\mathbb{H}, a^\dagger(k)] = + \epsilon_k a^\dagger(k) + J^\dagger(k) \tag{3.38a}$$

$$[\mathbb{H}, a(k)] = - \epsilon_k a(k) - J(k) \tag{3.38b}$$

where

$$J^\dagger(k) = [\mathbf{V}, a^\dagger(k)] = \sum_{\beta\gamma\delta} a^\dagger_\beta (k\beta|V|\gamma\delta) a_\delta a_\gamma \tag{3.39}$$

(Notice that the representation $\beta\gamma\delta$ need not be specified.) From (3.38) we have

$$[\mathbb{H}, a^\dagger(k)]|n_A\gg = \begin{cases} (\mathbb{H} - E_{n_A}) a^\dagger(k)|n_A\gg \\ \epsilon_k a^\dagger(k)|n_A\gg + J^\dagger(k)|n_A\gg \end{cases}$$

and hence

$$(\mathbb{H} - (E_{n_A} + \epsilon_k)) a^\dagger(k)|n_A\gg = J^\dagger(k)|n_A\gg \tag{3.40a}$$

Similarly, we find

$$(\mathbb{H} - (E_{n_A} - \epsilon_k)) a(k)|n_A\gg = - J(k)|n_A\gg \tag{3.40b}$$

We now invert Eq. (3.40a) by means of the Green's-function $(E-\mathbb{H})^{-1}$, adding a solution of the homogeneous equation (3.37):

$$a^\dagger(k)|n_A\gg = \lambda |n_A, k^{(\pm)}\gg - \frac{1}{E - \mathbb{H} + i\eta} J^\dagger(k)|n_A\gg$$

This equation gives $|n_A k^{(\pm)}\gg$ in terms of $|n_A\gg$; it turns out, as we shall see, that $\lambda = 1$ is the proper normalization:

So finally:

$$|n_A, k^{(\pm)}\gg = a^\dagger(k) n_A\gg + \frac{1}{E - \mathbb{H} + i\eta} J^\dagger(k)|n_A\gg \tag{3.41}$$

With this, we can check the orthogonality, and also find an expression for the S-matrix elements $(n'k'|S|nk)$. To this end, we need a formal relation obtainable from the commutation rules (3.38):

$$(\mathbb{H} + \epsilon_{k'} - E) a(k') = a(k') (\mathbb{H} - E) - J(k')$$

giving

$$a(k)\frac{1}{E-\mathbb{H}\pm i\eta}=\frac{1}{E-\epsilon_{k'}-\mathbb{H}\pm i\eta}a(k')+\frac{1}{E-\epsilon_{k'}-\mathbb{H}\pm i\eta}J(k')\frac{1}{E-\mathbb{H}\pm i\eta} \tag{3.42}$$

Then, writing simple E and E' for the energies of initial and final states:

$$\langle\langle n'k'^{(\pm)}|nk^{(\pm)}\rangle\rangle=\left(\langle\langle n'|J(k')\frac{1}{E'-\mathbb{H}\mp i\eta}+\langle\langle n'|a(k')\right)|nk^{(+)}\rangle\rangle$$

$$=\frac{\langle\langle n'|J(k')|nk^{(+)}\rangle\rangle}{E'-E\mp i\eta}+\langle\langle n'|a(k')\,a^{\dagger}(k)|n\rangle\rangle+\langle\langle n'|a(k')\frac{1}{E-\mathbb{H}+i\eta}J^{\dagger}(k)|n\rangle\rangle$$

The last term, using (3.42) can be written as

$$\langle\langle n'|\left(a(k')+J(k')\frac{1}{E-\mathbb{H}+i\eta}\right)J^{\dagger}(k)|n\rangle\rangle\frac{1}{E-E'+i\eta}$$

$$=\left\{\langle\langle n'|a(k')J^{\dagger}(k)|n\rangle\rangle+\langle\langle n'|J(k')\left(|nk^{(+)}\rangle\rangle-a^{\dagger}(k)|n\rangle\rangle\right)\right\}\frac{1}{E-E'+i\eta}$$

Hence

$$\langle\langle n'k'^{(-)}|nk^{(+)}\rangle\rangle=\langle\langle n'|J(k')|nk^{(+)}\rangle\rangle\left(\frac{1}{E'-E\mp i\eta}+\frac{1}{E-E'+i\eta}\right)$$

$$+\langle\langle n'|a(k)\,a^{\dagger}(k')|n\rangle\rangle+\frac{\langle\langle n'|a(k')J^{\dagger}(k)-J(k')a^{\dagger}(k)|n\rangle\rangle}{E-E'+i\eta}$$

The second line of this expression just gives

$$\delta(k'-k)\,\delta_{n'n}:$$

Using Eqs. (3.38) for J and $J^{\dagger}$, and the equality $\{a(k'),\ J^{\dagger}(k)\}=\{J(k'),\ a^{\dagger}(k)\}$, one obtains

$$\langle\langle n'|a(k')\,a^{\dagger}(k)+\frac{a^{\dagger}(k)\left((E_n-\epsilon_{k'}-\mathbb{H})-(E_{n'}-\epsilon_k-\mathbb{H})\right)a(k')}{E-E'+i\eta}|n\rangle\rangle$$

which, at once reduces to

$$\langle\langle n'|a(k')\,a^{\dagger}(k)+a^{\dagger}(k)\,a(k')|n\rangle\rangle=\delta(k'-k)\,\delta_{n'n}$$

This gives at once

$$\langle\langle n'k'^{(+)}|nk^{(+)}\rangle\rangle=\delta(k'-k)\,\delta_{n'n} \tag{3.43}$$

and

$$\langle\!\langle n'k'^{(-)} | n k^{(+)} \rangle\!\rangle = \delta(k'-k)\,\delta_{n'n} - 2\pi i \delta(E'-E)\,\langle\!\langle n' | J(k') | n k^{(+)} \rangle\!\rangle \qquad (3.44)$$

So the T-matrix for nucleon scattering is

$$\langle n'k | T | nk \rangle = \langle\!\langle n' | J(k') | n k^{(+)} \rangle\!\rangle \qquad (3.45a)$$

We might have proceeded slightly differently, using the expression (3.41) for $|nk^{(+)}\rangle\!\rangle$ rather than for $\langle\!\langle n'k'^{(+)}|$. In this case, we would have ended up with

$$\langle n'k' | T | n k \rangle = \langle\!\langle n'k'^{(-)} | J^{\dagger}(k) | n \rangle\!\rangle \qquad (3.45b)$$

The two expressions are in fact identical, but only on the energy shell.

There is a slight modification of this result, if the Hartree-Fock representation (3.26) for $\mathrm{I\!H}$ is used. It is then natural to use the creation - and annihilation - operators for H.F. single particle states, in particular, the operators $a(k^{(+)})$ and $a^{\dagger}(k^{(+)})$ for the continuum.

By completely analogous procedure, we now have

$$|n k^{(\pm)}\rangle\!\rangle = a^{\dagger}(k^{(\pm)}) | n \rangle\!\rangle + \frac{1}{E - \mathrm{I\!H} \pm i\eta}\, J^{\dagger}(k^{(\pm)}) | n \rangle\!\rangle \qquad (3.46)$$

This does not affect the orthogonality relations. But in the expression for the S-matrix we now deal with two different representations. Instead of (3.49) we get

$$\langle\!\langle n'k'^{(-)} | n k^{(+)} \rangle\!\rangle = \langle\!\langle n' | a(k'^{(-)})\, a^{\dagger}(k^{(+)}) + a^{\dagger}(k^{(+)})\, a(k'^{(-)}) | n \rangle\!\rangle$$
$$- 2\pi i \delta(E'-E)\,\langle\!\langle n' | J(k'^{(-)}) | n k^{(+)} \rangle\!\rangle \qquad (3.47)$$

The top line can be reduced by the relation

$$a(k'^{(-)}) = \int d^3k''\, (k' | s | k'')\, a(k''^{(+)}) \qquad (3.48)$$

with which this line may be written as

$$\int d^3k''\, (k' | s | k'')\, \langle\!\langle n' | a(k''^{(+)})\, a^{\dagger}(k^{(+)}) + a^{\dagger}(k^{(+)})\, a(k''^{(+)}) | n \rangle\!\rangle$$
$$= \int d^3k''\, (k' | s | k'')\, \langle\!\langle n' | \delta(k''-k) | n \rangle\!\rangle = (k' | s | k)\, \delta_{n'n}$$

Now $(k'|s|k)$ is the one-particle S-matrix for scattering of a nucleon in the Hartree-Fock potential, and has the form

$$(k' | s | k) = \delta(k'-k) - 2\pi i \delta(\epsilon_{k'} - \epsilon_k)\, (k' | t | k) \qquad (3.49)$$

Inserting this into (3.47), we finally have

$$\langle n'k' | T | n k \rangle = \delta_{n'n}\, (k' | t | k) + \langle\!\langle n' | J(k'^{(-)}) | n k^{(+)} \rangle\!\rangle \qquad (3.50)$$

This is again the familiar expression for the scattering from the sum of two potentials.

These considerations and results can be generalized to cases involving a composite projectile, say a deuteron. A deuteron of centre-of-mass momentum K and in spin state S has the wave function

$$\phi_D(\vec{r}_1 - \vec{r}_2,\ s_1 s_2)\ \langle \vec{r}_1 + \vec{r}_2\ |2|\vec{K}\rangle \tag{3.51}$$

(that is, a product of an intrinsic wave function and a momentum wave function $(\exp[i\vec{K}\cdot(\vec{r}_1+\vec{r}_2)/2])/(2\pi)^{\frac{3}{2}}$. We shall abreviate it as $\langle 12|DK\rangle$. By means of this wave function one constructs the deuteron creation operator

$$A_D^\dagger(k) = \frac{1}{\sqrt{2}} \int d\tau_1\, d\tau_2 \langle 12|DK\rangle \psi^\dagger(1)\, \psi^\dagger(2) \tag{3.52}$$

This operator is normalized such that

$$\langle 0|A_D(\vec{K}'S')\ A_D^\dagger(\vec{K}, S)|0\rangle\!\rangle = \delta(\vec{K}'-\vec{K})\ \delta_{S'S} \tag{3.53}$$

The state $A_D^\dagger(K)|0\rangle$ is the free deuteron, and is an eigenstate of $\mathbb{H}$.

$$\mathbb{H}\ A_D^\dagger(K)|0\rangle = E_{DK} A_D^\dagger(K)|0\rangle \tag{3.54}$$

with $E_{DK}^\dagger = \hbar^2K^2/|4m - |\epsilon_D|$, ϵ_D being the deuteron binding energy. This property is also expressed in the more general commutation relation

$$[\mathbb{H},\ A_D^\dagger(K)] = E_{DK} A_D^\dagger(K) + J_D^\dagger(K) \tag{3.55}$$

which is the analog of Eq. (3.38) for nucleons. The operator $J_D^\dagger$ gives zero on the vacuum: $J_D^\dagger|0\rangle = 0$.

The construction of scattering states, proof of their orthogonality, and the construction of the S-matrix follows exactly the pattern for the case of nucleon scattering. In general, we can state: let $A_a^\dagger(k)$ be the creation operator for any projectile of kind a (elementary or composite). It will satisfy a relation

$$[\mathbb{H},\ A_a^\dagger(K)] = E_a(k)\ A_a^\dagger(k) + J_a^\dagger(k) \tag{3.56}$$

Such a particle, interacting with a nucleus (target) in state $|n\rangle\!\rangle$ is described by a scattering state

$$|n_A,\ k_a^{(+)}\rangle\!\rangle = A_a^\dagger(k)|n_A\rangle\!\rangle + \frac{1}{E - \mathbb{H} + i\eta} J_a^\dagger(k)|n_A\rangle\!\rangle \tag{3.57}$$

and the T-matrix for the process ([n] ≡ target in state n)

$$[n_A] + a \rightarrow [n'_{A'}] + b$$

is given by

$$\langle n'_{A'}, k'_b \,|\, T \,|\, n_A k_a \rangle = \langle\!\langle n'_{A'} \,|\, J_b(k'_b) \,|\, n_A k_a^{(+)} \rangle\!\rangle \tag{3.58a}$$

$$= \langle\!\langle n'_{A'} k'^{(-)}_b \,|\, J_a^\dagger(k_a) \,|\, n_A \rangle\!\rangle \tag{3.58b}$$

Again, expressions (3.58a, 58b) are equal on the energy shell only. The equivalence of these two expressions can be made explicit by developing it a bit further.

Inserting the expressions (3.57) for the scattering states into (3.58a), one has

$$\langle\!\langle n'_{A'} | J_b(k'_b) | n_A k_a^{(+)} \rangle\!\rangle = \langle\!\langle n'_{A'} | J_b(k'_b)\, A_a^\dagger(k_a) | n_A \rangle\!\rangle$$

$$+ \langle\!\langle n'_{A'} | J_b(k'_b) \frac{1}{E - \mathbb{H} + i\eta} J_a^\dagger(k_a) | n_A \rangle\!\rangle$$

Now

$$J_b(k') A_a^\dagger(k) = [J_b(k'), A_a^\dagger(k)]_\mp \pm A_a^\dagger(k)\, J_b(k')$$

where we use the anti-commutator if a, b are both fermions, and the commutator in all other cases.
Then with

$$\langle\!\langle n' | A_a^\dagger(k) (E_{n'} - E_{k_a} - \mathbb{H}) = \langle\!\langle n' | J_a^\dagger(k)$$

$$\langle n'_{A'}, k'_b | T | n_A k_a \rangle = \langle\!\langle n'_{A'} | [J_b(k'), A_a^\dagger(k)]_\mp | n_A \rangle\!\rangle$$

$$+ \langle\!\langle n'_{A'} | J_b(k') \frac{1}{E - H + i\eta} J_a^\dagger(k) | n_A \rangle\!\rangle$$

$$\mp \langle n'_{A'} | J_a^\dagger(k) \frac{1}{E_{k_a} - E_{n'_{A'}} + \mathbb{H}} J_b(k') | n_A \rangle\!\rangle \tag{3.59}$$

Using (3.58b) would have given $\langle\!\langle n_{A'} | [A_b(k'), J_a^\dagger(k)]_\pm | n_A \rangle\!\rangle$ as the "Born" term in the above equation. These two expressions are easily seen to be identical on the energy shell; also in the last term $E_{k'_b} - E_{n_A}$ would have appeared, which is equal to $E_{k_a} - E'_{n_{A'}}$.

3.E. T-matrix and Green's-functions

The form (3.59) has the structure of the "low-equation", and in fact is nothing but the time-independent version of the well known expression for the T-matrix based on the Lehmann-Zimmermann-Symanzik formalism of collision. In this formalism one shows that

$$-2\pi i \delta(E'-E) \langle n'_{A'}, k'_b | T | n_A k_a \rangle$$

$$= \int_{-\infty}^{+\infty} dt \int_{-\infty}^{+\infty} dt'\, e^{+iE_{k'_b} t' - iE_{k_a} t} \left(i \frac{\partial}{\partial t'} - E_{k'_b}\right) \left(i \frac{\partial}{\partial t} + E_{k_a}\right)$$

$$\times \langle\!\langle n'_{A'} | T(\underline{A}_b(k', t'), \underline{A}_a(k, t) | n_A \rangle\!\rangle \tag{3.60}$$

$\underline{A}^{\dagger}(k,t)$ $\underline{A}(k',t')$ being the Heisenberg operators $(\exp[iHt])\,A^{\dagger}(k)\,(\exp[iHt])$ etc. and $T(x(t'),\ y(t))$ being the time ordered product

$$T(X(t'),\ Y(t)) = \begin{matrix} X(t')\ Y(t) & \text{for } t' > t \\ \pm\, Y(t)\ X(t') & \text{for } t > t' \end{matrix}$$

(the - sign valid for two fermion operators, the + sign otherwise).

Carrying out the t and t' integrations in (3.60) leads at once back to the Eq. (3.59).

Let us look at this expression in somewhat more detail, for the case of elastic scattering of nucleons from the target ground state $|0\rangle\!\rangle$. Then, in the LSZ formula for T appears the one-particle Green's-function.

$$\mathcal{G}(k',k;\,t'-t) = \frac{1}{i}\,\langle\!\langle\, 0 \,|\, T(\underline{a}(k',t'),\ a^{\dagger}(k,t)) \,|\, 0 \,\rangle\!\rangle \tag{3.61}$$

Now as the LSZ formula shows, there is a simple relation between the T-matrix for elastic scattering and the corresponding one-particle Green's-function. We shall formulate this relation in the time-independent language and first illustrate it for the case of a particle scattered by a potential V(r), as described in section 1. We define (using one particle plane wave states $|k\rangle$)

$$\mathcal{G}(k',k;\,\omega) = \langle k' \,|\, \frac{1}{\omega - H + i\eta} \,|\, k \rangle \tag{3.62}$$

(Notice that ω is an independent parameter, not equated with either E_k or $E_{k'}$.)

Since

$$\langle k' \,|\, H \,|\, k \rangle = \epsilon_k\, \delta(k'-k) + \langle k' \,|\, V \,|\, k \rangle$$

one has clearly

$$(\omega - \epsilon_{k'})\,\mathcal{G}(k',k;\,\omega) = \delta(k'-k) - \int d^3k''\, \langle k' \,|\, V \,|\, k'' \rangle\, \mathcal{G}(k'',k;\,\omega) \tag{3.63}$$

In shorthand, we can write this (and the "adjoint" equation) as

$$(\omega - \epsilon_{k'})\,\mathcal{G}(k',k;\,\omega) = \delta(k'-k) + \langle k' \,|\, V \frac{1}{\omega - H + i\eta} \,|\, k \rangle$$

$$(\omega - \epsilon_{k})\,\mathcal{G}(k',k;\,\omega) = \delta(k'-k) + \langle k' \,|\, \frac{1}{\omega - H + i\eta}\, V \,|\, k \rangle$$

and

$$(\omega - \epsilon_k)(\omega - \epsilon_{k'})\,\mathcal{G}(k',k;\,\omega) = (\omega - \epsilon_k)\,\delta(k'-k) + \langle k' \,|\, V \frac{1}{\omega - H + i\eta}(\omega - H + V) \,|\, k \rangle$$

$$= (\omega - \epsilon_k)\,\delta(k'-k) + \langle k' \,|\, V \,|\, k \rangle + \langle k' \,|\, V \frac{1}{\omega - H + i\eta}\, V \,|\, k \rangle$$

Clearly then, by using Eq. (1.31), we get the desired result:

$$\lim_{\substack{\omega-\epsilon_k\to 0\\ \omega-\epsilon_{k'}\to 0}} (\omega-\epsilon)(\omega-\epsilon')\,\mathcal{G}(k',k;\omega) = \langle k'|V|k\rangle + \langle k'|V\frac{1}{\epsilon-H+i\eta}V|k\rangle$$
$$= \langle k'|T|k\rangle \qquad (3.64)$$

All these simple relations remain valid in the case of scattering of a nucleon by a nuclear target (assumed in the ground state). We first define a $\mathcal{G}(k',k;\omega)$ as the Fourier transform of (3.60) (for nucleons):

$$\mathcal{G}(k',k;\omega) = \int_{-\infty}^{+\infty} d\tau\, e^{-\eta|\tau|}\; e^{i\omega\tau}\,\mathcal{G}(k',k;\tau)$$

For simplicity, choose the zero point energy of H such that $H|0\rangle\!\rangle = 0$; then

$$\mathcal{G}(k',k;\omega) = \langle\!\langle 0|a(k')\frac{1}{\omega-\mathbb{H}+i\eta}a^\dagger(k)|0\rangle\!\rangle$$
$$+ \langle\!\langle 0|a^\dagger(k)\frac{1}{\omega+\mathbb{H}-i\eta}a(k')|0\rangle\!\rangle \qquad (3.65)$$

By means of Eq. (3.38) it is then straightforward to see that we have

$$\lim_{\substack{\omega-\epsilon\to 0\\ \omega-\epsilon'\to 0}} (\omega-\epsilon)(\omega-\epsilon')\,\mathcal{G}(k',k;\omega) = \langle\!\langle 0|[J(k'),\,a^\dagger(k)]_+|0\rangle\!\rangle$$
$$+ \langle\!\langle 0|J(k')\frac{1}{\epsilon-\mathbb{H}+i\eta}J^\dagger(k)|0\rangle\!\rangle + \langle\!\langle 0|J^\dagger(k)\frac{1}{\epsilon+\mathbb{H}}J(k')|0\rangle\!\rangle$$
$$= \langle k'|T|k\rangle \qquad (3.66)$$

In the next section, we shall study the structure of $\mathcal{G}$, and derive perturbation expansion of $\mathcal{G}$ and therefore of T.

We terminate this section by defining the concept of the 'generalized' optical potential. This concept originates as follows. One may ask whether the one-particle Green's-function (3.65) satisfies an equation similar to Eq. (3.63) for the simple potential scattering case.

Now it is easy to see that the definition of $\mathcal{G}$ (3.65) gives a result

$$(\omega-\epsilon_{k'})\,\mathcal{G}(k',k;\omega) = \delta(k'-k) + R(k',k;\omega)$$

We shall see that the 'residue' R has the structure $\int dk''\,\langle k'|\mathcal{V}(\omega)|k''\rangle\mathcal{G}(k'',k;\omega)$; this defines the generalized optical potential $(k'|\mathcal{V}(\omega)|k)$. Thus $\mathcal{G}$ satisfies the equation

$$(\omega-\epsilon_{k'})\,\mathcal{G}(k',k;\omega) = \delta(k'-k) - \int d^3k''\,\langle k'|\mathcal{V}(\omega)|k''\rangle\,\mathcal{G}(k'',k;\omega) \qquad (3.67)$$

or equivalently

$$(\omega-\epsilon_{k'}) - \langle k'|\mathcal{V}(\omega)|k\rangle = \langle k'|\mathcal{G}^{-1}(\omega)|k\rangle$$

The l.h.s. is the 'inverse' Green's function. [In finite system, $\mathscr{V}(\omega)$ is generally written as $\Sigma(\omega)$ and called the mass- or self-energy operator.] The potential $\mathscr{V}(\omega)$ reduces elastic nucleon scattering from a composite target to a one-particle problem. Indeed, the one-particle T-matrix, calculated on the basis of the Lippman Schwinger equations (see Eqs(1.16, 17)):

$$\langle k' | k^{(+)} \rangle = \delta (k'-k) + \frac{\langle k' | T | k \rangle}{\epsilon_k - \epsilon_{k'} + i\eta} \tag{3.68}$$

where

$$\langle k' | T | k \rangle = \langle k' | \mathscr{V}(\omega) | k^{(+)} \rangle = \int d^3k'' \, \langle k' | \mathscr{V}(\omega) | k'' \rangle \langle k'' | k^{(+)} \rangle \Big|_{\omega = \epsilon_k}$$

is in fact identical with the T-matrix $\langle k' | T | k \rangle$ of Eq. (3.45). It is therefore of great interest and importance to get hold of $\mathscr{V}(\omega)$. This matter is taken up in the next section.

3.F. Green's-functions and the generalized optical potential

In this section, we derive an expression for the generalized optical potential $\langle k' | \mathscr{V}(\omega) | k \rangle$. The aim is to express $\mathscr{V}(\omega)$ as a matrix-element with respect to the Hartree-Fock ground state of the system; this will be achieved by expressing the Green's function by means of a linked diagram perturbation series, and extracting $\mathscr{V}(\omega)$ from this series.

We recall some premises and notations. We adjust a constant energy term in $\mathbb{H}$ such as to have $\mathbb{H} | 0 \gg = 0$; in that case, the Hartree-Fock representation of $H|$ is

$$\mathbb{H} = \mathbb{H}_0 + \mathbb{V} + \Delta E \tag{3.69}$$

ΔE being the difference $E_0^0 - E_0$ between the H.F. approximate and free ground state energy:

$$\Delta E = \langle 0 | \mathbb{H} | 0 \rangle - \ll 0 | \mathbb{H} | 0 \gg$$

The H.F. ground state $|0\rangle$ satisfies:

$$\mathbb{H}_0 | 0 \rangle = 0 \quad \text{and} \quad \langle 0 | \mathbb{V} | 0 \rangle = 0$$

The Green's function (or one-particle propagator) is defined by means of the equation

$$(k' | \mathscr{G}(t) | k) = \frac{1}{i} \ll 0 | T \, (\underline{a} \, (k', t_1 + t), \, \underline{a}^\dagger (k, t_1)) | 0 \gg \tag{3.70}$$

In this expression, $a^\dagger(k)$ and $a(k)$ are the usual plane wave state creation and annihilation operators, and $\underline{a}^\dagger(k, t)$, $\underline{a}\,(k, t)$ the associated Heisenberg operators

$$\underline{a}\,(k, t) = e^{\frac{i}{\hbar} \mathbb{H} t} \, a(k) \, e^{-\frac{i}{\hbar} \mathbb{H} t} \tag{3.71}$$

Finally

$$T\,(A_2(t_1),\ B(t_1)\,) \equiv \begin{cases} A(t_2)\,B(t_1), & t_2 > t_1 \\ -B(t_1)\,A(t_2), & t_1 > t_2 \end{cases} \tag{3.72}$$

is the time ordered product. (The - sign for $t_1 > t_2$ holds if <u>both</u> A and B are fermions; in all other cases the + sign applies.)

The Fourier transform of $\mathcal{G}$ is then

$$(k'\,|\,\mathcal{G}(\omega)\,|\,k) = \int_{-\infty}^{+\infty} dt\; e^{-\omega t - \eta|t|}\,(k'\,|\,\mathcal{G}(t)\,|\,k)$$

$$+ \langle\!\langle\, 0\,|\,a(k')\,\frac{1}{\omega - \mathbb{H} + i\eta}\,a^{\dagger}(k)\,|\,0\,\rangle\!\rangle + \langle\!\langle\, 0\,|\,a^{\dagger}(k)\,\frac{1}{\omega + \mathbb{H} - i\eta}\,a(k')\,|\,0\,\rangle\!\rangle \tag{3.73}$$

We shall first work with $\mathcal{G}(t)$; develop an expression which establishes the integral equation

$$\mathcal{G}(t) = \mathcal{G}_0(t) + \int_{-\infty}^{+\infty} dt' \int_{-\infty}^{+\infty} dt''\; \mathcal{G}_0(t - t') \sum (t' - t'')\,\mathcal{G}(t'') \tag{3.74a}$$

and hence a Fourier transform

$$\mathcal{G}(\omega) = \mathcal{G}_0(\omega) + \mathcal{G}_0(\omega) \sum (\omega)\,\mathcal{G}(\omega) \tag{3.74b}$$

$\langle k'\,|\,\mathcal{G}_0(\omega)\,|\,k\rangle$ is the zero order (in one case, Hartree-Fock) approximation to $\mathcal{G}$:

$$(k'\,|\,G_0(t)\,|\,k) = \frac{1}{i}\,\langle 0\,|\,T\,(a(k', t + t_1),\ a^{\dagger}(k, t_1)\,|\,0\rangle$$

where

$$a(k, t) = e^{i\mathbb{H}_0 t}\ a(k)\ e^{-i\mathbb{H}_0 t}$$

Its Fourier transform is

$$(k'\,|\,\mathcal{G}(\omega)\,|\,k) = \langle 0\,|\,a(k')\,\frac{1}{\omega - \mathbb{H} + i\eta}\,a^{\dagger}(k)\,|\,0\,\rangle$$

$$+ \langle 0\,|\,a^{\dagger}(k)\,\frac{1}{\omega + \mathbb{H}_0 - i\eta}\,a(k')\,|\,0\rangle$$

This may be reduced further by writing $a(k')$ and $a^{\dagger}(k)$ as a superposition of Hartree-Fock operators, by means of the Hartree-Fock wave function[4]

[4] These are the Fourier-transform of the previously introduced $\varphi_\alpha(x)$.

$\langle k|\alpha\rangle$ (or more specifically, the wave functions

$\langle k'|\mu\rangle$ for hole states $1 \leq \mu \leq A$

$\langle k'|\sigma\rangle$ for bound particle states

$\langle k'|k^{(+)}\rangle$ for continuum states).

$$a(k') = \sum_{\mu} \langle k'|\mu\rangle\, a_{\mu} + \sum_{\sigma} \langle k'|\sigma\rangle\, a_{\sigma} + \int d^3k\, \langle k'|k^{(+)}\rangle\, a(k^{(+)}) \tag{3.75}$$

This gives us an expression for $\mathcal{G}_0(\omega)$:

$$\langle k''|\mathcal{G}_0(\omega)|k'\rangle = \sum_{\sigma} \frac{\langle k''|\sigma\rangle\langle\sigma|k'\rangle}{\omega - \epsilon_{\sigma} + i\eta} + \int d^3k\, \frac{\langle k''|k^{(+)}\rangle\langle k^{(+)}|k'\rangle}{\omega - \epsilon_k + i\eta}$$

$$\sum_{\mu} \frac{\langle k''|\mu\rangle\langle\mu|k'\rangle}{\omega - \epsilon_{\mu} - i\eta} \tag{3.76}$$

Notice that this is just the form of $\mathcal{G}(\omega)$ we had found for the case of the scattering of a particle by a given potential well; except for the position of the hole-state poles in our case, this well is the H.F. potential well:

$$\langle k''|U_{HF}|k'\rangle = \sum_{\mu \leq A} \langle k''\mu|v|k'\mu\rangle - \langle k''\mu|v|\mu k'\rangle$$

We may also remark that one could of course define g in terms of Hartree-Fock operators a_{α}, $a_{\alpha}^{\dagger}$ instead of using plane wave operators. In this case $\mathcal{G}_0(\omega)$ is <u>diagonal</u>, and takes the simpler form

$$\langle\alpha|\mathcal{G}_0(\omega)|\beta\rangle = \frac{\delta_{\alpha\beta}}{\omega - \epsilon_{\alpha} + i\eta} \quad \text{for particle states (including continuum states)}$$

$$\langle\alpha|\mathcal{G}_0(\omega)|\beta\rangle = \frac{\delta_{\alpha\beta}}{\omega - \epsilon_{\alpha} - i\eta} \quad \text{for hole states} \tag{3.77}$$

If we choose the plane wave representation (3.76), then the optical potential will appear as the sum of two terms. $\mathcal{G}_0$ itself will satisfy the equation:

$$(\omega - \epsilon_{k''})\,\langle k''|\mathcal{G}_0(\omega)|k'\rangle = \int \langle k''|U_{HF}|k'''\rangle\, d^3k'''\, \langle k'''|\mathcal{G}_0(\omega)|k'\rangle + \delta(k'' - k') \tag{3.78}$$

Using this equation and the integral equation (3.74) for g in terms of $\mathcal{G}_0$, $\mathcal{G}$ is seen to satisfy the equation

$$(\omega - \epsilon_{k''})\,\langle k''|\mathcal{G}(\omega)|k'\rangle = \delta(k''-k')$$

$$+ \int d^3k'''\, \left\{ \langle k''|U_{HF}|k'''\rangle + \langle k''|\Sigma(\omega)|k'''\rangle \right\} \langle k'''|\mathcal{G}(\omega)|k'\rangle \tag{3.79}$$

which shows that the generalized optical potential $\mathscr{V}(\omega)$ is defined by

$$\mathscr{V}(\omega) = U_{HF} + \Sigma(\omega) \tag{3.80}$$

Now that we know what to look for, let us proceed to the determination of Σ.

The perturbation series for $\mathscr{G}$ and Σ is obtained by using the 'interaction' representation for operators, in which their time dependence is given by

$$\Omega(t) = e^{i\mathbb{H}_0 t}\ \Omega(0)\ e^{-i\mathbb{H}_0 t} \tag{3.81}$$

for any operator Ω. The relation of this to the previously introduced Heisenberg representation is expressed by means of the operators $(\exp[+i\mathbb{H}_0 t])(\exp[-i\mathbb{H}t])$ and $(\exp[i\mathbb{H}t])(\exp[-i\mathbb{H}_0 t])$. More precisely, we define

$$U(t_1, t_2) = e^{i(\mathbb{H}_0 + \Delta E)t_1}\ e^{-i\mathbb{H}(t_1 - t_2)}\ e^{-i(\mathbb{H}_0 + \Delta E)t_2}$$

$$= U(t_1, 0)\, U(0, t_2) \tag{3.82}$$

(ΔE is thrown in because $\mathbb{H} = \mathbb{H}_0 + \mathbf{V} + \Delta E$). This definition is assumed to hold for <u>real or complex</u> values of t_1 and t_2. U satisfied: $U(t_1, t_2) + U(t_1, t_i)U(t_i, t_2)$ (any t_i) and $U(t_1, t_1) = 1$. In addition, the differential equation

$$\frac{dU(t_1, t_2)}{dt_1} = -iV(t_1)\, U(t_1, t_2) \tag{3.83}$$

which has the formal solution

$$U(t_1, t_2) = 1 + \sum_{n=1}^{\infty} (-i)^n \int_{t_2}^{t_1} du_1 \int_{t_2}^{u_1} du_2 \ldots \int_{t_2}^{u_{n-1}} du_n\, V(u_1)\ V(u_2) \ldots V(u_n) \tag{3.84}$$

We can now write the Heisenberg operators $\underline{\Omega}(t)$ as

$$\underline{\Omega}(t) = e^{i\mathbf{H}t}\, \Omega\, e^{-\mathbf{H}t} = U(0, t)\, \Omega(t)\, U(t, 0) \tag{3.85}$$

The same operator U may also be used to express the true ground state $|0\gg$ in terms of the H. F. ground state $|0\rangle$:

$$|0\gg = \lim_{\beta \to \infty} U(0, i\beta)|0\rangle \Big/ \ll 0|0\rangle e^{\beta \Delta E} \tag{3.86}$$

Indeed,

$$U(0, i\beta)|0\rangle = e^{-\beta \mathbb{H}}|0\rangle e^{\beta \Delta E} = \sum_n |n\gg e^{-\beta E_n} \ll n|0\rangle e^{\beta \Delta E}$$

Assuming $E_n > 0$ for all $n > 0$ (notice $E_0 = 0$), Eq. (3.86) follows.

In this way, we may write

$$\mathcal{G}(t_2, t_1) = \lim_{\beta\to\infty} \frac{e^{-2\beta\Delta E}}{|\langle\langle 0|0\rangle|^2} \begin{cases} \langle 0|U(-i\beta, t_2)a(t_2)\,U(t_2, t_1)a^\dagger(t_1)\,U(t_1, i\beta)|0\rangle; & t_2 > t_1 \\ -\langle 0|U(-i\beta, t_1)a^\dagger(t_1)\,U(t_1, t_2)\,a(t_2)\,U(t_2, i\beta)|0\rangle; & t_1 > t_2 \end{cases}$$

Because of time displacement in variance of this expression, we may put $t_1 = 0$ and $t_2 = t$.

Notice that we assumed $\langle\langle 0|0\rangle\rangle = 1$, that is, we have:

$$\lim_{\beta\to\infty} \frac{e^{-2\beta\Delta E}}{|\langle\langle 0|0\rangle|^2} \langle 0|U(-i\beta, i\beta)|0\rangle = 1 \tag{3.87}$$

Upon inserting the expansion (3.84) for $U(t_2, t_1)$ into these expressions, a trivial identity may be made use of, the simplest example of which is

$$I = \int_a^b dx \int_a^x dy\, f(x)\, f(y) = \int_a^b dy \int_y^b dx\, f(x)\, f(y) = \int_a^b dx \int_x^b dy\, f(y)\, f(x)$$

or

$$I = \frac{1}{2} \int_a^b dx \int_a^b dy \begin{cases} f(x)\, f(y) & (\text{if } x > y) \\ f(y)\, f(x) & (\text{if } y > x) \end{cases}$$

$$= \frac{1}{2} \iint_a^b dx\, dy\, T(f(x), f(y))$$

where $T(f(x), f(y))$ stands for the ordered (according to the value of the argument) product of $f(x)$ and $f(y)$. The f's for different values of the argument need not commute, and in the application made here, $f \to V$, $V(t_1)$ and $V(t_2)$ in fact do *not* commute for $t_1 \neq t_2$. If the end points a, b are complex, then ordering is understood in terms of the relative position of x, y along the integration path from a to b. In a generalization of this to n-fold integrals, we have

$$\langle 0|U(-i\beta, i\beta)|0\rangle = \sum_{n=0}^{\infty} \frac{(-i)^n}{n!} \int_{i\beta}^{-i\beta} du_1 \ldots du_n \langle 0|T(V(u_1), V(u_2), \ldots V(u_n))|0\rangle$$

the ordering being defined in terms of the relative position of the variables $u_1, u_2 \ldots u_n$ on a path leading from $i\beta$ to $-i\beta$.

Another slight generalization of the argument makes it also applicable to the expression for $\mathcal{G}$:

$$\mathcal{G}(t) = \lim_{\beta\to\infty} \frac{e^{-2\beta\Delta E}}{|\langle\langle 0|0\rangle|^2}$$

$$\times \sum_{n=0}^{\infty} (-i)^n/n! \int_{i\beta}^{-i\beta} du_1 \ldots du_n \langle 0|T(V(u_1), V(u_2), \ldots V(u_n), a(t), a^\dagger(0))|0\rangle \tag{3.88}$$

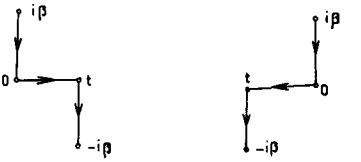

FIG. 3. Illustration path to illustrate ordering for $t > 0$ and $t < 0$. At a later stage it will be realized that the integration path may be changed so as to run from $-\infty \pm i\epsilon$ to $+\infty - i\epsilon$

The integration path runs here from $i\beta$ to 0, then to t, then from t to $-i\beta$ (Fig. 3). $a(t)$ and $a^\dagger(0)$ are included in the ordering; also the extra - sign occurring when $t < 0$ and hence $a^\dagger$ comes after a, is implied in the definition of $T(\ )$. (See Eq. 3.72.)

At this point, we invoke a result of Wick's theorem, stating that the vacuum expectation value of an ordered product is the sum of all possible total contraction.

Total contraction is a pairing off of all creation operators $a^\dagger(u_i)$ with an annihilation operator $a(u_j)$, and replacing this pair by

$$\pm \langle 0 | T(a(u_j),\ a^\dagger(u_i)) | 0 \rangle = \pm i\, \mathcal{G}_0(u_j - u_i)$$

For a given order n in the expression (3.88) for $\mathcal{G}$, there are a large number of possible patterns of contractions, graphically represented by diagrams. The elements of this description are

particle creation operator

particle annihilation operator

hole creation operator

hole annihilation operator

The operator $V(t)$ describes the processes:

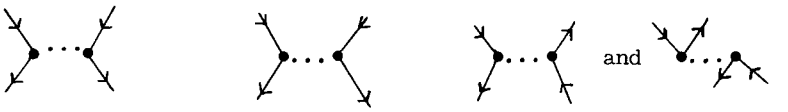

particle scattering hole scattering particle hole scattering

creation of particle hole pair annihilation of particle hole pair

Contraction: $\mathcal{G}_0(t_2 - t_1)$

Contraction $\mathcal{G}_0(t_1 - t_2)$

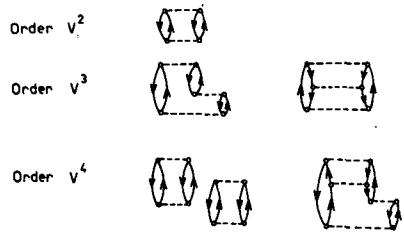

FIG. 4. Some diagrams in $\langle 0|U(=i,fi)|0\rangle$

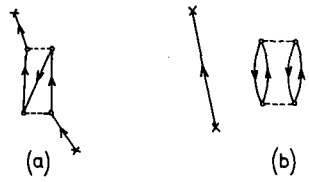

FIG. 5. Examples of diagrams in $\mathcal{G}$ (of order V^2): (a) linked diagram, (b) diagram with unlinked part

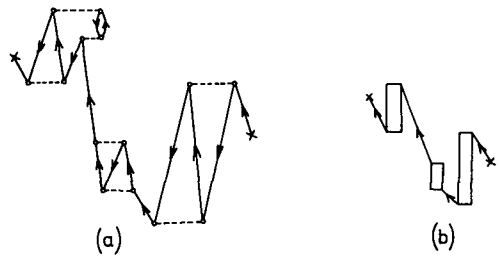

FIG. 6. (a) Example of a complex linked diagram; (b) its structure

As examples, we give in Fig. 4 some diagrams in $\langle 0|U(=i,fi)|0\rangle$.

Examples of diagrams in $\mathcal{G}$ (of order V^2) are shown in Figs 5a and b.

An example of a complex linked diagram and its structure is shown in Figs 6a and 6b.

The main points are now:

Call $G^{(n)}$ the contribution to $\mathcal{G}$ (discarding the factor $\exp[-2\beta\Delta E/|\langle\langle 0|0\rangle|^2]$) from all linked diagram of order n. The contribution of a diagram of order n with unlinked parts is then $\sum_{\ell=0}^{n-2} \mathcal{G}^{(\ell)} S^{(n-\ell)}$; that is, each unlinked part provides just a weight factor. Then

$$\mathcal{G} = \lim \frac{e^{-2\beta\Delta E}}{|\langle\langle 0|0\rangle|^2} \sum_n \left(\mathcal{G}^{(n)} + \sum_{\ell=0}^{n-2} \mathcal{G}^{(\ell)} S^{(n-\ell)}\right)$$

$$= \lim \frac{e^{-2\beta\Delta E}}{|\langle\langle 0|0\rangle|^2} \left(1 + \sum_{n=2}^{\infty} S^{(n)}\right) \sum_{\ell} \mathcal{G}^{(\ell)} \qquad (3.89)$$

It is easily seen that $(1 + \sum S^{(n)})$ is just $\langle 0 | U(-i\beta, i\beta | 0 \rangle$, and by Eq. (3.87) therefore

$$\mathcal{G} = \sum_{\ell=0}^{\infty} \mathcal{G}^{(\ell)} = \lim \sum_{\ell=0}^{\infty} \frac{(-i)^{\ell}}{\ell!} \int_{+i\beta}^{-i\beta} du_1 \ldots du_{\ell} \langle 0 | T(V(V(u_1), V(u_2) \ldots$$

$$\ldots V(u_{\ell}), a(t), a^{+}(0) | 0 \rangle_{\text{linked}} \qquad (3.90)$$

The general linked diagram has the structure indicated in Fig. 4a, and its contribution to g is therefore a sequence of convolutions of factor $\mathcal{G}_0(u, u')$ with 'boxes' $K^{(s)}(u, u')$ (as in Fig. 4b).

Abbreviating convolution by a dot, that is, writing

$$C = A \cdot B \quad \text{for} \quad C(t_2, t_1) = \int dt' \, A(t_2, t') \, B(t', t_1), \quad \text{etc.}$$

one has

$$\mathcal{G} = \mathcal{G}_0 + \mathcal{G}_0 \cdot (\sum K^{(s)}) \cdot \mathcal{G}_0 + \mathcal{G}_0 \cdot (\sum K^{(s)}) \cdot \mathcal{G}_0 (\sum K^{(t)}) \cdot \mathcal{G}_0 + \ldots$$

or

$$\mathcal{G} = \mathcal{G}_0 + \mathcal{G}_0 \cdot (\sum K^{(s)}) \cdot \mathcal{G}$$

Hence the self energy term $\sum$ is given by $\sum K^{(s)}$, the sum of all distinct 'boxes'.

A 'box' is characterized as a connected diagram, that is, it cannot be separated into two parts by cutting a single solid line; in other words, there is no decomposition $K = K' \cdot \mathcal{G}_0 \cdot K''$.

$\sum^{(n)}$, the sum of all $K^{(s)}$ of a given order n, is then contained in the term

$$\mathcal{G}_0 \cdot \sum^{(n)} \cdot \mathcal{G}_0$$

$$= \frac{(-i)^n}{n!} \int du_1 \ldots du_n \langle 0 | T(V(u_1), V(u_2) \ldots V(u_n), a(t), a^{\dagger}(0)) | 0 \rangle_{\substack{\text{linked and} \\ \text{connected}}}$$

To extract $\sum^{(n)}$ from this, observe that $a^{\dagger}(0)$ may contract with any $a(u_i)$ in $V(u_i)$. That contraction is

$$\langle 0 | T(a(u_i), a^{\dagger}(0)) | 0 \rangle = i \mathcal{G}_0(u_i, 0)$$

a(t) may contract with any $a^{\dagger}(u_j)$ in $V(u_j)$, and this gives a factor

$$\langle 0 | T(a(t), a^{\dagger}(u_j)) | 0 \rangle = i \mathcal{G}_0(t, u_j)$$

since u_i, u_j are different, but otherwise from any one of the n variables u_i, we get a factor n(n-1).

The removing of an $a(u_i)$ from $V(u_i)$ leaves the operator $J^\dagger(u_i)$ defined previously, and removal of an $a^\dagger(u_j)$ from $V(u_i)$ leaves a $J(u_j)$ (see Eqs (3.38, 3.39). Therefore

$$\mathcal{G}_0 \cdot \sum^{(n)} \cdot \mathcal{G}_0$$

$$= \frac{(-i)^{n-1}}{(n-2)!} \int_{-\infty}^{+\infty} dt' \int_{-\infty}^{+\infty} dt'' \, \mathcal{G}_0(t, t') \int_{-\infty}^{+\infty} du_1 \ldots du_{n-2} \langle 0 | T(V(u_1), V(u_2) \ldots$$

$$\ldots V(u_{n-2}), J(t'), J^\dagger(t'')) | 0 \rangle_{L.C.} \mathcal{G}_0 | t'', 0)$$

and $\sum$ itself is thus given by

$$(k' | \sum^{(n+2)}(t', t'') | k) = \frac{(-i)^{n+1}}{n!} \int_{-\infty}^{+\infty} dt_1 \ldots dt_n \langle 0 | T(V(t_1), \ldots V(t_n), J(k', t'), J^\dagger(k, t'')) | 0 \rangle_{L.C.}$$

We may now Fourier-transform this expression and get (we exploit here the time-translation invariance of $\sum$):

$$\sum^{(n+2)}(\omega) = \int_{-\infty}^{+\infty} dt \, e^{i\omega t - \eta |t|} \sum^{(n+2)}(t, 0)$$

or

$$\sum^{(n+2)}(\omega) = \frac{(-i)^{n+1}}{n!} \int_{-\infty}^{+\infty} dt \, e^{i\omega t - \eta |t|} \int_{-\infty}^{+\infty} dt_1 \ldots dt_n \langle 0 | T(V(t_1), \ldots V(t_n), J(t), J^\dagger(0)) | 0 \rangle_{L.C.}$$

At this point, a previously used algebraic identity is used in reverse, giving

$$\sum^{(n+2)}(\omega) =$$

$$\sum_{p+q+v=u} (-i)^{n+1} \left\{ \int_0^\infty dt \, e^{i(\omega + i\eta)t} \int_t^\infty du_1 \int_t^{u_1} du_2 \ldots \int_t^{u_{p-1}} du_p \int_0^t dw_1 \ldots \int_0^{w_{r-1}} dw_r \int_{-\infty}^0 dv_1 \int_{-\infty}^{v_1} dv_2 \ldots \int_{-\infty}^{v_{q-1}} dv_q \right.$$

$$\times \langle 0 | V(u_1) V(u_2) \ldots V(u_p) J(t) V(\omega_1) \ldots V(\omega_r) J^\dagger(0) V(v_1) \ldots V(v_q) | 0 \rangle_{L.C.}$$

$$- \int_{-\infty}^0 dt \, e^{i(\omega - i\eta)t} \int_0^\infty du_1 \int_0^{u_1} du_2 \ldots \int_0^{u_{p-1}} du_p \int_{-t}^0 dw_1 \ldots \int_{-t}^{w_{r-1}} dw_r \int_{-\infty}^t dv_1 \int_{-\infty}^{v_1} dv_2 \ldots \int_{-\infty}^{v_{q-1}} dv_q$$

$$\left. \langle 0 | V | u_1) \ldots V(u_p) J^\dagger(0) V(w_1) \ldots V(w_r) J(t) V(v_1) \ldots V(v_q) | 0 \rangle_{L.C.} \right\}$$

(3.91)

The time limits involved in these two multiple integrals are graphically illustrated as follows:

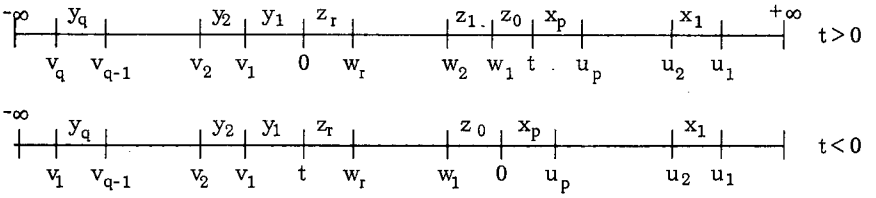

We now introduce, in place of the variables u, v, w, t, the n+1 positive intervals $x_1 \ldots x_p$, $z_0 \ldots z_r$, $y_i \ldots y_q$, illustrated above. Notice that

$$t = z_0 + z_1 t \ldots + z_r \quad \text{for } t > 0$$

and

$$t = -(z_0 + z_1 + \ldots + z_r) \quad \text{for } t < 0$$

All these intervals have now integration limits $0 < \ldots < \infty$. These intervals are the only variables occurring in the two matrix-elements of Eq. (3.91); indeed, we have:

$$\sum^{(n+2)}(\omega) = \sum_{p+q+r=n} (-i)^{n+1} \left\{ \int_0^\infty dx_1 \ldots dz_r \, e^{i(\omega+i\eta)(z_0+z_1+\ldots+z_r)} \right.$$

$$\langle 0 | V e^{-iH_0 x_1} V \ldots V e^{-iH_0 x_p} J e^{-iH_0 z_r} V \ldots V e^{-iH_0 z_r} J^\dagger e^{-iH_0 y_1} V \ldots e^{-iH_0 y_q} V | 0 \rangle_{L.C.}$$

$$- \int_0^\infty dx_1 \ldots dz_r \, e^{-i(\omega-i\eta)(z_0+z_1+\ldots+z_r)}$$

$$\left. \langle 0 | V e^{-iH_0 x_1} V \ldots V e^{-iH_0 x_p} J^\dagger e^{-iH_0 z_0} V \ldots V e^{-iH_0 z_r} J e^{-iH_0 y_1} V \ldots e^{-iH_0 y_q} V | 0 \rangle_{L.C.} \right\}$$

These integrations introduce the energy denominators, and give finally:

$$\langle k' | \sum^{(n+2)}(\omega) | k \rangle = \sum_{p+q+r=n} \left\{ \langle 0 | \left(V \frac{1}{-H_0} \right)^p J(k') \frac{1}{\omega - H_0 + i\eta} \left(V \frac{1}{\omega - H_0 + i\eta} \right)^r J^\dagger(k) \left(\frac{1}{-H_0} V \right)^q | 0 \rangle_{L.C.} \right.$$

$$\left. - \langle 0 | \left(V \frac{1}{-H_0} \right)^p J^\dagger(k) \frac{-1}{\omega + H_0 - i\eta} \left(V \frac{-1}{\omega + H_0 - i\eta} \right)^r J(k') \left(\frac{+1}{-H_0} V \right)^q | 0 \rangle_{L.C.} \right\}$$

the subscript C is a reminder that only those sequences of intermediate states which correspond to a connected diagram do contribute to $\sum$.

The lowest order term n=0 gives:

$$\sum^{(2)}(\omega) = \langle 0 | J(k') \frac{1}{\omega - H_0 + i\eta} J^\dagger(k) | 0 \rangle + \langle 0 | J^\dagger(k) \frac{1}{\omega + H_0 - i\eta} J(k') | 0 \rangle \qquad (3.92)$$

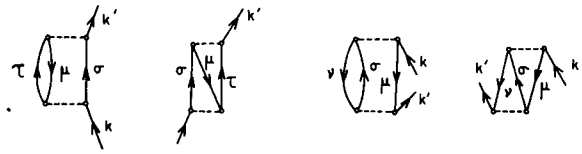

FIG. 7. Diagram of direct and exchange contributions of (a) first term, (b) second term of Eq. 3.92

We recall that the operators $J(k')$ and $J^\dagger(k)$ are given by

$$J(k') = \frac{1}{2} \sum_{\beta\gamma\delta} : a^\dagger_\beta (k'\beta | v_A | \gamma\delta) a_\delta a_\gamma :$$

$$J^\dagger(k) = \frac{1}{2} \sum_{\alpha\beta\delta} : a^\dagger_\alpha a^\dagger_\beta (\alpha\beta | v_A | k\delta) a_\delta : \qquad (3.93)$$

where we have introduced the anti-symmetrized matrix elements,

$$(\alpha\beta | v_A | \gamma\delta) = (\alpha\beta) V | \gamma\delta) - (\alpha\beta | V | \delta\gamma)$$

and therefore also a factor $\frac{1}{2}$ in (3.93).

The evaluation of (3.92) is now straightforward. To indicate the intermediate states involved in evaluating the two terms, we can draw the associated diagrams (see Fig. 7).

Algebraically, one has

$$(k' | \sum{}^{(2)}(\omega) | k) = \tfrac{1}{2} \sum_{\mu\sigma\tau} \frac{(k'_\mu | v_A | \sigma\tau)/\sigma\tau | v_A | k_\mu)}{\omega + \epsilon_\mu - \epsilon_\sigma - \epsilon_\tau + i\eta}$$

$$+ \tfrac{1}{2} \sum_{\mu\nu\sigma} \frac{(\mu\nu | v_A | k\sigma)(k'\sigma | v_A | \mu\nu)}{\omega + \epsilon_\sigma - \epsilon_\mu - \epsilon_\nu - i\eta} \qquad (3.94)$$

If we apply this to scattering problems, we must choose $\omega = e_k$; in that case, the first term in (3.94) is complex, the second real, since $\epsilon_k + \epsilon_\mu - (\epsilon_\mu + \epsilon_\tau)$ may have a zero, but $\epsilon_k + \epsilon_\sigma - (\epsilon_\mu + \epsilon_\nu)$ is > 0. The imaginary part of $\sum$ is then

$$\mathrm{Im}\,(\sum(\omega)) = -\frac{\pi}{2} \sum_{\sigma\mu\tau} \delta(\omega + \epsilon_\mu - \epsilon_\sigma - \epsilon_\tau)(k'\mu | v_A | \sigma\tau)(\sigma\tau | v_A | k\mu)$$

These formulae have been applied to the case of nuclear matter (in which case Σ has no space-dependence and is hence diagonal in k, k'); but no calculations of $(k' | \Sigma | k)$ using Hartree-Fock solutions for finite nuclei seem to exist yet. For a more detailed discussion of these matters, see Thouless [1] and Bell [2].

Another interesting question is the relation of the optical potential as defined here to the potential used to describe the energy averaged scattering

amplitudes. For these matters, we refer to the papers by Feshbach [3] and Brown [4].

REFERENCES

[1] THOULESS, D.J., The Quantum Mechanics of Many-body Systems, Academic Press, N.Y. (1961).
[2] BELL, T.S., "Formal theory of the optical model", in Lectures on the Many-body Problem, (CAIANELLO, E.R., Ed.), Academic Press, New York (1962).
[3] FESHBACH, H., The optical potential and its justification, A. Rev. nucl. Sci. 8 (1958) 49.
[4] BROWN, G.E., Rev. mod. Phys. 31 (1959) 893.

GENERAL BIBLIOGRAPHY

Textbooks: WU, T.-Y., CHMURA, T., Quantum Theory of Scattering, Prentice-Hall, N.J. (1962)
GOLDBERGER, M.L., WATSON, K.M., Collision Theory, John Wiley, New York (1964)
MOTT, N.F., MASSEY, H.S.W., The Theory of Atomic Collisions (3rd edn), Oxford University Press (1965)

Lecture notes: LOW, F., The Quantum Theory of Scattering, Brandeis University Summer School (1959)

Papers: LIPPMAN, B., SCHWINGER, J., Phys. Rev., 79 (1950) 469
GELL-MANN, M., GOLDBERGER, M., Phys. Rev. 91 (1953) 398
BRENIG, W., HAAG, R., Fortschritte der Physik 7 (1959) 183
NEWTON, R., J. math. Phys. 1 (196) 319

These papers are also found in the collection of Reprints:

ROSS, M. (ed.), Quantum Scattering Theory, Indiana University Press, Bloomington (1963)

CHAPTER 6

MULTICHANNEL SCATTERING FORMALISM AND THRESHOLD EFFECTS

L. FONDA

INTRODUCTION

The purpose of these notes is purely didactical. Most of the material covered here has been dealt with already in the literature. The reader is supposed to have good knowledge of quantum mechanics and some familiarity with ordinary potential scattering (see, for example, Chapter 5).

In sections 1-4 the general multichannel scattering formalism is considered in detail. Scattering systems are covered for which a Hamiltonian can be defined and can be split into two parts, one of which describes the free and internal motion of the fragments of a given configuration. The splitting of the Hamiltonian varies from one configuration to another. Accordingly, the formalism is general enough to cover any kind of nuclear reaction such as stripping, pick-up, rearrangement collisions and nucleon production. In section 4 a simple proof of the unitarity of the S-matrix is given.

Sections 5-7 give a brief account of the anomalies which show up in the scattering and reaction cross-sections as functions of energy at the opening of a new inelastic process. These effects usually amount to a cusp ('Wigner cusp') or to a rounded step, due to the sudden removal of flux from the incident beam at the onset of the new inelastic cross-section starting with infinite slope as a function of energy. No cusps or rounded steps appear, however, if Coulomb forces are present in the newly opened channel. In the case of Coulomb repulsion no anomaly is observed, while for Coulomb attraction a finite jump appears in the various old cross-sections due to the non-zero value of the new inelastic cross-section at its own threshold. The foregoing applies only when the new channel is a two-body channel. If, however, the new channel contains three or more particles no anomaly appears in the scattering and reaction cross-sections at its threshold energy.

The observation of threshold effects, as will be discussed below, turns out to be useful for the experimental determination of: relative parities and spins of the reaction products, scattering phase shift at the threshold for the new channel and cross-sections for processes which are often not feasible experimentally. They can even be used in the search for new particles.

The author is at the Istituto di Fisica Teorica dell' Università, Trieste.

Threshold effects were first pointed out by Wigner [1]. Their physical implications have been investigated by various authors such as Breit, Baz, Newton, Fonda, Okun, Adair, Delves and others. A list can be found in the review article by Fonda [2] and in the recent book by Newton [3], where proper reference is made to the original contributions.

1. GENERAL REMARKS

When we have a beam of particles focused on a given target, experimentally part of the beam will be found unaltered on the other side of the target while the rest will be found deviated in all directions, having possibly changed its characteristics (such as spin, type and number of particles, etc.). The knowledge of the intensity and characteristics of the deviated part of the beam in the various directions furnishes one of the most powerful means of obtaining information on the nature of the interparticle interactions and on the structure of the impinging and scattered particles. We shall now try to describe this kind of experiment by means of quantum mechanics.

We first point out that the experimenter must arrange the experimental apparatus in such a way that no interference occurs between different particles of the beam. We can therefore suppose that one particle at a time reaches the target. Besides, the experimental apparatus is set up in such a way that the particle takes an extremely long time to get on the target, i.e. in the region of interaction, so that by abstraction we can suppose that we had shot it in the remote past. If $\Psi^{(i)}(t)$ is the state associated with the physical system at the instant t of time we can then write:

$$\Psi^{(i)}(t) \underset{t \to -\infty}{\sim} \phi^{(i)}(t) \tag{1.1}$$

$\Psi^{(i)}(t)$ and $\phi^{(i)}(t)$ are unit vectors in the Hilbert space. The index (i) means a particular initial configuration. Of course, the "extremely long time" mentioned above is measured on atomic or sub-atomic scale by taking as reference, for example, the time of transit of the considered particle through the region of interaction. We shall suppose that the 'wave packet' $\phi^{(i)}(t)$ and the target have been prepared by the experimenter in such a way that when $\phi^{(i)}(t)$ gets on the target it overlaps at most one of the particles there. The initial state is then a two-particle state and we can forget about the other particles of the target which do not take part in the scattering process. Of course, the target, from time to time, must be regenerated from the loss of its particles which recoil out as a result of the collision process.

The evolution in time of $\phi^{(i)}(t)$ will be different from the evolution of $\Psi^{(i)}(t)$. In fact the last state suffers from the presence of the mutual interaction between the incoming and the target particles. $\Psi^{(i)}(t)$ being governed by the Hamiltonian H, $\phi^{(i)}(t)$ will be governed by the Hamiltonian obtained from H, via suppression of the mutual interaction mentioned above. We imagine then that H can be split into two terms K_i and V_i, such that if K_i were the entire Hamiltonian the impinging and the target particles would have the same internal structure and suffer no scattering one from the other. V_i is then the representative of the mutual inter-

particle interactions, while K_i describes the free and the internal motion of the fragments in the configuration considered. In the Schrödinger picture of motion, $\Psi^{(i)}(t)$ and $\phi^{(i)}(t)$ satisfy the following Schrödinger equations:

$$i\hbar \frac{d\Psi^{(i)}(t)}{dt} = H\Psi^{(i)}(t) \tag{1.2}$$

$$i\hbar_i \frac{d\phi^{(i)}(t)}{dt} = K_i \phi^{(i)}(t) \tag{1.3}$$

H and K_i are self-adjoint operators. In the language common to physicists, their eigenstates therefore form complete systems of vectors in Hilbert space.

As time goes on, the particle crosses the interaction region and gives rise to a reaction whose products are finally analysed by the experimenter very far away from the target. So, by abstraction again, we can say that experimental measurements are made on the state evolved from $\Psi^{(i)}(t)$ up to the distant future. Superposition principle tells us that the final state will be partly that evolved from the initial without having undergone scattering and partly a state which is the result of the interparticle interactions. We write:

$$\Psi^{(i)}(t) \underset{t \to +\infty}{\sim} \phi^{(i)}(t) + \chi^{(i)}(t) \tag{1.4}$$

$\chi^{(i)}(t)$ will be a superposition of all possible scattered states and, in general, will not evolve with a given Hamiltonian as $\phi^{(i)}(t)$ does. In fact, at $t \to +\infty$, besides the configuration containing the same, possibly energetically excited fragments of the initial state, we can have configurations belonging to different splittings of the total Hamiltonian H. In these configurations the free motion of the fragments is governed by $K_f \neq K_i$ and the number of fragments can even be greater than two.

There are many problems where the splitting of H is trivial, complicated situations may, however, arise when the definition of a non-interacting system cannot be given unambiguously. Quantum meson theory is an example: nucleons, even though far away from each other, interact indefinitely with their own meson field giving rise to the so called self-effects. In this kind of problem there are persistent effects in the interaction operators which do not vanish as the particles depart from one another. In what follows we shall not deal with systems of this kind and shall consequently impose due restrictions on the interaction operators to exclude the occurrence of persistent effects. Also, not being concerned with relativistic covariance, we shall work throughout in the centre-of-mass reference system. In this way the formalism is slightly simplified. The Schrödinger picture of motion will be used.

2. DETERMINATION OF THE SCATTERING AMPLITUDE

Suppose that various splittings of H are possible:

$$H = K_j + V_j \,. \qquad j = 1, 2, \ldots$$

For each splitting there is a corresponding configuration in which K_j is the Hamiltonian for the fragments when they are separated and do not interact, while V_j describes their mutual interaction. We assume that K_j has only a continuous spectrum bounded from below. Let us consider the eigenvalue problem for K_j

$$K_j \cdot \bar{\varphi}_j(a) = E_a \cdot \bar{\varphi}_j(a) \tag{2.1}$$

Here a is a set of continuous and discrete quantum numbers, necessary to specify $\bar{\varphi}_j$ completely. a varies with j. The $\bar{\varphi}$'s are normalized according to

$$(\bar{\varphi}_j(a), \bar{\varphi}_j(a')) = \delta(a - a') \tag{2.2}$$

From the $\bar{\varphi}_j$'s we pick up the eigenstates $\varphi_j(a)$ of K_j which are given by the product of the plane waves of the relative motion of the given fragments times the internal wave functions describing their bound states. These states $\varphi_j(a)$ define a 'channel' and will be referred to as 'channel eigenfunctions'. Channels will differ either because, belonging to the same K_j, they describe different bound states of the fragments, or because they belong to different splittings of H. The K_j's have continuous spectra which start at different energies $\bar{E}_j$. Due to the supposed absence of persistent effects, there is one K, call it K_1, whose continuous spectrum coincides with the continuous spectrum of H. All the other K's have energies $\bar{E}_j$ greater than E_1. The $\bar{E}_j$ are threshold energies for channels. However, we have more thresholds if the fragments belonging to K_j admit stable excited states. It goes without saying that, while the set $\{\bar{\varphi}_j(a)\}$ is complete, the set $\{\varphi_j(a)\}$ is not [1]. In what follows the sub-index j of the channel eigenfunctions will, for simplicity, label the channels (rather than only the possible splittings of H as done above).

$\delta(a - a')$ is a product of δ-functions and Kronecker δ's. The integral sign over a will be a symbol to represent the integrations over the continuous variables and the summations over the discrete ones. Sometimes we shall give separate consideration to the total energy variable contained in a, then we shall call α_a the aggregate of commuting observables which commute with K_j and together with it form a complete set. We shall write

$$da = dE_a \, d\alpha_a \,, \tag{2.3}$$

$$\delta(a - a') = \delta(E_a - E_{a'}) \, \delta(\alpha_a - \alpha_{a'})$$

[1] To clarify these ideas, take the case of proton-deuteron scattering. We can define two splittings of the total Hamiltonian, $H = K_1 + V_1$ and $H = K_2 + V_2$. K_2 is the kinetic energy of the three nucleons in the centre of mass system, K_1 is instead given by $K_1 = K_2 + V$ where V is the proton-neutron potential. If the continuous spectrum of K_2 starts from zero, that of K_1 will clearly start at $-|B|$, and will coincide with the spectrum of H. B is the binding energy of the deuteron. $\varphi_1(a)$ are the eigenstates of K_1 which are the product of the deuteron bound state wave function times the plane waves of the proton-deuteron relative motion. The set $\{\bar{\varphi}_1(a)\}$ contains the set $\{\varphi_1(a)\}$ and also eigenstates which describe the three nucleons completely unbound in the potential V. The set $\{\varphi_1(a)\}$ is clearly not complete. Instead, the set $\{\varphi_2(a)\} \equiv \{\bar{\varphi}_2(a)\}$ happens to be complete. We could have more than two channels if the deuteron had a stable excited state of energy B^*, in that case we can, in fact, define a set $\{\varphi'_1(a)\}$ of eigenstates of K_1 to describe this situation. Of course, the set $\{\varphi'_1(a)\}$ would be contained in $\{\bar{\varphi}_1(a)\}$ and would be orthogonal to the set $\{\varphi_1(a)\}$. Energetically we would then have three thresholds, precisely at $-|B|$, $-|B^*|$ and zero.

Next we introduce the set $\{\psi_j^{(\pm)}(a)\}$ of eigenstates of H satisfying:

$$\psi_j^{(\pm)}(a) = \varphi_j(a) + (E_a \pm i\epsilon - K_j)^{-1} V_j \quad \psi_j^{(\pm)}(a)$$

$$= \varphi_j(a) + (E_a \pm i\epsilon - H)^{-1} V_j \varphi_j(a) \tag{2.4}$$

(the limit $\epsilon \to 0^+$ is understood).
As can be easily shown, the $\psi^{(+)}$'s and $\psi^{(-)}$'s have the same normalization of their corresponding φ's:

$$(\psi_j^{(+)}(a),\ \psi_j^{(+)}(a')) = (\psi_j^{(+)}(a),\ \varphi_j(a')) + (\psi_j^{(+)}(a),\ (E_{\alpha'} + i\epsilon - H)^{-1} V_j \varphi_j(a'))$$

$$= (\varphi_j(a),\ \varphi_j(a')) + ((E_a + i\epsilon - K_j)^{-1} V_j \psi_j^{(+)}(a),\ \varphi_j(a'))$$

$$+ (\psi_j^{(+)}(a),\ (E_{a'} + i\epsilon - E_a)^{-1} V_j \varphi_j(a'))$$

$$= (\varphi_j(a),\ \varphi_j(a')) \tag{2.5}$$

The same holds for the $\psi^{(-)}$'s.

We now want to describe the following situation: the incoming and the final particles are fragments belonging to certain splittings of H. This defines a reaction from the initial channel i to a final channel f. The initial state $\phi^{(i)}$ will then be chosen as follows:

$$\phi^{(i)}(t) = \int da\ e^{-iE_a t/\hbar} \quad \varphi_i(a)(\varphi_i(a),\ \phi^{(i)}(0)) \tag{2.6}$$

Of course, the state $\phi^{(i)}(t)$ satisfies the time-dependent Schrödinger equation with Hamiltonian K_i. $\chi^{(i)}(t)$ is the unknown of our scattering problem. $\phi^{(i)}(t)$ is in fact perfectly known, it is the state prepared by the experimenter in the remote past. Equation (1.1) is therefore the boundary condition for the state vector $\Psi^{(i)}(t)$ satisfying the first order differential Eq. (1.2).

To evaluate $\chi^{(i)}(t)$ we have to take the limit of $\Psi^{(i)}(t)$ for $t \to +\infty$. This procedure will make sense once we know $\Psi^{(i)}(t)$ for finite times. Therefore the first step to take is to see how $\Psi^{(i)}(t)$ builds up from $\phi^{(i)}(t)$ at finite times.

By Eq. (1.1) we mean that:

$$\lim_{t \to -\infty} \left|\left| \Psi^{(i)}(t) - \phi^{(i)}(t) \right|\right| = 0$$

that is, strong convergence of $\Psi^{(i)}(t)$ to $\phi^{(i)}(t)$ is assumed.[2] We have

---

[2] For $\psi(t)$ to converge strongly to $\phi(t)$, it must converge weakly to zero. This is just what the experimenter realizes in practice: $\lim_{t \to \pm\infty} \psi(t, \vec{r}) = 0$ for any fixed $\vec{r}$, relative distance vector of the final ($t \to +\infty$) or initial ($t \to -\infty$) fragments. See also H. Ekstein, Phys. Rev. 101 (1956) 880.

$$\left|\left| e^{-iHt/\hbar}\, \Psi^{(i)}(0) - \phi^{(i)}(t) \right|\right| = \left|\left| \Psi^{(i)}(0) - e^{iHt/\hbar}\, \phi^{(i)}(t) \right|\right|$$

Therefore Eq. (1.1) is equivalent to

$$\lim_{t \to -\infty} e^{iHt/\hbar}\, \phi^{(i)}(t) = \Psi^{(i)}(0) \tag{2.7}$$

Let us compute the left-hand side

$$\lim_{t \to -\infty} e^{iHt/\hbar}\, \phi^{(i)}(t) = \lim_{t \to -\infty} \int da\, e^{i(H - E_a)t/\hbar}\, \varphi_i(a)(\varphi_i(a), \phi^{(i)}(0))$$

$$= \int da \left[1 + (E_a + i\epsilon - H)^{-1} (H - E_a) \right] \varphi_i(a)(\varphi_i(a), \phi^{(i)}(0))$$

$$= \int da\, \psi_i^{(+)}(a)(\varphi_i(a), \phi^{(i)}(0)) \tag{2.8}$$

where we have used the relation (see Ekstein, footnote 2)

$$\lim_{t \to \pm \infty} e^{iAt}\, g = \lim_{\epsilon \to 0^+} \left[1 - (A \pm i\epsilon)^{-1} A \right] g \tag{2.9}$$

g being independent of time.

From Eq. (2.8) we get the state vector at the generic time t:

$$\Psi^{(i)}(t) = \int da\, e^{-iE_a t/\hbar}\, \psi_i^{(+)}(a)(\varphi_i(a), \phi^{(i)}(0)) \tag{2.10}$$

Now that we have determined $\Psi^{(i)}(t)$ through (1.1) we could take the limit $t \to +\infty$ on it to determine $\chi^{(i)}(t)$. The direct knowledge of $\chi^{(i)}(t)$ is, however, not necessary. In fact, as we shall see in the next section, what is needed to compute cross-sections is the limit for $t \to +\infty$ of the amplitudes:

$$A_{fi} \equiv \lim_{t \to +\infty} (\phi^{(f)}(t),\ \chi^{(i)}(t)) = \lim_{t \to +\infty} (\phi^{(f)}(t),\ \Psi^{(i)}(t) - \phi^{(i)}(t)) \tag{2.11}$$

Here $\phi^{(f)}(t)$ is a 'trial' normalized state vector used by the experimenter to make observations on our scattering system. It evolves with the Hamiltonian K_f and is defined by:

$$\phi^{(f)}(t) = \int db\, e^{-iE_b t/\hbar}\, \varphi_f(b)(\varphi_f(b),\ \phi^{(f)}(0)) \tag{2.12}$$

$\phi^{(f)}$, by construction, has projections only on channel f.

To evaluate Eq.(2.11), it is convenient to introduce the normalized vector $\Psi_-^{(f)}(t)$, solution of the time dependent Schrödinger equation (1.2) with boundary condition:

$$\lim_{t\to+\infty} \left|\left|\Psi_-^{(f)}(t) - \phi^{(f)}(t)\right|\right| = 0 \tag{2.13}$$

Building $\Psi_-^{(f)}(t)$ at finite times from Eq.(2.13) is a straight-forward process. We have only to follow the very same procedure employed for the derivation of Eq.(2.10). We get:

$$\Psi_-^{(f)}(t) = \int db\, e^{-iE_b t/\hbar}\, \psi_f^{(-)}(b)(\varphi_f(b),\, \phi^{(f)}(0)) \tag{2.14}$$

Application of the Schwartz inequality shows that:

$$\left|(\Psi_-^{(f)}(t) - \phi^{(f)}(t),\ \Psi^{(i)}(t) - \phi^{(i)}(t))\right| \leqslant \left|\left|\Psi_-^{(f)}(t) - \phi^{(f)}(t)\right|\right|\ \left|\left|\Psi^{(i)}(t) - \phi^{(i)}(t)\right|\right|$$

so that, using Eq.(2.13), we can write for the scattering amplitude:

$$A_{fi} = \lim_{t\to+\infty} (\Psi_-^{(f)}(t),\ \Psi^{(i)}(t) - \phi^{(i)}(t)) \tag{2.15}$$

Substituting in Eq.(2.15) the equations for $\Psi_-^{(f)}(t)$, $\Psi^{(i)}(t)$ and $\phi^{(f)}(t)$ we obtain:

$$A_{fi} = \lim_{t\to+\infty} \int dbda\, \frac{e^{-i(E_a - E_b)t/\hbar}}{E_a - E_b + i\epsilon}\, (\phi^{(f)}(0),\, \varphi_f(b))$$

$$\times\, (\psi_f^{(-)}(b),\, V_i\, \varphi_i(a))(\varphi_i(a),\, \phi^{(i)}(0))$$

By application of the well known formula:

$$\lim_{\epsilon\to 0^+} \int_{-|M|}^{+|N|} dx\, \frac{e^{-ixt}}{x + i\epsilon}\, f(x) = \begin{cases} 0 & ,\quad t\to-\infty \\ -2i\pi f(0), & t\to+\infty \end{cases} \tag{2.16}$$

we finally have for the scattering amplitude:

$$A_{fi} = -2i\pi \int db\, da\, \delta(E_a - E_b)\, (\phi^{(f)}(0),\, \varphi_f(b))$$

$$\times\, (\psi_f^{(-)},\, V_i\, \varphi_i(a))(\varphi_i(a),\, \phi^{(i)}(0)) \tag{2.17}$$

We define then as T-matrix the quantity:

$$T_{fi}(b,a) \equiv (\psi_f^{(-)}(b),\ V_i\,\varphi_i(a)) \tag{2.18}$$

On the energy shell it satisfies:

$$\begin{aligned} T_{fi}(b,a) &= \left(\left[1+(E_b - i\epsilon - H)^{-1} V_f\right]\varphi_f(b),\ V_i\,\varphi_i(a)\right) \\ &= \left(\varphi_f(b),\ \left[V_i + V_f(E_a + i\epsilon - H)^{-1} V_i\right]\varphi_i(a)\right) \\ &= \left(\varphi_f(b),\ V_f\left[1+(E_a + i\epsilon - H)^{-1} V_i\right]\varphi_i(a)\right) \\ &= \left(\varphi_f(b),\ V_f\,\psi_i^{(+)}(a)\right),\quad E_a = E_b \end{aligned} \tag{2.19}$$

where use has been made of the fact that on the energy shell:

$$(\varphi_f(b),\ V_i\,\varphi_i(a)) = (\varphi_f(b),\ V_f\,\varphi_i(a)),\quad E_a = E_b \tag{2.20}$$

In fact if $E_a = E_b$ we have:

$$(\varphi_f(b),\ V_i\,\varphi_i(a)) = (\varphi_f(b),[H-K_i]\,\varphi_i(a)) = (\varphi_f(b),\ [H-E_a]\,\varphi_i(a))$$

$$= ([H-E_b]\,\varphi_f(b),\ \varphi_i(a)) = ([H-K_f]\varphi_f(b),\ \varphi_i(a))$$

from which Eq. (2.20) follows.

3. EVALUATION OF CROSS-SECTIONS

The probability of finding the scattered system in the 'trial' normalized state $\phi^{(f)}(t)$ for $t \to +\infty$ is:

$$\lim_{t\to+\infty} \left|(\phi^{(f)}(t), \Psi^{(i)}(t))\right|^2 \tag{3.1}$$

$\{\phi^{(f)}(t)\}$ is a set of normalized vectors used by the experimenter to make observations on our scattering system. In this set we shall also have the initial state $\phi^{(i)}(t)$. We assume that the experimenter is smart enough to build wave packets $\phi^{(f)}(t)$ for large times which, unless $\phi^{(f)}(t) \equiv \phi^{(i)}(t)$ (forward elastic scattering), do not overlap with $\phi^{(i)}(t)$. Note however that,

if channel f is different from channel i, then the ϕ's are already asymptotically orthogonal. In fact, let us consider the scalar product:

$$(\phi^{(f)}(t),\ \phi^{(i)}(t)) = \int \mathrm{d}b\mathrm{d}a\, e^{i(E_b - E_a)t/\hbar} (\varphi_f(b),\ \varphi_i(a)) \times (\phi^{(f)}(0),\ \varphi_f(b))(\varphi_i(a),\ \phi^{(i)}(0))$$

If the splitting of the Hamiltonian is the same in channel i and in channel f, then from the hypothesis that the channels are different we have that the fragments in channel f have internal (bound) states orthogonal to those of channel i (the channels are said to be orthogonal in this case) so that $(\varphi_f(b), \varphi_i(a)) = 0$ and

$$(\phi^{(f)}(t),\ \phi^{(i)}(t)) = 0, \text{ orthogonal channels f and i.}$$

If the splitting of the Hamiltonian is not the same in the two channels considered, then $(\varphi_f(b),\ \varphi_i(a))$ is in general different from zero. Moreover, φ_f and φ_i being eigenvectors of different operators (K_f and K_i, respectively), no δ-function on the energy will be produced by this scalar product so that

$$(\phi^{(f)}(t),\ \phi^{(i)}(t)) \neq 0, \quad \text{non-orthogonal channels f and i}$$

Application of the Riemann-Lebesgue lemma[3] in the limits $t \to \pm\infty$ now gives the desired result

$$\lim_{t \to \pm\infty} (\phi^{(f)}(t),\ \phi^{(i)}(t)) = 0, \quad \text{channel f} \neq \text{channel i} \tag{3.2}$$

From the foregoing discussion it follows that in Eq. (3.1) we can substitute $\Psi^{(i)}(t) - \phi^{(i)}(t)$ for $\Psi^{(i)}(t)$ for all $\phi^{(f)}(t) \neq \phi^{(i)}(t)$:

$$P_{fi} = |A_{fi}|^2 \tag{3.3}$$

$$A_{fi} = \lim_{t \to +\infty} (\phi^{(f)}(t),\ \Psi^{(i)}(t) - \phi^{(i)}(t))$$

To obtain information about the forward elastic scattered part of the system, the experimenter will, however, not use Eq. (3.1), since this is tantamount to a measurement of the total flux there. This is clearly wrong, since the total flux in the forward direction contains contributions both from the incoming non-deviated beam and from its scattered part. Instead, the experimenter will define the limit of Eq. (3.3) to the forward direction as the forward elastic-scattered part of the system. We see therefore, that, after the correct interpretation of forward elastic scattering, P_{fi} represents, as defined by Eq. (3.3), the correct scattering probability irrespective of the chosen final state, i.e. also if $\phi^{(f)}(t) \equiv \phi^{(i)}(t)$.

---

[3] E.T. Whittaker and G.N. Watson, A Course of Modern Analysis, Cambridge Univ. Press, London and New York (1958) 172. In this book the interval of integration is assumed to be finite, but it is easy to see that the same result holds for an infinite interval, provided the integrand is a continuous function of limited total fluctuation.

We now construct $\phi^{(f)}(t)$ as follows:

$$\phi^{(f)}(t) = e^{-iK_f t/\hbar} \frac{1}{(\Delta b_f)^{1/2}} \int_b^{b+\Delta b_f} db'\, c_f(b')\, \varphi_f(b')$$

$$= e^{-iK_f t/\hbar} \frac{1}{(\Delta E\, \Delta\alpha_f)^{1/2}} \int_E^{E+\Delta E} dE' \int_{\alpha_f}^{\alpha_f+\Delta\alpha_f} d\alpha'\, c_f(b')\varphi_f(b') \tag{3.4}$$

$c_f(b') \equiv (\varphi_f(b'), \phi^{(f)}(0))(\Delta E \Delta\alpha_f)^{1/2}$ satisfies to:

$$(\Delta b_f)^{-1} \int db' \left| c_f(b') \right|^2 = 1 \tag{3.5}$$

and is supposed to be a continuous function of b'. We say then that P_{fi} is the probability of finding for $t \to +\infty$ the scattered system in channel f with quantum numbers between b and $b+\Delta b_f$.

By definition P_{fi} is given by:

$$P_{fi} = \nu \Delta\sigma_{fi} \tag{3.6}$$

$\Delta\sigma_{fi}$ is the cross-section for the given reaction $i \to f$ and νdS the probability that the initial particle crosses (at the time $t = 0$) the surface dS perpendicular to the direction of its motion relative to the target particle. ν will then be given in terms of the initial state $\phi^{(i)}(0)$. By making the experiment over and over, by continuously sending one wave packet after the other, by multiplying Eq. (3.6) times ΔN, the number of initial particles which hit the target during the interval of time Δt, and dividing by Δt, we get:

$$\Delta i_f = i_0 \Delta\sigma_{fi}$$

which is the usual formula for the cross-section. i_0 is the initial flux, i.e. the number of particles which hit the target per unit time and unit area, and Δi_f is the number of scattered particles which per unit time are detected in channel f with quantum numbers between b and $b+\Delta b_f$.

$\phi^{(i)}$ is the tensor product of three vectors, one $\phi^{(i)}_{rel}$ describing the relative motion of the initial particles, one being the product of the bound state wave functions of the fragments in channel i, and one representing the intrinsic degrees of freedom such as spin and isotopic spin. Using $\phi^{(i)}_{rel}$ we easily get for ν:

$$\nu = \int_{-\infty}^{+\infty} dz \left| \phi^{(i)}_{rel}(\vec{r}) \right|^2 \tag{3.7}$$

where $\vec{r} = \vec{r}(x, y, z)$ is the relative distance vector of the initial particles. The z-axis has been chosen along the direction of the incident beam. ν is a function of the point P(x, y). We point out, however, that Eq. (3.6) makes sense only if ν is, to a very good approximation, constant over

the region of interaction. To realize this condition, the initial state $\phi_{rel}^{(i)}$ must be sufficiently sharp in momentum space. We write it as follows:

$$\phi_{rel}^{(i)}(\vec{r}) = \frac{1}{(\Delta E\,\Delta\alpha_i)^{1/2}} \int_E^{E+\Delta E} dE' \int_{\alpha_i}^{\alpha_i+\Delta\alpha_i} d\alpha'\, c_i(E',\alpha') \frac{e^{i\vec{k}'_i\cdot\vec{r}}}{(2\pi)^{3/2}} \tag{3.8}$$

where $\vec{k}_i$ is the relative momentum of the two initial particles. We introduce Eq. (3.8) into Eq. (3.7) and integrate over z. $c_i(E',\alpha')$ is such that for our purposes $k'_{ix} \approx 0$, $k'_{iy} \approx 0$ and $k'_{iz} \approx k'_i$. We get:

$$\nu = \frac{1}{\Delta E\,\Delta\alpha_i (2\pi)^2} \int_E^{E+\Delta E} dE'' \int_E^{E+\Delta E} dE' \int_{\alpha_i}^{\alpha_i+\Delta\alpha_i} d\alpha'' \int_{\alpha_i}^{\alpha_i+\Delta\alpha_i} d\alpha'\, c_i^*(E'',\alpha'') c_i(E',\alpha') \delta(k'_i - k''_i)$$

Application of the integral theorem of mean value gives:

$$\nu = \frac{\Delta\alpha_i}{(2\pi)^2} c_i^*(E_1,\alpha_{2i}) c_i(E_1,\alpha_{1i}) \left.\frac{dE'}{dk'_i}\right|_{E'=E_1} \tag{3.9}$$

where by $f(E_1,\alpha_{2i},\alpha_{1i})$ we mean the average value of $f(E',\alpha'',\alpha')$ over the region of integration.

Let us now evaluate the left-hand side of Eq. (3.6). Using Eq. (2.17) and applying again the mean value theorem we get:

$$P_{fi} = (2\pi)^2 \Delta\alpha_i \Delta\alpha_f \times c_f^*(E_1,\alpha_{1f}) c_f(E_2,\alpha_{2f}) c_i^*(E_2,\alpha_{3i}) c_i(E_1,\alpha_{4i}) T_{fi}(E_1\alpha_{1f};E_1\alpha_{4i}) T_{fi}^*(E_2\alpha_{2f};E_2\alpha_{3i}) \tag{3.10}$$

The ratio of Eq. (3.10) to Eq. (3.9) furnishes the differential cross-section. The expression that one obtains is just the quantity which the experimenter measures and which depends critically on the forms of the wave packets used and on the fineness of the experimental techniques. We can, however, obtain a result of universal value, that is, the result that an ideal experimenter would get taking the limits ΔE, $\Delta\alpha_i$, $\Delta\alpha_f \to 0$. Due to the supposed continuity of the c's and of the T-matrix being in the limits: $\alpha_{1i} = \alpha_{2i} = \alpha_{3i} = \alpha_{4i} \equiv \alpha_i$, $\alpha_{1f} = \alpha_{2f} \equiv \alpha_f$, $E_1 = E_2 \equiv E$ and, due to (3.5), $|c_f|^2 = 1$, we finally get:

$$\frac{d\sigma_{fi}}{d\alpha_f} = (2\pi)^4 \left|T_{fi}(E\alpha_f; E\alpha_i)\right|^2 \left(\frac{dE}{dk_i}\right)^{-1} \tag{3.11}$$

$d\sigma_{fi}$ is the cross-section for the reaction channel i → channel f, at the energy E, in which the final products obtain quantum numbers between α_f and $\alpha_f + d\alpha_f$.

The computation of dE/dk_i is very simple. In the centre-of-mass system $|\vec{k}_i| = |\vec{k}_{1i}| = |\vec{k}_{2i}|$, so that:

$$\frac{dE}{dk_i} = \hbar \left[\frac{p_i c^2}{(m_{1i}^2 c^4 + p_i^2 c^2)^{1/2}} + \frac{p_i c^2}{(m_{2i}^2 c^4 + p_i^2 c^2)^{1/2}} \right] = \hbar |\vec{v}_{1i} - \vec{v}_{2i}| = \hbar v_i \tag{3.12}$$

m_{1i} and m_{2i} are the rest masses of the particles in channel i. Let us now consider the case of two final particles. Then, using Eq.(3.12), we have:

$$d\alpha_f \equiv k_f^2 \frac{dk_f}{dE_f} \, d\Omega_f = \frac{p_f^2}{\hbar^3 v_f} \, d\Omega_f$$

Eq.(3.12) tells us that:

$$p_f = \omega_f v_f \tag{3.13}$$

with ω_f given by:

$$\omega_f = \frac{(m_{1f}^2 + p_f^2/c^2)^{1/2} (m_{2f}^2 + p_f^2/c^2)^{1/2}}{(m_{1f}^2 + p_f^2/c^2)^{1/2} + (m_{2f}^2 + p_f^2/c^2)^{1/2}} \tag{3.14}$$

We then get:

$$d\alpha_f = \frac{\omega_f^2 v_f}{\hbar^3} \, d\Omega_f$$

For the differential cross-section in the centre-of-mass system we then have:

$$\frac{d\sigma_{fi}^{(2)}}{d\Omega_f} = \left(\frac{2\pi}{\hbar} \right)^4 \omega_f^2 \frac{v_f}{v_i} |T_{fi}|^2 \tag{3.15}$$

where the index (2) stands for two particle → two particle reactions. Had we used non-relativistic kinematics we would have found the same formula (3.15) with the reduced mass μ_f substituted for ω_f.

If the final state is an N-particle state, then:

$$dE \, d\alpha_f \equiv d^3k_{1f} d^3k_{2f} \ldots d^3k_{N-1,f}$$

Note that the momentum $\vec{k}_N$ of the N-th particle, in the considered centre-of-mass system, is a function of the remaining momenta. So for $d\alpha_f$ we get:

$$d\alpha_f = d^3k_{1f} \, d^3k_{2f} \ldots d^3k_{N-2,f} \, d\Omega_{N-1,f} \, k_{N-1,f}^2 \left(\frac{dE}{dk_{N-1,f}} \right)^{-1} \tag{3.16}$$

where the derivative $dE/dk_{N-1,f}$ is evaluated by keeping $\vec{k}_{1f}$, $\vec{k}_{2f}$, ... $\vec{k}_{N-2,f}$ and the solid angle $\Omega_{N-1,f}$ fixed.

4. UNITARITY OF THE S-MATRIX AND OPTICAL THEOREM

The proof of the unitarity of the S-matrix is trivial in the case in which the splitting of H is unique, as in potential scattering. In that case we define:

$$(\psi^{(-)}(b),\ \psi^{(+)}(a)) = \delta(E_b - E_a)S(b,a) \tag{4.1}$$

and using the completeness of the sets $\{\psi^{(+)}(c)\} + \{\psi_{\text{bound states}}\}$ and $\{\psi^{(-)}(c)\} + \{\psi_{\text{bound states}}\}$ in the scalar products $(\psi^{(-)}(b),\ \psi^{(-)}(a))$ and $(\psi^{(+)}(b),\ \psi^{(+)}(a))$, respectively, we get the two unitarity equations:

$$\int d\alpha_c S(b,c)S^*(a,c) = \int d\alpha_c S^*(c,b)S(c,a) = \delta(\alpha_b - \alpha_a) \tag{4.2}$$

In Eq. (4.2) all the S-matrix elements are given on the 'energy shell' $E_b = E_a = E_c$. In this case it is also customary to define an S-operator by:

$$(\varphi(b), S\varphi(a)) \equiv (\psi^{(-)}(b),\ \psi^{(+)}(a)) \tag{4.3}$$

From Eq. (4.2) and the completeness of the set $\{\varphi(c)\}$ it follows that S is unitary:

$$SS^\dagger = S^\dagger S = 1 \tag{4.4}$$

In the case of rearrangement collisions the S-matrix is defined by:

$$(\psi_f^{(-)}(b),\ \psi_i^{(+)}(a)) = \delta(E_b - E_a)\, S_{fi}(b,a) \tag{4.5}$$

Let us now consider the scalar product of two wave packets built with eigenstates of H belonging to channel f and i, respectively:

$$(\psi^{(f)}(0),\ \psi^{(i)}(0)) \equiv \left(\int dbc_f(b)\psi_f^{(+)}(b),\ \int dac_i(a)\psi_i^{(+)}(a)\right) \tag{4.6}$$

The scalar product (4.6) is independent of time:

$$(\psi^{(f)}(0),\ \psi^{(i)}(0)) = (\psi^{(f)}(t),\ \psi^{(i)}(t)) \tag{4.7}$$

so that we can evaluate it in the limit $t \to -\infty$ where we can substitute $\psi(t)$ with $\phi(t)$. Using Eq. (3.2) we get:

$$(\psi^{(f)}(0),\ \psi^{(i)}(0)) = \lim_{t \to -\infty} (\phi^{(f)}(t),\ \phi^{(i)}(t)) = \delta_{fi} \times \text{constant} \tag{4.8}$$

Equation (4.8) tells us that, $c_f(b)$ and $c_i(a)$ being arbitrary, the 'channel' eigenvectors $\psi^{(+)}$ of H, belonging to different channels, are orthogonal:

$$(\psi_f^{(+)}(b),\ \psi_i^{(+)}(a)) = \delta_{fi}\ \delta(b-a) \tag{4.9}$$

Using wave packets of the incoming wave solutions $\psi^{(-)}$ in (4.6) we get analogously:

$$\left(\psi_f^{(-)}(b),\ \psi_i^{(-)}(a)\right) = \delta_{fi}\,\delta(b-a) \tag{4.10}$$

It is now easy to build two completeness relations in the sub-space of the eigenvectors of H belonging to a fixed energy E:

$$\lim_{\Delta E\to 0} \sum_j \int d\alpha_j \int_{E-\Delta E}^{E+\Delta E} dE'\ \psi_j^{(+)}(E',\alpha_j) \times \psi_j^{(+)}(E',\alpha_j) = P_E \tag{4.11}$$

$$\lim_{\Delta E\to 0} \sum_j \int d\alpha_j \int_{E-\Delta E}^{E+\Delta E} dE'\ \psi_j^{(-)}(E',\alpha_j) \times \psi^{(-)}(E',\alpha_j) = P_E \tag{4.12}$$

P_E gives $P_E\psi(E) = \psi(E)$, with $\psi(E)$ generic eigenvector of H belonging to the eigenvalue E. That is, P_E is the identity operator in that subspace. Of course, the sum over j in Eqs. (4.11) and (4.12) runs over all channels which are open at the considered energy E. Equations (4.11) and (4.12), when used in the scalar products $(\psi_f^{(-)}(b),\ \psi_i^{(-)}(a))$ and $(\psi_f^{(+)}(b),\ \psi_i^{(+)}(a))$, respectively, give immediately the two unitarity equations (on the energy shell $E_a = E_b = E_j$):

$$\sum_j \int d\alpha(c_j)\, S_{fj}(b,c_j) S^*_{ij}(a,c_j) = \sum_j \int d\alpha(c_j)\, S^*_{jf}(c_j,b) S_{ji}(c_j,a) = \delta_{fi}\,\delta(\alpha_b - \alpha_a) \tag{4.13}$$

It is not possible to define in general a unitary operator through an equation similar to Eq. (4.3), since the set $\{\varphi_j(a)\}$ is not linearly independent.[4] We could write:

$$(\Psi_-^{(f)}(0),\ \Psi^{(i)}(0)) = \lim_{\substack{t\to+\infty \\ t_0\to-\infty}} \left(e^{iHt/\hbar}\,\Psi_-^{(f)}(t),\ e^{iHt_0/\hbar}\,\Psi^{(i)}(t_0)\right)$$

$$= (\phi^{(f)}(0),\ S_{fi}\,\phi^{(i)}(0))$$

with

$$S_{fi} = \left(\lim_{t\to+\infty} e^{iK_f t/\hbar}\, e^{-iHt/\hbar}\right)\left(\lim_{t_0\to-\infty} e^{iHt_0/\hbar}\, e^{-iK_i t_0/\hbar}\right) \tag{4.14}$$

---

[4] See also H. Ekstein (p. 886 of Ref. given in footnote 2) and J. M. Jauch, Helv. Phys. Acta 31 (1958) 661.

but S_{fi} depends on the chosen final and initial channels. For potential scattering only, $S_{fi} \equiv S$ is unitary on the whole Hilbert space. In the general case the definition of a unitary operator must be given using as representation basis the eigenvectors of H.[5]

The S-matrix is simply related to the T-matrix:

$$(\psi_f^{(-)}(b),\ \psi_i^{(+)}(a)) = (\psi_f^{(-)}(b),\ \psi_i^{(-)}(a) - 2\pi i\,\delta(E_a - H)\,V_i\,\varphi_i(a))$$

$$= \delta_{fi}\,\delta(b-a) - 2\pi i\,\delta(E_b - E_a)(\psi_f^{(-)}(b),\ V_i\,\varphi_i(a)) \qquad (4.15)$$

The S-matrix elements are connected to the experimentally measured cross-sections and the unitarity equations then give rise to relations between cross-sections. In particular, we get the optical theorem. Writing the second unitarity Eq. (4.13) in terms of the T-matrix, on the energy shell $E_f = E_i = E_j$ we get:

$$iT_{fi}(\alpha_f, \alpha_i) - iT_{if}^{*}(\alpha_i, \alpha_f) = 2\pi \sum_j \int d\alpha_j\, T_{jf}^{*}(\alpha_j, \alpha_f) T_{ji}(\alpha_j, \alpha_i)$$

Choosing $i = f$, $\alpha_i = \alpha_f$ and using Eq. (3.11), we get the optical theorem:

$$-\operatorname{Im} T_{ii}(\alpha_i, \alpha_i) = \pi \sum_j \left[\int d\sigma_{ji}\right] \frac{dE}{dk_i} \frac{\hbar v_i}{(2\pi)^4} \equiv \frac{\hbar v_i}{2(2\pi)^3}\,\sigma_i^{tot} \qquad (4.16)$$

$T_{ii}(\alpha_i, \alpha_i)$ is the elastic scattering element evaluated in the forward direction with beam in channel i. σ_i^{tot} is the total cross-section arising from the initial wave in channel i.

5. LOW-ENERGY BEHAVIOUR OF CROSS-SECTIONS

We shall first consider the behaviour of the various elements of the transition amplitude for two-particle → two-particle collisions, when either the final channel is considered at its own threshold energy E_f or the initial channel is considered at its threshold energy E_i. We first take the endoergic case ($E_f > E_i$) and the exoergic case ($E_f < E_i$), after which the properties for the elastic scattering case ($E_f = E_i$) will be deduced. The considerations which follow will hold provided the non-Coulomb interaction vanishes beyond a certain distance. In most cases of interest, however, this condition can be relaxed, for example when the interaction vanishes asymptotically like an exponential as a function of the distance of the fragments. At the end of this section consideration will be given to three-body final channels.

The cross-sections, in the centre-of-mass co-ordinate system in the presence of Coulomb forces, are obtained as follows[6] (for the derivation

---

[5] J. M. Jauch (see footnote 4) and J. M. Jauch and J. P. Marchand, Helv. Phys. Acta 39, 325 (1966).

[6] We assume for simplicity that the Coulomb interaction cannot give transitions between channels.

see Ref. [2]):

$$\frac{d\sigma_{fi}(\vec{\xi}_f, \vec{\xi}_i)}{d\Omega_f} = \left|\Theta_{fi}(\vec{\xi}_f, \vec{\xi}_i)\right|^2 \tag{5.1}$$

$$\Theta_{fi}(\vec{\xi}_f, \vec{\xi}_i) = -\left(\frac{2\pi}{\hbar}\right)^2 (\omega_f \omega_i k_f/k_i)^{1/2} T_{fi}(\vec{\xi}_f, \vec{\xi}_i) \tag{5.2}$$

$$T_{fi}(\vec{\xi}_f, \vec{\xi}_i) = T_{ci}(\vec{k}_f, \vec{k}_i)\delta_{fi}\delta_{S_f S_i}\delta_{\nu_f \nu_i} + (\varphi_{cf}^{(-)}(\vec{\xi}_f), \Pi_{fi}\varphi_{ci}^{(+)}(\vec{\xi}_i)) \tag{5.3}$$

T_{ci} describes the scattering in channel i in the presence of only Coulomb forces and is related, through Eq. (5.2), to the Rutherford amplitude:

$$\Theta_{ci}(\vec{k}_f, \vec{k}_i) = -\frac{a_i e^{2i\sigma_0^i}}{2k_i^2 \sin^2\frac{\theta}{2}} \exp\left[-i\eta_i \log \sin^2\frac{\theta}{2}\right] \tag{5.4}$$

where

$$\sigma_\ell^i = \arg\Gamma(\ell + 1 + i\eta_i), \quad \theta = \widehat{k_f k_i}$$

$$\eta_i = \frac{a_i}{k_i} = \frac{Z_{1i}Z_{2i}e^2}{\hbar v_i} \tag{5.5}$$

$\vec{\xi}_j$ indicates the relative momentum of the fragments in channel j, their total spin and its z-component:

$$\vec{\xi}_j \equiv \vec{k}_j, S_j, \nu_j$$

$\omega_j c^2$ is the relative reduced energy given by Eq. (3. 14).

The operator Π_{fi} is given by:

$$\Pi_{fi} = V_f - V_{cf} + \lim_{\epsilon \to 0^+} (V_f - V_{cf})(E + i\epsilon - H)^{-1}(V_i - V_{ci}) \tag{5.6}$$

where E is the total energy and $V_j - V_{cj}$ is the non-Coulomb part of the interaction (e.g. the nuclear interaction) between the fragments in channel j. $\varphi_{cj}^{(+)}$ and $\varphi_{cj}^{(-)}$ are the j-th channel Coulomb eigenfunctions satisfying an outgoing and an incoming wave boundary condition, respectively. The representative of $\varphi_{cj}^{(\pm)}$ in the relative co-ordinate representation is:

$$\varphi_{cj}^{(\pm)}(\vec{\xi}_j, \vec{r}_j) = (2\pi)^{-3/2}\psi_{B1j}\psi_{B2j}\chi_{S_j}^{\nu_j}$$

$$\times \sum_{\ell m} 4\pi i^\ell Y_{\ell m}^*(k_j) Y_{\ell m}(\hat{r}_j) e^{\pm i\sigma_\ell^j} \frac{F_\ell(k_j r_j)}{k_j r_j} \tag{5.7}$$

where $\vec{r}_j$ is the vector describing the relative distance of the fragments of channel j, and ψ_{B1j} and ψ_{B2j} are the eigenvectors describing their internal (bound) states. χ_s^ν is the spin eigenfunction, and the $Y_{\ell m}$'s are the spherical harmonics in the notation of Blatt and Weisskopf [4]. $F_\ell(\rho)$ is the real Coulomb wave function regular at the origin:

$$F_\ell(\rho) = \frac{\exp[-\eta\pi/2]}{(2\ell+1)!} \left|\Gamma(\ell+1+i\eta)\right| 2^\ell \rho^{\ell+1} \frac{M_{i\eta,\,\ell+1/2}(2i\rho)}{(2i\rho)^{\ell+1}}, \quad \rho = kr \tag{5.8}$$

with

$$\frac{M_{i\eta,\,\ell+1/2}(2i\rho)}{(2i\rho)^{\ell+1}} = 1 + \frac{\eta}{\ell+1}\rho + \frac{2\eta^2 - (\ell+1)}{2(\ell+1)(2\ell+3)}\rho^2 + \ldots \tag{5.9}$$

$F_\ell(\rho)$ goes asymptotically as follows:

$$F_\ell(\rho) \underset{\rho\to\infty}{\sim} \sin(\rho - \eta \log 2\rho - \frac{\ell\pi}{2} + \sigma_\ell) \tag{5.10}$$

and in the absence of Coulomb forces it goes over to the Riccati-Bessel function:

$$F_\ell(\rho)\Big|_{Z_1Z_2e^2=0} = \sqrt{\pi\rho/2}\, J_{\ell+\frac{1}{2}}(\rho) \equiv \rho j_\ell(\rho) \tag{5.11}$$

Using Eqs. (5.2), (5.3) and (5.7) we get

$$\Theta_{fi}(\vec{\xi}_f, \vec{\xi}_i) = \sum_{\ell_f\ell_i} \sum_{m_f m_i} Y_{\ell_f m_f}(k_f) Y^*_{\ell_i m_i}(k_i) \bar{\Theta}_{fi}^{(\ell_f, \ell_i)}(\xi_f, \xi_i) \tag{5.12}$$

Let us choose the z-axis along the direction of the incident beam thus obtaining $Y_{\ell_i m_i}(\hat{k}_i) = \delta_{m_i,0}\left(\frac{2\ell_i+1}{4\pi}\right)^{1/2}$. Conservation of total angular momentum then gives $m_f = \nu_i - \nu_f$, so that Eq. (5.12) simplifies as follows:

$$\Theta_{fi}(\vec{\xi}_f, \vec{\xi}_i) = \sum_{\ell_f\ell_i} Y_{\ell_f,\,\nu_i-\nu_f}(\hat{k}_f)\, \Theta_{fi}^{(\ell_f,\ell_i)}(\xi_f, \xi_i) \tag{5.13}$$

Through $\Theta_{fi}^{(\ell_f,\ell_i)}$ we define the partial cross-section $\sigma_{fi}^{(\ell_f)}$ for the reaction $i \to f$ leading to a wave of orbital angular momentum ℓ_f:

$$\sigma_{fi}^{(\ell_f)} \equiv \sum_m \left| \int d\Omega_f \, \Theta_{fi}(\vec{\xi}_f, \vec{\xi}_i) \, Y^*_{\ell_f m}(\hat{k}_f) \right|^2 = \left| \sum_{\ell_i} \Theta_{fi}^{(\ell_f,\ell_i)}(\xi_f, \xi_i) \right|^2 \tag{5.14}$$

Equation (5.14) makes sense when $f \neq i$, and for elastic scattering in channels in which there are no Coulomb forces, since the integral over Ω_f diverges in that case.
We have[7]:

$$\sigma_{fi} \equiv \int d\Omega_f \frac{d\sigma_{fi}(\vec{\xi}_f, \vec{\xi}_i)}{d\Omega_f} = \sum_{\ell_f} \sigma_{fi}^{(\ell_f)} \tag{5.15}$$

σ_{fi} is infinite for $f = i$ with Coulomb forces present in channel i. From Eqs. (5.2) and (5.7) we see that:

$$\Theta_{fi}^{(\ell_f,\ell_i)}(\xi_f, \xi_i) = \Theta_{ci}^{(\ell_i)} \delta_{fi} \delta_{\ell_f \ell_i} \delta_{s_f s_i} \delta_{\nu_f \nu_i}$$

$$+ \left(\frac{\omega_f \omega_i}{k_f k_i^3} \right)^{1/2} \iint dr_f dr_i \, e^{i\sigma_{\ell_f}^f} F_{\ell_f}(k_f r_f) e^{i\sigma_{\ell_i}^i} F_{\ell_i}(k_i r_i) \theta_{fi}^{(\ell_f,\ell_i)}(r_f, r_i) \tag{5.16}$$

where $\theta_{fi}^{(\ell_f,\ell_i)}$, apart from uninteresting energy independent coefficients, is the matrix element of the operator Π_{fi} in the relative co-ordinate representation. Under our hypothesis that the non-Coulomb interaction vanishes beyond a certain distance, the same then also holds for this matrix element. It follows that, to understand the low-energy behaviour of Eq. (5.16), we need to consider only the low-energy properties of the Coulomb wave functions F_{ℓ_f} and F_{ℓ_i}. Since $M_{i\eta,\ell+1/2}(2ikr)/(2ikr)^{\ell+1}$ goes to const. $+O(k^2)$ in the limit $k \to 0$, the behaviour of $e^{i\sigma_\ell} F_\ell(kr)$ at $k = 0$ is determined by the function:

$$k^{\ell+1} e^{-\eta\pi/2} \Gamma(\ell + 1 + i\eta)$$

$$= \ell! \, e^{i\sigma_\ell} \left(\frac{2\pi ak}{e^{2\pi\eta} - 1} \right)^{1/2} \left\{ \left[k^2 + \left(\frac{a}{1} \right)^2 \right] \left[k^2 + \left(\frac{a}{2} \right)^2 \right] \cdots \left[k^2 + \left(\frac{a}{\ell} \right)^2 \right] \right\}^{1/2} \tag{5.17}$$

---

[7] The total cross-section from channel i is then given by:

$$\sigma_i^{tot}(\vec{\xi}_i) = \sum_{f s_f \nu_f} \sigma_{fi} \, .$$

The limit gives

$$e^{i\sigma_\ell} F_\ell(kr) \underset{k\to 0}{\sim} \begin{cases} \ell!\, k^{\ell+1} & , \quad a = 0 \\ k^{1/2}\sqrt{2\pi}\, e^{i\sigma_0} e^{-\pi a/k} a^{\ell+1/2} i^{\ell} & , \quad a > 0 \\ k^{1/2}\sqrt{2\pi}\, e^{i\sigma_0} |a|^{\ell+1/2} (-i)^{\ell} & , \quad a < 0 \end{cases} \tag{5.18}$$

Let us then see how $\Theta_{fi}^{(\ell_f,\ell_i)}$ behaves in the various cases.

(a) Endoergic case. For an endoergic reaction channel i → channel f (two-body, $E_f > E_i$), the initial channel momentum k_i goes to a constant $\neq 0$ for $k_f \to 0$. We get

$$\Theta_{fi}^{(\ell_f,\ell_i)} \underset{k_f\to 0}{\sim} \begin{cases} k_f^{\ell_f+1/2} & , \quad a_f = 0 \\ \sqrt{2\pi}\, e^{i\sigma_0^f} e^{-\pi a_f/k_f} a_f^{\ell_f+1/2} i^{\ell_f}/\ell_f\,! & , \quad a_f > 0 \\ \sqrt{2\pi}\, e^{i\sigma_0^f} |a_f|^{\ell_f+1/2} (-i)^{\ell_f}/\ell_f\,! & , \quad a_f < 0 \end{cases} \tag{5.19}$$

(two-body endoergic reaction).

We see that in the case of Coulomb repulsion in the final channel f($a_f > 0$), $\Theta_{fi}^{(\ell_f,\ell_i)}$ starts from $k_f = 0$ like the exponential $\exp[-\pi a_f/k_f]$, while for Coulomb attraction ($a_f < 0$) $\Theta_{fi}^{(\ell_f,\ell_i)}$ is finite there. Consideration of the next term in the expansion of $\Theta_{fi}^{(\ell_f,\ell_i)}$ for $a_f < 0$ shows that it is proportional to k_f^2. The case of no Coulomb forces in channel f yields the well known energy dependence.

In Fig. 1 the various cross-sections are plotted as functions of the initial channel momentum k_i^2. In the case of no Coulomb forces in the final channel f, dk_f/dk_i being equal to $(k_i/k_f)(\omega_f/\omega_i)$, we have:

$$\left(\frac{d\sigma_{fi}^{(\ell_f)}}{dk_i}\right)_{(a_f = 0)} \underset{k_f\to 0}{\sim} k_f^{2\ell_f - 1} \begin{cases} = \infty & , \quad \ell_f = 0 \\ = 0 & , \quad \ell_f > 0 \end{cases} \tag{5.20}$$

so that we recognize that the $\ell_f = 0$ part of σ_{fi} exhibits an infinite derivative with respect to k_i, and, with respect to the total energy, at $k_f = 0$. Note

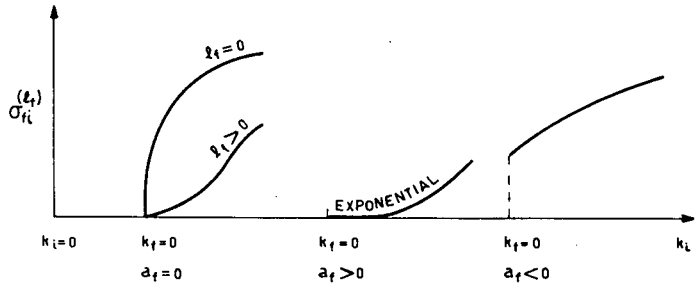

FIG.1. Cross-section behaviour in the endoergic case

that the derivative with respect to k_f is instead finite there. For Coulomb attraction the slope of $\sigma_{fi}^{(\ell_f)}$ is zero as a function of k_f and finite as a function of k_i.

At the onset of the neutral channel f there is then a sudden flux removal from the incident beam. This, as we shall see, will give rise to anomalies in the scattering and reaction cross-sections already present at that energy.

(b) Exoergic case. For an exoergic reaction, channel i → channel f, (two-body, $E_f < E_i$) the final channel momentum k_f goes to a constant $\neq 0$ for $k_i \to 0$. We get:

$$\Theta_{fi}^{(\ell_f,\ell_i)} \underset{k_i\to 0}{\sim} \begin{cases} k_i^{\ell_i - 1/2}, & a_i = 0 \\ k_i^{-1}\sqrt{2\pi}\, e^{i\sigma_0^i} e^{-\pi a_i/k_i}\, a_i^{\ell_i+1/2}\, i^{\ell_i}/\ell_i!, & a_i > 0 \\ k_i^{-1}\sqrt{2\pi}\, e^{i\sigma_0^i} |a_i|^{\ell_i+1/2}\, (-i)^{\ell_i}/\ell_i!, & a_i < 0 \end{cases} \qquad (5.21)$$

(two-body exoergic reaction).

The characteristic exponential $\exp[-\pi a_i/k_i]$ is still present for Coulomb repulsion ($a_i > 0$). In the case of Coulomb attraction ($a_i < 0$), $\Theta_{fi}^{(\ell_f,\ell_i)}$ goes to infinity in the limit $k_i \to 0$. The energy dependence for $a_i = 0$ is well known and yields the $1/v$ law for the absorption of slow neutrons by nuclei [1]. In Fig. 2 the various behaviours are shown.

For the case $a_i = 0$ if the ℓ_f wave is coupled to the $\ell = 0$ wave then $\sigma_{fi}^{(\ell_f)}$ is infinite at $k_i = 0$. If that is not the case, then $\sigma_{fi}^{(\ell_f)}$ vanishes at $k_i = 0$ with finite slope if $\ell_i = 1$ and with zero slope if $\ell_i > 1$.

(c) Elastic scattering. If Coulomb forces are not present, we obtain the well-known formula

$$\Theta_{ii}^{(\ell_i',\ell_i)} \underset{k_i\to 0}{\sim} k_i^{\ell_i'}\, k_i^{\ell_i} \quad (a_i = 0, \text{ two-body elastic scattering}) \qquad (5.22)$$

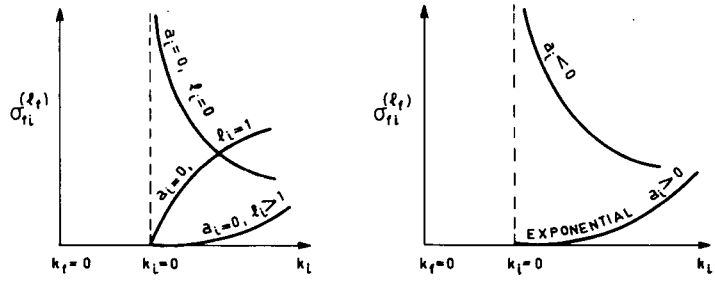

FIG. 2. Cross-section behaviour in the exoergic case

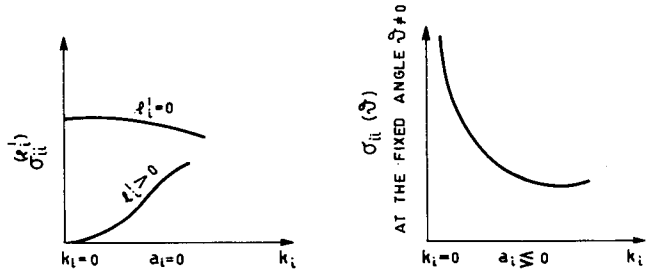

FIG. 3. Cross-section behaviour in the elastic scattering case

which shows that the scattering cross-section is finite at zero energy when Coulomb forces are not present. If Coulomb forces are present, then consideration of the pure Coulomb scattering amplitude $\Theta_{ci}(\vec{k}_f, \vec{k}_i)$ shows that at very low energy only pure Coulomb scattering survives, since $\Theta_{ci}(\vec{k}_f, \vec{k}_i) \underset{k_i \to 0}{\sim} k_i^{-2}$. The nuclear scattering amplitude has, of course, the behaviour in Eq. (5.22). In Fig. 3 the elastic cross-sections are plotted for the various cases. For $a_i = 0$ the slope of $\sigma_{ii}^{(\ell_i')}$ is zero for all ℓ_i' at $k_i = 0$.

(d) Three-body final channel. We shall consider here the low-energy properties of an endoergic reaction cross-section leading to a final neutral three-body channel. For the transition amplitude Θ_{fi}, we have

$$\Theta_{fi}(\vec{\xi}_1, \vec{\xi}_{23}; \vec{\xi}_i) = -\left(\frac{2\pi}{\hbar}\right)^2 (\omega_i \omega_{23} k_{23}/k_i)^{1/2} (\varphi_0(\vec{\xi}_1)\varphi_0(\vec{\xi}_{23}), V\psi^{(i)}) \qquad (5.23)$$

Θ_{fi}, as given here, yields the cross-section for the reaction leading to the three-body channel f, in which the first particle (n. 1) obtains a momentum between $\hbar\vec{k}_1$ and $\hbar\vec{k}_1 + d\hbar\vec{k}_1$, and the particles 2 and 3 receive a relative momentum $\hbar k_{23}$ in the direction between Ω_{23} and $\Omega_{23} + d\Omega_{23}$:

$$\bar{\sigma}_{fi} \equiv \frac{d\sigma_{fi}}{d^3\vec{k}_1 d\Omega_{23}} = |\Theta_{fi}(\vec{\xi}_1, \vec{\xi}_{23}; \vec{\xi}_i)|^2 \qquad (5.24)$$

where the φ_0's are free waves times the bound-state wave functions. ω_i is the reduced energy in the incoming two-body channel i, ω_{23} is the reduced energy of the system 2+3 in the final channel f.

We assume, as before, that the interaction V vanishes beyond finite values of r_1 and r_{23}. $\vec{r}_1$ is the distance separating particle 1 from the centre of mass of the system 2+3; $\vec{r}_{23}$ is the relative distance between 2 and 3. In the limit, as the total energy E approaches the threshold for the channel f from above, we have:

$$\Theta_{fi}(\ell_1, \ell_{23}) \underset{E \to E_f}{\sim} k_1^{\ell_1} k_{23}^{\ell_{23}+1/2} \tag{5.25}$$

where we have separated Θ_{fi} into the contributions from the various values of ℓ_1 and ℓ_{23}, orbital angular momentum of particle 1, and of particle 2 relative to 3, respectively. $\bar{\sigma}_{fi}$ vanishes at the threshold energy E_f for channel f. Using the conservation energy at low energy:

$$E \cong E_f + \frac{\hbar^2 k_1^2}{2\mu_1} + \frac{\hbar^2 k_{23}^2}{2\mu_{23}}$$

with $\mu_1 = m_1(m_2+m_3)/(m_1+m_2+m_3)$, $\mu_{23} = m_2 m_3/(m_2+m_3)$, and the fact that:

$$\int_0^{k_1^{max}} dk_1 k_1^{2\ell_1+2} \left(E - E_f - \frac{\hbar^2 k_1^2}{2\mu_1}\right)^{\ell_{23}+1/2} \underset{E \to E_f}{\sim} (E - E_f)^{\ell_1+\ell_{23}+2}$$

we get for the integrated cross-section:

$$\lim_{E \to E_f} \int_0^{k_1^{max}} d^3k_1 \bar{\sigma}_{fi} = 0, \quad \lim_{E \to E_f} \frac{d}{dk_i} \int_0^{k_1^{max}} d^3k_1 \bar{\sigma}_{fi} = 0, \tag{5.26}$$

$$\lim_{E \to E_f} \frac{d^2}{dk_i^2} \int_0^{k_1^{max}} d^3k_1 \bar{\sigma}_{fi} = \text{finite}$$

where the second derivative is different from zero only if the S-waves $\ell_1 = \ell_{23} = 0$ appear in the final channel.

6. THRESHOLD EFFECTS

We are now interested in the study of the energy behaviour of the various elements of the transition amplitude Θ around the threshold energy E_n for the two-body channel n. In this section we shall consider the case in which Coulomb forces are not present in channel n. Coulomb effects will be discussed in section 7.

In this case the threshold effects are most easily exploited by using the unitarity equations of the S-matrix. $\Theta_{fi}(\vec{\xi}_f, \vec{\xi}_i)$ in terms of the S-matrix reads as follows:

$$\Theta_{fi}(\vec{\xi}_f, \vec{\xi}_i) = \Theta_{ci}(\vec{k}_f, \vec{k}_i)\,\delta_{fi}\,\delta_{s_f s_i}\delta_{\nu_f \nu_i} + \frac{2\pi i}{k_i}\sum_{JM\ell_f\ell_i} Y_{\ell_f}^{M-\nu_f}(\hat{k}_f) Y_{\ell_i}^{*M-\nu_i}(\hat{k}_i)$$

$$\times C_{\ell_f s_f}(J, M;\, M-\nu_f, \nu_f) C_{\ell_f s_i}(J, M;\, M-\nu_i, \nu_i)\left[e^{2i\delta_{\ell_i}}\,\delta_{fi}\,\delta_{\ell_f \ell_i}\,\delta_{s_f s_i} - S^J_{f\ell_f s_f, i\ell_i s_i}(E)\right] \tag{6.1}$$

where the C's are the Clebsch-Gordan coefficients in the notation of Blatt and Weisskopf [4]. In Eq. (6.1) we have taken already into account rotational invariance. The unitarity of the S-matrix is then expressed by the two equations (use Eq. (4.13)):

$$\sum_{j,\alpha_j} S^{J*}_{j\alpha_j, f\alpha_f}(E)\, S^J_{j\alpha_j, i\alpha_i}(E) = \delta_{fi}\,\delta_{\alpha_f \alpha_i}, \tag{6.2}$$

$$\sum_{j,\alpha_j} S^J_{f\alpha_f, j\alpha_j}(E)\, S^{J*}_{i\alpha_i, j\alpha_j}(E) = \delta_{fi}\,\delta_{\alpha_f \alpha_i}, \tag{6.3}$$

where by α_j we mean both indices ℓ_j and s_j. The sum over j runs over the channels which are open at the considered total energy E. The total angular momentum J is fixed, consequently the sum over α_j runs over the values of ℓ_j and s_j which can make up a total angular momentum J. Just moving across the threshold E_n of the channel n, the S-matrix enriches itself of another row and column labelled by the index n. Therefore, above the threshold energy E_n consideration must be given to $S^J_{n\alpha_n, j\alpha_j}$. From Eqs. (6.1), (5.19) and (5.21) we see that at low k_n:[8]

$$S^J_{n\alpha_n, j\alpha_j}(E) \underset{k_n \to 0}{\sim} k_n^{\ell_n + 1/2}\, \mathcal{M}^J_{n\alpha_n, j\alpha_j}, \tag{6.4}$$

$$S^J_{j\alpha_j, n\alpha_n}(E) \underset{k_n \to 0}{\sim} k_n^{\ell_n + 1/2}\, \mathcal{M}^J_{j\alpha_j, n\alpha_n} \tag{6.5}$$

where $\mathcal{M}^J$ is constant in the limit $k_n \to 0$. In the same manner it can be seen from Eqs. (6.1) and (5.22) that the matrix element $S^J_{n\alpha_n, n\alpha'_n}$

[8] Time reversal invariance implies that $S^J_{i\alpha_i, f\alpha_f} = S^J_{f\alpha_f, i\alpha_i}$. However, we do not need this symmetry of the S-matrix in what follows.

goes like:

$$S^J_{n\alpha_n, n\alpha'_n}(E) \underset{k_n \to 0}{\sim} \delta_{\alpha_n \alpha'_n} - k_n^{\ell_n + \ell'_n + 1} \mathcal{N}^J_{\alpha_n, \alpha'_n} \tag{6.6}$$

with $\mathcal{N}^J$ constant in the limit $k_n \to 0$. For the remaining S-matrix elements, we suppose that they can be expanded in a power series of k_n:

$$S^J_{f\alpha_f, i\alpha_i}(E) = S^J_{f\alpha_f, i\alpha_i}(E_n) + k_n A^J_{f\alpha_f, i\alpha_i} + k_n^2 B^J_{f\alpha_f, i\alpha_i} + \ldots, \quad E \gtrsim E_n \tag{6.7}$$

$(f, i \neq n)$

We analytically continue the expansion (6.7) below the threshold energy E_n. In doing this we still require conservation of energy in channel n:

$$\left(m_{1n}^2 + \frac{\hbar^2 k_n^2}{c^2}\right)^{1/2} + \left(m_{2n}^2 + \frac{\hbar^2 k_n^2}{c^2}\right)^{1/2} = \frac{E}{c^2} \tag{6.8}$$

From Eq. (6.8) we see that k_n^2 must become negative for energies less than $E_n \equiv (m_{1n} + m_{2n})c^2$. k_n is then purely imaginary below threshold. From the two possibilities we choose this continuation

$$k_n \to i\,|k_n|, \qquad E < E_n \tag{6.9}$$

In fact, with the choice of the expression (6.9) the eigenfunction relative to channel n, which asymptotically reads:

$$\psi_n(\vec{r}_n) \underset{r_n \to \infty}{\sim} \text{const.} \frac{e^{ik_n r}}{r}$$

becomes normalizable as it should. This means that even though below the threshold energy E_n the fragments of channel n cannot be found asymptotically, we can still find them in a localized region of space of dimensions $\Delta R \sim \hbar/|k_n|$. We then obtain:

$$S^J_{f\alpha_f, i\alpha_i}(E) = S^J_{f\alpha_f, i\alpha_i}(E_n) + i\,|k_n| A^J_{f\alpha_f, i\alpha_i} - |k_n|^2 B^J_{f\alpha_f, i\alpha_i} + \ldots, \quad E \lesssim E_n \tag{6.10}$$

$(f, i \neq n)$

The linear term is, as we immediately see, responsible for the threshold anomaly. In fact:

$$\left.\frac{\partial S^J_{f\alpha_f, i\alpha_f}(E)}{\partial k_i}\right|_{k_n = 0} = \begin{pmatrix} 1 \\ -i \end{pmatrix} A^J_{f\alpha_f, i\alpha_i} \left.\frac{\mu_n k_i}{\omega_i |k_n|}\right|_{k_n = 0} + 2B^J_{f\alpha_f, i\alpha_i} \left.\frac{\mu_n k_i}{\omega_i}\right|_{k_n = 0} \tag{6.11}$$

$(f, i \neq n)$

The symbol $\binom{a}{b}$ means that a should be used above the threshold and b below. If $A^J_{fi} \neq 0$ the derivative of S^J_{fi} (f and $i \neq n$) is infinite at $k_n = 0$ and not the same above and below. Accordingly, all cross-sections σ_{fi} (f and $i \neq n$) therefore have (if $A^J_{fi} \neq 0$) infinite derivatives with respect to k_i (or with respect to the total energy) at $k_n = 0$. Notice that the derivatives of S^J_{fi} and σ_{fi} with respect to k_n are finite at $k_n = 0$ and different above from below. We have seen in section 1 that all this was also true for the cross-sections $\sigma_{n \leftarrow i}$. Now we understand how it comes about that conservation of total flux (unitarity of S-matrix also makes infinite the derivatives of the 'old' cross-sections σ_{fi} (f and $i \neq n$) at the opening up of the channel n. If $A^J_{fi} = 0$, then the derivative of S^J_{fi} (f and $i \neq n$) is finite at $k_n = 0$ and the same above and below. We do not have any threshold anomaly in this case. Let us then see the condition for which $A^J_{fi} \neq 0$ and find its formal expression.

When Eq.(6.7) is used, the unitarity equation (6.2) above the threshold energy E_n for $f \neq n$ and $i \neq n$ becomes:

$$\sum_{\substack{j,\alpha_j \\ j \neq n}} S^{J*}_{j\alpha_j, f\alpha_f}(E_n) S^J_{j\alpha_j, i\alpha_i}(E_n) = \delta_{fi}\delta_{\alpha_f\alpha_i}, \tag{6.12}$$

$$\sum_{\substack{j,\alpha_j \\ j \neq n}} \left[S^{J*}_{j\alpha_j, f\alpha_f}(E_n) A^J_{j\alpha_j, i\alpha_i} + A^{J*}_{j\alpha_j, f\alpha_f} S^J_{j\alpha_j, i\alpha_i}(E_n) \right]$$

$$= -\delta_{\ell_n, 0}\, \mathscr{M}^{J*}_{n\alpha_n, f\alpha_f}\, \mathscr{M}^{J}_{n\alpha_n, i\alpha_i} \tag{6.13}$$

. . . .

Equation (6.12) expresses the unitarity of the S-matrix at the threshold energy E_n. Equation (6.13) comes from the identification of the first order terms in Eq.(6.2). The dots underneath it stand for all the other equations which come from higher order terms of Eq.(6.2).

Below the threshold energy E_n in Eq.(6.2) the sum over j runs, of course, only up to channel n-1. Using Eq.(6.10) we again get Eq.(6.12) and:

$$\sum_{\substack{j,\alpha_j \\ j \neq n}} \left[S^{J*}_{j\alpha_j, f\alpha_f}(E_n) A^J_{j\alpha_j, i\alpha_i} - A^{J*}_{j\alpha_j, f\alpha_f} S^J_{j\alpha_j, i\alpha_i}(E_n) \right] = 0 \tag{6.14}$$

Consider now the case $\ell_n \neq 0$. Equations (6.13) and (6.14) give

$$\sum_{\substack{j,\alpha_j \\ j \neq n}} S^{J*}_{j\alpha_j, f\alpha_f}(E_n) A^J_{j\alpha_j, i\alpha_i} = 0, \qquad \ell_n \neq 0 \tag{6.15}$$

Let us multiply Eq. (6.15) by $S^J_{h\alpha_h, f\alpha_f}(E_n)$ and sum the resulting expression over f and α_f. Since $S^J(E_n)$ also satisfies the second unitarity Eq. (6.3), we get:

$$A^J_{f\alpha_f,\, i\alpha_i} = 0, \quad \ell_n \neq 0 \tag{6.16}$$

We have A^J_{fi} equal to zero if the orbital angular momentum of channel n, which intervenes in the reaction process, is different from zero. Therefore, waves in the various channels $j (j \neq n)$ which are not coupled to the S-wave of channel n do not feel the opening up of that channel. This is again quite understandable on physical grounds, since the reaction cross-sections $\sigma^{(\ell_n \neq 0)}_{n \leftarrow i}$ vanish smoothly at $k_n = 0$ and there is, then, no violent variation of flux in the other channels.

Let us now consider the case $\ell_n = 0$. In this case Eqs. (6.13) and (6.14) give instead:

$$\sum_{\substack{j, \alpha_j \\ j \neq n}} S^{J\,*}_{j\alpha_j, f\alpha_f}(E_n) A^J_{j\alpha_j, i\alpha_i} = -\frac{1}{2} \mathscr{M}^{J\,*}_{ns_n = J, f\alpha_f} \mathscr{M}^J_{ns_n = J, i\alpha_i}, \quad \ell_n = 0 \tag{6.17}$$

Multiplying Eq. (6.17) by $S^J_{h\alpha_h, f\alpha_f}(E_n)$, summing over f and α_f and using the unitarity of $S^J(E_n)$ we get:

$$A^J_{f\alpha_f, i\alpha_i} = -\frac{1}{2} \sum_{\substack{j, \alpha_j \\ j \neq n}} S^J_{f\alpha_f, j\alpha_j}(E_n) \mathscr{M}^{J\,*}_{ns_n = J, j\alpha_j} \mathscr{M}^J_{ns_n = J, i\alpha_i} \tag{6.18}$$

f not being equal to n, the unitarity Eq. (6.3) also gives:

$$\sum_{\substack{j\alpha_j \\ j \neq n}} S^J_{f\alpha_f, j\alpha_j}(E_n) \mathscr{M}^{J\,*}_{n\alpha_n, j\alpha_j} = -\left[\sum_{\alpha'_n} S^J_{f\alpha_f, n\alpha'_n}(E) S^{J\,*}_{n\alpha_n, n\alpha_n}(E) \right] k_n^{-\ell_n - \frac{1}{2}} \Bigg|_{k_n = 0} = -\mathscr{M}^J_{f\alpha_f, n\alpha_n} \tag{6.19}$$

where we have also used (6.6). We then get:

$$A^J_{f\alpha_f, i\alpha_i} = \frac{1}{2} \mathscr{M}^J_{f\alpha_f, ns_n = J} \mathscr{M}^J_{ns_n = J, i\alpha_i} \tag{6.20}$$

A^J_{fi} clearly arises from the virtual transition of the incident wave to the S-wave of channel n followed by the transition from this wave to a wave in channel f. This explains the threshold effects from the dynamical point

of view. We now write again the S-matrix elements embodying all the information we have gathered so far in only one formula:

$$S^J_{f\ell_f s_f,\, i\ell_i s_i}(E) = S^J_{f\ell_f s_f,\, i\ell_i s_i}(E_n) + \delta_{\ell_n,0}\frac{1}{2}\begin{pmatrix}1\\ i\end{pmatrix}|k_n|\mathcal{M}^J_{f\ell_f s_f,\, n0J}\mathcal{M}^J_{n0J,\, i\ell_i s_i} + \ldots \quad (6.21)$$

Equation (6.21) allows us to write explicitly the transition amplitude near threshold[9], neglecting terms in k_n^2, k_n^3, etc., as follows:

$$\Theta_{fi}(\vec{\xi}_f, \vec{\xi}_i) = \Theta_{fi}(\vec{\xi}_f, \vec{\xi}_i)\Big|_{k_n=0} + \begin{pmatrix}i\\ -1\end{pmatrix}|k_n|\sum_{s_n\nu_n}\Theta_{fn}(\vec{\xi}_f, \vec{\xi}_n)\Theta_{ni}(\vec{\xi}_n, \vec{\xi}_i)\,\delta_{\nu_n\nu_i} \quad (6.22)$$

Only the S-wave of channel n contributes to (6.22).

From Eq. (6.22) one can easily obtain the differential cross-sections around $k_n = 0$.

$$\frac{d\sigma_{fi}(\vec{\xi}_f, \vec{\xi}_i)}{d\Omega_f} = \frac{d\sigma_{fi}(\vec{\xi}_f, \vec{\xi}_i)}{d\Omega_f}\Big|_{k_n=0} - 2\begin{pmatrix}\mathrm{Im}\\ \mathrm{Re}\end{pmatrix}|k_n|\sum_{s_n\nu_n}\Theta^*_{fi}(\vec{\xi}_f, \vec{\xi}_i)\Theta_{fn}(\vec{\xi}_f, \xi_n)\Theta_{ni}(\xi_n, \vec{\xi}_i)\,\delta_{\nu_n\nu_i} \quad (6.23)$$

and the total cross-section:

$$\sigma_i^{tot}(\vec{\xi}_i) = \sigma_i^{tot}(\vec{\xi}_i)\Big|_{k_n=0} + \frac{4\pi}{k_i}|k_n|\begin{pmatrix}\mathrm{Re}\\ -\mathrm{Im}\end{pmatrix}\sum_{s_n\nu_n}\Theta_{in}(\vec{\xi}_i, \xi_n)\Theta_{ni}(\xi_n, \vec{\xi}_i)\,\delta_{\nu_n\nu_i}. \quad (6.24)$$

Equation (6.22) also holds true for $\sum_{\ell i}\Theta^{(\ell_f,\ell_i)}_{fi}(\xi_f, \xi_i)$ with the substitution of $\Theta_{fn}(\vec{\xi}_f, \xi_n)$ with $\Theta^{(\ell_f,0)}_{fn}(\xi_f, \xi_n)$ on the right-hand side. The following equation for the ℓ_f-partial cross-section integrated over angles is then

[9] The $\delta_{\nu_n\nu_i}$ comes from the fact that, n not being equal to i, near $k_n = 0$ we can write $\Theta_{ni}(\vec{\xi}_n, \vec{\xi}_i) \sim \delta_{\nu_n\nu_i}\Theta^{(\ell_n=0)}_{ni}(\vec{\xi}_n, \vec{\xi}_i)/\sqrt{4\pi}$

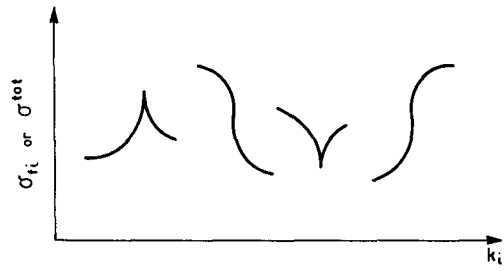

FIG. 4. Various forms of cross-section behaviour at the threshold for channel n

obtained:

$$\sigma_{fi}^{(\ell_f)} = \sigma_{fi}^{(\ell_f)}\Big|_{k_n=0} - 2|k_n| \begin{pmatrix} \mathrm{Im} \\ \mathrm{Re} \end{pmatrix} \sum_{s_n \nu_n \ell_i \ell'_i} \Theta_{fi}^{(\ell_f,\ell_i)*}(\xi_f, \xi_i)\Theta_{fn}^{(\ell_f,0)}(\xi_f, \xi_n)\Theta_{ni}^{(0,\ell'_i)}(\xi_n, \xi_i) \tag{6.25}$$

In Eqs. (6.23), (6.24) and (6.25) also, the derivative with respect to $|k_n|$ is finite, while the derivative with respect to any other channel momentum (for example k_i or k_f) or with respect to the total energy is infinite both from above and from below the threshold. The measurement of the cross-sections (differential, integrated over angles, total), at the threshold of channel n, will exhibit a characteristic 'cusp' or 'rounded step' as shown in Fig. 4.

The downward cusp and the S-like step (3rd and 4th cases in Fig. 4) are not possible for the scattering cross-section when only one channel (channel 1) is open below the threshold considered. Let us see this in detail.

Let us consider for simplicity the case in which the threshold effect appears in the $\ell = 0$ wave of channel 1 and let us forget about spins and Coulomb forces in this channel. For the $\ell = 0$ partial cross-section at threshold we have:

$$\frac{\partial}{\partial|k_n|}\sigma_{11}^{(0)} = \frac{\pi}{k_{10}^2}\frac{\partial}{\partial|k_n|}|1 - S_{11}|^2 \tag{6.26}$$

where S_{11} refers to $J = \ell_f = \ell_i = 0$ and k_{10} is k_1 evaluated at $k_n = 0$. Below the threshold for channel n, S_{11} is unitary and can be expressed as $\exp[2i\delta_{11}]$ with δ_{11} real number. Above the threshold the scattering phase shift δ_{11} becomes complex, but since $|S_{11}|^2 \leqslant 1$ from unitarity, its imaginary part must be non-negative. Near the threshold we therefore have:

$$\delta_{11} = \delta_{110} + \begin{pmatrix} i \\ -1 \end{pmatrix} \alpha |k_n| \tag{6.27}$$

where we have neglected terms in k_n^2, k_n^3, etc.; $\alpha \geqslant 0$ and δ_{110} is δ_{11} evaluated at $k_n = 0$. By the use of Eq. (6.27) we easily evaluate Eq. (6.26)

above and below the threshold for channel n. In the limit as $k_n \to 0$, we obtain:

$$\frac{\partial}{\partial k_n} \sigma_{11}^{(0)} \Big|_a = -\frac{8\pi}{k_{10}^2} \alpha \sin^2 \delta_{110}, \quad \text{above} \tag{6.28a}$$

$$\frac{\partial}{\partial |k_n|} \sigma_{11}^{(0)} \Big|_b = -\frac{8\pi}{k_{10}^2} \alpha \sin \delta_{110} \cos \delta_{110} \quad \text{below} \tag{6.28b}$$

Equation (6.28a) gives us the desired result that above the threshold the derivative of $\sigma_{11}^{(0)}$ is always negative.

The ratio of (6.28a) to (6.28b) gives:

$$\frac{\dfrac{\partial}{\partial k_n} \sigma_{11}^{(0)} \Big|_a}{\dfrac{\partial}{\partial |k_n|} \sigma_{11}^{(0)} \Big|_b} = \operatorname{tg} \delta_{110} \tag{6.29}$$

Because of the fact that:

$$\frac{d|k_n|}{dk_i} = \begin{pmatrix} + \\ - \end{pmatrix} \frac{k_i}{|k_n|} \frac{\omega_n}{\omega_i}$$

if $\operatorname{tg} \delta_{110}$ is positive then the threshold anomaly is a cusp (1st case in Fig. 4), if $\operatorname{tg} \delta_{110}$ is negative then the anomaly is a rounded step (2nd case in Fig. 4)[10]

Equation (6.28) enables us to obtain the scattering phase shift at the threshold for channel n by the measurement of the slope of $\sigma_{11}^{(0)}$ above and below the threshold in the experimental curve.

Various other examples in which direct use of Eqs. (6.23) and (6.24) furnishes information about scattering phase shifts have been considered in detail by Newton [5], and Baz, Puzikov and Smorodinskii [6].

It is clear from our method that the reason why the energy derivative of cross-sections is also infinite below the threshold for channel n is a purely quantum mechanical one. No explanation on classical grounds can be found for it as for the same phenomenon from above, which can be interpreted on the basis of the conservation of total flux (see also Refs. [5] and [7]).

It is clear how a phenomenon of this kind can give information about relative parities and spins. In fact, only the $\ell_n = 0$ part of the wave in channel n contributes to Eqs. (6.23), (6.24) and (6.25). Therefore, if it is possible to tell experimentally in which partial wave, in the initial or

[10] An equation similar to Eq. (6.29) holds true for any scattering cross-section, at the threshold of a generic channel n, in the perturbation approximation which assumes the off-diagonal potentials to be weak; see Eq. (5.9) of the first part of Ref. [5].

in the final channel, the cusp (or step) appears, the parity or spin of that channel will result from conservation of total angular momentum and parity, if any. For example: if one discovers that in the cross-section σ_{fi} the cusp appears for $\ell_f = 0$, then $P_{nf} = +1$, P_{nf} being the relative parity between channel n and channel f. If, instead, the cusp appears for $\ell_f = 1$, then $P_{nf} = -1$. This kind of analysis can be profitably applied, for example, to strange particle processes. The example just given works beautifully for $i = \pi^- p$, $f = \Lambda K$, $n = \Sigma K$. The experimental determination of the final partial wave, in which the cusp appears for the reaction $\pi^- p \to \Lambda K$ at the threshold for Σ production, can determine the $P_{\Lambda\Sigma}$ relative parity. And, for $P_{\Lambda\Sigma} = +1$, only a spin 1/2 for Σ is compatible with a spin 1/2 of Λ (spin of the K-meson taken = 0).

Threshold effects can also be useful for the determination of the reaction cross-section σ_{fn}, which in many instances is out of reach of direct experimental measurement. For the case in which one of the particles in channel n has spin zero so that s_n is given, taking the square of Eq.(6.25) above and below we get at threshold:

$$\left(\frac{\partial}{\partial k_n}\,{}^{(\ell_f)}\sigma_{fi}\Big|_a\right)^2 + \left(\frac{\partial}{\partial |k_n|}\,{}^{(\ell_f)}\sigma_{fi}\Big|_b\right)^2 = \pi^{-1}\,{}^{(\ell_f)}\sigma_{fi}\left(k_n\,{}^{(\ell_f)}\sigma_{fn}\right)\left(k_n^{-1}\,{}^{(\ell_n=0)}\sigma_{ni}\right) \qquad (6.30)$$

where it is understood that $\nu_n = \nu_i$. Since ${}^{(\ell_f)}\sigma_{fn}$ goes to infinity linearly in the limit $k_n \to 0$, a k_n has been placed to counterbalance this effect. Analogously, ${}^{(\ell_n=0)}\sigma_{ni}$ goes to zero linearly and k_n^{-1} makes it non-zero in the limit. Clearly only ℓ_f-waves which are coupled to the $\ell_n = 0$ wave satisfy Eq.(6.30). From measurements of the slope of ${}^{(\ell_f)}\sigma_{fi}$ above and below the threshold and of $\left(k_n^{-1}\,{}^{(\ell_n=0)}\sigma_{ni}\right)$, one can determine the ${}^{(\ell_f)}\sigma_{fn}$ cross-section at zero energy. If its right-hand side is known, Eq.(6.30) can be used to predict the size of the cusp (or rounded step)[11].

Equation (6.22) does not hold if the final channel is the new channel n. An equation analogous to Eq.(6.25) can, however, also be obtained for f = n:

$$\frac{\partial}{\partial k_n}\left(k_n^{-1}\,{}^{(\ell_n=0)}\sigma_{ni}\right) = -\frac{1}{2\pi}\left(k_n\sigma_n^{tot}\right)\left(k_n^{-1}\,{}^{(\ell_n=0)}\sigma_{ni}\right) \qquad (6.31)$$

where $\nu_n = \nu_i$. Equation (6.31) allows the determination of σ_n^{tot} from the slope and intercept of the curve $\left(k_n^{-1}\,{}^{(\ell_n=0)}\sigma_{ni}\right)$ near the threshold.

For the example considered above of production of strange particles in pion-nucleon collisions, by using Eq.(6.30) one can determine at zero energy the cross-section ${}^{(\ell_\Sigma=0)}\sigma_{\Sigma K \to \Lambda K}$ for the process $\Sigma K \to \Lambda K$, which is not feasible experimentally. Analogously, use of Eq.(6.31) at the ΛK and ΣK

---

[11] The size of a cusp or rounded step can actually be conspicuous; see, for example, the anomalies obtained by Fonda, L., and Newton, R. G., Nuovo Cimento 14 1027 (1959) and those obtained in Ref.[8].

thresholds yields the non-directly-measurable cross-sections $\sigma^{tot}_{\Lambda K}$ and $\sigma^{tot}_{\Sigma K}$, respectively.

Threshold anomalies can also give information about the existence of new particles. A typical example is that given by di-neutron: the discovery of a rounded step in neutron-deuteron scattering below the threshold for break-up of the deuteron would give information about the existence of the di-neutron. A calculation shows that in this case the effect can be large [8][12].

The threshold anomalies considered in this section have been observed experimentally in the elastic scattering ^{3}H (p, p) ^{3}H at the threshold for the reaction ^{3}H (p, n) ^{3}He in the form of a downward step [9], and in the scattering Li (p, p) Li at the threshold for Li (p, n) Be in the form of a cusp [10].

The method used in this section (unitarity and analyticity of the S-matrix) to obtain the threshold effects was first considered by Baz and Okun [11].

We end this section with a brief discussion of the case in which three particles are present in the new channel n (for example, the production of an extra nucleon in nucleon-nucleus collisions).

The quantity which exerts an influence on the scattering and reaction cross-sections σ_{fi} via removal of flux is now the reaction cross-section $\bar{\sigma}_{ni}$ integrated over the energy range available to one of the particles in channel n: $\int_0^{k_1^{max}} d^3k_1 \bar{\sigma}_{ni}$. The quantity (see Eq. (5.26)) and its first derivative with respect to k_i are zero at threshold, on the assumption that the interaction vanishes at large distances, so that no threshold effect of the cusp (or rounded step) type is expected in σ_{fi}. Since the second derivative is different from zero and finite, a discontinuity is instead expected in the second derivative of σ_{fi} with respect to k_i at threshold. Such expectations are confirmed by a quantitative analysis, on the same line as before, that we omit. Note that again only the waves in the initial and final channels, coupled to the S-waves $\ell_1 = \ell_{23} = 0$ of the three-body channel, will exhibit the anomaly in the second derivative.

7. COULOMB EFFECTS

From Fig. 1 we see that when a repulsive Coulomb force is present in channel n, then σ_{ni} starts at the threshold like $\exp[-\pi a_n/k_n]$, while in the case of Coulomb attraction in n, σ_{ni} starts with a finite value at the threshold and in general with non-zero and finite slope as a function of k_i. We expect, therefore, that in the case of Coulomb repulsion the new channel n makes itself felt in the other cross-sections very smoothly and no cusp (or rounded step) will consequently appear in them [12, 13]. Also, in the case of Coulomb attraction no cusp is expected, but instead

---

[12] Incidentally, recent experimental work seems to exclude the occurrence of a large anomaly in the total cross-section (H.B. Willard, J.K. Bair and C.M. Jones, Phys. Lett. 9 (1964) 339. If the set of scattering lengths which favours the doublet scattering is chosen to be correct, this experiment excludes the existence of the di-neutron; on the other hand, if the other set of scattering lengths is chosen, nothing can be said about the existence of the di-neutron, since, in this case, the threshold effect would be very small.

another type of anomaly is to be observed. As the energy of the incident particle approaches the threshold for channel n from below, we will observe in σ_{fi} a series of ever more rapid oscillations due to the physical possibilities of excitation of the infinitely many Coulomb bound states of channel n. The limit of σ_{fi} below the threshold will not exist, since these Coulomb bound states, and therefore the corresponding resonances in σ_{fi}, have the threshold energy as an accumulation point. What will be seen experimentally is the average of σ_{fi} below the threshold of channel n, and this quantity will eventually exhibit a step-like discontinuity at threshold, to counterbalance the sudden leakage of flux to the new channel n [13].

The Coulomb effects are therefore able, in both the repulsive and the attractive case, to wash out the cusp (or rounded step), as given in Fig. 4, in the old cross-sections at the threshold for the new channel n. In most cases of interest, however, such as in processes in which nuclear particles take place, the Coulomb effects described above cover an energetic region around the threshold of the order of 10^{-3} MeV, which is out of reach of the present techniques due to the poor energy resolution in the incoming beam. In these cases the overall energy behaviour of the various σ_{fi} at the threshold for channel n will look like a cusp (or a rounded step), even though σ_{fi} does <u>not</u> exhibit infinite derivatives at either side of the threshold in either case (repulsive or attractive). In these cases, therefore, arguments like the ones given before on the determination of parity, spins, etc., will still be applicable.

The above considerations cannot be put into a quantitative form by using the method of section 6. In fact that method is not applicable now, since the S-matrix has an essential singularity at $k_n = 0$. Use must instead be made of the properties of the complete resolvent $(E + i\epsilon - H)^{-1}$. The method sketched here follows Ref. [2]. We obtain, after few formal manipulations:

$$\Delta\Theta_{fi}(\vec{\xi}_f, \vec{\xi}_i) = -\left(\frac{2\pi}{\hbar}\right)^2 (\omega_i \omega_f k_f / k_i)^{1/2} \left(\varphi_{cf}^{(-)}, \Pi_{fn} \frac{1}{[\Delta G_{cn}]^{-1} + \Pi_{nn}} \Pi_{ni} \varphi_{ci}^{(+)} \right), \quad (7.1)$$

where G_{cn} is the Coulomb Green's function for channel n:

$$\langle \vec{r} | G_c | \vec{r}' \rangle = -\frac{\omega}{2\pi\hbar^2} \sum_{\ell} \frac{2^\ell}{(2\ell)!} \frac{r_<^\ell}{r_>} P_\ell(\cos \hat{rr'}) \frac{M_{i\eta,\, \ell+1/2}(2ikr_<)}{(2ikr_<)^{\ell+1}}$$

$$\times \left[(-ik)^\ell \Gamma(\ell + 1 + i\eta) W_{-i\eta,\, \ell+1/2}(-2ikr_>) \right] \quad (7.2)$$

W is the irregular confluent hypergeometric function in the notation of Whittaker and Watson [14]. By $\Delta f(k_n)$ we mean

$$\Delta f(k_n) \equiv \lim_{\bar{k}_n \to 0^+} f(\bar{k}_n) - f(k_n) \quad (7.3)$$

with k_n given below the threshold energy E_n.

By using Eq. (7.2) we can evaluate explicitly the jump experienced by the Coulomb Green's function G_{cn}. The quantity which is responsible for such a jump across the threshold is:

$$(-ik_n)^{\ell}\,\Gamma(\ell+1+i\eta_n)W_{-i\eta_n,\,\ell+1/2}(-2ik_n r_>) \tag{7.4}$$

while at the threshold $M_{i\eta,\,\ell+1/2}(2i\rho_<)/(2i\rho_<)^{\ell+1}$ is a continuous function of the energy. The quantity (7.4) has been considered in great detail in Ref. [13]. Using Eq. (16) of that paper we get for the Coulomb Green's function:

$$\Delta\langle\vec{r}|G_{cn}|r'\rangle = \begin{cases} = -\dfrac{i\omega_n|k_n|}{\pi\hbar^2}\left[1-e^{-2i\pi|\eta_n|}\right]^{-1} \\ \quad \times\displaystyle\sum_{\ell}(2\ell+1)P_{\ell}(\cos\hat{rr'})\,\frac{F_{\ell}(|k_n|r_<)}{|k_n|r_<}\,\frac{F_{\ell}(|k_n|r_>)}{|k_n|r_>}, & a_n<0 \\ = 0, \quad a_n>0 \end{cases} \tag{7.5}$$

For attractive Coulomb forces ($a_n<0$) in channel n we then obtain a jump in G_{cn}, and in Θ_{fi}, when we go across the threshold, while the jump is zero for repulsive Coulomb forces ($a_n>0$) so that no anomaly is observed, as expected, in this last case.

Substitution of Eq. (7.5) into Eq. (7.1) yields a simple expression for $\overline{\Delta\Theta}_{fi} \equiv e^{-i\sigma_0^f}\,\Delta\Theta_{fi}\exp^{-i\sigma_0^i}$ only if we expand in spherical harmonics:

$$\overline{\Delta\Theta}_{fi}(\vec{\xi}_f,\vec{\xi}_i) = -\frac{2\pi i}{k_i}\sum_{\substack{JM\ell_i\ell_f \\ \ell_n S_n \ell_n' S_n'}} Y_{\ell_f}^{M-\nu_f}(\hat{k}_f)Y_{\ell_i}^{M-\nu_i\,*}(\hat{k}_i)C_{\ell_f s_f}(J,M;\,M-\nu_f,\nu_f)$$

$$\times\, C_{\ell_i s_i}(J,M;\,M-\nu_i,\nu_i)\bar{S}^J_{f\ell_f s_f,\,n\ell_n s_n}\left(\frac{1}{\bar{S}_n^J-\exp\left[i\pi(\ell-2|\eta_n|)\right]}\right)_{n\ell_n s_n,\,n\ell_n' s_n'}\bar{S}^J_{n\ell_n' s_n',\,i\ell_i s_i}, \tag{7.6}$$

$$a_n<0$$

where $\bar{S}_n^J$ is the sub-matrix whose elements refer only to channel n; $\exp[i\pi\ell]$ is a diagonal matrix in the ℓ-representation for channel n. We

have renormalized the definition of the S-matrix by

$$\bar{S}_{jk} \equiv e^{-i\sigma_0^j} S_{jk} e^{-i\sigma_0^k} \tag{7.7}$$

which does not alter any of the observable quantities, and have taken into account the fact that

$$\lim_{k_n \to 0} \exp[2i(\sigma_\ell^n - \sigma_0^n)] = \exp[i\pi\ell]$$

From Eqs. (7.6) and (6.1) we obtain the energy behaviour of the elements of the S-matrix (for $i \neq n$, $f \neq n$) at the threshold for channel n:

$$\Delta\bar{S}^J_{f\ell_f s_f, i\ell_i s_i} = \sum_{\ell_n s_n \ell'_n s'_n} \bar{S}^J_{f\ell_f s_f, n\ell_n s_n} \left(\frac{1}{\bar{S}^J_n - \exp[i\pi(\ell - 2|\eta_n|)]} \right) \bar{S}^J_{n\ell_n s_n, n\ell'_n s'_n, i\ell_i s_i}$$

$$a_n < 0. \tag{7.8}$$

The oscillatory denominator in Eqs. (7.6) and (7.8) represents the resonances at each of the infinitely many Coulomb bound states of the channel n. These oscillations become infinitely fast near $k_n = 0^-$, point of accumulation for the Coulomb bound states. Therefore only the average of the various observable quantities will be detected experimentally. The averaging procedures for the differential reaction cross-sections and for the total cross-section have been given in Ref. [15]. The result is that, while the various averaged differential cross-sections exhibit a jump across the threshold for channel n, the averaged total cross-section turns out to be continuous there.

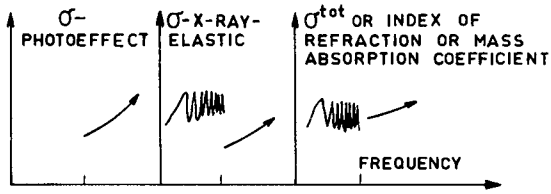

FIG. 5. Photoeffect

A phenomenon of this kind is, for example, expected to occur in the elastic scattering of X-rays by atoms at the threshold for the photoelectric effect [15]. Figure 5 shows the details of the phenomenon. An analogous effect will occur in nucleon-nucleus scattering of the threshold for π^- production.

In this report I have not discussed the case where, even though the two particles are not both charged in the considered channel, the Coulomb interaction manages to give a potential α/r^2. This occurs,

for example, in the case of the scattering of an electron on hydrogen atom. The treatment of this case is a simple generalization of the non-Coulomb case considered in this report. We have only to substitute in place of the orbital angular momentum quantum number ℓ the quantity λ obtained from the equation

$$\ell(\ell+1)+\alpha = \lambda(\lambda+1)$$

For details see Ref. [16].

REFERENCES

[1] WIGNER, E.P., Phys. Rev. 73 (1948) 1002.
[2] FONDA, L., Supplemento Nuovo Cimento 20 (1961) 116.
[3] NEWTON, R.G., Scattering Theory of Waves and Particles, Mc Graw-Hill Inc., New York (1966).
[4] BLATT, J.M., WEISSKOPF, V.F., Theoretical Nuclear Physics, Appendix A, J. Wiley and Sons, New York (1952).
[5] NEWTON, R.G., Annals of Physics 4 29 (1958); Phys. Rev. 114 (1959) 1611.
[6] BAZ, A.I., PUZIKOV, L.D., SMORODINKSKII, Ya.A., Zh. eksp. teor. Fiz. 42 (1962) 1249. Transl.: Sov. Phys. JETP 15 (1962) 865.
[7] FONDA, L., Nuovo Cimento 13 (1959) 956.
[8] ALZETTA, R., GHIRARDI, G.C., RIMINI, A., Phys. Rev. 131 (1963) 1740.
[9] ENNIS, M.E., HEMMENDINGER, A., Phys. Rev. 95 (1954) 772.
[10] MALMBERG, P.R., Phys. Rev. 101 (1956) 114.
[11] BAZ, A.I., OKUN, L.B., Z. eksp. teor. Fiz. 35 (1958) 757. Transl.: Sov. Phys. JETP 8 (1959) 526.
[12] BREIT, G., Phys. Rev. 107 (1957) 1612; Handbuch der Physik, Band XLI/1, Berlin (1959) 1.
[13] FONDA, L., NEWTON, R.G., Ann. Phys. 7 (1959) 133.
[14] WHITTAKER, E.T., WATSON, G.N., A Course of Modern Analysis, Cambridge University Press, London and New York (1958).
[15] NEWTON, R.G., FONDA, L., Ann. Phys. 9 (1960) 416.
[16] GAILITIS, M., DAMBURG, R., Proc. phys. Soc. 82 (1963) 192.

The references given above cover only papers related to threshold effects. For more material on scattering theory, in addition to the papers by Ekstein and Jauch quoted in the text and to the book by Newton (Ref. [3]), the reader is referred to:

SCHWEBER, S.S., An Introduction to Relativistic Quantum Field Theory, Chap. 11, Row-Peterson, Evanston, Illinois (1961).

GOLDBERGER, M.L., WATSON, K.M., Collision Theory, John Wiley & Sons, Inc., New York (1964).

BRENIG, W., HAAG, R., Fortschr. Phys. 7 (1959) 183; Quantum Scattering Theory, (ROSS, M., Ed.) Indiana University Press, Bloomington, Indiana (1963) 13.

CHAPTER 7

S-MATRIX THEORY OF NUCLEAR RESONANCE REACTIONS

J. HUMBLET

INTRODUCTION

The theory of nuclear reactions has considerably expanded during the last few years. Its ultimate object is obviously the computation of cross-sections. This is basically a dynamical problem. For a given set of nucleons, one should be able to write down its Hamiltonian and to derive from it the bound states, the reaction channels, their thresholds and the elements of the collision matrix as a continuous function of the total energy of the system. If this could be achieved, the elements of the collision matrix would then give the cross-sections which are the quantities measured in the laboratory. In practice however, this approach to the theory of nuclear reactions is still far from realizable.

Nevertheless, for more than thirty years, experimental data on nuclear reactions have been accumulated; in many cases they include the energy dependence of the integrated and differential cross-sections. Prominent features such as the resonances were discovered. Lacking a dynamical theory of resonance reactions, the theoretical analysis of an experimental cross-section consisted only in its parametrization, i.e. its description in terms of a small number of parameters. In particular, many resonances have been fitted to the well-known Breit-Wigner formula [1-3]. This led to a systematic determination of such parameters as the energy of a resonance, its total and partial widths. The original Breit-Wigner formula being only a "one-level" approximation and its justification being partly phenomenological [4], it followed that the first theories of nuclear reactions were mainly concerned with the formal derivation of an exact dispersion formula for the collision matrix. We refer to the theories such as those of Bethe and Placzek [5, 6], Kapur and Peierls [7, 8], and the R-matrix theory of Wigner and collaborators [9, 10, 11]. In practice however, only the R-matrix theory, or rather the approximations derived from it [12], has been extensively used for parametrizing experimental data.

The author is at the Institut de Mathématique (Physique Nucléaire Théorique), University of Liège, Belgium.

Unfortunately, the definition of the basic parameters introduced in the R-matrix theory, namely the energy eigenvalues E_λ and the reduced width amplitudes $\gamma_{\lambda c}$, is largely arbitrary. They strongly depend on the (free) choice of boundary condition constants and also on the exact value adopted for the channel radii, although the latter quantities cannot be sharply defined from a physical point of view. Moreover, the derivation of the collision matrix from the parametrized R-matrix involves the inversion of a matrix. It results in a very complicated dependence of the collision matrix elements on the energy and basic parameters (Ref. [12], p. 294). Under such conditions, one is justified in questioning the validity of the assumptions and approximations which are usually made in deriving the approximate parametrized cross-sections which have been used for fitting experimental data. A discussion of the validity of some of these approximations may be found in the original literature (see Refs [15, 16]).

Here, we present an alternative way of parametrizing the collision matrix; it has been developed in a series of recent papers [17-25] and is often referred to as the S-matrix theory of nuclear reactions. In contrast with the R-matrix theory, it parametrizes directly the S-matrix itself; it introduces a set of complex eigenvalues, the real and imaginary parts of which correspond to the position and total width of the resonances.

Neither the R-matrix nor the S-matrix theories have been designed to be a dynamic theory. Nevertheless, the accumulation of data from parametrized cross-sections and shell model calculations have suggested approaching the dynamical aspect of the theory of nuclear reactions in a less ambitious but more realistic way than the above-mentioned one. Very schematically, most of the recent dynamical theories can be characterized as follows: they assume as a starting point the knowledge of an approximate Hamiltonian and its complete set of eigenfunctions; some [26-28] aim at a direct computation of the cross-sections as a function of the energy, but most [29-36] are basically oriented towards the theoretical calculation of the main reaction parameters (energy, total and partial widths of resonances).

Under such conditions, the formal derivation of a parametrized collision matrix retains all its former importance. The question of deciding which parametrization is better adapted to dynamical computations is also of current interest [16, 34-36].

AUTHOR'S NOTE

It is assumed that the reader is familiar with the phenomenological aspect of the theory of nuclear reactions [4]. For didactic reasons, however, a preliminary discussion on the one-channel case (elastic scattering by a central force) will introduce the subject. It will summarize the first twenty pages of Ref. [17] and will not be reproduced in this text. In the first sections of this chapter, we follow rather closely Sections 4 to 7 of Ref. [17]; then we progressively introduce the improvements of the theory as given mainly in Refs. [20] and [22].

1. THE CONFIGURATION SPACE AND THE WAVE-FUNCTION

1.1. Channels

Our general assumptions will be the usual ones: conservation of probability, time reversability and causality in the framework of non-relativistic mechanics.

As usual also, we call channel a situation in which the A nucleons we consider are separated into two fragments containing A_1 and A_2 nucleons respectively, each of which is in a stationary state, while their state of relative motion is also specified. We confine the discussion to channels of this restricted type, i.e. we disregard the photons and possibility of a three-body break-up; photon channels have been introduced in the S-matrix theory of nuclear reactions by Mahaux [23], but the three-body break-up is obviously a much more difficult and unsolved problem.

The state of a fragment A_j is characterized by a total spin quantum number I_j, its projection i_j and a set of other quantum numbers specifying its energy, which we denote by α_j. Instead of i_1, i_2, we may also use the quantum numbers s, ν specifying the channel spin

$$\vec{s} = \vec{I}_1 + \vec{I}_2$$

$$|I_1 - I_2| \leqslant s \leqslant I_1 + I_2$$

and its projection ν. We shall consider states of relative motion of orbital momentum with quantum numbers ℓ, m. Because of the conservation of the total angular momentum $\vec{J} = \vec{\ell} + \vec{s}$, of quantum numbers J, M, we may also replace the quantum numbers ν, m by J, M in the definition of the channel. Accordingly, the channel symbol c will be used to represent any one of the sets of quantum numbers:

$$\begin{aligned} &\{\alpha_1\alpha_2,\ I_1I_2,\ i_1i_2,\ \ell m\} \\ &\{\alpha_1\alpha_2,\ I_1I_2,\ s\nu,\ \ell m\} \\ &\{\alpha_1\alpha_2,\ I_1I_2,\ s\ell,\ JM\} \end{aligned} \qquad (1.1.1)$$

For each mode of subdivision into two fragments A_1, A_2, we use an appropriate set of co-ordinates to which we attach an index α chosen as the same letter α by which we denote the states of excitation α_1, α_2, of the fragments. Thus for the two fragments we shall take two sets of internal co-ordinates $q_{\alpha 1}$, $q_{\alpha 2}$ (including the spin of the individual nucleons), while $\vec{r}_\alpha$ will be used to designate the relative position of their respective centre-of-mass:

$$\vec{r}_\alpha = \vec{r}_{\alpha_2} - \vec{r}_{\alpha_1} \qquad (1.1.2)$$

As usual, we assume that the motion of the centre-of-mass of the total system has been eliminated.

For each channel c we also assume the existence of a "channel radius" a_α such that for $r_\alpha > a_\alpha$ only Coulomb forces act between the two fragments. This is not, of course, a very accurately defined quantity, but, as we shall see later, this is precisely one of the main features of the S-matrix theory to be independent of the exact values of the channel radii; they may be chosen much larger than the range of the nuclear forces.

Let us consider the configuration space of the A nucleons. The region of this space corresponding to the A nucleons being close together in

physical space is called the interior region, more precisely, it is defined by

$$r_\alpha < a_\alpha \text{ for all } \alpha . \tag{1.1.3}$$

The boundary surface $\mathscr{S}$ of this interior region is then composed of an assembly of parts of the surfaces $r_\alpha = a_\alpha$. Any point which is not in the interior region or on its boundary $\mathscr{S}$ is said to be in the exterior region.

1.2. The wave-function in the exterior region

Let Ψ_c be the total wave-function in channel c. It contains a sum of products of internal wave-functions of the two fragments

$$\psi_{\alpha_1 I_1 i_1} \; \psi_{\alpha_2 I_2 i_2} \tag{1.2.1}$$

which may be grouped in a channel-spin wave-function

$$\psi_{\bar{\alpha} s \nu} = \sum_{i_1+i_2=\nu} (I_1 I_2 i_1 i_2 \,|\, s \nu) \psi_{\alpha_1 I_1 i_1} \; \psi_{\alpha_2 I_2 i_2} \tag{1.2.2}$$

where $\bar{\alpha}$ is written for $\alpha_1\alpha_2$, while the indices $I_1 I_2$ are generally omitted. Representing the relative motion of the fragments by

$$i^\ell Y_m^\ell(\Omega_\alpha) u_c(r_\alpha)/r_\alpha \tag{1.2.3}$$

it is convenient to define a surface factor

$$\varphi_{\bar{\alpha} s \ell \nu m} = i^\ell Y_m^\ell \; \psi_{\bar{\alpha} s \nu} \tag{1.2.4}$$

in the $\{\bar{\alpha}\, s\, \ell\, \nu\, m\}$ representation, or

$$\varphi_{\bar{\alpha} s \ell, J M} = \sum_{\nu+m=M} (s\, \ell\, \nu\, m \,|\, J\, M)\, \varphi_{\bar{\alpha} s \ell \nu m} \tag{1.2.5}$$

in the $\{\bar{\alpha}\, s\, \ell\, J\, M\}$ representation.

For all channels corresponding to the mode of fragmentation α, the surface functions φ_c may be chosen to form an orthonormal set, which may be assumed to be complete in the subspace of all co-ordinates except r_α. In this subspace we write the orthonormality relation in the form

$$\int \varphi_c^* \, \varphi_{c'} \, dS_\alpha = \delta_{cc'} \tag{1.2.6}$$

with

$$dS_\alpha = d\Omega_\alpha dq_{\alpha_1} dq_{\alpha_2} \tag{1.2.7}$$

The completeness of the set φ_c allows us to express the exterior wave-function Ψ_{ext}, in its most general form, at any point of the exterior region

corresponding to the fragmentation α, as a superposition of all the channel wave-functions Ψ_c belonging to this mode of fragmentation α:

$$\Psi_{\text{ext}(\alpha)} = \sum_{c(\alpha)} \Psi_c = \sum_{c(\alpha)} \varphi_c \frac{u_c(r_\alpha)}{r_\alpha} \tag{1.2.8}$$

where the symbol $\sum_{c(\alpha)}$ indicates a summation over all channels for which the mode of fragmentation of the compound system is α. Moreover, since the very existence of the channels implies that the overlapping of two functions $\Psi_{\text{ext}(\alpha)}$, $\Psi_{\text{ext}(\alpha')}$ is completely negligible, the general form of the total wave-function Ψ in the exterior region is

$$\Psi = \sum_{\alpha} \Psi_{\text{ext}(\alpha)} \tag{1.2.9}$$

or

$$\Psi = \sum_{c} \Psi_c = \sum_{c} \varphi_c u_c(r_\alpha)/r_\alpha \tag{1.2.10}$$

in Eq. (1.2.9), only one term can be different from zero at some specified point of the exterior region, while the sums in Eqs (1.2.10) are extended to all possible channels, irrespective of the fragmentation.

The total energy $\mathscr{E}$ of the compound system is expressed in a given channel c as a sum of the internal energy $E_{\bar{\alpha}} = E_{\alpha_1} + E_{\alpha_2}$ of the fragments and the energy E_c of their relative motion:

$$\mathscr{E} = E_c + E_{\bar{\alpha}} \tag{1.2.11}$$

If $E_c > 0$, the channel c is said to be "open"; if $E_c < 0$, it is said to be "closed". The relative motion in an open channel is characterized by a real positive wave-number defined by

$$k_c = \frac{+(2M_\alpha E_c)^{\frac{1}{2}}}{\hbar} \tag{1.2.12}$$

where $M_\alpha = M_{\alpha_1} M_{\alpha_2}/(M_{\alpha_1} + M_{\alpha_2})$ is the reduced mass of the fragments. The corresponding relative velocity is

$$v_c = \hbar k_c / M_\alpha \tag{1.2.13}$$

In a closed channel, the wave-number defined by Eq. (1.2.12) is imaginary; it will be taken with

$$\text{Im}\, k_c > 0 \tag{1.2.14}$$

For a state of the system of given energy $\mathscr{E}$, the various channel wave-numbers are not independent, but are connected by the relations of the

form (1.2.11) expressing the conservation of energy in the processes concerned:

$$\mathscr{E} = \frac{\hbar^2}{2M_\alpha} k_c^2 + E_{\bar{\alpha}} = \frac{\hbar^2}{2M_{\alpha'}} k_{c'}^2 + E_{\bar{\alpha}'} = \ldots \tag{1.2.15}$$

The radial factor $u_c(r_\alpha)$ of the channel wave-function Ψ_c appearing in Eq.(1.2.10) may be written, as in the single-channel case,

$$u_c(r_\alpha) = x_c O_\ell(r_\alpha, k_c) + y_c I_\ell(r_\alpha, k_c) \tag{1.2.16}$$

where the functions O_ℓ, I_ℓ correspond to outgoing and ingoing waves respectively. We define them in terms of the Coulomb wave-functions F_ℓ, G_ℓ, as

$$O_\ell = (G_\ell + iF_\ell) e^{-i\sigma_\ell}, \quad I_\ell = (G_\ell - iF_\ell) e^{i\sigma_\ell} \tag{1.2.17}$$

and they satisfy the Wronskian relation

$$W(O_\ell, I_\ell; r_\alpha) = -2ik \tag{1.2.18}$$

1.3. The interior wave-function and the boundary conditions

For the total wave-function in the interior region Ψ_{int}, no factorization of type (1.2.10) is possible because of the coupling of the channels. Nevertheless, considering the product $r_\alpha \Psi_{int}$ on the portion $\mathscr{S}_\alpha$ of $\mathscr{S}$ corresponding to $r_\alpha = a_\alpha$, we may write

$$(r_\alpha \Psi_{int})_{\mathscr{S}_\alpha} = \sum_{c(\alpha)} \Phi_c \varphi_c \tag{1.3.1a}$$

where the expansion coefficient Φ_c is defined as

$$\Phi_c = \int \varphi_c^* (r_\alpha \Psi_{int})_{r_\alpha = a_\alpha} dS_\alpha \tag{1.3.2a}$$

Similarly, for the radial derivative, we have

$$\left[\frac{\partial}{\partial r_\alpha}(r_\alpha \Psi_\alpha)\right]_{\mathscr{S}_\alpha} = \sum_{c(\alpha)}' \Phi_c' \varphi_c \tag{1.3.1b}$$

with

$$\Phi_c' = \int \varphi_c^* \left[\frac{\partial}{\partial r_\alpha}(r_\alpha \Psi_{int})\right]_{r_\alpha = a_\alpha} dS_\alpha \tag{1.3.2b}$$

It is clear that Φ_c, Φ_c' correspond to the radial factors $u_\ell(a)$, $u_\ell'(a)$ of the one-channel case. It will be convenient to call Φ_c' the "derivative" of Φ_c and speak of an expression like $\Phi_c O_c'(a_\alpha) - \Phi_c' O_c(a_\alpha)$ as the "Wronskian" of Φ_c and O_c at $r_\alpha = a_\alpha$, which we shall denote by $W(\Phi_c, O_c; a_\alpha)$.

Because we neglect the overlapping of two functions φ_c corresponding to different fragmentations, we may also give to the expansions (1.3.1 and 1.3.2) the following form

$$(r\,\Psi_{int})_{\mathcal{S}} = \sum_c \Phi_c\,\varphi_c \tag{1.3.3a}$$

$$\left[\frac{\partial}{\partial r}\,(r\,\Psi_{int})\right]_{\mathcal{S}} = \sum_c \Phi'_c\,\varphi_c \tag{1.3.3b}$$

where the left-hand side is taken at any point of $\mathcal{S}$, while in the right-hand side the summation is now extended to all channels independently of the fragmentation to which they belong.

With the help of the representation (1.3.1) of the interior wave-function and its normal derivative on the partial boundary surface $r_\alpha = a_\alpha$, we immediately obtain, by comparison with the expansion (1.2.8) of the exterior wave-function, the continuity conditions on this surface. Because of the linear independence of the φ_c, these conditions become, with the expression (1.2.16) for u_c,

$$\Phi_c = x_c O_\ell(a_\alpha, k_c) + y_c I_\ell(a_\alpha, k_c) \tag{1.3.4a}$$

$$\Phi'_c = x_c O'_\ell(a_\alpha, k_c) + y_c I'_\ell(a_\alpha, k_c) \tag{1.3.4b}$$

for all channels c belonging to the mode of subdivision α. Repeating the argument for all the subdivisions, we thus arrive at a complete formulation of the boundary conditions for all channels, which has the advantage of yielding the amplitudes x_c, y_c in explicit form for each channel separately:

$$x_c = -\frac{1}{2ik_c}\,W(\Phi_c, I_\ell; a_\alpha) \tag{1.3.5a}$$

$$y_c = +\frac{1}{2ik_c}\,W(\Phi_c, O_\ell; a_\alpha) \tag{1.3.5b}$$

It is through the factors Φ_c, Φ'_c that a coupling is implicitly established between the amplitudes in the various channels, inasmuch as specification of the incoming amplitudes fixes the interior wave-function and all the radial factors Φ_c, Φ'_c which then, by Eqs (1.3.5a), determine the outgoing amplitudes for all channels.

From now on, when no confusion is to be feared, we shall often find it convenient to use the channel index c instead of more specific indices such as ℓ or α for quantities like O_ℓ, I_ℓ, a_α.

1.4. Collision matrix

Let us consider now a wave-function $\Psi^{(c)}$ with only one incoming channel c and let us add an upper index (c) to all the corresponding physical quantities. According to Eq. (1.3.5b) we have

$$y_{c'}^{(c)} = 0 \text{ for all } c' \neq c \tag{1.4.1a}$$

or more explicitly

$$W(\Phi_{c'}^{(c)}, O_{c'}; a_{c'}) = 0 \text{ for all } c' \neq c \tag{1.4.1b}$$

Hence, in the exterior region we have

$$\Psi^{(c)} = \sum_{c'} x_{c'}^{(c)} O_{c'}(r_{c'}, k_{c'}) \varphi_{c'}/r_{c'} + y_c^{(c)} I_c(r_c, k_c) \varphi_c/r_c \tag{1.4.2}$$

We may consider the Eqs (1.4.1) as a set of boundary conditions defining $\Psi^{(c)}$ completely, except for a normalizing factor $y_c^{(c)}$. Under such conditions, it is convenient to rewrite (1.4.2) in the form

$$\Psi^{(c)} = y_c^{(c)} \left[I_c(r_c, k_c) \varphi_c/r_c - \sum_{c'} U_{c'c} O_{c'}(r_{c'}, k_{c'}) \varphi_{c'}/r_{c'} \right] \tag{1.4.3}$$

where $U_{c'c}$ is defined by

$$x_{c'}^{(c)} = -U_{c'c} y_c^{(c)} \tag{1.4.4}$$

or, according to Eqs (1.3.5),

$$U_{c'c} = \frac{W(\Phi_{c'}^{(c)}, I_{c'}; a_{c'})/k_{c'}}{W(\Phi_c^{(c)}, O_c; a_c)/k_c} \tag{1.4.5}$$

These are the elements of a matrix U related to those of the collision matrix $\mathscr{U}$ by the relation

$$\mathscr{U}_{c'c} = \sqrt{\frac{v_{c'}}{v_c}} U_{c'c} \tag{1.4.6}$$

where

$$v_c = \hbar k_c / M_c \tag{1.4.7}$$

is the velocity in channel c.

Although the unitarity and symmetry properties take a simpler form for $\mathscr{U}$ than for U, namely

$$\sum_{c^+} \mathscr{U}_{cq}^* \mathscr{U}_{cp} = \delta_{pq}, \quad \sum_{c^+} v_c U_{cq}^* U_{cp} = v_q \delta_{qp} \tag{1.4.8}$$

$$\mathscr{U}_{pq} = \mathscr{U}_{qp}, \quad v_p U_{pq} = v_q U_{qp} \tag{1.4.9}$$

we shall often find it more convenient to consider the matrix elements of U rather than those of $\mathscr{U}$. In Eqs (1.4.8), the sums extend over the open channels only. The matrix U will also be called "collision matrix", but no confusion can arise.

In the representation $\{\bar{\alpha}\, s\, \ell,\ J\, M\}$, it is clear that, because of the conservation properties of J and M, we have

$$\Phi^{(c)}_{c'} = \Phi^{(c)'}_{c'} = 0 \text{ when } J, M \neq J', M'. \tag{1.4.10}$$

Moreover, since $\Phi^{(\bar{\alpha}\, s\, \alpha, JM)}_{\bar{\alpha}'\, s'\, \ell',\, JM}$ and $\Phi^{(\bar{\alpha}\, s\, \ell,\, JM)'}_{\alpha\ s'\, \ell',\, JM}$ are scalar products, they are independent of M. In particular, if the notation $-c$ is used to designate the channel $\{\bar{\alpha}\, s\, \ell,\ J-M\}$, we have

$$\Phi^{(c)}_{c'} = \Phi^{(-c)}_{-c'} \tag{1.4.11}$$

The definition (1.4.5) of the matrix element $U_{c'c}$ shows that it is entirely determined by the consideration of the wave-function with the single entrance channel c. The most convenient channel designation scheme for representing the matrix U is obviously $c = \{\bar{\alpha}\, s\, \ell,\ J\, M\}$: in this scheme, according to Eqs (1.4.10), the matrix is diagonal with respect to the angular momentum quantum numbers J, M. Moreover, its elements (like the radial factors $\Phi^{(c)}_{c'}$ on which they depend) are independent of M and may therefore be written

$$U_{c'c} = \delta_{M'M}\ \delta_{J'J}\ U^{J}_{\alpha'\, s'\, \ell',\, \bar{\alpha}\, s\, \ell} \tag{1.4.12}$$

One easily passes from the representation $\{\bar{\alpha}\, s\, \ell\, J\, M\}$ to the scheme $\{\bar{\alpha}\, s\, \ell\, \nu\, m\}$, for instance, by relations of the form

$$U_{\bar{\alpha}'\, s'\, \ell'\, \nu'\, m';\, \bar{\alpha}\, s\, \ell\, \nu\, m} = \sum_{JM} (s'\ell'\nu'm' \,|\, J\, M)\, U^{J}_{\bar{\alpha}'\, s'\, \ell',\, \bar{\alpha}\, s\, \ell}\ (s\, \ell\, \nu\, m \,|\, J\, M) \tag{1.4.13}$$

2. THE RESONANCE STATES

2.1. Definition

Let us consider a wave-function with only one incoming channel $\Psi^{(c)}$. It satisfies, on $\mathscr{S}$, the boundary conditions

$$y^{(c)}_{c'} = W(\Phi^{(c)}_{c'},\ O_{c'}\,;\, a_{c'}) = 0 \quad \text{for} \quad c' \neq c \tag{2.1.1}$$

while its asymptotic behaviour is given by

$$\Psi^{(c)} = y^{(c)}_{c}\, \varphi_c I_c(r_c, k_c)/r_c + \sum_{c'} x^{(c)}_{c'}\, \varphi_{c'}\, O_{c'}(r_{c'}, k_{c'})/r_{c'} \tag{2.1.2}$$

If we add one more boundary condition for $\Psi^{(c)}$, we shall define a set of eigenvalues $\mathscr{E}^{(c)}_n$ of the total energy $\mathscr{E}$ and of eigenfunctions $\Psi^{(c)}_n = \Psi^{(c)}(\mathscr{E}^{(c)}_n)$.

Another wave-function $\Psi^{(d)}$ with asymptotic behaviour

$$\Psi^{(d)} = y^{(d)}_{d}\, \varphi_d I_d(r_d, k_d)/r_d + \sum_{c'} x^{(d)}_{c'}\, \varphi_{c'}\, O_{c'}(r_{c'}, k_{c'})/r_{c'} \tag{2.1.3}$$

satisfying the boundary conditions

$$y_{c'}^{(d)} = W(\Phi_{c'}^{(d)}, O_{c'}; a_{c'}) = 0 \text{ for } c' \neq d \tag{2.1.4}$$

will, when an extra boundary condition is added, lead to different sets of eigenvalues $\mathscr{E}_n^{(d)}$ and eigenfunctions $\Psi_n^{(d)} = \Psi^{(d)}(\mathscr{E}_n^{(d)})$.

If, however, on the basis of what is known for the resonance states in nuclei, we want the two sets $\mathscr{E}_n^{(c)}$, $\mathscr{E}_n^{(d)}$ to be identical, we are not free to choose arbitrarily the extra boundary conditions. They must be $y_c^{(c)} = 0$ for $\Psi_d^{(c)}$ and $y_d^{(d)} = 0$ for $\Psi^{(d)}$. Taking Eqs (2.1.1) and (2.1.4) into account, these conditions imply that on the most general wave function Ψ, we must impose the following set of boundary conditions

$$y_c = 0 \quad \text{for all } c \tag{2.1.5a}$$

i.e.

$$W(\Phi_c, O_c; a_c) = 0 \text{ for all } c \tag{2.1.5b}$$

corresponding formally to a situation without incoming wave in any of the channels. The corresponding states with eigenfunctions Ψ_n and energy $\mathscr{E}_n$ will be, by definition, the resonance states of our system.

Let us decide that any quantity to be taken at the resonance, i.e., for $\mathscr{E} = \mathscr{E}_n$, will simply be written with an extra index n. Under such conditions the following quantities $\Phi_{cn}^{(c)}$, $\Phi_{cn}^{(d)}$, ... $\Phi_{cn}^{(c)'}$, $\Phi_{cn}^{(d)'}$, ... are independent of (c), (d), ..., just as $\mathscr{E}_n^{(c)}$, $\Psi_n^{(c)}$ ... and we are justified in writing

$$\Phi_{cn}^{(c)} = \Phi_{cn}^{(d)} = \ldots \equiv \Phi_{cn} \tag{2.1.6a}$$

$$\Phi_{cn}^{(c)'} = \Phi_{cn}^{(d)'} = \ldots \equiv \Phi_{cn}' \tag{2.1.6b}$$

However, one should not overlook the fact that $\mathscr{E}_n$, Ψ_n should rather be written as

$$\mathscr{E}_{J,n}, \quad \Psi_{JM,n} \tag{2.1.7}$$

the indices J, M being dropped when no confusion is possible.

A resonance energy $\mathscr{E}_n$ is in general complex, since, for any real energy, the flux is conserved, which is not possible when there is no incoming flux. The only exceptions correspond to the bound states which are obviously included in the above definition of the resonant states $\mathscr{E}_n$; both the incoming and outgoing fluxes are then vanishing.

In order to be in a position to discuss the possible locations in the complex k_c-plane of the complex wave-number k_{cn}, i.e., k_c for $\mathscr{E} = \mathscr{E}_n$, we shall now give some properties of the functions I_ℓ and O_ℓ defined by Eqs (1.2.17). Other properties of the same functions in the complex k_c-plane, useful later in the derivation of the expansion of $U_{c'c}$, will also be given in the next paragraph.

2.2. Coulomb wave-functions

In this paragraph, let us drop the index c when no confusion can arise; we follow closely Section 2 of Ref.[20], although here the Coulomb

parameter η will be given its most common definition, namely the energy dependent quantity

$$\eta = Z_1 Z_2 e^2 M/(\hbar^2 k) \tag{2.2.1}$$

while α will be the independent one

$$\alpha = Z_1 Z_2 e^2 M/\hbar^2 \tag{2.2.2}$$

$$= \eta k \tag{2.2.3}$$

Moreover, as in [20], we adopt here the so-called "old" normalization (1.2.17) of I_ℓ and O_ℓ; only later shall we drop the phase $\exp(\pm i\sigma_\ell)$, after the expansion of the collision matrix has been derived.

Two solutions of the equation

$$\left(\frac{d^2}{dr^2} + k^2 - \frac{\ell(\ell+1)}{r^2} - \frac{2\alpha}{r}\right) u_\ell(r,k) = 0 \tag{2.2.4}$$

satisfied by the radial factor of a Coulomb wave-function, are the well known regular function F_ℓ and irregular function G_ℓ. For complex k, with

$$-\pi < \arg k < +\pi \tag{2.2.5}$$

their asymptotic behaviour for large kr is

$$F_\ell \sim \sin(kr - \eta \log(2kr) - \tfrac{1}{2}\ell\pi + \sigma_\ell) \tag{2.2.6a}$$

$$G_\ell \sim \cos(kr - \eta \log(2kr) - \tfrac{1}{2}\ell\pi + \sigma_\ell) \tag{2.2.6b}$$

where σ_ℓ is defined by

$$e^{2i\sigma_\ell} = \frac{\Gamma(\ell+1+i\eta)}{\Gamma(\ell+1-i\eta)} \tag{2.2.7}$$

For small kr, in terms of a well known notation [37] (or see Eqs (2.2.10) below), we have

$$F_\ell \sim (kr)^{\ell+1} C_\ell, \quad G_\ell \sim \frac{1}{(2\ell+1)C_\ell} (kr)^{-\ell} \tag{2.2.7'}$$

The quantities F_ℓ, G_ℓ, η and σ_ℓ are real when k itself is real.

The first solution F_ℓ is proportional to the regular Whittaker function $\mathcal{M} = \mathcal{M}_{i\eta,\,\ell+\frac{1}{2}}(2ikr)$, since

$$F_\ell = \tfrac{1}{2}\epsilon_\ell \ell!\,(-i)^{\ell+1} \mathcal{M}_{i\eta,\,\ell+\frac{1}{2}}(2ikr) \tag{2.2.8}$$

where

$$\epsilon_\ell = \frac{1}{\ell!} e^{-\pi\eta/2} [\Gamma(\ell+1+i\eta)\,\Gamma(\ell+1-i\eta)]^{\frac{1}{2}} \tag{2.2.9}$$

The function $\mathscr{M}$ is defined according to Buchholz [38], i.e.,

$$\mathscr{M} = M_{i\eta,\, \ell+\frac{1}{2}}(2ikr)/(2\ell+1)!$$

for fixed r, $\mathscr{M}/k^{\ell+1}$ is an integral function of k^2. We also have

$$\epsilon_\ell = (2\ell+1)!!\, C_\ell = \frac{1}{\ell!}\left[(\ell^2+\eta^2)\ldots(1+\eta^2)\frac{2\pi\eta}{e^{2\pi\eta}-1}\right]^{\frac{1}{2}} \quad (2.2.10a)$$

$$= \frac{1}{\ell!}\left[(\ell^2+\eta^2)\ldots(1+\eta^2)\right]^{\frac{1}{2}} C_0 \quad (2.2.10b)$$

the latter quantity has been normalized in order that $\epsilon_\ell = 1$ for $k = \infty$ or for a neutron channel ($\alpha = 0$).

Two other solutions of Eq. (2.2.4) are conveniently defined as

$$I_\ell(r,k) = (G_\ell - iF_\ell)\, e^{i\sigma_\ell} = i^\ell e^{\frac{\pi\eta}{2}}\, W_- \quad (2.2.11a)$$

$$O_\ell(r,k) = (G_\ell + iF_\ell)\, e^{-i\sigma_\ell} = (-i)^\ell e^{\frac{\pi\eta}{2}}\, W_+ \quad (2.2.11b)$$

where

$$W_- = W_{i\eta,\,\ell+\frac{1}{2}}(e^{\frac{i\pi}{2}}\, 2kr), \quad W_+ = W_{-i\eta,\,\ell+\frac{1}{2}}(e^{-\frac{i\pi}{2}}\, 2kr) \quad (2.2.12)$$

are irregular Whittaker functions. Considered as functions of k, W_+ and W_- have $k = 0$ and $k = \infty$ as essential singularities, but they have no other singularity in the complex k-plane. They are multivalued, according to the relations [38]

$$W_{i\eta,\,\ell+\frac{1}{2}}(e^{i\pi/2}\, 2kr\, e^{i2\pi n}) = W_{i\eta,\,\ell+\frac{1}{2}}(e^{i\pi/2}\, 2kr) + 2in\pi\frac{\mathscr{M}_{i\eta,\,\ell+\frac{1}{2}}(2ikr)}{\Gamma(-\ell-i\eta)} \quad (2.2.13a)$$

$$W_{-i\eta,\,\ell+\frac{1}{2}}(e^{-i\pi/2}\, 2kr\, e^{i2\pi n}) = W_{-i\eta,\,\ell+\frac{1}{2}}(e^{-i\pi/2}\, 2kr) + 2in\pi\frac{\mathscr{M}_{-i\eta,\,\ell+\frac{1}{2}}(2ikr)}{\Gamma(-\ell+i\eta)} \quad (2.2.13b)$$

where n is an integer and $\mathscr{M}_{-i\eta,\,\ell+\frac{1}{2}}(-2ikr) = (-1)^{\ell+1}\mathscr{M}_{i\eta,\,\ell+\frac{1}{2}}(2ikr)$. Together with the regular function $\mathscr{M}$, the functions $W_\pm$ satisfy the relation [37, 38]

$$\mathscr{M} = \frac{e^{\pi\eta}}{\Gamma(\ell+1-i\eta)}\, W_+ - \frac{e^{\pi(\eta+i\ell)}}{\Gamma(\ell+1+i\eta)}\, W_- \quad (2.2.14)$$

and the Wronskian relations [38]

$$W(\mathscr{M}, W_\pm) = -2ik\,\frac{e^{i\pi(\ell\pm\ell)/2}}{\Gamma(\ell+1\pm i\eta)} \quad (2.2.15a)$$

$$W(W_+, W_-) = -2ik\, e^{-\pi\eta} \quad (2.2.15b)$$

According to Eqs (2.2.11), the relations (2.2.14) and (2.2.15) may be rewritten as

$$-2i F_\ell = e^{-i\sigma_\ell} I_\ell - e^{i\sigma_\ell} O_\ell \tag{2.2.16a}$$

$$W(F_\ell, O_\ell) = -k e^{-i\sigma_\ell}, \quad W(O_\ell, I_\ell) = -2ik \tag{2.2.17}$$

we also have

$$2G_\ell = e^{-i\sigma_\ell} I_\ell + e^{i\sigma_\ell} O_\ell \tag{2.2.16b}$$

For large values of $|kr|$, the asymptotic behaviour of $W_\pm$ is such that [38]

$$I_\ell \sim \exp[-i(kr - \eta \log(2kr) - \tfrac{1}{2}\pi\ell)] \quad (-2\pi < \arg k < +\pi) \tag{2.2.18a}$$

$$O_\ell \sim \exp[+i(kr - \eta \log(2kr) - \tfrac{1}{2}\pi\ell)] \quad (-\pi < \arg k < 2\pi) \tag{2.2.18b}$$

and accordingly they correspond to incoming and outgoing waves respectively. Later, we shall also need the behaviour of $\mathscr{M}$ and $W_\pm$ for very small k. We have

$$\mathscr{M} = \tfrac{1}{2}\left(\frac{ik}{\alpha}\right)^{\ell+1} x I_{2\ell+1}(x)[1 + O(k^2)] \text{ (any arg k)} \tag{2.2.19a}$$

$$\Gamma(\ell + 1 \pm i\eta) W_\pm = \left(\frac{\pm i\alpha}{k}\right)^{\ell} x K_{2\ell+1}(x)[1 + O(k^2)], \quad |\arg k \mp \tfrac{1}{2}\pi| \leqslant \pi - \theta \tag{2.2.19b}$$

where

$$x = (8\eta kr)^{\frac{1}{2}} = (8\alpha r)^{\frac{1}{2}} \tag{2.2.20}$$

and θ are positive quantities, the latter being an arbitrarily small constant.

Because of the definition (2.2.11) of I_ℓ and O_ℓ, we have

$$I_\ell(r, ke^{-i\pi}) = (-1)^\ell O_\ell(r, k) e^{-\pi\eta} \tag{2.2.21a}$$

$$O_\ell(r, ke^{i\pi}) = (-1)^\ell I_\ell(r, k) e^{-\pi\eta} \tag{2.2.21b}$$

Further, if k* is properly defined as $|k| \exp(-i \arg k)$, we have

$$O_\ell(r, k)^* = i^\ell e^{\frac{1}{2}\pi\alpha/k^*} W_{i\eta/k^*, \ell+\frac{1}{2}}(e^{i\frac{1}{2}\pi} 2k^* r)$$

$$= I_\ell(r, k^*) = (-1)^\ell O_\ell(r, k^* e^{i\pi}) e^{\pi\eta^*}, \tag{2.2.22a}$$

$$I_\ell(r, k)^* = O_\ell(r, k^*) = (-1)^\ell I_\ell(r, k^* e^{-i\pi}) e^{\pi\eta^*} \tag{2.2.22b}$$

In an open channel, k is a real and positive quantity and we have in particular

$$O_\ell(r, k)^* = I_\ell(r, k), \quad I_\ell(r, k)^* = O_\ell(r, k) \quad \text{(open)} \tag{2.2.23}$$

In a closed channel, $\arg k = \frac{1}{2}\pi$ and

$$O_\ell(r,k)^* = (-1)^\ell O_\ell(r,k)\, e^{-\pi\eta} \quad \text{(closed)} \tag{2.2.24a}$$

$$I_\ell(r,k)^* = (-1)^\ell I_\ell(r, ke^{-2i\pi})e^{-\pi\eta} \quad \text{(closed)} \tag{2.2.24b}$$

the last relation, which corresponds to a change of Riemann sheet, is however, not needed for deriving the time-reversal properties of $\Psi^{(c)}$ and U.

From now on, we shall make I_ℓ and O_ℓ single-valued functions of k by introducing a cut in the complex k-plane along the negative imaginary axis. Then

$$-\tfrac{1}{2}\pi < \arg k < \tfrac{3}{2}\pi \tag{2.2.25a}$$

and also

$$-\tfrac{1}{2}\pi < \arg(k^* e^{i\pi}) < \tfrac{3}{2}\pi \tag{2.2.25b}$$

2.3. Time-reversal properties

Let us consider the wave-function $\Psi^{(c)}$ defined by the boundary conditions

$$\Phi'_d - L_d \Phi_d = 0 \quad (\text{all } d \neq c) \tag{2.3.1}$$

where

$$L_d = L_\ell(a_d, k_d) = \frac{O'_\ell(a_d, k_d)}{O_\ell(a_d, k_d)} \tag{2.3.2}$$

Let us express the total energy $\mathscr{E}$ in terms of k_c according to the first relation (1.2.15), but let us disregard temporarily the fact that the wave numbers k_d of Eqs (2.3.1) and (2.3.2) are related to each other and to k_c according to the relations (1.2.15). In other words, let us consider the k_d as independent parameters. Under such conditions, $\Psi^{(c)}$, besides being a function of the space and spin co-ordinates, is also a function of <u>all</u> the wave numbers

$$\Psi^{(c)} = \Psi^{(c)}(k_c, k_d, \ldots) \tag{2.3.3}$$

The first one comes in because of the Schrödinger equation

$$H\Psi^{(c)} = (E_{\tilde{\alpha}_c} + \frac{\hbar^2}{2M_c} k_c^2)\, \Psi^{(c)} \tag{2.3.4}$$

the others because of the boundary conditions (2.3.1).

The relations (2.2.22) derived earlier must be considered as the time-reversal property of the functions I_ℓ, O_ℓ valid for real and complex wave-numbers as well.

In the channel spin $\{\bar{\alpha}\, s\, \nu\}$ representation, the time-reversal property of the product $\psi_{\bar{\alpha}s\nu}$ reads [12]

$$K\psi_{\bar{\alpha}s\nu} = (-1)^{s-\nu}\psi_{\bar{\alpha}s-\nu} \tag{2.3.5}$$

and hence, in the $\{\bar{\alpha}\, s\, \ell\, J M\}$ representation, the complete surface factor (1.2.5) satisfies the equation

$$K\varphi_c = (-1)^{J-M}\varphi_{-c} \tag{2.3.6}$$

while

$$K[\varphi_c O_c(r_c, k_c)] = (-1)^{J-M}\varphi_{-c} I_c(r_c, k_c^*) \tag{2.3.7a}$$

$$= (-1)^{J-M}\varphi_{-c} O_c(r_c, e^{i\pi}k_c^*)\cdot(-1)^{\ell}e^{\pi\eta^*} \tag{2.3.8a}$$

$$K[\varphi_c I_c(r_c, k_c)] = (-1)^{J-M}\varphi_{-c} O_c(r_c, k_c^*) \tag{2.3.7b}$$

$$= (-1)^{J-M}\varphi_{-c} I_c(r_c, e^{-i\pi}k_c^*)\cdot(-1)^{\ell}e^{\pi\eta^*} \tag{2.3.8b}$$

where as usual $-c = \{\bar{\alpha}\, s\, \ell\, J - M\}$; in the I and O radial functions, indices c may of course be used instead of -c.

In terms of these notations, the time reversal property assumed for the wave-function $\Psi^{(c)}$, when the channel wave numbers are considered as complex and independent of each other, reads

$$K\Psi^{(c)}(k_c, k_d, \ldots) = (-1)^{J-M}\Psi^{(-c)}(e^{i\pi}k_c^*, e^{i\pi}k_d^*, \ldots) \tag{2.3.9}$$

It seems at first sight that Eq.(2.3.9) agrees only with the time-reversal property (2.3.8a) of $\varphi_c O_c$, but not with the corresponding one (2.3.8b) of $\varphi_c I_c$. We shall now see that this is not the case by giving to $\Psi^{(c)}$ in the channel region a form in which all the radial factors satisfy an equation of the type (2.3.8a).

In the exterior region of the configuration space, we have from Eq.(2.2.16a)

$$\Psi^{(c)} = \varphi_c(x_c^{(c)}O_c + y_c^{(c)}I_c)/r_c + \sum_{c'\neq c}\varphi_{c'}\, x_{c'}^{(c)}O_{c'}/r_{c'}$$

$$= \varphi_c\, y_c^{(c)}(O_c e^{2i\sigma_c} - 2iF_c e^{i\sigma_c})/r_c + \sum_{c'}\varphi_{c'}\, x_{c'}^{(c)}O_{c'}/r_{c'} \tag{2.3.10}$$

In the latter expression of $\Psi^{(c)}$, we have eliminated I_c by introducing the radial wave-function

$$iF_c e^{i\sigma_c} = \tfrac{1}{2}(-i)^{\ell}e^{-\pi\eta/2}\Gamma(\ell+1+i\eta)\mathscr{M}_{i\eta,\,\ell+\frac{1}{2}}(2ikr) \tag{2.3.11}$$

which obviously satisfies the equations

$$(iF_\ell e^{i\sigma_\ell})^* = \tfrac{1}{2}i^{\ell}e^{-\pi\eta^*/2}\Gamma(\ell+1-i\eta^*)\mathscr{M}_{-i\eta^*,\,\ell+\frac{1}{2}}(-2ik^*r)$$

$$= e^{-\pi\eta^*}(iF_\ell e^{i\sigma_\ell})_{k\to e^{\pm i\pi}k^*} \tag{2.3.12}$$

since $\mathscr{M}/k^{\ell+1}$ is an integral function of k^2. Choosing the + sign in Eq. (2.3.12), we see that Eq. (2.3.9) agrees with Eqs (2.2.22a) and (2.3.12). Moreover, though the relation (2.2.16a) may also be used to write $\Psi^{(c)}$ in terms of F_ℓ and I_ℓ functions only, this is not a sufficient reason to justify the assumption that $\Psi^{(c)}$ satisfies a time-reversal property with $e^{-i\pi} k_b^*$ rather than with $e^{+i\pi} k_b^*$ for any b. Indeed, we must also require that for real total energies, the time-reversal property should not be different from the usual one. We know from Eq. (2.2.24b) that this is not the case for I_ℓ.

From Eq. (2.3.9), the time-reversal property of the radial factors $\Phi_{c'}^{(c)}$, $\Phi_{c'}^{(c)'}$ are easily derived. We have

$$\Phi_{c'}^{(c)}(k_c, k_d, \ldots)^* = \int (K\varphi_{c'})^* (r_\alpha K\Psi_{\text{int}}^{(c)})_{r_\alpha = a_\alpha} \, dS_\alpha$$

or

$$[\Phi_{c'}^{(c)}(k_c, k_d, \ldots)]^* = \Phi_{c'}^{(c)}(e^{i\pi} k_c^*, e^{i\pi} k_d^*, \ldots) \tag{2.3.13a}$$

and similarly

$$[\Phi_{c'}^{(c)'}(k_c, k_d, \ldots)]^* = \Phi_{c'}^{(c)'}(e^{i\pi} k_c^*, e^{i\pi} k_d^*, \ldots) \tag{2.3.13b}$$

These relations simply exhibit the fact that $\Phi_{c'}^{(c)}$ and $\Phi_{c'}^{(c)'}$ have been defined as real functions of ik_c, ik_d, ... This is obviously related to the fact that we assumed the Hamiltonian H to be a real operator, while $\mathscr{E} = E_{\alpha} - \hbar^2(ik_c)^2/(2M_c)$ and $L_d(a_d, k_d)$ are real functions of ik_c and ik_d respectively[1]; from Eqs (2.3.2) and (2.2.22a), we have indeed

$$[L_d(a_d, k_d)]^* = L_d(a_d, e^{i\pi} k_d^*). \tag{2.3.14}$$

The relations (2.3.13) have two straightforward consequences. Firstly we see that if k_{cn}, k_{dn}, ... is a set of complex wave numbers satisfying the boundary conditions (2.1.5) which define a resonance state, the same boundary conditions will also be satisfied for $k_c = e^{i\pi} k_{cn}^*$, $k_d = e^{i\pi} k_{dn}^*$, ... This eigenstate will be designated by an index $-n$, i.e. for the wave numbers

$$k_{b,-n} = e^{i\pi} k_{bn}^* \qquad \text{(all b)} \tag{2.3.15a}$$

and for the wave-function

$$\Psi_{-n} = \Psi(k_{c,-n}, k_{d,-n}, \ldots) \tag{2.3.15b}$$

hence

$$K\Psi_{JM,n} = (-1)^{J-M} \Psi_{J-M,-n} \tag{2.3.15c}$$

the indices J, M being dropped only when no confusion is possible.

---

[1] By definition, the operator H is real if it commutes with the time reversal operator K, while the function f(z) is real if $[f(z)]^* = f(z^*)$.

Secondly, defining the elements of a T-matrix by

$$T_{c'c} = \delta_{c'c}\, e^{2i\sigma_c} - U_{c'c} \tag{2.3.16}$$

$$= 2\, \frac{W(\Phi_c^{(c)},\, i F_{c'}\, e^{i\sigma_{c'}})/k_{c'}}{W(\Phi_c^{(c)},\, O_c)/k_c} \tag{2.3.17}$$

we immediately get

$$[\, T_{c'c}(k_c,\, k_d,\, \ldots)]^* = (-1)^{\ell'+\ell}\, e^{-\pi\eta_c^* - \pi\eta_{c'}^*}\, T_{c'c}\, (e^{i\pi} k_c^*,\, e^{i\pi} k_d^*,\, \ldots) \tag{2.3.18}$$

when Eqs (2.2.22a), (2.3.12) and (2.3.13) are taken into account.

Formal papers on inelastic scattering, such as the one by Newton [39], have been concerned with analyzing more closely the structure of the T-matrix considered as a function of several independent complex variables k_c, k_d, ... Other authors, such as Peierls [40], Le Couteur [41] and Weidenmüller [13]) take the relations (1.2.15) into account and study the structure of the T-matrix on a complete Riemann surface when one channel wave number is chosen to be the only independent variable; then there are obviously branch-points at the thresholds. Here we want to deal with proper nuclear reactions and accordingly we have not only branch-points, but also logarithmic essential singularities introduced at the thresholds by the Coulomb interaction. Therefore, we shall restrict ourselves to the study and expansion of the collision matrix on one Riemann sheet only.

2.4. The physical k-plane

Let us now decide that an arbitrary channel wave number, say k_b, is chosen as the independent variable. The corresponding complex k_b-plane, with appropriate cuts, that is going to be defined now, will be called the physical k_b-plane.

From now on, we assume that the only singularities of the wave-function $\Psi^{(c)}$ are located at the thresholds $k_o = 0$, $k_a = 0$, $k_b = 0$, ...

Under such conditions, by drawing in the complex k_b-plane the set of cuts indicated in Fig. 1, the wave-function $\Psi^{(c)}$ becomes holomorphic at any interior point of the k_b-plane, i.e. at any point lying neither on a cut nor between those cuts starting at $k_b = 0$. The phase of any wave number

$$k_d = [(k_b^2 - K_{db}^2)\, M_d / M_b]^{\frac{1}{2}} \tag{2.4.1}$$

is chosen in such a way that $k_d = \pm\, |k_d|$ for $k_d \to \pm\infty + 0i$. In relation (2.4.1), we have, according to Eq. (1.2.15),

$$\hbar^2 K_{db}^2 / (2M_b) = E_{\tilde{\alpha}_d} - E_{\tilde{\alpha}_b} \tag{2.4.2}$$

The quantity K_{db} will be chosen positive real or positive imaginary.

The cuts starting at $+K_{db}$ and $-K_{db}$ are not necessarily straight lines, but they must be drawn in the lower half plane and symmetrically with regard to the imaginary axis; they join the cut starting at $k_b = 0$ at an arbitrary distance from the real axis or at infinity. Under such conditions,

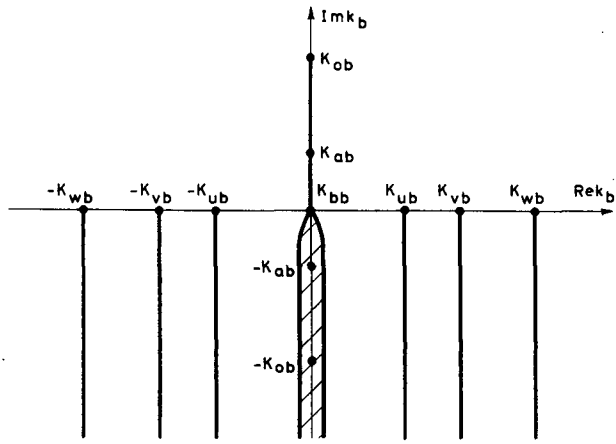

FIG. 1. The physical k_b-plane

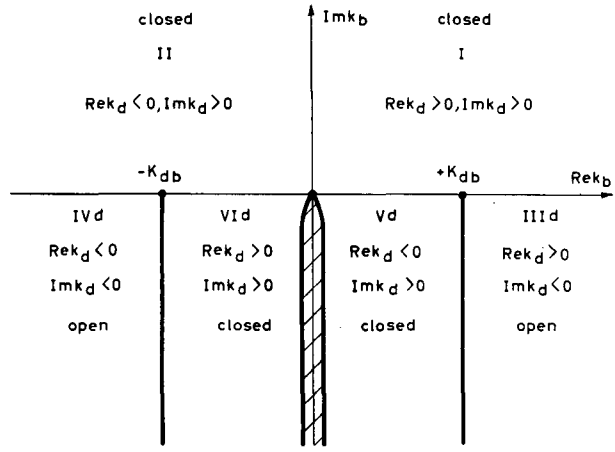

FIG. 2. Signs of (Re k_d) and (Im k_d) in the physical k_b-plane when $E_{\bar{\alpha}_d} > E_{\bar{\alpha}_b}$

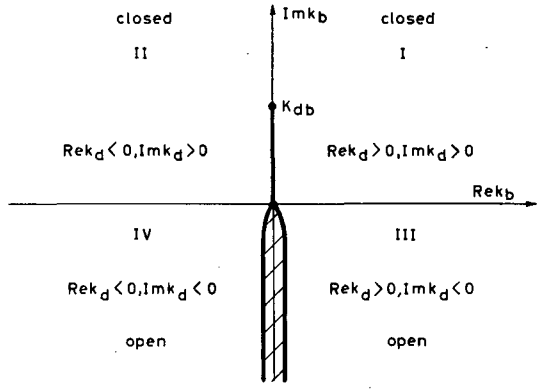

FIG. 3. Signs of (Re k_d) and (Im k_d) in the physical k_b-plane when $E_{\bar{\alpha}_d} < E_{\bar{\alpha}_b}$

the important relations (2.2.25) are satisfied for each channel wave number and, for any d, we have

$$k_d(e^{i\pi}k_b^*) = e^{i\pi}\,[k_d(k_b)]^* \tag{2.4.3}$$

where $k_b^* = |k_b|\exp(-i\arg k_b)$. Similarly, when the different regions of the k_b-plane defined by the cuts starting at $k_b = 0$ and $\pm K_{db}$ are numbered as indicated in Figs 2 and 3, the following relations are easily verified:

$$k_d(e^{i\pi}k_b) = -k_d(k_b) \text{ for } k_b \text{ in III d} \tag{2.4.4a}$$

$$k_d(e^{-i\pi}k_b) = -k_d(k_b) \text{ for } k_b \text{ in IV d} \tag{2.4.4b}$$

$$k_d(e^{i\pi}k_b) = +k_d(k_b) \text{ for } k_b \text{ in V d} \tag{2.4.4c}$$

$$k_d(e^{-i\pi}k_b) = +k_d(k_b) \text{ for } k_b \text{ in VI d} \tag{2.4.4d}$$

This is easily seen from Figs 4 and 5, which have been adapted from Fig. 4.17 of Morse and Feshbach [42]; here, u is interpreted as $\mathrm{Re}\,k_d = \kappa_d$ and v as $\mathrm{Im}\,k_d = -\gamma_d$. When the cut in Fig. 4 is deformed to become parallel to the imaginary axis at finite distance, as in Fig. 2, the signs of κ_d and γ_d are changed in the regions Vd and VI d; there is a change of sign for κ_d and γ_d along the lines $\kappa_d = \text{const.}$ and $\gamma_d = \text{const.}$ when these lines cross the cuts. Similarly, the indications reported in Fig. 3 are easily related to those given in Fig. 5.

Finally, in connection with Eq. (2.2.19b), we must point out that by drawing the cuts in the lower k_b-plane, we have restricted the values of $\arg k_d$ to the appropriate range. More precisely, for any d, we have

$$-\tfrac{1}{2}\pi + \theta_{db} \leqslant \arg k_d \leqslant \tfrac{3}{2}\pi - \theta_{db} \tag{2.4.5}$$

where θ_{db} is a non-vanishing positive constant. The condition (2.4.5) is obviously satisfied for[2] $d = b$, while near the other thresholds $d \neq b$, because of the phase chosen for k_d, we have

$$0 \leqslant \arg k_j \leqslant \pi \text{ for } k_b \text{ near } +K_{jb}\,. \tag{2.4.6a}$$

when K_{jb} is lying on the imaginary axis and

$$\mp\tfrac{1}{4}\pi \leqslant \arg k_j \leqslant \pi \mp \tfrac{1}{4}\pi \text{ for } k_b \text{ near } \mp K_{jb} \tag{2.4.6b}$$

when K_{jb} is located on the real axis and the cuts are orthogonal to that axis near $k_j = 0$. Hence, we see that the condition (2.4.5) is satisfied near the thresholds; it is easily extended to the whole physical k_b-plane by considering Figs 4 and 5 and their transformation into Figs 2 and 3, respectively.

---

[2] When b is a neutron channel, one is of course justified in taking a vanishing width for the cut starting at $k_b = 0$, i.e. in taking simply the negative imaginary axis.

Up to now, the concept of open and closed channels has been used for real total energies only. We are now in a position to extend it to any point of the physical k_b-plane. The channel d will be called open if

$$\mathrm{Im}\, k_d \leqslant 0 \qquad \text{(open)} \tag{2.4.7}$$

and closed if

$$\mathrm{Im}\, k_d > 0 \qquad \text{(closed)}. \tag{2.4.8}$$

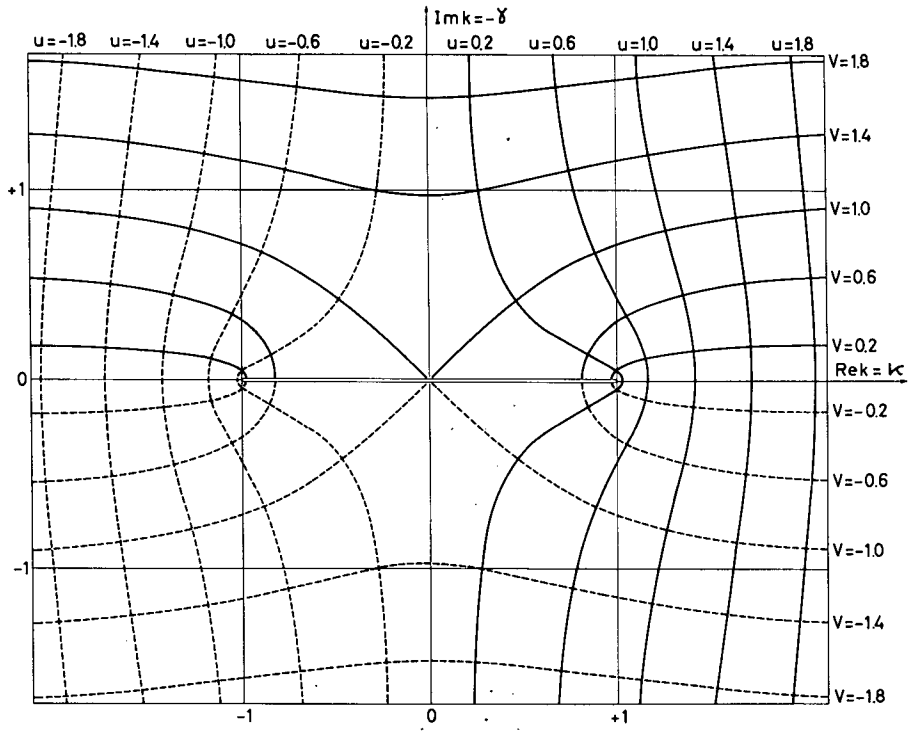

FIG. 4. Real and imaginary parts of $f(k) = \sqrt{(k^2 - 1)} = u + iv$ in the physical k-plane

In the former case, k_b lies in one of the regions I, II, Vd, VId shown in Figs 2 and 3, while in the latter case, k_b lies in regions IIId or IVd. Such a definition includes the usual one for real energies, since beyond K_{db} the positive real axis corresponds to an actual physical situation where d is open, while the positive imaginary axis and the segment $K_{bb} - K_{db}$ are associated with a closed channel.

The above definition applies in particular to a resonance state. Then, since for $r_d > a_d$ we have

$$u_{dn} = u_d(r_d, k_{dn}) \propto \exp(ik_{dn} r_d) \tag{2.4.9}$$

we see that the wave-function Ψ_n is exponentially decreasing in a closed channel and increasing in an open one, except however when $\mathrm{Im}\, k_d = 0$.

In the physical k_b-plane the properties (2.3.9) of the wave-function and (2.3.13) of the radial factors may now be rewritten as

$$K\Psi^{(c)}(k_b) = (-1)^{J-M}\Psi^{(-c)}(e^{i\pi}k_b^*) \tag{2.4.10}$$

$$\Phi_{c'}^{(c)}(k_b)^* = \Phi_{c'}^{(c)}(e^{i\pi}k_b^*),\quad \Phi_{c'}^{(c)'}(k_b)^* = \Phi_{c'}^{(c)'}(e^{i\pi}k_b^*) \tag{2.4.11}$$

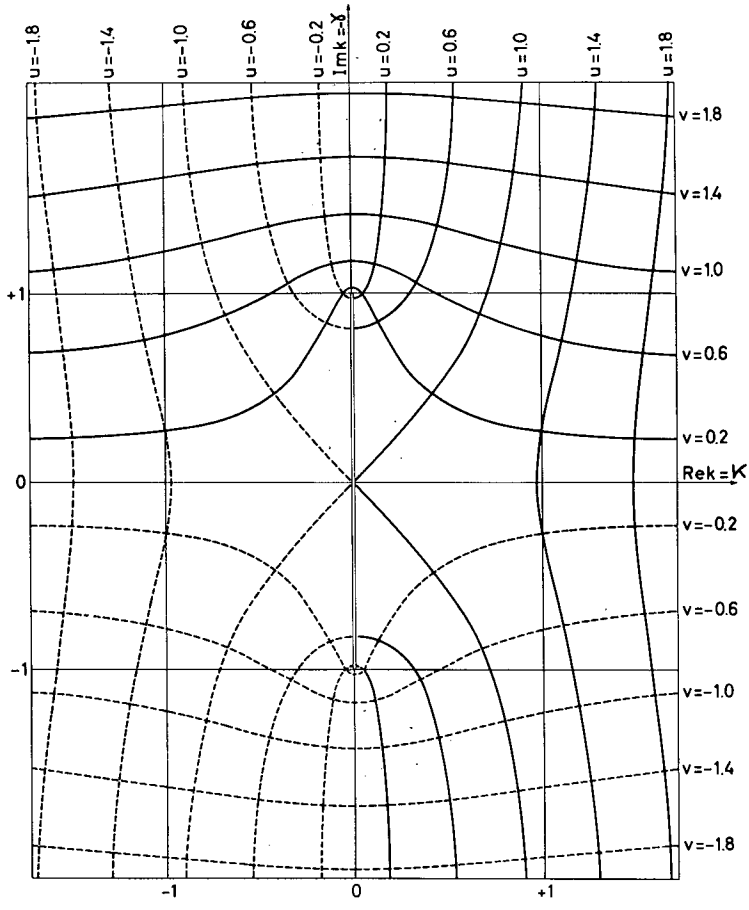

FIG. 5. Real and imaginary parts of $f(k) = \sqrt{(k^2+1)} = u + iv$ in the physical k-plane

while if k_{bn} corresponds to a resonance state, the same may be said of its symmetrical $e^{i\pi}k_{bn}^*$. Accordingly, if we write

$$k_{bn} = \kappa_{bn} - i\gamma_{bn} \tag{2.4.12a}$$

we may always assume that $\kappa_{bn} \geqslant 0$, since then

$$k_{b,-n} = e^{i\pi}k_{bn}^* = -\kappa_{bn} - i\gamma_{bn}. \tag{2.4.12b}$$

After deriving Green's theorem, we prove that in the upper half of the physical k_b-plane, there are no resonance states k_{bn} located outside the imaginary axis, just like in the one-channel case.

2.5. Green's theorem

Let us consider two solutions Ψ_1, Ψ_2 of the wave equation $H\Psi = \mathscr{E}\Psi$, corresponding to two different real or complex energies $\mathscr{E}_1$, $\mathscr{E}_2$. Then we may write

$$(\mathscr{E}_2^* - \mathscr{E}_1) \int_\omega \Psi_2^* \Psi_1 d\omega = \int_\omega [(H\Psi_2)^* \Psi_1 - \Psi_2^* (H\Psi_1)] d\omega \qquad (2.5.1)$$

where the integration in configuration space is extended to the interior region ω bounded by the surface $\mathscr{S}$. If we assume the potential V to be self-adjoint, i.e.

$$\int_\omega [(V\Psi_2)^* \Psi_1 - \Psi_2^* (V\Psi_1)] d\omega = 0 \qquad (2.5.2)$$

only the terms of H corresponding to the kinetic energies contribute to the right-hand side of (2.5.1) and these are transformed by Green's theorem into an integral over the surface $\mathscr{S}$. For the part of the surface $\mathscr{S}$ corresponding to $r_\alpha = a_\alpha$, this integral

$$-\frac{\hbar^2}{2M_\alpha} \int \left[\frac{\partial \Psi_2^*}{\partial r_\alpha} \Psi_1 - \Psi_2^* \frac{\partial \Psi_1}{\partial r_\alpha} \right]_{r_\alpha = a_\alpha} a_\alpha^2 dS_\alpha$$

$$= -\frac{\hbar^2}{2M_\alpha} \int \left[\frac{\partial (r_\alpha \Psi_2^*)}{\partial r_\alpha} r_\alpha \Psi_1 - r_\alpha \Psi_2^* \frac{\partial (r_\alpha \Psi_1)}{\partial r_\alpha} \right] dS_\alpha$$

or, on account of the expansions (1.3.1) and the orthonormality relations between the φ_c,

$$-\frac{\hbar^2}{2M_\alpha} \sum_{c(\alpha)} (\Phi'^*_{2c} \Phi_{1c} - \Phi^*_{2c} \Phi'_{1c})$$

The integral over the whole surface $\mathscr{S}$ is the sum of similar expressions for the different modes of fragmentation α, and Eq. (2.5.1) thus becomes

$$(\mathscr{E}_2^* - \mathscr{E}_1) \int_\omega \Psi_2^* \Psi_1 d\omega = \sum_c \frac{\hbar^2}{2M_c} W(\Phi_{2c}^*, \Phi_{1c}) \qquad (2.5.3)$$

where the summation now extends to all channels and where we have written M_c instead of M_α for the reduced mass in channel c.

Let us now apply this relation (2.5.3) to the case where Ψ_1 and Ψ_2 are the same eigenfunction Ψ_n with resonance energy

$$\mathscr{E}_n = E_n - \tfrac{1}{2} i \Gamma_n \qquad (2.5.4)$$

the real and imaginary parts of which are given by

$$E_n = \frac{\hbar^2}{2M_c}(\kappa_{cn}^2 - \gamma_{cn}^2) + E_{\bar{\alpha}_c} = \frac{\hbar^2}{2M_d}(\kappa_{dn}^2 - \gamma_{dn}^2) + E_{\bar{\alpha}_d} = \ldots \qquad (2.5.5a)$$

$$\Gamma_n = \frac{2\hbar^2}{M_c}\kappa_{cn}\gamma_{cn} = \frac{2\hbar^2}{M_d}\kappa_{dn}\gamma_{dn} = \ldots \qquad (2.5.5b)$$

Let us also assume that the integration is not limited to the interior region ω of the configuration space, but that it rather extends to a region ω_n composed of ω plus that part of the exterior region corresponding to the channels which are closed at the energy $\mathscr{E}_n$. In the latter channels, according to Eqs (2.4.8) and (2.4.9), we have $\mathrm{Im}\, k_{cn} = -\gamma_{cn} > 0$ and $u_{cn}(r_c, k_{cn})$ vanishes like $\exp(-|\gamma_{cn}|r_c)$ for $r_c \to \infty$. Accordingly, we are left with

$$i\Gamma_n \int_{\omega_h} |\Psi_n|^2 \, d\omega = \sum_{c^+} \frac{\hbar^2}{2M_c}(\Phi_{cn}^* \Phi_{cn}' - \Phi_{cn}'^* \Phi_{cn}) \qquad (2.5.6a)$$

$$= \sum_{c^+} \frac{\hbar^2}{2M_c} \Phi_{cn}^* \Phi_{cn} (L_{cn} - L_{cn}^*) \qquad (2.5.6b)$$

where the integral is finite, while the sums in the right-hand sides extend over the open channels only.

2.6. Bound states

We shall now use the relation (2.5.6b) just derived to prove that in the upper physical k_b-plane there are no resonance states outside the imaginary axis. Assuming only that $\gamma_{bn} < 0$, we see from Figs 2 and 3 that in fact

$$\gamma_{dn} < 0 \text{ for all } d \qquad (2.6.1)$$

i.e. that all the channels are closed. Under such conditions Eqs (2.5.6) become

$$\Gamma_n \int_{\infty} |\Psi_n|^2 \, d\omega = 0 \qquad (2.6.2)$$

or, the integral being finite,

$$\Gamma_n = 0 \qquad (2.6.3)$$

From Eqs (2.5.5b) and (2.6.1), this is equivalent to

$$\kappa_{dn} = 0 \text{ for all } d \qquad (2.6.4)$$

and hence k_{bn} is necessarily located in the upper half of the imaginary axis. The resonance state considered is in fact a bound state.

This result completes, for the upper half, the one derived at the end of sub-section 2.4 for the location of the resonance states in the lower half of the physical k_b-plane.

2.7. Channel radii and resonance states

Before we close this section we still have to point out one important property of the resonance states when they are defined according to Eq.(2.1.5).

Let us first recall the definition (1.4.4) of the collision matrix, namely

$$U_{c'c} = -x_{c'}^{(c)} / y_c^{(c)} \tag{2.7.1}$$

Being a ratio of two amplitudes, its value will not be changed if the channel radii taken are larger than a_c, $a_{c'}$, ... in some or all channels, still assuming, however, that in the portion of the configuration space between the surfaces $\mathscr{S}$ and $\mathscr{S}'$, the latter surface being defined by

$$r_d = a_d' \quad \text{(all d)} \tag{2.7.2}$$

only the Coulomb forces act between the fragments. Accordingly, the eigenvalues $\mathscr{E}_n$ are also independent of the fact that the boundary surface chosen is $\mathscr{S}$ or $\mathscr{S}'$.

Until now this argument has been rather formal, but nevertheless it has a practical importance when it is reformulated as follows: Let us assume that the nuclear interaction of two fragments is very small, but not zero, when their representative point in the configuration space lies between $\mathscr{S}$ and $\mathscr{S}'$. If this interaction is not neglected in the definition of the collision matrix, i.e., if the boundary surface chosen is $\mathscr{S}'$ rather than $\mathscr{S}$, we have with obvious notations

$$\begin{gathered} x_{c'}^{(c)}(\mathscr{S}') \approx x_{c'}^{(c)}(\mathscr{S}), \qquad y_c^{(c)}(\mathscr{S}') \approx y_c^{(c)}(\mathscr{S}) \\ U_{c'c}(\mathscr{S}') \approx U_{c'c}(\mathscr{S}) \end{gathered} \tag{2.7.3}$$

Hence, for the corresponding eigenvalues, we also have

$$\mathscr{E}_n(\mathscr{S}') \approx \mathscr{E}_n(\mathscr{S}) \tag{2.7.4}$$

even if a_c', $a_{c'}'$, ... are chosen much larger than a_c, $a_{c'}$, ..., respectively. They may even be taken much larger than the range of the nuclear forces for open and closed channels as well; for the latter channels they may be taken as infinite.

When later we want to refer to this property of the collision matrix and of the resonant states, we shall simply say that they are "independent of the channel radii" or "a-independent".

3. EXPANSION OF THE COLLISION MATRIX

In this section, we want to derive an expansion of the collision matrix which could fit the experimental data on resonance reactions at low ener-

gies. Among the parameters introduced in such an expansion, the eigenvalues $\mathscr{E}_n = E_n - \frac{1}{2} i\Gamma_n$ should play a major part, since we know that, just like the observed resonances, their positions E_n and total widths Γ_n are independent of what the incoming channel is; they characterize the compound nucleus itself. Since in practice only one- or few-level approximations of the expansion of the collision matrix are used, one must also look for an expansion, the one- and few-level approximations of which have the same general property as the exact collision matrix: (i) symmetry, (ii) independence of the channel radii, (iii) threshold behaviours, (iv) time-reversal property, (v) unitarity.

Since our definition of the resonance states satisfies requirement (ii), it is very likely that the most appropriate type of expansion should exhibit the fact that these resonance states have been defined as the poles of the collision matrix. Accordingly, it seems we have no choice but to expand the U-matrix directly according to its poles, rather than expanding first an auxiliary matrix as in the R-matrix theory. Under such conditions, one must however expect that the one- and few-level approximations will not rigorously satisfy the unitarity requirement (v), because U is not a real matrix. All the other requirements (i) to (iv) will be satisfied by the expansions we derive later, except when otherwise stated.

After we have specified in the next paragraph the analyticity hypothesis assumed for the wave-function and the radial factors $\Phi_c^{(c)}$, $\Phi_c^{(c)'}$, we derive the threshold factors of the collision matrix elements and an expansion theorem applicable in the physical k_b-plane. In fact, however, we shall find it easier to write the expansion of the collision matrix elements first in a physical $\mathscr{E}$-plane still to be defined and then in the physical k_b-plane.

3.1. Analyticity of the wave-function, radial factor and collision matrix

In most of the formal theories of nuclear reactions, one assumes the existence in the interior region of an expansion of the wave-function in terms of a complete orthonormal set of eigenfunctions. Here, since the Ψ_n do not form an orthogonal set in the interior region ω (nor in the region ω_n) and since the resonance states have been defined as the poles of the collision matrix, we rather assume analyticity properties for the wave-function, namely:

(1) on the boundary surface, the wave-function $\Psi^{(c)}$ and its normal derivatives are holomorphic functions of the wave number k_b at any interior point of the physical k_b-plane and on its boundary, except at the thresholds.

(2) It is possible to normalize $\Psi^{(c)}$ in such a way that the Φ_{dn} do not vanish simultaneously for all d, and

(3) that $\Phi_d^{(c)}$, $\Phi_d^{(c)'}$ (any d) are continuous at the thresholds $\pm K_{eb}$ (any e), i.e. that

$$\lim_{k_b \to \pm K_{eb}} \Phi_d^{(c)}(k_b) = \Phi_d^{(c)}(\pm K_{eb}) = \text{finite constant} \qquad (3.1.1)$$

$$\lim_{k_b \to \pm K_{eb}} \Phi_d^{(c)'}(k_b) = \Phi_d^{(c)'}(\pm K_{eb}) = \text{finite constant} \qquad (3.1.2)$$

when k_b is an interior point of the physical k_b-plane.

(4) All the roots of the equation

$$W(\Phi_c^{(c)}, O_c) = 0 \tag{3.1.3}$$

are simple and we disregard the case where a resonance lies at a threshold.

Under such conditions, the only singularities of the collision matrix elements in the physical k_b-plane are:

(i) the thresholds K_{eb} on its boundary,

(ii) the simple poles k_{bn} and k_{b-n} corresponding to the resonance states in its interior.

3.2. The threshold factor

As a consequence of the analytical properties of $\Phi_c^{(c)}$, $\Phi_{c'}^{(c)}$, it seems at first sight that turning to the collision matrix element (1.4.5), we have to deal with its poles $\mathscr{E}_n$ and the threshold singularities of O_ℓ and $I_{\ell'}$. In fact, however, since the quantity of physical interest is $T_{c'c}$ rather than $U_{c'c}$, let us rather analyse the behaviour at the thresholds of the former matrix, as defined by Eq. (2.3.17).

For that purpose, let us rewrite $T_{c'c}$ as

$$T_{c'c} = i\epsilon_{c'}\epsilon_c e^{i(\sigma_{c'}+\sigma_c)}\, k_{c'}^{\ell'} k_c^{\ell+1} M_{c'}^{\frac{1}{2}} M_c^{-\frac{1}{2}} t_{c'c} \tag{3.2.1}$$

where $t_{c'c}$ is defined according to

$$t_{c'c} = 2\,\frac{M_c^{\frac{1}{2}}\, W(\Phi_{c'}^{(c)}, F_{c'}\epsilon_{c'}^{-1}k_{c'}^{-\ell'-1})}{M_{c'}^{\frac{1}{2}}\, W(\Phi_c^{(c)}, O_c\epsilon_c e^{i\sigma_c} k_c^{\ell})} \tag{3.2.2}$$

In the latter matrix element, we have

$$F_{c'}\epsilon_{c'}^{-1}k_{c'}^{-\ell'-1} = \tfrac{1}{2}\ell'!\,(ik_{c'})^{-\ell'-1}\,\mathscr{M}_{i\eta_{c'},\,\ell'+\frac{1}{2}}(2ik_{c'}r_{c'}) \tag{3.2.3}$$

$$O_c\epsilon_c e^{i\sigma_c} k_c^{\ell} = (\ell!)^{-1}(-ik_c^{\ell})\,\Gamma(\ell+1+i\eta_c)\,W_+ \tag{3.2.4}$$

The former of these two quantities is an integral function of $k_{c'}^2$ with a finite asymptotic behaviour for small $k_{c'}$ given according to Eq. (2.2.19a) by

$$F_{c'}\epsilon_{c'}^{-1}k_{c'}^{-\ell'-1} = \tfrac{1}{4}\ell'!\,\alpha_{c'}^{-\ell'-1}\, x_{c'} I_{2\ell'+1}(x_{c'})\,[1+0(k_{c'}^2)] \tag{3.2.5}$$

The product (3.2.4) has singularities corresponding to the poles of the Γ function, namely

$$k_c = -i\alpha_c/(\ell+n) \quad (n = 1, 2, \ldots) \tag{3.2.6}$$

and at the essential singularity of Γ and W_+ at $k_c = 0$. Nevertheless, according to Eq. (2.2.19b) for small k_c and

$$-\tfrac{1}{2}\pi + \theta \leqslant \arg k_c \leqslant \tfrac{3}{2}\pi - \theta \tag{3.2.7a}$$

where θ is an arbitrarily small positive constant, we have the simple asymptotic behaviour

$$O_c \epsilon_c e^{i\sigma_c} k_c^{\ell} = (\ell!)^{-1} \alpha_c^{\ell} x_c K_{2\ell+1}(x_c) [1 + 0(k_c^2)]. \qquad (3.2.7b)$$

The relations (3.2.7a) are satisfied in the physical k_b-plane and on its boundary, since they do not differ from the relations (2.4.5). Accordingly, the matrix element $t_{c'c}$ is a continuous function of k_b on the boundary of the physical k_b-plane, including all the thresholds, while, in the interior of this boundary, it has simple poles at the resonances[3].

From Eqs (2.3.13) and (3.2.1 - 3.2.3), it is easy to verify that the time reversal property satisfied by the matrix elements $t_{c'c}$ reads

$$t_{c'c}(k_b)^* = t_{c'c}(e^{i\pi} k_b^*) \qquad (3.2.8)$$

and is equivalent to the property (2.3.18) of $T_{c'c}$. The derivation of the two other general properties of $t_{c'c}$, namely the symmetry and unitarity properties in the physical k_b-plane will not be given here; the reader should refer to Ref.[22]. They read

$$t_{c'c} = t_{cc'} \qquad (3.2.9)$$

and

$$i \sum_{d^+} k_d^{2\ell_d+1} \epsilon_d^2 t_{dc}^* t_{dc'} + t_{cc'} - t_{c'c}^* = 0$$

or

$$i \sum_{d^+} k_d^{2\ell_d+1} \epsilon_d^2 t_{dc}(e^{i\pi} k_b^*) t_{dc'}(k_b) + t_{cc'}(k_b) - t_{c'c}(e^{i\pi} k_b^*) = 0 \qquad (3.2.10)$$

3.3. The expansion theorem

The well-known Mittag-Leffler expansion [43, 44] being concerned with single-valued functions of a complex variable, the expansion of $t_{c'c}(k_b)$ in terms of its poles k_{bn}, k_{b-n} is not a straightforward application of this theorem. Nevertheless, in the physical k_b-plane, it is possible to justify the existence of an expansion similar to the Mittag-Leffler expansion and directly applicable to $t_{c'c}$.

Let $f(k)$ be a function defined in a complex k-plane in which a series of cuts have been introduced to make it single-valued. Outside the cuts, let its only singularities be an infinite number of simple isolated poles $k_1, k_2, \ldots$ with residues $\rho_1, \rho_2, \ldots$; let us assume that

$$0 < |k_1| \leqslant |k_2| \leqslant \ldots \qquad (3.3.1)$$

and that the series

$$\sum_{n=1}^{\infty} |\rho_n / k_n| \qquad (3.3.2)$$

[3] This result does not imply that $t_{c'c}$ is free from essential singularities at the thresholds; see Ref.[22].

is convergent. Under such conditions, it is easy to verify that the series

$$\sum_{n=1}^{\infty} \rho_n / (k - k_n) \tag{3.3.3}$$

is also convergent for any finite value of k uniformly distant from the poles.

Let now C_m be a circle with indentations corresponding to the cuts and having the poles $k_1, \ldots k_m$, but no other, as interior points. Then according to the theorem of residues,

$$\frac{1}{2i\pi} \int_{C_m} f(k')/(k - k')\, dk' = -f(k) + \sum_{n=1}^{m} \rho_n/(k - k_n) \tag{3.3.4}$$

Hence, if we let m go to infinity

$$f(k) = Q(k) + \sum_{n=1}^{\infty} \rho_n / (k - k_n) \tag{3.3.5}$$

where

$$Q(k) = \lim_{m \to \infty} \int_{C_m} \frac{f(k')}{k' - k}\, dk' \tag{3.3.6}$$

is a continuous function of k in the k-plane and on its cuts.

It is important to recall that the fundamental Cauchy theorem and the theorem of residues used to derive Eq. (3.3.4) do not require that each point of the contour be a point of holomorphy of f(k). It is sufficient that f(k) be continuous on the contour C_m; then, for any point k' on C_m, we have

$$\lim_{k \to k'} [f(k) - f(k')] = 0 \tag{3.3.7}$$

when k is an interior point tending to k'. Accordingly, the expansion (3.3.5) is applicable to $t_{c'c}$ and not to $T_{c'c}$. Only for the former matrix elements is it possible to extend the cuts just to the thresholds, rather than turning round them at a non-vanishing distance.

3.4. Expansion of the collision matrix in the physical $\mathscr{E}$-plane

Let o be the channel with the smallest internal energy $E_{\bar{\alpha}_0}$ and let us take $E_{\bar{\alpha}_0}$ as the origin of the energy scale. Let us define a physical $\mathscr{E}$-plane as the conformal mapping of the right-half of the physical k_0-plane and in accordance with the relation

$$\mathscr{E} = \frac{\hbar^2}{2M_0} k_0^2 \tag{3.4.1}$$

If there are bound states on the positive imaginary axis k_0, they will be included in the k_0-plane and in the corresponding $\mathscr{E}$-plane as indicated in Fig. 6; it is known that the cut starting at $k_0 = 0$ in the k_0-plane must have

a finite width when o is not a neutron channel (see Figs 2 and 3). An alternative way of drawing cuts is given in Fig. 7.

Let us now compute the residue of $t_{c'c}$ at a pole $\mathscr{E}_n$, namely,

$$r_{c'cn} = \frac{M_c^{\frac{1}{2}}}{M_{c'}^{\frac{1}{2}}} \frac{2W(\Phi_{c'n}, F_{\ell'n})}{\epsilon_{c'n} k_{c'n}^{\ell'+1} \epsilon_{cn} k_{cn}^{\ell} e^{i\sigma_{cn}} \left[\frac{d}{d\mathscr{E}} W(\Phi_c^{(c)}, O_c)\right]_{\mathscr{E}=\mathscr{E}_n}} \qquad (3.4.2)$$

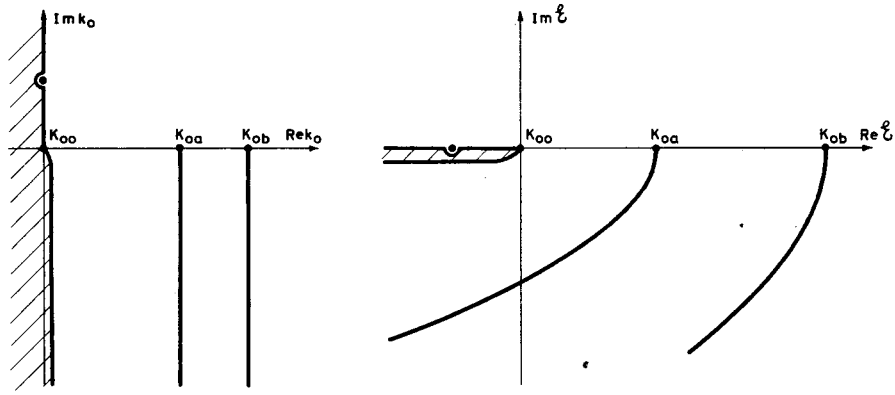

FIG. 6. The right-half of a physical k_0-plane and the corresponding $\mathscr{E}$-plane. Straight-line cuts in the former correspond to parabolic ones in the latter

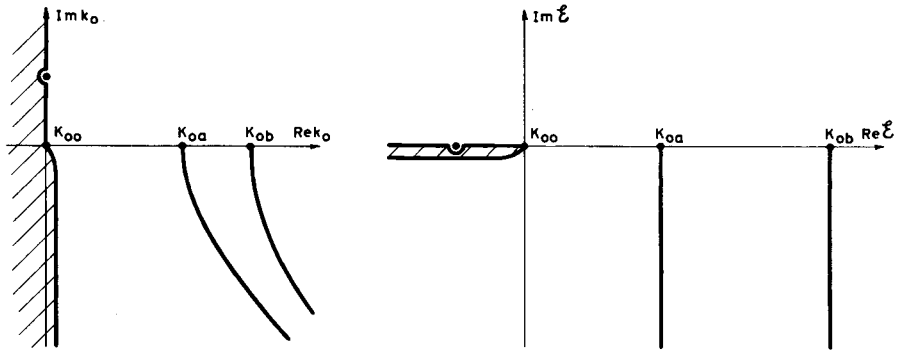

FIG. 7. An alternative way of drawing cuts in the right-half of the physical k_0-plane and in the $\mathscr{E}$-plane: straight-line cuts in the latter correspond to hyperbolic ones in the former

Taking account of Eq. (2.2.16a), the condition

$$W(\Phi_{c'n}, O_{c'n}) = 0 \quad \text{for all } c' \qquad (3.4.3)$$

and the Wronskian relation (2.2.17) easily give

$$2W(\Phi_{c'n}, F_{\ell'n}) = 2k_{c'} e^{-i\sigma_{c'n}} \Phi_{c'n} / O_{c'n} \qquad (3.4.4)$$

In order to calculate $(d/d\mathscr{E})\,W(\Phi_c^{(c)}, O_c)$ we start from the Green theorem (2.5.6), in which we take

$$\Psi_1 \equiv \Psi^{(c)}(k_0), \qquad \Psi_2 \equiv \Psi^{(c)}(e^{i\pi} k_{on}^*) = \Psi_{-n} \tag{3.4.5}$$

It reads then

$$(\mathscr{E}_n - \mathscr{E}) \int_\omega \Psi_{-n}^* \Psi^{(c)}(k_0)\, d\omega = \sum_{c'+} \frac{\hbar^2}{2M_{c'}} W(\Phi_{c'-n}^*, \Phi_{c'}^{(c)}(k_0)) \tag{3.4.6}$$

By virtue of Eqs (2.4.11), the Wronskian on the right-hand side is transformed into

$$W(\Phi_{c'n}, \Phi_{c'}^{(c)}(k_0)) = \Phi_{c'n}\Phi_{c'}^{(c)}(k_0)\left[\frac{\Phi_{c'}^{(c)\prime}}{\Phi_{c'}^{(c)}} - L_{c'n}\right] \tag{3.4.7}$$

when account is taken of Eqs (3.4.3) and the notation (2.3.2) is used. The last expression may be split further as follows:

$$W(\Phi_{c'n}, \Phi_{c'}^{(c)}(k_0)) = \Phi_{c'n}\Phi_{c'}^{(c)}(k_0)[L_{c'}(k_{c'}) - L_{c'n}] - \frac{\Phi_{c'n}}{O_{c'}(k_{c'})} W(\Phi_{c'}^{(c)}, O_{c'})$$

the last term vanishing, by virtue of the conditions (2.1.1), for all channels except c. We therefore get

$$(\mathscr{E}_n - \mathscr{E}) \int \Psi_{-n}^* \Psi^{(c)}(k_0)\, d\omega = -\frac{\hbar^2}{2M_c} \frac{\Phi_{cn}}{O_c(k_c)} W(\Phi_c^{(c)}, O_c)$$

$$+ \sum_{c'+} \frac{\hbar^2}{2M_{c'}} \Phi_{c'n}\Phi_{c'}^{(c)}(k_0)[L_{c'}(k_{c'}) - L_{c'n}] \tag{3.4.8}$$

We now take the derivative with respect to $\mathscr{E}$ and we then let $\Psi^{(c)}(k_0)$ coincide with Ψ_n; it is clear, on account of the condition (3.4.3) and the special form of the various terms, that the result of this operation is

$$-\int_\omega \Psi_{-n}^* \Psi_n\, d\omega = -\frac{\hbar^2}{2M_c}\frac{\Phi_{cn}}{O_{cn}}\left[\frac{d}{d\mathscr{E}} W(\Phi_c^{(c)}, O_c)\right]_{\mathscr{E}=\mathscr{E}_n} + \sum_{c'} \frac{\hbar^2}{2M_{c'}} \Phi_{c'n}^2 \frac{dL_{c'n}}{d\mathscr{E}_n} \tag{3.4.9}$$

whence,

$$\left[\frac{d}{d\mathscr{E}} W(\Phi_c^{(c)}, O_c)\right]^{-1}_{\mathscr{E}=\mathscr{E}_n} = \frac{\hbar^2}{2M_c}\frac{\Phi_{cn}}{O_{cn}}\frac{1}{\nu_n} \tag{3.4.10}$$

with

$$\nu_n = \int_\omega \Psi_{-n}^* \Psi_n\, d\omega + \sum_c \frac{\hbar^2}{2M_c} \Phi_{cn}^2 \frac{dL_{cn}}{d\mathscr{E}_n} \tag{3.4.11a}$$

or

$$\nu_n = \int_{\omega_n} \Psi^*_{-n} \Psi_n \, d\omega + \sum_{c^+} \frac{\hbar^2}{2M_c} \Phi^2_{cn} \frac{dL_{cn}}{d\mathscr{E}_n} \tag{3.4.11b}$$

when the volume of integration is extended to infinity in the closed channels.

Inserting the results (3.4.4) and (3.4.10) into Eq.(3.4.2), we obtain for the residue the symmetrical expression

$$r_{c'cn} = \frac{\hbar^2}{\sqrt{M_{c'} M_c}\, \nu_n} \times \frac{\Phi_{c'n}/O_{c'n}}{\epsilon_{c'n} e^{i\sigma_{c'n}} k^{\ell'}_{c'n}} \times \frac{\Phi_{cn}/O_{cn}}{\epsilon_{cn} e^{i\sigma_{cn}} k^{\ell}_{cn}} \tag{3.4.12}$$

$$= g_{c'n}\, g_{cn} \tag{3.4.13}$$

where $g_{c'n}$, g_{cn} are complex quantities according to

$$g_{cn} = \frac{\hbar}{\sqrt{M_c \nu_n}} \times \frac{\Phi_{cn}}{O_{cn}} \times \frac{1}{\epsilon_{cn} e^{i\sigma_{cn}} k^{\ell}_{cn}} \tag{3.4.14a}$$

$$= \frac{\hbar}{\sqrt{M_c \nu_n}} \frac{\ell!\, \Phi_{cn}}{(-i k_{cn})^{\ell} \Gamma(\ell + 1 + i\eta_c) W_{+,cn}} \tag{3.4.14b}$$

We assume here that

$$\Phi_{cn} \neq 0, \qquad \Phi_{c'n} \neq 0, \tag{3.4.15}$$

otherwise $\mathscr{E}_n$ would not be a pole of the matrix element $t_{c'c}$.

According to Eq.(3.3.5), the expansion of $t_{c'c}$ according to its poles reads

$$t_{c'c} = -i Q_{c'c}(\mathscr{E}) + \sum_{n=1}^{\infty} \frac{g_{c'n}\, g_{cn}}{\mathscr{E} - \mathscr{E}_n} \tag{3.4.16}$$

where $-iQ_{c'c}(\mathscr{E})$ corresponds to the function Q(k) of the expansion theorem (3.3.5).

The expansion of the transition matrix $\mathscr{T}$, defined according to

$$\mathscr{T}_{c'c} = e^{2i\sigma_c} \delta_{c'c} - \mathscr{U}_{c'c} \tag{3.4.17}$$

is easily derived from equations (1.4.6), (2.3.17) and (3.2.1); it reads

$$\mathscr{T}_{c'c} = \epsilon_{c'} \epsilon_c e^{i(\sigma_{c'} + \sigma_c)} k^{\ell' + \frac{1}{2}}_{c'} k^{\ell + \frac{1}{2}}_{c} \left\{ Q_{c'c}(\mathscr{E}) + \sum_{n=1}^{\infty} \frac{g_{c'n}\, g_{cn}}{\mathscr{E} - \mathscr{E}_n} \right\} \tag{3.4.18}$$

The denominators of the resonance terms of this expansion may be given the familiar form

$$\mathscr{E} - \mathscr{E}_n = E_c - E_{cn} + \tfrac{1}{2} i \Gamma_n = E_{c'} - E_{c'n} + \tfrac{1}{2} i \Gamma_n \tag{3.4.19a}$$

where

$$E_c = \frac{\hbar^2}{2M_c} k_c^2, \quad E_{cn} = E_n - E_{\bar{\alpha}_c} = \frac{\hbar^2}{2M_c} (\kappa_{cn}^2 - \gamma_{cn}^2) \tag{3.4.19b}$$

$$\Gamma_n = \frac{2\hbar^2}{M_c} \kappa_{cn}\gamma_{cn} = \frac{2\hbar^2}{M_{c'}} \kappa_{c'n}\gamma_{c'n} \tag{3.4.19c}$$

the quantities κ_{cn} and γ_{cn} are easily expressed in terms of the resonance energy parameter E_{cn} and the total width Γ_n as

$$\kappa_{cn} = M_c^{\frac{1}{2}} \hbar^{-1} \left(E_{cn} + \sqrt{E_{cn}^2 + \Gamma_n^2/4} \right)^{\frac{1}{2}} \tag{3.4.20a}$$

$$\gamma_{cn} = \tfrac{1}{2} M_c^{\frac{1}{2}} \hbar^{-1} \Gamma_n \left(E_{cn} + \sqrt{E_{cn}^2 + \Gamma_n^2/4} \right)^{-\frac{1}{2}} \tag{3.4.20b}$$

In Eq. (3.3.18), the elements of the $\mathcal{T}$ matrix appear as a sum of resonance term plus a background term. Both have the same behaviour at the thresholds $k_c = 0$, $k_{c'} = 0$ as $\mathcal{T}_{c'c}$ itself. The function $Q_{c'c}$ is expected to be slowly varying with the energy $\mathscr{E}$, although it must account for "cusps" at the channel thresholds different from c and c', when such cusps are really observed in a cross-section. It is probably impossible to make any general statement about the relative contribution of $Q_{c'c}$ to $\mathcal{T}_{c'c}$. However, in the applications made so far, such as in [25], it appeared that the background term could be completely neglected or approximated by a constant.

The expansion (3.4.18) of $\mathcal{T}_{c'c}$ satisfies the requirements (i) - (iii) introduced at the beginning of section 3. This is obvious, not only as far as symmetry and threshold behaviour at $k_c = 0$ and $k_{c'} = 0$ are concerned, but for the a-independence as well. Indeed, the residue $r_{c'cn}$ is a-independent because this is the limit of an a-independent quantity, namely $(\mathscr{E} - \mathscr{E}_n) t_{c'c}$; its factors Φ_{cn}/O_{cn}, $\Phi_{c'n}/O_{c'n}$ are a-independent because they are amplitudes of purely outgoing waves; accordingly, the factor ν_n is also a-independent. A direct proof of it has been given in Ref. [19].

The time-reversal property (3.2.8) of $t_{c'c}$ is not individually satisfied by each term of its expansion (3.4.16). This was to be expected a priori, since the very consideration of the physical $\mathscr{E}$-plane removes the contributions of the poles $k_{0-n} = (\exp i\pi) k_{0n}^*$ from the "resonance part" of the expansion. To avoid this, one must obviously expand $t_{c'c}$ in a physical k-plane.

3.5. Expansion of the collision matrix in the physical k_c-plane

Let us derive the expansion of $t_{c'c}$ in the physical k_c-plane. The residue of $t_{c'c}$ at $k_{c'} = k_{c'n}$ is given by

$$\lim_{k_c = k_{cn}} [(k_c - k_{cn}) t_{c'c}] = \frac{2M_c}{\hbar^2 2k_{cn}} \lim_{\mathscr{E} = \mathscr{E}_n} [(\mathscr{E} - \mathscr{E}_n) t_{c'c}]$$

$$= \frac{M_c}{\hbar^2 k_{cn}} r_{c'cn} = \frac{M_c}{\hbar^2 k_{cn}} g_{c'n} g_{cn} \tag{3.5.1a}$$

The residue at $k_{c-n} = e^{i\pi} k^*_{cn}$ is

$$\frac{M_c}{\hbar^2 k_{c-n}} g_{c'-n}\, g_{c-n} = -\frac{M_c}{\hbar^2 k^*_{cn}}\, g^*_{c'n}\, g^*_{cn} \tag{3.5.1b}$$

since, according to the definitions (3.4.11) and (3.4.14), we have

$$\nu_{-n} = \nu^*_n \tag{3.5.2}$$

and

$$g_{c-n} = g^*_{cn} \tag{3.5.3}$$

Comparing Eqs (3.5.1) with Eq. (3.4.13), we see that the expansion of $t_{c'c}$ may also be written as

$$t_{c'c} = -i Q^1_{c'c} + \hbar^{-2} \sum_n \left(g_{c'n}\, g_{cn} \frac{M_c/k_{cn}}{k_c - k_{cn}} - g^*_{c'n} g^*_{cn} \frac{M_c/k^*_{cn}}{k_c + k^*_{cn}} \right) \tag{3.5.4}$$

As expected, each resonance term is not symmetrical in c', c. To reintroduce such a symmetry, let us notice that if the sum over n in Eq. (3.5.4) is convergent, the following expansion

$$\sum_n \left(\frac{g_{c'n}\, g_{cn}}{k_{c'n} k_{cn}} \frac{M_c}{k_c - k_{cn}} + \frac{g^*_{c'n}\, g^*_{cn}}{k^*_{c'n}\, k^*_{cn}} \frac{M_c}{k_c + k^*_{cn}} \right) \tag{3.5.5}$$

is also convergent if one assumes that, as in the one-channel case, k_{cn} is O(n) for large n. Under such conditions let us define $Q^2_{c'c}$ by

$$t_{c'c} = -i Q^2_{c'c} + \hbar^{-2} k_{c'} \sum_n \left(\frac{g_{c'n}\, g_{cn}}{k_{c'n} k_{cn}} \frac{M_c}{k_c - k_{cn}} - \frac{g^*_{c'n} g^*_{cn}}{k^*_{c'n}\, k^*_{cn}} \frac{M_c}{k_c + k^*_{cn}} \right) \tag{3.5.6}$$

and $Q^{c'c}$ as

$$Q^{c'c} = \tfrac{1}{2} (Q^1_{c'c} + Q^2_{c'c}) \tag{3.5.7}$$

Hence, we have

$$\mathcal{T}_{c'c} = \epsilon_{c'} \epsilon_c e^{i(\sigma_{c'} + \sigma_c)} k_{c'}^{\ell+\frac{1}{2}} k_c^{\ell+\frac{1}{2}}$$
$$\times \left(Q^{c'c} + \tfrac{1}{2} i \hbar^{-2} M_c \sum_n \left(\frac{g_{c'n} g_{cn}}{k_{c'n} k_{cn}} \frac{k_{c'} + k_{c'n}}{k_c - k_{cn}} + \frac{g^*_{c'n} g^*_{cn}}{k^*_{c'n} k^*_{cn}} \frac{k_{c'} - k^*_{c'n}}{k_c + k^*_{cn}} \right) \right) \tag{3.5.8}$$

The symmetry holds now for each resonance term, since from Eqs (1.2.15), we have

$$M_c \frac{k_{c'} + k_{c'n}}{k_c - k_{cn}} = M_{c'} \frac{k_c + k_{cn}}{k_{c'} - k_{c'n}}, \quad M_c \frac{k_{c'} - k^*_{c'n}}{k_c + k^*_{cn}} = M_{c'} \frac{k_c - k^*_{cn}}{k_{c'} + k^*_{c'n}} \tag{3.5.9}$$

The expansion (3.5.8) introduces exactly the same parameters as the expansion in the $\mathscr{E}$-plane (3.4.18), namely the g_{cn} and k_{cn}, but the background terms $Q_{c'c}$ and $Q^{c'c}$ are obviously different. Under such conditions,

when fitting experimental data, it is not exactly equivalent to neglect one background or the other and it might be useful to try both alternatives. One should also notice that the second term in the brackets of Eq. (3.5.8) is not "resonant" in the sense that the real part of its denominator $k_c + k_{cn}^*$ does not vanish for $k_c = \kappa_{cn}$. Moreover, for a bound state, this term should be dropped from the bracket, since in this case $-k_{cn}^* = k_{cn}$.

4. TOTAL, PARTIAL AND REDUCED WIDTHS; PENETRATION AND THRESHOLD EFFECTS

4.1. Partial and total widths

The factor $\exp[-i(\sigma_{c'n} + \sigma_{cn})]$ in the product $g_{c'n}\, g_{cn}$ seems at first sight to introduce an unexpected complication in the practical computation of cross-sections, since σ_{cn} and $\sigma_{c'n}$ are not real quantities. However, the occurrence of these factors is only the result of the definition adopted for I_ℓ and O_ℓ for the purpose of analytical arguments, and we may now go over to a more practical notation.

The definitions (2.2.11) were in fact chosen because they made I_ℓ and O_ℓ free of poles and zeros independent of r. Under such conditions, the amplitudes x_c and y_c were properly defined in the complex k_c-plane. Now that the expansions (3.4.18) and (3.5.8) have been established, we may define new ingoing and outgoing wave-functions by

$$I_\ell^{new} = G_\ell - i F_\ell = I_\ell^{old}\, e^{-i\sigma_\ell} \tag{4.1.1a}$$

$$O_\ell^{new} = G_\ell + i F_\ell = O_\ell^{old}\, e^{+i\sigma_\ell} \tag{4.1.1b}$$

and for real energies, new amplitudes X_c and Y_c by

$$u_c(r_c, k_c) = X_c O_c^{new} + Y_c I_c^{new} \tag{4.1.2}$$

leading to a new collision matrix elements

$$U_{c'c}^{new} = -\frac{X_{c'}^{(c)}}{Y_c^{(c)}} = U_{c'c}^{old}\, e^{-i(\sigma_{c'} + \sigma_c)} \tag{4.1.3}$$

and hence

$$\mathscr{U}_{c'c}^{new} = \mathscr{U}_{c'c}^{old} e^{-i(\sigma_{c'} + \sigma_c)}, \quad \mathscr{T}_{c'c}^{new} = \mathscr{T}_{c'c}^{old} e^{-i(\sigma_{c'} + \sigma_c)} \tag{4.1.4}$$

This change in the notation does not modify either the definition of Φ_{cn} or the numerical value of g_{cn} as given by Eq. (3.4.14). For further reference, let us rewrite it in terms of O_{cn}^{new} and let us also write the expansions of $\mathscr{T}_{c'c}^{new}$ corresponding to those of $\mathscr{T}_{c'c}^{old}$. Dropping from now on the indices "new" everywhere, they read

$$g_{cn} = \frac{\hbar}{\sqrt{M_c \nu_n}} \frac{1}{\epsilon_{cn} k_{cn}^\ell} \frac{\Phi_{cn}}{O_{cn}} \tag{4.1.5}$$

$$\mathcal{T}_{c'c} = \epsilon_{c'}\epsilon_c k_{c'}^{\ell'+\frac{1}{2}} k_c^{\ell+\frac{1}{2}} \left\{ Q_{c'c} + i \sum_n \frac{g_{c'n}\, g_{cn}}{\mathcal{E} - \mathcal{E}_n} \right\} \tag{4.1.6}$$

$$\mathcal{T}_{c'c} = \epsilon_{c'}\epsilon_c k_{c'}^{\ell'+\frac{1}{2}} k_c^{\ell+\frac{1}{2}} \left\{ Q^{c'c} + \right.$$

$$\left. + i\,\tfrac{1}{2}\hbar^{-2} \sum_n \left[\frac{g_{c'n}\, g_{cn}}{k_{c'n} k_{cn}} M_c \frac{k_{c'} + k_{c'n}}{k_c - k_{cn}} + \frac{g^*_{c'n}\, g^*_{cn}}{k^*_{c'n}\, k^*_{cn}} M_c \frac{k_{c'} - k^*_{c'n}}{k_c + k^*_{cn}} \right] \right\} \tag{4.1.7}$$

Similar expansions are usually written in terms of "partial widths" which we will now define. For that purpose, when $\Gamma_n \neq 0$, let us consider Eq. (2.5.6b) derived from Green's theorem, namely

$$i\,\Gamma_n \int_{\omega_n} |\Psi_n|^2 \, d\omega = \sum_{c^+} \frac{\hbar^2}{2M_c} \Phi^*_{cn} \Phi_{cn} (L_{cn} - L^*_{cn}) \tag{4.1.8}$$

Let us also define a real quantity N_{cn} by

$$N_{cn} = \frac{1}{2\gamma_{cn}} \left[1 + \frac{i}{2\kappa_{cn}} (O^*_{cn} O'_{cn} - O'^*_{cn} O_{cn}) \right] \tag{4.1.9}$$

it satisfies the equation

$$|O_{cn}|^2 (L_{cn} - L^*_{cn}) = 2i\kappa_{cn} - 2iM_c \hbar^{-2} \Gamma_n N_{cn}$$

When the latter equation is introduced in Eq. (4.1.8), one gets easily

$$\Gamma_n = \frac{1}{\mu_n} \sum_{c^+} \frac{\hbar^2 \kappa_{cn}}{M_c} \left| \frac{\Phi_{cn}}{O_{cn}} \right|^2 \tag{4.1.10}$$

provided μ_n is defined as

$$\mu_n = \int_{\omega_n} |\Psi_n|^2 \, d\omega + \sum_{c^+} N_{cn} \left| \frac{\Phi_{cn}}{O_{cn}} \right|^2 \tag{4.1.11}$$

This is a positive quantity because in Eq. (4.1.10) Γ_n and all the κ_{cn} are themselves positive. Under such conditions, Eq. (4.1.10) suggests defining a partial width Γ_{cn} in order that

$$\Gamma_n = \sum_{c^+} \Gamma_{cn} \tag{4.1.12}$$

i.e., according to

$$\Gamma_{cn} = \frac{1}{\mu_n} \frac{\hbar^2 \kappa_{cn}}{M_c} \left| \frac{\Phi_{cn}}{O_{cn}} \right|^2 \tag{4.1.13}$$

Before introducing such partial widths in the expansions of $\mathcal{T}_{c'c}$, let us still define a real phase ξ_{cn} and a positive ratio q_n according to

$$g_{cn} = |g_{cn}| e^{i\xi_{cn}} \tag{4.1.14}$$

and

$$q_n = \frac{\mu_n}{|\nu_n|} \tag{4.1.15}$$

In terms of the real quantities Γ_{cn}, ξ_{cn} and q_n, the expansions (4.1.6) and (4.1.7) read

$$\mathcal{T}_{c'c} = \epsilon_{c'} \epsilon_c k_{c'}^{\ell'+\frac{1}{2}} k_c^{\ell+\frac{1}{2}} Q_{c'c}(\mathcal{E}) \tag{4.1.16}$$

$$+ i \sum_n q_n \sqrt{\frac{k_{c'} k_c}{\kappa_{c'n} \kappa_{cn}}} \frac{k_{c'}^{\ell'} k_c^{\ell}}{|k_{c'n}^{\ell'} k_{cn}^{\ell}|} \frac{\epsilon_{c'} \epsilon_c}{|\epsilon_{c'n} \epsilon_{cn}|} e^{i\xi_{c'n}} \frac{\Gamma_{c'n}^{\frac{1}{2}} \Gamma_{cn}^{\frac{1}{2}}}{\mathcal{E} - \mathcal{E}_n} e^{i\xi_{cn}}$$

$$= \epsilon_{c'} \epsilon_c k_{c'}^{\ell'+\frac{1}{2}} k_c^{\ell+\frac{1}{2}} Q^{c'c} + \tfrac{1}{2} i \hbar^{-2} \sum_n q_n \sqrt{\frac{k_{c'} k_c}{\kappa_{c'n} \kappa_{cn}}} \frac{k_{c'}^{\ell'} k_c^{\ell}}{|k_{c'n}^{\ell'} k_{cn}^{\ell}|} \frac{\epsilon_{c'} \epsilon_c}{|\epsilon_{c'n} \epsilon_{cn}|}$$

$$\times M_c \Gamma_{c'n}^{\frac{1}{2}} \Gamma_{cn}^{\frac{1}{2}} \left\{ \frac{e^{i(\xi_{c'n} + \xi_{cn})}}{k_{c'n} k_{cn}} \frac{k_{c'} + k_{c'n}}{k_c - k_{cn}} \right.$$

$$\left. + \frac{e^{-i(\xi_{c'n} + \xi_{cn})}}{k_{c'n}^* k_{cn}^*} \frac{k_{c'} - k_{c'n}^*}{k_c + k_{cn}^*} \right\} \tag{4.1.17}$$

For simplicity, in the above expansions and in those we are going to write later, we have omitted the terms corresponding to the bound states ($\Gamma_n = 0$). They cannot of course be expressed in terms of partial widths and they always retain the form they have in Eqs (4.1.6) and (4.1.7).

The definition of Γ_{cn} according to Eq. (4.1.13) and the simultaneous introduction of q_n in the expansions (4.1.16) and (4.1.17) implies a choice between two alternatives. Indeed, considering first the expansions (4.1.6) and (4.1.7), one should rather define an "observable" partial width Γ_{cn}^0 as

$$\Gamma_{cn}^0 = \frac{1}{|\nu_n|} \frac{\hbar^2 \kappa_{cn}}{M_c} \left| \frac{\Phi_{cn}}{O_{cn}} \right|^2 \tag{4.1.18a}$$

$$= q_n \Gamma_{cn} \tag{4.1.18b}$$

and in order that

$$q_n \Gamma_{c'n}^{\frac{1}{2}} \Gamma_{cn}^{\frac{1}{2}} = \Gamma_{c'n}^{0\,\frac{1}{2}} \Gamma_{cn}^{0\,\frac{1}{2}} \tag{4.1.19}$$

the sum of the Γ_{cn}^0 satisfies the following relation:

$$\Gamma_n = \frac{1}{q_n} \sum_{c^+} \Gamma_{cn}^0 \tag{4.1.20}$$

where q_n is still defined according to Eq. (4.1.15).

It is obvious that the fitting of experimental data will lead first to the determination of Γ_n and the Γ^0_{cn} ; hence, the factor q_n will be deduced from Eq.(4.1.20) only if one has enough experimental data to determine all the observable partial widths Γ^0_{cn} of the channels which are open at the energy $\mathscr{E} = \mathscr{E}_n$.

Under such conditions, a theoretical estimate of q_n is very desirable, but in the present general framework the only theoretical result so far available refers to a limiting case, namely (see [22]),

$$q_n \to 1 \text{ for } \Gamma_n \to 0 \tag{4.1.21}$$

This is a generalization of a result first obtained by Weidenmüller [14] in his model of many-channel scattering.

In order to prove the property (4.1.21), let us consider a resonance state for which $k_{bn} = \kappa_{bn} - i\gamma_{bn}$ is lying in the lower half k_b-plane, very close to the positive real axis, but not very close to a threshold. Then,

$$\Gamma_n = 2\hbar^2 \kappa_{dn} \gamma_{dn} / M_d \approx 0 \tag{4.1.22}$$

with

$$\gamma_{dn} \approx 0, \quad \kappa_{dn} \gg \gamma_{dn} > 0 \quad (\text{d open}) \tag{4.1.23a}$$

or

$$\kappa_{dn} \approx 0, \quad \gamma_{dn} \gg \kappa_{dn} > 0 \text{ (d closed)}. \tag{4.1.23b}$$

The quantity μ_n remains finite for $\Gamma_n \to 0$, because N_{c^+n} is itself finite for $\gamma_{c^+n} = 0$. Then, considering Eq.(4.1.10) where, according to Eq.(4.1.23a), κ_{c^+n} is positive, we see that if $\Gamma_n \approx 0$, one must also have

$$\Phi_{c^+n} \approx 0 \text{ for all } c^+; \tag{4.1.24}$$

consequently,

$$\nu_n \approx \int_{\omega_n} \Psi^*_{-n} \Psi_n \, d\omega, \quad \mu_n \approx \int_{\omega_n} |\Psi_n|^2 \, d\omega \tag{4.1.25}$$

In the limiting case $\Gamma_n = 0$, i.e. when

$$\kappa_{c^-n} = \gamma_{c^+n} = 0 \quad (\Gamma_n = 0) \tag{4.1.26}$$

we have

$$e^{i\pi} k^*_{c^-n} = +k_{c^-n}, \quad e^{i\pi} k^*_{c^+n} = -k_{c^+n} \tag{4.1.27}$$

But, the wave equation as well as the boundary conditions for open channels, namely, in the present case,

$$\Phi_{c^+n} = 0 \text{ or } \Phi'_{c^+n} = 0 \tag{4.1.28}$$

being even in k_{c^+n}, it is possible to normalize Ψ_n in order that $\Psi_n = \Psi_{-n}$. Moreover, since $L_{c^-n} = O'_{c^-n}/O_{c^-n}$ is real when k_{c^-n} is imaginary, all the boundary conditions defining Ψ_n in the present case are real and $\Psi^*_n = \Psi_n$.

Hence, when the total width Γ_n is very small, we have

$$\Psi_n \approx \Psi_{-n} \approx \Psi_n^* \tag{4.1.29}$$

From Eqs (4.1.15), (4.1.25) and (4.1.29) we may conclude that

$$q_n \approx 1 \quad \text{when } \Gamma_n \approx 0. \tag{4.1.30}$$

This is an important relation in view of practical applications (see subsection 4.6 below).

4.2. General remarks on the penetration of the Coulomb and centrifugal barriers

Before discussing the penetration and threshold effects in the framework of the S-matrix theory, let us first briefly review the arguments justifying the introduction of a penetration factor in any theory of nuclear resonance reactions at low energy. We follow very closely a discussion given by Jeukenne in Ref. [21].

Many experimental data on isolated resonances at low energy have been fitted to a theoretical cross-section of the Breit-Wigner type. The exact energy dependence of such a cross-section depends on the phenomenological or formal theory adopted for its derivation. In any case, it appears, however, as a product of two factors. One is related to extranuclear effects only, namely the penetration of the Coulomb and centrifugal barriers; near a threshold, it behaves according to the Gamow factor. The other factor contains all the nuclear effects; it has exactly or approximately the form of a Lorentz factor.

From a qualitative point of view, this factorization is undoubtedly well supported by the experimental data. But, considered from the point of view of quantum mechanics, it is also obvious that an exact and complete separation of the penetration and nuclear effects is impossible: the penetrability of a particle through a barrier depends not only on the barrier itself, but also on the potential on the other side of the barrier. In the case of a nuclear reaction, the Coulomb and centrifugal potentials in a channel are separable from the total Hamiltonian in the exterior region of the configuration space associated with that channel, but not in the interior region of the configuration space. Accordingly, it is impossible to define a priori a unique and exact form of the penetration factor.

In particular, although there are good physical arguments in favour of defining a penetration factor according to

$$P_\ell = \frac{1}{F_\ell^2 + G_\ell^2} = \frac{1}{O_\ell I_\ell} \tag{4.2.1}$$

they are nevertheless only qualitative and phenomenological. This being often overlooked, we shall now briefly recall these arguments.

Let us consider the following approximate picture of the first stage of a nuclear reaction leading to the formation of the compound nucleus [4]. A beam of charged particles with the angular momentum ℓ comes from $r = +\infty$, undergoes an electrostatic repulsion up to $r = a$ and then "proceeds

to $r = -\infty$" in a potential well of finite depth U_0 and infinite width extending up to $r = -\infty$ as indicated on Fig. 8.

Defining K and K_0 according to the equations

$$K = (k^2 + 2MU_0/\hbar^2)^{\frac{1}{2}} = (k^2 + K_0^2)^{\frac{1}{2}}$$

the transmission factor for the electrostatic and centrifugal barriers from $r = +\infty$ to $r = a$ is easily seen to be

$$T_\ell = \frac{4K k P_\ell}{S_\ell^2 + (kP_\ell + K)^2} \qquad (4.2.2)$$

where

$$S_\ell = P_\ell (F_\ell F'_\ell + G_\ell G'_\ell)_{r=a}$$

When the energy of the incoming particles is sufficiently small, namely when $k \ll K_0$, then K is much larger than kP_ℓ and S_ℓ. Hence, we have

$$T_\ell \approx \frac{4k}{K_0} P_\ell \qquad (4.2.3)$$

This is the relation which is usually considered as justifying the interpretation of P_ℓ as a penetration factor.

Let us postpone until the next sub-section the discussion of the choice of the best penetration factor one can make in the framework of the S-matrix theory.

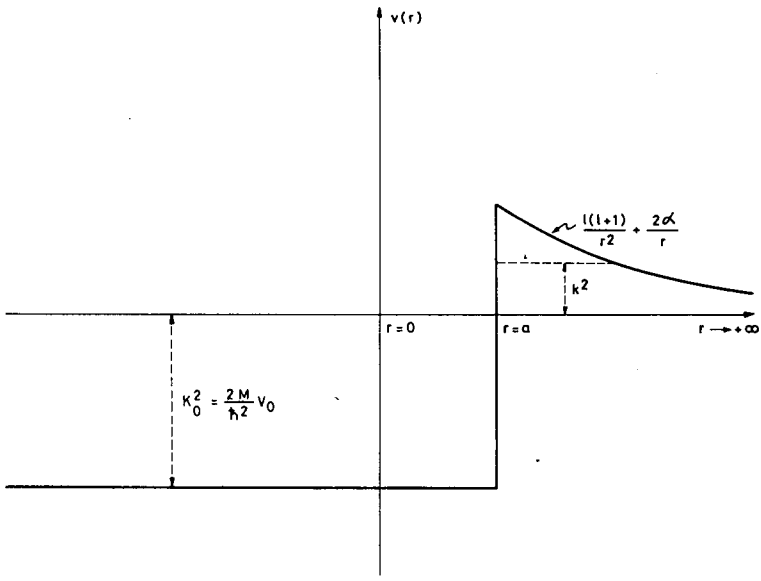

FIG. 8. Phenomenological potential extending from $r = +\infty$ to $r = -\infty$ used in the interpretation of P_ℓ as a penetration factor

4.3. Threshold and penetration effects in the S-matrix theory

Let us go back to the expansions (4.1.16) and (4.1.17) and define a "threshold factor" in channel c as[4]

$$\Pi_c = \epsilon_c k_c^{\ell} \tag{4.3.1}$$

This factor depends only on the Coulomb and centrifugal interactions in channel c; it is however a-independent.

On the one hand, because of its very definition, Π_c is obviously a good penetration factor for a resonance located near the threshold $k_c = 0$; in particular, according to Eqs (2.2.10), it contains the Gamow factor

$$2\pi\eta_c / [\exp(2\pi\eta_c) - 1] \tag{4.3.2}$$

On the other hand, when a resonance is far above a threshold, there is no reason why the threshold factor Π_c should still simultaneously be a good penetration factor. In this case, one expects the Coulomb and centrifugal barriers to play a minor part in the cross-section and in the limiting case of $k_c \to \infty$, one must be justified in ignoring them completely. In the product Π_c, only ϵ_c tends toward unity for $k_c \to \infty$.

Under such conditions, one must expect that a broad[5] resonance far above the thresholds $k_c = 0$ and $k_{c'} = 0$ is better parametrized by

$$\epsilon_{c'} \epsilon_c \frac{\text{const.}}{\mathscr{E} - \mathscr{E}_n} \tag{4.3.3a}$$

than by

$$k_{c'}^{\ell'} k_c^{\ell} \epsilon_{c'} \epsilon_c \frac{\text{const.}}{\mathscr{E} - \mathscr{E}_n} \tag{4.3.3b}$$

This brings up the following question: Is the expansion (4.1.16) the only one which corresponds to a pole expansion of $\mathscr{T}_{c'c}$ in the physical $\mathscr{E}$-plane (and correspondingly for the expansion (4.1.17) in the physical k_c-plane)? The answer is no, since one is just as well justified in applying the expansion theorem to the second factor of

$$\frac{1}{f(\mathscr{E})} \times \left[f(\mathscr{E})\, t_{c'c} \right]$$

provided $f(\mathscr{E})$ has no pole in the complex $\mathscr{E}$-plane, is continuous on its boundary and that the residue of $f(\mathscr{E})t_{c'c}$, namely $f(\mathscr{E}_n)r_{c'cn}$, satisfies the convergence condition (3.3.2).

---

[4] It is more convenient not to include $k_c^{\frac{1}{2}}$ in the definition of Π_c because, as it is defined, Π_c reduces to unity for an s-wave neutron channel.

[5] For a narrow resonance, the variation of $k_c^{\ell'} \cdot k_c^{\ell}$ over the width of the resonance might not be very significant.

These conditions are obviously satisfied when $f(\mathscr{E}) = k_{c'}^{\ell'} k_c^{\ell}$ and one obtains immediately the corresponding expansions for $\mathscr{T}_{c'c}$; they read

$$\mathscr{T}_{c'c} = \epsilon_{c'} \epsilon_c k_{c'}^{\frac{1}{2}} k_c^{\frac{1}{2}} \overline{Q}_{c'c} + i \sum_n q_n \sqrt{\frac{k_{c'} k_c}{\kappa_{c'n} \kappa_{cn}}} \frac{\epsilon_{c'} \epsilon_c}{|\epsilon_{c'n} \epsilon_{cn}|} e^{i\bar{\xi}_{c'n}} \frac{\Gamma_{c'n}^{\frac{1}{2}} \Gamma_{cn}^{\frac{1}{2}}}{\mathscr{E} - \mathscr{E}_n} e^{i\bar{\xi}_{cn}} \Bigg\} \tag{4.3.4}$$

$$= \epsilon_{c'} \epsilon_c k_{c'}^{\frac{1}{2}} k_c^{\frac{1}{2}} \overline{Q}^{c'c} + \tfrac{1}{2} i \hbar^{-2} \sum_n q_n \sqrt{\frac{k_{c'} k_c}{\kappa_{c'n} \kappa_{cn}}} \frac{\epsilon_{c'} \epsilon_c}{|\epsilon_{c'n} \epsilon_{cn}|} \times \Gamma_{c'n}^{\frac{1}{2}} \Gamma_{cn}^{\frac{1}{2}} \left\{ \frac{e^{i(\bar{\xi}_{c'n} + \bar{\xi}_{cn})}}{k_{c'n} k_{cn}} M_c \frac{k_{c'} + k_{c'n}}{k_c - k_{cn}} + \frac{e^{-i(\bar{\xi}_{c'n} + \bar{\xi}_{cn})}}{k_{c'n}^* k_{cn}^*} M_c \frac{k_{c'} - k_{c'n}^*}{k_c + k_{cn}^*} \right\} \tag{4.3.5}$$

where

$$\bar{\xi}_{cn} = \xi_{cn} - \arg(k_{an}^{\ell}) \tag{4.3.6}$$

The background terms $\overline{Q}_{c'c}$, $\overline{Q}^{c'c}$ are different in the expansions (4.1.16), (4.1.17) and (4.3.4), (4.3.5). From a purely mathematical point of view, these four expansions are rigorously equivalent; this is no longer so if one turns to physical applications corresponding to one- or few-level approximations. It is a priori better justified to neglect the background term and the "faraway levels" in the expansion (4.3.4), rather than in the expansion (4.1.16), if one wants to fit one or a few resonances far above the thresholds $k_c = 0$, $k_{c'} = 0$.

Obviously, if a resonance is far above the threshold of channel c, but close to the threshold of channel c', $f(\mathscr{E})$ will be chosen as $f(\mathscr{E}) = k_c^{\ell}$. The corresponding expansions of $\mathscr{T}_{c'c}$ are easily written down.

But there is still the case of a very broad resonance extending from close to a threshold to far above it! In this case the arguments just given suggest fitting the low-energy part of the resonance according to the expansion (4.1.16) or (4.1.17) and its high-energy part according to (4.3.4) or (4.3.5). Although each of these two analyses should in principle lead to the same values of E_n, Γ_n and $q_n \Gamma_{c'n}^{\frac{1}{2}} \Gamma_{cn}^{\frac{1}{2}}$, this is obviously not a very satisfactory way of analyzing such a resonance. One must rather look for some way of introducing a smooth transition from $\epsilon_c k_c^{\ell}$ for small k_c to ϵ_c or 1 for large k_c.

This is precisely one property of the a-dependent quantity $P_{\ell}^{\frac{1}{2}}$ when P_{ℓ} is defined according to Eq. (4.2.1). Indeed, from Eqs (2.2.9), (2.2.11) and (2.2.19b), we have

$$P_{\ell} = \frac{1}{e^{\pi\eta} W_+ W_-} \tag{4.3.7}$$

$$= \frac{1}{[\ell!\, \alpha^{\ell} x_c K_{2\ell+1}(x_c)]^2} \epsilon_{\ell}^2 k_c^{2\ell} [1 + 0(k_c^2)] \tag{4.3.8}$$

for small k and $\alpha \neq 0$, while for $\alpha = 0$, the asymptotic properties of the spherical Hankel immediately give

$$P_\ell = \frac{1}{\mathscr{H}_\ell^{(1)}(k_c a_c)\,\mathscr{H}_\ell^{(2)}(k_c a_c)} \tag{4.3.9}$$

$$= \left(\frac{(2\ell)!}{\ell!\,2^\ell}\right)^2 (k_c a_c)^{2\ell} \quad [1 + 0(k_c^2 a_c^2)] \tag{4.3.10}$$

Moreover, from Eqs (2.2.18), for large energies, we have

$$P_\ell \to 1 \text{ for } ka \to \infty \tag{4.3.11}$$

Hence, $P_\ell^{\frac{1}{2}}$ indeed behaves like π_c near $k_c = 0$, while at large energies it has the other desired property of tending to unity.

An expansion for $\mathscr{T}_{c'c}$ in which the resonance terms are proportional to $P_{\ell'}^{\frac{1}{2}}\, P_\ell^{\frac{1}{2}}$ is derived in the next paragraph. An extra factor $k_c a_c$ is often included in the definition of P_ℓ; here we have adopted for the penetration factor P_ℓ the definition (4.2.1) which reduces to unity in the absence of Coulomb and centrifugal barriers (for an s-wave neutron: $\alpha_c = 0$, $P_0 \equiv 1$) and tends towards unity at large energies (cf. (4.3.11)).

4.4. An alternative expansion of $\mathscr{T}_{c'c}$ ([20])

Let us first consider the matrix element

$$\mathscr{U}_{c'c} = \sqrt{\frac{k_c M_c}{k_{c'} M_{c'}}}\, \frac{W(\Phi_c^{(c)}, I_{c'})}{W(\Phi_c^{(c)}, O_c)} \tag{4.4.1}$$

and, use being made of the relations (2.1.1) and (2.2.17), let us rewrite its numerator as

$$W(\Phi_{c'}^{(c)}, I_{c'}) = \frac{I_{c'}}{O_{c'}} \left[\Phi_{c'}^{(c)} O_{c'}' - \Phi_{c'}^{(c)\prime} O_{c'} + O_{c'} \Phi_{c'}^{(c)} \left(\frac{I_{c'}'}{I_{c'}} - \frac{O_{c'}'}{O_{c'}} \right) \right]$$

$$= \frac{I_{c'}}{O_{c'}} \left[\delta_{c'c} W(\Phi_c^{(c)}, O_c) - 2ik_c \Phi_{c'}^{(c)} / I_{c'} \right] \tag{4.4.2}$$

Hence, defining the phase factor Ω_c according to

$$(I_c / O_c)^{\frac{1}{2}} = \Omega_c = e^{i\varphi_c} \tag{4.4.3}$$

and noticing that one has

$$\frac{1}{O_c} = P_c^{\frac{1}{2}} \Omega_c \tag{4.4.4}$$

the matrix element $\mathscr{U}_{c'c}$ reads also

$$\mathscr{U}_{c'c} = \Omega_{c'} \Omega_c \left[\delta_{c'c} - 2i \sqrt{\frac{M_c}{M_{c'}}}\, k_{c'}^{\frac{1}{2}} k_c^{\frac{1}{2}} P_{c'}^{\frac{1}{2}} P_c^{\frac{1}{2}} \frac{\Phi_{c'}^{(c)}}{\Phi_c^{(c)\prime} - L_c \Phi_c^{(c)}} \right] \tag{4.4.5}$$

According to our analyticity hypothesis, the poles of $\Phi_c^{(c)} / (\Phi_c^{(c)'} - L_c \Phi_c^{(c)})$ are exactly the same as those[6] of $\mathscr{U}_{c'c}^{old}$; moreover, according to Eq.(2.2.19b), L_c is continuous for $k_c \to 0$, when k_c remains an interior point of the physical plane considered.

Taking Eq.(3.4.10), into account, we easily get the following expansion:

$$2i \sqrt{\frac{M_c}{M_{c'}}} \frac{\Phi_c^{(c)}}{\Phi_c^{(c)'} - L_c \Phi_c} = \mathscr{Q}_{c'c} + i \frac{\hbar^2}{\sqrt{M_{c'} M_c}} \sum_n \frac{1}{\nu_n} \frac{\Phi_{c'n} \Phi_{cn}}{\mathscr{E} - \mathscr{E}_n} \tag{4.4.6}$$

and hence

$$\mathscr{U}_{c'c} = \Omega_{c'} \Omega_c \left[\delta_{c'c} - k_{c'}^{\frac{1}{2}} k_c^{\frac{1}{2}} P_{c'}^{\frac{1}{2}} P_c^{\frac{1}{2}} \left(\mathscr{Q}_{c'c} + i \frac{\hbar^2}{\sqrt{M_{c'} M_c}} \sum_n \frac{1}{\nu_n} \frac{\Phi_{c'n} \Phi_{cn}}{\mathscr{E} - \mathscr{E}_n} \right) \right] \tag{4.4.7}$$

$$\mathscr{T}_{c'c} = 2 i \delta_{c'c} F_c / O_c + \Omega_{c'} \Omega_c k_{c'}^{\frac{1}{2}} k_c^{\frac{1}{2}} P_{c'}^{\frac{1}{2}} P_c^{\frac{1}{2}} \left[\mathscr{Q}_{c'c} + i \frac{\hbar^2}{\sqrt{M_{c'} M_c}} \sum_n \frac{1}{\nu_n} \frac{\Phi_{c'n} \Phi_{cn}}{\mathscr{E} - \mathscr{E}_n} \right] \tag{4.4.8}$$

Defining a real phase ξ_{cn} according to

$$\frac{1}{\sqrt{\nu_n}} \Phi_{cn} = \left| \frac{1}{\sqrt{\nu_n}} \Phi_{cn} \right| e^{i \zeta_{cn}} \tag{4.4.9}$$

this expansion may be given the following form:

$$\mathscr{T}_{c'c} = 2 i \delta_{c'c} F_c / O_c + \Omega_{c'} \Omega_c P_{c'}^{\frac{1}{2}} P_c^{\frac{1}{2}} \left(k_{c'}^{\frac{1}{2}} k_c^{\frac{1}{2}} \mathscr{Q}_{c'c} + i \sum_n q_n \sqrt{\frac{k_{c'} k_c}{\kappa_{c'n} \kappa_{cn}}} \left| O_{c'n} O_{cn} \right| e^{i \zeta_{c'n}} \frac{\Gamma_{c'n}^{\frac{1}{2}} \Gamma_{cn}^{\frac{1}{2}}}{\mathscr{E} - \mathscr{E}_n} e^{i \zeta_{cn}} \right) \tag{4.4.10}$$

where the partial widths are defined according to Eq.(4.1.13).

It is of interest to point out that from a formal point of view, there is a relation between P_ℓ and $\epsilon_\ell k_c^\ell$, according to which expansion (4.1.16) is nothing else than the limit of expansion (4.4.10) for vanishing channel radii a_c and $a_{c'}$. Considering the relations (2.2.7') and the factor $|O_{cn}| P_c^{\frac{1}{2}}$ which appears in the expansion (4.4.10), we have

$$\lim_{a_c \to 0} |O_{cn}| P_c^{\frac{1}{2}}(a_c, k_c) = \lim_{a_c \to 0} \left| \frac{G_\ell(a_c, k_{cn})}{G_\ell(a_c, k_c)} \right| = \frac{\epsilon_c k_c^\ell}{|\epsilon_{cn} k_{cn}^\ell|} \tag{4.4.11}$$

Although this result suggests to consider $\pi_c = \epsilon_c k_c^\ell$ as related to a penetration down to the "centre" of the target nuclei, such an interpretation should not be taken too literally. The result (4.4.11) is simply related to the fact that the a_c- and k_c-dependence of P_ℓ are separable when $a_c \to 0$ or when $k_c \to 0$.

---

[6] Eqs (4.4.1) to (4.4.5) hold for $\mathscr{U}_{c'c}^{new}$ and $\mathscr{U}_{c'c}^{old}$ as well, assuming that, according to the definition (4.4.3), we have $\Omega_c^{new} = \Omega_c^{old} \, e^{-i\sigma_\ell}$; Eq.(4.4.8) holds for $\mathscr{T}_{c'c}^{new}$ only.

4.5. Reduced widths

When experimental data can be fitted to a one- or few-level approximation of the expansion (4.4.10) just obtained, they lead to the determination of the products $|O_{cn}|^2 \Gamma_{cn}$ and hence, in principle, to the knowledge of the a-independent partial widths Γ_{cn}. In practice, however, it implies the difficult computation of the O_{cn}, i.e. the computation of Whittaker functions W_+ for complex $k_c = k_{cn}$.

This justifies the introduction of a real reduced width w_{cn}^2 defined according to

$$w_{cn}^2 = \frac{1}{2\kappa_{cn} a_c} |O_{cn}|^2 \Gamma_{cn} \tag{4.5.1a}$$

$$= \frac{1}{\mu_n} \frac{\hbar^2}{2 a_c M_c} |\Phi_{cn}|^2 \tag{4.5.1b}$$

in terms of which the expansion (4.4.10) reads

$$\mathscr{T}_{c'c} = 2i\delta_{c'c} F_c/O_c + \Omega_{c'} \Omega_c P_{c'}^{\frac{1}{2}} P_c^{\frac{1}{2}} \Big(\sqrt{k_{c'} k_c}\, \mathscr{Q}_{c'c} + 2i \sum_n q_n \sqrt{k_{c'} a_{c'} k_c a_c}\, e^{i\zeta_{c'n}} \frac{w_{c'n} w_{cn}}{\mathscr{E} - \mathscr{E}_n} e^{i\zeta_{cn}} \Big) \tag{4.5.2}$$

where we chose $w_{cn} > 0$. Obviously, one could just as well introduce observable reduced widths

$$w_{cn}^{o2} = q_n w_{cn}^2 \tag{4.5.3a}$$

$$= \frac{\hbar^2}{2 a_c M_c} \left| \frac{1}{\nu_n} \Phi_{cn}^2 \right| \tag{4.5.3b}$$

4.6. Sum rules and single-particle limit

As we noticed in sub-section 4.1, the definition of the partial widths Γ_{cn} suggested by the expansion (4.1.6) is not unique. We chose to normalize them in order to satisfy exactly the relation

$$\Gamma_n = \sum_{c^+} \Gamma_{cn} \tag{4.6.1}$$

although the quantities directly related to the experimental data are rather the observed partial widths Γ_{cn}^0 satisfying the relation

$$\Gamma_n = \frac{1}{q_n} \sum_{c^+}' \Gamma_{cn}^0 \tag{4.6.2}$$

An exact theoretical determination of q_n is at present impossible, because it implies the computation of Ψ_n in the interior region of the configuration space. Nevertheless, we believe that the relation (4.6.2)

amounts to a good and useful sum rule in the fitting of experimental data. The very analytical definitions (3.4.11) and (4.1.11) of ν_n and μ_n, not only allowed us to prove that $q_n \to 1$ for $\Gamma_n \to 0$, but make it also very likely that q_n is of the order of unity not just for very narrow levels, but for "rather broad" levels as well. Up to now, however, this is supported only by the following results.

On the one hand, in his model for many-channel scattering, Weidenmüller [14] has computed q_n for one resonance state, using different values of the parameter coupling the two channels he considers; when the total width varies from $\Gamma_n = 0$ to 1.5 MeV, the corresponding values of q_n range from $q_n = 1$ to 0.94.

On the other hand [45-47] q_n has been determined from experimental data for two levels of ^{7}Be. The available differential and integrated cross-sections for the three reactions

$$^6\mathrm{Li}(p, p), \quad ^4\mathrm{He}(^3\mathrm{He}, ^3\mathrm{He}), \quad ^6\mathrm{Li}(p, ^4\mathrm{He}) \tag{4.6.3}$$

have been simultaneously fitted using a two-level approximation for the collision matrix elements. The investigated region of excitation energy of ^{7}Be extends from 6.0 to 8.4 MeV; two $5/2^-$ resonances are observed around 6.40 and 7.20 MeV. Let E_n, E_m, Γ_n, Γ_m be the positions and total widths of these resonances. The resonance terms of the collision matrix elements have numerators proportional to

$$q_i\Gamma_{pi}, \quad q_i\Gamma_{\alpha i}, \quad q_i\Gamma_{pi}^{\frac{1}{2}}\,\Gamma_{\alpha i}^{\frac{1}{2}} \quad (i = n, m) \tag{4.6.4}$$

for the three reactions (4.6.3), respectively. Least square adjustments have been performed taking into account the obvious relation existing between the products (4.6.4). Good fits were achieved using the values given in the first four lines of Table I. The relations $\Gamma_i = \Gamma_{pi} + \Gamma_{\alpha i}$ $(i = n, m)$ together with the third and fourth lines of Table I, easily lead to the results given in the last three lines of Table I. Both q_n and q_m turn out to be close to unity, although the corresponding levels are not narrow.

Let us now turn to the reduced widths and derive the so-called single-particle limit. Although derived under very crude assumptions, it has nevertheless proved very useful. Let us only consider the observable

TABLE I. ENERGY, TOTAL AND PARTIAL WIDTHS IN MeV AND q_i FACTORS FOR TWO RESONANCES IN ^{7}Be

	i=n	i=m
E_i	6.497	7.078
Γ_i	1.086	0.469
$q_i\Gamma_{pi}$	0.0171	0.3895
$q_i\Gamma_{\alpha i}$	1.056	0.0237
Γ_{pi}	0.0174	0.442
$\Gamma_{\alpha i}$	1.069	0.027
q_i	0.988	0.881

reduced width w_{cn}^{o2}, since it differs from the formal reduced width w_{cn}^2 only by a factor q_n, the value of which has just been discussed.

Let us assume that in the interior as well as in the exterior region of the configuration space, the wave-function at the resonance energy can be given the following form:

$$\Psi_n \approx \varphi_c u_{cn}(r_c, k_{cn})/r_c \tag{4.6.5}$$

where the single channel considered has one and A-1 nucleons in the two fragments respectively. If, moreover, we assume that the probability density $|\Psi_n|^2$ at any point of the interior region is the same as on the boundary surface $\mathscr{S}_c$, we get

$$\nu_n \approx \int\int [\varphi_c \Phi_c (e^{i\pi} k_{cn}^*)/a_c]^* [\varphi_c \Phi_{cn}/a_c] r_c^2 \, dr_c \, dS_c + \frac{\hbar^2}{2M_c} \Phi_{cn}^2 \frac{dL_{cn}}{d\mathscr{E}_n}$$

$$\approx \Phi_{cn}^2 \left[\frac{a_c}{3} + \frac{1}{2k_{cn}} \frac{dL_{cn}}{dk_{cn}} \right] \tag{4.6.6}$$

The last term in the bracket is in general not easily evaluated; however, for an s-wave neutron channel it reduces to $i/2k_{cn}$, while, according to Eq. (2.2.19b), for a proton channel, it can be neglected when $|k_{cn}| a_c \ll 1$. Hence, only considering the latter case, we easily obtain

$$w_{cn}^{o2} = \frac{3}{2} \frac{\hbar^2}{a_c^2 M_c} \tag{4.6.7}$$

In most cases, this result must only be considered as an approximate upper limit of w_{cn}^{o2} for the following reasons. On the one hand, the contribution of the closed channels to ν_n has been neglected; on the other hand, we have most probably largely underestimated $|\Psi_n|^2$ in the interior region, since, according to sub-section 4.1, Φ_{cn} (i.e. u_{cn} on $\mathscr{S}_c$) can be very small for an open channel.

4.7. Final remarks

Although there are several ways of defining a set of eigenstates of a compound nucleus, the one we have adopted here is the only one which, when it is applied to a physical wave-function with only one entrance channel $\Psi^{(c)}$, $\Psi^{(d)}$, ..., leads directly to a set of constant eigenvalues $\mathscr{E}_n$ independent of the entrance channel considered (c), (d), ... But, since the corresponding eigenfunctions Ψ_n do not form an orthogonal set, we had to turn to the analytical properties of the wave-functions $\Psi^{(c)}$, $\Psi^{(d)}$, ..., for the derivation of an expansion of the collision matrix. The fact that the eigenvalues $\mathscr{E}_n$ are precisely the poles of the collision matrix suggested not just one, but several, possible expansions of the collision matrix according to its poles; all these expansions introduce different background terms. The physical reason for the existence of such background terms is clear: they must contain the non-resonant part of the collision matrix. But, still, from a purely physical point of view, it is also obvious that the separation of resonant and non-resonant effects cannot be a sharp one. This agrees with the fact that the various expansions of the collision matrix have different background terms.

In the same line of argument, we should also point out the fact that an expansion derived in a physical plane, i.e. on a single Riemann sheet with cuts, does not contain in the resonant part of the expansion all the poles defined by Eq.(2.1.5). Under such conditions, it is important that the cuts should be drawn in such a way that all the physically important ones, i.e. the narrow ones, appear in the resonance part. Except for poles located very close to the thresholds, the two sets of cuts given in Figs (6) and (7) are adapted to that purpose. From that point of view they are in fact practically equivalent, since in both cases the immediate neighbourhood of the real positive k_0- and $\mathscr{E}$-axis is part of the physical plane considered, all the cuts being orthogonal to the real axis.

Applied to the fitting of experimental data on low energy resonances, all these expansions should in principle give the same values for the parameters E_n, Γ_{cn}, q_n, ... In practice, small differences are observed because the few-level approximations are obtained by neglecting (or approximating by a constant) different background terms. One can decide which are the "best" parameters only if several reactions leading to the formation of the same compound nucleus are analysed simultaneously; the position and total width of a resonance should be independent of the reaction used for their determination.

We are now in a position to conclude our discussion on the best choice of the penetration factor; should it be simply the threshold factor $\epsilon_c k_c^{\ell}$ or the conventional $P_{\ell}^{\frac{1}{2}}$? Besides those given above, the main argument often invoked in favour of the latter choice is that it gives a more physical character to the parametrization of the collision matrix, since the channel radii introduce the dimensions of the nuclei in that parametrization. This might be true in some cases, but in many cases this is only illusory. Indeed, since many resonances can be fitted to the one-level approximation of the expansions (4.1.16) and (4.4.10) as well, it is clear that the size of the nuclei, i.e. the channel radii, is not given by such experimental data. In such cases, the determination of reduced widths from the expansion (4.4.10) amounts to defining them according to

$$w_{cn}^2 = \Gamma_{cn} \frac{|O_c(a_c, k_{cn})|^2}{2\kappa_{cn} a_c} \qquad (4.7.1)$$

where κ_{cn} and Γ_{cn} are determined from the one-level approximation of the expansion (4.1.16) and the a priori choice a_c.

This argument should be less valid when one deals with very large resonances, since the k_c- and a_c-dependences in

$$f(a_c, k_c) \equiv \frac{[P_{\ell}(a_c, k_c)]^{\frac{1}{2}}}{\epsilon_c k_c^{\ell}} \qquad (4.7.2)$$

are not separable[7]. As explained in sub-section 4.2, it is only for very broad resonances that the expansion (4.4.10) has an obvious advantage over the expansions (4.1.16). The fact that the best fit corresponds precisely to the "best" channel radii will however remain uncertain, since the a-dependence of $P_c^{\frac{1}{2}} P_c^{\frac{1}{2}}$ must be contrasted to the a-independence of the exact collision matrix.

[7] This non-separability entails a dependence of Γ_n and E_n upon the channel radii when a resonance is analysed with the one-level approximation of the expansion (4.4.10); this dependence has been discussed and estimated by Jeukenne [21] for the reactions ^{3}He(d, p) and ^{3}H(d, n).

Finally, let us also notice that most of the recent dynamical approaches to the theory of nuclear reactions [26-36] completely avoid the introduction of channel radii and the corresponding division of the configuration space into a clear-cut interior and exterior region. Mahaux [48] has shown that this is also possible in the present formal theory, at least as far as the derivation of an expansion of the form (4.1.6) is concerned. Only the Green's theorem and the applications we made of it require the explicit reference to channel radii.

5. DIFFERENTIAL CROSS-SECTION AND APPLICATIONS

For easier reference, we give hereafter the differential cross-section for a reaction $\alpha_1\alpha_2 s\nu \rightarrow \alpha_1'\alpha_2' s'\nu'$. With our usual notation $\bar{\alpha} \equiv \alpha_1, \alpha_2$ and adopting the following definitions [12]

$$C_{\bar{\alpha}}(\theta_{\bar{\alpha}}) = (4\pi)^{-\frac{1}{2}} \eta_{\bar{\alpha}} \mathrm{cosec}^2(\tfrac{1}{2}\theta_{\bar{\alpha}}) \exp[-2i\eta_{\bar{\alpha}} \log \sin(\tfrac{1}{2}\theta_{\bar{\alpha}})] \tag{5.1}$$

$$\omega_{\bar{\alpha}\ell} = \sigma_{\bar{\alpha}\ell} - \sigma_{\bar{\alpha}0} \equiv \sigma_\ell - \sigma_0 (\text{for } \eta = \eta_\alpha) \tag{5.2}$$

the differential cross-section $d\sigma_{\bar{\alpha}s\nu,\ \bar{\alpha}'s'\nu'}$ may be written as

$$d\sigma_{\bar{\alpha}s\nu,\ \bar{\alpha}'s'\nu'} = \left| A_{\bar{\alpha}'s'\nu',\ \bar{\alpha}s\nu}(\Omega_{\bar{\alpha}'}) \right|^2 d\Omega_{\bar{\alpha}'} \tag{5.3}$$

where

$$A_{\bar{\alpha}'s'\nu',\ \bar{\alpha}s\nu} = \pi^{\frac{1}{2}} k_{\bar{\alpha}}^{-1} \Big[C_{\bar{\alpha}'}(\theta_{\bar{\alpha}'}) \delta_{\bar{\alpha}'s'\nu',\ \bar{\alpha}s\nu} + i \sum_{\ell' m' \ell} \sqrt{2\ell+1}\ e^{i(\omega_{\bar{\alpha}'\ell'} + \omega_{\bar{\alpha}\ell})} \mathscr{T}_{\bar{\alpha}'s'\ell'\nu'm',\ \bar{\alpha}s\ell\nu 0}\ Y_\ell^m(\Omega_{\bar{\alpha}'}) \Big] \tag{5.4}$$

Either of the expansions derived earlier for $\mathscr{T}_{c'c}^{new}$ may be introduced in the amplitude (5.4); for further details, see Ref. [12].

In this chapter no space can be given to reviewing some of the applications of the general theory which have been made recently. The reader should refer to the original papers: to Refs [49, 21, 25] for various applications of the one- and two-level approximations; to [45-47] for the analysis of an elastic scattering reaction and two experimental determinations of q_n; to [50, 51] for the application of a perturbation formula for the resonance levels to the computation of the shift of the levels in mirror nuclei; and to Refs [21, 45-47, 52] for applications of the expansion (4.5.2) using the P_ℓ as penetration factors.

ACKNOWLEDGEMENTS

The author thanks Professor Abdus Salam and the IAEA for the hospitality extended to him at the International Centre for Theoretical Physics, Trieste. He is also grateful to Professors A. de-Shalit and C. Villi for the opportunity offered to him to write up these lecture notes on the occasion of the International Course on Nuclear Physics held in Trieste in October-December 1966. The very effective collaboration of the editorial staff of the Centre has also been appreciated.

REFERENCES

[1] WIGNER, E.P., Z. Physik 83 (1933) 253.
[2] WIGNER, E.P., BREIT, G., Phys. Rev. 49 (1936) 519, 612.
[3] BREIT, G., Handb. Physik 41/1 Springer-Verlag, Berlin (1959).
[4] BLATT, J.M., WEISSKOPF, V.F., Theoretical Nuclear Physics, Wiley (1952).
[5] BETHE, H.A., PLACZECK, G., Phys. Rev. 51 (1937) 450.
[6] BETHE, H.A., Rev. mod. Phys. 9 (1937) 69.
[7] KAPUR, P.L., PEIERLS, R.E., Proc. Roy. Soc., Lond. A 166 (1937) 277.
[8] PEIERLS, R.E., Proc. Cambridge phil. Soc. 44 (1947) 242.
[9] WIGNER, E.P., Phys. Rev. 70 (1946) 15.
[10] WIGNER, E.P., EISENBUD, L., Phys. Rev. 72 (1947) 29.
[11] TEICHMAN, T., WIGNER, E.P., Phys. Rev., 87 (1952) 123.
[12] LANE, A.M., THOMAS, R.G., Rev. mod. Phys. 30 (1958) 257.
[13] WEIDENMÜLLER, H.A., Ann. Phys. 28 (1964) 60.
[14] WEIDENMÜLLER, H.A., Ann. Phys. 29 (1964) 378.
[15] MAHAUX, C., WEIDENMÜLLER, H.A., Ann. Phys. 32 (1965) 259.
[16] MAHAUX, C., WEIDENMÜLLER, H.A., Comparison between R-matrix and shell-model approach to nuclear reactions, Nucl. Phys. (1967, in press).
[17] HUMBLET, J., ROSENFELD, L., Nucl. Phys. 26 (1961) 529.
[18] ROSENFELD, L., Nucl. Phys. 26 (1961) 594.
[19] HUMBLET, J., Nucl. Phys. 31 (1962) 544.
[20] HUMBLET, J., Nucl. Phys. 50 (1964) 1.
[21] JEUKENNE, J.P., Nucl. Phys. 58 (1964) 1.
[22] HUMBLET, J., Nucl. Phys. 57 (1964) 386.
[23] MAHAUX, C., Nucl. Phys. 68 (1965) 481.
[24] ROSENFELD, L., Nucl. Phys. 70 (1965) 1.
[25] MAHAUX, C., Nucl. Phys. 71 (1965) 241.
[26] BLOCH, C., GILLET, V., Physics Lett. 16 (1965) 62.
[27] GILLET, V., BLOCH, C., Physics Lett. 18 (1965) 58.
[28] DANOS, M., GREINER, W., Phys. Rev. 146 (1966) 708.
[29] FESHBACH, H., Ann. Phys. 5 (1958) 357; and 19 (1962) 287.
[30] MacDONALD, W.M., Nucl. Phys. 54 (1964) 393; 56 (1964) 636; and 56 (1964) 647.
[31] HERZENBERG, A., KWOK, K.L., MANDL, F., Proc. phys. Soc., Lond. 84 (1964) 477.
[32] WEIDENMÜLLER, H.A., Nucl. Phys. 75 (1965) 189.
[33] WEIDENMÜLLER, H.A., DIETRICH, K., Nucl. Phys. 83 (1966) 332.
[34] HAGLUND, M.E., ROBSON, D., Phys. Lett. 14 (1965) 225.
[35] LANE, A.M., ROBSON, D., Phys. Rev. 151 (1966) 774.
[36] MAHAUX, C., WEIDENMÜLLER, H.A., Nucl. Phys. A 91 (1967) 241.
[37] HULL, M.H., BREIT, G., Handb. Phys. 41/1 Springer-Verlag, Berlin (1959).
[38] BUCHHOLZ, H., Die Konfluente Hypergeometrische Funktion, Springer-Verlag, Berlin (1953).
[39] NEWTON, R.G., J. Math. Phys. 2 (1961) 188.
[40] PEIERLS, R.E., Proc. Roy. Soc., Lond. A.253 (1959) 16.
[41] Le COUTEUR, K.J., Proc. Roy. Soc., Lond. A.256 (1960) 115.
[42] MORSE, P.M., FESHBACH, H., Methods of Theoretical Physics, McGraw-Hill, New York (1953).
[43] HURWITZ, A., COURANT, R., Funktionentheorie, Springer-Verlag, Berlin (1922).
[44] TITCHMARSH, E.C., Theory of Functions, Oxford University Press (1939).
[45] LEJEUNE, A., Bull. Soc. roy. Sci. de Liège 35 (1966) 566.
[46] HUMBLET, J., LEJEUNE, A., Phys. Lett. 23 (1966) 561.
[47] LEJEUNE, A., Ph.D. Thesis (to be published in 1967).
[48] MAHAUX, C., Nucl. Phys. 79 (1966) 481.
[49] MAHAUX, C., ROBAYE, G., Nucl. Phys. 74 (1965) 161.
[50] LEBON, G., Mém. Soc. roy. Sci. de Liège, 5ème série, 13 4 (1966).
[51] LEBON, G., HUMBLET, J., Nucl. Phys. A 96 (1967) 593.
[52] HARRISON, W.D., Ph.D. Thesis, California Institute of Technology (1966); Nucl. Phys. A 92 (1967) 253, 260.

CHAPTER 8

NUCLEAR RESONANCE REACTIONS AND S-MATRIX ANALYTICITY

K. W. McVOY

1. INTRODUCTION

Although the complex poles and residues of the S-matrix provide a remarkably concise means of parametrizing scattering resonances, they are not a familiar ingredient of traditional nuclear reaction formalisms and have often been viewed as mathematical oddities, only tenuously connected with physical reality. The present review is an attempt to increase their familiarity by examining in non-mathematical terms their relations to a variety of physical scattering properties such as barrier penetrability, branching ratios, resonance circles, Levinson's Theorem, and bound states.

Elastic resonances are considered in sections 1—3, which include a discussion of overlapping resonances and the difference between their R-matrix and S-matrix widths (section 3.4.). Many-channel resonances are discussed in section 4. In this case the one-pole approximation to S, when made unitary, is found to include the Breit-Wigner approximation and to provide its generalization to the case of a non-elastic background. It agrees exactly with the form of the general R-matrix result ($R^\circ L^\circ$ unrestricted), but is parametrized in such a way as to be suitable for practical resonance curve fitting. The (unitary) two-pole expression for two overlapping resonances is given as well.

Multi-channel resonances are discussed in terms of the eigenchannels of S in Appendix B. It is found that the eigenphase-repulsion phenomenon normally forces them to occur in several eigenchannels at once.

Since the nucleon-nucleon force is short ranged, a fundamental characteristic of nuclear reactions is the fact that in the asymptotic wave zone, where the interaction between the scattered particles[1] is very small,

---

The author is in the Department of Physics, University of Wisconsin, Madison, Wis., United States of America.

[1] The discussion here is restricted, as usual, to two-body channels.

the wave function for their relative motion in the centre-of-mass system is simply a superposition of incoming and outgoing free-particle (or Coulomb) waves. Since the incoming flux is determined by experimental conditions, the influence of the interactions on the wave function in the asymptotic region, where the measurements are made, appears only in the relative amplitudes of the outgoing waves in the various open channels. These amplitudes are the elements of the S-matrix, and since the outgoing flux, and hence the cross-sections, are linear or quadratic functions of them, it is their energy dependence which directly determines the shapes of the scattering and reaction cross-sections as a function of energy.

The S-matrix elements, as complex-valued functions of the energy, are thus a natural meeting-ground for theory and experiment, and this review aims to provide a utilitarian compendium of their properties for the types of potentials employed in nuclear physics. An elegant mathematical treatment of the S-matrix for potential scattering problems is available in the work of Newton [1] and of Humblet and Rosenfeld [2], but a great deal more is known about the subject, of a practical, intuitive nature, and it is to this 'folklore' that attention is directed here, particularly that aspect involving the analytic continuation of S(E) into the complex E-plane and the use of its complex poles and zeros for the parametrization of resonance amplitudes.

Wigner's R-matrix has long provided a useful model for the computation of S-matrix elements for the case of a cutoff potential, which contains as free parameters the energies and reduced widths necessary to fit experimental resonance data. Unfortunately, in practical applications it has certain disadvantages, one being the occurrence of arbitrary and unphysical 'fitting radii', and another being the fact that the energy and width parameters, which produce one resonance curve in isolation, produce a totally different one if the resonance in question is overlapped by another. For the purpose of extracting resonance data from cross-sections, however, it is possible to bypass R altogether and parametrize the energy dependence of S itself directly in terms of the desired resonance energies and widths. For a variety of reasons set forth below, we feel that in many cases this may provide a more direct and less ambiguous means of obtaining experimental resonance parameters.

Several different resonance expansions of S are known, however, none without its disadvantages. It is an open question at the moment which of them will prove the most useful experimentally, a question likely to be answered only after a good deal of practical trial and error. It is hoped that a review of this kind may stimulate this programme by collecting in one place many of the necessary bits of practical S-matrix lore.

As for units and other conventions, we employ 'natural' units throughout, in which $\hbar = c = 1$, so that, for example, a resonance of width Γ has lifetime $1/\Gamma$. We shall deal, as usual, only with two-body channels and always work in the centre-of-mass system, so that m is the reduced mass of the two fragments in the channel at hand. Non-relativistic kinematics are presumed throughout, even when limits such as $k \to \pm \infty$ are considered. Since our primary concern is with the energy-dependence of S-matrix elements, we do not deal with the complications due to spin; they mainly affect the relation between S and the cross-sections, a subject dealt with in detail by Newton [3] and by Goldberger and Watson [4]. Thus although only spinless particles are considered in detail here, the concepts and

phenomena involved are equally applicable to particles with spin, at the price of the usual angular momentum algebra.

The lion's share of attention is devoted to the single-channel case; for a discussion of the general properties of S considered here it is quite general enough, the n-coupled channel situation being obtainable by a 'rotation' from a set of n uncoupled eigenchannels.

2. SINGLE-CHANNEL POTENTIAL SCATTERING OF SPINLESS PARTICLES

We consider two point particles interacting via a central potential $V(r)$ defined on the interval $(0, \infty)$, where $\vec{r}$ is their separation in the centre-of-mass system. Since we have nuclear applications in mind, we assume $V(r)$ to be 'reasonable' in that context, i.e. short-ranged and non-singular. This will often simply mean that its first two absolute moments exist,

$$\int_0^\infty r\,|V(r)|\,dr < \infty, \quad \int_0^\infty r^2|V(r)|\,dr < \infty \tag{2.1}$$

but in many cases the simplest analyticity properties of its S-matrix are obtainable only by accepting the additional restriction that $V(r)$ vanish as $r \to \infty$ faster than any exponential; a cutoff potential, $V(r) \equiv 0$, $r > a$, is one such example and a Gaussian potential is another.

Whenever $V(r)$ simply vanishes at ∞ faster than $1/r$, the asymptotic form of the scattering wave function is, to within a normalization constant,

$$\psi(\vec{r}; \vec{k}_0, \vec{k}) \to e^{i\vec{k}_0 \cdot \vec{r}} + f(\vec{k}_0, \vec{k})\,\frac{e^{ikr}}{r} \tag{2.2}$$

where the only angular dependence of the scattering amplitude $f(\vec{k}_0, \vec{k})$ in the central force case is on $\hat{k}_0 \cdot \hat{k}$. Its partial-wave expansion,

$$f(\vec{k}_0, \vec{k}) = \sum_\ell (2\ell+1)\left(\frac{S_\ell - 1}{2ik}\right) P_\ell(\hat{k}_0 \cdot \hat{k}) \tag{2.3}$$

defines the infinite set of constants (i.e., functions of ℓ and E but not of r) $S_\ell(E)$, the 'S-matrix elements' for the given potential, which in turn determine the scattering cross-section by

$$\frac{d\sigma}{d\Omega} = |f(\vec{k}_0, \vec{k})|^2 \tag{2.4}$$

It is these partial wave S-matrix elements $S_\ell(E)$ with which we shall be concerned; if the potential is not central or if further degrees of freedom are involved, they are labelled not by ℓ but by j and any further quantum numbers conserved by the interaction.

Alternatively, if ψ itself is expanded in Legendre functions of the direction of $\vec{r}$ (which is that of $\vec{k}$),

$$\psi(\vec{r}, \vec{k}_0, \vec{k}) = \sum_{\ell} \frac{u_\ell(r, k)}{r} P_\ell(\hat{r} \cdot \hat{k}_0) \tag{2.5}$$

the S_ℓ appear in its asymptotic form as the familiar coefficients of the outgoing wave,

$$u_\ell(r, k) \to A_\ell(e^{-ikr} - (-1)^\ell S_\ell(E)\, e^{ikr}) \tag{2.6}$$

In the limit of no potential at all $S_\ell \to 1$, for all ℓ, and there is no scattering. If the potential is elastic, i.e., neither absorbs nor emits flux, it is then clear from Eq. (2.6) that all S_ℓ must be unitary,

$$|S_\ell(E)| \equiv 1 \tag{2.7}$$

so that the asymptotic wave function in each partial wave is described by a single real parameter, the phase shift $\delta_\ell(E)$, which is most conveniently taken as half the phase of S_ℓ,

$$S_\ell(E) = e^{2i\delta_\ell(E)} \tag{2.8}$$

The asymptotic partial wave function then takes the simple and familiar form

$$u_\ell(r, k) \to -2i\, A_\ell\, e^{i(\delta_\ell - \pi/2)} \sin(kr - \ell\pi/2 + \delta_\ell) \tag{2.9}$$

which is responsible for the name 'phase shift'; a positive phase shift corresponds to the wave being 'pulled in' toward the origin (relative to an unscattered wave), and a negative δ_ℓ corresponds to the wave being 'pushed out'.

2.1. Phase shifts for simple representative potentials; high- and low-energy limits

As a guide to what functions $\delta_\ell(E)$ can be expected from a given potential, we recall a few elementary examples. In the high-energy limit the phase is given directly in terms of the potential by the short wavelength limit of the Born approximation,

$$\delta_\ell(E) \to -\frac{m}{k} \int_0^\infty V(r)\, dr + n\pi \tag{2.10}$$

(for all ℓ). δ_ℓ is clearly only defined by Eqs. (2.6) and (2.9) modulo π, and because of Levinson's theorem, which we discuss below, it is traditional and convenient to choose $n = 0$ in Eq. (2.10), so that $\delta_\ell(\infty) = 0$, and an attractive potential produces a positive phase shift and a repulsive one a negative

phase shift, at least at high energy. Of course the function $\delta(E)$ can change sign at one or more E-values (typically if V(r) changes sign), but if V(r) is predominantly attractive outside the centrifugal barrier $(r > (\ell(\ell+1))^{\frac{1}{2}}/k)$, where the free wave is oscillatory, it will decrease the local wavelength and pull the wave in, giving a positive phase shift at that value of k; the sign of V(r) is less important inside the barrier, where the incident wave is small.

As for the low-energy behaviour of $\delta_\ell(E)$, we recall that the barrier radius or classical turning point (for the non-interacting wave), $r = (\ell(\ell+1))^{\frac{1}{2}}/k$, increases with increasing ℓ and decreasing k and we can expect $\delta_\ell(E)$ to become small whenever ℓ becomes large enough or E becomes small enough so that this radius significantly exceeds the range of the potential – and thus prevents the incident wave from feeling it – provided, of course, that V(r) has a 'range'. In particular, V(r) must certainly fall off with increasing r more rapidly than $1/r^2$ if the long-range behaviour (which is all that the incident wave is sensitive to in the long wavelength limit) is to be dominated by the centrifugal potential $\ell(\ell+1)/2mr^2$. This centrifugal shielding is of course the origin of the familiar threshold behaviour,

$$\delta_\ell(E) \to a_\ell k^{2\ell+1} (\text{modulo } \pi) \text{ as } k \to 0 \tag{2.11}$$

which for a sufficiently weak potential follows directly from the Born approximation

$$\delta_\ell(E) \approx -2mk \int_0^\infty [j_\ell(kr)]^2 \, V(r) \, r^2 \, dr \tag{2.12}$$

by using the low-energy form of $j_\ell(kr)$, and is actually true in general; see, for example, Ref. [3].

Since $[\delta_\ell(k) - \delta_\ell(0)]$ vanishes at k = 0 like an odd power of k, it is necessarily an odd function of k near the origin and its analytic continuation to the negative k-axis is in fact odd for all k. Note also that since the angle-integrated partial wave cross-section is

$$\sigma_\ell(E) = \pi \lambda\!\!\!^{-2} (2\ell+1) \, 2[1 - \mathrm{Re}(S_\ell)] = 4\pi \lambda\!\!\!^{-2} (2\ell+1) \sin^2 \delta_\ell \tag{2.13}$$

Eq. (2.11) implies that

$$\sigma_\ell(E) \sim k^{4\ell} \tag{2.14}$$

at low energy, only the S-wave cross-section remaining finite as $k \to 0$.

A few examples may make these limits clearer. First we note from Eq. (2.9) that, even in the absence of a scatterer, different partial waves have different asymptotic forms, due, of course, to the different centrifugal potentials they experience; from Eq. (2.9) it is clear that the 'centrifugal phase shift' is simply $-\ell\pi/2$, so that a pure $1/r^2$ potential has an energy-independent phase shift. Of course, if it were A/r^2 only for $r > R$, and finite for $r < R$, it would have essentially the same effect on any wave with $E \ll A/R^2$, and the phase would vanish like 1/k as $k \to \infty$, so the potential of Fig. 1(a) produces the phase shift of Fig. 1(b); the constant section of the phase shift has different values for different ℓ's.

Conversely, a $1/r^2$ potential cutoff 'the other way' will show hard-sphere behaviour at low energy, where it presents a thick barrier to the incident wave, which goes over into a constant phase shift at high energy, giving the correlation shown in Figs. 1(c) and 1(d), for $\ell = 0$. This phase does not vanish as $E \to \infty$, and indeed Levinson's theorem is violated by a $1/r^2$ singularity.

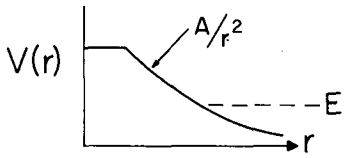

FIG. 1(a) Potential $V = A/r^2$ for $r > R$

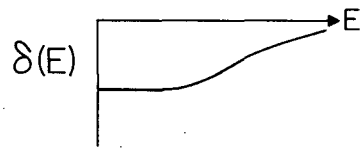

FIG. 1(b) Phase shift $\delta(E)$ corresponding to A/r^2

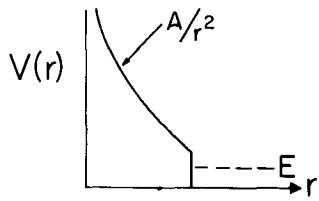

FIG. 1(c) Potential A/r^2 with a cut-off

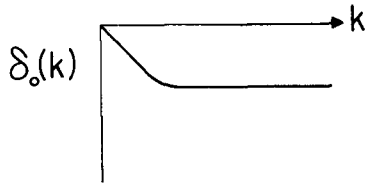

FIG. 1(d) Phase shift corresponding to Fig. 1c

Finally we recall the hard-sphere phase shifts themselves. If $V(r)$ is $+\infty$ for $r < a$ and zero for $r > a$, the free particle radial wave function

$$2j_\ell(kr) = h_\ell^-(kr) + h_\ell^+(kr)$$

is readily seen to become

$$h_\ell^-(kr) + S_\ell h_\ell^+(kr)$$

in the presence of the hard core, for $r > a$, so from the condition that it vanish at $r = a$, the S-matrix elements are

$$S_\ell(k) = -\frac{h_\ell^-(ka)}{h_\ell^+(ka)} = -\frac{[h_\ell^+(ka)]^*}{h_\ell^+(ka)} \quad \text{(hard core)} \tag{2.15}$$

In particular,

$$S_0(k) = e^{-2ika},$$

$$S_1(k) = -e^{-2ika}\left(\frac{ka - i}{ka + i}\right) \tag{2.15a}$$

and the phase shifts behave as indicated in Fig.2. Clearly the low-energy $k^{2\ell+1}$ behaviour is again due to the core being shielded by the centrifugal potential; for $ka \gg \ell$, the shielding is ineffective and the high-energy phase shift settles down to the S-wave value (modulo π) for all finite ℓ.

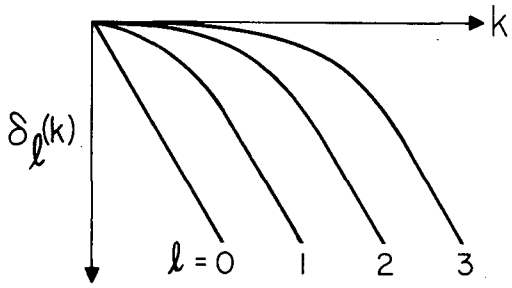

FIG.2. Phase shifts for a hard-sphere potential

It is interesting to note that these S-matrix elements, considered as analytic functions of the complex variable k, are in N(k)/D(k) form, with $N = D^*$ by unitarity and $D_\ell(k)$ having ℓ zeros ($S_\ell(k)$ having ℓ poles) in the lower half k-plane. They are clustered in the vicinity of the origin and have as their 'purpose' the generation of the polynomial which assures the $k^{2\ell+1}$ behaviour of $\delta(k)$ near the origin, but which $\to 1$ as k moves out of the pole region. For $|ka| \gg \ell$, $S_\ell(k)$ is dominated by its essential singularity at infinity, e^{-2ika} (a feature possessed, incidentally, by all cutoff potentials), which is how the mathematics represents the domination of reflection from the core at high energy. The resulting cross-section is oscillatory, $\sigma_\ell(E) \sim (\sin^2 ka)/k^2$, with infinitely many (low) maxima caused by the phase shift passing downward through $\pi/2$.

2.2. Wigner and Levinson theorems

The Wigner and Levinson theorems are two very important theorems on general properties of the function $\delta_\ell(k)$. The first [5] provides a physical interpretation of the first derivative of the function, $d\delta/dk$, and can be derived by a consideration of the incoming 'radial wave packet' which is the partial wave manifestation of a 'plane wave packet' passing by the point in question,

$$\varphi_\ell(r, t) = \int \rho_\ell(k)\, e^{-i(kr + \nu(k)t)}\, dk$$

If the momentum spectrum $\rho_\ell(k)$ is sharply peaked (and the result is valid only for this nearly-monochromatic case), ϕ will have its maximum where the phase of the exponential is stationary,

$$\frac{d}{dk}[kr + \nu(k)t] = 0$$

so the position of the centre of the packet is at

$$r_{max} = -\frac{d\nu}{dk}t$$

moving with group velocity $-d\nu/dk$. The corresponding scattered wave packet is

$$\psi_\ell(r,t) = \int \rho_\ell(k)\, e^{i[kr-\nu t + 2\delta_\ell(k)]}\, dk$$

whose maximum is at

$$r_{max} = \frac{d\nu}{dk}t - 2\frac{d\delta_\ell}{dk}$$

i.e. displaced from the maximum of a corresponding unscattered packet by the amount

$$\Delta r = -2\, d\delta/dk \qquad (2.16)$$

Equivalently, the scattered packet may be thought of as <u>delayed</u> in time by the amount

$$\text{Time delay} = +2\frac{d\delta}{dE} \qquad (2.17)$$

Thus a phase shift which increases as a function of energy indicates a time delay of the scattered packet, usually due to trapping in a resonant state at that energy, while a falling phase indicates a time advance. This may be due, as in the hard core example, to reflection from the 'surface' of the potential (an <u>unscattered</u> incoming wave must proceed all the way in to the origin before it reverses direction and comes out again), or it may simply be due to an attractive potential through which the wave proceeds at a higher velocity than in free space. If the potential is cut off at $r = a$, the maximum phase advance permitted by causality (the incoming wave cannot scatter before it reaches the potential) is $2a$, from which Wigner's theorem follows,

$$\frac{d\delta}{dk} \geq -a \qquad (2.18)$$

A repulsive barrier will normally force the phase downward as a function of energy, at energies below the top of the barrier (e.g. Fig. 1(d)), with

steeper negative slope, the more the wave is excluded from the interior of the barrier, and in the limit of complete exclusion (hard core), the phase decreases like -ka.

Actually, of course, the assumption of a sharply localized packet is only a short wavelength idealization, which is surely invalid if $\lambda \gtrsim a$; for the s-wave the more precise form of the limit is

$$\frac{d\delta_0}{dk} \geq -a + \frac{\sin 2\,(ka + \delta)}{2k} \tag{2.19}$$

which becomes Eq. (2.18) for $ka \gg 1$, but imposes no restriction for $ka \ll 1$, where $d\delta_0/dk$ is simply the negative of the scattering length. This can have an arbitrarily large negative value, but only if the potential has a bound state very near zero energy, in which case its 'radius', which is equal to the scattering length, plays the role of 'radius' for the potential if it exceeds the true radius a.

Levinson's theorem [6] might be thought of as the integral of Wigner's theorem, for it considers the total amount by which δ_ℓ decreases over the energy range from zero to infinity. Provided only that both the first and second absolute moments of V(r) exist, it states that

$$\delta(0) - \delta(\infty) = n\pi \tag{2.20}$$

where n is the number of bound states that the potential has.

A mathematical derivation is given below in terms of analytic properties of S(k), but we record here a heuristic argument due to C. J. Goebel. $S(\infty) = S(0) = 1$ if the moments exist, and we wish to observe the changes undergone by the wave function as the energy is changed from ∞ to zero; to simplify the argument as much as possible, we assume V(r) vanishes for $r > a$. At $E \to \infty$, $\lambda = 0$, and the entire r-axis is packed tight with such waves. At this energy the potential has no effect whatever, and $\delta = 0$, so the nodes of the actual wave function coincide with those of a free-particle function. As E is lowered and waves move out to $r \to \infty$, the nodes for the two functions begin to separate by an amount Δr, in particular in the asymptotic region, where the phase shift can be measured as $\delta = k\,\Delta r = 2\pi(\Delta r/\lambda)$. If, for instance, the potential is attractive, the interacting wave will be pulled in relative to the free wave, and whenever (as E decreases) a free node moves out past an interacting one, δ has increased by π. Finally, at $E = 0$, all the free-wave nodes have moved out to ∞, so $\delta(0) = n\pi$, where n is the number of nodes in the interacting wave function which remain at finite r in the zero-energy limit. However, a simple examination of the zero-energy function in terms of the scattering length shows n also to be the number of bound states.

We note that the theorem is violated by the hard core potential and by any potential which behaves like $1/r^2$ as $r \to 0$ or $r \to \infty$.

2.3. Elastic resonances. Elementary properties and simple examples

Because the Schrödinger equation for single-channel scattering is a wave equation (with the potential, possibly momentum-dependent, playing the role of refractive index), the resonances ('single-particle resonances')

which occur in potential scattering problems are identical, both mathematically and physically, with the standing-wave or cavity resonances familiar in wave guides, band-pass filters, Fabry-Perot interferometers and other examples of cavity resonators. That is, the essential mechanism is the establishment of a spatial cavity with a reflecting wall (typically a potential barrier), within which incident waves can be temporarily trapped. If the walls could be made completely reflecting, the 'resonant states' would actually be bound, with infinite lifetimes and sharp energies, and would occur only at those discrete energies at which their wavelengths are tuned to the cavity in such a way as to put nodes of the wave function at the walls. If the walls are highly, but not completely, reflecting, the Q of the cavity will be high but not infinite. The interior of the cavity will communicate weakly with the exterior at all energies, but only at those energies determined by the same nodal tuning condition as above (integral number of internal half wavelengths in the cavity) will successive sections of the incoming wave interfere constructively inside, to give a steady-state solution with a much larger amplitude inside the cavity than outside. The resonance energies will thus be discrete but not sharp, because of the finite lifetimes of the states.

In nuclear physics these single-particle resonances are customarily caused by a central potential, so they occur in one partial wave at a time (labelled by its quantum numbers), and are due to the internal reflection of the corresponding centrifugal or Coulomb barrier. This is shown in Fig. 3(a) which also indicates that the most striking feature of the resonance is the very large amplitude which the steady-state wave function develops

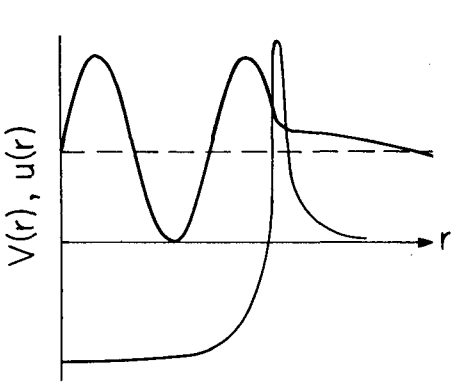

FIG. 3(a) Example of a resonance in a central potential

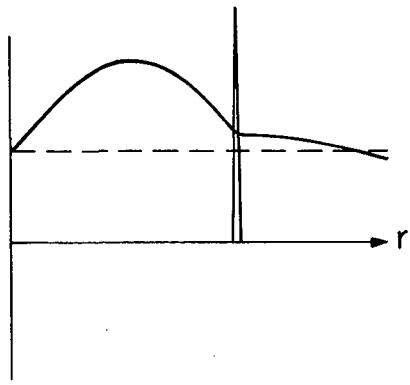

FIG. 3(b) An idealization of Fig. 3(a)

inside the barrier at each resonance energy. In customary scattering experiments, however, both this internal region and the trapping-time of an incident pulse (Fig. 3b) are inaccessible to measurement, and the resonance must be recognized from its effect on the energy dependence of the asymptotic wave function, i.e. on the phase shift. That it should cause a sharp rise in the phase shift as a function of energy follows in general from Wigner's interpretation of $d\delta/dE$, but it is also interesting to see how this phase rise (a 'pulling in' of the external wave function as the energy increases over the resonance) is correlated with the large internal amplitude.

It is most clearly seen for the case of a thin spherical shell of attractive potential [$V(r) = c\delta(r-a)$, $c < 0$], for which the $\ell = 0$ phase shift vanishes (see Ref. [7]) just below the resonance energy, due to the wave function having a node at $r = a$. The wave functions just below, at and just above a resonance are shown in Fig. 4, in which the external node indicated by an arrow is seen to be pulled in by nearly half a wavelength as the energy increases over the resonance width. Since $\delta = 0$ just below resonance in this case, the phase shift is +90° at the centre of the resonance, which causes a sharp maximum in the energy dependence of $\sin^2\delta$ and the partial wave cross-section. In general, however, the background phase is not zero; δ then increases through both $\pi/2$ and π, and the resonance is typically characterized by a sharp maximum and a zero of $\sigma_\ell(E)$ occurring near each other, of which only the maximum is generally visible experimentally. In any case it is the sharp rise of $\delta(E)$, not the 90° value, which signals the presence of the resonance.

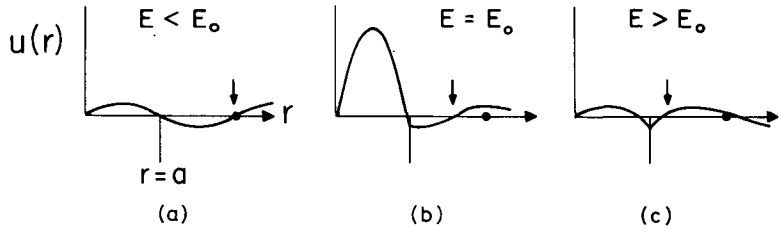

FIG. 4. An attractive potential $V(r) = c\,\delta(r-a)$ with the corresponding wave functions for (a) $E < E_0$; (b) $E = E_0$; (c) $E > E_0$

It is the shape of this phase rise, especially in the case of inelastic and overlapping resonances, which we wish to relate to the analytic properties of the function $\delta(E)$ (or equivalently $S(E)$) in the complex E-plane. By way of introduction we recall, without proof at the moment, the long-recognized fact that in the immediate vicinity of a resonance the energy dependence of $S_\ell(E)$ is very accurately reproduced by the simple rational function

$$S_\ell(E) = e^{2i\varphi}\left[1 - i\,\frac{\Gamma}{E-E_0+i\Gamma/2}\right] = e^{2i\varphi}\,\frac{E-E_0-i\Gamma/2}{E-E_0+i\Gamma/2} \tag{2.21}$$

the (manifestly unitary) Breit-Wigner approximation. $\varphi(E)$ is the constant or slowly-varying background phase, and, in the simplest version of the approximation, E_0 and Γ are constants, the position and width of the resonance. In the particular case $\varphi = 0$, Eq. (2.21) yields for the partial wave cross-section in the vicinity of the resonance the familiar expression

$$\sigma_\ell(E) = \pi\lambda\!\!\!^{-2}(2\ell+1)\,\frac{\Gamma^2}{(E-E_0)^2+\Gamma^2/4} \tag{2.22}$$

which indeed peaks at $E = E_0$(neglecting the slow energy variation of λ^2). If $\varphi \neq 0$, the algebra becomes more opaque and the cross-section shape more involved, but it is readily followed geometrically by recognizing that, as the energy passes over the resonance and δ_ℓ increases by π, $S_\ell(E)$ simply travels once counterclockwise around the unitary circle, starting and stopping at the background value, $S_\ell = e^{2i\varphi}$. Then recalling that only the real part of S_ℓ counts, since by Eq.(2.13)

$$\sigma_\ell(E) = \pi\lambda^2(2\ell+1)\,2(1 - \mathrm{Re}[S_\ell(E)]) \qquad (2.13)$$

cross-section curves such as those shown in Figs. 5 and 6 are direct consequences of the corresponding S-diagrams. In particular, $\sigma_\ell(E)$ has a maximum where $\mathrm{Re}\,S_\ell = -1$ and a zero where $\mathrm{Re}\,S_\ell = +1$; the centre of the resonance occurs halfway around the circle, which is at the maximum only if $\varphi = 0$.

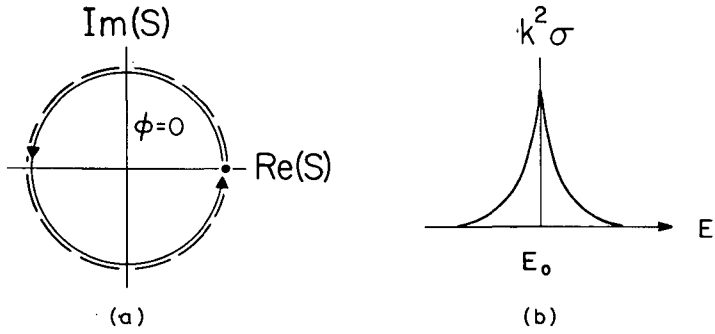

FIG. 5. (a) Imaginary part of the S-matrix versus its real part for $\varphi = 0$. (b) Cross-section in the vicinity of a resonance

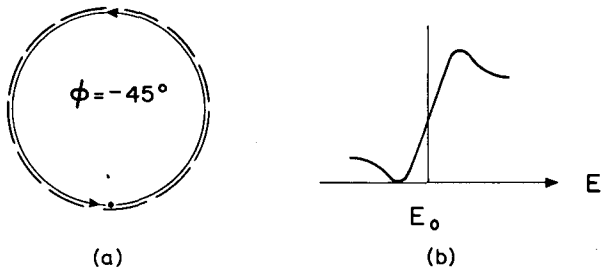

FIG. 6. (a) Imaginary part of the S-matrix versus its real part for $\varphi = 45°$. (b) Corresponding cross-section

The resonant factor in the Breit-Wigner expression for $S_\ell(E)$, Eq.(2.21), is immediately continuable into the complex E-plane, where its 'structure' consists of a pole at $E_R = E_0 - i\Gamma/2$ in the lower half plane and a zero at E_R^* in the upper half plane. The occurrence of poles and zeros in the complex frequency plane has long been familiar in the study of circuit and cavity resonances, and as far as is known it is completely general: every elastic

resonance of any physical system is believed to be characterized by a pole and zero of the response function, in its complex energy or wave-number plane. Completely non-analytic response functions could, of course, be imagined, but the customary mathematics of physical resonators has not produced them, and an overwhelming number of fits to experimental data stands behind the Breit-Wigner assumption.

Although we have introduced it in the context of time-independent solutions of the Schrödinger or wave equation, a familiar consideration of the time dependence of the scattering of a wave packet at a resonance energy lends further support to the reasonableness of the complex pole assumption. If the incident wave packet (in a single partial wave) has the energy spectrum $\rho(E)$, its time dependence (at a fixed radial position) is

$$\varphi(t) = \int \rho(E)\, e^{-iEt}\, dE$$

and the corresponding resonantly scattered packet is

$$\psi(t) = \int \rho(E)\, [S(E)-1]\, e^{-iEt}\, dE$$

$$\approx \int \rho(E) \left[e^{2i\varphi}\, \frac{E-E_R^*}{E-E_R} - 1 \right] e^{-iEt}\, dE$$

$$\approx C\, e^{-iE_R t}$$

doing the integral by contour integration in the lower half E-plane and retaining only the term giving the long-time dependence, which comes from the pole nearest the real axis. (This assumes $\rho(E)$ to be broader than the resonance width.) Thus the long-time dependence of the scattered packet at fixed r is

$$|\psi(t)|^2 = |C|^2\, e^{-\Gamma t} \qquad (2.23)$$

indicating the direct relation between the Breit-Wigner resonance pole and the exponential decay of the resonant state, with 'lifetime' $\tau = 1/\Gamma$.

Two elementary S-wave examples (Ref. [7]) which illustrate both resonances and the importance of the background on which they are superimposed are (1) the thin-walled spherical cavity like that of Fig. 4 (delta-function potential barrier, $V(r) = c\,\delta(r-a)$ with $c > 0$) and (2) the attractive square well.

The transmission coefficient of the delta function is energy-dependent and has the (monotonic increasing) form

$$T(k) = [1 + A/k^2a^2]^{-1} \qquad (2.24)$$

with $A = 400$ for the case illustrated in Fig. 7. If the barrier were completely impenetrable, the cavity would posses bound states with momenta $k_n a = n\pi$, so with nearly impenetrable walls it has resonances near these momenta, which cause the rapid increases in the phase shift indicated in Fig. 7(a); note that for this potential the phase shift vanishes identically at $ka = n\pi$, since the wave function has a node at the barrier in that case and so is not

scattered. Figure 7(b) shows how the ratio of internal to external wave amplitude increases sharply at these resonance energies, and Fig. 7(c) indicates the corresponding energy dependence of the S-wave cross-section.

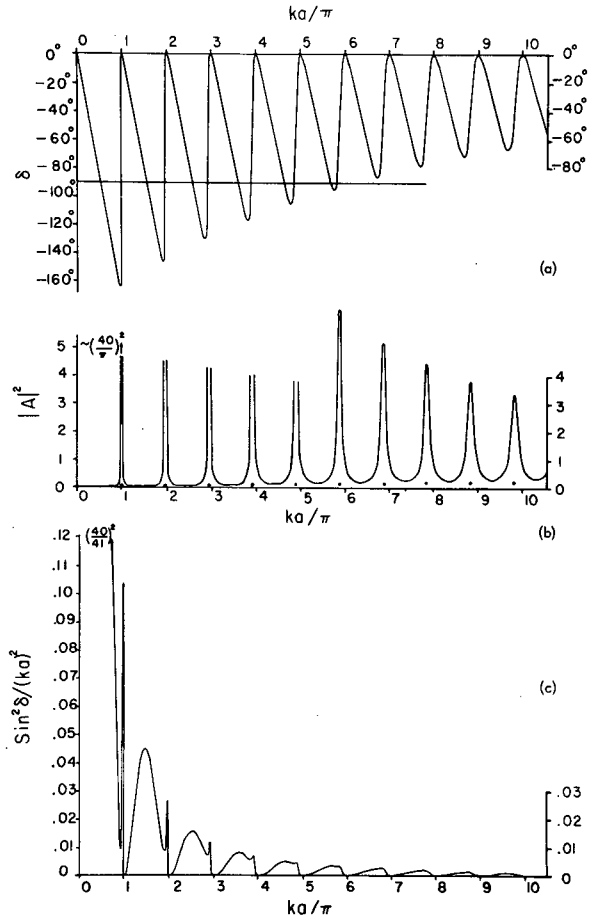

FIG. 7. Scattering characteristics of the δ-function potential $V(r) = c\,\delta(r-a)$. (a) Phase shift, (b) square of internal wave amplitude and (c) cross-section, all as functions of the bombarding momentum

At low energy, where the barrier is nearly impenetrable (from outside as well as inside), the phase shift is nearly the hard core result, decreasing at the Wigner limit, but interrupted by abrupt rises at the resonance energies Consequently the cross-section displays both the broad, non-resonant hard core maxima due to the phase passing downward through $-\pi/2$, as well as the sharp resonant maxima due to the abrupt phase rises.

At higher energies the barrier becomes leaky and the resonances broaden, so that the hard core component of the phase decreases by a significant amount across the resonance width. As a result, the net rise in the total phase shift becomes less than 180°, and if the resonance becomes

sufficiently broad it will even be less than 90°. The resonant and non-resonant maxima in the cross-section then merge into a single asymmetric bump, whose steep upper wing is the only remnant of the resonance. The resonances are still visible in the energy dependence of $|A|^2$ (Fig. 7(b)), which is not confused by background phase effects, but even these maxima begin to overlap significantly as the energy increases still further.

The lifetimes of the narrow resonances are readily found [7] to be given by

$$1/\Gamma = (2a/v_0)\,T^{-1} \tag{2.25}$$

i.e. longer than the free-particle transit time across the sphere by the factor T^{-1}, indicating how the resonances become broader and merge into the background as the barrier transmission increases. The relative positions of the complex zeros of S(k) in the ka-plane are indicated in Fig. 7(b); both they and the poles (at the complex conjugate positions) move farther off the real axis for the higher energy (overlapping) resonances until at very high energies, where the scattering vanishes, they are so far off into the k-plane that they produce no resonant effects at all on the real axis.

In the case of an attractive square well, the descending background phase (time advance) is due primarily to the higher group velocity of the wave packet inside the potential than outside. Because the potential has no surface barrier for $\ell = 0$, the resonances it superimposes on this background are very broad, as is implied by the familiar fact that the internal wave amplitude is less than or equal to the external amplitude at all energies. They are so broad, in fact, that the resonant state nearest zero energy produces a phase rise of only $\pi/2$ at most, and all higher energy states produce almost no phase rise at all! Explicit details can be found in Ref.[7] but the essential point is that a step-down potential of this sort is asymmetric and reflects more effectively on the outside than on the inside. If the well is deep enough to have several bound states, this produces a net downward trend of the phase shift as a function of energy (in agreement with Levinson's theorem), which is simply interrupted by small flat shoulders at the energies of the weak resonances. The relevant functions for a well with 25 bound states are indicated in Fig. 8(a), which shows the background phase to be so dominant that all the maxima seen in $\sin^2\delta$ and the cross-section as a function of energy are due to the phase passing downward through $\pi/2$, as in the hard core case. Fig. 8(b) describes the scattering by a repulsive square well.

2.4. Resonances and bound states

There is, of course, a very close connection between resonances and bound states, for a slight change in interaction can change one into the other. For instance, consider the case of the resonance shown in Fig. 3(a), whose energy is determined by the requirement that an integral number of internal half-wavelengths fits inside the well. If the well radius is increased slightly, this wavelength must increase, thus decreasing the internal kinetic energy of the particle. The resonance drops to a lower total energy, where it sees a thicker centrifugal barrier which traps it for a longer time and so decreases its width. As $E = 0$ is approached, the barrier

becomes infinitely thick, the resonance width decreases to zero and the resonance becomes a bound state – whose energy, of course, continues to decrease if the well radius is increased still further.

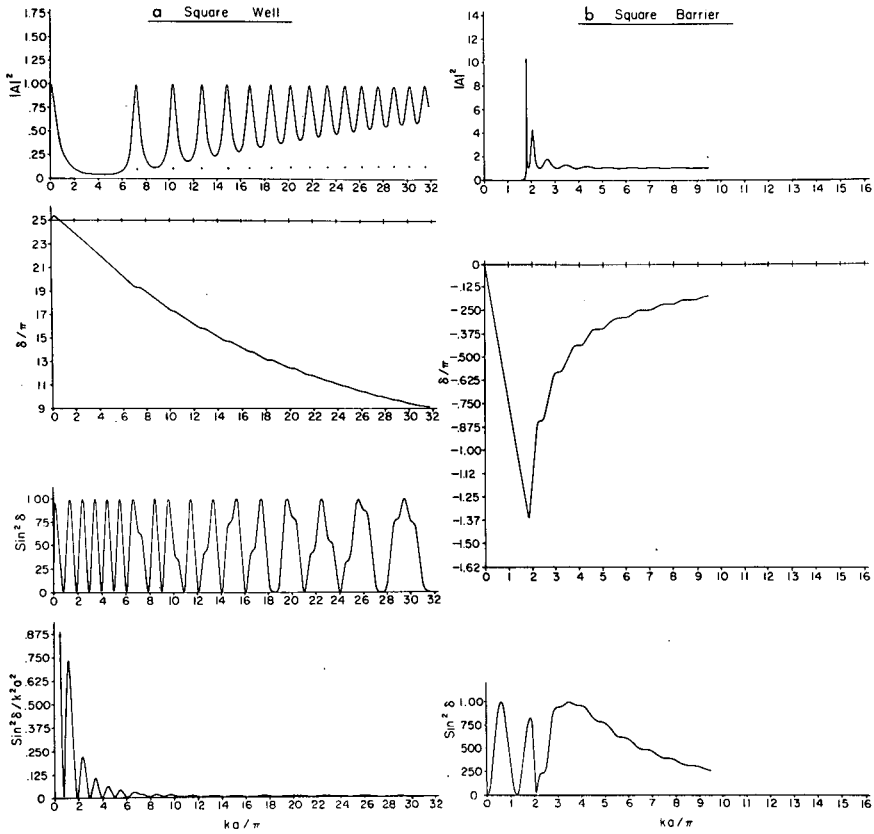

FIG. 8. $|A|^2$, δ/π, $\sin^2\delta$ for (a) a square well potential, (b) a square barrier

Stated in terms of the phase shift function $\delta_\ell(E)$, if the resonance is at an energy near the top of the barrier, it will be very broad; the background phase will decrease with energy nearly as fast as the resonant part of the phase increases, giving only a small net rise in the observed phase shift. Increasing the well size to get a lower-energy, narrower resonance produces a sharper, larger phase rise, and when the resonance is very near E = 0 the phase rises very rapidly with energy to nearly π. Finally, when the state binds, the phase may be thought of as starting at π and decreasing to zero at high energy in agreement with Levinson's theorem. This phase shift behaviour, as well as the resulting cross-sections, is shown in Fig. 9 for the p-wave in a Woods-Saxon well of depth 50 MeV and radius R = 1.25 $A^{\frac{1}{3}}$F.; the curves are labelled by the corresponding A-values. Although this example is a single-particle 'level', multi-particle or compound-nucleus levels respond in exactly the same way to a change in interaction strength.

On the other hand, a single-particle s-wave resonance for an uncharged particle in a Woods-Saxon type well has a very different behaviour for, as was noted earlier, in this case there is no surface barrier to provide efficient trapping of the internal wave. The resonances in such a well are not only very weak, they even, in effect, move to a negative energy (where

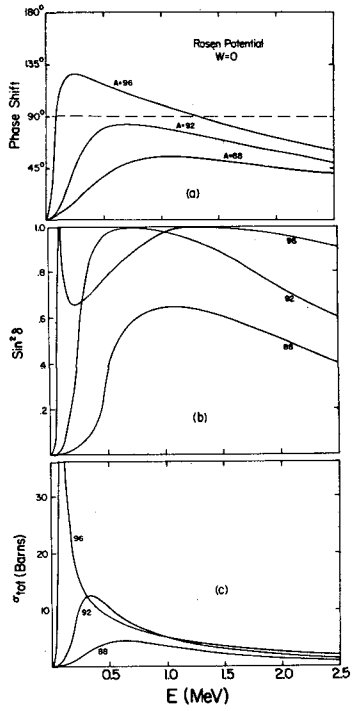

FIG. 9. Phase-shift behaviour and resulting cross-sections in a Woods-Saxon well of depth 50 MeV and radius $R = 1.25\ A^{\frac{1}{3}}$ F

they are called virtual states) with increasing interaction strength before becoming bound. For this reason only their 'tails' are seen in the phase-shift behaviour at positive energy, and in consequence $\delta_0(E)$ never rises by more than $\pi/2$ at any such resonance. The square well is an example of such a potential, whose phase-shift curves for a series of increasing well depths are shown schematically in Fig. 10. The lowest one is for a well just too weak to bind the 1s state, whose influence (as a virtual state) is seen in the sharp rise in the phase shift by $\pi/2$ at low energy (large negative scattering length). The influence of the 2s state, which was shown in Fig. 8(a) as simply a flat shoulder on the descending phase, is here magnified for clarity to indicate that it actually does produce a small but distinct maximum and minimum in $\delta(k)$).

In the next curve up, the 1s state is just bound, and produces the sharp drop in $\delta(E)$ (large positive scattering length) which was noted in connection with the low-energy form of Wigner's interpretation of $d\delta/dk$. The successive curves show how the scattering length (i.e. $-d\delta(0)/dk$)

decreases to zero and becomes negative as the potential is deepened further, and also indicate how the size of the 2s 'bump' in $\delta(E)$ progressively increases until it also attains a height of $\pi/2$ just before becoming bound.

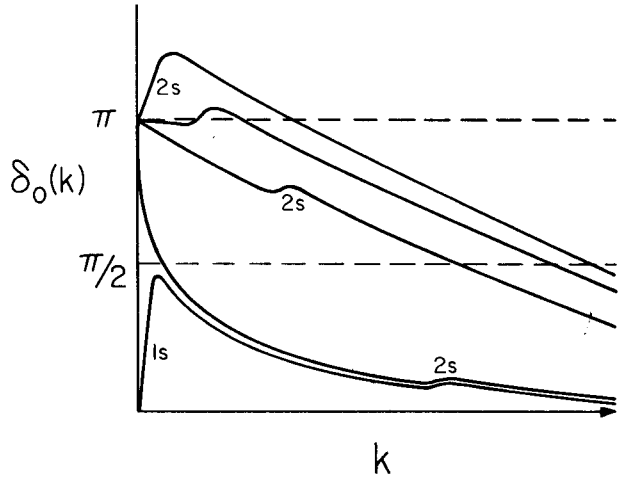

FIG.10. S-wave phase shift curves for a series of increasing well depths

It is rather remarkable that this steep rise in phase never causes a peak in the cross-section $\sigma_0(E)$. This is simply because at low energy the s-wave phase increases linearly in k, but sin δ increases slightly less rapidly than δ, so that $\sigma_0 = 4\pi(\sin^2\delta)/k^2$ in general decreases from its $k = 0$ value. This is seen more explicitly by including the k^3 contribution through the effective range expansion

$$k \cot \delta = -\frac{1}{a} + \frac{1}{2} r_0 k^2 \tag{2.26}$$

which gives

$$\sigma_0(E) = \frac{4\pi a^2}{1 + k^2a^2\left(1 - \frac{r_0}{a}\right) + \frac{1}{4} a^2 r_0^2 k^2} \tag{2.27}$$

This is a decreasing function of E near $E = 0$ unless $r_0 > a > 0$ or $r_0 < a < 0$ but this can only happen 'between' zero-energy bound states, whereas we are interested in the opposite case - $a \gg |r_0| \sim R$, very near a zero-energy bound state, to get a sharply rising phase shift. Consequently, these single-particle s-wave resonances are so weak that they never produce a maximum in $\sigma_0(E)$; any such maximum which occurs is of the hard-sphere type, caused by $\delta(E)$ decreasing through $\pi/2$.

Incidentally, in this context it is worth recalling that for the square well the scattering length is given in terms of the well parameters by

$$a = R - \frac{1}{K_0} \tan K_0 R \tag{2.28}$$

with $K_0^2 = 2mV_0$. This is a monotonic-decreasing function of V_0 with poles where $K_0R = (n+\frac{1}{2})\pi$ (the zero-energy bound-state conditions); for $K_0R \gg 1$ it is 'usually' positive, corresponding to $\delta'(k) < 0$ at $k = 0$.

3. ANALYTICITY PROPERTIES OF SINGLE-CHANNEL POTENTIAL SCATTERING AMPLITUDES

3.1. Jost functions and isolated poles of S(k)

From a practical point of view, any potential of interest in nuclear physics will provide phase shifts $\delta_\ell(E)$ sufficiently analytic in E so that their energy dependence in the neighbourhood of a resonance can be adequately represented by a one-pole or Breit-Wigner approximation. This is a 'local' property of the function $\delta_\ell(E)$ in the complex E-plane, which is simple enough to require no further mathematical background. In addition, however, it is important to know something about the distribution of poles in the energy plane, particularly their symmetry about $E = 0$ (which is related to the threshold energy dependence of δ_ℓ) and their asymptotic distribution for $|E| \to \infty$ (which determines the high-energy behaviour of δ_ℓ). These more detailed properties are thoroughly understood only for sufficiently well-behaved potentials, and are obtained most directly from the mathematical properties of the so-called Jost functions, which we summarize briefly in this section.

The radial Schrödinger equation in the ℓ-th partial wave for a spherically-symmetric potential is

$$-u''(r) + \left[\frac{\ell(\ell+1)}{r^2} + 2mV(r)\right]u(r) = k^2 u(r) \tag{3.1}$$

the physical scattering solution of which vanishes like $r^{\ell+1}$ at the origin; if it is normalized so that $\int_0^\infty u^*(k', r)\,u(k, r) = \delta(E - E')$, it has the asymptotic behaviour

$$u(k, r) \to \frac{1}{2} e^{i(\ell+1)\pi/2}\left(e^{-ikr} - (-1)^\ell S_\ell(k) e^{ikr}\right) \tag{3.2}$$

Equation (3.1) and its solution u(k, r) depend on the parameter k, and for some potentials V(r) may make sense for complex as well as real values of this parameter, thereby permitting us to continue analytically the solution u(k, r) and hence its S-matrix element $S_\ell(k)$ into the complex k-plane. (For instance $V(r) \equiv 0$ is such a case, for the solutions $k^\ell h_\ell^\pm(kr)$ exist and are analytic in k everywhere in the k-plane.) The region of analyticity of $S_\ell(k)$ permitted by a given potential is obtained most readily by considering another solution $\varphi(k, r)$ of the differential equation, regular at the origin and therefore proportional to u(k, r), but normalized by the different condition

$$\lim_{r \to 0} r^{-\ell-1}\varphi(k, r) = 1 \tag{3.3}$$

The importance of this type of normalization is that it is independent of k, for this permits us to use a celebrated theorem due to Poincaré (see Newton [1]) which states that if the parameter k appears in the differential equation only as an entire function (such as k^2), then any solution such as $\varphi(k, r)$, which is specified by a k-independent boundary condition, will itself be an entire function of k, i.e. analytic in the entire k-plane.

Secondly, because both the differential equation and the boundary condition are invariant under $k \to -k$ (i.e. the energy is an even function of k), and φ is uniquely specified by them, φ must be even in k,

$$\varphi(-k, r) = \varphi(k, r) \tag{3.4}$$

And finally, if the potential is real (i.e. neither absorptive nor emissive in the optical model sense), then for real k the equation and the boundary condition are invariant under complex conjugation and so define a real solution, $\varphi^*(k, r) = \varphi(k, r)$ for k and r real. If φ has a region of analyticity along the real k-axis, the continuation of this condition is clearly

$$\varphi^*(k^*, r) = \varphi(k, r) \tag{3.5}$$

Physically, this expresses the conservation of probability current and directly implies the unitarity of $S_\ell(k)$.

$\varphi(k, r)$ is regular at $r = 0$ but, in general, has both incoming and outgoing waves in the asymptotic region. These irregular, running-wave solutions we define by the necessarily k-dependent boundary conditions

$$\lim_{r \to \infty} e^{\mp ikr} f_\pm(k, r) = 1 \tag{3.6}$$

Although they are linearly independent, they are closely related, for they clearly satisfy

$$f_-(k, r) = f_+(-k, r) \tag{3.7a}$$

and (if V(r) is real)

$$f_-^*(k^*, r) = f_+(k, r) \tag{3.7b}$$

both equations holding in whatever corresponding analyticity domains the functions possess. Their singularities in the k-plane depend critically on the long-range behaviour of V(r); Newton [1] finds explicitly that if

$$\int_0^\infty r\,|V(r)|\,e^{pr}\,dr < \infty \tag{3.8}$$

then $f_+(k, r)$ has no singularities in the entire upper half of the k-plane specified by $\mathrm{Im}\ k > -p/2$ (and f_- has none for $\mathrm{Im}\ k \leq p/2$). That is, the more rapidly V(r) vanishes as $r \to \infty$, the farther from the real k-axis are the singularities of $f_\pm(k, r)$. For instance, two familiar examples are the

Yukawa potential $V(r) = e^{-\mu r}/r$ which produces logarithmic branch points at $k = \mp i\mu/2$, and any non-singular potential which vanishes beyond a fixed radius, whose $f_\pm$ are entire functions of k.

Since $f_\pm(k, r)$ are linearly independent, any other solution of the equation such as $\varphi(k, r)$ is a linear combination of them, and we choose to define the expansion coefficients $f_\ell^\pm(k)$ such that

$$\varphi(k, r) = \frac{i}{2k^{\ell+1}}\left\{e^{i\ell\pi/2} f_\ell^+(k) f_-(k, r) - e^{-i\ell\pi/2} f^-(k) f_+(k, r)\right\} \tag{3.9}$$

These expansion coefficients have the following simple and important properties: from Eqs.(3.5) and (3.7b),

$$[f_\ell^+(k^*)]^* = f_\ell^-(k) \qquad \text{(unitarity)} \tag{3.10}$$

if V(r) is real, and from Eqs.(3.4) and (3.7a),

$$f_\ell^+(-k) = f_\ell^-(k) \tag{3.11}$$

so within the analyticity domain where these relations hold, we are really dealing with only one function of the momentum,

$$f_\ell(k) \equiv f_\ell^+(k) \tag{3.12}$$

which is known as the Jost function.

Since $\varphi(k, r)$ is everywhere analytic in k, Eq.(3.9) shows the domain of analyticity of $f_\ell(k)$ to be exactly that of $f_+(k, r)$, at least the upper half of the k-plane for 'reasonable' potentials, with a lower boundary determined by the tail of the potential. In particular, for a cutoff potential ($V(r) \equiv 0$ for $r > R$), $f_\pm(k, r) = h_\ell^\pm(k, r)$ in this region, so f(k) is clearly an entire function of k.

The significance of the Jost function in scattering theory is seen at once from the asymptotic form of Eq.(3.9),

$$\begin{aligned}\varphi(k, r) &= \frac{e^{i(\ell+1)\pi/2} f_\ell^+(k)}{2k^{\ell+1}}\left\{f_-(k, r) - (-1)^\ell \frac{f_\ell^-(k)}{f_\ell(k)} f_+(k, r)\right\} \\ &\to \frac{e^{i(\ell+1)\pi/2} f_\ell^+(k)}{2k^{\ell+1}}\left\{e^{-ikr} - (-1)^\ell \frac{f_\ell^-(k)}{f_\ell^+(k)} e^{ikr}\right\}\end{aligned} \tag{3.13}$$

from which we have the relation of φ to the physical wave function,

$$u(k, r) = \frac{k^{\ell+1}}{f_\ell(k)} \varphi(k, r) \tag{3.14}$$

and the more important result that the S-matrix element is given in terms of the Jost function by

$$S_\ell(k) = \frac{f_\ell^-(k)}{f_\ell^+(k)} = \frac{f_\ell(-k)}{f(k)} \tag{3.15}$$

valid throughout the appropriate analyticity domain of $f_\ell(k)$ in the k-plane (which in particular certainly includes the real axis for any potential of interest in nuclear physics). Within this domain, Eqs.(3.10) and (3.11) guarantee the essential symmetry properties of S,

$$S^*(k^*)\,S(k) = 1 \qquad \text{(continued unitarity)} \tag{3.16}$$

and

$$S(-k)\,S(k) = 1 \tag{3.17}$$

which, together, of course imply

$$S^*(-k^*) = S(k) \tag{3.18}$$

We note that Eq.(3.16) is a 'local' property, relating the values of S at two nearby points in the k-plane, if k is near the real axis, and Eq.(3.18) is local near the imaginary axis, but Eq.(3.17) is very non-local except near the single point k = 0. Finally, since unitarity Eq.(3.10) guarantees that $f_\ell^+(k)$ and $f_\ell^-(k)$ have equal and opposite phases for real k, we see from Eq.(3.15) that, on the real k axis, the phase of $f_\ell(-k)$ is the scattering phase shift:

$$f_\ell(-k) = e^{i\delta(k)}\,|f_\ell(k)| \qquad \text{(for real k)} \tag{3.19}$$

The most interesting features of an analytic function are its singular points, and from Eq.(3.15) the singularities of $S_\ell(k)$ in the complex k-plane can be of two kinds:

(1) Poles, branch points and essential singularities caused by these singularities in $f_\ell(-k)$.

(2) Poles caused by zeros of $f_\ell(k)$.

Branch points seem to be a general characteristic of 'realistic' potentials, such as the Yukawa potential mentioned above (which has, in fact, an infinite number of them, at $\pm\, i n\mu/2$). The shorter the range of the potentials, the farther they recede from the real k-axis and, in the limit of a potential cut off completely beyond $r = R$,[2] they are replaced by an essential singularity of the e^{-2ikR} type which is caused physically by reflections from the non-analytic termination of the potential at r = R. Both these kinds of singularities have as their 'purpose' the generation of the 'background' part of the phase shift $\delta_\ell(k)$, which decreases as k proceeds along the real axis,

---

[2] Incidentally, this is a completely non-uniform limit, in the sense that a Yukawa potential, say, cut off at r=R, has an S-matrix element $S_\ell(k;R)$ which in the limit $R\to\infty$ is not that for a true Yukawa potential except within the 'stable zone' $|\mathrm{Im}\ k| < \mu/2$ along the real k-axis.

for all the poles of $S_\ell(k)$ due to zeros of $f_\ell(k)$ (except the bound states) contribute only a rising component to the phase shift. Taking the branch points seriously inevitably leads one into a consideration of integrals along the corresponding cuts, and thence into the elaborate mathematics of dispersion relations. In many contexts this indeed appears unavoidable because of the important dynamical role played by the cuts, but in the low-energy nuclear physics situation, where static potential interactions seem entirely adequate, the branch points are far from the real axis and so exert only a weak influence on the energy dependence of the phase shifts. For the purpose of parametrizing the background part of the phase shift along the real k-axis, the 'hard-sphere' factor e^{-2ikR} seems by far the simplest to use, so for the most part we shall employ it and thus confine our dicussion to the case of cutoff potentials. In this case $f_\ell(k)$ is an entire function, so $S_\ell(k)$ is meromorphic.

Although $f_\ell(-k)$ can have poles (far from the real axis) for certain potentials (e.g. the 'redundant poles' of the exponential potential $\exp-\mu r$, at the same positions on the imaginary axis as the Yukawa branch points), by far the most important singularities of $S_\ell(k)$ (and its only singularities in the case of a cutoff potential) are those caused by zeros of $f_\ell(k)$. These occur at discrete points, infinite in number for a cutoff potential, which in a sense form the most natural 'spectrum' of the Hamiltonian of the problem. This is because, according to the expansion (3.9), they are the points in the complex k-plane at which the solution $\varphi(k, r)$, which is regular at the origin, contains no incoming wave component – i.e. they are the (discrete) eigenvalues k_n determined by the two boundary conditions that the eigenfunction vanish at $r = 0$ and behave like $\exp+ik_n r$ as $r \to \infty$. Because one boundary condition is complex, the operator is non-hermitian and the eigenvalues complex, and because the boundary condition depends on the eigenvalue, the corresponding 'pole-eigenfunctions' are in general not orthogonal; most of them, in fact, are not even normalizable in terms of the customary inner product.

If k_n is positive imaginary, $k_n = i\lambda$, then $\exp ik_n r = \exp-\lambda r$ and the eigenfunction is a bound state of the potential, with real energy $E_n = -\lambda^2/2m$. Thus the bound states are included in the 'spectrum' of eigenvalues k_n, and they have the additional distinction of being its only points which occur in the upper half of the k-plane (for a real potential). This is readily seen by forming the Wronskian of an eigenfunction u_n with its conjugate, which for a real potential is

$$-\frac{d}{dr}(u_n^* u_n' - u_n'^* u_n) = (k_n^2 - k_n^{2*}) |u_n|^2$$

If $\mathrm{Im}\, k_n > 0$, the functions vanish at $r \to \infty$ as well as at $r = 0$, so

$$[\mathrm{Im}\,(k_n^2)] \int_0^\infty |u_n|^2 \, dr = 0,$$

and $\mathrm{Im}\,(k_n^2) = 0$. But by assumption k_n is not pure real, hence in the upper half plane it is necessarily pure imaginary. In addition, no k_n can occur on the real axis (except at $k = 0$), for it it did both f^+ and f^-, and so φ, would

vanish there, contrary to Eq.(3.3), hence the important result: poles of S can cross the real k-axis only at k = 0, and as a pole crosses into the upper half plane, a zero crosses into the lower.

In the lower half of the k-plane the poles of $S_\ell(k)$ are unrestricted, but the symmetry properties (3.16) – (3.18) ensure that poles and zeros of S occur in an interesting pattern, namely, a pole of S at k_n is necessarily accompanied by another at $-k_n^*$, and by zeros in the upper half plane at the conjugates of these two points (Fig. 11). A pole on the imaginary axis is accompanied only by the conjugate zero. It is the conjugate zero, equidistant from the real axis, which prevents S from violating the unitarity condition $|S|^2 = 1$ on the real axis when a pole occurs nearby (e.g. 1 and 2 of Fig. 11).

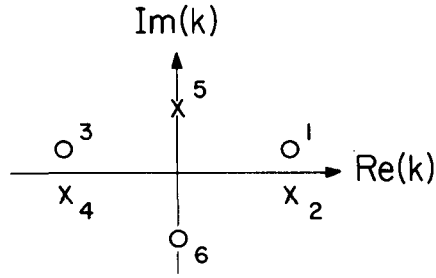

FIG. 11. Poles of $S_\ell(k)$ in the k-plane

The physical importance of these pole-zero pairs lies, as was indicated in section II, in their close relation to resonances, for if such a conjugate pair lies 'close' to the real axis, it necessarily contributes a rapidly-rising component to the phase shift $\delta_\ell(E)$ along the region of the real axis which passes 'through' the pair. The relation of the pole to a physical resonance is also emphasized by the fact that k_n is exactly the complex momentum a solution must have if it is to be both regular at r = 0 and a pure 'decaying state', i.e. have only an outgoing wave component, exp+ikr, in the asymptotic region. Finally and more physically, from Eq.(3.14) and the normalization condition on u(k, r), the corresponding condition for $\varphi(k, r)$ is

$$\int_0^\infty \varphi(k', r)\,\varphi(k, r)\,dr = |f_\ell(k)|^2 k^{-2(\ell+1)}\,\delta(E-E') \qquad (3.20)$$

which shows that the 'normalization constant' becomes very small at a real momentum k close to a zero of $f_\ell(k)$ [pole of $S_\ell(k)$]. However, the magnitude of the leading term in the small-r expansion of φ is fixed by its energy-independent boundary condition (3.3), which in essence fixes the amplitude of φ inside the potential region at the same value for all energies. Consequently, the small normalization constant near a resonance must indicate a decreased amplitude of the wave function in the external region: although both u(k, r) and $\varphi(k, r)$ are continuum functions which oscillate at large r, they do their best to look like bound-state wave functions near a resonance energy, by making their internal amplitudes much greater than the external ones if a zero of the Jost function is nearby.

Before considering the effects of these poles on the phase shift in more detail, it is well to recall that because the asymptotic functions $f_{\pm}(k, r)$ depend in an essential way on k rather than on k^2, we were led automatically to consider S_ℓ as a function of k rather than of E. Of course, $S_\ell(k) = S_\ell[k(E)]$ is a function of E if it is a function of k, but because $k = (2mE)^{\frac{1}{2}}$ has a square root branch point at E = 0 ('threshold'), $S_\ell(E)$ does also. By $S_\ell(E)$ and $S_\ell(k)$ we shall mean two different functions distinguished by their arguments, which have equal values at corresponding values of their arguments. However, because $E = k^2/2m$ is the same for $\pm k$, we must as usual introduce for $S_\ell(E)$ a branch cut and two sheets of the Riemann energy-surface to correspond to the single sheet of the k-plane. Traditionally, the cut (usually called the physical cut, to distinguish it from cuts associated with branch points on the imaginary k-axis of the type noted above for the Yukawa potential) is taken from E = 0 to $E \to +\infty$ along the

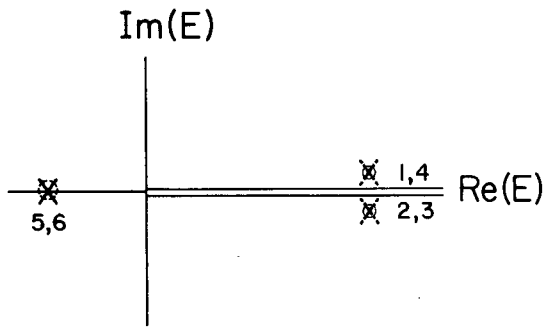

FIG. 12. E-plane corresponding to the k-plane of Fig. 11

positive real axis, so that the upper half of the k-plane is mapped onto the first E-sheet (called the 'physical sheet') and the lower half onto the second E-sheet. Thus a resonance pole-zero pair which straddles the positive real k-axis is also found at E_p and $E_z = E_p^*$ in E, but on opposite sides of the cut, with the zero on the physical sheet and the pole near to it on the second sheet, reached from the zero by passing directly through the cut (rather than by passing around the branch point). Since a pole at k_p always implies a zero at $-k_p$ and hence at the same position in E, but on the other sheet, the E-plane picture corresponding to the k-plane of Fig. 11 is shown in Fig. 12, in which both the zeros just above the real k-axis are on the physical E-sheet (the one reached from the other by a path passing around the branch point) and their poles are at these same E-positions, but on the second sheet. The upper half of the imaginary k-axis is the negative E-axis (bound states) of the physical E-sheet and the lower imaginary k-axis is the negative E-axis on the second E-sheet; consequently, the bound-state pole and zero are also 'on top' of one another in E. The crucial point is that any point near the positive real k-axis (the physical scattering region) is also near the upper rim of the cut along the positive real energy axis, whichever E-sheet it is on; a pole-zero pair which causes a resonance at positive real k also, of course, produces it at positive real E.

Incidentally, it is worth noting that the symmetry property (3.18), $S^*(-k^*) = S(k)$, which relates the values of S at two points on the same E-sheet [same Im (k)], in energy becomes

$$S^*(E^*) = S(E) \tag{3.18a}$$

i.e. S is a real analytic function of E. If Re (E) > 0, Eq. (3.18a) relates its values on the same sheet on opposite sides of the cut and, as E moves onto the cut, gives the discontinuity across the cut as 2 Im [S(E)]. If E is real and negative, on the other hand (i.e. below the threshold branch point), Eq. (3.18a) ensures that S(E) is real (and hence $\delta(E)$ is pure imaginary) on each E-sheet. Consequently, the residue of S(E) at any bound state pole must be real, and that of S(k) (which is on the imaginary k-axis) must be pure imaginary.

To see explicitly how such pairs affect the phase shift, the simplest 'local' (and unitary) approximation to $S_\ell(k)$, valid near a pole at $k = k_n$ and its conjugate zero at k_n^*, is $S_\ell(k) = S_\ell^B(k)\, S_\ell^{(n)}(k)$, where S_ℓ^B is the slowly varying 'background' part of S, and

$$S_\ell^{(n)}(k) = \frac{k_n^* - k}{k_n - k} \tag{3.21}$$

the 'Breit-Wigner' or one-pole approximation in the k-plane. Since the resonant part δ_n of the scattering phase shift is half the phase of this complex function, it is given (within the narrow energy range $|k - \mathrm{Re}\,(k_n)| \lesssim |\mathrm{Im}\,(k_n)|$ indicated by the dashed curve) by the simple geometrical construction of Fig. 13, which shows how $\delta_n(k)$ increases rapidly by about π as k passes through the narrow 'gate' formed by the pole and zero of the resonance.

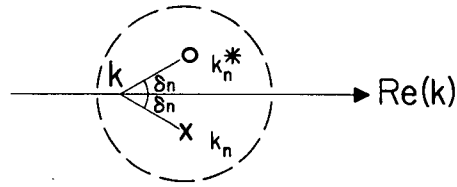

FIG. 13. Geometrical construction showing $\delta_n(k)$ as a function of k

It should be pointed out that, although all forms of the 1-pole approximation must, of course, have the same pole, there is no 'best' numerator function and different ones are employed for different purposes. Ours was chosen to satisfy unitarity (so the resonant phase shift δ_n is real) and to exhibit directly the role played in its energy dependence by both the pole and the zero. Its main defect is in its failure to satisfy the condition $S^{(n)}(-k) = 1/S^{(n)}(k)$, important near $k = 0$, which is reflected in the fact that $\delta_n(0)$ is not zero. If the k-range covered by the resonance includes the origin, $\mathrm{Im}\,(k_n) \sim \mathrm{Re}\,(k_n)$, this becomes a serious defect. We discuss below a variety of ways of rectifying it, the simplest of which is to include

the left-hand pole-zero pair of Fig. 11 as a second factor (note that this cannot be done in the E-plane), to give

$$S_\ell^{(n)} = e^{2i(\delta_n^r + \delta_n^\ell)} = \left(\frac{k_n^* - k}{k_n - k}\right)\left(\frac{-k_n - k}{-k_n^* - k}\right) \tag{3.22}$$

The second factor is seen from Fig. 14 to have a negative phase, which is the (-k) image of $\delta_n^r(k)$, so that only its 'tail' extends to positive energies, but with just a large enough amplitude to allow the two to cancel one another at k = 0. However, the resulting total phase shift is given in terms of the pole parameters by

$$\tan \delta_n = \frac{-2\,k\,\mathrm{Im}\,(k_n)}{|k_n|^2 - k^2} \tag{3.23}$$

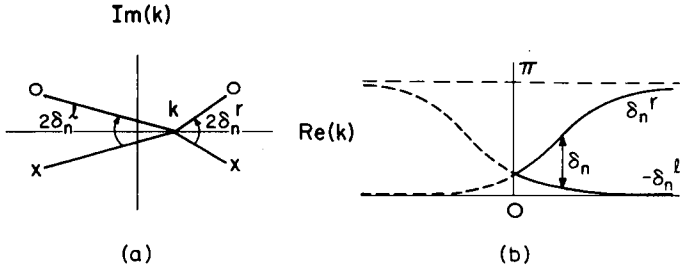

FIG. 14. (a) Poles and zeros of Eq. (3.22). (b) The corresponding phases $\delta_n^r(k)$ and $\delta_n^\ell(k)$

which, although it does vanish at k = 0, does so linearly in k. Hence this 2-pole approximation may suffice for s-waves, but is clearly not adequate for higher partial waves if it is to be believed near threshold.

A pole-zero pair on the imaginary k-axis has a significantly different effect on the phase shift, for threshold then stands exactly in the middle of their 'gate', the influence of which on δ is in a sense reduced by half. In this case it is convenient to choose $\delta_n = 0$ at k = 0, in which case the 1-pole approximation to S (k), when the pole is on the lower imaginary axis at $k = -i\beta$, becomes

$$e^{2i\delta_n} = \frac{1 + i \tan \delta_n}{1 - i \tan \delta_n} = \frac{i\beta_n - k}{i\beta_n + k} \tag{3.24}$$

or

$$\tan \delta_n = k/\beta_n \tag{3.25}$$

Consequently, the contribution of a pole-zero pair of this type to δ (k) is a phase-rise of only π/2, as indicated in Fig. 15, half of which is accomplished between k = 0 and $k = \beta_n$; it is most appropriately thought of as the second

or upper half of a curve like $\delta_n^r(k)$ of Fig. 14 (b). Incidentally it is interesting to note from Eq. (2.26) that Eq. (3.25) is the scattering length or zero-effective-range approximation, giving a $\delta_n(k)$ which vanishes linearly in k at the origin. As an approximation to $\delta(k)$ itself, it can only be valid for s-waves, and then only at very low energy, but as a component of the net energy dependence of the phase shift, it does correctly (at any energy and for any ℓ) describe the contribution of a pole on the negative imaginary axis.

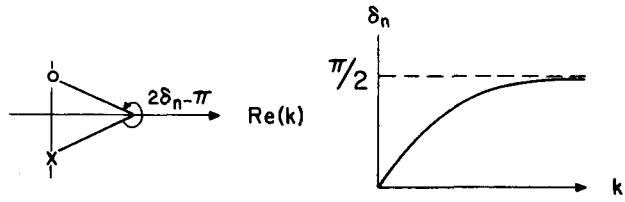

FIG. 15. The phase shift produced by a 'virtual state' pole

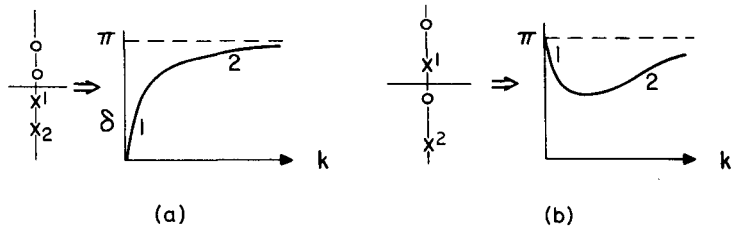

FIG. 16. (a) Phase shift produced by two 'virtual state' poles. (b) Phase shift produced by one virtual and one bound state pole

Similarly, putting the pole at $+ i\beta_n$ we see that a bound state of the system contributes a net decrease of $\pi/2$ to the phase shift, half of it again occurring for $0 < k < \beta_n$, which in terms of the binding energy B of the state is $0 < k < (2\,m\,B)^{\frac{1}{2}}$; a very weakly bound (s-wave) state causes the phase to decrease rapidly by $\pi/2$ very near threshold, whereas a deeply-bound state (any ℓ) spreads its $\pi/2$ over a large energy range. Since bound states are the only upper-plane poles, they are the only ones which can make a negative contribution to the energy-derivative of the phase shift, $d\delta/dE$.

Incidentally, the shift from a phase increase of $\pi/2$ to a phase decrease of $\pi/2$ as a pole moves from the lower half to the upper half of the imaginary k-axis is an alternative statement of Levinson's theorem, for, as we found above, a resonance can become a bound state only by moving from the lower half plane through the origin and onto the upper imaginary axis, and it necessarily contributes a net phase-decrease of π by so doing.

As will become clear from examples given below, poles on the imaginary k-axis almost always occur in pairs, either with both poles below the origin (this happens only for s-waves) or one above and one below. Their phase shift contributions are additive and produce results of the kind indicated in Fig. 16 for $\delta^{(1)}(k) + \delta^{(2)}(k)$, the rapid rise or fall at low k being due to the pole nearest the origin and the slower rise at higher energy coming from the further pole, which we have put in the lower half

plane, as is the case for $\ell = 0$. Fig.16(a) would seem to predict that $\delta(k)$ rises through $\pi/2$ for a potential with an almost-bound s-state. As we saw in the discussion of Fig.10, however, the phase actually turns over and decreases before reaching $\pi/2$ for a square-well or Woods-Saxon type of potential. This is a useful warning that the nearest-pole approximation is not always adequate, especially near threshold, where the 'background phase' also has a $k^{2\ell+1}$-dependence and in this case is exactly large enough (e.g. - kR if the potential is cut off at r = R) to prevent the phase shift curve of Fig.16(a) from rising to $\pi/2$.

Finally, before looking at examples, we consider how Levinson's theorem is related to the zeros of the Jost function. From

$$f_\ell(k) = e^{-\delta_\ell(k)} \left| f_\ell(k) \right| \tag{3.19}$$

and the symmetry $f_\ell^*(-k^*) = f_\ell(k)$ we obtain

$$\delta_\ell^*(-k^*) = -\delta_\ell(k) \tag{3.26}$$

i.e. $\delta_\ell(k)$ is odd for real k, as was noted earlier from its threshold behaviour; in similar fashion $\left| f_\ell \right|$ is even in k. Rouché's theorem states that

$$\frac{1}{2\pi i} \oint \frac{f_\ell'}{f_\ell} \, dk = n \tag{3.27}$$

where n is the number of zeros of $f_\ell(k)$ enclosed by the contour. If we take the contour to be the real k-axis plus a semicircle in the upper half plane, then under the conditions (2.1) Newton [1] shows that $f_\ell(k)$ is given by the Born approximation, $f_\ell(k) \to 1 + c/k$ along the large semicircle, so that as its radius tends to infinity its contribution to Eq.(3.27) vanishes. Then, because of the above symmetries, the $\left| f_\ell \right|$ contributions cancel on the two halves of the real axis, and those from δ_ℓ add, giving

$$-\int_0^\infty \delta_\ell'(k) \, dk = \delta_\ell(0) - \delta_\ell(\infty) = n\pi \tag{3.28}$$

but, as we have seen, n is just the number of zeros on the upper imaginary axis, i.e. the number of bound states.

3.2. Examples of pole distributions

From the preceding section we see that the translation of physics into complex-plane mathematics which emerges is that any potential V(r) determines a function $S_\ell(k)$ (for each partial wave), which has a certain distribution of poles and zeros in the complex k-plane. If a pole-zero pair occurs close enough to the positive real axis, it will 'cause' a resonant rise in the phase shift $\delta_\ell(k)$. Furthermore, if the potential is made a little more attractive, the resonance energy will decrease, so $\mathrm{Re}(k_n)$

must decrease. Im (k_n) will also decrease, for the resonance necessarily becomes narrower as its energy decreases. In fact, if the pole is at $k_n = \alpha_n - i\beta_n$ in the k-plane, it is at $E_0 - i\Gamma/2 = k_n^2/2m = (\alpha_n^2 - \beta_n^2)/2m - i\alpha_n\beta_n/m$ in the energy plane, and from the familiar fact that $\Gamma \sim k_0^{2\ell+1}$ near threshold, where $k_0^2/2m = E_0$, we conclude that the pole motion near the origin is determined by the centrifugal barrier to be

$$\beta_n \sim \alpha_n^{2\ell} \tag{3.29}$$

Thus for $\ell > 0$ the centrifugal barrier causes the pole to approach the origin tangent to the real axis. The resonance width decreases to zero just as the pole reaches the origin, where it then collides with its partner coming from the other side of the imaginary axis at $-k_n^*$, one 'scattering' down along the imaginary axis and one up it into the upper half plane where it is a bound state, as indicated in Fig. 17(a). (The zeros, meanwhile, are following complex conjugate trajectories.) Although they of course lose their identity at the collision, if the potential is made slightly absorptive they 'miss', and one finds that it is the left-hand pole which becomes the bound state even though the right-hand one is the resonance. In the s-wave case, on the other hand, which has no centrifugal barrier, the poles meet (as the potential is strengthened) on the imaginary axis a finite distance below the origin (Fig. 17(b)), generally near the point -i/R, where R is

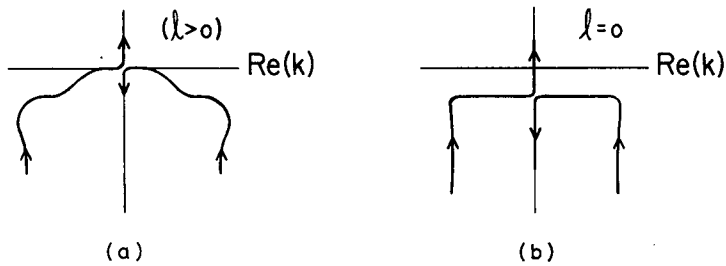

FIG. 17. Pole motion caused by the centrifugal barrier (a) for $\ell > 0$, (b) for $\ell = 0$

the 'range' of the potential, appropriately interpreted (e.g. $R = \mu^{-1}$ for a Yukawa potential), if the potential itself has no surface barrier. After collision, the 'left-hand' pole moves up the imaginary axis and becomes a bound state by passing through the origin alone, causing the low-energy phase shift behaviour shown in Figs. 16(a) and 16(b), while on the imaginary axis below the origin, it is known as a 'virtual state' (e.g. the singlet state of the deuteron). It is a well-defined pole, of course, but in the energy plane is at a negative energy on the second sheet, which is why it fails to produce the customary resonance effects, at a definite positive energy. The fact that the s-wave poles never approach the positive k-axis more closely than 1/R also explains why the square-well resonances of Fig. 8(a) are so weak, for, from the 1-pole approximation (3.21), one finds that the maximum positive slope $d\delta/dk$ contributed by the resonance in this case is $d\delta_n/dk = R$, which is exactly cancelled by the background-phase contribution $d(-kR)/dk = -R$; it is only when the pole begins climbing the imaginary axis that it gets close enough to the physical region to cause a significant phase rise.

This behaviour is nicely illustrated by the work of Ferreira and Teixeira [8], who obtained numerically the pole pattern for an attractive $1/r$ potential cutoff at $r = b$, and studied its behaviour as a function of b, which in this case serves as both a strength and a range. Figure 18 shows their results for the s-wave. Since each pair of poles in the lower half plane will eventually lead to a bound state if the potential strength is made great enough, they could be labelled by the radial quantum numbers of the bound states. Ferreira and Teixeira have chosen the other alternative, of labelling them by the asymptotic positions they asume when the potential is turned off, $b \to 0$. Since there is no scattering in this limit, the poles must be far from the physical region, and they are found to recede to the equally-spaced points $(\pm N\pi/2 - i\infty)$, with N even for even ℓ and odd for odd. An exactly similar behaviour is found for the poles of the delta-function potential

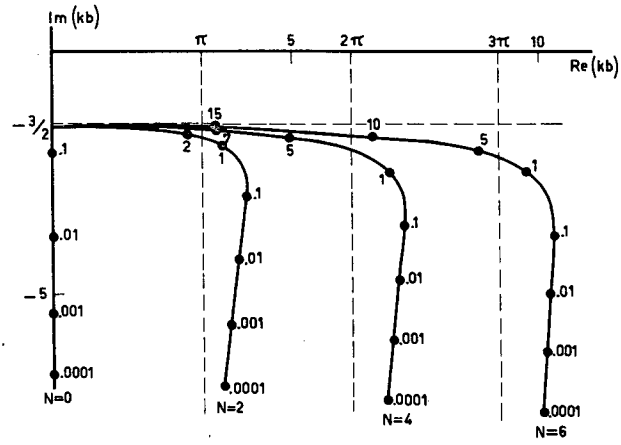

FIG. 18. Poles for the S-matrix for s-wave scattering by a screened attractive Coulomb potential of range b. The values of b are shown on the curves. The trajectory N = 0 is always on the imaginary axis. Each trajectory has a symmetric one for negative values of Re(kb). After two symmetric poles reach the imaginary axis as b increases, one moves upwards and the other moves downwards along the imaginary axis. (Taken from J. math. Phys. 7 (1966) 1207)

whose zeros are shown in Fig. 7(b). As the 'coupling constant' vanishes, the poles and zeros move off to $\pm i\infty$, where they succeed in exactly cancelling the essential singularity at infinity exp-2ikR. In the opposite extreme of infinite coupling constant, the barrier becomes completely reflecting; the resonances become infinitely narrow and the poles and zeros cancel one another in pairs on the real axis, leaving only the reflection factor $S = \exp -2ikR$.

Figure 19(a) shows the pole trajectories for the p-wave in the cutoff Coulomb well. Their behaviour near the origin reflects the existence of narrow resonances there, which may be thought of as 'materializing' at an energy somewhere near the top of the centrifugal barrier (Fig. 3(a)) and then moving down in energy as the well is made more attractive. This is accomplished neatly in the complex plane by the pole always 'being there', but remaining far off the real axis when the real part of its energy exceeds the top of the barrier. Following the trajectories of Fig. 19(a) 'backwards'

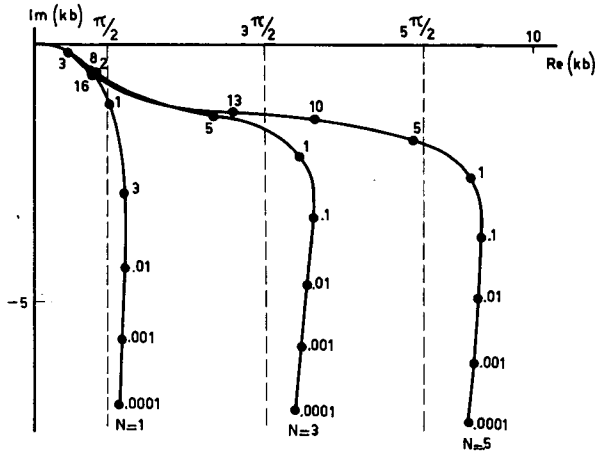

FIG.19(a) Trajectories of the poles for p-wave scattering by attractive potentials. The values of the range b are indicated on the curves. All trajectories enter the imaginary axis at the origin, and then run upwards and downwards along the imaginary axis. (Taken from J. math. Phys. 7 (1966) 1207)

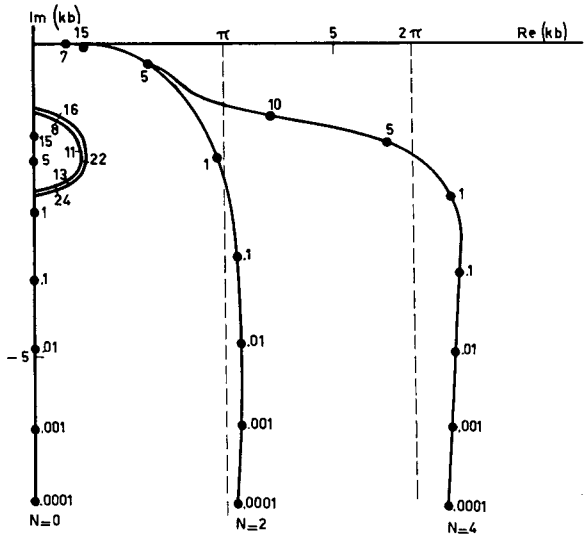

FIG.19(b) d-wave poles for attractive potentials. As b increases the complex poles move towards the origin, and then follow the imaginary axis. Those which run along the negative imaginary axis pass again to the complex plane, describing "semicirles", and turning back to the imaginary axis. When $\delta \to \infty$ there will be poles on the imaginary axis and at the points $\mp \frac{1}{2}\sqrt{3} - \frac{1}{2}i$. (Taken from J. math. Phys. 7 (1966) 1207)

(decreasing b), we see that indeed at a momentum near the top of the barrier the poles move away from the real axis. Being above the barrier they are then similar to s-wave poles, so as b is decreased further they follow closely along the s-wave trajectory at a distance $\sim 3/2b$ from the real axis and finally plunge decisively into the depths of the lower k-plane, losing their individual identity as they become a part of the 'background phase'.

This is a typical example of a general result which seems to emerge: for a pole in the k-plane to have a strong individual effect on the phase shift $\delta(k)$, it must lie closer to the real axis than the reciprocal range of the force, for only in this way can it win out against the decreasing background phase $\delta_B \sim -k\,R$. Once a pole gets further than this off the real axis, it simply becomes a part of the background itself. It is just these far-off poles which normally prevent the phase shift from decreasing at the Wigner limit (e.g. the low-energy poles in the hard-sphere case for $\ell > 0$), and it is not hard to see that a distribution of them far from the real axis, with equal spacing between their real parts as in Figs. 18 and 19 for large N, is precisely what is needed to cancel out the exp-2ikR factor in S(k) and give a phase shift which tends to a constant as $k \to \infty$. Indeed, for a general cutoff potential the asymptotic pole distribution for s-waves is found to be [1]

$$\begin{aligned} \mathrm{Re}\,(k_n) &\to \pm n\pi/R \\ \mathrm{Im}\,(k_n) &\to \text{const.} \times \log(n) \end{aligned} \qquad (3.30)$$

Fig. 19(b) shows the d-wave poles, which are 'tangent' to the real axis out to higher energy than the p-wave ones because of the higher centrifugal barrier.

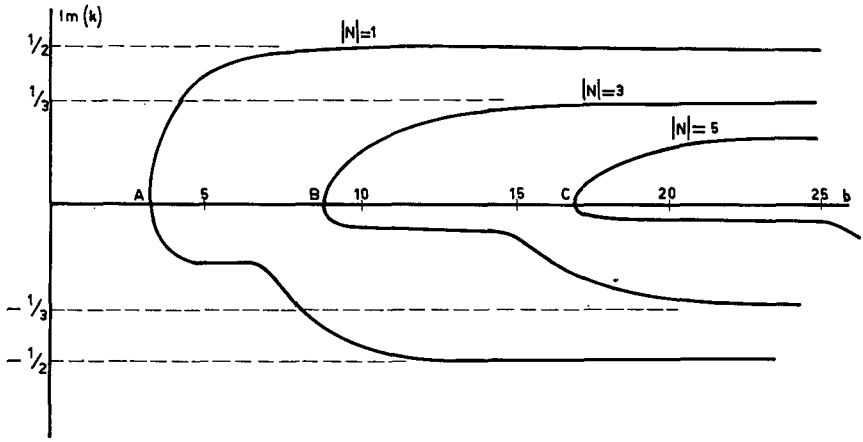

FIG. 20. Purely imaginary poles for p-wave scattering by attractive potentials. The points A, B, C give the values of b for which the poles reach the origin and new bound states are formed. As $b \to \infty$ the bound-state poles tend to the values of Im (k) corresponding to the binding energies given by Rydberg formula. In the Coulomb limit there are symmetric poles in the negative imaginary axis. (Taken from J. math. Phys. 7 (1966) 1207)

Finally, Fig. 20 shows in detail how the pairs of p-wave poles behave as a function of b after they have reached the imaginary axis. In the s-wave case the lower pole, which had a 'head start', remains further from the real axis than the upper pole for all values of b, so their joint contribution to the phase shift is of the form shown in Fig. 16(b). Figure 20, on the other hand, indicates that the converse is true for the p-wave in this well,

i.e. immediately after the poles collide at k = 0, the one on the upper imaginary k-axis moves away from the origin faster than the lower-axis pole, so in this case (and the same is true for the d-wave) the bound-state pole, together with its partner, produces a phase shift contribution which is the negative of that of Fig. 16(b), i.e. an increasing phase at low energy followed by a slower decrease at higher energy. When the state becomes more strongly bound (approaching its value for a true Coulomb field as $b \to \infty$), the lower pole catches up; they become equidistant from the origin, each being stifled by the other's zero (i.e. residue $\to 0$), so for this potential strongly-bound states contribute nothing to the energy dependence of the phase shift. At the moment it is not known whether this behaviour is to be expected in general, but it is clearly a point of considerable practical importance.

3.3. Pole collisions

The phase shift curve of Fig. 10 has the property that at a certain potential strength it is tangent to the line $\delta = \pi$, and for a larger strength it intersects the line at two real momenta, which move apart as the strength is increased still further. In discussing the effective range expansion below, we shall be interested in these points as poles of cot $\delta(k)$, and from Fig. 10 it would appear that as a function of the potential depth these poles suddenly spring into existence on the real k-axis and then move apart along it. This is a very common occurrence in the motion of poles, and what really happens is covered by the following two theorems; since the poles of interest to us arise from zeros of a denominator, we consider the motion of zeros instead (see Fig. 21).

Theorem I: If $F(k, \lambda)$ is analytic in both k and λ and has zeros in the k-plane, $k_n(\lambda)$, it is impossible for two zeros to 'vanish' by colliding with each other.

Proof:
$$(2\pi i)^{-1} \oint (\partial_k F / F)\, dk = n(\lambda)$$

is the number of zeros inside the contour, and is clearly an analytic function of λ provided no zero crosses the contour. But it is a constant function of λ and so cannot change when two zeros collide within the contour.

Theorem II: If $F(k, \lambda)$ is analytic in both k and λ in the joint neighbourhood of $k = 0$ and $\lambda = 0$, then if two of its zeros in the k-plane meet at $k = 0$ as λ passes through zero along its real axis, the k-zeros must approach and recede from one another along straight lines passing through the collision point, at equal 'speeds', and they will 'scatter' through right angles.

Proof: The choice of $k = 0$ and $\lambda = 0$ for the collision point is purely for convenience, and any others would clearly do as well. The double Taylor's expansion about this point is

$$F(k, \lambda) = F(0, 0) + kF_1 + \lambda F_2 + \tfrac{1}{2}\left[k^2 F_{11} + \lambda^2 F_{22} + 2\lambda k F_{12}\right] + \cdots \quad (3.31)$$

But $F(0, 0) = 0$ and, since at $k = \lambda = 0$ the zero is double in k, $F_1(0, 0) = 0$. Then in lowest order the zero positions in the k-plane are at

$$k(\lambda) = \pm (2 F_2 / F_{11})^{\frac{1}{2}} \lambda^{\frac{1}{2}} \tag{3.32}$$

the other terms clearly giving higher-order corrections in $\lambda^{\frac{1}{2}}$. Hence the two k-values are on a line passing through $k = 0$, and acquire a factor of (i) when λ passes from positive to negative values, so the line of recession is at right angles to the line of approach. More generally, a 3-body collision is given by

$$k_n(\lambda) = c \lambda^{\frac{1}{3}} e^{2\pi i n/3}, \quad n = 1, 2, 3, \tag{3.33}$$

etc. from which the general situation is clear: the 'particles' always divide the plane symmetrically among themselves, and rotate the paths by half the angle separating them upon colliding.

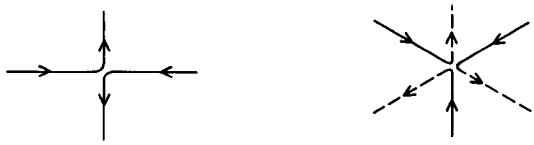

FIG. 21. Two- and three-pole collisions

Of course, it was crucial that λ passed through the collision value along a straight line; e.g. thought of as a coupling constant, well depth, etc., it will normally be a real number. That F should depend on it analytically follows in most cases from the Poincaré theorem quoted in connection with Eq. (3.3), for λ will generally occur as a parameter in the differential equation, but not in the boundary condition.

Incidentally, Theorem II provides a very simple explanation of the repulsion-of-levels phenomenon familiar for bound states. Two bound levels are prevented from crossing (as some interaction parameter is varied) by the fact that if their poles did collide, they would have to scatter off the imaginary k-axis, which we found above to be an impossibility in the upper k-plane. No such restriction impedes the collision of resonance poles.

Returning to the poles of $\cot \delta(k)$ in Fig. 10, it is clear that they didn't simply appear on the real k-axis at a certain potential strength; they were present even before the curve intersected the straight line, moving towards the real axis parallel to the imaginary axis.

3.4. Two overlapping resonances; double poles

Although bound levels cannot cross, we have seen in many examples that poles in the lower half plane can and do collide if the potential is appropriately varied, producing, at the instant of collision, a double pole of $S_\ell(k)$. None of the collisions in those examples occurred near enough to the real axis for the poles concerned to correspond to a sharp resonance,

however, since the potentials used were not constructed for that purpose. A hint as to how a double resonance pole might be achieved can be obtained from recalling that a one-dimensional attractive potential, symmetric about its midpoint (e.g. a square well), has bound states which are successively (in energy) even and odd about this midpoint, and that if a repulsive barrier is raised up at this midpoint (as, for example, in the 'inversion oscillations' of the NH_3 molecule or deformed nuclei), the levels become degenerate in pairs – but only in the limit that this barrier is completely impenetrable. Bell and Goebel [9] have recently generalized this idea to resonances rather than bound states by allowing one wall of the potential well to leak; specifically, they replaced it by a delta-function barrier at $r = 2R$ as in Fig.3(b), whose resonance wave functions are successively approximately symmetric and anti-symmetric about $r = R$ if the barrier is quite impenetrable. Then by raising a second such barrier, $V(r) = c\delta(r - R_1)$ with $R_1 \approx R$(two concentric spherical shells, in three dimensions), they found that the resonance poles could be driven together in pairs (one pair at a time) for finite values of c, producing double poles of S as they collided. Such a double pole near the real axis affects the phase shift very much in the way two nearby poles (overlapping resonances) would, merely producing a smooth and rapid rise of 2π rather than π, but it radically alters the decay rate of the resonant state, which becomes $(1 - a\Gamma t)e^{-\Gamma t}$, where a depends explicitly on how the resonance was excited, i.e. on the shape of the incident wave packet; $a \to \frac{1}{2}$ if the bandwidth of the packet is much larger than Γ, which is necessary if the decay curve is to be clearly observed.

In a rather more formal context, Lynn [10] has noticed that S-matrix poles can be made to collide by forcing two R-matrix poles close together – something which happens, for instance, in heavy nuclei, where the level density is high. Considering the 1-channel s-wave case for simplicity, the relation between R and S is

$$S_0(k) = e^{-2ika}\ \frac{1 + ika\,R(E)}{1 - ika\,R(E)} \tag{3.34}$$

if the potential is cut off at $r = a$. R(E) is real for real E, so Eq.(3.34) is simply a transformation which maps the real axis of the complex plane (along which R moves as E is varied) onto the unit circle (along which S moves as E is varied) in such a way that one traversal of the entire real axis by R produces one complete circuit of the unit circle by S (i.e. phase rise of π). In algebraic terminology, since

$$\tan(\delta + ka) = ka\,R(E) \tag{3.35}$$

where $\delta(k)$ is the phase shift, a rapid increase in R (R'(E) is positive everywhere on the real energy axis) causes a rapid increase in δ and, in particular, an isolated pole of R(E) (they occur only on the real axis) causes a rapid rise of π in $(\delta + ka)$, i.e. a resonance, whose width is determined by the slope R'(E) near the pole, that is to say by the residue of the pole. If two resonances overlap, however, the shape of R(E) between them may be so drastically altered that the one-to-one relation between poles of R(E) and resonances breaks down completely, with the result that the widths of the observed resonances (there are still two of them) are no longer even approximately given by the residues of the R-poles.

That is, in the 2-pole approximation,

$$ka\,R(E) \approx \frac{ka\gamma_1^2}{E_1-E} + \frac{ka\gamma_2^2}{E_2-E} \equiv \frac{\Gamma_1/2}{E_1-E} + \frac{\Gamma_2/2}{E_2-E} \tag{3.36}$$

where, if we neglect the variation of k over the energy range covering the two resonances[3], Γ_1 and Γ_2 are the widths which these two resonances (at E_1 and E_2) would have if they did not overlap.

The poles of $S_0(k)$ are then given by the zeros of the denominator of Eq.(3.34)

$$1 - ikaR = \frac{(E_1-E)(E_2-E) - \frac{i}{2}\Gamma_1(E_2-E) - \frac{i}{2}\Gamma_2(E_1-E)}{(E_1-E)(E_2-E)} \tag{3.37}$$

The most interesting case, and also the one in which the algebra is most transparent, is that of equal residues for the R-poles, $\Gamma_1 = \Gamma_2$, in which case the S-poles are at

$$E_p = \tfrac{1}{2}(E_1 - \tfrac{1}{2}\Gamma + E_2 - \tfrac{i}{2}\Gamma) \pm \tfrac{i}{2}\left((E_1-E_2)^2 - \Gamma^2\right)^{\frac{1}{2}} \tag{3.38}$$

If $|E_1 - E_2| \gg \Gamma$, the resonances are well separated and the S-poles (which both have width Γ) occur directly below the R-poles in the E-plane, giving the two separate phase-rises of π for the resonant part of the phase shift, as indicated schematically in Fig. 22(a). The R-matrix and S-matrix widths are the same in this case. If the R-poles are moved closer together (holding Γ constant) until the resonances begin to overlap, the S-poles move along with them, parallel to the real axis, but getting somewhat 'ahead' of the R-poles, and at $|E_1 - E_2| = \Gamma$ the S-poles collide, giving the double-pole resonance shown in Fig. 22(b). After collision the S-poles move vertically, maintaining exactly equal real parts (this would not quite hold true if we had retained the effect of threshold by allowing k to vary) and in the limit that the R-poles are moved very close together, $|E_1 - E_2| \ll \Gamma$, one S-pole approaches the real axis and the other recedes to a distance Γ from the real axis. In this case we are clearly dealing with two resonances at exactly the same energy, one broad and one very narrow. The corresponding phase shift, Fig. 22(c), shows a slow rise of $\pi/2$ due to the 'lower half' of the broad resonance, on top of which the rapid rise of π from the narrow resonance is superimposed, followed by the second $\pi/2$ of the broad one. The curves of $\sin^2\delta_r$, i.e. $k^2\sigma_0^2$, are given in Fig. 23, (for simplicity we assume $ka \ll 1$ and so neglect any background phase from the first factor of Eq.(3.53)) indicating that in case (c) the 90° 'background phase' provided by the broad resonance means that the effect of the narrow resonance appears as a sharp dip in the cross-section, instead of a sharp rise. It is, of course, the same dip which appears between the two maxima in (a) and (b), but its walls are greatly steepened in (c). To indicate how

[3] The present considerations are of greatest relevance to the narrow compound-nucleus type of resonance, for such resonances are much more likely to occur close together than the single-particle potential resonances discussed above.

confusing the analysis of experimental data can be in such a case, Fig.23(d) shows how the cross-section for the same pair of poles as in (c) is changed by adding a constant background phase of about +45°. The total phase then reaches 90° below the energy of the narrow resonance, which consequently rides on the descending flank of the broad one. If one is guided by the two maxima in the cross-section, the two resonances appear to occur at different energies, but if properly analysed and the background phase extracted, they will, of course, be found at the same energy.

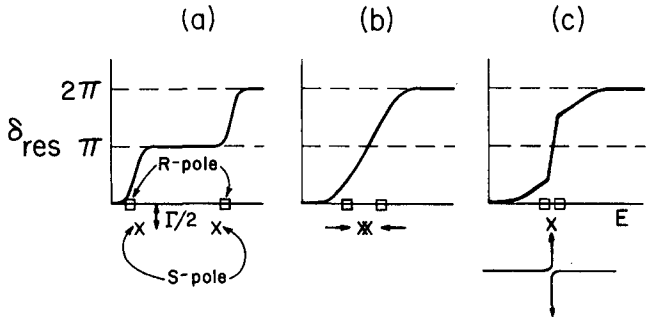

FIG. 22. Two resonances: phase shifts and corresponding S- and R-poles

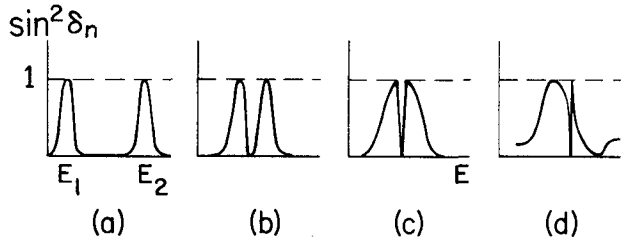

FIG. 23. Curves of $\sin^2\delta_n$, i.e., $k^2\sigma^2$, corresponding to Fig. 22

Quite aside from such additional complexities as this, this example seems to us to provide a compelling argument for the use of S-matrix rather than R-matrix parameters to describe overlapping resonances, for the influence of an S-pole on the phase shift is seen to be the same whether another pole is nearby or not (though the phase rise of the broad resonance is, of course, 'split in two' in (c) by the intervention of the narrow resonance). This is because, as we shall see from Eq. (3.58) below, the phase shifts associated with different S-poles are additive, whether they overlap or not. The effects of R-poles, on the other hand, distinctly interfere with each other when they overlap, so that although the width of an isolated resonance is given directly in terms of the residue of the corresponding R-pole, this is not necessarily true at all if the resonance is overlapped by another.

Exactly how this 'interference' comes about is evident from Fig. 24. Recalling that as R(E) increases rapidly by an infinite increment, the phase shift increases rapidly by π, Fig. 24(a) indicates a typical R-curve for two

isolated resonances, indicating that the shape of R(E) near each pole is very little influenced by the other far-away pole, so that the shape of each resonant phase rise is determined only by the residue at the corresponding R-pole. On the other hand, if the poles occur close enough together, as in (b), the curve between them is forced to rise by an infinite amount over the energy-range $(E_2 - E_1)$. It is this increase in R(E) which then corresponds to the narrower of the two resonances, whose width, when $|E_2 - E_1|$ is much smaller than the residue at either pole, is clearly determined by $|E_2 - E_1|$ rather than by these residues[4].

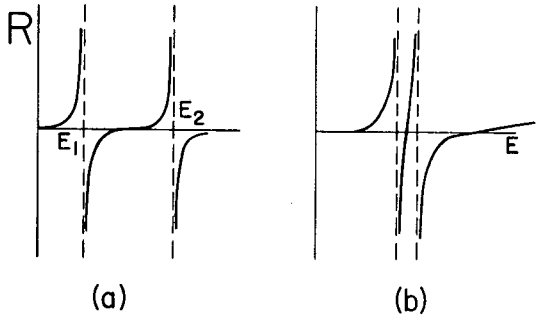

FIG. 24. Interference of levels in the R-function

It thus becomes clear that a one-to-one association of R-matrix poles (or their corresponding states) with resonances is only possible for completely isolated resonances. When two R-poles overlap severely, they necessarily produce one narrow and one broad resonance by pooling their resources. Their two 'central halves' combine to produce the narrow resonance, and the remaining outer tails are responsible for the broad one, which explains why the width of neither resonance is given by either of the pole residues. This is of course directly connected with the fact that the resonances in this case do not occur at the points where the phase of the second factor of Eq. (3.34) is 90°, i.e. at the poles of R(E), where the curves of Fig. 23 have their maxima; it is the slope of $\delta(E)$ which marks the resonance, so that in Fig. 23(c) the broad resonance indeed occurs where the phase is 90°, but the centre of the narrow one occurs where it is 180°, i.e. at a zero of the cross-section.

If N rather than 2 R-poles (with roughly but not necessarily exactly equal residues) are 'squeezed together', N-1 of the resonances will clearly become narrow, and only one S-pole (a composite of the outside tails of the two end R-poles) will drop away from the real axis to produce a single broad resonance. The mathematical reasoning is not unlike that of the Brown-Bolsterli model of the giant dipole resonance, in which a pairing interaction separates one pole of a cluster widely (along the real axis in this case) from the rest.

Finally, we note from Figs. 23(c) and (d) that two overlapping resonances can produce readily-distinguishable effects on the energy-dependence of the cross-section, provided that their widths are very different – i.e.

[4] This will be true, of course, whether the residues of the two poles are equal or not.

that their S-poles are widely separated vertically. The only case in which two resonances are likely to be very difficult to distinguish is that of nearly-coincident S-poles, i.e. overlapping resonances of nearly equal widths (Fig. 23(b)). The exact positions of such poles will be difficult to ascertain from experimental data, and for this reason may, in fact, no longer provide the most useful parametrization for the shape of $\sigma(E)$.

3.5. Threshold behaviour and energy-dependent widths; the effective range expansion

There are two situations (apart from overlapping resonances) in which the 1-pole approximation in the unitary form (2.21) or (3.21) will fail to account adequately for the shape of $\delta_\ell(k)$ at nearby real energies. The first is simply the case in which the pole is too far off the real axis to dominate over the background; arguments presented above suggest that this will occur whenever the inequality $\mathrm{Im}\,(k_n) \ll 1/R$ is violated, where R is in some sense the range of the force.

The second case is that in which the resonance occurs at a low enough energy to 'overlap threshold', i.e. if $(\mathrm{Im}\,k_n) \gtrsim \mathrm{Re}\,(k_n)$. That is, the 1-pole approximations used above yield a $\delta_n(k)$ which is completely symmetric about $k = \mathrm{Re}\,(k_n)$, so that a fraction of its left-hand 'tail' extends below $k = 0$. If $\mathrm{Im}\,(k_n) \ll \mathrm{Re}\,(k_n)$ (i.e. phase of k_n is much smaller than 45°), this is not serious, but if a significant fraction of the tail is 'lost' in this way, the 1-pole approximation will certainly not be accurate over the full width of the resonance, as Fig. 25 makes clear, for it seriously violates the thres-

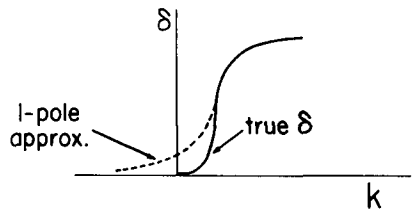

FIG. 25. The effect of threshold on a phase shift

hold condition, $\delta_\ell(k) \sim k^{2\ell+1}$ near $k = 0$. This additional constraint not only forces the phase shift to zero at $k = 0$, but also (for $\ell > 0$) holds it near zero out to a finite energy, thus steepening the resonant rise when it finally does appear. Because this steepening effect occurs only on the low-energy side of the resonance, the cross-section is distorted from the symmetric Breit-Wigner shape (2.22) to one which is 'narrower' on the low-energy side than on the high-energy side.

In other words, if we take the 'background phase' to mean the difference between the two curves of Fig. 25, it will vary over the resonance region even more rapidly than the resonant part of the phase shift and so must be handled with great care. In fact, in a case like that of Fig. 25, any useful approximation must be valid throughout a k-range including $k = 0$, so it may be most advantageous in this case not to separate $S_\ell(k)$ explicitly into 1-pole and background parts at all, but to lump them together and instead

treat the total phase by an expansion in powers of k. Since it is very difficult to ensure the unitarity of such an expansion of $S_\ell(k)$ itself, a convenient alternative is to write $S_\ell(k)$ in the form $D_\ell^*(k)/D_\ell(k)$ (for real k) and use a power series expansion for $D_\ell(k)$. By writing S as

$$S_\ell(k) = \frac{\cos\delta_\ell + i\sin\delta_\ell}{\cos\delta_\ell - i\sin\delta_\ell} \tag{3.39}$$

we see that not only should $\mathrm{Re}(D_\ell)$ be even in k and $\mathrm{Im}(D_\ell)$ odd, but to get threshold right we also need

$$\frac{\mathrm{Im}\ D_\ell(k)}{\mathrm{Re}\ D_\ell(k)} \longrightarrow k^{2\ell+1} \text{ as } k \to 0 \tag{3.40}$$

The simplest approximation satisfying these conditions, the one which contains the smallest number of parameters, is

$$\begin{aligned} \mathrm{Re}\ D_\ell &= A + Bk^2 \\ \mathrm{Im}\ D_\ell &= Ck^{2\ell+1} \end{aligned} \tag{3.41}$$

which in terms of E may be written in the more suggestive form[5]

$$\begin{aligned} S_\ell(k) &\approx \frac{E - E_0 - i\Gamma/2}{E - E_0 + i\Gamma/2} \\ &= \frac{E - E_0 - i\,C_\ell k^{2\ell+1}}{E - E_0 + i\,C_\ell k^{2\ell+1}} \end{aligned} \tag{3.42}$$

with two real free parameters, E_0 and C_ℓ. If $\Gamma(k_0) \ll E_0$, it will describe a resonance near E_0, and is known as the 'energy-dependent width' approximation, for it indeed does make the resonance 'wider' on the high-energy side. If thought of in terms of a single pseudo or effective pole, it describes a pole which moves vertically as a function of k, and from a diagram like Fig. 13 it is clear why the approximation works, for as $k \to 0^+$, the pole and zero approach one another, 'closing the gate' behind it at just the rate necessary to give the correct threshold dependence for $\delta_\ell(k)$.

More explicitly, the $S_\ell(k)$ given by Eq. (3.42) actually has $2\ell+1$ 'fixed' poles (2 for $\ell = 0$), given by the roots of

$$E - E_0 + iC_\ell k^{2\ell+1} = 0 \tag{3.43}$$

(from the real axis they look like a single moving pole) which, like the set of ℓ poles we found earlier for the hard sphere case, are positioned in the

[5] It may often be advantageous to factor off an additional 'background' piece of $S_\ell(k)$ (e.g. a hard-core factor), as was done in Eq. (3.21), in which case Eq. (3.42) is an expansion of only a part of $S_\ell(k)$. In this case the 'background' factor must also have the correct threshold behaviour.

k-plane in just such a way as to ensure the correct threshold behaviour for $S_\ell(k)$. (Because this approximation satisfies both the symmetries (3.16) and (3.17), its poles occur in the same type of pattern as those of the exact S.) If threshold is to be attained by brute force of poles, in other words, $(2\ell + 1)$ is the smallest number which will do it.

If a single narrow resonance occurs within the range of validity of the approximation, the inequality

$$C_\ell k_0^{2\ell+1} \ll E_0 \tag{3.44}$$

will be satisfied, and its pole k_n (together with a mirror-image one at $-k_n^*$) will occur among the roots of Eq. (3.43), in energy near $E = E_0 - i\Gamma(k_0)/2$, and so most readily found by iterations based on (3.44).[6]

The remaining $(2\ell-1)$ poles will lie much further from the real axis (otherwise δ would rise rapidly by more than π), and in fact will often lie outside the range of validity of the approximation (3.42) itself. In this case they are not true, individual poles of $S_\ell(k)$, but merely a representation, valid near $k = 0$, of all the distant singularities of S.

For the purpose of obtaining resonance parameters, the practical point of importance is that the positions of all these poles, including the 'real' one, are determined by the two parameters E_0 and C_ℓ, so once they are obtained from a fit to experimental data, the true pole parameters are readily obtained, if desired, from the iterative solution of Eq. (3.43).

All this is, of course, very familiar from R-matrix theory for cutoff potentials, in which the single-R-pole approximation gives for the S-matrix element,

$$S_\ell(k) = E^{-2i\delta_\ell^c} S_{res}(k) \tag{3.45}$$

where $\delta_\ell^c(k)$ is the hard-sphere phase (with correct threshold behaviour) and

$$S_{res}(k) = \frac{E - E_0 - i\gamma^2 P_\ell(kr)}{E - E_0 + i\gamma^2 P_\ell(kr)} . \tag{3.46}$$

Here γ^2 (the 'reduced width') and E_0 are constants and $P_\ell(kR)$, the 'penetration factor' in the ℓ-th partial wave, is a known function with the correct threshold behaviour, $P_\ell(x) \sim x^{2\ell+1}$ for $x \ll \ell$.

Generalizing slightly, a multi-pole approximation of the general form

$$S_\ell(k) = S_\ell^B(k) \frac{E - E_0 - i\gamma^2 P_\ell(k)}{E - E_0 + i\gamma^2 P_\ell(k)} \tag{3.47}$$

seems an attractive one to use for fitting isolated low-energy resonances, for, subject only to the condition that $P_\ell(-k) = -P_\ell(k)$ and $P_\ell(k) \sim k^{2\ell+1}$ as

[6] E. g. if in the p-wave case we write Eq. (3.43) as $k^2 - k_0^2 + ibk^3 = 0$ with $bk_0 \ll 1$, the solution near $k^2 = k_0^2 - ibk_0^3$, through order $(bk_0)^3$, is $k^2 = k_0^2(1 - \frac{3}{2} b^2 k_0^2) - ibk_0^3$.

$k \to 0$, its resonant factor possesses both the symmetry properties (3.16) and (3.17), has the correct threshold behaviour and contains the two parameters needed to fit an elastic resonance. $P_\ell(k)$ should be a function which accounts as well as possible for the reduction of the wave amplitude as it penetrates the centrifugal and/or Coulomb barrier as well as for reflections from the inside of the barrier which depend on the surface thickness of the potential well (i.e. those single-particle effects which also occur in the realistic nuclear problem and which it is desirable to separate as much as possible from the specifically many-body effects associated with the nuclear interior). Although it must vanish like $k^{2\ell+1}$ at low energies, it should approach unity as the energy is increased above the top of the barrier, thus permitting the use of Eq. (3.47) for higher energy resonances as well, if desired. In addition, the remaining effects of the barrier ought to be incorporated into the background factor; the experience accumulated over the years from fitting nuclear resonance data seems to suggest that the hard core factor of Eq. (3.45) provides a useful approximation over a limited energy range; one expects that the radius R which enters should be chosen somewhat smaller than the nuclear radius, to allow for the fact that the reflection is not complete, so that the background phase does not descend at the Wigner limit. Of course, if more than one channel is open, there is no reason to expect S^B to be elastic, but for small inelasticity the background phase of the diagonal S-matrix element is probably well approximated in the same way.

Exactly what choice of penetration function $P_\ell(k)$ is most appropriate, especially if the Yukawa tail of a realistic well is taken into consideration, is an open question at the moment; Humblet discusses several possibilities in chapter 7 of this volume. Clearly the separation of resonance and threshold effects cannot be accomplished completely, nor can it be done uniquely, so the choice of function $P_\ell(k)$, and hence the value of the reduced width γ^2, is to some extent a matter of convention. If a specific convention is adopted, however, the energy-dependent width approximation could be used for resonances occurring over a wide energy range, even above the barrier height. (Isobaric analogue states, for example, often do this, but of course the single-particle potential resonances discussed above cannot.) Near threshold where the energy dependence is severe, Eq. (3.43) would have to be solved to determine the actual pole position in terms of E_0 and γ^2, but for many-particle resonances at energies high enough so that $P_\ell(k)$ becomes nearly constant, the 'background poles' recede very far from $k = 0$, and E_0 and γ^2 give the pole position directly. Of course, for nuclear structure purposes it is often the reduced width which is of more interest than the 'pole width' $\mathrm{Im}(k_n)$; in any case the two descriptions (E_0, γ^2) and $[\mathrm{Re}(k_n); \mathrm{Im}(k_n)] \equiv (\alpha_n, -\beta_n)$ are entirely equivalent (once P is chosen) and can be obtained from one another as desired. In fact, if the resonance is sufficiently narrow, $\beta_n \ll \alpha_n$,

$$E_0 = \frac{\alpha_n^2 - \beta_n^2}{2m} \approx \frac{\alpha_n^2}{2m} \qquad \gamma^2 \approx \frac{1}{P_\ell(\alpha_n)} \frac{\alpha_n \beta_n}{m} \tag{3.48}$$

Finally we note briefly that Eq. (3.42) and the effective range approximation are very closely related, as they must be since both are valid in the vicinity of $k = 0$. By writing

$$S_\ell(k) = \frac{\cot \delta_\ell + i}{\cot \delta_\ell - i} \tag{3.49}$$

or conversely

$$\cot \delta = i \frac{S+1}{S-1} \tag{3.50}$$

we see that cot $\delta(k)$ is analytic in k throughout the domain of analyticity of S(k), even at its poles, except for the points where $S = +1$ ($\delta = \pi$), where cot δ has poles. One such point is $k = 0$, where cot δ_ℓ has a pole of order $2\ell + 1$, which we can remove by considering instead $k^{2\ell+1} \cot \delta_\ell(k)$. Since this function is even in k it has a power series expansion in k^2, whose radius of convergence is equal to the distance from $k = 0$ to the nearest pole (assuming S(k) to have no branch points closer). The first two terms of this expansion,

$$k^{2\ell+1} \cot \delta_\ell(k) \approx - \frac{1}{a^{2\ell+1}} + \frac{1}{2} r_0^{1-2\ell} k^2 \tag{3.51a}$$

are known as the effective range expansion (with a and r_0 real because of Eq. (3.26)) which in turn can be used to approximate $S_\ell(k)$ for k sufficiently near the origin,

$$\begin{aligned} S_\ell(k) &\approx \frac{- \frac{1}{a^{2\ell+1}} + \frac{1}{2} r_0^{1-2\ell} k^2 + i k^{2\ell+1}}{- \frac{1}{a^{2\ell+1}} + \frac{1}{2} r_0^{1-2\ell} k^2 - i k^{2\ell+1}} \\ &\equiv \frac{E - E_0 - i C_\ell k^{2\ell+1}}{E - E_0 + i C_\ell k^{2\ell+1}} \end{aligned} \tag{3.52}$$

identically the energy-dependent width approximation. Although we introduced it as a resonance approximation, it is clearly valid in general, within the circle of convergence of the expansion (3.51).

It is useful to recall that the radius of this circle is determined by the pole of cot $\delta(k)$ nearest the origin, which is a position in the k-plane at which $\delta = 0 \pmod{\pi}$. Such points can occur on the real axis[7] and, as Fig. 10 indicates, if the potential strength is appropriately varied, may even move toward $k = 0$, forcing the radius of convergence of the effective range expansion to zero. Indeed, this happens for any potential at that value of the coupling constant which makes the scattering length vanish, i.e. when the normal $(2\ell+1)$ - order zero of $\delta_\ell(k) \sim k^{2\ell+1}$ at $k = 0$ becomes a $(2\ell+3)$ - order zero. This is because $\delta(k) = -\delta(-k)$, so its zeros, if

[7] Incidentally, this is a reminder that no finite approximation to $k^{2\ell+1} \cot \delta(k)$, such as (3.51), is adequate to describe two nearby resonances, since they would necessarily force the phase shift up through π, at which energy the entire power series diverges. A discussion of how the approximation can be extended to handle two resonances near threshold is given in Appendix A.

they approach the origin at all, must do so in pairs, thus increasing the order of the 'fixed' zero there by two when they collide.

For most attractive potentials this seems to occur (as the potential strength is increased) in the manner indicated in Fig. 26(a), involving only two poles, which after collision mark the energy at which the phase shift decreases through π as a function of energy, and so move further from the origin as the potential strength is increased. For s-wave scattering by a square well, however, the peculiar 'bumps' shown in Fig. 10 cause two such pole collisions to occur, at finite k, as the bump becomes tangent to $\delta = \pi$, after which two of the poles approach one another along the real axis and produce a third collision at the origin, when the scattering length vanishes. The net result in either case is to give a radius of convergence of the effective range expansion and hence of the low-energy form (3.42) of the

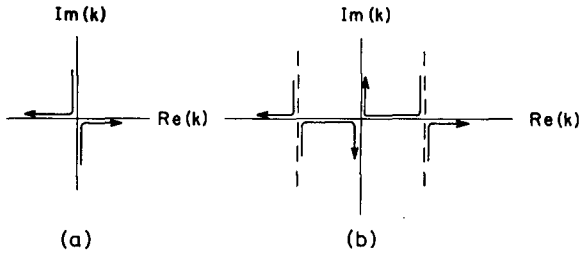

FIG. 26. Collisions of poles of cot $\delta(E)$

energy-dependent-width approximation, which oscillates as a function of coupling strength (because of successive poles approaching the origin) and passes through zero whenever the scattering length vanishes.

As for poles of $S_\ell(k)$ (points at which cot δ = i), in the s-wave case the effective range expansion predicts them at

$$k = \frac{i}{r_0} \pm \frac{1}{r_0}\sqrt{\frac{2r_0}{a} - 1} \tag{3.53}$$

As $a \to 0$ these solutions move far from the origin and so are surely outside the radius of convergence of the expansion, where they are physically meaningless. In the opposite extreme, $|r_0/a| \ll 1$, which is near the potential strength necessary to give a zero-energy bound state, the solutions are pure imaginary,

$$k_{1,2} = \frac{2i}{r_0}, \frac{i}{a} \tag{3.54}$$

Presumably only the second, which is the closer to the origin, lies within the circle of convergence, where it is either a virtual ($a < 0$) or bound ($a > 0$) state, the latter having a wave function whose asymptotic form is exp-r/a. The other pole is much further from the origin; if $r_0 > 0$ it is apparently trying to represent branch points or essential singularities of $S_\ell(k)$ in the upper half-plane, and if $r_0 < 0$, distant poles in the lower half-plane.

In the p-wave case there are 3 poles, and one readily finds that the scattering length is given in terms of the two closest to the origin by

$$a^3 = -i\frac{k_1+k_2}{(k_1k_2)^2} \tag{3.55}$$

In the case of a very weakly-bound state, with k_1 and k_2 on the imaginary axis on opposite sides of the origin, the phase shift starts downward from its $k = 0$ value so that $a > 0$, meaning the upper or bound-state pole is slightly further from the origin than the lower one, in agreement with the result of Ferreira and Teixeira (Fig. 20). They evidently nearly cancel one another's effects on the phase shift, however, for even though together they contribute a rising phase near $k = 0$, the total phase shift decreases with k.

Finally, we reiterate that, although the effective range expansion is always valid near $k = 0$ (within the circle of convergence), it represents a low-energy resonance only if $C_\ell k_0^{2\ell+1} \ll E_0$, in which case the resonance parameters C_ℓ and E_0 are simply the scattering length and effective range in disguise.

3.6. Pole expansion of $S_\ell(k)$

$S_\ell(k)$ for a cutoff potential is meromorphic in k and so is determined, to within an entire function, by its pole positions. Furthermore, because of the rate at which its poles recede from the origin with increasing n (Eq. (3.30)), $S_\ell(k)$ possesses two simple expansions which exhibit this dependence on its poles explicitly. One is the Mittag-Leffler sum over poles discussed by Humblet and Rosenfeld [2],

$$S_\ell(k) = 1 + Q_\ell(k) + k^{2\ell+1}\sum_{n=1}^{\infty}\frac{R_n}{k-k_n} \tag{3.56}$$

the sum being over all poles in the k-plane; $Q_\ell(k)$ is the entire function which is not determined by the poles, whose slow energy dependence, together with the poles far from the real axis, describes the background part of the phase shift. Note that the zero positions do not appear explicitly in Eq. (3.56) but are, of course, determined by $Q_\ell(k)$ and the residues at the poles, R_n. The symmetries (3.16) and (3.17) impose very complicated conditions on $Q_\ell(k)$ and the residues.

The other expansion [1] is the Ning Hu or product representation,

$$S_\ell(k) = e^{-2ikR}\prod_{n=1}^{\infty}\frac{k-k_n^*}{k-k_n} \tag{3.57}$$

where again the product is over all the pole positions of $S_\ell(k)$. In this case the entire function exp-2ikR is given explicitly in terms of the cutoff radius R, the symmetries are automatically satisfied because of the pole-zero pattern (Fig. 11) and S is written as a product of factors, each one of which is individually unitary. All the few-pole expansions we used above,

in fact, were simply truncations of this expression. It has the further attractive feature that by taking logarithms one automatically gets an expression for the phase shift as a sum over contributions from the individual pole-zero pairs,

$$\delta(k) = -kR + \sum_{n=1}^{\infty} \delta_n(k) \tag{3.58}$$

a two-pole approximation to which was considered in Fig. 14. If a single pole occurs near the real axis, Eq. (3.58) gives an expression for the background phase if we remove this resonant contribution from the sum; since all the poles but the finite number of bound states contribute rising phases, this explains in pole terms why the background term generally decreases with momentum at a rate smaller than the Wigner limit.

In spite of these attractions, Eq. (3.57) has two serious practical disadvantages. One is that it has no known generalization to the N-channel case (with the exception of N = 2), and it does not exhibit threshold behaviou in any obvious way. In fact, if a small-k expansion is made, Eq. (3.57) appears to contain all powers of k, and the first 2ℓ of them have vanishing coefficients only if the poles k_n are distributed in a very special way; e.g. the coefficient of the linear term is $(-2iR + 2\Sigma\, k_n^{-1})$, and must vanish for any $\ell > 0$. Of course, these conditions can be satisfied even by a finite number of poles if the ones further from the origin are 'moved' somewhat from their true positions; $(2\ell+2)$ seems to be the minimum number of poles needed, one more than the effective range expansion, which economizes by replacing a far-away pair symmetric about the imaginary axis by a single pole on the axis.

Actually the existence of the complete expansions (3.56) and (3.57) is somewhat irrelevant for the purposes of fitting resonance data, since the infinitely many far-away poles serve only to determine the uninteresting background phase. The more relevant question is the usefulness of their few-pole truncations to approximate $S_\ell(k)$ locally in a region near the real axis, and in this regard it is interesting to note that the few-pole truncations of the two expansions are in a sense complementary. That is, the truncated product expansion is automatically unitary but certainly gives the residues of the poles (which are determined by the positions of all the other poles), as well as threshold behaviour, incorrectly, whereas the truncated sum expansion is unavoidably non-unitary, but has the correct residues for those poles it retains. The product expansion does have the advantage that if 'extra' poles, beyond the resonance one, are kept and moved somewhat from their true positions, they can give an approximation to $S_\ell(k)$ (the effective range expansion) which satisfies all the necessary symmetries and behaves properly at threshold; provided the resonance pole occurs well within the radius of convergence of the expansion, its residue will also be given accurately.

4. MANY-CHANNEL RESONANCES

In many respects a many-channel resonance is merely an extension of the one-channel case, more complicated but not basically different, which

is why we have devoted so much time to one-channel analyticity. There is, however, one entirely new element in the many-channel situation, which is a mechanism for resonances quite different from the trapping-by-a-barrier which causes single-particle resonances. This is the so-called 'bound state in the continuum' or 'bound state in a closed channel' mechanism, in which the state which appears as a resonance in an open channel is 'really' a bound state of a higher, closed channel. It is a mechanism which can only operate if there are two or more coupled channels, and in the limit of zero coupling produces a resonance of zero width. It thus provides a very natural explanation for narrow resonances and is presumably the mechanism behind all narrow, many-particle, compound nucleus resonances.

4.1. Introduction

The basic physical ingredient of the many-channel situation is the set of real energies

$$\mathscr{E}_1 < \mathscr{E}_2 < \mathscr{E}_3 \text{-------} \tag{4.1}$$

at which the successive (2-body) channels open up, in terms of which the channel momenta are defined by

$$k_a(E) = \sqrt{2m_a(E - \mathscr{E}_a)} \tag{4.2}$$

We shall use this definition for all E, complex as well as real, with the phase fixed by insisting that for E on the physical region of the real axis, k_a is positive real if $E > \mathscr{E}_a$ (channel a open) and positive imaginary (exactly as in the 1-channel case) if $E < \mathscr{E}_a$ (channel a closed). m_a is the reduced mass of the two fragments which define channel a, and the zero of energy is often chosen at the lowest threshold $\mathscr{E}_1$.

With the definition (4.2) the meaning of incoming and outgoing waves is unambiguous for any channel, open or closed, and, as Humblet has discussed in chapter 7, for example, the S-matrix elements S_{ba} (with rows and columns labelled by the channels) can be defined in terms of the ratio of outgoing flux in channel b to that of the incoming flux in channel a, in complete analogy to the 1-channel case. Since the flux necessarily depends on the channel momenta themselves (rather than on their squares), the matrix elements $S_{ba}(E)$ have square-root branch points at all thresholds $\mathscr{E}_i$. It is customary to take their cuts along the real energy axis from $\mathscr{E}_i$ to $+\infty$, so that, as in the 1-channel case, the two sheets of the energy Riemann surface associated with $\mathscr{E}_a$ are distinguished by the sign of Im (k_a). Each sheet of the full surface is then labelled by the sequence of signs of Im k_1, Im k_2, etc., e.g., (++-+-...); if there are M channels in all, there are M entries, with two choices for each, or 2^M sheets altogether.

Fortunately only a small fraction of them are normally of physical interest, the principal one being the 'physical sheet', labelled by (+++... +). If the cuts are positioned along the positive real axis as indicated in Fig.27, then crossing the real axis from P at an energy between $\mathscr{E}_1$ and $\mathscr{E}_2$ crosses only the $\mathscr{E}_1$-cut and so only changes the sign of Im k_1, exactly as in the 1-channel case. The sheet reached in this way is 'near' the physical sheet P along the interval of the real axis between $\mathscr{E}_1$ and $\mathscr{E}_2$; it is labelled

by (- ++... +), or more simply as E_1. Similarly crossing the real axis between $\mathcal{E}_1$ and $\mathcal{E}_2$ leads across both the $\mathcal{E}_1$ and $\mathcal{E}_2$ cuts, to (- - ++... +), or E_2, etc. The physical sheet P, together with the sheets E_a reached from it by crossing the real axis between thresholds are the most important ones physically because they possess regions near to the 'physical region' where scattering experiments are done, the upper edge of the real axis, $E+i\epsilon$, as reached from P.

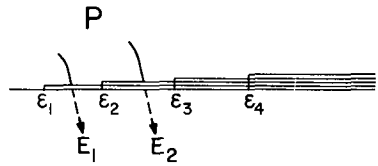

FIG. 27. Threshold branch points and cuts in the complex energy plane

We are concerned, then, with the set of complex functions $S_{ba}(E)$ and their analytic properties throughout the many-sheeted E-surface. It should be emphasized that there is only one set of these functions, which has nothing to do with channels being open or closed, (the concept is not even defined off the real axis) and in fact are continuous functions of E along the real axis even at thresholds (where, however, their derivatives may be discontinuous). Of course $\exp ik_a r$ carries no flux if k_a is pure imaginary (i.e. below threshold $\mathcal{E}_a$), so only the open channels contribute to the cross-sections, which are given, in terms of the open channel S-matrix elements, by the familiar formulae,

$$\sigma_{ba}^{\ell} = \pi \lambda\!\!\!^{-2}_a (2\ell+1) \left|S_{ba}^{\ell}\right|^2 ; \qquad \sigma_{aa}^{\ell} = \pi \lambda\!\!\!^{-2}_a (2\ell+1) \left| 1 - S_{aa}^{\ell}\right|^2 \tag{4.3}$$

a being the entrance channel. The total reaction cross-section, for incoming particles in channel a, is $\sigma_{a,r}^{\ell} \equiv \sum_{b \neq a} \sigma_{b,a}$, which by the conservation of flux can be written in terms of the particles which do not reappear in channel a; the resulting expressions for the reaction and total cross-sections in one partial wave are

$$\sigma_{a,r}^{\ell} = \pi \lambda\!\!\!^{-2}_a (2\ell+1)\,(1 - \left|S_{aa}\right|^2);$$

$$\sigma_{a,t}^{\ell} = \sigma_{aa}^{\ell} + \sigma_{a,r}^{\ell} = \pi \lambda\!\!\!^{-2}_a (2\ell+1)\, 2(1 - \mathrm{Re}\, S_{aa}) \tag{4.4}$$

From unitarity, $\left|S_{aa}\right| \leq 1$, so $S_{aa}(E)$ moves inside the unit circle as the energy moves along the real axis; Eq. (4.4) shows exactly how the cross-sections $\sigma(E)$ depend on its path. In particular, they all vanish if $S_{aa} = +1$, and σ_{aa} and σ_t reach their maximum possible values $4\pi \lambda\!\!\!^{-2}(2\ell+1)$ ('unitarity limit') when $S_{aa} = -1$.

4.2. Analyticity and unitarity

The domain of analyticity of the functions $S_{ba}(E)$ will, of course, depend on the type of interaction responsible for the scattering, and, in general,

about all that can be said is that, as in the 1-channel case, 'resonance poles' of S_{ba} cannot occur on the physical sheet, though of course bound-state poles and branch points may. If all the interactions involved in the scattering, within a channel as well as between channels, are cutoff interactions, then just as in the 1-channel case, the $S_{ba}(E)$ will have only 'resonance-pole' (and bound-state pole) singularities, the closest ones to the real axis occurring on the sheets E_a described above. They are in any case likely to be the singularities nearest the real axis, and are the only ones (aside from the threshold branch points) which we shall take into consideration.

Although the $S_{ba}(E)$ are all well-defined everywhere along the real axis, it is only those with both b and a open that contribute to the outgoing flux. Thus in the energy range $\mathscr{E}_N < E < \mathscr{E}_{N+1}$, there are N open channels whose N x N open-channel sub-matrix contains the elements of direct physical interest in this energy range. It is this sub-matrix S^N which must satisfy the important unitarity or flux-conservation condition,

$$S^{N\dagger}(E)\, S^N(E) = 1, \quad \mathscr{E}_N < E < \mathscr{E}_{N+1} \tag{4.5}$$

which is of central importance in describing resonances (whose poles are found on the sheets E_a), for its analytic continuation off the real axis necessarily connects values of S^N on P and on E_N,

$$S^{N\dagger}(E_N^*)\, S^N(E) = 1 \qquad \text{(continued unitarity)} \tag{4.6}$$

with E on the physical sheet.[8] In fact this immediately gives $S^N(E_N)$ in terms of the matrix elements of S on E, as

$$\begin{aligned} S^N(E_N^*) &= [S^{N\dagger}(E)]^{-1} \\ &= \frac{C^N(E)}{D^{N*}(E)} \end{aligned} \tag{4.7}$$

where $D^N(E) = \det [S^N(E)]$ and C^N is the usual matrix of co-factors of $S^{N\dagger}$.

From this we see that the single function (not matrix) $D^N(E)$ plays a central role in the description of resonances, for S^N will have a pole (this is what we mean by a 'resonance pole', though it will signify a resonance only if sufficiently near the physical region) at E^* on sheet E_N whenever $D^N(E)$ has a zero at E on P - and furthermore such a zero will 'cause' poles in all open-channel matrix elements S_{ba} at once, unless by chance (or because of a selection rule) the corresponding $C^N_{ba}(E)$ also vanish at the zero of D^N. A many-channel resonance, in other words, is a property of a resonance 'state', which decays through all open channels unless it happens to be decoupled from one of them. In pole terms, although the pole occurs in all elements of S_{ba}, they will have different residues there, those corre-

[8] We shall consistently use E_N to denote both an entire sheet of the Riemann surface and, when necessary, a particular point on this sheet. Thus E and E_N^* are at complex conjugate positions but on different sheets.

sponding to channels coupled most strongly to the resonance having the largest residues.

The simplest generalization of the pole-zero relation which is responsible for unitarity in the 1-channel case is obtained by taking the determinant of Eq. (4.6) to get

$$D^{N*}(E_N^*)\, D^N(E) = 1 \tag{4.8}$$

so that the poles and zeros of $D^N(E)$ occur in exactly the same pattern as those of the 1-channel S-matrix element (which is its own determinant) (Fig. 12). There is no such relation between the poles and zeros of a single S_{ba}. A pole of $S_{ba}(E)$ on E_N only implies a zero of $D^N(E)$ at the conjugate energy on P; in general, it is not unlikely for at least the diagonal elements S_{aa} to have a zero somewhere in the same neighbourhood, and it will certainly have one near the zero of D^N if most of the partial width of the resonance is in channel a, as we shall see below.

It is quite illuminating to consider the motion of these zeros as a function of the strength of the 'channel coupling'. We shall say that a channel a is decoupled from the rest of the S-matrix if all the off-diagonal elements S_{ba} coupled to a (i.e. one row and one column of S, except for S_{aa}) are zero, and if the remaining elements S_{bc} do not have a branch point at $\mathscr{E}_a$; in this case channel a simply scatters elastically, entirely independently of the others. If we imagine, for instance, that all channels could be decoupled from one another, S would be diagonal and each S_{aa} would have a pole-zero pattern like that of Fig. 12. The way this comes about is through the motion of the zeros, for if a resonance 'belongs' to channel a, the corresponding zero of S_{aa} will move to the position conjugate to the pole in the decoupled limit, whereas the residue of this pole will vanish for all other S_{bb} by their zeros moving directly onto the pole;[9] Fig. 28 shows a few typical examples. In particular if $S_{N+1,N+1}$ has a

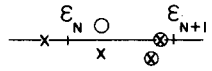

FIG. 28. Poles and zeros of S_{NN} in the limit that it is decoupled from other channels

bound state pole in the decoupled limit, it will sit on the real axis in the physical region of channel N where it is called a 'bound state in the continuum' of this channel, and must certainly be cancelled by a zero (in S_{NN}) in order to prevent an infinite cross-section there. Such bound states in closed channels are of extreme importance in nuclear physics, where (when the channel coupling or 'residual interaction' is turned back on) they are responsible for all 'compound nucleus' resonance levels; they play exactly the same role for the narrow resonances of atomic and of high-energy physics.

It is important to realize that the continued unitarity relation (4.6) defines the analytic continuation of the open-channel S-matrix elements

[9] Following this zero motion 'backwards', starting from the decoupled limit, provides a vivid indication that the principal difference between the 1-channel and many-channel cases derives from the greater freedom of motion enjoyed by the zeros of the S-matrix elements in the latter case.

onto sheet E_N only. On the interval $\mathscr{E}_{N+1} < E < \mathscr{E}_{N+2}$, the next-largest sub-matrix S^{N+1} satisfies a different condition (i.e. Eq. (4.6) with $N \to N+1$), which is the one that provides the continuation onto sheet E_{N+1}, etc. Although the elements of the sub-matrix S^N are thus given continuations onto both E_N and E_{N+1}, the continuations are accomplished via different equations and consequently are, in general, different on the two sheets.

4.3. Resonance poles and resonance circles

From the above discussion we may conclude that if S has a pole on E_N near the real axis between $\mathscr{E}_N$ and $\mathscr{E}_{N+1}$, it is generally reasonable to expect S_{NN} (or any other diagonal element) to have a zero not far away, either on P or on E_N. If this is the case, and if there are no other nearby singularities, we may expect that a reasonable approximation to $S_{NN}(E)$, along the real axis near the pole, will be given by the generalized pole-zero approximation of the 1-channel case,

$$S_{NN}(E) \approx S_B\left(\frac{E - E_z}{E - E_p}\right) \tag{4.9}$$

where S_B is a constant or slowly-varying 'background' factor; E_z and E_p must, of course, be so located that, together with $|S_B|$, they insure that $|S_{NN}| \leq 1$ over the energy range of the approximation.

As was noted in connection with Eq. (4.4), the path followed by the complex number S_{NN} inside the unit circle as E passes over the resonance determines the shapes of the cross-sections in this region, and a simple way of finding this path is to rewrite Eq. (4.9) in the form

$$S_B\left(\frac{E - E_z}{E - E_p}\right) = S_B\left[\frac{E_p^* - E_z}{E_p^* - E_p} + \frac{E_z - E_p}{E_p^* - E_p}\left(\frac{E - E_p^*}{E - E_p}\right)\right] \tag{4.10}$$

which clearly traces out a counter-clockwise circle as E passes along the real axis between E_p and E_p^*.

It is this 'rapid circle' which is the signature of a resonance, as can be seen most convincingly from the associated time-delay of the wave packet. If $E_z = E_p^*$, the circle coincides with the unit circle and describes a rise in the phase shift by π, whose slope $d\delta/dE$ gives the time-delay; the resonance in this case is elastic. If $E_z \neq E_p^*$ the resonance is inelastic, i.e. is coupled to more than one channel; its circle in S_{NN} is then smaller, because part of its 'strength' is in other channels, and the time-delay in this case is determined not by dS_{NN}/dE alone, but by the derivatives of all open-channel elements connected to N. The details were worked out by Smith [11], but the result is the same as in the 1-pole case: in terms of the pole position $E_p = E_0 - i\Gamma/2$, the lifetime of the resonant state is still $1/\Gamma$, so a pole near the real axis corresponds to a narrow, long-lived resonance and produces 'rapid circles' in all S-matrix elements.

In the diagonal elements, the size and position of the circle are often given conveniently in terms of the nearby zero, as in Eq. (4.10). Since its energy-dependent factor becomes unity above and below the resonance,

the circle 'starts' and 'stops' at $S_{NN} = S_B$ and its radius is given in terms of the pole and zero positions by

$$\rho_N = |S_B| \cdot \left| \frac{E_z - E_p}{E_p^* - E_p} \right| \tag{4.11}$$

In Fig. 29 we have defined the two distances

$$\begin{aligned} i\,''\Gamma_r'' &\equiv E_p^* - E_z \\ i\,''\Gamma_N'' &\equiv E_z - E_p \end{aligned} \tag{4.12}$$

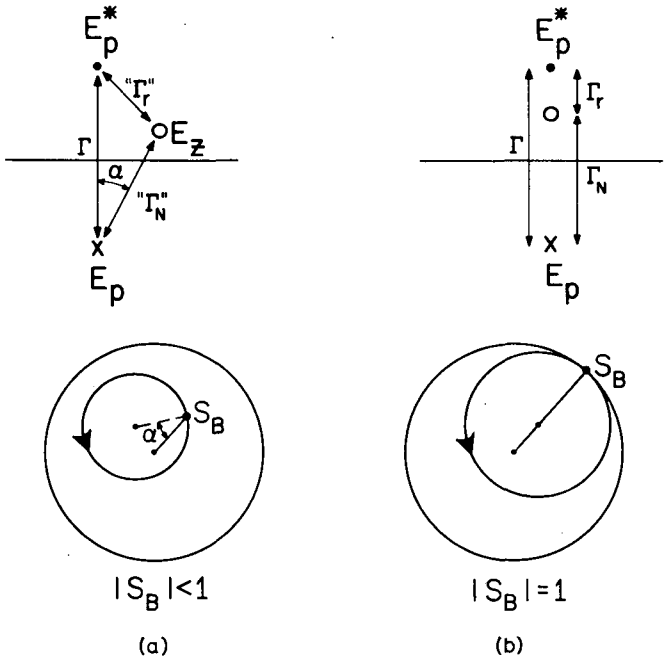

FIG. 29. Resonance circle in a diagonal S-matrix element, together with its pole and zero. (a) Non-elastic background ($|S_B| < 1$) and non-zero tip-angle α. (b) Elastic background ($|S_B| = 1$) with untipped circle

and given them these names, not because their magnitudes are the reaction and elastic widths seen from entrance channel N, but because if it should happen that the background matrix $(S_B)_{ba}$ is diagonal, then (as we show below) $\mathrm{Re}(E_z) = \mathrm{Re}(E_p)$, as in Fig. 29 (b), and $''\Gamma_r''$ and $''\Gamma_N''$ become exactly

these widths. Equation (4.11) then reduces to the familiar Breit-Wigner form for an inelastic resonance,

$$S_{NN}(E) \approx S_B\left[\frac{\Gamma_I}{\Gamma} + \frac{\Gamma_N}{\Gamma}\left(\frac{E - E_p^*}{E - E_p}\right)\right]$$

$$= S_B\left[1 - i\,\frac{\Gamma_N}{E - E_0 + i\Gamma/2}\right] \tag{4.13}$$

In this case the radius of the resonance circle is given simply by

$$\rho_N = \frac{\Gamma_N}{\Gamma} \tag{4.14}$$

the branching ratio for decay of the resonance into channel N, which is also the amount by which the maximal excursion of the total cross-section away from the background is reduced below that for an elastic resonance. We shall find below that this expression is valid independently of the orientation of the zero relative to the pole.

In the Breit-Wigner case, Eq.(4.13), the centre of the circle is at $S_B(\Gamma_I/\Gamma)$, and so lies on the line through the origin and S_B. (Furthermore, E_z is in the upper half-plane (i.e. on P) if $\Gamma_N > \Gamma/2$, on the real axis if $\Gamma_N = \Gamma/2$, and on E_N if $\Gamma_N < \Gamma/2$.) In the more general case (4.10), the circle will be 'tipped' from this orientation by the phase of $(E_z - E_p)/(E_p^* - E_p)$, which is the angle of tip, α, of the zero relative to the pole in Fig. 29(a). This makes the necessary relation between $|S_B|$, E_z and E_p clear: for a given degree of inelasticity of the background, $|S_p|$, the pole and the zero must be so positioned that the entire resonance circle is inside the unit circle. Thus the background in channel N distinctly limits the branching ratio of the resonance into this channel,

$$\frac{\Gamma_N}{\Gamma} \leq \frac{1 + |S_B|}{2} \tag{4.15}$$

and even this limit is permissible only if the angle of tip is zero.

Incidentally, Eq.(4.10) is also often written as

$$S_B\left(\frac{E - E_z}{E - E_p}\right) = S_B\left[1 - \frac{E_z - E_p}{E - E_p}\right]$$

$$= S_B\left[1 - i\,e^{-i\alpha}\,\frac{R}{E - E_p}\right] \tag{4.16}$$

with $R = |E_z - E_p|$, so that the tip angle of the circle is also the 'phase of the resonance relative to the background'. Although it can in general be non-zero, in the special case that the background in channel N is elastic,

$|S_B| = 1$, it is obvious geometrically that α must vanish to satisfy unitarity.[10]

As typical examples of resonance circles and the corresponding cross-sections (angle-integrated, in one partial wave), Fig. 30(a) shows a resonance whose width is 3/4 in channel N, sitting on a background which is elastic, with a phase of -45°. Rather than actual cross-sections the curves are for $|1-S_{NN}|^2$ (el.), $1-|S_{NN}|^2$ (r.) and their sum, $2[1-\mathrm{Re}\,(S_{NN})]$ (tot), for which the unitarity limit is simply 4. Figure 30(b) shows a resonance with $\Gamma_N/\Gamma = 0.5$ and $S_B = +1$. The corresponding circle happens to be the curve along which $\sigma_{NN} \equiv \sigma_{N,r}$ (inside the circle the reaction cross-section is the larger of the two and outside of it the elastic cross-section is the larger), so the total cross-section is just twice as large.

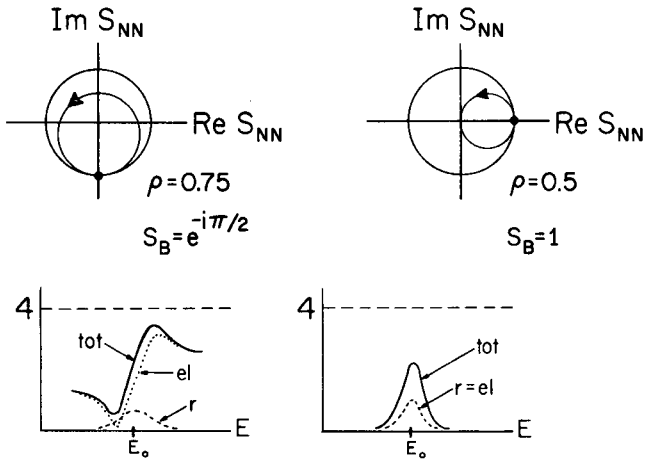

FIG. 30. Resonance circles in a diagonal S-matrix element and the corresponding cross-sections. The background is elastic in both cases

The reason the resonance circles close completely in these examples is that S_B is taken completely independent of energy. Of course, in any realistic situation, the background phase will change somewhat over the width of the resonance; since it is normally a decreasing function of energy, $S_B(E)$ will move slightly clockwise and prevent the resonance circle from closing completely. The broader the resonance, the less the circle will close, and the less of it will be 'visible' in the face of the background. Figure 31 shows a specific 2-channel example, (the details can be found in Ref. [7]) indicating how $S_{11}(E)$ shows a rising-phase behaviour in the neighbourhood of the resonance, followed by a falling-phase behaviour beyond the resonance. As the decay width into channel 1 is decreased, (and the resonance simultaneously broadened) the background phase contribution becomes more and more important, until when $\Gamma_1 \ll \Gamma_2$ the resonance circle is invisibly small and produces no effect on the total cross-section.

[10] Because isobaric analogue resonances often sit on a very inelastic background, α is generally non-zero for them, and it is indeed found that their shapes can be fitted only by the general form of the one-pole approximation (4.16), rather than by the special Breit-Wigner form (4.13).

4.4. Unitary one- and two-pole approximations

The one-pole approximation most commonly used to fit data on isolated resonances is the Breit-Wigner expression,

$$S_{ba}(E) = e^{i(\varphi_a + \varphi_b)} \left[\delta_{ba} - i \frac{\Gamma_b^{1/2} \Gamma_a^{1/2}}{E - E_p} \right] \tag{4.17}$$

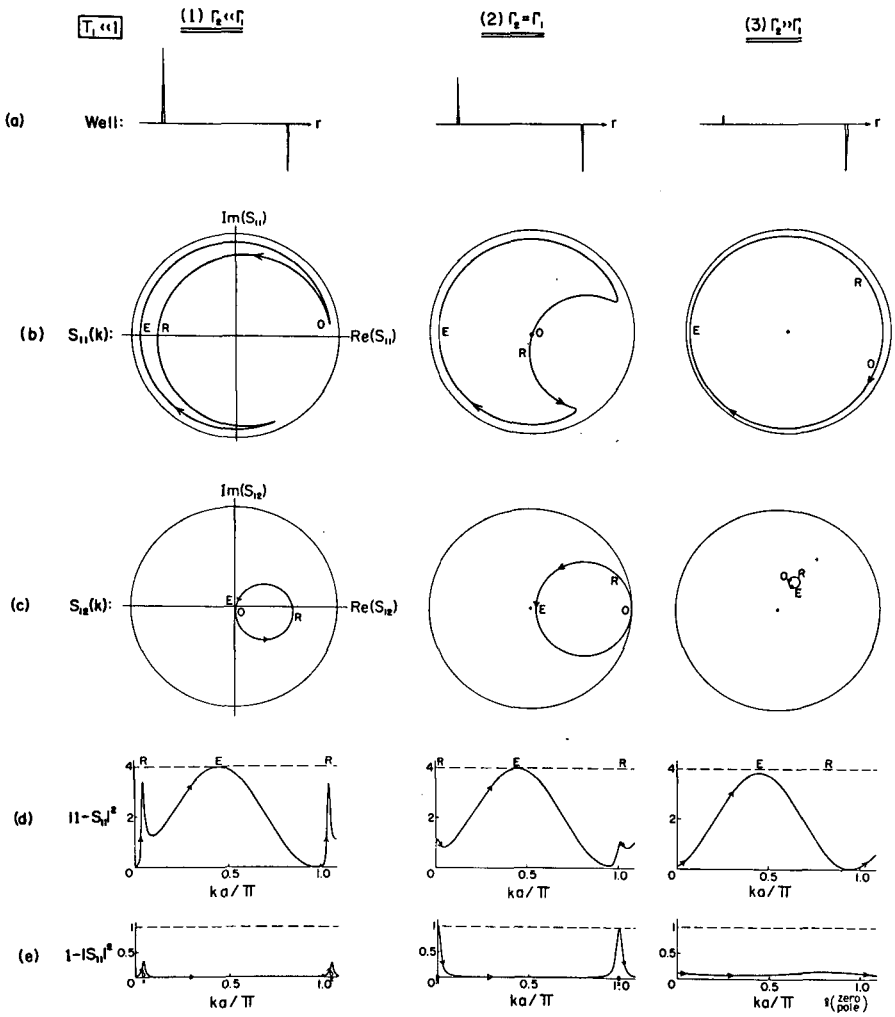

FIG.31. Resonance circles in a two-channel model, indicating how their radii depend on the branching ratios

Provided that $\sum_{\substack{b \\ \text{open}}} \Gamma_b = -2 \text{ Im } (E_p)$, this S-matrix is unitary, as it should be, but it is quite special in having a diagonal background part (hence zero

tip-angles) and so can only describe resonances which sit on an elastic background. Our purpose in this section is to indicate a natural generalization to the case of non-diagonal background (i.e. direct reactions as well as reactions which proceed through the resonance), as well as to the case of two or more overlapping resonances (of the same spin and parity). The derivation used here is an obvious extension of that given by Davies and Baranger [12]; an alternative derivation in terms of eigenchannels is given in Appendix B. We consider N open channels and designate the corresponding NxN matrix simply S(E), with elements $S_{ba}(E)$.

(a) The generalized Breit-Wigner approximation

We consider an isolated resonance far from threshold, by which we mean that S(E) has a pole near the real energy axis between $\mathcal{E}_N$ and $\mathcal{E}_{N+1}$, which in the small energy region around it is the only singularity present, so that for E sufficiently near the pole it is reasonable to approximate S as

$$S(E) = B - i \frac{T}{E - E_p} \tag{4.18}$$

both B and T must be symmetric in order to make S symmetric. T is the matrix of residues at the pole, which has the crucial property of being factorable channelwise, $T = tt^T$, or $T_{ba} = t_b t_a$, where t is a column vector. It is this factorizability of the residues which permits the definition of partial widths for decay of the resonance into the various channels, for the entry t_a is, to within a phase factor, $\Gamma_a^{1/2}$. The factorizability follows directly from the assumption that the pole occurs in only one eigenvalue of S(E) on a given sheet of the energy surface. (This does not assume that the resonance occurs in only one eigenchannel; see Appendix B for a detailed discussion.) The coincidence of poles in two different eigenchannels is not impossible, but is surely highly improbable. We do not consider it further here, but return to it in connection with Eq. (4.39) below. The factorizability of the residues may also be arrived at in quite different ways [2, 12, 13], which are, however, alternative statements of this same assumption.

Equation (4.18) is identical in form to the one-pole approximation to the Humblet-Rosenfeld expansion [2], and our only reason for reconsidering it here is that the relations which are necessary between their background matrix Q and the various poles parameters in order to guarantee the unitarity of S, which in general are extremely complex, become very simple at energies near enough to a specific pole that the net background matrix there (Q plus the faraway poles) can be considered constant.

That is, the exact S-matrix is identically unitary in E, and if we define B (which will in general depend slowly on the energy) so that Eq. (4.18) is the exact S, this requires that

$$B^\dagger(E)B(E) + i\left(\frac{T^\dagger B(E)}{E - E_p^*} - \frac{B^\dagger(E)T}{E - E_p}\right) + \frac{T^\dagger T}{|E - E_p|^2} = \mathbb{1} \tag{4.19}$$

(as well as the adjoint equation) be satisfied identically in E for real E. In particular, if B should happen to be exactly constant across the resonance, Eq. (4.19) requires B itself to be unitary there, so that if B is

nearly constant across the resonance, it must be nearly unitary there. The simplest approximation is obtained by assuming B constant, but a slightly more flexible one is obtained by assuming that, whatever its energy dependence across the resonance, B(E) is identically unitary there (as, for example, in the Breit-Wigner approximation with slowly-varying but real phases φ_a). This is the crux of the present approximation, which greatly simplifies the unitarity condition (4.19).

To see how, we recall that since B is both unitary and symmetric, its eigenvectors can be chosen real,[11] so that B can be diagonalized by a real orthogonal matrix V (the matrix of eigenvectors): $V^T B\, V = \exp 2i\beta$, or $(\exp -i\beta)V^T B\, V\, (\exp -i\beta) = \mathbb{1}$, where $\exp 2i\beta$ is the diagonal matrix of eigenvalues of B, $(\exp 2i\beta)_{ba} = \delta_{ba} \exp 2i\beta_a$. It is convenient to consider the transform of S(E) itself by the nearly-constant matrix $\exp -i\beta V^T$.

$$\begin{aligned} \hat{S}(E) &\equiv e^{-i\beta} V^T S(E)\, V\, e^{-i\beta} \\ &= \mathbb{1} - i \frac{\Gamma}{E - E_p} u\, u^T \end{aligned} \tag{4.20}$$

$$\text{with} \quad u = \Gamma^{-1/2} (e^{-i\beta} V^T t)$$

Although this transformation is not unitary, one readily verifies that if S is unitary and symmetric, $\hat{S}$ is as well, so we require $\hat{S}(E)$ to be unitary for E real. Since by inspection u is seen to be an eigenvector of $\hat{S}$, it can be chosen real,[12]

$$u^* = u \tag{4.21}$$

and one then readily verifies that the $\hat{S}(E)$ of Eq. (4.20) is indeed unitary, provided that in addition u has unit normalization,

$$\begin{aligned} u^T u &= 1 \\ \text{or} \quad \Sigma u_b^2 &= 1 \end{aligned} \tag{4.22}$$

This is just the requirement that the sum of the partial widths equal the total width, for, transforming from $\hat{S}$ back to S, we can write S in terms of u, V and $\exp i\beta$ as

$$\begin{aligned} S(E) &= V\, e^{2i\beta} V^T - i \frac{\Gamma}{E - E_p} (V e^{i\beta} u)(V e^{i\beta} u)^T \\ \text{or} \quad S_{ba}(E) &= B_{ba} - i \frac{e^{i\varphi_b} \Gamma_b^{1/2}\, \Gamma_a^{1/2} e^{i\varphi_a}}{E - E_0 + i\Gamma/2} \end{aligned} \tag{4.23a}$$

---

[11] If ν is an eigenvector of B, $B\nu = \lambda\nu$, then $B^* \nu^* = B^{-1} \nu^* = \lambda^* \nu^* = \lambda^{-1} \nu^*$ since $BB^* = 1$, so $B\nu^* = \lambda\nu^*$; hence $(\nu + \nu^*)$, which is real, is also an eigenvector.

[12] That is, $e^{i\beta} V^T t$ is real. This implies a specific relation between the phases of the residues of the S_{ba} and the eigenphases of B; the Breit-Wigner approximation provides a particularly simple example. It is worth noting that the residue of $\hat{S}(E)$ at E_p is not $-i\Gamma u\, u^T$, but the analytic continuation of this expression to the pole, where it is in general not pure imaginary.

$$\text{with } B_{ba} = \sum_c V_{bc}\, e^{2i\beta_c} V_{ac} \tag{4.23b}$$

$$e^{i\varphi_a}\, \Gamma_a^{1/2} = \Gamma^{1/2} \sum_c V_{ac} e^{i\beta_c}\, u_c \tag{4.23c}$$

and $$\Sigma \Gamma_a = \Gamma (u^T e^{i\beta}\, V^T V\, e^{i\beta} u) = \Gamma$$

V is real and orthogonal, and the u_c and β_c are real.

This is the desired generalization[13] of the Breit-Wigner expression. It agrees with the one-pole R-matrix approximation [14], is unitary for all real E, and reduces to the Breit-Wigner expression if B is diagonal, i.e. if $V = \mathbb{1}$. Whereas with N open channels the Breit-Wigner approximation contains $(2N+1)$ real parameters, Eq. (4.23a) contains in addition the $N(N-1)/2$ parameters specifying V (which account for the off-diagonal elements of B), making $(N^2/2 + 3N/2 + 1)$ altogether, e.g. 6 parameters for $N = 2$, 10 for $N = 3$, 15 for $N = 4$.

It is perhaps worthwhile writing out the $N = 2$ case explicitly. The real orthogonal V can be written in terms of a single parameter λ, as

$$V = \begin{pmatrix} \cos\lambda & -\sin\lambda \\ \sin\lambda & \cos\lambda \end{pmatrix}$$

in terms of which

$$B = \begin{bmatrix} \cos^2\lambda\, e^{2i\beta_1} + \sin^2\lambda\, e^{2i\beta_2} & \cos\lambda \sin\lambda\, (e^{2i\beta_1} - e^{2i\beta_2}) \\ \cos\lambda \sin\lambda\, (e^{2i\beta_1} - e^{2i\beta_2}) & \sin^2\lambda\, e^{2i\beta_1} + \cos^2\lambda\, e^{2i\beta_2} \end{bmatrix} \tag{4.24}$$

and

$$e^{i\varphi_1}\, \Gamma_1^{1/2} = \Gamma^{1/2} (\cos\lambda\, e^{i\beta_1} u_1 - \sin\lambda\, e^{i\beta_2} u_2)$$
$$e^{i\varphi_2}\, \Gamma_2^{1/2} = \Gamma^{1/2} (\sin\lambda\, e^{i\beta_1} u_1 + \cos\lambda\, e^{i\beta_2} u_2)$$

S(E) depends on the six real parameters u_1, u_2, E_0, β_1, β_2, and λ; more physically, they are equivalent to Γ_1, Γ_2, E_0 and three parameters for the background B.

The point of writing S(E) in the form (4.24) is that it is guaranteed unitary for any values of these real parameters which satisfy $u_1^2 + u_2^2 = 1$. On the other hand, it is awkward that none of these parameters are quantities which are directly measured, and that values must be assumed for all of them, even to fit data which are available in only one channel.

---

[13] Since the residue of $S_{aa}(E)$ at E_p is $(\exp 2i\beta_a)\, \Gamma_a$, it would appear from Eq. (4.23d) that the sums of the absolute values of the residues of the diagonal elements of S must identically be Γ. This is inexact to the extent that B, which we have assumed unitary at $E = E_r$, is not precisely unitary.

Consequently for the practical analysis of data it is perhaps preferable to write Eq.(4.23) in the more conventional form

$$S(E) = B - i\frac{tt^T}{E - E_p} \qquad (4.25a)$$

$$\text{or} \qquad S_{ba}(E) = B_{ba} - i\frac{t_b t_a}{E - E_p}$$

In this case no reference is made at all to the real parameters V_{ba}, β_a, and u_a, which are replaced by the more physical complex parameters B_{ba} and t_a themselves; here t is the complex column vector with entries

$$t_a = e^{i\varphi_a}\Gamma_a^{1/2} \qquad (4.25b)$$

The above expression for S is of course not unitary in general, but will be so if B and t satisfy the additional constraints (equivalent to Eqs.(4.23b) and (4.23c); cf. Ref. [14])

$$BB^\dagger = B^\dagger B = 1 \qquad (4.25c)$$

$$t^\dagger t = \sum_a \Gamma_a = \Gamma \qquad (4.25d)$$

and $Bt^* = t$

$$\text{i.e.} \quad \sum_c B_{bc} e^{i\varphi_c} \Gamma_c^{1/2} = e^{i\varphi_b}\Gamma_b^{1/2} \qquad (4.25e)$$

As is to be expected, these unitarity conditions can be checked only if data are available in all open channels.

The practical problem of fitting data with Eq.(4.25a) can be greatly facilitated by using the fact that the trajectory of each $S_{ba}(E)$ as the energy passes over the resonance is simply a circle, for the parameters which determine the size and orientation of the circle are precisely the ones which occur in Eq.(4.25). This is best seen by rewriting Eq.(4.25a) in the form

$$S_{ba}(E) = \left[B_{ba} - \frac{t_b t_a}{\Gamma}\right] + \frac{t_b t_a}{\Gamma}\left(\frac{E - E_p^*}{E - E_p}\right)$$

which exhibits the resonance circle more explicitly. Its radius is given directly in terms of the branching ratios as

$$\rho_{ba} = \frac{|t_b t_a|}{\Gamma} = \frac{(\Gamma_b \Gamma_a)^{1/2}}{\Gamma} \qquad (4.26)$$

i.e. the absolute value of the residue divided by the total width (whether the background is elastic or not, in agreement with Eq.(4.14). The centre of the circle is at $(B_{ba} - t_b t_a)$, so that its tip-angle (Fig.29) is

$$\alpha_{ba} = \varphi_b + \varphi_a - 2\bar{\varphi}_{ba} \qquad (4.27)$$

where $2\bar{\varphi}_{ba}$ is the phase of B_{ba}.

A typical resonance trajectory is shown in Fig. 32, indicating how the slow motion of the background term is interrupted by the rapid counter-clockwise resonance circle, which would have started and stopped at the point B_{ba} if the background had been completely constant across the resonance. Consequently, if the experimental $S_{ba}(E)$ - trajectory is available

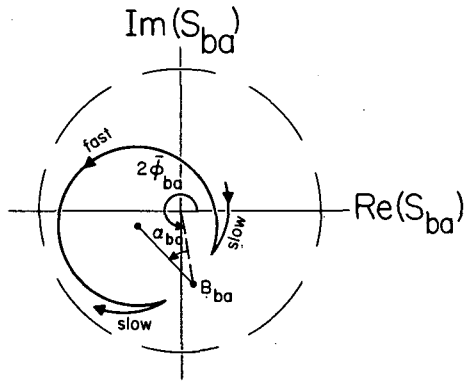

FIG. 32. Typical inelastic resonance circle ("fast") superimposed on an inelastic background, with a positive tip-angle α_{ba}. The 'gap' in the circle measures the change in the background across the bandwidth of the resonance

from a phase shift analysis, B_{ba}, α_{ba} and ρ_{ba} can be obtained from it geometrically,[14] which is extremely convenient, for Eq. (4.25a) can be written directly in terms of them, as

$$S_{ba}(E) = B_{ba} - i\, e^{i(\varphi_b + \varphi_a)} \frac{\Gamma_b^{1/2}\Gamma_a^{1/2}}{E - E_p} \tag{4.28a}$$

$$= e^{2i\bar{\varphi}_{ba}}\left[\,|B_{ba}| - i\, e^{i\alpha_{ba}} \frac{\Gamma_b^{1/2}\Gamma_a^{1/2}}{E - E_p}\right] \tag{4.28b}$$

$$= e^{2i\bar{\varphi}_{ba}}\left[\,|B_{ba}| - i\, e^{i\alpha_{ba}} \frac{\rho_{ba}\Gamma}{E - E_p}\right] \tag{4.28c}$$

These parameters being known, only E_0 and Γ remain to be found by fitting Eq. (4.28) to the data.

Equation (4.28) is doubtless the most convenient form of the approximation for practical curve-fitting. It (especially Eq. (4.28b)) is very similar in form to the Breit-Wigner expression (4.17), but contains the two extra parameters $|B_{ba}|$ and α_{ba} to allow the background to be inelastic and the residue to have a different phase from the background. Precisely because of these parameters, however, it is slightly more 'dangerous' than the Breit-Wigner approximation, in the following sense. Provided only that $\Gamma_a \leq \Gamma$ for each channel, each Breit-Wigner S-matrix element satisfies $|S_{ba}| \leq 1$, i.e. has a trajectory which remains entirely within

[14] We emphasize that the sign of α_{ba} is significant, and, as defined in (4.27) is positive in Fig. 32.

the unit circle, in accord with the minimal requirement of unitarity. Once a non-zero tip angle α_{ba} is allowed, however, it is very easy for the resonance circle to cross the unit circle if α_{ba} is chosen too large. Of course, this is guaranteed not to happen if all the unitarity conditions (4.25c through 4.25e) are satisfied, but these can only be imposed if data are available in all open channels. When working with only one or a few channels, any fit to Eq.(4.28) should at least be checked to see that $|S_{ba}|^2 \leq 1$ is satisfied along each trajectory. Incidentally, other obvious consistency checks on the geometrical parameters are

$$(\alpha_{aa} - 2\bar{\varphi}_{aa}) + (\alpha_{bb} - 2\bar{\varphi}_{bb}) = 2(\alpha_{ba} - 2\bar{\varphi}_{ba}) \tag{4.29a}$$

$$\rho_{bb}\,\rho_{aa} = \rho_{ba}^2 \tag{4.29b}$$

and

$$\Sigma\,\rho_{aa} = 1 \tag{4.29c}$$

the last being the geometrical condition that the set of all resonance circles for the diagonal matrix elements should fit exactly on a diameter of the unit circle (Fig. 33).

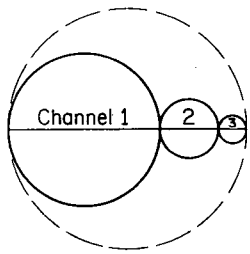

FIG. 33. Diagonal-element resonance circles

Regarding further properties of Eq.(4.28) in the complex energy plane, the position of the zero of $S_{ba}(E)$ is given by

$$E_z^{ba} - E_p = i\,\frac{e^{i(\varphi_b + \varphi_a)}}{B_{ba}}\,(\Gamma_b\Gamma_a)^{1/2} \tag{4.30}$$

so that Eq.(4.27) implies that α_{ba} is also the tip-angle of the zero relative to the pole (Fig. 29), in agreement with what we found above for the diagonal elements. If B is made diagonal, the zeros of the off-diagonal elements move off to infinity. As for the diagonal-element zeros, $B_{aa} = \sum_c V_{ac}^2\, e^{2i\delta_c}$, so that

$$|B_{aa}| \leq \sum_c V_{ac}^2 = 1 \tag{4.31}$$

and consequently

$$|E_z^{aa} - E_p| \geq \Gamma_a \tag{4.32}$$

the equality holding only in the Breit-Wigner case, when $V_{ac} = \delta_{ac}$ and the zero is directly above the pole.

As for the effect of penetration factors, we note briefly that at the N-th threshold we must have

$$S_{Na} = 0, \quad a \neq N$$

$$S_{NN} = 1$$

This can be achieved by requiring

$$V_{Na} = 0, \quad a \neq N$$

$$V_{NN} = 1$$

$$\beta_N = 0$$

and

$$u_N = 0$$

For the rates at which these limits are approached, and a general discussion of threshold effects, see Davies and Baranger [12].

In summary, the requirement that a one-pole approximation to S have a unitary background term and itself be identically unitary in E leads directly to the general result (4.23), whose resonance circles (extrapolated if necessary) pass through the points B_{ba}, have finite tip-angles, and are described by Eqs. (4.26), (4.27) and (4.28). In the special case that B is diagonal, the tip-angles become zero and Eq. (4.23) reduces to the Breit-Wigner approximation.

(b) The two-level approximation

If two resonances of the same spin and parity overlap, but are far from other resonances and from thresholds, the energy-dependence of S will be dominated by two poles rather than one. Putting them over a common denominator, its matrix elements can always be written, in this energy range, in the form

$$S_{ba}(E) = S_B\left(\frac{E - \hat{E}_1}{E - E_1}\right)\left(\frac{E - \hat{E}_2}{E - E_2}\right) \tag{4.33}$$

with poles at the complex energies E_1 and E_2 and zeros (which depend on b and a) at $\hat{E}_1$ and $\hat{E}_2$. The resulting S-trajectory is more complicated than a single circle and may, under certain conditions described below, be composed of two circles, one for each resonance.

(b.1) Poles in different eigenchannels of $\hat{S}(E)$: Such resonances can occur in two ways, depending on whether the two poles are in the same or in different eigenvalues of $\hat{S}(E)$. The latter, which would a priori appear more likely, corresponds to an S of the form

$$\begin{aligned} S(E) &= B - i\,\frac{T_1}{E - E_1} - i\,\frac{T_2}{E - E_2} \\ &= B - i\,\frac{t_1 t_1^T}{E - E_1} - i\,\frac{t_2 t_2^T}{E - E_2} \end{aligned} \tag{4.34}$$

We again assume B unitary and consider the transformed matrix,

$$\begin{aligned}\hat{S}(E) &\equiv e^{-i\beta} V^T S(E)\, V e^{i\beta} \\ &= \mathbb{1} - i\frac{\Gamma_1}{E-E_1} u_1 u_1^T - i\frac{\Gamma_2}{E-E_2} u_2 u_2^T\end{aligned} \tag{4.35}$$

If u_1 and u_2 are constant, it is readily verified that this matrix can be identically unitary in E only if u_1 and u_2 are real and satisfy[15]

$$\begin{aligned}u_1^T u_1 &= u_2^T u_2 = 1 \\ u_1^T u_2 &= 0\end{aligned} \tag{4.36}$$

in which case they are, of course, eigenvectors of $\hat{S}$. (Furthermore, as in the one-pole case, $\hat{S}(E)$ is even unitary for energy-dependent u's, provided they satisfy Eq.(4.36) at each real energy.) Assuming this to be true, we can again transform back to S, obtaining

$$S(E) = B - i\frac{t_1 t_1^T}{E-E_1} - i\frac{t_2 t_2^T}{E-E_2} \tag{4.37a}$$

which is unitary provided $t_j = V(\exp i\beta)u_j$, i.e.

$$B^\dagger B = BB^\dagger = 1 \tag{4.37b}$$

$$Bt_1^* = t_1, \quad Bt_2^* = t_2 \tag{4.37c}$$

and

$$t_i^\dagger t_j = \Gamma^i \delta_{ij} \tag{4.37d}$$

The last is the rather remarkable statement that S can have the form (4.37a), with overlapping resonances and unitary background, only if the 'partial width vectors' t_1 and t_2 of the two resonances are orthonormal. If the matrix B happens to be diagonal, V = 1 and Eq.(4.37a) reduces to the 'double Breit-Wigner form',

$$S_{ba}(E) = e^{i(\varphi_b + \varphi_a)}\left[\delta_{ba} - i\frac{(\Gamma_b^1\Gamma_a^1)^{1/2}}{E-E_1} - i\frac{(\Gamma_b^2\Gamma_a^2)^{1/2}}{E-E_1}\right] \tag{4.38a}$$

with

$$\sum_a (\Gamma_a^i \Gamma_a^j)^{1/2} = \delta_{ij}\ \Gamma^j \tag{4.38b}$$

Since the same background matrix suffices for both resonances, this expression contains only (N+1) more real parameters than the 1-pole formula, making $N^2/2 + 5N/2 + 2$ in all. Even so, this number of para-

[15] A more detailed discussion is given in Appendix B.

meters is large enough (9, 14 and 20 for N = 2, 3 and 4) to make their extraction from the experimental data seem quite difficult in general. Unfortunately, the shapes of the S(E)-trajectories may not be of great help in the two-pole case, for each pole corresponds to a circle, and two superimposed 'simultaneous' circles can produce a wide variety of curves.

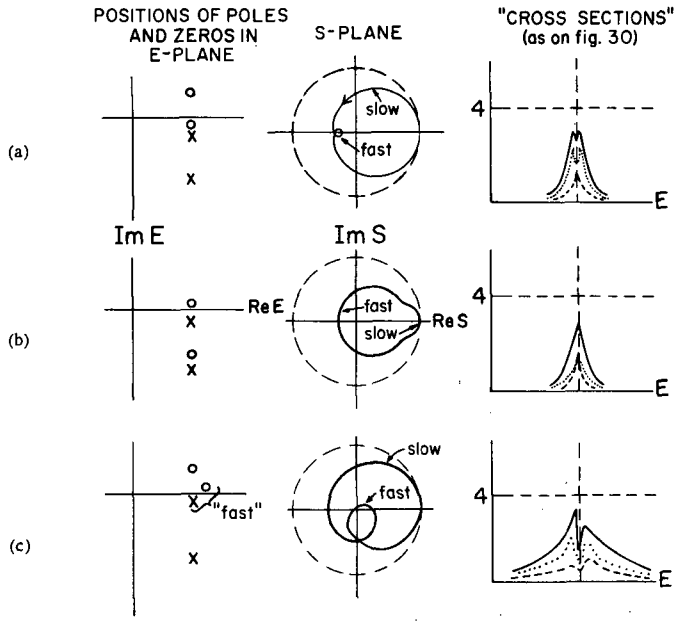

FIG. 34. Superimposed broad and narrow resonances of different inelasticities, showing pole-zero pairs and complex-plane trajectories of S_{aa}, together with corresponding cross-sections. See text for details

There are, however, two extremes in which the shape of the trajectory given by Eq. (4.37a) is readily interpreted. The first is the case in which one of the overlapping resonances is much broader than the other, since then the broad one in effect acts as a background for the narrow one. This is illustrated by a few examples for a diagonal element S_{aa} in Fig. 34, parametrized merely by the pole and zero positions, Eq. (4.33), with $S_B = 1$ for simplicity. In Fig. 34(a) a very inelastic (relative to this channel) narrow resonance is superimposed on the centre of a more elastic broad one, both untipped, and in Fig. 34(b) a nearly elastic narrow resonance sits on the centre of a very inelastic broad one, again both untipped to give symmetry of the cross-section about the central energy. Note that if the effective background, $S'_B \approx (E_2 - \hat{E}_1)/(E_2 - E_1)$, provided by the broad resonance (1) for the narrow one (2) is inelastic, the radius of the narrow one's circle is reduced below $(\hat{E}_2 - E_2)/\Gamma_2$ by the factor $|S'_B|$, in agreement with Eqs. (4.26) and (4.29). In Fig. 34(c), a narrow, inelastic, tipped resonance is superimposed on the centre of a broad, fairly elastic, untipped one, producing cross-sections similar to those of Fig. 34(a), but with symmetric wings and an asymmetric centre.

The other simple extreme of Eq. (4.37a) is that in which the resonances in the two eigenchannels 'overlap completely', i.e. when their two poles

occur at exactly the same complex energy, so that the resonances not only have equal energies but also equal widths. In this remarkable (and unlikely) event, the pole does not become double. A single, simple pole remains in S, but with the unusual property that its residue does not factor channel-wise, for S becomes

$$S(E) = B - i \frac{t_1 t_1^T + t_2 t_2^T}{E - E_1} \tag{4.39}$$

Thus each $S_{ba}(E)$ follows a single-circle path, and the resonance differs from a normal single-pole resonance only in the unusual relations between the various $S_{ba}(E)$ trajectories. In particular, the relations (4.29) will fail, for partial widths defined in the usual way simply do not exist. This extreme is not of great practical interest for its own sake, but it does imply the important result that as two poles in different eigenchannels of $\hat{S}$ are moved toward one another the resulting S(E)-trajectories tend toward a single circle (unless at the same time their residues tend to cancel, $t_1 t_1^T \to - t_2 t_2^T$).

(b.2) Both poles in the same eigenchannel of S(E): The above single circle is to be contrasted with the trajectory produced by the other possibility for the two-resonance case, that in which both poles occur in the same eigenvalue of $\hat{S}(E)$. In this event S(E) has the form

$$S(E) = B - i A(E) \frac{t\, t^T}{(E - E_1)(E - E_2)} \tag{4.40}$$

Although the residues now certainly factor at each pole, the numerator of the second term is necessarily energy-dependent, for in this case

$$\hat{S}(E) = \mathbb{1} - i \frac{A(E)}{(E - E_1)(E - E_2)} u\, u^T \tag{4.41}$$

and the condition that a matrix of the general form

$$\mathbb{1} - iF\, u\, u^T$$

(with F a number, not a matrix, and $u^T u = 1$) be unitary is that u be real, and

$$2\,\mathrm{Im}\,(F) = - |F|^2$$

This requires $A(E) = \Gamma^1(E - E_{02}) + \Gamma^2(E - E_{01})$, if $E_1 = E_{01} - i\,\Gamma^1/2$ and $E_2 = E_{02} - i\,\Gamma^2/2$, so that

$$\hat{S}(E) = \mathbb{1} - i \frac{\Gamma^1(E - E_{02}) + \Gamma^2(E - E_{01})}{(E - E_1)(E - E_2)} u\, u^T \tag{4.42}$$

which is more neatly written as

$$\hat{S}(E) = \mathbb{1} + \left\{\left(\frac{E - E_1^*}{E - E_1}\right)\left(\frac{E - E_2^*}{E - E_2}\right) - 1\right\} u u^T \tag{4.43}$$

Transforming back to S, it is expressed in terms of $\exp i\beta$, V, and u as

$$S(E) = B + \left\{\left(\frac{E - E_1^*}{E - E_1}\right)\left(\frac{E - E_2^*}{E - E_2}\right) - 1\right\} \tilde{t}\,\tilde{t}^T \tag{4.44a}$$

with $\tilde{t} = Ve^{i\beta}u$, i.e.

$$\begin{aligned} B^\dagger B &= BB^\dagger = 1 \\ B\tilde{t}^* &= \tilde{t} \end{aligned} \tag{4.44b}$$

and

$$u^T u = \tilde{t}^\dagger \tilde{t} = \sum_a |\tilde{t}_a|^2 = 1 \tag{4.44c}$$

The numbers $|\tilde{t}_a|^2$ are to be regarded as dimensionless partial widths, and remarkably enough play the same role for both resonances. Although, of course, they may vary somewhat between the resonances, they will normally be nearly the same at the two resonance energies E_{01} and E_{02}, meaning that in this case the distribution of partial widths over the channels is the same for both resonances. (The two total widths, on the other hand, are unrelated.) This implies very distinctive S-trajectories, as is best seen by writing Eq.(4.44a) in terms of channel labels,

$$S_{ba}(E) = B_{ba} - \tilde{t}_b \tilde{t}_a + \left(\frac{E - E_1^*}{E - E_1}\right)\left(\frac{E - E_2^*}{E - E_2}\right)\tilde{t}_b \tilde{t}_a \tag{4.45}$$

Since the last term has absolute magnitude $|\tilde{t}_b \tilde{t}_a|$ for all real E, the trajectory followed by this matrix element as E passes over the two resonances is made up of two circles of (nearly) the same radius, $|\tilde{t}_b \tilde{t}_a|$, and (nearly) the same centre, $(B_{ba} - \tilde{t}_b \tilde{t}_a)$ -- a trajectory readily distinguished from those of Eq.(4.37), whose poles are in different eigenchannels. For instance, if the two poles were at the same place, $E_1 = E_2$, Eq.(4.45) would execute two successive, superimposed circles at uniform 'speed', in contrast to the single circle of Eq.(4.37) when $E_1 = E_2$. If the two resonances in Eq.(4.45) have very different widths, on the other hand, the slow circle of the broad one will be interrupted by the fast circle of the narrow one (somewhat as in Fig. 34), but both will run 'on the same track'. The tip angle of the double circle is in any event given by Eq.(4.27), where φ_b and φ_a are the phases of $\tilde{t}_b$ and $\tilde{t}_a$. Also, the number of free parameters in Eq.(4.41) is only $N^2/2 + 3N/2 + 2$.

If the background matrix B is diagonal, Eq.(4.45) again reduces to a Breit-Wigner-like form,

$$S_{ba}(E) = e^{i(\varphi_b + \varphi_a)}\left[\delta_{ba} + \left\{\left(\frac{E - E_1^*}{E-E_1}\right)\left(\frac{E - E_2^*}{E - E_2}\right) - 1\right\} |\tilde{t}_b\tilde{t}_a|\right] \tag{4.46}$$

$$\Sigma\, |\tilde{t}_a|^2 = 1$$

5. ANALYTICITY AND NUCLEAR REACTION CALCULATIONS

Although it is too large and too active a subject to be discussed in detail here, a few brief remarks may be in order on shell model calculations in the continuum. In a customary shell model calculation for bound levels, the Hamiltonian is written as $H = H_0 + V$, with H_0 the single-particle average Hamiltonian and V the sum of two-body residual interactions. H_0 describes the 'unperturbed' system, and the purpose of the calculation is to see how a set of its degenerate or nearly-degenerate bound-state poles is split and moved to 'perturbed' positions along the real energy axis as V is turned on. In the corresponding scattering problem, in which such a calculation is extended to energies above a particle emission threshold, the most obvious difference is that the poles are no longer confined to the real axis, but can wander in two dimensions, and the purpose of this calculation is to predict the positions in the complex plane to which they move as V is turned on[16], i.e. the widths as well as the energies of the resonances.

Perhaps a more fundamental distinction is that in the scattering problem V also has the effect of coupling channels which in the limit $H = H_0$ are uncoupled. That is, H_0 describes the scattering of a single particle by a static target, whose possible states of internal excitation (the various configurations of the nucleons of the target nucleus) specify the channels of this single-particle problem. H_0 by definition cannot connect these channels, but turning on V, which allows the incident particle to interact individually with those of the target, does so, in this way enabling the projectile to excite states of the target (many-particle configurations), and so undergo inelastic as well as elastic scattering.

An elementary example can perhaps make this clearest. Consider a system whose 'compound nucleus' or 'intermediate state' consists of two particles in a potential well, which for simplicity has only two levels. It is perhaps clearest to take the zero of energy at the bottom of the well (of depth V_0), with the levels at energies E_1 and E_2 above it; it is important for our purpose to choose

$$E_2 - E_1 > V_0 - E_2 \tag{5.1}$$

If one of the particles is thought of as a projectile, we have a two-channel scattering problem, with the channels specified, in the limit of vanishing interaction between the two particles, by the level in which the target particle is found. With our choice of zero the lower threshold

[16] In the scattering problem V continues to mean the sum of all two-body interactions, including the incident nucleon as well as those in the target.

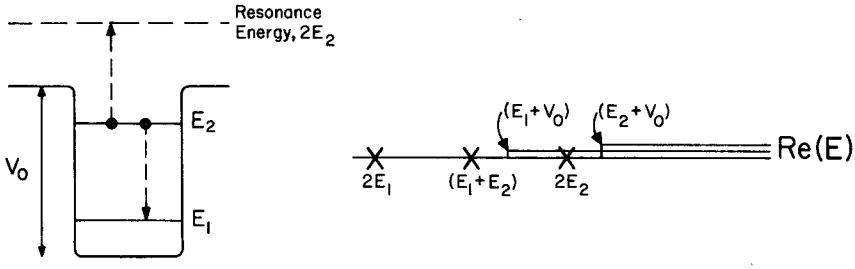

FIG. 35. 2-particle, 1-hole (Auger) resonance and corresponding pole positions in the limit of no residual interaction

corresponds to one particle (target) at energy E_1 and the other (projectile) at V_0, giving threshold energy $\mathcal{E}_1 = E_1 + V_0$; similarly the second threshold, corresponding to scattering on an excited target, is at $\mathcal{E}_2 = E_2 + V_0$. With no 'residual interaction' between the particles, the problem has two true bound states, at $2E_1$ and $E_1 + E_2$, both in the lower channel (i.e. with the target particle in E_1), as well as a bound state in the upper channel, at $2E_2$, which because of Eq. (5.1) is above the lower threshold but below the upper one.

This is an example of the 'bound state in the continuum' mentioned in section 4, for with no residual interaction (i.e. no channel coupling), its energy $2E_2$ is real and directly in the lower channel continuum, so the residue of the corresponding pole must be zero for S_{11} and S_{21} (but, of course, not for S_{22}). This merely means, physically, that the state with two particles in the upper level, though energetically capable of emitting one particle by allowing the other to drop into the lower level, is dynamically incapable of doing so if there is no coupling between the particles. In atomic physics this is, of course, known as an Auger or auto-ionizing state, and in nuclear physics is called a 2-particle 1-hole state (the 'hole' of the target being in level E_1). In the $V = 0$ limit it can be thought of as a resonance of zero width (technically, the channel 1 phase shift has a discontinuous, and thus unobservable, jump of π at this energy), for if V is 'turned on' slightly, the state can decay into channel 1 and the pole will correspondingly move off the real axis (with width proportional to V^2 for small V). Looked at the other way, a projectile incident on the target in its ground state will, at bombarding energy $2E_2 - E_1 - V_0$, be able to excite the 2-particle 1-hole intermediate state and so will see a narrow resonance caused by this closed channel state (see Fig. 35).

Of course, if the potential well has a barrier (centrifugal and/or Coulomb) at its edge, it can also have single-particle resonances (whose poles are off the real axis even when $V = 0$), and they together with the many-particle bound states in closed channels provide the only two known resonance mechanisms. Consequently a shell model calculation in the continuum may be characterized by a pole diagram which in the independent particle limit has a few poles off the real axis (single-particle states, of low level density) and many on it (many-particle states, high level density). When the residual interaction V is turned on, the many-particle poles move down off the real axis as their configurations absorb some single-particle admixture from nearly single-particle poles, and the single-particle states move correspondingly toward the real axis as they become diluted with

many-particle or closed-channel configurations. The principal fascination of the sport is in observing the interactions between the poles as they move, for the familiar second-order repulsion of poles along the real direction is readily seen to become an attraction along the imaginary direction, and the combination of the two leads to quite complicated pole trajectories.

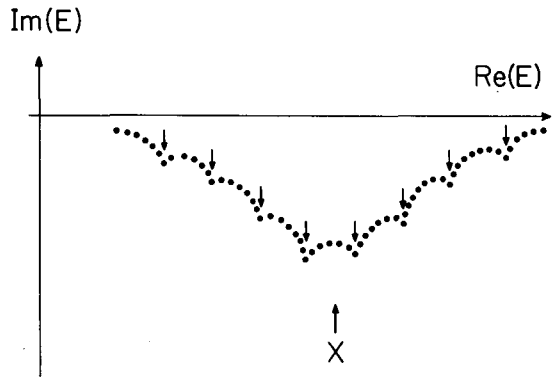

FIG. 36. Lane-Thomas-Wigner giant resonance in the total widths of compound levels, with superimposed intermediate structure and doorway states (arrows)

One interesting configuration which can result is a trough-shaped string of many-particle poles pulled down from the real axis by an isolated single-particle pole (Fig. 36), which is the complex-plane description of a Lane-Thomas-Wigner giant resonance. If in addition V couples some of the many-particle states ('doorway states') to the continuum more strongly than others, the corresponding poles will get ahead of their many-particle neighbours in the general downward motion, at least for small V, thus superimposing an 'intermediate structure' on the overall giant resonance indicated schematically by the scallops in Fig. 36. The ramifications and subtleties which these and similar phenomena can be expected to produce should make the next few years interesting ones indeed, as the calculational techniques for following such pole motions are developed. The subject is clearly too large and complex to be treated in detail here, but many of its facets are treated in the publications listed in Ref. [16].

ACKNOWLEDGEMENTS

It is a pleasure to express thanks to the many colleagues with whom this material has been discussed over the years, and from whom I have learned a great deal about the mysterious depths of the complex energy plane. Special thanks are due to C. J. Goebel, but I am also much indebted to A. M. Bincer, L. Durand, III, and L. Heller.

REFERENCES

[1] NEWTON, R. G., J. math. Phys. 1 (1960) 319, reprinted in Quantum Scattering Theory (ROSS, M. H., Ed.) Indiana Univ. Press, Bloomington, Ind. (1963); J. math. Phys. 2 (1961) 188.

[2] HUMBLET, J., ROSENFELD, L., Nucl. Phys. 26 (1961) 529.

[3] NEWTON, R.G., Scattering Theory of Waves and Particles, McGraw-Hill, New York (1966).
[4] GOLDBERGER, M.L., WATSON, K.M., Collision Theory, Wiley, New York (1964).
[5] WIGNER, E.P., Phys. Rev. 98 (1955) 145.
[6] LEVINSON, N., Kgl. Danske Videnskab. Selskab, Mat. fys. Medd. 25 (9) (1949).
[7] McVOY, K.W., HELLER, L., BOLSTERLI, M., Rev. mod. Phys. 39 (1967) 245.
[8] FERREIRA, E.M., TEIXEIRA, A.F.F., J. math. Phys. 7 (1966) 1207.
[9] BELL, J.S., GOEBEL, C.J., Phys. Rev. 138 (1965) B1198.
[10] LYNN, J.E., Proc. Int. Conf. Study of Nuclear Structure with Neutrons, (Neve de Mévergnies, M., Ed) North Holland, Amsterdam (1966) 125.
[11] SMITH, F.T., Phys. Rev. 118 (1960) 349.
[12] DAVIES, K.T.R., BARANGER, M., Ann. Phys. (N.Y.) 19 (1962) 383.
[13] BREIT, G., Handbuch der Physik XLI/1, Springer Verlag, Berlin (1959) 43.
[14] LANE, A.M., THOMAS, R.G., Rev. mod. Phys. 30 (1958) 297 and 321.
[15] GOLDBERGER, M.L., JONES, C.E., to be published.
[16] WEIDENMUELLER, H.A., Nucl. Phys. 75 (1966) 189; WEIDENMUELLER, H.A., DIETRICH, K., Nucl. Phys. 83 (1966) 332; MacDONALD, W.M., Nucl. Phys. 54 (1964) 393 and 56 (1966) 636; FESHBACH, H., KERMAN, A.K., LEMMER, R.H., to be published.

APPENDIX A

WIGNER'S R-MATRIX EXPANSION AS AN EXTENSION OF THE EFFECTIVE RANGE APPROXIMATION

Two useful ways of writing the single-channel S-matrix element are

$$S_\ell = \frac{\cot \delta_\ell + i}{\cot \delta_\ell - i} = \frac{1 + i \tan \delta_\ell}{1 - i \tan \delta_\ell} \tag{A1}$$

Since both $k^{2\ell+1} \cot \delta_\ell$ and $k^{-(2\ell+1)} \tan \delta_\ell$ are in general analytic near $k = 0$, either could be expanded in a power series in k to obtain a low-energy approximation to $S_\ell(k)$. If the phase shift rises or falls through $\pi/2$ in this region, the first series is somewhat preferable to the second because its circle of convergence extends out to the energy at which the phase passes through π (pole of $\cot \delta_\ell$), whereas that of the second series is determined by the smaller energy at which δ_ℓ passes through $\pi/2$ (pole of $\tan \delta_\ell$).

The first two terms of the first series give the effective range or energy-dependent width approximation to $S_\ell(k)$, Eq. (3.42), containing two free parameters. On the other hand, if the potential is cut off at $r = a$, $S_\ell(k)$ is meromorphic in k so that $k^{-(2\ell+1)} \tan \delta_\ell$ is meromorphic in E, and it is readily seen that a one-pole approximation (actually two, at E_n and E_n^*) to $k^{-(2\ell+1)} \tan \delta_\ell$ also produces an approximation to S_ℓ of exactly the effective-range form (3.42) at low energy. Although the same final result is obtained, this is an awkward route to it, for in general the poles and residues of $\tan \delta_\ell(k)$ are complex, and only certain two-parameter combinations of the 4 real numbers inherent in a 1-pole approximation actually appear in Eq. (3.42). This is important because it appears that an extension of the effective-range approximation to a form capable of accommodating two or more resonances can be accomplished more systematically by extending the one-pole approximation to $\tan \delta_\ell$ to two poles (allowing δ_ℓ to pass through $\pi/2$ and $3\pi/2$) than by including a pole of $\cot \delta_\ell$ (to allow δ_ℓ to pass through π).

It was Wigner who recognized that this could be done most efficiently (for a potential cutoff at r = a) in still a third way, by using the important theorem that, even though the poles of cot $\delta(E)$ are in general complex, those of cot $(\delta-\delta_c)$ occur only on the real energy axis, where δ_c is the phase shift for scattering by a hard core of radius a. The proof of the theorem is immediate, for if $\delta = \delta_c \pmod{\pi}$, then since both potentials vanish for r > a, their wave functions are identical over this range. Hence the scattering wave function at this (discrete) energy is required to vanish at r = 0 and at r = a – a real boundary condition which determines a real spectrum.

Similarly, for $\ell = 0$ the energies at which $\delta = \delta_c \pm \pi/2 \pmod{\pi}$, at which the derivative of the wave function vanishes at r = a, are also real, so the poles of $k^{-1} \tan(\delta-\delta_c)$ occur only on the real energy axis and hence have real residues. Since this function is also meromorphic in E, one can write, for example,

$$\frac{S(E)}{S_c(E)} = e^{2i(\delta-\delta_c)} = \frac{1+ik\,[k^{-1}\tan(\delta-\delta_c)]}{1-ik\,[k^{-1}\tan(\delta-\delta_c)]} \tag{A2}$$

and use a truncation of the Mittag-Leffler expansion for $k^{-1}\tan(\delta-\delta_c)$ to obtain a local approximation to $S_\ell(E)$. In particular, if only low-energy poles are kept, it provides a low-energy expansion; the one-pole approximation is exactly the effective range approximation (for $\delta-\delta_c$), which can describe a single resonance, and more resonances can be accommodated by including more poles.

Of course this is exactly the R-matrix expansion, since

$$R(E) = (ka)^{-1}\tan(\delta-\delta_c) \quad \text{for } \ell = 0 \tag{A3}$$

For $\ell > 0$, however, some of the poles of $\tan(\delta-\delta_c)$ may be complex, whereas all of those of R(E) remain real. Consequently the two pole expansions are different, and that of R(E) is clearly preferable for the parametrization of resonances, since each of its poles adds just two real parameters (pole energy and residue, equivalent to resonance energy and width) to the energy-dependence of $\delta(E)$. Once the values of these R-pole parameters are determined, the corresponding pole positions of the S-matrix can be obtained from the familiar expression

$$\frac{S(E)}{S_c(E)} = \frac{1-L_\ell^* R}{1-L_\ell R} \approx \frac{1-L_\ell^* \sum_1^N \frac{\gamma_i^2}{E_i-E}}{1-L_\ell \sum_1^N \frac{\gamma_i^2}{E_i-E}} \tag{A4}$$

by searching for the complex roots of

$$1 - L_\ell(ka) \sum_1^N \frac{\gamma_i^2}{E_i-E} = 0 \tag{A5}$$

which lie nearest the origin, as described in section 3.5.

Thus our conclusion is that, although the poles of S are related one-to-one to the resonances much more directly than are the poles of R, the S-poles do not seem to occur simply in unitary low-energy approximations; for the case of several resonances near threshold, the R-matrix (or K-matrix) expansion appears to provide as efficient a unitary approximation as any, although the extraction of S-poles and residues from it is not particularly convenient.

APPENDIX B

EIGENVALUE EXPANSIONS OF THE S-MATRIX

(a) The one-level case

The open channel sub-matrix S(E) is symmetric and unitary on the real energy axis and so can be expanded in terms of its eigenvectors v_μ and eigenvalues σ_μ in the form

$$S(E) = \sum_{\mu=1}^{N} \sigma_\mu(E)\, v_\mu(E)\, v_\mu^T(E) \tag{B1}$$

v_μ being a vector,

$$v_\mu = \begin{bmatrix} v_\mu^1 \\ v_\mu^2 \\ \vdots \\ v_\mu^N \end{bmatrix} \tag{B2}$$

identified by the eigenchannel μ, whose elements are labelled by the physical channels a. On the real axis the $v_\mu(E)$ are real and satisfy the usual orthonormality and completeness relations, and the $\sigma_\mu(E)$ have unit absolute magnitude there ($\sigma_\mu = \exp 2i\delta_\mu$, where δ_μ is the real 'eigenphase'), so their analytic continuations satisfy

$$\begin{aligned} \sum_a v_\mu^a(E)\, v_\nu^a(E) &= \delta_{\mu\nu} \\ \sum_\mu v_\mu^b(E)\, v_\mu^a(E) &= \delta_{ba} \end{aligned} \tag{B3}$$

and

$$\sigma_\mu^*(E_N^*)\, \sigma_\mu(E) = 1$$

throughout their regions of analyticity, indicating that the eigenvectors can have no poles, and that the poles and zeros of the eigenvalues occur

in conjugate pairs on E_N and P, like those of the determinant $D_N(E)$ (since of course the determinant is the product of the eigenvalues).

In this context it is tempting to conjecture that an isolated resonance is due to an isolated pole in one of the eigenvalues $\sigma_\mu(E)$,

$$\sigma_\rho(E) \approx \bar{\sigma}_\rho \left(\frac{E-E_p^*}{E-E_p}\right) = \bar{\sigma}_\rho \left(1 - i\,\frac{\Gamma}{E-E_p}\right) \tag{B4}$$

where σ_ρ is the background eigenvalue. Assuming all eigenvectors and all other eigenvalues constant in this energy region, this would give

$$S(E) = \sum_\mu \bar{\sigma}_\mu v_\mu v_\mu^T - i\bar{\sigma}_\rho \;\Gamma \frac{v_\rho v_\rho^T}{E-E_p} \tag{B5}$$

Although at first sight it appears eminently reasonable, this conjecture is in general false for a narrow resonance. The difficulty is that $\sigma_\rho(E)$, as well as at least one other eigenvalue $\sigma_\tau(E)$, will normally also have a branch point near the pole, and if σ_ρ has a pole on E_N, σ_τ will also have one, at the 'same' place but on the sheet reached from E_N by passing through this branch cut. If one pole is near the real axis, the other is as well, so both eigenvalues (as well as their eigenvectors) are rapidly varying in this energy region, and the resonance in effect passes from one eigenvalue to the other as the energy is varied past the branch point.

Another way of seeing that at least two eigenvalues must become involved in a narrow resonance is to note that if a single eigenphase δ_ρ were to be responsible for the entire resonance, it would necessarily rise by about π. This would normally force it to cross one of the other eigenphases (which are only defined modulo π), and thus violate the theorem that eigenphases (or eigenvalues) normally cannot cross as a function of the energy.

Because of the central role played by this theorem, it is perhaps worth remarking that it can be proved by the same argument used above to demonstrate that bound-state poles cannot cross one another. That is, the eigenvalues are obtained as functions of the energy by solving a secular equation of the form

$$\left| S(E) - \sigma\, \mathbb{1} \right| \equiv F(\sigma, E) = 0$$

If the $S_{ba}(E)$ are assumed analytic in the vicinity of E_0, where the eigenvalue under consideration equals σ_0, F will be analytic in both σ and E there. Expanding it in powers of $\Delta E = E-E_0$ and $\Delta\sigma = \sigma - \sigma_0$,

$$F_0 + (\Delta\sigma) F_1 + (\Delta E) F_2 + \frac{1}{2}\left[(\Delta\sigma)^2 F_{11} + 2(\Delta\sigma)(\Delta E) F_{12} + (\Delta E)^2 F_{22}\right] + \ldots = 0 \tag{B6}$$

$F_0(E_0) = 0$, and if two solutions σ coincide at E_0, $F_1(E_0) = 0$, so to lowest order in ΔE,

$$\Delta\sigma(E) = \left(\frac{2F_2}{F_{11}}\right)^{1/2} (\Delta E)^{1/2} \tag{B7}$$

Consequently the two σ's have square root branch points at $E = E_0$, and must scatter at right angles after colliding at σ_0 – which they cannot do if E moves through E_0 along the real axis because both σ's are constrained to the unit circle for real E. The only exception is if $F_2(E_0) = 0$ also, in which case $\Delta\sigma \sim \Delta E$; then neither eigenvalue has a branch point at E_0, and they are free to pass through one another without leaving the unit circle. This, however, is the exception rather than the rule.

Exactly like bound energy levels, eigenphases normally avoid crossing by repelling one another, as indicated by the solid curves in Fig. 37, the sharp bends in the curves being caused by the 'extra' branch points mentioned. It may seem strange that the eigenvalues (and indeed eigenvectors) have branch points which do not occur in the physical S-matrix elements themselves, but these are simply the N-th root branch points which come from solving the (algebraic) secular equation, illustrated most simply in the two-channel case, where the eigenvalues are

$$\sigma_\pm = \frac{1}{2}(S_{11} + S_{22}) \pm \frac{1}{2}\sqrt{(S_{11} - S_{22})^2 + 4\,S_{12}^2} \qquad \text{(B8)}$$

The branch points are the energies E_c (generally complex) at which the discriminant vanishes, for if the $S_{ba}(E)$ are proportional to $(E-E_c)$ near E_c, as they normally are, E_c is a square root branch point of the eigenvalues; encircling E_c once crosses the corresponding cut and simply interchanges the values of $\sigma_+(E)$ and $\sigma_-(E)$.

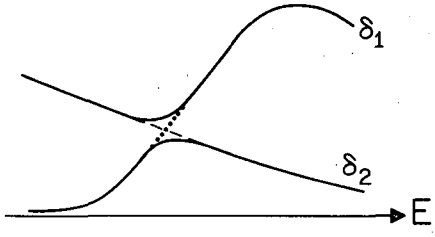

FIG. 37. Repulsion of eigenphases at a resonance

The branch points E_c occur in pairs at complex conjugate energies, and in the unlikely event that the two members of a pair coincide on the real axis, σ_+ and σ_- are equal there without having a branch point. This is the case in which F_2 of Eq. (B6) vanishes, allowing $\sigma_+(E)$ and $\sigma_-(E)$ to cross rather than repel, as indicated by the dashed curves of Fig. 37. We note from Eq. (B8) that this will certainly happen if $S_{12}(E) \equiv 0$ (making $\sigma_+ = S_{11}$ and $\sigma_- = S_{22}$), and this result is general, for the phases of decoupled scattering problems can cross with impunity. They will almost surely do so whenever one exhibits a sharp resonance and rises by nearly π, but turning on a coupling between the channels will move the crossing points off the real axis in conjugate pairs. Consequently, any eigenphase which has a resonance pole will almost certainly have such a branch point nearby, coupling it to the other eigenphase which it might have crossed and causing the two to repel one another. It is in this way that the two eigenphases become involved in the resonance.

These 'crossing point' singularities have recently been discussed in some mathematical detail by Goldberger and Jones [15], but the rather remarkable energy-dependence caused by the repulsion can perhaps be understood most simply in terms of the geometry of Fig. 38. The eigenphases $\delta_1(E)$ and $\delta_2(E)$ are both active in the resonance region because each has a pole near the real axis, one on the 'normal' sheet of the energy surface, and one at the same position, but on the sheet reached from the first pole by encircling the nearby branch point[17]. Consequently, for energies on the low-energy wing of the resonance, the pole in $\delta_2(E)$ is closest to the physical energy, causing $\delta_2(E)$ to rise rapidly while $\delta_1(E)$ remains nearly constant. On the high-energy wing, however, the δ_1-pole is closer to the physical energy, so the activity is shifted into this eigenchannel. Of course, if more phases are present, there can be several branch points and several eigenphase-repulsions, as the resonance activity is handed on from one eigenchannel to the next.

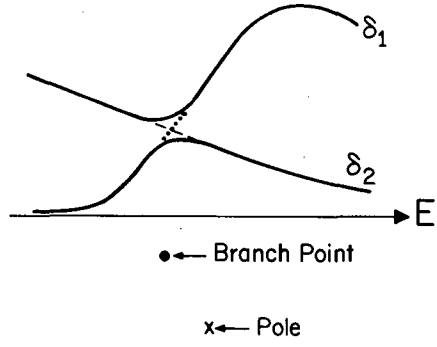

FIG. 38. Repulsion of eigenphases at a resonance, indicating relative pole and crossing-point positions in the complex energy plane

Thus the non-crossing of eigenphases means that a sharp resonance is normally not found in a single eigenchannel of S any more than it is confined to a single physical channel. The exceptional case (aside from decoupled channels) in which the resonance could remain in one eigenchannel is that in which all the eigenphases are equal (mod π) off-resonance, so that the resonating phase can rise by π without crossing another phase; this corresponds to the branch point being very distant from the pole, so that the phase-repulsion, if it occurs, happens well outside the resonance region.

It is precisely this happy property which is possessed by the matrix $\hat{S}(E)$ which plays a central role in the arguments of section 4.4. If

$$S(E) = B - i \frac{tt^T}{E-E_p} \qquad (B9)$$

with t a constant column vector and B a constant, symmetric and unitary matrix, we can write $B = V(\exp 2i\beta)V^T$ in terms of its eigenvalues

[17] Of course, the physical $S_{ba}(E)$ only have a single pole on the normal sheet, and only one eigenvalue has its pole there, thus guaranteeing factorability of the residue of S_{ba} at the pole.

exp $2i\beta_\mu$ and its matrix of real eigenvectors V. The corresponding inverse transform of S,

$$\hat{S}(E) \equiv e^{-i\beta}\, V^T S(E)\, V\, e^{-i\beta}$$
$$= \mathbb{1} - i\frac{\Gamma}{E-E_p}\, u\, u^T \qquad \text{(B10)}$$

$$\text{with } u = \Gamma^{-1/2}(e^{-i\beta}\, V\, {}^T t)$$

is itself symmetric and unitary. Hence u, which by inspection is one of its eigenvectors, must be real and normalized,

$$u^T u = 1 \qquad \text{(B11)}$$

Its corresponding eigenvalue is

$$\sigma = 1 - i\frac{\Gamma}{E-E_p} = \frac{E-E_p^*}{E-E_p} \qquad \text{(B12)}$$

and the others are all identically unity across the resonance. Hence, even though the eigenvalues of S(E) in Eq.(B9) do repel one another, those of $\hat{S}(E)$ (obtained from the elements S_{ba} by a simple linear transformation) are all equal off-resonance and so neither exhibit repulsion nor have branch points near the pole; the resonance 'stays' in a single eigenphase of $\hat{S}(E)$[18].

The great difference between the eigenvalues of S and $\hat{S}$ is conveniently illustrated by the two-channel case, where the algebra is transparent. The eigenvalues of $\hat{S}(E)$, (B12), have no branch points near the pole by construction, but those of S(E) in Eq.(B9) do. They can be obtained from Eqs.(B8) and (B9) and are located at the conjugate points

$$E_c = E_0 + \frac{\Gamma}{2}(u_1^2 - u_2^2)\,\frac{i(e^{2i\beta_1} + e^{2i\beta_2})}{e^{2i\beta_1} - e^{2i\beta_2}} \pm 2\Gamma u_1 u_2 \frac{e^{i(\beta_1+\beta_2)}}{e^{2i\beta_1} - e^{2i\beta_2}} \qquad \text{(B13)}$$

where $E_0 = \mathrm{Re}(E_p)$. They coincide on the real axis if either u_1 or u_2 vanishes (this puts the resonance completely in one eigenchannel of S), and recede infinitely far from the pole if $\beta_1 \to \beta_2$, since then $S \to \hat{S}$. Incidentally, if the background phases φ_1 and φ_2 of (4.17) are identified with β_1 and β_2, Eq.(B13) also gives the crossing points of the two-channel Breit-Wigner S-matrix, showing that they also lie near the pole unless the φ_i are equal; even a Breit-Wigner resonance does not remain in a single eigenchannel of S, unless the background phases φ_i are equal in all channels.

In summary, an eigenvalue expansion of S(E) does not in general provide a useful parametrization of a resonance, but that of the closely-related $\hat{S}(E)$ does – and is the one employed in section 4.4.

---

[18] In this sense it can be thought of as an 'elastic' resonance (B12), confined entirely to one eigenchannel of $\hat{S}(E)$, whose width is, however, distributed over the various physical channels by the transformation (B10) which expresses S in terms of $\hat{S}$.

(b) Two overlapping levels

For simplicity we assume that S can be approximated by

$$S(E) = B + T(E) \tag{B14}$$

with B constant. If T(E) is rapidly-varying because of nearby poles, B must itself be unitary and symmetric.[19]

As before, it is then simplest to consider the transformed matrix,

$$\hat{S}(E) \equiv e^{-i\beta}\, V^T S(E)\, V e^{-i\beta} \tag{B15}$$

$$= \mathbb{1} + W(E)$$

defined by the condition that the B-term is transformed into the unit matrix. Since $\hat{S}(E)$ is itself symmetric and unitary for real E, W is symmetric and must satisfy

$$W + W^* + WW^* = 0 \tag{B16}$$

A single resonance, associated with a single phase-rise of π, implies only a single 'set' of crossing points (where the rising eigenphase would cross the others if it could), which can be driven infinitely far away in $\hat{S}(E)$ by making all its background eigenphases equal. This can no longer be accomplished if two resonances overlap because the attendant phase-rise is 2π, and making the background phases of $\hat{S}(E)$ equal just below the resonance region, say, only solves half the problem. We investigate the consequences in this section, which is based only on the two assumptions that B is symmetric-unitary and constant, and that the residues of all S-matrix elements factor at each pole.

The simplest case is that in which both resonances occur in a single eigenphase of $\hat{S}$, i.e. in which T is factorable, in the form $T = f(E)\, tt^T$; f(E), which has two nearby poles, must be otherwise free of singularities and in particular contains no crossing-type branch points, for it occurs in S(E), not in its eigenvalues. Then

$$\hat{S}(E) = \mathbb{1} + f(E)\, uu^T \tag{B17}$$

of which u is clearly an eigenvector and so real. If we normalize it by $u^T u = 1$, $1 + f(E)$ is the corresponding eigenvalue, which must satisfy

$$\left|1 + f(E)\right|^2 = 1 \tag{B18}$$

in agreement with Eq.(B16). If f has poles at E_1 and E_2, it is determined uniquely by Eq.(B18) and the resulting S is

$$S(E) = B + \left\{\left(\frac{E-E_1^*}{E-E_1}\right)\left(\frac{E-E_2^*}{E-E_2}\right) - 1\right\} tt^T \tag{B19}$$

with $t^\dagger t = 1$ and $Bt^* = t$, as in Eq.(4.25).

---

[19] Everything which follows will also be true even if B varies slowly in the energy region concerned, provided it is unitary across the region.

Our assumption that T has the factorable form $f(E)\,tt^T$ across the double resonance region has forced both resonances into the same eigenchannel of $\hat{S}$. Hence this $\hat{S}$-eigenphase rises by a total of 2π, so it must cross the other eigenphases, which are dormant at $\delta = 0 \pmod{\pi}$. The crossing thus occurs where $1+f(E) = 1$, i.e. $f(E) = 0$, making $\hat{S}$ diagonal at this energy. This is the exceptional situation mentioned above, in which two branch points of $\hat{S}$ have coalesced on the real axis to permit the eigenphases to cross.

Because of the constraint that the residues must factor at both poles, the only other form of S which admits of two poles is

$$S(E) = B + f(E)\,tt^T + g(E)\,rr^T \tag{B20}$$

which is of course just the form of two-pole approximation to the Humblet-Rosenfeld series [2]. Again assuming B constant and unitary over the region of the two resonances,

$$\hat{S}(E) = \mathbb{1} + f(E)\,uu^T + g(E)\,vv^T \tag{B21}$$

But a matrix of this special form, with u and v constant vectors and f(E) and g(E) different functions, can be identically unitary in E only if u and v are (orthogonal) eigenvectors of S. One way of seeing this is to write it as $1+U+V$, with U and V symmetric so that $U^\dagger$ equals U^* making the unitarity condition (B16)

$$U+U^*+V+V^*+UU^*+VV^*+UV^*+VU^* = 0 \tag{B22}$$

Since the sum of the first four terms is real and symmetric, that of the second four must be real and symmetric as well. This means, for example, that

$$\mathrm{Im}\,[\,|f|^2(u^\dagger u)\,uu^\dagger] = \mathrm{Im}(UU^*) = -\mathrm{Im}(VV^*+VU^*+UV^*), \tag{B23}$$

but since the two sides have entirely different energy dependences for arbitrary u and v, this can only be true if u and v are such that both sides are separately real, i.e. $uu^\dagger$ is real, or $u_b u_a^* = u_b^* u_a$, which can be true for all a and b only if u is a real vector (to within an overall phase, which we absorb in F(E)). Similarly v must be real, and if we normalize them according to

$$u^T u = v^T v = 1 \tag{B24}$$

Eq. (B22) becomes

$$(f+f^*+|f|^2)\,uu^T + (g+g^*+|g|^2)\,vv^T + (u^Tv)\,[fg^*\,uv^T + f^*g\,vu^T] = 0 \tag{B25}$$

Either u or v (which are directly related to the partial width vectors t and r of Eq. (B20)) can be chosen arbitrarily (consistent with Eq. (B24)). In particular, if $u^T = (1, 0, 0, \ldots 0)$, or if $v^T = (1, 0, 0, \ldots 0)$, Eq. (B25) implies

$$f+f^*+|f|^2 = 0 \tag{B26}$$

and $$g + g^* + |g|^2 = 0$$

just as in the one-pole case. Consequently, either $f^* g = 0$, which is impossible, or

$$u^T v = 0 \tag{B27}$$

q.e.d.

This means that u and v are necessarily eigenvectors of $\hat{S}$, with eigenvalues $1 + f(E)$ and $1 + g(E)$; the latter have no branch points by assumption and in general will cross at a real energy E_c where again two branch points have been forced to coalesce.

Although one or both of f(E) and g(E) could have two poles, with one of the poles also occurring in the other function, this is unlikely, and the normal situation is one pole in each function. In this case Eq.(B26) determines the functions as in Eq.(B10, giving

$$S(E) = B - i \frac{\Gamma^1}{E-E_1} t t^T - i \frac{\Gamma^2}{E-E_2} r r$$

$$\text{with } t^\dagger t = r^\dagger r = 1, \; t^\dagger r = 0$$
$$\text{and } Bt^* = t, \; Br^* = r$$

Thus one of the consequences of writing S(E) in this form, with B constant, is that the 'partial width vectors' t and r of the two resonances are necessarily orthogonal.

CHAPTER 9

APPLICATIONS OF RESONANCE SCATTERING THEORY IN NUCLEAR PHYSICS

R. H. LEMMER

1. INTRODUCTION

In this chapter we shall be primarily interested in the possible applications of scattering theory to problems of nuclear structure. However, in order to give proper background to our discussion, it will be necessary to discuss the relevant scattering formalism in some detail. No exhaustive treatment of scattering theory is intended here since this has already been covered from various points of view in Chapters 5 and 7. Rather we wish to define the notation and concepts that will be used in the subsequent discussion.

Let us outline a typical problem: A nucleon of energy E collides with a nucleus A containing A nucleons. If E is low enough we know from experiment that elastic scattering of the nucleon and its radiative capture via a (n, γ) process are the most likely reaction processes. If we examine the total cross-section $\sigma_T(E)$ as a function of E we observe a smooth dependence except in the vicinity of certain special energies E_s, e.g. where σ_T fluctuates rapidly with E over an interval Γ_s. This fluctuation is called a resonance and, as we shall see shortly, can be associated with the formation of quasi-bound states of the compound nucleus (A + 1) that forms during the collision. We shall refer to such states as compound states. These states are not stable, but possess a width Γ_s (or lifetime $\hbar/\Gamma_s$) for decay into whatever final channels are open to the compound state in question.

At low energies the average width to spacing ratio Γ/D is small and we observe isolated resonances. As the energy is increased, the number of possible open channels increases with a corresponding increase in Γ until the situation of strongly overlapping levels, $\Gamma/D \gg 1$, develops. Our considerations will for the most part apply to the region of isolated resonances. Typically this will mean incident nucleon energies below 3 MeV or so, always having in mind, however, that such features vary strongly from nucleus to nucleus.

The author is at the Laboratory for Nuclear Science and Physics Dept., Massachusetts Institute of Technology, Cambridge, Massachusetts, United States of America.

The text has been compiled by C. A. Engelbrecht, of the South African Atomic Energy Board, Pelindaba, South Africa, from notes taken at the author's lectures.

It has been known for a long time that the cross-section in the vicinity of an isolated resonance is very accurately described by the Breit-Wigner [1] one-level formula. For example, for an s-wave resonance this reads

$$\sigma_T(E) = \frac{4\pi}{k^2}\left|-e^{i\delta}\sin\delta + e^{2i\delta}\,\frac{\Gamma_s^{(n)}/2}{E - E_s + i\Gamma_s/2}\right|^2 \qquad (1.1)$$

where k = incident wave number
δ = potential scattering phase shift
$\Gamma_s^{(n)}$ = partial width for emitting a nucleon
Γ_s = total width.

This formula provides us with a means to extract the parameters listed below it from experiment. But it tells us nothing about why resonances occur at particular energies and what determines their widths. Thus, in order to make contact between such measured quantities and the properties of the many-body system (i.e. the compound nucleus) that exhibits them, we must introduce a nuclear dynamics, i.e. the mutual interactions between nucleons and the equations of motion that govern nucleon motion under these interactions. This is of course an obvious statement, and how we implement it for the discussion of compound nucleus resonances leads directly into the various scattering formalisms that have been developed during the past 20 years (starting perhaps with Wigner and Eisenbud [1] in 1947). Since the applications we wish to discuss have been based on the formalism developed by Feshbach [2], we proceed to give a very brief outline of his approach.

Formalism. Our problem can be stated as follows. A nucleon a interacts with the target nucleus A via a mutual interaction V(a, A). (As our notation suggests, the symbols a and A now stand for all the co-ordinates of the incident and target systems.) The Hamiltonian of our system is thus

$$H = H(A) + T_a + V(a, A)$$

consisting of the target Hamiltonian H(A), the kinetic energy T_a of a and their mutual interaction. We next expand the full wave function $\Psi(a, A)$ in terms of a complete set of target states. Call these states $\phi_\alpha(A)$. Then we write

$$\Psi(a, A) = \sum_\alpha u_\alpha(a)\,\phi_\alpha(A) \qquad (1.2)$$

Inserting this expansion into the wave equation $(H - E)\Psi(a, A) = 0$ we immediately obtain an infinite set of coupled equations for the $u_\alpha(a)$. However, if we are at energies for which elastic scattering is the only open channel, all the scattering information is contained in the amplitude $u_0(a)$, since all the remaining u_α's will vanish as $a \to \infty$. This observation suggests that it will be convenient to isolate u_0 from the other amplitudes and derive an equation for u_0. This is Feshbach's procedure. He introduces the projection operators P and $Q = 1 - P$ such that

$$P\Psi = u_0(a)\phi_0(A) \qquad (1.3)$$

where $\phi_0(A)$ symbolizes the ground state of the target nucleus. Thus P projects onto open channels, Q onto closed channels. Then, writing the wave equation as $(H - E)(P + Q)\Psi = 0$, it is a simple matter to derive an equation for $P\Psi$:

$$\begin{aligned} &(E - H_{PP} - H_{PQ}\frac{1}{E - H_{QQ}}H_{QP})P\Psi = 0 \\ &H_{PP} = PHP \\ &H_{QQ} = QHQ \\ &H_{QP} = QHP = H_{PQ}^{\dagger} \end{aligned} \tag{1.4}$$

If, as here, we are looking at elastic scattering only (and ignoring anti-symmetry), we can write for P,

$$P = |\phi_0)(\phi_0| \tag{1.5}$$

in which case Eq. (1.4) becomes, after operating with $(\phi_0|$ from the left,

$$\left[E - T_a - V_a - \left(\phi_0 \middle| VQ\frac{1}{E - H_{QQ}}QV \middle| \phi_0\right)\right]u_0 = 0 \tag{1.6}$$

where $V_a = (\phi_0|V(a, A)|\phi_0)$, $(\phi_0|H_{PQ} = (\phi_0|VQ$. The round brackets imply integration over target co-ordinates only. We shall use sharp brackets $\langle \ldots | \ldots \rangle$ when an integration over all co-ordinates is intended.

The structure of Eq. (1.6) is significant in that it contains interaction terms that behave quite differently with energy. V_a does not depend explicitly on E, while the last term varies very rapidly with E if the spectrum of the system defined by the Hamiltonian H_{QQ} is dense. The significant quantities are the energies E_s, where

$$(E_s - H_{QQ})\Phi_s = 0 \tag{1.7}$$

which are poles in the last term of Eq. (1.6). Equation (1.7) is an $(A + 1)$-particle problem, and, as we shall show in a moment, provides a very convenient definition for the compound states of the $(A + 1)$ nucleus. To see this, consider an isolated level, E_s, of H_{QQ} that lies in the continuum of the incident nucleon (see Fig. 1).

We display the operator $(E - H_{QQ})^{-1}$ in terms of the (assumed) complete set of states Φ_s, but keep only the term with a pole at $E = E_s$ explicitly and regard the rest as a modification of the potential V_a, replacing it by V_a'. Then (1.6) reads

$$(E - T_a - V_a')u_0 = \frac{(\phi_0|VQ|\Phi_s\rangle\langle\Phi_s|QV|\phi_0 u_0\rangle}{E - E_s} \tag{1.8}$$

Knowing the scattering solutions of the left-hand side of this equation,

$$(E - T_a - V_a')\psi_0^{(\pm)} = 0 \tag{1.9}$$

for both incoming and outgoing wave boundary conditions, we can solve for the transition amplitude. The result is easily found to be

$$T = T_0 + \frac{\langle \psi_0^{(-)} \phi_0 | VQ | \Phi_s \rangle \langle \Phi_s | QV | \phi_0 \psi_0^{(+)} \rangle}{E - E_s - \Delta_s + i\Gamma_s/2} \tag{1.10}$$

where

$$\begin{aligned} \Delta_s &= \langle \Phi_s | QV | \phi_0 \rangle \frac{P}{E - T_a - V_a'} (\phi_0 | VQ | \Phi_s \rangle \\ \Gamma_s &= 2\pi \langle \Phi_s | QV | \phi_0 \rangle \delta(E - T_a - V_a') (\phi_0 | VQ | \Phi_s \rangle \end{aligned} \tag{1.11}$$

P means principal value, not projection, and T_0 is the scattering amplitude for the problem defined by (1.9), i.e. the scattering caused by V_a' acting alone. We note that T(E) in (1.10) has a pole at the complex energy

$$E_s + \Delta_s - \frac{i}{2}\Gamma_s$$

indicating a resonance at energy $E_s + \Delta_s$ with a width Γ_s. Thus if the shift Δ_s is small, the resonances occur very close to the eigenvalues of the system with Hamiltonian H_{QQ}. Since the coupling with the entrance channel has been reduced to zero in H_{QQ}, we are in a sense dealing with an "internal" problem involving the interaction of A + 1 particles. Restoring the coupling H_{QP} with the entrance channel then endows all states of H_{QQ} with an energy shift Δ_s, and those states above threshold with an escape width Γ_s in addition.

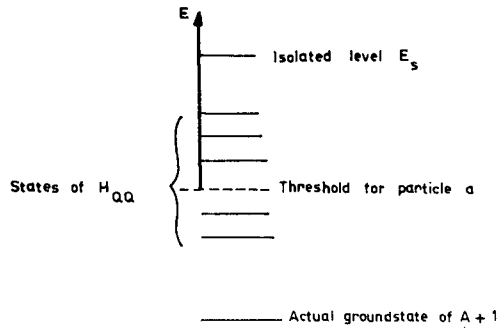

FIG.1. An isolated level E_s of H_{QQ}, lying in the continuum of the incident nucleon

By contrast, the first term T_0 in (1.10) is expected to vary slowly with energy and is usually referred to as the potential scattering.

Equation (1.10) almost has the form of the one-level Breit-Wigner amplitude used in (1.1), except that we have not broken T up into a partial wave expansion. However, it is instructive to do so in order to appreciate the point that a given resonance in T in (1.10) can only be excited by certain partial waves that are determined by angular momentum conservation.

Let us assume that V_a' is spherically symmetric and also ignore intrinsic spin of all particles. Then the scattering solutions $\psi_0^{(+)}$ may be displayed in partial waves according to

$$\psi^{(+)}_{0,\vec{k}}(\vec{r}) = \sum_{\ell m} \psi^{(+)}_{\ell m}(\vec{r}) Y_{\ell m}(\hat{k}) \tag{1.12}$$

where $\hat{k}$ is the direction of the incident plane wave. The incoming wave solutions $\psi_0^{(-)}$ have a similar display, with $\psi^{(+)}_{\ell m}$ replaced by $\psi^{(-)}_{\ell m} = e^{-2i\delta_\ell}\,\psi^{(+)}_{\ell m}$ where δ_ℓ is the potential scattering phase shift for the ℓ-th partial wave. Since the compound states Φ_s carry a good angular momentum (they are eigenstates of a rotationally invariant system), we see from the matrix elements, e.g.

$$\langle \Phi_s^J \,|\, QV \,|\, \psi_s^{(+)} \phi_0 \rangle$$

same total
angular momentum

that a resonance of angular momentum J is only excited by the $\ell = J$ partial wave in the incident beam. Writing $T(\hat{k}', \hat{k}) = \sum_{\ell m} Y_{\ell m}(\hat{k}')\, T_\ell\, Y_{\ell m}(\hat{k})$ where $\hat{k}'$ is the direction of the scattered particles and inserting the expansions for $\psi_0^{(\pm)}$ in (1.10) we find that

$$T_\ell = -\frac{1}{\pi} e^{i\delta_\ell} \sin\delta_\ell + e^{2i\delta_\ell} \frac{\left| \langle \Phi_s^J \,|\, QV \,|\, \psi^{(+)}_{\ell m} \phi_0 \rangle \right|^2}{E - E_s - \Delta_s + i\Gamma_s/2} \tag{1.13}$$

for $\ell = J$. For other values of ℓ only the potential scattering term is present. We can also identify the width Γ_s belonging to the state Φ_s^J. From (1.11) this is just

$$\Gamma_s^{J=\ell} = 2\pi \left| \langle \Phi_s^J \,|\, QV \,|\, \psi^{(+)}_{\ell m} \phi_0 \rangle \right|^2 \tag{1.14}$$

a result that is immediate upon expressing $\delta(E - T_a - V_a')$ in terms of the (energy-normalized) states $\psi^{(+)}_{\ell m}$. Note that the bound states of $T_a + V_a'$ do not contribute because E always refers to an energy above threshold for the particle a. Equation (1.13) is precisely the one-level Breit-Wigner formula in its more usual form. The corresponding total cross-section for elastic resonance scattering of the partial wave $\ell = J$ is

$$\sigma_\ell = \frac{4\pi^3}{k^2}(2\ell + 1) \left| -\frac{1}{\pi} e^{i\delta_\ell} \sin\delta_\ell + \frac{1}{\pi} e^{2i\delta_\ell} \frac{\Gamma_s/2}{E - E_s - \Delta_s + i\Gamma_s/2} \right|^2 \tag{1.15}$$

if we make use of (1.14) for the matrix element $\langle \Phi_s \,|\, QV \,|\, \psi^{(+)}_{\ell m} \phi_0 \rangle$.

Thus far we have pretended that a single, isolated level at E_s is responsible for resonance scattering. However, we shall also be interested in the case that several levels E_s have to be considered. The procedure for obtaining the transition amplitude in this case is still straightforward.

For N levels E_s the equation (1.8) is replaced by

$$(E - T_a - V_a'')u_0 = \sum_{s=1}^{N} \frac{(\phi_0|VQ|\Phi_s\rangle\langle\Phi_s|QV|\phi_0 u_0\rangle}{E - E_s} \tag{1.16}$$

where, as before, V_a'' indicates that the remaining non-resonant levels have been included in V_a. Feshbach [2] has shown that in this case the transition amplitude is of the form

$$T = T_0 + \sum_{\mu} \frac{A_\mu}{E - \mathscr{E}_\mu} \tag{1.17}$$

where the $\mathscr{E}_\mu$ are the complex roots of

$$\sum_{s'} \left[(\mathscr{E}_\mu - E_s)\delta_{ss'} - \Delta_{ss'} + \frac{i}{2}\Gamma_{ss'} \right] \chi_{\mu,s'} = 0$$

i.e. the energy shift and width factors in (1.11) are replaced by matrices. However, if we neglect the coupling between compound states that arises through their mutual interaction with the entrance channel by setting the off-diagonal elements $\Delta_{ss'}$ and $\Gamma_{ss'}$ to zero we regain a simple structure for T that will be adequate for our purposes:

$$T \approx T_0 + \sum_{s} \frac{\langle\psi_0^{(-)}\phi_0|VQ|\Phi_s\rangle\langle\Phi_s|QV|\psi_0^{(+)}\phi_0\rangle}{E - E_s - \Delta_{ss} + i\Gamma_{ss}/2} \tag{1.18}$$

Note in passing that, because of the approximation we have introduced, T in (1.18) is not properly unitary, while T in (1.17) is.

2. ANTISYMMETRIZATION

So far we have disregarded the requirement of antisymmetry between the incident nucleon and the nucleons in the target. For bound state problems this requirement can easily be satisfied but in scattering problems non-trivial changes are necessary. This can be illustrated by considering a very simple model for the target nucleus. Let us assume that it consists of a completely filled Fermi sea which is never excited, and an additional nucleon whose co-ordinates will be denoted by b. This nucleon can occupy bound levels ϕ_0 or ϕ_1 or continuum levels $\phi_\epsilon^{(+)}$ (with energy ϵ) of the Hamiltonian for the target nucleus. If we do not antisymmetrize, the wave function of the complete system (incident nucleon plus target) can be expanded according to

$$\Psi(a, b) = u_0(a)\phi_0(b) + u_1(a)\phi_1(b) + \int_0^\infty d\epsilon\, u_\epsilon(a)\phi_\epsilon^{(+)}(b) \tag{2.1}$$

If the target is initially in state $\phi_0(b)$ and the energy of the incident nucleon is less than the energy difference between states ϕ_1 and ϕ_0, the coefficients

$u_1(a)$ and $u_\epsilon(a)$ will asymptotically tend to zero so that the scattering is completely determined by the overlap

$$(\phi_0, \Psi) = u_0(a) \tag{2.2}$$

whose s-wave component, for example, asymptotically becomes proportional to

$$\frac{1}{r}(e^{-ikr} - Se^{ikr}) \tag{2.3}$$

To obtain the value of the transition amplitude (S - 1), the Schrödinger equation for $u_0(a)$ must be solved everywhere.

Let us now consider what happens when (2.1) is antisymmetrized. The result is ($\mathscr{A}$ denotes antisymmetrization)

$$\mathscr{A}\Psi = u_0(a)\phi_0(b) - u_0(b)\phi_0(a) + u_1(a)\phi_1(b) - u_1(b)\phi_1(a)$$
$$+ \int_0^\infty d\epsilon \left[u_\epsilon(a)\phi_\epsilon^{(+)}(b) - u_\epsilon(b)\phi_\epsilon^{(+)}(a) \right] \tag{2.4}$$

Because of the orthogonality of the target states, the overlap with the ground state of the target is given by

$$(\phi_0, \mathscr{A}\Psi) = u_0(a) - (u_0, \phi_0)\phi_0(a) - (u_1, \phi_0)\phi_1(a)$$
$$- \int d\epsilon\, (u_\epsilon, \phi_0)\phi_\epsilon^{(+)}(a) \tag{2.5}$$

Since (2.4) is completely antisymmetric, it does not matter which particle we consider as the "detected" particle - one simply obtains the same expression but with opposite sign. We have here chosen a to be the "detected" particle. Letting its co-ordinates tend to infinity, we obtain

$$(\phi_0, \mathscr{A}\Psi) \to u_0(a) - \int d\epsilon\, (u_\epsilon, \phi_0)\phi_\epsilon^{(+)}(a) \tag{2.6}$$

Equation (2.6) indicates the complication, namely that u_0 no longer contains all information about the scattering. The second term in (2.6) also contributes to the outgoing wave part of u_0. It is thus essential that in (2.4) we expand in terms of a complete set of target states including the continuum.

The complication arises because $\mathscr{A}(\Psi - u_0\phi_0)$ (see (2.4)) is no longer orthogonal to ϕ_0. We shall now outline a procedure which regains the simplicity of having all scattering information contained in a single u_0 (which will of course be different from the one defined above) but at the price of introducing a more complicated projection operator P. For this purpose we return to the general formulation where $\phi_0(1 \ldots A)$ simply denotes the target ground state and does not refer to the simple model which we have just discussed.

We now start with a wave function $\Psi(a\ 1\ 2\ \ldots\ A)$ of the complete system which is already completely antisymmetric and demand that

$$P\Psi(a\ 1\ \ldots\ A) = \mathcal{A}[u_0(a)\phi_0(1\ \ldots\ A)]$$

$$= u_0(a)\phi_0(1\ \ldots\ A) - \sum_{i=1}^{A} u_0(i)\phi_0(1\ \ldots\ i-1,\ a,\ i+1\ \ldots\ A) \quad (2.7)$$

where u_0 is still undefined. If it is supposed to contain the complete scattering information, we must guarantee that $(\Psi - P\Psi)$ does not contain the ground state and by this process complete the definition of P. Thus we demand

$$(\phi_0,\ \Psi - P\Psi) = 0 \quad (2.8)$$

From (2.7) we thus obtain

$$v(a) \equiv (\phi_0,\ \Psi) = (\phi_0,\ P\Psi)$$

$$= u_0(a) - A\int d(1\ \ldots\ A)\phi_0^*(1\ 2\ \ldots\ A)\phi_0(a\ 2\ \ldots\ A)u_0(1) \quad (2.9)$$

where the complete antisymmetry enabled us to replace the summation sign by the number of equal terms A. Let us define

$$K(a, 1) \equiv A\int d(2\ \ldots\ A)\phi_0^*(1\ 2\ \ldots\ A)\phi_0(a\ 2\ \ldots\ A) \quad (2.10)$$

which is just the density matrix for the target nucleus in its ground state. Then (2.9) reads

$$v(a) = u_0(a) - \int d(1)K(a, 1)u_0(1) \quad (2.11)$$

which we wish to solve for u_0 in terms of v. The integral operator K is obviously hermitian (i.e. $K^*(a, 1) = K(1, a)$); we can use its set of eigenfunctions u_λ defined by

$$\int d(1)K(a, 1)u_\lambda(1) = \lambda u_\lambda(a) \quad (2.12)$$

to express

$$K(a, 1) = \sum_\lambda u_\lambda(a)\lambda\, u_\lambda^*(1) \quad (2.13)$$

Equation (2.11) can be written symbolically as

$$v = u - Ku \quad (2.14)$$

which can be solved formally by

$$u = \frac{1}{1 - K} v + w \tag{2.15}$$

where w is a solution of the homogeneous equation $(1 - K)w = 0$.

It is obvious that the discussion of the homogeneous solution w as well as the treatment of poles in the operator $(1 - K)^{-1}$ requires an investigation of the possible eigenvalue $\lambda_1 = 1$ in (2.12). The definition (2.10) implies that we can write, for any function u_{λ_1}, that

$$(\phi_0, \mathscr{A} u_{\lambda_1} \phi_0) = u_{\lambda_1} - K u_{\lambda_1} \tag{2.16}$$

just as in (2.9). If u_{λ_1} is now an eigenfunction corresponding to $\lambda_1 = 1$, it follows from (2.12) that the right-hand side of (2.16) vanishes and hence also

$$\langle \mathscr{A} u_{\lambda_1} \phi_0, \mathscr{A} u_{\lambda_1} \phi_0 \rangle$$

which implies

$$\mathscr{A} u_{\lambda_1} \phi_0 = 0 \tag{2.17}$$

and hence also

$$(u_{\lambda_1}, v) = (\mathscr{A} u_{\lambda_1} \phi_0, \Psi) = 0 \tag{2.18}$$

In the special case where ϕ_0 is a single Slater determinant (Hartree-Fock ground state), K is simply a sum over occupied single-particle states

$$K(a, 1) = \sum_{\alpha(\text{occ})} \varphi_\alpha(1) \varphi_\alpha^*(a)$$

Since u_{λ_1} is a linear combination of precisely these states, the result (2.17) then follows from the vanishing of a determinant with equal rows.

Equation (2.15) can now be expanded in terms of the set of eigenfunctions u_λ

$$u_0(a) = \sum_{\lambda \neq 1}' \frac{u_\lambda(a)\,(u_\lambda, v)}{1 - \lambda} + \sum_{\lambda_1} b_{\lambda_1} u_{\lambda_1}(a) \tag{2.19}$$

where the terms $\lambda = 1$ may be omitted from the first sum on account of (2.18) and where the coefficients b_{λ_1} are undetermined but unimportant since they drop out of the formalism as we shall now see. First rewrite (2.19):

$$u_0(a) = v(a) + \sum_{\lambda \neq 1}' \frac{\lambda}{1 - \lambda} u_\lambda(a)\,(u_\lambda, v) + \sum_{\lambda_1} b'_{\lambda_1} u_{\lambda_1}(a) \tag{2.20}$$

and now compute

$$P\Psi = \mathscr{A}u_0(a)\phi_0(1 \ldots A)$$

$$= \mathscr{A}\left[v\phi_0 + \sum_{\lambda \neq 1} \frac{\lambda(u_\lambda, v)}{1 - \lambda} u_\lambda \phi_0\right] \tag{2.21}$$

where we have made use of (2.17). The first term on the right-hand side can be written as

$$v_0(a)\phi_0(1 \ldots A) = \int d(1' \ldots A')\phi_0^*(1' \ldots A')\Psi(a, 1' \ldots A')\phi_0(1 \ldots A)$$

$$= (1 \ldots A | \phi_0)(\phi_0 | \Psi\rangle$$

Similarly,

$$u_\lambda \phi_0(u_\lambda, v) = \langle a\ 1 \ldots A | u_\lambda \phi_0 \rangle \langle u_\lambda \phi_0 | \Psi \rangle$$

so that the operator P can finally be expressed [2] as

$$P = \mathscr{A}\left\{\phi_0)(\phi_0 + \sum_{\lambda \neq 1} \frac{u_\lambda \phi_0 \rangle \lambda \langle u_\lambda \phi_0}{1 - \lambda}\right\} \tag{2.22}$$

Sometimes the more symmetrical form

$$P = \frac{\mathscr{A}}{\sqrt{A + 1}} \left\{\phi_0)(\phi_0 + \sum_{\lambda \neq 1} \frac{u_\lambda \phi_0 \rangle \lambda \langle u_\lambda \phi_0}{1 - \lambda}\right\} \frac{\mathscr{A}}{\sqrt{A + 1}}$$

is used.

It can be shown that, with this definition, $P^2 = P$ so that this is indeed a projection operator. If the form (2.22) rather than (1.5) is used, (1.4) still holds for $P\Psi$ which still contains all the scattering information. Since P is differently defined, operators such as H_{PP}, H_{PQ} and H_{QQ} may have different meanings, however. The second term in (2.22) contributes only for λ which differ from 0 and 1. If the ground state of the target nucleus can be represented as a single Slater determinant of single nucleon wave functions, this term vanishes. Even for simple cases like closed shell plus one or plus two nucleons in the target, angular momentum coupling would, however, cause it to play a role.

As one might suspect, all of the preceding discussion can be carried out in a second quantized version [3]. Define anticommuting field operators $\psi(\xi)$ and $\psi^\dagger(\xi)$ which destroy and create a nucleon with co-ordinates (space, spin, and isospin) ξ and consider the expression

$$\int d\xi\, \psi^\dagger(\xi) | G \rangle u_0(\xi)$$

where the amplitude $u_0(\xi)$ appeared in (2.7) while $|G\rangle$ denotes the ground state of the target nucleus. The overlap with $\psi^\dagger(a)|1, \ldots, A\rangle$, i.e. an

antisymmetrized state containing nucleons with co-ordinates (a, 1, 2, . . . , A), is given by

$$\int d\xi \, \langle 1 \ldots A | \psi(a) \psi^\dagger(\xi) | G \rangle u_0(\xi)$$

$$= u_0(a) \phi_0(1 \ldots A) - \int d\xi \, \langle 1 \ldots A | \psi^\dagger(\xi) \psi(a) | G \rangle \, u_0(\xi) \tag{2.23}$$

where we have set

$$\langle 1 \ldots A | G \rangle = \phi_0(1 \ldots A) \tag{2.24}$$

If we now express

$$| 1 \ldots A \rangle = \left(\frac{1}{A!} \right)^{\frac{1}{2}} \psi^\dagger(1) \psi^\dagger(2) \ldots \psi^\dagger(A) | 0 \rangle$$

and use the anticommutation properties of the ψ's, it is easy to show that the right-hand side of (2.23) reduces to

$$\mathscr{A} \{ u_0(a) \phi_0(1 \ldots A) \}$$

which is identical with (2.7). It follows that the density matrix (2.10) is given by

$$K(a, 1) = \langle G | \psi^\dagger(1) \psi(a) | G \rangle \tag{2.25}$$

while the projection operator P (2.22) may be written as

$$P = \int d\xi \psi^\dagger(\xi) | G \rangle \langle G | \psi(\xi)$$

$$+ \sum_{\lambda \neq 1} \int\int d\xi d\eta \, \psi^\dagger(\xi) | G \rangle \, u_\lambda(\xi) \frac{\lambda}{1 - \lambda} \, u_\lambda^*(\eta) \langle G | \psi(\eta) \tag{2.26}$$

where the $u_\lambda(\xi)$ are eigenfunctions of K as in (2.12).

As an example consider the scattering of a nucleon from a target nucleus described in the shell model by a single hole state

$$| G \rangle = a_{n_0 j_0 m_0} | 0 \rangle \tag{2.27}$$

where the nucleon destruction operator $a_{n_0 j_0 m_0}$ creates a hole of angular momentum $(j_0, -m_0)$ in the Fermi sea $| 0 \rangle$. If $\vec{j}_0$ and the partial wave $\vec{j}$ of the incident nucleon are coupled to a total angular momentum $\vec{J}$, the density matrix becomes

$$K(\vec{r}, \vec{r}') \equiv K_{jm}(r, r')$$

$$= \langle G | a_{jm}^\dagger(r') a_{jm}(r) | G \rangle$$

$$= \sum_{J, M} (j m j_0 \; -m_0 \, | J M)^2 \, K_{j j_0}^J(r, r') \tag{2.28}$$

The matrix $K^J_{jj_0}(r, r')$ is

$$K^J_{jj_0}(r, r') = \sum_{n(occ)} R_{n_j}(r) R_{n_j}(r') - (2j_0 + 1)\delta_{J,0}\,\delta_{jj_0} R_{n_0 j_0}(r) R_{n_0 j_0}(r') \tag{2.29}$$

where we have used the expansion

$$a_{jm}(r) = \sum_n R_{nj}(r)\, a_{njm} \tag{2.30}$$

for $a_{jm}(r)$ in terms of a complete set of radial "orbitals" R_{nj} of angular momentum j. Note that the sum in (2.29) is over occupied orbitals in the Fermi sea $|0\rangle$ only.

When $J > 0$, only the first term in (2.29) contributes. The eigenfunctions and associated eigenvalues are easily seen to be

$$u_\lambda(r) = R_{nj}(r), \quad \lambda = 1 \quad \text{if } n_j \text{ is occupied in } |0\rangle$$

$$\lambda = 0 \quad \text{if } n_j \text{ is unoccupied in } |0\rangle$$

If $J = 0$ (hence $j = j_0$) we have, on the other hand,

$$u_\lambda(r) = R_{nj}(r), \quad \lambda = -2j_0 \quad \text{if n is the occupied state } n_0$$

$$\lambda = 1 \quad \text{if n is any other occupied state}$$

$$\lambda = 0 \quad \text{if n is unoccupied in } |0\rangle$$

We notice that the eigenfunctions $u_\lambda(r)$ form a complete set in each case. These results show that in this example the last term in (2.26) contributes only if $J = 0$ and $n = n_0$.

3. OPTICAL MODEL

It is a well-established fact that the energy averages of total and scattering cross-sections are adequately described by the optical model. In this model one considers the scattering of the incident particle by a complex potential well

$$[E - T_a - (V - iW)]\chi(a) = 0 \tag{3.1}$$

which embodies in W all our ignorance concerning the nuclear many-body problem. We shall now investigate if anything can be learned about this complex potential by the application of our formalism to the problem of average cross-sections.

We have seen (Eq. (1.16)) that the complete scattering properties are contained in a function u_0 which satisfies the equation

$$\left[E - T_a - V_a'' - \sum_s \frac{(\phi_0 | VQ | \Phi_s\rangle\langle\Phi_s | QV | \phi_0)}{E - E_s}\right] u_0(a) = 0 \tag{3.2}$$

Unlike χ, which describes only the average properties of the reaction (solid line on Fig. 2), u_0 contains the actual resonance properties (broken line).

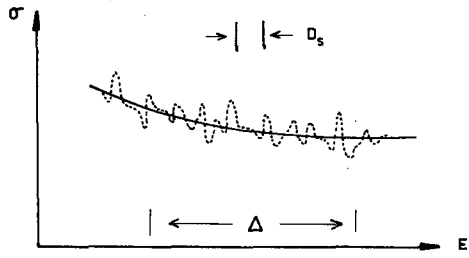

FIG. 2. Average properties of the reaction (solid line) and actual resonance properties (broken line)

If we wish to derive an optical model from (3.2), it is clear that we have to average over many resonances, and thus have to use an averaging interval of energy width Δ which is large compared to the average spacing D_s between resonances. The transition matrix corresponding to (3.2) was seen (Eq. (1.18)) to be given

$$T \approx T_0 + \sum_s \frac{\langle \psi_0^{(-)} \phi_0 | VQ | \Phi_s \rangle \langle \Phi_s | QV | \phi_0 \psi_0^{(+)} \rangle}{E - E_s - \Delta_{ss} + \frac{i}{2}\Gamma_{ss}} \tag{3.3}$$

if the coupling between resonances (non-diagonal terms $\Delta_{ss'}$ and $\Gamma_{ss'}$) is neglected.

The optical model potential is defined in such a way (see for example Ref. [2]) that its T-matrix corresponds to the energy average of the actual T-matrix. We thus have to average (3.3) by means of a normalized weight function $\rho(E, E')$:

$$\langle T \rangle = \int \rho(E, E')\, T(E')\, dE' \tag{3.4}$$

An example of a weight function would be the one used by Feshbach, Porter and Weisskopf [4] in their original paper on the optical model:

$$\rho(E, E') = \begin{cases} \frac{1}{\Delta} & \text{if} \quad |E - E'| < \Delta/2 \\ 0 & \text{if} \quad |E - E'| > \Delta/2 \end{cases} \tag{3.5}$$

To avoid having to worry about end effects, it is simpler to use the Lorentzian form

$$\rho(E, E') = \frac{\Gamma/2\pi}{(E - E')^2 + (\Gamma/2)^2} \tag{3.6}$$

where $I \simeq 2\Delta/\pi$. Cauchy's theorem shows that this latter weight function has the property

$$\int \rho(E, E')\, F(E')\, dE' = F(E \pm \tfrac{i}{2} I) \tag{3.7}$$

for any function F which has no poles in the upper half plane and satisfies certain criteria of boundedness.

When averaging (3.3), we shall assume that all rapid fluctuations of T over the averaging interval I are contained in the sum term so that the energy dependence of T_0 may be disregarded in the interval I and $\langle T_0 \rangle$ set equal to T_0. In the sum term the $\psi_0^{(\pm)}$ also depend on E through the equation

$$(E - T_a - V_a'')\, \psi_0^{(\pm)} = 0$$

but this dependence will be slow so that the average can be calculated approximately by the application of (3.7). The result is

$$\langle T \rangle = T_0 + \sum_s \frac{\langle \psi_0^{(-)} \phi_0 | VQ | \Phi_s \rangle \langle \Phi_s | QV | \phi_0 \psi_0^{(+)} \rangle}{E - E_s - \Delta_{ss} + \frac{i}{2}\Gamma_{ss} + \frac{i}{2} I} \tag{3.8}$$

The only difference between this expression and (3.3) is that the E in the denominator of the sum is replaced by E + iI/2. Since the T-matrix of (3.3) followed from the solution of (3.2), we see that the average $\langle T \rangle$-matrix will follow from the solution of the equation obtained by replacing E by E + iI/2 in the denominator of the sum in (3.2). The resulting equation is a one-particle equation whose solution leads to the average $\langle T \rangle$-matrix and is thus by definition the optical model equation. This observation enables us to identify the optical model potential as

$$V - iW = V_a'' + \sum_s \frac{(\phi_0 | VQ | \Phi_s \rangle \langle \Phi_s | QV | \phi_0)}{E - E_s + \frac{i}{2} I} \tag{3.9}$$

We shall be especially interested in the imaginary part of the optical potential, which is

$$W = \frac{2}{I} \sum_s \frac{(\phi_0 | VQ | \Phi_s \rangle \langle \Phi_s | QV | \phi_0)}{1 + 4(E - E_s)^2 / I^2}$$

The denominator has the effect of damping the contributions from levels with $|E - E_s| \gg I/2$. In fact most of the contribution to this sum comes from levels within I, and we find

$$W \approx \frac{\pi}{\Delta} \sum_{s=1}^{N} (\phi_0 | VQ | \Phi_s \rangle \langle \Phi_s | QV | \phi_0) \tag{3.10}$$

where we disregard end effects and simply sum over the N levels whose energies E_s fall inside the interval $\Delta \sim \pi I/2$.

Two features of W emerge directly from this expression. In the first place it contains an intrinsic energy-dependence on account of the fact that a different set of levels E_s will be included in the sum at different energies E. Furthermore, the potential is non-local, as we can see by writing (3.10) in configuration space

$$W(a, a') = \frac{\pi}{\Delta} \sum_s \int d(1 \ldots A) d(1' \ldots A') \phi_0^*(1 \ldots A) V(a, 1 \ldots A) \Phi_s(a, 1 \ldots A)$$

$$\times \Phi_s^*(a', 1' \ldots A') V(a', 1' \ldots A') \phi_0(1' \ldots A') \qquad (3.11)$$

This would introduce an additional energy-dependence if an equivalent local optical potential is used for W.

To investigate the physical meaning of (3.10), let us make some extreme assumptions. In particular, consider a closed shell plus one nucleus such as ^{17}O, ^{41}Ca, ^{209}Pb and suppose that their ground state ϕ_0 can be written as a single Slater determinant of shell model single-particle wave functions. The operator QV which causes excitations can then be identified with the residual interaction V_R of the nuclear shell model. If it is assumed to be pure two-body interaction, the only effect it has on ϕ_0 is to excite the odd nucleon from its ground state level 0 to another level β, or to excite a nucleon out of the completely filled Fermi sea, while the incident nucleon drops into a single-particle α. This suggests that we expand Φ_s in terms of such simple excitations, ψ_d say:

$$\Phi_s = \sum_d a_{sd} \psi_d + \text{other terms} \qquad (3.12)$$

where the "other terms" are not coupled to $\phi_0 \psi_0^{(+)}$ through V_R.

The expression for W then becomes:

$$W \approx \frac{\pi}{\Delta} \sum_d \left[\sum_s |a_{sd}|^2 \right] (\phi_0 | V_R | \psi_d \rangle \langle \psi_d | V_R | \phi_0)$$

$$\approx \frac{\pi}{\Delta} \sum_d (\phi_0 | V_R | \psi_d \rangle \langle \psi_d | V_R | \phi_0) \qquad (3.13)$$

where $\sum_s |a_{sd}|^2$ should approach unity if a sufficiently large set of "compound states" Φ_s is included in Δ. Although (3.13) has the same form as (3.10), the simple excitations ψ_d will in general be expected to be much further apart in energy than the compound states Φ_s (i.e. $D_d \gg D_s$) so that the sum includes far fewer terms.

Let us return to the simple case we are discussing and simplify the model further by disregarding excitations of the Fermi sea. Thus the excitations

$$\psi_d(a, b) = \phi_\alpha(a) \phi_\beta(b)$$

are simply two-particle states in the shell-model potential. (We denote

the co-ordinates of the incident and target nucleons by a and b, respectively, and neglect antisymmetry.) If we define

$$V_{0\beta}(a) \equiv (\phi_0(b),\ V_R(a,b)\,\phi_\beta(b))$$

it is easy to see that the imaginary part of the optical potential becomes

$$W(a,a') = \frac{\pi}{\Delta}\left[\sum_\beta V_{0\beta}(a)\,V_{\beta 0}(a')\right]\left[\sum_\alpha \phi_\alpha(a)\,\phi_\alpha^*(a')\right] \qquad (3.14)$$

where the separation into the product of two sums is a consequence of using a simple product wave function.

This simple expression can serve as basis for a few remarks concerning $W(a,a')$. In the first place, we observe that the radial distribution of the imaginary potential is determined mainly by the single-particle wave functions. We also obtain an explicit representation of the non-locality and notice that it is of a separable form, quite unlike the forms that are usually used for phenomenological studies. In our model the non-locality is determined by the density distribution of the "extra core" particles and could thus have a range of the same order as the dimensions of the nucleus. If the interval Δ had contained a complete set of states, closure would have reduced the second bracket to $\delta(a - a')$ and the potential would have become a local one. Of course, the model is a very simple one and even coupling to a definite angular momentum would destroy the single-product nature of our wave function.

4. INTERMEDIATE STRUCTURE AND DOORWAY STATES

When the cross-section for a nuclear reaction is measured with good energy resolution (1 keV, say, for light nuclei and better for heavy nuclei) at low excitation energies, one usually observes isolated resonances with widths Γ_s and spacing D_s. In the first section we saw how these resonances can be associated with compound nuclear levels or eigenstates of H_{QQ} (see Eq. (1.7)) in our formalism. At higher energies these resonance peaks merge and are replaced by Ericson fluctuations. If, on the other hand, the energy resolution is poor (say 2 MeV), one only observes the very broad peaks described by the optical model [4].

If an intermediate energy resolution (say 50 keV) is used, an intermediate type of structure (widths Γ_d, spacings D_d) is often seen. This is shown in Fig. 3 for the total cross-section of ^{19}F for neutrons.

One could speculate that this intermediate structure is caused by random fluctuations but would then find it difficult to explain the large widths $\Gamma_d \gg \Gamma_s$. In many cases the correlated structure in different reaction channels makes this interpretation untenable. An alternative explanation that has been advanced since 1963 [5] is in terms of simple excitations of the compound system.

As an example we may consider the case of a nucleon incident on a closed-shell nucleus which is described by means of a completely filled Fermi sea with additional empty bound levels (Fig. 4).

If the residual interactions consist of pure two-body forces, the most complicated state they could produce when acting once only would consist of the incident nucleon dropping down into an empty bound level while another nucleon is lifted out of the sea to another empty level (these levels could in general also be in the continuum). If no further couplings to the Fermi sea are allowed, this two-particle - one-hole (2p-1h) state (which we denote ψ_d) is all that can form and according to (1.14) we expect to see a resonance of width

$$\Gamma^{\uparrow} = 2\pi \left| \langle \psi_d \left| V \right| \phi_0 \psi_0^{(+)} \rangle \right|^2 \tag{4.1}$$

Actually, the state ψ_d is not stationary and more complicated states Φ_s evolve. Since they contain ψ_d only partly, the matrix elements that determine Γ_s are much smaller, so that $\Gamma_s \ll \Gamma^{\uparrow}$. The simple excitations ψ_d were called doorway states by Block and Feshbach [5], since they provide the entrance into the states Φ_s of the compound system. We shall later see under what circumstances the average cross-sections are dominated by their structure.

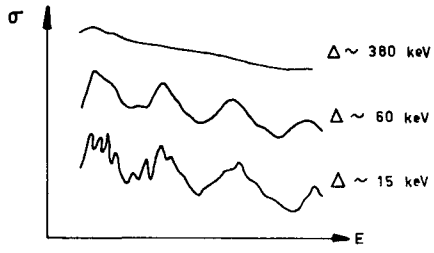

FIG. 3. Total cross-section of ^{19}F for neutrons showing that if an intermediate energy resolution is used, an intermediate type of structure appears

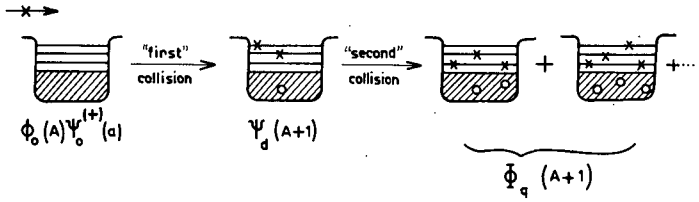

FIG. 4. Case of a nucleon incident on a closed-shell nucleus described by means of a completely filled Fermi sea with additional bound levels

More generally, we can always decompose the eigenfunction Ψ of the complete Hamiltonian H into three parts

$$\Psi = P\Psi + d\Psi + q\Psi \tag{4.2}$$

where the projection operator P is defined to project onto the part where the target is in its ground state, q projects onto the part which is orthogonal to $H\Psi$, and $d = 1 - P - q$. If only one doorway state ψ_d is important,

it is proportional to $d\Psi$. The eigenstates of H_{QQ} can then be decomposed according to

$$\Phi_s = a_{sd}\psi_d + q\Phi_s \tag{4.3}$$

and a typical matrix element becomes

$$\langle \psi_0^{(-)} \phi_0 | VQ | \Phi_s \rangle = a_{sd} \langle \psi_0^{(-)} \phi_0 | V | \psi_d \rangle \tag{4.4}$$

since d and q have been defined in such a way that $P\psi_d = 0$ and $V_{Pq} = 0$.

The spectra of the operators H_{PP}, H_{dd} and H_{qq} can be pictured as shown in Fig. 5.

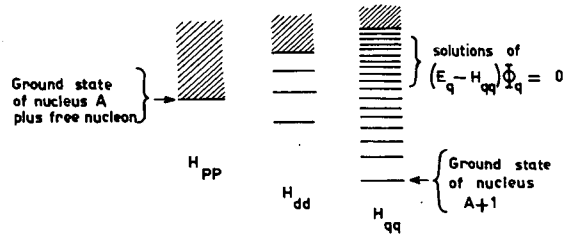

FIG. 5. Spectra of the operators H_{PP} H_{dd} H_{qq}

When the coupling term V_{dq} is included, the eigenstates Φ_s of H_{QQ} are linear combinations of the ψ_d and the Φ_q. There may be small energy shifts but in general the spectrum of the E_s will be very similar to that of the E_q. When V_{Pd} is also included, further shifts of the levels below threshold may occur while the discrete states above the lowest threshold become resonances.

To investigate the coupling between H_{dd} and H_{qq}, let us consider the following schematic model:

(1) Assume that we have a single doorway state ψ_d against a background of equidistant (spacing D) levels Φ_q.

(2) Assume that the matrix elements $\langle \Phi_q | V | \psi_d \rangle$ are independent of q (= V, say).

To obtain the coefficients a_{sd}, one could diagonalize H_{QQ} in the basis $\{\psi_d, \Phi_q\}$. However, it is simpler to consider the Green's function

$$G(E) \equiv \langle \psi_d | d \frac{1}{E - H_{QQ}} d | \psi_d \rangle \tag{4.5}$$

$$= \sum_s \langle \psi_d | \frac{1}{E - H_{QQ}} | \Phi_s \rangle \langle \Phi_s | \psi_d \rangle$$

$$= \sum_s \frac{|a_{sd}|^2}{E - E_s} \tag{4.6}$$

since its poles are the actual resonances while the residues are precisely $|a_{sd}|^2$. Using the identity

$$d\,\frac{1}{E - H_{QQ}}\,d = d\,\frac{1}{E - H_{dd} - H_{dq}\,\dfrac{1}{E - H_{qq}}\,H_{qd}}\,d \tag{4.7}$$

we obtain

$$G(E) = \left\{E - E_d - \sum_q \frac{|\langle \psi_d | H_{dq} | \Phi_q \rangle|^2}{E - E_q}\right\}^{-1}$$

$$= \left\{E - E_d - \frac{\pi |V|^2}{D} \cot\left(\frac{\pi E}{D}\right)\right\}^{-1} \tag{4.8}$$

where we have made use of the assumptions of our model. The poles E_s of G(E) are thus given by the solutions of

$$E_s - E_d - \frac{\pi |V|^2}{D} \cot\left(\frac{\pi E_s}{D}\right) = 0 \tag{4.9}$$

while the residues are given by

$$|a_{sd}|^2 = \lim_{E \to E_s} [(E - E_s)\,G(E)]$$

$$= \left\{1 + \frac{\pi^2}{D^2} |V|^2 \operatorname{cosec}^2\left(\frac{\pi E_s}{D}\right)\right\}^{-1}$$

$$= \frac{|V|^2}{(E_s - E_d)^2 + (\pi |V|^2/D)^2 + V^2} \tag{4.10}$$

This is simply a Lorentzian form as shown in Fig. 6. If $|V| \gg D$, we can write

$$\frac{2\pi}{D} |a_{sd}|^2 = \frac{\Gamma^{\downarrow}}{(E_s - E_d)^2 + (\Gamma^{\downarrow}/2)^2} \tag{4.11}$$

$$\Gamma^{\downarrow} = \frac{2\pi}{D} |\langle \Phi_q | V | \psi_d \rangle|^2 \tag{4.12}$$

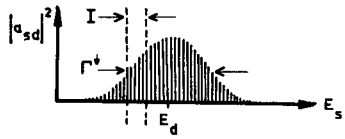

FIG. 6. The residues $|a_{sd}|^2$ as a function of E_s

The "strength" of the doorway state is thus distributed among actual compound states Φ_s in an energy interval of order $\Gamma^{\downarrow}$ around E_d. The distribution of eigenvalues E_s differs very little from the distribution of E_q. Although these results were derived from a very simple model, they

remain qualitatively true for a more realistic model and will thus be repeatedly used in the further discussion.

If we consider energy averages over an interval $I \gg \Gamma_{ss}$, neglect the shifts Δ_{ss}, and introduce expansion (4.3), the average T-matrix of Eq. (3.8) becomes

$$\langle T \rangle = T_0 + \langle \psi_0^{(-)} \phi_0 | Vd | \psi_d \rangle \langle \psi_d | dV | \phi_0 \psi_0^{(+)} \rangle \sum_s \frac{|a_{sd}|^2}{E - E_s + iI/2} \tag{4.13}$$

For $I \gg D_s \approx D$, we could write

$$\sum_s \frac{|a_{sd}|^2}{E - E_s + iI/2} \approx \frac{1}{D} \int \frac{\langle |a_{sd}|^2 \rangle \, dE_s}{E - E_s + iI/2}$$

$$= \int dE_s \frac{\Gamma^{\downarrow}/2\pi}{(E_s - E_d)^2 + (\Gamma^{\downarrow}/2)^2} \cdot \frac{1}{E - E_s + iI/2}$$

$$= \frac{1}{E - E_d + \frac{i}{2}(\Gamma^{\downarrow} + I)} \tag{4.14}$$

where we have introduced the result (4.11) and made use of (3.7).

The width $\Gamma^{\downarrow}$ of (4.12) contains the coupling of the doorway state with the states Φ_q. The coupling with the entrance channel adds the width $\Gamma^{\uparrow}$ of (4.1) so that the average T-matrix becomes

$$\langle T \rangle = T_0 + \frac{\langle \psi_0^{(-)} \phi_0 | Vd | \psi_d \rangle \langle \psi_d | dV | \phi_0 \psi_0^{(+)} \rangle}{E - E_d + \frac{i}{2}(\Gamma^{\uparrow} + \Gamma^{\downarrow} + I)} \tag{4.15}$$

It now becomes clear that intermediate structure associated with a doorway state will become evident in an average cross-section whenever an averaging interval I can be chosen which satisfies the criteria

$$D_d > \Gamma_d > I \gg D_s, \Gamma_s \tag{4.16}$$

where $\Gamma_d = \Gamma^{\uparrow} + \Gamma^{\downarrow}$ is the total width. Equations (4.1) and (4.12) both have the form of the "golden rule" with the density of states represented, respectively, by 1 (on account of the energy normalization of the continuum states $\psi^{(+)}$) and by D^{-1}. They represent the transition probability per unit time for the escape of the nucleon back into the entrance channel and for the decay of the doorway state into more complicated states. For this reason $\Gamma^{\uparrow}$ and $\Gamma^{\downarrow}$ are called the escape width and the decay width of the doorway state, respectively.

It is interesting to see what optical model potential would produce the average cross-sections which include intermediate structure. Let us

first generalize the situation somewhat by allowing for contributions from more than one doorway state.

$$\Phi_s = \sum_d a_{sd}\psi_d + q\Phi_s \tag{4.17}$$

The last term in (4.13) then becomes

$$\sum_d \sum_{d'} \langle \psi_0^{(-)} \phi_0 | V | \psi_{d'} \rangle \langle \psi_d | V | \phi_0 \psi_0^{(+)} \rangle \sum_s \frac{a_{sd}^* a_{sd'}}{E - E_s + iI/2} \tag{4.18}$$

If the cross terms in the sum over s are assumed to vanish or to cancel, we may again apply (4.11) as before. By analogy with (3.9), the corresponding optical potential is then given by

$$V - iW = \sum_d \frac{(\phi_0 | V | \psi_d \rangle \langle \psi_d | V | \phi_0)}{E - E_d + \frac{i}{2}(I + \Gamma^{\downarrow})} \tag{4.19}$$

If $I \gg \Gamma_d^{\downarrow}$, we recover the ordinary optical potential of (3.13) expressed as a sum over doorway states. When $I < \Gamma^{\downarrow}$, the potential is very different, however. Among other things, it is much more strongly energy-dependent.

In this formulation in terms of doorway states, the complexity of the many-body problem is shifted to the coefficients a_{sd} and finally to the decay width $\Gamma^{\downarrow}$. To be able to see non-overlapping doorway states, $\Gamma^{\downarrow}$ should not become too large. This restriction would for example be satisfied if the number of states Φ_q which are connected to ψ_d through the matrix elements which occur in (4.12) is cut down due to some selection rule such as conservation of total angular momentum, parity or isospin. This is what happens in the case of analog states. It also leads us to expect doorway phenomena to stand out more clearly near closed shells where the states are simpler and the selection rules more effective. The decay width $\Gamma^{\downarrow}$ would nevertheless be spread over several compound states s so that (4.11) indicates that for all states

$$|a_{sd}|^2 < \frac{D_s}{\Gamma^{\downarrow}} \ll 1 \tag{4.20}$$

This also implies

$$\Gamma_s = |a_{sd}|^2 \Gamma^{\uparrow} \ll \Gamma^{\uparrow} \tag{4.21}$$

The effects of the coupling between the Φ_q states and the doorway state can also be looked at from a time-dependent point of view. If we neglect coupling to the entrance channel, we may expand the total time-dependent function $\Psi(t)$ in terms of the complete set Φ_s:

$$\Psi(t) = \sum_s A_s \Phi_s e^{-iE_s t}$$

Let us assume $\Psi(0) = \psi_d$ at $t = 0$ and consider the expansion

$$\Phi_s = a_{sd}\,\psi_d + \text{terms which we disregard.}$$

Then it is easy to see that

$$\Psi(t) = \sum_s |a_{sd}|^2\, e^{-iE_s t}\, \psi_d$$

By inserting (4.11) and changing the sum into an integral which can be done by completing the contour in the lower half of the E_s-plane, we find

$$\Psi(t) = \psi_d e^{-iE_d t}\, e^{-\Gamma^{\downarrow} t/2} \tag{4.22}$$

This shows once more that the doorway state is not stationary and that $1/\Gamma^{\downarrow}$ measures the lifetime with respect to decay into the compound states.

5. ANALOG RESONANCES

Having investigated some of the conditions under which doorway states could produce intermediate structure in cross-sections, let us now discuss a specific type of doorway state which to date offers perhaps the clearest example of this phenomenon.

As a specific example let us take the resonance structure which has been seen [6] in the scattering of 5-7 MeV protons from ^{88}Sr (see Fig. 8). At 5.06, 6.06 and 7.06 MeV one observes strong structure with widths 16, 70 and 50 keV. Compound nuclear widths in this region should be only about 200 eV so that another explanation is required.

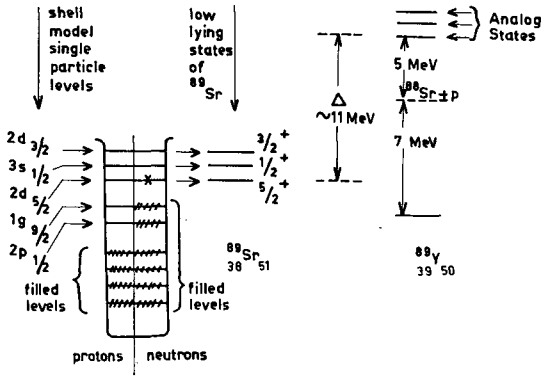

FIG. 7. Comparison of resonance structure with the isobaric spin analogs of the $5/2^+$, $1/2^+$ and $3/2^+$ ground and first two excited states of ^{89}Sr

The correct interpretation seems to be to identify these resonances with the isobaric spin analogs of the $5/2^+$, $1/2^+$ and $3/2^+$ ground and first two excited states of ^{89}Sr. This is illustrated in Fig. 7.

The excited states of ^{89}Y with which the resonances are identified are obtained from the low-lying states of ^{89}Sr by a charge exchange process. In the figure Δ means the energy difference

$$\Delta = \Delta E_c - (m_n - m_p) \tag{5.1}$$

where ΔE_c is the Coulomb energy difference.

These analog states are, however, surrounded by a very dense distribution of other states of ^{89}Y and we must provide an explanation for the fact that only these states give rise to intermediate structure in the cross-section before the interpretation becomes convincing.

Robson [7] suggested that this comes about because the conservation of isospin is also valid in heavy nuclei. Thus we can characterize states by the values (T, T_3) of the total isospin and its 3-component. We shall use the convention that the nucleon ($T = \frac{1}{2}$) state corresponds to a neutron if $T_3 = +\frac{1}{2}$ and a proton if $T_3 = -\frac{1}{2}$. All the states of a given nucleus must thus have

$$\left.\begin{aligned} T_3 &= \tfrac{1}{2}(N - Z) \\ T &\geq |T_3| \end{aligned}\right\} \tag{5.2}$$

Nuclear forces produce greater binding for low T-values so that the ground states almost always have $T = T_3$. The ground state isospin of the target nucleus is denoted T_0. (In our example of ^{88}Sr, $T_0 = 6$.)

The states of ^{89}Sr which were drawn on Fig. 7 must all have $T = T_0 + \frac{1}{2}$. If isospin is a good quantum number, the analog states in ^{89}Y will also have $T = T_> \equiv T_0 + \frac{1}{2}$. On the other hand, the dense distribution of states surrounding the analog states will have $T = T_< \equiv T_0 - \frac{1}{2}$. From Eq. (4.12) we thus have

$$\Gamma^{\downarrow} = \frac{2\pi}{D} \left| \langle T_0 - \tfrac{1}{2} | V | T_0 + \tfrac{1}{2} \rangle \right|^2 \tag{5.3}$$

If nuclear forces conserve isospin, the only contribution to the matrix element could come from the long-range Coulomb force, but this has very small matrix elements between different orbital states and yields widths of at most 5 keV [8]. The actual widths are appreciably larger so that we can to a good approximation set

$$\Gamma^{\downarrow} \approx 0 \tag{5.4}$$

Thus isospin conservation provides a possible explanation why the analog states manifest themselves so strongly as doorway states.

The question arises as to how the compound states are in fact formed if the doorway states cannot decay into them, as (5.4) indicates. The answer lies partially in the fact that the actual physical state of proton plus target is a mixture of different isospin states. This is most easily seen in terms of a model developed by Lane [7]. Let us denote the target state by $|C\rangle$ and its analog state by $|A\rangle$. This is, namely, the state obtained by operating on $|C\rangle$ with the isospin lowering operator T_- and normalizing. In our example it would be a linear combination of

states having a hole in one of the neutron $g_{9/2}$ or $p_{1/2}$ levels and a particle in the corresponding proton level. The analog states in ^{89}Y are obtained by applying T_- to the low-lying states in ^{89}Sr. It is easy to show that this gives

$$|T_0 + \tfrac{1}{2},\ T_0 - \tfrac{1}{2}\rangle = \frac{1}{\sqrt{2T_0 + 1}}\ T_-|T_0 + \tfrac{1}{2},\ T_0 + \tfrac{1}{2}\rangle$$

$$= \frac{1}{\sqrt{2T_0 + 1}}\ |pC\rangle + \sqrt{\frac{2T_0}{2T_0 + 1}}\ |nA\rangle \qquad (5.5)$$

so that the overlap between the incident state $|pC\rangle$ (proton plus target) with the analog state $|T_0 + \tfrac{1}{2},\ T_0 - \tfrac{1}{2}\rangle$ is indeed small.

In Lane's model, we can write the Hamiltonian as

$$H = H_{T_0} + T_a + V_a + V_1 \vec{t}\cdot\vec{T}_0 + V_c(\tfrac{1}{2} - t_3) \qquad (5.6)$$

where V_c is the Coulomb force ($1/2 - t_3 = 1$ for protons and 0 for neutrons) while the surface-peaked isospin-dependent term $V_1 \vec{t}\cdot\vec{T}$ is an idealization of a term $\sum_i V_{ai}\,\vec{t}\cdot\vec{t}_i$ obtained by assuming that the coupling matrix elements V_{ai} between incident and target nucleons are independent of the orbit involved. To describe averaged cross-sections, we should add to the Hamiltonian (5.6) an imaginary potential -iW which contains absorption into the background of $T = T_<$ states. To prevent this potential from acting in $T = T_>$ states (since the analog state is not damped to a first approximation), we append to -iW the projection operator

$$P_< = \frac{T_0 - 2\vec{t}\cdot\vec{T}_0}{2T_0 + 1} \qquad (5.7)$$

onto $T = T_<$ states.

Rearranging, we obtain for the Hamiltonian

$$H = H_{T_0} + T_a + V_a + V_c(\tfrac{1}{2} - t_3) - \frac{iWT_0}{2T_0 + 1} + \left(V_1 + \frac{2iW}{2T_0 + 1}\right)\vec{t}\cdot\vec{T}_0 \qquad (5.8)$$

If we now expand the solution of the Schrödinger equation $(E - H)\Psi = 0$ as

$$\Psi = u_p|pC\rangle + u_n|nA\rangle \qquad (5.9)$$

we obtain the following coupled equations

$$\left.\begin{aligned}\left(T_p + V_p + V_c - iW\frac{2T_0}{2T_0 + 1} - V_1\frac{T_0}{2}\right)u_p - Eu_p + \sqrt{\frac{T_0}{2}}\left(V_1 + \frac{2iW}{2T_0 + 1}\right)u_n = 0\\ \left(T_n + V_n - iW\frac{1}{2T_0 + 1} + V_1\frac{T_0 - 1}{2}\right)u_n - (E - \Delta)u_n + \sqrt{\frac{T_0}{2}}\left(V_1 + \frac{2iW}{2T_0 + 1}\right)u_p = 0\end{aligned}\right\} \qquad (5.10)$$

where use has been made of the matrix elements

$$\langle pC|\vec{t}\cdot\vec{T}_0|pC\rangle = -T_0/2$$

$$\langle nA|\vec{t}\cdot\vec{T}_0|nA\rangle = (T_0 - 1)/2$$

$$\langle nA|\vec{t}\cdot\vec{T}_0|pC\rangle = \sqrt{T_0/2}$$

and the eigenvalue equations

$$H_{T_0}|C\rangle = 0 \qquad H_{T_0}|A\rangle = \Delta|A\rangle$$

Equations (5.10) correspond closely to what we would expect on the basis of physical intuition, for example, that for large T_0 (i.e. heavy nuclei) the absorptive potential W acts mostly on the entrance channel $|pC\rangle$ and hardly at all on the analog state $|nA\rangle$. The only feature which is perhaps unexpected is the appearance of the absorptive potential in the coupling terms between the two equations.

To solve (5.10), one could proceed as before, eliminating u_n between the two equations and deriving a resonance formalism (complicated by the imaginary potential iW) for u_p. Actually it is simpler to solve the coupled equations directly by numerical integration. For this purpose one requires real proton and neutron potential wells V_p and V_n for which the usual optical model Saxon-Woods potentials may be used, and similarly an imaginary well W. The energy shift Δ is obtained from empirical data while V_1 can be estimated on the basis of the shell model.

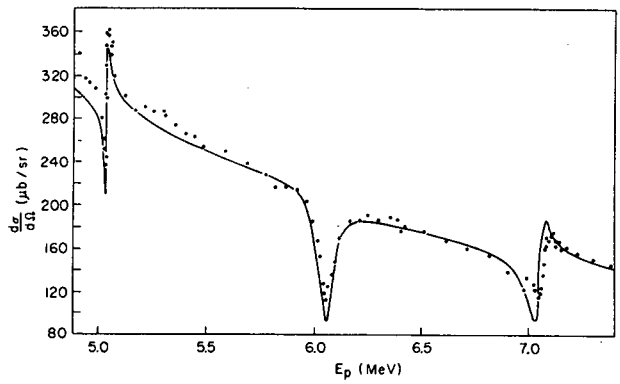

FIG. 8. Calculated differential cross-sections at 90° for p + ^{88}Sr. The resonances at 5.06, 6.06 and 7.07 MeV are $d_{5/2}$, $s_{1/2}$ and $d_{3/2}$, respectively (Courtesy of American Institute of Physics)

The results of such a calculation are indicated by the curves on Fig. 8. The positions of the three resonances are easily fitted by adjusting V_n and the spin-orbit potential, although it is important that the required strengths are consistent with those normally used in the shell model and the optical model. The real success of the model lies, however, in the fitting of the resonance shape. Since the resonance term itself is small, the largest effect comes from its interference with the potential scattering. Since

this is very sensitive to relative phases, one must be able to influence the relative phase in order to get a good fit. It turns out that for this to be possible, the appearance of W in the coupling terms plays a decisive role.

6. APPLICATIONS

If we consider an appropriate energy-averaging interval and include contributions from more than one doorway state, the average transition matrix (4.15) is given by

$$\langle T \rangle = T_0 + \sum_d \frac{\langle \psi_0^{(-)} \phi_0 | V_R | \psi_d \rangle \langle \psi_d | V_R | \phi_0 \psi_0^{(+)} \rangle}{E - E_d + \frac{i}{2}(\Gamma_d^{\uparrow} + \Gamma_d^{\downarrow})} \tag{6.1}$$

(this is actually only true when $\sum_s a_{sd}^* a_{sd'}$ vanishes for $d' \neq d$, as we have seen). How should we now go about to do an actual calculation with this expression?

The transition matrix T_0 and the wave functions $\psi_0^{(\pm)}$ are simply obtained from the solutions of the single-particle equation

$$(T_a + V_a') \psi_0^{(\pm)} = E \psi_0^{(\pm)} \tag{6.2}$$

where V_a' is a real potential for which we could for example use a Woods-Saxon well. This part of the calculation simply produces a nuclear size effect and corresponds in the bound state problem to finding the zero-order energy levels before diagonalizing the residual interactions.

To calculate the matrix elements in (6.1), one further needs the residual interaction V_R, the target wave function ϕ_0 and the doorway wave function ψ_d. These are all obtained by means of some dynamical nuclear model. We could for example in light nuclei use a pure shell model, for heavier nuclei introduce a vibrational collective model and in the rare earth region include rotations. Once the matrix elements are known, so is the escape width $\Gamma_d^{\uparrow}$ (Eq.(4.1)) which is just 2π times the absolute value of the denominator in (6.1).

The only unknown that is left is therefore the decay width $\Gamma_d^{\downarrow}$. It contains our ignorance concerning the many-particle compound system. In some cases it may become small compared with $\Gamma_d^{\uparrow}$ due to the operation of a selection rule such as angular momentum or isospin. Otherwise it could be retained as an unknown parameter.

Let us look in somewhat more detail at a few examples where this formalism has been applied to light nuclei, assuming that the decay width vanishes, so that the ψ_d are already compound states.

6.1. ^{15}N + p or n

In the shell model, the ground state of ^{15}N is represented by a hole in the proton $1p_{1/2}$ level. For giant dipole states Brown [9] has suggested a particle-hole description. This can be extended to all the excited states

of the A = 16 system rather than only the 1^- states. As a basis for the ψ_d, one can thus use states consisting of a $1p_{3/2}$ hole plus a particle in the $1d_{5/2}$, $2s_{1/2}$, or $1d_{3/2}$ level. Adding a residual interaction term of the form

$$(a + b\vec{\sigma}_1 \cdot \vec{\sigma}_2)\,\delta(\vec{r}_1 - \vec{r}_2)$$

one can now diagonalize the Hamiltonian in this basis, thus constructing the eigenstates which are identified with the ψ_d. The widths as well as the energy shifts can now be calculated. The results of such a calculation [10] are shown on Fig. 9.

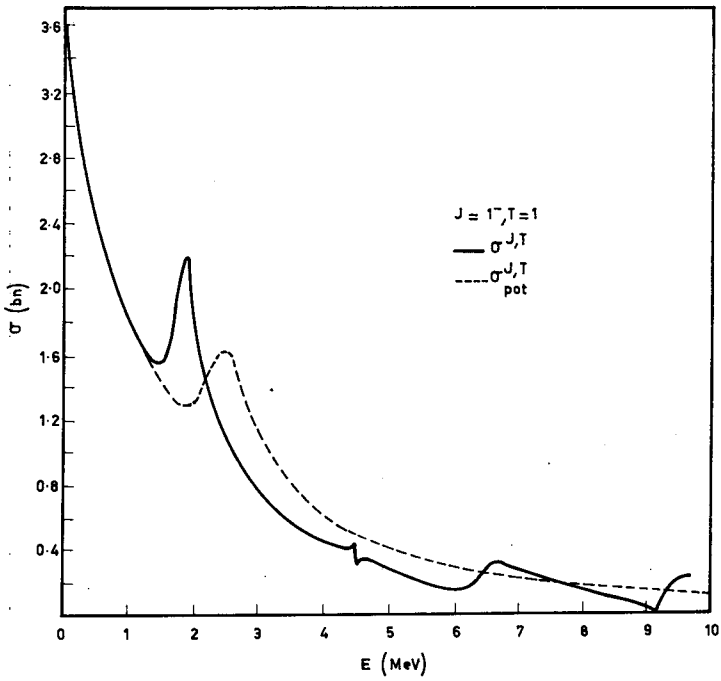

FIG. 9. Calculated cross-section as a function of energy for the $J = 1^-$ channel in nucleon + A = 15

Each angular momentum and parity defines a different channel. The 1^- channel is shown on the figure. Resonances are found at 1.85, 4.52, 6.54 and 9.28 MeV with widths 300, 9, 800 and 580 keV, the last two corresponding to giant dipole states. Notice the wide range of widths obtained from this formulation in spite of the fact that the states all have the simple 1p-1h structure.

6.2. $^{12}C + n$

The same techniques have been applied to the scattering of neutrons from ^{12}C [11] except that the pertinent states of ^{13}C are now 2p-1h states. The comparison between the calculated (broken line) and measured (solid line) cross-sections is shown on Fig. 10. The resonances at 1.9, 2.7

and 3.2 MeV have calculated widths of 80, 200, and 500 keV and correspond (tentatively) to $5/2^+$, $3/2^+$, and $3/2^+$ states. What is again impressive is not so much that the correct resonance energies could be fitted but that the estimates of the widths agree so well with experiment.

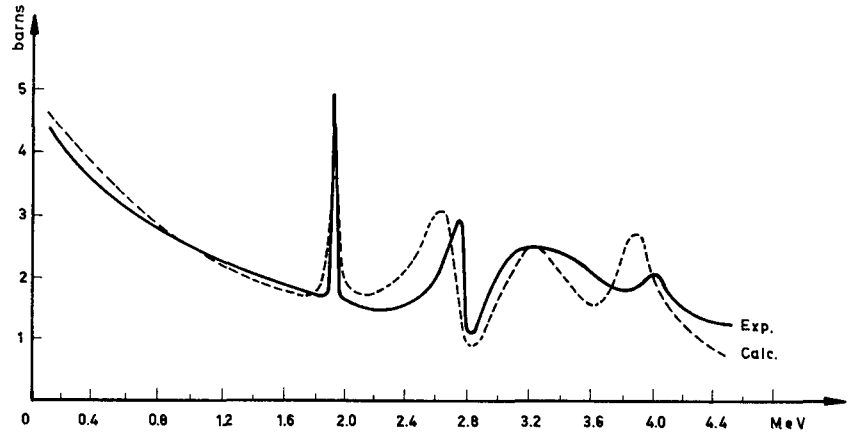

FIG.10. Comparison between the calculated (broken line) and measured (solid line) cross-sections for the scattering of neutrons from ^{12}C

It is interesting to note that the same system has also been studied assuming that the states of ^{13}C consist of a deformed ^{12}C core with an extra neutron coupled to the rotational band [12]. Here the states ψ_d were not described as 2p-1h states of the shell model but by means of wave functions

$$\psi_d = \{\phi_j(a)\, \mathcal{D}^J_{MK}\}$$

where the curly brackets denote that coupling to definite total angular momentum must be performed. A surface quadrupole residual interaction was used. The analysis was not performed by means of the Feshbach formalism but in terms of R-matrix theory. The compound nuclear levels were, however, calculated by the diagonalization of a realistic interaction. The results are very similar to those obtained by means of the shell-model calculation described before.

6.3. The giant dipole state

In the case of analog resonances, conservation of isospin resulted in small decay widths $\Gamma^{\downarrow}$ so that essentially only the escape widths $\Gamma^{\uparrow}$ had to be calculated. The opposite situation occurs for the giant dipole resonance, whose width of about 5 MeV is much larger than typical calculated escape widths ($\sim$ 50 keV) and consists almost entirely of the decay width.

This resonance occurs in photodisintegration (γ, n) reactions at about 15 MeV in a typical heavy nucleus like ^{208}Pb. Since photons of

this energy transfer small momenta, we expand the transition operator into multipoles and keep only the electric dipole part:

$$\sum_{i=1}^{Z} e\, x_i \tag{6.3}$$

However, since we are not interested in photon scattering by the total nuclear charge but rather in excitations, we should use a dipole operator with co-ordinates measured with respect to the centre of mass $X = \sum_{1}^{A} x_i/A$ of the nucleus. Thus we obtain

$$D = \sum_{i=1}^{Z} e\left(1 - \frac{Z}{A}\right)x_i - \sum_{i=1}^{N} e\,\frac{Z}{A}\,x_i$$

$$= \sum_{i=1}^{A} e\left(\frac{1}{2} - \frac{Z}{A} - t_3(i)\right)x_i = D^{(0)} + D^{(1)} \tag{6.4}$$

where we have decomposed D into parts which transform like a scalar and the third component of a vector in isospin. The factor $e(1/2 - Z/A - t_3)$ where t_3 is the third component of the nucleon isospin $\vec{t}$, summarizes the effective charges carried by protons and neutrons.

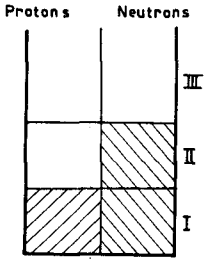

FIG.11. Schematic filling of proton and neutron shells in a heavy nucleus

Denote the ground state of the target nucleus by $|T = T_0,\ T_{03} = T_0\rangle$. Operating on this with $D^{(0)}$ and $D^{(1)}$ of Eq. (6.4) produces respectively a state with $T = T_0$ and a linear combination of states with $T = T_0$ and $T = T_0 + 1$. Now since the D's are one-particle operators these excitations are of a particle-hole type. Let us analyse their structure in more detail. Figure 11 indicates the schematic filling of proton and neutron shells in a heavy nucleus. We divide the levels into three groups: I is filled by protons and neutrons, II by neutrons only, and III is empty. The possible excitations produced by D can be grouped according to

(1) proton-proton hole $a_p^{\dagger}(\mathrm{II})\, a_{\tilde{p}}(\mathrm{I})$

(2) neutron-neutron hole $a_n^\dagger(\mathrm{III})\, a_{\bar{n}}(\mathrm{II})$

(3) nucleon-nucleon hole $a_i^\dagger(\mathrm{III})\, a_{\bar{i}}(\mathrm{I})$

where each particle-hole pair is coupled to $J = 1^-$, and the notation is p or n for particle, $\bar{p}$ or $\bar{n}$ for hole.

Now while excitations of type (1) or (2) cannot change the isospin of the target nucleus, this is no longer true for type (3) in which the nucleon-nucleon hole pair can couple to isospin $T_{ph} = 0$ and 1. Type (3) therefore contributes to isospin states of the total system with $T = T_0$ and $T = T_0 + 1$ according to

$$|(T_{ph}, T_0)T, T_0\rangle = \sum (T_{ph}\, T_Z T_0\, T_{03} \,|\, T\, T_0)[a_i^\dagger(\mathrm{III})\, a_{\bar{i}}(\mathrm{I})]^{T_{ph}}_{T_Z} |\, T_0\, T_{03}\rangle \qquad (6.5)$$

in an obvious notation. In particular

$$|(1, T_0)T_0, T_0\rangle = \frac{1}{\sqrt{T_0+1}} \left\{ \sqrt{\frac{T_0}{2}} [a_n^\dagger(\mathrm{III})\, a_{\bar{n}}(\mathrm{I}) - a_p^\dagger(\mathrm{III})\, a_{\bar{p}}(\mathrm{I})] |\, T_0, T_0\rangle + a_n^\dagger(\mathrm{III}) a_{\bar{p}}(\mathrm{I}) |T_0, T_0 - 1\rangle \right\} \qquad (6.6)$$

for $T_{ph} = 1$, $T = T_0$ and

$$|(1, T_0)T_0 + 1, T_0\rangle = \frac{1}{\sqrt{T_0+1}} \left\{ \frac{1}{\sqrt{2}} [a_n^\dagger(\mathrm{III})\, a_{\bar{n}}(\mathrm{I}) - a_p^\dagger(\mathrm{III}) a_{\bar{p}}(\mathrm{I})] \,|\, T_0, T_0\rangle - \sqrt{T_0}\, a_n^\dagger(\mathrm{III}) a_{\bar{p}}(\mathrm{I}) |T_0, T_0 - 1\rangle \right\} \qquad (6.7)$$

for $T_{ph} = 1$, $T = T_0 + 1$.

To construct $|T_0, T_0 - 1\rangle$ we use the isospin lowering operator T_- defined in Eq. (5.5). Thus the second term in both (6.6) and (6.7) reads

$$a_n^\dagger(\mathrm{III})\, a_{\bar{p}}(\mathrm{I}) |\, T_0, T_0 - 1\rangle = a_n^\dagger(\mathrm{III})\, a_{\bar{p}}(\mathrm{I}) \frac{T_-}{\sqrt{2T_0}} |\, T_0, T_0\rangle$$

$$= \frac{1}{\sqrt{2T_0}}\, a_n^\dagger(\mathrm{III})\, a_{\bar{p}}(\mathrm{I})\, a_p^\dagger(\mathrm{II}) a_{\bar{n}}(\mathrm{II}) |\, T_0, T_0\rangle \qquad (6.8)$$

i.e. it is a two-particle - two-hole excitation with the pair $a_p^\dagger(\mathrm{II})\, a_{\bar{n}}(\mathrm{II})$ coupled to spin $J = 0^+$ and the pair $a_n^\dagger(\mathrm{III})\, a_{\bar{p}}(\mathrm{I})$ coupled to $J = 1^-$ as indicated in Fig. 12. The 1^- states with $T = T_0$ therefore have the structure

$$\psi_D = \left\{ \sum A_{n\bar{n}} a_n^\dagger a_{\bar{n}} + \sum B_{p\bar{p}} a_p^\dagger a_{\bar{p}} \right\} |\, T_0, T_0\rangle + \sum C_{i\bar{i}} |(0, T_0)T_0, T_0\rangle + \sum D_{i\bar{i}} |(1\, T_0)T_0, T_0\rangle \qquad (6.9)$$

while states with $T = T_0 + 1$ are given by $\sum F_{ij} |(1, T_0)\, T_0 + 1,\ T_0\rangle$. For a heavy nucleus ($T_0 = (N - Z)/2$ large) we note (a) that the 2p - 2h component in the state $|(1, T_0)\, T_0,\ T_0\rangle$ is effectively suppressed by the factor $(T_0 + 1)^{-\frac{1}{2}}$, and (b) the part of $|(1, T_0)\, T_0 + 1,\ T_0\rangle$ that is reached directly by the dipole operator is suppressed by the same factor. One therefore expects ψ_D in (6.9) to carry most of the dipole strength. Peterson [14] has estimated the contribution to the total width of the dipole state in ^{208}Pb coming from the nucleon decay (mostly neutrons) of ψ_D as given by (6.9). He finds a total escape width $\Gamma^{\uparrow} \lesssim 500$ keV which is about one tenth of the observed total width.

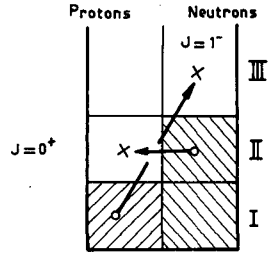

FIG.12. Two-particle - two-hole excitation required to make up a state of good total isospin in Eq.(7.4)

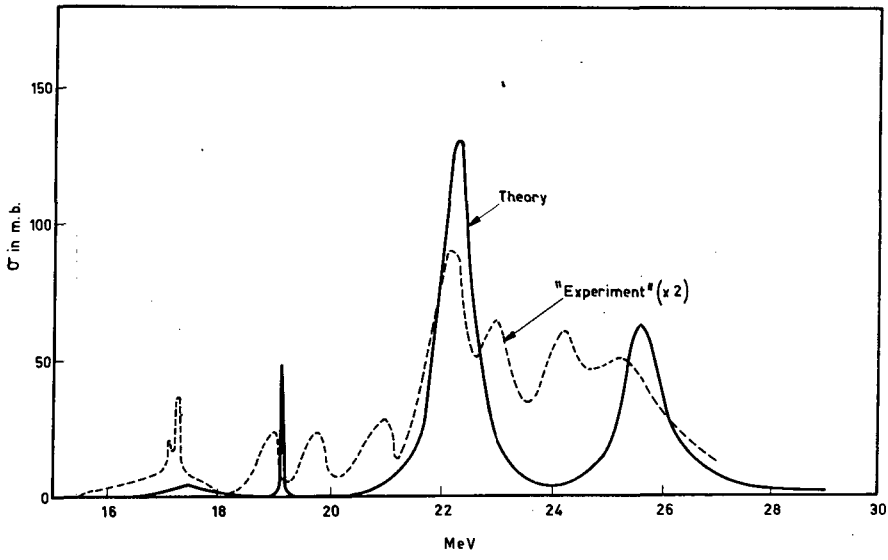

FIG.13. Result of a shell-model calculation for ^{16}O

An estimate of the damping width $\Gamma^{\downarrow}$ can be obtained by considering higher excitations such as 2p-2h, 3p-3h etc. It turns out that energy considerations only allow the first type to make a substantial contribution. Estimates of 2p-2h level densities in the energy region of the dipole state [15] lead to a value of about 50 levels per MeV. Thus more than 200 levels would be within the experimental width. This determines

the density D^{-1} which enters Eq. (4.12). Depending on the strength of the interaction, one obtains a damping width $\Gamma^{\downarrow}$ between 500 keV and 2.5 MeV for ^{208}Pb which, when supplemented with $\Gamma^{\uparrow}$, is at least beginning to approach the observed width.

In heavy nuclei the damping width is much larger than the escape width. The opposite situation holds for light nuclei. In fact, the shell model already overestimates the escape width. Figure 13 shows the result of a shell-model calculation for the ^{16}O absorption cross-section [16].

The structure of the giant dipole state is still not fully understood. It does seem to fit into our general treatment of intermediate resonances, but unlike the analog states, it is not prevented from being damped away by selection rules, and the reason why it does not damp too strongly may be a consequence of its coherent nature. To obtain better insight into its structure, it may be useful to look at 1^- states in nuclei other than the dipole state.

REFERENCES

[1] BREIT, G., WIGNER, E.P., Phys. Rev. 49 (1936) 519; WIGNER, E.P., EISENBUD, L., Phys. Rev. 72 (1947) 29.
[2] FESHBACH, H., Ann. Phys., N.Y. 5 (1958) 357; 19 (1962) 287.
[3] KERMAN, A.K., Lectures in Theoretical Physics, University of Colorado, Boulder, Colorado (1966); VILLARS, F. (1963) unpublished; FRIEDMAN, W., Ph.D. thesis, M.I.T. (1966).
[4] FESHBACH, H., PORTER, C.E., WEISSKOPF, V.F., Phys. Rev. 96 (1954) 448.
[5] BLOCK, B., FESHBACH, H., Ann. Phys., N.Y. 23 (1963) 47; KERMAN, A.K., RODBERG, L., YOUNG, J.E., Phys. Rev. Lett. 11 (1963) 422; FESHBACH, H., KERMAN, A.K., LEMMER, R.H., to be published.
[6] COSMAN, E.R., ENGE, H.A., SPERDUTO, A., Phys. Lett. 22 (1966) 195; AUERBACH, E.H., DOVER, C.B., KERMAN, A.K., LEMMER, R.H., SCHWARZ, E.H., Phys. Rev. Lett. 17 (1966) 1184.
[7] ROBSON, D., Phys. Rev. 137 (1965) B 535; LANE, A.M., Nucl. Phys. 35 (1962) 676.
[8] de TOLEDO PIZA, A.F.R., KERMAN, A.K., FALLIEROS, S., VENTER, R.H., to be published.
[9] BROWN, G.E., CASTILLEJO, L., EVANS, J.A., Nucl. Phys. 22 1 (1961).
[10] LEMMER, R.H., SHAKIN, C.M., Ann. Phys., N.Y. 27 13 (1964).
[11] LOVAS, I., Nucl. Phys. 81 (1966) 353.
[12] HAGLUND, M.E., to be published.
[13] AFNAN, I., Ph.D. thesis, M.I.T. (1966).
[14] PETERSON, L.R., Ph.D. thesis, M.I.T. (1966)
[15] DANOS, M., GREINER, W., Phys. Rev. 138 (1965) B 876.
[16] MIKESKA, H.J., Z. Phys. 177 (1964) 441.

CHAPTER 10

MICROSCOPIC COLLECTIVE THEORIES

D.J. ROWE

1. INTRODUCTION

The problem of nuclear structure is, of course, the many-body problem. Before tackling it, therefore, we should look around at other branches of many-body theory, notably atomic physics, solid-state physics, elementary particle physics, etc., and see if some of the same techniques can be applied. Frequently they can, and in fact most of the important advances have been stolen from other fields. For example, the Hartree-Fock theory comes from atomic physics; pairing force theory from the theory of superconductivity; vibration theory from the Bohm-Pines theory of plasma oscillations of electrons in metals; methods of quantized field theory from elementary particles, etc. In return, some of the group theoretic methods developed for nuclear physics have now found an application to elementary particles.

Although the nucleus has much in common with other many-body systems, it has its own distinctive features. For example, the nuclear particles are bound together solely by their mutual attraction without the aid of any external field, as for atomic electrons, making the application of self-consistent field methods less certain. Unlike solid-state

The author, previously at the Atomic Energy Research Establishment, UKAEA Harwell, Berks, United Kingdom, is now in the Department of Physics and Astronomy, The University of Rochester, Rochester, N.Y., United States of America.

systems, the nucleus is a finite many-body system, containing perhaps only a few or at most a few hundred particles. Approximations which are valid to order 1/N, where N is the particle number, are therefore not always very reliable. On the other hand, there are usually too many particles for a few-body treatment. Thus the nucleus poses its own special problems, which makes it often infuriating but rarely dull. On the credit side, it has the simplifying feature of being essentially always at zero temperature; nuclear excitations are usually of the order of an MeV or a keV, whereas room temperature corresponds only to 1/40 eV, so that, at equilibrium, the nucleus remains in its lowest energy eigenstate.

In this paper we shall be concerned principally with many-body methods, which have application over a wide range of nuclei, but which may not necessarily be the best in specific cases. Thus we are concerned mostly with systematic properties of nuclei, such as collective phenomena, rather than the idiosyncrasies of particular nuclei or local shell structure.

Although we describe several theories, there is a common theme runing throughout. This is the Hartree-Fock method. Essentially it is an approximation for reducing the problem of many interacting particles to one of non-interacting particles in a field. Clearly this effects an enormous simplification of the problem, but it is an approximation and neglects a large part of the interparticle forces. These neglected forces we call the residual interactions. The major problem of nuclear structure, and to a large extent of nuclear reactions also, is how to include these residual interactions.

Most of the methods that I shall describe can be regarded as extensions of the simple HF theory. For example, BCS theory, which is designed to account for the short-range part of the residual interactions, can be regarded as a special case of a generalized HF (or GHF) theory. HF theory can also be made time-dependent (TDHF theory) to describe excited states and to take into account, in particular, the long-range or field-producing part of the residual interactions. This theory is also expressed in other language as the random phase approximation (RPA). The advantages of both extensions can furthermore be incorporated in a generalized TDHF (or GTDHF) theory, which is equivalent to the perhaps better known quasi-particle RPA (or QRPA).

Thus we might have entitled this course 'A unified theory of nuclear structure' which, together with a 'unified (or HF) theory of nuclear reactions', would provide a unified theory of nuclear physics.

2. HARTREE-FOCK SELF-CONSISTENT FIELD THEORY

2.1. Hartree theory

The physical principles of HF theory are illustrated by deriving it intuitively and neglecting particle exchange. Consider the Hamiltonian for atomic electrons

$$H = \sum_{i}^{A} \{T_i + u_0(i)\} + \frac{1}{2}\sum_{ij}^{A} V(i,j)$$

where T is the kinetic energy, u_0 the central Coulomb field of the nucleus, and V(i, j) is the electrostatic interaction between electrons. Neglecting the interaction, the particles are independent and have wave functions satisfying the wave equation

$$\left\{-\frac{\hbar^2}{2m}\nabla^2 + u_0(r)\right\}\psi_i(\vec{r}) = \epsilon_i\psi_i(\vec{r})$$

The total nuclear wave function, neglecting anti-symmetrization, is then

$$\varphi = \psi_1(1)\,\psi_2(2).....\psi_A(A)$$

Now include interactions. The average interaction felt by particle i, due to all other electrons, is

$$u_1(\vec{r}_i) = \sum_{j\neq i}\int d\vec{r}_j\,\psi_j^*(\vec{r}_j)\,\psi_j(\vec{r}_j)\,V(\vec{r}_i, \vec{r}_j)$$

Thus we get the modified Schrödinger equation

$$\left\{-\frac{\hbar^2}{2m}\nabla^2 + u_0(r) + u_1(\vec{r})\right\}\psi_i(\vec{r}) = \epsilon_i\psi_i(\vec{r})$$

which is still a single-particle equation and solvable. Better single-particle wave functions can now be calculated, which can in turn be used to generate a better field. Iterating in this way, one finally achieves self-consistency between the field and the particle density.

This intuitively appealing method can be made more rigorous by deriving it from a variational principle. This we now do and at the same time correct for the major deficiency of Hartree theory, which is that it neglects exchange terms which only appear when the wave function is anti-symmetrized.

2.2. Hartree-Fock theory

The variational principle is that, for an eigenstate, the expectation of the energy is stationary. Thus the best approximation φ of a given type, to the ground state wave function, is given by the variational equation

$$\delta\langle\varphi|(H - E_0)|\varphi\rangle = 0 \qquad (2.1)$$

where E_0 is a Lagrangian multiplier, providing the normalization constraint, which takes the role of the ground state energy.

If φ is the anti-symmetrized product of single-particle wave functions

$$\varphi = \mathscr{A}\psi_1(1)\,\psi_2(2)....\psi_A(A) \qquad (2.2)$$

the energy expectation of the Hamiltonian

$$H = \sum_i^A T_i + \frac{1}{2}\sum_{ij}^A V(\vec{r}_i, \vec{r}_j) \qquad (2.3)$$

is

$$\langle \varphi | H | \varphi \rangle = \sum_i \int d\vec{r}\, \psi_i^*(\vec{r})\, T\psi_i(\vec{r})$$

$$+ \frac{1}{2} \sum_{ij} \int\int d\vec{r}\, d\vec{r}'\, \psi_i^*(\vec{r})\, \psi_j^*(\vec{r}')\, V(\vec{r}, \vec{r}')\, \psi_i(\vec{r})\, \psi_j(\vec{r}')$$

$$- \frac{1}{2} \sum_{ij} \int\int d\vec{r}\, d\vec{r}'\, \psi_i^*(\vec{r})\, \psi_j^*(\vec{r}')\, V(\vec{r}, \vec{r}')\, \psi_i(\vec{r}')\, \psi_j(\vec{r}) \qquad (2.4)$$

Applying the variation, we obtain the single-particle wave equation

$$T\psi_i(\vec{r}) + \sum_j \int d\vec{r}'\, \psi_j^*(\vec{r}')\, V(\vec{r}, \vec{r}')\, \psi_j(\vec{r}')\, \psi_i(\vec{r})$$

$$- \sum_j \int d\vec{r}'\, \psi_j^*(\vec{r}')\, V(\vec{r}, \vec{r}')\, \psi_j(\vec{r})\, \psi_i(\vec{r}') = \epsilon_i\, \psi_i(\vec{r}) \qquad (2.5)$$

where ϵ_i is a Lagrangian multiplier constraining the $\psi_i(\vec{r})$ to be normalized and taking the role of a single-particle energy. Equation (2.5) can be written more concisely

$$-\frac{\hbar^2}{2m} \nabla^2 \psi_i(\vec{r}) + \int d\vec{r}'\, u(\vec{r}, \vec{r}')\, \psi_i(\vec{r}') = \epsilon_i\, \psi_i(\vec{r}) \qquad (2.6)$$

where $u(\vec{r}, \vec{r}')$ is the self-consistent field

$$u(\vec{r}, \vec{r}') = \delta(\vec{r} - \vec{r}') \sum_j \int d\vec{r}''\, V(\vec{r}, \vec{r}'')\, \psi_j(\vec{r}'')\, \psi_j^*(\vec{r}'')$$

$$- \sum_j V(\vec{r}, \vec{r}')\, \psi_j(\vec{r})\, \psi_j^*(\vec{r}') \qquad (2.7)$$

The first term is the direct term, corresponding to the Hartree field, the second is the exchange contribution which is non-local. It is seen that the range of non-locality of the HF field is of the order of the range of the two-body interaction $V(\vec{r}, \vec{r}')$.

Generally the two-body interaction itself is non-local; it contains velocity dependence and exchange forces. The more general expression for the field is then

$$u(\vec{r}_1, \vec{r}_1') = \sum_j \int\int d\vec{r}_2\, d\vec{r}_2'\, v(\vec{r}_1 \vec{r}_2;\ \vec{r}_1' \vec{r}_2')\, \psi_j(\vec{r}_2')\, \psi_j^*(\vec{r}_2)$$

$$- \sum_j \int\int d\vec{r}_2\, d\vec{r}_2'\, v(\vec{r}_1 \vec{r}_2;\ \vec{r}_2' \vec{r}_1')\, \psi_j(\vec{r}_2')\, \psi_j^*(\vec{r}_2)$$

or, more compactly,

$$u(\vec{r}_1, \vec{r}_1') = \int\int d\vec{r}_2\, d\vec{r}_2'\, V(\vec{r}_1\vec{r}_2;\ \vec{r}_1'\vec{r}_2')\, \rho(\vec{r}_2'\vec{r}_2) \equiv \mathcal{S}r_2 (V\rho) \tag{2.8}$$

where V is the anti-symmetrized interaction

$$V(\vec{r}_1\vec{r}_2;\ \vec{r}_1'\vec{r}_2') = v(\vec{r}_1\vec{r}_2;\ \vec{r}_1'\vec{r}_2') - v(\vec{r}_1\vec{r}_2;\ \vec{r}_2'\vec{r}_1') \tag{2.9}$$

and $\rho(\vec{r}', \vec{r})$ is the single-particle density, which for a product wave (Eq. (2.2)) is

$$\rho(\vec{r}', \vec{r}) \equiv \langle a_r^\dagger a_{r'} \rangle = \sum_j^A \psi_j(\vec{r}')\, \psi_j^*(\vec{r}) \tag{2.10}$$

To solve these equations, we must again proceed iteratively in the cycle

$$u \rightarrow \psi_i \rightarrow \rho \rightarrow u = \int V\rho$$

starting now from an inspired guess for the field u. We finally obtain a set of single-particle states. In the HF ground state $|\ \rangle$, these are all occupied from the lowest energy state up to the Fermi surface.

In the following, we shall often have cause to refer to the HF state $|\ \rangle$ as the vacuum. Single-particle states above the Fermi surface are then particle states and will be labelled by the subscripts m, n (see Fig. 1), while single-particle states below the Fermi surface are hole states and labelled by the subscripts i, j.

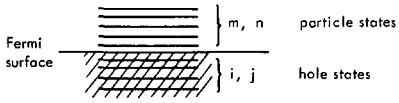

FIG. 1. Particle and hole states

A disadvantage of variational methods generally is that one does not know how good the answer is. Fortunately it is possible to express HF theory in another manner to exhibit the residual interactions explicitly. For this purpose it is convenient to go over to the language of second quantization.

The Hamiltonian becomes

$$H = \sum_{\nu\nu'} T_{\nu\nu'} a_\nu^\dagger a_{\nu'} + \frac{1}{4} \sum_{\mu\nu\mu'\nu'} V_{\mu\nu\mu'\nu'} a_\nu^\dagger a_\mu^\dagger a_{\mu'} a_{\nu'} \tag{2.11}$$

where we now take $V_{\mu\nu\mu'\nu'}$ to be anti-symmetrized

$$V_{\mu\nu\mu'\nu'} = \langle \mu\nu | V | \mu'\nu' \rangle$$

$$= \int\int d\vec{r}\, d\vec{r}\,' \varphi_\mu^*(\vec{r})\, \varphi_\nu^*(\vec{r}\,')\, V(\vec{r}, \vec{r}\,')\, \varphi_{\mu'}(\vec{r})\, \varphi_{\nu'}(\vec{r}\,')$$

$$- \int\int d\vec{r}\, d\vec{r}\,' \varphi_\mu^*(\vec{r})\, \varphi_\nu^*(\vec{r}\,')\, V(\vec{r}, \vec{r}\,')\, \varphi_{\mu'}(\vec{r}\,')\, \varphi_{\nu'}(\vec{r})$$

hence the factor 1/4. Now expand the interaction in normal order, with respect to the HF vacuum, using Wick's theorem

$$H = \sum T_{\nu\nu'} a_\nu^\dagger a_{\nu'} + \frac{1}{2} \sum V_{\mu\nu\mu'\nu'} \langle | a_\mu^\dagger a_{\mu'} | \rangle \langle | a_\nu^\dagger a_{\nu'} | \rangle$$

$$+ \sum V_{\mu\nu\mu'\nu'} \langle | a_\mu^\dagger a_{\mu'} | \rangle \{ a_\nu^\dagger a_{\nu'} \} + \frac{1}{4} \sum V_{\mu\nu\mu'\nu'} \{ a_\nu^\dagger a_\mu^\dagger a_{\mu'} a_{\nu'} \}$$

Now

$$\{ a_\nu^\dagger a_{\nu'} \} = a_\nu^\dagger a_{\nu'} - \langle | a_\nu^\dagger a_{\nu'} | \rangle$$

so that

$$H = \sum_{\nu\nu'} \left[T_{\nu\nu'} + \sum_{\mu\mu'} V_{\mu\nu\mu'\nu'} \langle | a_\mu^\dagger a_{\mu'} | \rangle \right] a_\nu^\dagger a_{\nu'}$$

$$- \frac{1}{2} \sum V_{\mu\nu\mu'\nu'} \langle | a_\mu^\dagger a_{\mu'} | \rangle \langle | a_\nu^\dagger a_{\nu'} | \rangle$$

$$+ \frac{1}{4} \sum V_{\mu\nu\mu'\nu'} \{ a_\nu^\dagger a_\mu^\dagger a_{\mu'} a_{\nu'} \} \qquad (2.12)$$

The first term is a single-particle operator and can be diagonalized by a suitable choice of the single-particle basis

$$T_{\nu\nu'} + \sum_{\mu\mu'} V_{\mu\nu\mu'\nu'} \langle | a_\mu^\dagger a_{\mu'} | \rangle = \delta_{\nu\nu'} \epsilon_\nu \qquad (2.13)$$

This basis is of course the HF basis and this equation the HF equation; compare this equation in the form

$$T_{\nu\nu'} + u_{\nu\nu'} = \delta_{\nu\nu'} \epsilon_\nu \qquad (2.14)$$

where

$$u_{\nu\nu'} = \sum_{\mu\mu'} V_{\mu\nu\mu'\nu'} \rho_{\mu'\mu} = \langle \nu | \mathscr{F}_{r_2}(V\rho) | \nu' \rangle \qquad (2.15)$$

with Eqs. (2.6) and (2.8).

In this HF basis, the density matrix elements are diagonal and are equal to 1 for a hole state, and 0 for a particle state;

$$\langle | a_\mu^\dagger a_{\mu'} | \rangle = \delta_{\mu\mu'} \sum_i \delta_{\mu i}$$

Equation (2.12) therefore becomes

$$H = \sum_\nu \epsilon_\nu a_\nu^\dagger a_\nu - \frac{1}{2} \sum_{ij} V_{ijij} + \frac{1}{4} \sum V_{\mu\nu\mu'\nu'} \{a_\nu^\dagger a_\mu^\dagger a_{\mu'} a_{\nu'}\} \tag{2.16}$$

where

$$\epsilon_\nu = T_{\nu\nu} + \sum_j V_{j\nu j\nu} \tag{2.17}$$

(cf. Eq. (2.5) for $\nu = i$).

The HF approximation is now clear. The HF wave function is an eigenstate of

$$H_0 = \sum_\nu \epsilon_\nu a_\nu^\dagger a_\nu - \frac{1}{2} \sum_{ij} V_{ijij} \tag{2.18}$$

and hence the residual interaction V_{res} is

$$V_{res} = \frac{1}{4} \sum V_{\mu\nu\mu'\nu'} \{a_\nu^\dagger a_\mu^\dagger a_{\mu'} a_{\nu'}\} \tag{2.19}$$

To show that $|\rangle$ satisfies the variational equation, we can invoke Thouless' theorem. A variation of the product wave function can be expressed (see Appendix)

$$|\rangle \rightarrow (1 + \sum_{mi} C_{mi} a_m^\dagger a_i + \ldots) |\rangle$$

so that an infinitesimal variation can be written

$$\delta |\rangle = \sum_{mi} \delta C_{mi} a_m^\dagger a_i |\rangle$$

for arbitrary δC_{mi}. Thus we require

$$\langle | a_i^\dagger a_m H | \rangle = \langle | H a_m^\dagger a_i | \rangle = 0, \quad \text{all } m, i \tag{2.20}$$

which is satisfied separately for H_0 and V_{res}.

Another expression of the variational equation, which we will have cause to use, is in terms of the density matrix. If $|\rangle$ is any wave function, not necessarily an eigenstate, which is specified at time t and allowed to develop in time according to the time-dependent Schrödinger equation, the expectation of any operator, in particular the density matrix

$$\rho_{\alpha\beta} = \langle | a_\beta^\dagger a_\alpha | \rangle$$

will also develop in time. The time derivative at time t is given by the Heisenberg equations of motion

$$i\hbar \frac{\partial \rho_{\alpha\beta}}{\partial t} = \langle | [a_\beta^\dagger a_\alpha, H] | \rangle$$

If $|\rangle$ were an eigenstate, the expectation of any operator would be a constant in time. The HF condition requires only that this be true for single-particle operators i.e.

$$\langle | [a_\beta^\dagger a_\alpha, H] | \rangle = 0, \quad \text{all } \alpha, \beta \tag{2.21}$$

This is a generalization of Eq. (2.20) and is readily seen to hold for both H_0 and V_{res}.

The HF Hamiltonian H_0 has been tailor-made to give a good approximation to the ground state. It can nevertheless be used to set up a complete basis. Thus we have 1ph (1 particle-hole) states

$$H_0 a_m^\dagger a_i | \rangle = (E_0 + \epsilon_m - \epsilon_i) a_m^\dagger a_i | \rangle \tag{2.22}$$

where

$$H_0 | \rangle = E_0 | \rangle$$

with

$$E_0 = \sum_i \epsilon_i - \frac{1}{2} \sum_{ij} V_{ijij} \tag{2.23}$$

2ph states

$$H_0 a_m^\dagger a_n^\dagger a_i a_j | \rangle = (E_0 + \epsilon_m + \epsilon_n - \epsilon_i - \epsilon_j) a_m^\dagger a_n^\dagger a_i a_j | \rangle$$

etc. One can then hope to use these as a basis in which to diagonalize the residual interactions.

2.3. Realistic forces and hard cores

It almost goes without saying that a necessary condition for the success of the HF method is that the two-body interaction should have no singularities. Unfortunately, phase shift analysis of high energy ($\sim$300 MeV) nucleon-nucleon scattering leads one to believe that the interaction is infinitely repulsive at a distance of $\sim$0.4 f. In other words, the nucleus has a hard core.

At first sight, this is disastrous for the HF method. Why? Because matrix elements of a hard core interaction, taken between independent particle wave functions, are infinite. The particles may therefore be expected to scatter far and wide out of their HF orbits. Nevertheless, in spite of the hard core, the shell model seems to work very well, so how can this be?

Consider the wave function for the relative motion of two independent particles in a potential well. In a relative s-state, the unperturbed wave function penetrates the core and leads to an infinite energy expectation (see Fig. 2). The perturbed wave function, then, must clearly not penetrate the core. It must go to zero at its boundary.

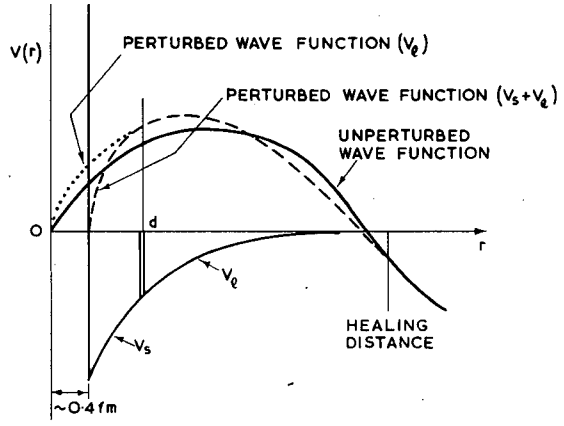

FIG. 2. Unperturbed and perturbed wave functions for the relative motion of two independent particles in a potential well

Now a perturbation correction for the hard core is not going to work, unless one is prepared to go to infinite order when each order alone diverges. However as Moszkowski and Scott [1] point out, the strong attractive forces, just outside the hard core, rapidly compensate. The perturbed wave function bends over faster than the unperturbed and, at the 'separation distance' d, reaches the same logarithmic derivative.

Moszkowski and Scott suggest therefore that one should separate the potential into two parts, V_s (for $r < d$) which is singular, and V_ℓ (for $r > d$) which is well behaved. As far as the wave function for $r > d$ is concerned, one can, to a good approximation, discard V_s and retain only V_ℓ. The total volume of space, for which $r < d$, is a small fraction of the nuclear volume and, unless one is specifically interested in short-range two-body correlations, the error in the wave function in this region will not much matter.

V_ℓ, being well behaved, can now be used in a HF calculation. There is a complication however, in that the separation distance depends on the relative momentum of the particles (it is defined by the condition that V_s gives zero phase shift for a particular relative state). This means that the effective interaction has a rather complicated velocity (or state) dependence.

Even after the removal of V_s, the force is still comparatively short ranged and is not taken fully into account in the HF self-consistent field.

In brief, there are residual interactions. Fortunately for HF theory, they are not too strong and are prevented from doing too much damage by the Pauli principle. In particular, they are restrained from scattering particles which are deeply embedded in the Fermi sea, just because there are no free states for them to scatter into. In terms of the relative wave function, the Pauli principle effects a healing of the wave function within a comparatively short distance. (This distance is of the order $1/k_F$, where k_F is the average momentum of a particle at the Fermi surface.)

The short-range forces are not restrained, however, from scattering particles near the top of the Fermi sea, where they bring about a diffuseness of the Fermi surface. In this way, they are responsible, as we discussed in the phenomenological course, for stabilizing the spherical shape of the near closed shell nuclei. We shall return to the treatment of the short-range residual interactions later, in terms of 'pairing force theory'.

2.4. The shell model

Although HF theory presents a formally solvable problem, in practice it is not trivial and only recently is it being seriously tackled. However, if we could determine the self-consistent field directly, we could start with that, rather than the two-body interaction, and so by-pass all the hard work. This is the principle behind the shell model.

The shell model potential was constructed historically to reproduce the shell closure, or 'magic numbers'. The essential ingredients were found to be a central potential, intermediate between a harmonic oscillator and a square well, and a spin orbit potential:

$$u(\vec{r}) = V(r) + f(r)(\vec{l} \cdot \vec{s})$$

A potential which meets these requirements, and is also consistent with our knowledge of nuclear distributions, is the Woods-Saxon potential

$$V(r) = -\frac{V_0}{1 + e^{(r-R)/a}}$$

illustrated in Fig. 3, together with the spin-orbit potential

$$f(r) \propto \frac{1}{r}\frac{dV(r)}{dr}$$

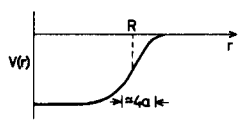

FIG. 3. Woods-Saxon potential

Suppose now we use this shell model potential to calculate a set of single-particle wave functions and energy levels for a closed shell nucleus, such as ^{208}Pb. How can we check the results with experiment?

The best we can do is to look at the neighbouring nuclei, e.g. ^{209}Pb and ^{207}Pb and observe what energy levels the extra particle, or hole, goes into. Figure 4 shows the result of such a comparison. The agreement is very good. It is not perfect, but then it is not supposed to be. Since the extra particle modifies the field, the energy levels in ^{209}Pb and ^{207}Pb are not quite the same as those in ^{208}Pb. In shell model language, the extra particle polarizes the core. Allowing for such polarization, even better agreement can be obtained.

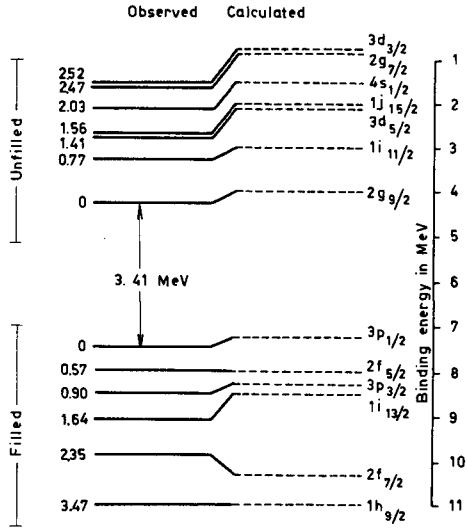

FIG. 4. Comparison of experimental neutron energies in ^{208}Pb with shell-model energies as calculated by Blomquist and Wahlborn [2]. (diagram taken from Brown's book [2], courtesy of North-Holland Publishing Co.)

For closed shell nuclei, the shell model is simply a first approximation to HF theory. How good an approximation it is depends on how closely the potential well resembles the self-consistent field. For nuclei with particles outside a closed shell, the conventional shell model is no longer an approximation to HF theory. Its method is to set up a basis of wave functions by putting the extra-core particles into the various unoccupied levels of the unperturbed closed shell core. The two-body interaction is introduced explicitly and diagonalized within this configuration space. By eliminating the core in this way, that is, by taking it into account only via the exclusion principle and the potential well it generates, the shell model reduces the many-body problem to a few-body problem. For two or three extra-core particles this works very well. If it is generalized to include core excitations it is potentially exact, although in practice it is very much limited by the volume of configuration space that can be handled by a computer. For this reason its usefulness is restricted to the near closed shell nuclei.

2.5. The deformed shell model

The HF method treats all particles in the nucleus, core and extra-core, on an equal basis, as a many-body problem. However there is a

fundamental difference between the results for a closed shell and a non-closed shell nucleus. Because of the independent particle constraint, the HF state, for a non-closed shell nucleus, turns out to be deformed.[1]

Consequently, the wave-function does not have good angular momentum and cannot represent an eigenstate of the nucleus. To obtain physical states from the HF wave function, we have the choice of projecting from it components of good angular momentum, inserting it as an intrinsic wave function into the rotational model, or following some other approximate procedure. Clearly there are going to be problems of mathematical rigour, but the fact that the HF method produces wave functions of large deformation, in just those regions of the periodic table where rotational spectra are observed, is physically appealing.

Although we can speculate about the nature of the HF solutions, they are difficult to carry through. But, again, we can introduce a deformed shell model or Nilsson model (which has already been described in Chapter 2), as a first approximation. What to do with the wave function when we have it, is anothe problem. Since this is a paper on microscopic theory, we would prefer not to introduce phenomenology or, for that matter, dubious theory, by blatantly labelling it an intrinsic wave function and employing redundant rotational variables. However Kurath and Picman [3] have found the following very encouraging result. They calculate the wave functions for nuclei in the 1p shell, and early 2s-1d, in two different ways. Firstly, they use the conventional shell model approach of interacting particles in a spherical potential. Secondly, they project out components of good angular momentum from the deformed shell model wave function - independent particles in a deformed potential. The overlap between the two results is in most cases better than 98%.

Since the projection method seems to yield such good results in cases where it can be tested, it gives us some degree of confidence in its reliability generally. As we shall see in section 3, this projection method does have considerable theoretical backing.

3. ROTATION THEORY

3.1. Peierls-Yoccoz theory [4]

If the HF wave function $\varphi(\vec{x})$ has a non-spherical density distribution, it defines a direction in space. Now, since the Hamiltonian is invariant under rotations, HF wave functions $\varphi(\theta, \vec{x})$ with different orientations are all degenerate in energy. This degeneracy can be used to construct a better trial wave function, by taking the linear combination

$$\psi(\vec{x}) = \int f(\theta)\, \varphi(\theta, \vec{x})\, d\theta \qquad (3.1)$$

[1] For a discussion of this, see the notes on the aligned coupling scheme (Phenomenological collective models, chapter 2); the aligned coupling scheme is nothing more than the phenomenological approach to HF theory.

The function $f(\theta)$ is to be determined variationally by minimizing $\langle\psi|H|\psi\rangle$ subject to the constraint that $\psi(\vec{x})$ remains normalized. Thus we get the variational equation

$$\langle\delta\psi|(H - \lambda)|\psi\rangle = 0$$

which gives the integral equation for $f(\theta)$

$$\int h(\theta' - \theta)\, f(\theta)\, d\vec{\theta} - \lambda \int n(\theta' - \theta)\, f(\theta)\, d\theta = 0 \qquad (3.2)$$

where

$$\begin{aligned} h(\theta' - \theta) &= \langle \varphi(\theta')|H|\varphi(\theta)\rangle \\ n(\theta' - \theta) &= \langle \varphi(\theta')|\varphi(\theta)\rangle \end{aligned} \qquad (3.3)$$

For HF solutions with axial symmetry, which is the only case we shall consider, the z-projection of angular momentum is a good quantum number, K say. It can then be shown that

$$f(\theta) = \mathscr{D}^{I}_{MK}(\theta) \qquad (3.4)$$

satisfies the above integral equation.

The physical significance of the Peierls-Yoccoz wave function is readily seen. Expand

$$\varphi_K(\vec{x}) = \sum_J c_J \varphi^J_K(\vec{x})$$

Then, rotating this wave function to an angle θ, we get

$$\varphi_K(\theta, \vec{x}) = \sum_J \sum_{M'} c_J \mathrm{III}^{*J}_{M'K}(\theta)\, \varphi^J_{M'}(\vec{x})$$

The Peierls-Yoccoz wave function is therefore

$$\psi_{IKM}(\vec{x}) = \int \mathscr{D}^{I}_{MK}(\theta)\, \varphi_K(\theta, \vec{x})\, d\theta = \frac{8\pi^2}{2I+1} c_I \varphi^I_M(\vec{x}) \qquad (3.5)$$

which is just the component, of $\varphi_K(\vec{x})$, of angular momentum I.

This variational method provides the justification for projecting out states of good angular momentum from the Nilsson wave function. By the nature of variational methods, it is difficult to say what approximation is involved, but the results of Kurath and Picman indicate that the trial wave function is of sufficient generality to provide a very good approximation.

One of the first things that strikes one about the wave function $\psi_{IKM}(\vec{x})$, is its similarity to the unified model wave function for rotations. If, for a specified set of co-ordinates $\vec{x}$, the wave function $\varphi_K(\theta, \vec{x})$ is sufficiently sharply peaked about a particular value of $\theta = \theta(\vec{x})$, (sufficiently

sharp, that is, that $\mathscr{D}^I_{MK}(\theta)$ varies little over this peak) then the integral in the wave function can be dropped and we get the rotational wave function

$$\psi_{IKM}(\vec{x}) \rightarrow \mathscr{D}^I_{MK}(\theta(\vec{x}))\varphi_K(\theta(\vec{x}), \vec{x})$$

This should happen in the limit of very large deformation, when the wave function $\varphi_K(\theta, \vec{x})$ becomes virtually 'intrinsic'.

The spectrum of energy levels is given in the Peierls-Yoccoz theory by

$$E_{IK} = \frac{\int h(\beta)\, d^I_{KK}(\beta)\, d(\cos\beta)}{\int n(\beta)\, d^I_{KK}(\beta)\, d(\cos\beta)} \tag{3.6}$$

where

$$\begin{aligned} h(\beta) &= h(0, \beta, 0) \\ n(\beta) &= n(0, \beta, 0) \end{aligned} \tag{3.7}$$

These overlap integrals are generally assumed to be small, for nuclei of sizeable deformation, except in the region of $\beta = 0$. So we expand

$$d^I_{KK}(\beta) = 1 - \frac{1}{4}[I(I+1) - K^2]\beta^2 + \ldots$$

It is easy to see that inserting this expansion in Eq. (3.6) will lead to a rotational I(I + 1) spectrum, to leading order. It has been pointed out by Verhaar [5] that the overlap integrals are also sizeable in the region $\beta = \pi$, i.e. when the nuclei are pointing in exactly opposite directions. Thus there are important corrections from $d^I_{KK}(\pi - \beta)$. For K = 1/2, for example

$$d^I_{\frac{1}{2}\frac{1}{2}}(\pi - \beta) = -\frac{1}{2}(-1)^{I+\frac{1}{2}}\left(I + \frac{1}{2}\right)\beta + \ldots$$

giving an energy spectrum of the form

$$E_{IK=\frac{1}{2}} = E_0 + \frac{\hbar^2}{2\mathscr{I}}\left[I(I+1) + a(-1)^{I+\frac{1}{2}}\left(I + \frac{1}{2}\right)\right] + \ldots \tag{3.8}$$

Important corrections to the rotational I(I + 1) spectrum are also found for other K-bands. But these do not always correspond to the correction turns in the rotational model.

The evaluation of the moment of inertia and other parameters is formally possible, although in practice not very easy. The major problem is the evaluation of the overlap integrals $h(\beta)$ and $n(\beta)$. (For a further discussion of this approach see chapter 11.)

A good test of the model is to see how well it works for translational motion, where the answer is known beforehand. The corresponding Peierls-Yoccoz wave function is

$$\psi_{\vec{k}}(\vec{x}) = \int e^{i\vec{k}.\vec{r}}\, (\vec{x} - \vec{r})\, d\vec{r}$$

It is found that the energy expectation of this state $\langle \psi_{\vec{k}} | H | \psi_{\vec{k}} \rangle$ is not quite equal to

$$E(\vec{k}) = E_0 + \frac{1}{2AM} k^2$$

as it should be, if the method were exact. It is very easy to see what is wrong. Expand

$$\varphi(\vec{x}) = \sum_n \int d\vec{k}\, C_n(\vec{k})\, e^{i\vec{k}.\vec{X}} \chi_n(q)$$

where $\vec{X}$ is the centre-of-mass co-ordinate, and χ_n are the eigenstates of the intrinsic Hamiltonian. The Peierls-Yoccoz wave function is therefore

$$\psi_{\vec{k}}(\vec{x}) = e^{i\vec{k}.\vec{X}} \sum_n C_n(\vec{k})\, \chi_n(q)$$

which is just the component of good centre-of-mass momentum $\vec{k}$. However, it will not lead to the correct mass, since the intrinsic part of the wave function is $\vec{k}$-dependent.

An exception occurs for a harmonic oscillator potential, when the intrinsic and centre-of-mass parts of the wave-function are separable. In this particular case, Peierls-Yoccoz theory leads to the correct result. The corresponding condition that Peierls-Yoccoz theory give the correct result for rotations is that the HF wave function should be made up of a superposition of states belonging only to the ground state band.

To obtain the correct result for translations, for a general potential well, Peierls and Thouless [6] have proposed taking the more general linear combination of wave functions

$$\Psi_{\vec{k}}(\vec{x}) = \int\int G_{\vec{k}}(\vec{v}, \vec{r})\, \varphi_{\vec{v}}(\vec{x} - \vec{r})\, d\vec{r}\, d\vec{v}$$

where $\varphi_{\vec{v}}(\vec{x})$ is the HF wave function in a reference frame moving with velocity $\vec{v}$. This leads to a wave function of the form

$$\Psi_{\vec{k}}(\vec{x}) = e^{i\vec{k}.\vec{X}} \int d\vec{k}'\, g(\vec{k}') \sum_n C_n(\vec{k}')\, \chi_n(q)$$

The co-factor of exp $i\vec{k}.\vec{X}$ is now $\vec{k}$-independent and must clearly lead to the correct mass.

The corresponding trial function for rotations is

$$\Psi_I(\vec{x}) = \int\int G_I(\vec{\omega}, \theta)\, \varphi_{\vec{\omega}}(\theta, \vec{x})\, d\vec{\theta}\, d\vec{\omega} \qquad (3.9)$$

This wave function should give better results, simply because of the extra generality of the trial function. Unfortunately it is much harder to work with.

3.2. The moment of inertia

A method for deriving the moment of inertia directly is due to Thouless [7]. It is very similar to the cranking model which, as we shall see, appears as an approximation to the Thouless method. The method is to find the best product wave function for the nucleus, subject to the constraint that it have a small but specified mean angular momentum. Thus we get the variational equation

$$\delta \langle \psi | (H - E_0 - \omega J_x) | \psi \rangle = 0 \tag{3.10}$$

where ω is a second Lagrangian multiplier, which has the significance of an angular velocity. The moment of inertia is deduced by equating

$$\langle \psi | J_x | \psi \rangle = \omega \mathcal{I}_x \tag{3.11}$$

A convenient way to carry out the variation is to use Thouless' theorem, and write the wave function

$$|\psi\rangle = \exp\left[\sum_{mi} C_{mi} a_m^\dagger a_i \right] | \rangle \tag{3.12}$$

Because of gauge invariance, we can vary $|\psi\rangle$ and $\langle\psi|$ independently. To leading order in C_{mi}

$$\frac{\partial}{\partial C_{mi}^*} \langle \psi | (H - E_0 - \omega J_x) | \psi \rangle$$

$$= \langle | a_i^\dagger a_m (1 + \sum_{nj} C_{nj}^* a_j^\dagger a_n)(H - E_0 - \omega J_x)(1 + \sum_{nj} C_{nj} a_n^\dagger a_j) | \rangle = 0 \tag{3.13}$$

The Hamiltonian in the HF representation is

$$H = \sum \epsilon_\nu a_\nu^\dagger a_\nu + \frac{1}{4} \sum V_{\mu\nu\mu'\nu'} \{ a_\nu^\dagger a_\mu^\dagger a_{\mu'} a_{\nu'} \} - \frac{1}{2} \sum V_{ijij}$$

Thus we get

$$(\epsilon_m - \epsilon_i) C_{mi} + \sum (V_{mjin} C_{nj} + V_{mnij} C_{nj}^*) = \omega (J_x)_{mi} \tag{3.14}$$

Similarly, from

$$\frac{\partial}{\partial C_{mi}} \langle \psi | (H - E_0 - \omega J_x) | \psi \rangle = 0$$

we get the complex conjugate equation.

Now the moment of inertia is given from Eq. (3.11) as

$$\mathcal{I}_x = \frac{1}{\omega} \sum_{mi} \left[(J_x)_{im} C_{mi} + (J_x)_{mi} C^*_{mi} \right] \tag{3.15}$$

where the C_{mi} are defined by Eq. (3.14). The solution for these coefficients involves a matrix inversion. However, if we neglect the interaction terms the matrix is diagonal and the inversion trivial. We get

$$\mathcal{I}_x = 2 \sum \frac{|(J_x)_{mi}|^2}{\epsilon_m - \epsilon_i} \tag{3.16}$$

If the HF theory is approximated by the deformed shell model, this expression is just the cranking model result. The full Thouless treatment, by working with H rather than H_{HF}, in the initial variational equation, allows for a modification of the self-consistent field due to the rotation, which the cranking model does not do. A change in the field can after all be expected due to the centrifugal and Coriolis forces.

The effect of the interaction terms may well be important. Certainly the residual interactions, which are neglected altogether in this treatment, are very important. The most important of these, namely the short-range pairing forces, can be included in a generalized HF treatment, and bring the cranking model expression down from the rigid body value to something 2 to 5 times smaller and more in line with experiment. We shall describe the generalized HF theory in the succeeding chapter, but the modification to the cranking model formula has already been discussed in Chapter 2.

Since it is a semi-classical method and uses HF wave functions which are not eigenstates of a rotationally invariant Hamiltonian, it is not easy to say what approximations are involved in Thouless' derivation. However, like the cranking model, we can show that it leads to exact results in the translational case. The translational equivalent to Eq. (3.13) is

$$\langle | a^\dagger_i a_m (1 + \sum_{nj} C^*_{nj} a^\dagger_j a_n)(H - E_0 - vP)(1 + \sum_{nj} C_{nj} a^\dagger_n a_j) | \rangle = 0 \tag{3.17}$$

Making use of the fact that

$$a^\dagger_j a_n | \rangle \equiv 0$$

and

$$\langle | a^\dagger_i a_m (H - E_0) | \rangle = 0$$

this equation can also be written

$$\langle | a^\dagger_i a_m \left[(H - E_0), \sum_{nj} (C_{nj} a^\dagger_n a_j - C^*_{nj} a^\dagger_j a_n) \right] | \rangle = vP_{mi} \tag{3.18}$$

We can now drop E_0 in the commutator, since it is just a number. In this form, the solution for the C_{nj} can be deduced by comparison with the equation

$$\langle|a_i^\dagger a_m[H, X]|\rangle = -\frac{i\hbar}{AM} P_{mi}$$

We find

$$C_{nj} = i\frac{AM}{\hbar} vX_{nj}$$

Putting this solution into the expression for the mass (cf Eq. (3.15))

$$\mathcal{M} = \frac{1}{v}\sum_{mi}[P_{im}C_{mi} + P_{mi}C_{mi}^*]$$

$$= i\frac{AM}{\hbar}\sum_{mi}(\langle|P|mi\rangle\langle mi|X|\rangle - \langle|X|mi\rangle\langle mi|P|\rangle)$$

$$= i\frac{AM}{\hbar}\langle|[P, X]|\rangle = AM \qquad (3.19)$$

An interesting question now arises: If both the pushing model and the Thouless model for translations give the exact answer, what has happened to the interaction terms? The answer is that the pushing model only gives the correct answer for a local shell model potential, i.e. when

$$[u_{SM}(r), X] = 0$$

It would not give the correct answer if it were used with the non-local HF potential, since

$$[u_{HF}(\vec{r}, \vec{r}'), X] \neq 0$$

Thus, if the HF potential were used, the interaction terms of the Thouless method are also needed to get the correct answer. But, conversely, if the HF potential ia approximated by the shell model in the Thouless method it is inconsistent to include also the interaction terms.

Unfortunately it is difficult to make corresponding statements in the rotational case.

3.3. Villars' theory [8]

The microscopic theory of rotations is really not in a very satisfactory state. The rotation-like spectra and also the wave functions can be derived well enough with Peierls-Yoccoz theory. Such spectra also have a simple explanation in terms of the shell model and the SU(3) coupling scheme. But these are not really rotational theories. They are very enlightening in themselves but they do not explain directly the very con-

siderable success of the phenomenological rotational models. A recent and very promising onslaught on this problem has been made by Villars, which I shall present in outline.

The objective is to introduce collective co-ordinates and effect a transformation of the Hamiltonian into rotational and intrinsic parts, together with the inevitable coupling terms. This is an old idea which has not hitherto been very successful. The major problem has been that the intrinsic co-ordinates are complicted. They do not have a simple one-to-one correspondence with the individual particles and consequently the possibility of independent particle wave functions is lost. Villars gets around this problem by never introducing intrinsic co-ordinates explicitly, but working always in the original particle basis.

The method is most easily demonstrated for translations. Here we already know the answer

$$H = H_{\text{intr.}} + H_{\text{trans.}} \tag{3.20}$$

where

$$H_{\text{trans.}} = \frac{P^2}{2AM}, \qquad H_{\text{intr.}} = H - \frac{P^2}{2AM}$$

But can we find a systematic way of achieving this separation without using our a priori knowledge?

Given that the Hamiltonian is translation-invariant, i.e.

$$[H, P] = 0 \tag{3.21}$$

it follows that H is a function only of P and not of X. So we expand

$$H(P) = H^{(0)} + P\,H^{(1)} + \frac{1}{2!}\,P^2\,H^{(2)} + \ldots \tag{3.22}$$

where the $H^{(n)}$ are functions only of the intrinsic co-ordinates:

$$[H^{(n)}, X] = [H^{(n)}, P] = 0$$

The problem therefore reduces to finding the set of intrinsic functions $H^{(n)}$. We now use a general property of conjugate co-ordinates, which enables us to derive all the derivatives of H(P) with respect to P; namely

$$\frac{i}{\hbar}\left[f(P),\ X\right] = \frac{\partial f(P)}{\partial P}$$

for any function f(P). Thus we define

$$X^{(0)}(P) = H = H^{(0)} + P\,H^{(1)} + \frac{1}{2!}\,P^2 H^{(2)} + \cdots$$

$$X^{(1)}(P) = \frac{i}{\hbar}\left[X^{(0)},\ X\right] = \frac{\partial H}{\partial P} = H^{(1)} + P\,H^{(2)} + \frac{1}{2!}\,P^2\,H^{(3)} + \cdots \tag{3.23}$$

$$X^{(1)}(P) = \frac{i}{\hbar}\left[X^{(1)},\ X\right] = \frac{\partial^2 H}{\partial P^2} = H^{(2)} + P\,H^{(3)} + \frac{1}{2!}\,P^2\,H^{(4)} + \cdots$$

etc.

These equations can be inverted, using the relations

$$H^{(0)} = H(P=0), \qquad H^{(1)} = \left.\frac{\partial H}{\partial P}\right|_{P=0} \qquad \text{etc.},$$

and a Taylor expansion about arbitrary P. We get

$$H^{(n)} = \sum_k \frac{(-1)^k}{k!} X^{(k+n)} P^k \tag{3.24}$$

To see how this works out, let us evaluate these functions:

$$\begin{aligned} X^{(0)} &= H \\ X^{(1)} &= \frac{i}{\hbar}\left[H, X \right] = \frac{P}{AM} \\ X^{(2)} &= \frac{i}{\hbar}\left[\frac{P}{AM}, X \right] = \frac{1}{AM} \\ X^{(3)} &= 0, \quad \text{etc.} \end{aligned} \tag{3.25}$$

Whence

$$\begin{aligned} H^{(0)} &= H - \frac{P^2}{2AM} \\ H^{(1)} &= 0 \\ H^{(2)} &= \frac{1}{AM} \\ H^{(3)} &= H^{(4)} = \cdots = 0 \end{aligned} \tag{3.26}$$

which is the required result.

Now let us apply this method to the case of two-dimensional rotations. Rotational invariance

$$[H, J] = 0 \tag{3.27}$$

implies that H can be expanded

$$H = H^{(0)} + J\, H^{(1)} + \frac{1}{2!} J^2 H^{(2)} + \cdots$$

To derive the $H^{(n)}$ we must introduce a co-ordinate angle φ conjugate to J, i.e. satisfying the equation

$$[J, e^{i\varphi}] = e^{i\varphi} \tag{3.28}$$

A natural choice for φ is the angle specifying the orientation of the principal axes of the inertia tensor. If φ is a function simply of the particle co-

ordinates, then, provided that the two-body interactions are local, the rotational sequence, like the translational, cuts off at $H^{(2)}$.

How can we use this separation to derive, for example, the moment of inertia? First we must find the eigenstates, or some approximation to them. These must be eigenstates of angular momentum. Consider an eigenstate with eigenvalue K of J. The wave function is of the form

$$\Psi_K(\varphi, q) = e^{iK\varphi}\,\psi^K(q) \tag{3.29}$$

where q is the set of intrinsic co-ordinates. Thus $\psi^K(q)$ is an eigenstate of the intrinsic Hamiltonian H^K,

$$H^K\psi^K(q) = E(K)\,\psi^K(q) \tag{3.30}$$

where

$$H^K = H^{(0)} + K\,H^{(1)} + \frac{1}{2!}\,K^2\,H^{(2)} \tag{3.31}$$

An exact solution is not easy, because of the complicated nature of the intrinsic co-ordinates for one thing. Villars' idea is to diagonalize in terms of the original particle co-ordinates, in which it is, in any case, already expressed. This is, of course, a redundant basis and, in an exact solution, leads to degeneracies. Thus

$$H^K\chi^K(\varphi, q) = E(K)\chi^K(\varphi, q) \tag{3.32}$$

where

$$\chi^K(\varphi, q) = \psi^K(q)\,g(\varphi) \tag{3.33}$$

with arbitrary $g(\varphi)$. In an approximate HF diagonalization, this degeneracy will be lifted, but that is of little consequence unless we are also interested in intrinsic excited states, when the problem of recognizing spurious states will arise.[2]

Thus the HF ground state energies E(K) are, for quantized K, the energy levels of the ground state rotational band. What result does this give for the moment of inertia?

The HF determinant χ^K can be related to the determinant χ^0 using Thouless' theorem.

$$\chi^K = e^{iKF}\,\chi^0 \tag{3.34}$$

where F is a single-particle operator. Having found χ^0 we can derive F from the variational equation

$$\delta\left\langle \chi^0 \middle| e^{-iKF}\,H^K e^{iKF} \middle| \chi^0 \right\rangle = 0 \tag{3.35}$$

---

[2] This problem can be handled with the RPA, when the spurious states come out with zero excitation energy. For the ground state band, we are only concerned with obtaining a good relative approximation for E(K); relative, that is, to E(K') for other $K' \neq K$.

Using this equation, and expanding E(K), we obtain from the coefficient of the K^2 term

$$\frac{1}{\mathcal{I}} = \langle \chi^0 | \{ H^{(2)} + i[(H^{(1)} + \tfrac{1}{2} K H^{(2)}), F] \} | \chi^0 \rangle \tag{3.36}$$

Villars shows that with certain approximations, this leads once again to the Thouless result.

If we want the wave functions, these can also be obtained by projection from $\chi^K(\varphi, q)$. Thus

$$\Psi(\varphi, q) \propto \int e^{iK\varphi'} \chi^K(\varphi - \varphi', q)\, d\varphi'$$

$$\approx e^{iK\varphi} \psi^K(q) \int e^{-iK\varphi'} g(\varphi')\, d\varphi' \tag{3.37}$$

which is similar to, but an improvement on, the Peierls-Yoccoz wave functions.

4. PAIRING FORCE THEORY

4.1. The inadequacy of HF theory

HF theory takes into account only that part of the two-body interaction which can be expressed in terms of a static field. The reason it works so well is because the Pauli principle inhibits particles from scattering strongly, due to the shortage of unoccupied status to scatter into. The situation where HF theory works particularly well is for closed-shell nuclei. This is because it costs a lot of energy for two particles to scatter out of their HF orbitals; the energy required $\sim 2\hbar\omega$, where $\hbar\omega$ is the shell spacing (see Fig. 5).

FIG. 5. A 2 ph configuration weakly coupled to the HF wave-function by the residual interactions, for a closed-shell nucleus

For a partly filled shell, on the other hand, very little energy is required and the residual interactions can be very important (see Fig. 6). The result is a smearing of the Fermi surface and with it the loss of an independent particle description of the nucleus, as a good zero order approximation. This is a serious loss, because without this enormous simplification the many-body problem is not manageable. Fortunately, it is possible to generalize HF theory and consider independent quasi-particles, which again proves a good zero order description of the non-closed shell nuclei and at the same time retains most of the simplicity of standard HF theory.

We first consider how the problem of a schematic short range residual interaction, namely the 'pairing force', can be solved in terms of the shell model. In the following chapter we will then apply the methods developed to the more general HF problem.

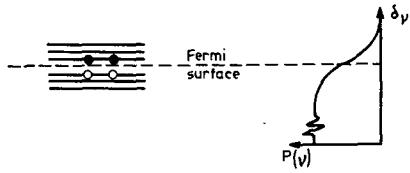

FIG. 6. A strongly coupled 2 ph configuration for a partially filled shell and the resultant smearing of the Fermi surface

4.2. Particles in a degenerate j-shell

A characteristic of short-range attractive interactions is that two particles, in a j^2 configuration, are strongly bound when coupled to $J = 0$ and weakly bound otherwise. (See Chapter 2.) Furthermore, the $J \neq 0$ states cluster within an energy region narrow compared with the separation of the $J = 0$ state. This suggests the use of a simple schematic interaction which acts only in $J = 0$ states. Such an interaction is the 'pairing force':

$$H = -G \sum^{(+)} a^\dagger_m a^\dagger_{\bar{m}} a_{\bar{m}'} a_{m'}, \qquad (a^\dagger_m \equiv a^\dagger_{jm}) \tag{4.1}$$

where the + sign over the summation index means that summation is only required over magnetic projections $m > 0$, and a barred suffix refers to a time-reversed single-particle state. It turns out that the pairing force exactly diagonalizes Racah's seniority coupling scheme.

In the $(m, \bar{m})$ two-particle sub-space, H has the form

$$H = -G \begin{pmatrix} 1\,1\,1\,\ldots \\ 1\,1\,1\,\ldots \\ \ldots\quad\ldots \\ 1\,1\,1\quad\ldots \end{pmatrix} \tag{4.2}$$

It is clear that for two particles this matrix has lowest energy eigenfunction

$$\varphi_0 = \frac{1}{\sqrt{\Omega}} \begin{pmatrix} 1 \\ 1 \\ 1 \\ . \\ . \\ . \\ 1 \end{pmatrix} \equiv \frac{1}{\sqrt{\Omega}} \sum^{(+)} a^\dagger_m a^\dagger_{\bar{m}} |-\rangle \equiv |(j)^2 J = 0\rangle \tag{4.3}$$

where $|-\rangle$ is the bare vacuum and

$$\Omega = \tfrac{1}{2}(2j + 1)$$

is the number of pair states $(m, \bar{m})$ with $m > 0$. The energy of this $J = 0$ state is

$$E_0 = -G\Omega \tag{4.4}$$

while all orthogonal two-particle states have energy zero.

To solve the N-particle problem, let us define the operator

$$A^\dagger = \frac{1}{\sqrt{\Omega}} \sum^{(+)} a^\dagger_m a^\dagger_{\bar{m}} \tag{4.5}$$

which creates a two-particle $J = 0$ state. In terms of this operator

$$H = -G\Omega A^\dagger A \tag{4.6}$$

The commutation relations are

$$[A, A^\dagger] = 1 - \frac{n}{\Omega} \tag{4.7}$$

where n is the number operator

$$n = \sum^{(+)} (a^\dagger_m a_m + a^\dagger_{\bar{m}} a_{\bar{m}}) \tag{4.8}$$

The seniority zero eigenstates of the Hamiltonian now follow from the equation of motion

$$[H, A^\dagger] = -GA^\dagger(\Omega - n) = -G(\Omega - n + 2)A^\dagger \tag{4.9}$$

Starting from the bare vacuum $|-\rangle$ of zero particles we get

$$\begin{aligned} H A^\dagger |-\rangle &= -G\Omega A^\dagger |-\rangle &&= -G\Omega |N = 2,\ v = 0\rangle \\ H(A^\dagger)^2 |-\rangle &= -2G(\Omega - 1)(A^\dagger)^2 |-\rangle &&= -2G(\Omega - 1)|4, 0\rangle \\ H(A^\dagger)^{N/2} |-\rangle &= -\frac{G}{4} N(2\Omega - N + 2)(A^\dagger)^{N/2} |-\rangle &&= -\frac{G}{4} N(2\Omega - N + 2)|N, 0\rangle \end{aligned} \tag{4.10}$$

In addition one can define $(\Omega - 1)$ operators $B^\dagger_i$, which create two-particle states orthogonal to $A^\dagger$ and obey the equation

$$[H, B^\dagger_i] = 0 \tag{4.11}$$

With these operators we can now construct the complete set of eigenstates for the even nuclei

$$\begin{aligned} H\, B_i^\dagger |-\rangle &= H|N=2, v=2\rangle = 0 \\ H\, B_i^\dagger B_j^\dagger |-\rangle &= H|4,\ 4\rangle = 0 \\ H\, A^\dagger B_i^\dagger |-\rangle &= H|4,\ 2\rangle = -G(\Omega-2)|4,\ 2\rangle \end{aligned} \qquad (4.12)$$

etc.

Thus for N = 4 we get the energy spectrum of Fig. 7.

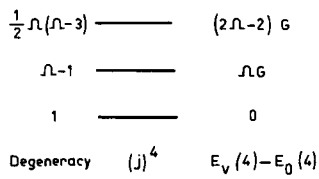

FIG. 7. Four-particle spectrum corresponding to a pure pairing force Hamiltonian

For odd nuclei, we can similarly generate eigenstates

$$H\, A^\dagger a_\nu^\dagger |-\rangle = -G(\Omega-1)\, A^\dagger a_\nu^\dagger |-\rangle = -G(\Omega-1)|N=3,\ v=1\rangle$$

etc. Generally one obtains the eigenvalues

$$E_v(N) = -\frac{G}{4}(N-v)(2\Omega - N - v + 2) \qquad (4.13)$$

giving the excitation energies

$$E_v(N) - E_0(N) = \frac{G}{4} v(2\Omega - v + 2) \qquad (4.14)$$

The interesting feature of this result is that the energy spectra for all nuclei are identical regardless of N. This, as we shall see, has very important consequences.

4.3. Two particles in non-degenerate levels

Suppose now that there are several non-degenerate levels lying within the range of the short-range interactions. For a short-range interaction it transpires that

$$|\langle (j_\alpha)^2 J=0|V|(j_\beta)^2 J=0\rangle| \gg |\langle (j_\alpha)^2 J\neq 0|V|(j_\beta)^2 J\neq 0\rangle| \qquad (4.15)$$

and that the J = 0 matrix elements do not vary over a very wide range (see Lane [9]). We therefore set up the more general pairing Hamiltonian.

$$H = \sum \epsilon_\nu^{(0)} a_\nu^\dagger a_\nu - G \sum^{(+)} a_\mu^\dagger a_{\bar{\mu}}^\dagger a_{\bar{\nu}} a_\nu \qquad (4.16)$$

where the $\epsilon_\nu^{(0)}$ are the unperturbed single-particle energies.

For two particles, the wave functions $|\alpha\rangle$ (N = 0 states only) can be expanded

$$|\alpha\rangle = \sum^{(+)} C_{\alpha\nu}\, a_\nu^\dagger a_{\bar{\nu}}^\dagger |-\rangle \tag{4.17}$$

where the $C_{\alpha\nu}$ are solutions of the equations

$$(2\epsilon_\nu^{(0)} - E_\alpha)C_{\alpha\nu} - G \sum_\mu^{(+)} C_{\alpha\mu} = 0 \tag{4.18}$$

This equation yields the eigenvalue equation

$$\sum_\nu^{(+)} \frac{1}{2\epsilon_\nu^{(0)} - E_\alpha} = \frac{1}{G} \tag{4.19}$$

which is solved by graphical means, as illustrated in Fig. 8.

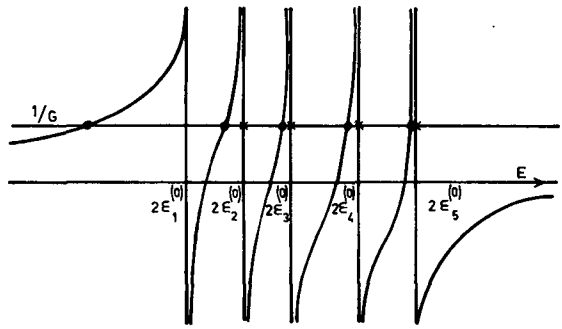

FIG. 8. Graphical solution of the eigenvalue equation. The eigenvalues are sandwiched between the unperturbed energies $2\epsilon_\nu^{(0)}$. For spherical nuclei the $\epsilon_\nu^{(0)}$ are degenerate, corresponding to j - sub-shells, with the result that most of the solutions are unperturbed. These are pure $|(j)^2 J \neq 0\rangle$ states and are marked by crosses. The J = 0 states, marked by dots, are all depressed but one is depressed much more than the rest. For non-spherical nuclei, the unperturbed energy levels are not degenerate and the crosses disappear, together with J as a good quantum number in the intrinsic frame.

4.4. N particles in non-degenerate levels (BCS theory)

For this problem there is no known exact treatment and we have to resort to approximate methods.

By analogy with the degenerate case, one would guess that the N-particle ground state (N even) is of the form

$$|N\rangle = \left(\sum^{(+)} C_\nu^{(N)}\, a_\nu^\dagger a_{\bar{\nu}}^\dagger\right)^{N/2} |-\rangle \tag{4.20}$$

(cf. Eq. 4.10)

This expression could be used as a trial function in a variational equation. Unfortunately, it is not an independent particle wave function which makes the variational calculation rather difficult.

However, we can regard $|N\rangle$ as the projection onto the N-particle space of the wave function

$$|\rangle = \prod_{\nu>0} (u_\nu + v_\nu a_\nu^\dagger a_{\tilde{\nu}}^\dagger)|-\rangle \tag{4.21}$$

namely

$$P_N|\rangle = \prod_{\mu>0} u_\mu \frac{1}{(N/2)!}\left[\sum_\nu^{(+)} \frac{v_\nu}{u_\nu} a_\nu^\dagger a_{\tilde{\nu}}^\dagger\right]^{\frac{N}{2}}|-\rangle \tag{4.22}$$

which means that

$$C_\nu^{(N)} \propto \frac{v_\nu}{u_\nu}$$

The wave function $|\rangle$ is very much easier to work with than $|N\rangle$, for the simple reason that it is the vacuum of a set of single-particle operators:

$$(u_\mu a_\mu - v_\mu a_{\tilde{\mu}}^\dagger) \prod_{\nu>0} (u_\nu + v_\nu a_\nu^\dagger a_{\tilde{\nu}}^\dagger)|-\rangle = 0 \qquad \text{all } \mu \tag{4.23}$$

Thus $|\rangle$ is the vacuum for quasi-particles, as defined by

$$\begin{aligned}
\alpha_\nu^\dagger &= u_\nu a_\nu^\dagger - v_\nu a_{\tilde{\nu}} & a_\nu^\dagger &= u_\nu \alpha_\nu^\dagger + v_\nu \alpha_{\tilde{\nu}} \\
\alpha_{\tilde{\nu}}^\dagger &= u_\nu a_{\tilde{\nu}}^\dagger + v_\nu a_\nu & a_{\tilde{\nu}}^\dagger &= u_\nu \alpha_{\tilde{\nu}}^\dagger - v_\nu \alpha_\nu \\
\alpha_\nu &= u_\nu a_\nu - v_\nu a_{\tilde{\nu}}^\dagger & a_\nu &= u_\nu \alpha_\nu + v_\nu \alpha_{\tilde{\nu}}^\dagger \\
\alpha_{\tilde{\nu}} &= u_\nu a_{\tilde{\nu}} + v_\nu a_\nu^\dagger & a_{\tilde{\nu}} &= u_\nu \alpha_{\tilde{\nu}} - v_\nu \alpha_\nu^\dagger
\end{aligned} \tag{4.24}$$

This is known as a Bogolubov-Valatin transformation. For the transformation to be unitary, we must require that

$$u_\nu^2 + v_\nu^2 = 1 \tag{4.25}$$

Now the quasi-particle vacuum $|\rangle$ does not have a definite number of physical particles. However, in the degenerate case we found that the spectrum was independent of particle number. There is every reason to believe that, in the non-degenerate case at least, near neighbours will have very similar spectra. Consequently some uncertainty in particle number should not make too much difference to the results. In the next section we shall apply the quasi-particle (or BCS) method to the degenerate case, where we know the exact solutions, and see how well it works.

The wave function $|\rangle$ is optimized by minimizing the expectation of $H' = H - \lambda n$

$$= \sum^{(+)} (\epsilon_\nu^{(0)} - \lambda)(a_\nu^\dagger a_\nu + a_{\bar{\nu}}^\dagger a_{\bar{\nu}}) - G \sum^{(+)} a_\mu^\dagger a_{\bar{\mu}}^\dagger a_{\bar{\nu}} a_\nu \tag{4.26}$$

where λ is a Lagrangian multiplier, chosen to ensure that the mean particle number is correct;

$$\langle|n|\rangle = N \tag{4.27}$$

Thus $\lambda(N)$ must have a value given by the condition

$$\frac{\partial \langle|H'|\rangle}{\partial N} = 0$$

or

$$\lambda = \frac{\partial \langle|H|\rangle}{\partial N} \tag{4.28}$$

which is just the chemical potential.

The vacuum expectation of H' can be obtained by picking out the constant U, in its normal order expansion with respect to quasi-particles

$$H' = U + H_{11} + H_{20} + H_{res} \tag{4.29}$$

where H_{11} is a single quasi-particle operator of the form $\alpha^\dagger\alpha$, H_{20} creates or annihilates pairs of quasi-particles ($\alpha^\dagger\alpha^\dagger + \alpha\alpha$) and H_{res} contains products of 4 quasi-particles in normal order and is the residual interaction, not included in the BCS treatment. U is given by

$$U = \sum_\nu^{(+)} (\epsilon_\nu^{(0)} - \lambda)(\langle|a_\nu^\dagger a_\nu|\rangle + \langle|a_{\bar{\nu}}^\dagger a_{\bar{\nu}}|\rangle)$$

$$-G \sum_{\mu\nu}^{(+)} (\langle|a_{\bar{\mu}}^\dagger a_{\bar{\nu}}|\rangle\langle|a_\mu^\dagger a_\nu|\rangle + \langle|a_\mu^\dagger a_{\bar{\mu}}^\dagger|\rangle\langle|a_{\bar{\nu}} a_\nu|\rangle)$$

$$= \sum^{(+)} [2(\epsilon_\nu^{(0)} - \lambda) v_\nu^2 - G v_\nu^4] - G\left(\sum^{(+)} u_\nu v_\nu\right)^2 \tag{4.30}$$

Carrying out the variation

$$\frac{\partial U}{\partial v_\nu} = 0$$

with the condition

$$u_\nu^2 + v_\nu^2 = 1$$

we obtain

$$4(\epsilon_\nu^{(0)} - \lambda)v_\nu - 4Gv_\nu^3 - 2G\left(\sum_\mu^{(+)} u_\mu v_\mu\right)\left(u_\nu + v_\nu \frac{\partial u_\nu}{\partial v_\nu}\right) = 0 \qquad (4.31)$$

Evaluating $\partial u_\nu/\partial v_\nu$ from Eq. (4.25) and multiplying through by u_ν, this equation reduces to

$$2(\epsilon_\nu - \lambda)u_\nu v_\nu - \Delta(u_\nu^2 - v_\nu^2) = 0 \qquad (4.32)$$

where

$$\begin{aligned} \epsilon_\nu &= \epsilon_\nu^{(0)} - G v_\nu^2 \\ \Delta &= G \sum_\mu^{(+)} u_\mu v_\mu \end{aligned} \qquad (4.33)$$

These equations have solution for u_ν, v_ν

$$u_\nu^2 = \frac{1}{2}\left\{1 + \frac{\epsilon_\nu - \lambda}{\sqrt{(\epsilon_\nu - \lambda)^2 + \Delta^2}}\right\}, \quad v_\nu^2 = \frac{1}{2}\left\{1 - \frac{\epsilon_\nu - \lambda}{\sqrt{(\epsilon_\nu - \lambda)^2 + \Delta^2}}\right\} \qquad (4.34)$$

where Δ and λ are solutions of the gap equation

$$\frac{G}{2}\sum^{(+)} \frac{1}{\sqrt{(\epsilon_\nu - \lambda)^2 + \Delta^2}} = 1 \qquad (4.35)$$

which follows from the definition of Δ, together with the number equation

$$\langle |n| \rangle = 2 \sum_\nu^{(+)} v_\nu^2 = N$$

or

$$\sum^{(+)} \left\{1 - \frac{\epsilon_\nu - \lambda}{\sqrt{(\epsilon_\nu - \lambda)^2 + \Delta^2}}\right\} = N \qquad (4.36)$$

Excited states in the BCS formalism are the quasi-particle excitations

$$\alpha^\dagger |\rangle, \quad \alpha^\dagger \alpha^\dagger |\rangle, \quad \alpha^\dagger \alpha^\dagger \alpha^\dagger |\rangle, \text{ etc.}$$

But note that

$$|\rangle, \quad \alpha^\dagger \alpha^\dagger |\rangle, \quad \text{etc}$$

contain only admixtures of even numbers of real particles, while

$$\alpha^\dagger |\rangle, \quad \alpha^\dagger \alpha^\dagger \alpha^\dagger |\rangle, \text{ etc.}$$

contain only odd numbers. The quasi-particle states of an even nucleus are consequently restricted to even numbers and vice-versa (cf. seniority).

The energy of a v-quasi-particle state is obtained from H_{11}. Now

$$H_{11} + H_{20} = \sum^{(+)} (\epsilon_\nu^{(0)} - \lambda) [\{a_\nu^\dagger a_\nu\} + \{a_{\bar{\nu}}^\dagger a_{\bar{\nu}}\}]$$

$$-G \sum^{(+)} [\langle |a_\mu^\dagger a_{\bar{\mu}}^\dagger| \rangle \{a_{\bar{\nu}} a_\nu\} + \langle |a_{\bar{\nu}} a_\nu| \rangle \{a_\mu^\dagger a_{\bar{\mu}}^\dagger\}$$

$$+ \langle |a_{\bar{\mu}}^\dagger a_{\bar{\nu}}| \rangle \{a_\mu^\dagger a_\nu\} + \langle |a_\mu^\dagger a_\nu| \rangle \{a_{\bar{\mu}}^\dagger a_{\bar{\nu}}\}] \qquad (4.37)$$

which gives

$$H_{11} = \sum^{(+)} E_\nu (\alpha_\nu^\dagger \alpha_\nu + \alpha_{\bar{\nu}}^\dagger \alpha_{\bar{\nu}}), \qquad H_{20} = 0 \qquad (4.38)$$

where

$$E_\nu = \sqrt{(\epsilon_\nu - \lambda)^2 + \Delta^2} \qquad (4.39)$$

Thus we see that the minimum excitation energy of an unperturbed 2-quasi-particle state is 2Δ, which is sometimes called the energy gap.

Although the pairing force is very schematic, it nevertheless explains in a most convincing manner many dramatic and systematic features of nuclear spectroscopy. For instance, it explains why the even-even nuclei have spin zero ground states and very few low-lying states; why odd nuclei, for which the low-lying states are 1-quasi-particle states, are more complex; and why odd-odd nuclei, for which low-lying states are a proton quasi-particle coupled to neutron quasi-particle, are still more complex (see Chapter 2, Fig. 6).

Also explained is the odd-even mass difference; a single quasi-particle state has a minimum energy of Δ.

4.5. Comments on the BCS approximation

For the degenerate problem, we already have an exact solution and the BCS equations are trivially solvable. It is possible therefore to make comparisons between the results and learn something of the accuracy of the BCS approximation.

The exact energy spectrum, for an N-particle nucleus, is given by

$$E_v(N) = -\frac{G}{4} N(2\Omega - N + 2) + \frac{G}{4} v(2\Omega - v + 2) \qquad (4.40)$$

The chemical potential $\lambda^{(N)}$ is

$$\lambda^{(N)} = \frac{\partial E_0(N)}{\partial N} = -\frac{G}{2} (\Omega - N + 1) \qquad (4.41)$$

The exact energy spectrum for the Hamiltonian

$$H' = H - \lambda^{(N_0)} n$$

is given, therefore, by

$$E'_\nu(N) = E_\nu(N) - \frac{GN}{2}(\Omega - N_0 + 1)$$

$$= \frac{G}{4}(N - N_0)^2 - \frac{G}{4}N_0^2 - \frac{G}{4}\nu(2\Omega - \nu + 2) \qquad (4.42)$$

and is shown in Fig. 9.

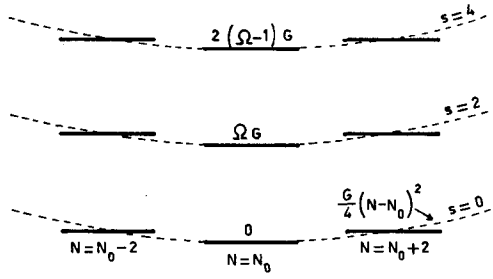

FIG. 9. Exact energy spectrum for the Hamiltonian $H' = H - \lambda^{(N_0)} n$

Now the component of the BCS wave function $|\rangle$, of definite particle number N,

$$P_N|\rangle \propto \left[\sum^{(+)} C_\nu a_\nu^\dagger a_{\bar{\nu}}^\dagger\right]^{N/2} |-\rangle \qquad (4.43)$$

has the correct form for the N-particle ground state. In the exact solution C_ν is independent of N and so it is possible to construct a wave function, of BCS form, from only ground state wave functions. It is also clear that all the C_ν of the BCS approximation are equal on symmetric grounds. This means that wave functions, of definite particle number, projected from the BCS wave function are exact ground states.

Unfortunately this is not true in the non-degenerate case, since the exact C_ν are not constants and do depend on N although often rather weakly, especially in the case of near degeneracies. But even if the projected components $P_N|\rangle$ are not exact, the particular component $P_{N_0}|\rangle$ should be pretty good, since the wave function is optimized for this number of particles.

In practice it is unusual to project and so we must enquire into the consequences of the number fluctuation. The spread in particle number may be defined by

$$(\Delta N)^2 = \langle|(n - N)^2|\rangle = 4\sum^{(+)} u_\nu^2 v_\nu^2 \qquad (4.44)$$

In the degenerate model the u_ν and v_ν are all equal and hence

$$v_\nu^2 = \frac{N}{2\Omega}, \qquad u_\nu^2 = 1 - \frac{N}{2\Omega} \tag{4.45}$$

Thus

$$(\Delta N)^2 = 2N\left(1 - \frac{N}{2\Omega}\right) \tag{4.46}$$

which means a fractional uncertainty in particle number

$$\frac{\Delta N}{N} \lesssim \sqrt{\frac{2}{N}} \tag{4.47}$$

What effect will this number fluctuation have on the ground state energy? Since the mean particle number is correct, only the quadratic term in $E_0(N)$ is affected and hence, from Eq. (4.42), the energy expectation of $|\rangle$ should be

$$\begin{aligned} E_0 &= E_0(N) + \frac{G}{4}\langle|(n - N)^2|\rangle \\ &= E_0(N) + \frac{G}{4}\,2N\left(1 - \frac{N}{2\Omega}\right) \end{aligned} \tag{4.48}$$

Thus the fractional error is of order $1/\Omega$ (cf. Eq. (4.40)). This is exactly the BCS energy

$$u = \langle|H|\rangle$$

obtained by putting the solutions of Eq. (4.45) into Eq. (4.30) for u.

Now the BCS wave function $|\rangle$ is only appropriate for an even nucleus. An odd N-particle nucleus is described in BCS theory by the quasi-particle state

$$\alpha_\mu^\dagger|\rangle = \frac{1}{u_\mu^{(N-1)}}\prod_{\nu>0}(u_\nu^{(N-1)} + v_\nu^{(N-1)}\,a_\nu^\dagger a_{\bar{\nu}}^\dagger)\,a_\mu^\dagger|-\rangle$$

where the coefficients $u_\nu^{(N-1)}$, $v_\nu^{(N-1)}$ are optimized for the even (N - 1) nucleus. Ideally these coefficients should be optimized directly for the N-particle nucleus. It is not difficult to see what the result would be If the single-particle level is occupied by a real particle, this level becomes 'blocked' and is no longer available for the pair correlations of the other particles. We therefore have the problem of N - 1 particles in Ω - 1 pair states. Similar effects can be expected in even-quasi-particle states so that the general solution fo a v-quasi-particle state can be obtained from the BCS ground state solution by the substitution

$$N \to N - v, \qquad \Omega \to \Omega - v$$

Taking into account the number fluctuation correction,

$$E_0(N) = -\frac{G}{4} N(2\Omega - N - v + 2)$$

generalizes to

$$E_v(N) = -\frac{G}{4} (N - v)(2\Omega - N - v + 2)$$

which is the exact answer.

While these blocking corrections are simple enough, there is a disadvantage to applying them in general. It is that they require a different quasi-particle basis for each energy level, which makes it difficult to relate wave functions or calculate transition matrix elements. It is usually more convenient therefore to optimize the basis for the even nucleus ground state and describe corrections, to other states, in terms of configuration mixing. The force responsible for the mixing is of course H_{res}, which is neglected in the BCS treatment. The unperturbed excited state energies are given by H_{11}, which, in the degenerate case, is easily shown to be

$$H_{11} = \frac{1}{2} G\Omega \sum^{(+)} (\alpha_\nu^\dagger \alpha_\nu + \alpha_{\bar{\nu}}^\dagger \alpha_{\bar{\nu}}) = \frac{1}{2} G\Omega\hat{v} \qquad (4.49)$$

where $\hat{v}$ is the quasi-particle number operator. It is seen that this gives exactly the right excitation energy for the 2-quasi-particle states and is generally correct to order v/Ω.

Now it may be noted that the BCS treatment gives Ω distinct 2-quasi-particle states, whereas the exact solution allows only $(\Omega - 1)$ seniority two states. The origin of the spurious state is easy to see; it is the state

$$(n - N)|\rangle$$

which is a superposition of 2-quasi-particle states and yet must be a super-position of only seniority zero ground states. If H_{res} is diagonalized in the 2-quasi-particle sub-space, because of the symmetry, $(\Omega - 1)$ combinations remain degenerate while the spurious state falls in energy. It will not fall to zero energy because it has a different number fluctuation to the BCS state. In the non-degenerate case, a spurious 2-quasi-particle state also exists but the problem of recognizing it may be more difficult, especially in any approximate diagonalization of the residual interaction.

In concluding this section we sould emphasize that the error in BCS theory arises solely from the neglect of H_{res}; or equivalently from the choice of trial wave function. No error is introduced by the Bogolubov-Valatin transformation. Consequently if H_{res} were diagonalized in the complete quasi-particle basis, exact eigenstates, with no particle fluctuations, must result.

In applying BCS theory to nuclei, it must also be remembered that the pairing force only simulates the short-range part of the shell model residual interactions. If one is interested in collective states, the long-

range part is also most important. Normally it is included, in a schematic treatment, by adding into H_{res} an appropriate multiple force, such as the P_λ force (see chapter 2).

4.6. Existence of a superconducting solution

It is clear that the basic BCS equations

$$\Delta = G \sum^{(+)} u_\mu v_\mu$$

$$N = 2 \sum^{(+)} v_\mu^2$$

always have the trivial solution

$$\Delta = 0, \qquad v_\mu = 1 \text{ or } 0 \qquad u_\mu = 0 \text{ or } 1$$

corresponding to a sharp Fermi surface. But generally there is a non-trivial superconducting solution of lower energy, for which $\Delta \neq 0$. However, if G is too small, it may transpire that no superconducting solution exists. For example, consider the two degenerate level situations, ϵ_1 and ϵ_2, and suppose that, in the unperturbed shell model, ϵ_1 is full and ϵ_2 empty. For a superconducting solution, λ must be somewhere intermediate between ϵ_1 and ϵ_2 (Fig. 10) in order to satisfy the number equation, when

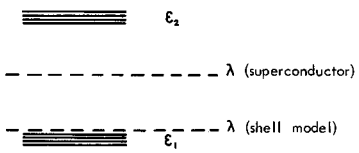

FIG. 10. Position of λ for a superconducting solution

not all particles are in ϵ_1. Now if, for such a value of λ, G is so small that

$$\frac{G}{2} \sum_{\nu}^{(+)} \frac{1}{\epsilon_\nu - \lambda} < 1$$

it is clear that a solution to the gap equation

$$\frac{G}{2} \sum^{(+)} \frac{1}{(\epsilon_\nu - \lambda)\sqrt{1 + \dfrac{\Delta^2}{(\epsilon_\nu - \lambda)^2}}} = 1$$

does not exist. This is the situation for closed shell nuclei, when the pairing force is not sufficiently strong to lift particle pairs into the next major shell.

For a nucleus with a partly filled degenerate level, a superconducting solution must always be possible, however weak the interaction.

Because a superconducting solution may not exist it does not mean that the pairing interaction has no effect. It simply means that no improvement, in the zero order approximation, results from extending independent particles to independent quasi-particles. In such a case the whole pairing interaction must be considered as a residual interaction.

4.7. Consequences of pairing and comparison with experiment

Throughout this chapter we have considered only one kind of particle, whereas in nuclei there are two kinds. To avoid the problems posed by the possibility of neutron-proton pairing, most calculations to date have either been with single closed shell nuclei, leaving effectively one kind of particle or have neglected the neutron-proton residual interaction, considering pairing only between like particles. We will discuss mostly the results of calculations carried out by Kisslinger and Sorensen [10] for single closed shell nuclei.

There are many phenomena which exhibit the consequences of pairing among which are the following:

(a) The odd-even mass difference: Because of pairing, the last particle in an odd mass nucleus is much less strongly bound than in the neighbouring even-even nuclei. The mass difference can be defined by

$$E_{N+1} + E_{N-1} - 2E_N = 2E_j \sim 2\Delta$$

where N is odd and the odd mass nucleus is supposed to be a single quasi-particle state j. A comparison of theory with experiment is shown in Fig. 11 and is seen to be very good.

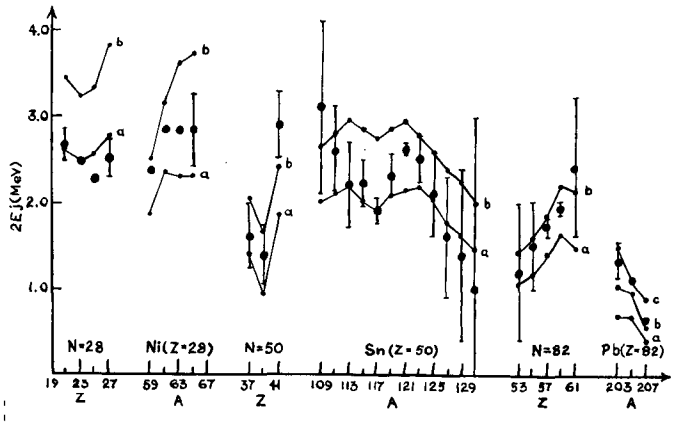

FIG. 11. Even-odd-A mass difference.
The dots are experimental mass differences $E_{N+1} + E_{N-1} - 2E_N$. The theoretical curves are simply $2E_j$, twice the energy of the lowest lying quasi-particle for the odd-A isotope. Curves a and b correspond to G = 19/A and 23/A, respectively. Curve c (for lead only) corresponds to G = 30/A. (Courtesy of Mate atisk Fysiske Meddelelser)

(b) Energy spectra: Apart from a few collective states, whose energies are depressed by the residual field interactions, no excited states are expected for spherical even-even nuclei, below the minimum 2-quasi-particle energy 2Δ. In contrast, odd or odd-odd nuclei exhibit no such energy gap and the low-lying spectra are expected to be, and indeed are, much less simple (see Fig. 6 of chapter 2).

(c) Matrix elements: Electromagnetic multipole moments and transitions are sometimes strongly modified by pairing and sometimes hardly at all. Consider the matrix element, between 1-quasi-particle states, of a general operator Q:

$$\langle|\alpha_\nu Q\alpha^\dagger_{\nu'}|\rangle = \sum_{\alpha\beta}\langle\alpha|Q|\beta\rangle\langle|\alpha_\nu a^\dagger_\alpha a_\beta\alpha^\dagger_{\nu'}|\rangle$$

$$= \langle\nu|Q|\nu'\rangle\,(u_\nu u_{\nu'} - \tau v_\nu v_{\nu'}) \qquad (4.50)$$

where $\tau = \pm 1$ according as Q is $\pm$ve., under time reversal. Thus electric moments, in particular electric quadrupole moments, and electric transitions, are oftent substantially reduced in odd nuclei, whereas magnetic moments and transitions are barely affected. For even nuclei the reverse occurs. The matrix element of Q between the ground state and a 2-quasi-particle state is

$$\langle|Q\alpha^\dagger_\nu\alpha^\dagger_{\tilde{\nu}'}|\rangle = \sum_{\alpha\beta}\langle\alpha|Q|\beta\rangle\langle|a^\dagger_\alpha a_\beta\alpha^\dagger_\nu\alpha^\dagger_{\tilde{\nu}'}|\rangle$$

$$= \langle\nu'|Q|\nu\rangle\,(u_\nu v_{\nu'} + \tau v_\nu u_{\nu'}) \qquad (4.51)$$

Thus electric moments are barely affected while magnetic moments are reduced.

(d) Spectroscopic factors: Experiments of particular interest, as far as pairing is concerned, are the stripping and pick-up reactions. After applying stripping theory, such experiments determine the spectroscopic factors

$$S(J, jJ_0) = \langle\Psi_{JM}|\Phi_{JM}(j, J_0)\rangle^2 \qquad (4.52)$$

where Ψ_{JM} is the odd-particle parent nucleus and Φ_{JM} is the coupled channel state of nucleon j and even daughter nucleus J_0. If we take the daughter nucleus as the quasi-particle vacuum $|\rangle$, with $J_0 = 0$, and suppose that the parent is the quasi-particle state

$$\Psi_{jm} = \alpha^\dagger_{jm}|\rangle$$

then we get

$$S(j, j\ 0) = \langle|\alpha_{jm}a^\dagger_{jm}|\rangle^2 = u_j^2 \qquad (4.53)$$

Thus spectroscopic factors are a means of measuring the coefficients u_ν, v_ν directly. In Fig. 12 are shown experimental values of v_j^2 obtained by Cohen and Price [11] from (d, p) and (d, t) experiments on the Sn isotopes; the theoretical values are from Kisslinger and Sorenson. The agreement is very satisfactory, especially considering the uncertainties both in stripping theory and in the pairing calculations.

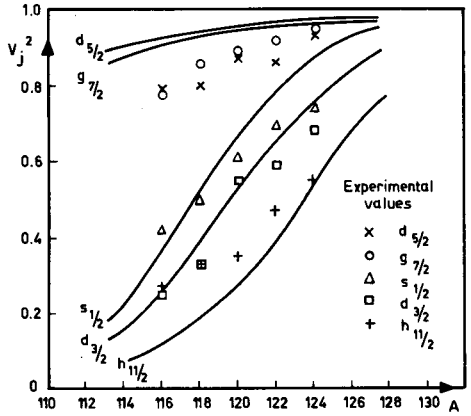

FIG. 12. Experimental values of V_j^2 obtained by B. L. Cohen and R. E. Price [11] from (d, p) and (α, t) experiments on the Sn isotopes as compared to the theoretical values of Kisslinger and Sørensen [10]

4.8. Charge-independent pairing forces

If both the neutron and proton shells are open, then we have two types of particle to consider. What is generally done is to allow pairing between the neutrons and between the protons independently. Thus one obtains a wave function

$$|\rangle = \prod_{\nu>0} [u_\nu(n) + v_\nu(n) a_\nu^\dagger(n) a_{\bar{\nu}}^\dagger(n)] \prod_{\nu>0} [u_\nu(p) + v_\nu(p) a_\nu^\dagger(p) a_{\bar{\nu}}^\dagger(p)] \, |-\rangle \qquad (4.54)$$

which is an eigenfunction of a pairing Hamiltonian $H_{nn} + H_{pp}$ (with neglect of $H_{res}(nn)$ and $H_{res}(pp)$). Clearly this Hamiltonian is not charge independent, and as a consequence $|\rangle$ does not have good isospin.

A charge-independent pairing Hamiltonian is

$$H = H_{nn} + H_{pp} + H_{np} \qquad (4.55)$$

where

$$H_{np} = -\frac{1}{2} G \sum_{\nu\nu'} a_\nu^\dagger(p) \, a_{\bar{\nu}}^\dagger(n) \, a_{\bar{\nu}'}(n) \, a_{\nu'}(p)$$

Expanded in normal order in terms of $|\rangle$, H_{np} becomes

$$H_{np} = -\frac{1}{2} G \sum_{\nu} \langle | a^{\dagger}_{\bar{\nu}}(n)\, a_{\bar{\nu}}(n) | \rangle \langle | a^{\dagger}_{\nu}(p)\, a_{\nu}(p) | \rangle$$

$$- \frac{1}{2} G \sum_{\nu} [\langle | a^{\dagger}_{\bar{\nu}}(n)\, a_{\bar{\nu}}(n) | \rangle \{ a^{\dagger}_{\nu}(p)\, a_{\nu}(p) \} + \langle | a^{\dagger}_{\nu}(p)\, a_{\nu}(p) | \rangle \{ a^{\dagger}_{\bar{\nu}}(n)\, a_{\bar{\nu}}(n) \}]$$

$$+ H_{res}(np) \qquad (4.56)$$

Now it was observed by Elliott and Lea [12] that the Hamiltonian

$$H^{(eff)}_{np} = -\frac{1}{2} G \sum_{\nu\nu'} a^{\dagger}_{\nu}(p)\, a^{\dagger}_{\nu'}(n)\, a_{\nu}(n)\, a_{\nu'}(p) \qquad (4.57)$$

gives exactly the same expansion as H_{np}, apart from differences in H_{res} which we neglect anyway.

$H^{(eff)}_{np}$ is in fact much easier to work with, since it can be expressed

$$H^{(eff)}_{np} = \frac{1}{4} G \sum_{\nu\nu'} a^{\dagger}_{\nu}(p)\, a_{\nu}(n)\, a^{\dagger}_{\nu'}(n)\, a_{\nu'}(p) - \frac{1}{4} G \sum_{\nu}{}' a^{\dagger}_{\nu}(p)\, a_{\nu}(p)$$

$$+ \frac{1}{4} G \sum_{\nu\nu'} a^{\dagger}_{\nu'}(n)\, a_{\nu'}(p)\, a^{\dagger}_{\nu}(p)\, a_{\nu}(n) - \frac{1}{4} G \sum_{\nu}{}' a^{\dagger}_{\nu}(n)\, a_{\nu}(n)$$

$$= \frac{1}{4} G (T_+ T_- + T_- T_+) - \frac{1}{4} G n \qquad (4.58)$$

$$= \frac{1}{4} G \left(T^2 - T_0^2 - \frac{1}{2} n \right)$$

Thus if the component of definite isospin (T, T_0) and particle number N, $|\rangle_{NTT_0}$ is projected from the wave function $|\rangle$, $H^{(eff)}_{np}$ is already diagonal, i.e.

$$H' |\rangle_{NTT_0} = [E_n + E_p + \tfrac{1}{2} G \{ T(T+1) - T_0^2 - \tfrac{1}{2} N \}] |\rangle_{NTT_0} \qquad (4.59)$$

In many cases of interest, where one is interested in energy differences, it appears that the extra terms, introduced by making the pairing force change independent, cancel. It is possible therefore that they can be neglected for most purposes with impunity, although this needs further investigation.

Unfortunately we cannot yet relax. The above charge-independent pairing force does not answer all the problems. In particular, it can only simulate the short range interactions in relative $T = 1$ states. It turns out, that, for a reasonable nucleon-nucleon force, the interaction

is every bit as strong in some T = 0, J = 1, 3, ... configurations as in the T = 1, J = 0. For the lighter nuclei, where neutrons and protons are filling the same shell, this is a particular problem. A brief review of some of the progress made is given in the book by Lane [9].

5. GENERALIZED HARTREE-FOCK THEORY

Having seen how to get a good approximate solution for a schematic short-range residual interaction in terms of the shell model, we can now apply these methods to the general HF problem using forces taken from 'nature' [13].

We right away start by making a Bogolubov-Valatin transformation to quasi-particles

$$a_\nu^\dagger = u_\nu \alpha_\nu^\dagger + v_\nu \alpha_{\bar{\nu}} \tag{5.1}$$

but with the single-particles basis ν and the coefficients u_ν, v_ν as yet undefined. We now seek the best wave function of the form of the quasi-particle vacuum

$$|\rangle = \prod_{\nu>0} (u_\nu + v_\nu a_\nu^\dagger a_{\bar{\nu}}^\dagger)|-\rangle \tag{5.2}$$

with the restraint that it should have the correct mean number of particles. Thus we must minimize the expectation of H', where

$$H' = \sum_{\nu\nu'} (T_{\nu\nu'} - \lambda\delta_{\nu\nu'})\, a_\nu^\dagger a_{\nu'} + \frac{1}{4}\sum_{\mu\nu\mu'\nu'} V_{\mu\nu\mu'\nu'}\, a_\nu^\dagger a_\mu^\dagger a_{\mu'} a_{\nu'} \tag{5.3}$$

Proceeding as in standard HF theory, arrange H' in normal order with respect to the quasi-particle vacuum $|\rangle$. We get, as in the schematic treatment

$$H' = U + H_{11} + H_{20} + H_{res} \tag{5.4}$$

where

$$\begin{aligned} U = &\sum_{\nu\nu'}\left[(T_{\nu\nu'} - \lambda\delta_{\nu\nu'}) + \frac{1}{2}\sum_{\mu\mu'} V_{\mu\nu\mu'\nu'} \langle|a_\mu^\dagger a_{\mu'}|\rangle\right] \langle|a_\nu^\dagger a_{\nu'}|\rangle \\ &+ \frac{1}{4}\sum_{\mu\nu\mu'\nu'} V_{\mu\nu\mu\nu'} \langle|a_\nu^\dagger a_\mu^\dagger|\rangle\langle|a_{\mu'} a_{\nu'}|\rangle \\ H_{11} + H_{20} = &\sum_{\nu\nu'}\left[(T_{\nu\nu'} - \lambda\delta_{\nu\nu'}) + \sum_{\mu\mu'} V_{\mu\nu\mu'\nu'} \langle|a_\mu^\dagger a_{\mu'}|\rangle\right]\{a_\nu^\dagger a_{\nu'}\} \\ &+ \frac{1}{4}\sum_{\mu\nu\mu'\nu'} V_{\mu\nu\mu'\nu'} [\langle|a_\nu^\dagger a_\mu^\dagger|\rangle\{a_{\mu'} a_{\nu'}\} + \langle|a_{\mu'} a_{\nu'}|\rangle\{a_\nu^\dagger a_\mu^\dagger\}] \\ H_{res} = &\frac{1}{4}\sum_{\mu\nu\mu'\nu'} V_{\mu\nu\mu'\nu'}\, \{a_\nu^\dagger a_\mu^\dagger a_{\mu'} a_{\nu'}\} \end{aligned} \tag{5.5}$$

These expressions can be expanded with the following useful identities:

$$\langle|a^\dagger_\alpha a_\beta|\rangle = \delta_{\alpha\beta}\, v^2_\alpha$$
$$\langle|a^\dagger_\alpha a^\dagger_{\bar\beta}|\rangle = \langle|a_\beta a_\alpha|\rangle = \delta_{\bar\alpha\beta}\, u_\alpha v_\alpha = -\delta_{\alpha\bar\beta}\, u_\beta v_\beta \tag{5.6}$$

$$\{a^\dagger_\alpha a_\beta\} = u_\alpha u_\beta \alpha^\dagger_\alpha \alpha_\beta - v_\alpha v_\beta \alpha^\dagger_{\bar\beta} \alpha_{\bar\alpha} + u_\alpha v_\beta \alpha^\dagger_\alpha \alpha^\dagger_{\bar\beta} + v_\alpha u_\beta \alpha_{\bar\alpha} \alpha_\beta$$
$$\{a^\dagger_\alpha a^\dagger_{\bar\beta}\} = u_\alpha v_\beta \alpha^\dagger_\alpha \alpha_{\bar\beta} - v_\alpha u_\beta \alpha^\dagger_{\bar\beta} \alpha_{\bar\alpha} + u_\alpha u_\beta \alpha^\dagger_\alpha \alpha^\dagger_\beta + v_\alpha v_\beta \alpha_{\bar\alpha} \alpha_{\bar\beta} \tag{5.7}$$
$$\{a_\alpha a_\beta\} = v_\alpha u_\beta \alpha^\dagger_{\bar\alpha} \alpha - u_\alpha v_\beta \alpha^\dagger_{\bar\beta} \alpha_\alpha + v_\alpha v_\beta \alpha^\dagger_{\bar\alpha} \alpha^\dagger_{\bar\beta} + u_\alpha u_\beta \alpha_\alpha \alpha_\beta$$

Consider first $(H_{11} + H_{20})$. This can be written in the abbreviated form

$$(H_{11} + H_{20}) = \sum (\epsilon_{\nu\nu'} - \lambda \delta_{\nu\nu'})\{a^\dagger_\nu a_{\nu'}\} - \frac{1}{2} \sum \Delta_{\nu\nu'} [\{a_{\bar\nu} a_{\nu'}\} + \{a^\dagger_\nu a^\dagger_{\bar\nu'}\}] \tag{5.8}$$

where

$$\epsilon_{\nu\nu'} = T_{\nu\nu'} + \sum_{\mu\mu'} V_{\mu\nu\mu\nu'} \langle|a^\dagger_\mu a_{\mu'}|\rangle = T_{\nu\nu'} + \sum_\mu V_{\mu\nu\mu\nu'} v^2_\mu$$

$$\Delta_{\nu\nu'} = -\frac{1}{2} \sum_{\mu\mu'} V_{\bar\mu\mu'\bar\nu\nu'} \langle|a^\dagger_{\mu'} a^\dagger_{\bar\mu}|\rangle = -\frac{1}{2} \sum_{\mu\mu'} V_{\nu\bar\nu'\mu\bar\mu'} \langle|a_\mu a_{\bar\mu'}|\rangle \tag{5.9}$$

$$= -\frac{1}{2} \sum_\mu V_{\bar\mu\mu\bar\nu\nu'} u_\mu v_\mu$$

Now a necessary and sufficient condition that $|\rangle$ minimize the expectation of H' is that

$$\langle|H_{20} = H_{20}|\rangle = 0 \tag{5.10}$$

which expresses the condition that

$$\langle|\alpha_\mu \alpha_\nu H'|\rangle = \langle|H'\alpha^\dagger_\mu \alpha^\dagger_\nu|\rangle = 0 \quad \text{all } \mu\nu$$

We also require that H_{11} should be diagonal, so that the quasi-particles should be independent. The latter condition gives us the single-particle basis wave functions ν and the former the coefficients u_ν, v_ν. Anticipating the results, we choose a single-particle representation in which $\epsilon_{\nu\nu'}$ is diagonal and assume for simplicity, although this is not strictly necessary, that this choice also diagonalizes $\Delta_{\nu\nu'}$.[3]

---

[3] For a spherical nucleus this is guaranteed in almost all practical cases by angular momentum conservation. Generally we have to postulate a conservation law

$$V_{\bar\mu\mu\bar\nu\nu'} = 0, \qquad \nu \neq \nu'$$

The problem could have been avoided by diagonalizing the whole of H_{11} directly, rather than in parts, but this complicates the formulae.

Thus we obtain

$$H_{11} = \sum_{\nu} \left[(\epsilon_\nu - \lambda)(u_\nu^2 - v_\nu^2) + 2\Delta_\nu u_\nu v_\nu \right] \alpha_\nu^\dagger \alpha_\nu$$

$$H_{20} = \sum_{\nu} \left[(\epsilon_\nu - \lambda) u_\nu v_\nu - \tfrac{1}{2}\Delta_\nu (u_\nu^2 - v_\nu^2) \right] (\alpha_\nu^\dagger \alpha_{\bar{\nu}}^\dagger + \alpha_{\bar{\nu}} \alpha_\nu) \tag{5.11}$$

Requiring that H_{20} vanishes gives

$$(\epsilon_\nu - \lambda) 2u_\nu v_\nu = \Delta_\nu (u_\nu^2 - v_\nu^2) \tag{5.12}$$

which, together with the normalization and number constraints

$$\begin{aligned} u_\nu^2 + v_\nu^2 &= 1 \\ \sum_\nu v_\nu^2 &= N \end{aligned} \tag{5.13}$$

is sufficient to determine u_ν, v_ν and λ. The following solutions emerge

$$u_\nu^2 = \frac{1}{2}\left\{1 + \frac{\epsilon_\nu - \lambda}{\sqrt{(\epsilon_\nu - \lambda)^2 + \Delta_\nu^2}}\right\} \qquad v_\nu^2 = \frac{1}{2}\left\{1 - \frac{\epsilon_\nu - \lambda}{\sqrt{(\epsilon_\nu - \lambda)^2 + \Delta_\nu^2}}\right\} \tag{5.14}$$

where Δ_ν and λ are solutions of the gap equation

$$\Delta_\nu = -\frac{1}{4} \sum_{\nu'} \frac{V_{\bar{\nu}\nu\bar{\nu}'\nu'}}{\sqrt{(\epsilon_{\nu'} - \lambda)^2 + \Delta_{\nu'}^2}} \Delta_{\nu'} \tag{5.15}$$

and the number equation

$$\frac{1}{2} \sum_\nu \left\{1 - \frac{\epsilon_\nu - \lambda}{\sqrt{(\epsilon_\nu - \lambda)^2 + \Delta_\nu^2}}\right\} = N \tag{5.16}$$

Gathering terms we finally end up with

$$\begin{aligned} u &= \sum_\nu \left[(\epsilon_\nu - \lambda) - \frac{1}{2} \sum_\mu V_{\mu\nu\mu\nu} \; V_\mu^2 \right] v_\nu^2 - \frac{1}{2} \sum_\nu \Delta_\nu u_\nu v_\nu \\ H_{11} &= \sum_\nu E_\nu \alpha_\nu^\dagger \alpha_\nu \\ H_{20} &= 0 \\ H_{res} &= \frac{1}{4} \sum_{\mu\nu\mu'\nu'} V_{\mu\nu\mu'\nu'} \; \{a_\nu^\dagger a_\mu^\dagger a_{\mu'} a_{\nu'}\} \end{aligned} \tag{5.17}$$

where

$$E_\nu = \sqrt{(\epsilon_\nu - \lambda)^2 + \Delta_\nu^2} \tag{5.18}$$

These equations are very similar to those obtained with the schematic pairing force. For practical purposes the only significant difference is that Δ_ν is no longer a constant but depends on ν. However, it appears that, for reasonable nuclear forces, Δ_ν varies very little in fact, with ν.

Results calculated with the schematic pairing force should therefore be pretty reliable.

If H_{res} is neglected, excited states are quasi-particle states. But if one is interested in collective states then H_{res} cannot sensibly be neglected. In the following sections we shall be concerned with collective vibrational states and how H_{res} can be taken into account.

6. THE TAMM-DANCOFF APPROXIMATION

We now come to a discussion of excited states. For simplicity we shall forget all about pairing for the time being in the knowledge that it can be simply included later, when we have worked out the essential many-body techniques.

6.1. The Tamm-Dancoff approximation

The Tamm-Dancoff approximation is a natural one. It is to accept the HF wave function $|\rangle$ for the ground state, and to set up a basis of excited HF configurations among which the residual interactions can be diagonalized.

The lowest unperturbed configurations are the 1 ph states

$$|mi\rangle = a_m^\dagger a_i |\rangle$$

(Remember that the subscripts m, n are reserved for particle states or single-particle states above the HF Fermi surface, while i, j are reserved for hole states or single-particle states below the HF Fermi surface.) Such configurations are coupled by the residual interaction

$$H_{res} = \frac{1}{4} \sum_{\mu\mu'\nu'} V_{\mu\nu\mu'\nu'} \{a_\nu^\dagger a_\mu^\dagger a_{\mu'} a_{\nu'}\}$$

not included in the self-consistent field (section 2). The coupling between two particle-hole states is

$$\langle mi | H_{res} | nj \rangle = V_{mjin}$$

$$\equiv \int\int \varphi_m^*(\vec{r})\, \varphi_j^*(\vec{r}')\, V(\vec{r}, \vec{r}')\, \varphi_i(\vec{r})\, \varphi_n(\vec{r}')\, d\vec{r}\, d\vec{r}'$$

$$- \int\int \varphi_m^*(\vec{r})\, \varphi_j^*(\vec{r}')\, V(\vec{r}, \vec{r}')\, \varphi_n(\vec{r})\, \varphi_i(\vec{r}')\, d\vec{r}\, d\vec{r}'$$

which is expressed graphically in Fig. 13.

Matrix elements of the full Hamiltonian, between particle-hole states, are

$$\langle mi|H|nj\rangle = \delta_{mn}\,\delta_{ij}\,(E_0 + \epsilon_{mi}) + V_{mjin}$$

where E_0 is the ground-state energy and $\epsilon_{mi} = \epsilon_m - \epsilon_i$ is the unperturbed particle-hole energy.

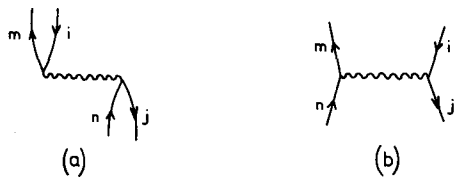

FIG. 13. Graphical expression of the matrix element V_{mjin}

(a) Direct term: $\iint \varphi_m^*(\vec{r})\,\varphi_j^*(\vec{r}')\,V(\vec{r},\vec{r}')\,\varphi_i(\vec{r})\,\varphi_n(\vec{r}')\,d\vec{r}\,d\vec{r}'$

(b) Exchange term: $\iint \varphi_m^*(\vec{r})\,\varphi_j^*(\vec{r}')\,V(\vec{r},\vec{r}')\,\varphi_n(\vec{r})\,\varphi_j(\vec{r}')\,d\vec{r}\,d\vec{r}'$

Assuming that an excited eigenstate $|\hbar\omega\rangle$, of excitation energy $\hbar\omega$, has the particle-hole form

$$|\hbar\omega\rangle = \sum_{mi} Y_{mi}\,|mi\rangle \tag{6.1}$$

we get the secular equation

$$(\epsilon_{mi} - \hbar\omega)\,Y_{mi} + \sum_{nj} V_{mjin}\,Y_{nj} = 0 \tag{6.2}$$

Matrix elements for a general one-body operator Q, which might, for example, be an electromagnetic multipole operator, are given by

$$\langle\hbar\omega|Q|\rangle = \sum_{mi} Y_{mi}^*\,Q_{mi} \tag{6.3}$$

where

$$Q_{mi} = \langle m|Q|i\rangle = \int \varphi_m^*(\vec{r})\,Q\,\varphi_i(\vec{r})\,d\vec{r}$$

For a closed-shell nucleus the Tamm-Dancoff method is immediately applicable. The shell model provides a good approximation to the HF wave functions and pairing can justifiably be neglected. In such a case the method is, of course, no more than a conventional shell model treatment, for which several calculations have been performed. Some of the earliest and most well-known are those of Elliott and Flowers [14] for the odd parity states of ^{16}O. Generally speaking, their fits to the experimental energies and lifetimes were good. But more interesting

than merely fitting data are some of the general trends that emerge from such calculations, in particular the appearance of collective states.

Consider the 1-, T = 1 states, for example. From among the unperturbed configurations, one linear combination separates out and is pushed up in energy by the residual interactions. Furthermore, it acquires collective properties by taking with it the bulk of the E1 strength. Thus the shell model with residual interactions explains rather well the energy and strength of the giant dipole resonance.[4]

For the 3-, T = 0 states, one state again gathers the bulk of the collective strength, but this time falls below the others in energy. It appears to be a general feature of such calculations that T = 1 states rise in energy, with the most collective among them having the highest energies, while T = 0 states are depressed and the most collective are the lowest. This is in general agreement with observation.

6.2. The schematic model

The physics behind the above results was explained rather nicely by Brown et al. [15] with the schematic interaction

$$V(\vec{r}_i, \vec{r}_j) = -\chi \sum_{\mu} r_i^J Y_{J\mu}(\theta_i)\, r_j^J Y_{J\mu}^*(\theta_j) \tag{6.4}$$

Neglecting exchange terms

$$V_{mjin} = -\chi D_{mi} D_{nj}^* \tag{6.5}$$

where

$$D_{mi} = \langle m | r^J Y_{J\mu} | i \rangle$$

The secular equation becomes

$$(\epsilon_{mi} - \hbar\omega) Y_{mi} = \chi D_{mi} \sum_{nj} D_{nj}^* Y_{nj}$$

which is easily solved, since $\sum_{nj} D_{nj}^* Y_{nj}$ is a constant. Hence

$$Y_{mi} = \frac{N D_{mi}}{\epsilon_{mi} - \hbar\omega} \tag{6.6}$$

where N is a normalization constant such that

$$\sum_{mi} |Y_{mi}|^2 = 1$$

[4] Its width and structure are also readily understandable in terms of particle emission broadening and coupling to more complicated configurations, although such aspects are not easy to calculate.

We also obtain a dispersion formula for the energy $\hbar\omega$

$$\sum_{mi} D^*_{mi} Y_{mi} = \chi \sum_{mi} \frac{|D_{mi}|^2}{\epsilon_{mi} - \hbar\omega} \sum_{nj} D^*_{nj} Y_{nj}$$

or

$$\sum_{mi} \frac{|D_{mi}|^2}{\epsilon_{mi} - \hbar\omega} = \frac{1}{\chi} \tag{6.7}$$

The graphical solution of this equation proves to be rather instructive, and is shown in Fig. 14.

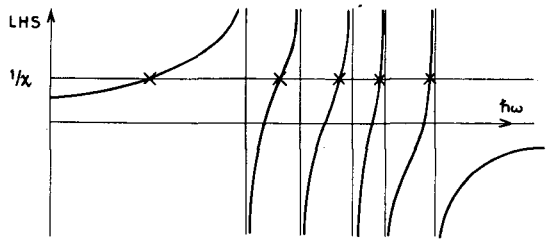

FIG. 14. Graphical solution of the dispersion formula for $\hbar\omega$, for $\chi > 0$

All the solutions, save one, are trapped between the unperturbed energies. The solution that is not trapped falls a long way below the rest and becomes collective, i.e. it acquires much more than its fair share of electromagnetic multipole strength.

This is demonstrated most forcefully in the degenerate limit, when all the particle-hole energies ϵ_{mi} are equal to a common ϵ. In this limit, all solutions save one are trapped at the unperturbed energy ϵ. For the solution that is not trapped

$$Y_{mi} = \frac{N D_{mi}}{\epsilon - \hbar\omega} = \frac{D_{mi}}{\sqrt{\sum_{nj} |D_{nj}|^2}}$$

and, from the dispersion equation,

$$\hbar\omega = \epsilon - \chi \sum_{mi} |D_{mi}|^2 \tag{6.8}$$

The multipole strength for this state is

$$|\langle \hbar\omega | r^J Y_{J\mu} | \rangle|^2 = \Big| \sum_{mi} Y^*_{mi} D_{mi} \Big|^2$$

$$= \sum_{mi} |D_{mi}|^2 \qquad (6.9)$$

which is equal to the sum of all the strength of the unperturbed states.

If the particle-hole interaction is repulsive, i.e. $\chi < 0$, similar results transpire. One state is then pushed up in energy above the rest and, in the degenerate limit, collects all the multipole strength.

Qualitatively similar, but less extreme results can be expected with non-degenerate levels and more realistic interactions.

6.3. The particle-hole interaction

Another question we may ask in trying to understand the behaviour of the Tamm-Dancoff solutions is "when should the particle-hole interaction be predominantly attractive and when repulsive?"

There are two sorts of particles in the nucleus, thus it is possible to construct both T = 0 and T = 1 particle-hole excitations. These can be written schematically

$$|ph\rangle = \frac{1}{\sqrt{2}} (P\bar{P} \pm N\bar{N}), \qquad T = 0,\ 1$$

where P refers to a proton particle state and $\bar{P}$ a proton hole state. If we suppose a simple attractive particle-particle interaction, the matrix elements for the different components are

$$\langle P\bar{P}|H|P\bar{P}\rangle = D - E$$

$$\langle P\bar{P}|H|N\bar{N}\rangle = D$$

where D is the direct matrix element (Fig. 13 (a)) and E is the exchange (Fig. 13 (b)). Thus for the particle-hole matrix elements we obtain

$$\langle ph|H|ph\rangle = 2D - E \quad \text{for} \quad T = 0$$

$$= -E \qquad \text{for} \quad T = 1$$

For a short range interaction, $D \approx E$ and we get the result that, for an attractive particle-particle interaction, the particle-hole interaction is attractive in T = 0 states and repulsive in T = 1 states. This result still holds good for any reasonable exchange mixture. The physical interpretation is that, since protons and neutrons move in anti-phase in a T = 1 excitation, the motion is opposed by the attractive force between them, whereas in a T = 0 excitation they move in phase and consequently the motion is favoured by their interaction.

7. THE RANDOM PHASE APPROXIMATION (RPA)

7.1. The philosophy of the RPA

The Tamm-Dancoff approximation works very well but it fails in at least one systematic way in that it does not satisfy the energy-weighted sum rule. As a consequence, it tends to underestimate, and often rather badly, the strength of the low-lying collective states. The 3-, T = 0 collective states of ^{16}O and ^{40}Ca, for example, are underestimated by something like a factor of three. Experimentally, these states are extremely strong. The ^{16}O octupole state actually over-exhausts the sum shell model strength for 1 $\hbar\omega$ excitations by a factor 2.13, and exhausts ~0.64 of the total strength.

There are three things we could try to do improve the situation:

(a) Enlarge the particle-hole configuration space to include 3 $\hbar\omega$ excitations. This helps a little but not nearly enough.

(b) Include more complicated configurations, 2ph, 3ph, etc. Such configurations have zero multipole strength and are unlikely to help very much.

(c) Take into account the effects of the residual interactions on the ground state. By modifying the ground state wave function, the non-energy weighted sum rule itself, which is very model-dependent, can be incremented.

Clearly we can do all of these things, but the complexity of the problem so rapidly escalates that it is not possible to take them very far. Fundamentally the problem is that wave functions really are extremely complicated, and however much effort is expended in calculating them, the result will inevitably be almost orthogonal to the exact wave function. This does not mean that we should abandon the problem, but it does mean that we should design our efforts to optimizing those aspects of the wave function that concern us.

What aspect of the nucleus does HF theory optimize? It is of course the single-particle aspect. For the exact ground state $|0\rangle$, the expectation of any arbitrary operator $\hat{Q}$,

$$Q = \langle 0|\hat{Q}|0\rangle$$

is a constant in time. This gives a condition on the wave function

$$i\hbar \frac{\partial Q}{\partial t} = \langle 0|[\hat{Q}, H]|0\rangle = 0, \qquad \text{all } \hat{Q}$$

This is a very stringent condition and, if satisfied for all possible $\hat{Q}$, ensures that $|0\rangle$ is an exact eigenfunction. Now the HF approximation $|\ \rangle$to $|0\rangle$ satisfies this equation only for Q, a single particle operator. Thus the HF approximation can be expected to give good results for observables corresponding to single-particle operators, such as nuclear density distributions, magnetic or quadrupole moments, etc. It cannot be expected to give good results for phenomena involving two or more particle correlations such as quasi-deuteron processes as evidence in

high-energy photo-absorption, etc. In physical terms, the probability that all the nucleons are simultaneously in their HF orbitals is surely rather small, but the chance that any particular orbital has its HF occupancy is very much larger.

We can similarly apply this principle to the calculations of excited states. The properties of an excited state that most interest us are its excitation energy and its single-particle matrix elements with the ground state. What we have been attempting to do is to calculate ground and excited state wave-function independently. But the above observables involve not so much the wave functions themselves as the relationships between them. We should therefore attempt a more direct onslaught of calculating the appropriate relationships rather than the separate wave functions, thereby optimizing our efforts to give the best possible values for the observables. This is the philosophy behind the random phase approximation RPA – at least as presented here. The RPA derives, as we shall now show, from the well-known equations of motion method for solving the harmonic oscillator problem.

The RPA also goes under other names, in particular the quasi-boson approximation, the method of linearized equations of motion and time-dependent Hartree-Fock theory. In all cases the final equations are identical, although it is not always immediately obvious that the approximations of the different methods are equivalent. Indeed some of the methods of linearizing the equations of motion are really not derivations at all but prescriptions. The variation described here is not (yet) to be found in the literature, but has the advantage of a much firmer basis, is simple and is readily extended to higher order.

7.2. The equations of motion

The equations of motion, for a harmonic oscillator Hamiltonian of frequency ω, are

$$\begin{aligned} [H,\ O^\dagger] &= \omega O^\dagger \\ [H,\ O] &= -\omega O \end{aligned} \tag{7.1}$$

where we put $\hbar = 1$, and where O, $O^\dagger$ are boson operators with the commutators

$$[O,\ O^\dagger] = 1 \tag{7.2}$$

From the solution to these equations, a set of eigenfunctions can be constructed, defined by

$$\begin{aligned} O|0\rangle &\equiv 0 \\ O^\dagger|0\rangle &= |1\rangle \\ O^\dagger|n\rangle &= \sqrt{(n+1)}\,|n+1\rangle \end{aligned} \tag{7.3}$$

Thus instead of solving the set of eigenfunction equations

$$H|n\rangle = (n + \tfrac{1}{2})\omega|n\rangle$$

the equations-of-motion method determines operators $O^\dagger$, O which relate eigenfunctions. This then is the sort of approach required for finding nuclear excited states. The problem is to generalize the method to a non-harmonic Hamiltonian.

The solution to the above equation for $O^\dagger$, in terms of eigenfunctions, is

$$O^\dagger = \sum_{n=0}^{\infty} \sqrt{(n+1)}\,|n+1\rangle\langle n|$$

Now suppose that the Hamiltonian is not completely harmonic, but has a harmonic spectrum of energy levels up to the m'th level. By this we mean that Eq. (7.3) holds for all $n \leq m$ and that

$$E_{n+1} - E_n = \omega, \quad \text{all } n \leq m$$

where ω is a constant independent of n. If $O^\dagger$ is given the form

$$O^\dagger = \sum_{n=0}^{m} \sqrt{(n+1)}\,|n+1\rangle\langle n| + \sum_{p,\,q>m} C_{pq}\,|p\rangle\langle q|$$

for arbitrary C_{pq}, it is seen that Eqs. (7.1) - (7.3) are still satisfied provided they are allowed to operate only in that sub-Hilbert space spanned by the eigenvectors $n \leq m$. In other words, the equations of motion can be written

$$\begin{aligned} [H,\, O^\dagger] &= \omega O^\dagger + P \\ [H,\, O] &= -\omega O - P^\dagger \end{aligned} \tag{7.4}$$

and the commutators

$$[O,\, O^\dagger] = 1 + Q \tag{7.5}$$

where

$$P|n\rangle = P^\dagger|n\rangle = Q|n\rangle \equiv 0, \quad \text{all } n \leq m$$

Equation (7.4) can be put into a much more tractable form: Premultiply the first equation by an arbitrary operator R and the second by $R^\dagger$, then take the expectation of the first plus the Hermitian conjugate of the second, with respect to a wave function $|\varphi\rangle$. Provided $|\varphi\rangle$ lies within the harmonic region of Hilbert space, we obtain

$$\langle\varphi|[R,\, ([H,\, O^\dagger] - \omega O^\dagger)]\,|\varphi\rangle = 0, \quad \text{all } R \tag{7.6}$$

Similarly

$$\langle\varphi|[R,\ ([H,\ O] + \omega O)]\,|\varphi\rangle = 0, \qquad \text{all } R$$

so that both $O^\dagger$ and O should appear as solutions of Eq. (7.6) with eigenfrequencies $\pm\omega$ respectively.

Now the nuclear Hamiltonian is mildly harmonic in the so-called vibrational modes, but not at all in the multitude of other modes. Thus the harmonic region of Hilbert space is rather small. But note that it never vanishes, regardless of the Hamiltonian. It must always contain at least the one-dimensional space of the ground state wave function. Thus if $|\varphi\rangle = |0\rangle$, Eq. (7.6) is exact for any Hamiltonian. But the great advantage of this approach is that the results of Eq. (7.6) should not depend very critically on the details of the wave function $|\varphi\rangle$ chosen.

7.3. The RPA

While Eq. (7.6) is exact, it cannot be solved without making some approximations. First we need a wave function $|\varphi\rangle$, which lies within the harmonic sub-space. The first approximation of the RPA is to suppose that this condition is satisfied by the HF wave function $|\ \rangle$. The RPA equation of motion is therefore

$$\langle\,|[R,\ ([H,\ O^\dagger] - \omega O^\dagger)]\,|\,\rangle = 0, \qquad \text{all } R \tag{7.7}$$

The second approximation is to limit the form of the operator $O^\dagger$ in order to have a problem of manageable dimensions. The form chosen is the simplest possible which leads to consistent solutions;[5] i.e. the particle-hole form

$$O^\dagger = \sum_{mi} (Y_{mi}\, a_m^\dagger a_i - Z_{mi}\, a_i^\dagger a_m) \tag{7.8}$$

We could equally well take $O^\dagger$ to be a general single-particle operator but it transpires that the particle-particle and hole-hole parts vanish in Eq. (7.7) leaving only the particle-hole components.

---

[5] The still simpler form of the Tamm-Dancoff approximation

$$O^\dagger = \sum_{mi} Y_{mi}\, a_m^\dagger a_i$$

does not lead to consistent solutions, for while

$$\langle\,|[a_i^\dagger a_m,\ [H,\ O^\dagger]]\,|\,\rangle = (\epsilon_m - \epsilon_i)\,Y_{mi} + \sum_{nj} V_{mjin}\, Y_{nj}$$

$$= \omega\,\langle\,|[a_i^\dagger a_m,\ O^\dagger]\,|\,\rangle$$

the conjugate equation is not simultaneously satisfied

$$\langle\,|[a_i^\dagger a_m,\ [H,\ O]]\,|\,\rangle = \sum_{nj} V_{mnij}\, Y_{nj}^* \neq \omega\,\langle\,|[a_i^\dagger a_m,\ O]\,|\,\rangle = 0$$

The problem is now well defined. Taking for R first $a_i^\dagger a_m$ and then $a_m^\dagger a_i$, we obtain the usual equations of the RPA

$$\left.\begin{aligned}(\epsilon_m - \epsilon_i)\,Y_{mi} + \sum_{nj}(V_{mjin}\,Y_{nj} + V_{mnij}\,Z_{nj}) &= \omega\,Y_{mi}\\ (\epsilon_m - \epsilon_i)\,Z_{mi} + \sum_{nj}(V_{inmj}\,Z_{nj} + V_{ijmn}\,Y_{nj}) &= -\omega\,Z_{mi}\end{aligned}\right\}\quad \text{all m, i} \qquad (7.9)$$

These equations may be written in matrix form

$$\begin{pmatrix} A & B \\ -B^* & -A^* \end{pmatrix}\begin{pmatrix} Y \\ Z \end{pmatrix} = \omega \begin{pmatrix} Y \\ Z \end{pmatrix} \qquad (7.10)$$

with obvious notation.

From the symmetry of the matrix, it is clear that the RPA is a consistent approximation. Thus if one solution is

$$O^\dagger \equiv \begin{pmatrix} Y \\ Z \end{pmatrix}$$

with frequency ω, another solution is

$$O \equiv \begin{pmatrix} Z^* \\ Y^* \end{pmatrix}$$

with frequency $-\omega$.

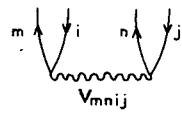

FIG. 15. Graph of a matrix element V_{mnij}

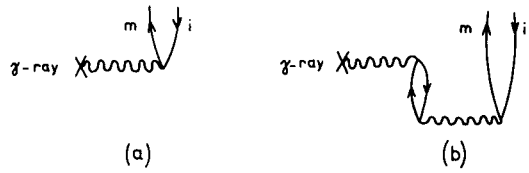

FIG. 16. (a) Creation of a particle-hole pair by a γ-ray. (b) Annihilation of a particle-hole pair already present in the ground state, by a γ-ray

If the matrix B were identically zero, then the RPA would reduce to the Tamm-Dancoff approximation. However, B is not zero. A matrix element of B is shown graphically in Fig. 15. The non-vanishing of B implies that coupled to the HF vacuum are 2ph configurations in first order, 4ph in second order, etc. The admixture of these configurations

into the ground state is referred to as 'ground-state correlations'. The existence of these correlations can be very important in calculating transition matrix elements. For example, the nucleus can be excited by absorption of a γ-ray in one of two ways. The γ-ray can either create a particle-hole pair, as in Fig. 16(a), or it can annihilate a particle-hole pair already present in the ground state, as in Fig. 16(b).

7.4. Properties of the solutions [16]

(a) Normalization

Provided the excitation operators $O_\alpha^\dagger$, O_α obey the pseudoboson commutation relations

$$\langle 0|[O_\alpha, O_\alpha^\dagger]|0\rangle = 1, \quad \omega_\alpha > 0 \tag{7.11}$$

the normalization of the excited state $|\alpha\rangle$is ensured;

$$\langle \alpha|\alpha\rangle = \langle 0|O_\alpha O_\alpha^\dagger|0\rangle = \langle 0|[O_\alpha, O_\alpha^\dagger]|0\rangle$$

Under the RPA assumption that $|\ \rangle$lies within the harmonic sub-space, we also require

$$\langle |[O_\alpha, O_\alpha^\dagger]|\ \rangle = 1, \quad \omega_\alpha > 0 \tag{7.12}$$

Now $[O_\alpha, O_\alpha^\dagger]$ is a single-particle operator, and since the ground state expectation of a single-particle operator is given well by the HF wave function, these two equations are fortunately simultaneously satisfiable to a good approximation. Equation (7.12) is most easily calculated and gives the normalization

$$\sum_{mi} (|Y_{mi}(\alpha)|^2 - |Z_{mi}(\alpha)|^2) = 1, \quad \omega_\alpha > 0 \tag{7.13}$$

Note that $O^\dagger$ and O are both solutions of the same Eq. (7.7), with $\omega_\alpha = \pm|\omega_\alpha|$ respectively. Thus for $\omega_\alpha < 0$ the role of the two operators becomes interchanged, giving the normalization

$$\langle |[O_\alpha, O_\alpha^\dagger]|\ \rangle = \sum_{mi} (|Y_{mi}(\alpha)|^2 - |Z_{mi}(\alpha)|^2) = -1, \quad \omega_\alpha < 0 \tag{7.14}$$

(b) Orthogonality

For the excited states $|\alpha\rangle$ and $|\beta\rangle$ to be orthogonal we require

$$\langle \alpha|\beta\rangle = \langle 0|[O_\alpha, O_\beta^\dagger]|0\rangle \approx \langle |[O_\alpha, O_\beta^\dagger]|\ \rangle = \delta_{\alpha\beta}, \quad \omega_\alpha > 0$$

or

$$\sum_{mi} (Y^*_{mi}(\alpha)\, Y_{mi}(\beta) - Z^*_{mi}(\alpha)\, Z_{mi}(\beta)) = \delta_{\alpha\beta}\,, \qquad \omega_\alpha > 0$$

Consider

$$(Y^*(\alpha)\, Z^*(\alpha)) \begin{pmatrix} A & B \\ B^* & A^* \end{pmatrix} \begin{pmatrix} Y(\beta) \\ Z(\beta) \end{pmatrix} = \omega_\beta \, (Y^*(\alpha)\, Z^*(\alpha)) \begin{pmatrix} Y(\beta) \\ -Z(\beta) \end{pmatrix}$$

Interchanging α and β and taking the hermitian conjugate, we find

$$(\omega_\alpha - \omega_\beta)\, (Y^*(\alpha)\, Z^*(\alpha)) \begin{pmatrix} Y(\beta) \\ -Z(\beta) \end{pmatrix} = 0$$

so that

$$(Y^*(\alpha)\, Z^*(\alpha)) \begin{pmatrix} Y(\beta) \\ -Z(\beta) \end{pmatrix} = \begin{cases} \delta_{\alpha\beta}\,, & \omega_\alpha > 0 \\ -\delta_{\alpha\beta}\,, & \omega_\alpha < 0 \end{cases} \tag{7.15}$$

(c) Spurious states

It is well known that in calculating excited states within the framework of the shell model, one has to be careful about spurious states corresponding to excitation of the centre-of-mass motion in the shell model potential. The problem arises because the shell model Hamiltonian is not translationally invariant; i.e.

$$[H_{SM},\, P] \neq 0$$

The problem is complicated by the fact that the spurious states do not separate out as eigenstates.

In this respect the RPA is much superior. Since the full translationally invariant Hamiltonian is used in the equation of motion, it follows that

$$\langle |[R, [H, P]]| \rangle = 0, \qquad \text{all } R$$

and hence that

$$\begin{pmatrix} A & B \\ B^* & A^* \end{pmatrix} \begin{pmatrix} P \\ -P^* \end{pmatrix} = 0 \tag{7.16}$$

where P in the last equation is the column vector P_{mi}. Thus, in the RPA, the centre-of-mass motion is an eigenstate with zero frequency. This is as it should be, since if the centre of mass is displaced there is no restoring force and no oscillation.

However, the mere existence of a zero frequency solution can cause problems. For instance it is self-orthogonal.

$$(P^* \quad P) \begin{pmatrix} P \\ -P^* \end{pmatrix} = 0$$

All tne other solutions are paired off with $\omega_\alpha = \pm|\omega_\alpha|$. However, if $\omega = 0$ the state is identical to its opposite. As a consequence, for every $\omega = 0$ solution the eigenvectors are one short of forming a complete set. In the above example it is easy to guess that the position co-ordinate X conjugate to P should provide the extra vector needed to complete the set. Because of Galilean invariance

$$[H, X] = \frac{-i}{AM} P$$

it follows that

$$\langle |[R, [H, \Psi]]| \rangle = \frac{1}{AM} \langle |[R, P]| \rangle$$

where $\Psi = iX$ and hence that

$$\begin{pmatrix} A & B \\ B^* & A^* \end{pmatrix} \begin{pmatrix} \Psi \\ \Psi^* \end{pmatrix} = \frac{1}{AM} \begin{pmatrix} P \\ P^* \end{pmatrix} \tag{7.17}$$

It is easy to show that the solution to this equation for Ψ provides the other vector needed to make up the complete set.

There can also be other zero frequency solutions corresponding to other invariances of the Hamiltonian. For example, for a deformed HF wave function, angular momenta is not a good quantum number, but

$$[H, J] = 0$$

and gives rise to a solution corresponding to a rotation. Again if we were to use the generalized HF wave function, for which the particle number is not a good quantum number, the invariance

$$[H, n] = 0$$

where n is the number operator, leads to a spurious state corresponding to a number fluctuation. This is the spurious two quasi-particle state discussed previously. The fact that these spurious states do separate out exactly is one of the significant advantages of the RPA.

7.5. Transitions and sum rules

The matrix elements between ground and excited state $|\alpha\rangle$, for a single-particle operator W, are

$$\begin{aligned} \langle 0|W|\alpha\rangle &= \langle 0|[W, O_\alpha^\dagger]|0\rangle \\ &\approx \langle |[W, O_\alpha^\dagger]| \rangle = \sum_{mi} (W_{mi}^* Y_{mi}(\alpha) + W_{mi} Z_{mi}(\alpha)) \end{aligned} \tag{7.18}$$

This result may be compared with the Tamm-Dancoff expression

$$\langle |W| \alpha \rangle = \sum_{mi} W^*_{mi} \, Y_{mi}(\alpha)$$

The extra term in Z can often bring about a considerable enhancement of the matrix element.

In the Tamm-Dancoff approximation the total multipole strength is limited by the sum rule

$$S^{TD}_{NEW} = \sum_{\alpha} |\langle |W| \alpha \rangle|^2 = \sum_{mi} |W_{mi}|^2$$

In the RPA, because of the admission of ground-state correlations, there is no simple limit to this sum rule. Because of the negative sign in the normalization (Eq. (7.13)) the Y_{mi} and Z_{mi} can become very much larger than Y_{mi} in Tamm-Dancoff, with the result that the matrix elements (Eq. (7.18)) can be much enhanced. There can also be cancellation, of course, if Y_{mi} and Z_{mi} have opposite sign, and this happens in some notable cases which we shall discuss later.

The energy weighted sum rule

$$S_{EW} = \tfrac{1}{2} \langle 0 | [W; [H, W]] | 0 \rangle = \sum_{\alpha} \omega_{\alpha} |\langle 0 | W | \alpha \rangle|^2$$

which should be pretty well model-independent, is obeyed exactly by the RPA. Evaluating the sum rule in the HF state

$$S_{EW} = \tfrac{1}{2} \langle | [W, [H, W]] | \rangle = \tfrac{1}{2} (W^* \; -W) \begin{pmatrix} A & B \\ B^* & A^* \end{pmatrix} \begin{pmatrix} W \\ -W^* \end{pmatrix} \tag{7.19}$$

If we assume that there are no spurious states with the angular momentum and parity of W, then

$$S_{EW} = \tfrac{1}{2} \sum_{\alpha} (W^* \; -W) \begin{pmatrix} A & B \\ B^* & A^* \end{pmatrix} \begin{pmatrix} Y(\alpha) \\ Z(\alpha) \end{pmatrix} (Y^*(\alpha) \; Z^*(\alpha)) \begin{pmatrix} W \\ W^* \end{pmatrix}$$

$$= \sum_{\alpha > 0} \omega_{\alpha} \, (W^* \; W) \begin{pmatrix} Y(\alpha) \\ Z(\alpha) \end{pmatrix} (Y^*(\alpha) \; Z^*(\alpha)) \begin{pmatrix} W \\ W^* \end{pmatrix}$$

$$= \sum_{\alpha > 0} \omega_{\alpha} |\langle 0 | W | \alpha \rangle|^2 \tag{7.20}$$

Thus the particle-hole excitations of the RPA completely exhaust the energy weighted sum rule.

If there is a spurious state with the quantum numbers of W (centre-of-mass motion has quantum numbers $J^\pi = 1^-$, $T = 0$), then before agreement can be obtained, it is necessary to subtract the spurious strength from the sum rule. This can be done and the RPA excited states ($\omega_\alpha > 0$) exactly exhaust the remainder.

7.6. The extended schematic model [17]

The behaviour of the RPA solutions is also illustrated very well by using a schematic interaction. Again neglecting exchange terms,

$$V_{mjin} = -\chi D_{mi} D^*_{nj} , \qquad V_{mnij} = -\chi D_{mi} D_{nj} \tag{7.21}$$

The RPA equations become

$$(\epsilon_{mi} - \omega) Y_{mi} - \chi D_{mi} \sum_{nj} (D^*_{nj} Y_{nj} + D_{nj} Z_{nj}) = 0$$

$$(\epsilon_{mi} + \omega) Z_{mi} - \chi D^*_{mi} \sum_{nj} (D_{nj} Z_{nj} + D^*_{nj} Y_{nj}) = 0$$

with solution

$$Y_{mi} = \frac{N D_{mi}}{\epsilon_{mi} - \omega} , \qquad Z_{mi} = -\frac{N D^*_{mi}}{\epsilon_{mi} + \omega} \tag{7.22}$$

where N is a constant given by

$$N = \chi \sum_{nj} (D^*_{nj} Y_{nj} + D_{nj} Z_{nj}) \tag{7.23}$$

and can be determined by the normalization, Eq. (7.13). From Eqs. (7.22) and (7.23) we get the dispersion equation

$$\sum_{mi} \frac{|D_{mi}|^2 \epsilon_{mi}}{\epsilon^2_{mi} - \omega^2} = \frac{1}{2\chi} \tag{7.24}$$

This equation may be solved graphically, just as in the Tamm-Dancoff case. If $\chi > 0$ (attractive force), one solution falls below all the rest and becomes collective, while if $\chi < 0$ one solution rises above the rest and again becomes collective.

To compare more quantitatively with the Tamm-Dancoff results we again go to the degenerate limit. All solutions but one are trapped at the energy $\omega = \epsilon$. For the solution that is not trapped

$$\omega^2 = \epsilon^2 - 2\chi\epsilon \sum_{mi} |D_{mi}|^2 \tag{7.25}$$

This may be compared with the square of Eq. (6.8)

$$\omega^2_{\text{T.D.}} = \epsilon^2 - 2\chi\epsilon \sum_{mi} |D_{mi}|^2 + \chi^2 \Big(\sum_{mi} |D_{mi}|^2 \Big)^2$$

Thus we see that, for a given interaction strength, the RPA energy is always lower than the Tamm-Dancoff.

The multipole strength for excitation of the state $|\omega\rangle$ is

$$|\langle \omega | r^J Y_{J\mu} | 0 \rangle|^2 = \Big[N \sum_{mi} |D_{mi}|^2 \frac{2\epsilon}{\epsilon^2 - \omega^2} \Big]^2$$

where the normalization N is given by comparison of Eq. (7.22) with (7.13);

$$N^2 \sum |D_{mi}|^2 \frac{4\omega\epsilon}{(\epsilon^2 - \omega^2)^2} = 1$$

We obtain

$$|\langle \omega | r^J Y_{J\mu} | 0 \rangle|^2 = \frac{\epsilon}{\omega} \sum_{mi} |D_{mi}|^2 \tag{7.26}$$

For some of the low-lying collective states, in particular the quadrupole and octupole vibrational states, $\epsilon/\omega \approx 2$, which means a very considerable enhancement of the sum rule due to ground-state correlations. (Equation (7.26) also follows directly from conservation of the energy-weighted sum rule.)

7.7. The validity of the RPA

The first major approximation of the RPA is to restrict the phonon operator to be a single-particle operator. Now as we saw in Chapter 2, the observed anharmonicities of vibrational spectra require a mixing of one- and two-phonon states. In other words, the true excitation operators should be a mixture of one- and two-body operators. The RPA can be generalized to a higher RPA in this way, although the problem of diagonalizing the matrix that results is pretty formidable.

The second major approximation is to use the HF wave function $|\,\rangle$ instead of the correlated wave function $|0\rangle$ in the equation of motion. If the admixtures of excited states in $|\,\rangle$ were all within the harmonic region, this would be no approximation at all. However, since hardly any excited states are really harmonic in practice, we may enquire what difference using $|0\rangle$ would make. Now it can be shown that the double commutator, in the equation of motion, is predominantly a single-particle operator. We have supposed that ground-state matrix elements of single-particle operators are given well in the HF approximation, so let us see if this is true.

The correlated ground state wave function is defined by

$$O_\alpha |0\rangle \equiv 0 \qquad \text{all } \alpha$$

This equation can be solved approximately, and one finds that

$$\langle 0|a_i^\dagger a_i|0\rangle \approx \langle |a_i^\dagger a_i| \rangle - \frac{1}{2}\sum_{\alpha m} |Z_{mi}(\alpha)|^2$$

$$\langle 0|a_m^\dagger a_m|0\rangle \approx \frac{1}{2}\sum_{\alpha i} |Z_{mi}(\alpha)|^2$$

The schematic model indicates that as $\omega/\epsilon \to 0$, Y_{mi} and Z_{mi} become more and more nearly equal. Thus to preserve the normalization they must get larger. This means that ground-state correlations build up as a collective state falls in energy and, in particular, the error of approximating a single-particle matrix element by its HF value becomes large. The RPA breaks down therefore in this adiabatic limit.

7.8. Comparison with experiment

A number of RPA and Tamm-Dancoff calculations have been made. Some of particular interest are due to Gillet et al. [18] for ^{12}C, ^{16}O and ^{40}Ca. The intention was to fit the various excited states of these nuclei

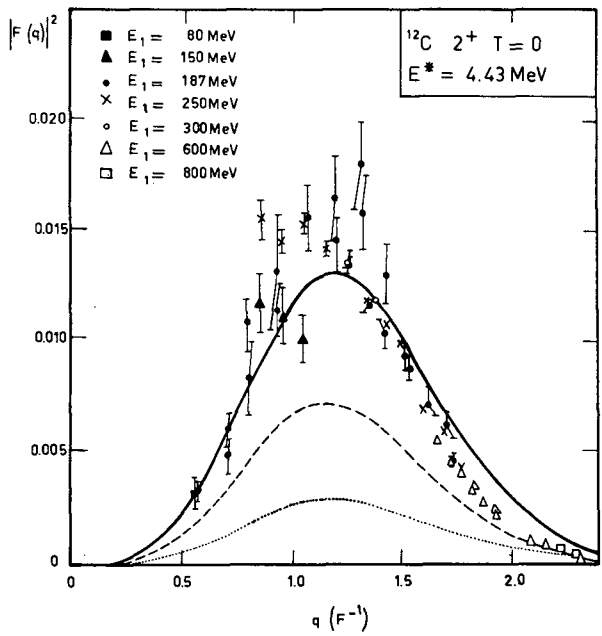

FIG. 17. Form factor of the 2^+ T = 0, 4.43-MeV state of ^{12}C. Dotted line, IP model; dashed line, Tamm-Dancoff approximation; solid line, RPH (Courtesy of American Institute of Physics) [19]

in both Tamm-Dancoff and the RPA to see which would give the better results. Their conclusion was that energy levels could be fitted more or less equally well with either. However, a common interaction could be used for all the nuclei in the RPA, whereas a different interaction was needed for each in Tamm-Dancoff.

Transition strengths, particularly for the low-lying collective states, are generally fitted very well in the RPA and poorly in Tamm-Dancoff. This is demonstrated rather forcefully by the calculations of Gillet and Melkanoff [19] of form factors for inelastic electron scattering, an example of which is shown in Fig. 17, for the 4.43 MeV, $J\pi = 2^+$ of ^{12}C.

8. TIME-DEPENDENT HARTREE-FOCK (TDHF) THEORY

We now present an alternative method of deriving the RPA, namely TDHF theory. This approach is often preferred as being more physical and it has even been claimed that it provides the justification for the 'more dubious' methods of the RPA.[6] This latter claim is completely false for, as we shall see, TDHF theory is completely equivalent to the RPA. However, it is indeed more physical and for this reason has a special merit of its own, in particular because it enables a microscopic derivation of the unified model.

8.1. The TDHF equations

What is the object of looking for a time-dependent wave function? Suppose we have at time $t = 0$ an arbitrary wave function ψ which we can expand in terms of eigenstates

$$\psi = \sum_n a_n \psi_n$$

If we can find the time development of this wave function,

$$\psi(t) = \sum_n a_n \psi_n e^{-iW_n t}$$

then by picking out the different frequency components we determine the corresponding eigenfunctions.

TDHF theory seeks a time-dependent wave function, which is at every instant in time a single-Slater determinant. Using Thouless' theorem we can write such a wave function

$$|\varphi(t)\rangle = e^{-iE_0 t} \exp\left[\sum_{mi} C_{mi}(t)\, a_m^\dagger a_i\right] |\rangle \qquad (8.1)$$

[6] The authors of such claims had not, of course, read section 7.

The coefficients C_{mi} are to be determined by the variational equation

$$\langle \delta \varphi(t) \left| \left(H - i \frac{\partial}{\partial t} \right) \right| \varphi(t) \rangle = O(C^2) \tag{8.2}$$

which is solved to leading order; the C_{mi}'s being taken as infinitesimals. Now

$$\langle \varphi(t) | H | \varphi(t) \rangle = E_0 \left(1 + \sum_{mi} |C_{mi}|^2 \right) + \sum_{mi} \epsilon_{mi} |C_{mi}|^2$$

$$+ \sum_{mnij} V_{mjin} C^*_{mi} C_{nj} + \frac{1}{2} \sum_{mnij} V_{mnij} C^*_{mi} C^*_{nj} + \frac{1}{2} \sum_{mnij} V_{ijmn} C_{mi} C_{nj} \tag{8.3}$$

and

$$\langle \varphi(t) | i \frac{\partial}{\partial t} | \varphi(t) \rangle = E_0 \left(1 + \sum_{mi} |C_{mi}|^2 \right) + \sum_{mi} C^*_{mi} \; i \frac{\partial}{\partial t} C_{mi}$$

Differentiating with respect to C^*_{mi} gives

$$\epsilon_{mi} C_{mi} + \sum_{nj} V_{mjin} C_{nj} + \sum_{nj} V_{mnij} C^*_{nj} = i \frac{\partial}{\partial t} C_{mi} \tag{8.4}$$

Since we are seeking oscillating solutions, let us put

$$C_{mi} \propto Y_{mi} e^{-i\omega t} + Z^*_{mi} e^{i\omega t} \tag{8.5}$$

Equating positive and negative frequency components, we get

$$\begin{aligned} \epsilon_{mi} Y_{mi} + \sum_{nj} V_{mjin} Y_{nj} + \sum_{nj} V_{mnij} Z_{mi} &= \omega Y_{mi} \\ \epsilon_{mi} Z_{mi} + \sum_{nj} V_{inmj} Z_{nj} + \sum_{nj} V_{ijmn} Y_{nj} &= -\omega Z_{mi} \end{aligned} \tag{8.6}$$

These are the equations of the RPA. In a way this is very nice, because it appears to be a natural extension of the stationary HF picture; it allows a self-consistent oscillation of the potential with the particles. However, there are problems ahead, concerned mainly with answering the question "what do these equations mean, in terms of the present time-dependent description?"

8.2. Problems of interpretation

The obvious interpretation, at first sight, is to extract the different frequency components and call these eigenstates. We find

$$|\varphi(t)\rangle = e^{-iE_0 t}\,|\,\rangle + \epsilon\, e^{-i(E_0+\omega)t} \sum_{mi} Y_{mi}\, a_m^\dagger a_i\,|\,\rangle + \epsilon\, e^{-i(E_0-\omega)t} \sum_{mi} Z_{mi}^*\, a_m^\dagger a_i\,|\,\rangle + O(\epsilon^2)$$

where ϵ is the infinitesimal proportionality constant of Eq. (8.5). Taken literally, this means that $|\,\rangle$ is the ground state and there are two states, for each solution, with energies ω above and below the HF energy. Clearly this interpretation will not do, particularly since the two states are not remotely orthogonal.

Another possibility is to adopt the attitude: " we recognize these equations and we know what they mean in terms of the RPA; what more do we need?" This is all right, but it means essentially that we discard TDHF theory as having nothing further to add to the RPA. This would be a pity since it has the potentiality of giving a very physical description of nuclear vibrations.

A third possibility is to go to the physical extreme and forget all about the structure of the wave function $|\varphi(t)\rangle$. The corresponding density distribution $\rho(t)$ is oscillating harmonically. Let us go to the classical limit of finite amplitude of oscillation. We know the frequency and can calculate the emission of radiation. Then extrapolating from our knowledge of the harmonic oscillator, we can deduce the energy spacing (which is just the frequency) and the transition strength of the low energy eigenstates. This is known as a semi-classical treatment. It leads to the same results as the RPA. However, it is not a very tenable interpretation for several reasons. In particular because TDHF theory is only valid for small amplitudes. If the amplitude is even as large as the RMS amplitude in just the first excited state, the method breaks down. Thus it is dubious to extrapolate the results to the limit of large oscillator quantum numbers. Again, harmonic states of large oscillator quanta do not exist in practice for any modes, let alone the non-collective modes.

However, this last approach does seem to have some promise and so we shall develop it properly in terms of the classical correspondence principle for a harmonic oscillator. As we shall see, there is no necessity to go to finite amplitudes or to large oscillator quantum numbers to get classical behaviour. Neither is it necessary to make any semi-classical approximation; we shall work always in the language of quantum mechanics.

8.3. Normal co-ordinates for a quantum system

Consider the harmonic oscillator Hamiltonian

$$H = \frac{1}{2\mathscr{B}}\, p^2 + \frac{\mathscr{C}}{2}\, q^2 \qquad (8.7)$$

The classical solution is

$$q = \epsilon \cos\omega t, \qquad p = -\omega \mathscr{B} \epsilon \sin\omega t, \qquad \text{where } \omega = \sqrt{\mathscr{C}/\mathscr{B}}$$
$$E = \frac{1}{2}\epsilon^2 \omega^2 \mathscr{B} \tag{8.8}$$

In quantum mechanics, p and q are interpreted as operators $\hat{p}$ and $\hat{q}$, with commutators

$$[\hat{q}, \hat{p}] = i, \qquad (\hbar = 1) \tag{8.9}$$

The harmonic oscillator problem is solved by defining phonon operators

$$O^\dagger = \sqrt{\frac{\omega\mathscr{B}}{2}}\left(\hat{q} - \frac{i}{\omega\mathscr{B}}\hat{p}\right)$$
$$O = \sqrt{\frac{\omega\mathscr{B}}{2}}\left(\hat{q} + \frac{i}{\omega\mathscr{B}}\hat{p}\right) \tag{8.10}$$

with commutators

$$[O^\dagger, O] = 1 \tag{8.11}$$

from which one can generate a set of eigenstates.

Now according to the correspondence principle it is always possible to regain the classical equations of motion from quantum mechanics, provided one replaces each classical variable by the expectation value of the corresponding quantal operator.

Consider the stationary state $|n\rangle$, and let its q-variable be displaced a distance ϵ at time t = 0,

$$|\psi_n(t=0)\rangle = \exp(-i\epsilon\hat{p})|n\rangle$$
$$= \exp\left[\epsilon\sqrt{\frac{\omega\mathscr{B}}{2}}(O^\dagger - O)\right]|n\rangle \tag{8.12}$$

substituting with Eq. (8.10). The time development of this wave function follows from the Heisenberg equation of motion

$$[H, O^\dagger(t)] = i\frac{\partial}{\partial t}O^\dagger(t) = \omega O^\dagger(t)$$

which has solution

$$O^\dagger(t) = O^\dagger e^{-i\omega t}$$

Thus

$$|\psi_n(t)\rangle = e^{-iW_n t}\exp\left[\epsilon\sqrt{\frac{\omega\mathscr{B}}{2}}(O^\dagger e^{-i\omega t} - Oe^{i\omega t})\right]|n\rangle \tag{8.13}$$

This wave function has all the required classical properties

$$\langle \hat{q} \rangle = \epsilon \cos \omega t, \qquad \langle \hat{p} \rangle = -\omega \mathscr{B} \epsilon \sin \omega t \tag{8.14}$$

$$\langle H \rangle = W_n + \tfrac{1}{2} \epsilon^2 \omega^2 \mathscr{B}$$

For the pure harmonic oscillator considered here there is no limit to the amplitude ϵ. In practice most systems become anharmonic for large amplitudes. We will now show that for infinitesimal amplitude any Hamiltonian has the classical correspondence properties of a harmonic oscillator.

The important point is that, to leading order in ϵ, the Eqs. (8.14) only involve in their derivation the stationary states $|n\rangle$ and $|n \pm 1\rangle$. They follow therefore, provided only that $|n\rangle$ is within the harmonic region. But if $|n\rangle = |0\rangle$, this condition is satisfied trivially for any Hamiltonian.

Thus for any excited state $|\alpha\rangle$ of a system governed by any Hamiltonian, it is possible to define the normal co-ordinates

$$\hat{q}_\alpha = \frac{1}{\sqrt{2\omega_\alpha \mathscr{B}_\alpha}} (O_\alpha^\dagger + O_\alpha)$$

$$\hat{p}_\alpha = i \sqrt{\frac{\omega_\alpha \mathscr{B}_\alpha}{2}} (O_\alpha^\dagger - O_\alpha) \tag{8.15}$$

and to generate a time-dependent wave function that describes small oscillations in these co-ordinates. It is meaningful, therefore, to describe them as normal co-ordinates and the corresponding oscillations as normal modes. They should perhaps be described as pseudo co-ordinates, since, just like the excitation operators $O^\dagger$, O, they only have the proper commutators when operating on the ground state, or any state within the harmonic region. Thus

$$[\hat{q}, \hat{p}] |0\rangle = i|0\rangle \tag{8.16}$$

8.4. Time-dependent Hartree-Fock theory

From the development of the last section, we see that, to leading order in ϵ,

$$|\psi_0(t)\rangle = e^{-iW_0 t} \exp\left[\epsilon \sqrt{\frac{\omega \mathscr{B}}{2}} (O^\dagger e^{-i\omega t} - O e^{i\omega t})\right] |0\rangle \tag{8.17}$$

is a good time-dependent wave function. This suggests the use of a variational equation

$$\langle \delta\psi_0(t) | \left(H - i \frac{\partial}{\partial t}\right) | \psi_0(t) \rangle = 0$$

to determine the excitation operators. Expanding, we get

$$\langle 0|R\left[1+\epsilon\sqrt{\frac{\omega\mathscr{B}}{2}}\,(Oe^{i\omega t}-O^{\dagger}e^{-i\omega t})\right]e^{iW_0t}\left(H-i\frac{\partial}{\partial t}\right)e^{-iW_0t}$$

$$\times\left[1+\epsilon\sqrt{\frac{\omega\mathscr{B}}{2}}\,(O^{\dagger}e^{-i\omega t}-Oe^{i\omega t})\right]|0\rangle=O(\epsilon^2),\qquad \text{all } R$$

or

$$\langle 0|R\left[\left(H-i\frac{\partial}{\partial t}\right),\,(O^{\dagger}e^{-i\omega t}-Oe^{i\omega t})\right]|0\rangle=0$$

Separating the positive and negative frequency components, we have

$$\left.\begin{aligned}\langle 0|R([H,\,O^{\dagger}]-\omega O^{\dagger})|0\rangle&=0\\ \langle 0|R^{\dagger}([H,\,O]+\omega O)|0\rangle&=0\end{aligned}\right\}\quad \text{all } R$$

which must be simultaneously satisfied. These can be put into the single equation

$$\langle 0|[R,\,([H,\,O^{\dagger}]-\omega O^{\dagger})]|0\rangle=0 \tag{8.18}$$

which is just the equation of motion on which the RPA was based.

Suppose now we make the RPA approximations to solve Eq. (8.18), i.e. give $O^{\dagger}$ the particle-hole form

$$O^{\dagger}=\sum_{mi}(Y_{mi}a_m^{\dagger}a_i-Z_{mi}a_i^{\dagger}a_m) \tag{8.19}$$

and substitute $|\ \rangle$ for $|0\rangle$. Clearly we get again the RPA Eqs. (7.9) or (8.6) The wave function becomes

$$|\psi_0(t)\rangle\rightarrow|\chi(t)\rangle=e^{-iE_0t}\ \exp\left[\epsilon\sqrt{\frac{\omega\mathscr{B}}{2}}\,(O^{\dagger}e^{-i\omega t}-Oe^{i\omega t})\right]|\ \rangle \tag{8.20}$$

which can also be written

$$|\chi(t)\rangle=e^{-iE_0t}\ \exp\left[\sum_{mi}(C_{mi}(t)a_m^{\dagger}a_i-C_{mi}^{*}(t)a_i^{\dagger}a_m)\right]|\ \rangle$$

Now since

$$a_i^{\dagger}a_m|\ \rangle\equiv 0$$

$|\chi(t)\rangle$ is essentially the TDHF wave-function $|\varphi(t)\rangle$. In fact

$$|\varphi(t)\rangle=\left(1+\frac{1}{2}\sum_{mi}|C_{mi}(t)|^2\right)|\chi(t)\rangle+O(\epsilon^3) \tag{8.21}$$

The difference is only one of normalization. However, the normalization factor is time dependent and one must be careful. Fortunately, it contributes nothing to the variational equation. Thus we see that the TDHF method must give the RPA equations with exactly the same meaning, and involving exactly the same approximations.

But what happens to all the classical correspondence properties when the RPA approximations are introduced? The fact that $|\ \rangle$ is now a mixture of eigenstates makes no difference to the oscillation of the q and p co-ordinates (provided $|\ \rangle$ lies within the harmonic sub-space);

$$\langle \varphi(t)|\hat{q}|\varphi(t)\rangle = \epsilon \cos \omega t, \quad \langle \varphi(t)|\hat{p}|\varphi(t)\rangle = -\omega \mathscr{B} \epsilon \sin \omega t \qquad (8.22)$$

However, it could make a difference to the energy expectation. Now if all components of $|\ \rangle$ are within the harmonic region of the spectrum, the diagonal contributions to the energy just add to give the classical increment. However, off-diagonal contributions may also occur, but since different eigenfunctions can only be coupled by an unequal number of excited state creation and destruction operators, such elements must be time dependent with zero time average. Up to second order, the time-dependent part of the energy increment $\Delta E(t)$ is

$$\Delta E(t) = \epsilon \sqrt{\frac{\omega \mathscr{B}}{2}} \langle |[H,\ O^\dagger]| \rangle\ e^{-i\omega t} + \text{c.c.}$$

$$- \frac{1}{4} \epsilon^2 \omega \mathscr{B} \langle |[O^\dagger,\ [H,\ O^\dagger]]| \rangle\ e^{-2i\omega t} + \text{c.c.} \qquad (8.23)$$

The first term vanishes identically for $O^\dagger$, a single-particle operator, just because $|\ \rangle$ is the HF wave function (see section 7.1). The second term vanishes under the RPA assumptions that $|\ \rangle$ lies within the harmonic sub-space. For the RPA solutions, $\Delta E(t)$ is readily shown to vanish identically, so that the RPA is at least consistent in this respect. Thus

$$\langle \varphi(t)|H|\varphi(t)\rangle = \left(1 + \sum |C_{mi}(t)|^2\right) E_0 + \frac{1}{2} \epsilon^2 \omega^2 \mathscr{B} + O(\epsilon^3) \qquad (8.24)$$

and all the classical correspondence properties hold.

9. ITERATIVE SOLUTION OF TDHF THEORY

9.1. Introduction

The usual method of solving TDHF theory is to diagonalize the non-hermitian RPA matrix, Eq. (7.10), as it stands, within some limited configuration space. However, there is no reason why the TDHF equations should not be solved in exactly the same way as the static equations. In the static problem we would start by making a guess $u_0^{(1)}(\vec{r})$ for the self-consistent field $u_0(\vec{r})$; for this guess calculate a wave function $\phi_0^{(2)}$, a

density distribution $\rho_0^{(2)}(\vec{r})$, and hence recalculate the field $u_0^{(2)}(\vec{r})$. In other words, we would follow the cycle

$$u_0^{(1)} \rightarrow \phi_0^{(2)} \rightarrow \rho_0^{(2)} \rightarrow u_0^{(2)}$$

and iterate until convergence is obtained, when the self-consistency equation

$$u_0^{(1)}(\vec{r}, \vec{r}') \equiv \int d\vec{r}_1 \, d\vec{r}_1' \, V(\vec{r}\,\vec{r}_1 ; \vec{r}'\,\vec{r}_1') \, \rho_0^{(2)}(\vec{r}_1', \vec{r}_1) = u_0^{(1)}(\vec{r}, \vec{r}') \qquad (9.1)$$

is satisfied.

Let us assume that the static problem has been solved. The time-dependent field u(t) can be expanded

$$u(t) = u_0 + u_1(t)$$

where $u_1(t)$ is the oscillating part of the field of infinitesimal amplitude. We can now attempt the cycle

$$u_1^{(1)}(t) \rightarrow \chi^{(2)}(t) \rightarrow \rho_1^{(2)}(t) \rightarrow u_1^{(2)}(t)$$

and iterate until the self-consistency equation

$$u_1^{(2)}(\vec{r}, \vec{r}'; t) \equiv \int d\vec{r}_1 \, d\vec{r}_1' \, V(\vec{r}\,\vec{r}_1 ; \vec{r}'\,\vec{r}_1') \, \rho_1^{(2)}(\vec{r}_1', \vec{r}_1; t) = u_1^{(1)}(\vec{r}, \vec{r}'; t) \qquad (9.2)$$

is satisfied. However, while we can guess the mode of oscillation of the field, we must not guess its frequency of oscillation. This is something that is quantized by the self-consistency equation, which of course is only achieved after many iterations. An intermediate self-consistency equation will therefore be required to quantize the frequency for each iteration.

9.2. The TDHF dispersion equations

The time-dependent wave function $|\chi(t)\rangle$, of Eq. (8.2), can be written

$$\begin{aligned} |\chi(t)\rangle &= e^{-iE_0 t} \exp\left[\epsilon \sqrt{\frac{\omega\mathscr{B}}{2}} \left(O^\dagger e^{-i\omega t} - O e^{i\omega t}\right)\right] |\rangle \\ &= e^{-iE_0 t} \exp\left[-i(\alpha \hat{p} + \omega\mathscr{B}\beta\hat{q})\right] |\rangle \end{aligned} \qquad (9.3)$$

where

$$\begin{aligned} \alpha &\equiv \langle \chi(t) | \hat{q} | \chi(t) \rangle = \epsilon \cos \omega t \\ \beta &\equiv -\frac{1}{\omega\mathscr{B}} \langle \chi(t) | \hat{p} | \chi(t) \rangle = \epsilon \sin \omega t \end{aligned} \qquad (9.4)$$

Thus it follows that the time-dependence of the density is contained in the parameters α, β;

$$\rho(t) = \rho(\alpha, \beta)$$

Now since α, β are infinitesimals, of amplitude ϵ, we can expand

$$\rho(\alpha, \beta) = \rho_0 + \alpha \left.\frac{\partial \rho}{\partial \alpha}\right|_{\alpha=\beta=0} + \beta \left.\frac{\partial \rho}{\partial \beta}\right|_{\alpha=\beta=0} + \ldots \tag{9.5}$$

Similarly the field

$$u(\vec{r}, \vec{r}'; t) = \int\int d\vec{r}_1 \, d\vec{r}_1' \, V(\vec{r}\,\vec{r}_1; \; \vec{r}'\,\vec{r}_1') \, \rho(\vec{r}_1', \vec{r}_1; t) \tag{9.6}$$

can be expanded in the same manner

$$u(\alpha, \beta) = u_0 + \alpha \left.\frac{\partial u}{\partial \alpha}\right|_{\alpha=\beta=0} + \beta \left.\frac{\partial u}{\partial \beta}\right|_{\alpha=\beta=0} + \ldots \tag{9.7}$$

where ρ_0 and u_0 are the static HF density and field respectively.

Suppose now that we have some guess $\partial u^{(1)}/\partial\alpha$ for $\partial u/\partial\alpha$, and $\partial u^{(1)}/\partial\beta$ for $\partial u/\partial\beta$, then, since α and β are infinitesimals, we can solve for $|\chi^{(2)}(t)\rangle$ in first order perturbation theory, keeping the frequency as an unknown parameter. Let us write $|\chi^{(2)}(t)\rangle$ in particle-hole form, using Eqs. (8.1) and (8.21):

$$|\chi^{(2)}(t)\rangle = e^{-iE_0 t}\left[1 - \frac{1}{2}\sum_{mi}|C_{mi}(t)|^2 + \sum_{mi} C_{mi}(t) a_m^\dagger a_i + \ldots\right]|\rangle \tag{9.8}$$

In first order perturbation theory,

$$C_{mi}(t) = \frac{\epsilon}{2}\langle m\left|\frac{\partial u^{(1)}}{\partial \alpha}\right|i\rangle\left[\frac{e^{-i\omega t}}{\omega - \epsilon_{mi}} - \frac{e^{i\omega t}}{\omega + \epsilon_{mi}}\right]$$

$$+ \frac{i\epsilon}{2}\langle m\left|\frac{\partial u^{(1)}}{\partial \beta}\right|i\rangle\left[\frac{e^{-i\omega t}}{\omega - \epsilon_{mi}} + \frac{e^{i\omega t}}{\omega + \epsilon_{mi}}\right]$$

$$= \epsilon \cos \omega t \left[\frac{\langle m\left|\frac{\partial u^{(1)}}{\partial \alpha}\right|i\rangle \epsilon_{mi} + \langle m\left|\frac{\partial u^{(1)}}{\partial \beta}\right|i\rangle i\omega}{\omega^2 - \epsilon_{mi}^2}\right]$$

$$+ \epsilon \sin \omega t \left[\frac{\langle m\left|\frac{\partial u^{(1)}}{\partial \beta}\right|i\rangle \epsilon_{mi} - \langle m\left|\frac{\partial u^{(1)}}{\partial \alpha}\right|i\rangle i\omega}{\omega^2 - \epsilon_{mi}^2}\right] \tag{9.9}$$

where $\partial u^{(1)}/\partial\alpha$ and $\partial u^{(1)}/\partial\beta$ are to be evaluated at $\alpha = \beta = 0$ and ϵ_{mi} is the particle-hole energy $(\epsilon_m - \epsilon_i)$.

The next stage of the cycle is to calculate the density $\rho_1^{(2)}(t)$ from the coefficients C_{mi}. Right away we have the density matrix elements

$$\langle m|\rho_1^{(2)}(t)|i\rangle = \langle \chi^{(2)}(t)|a_i^\dagger a_m|\chi^{(2)}(t)\rangle = C_{mi}(t) \tag{9.10}$$

and hence from Eq. (9.9)

$$\begin{aligned}\left\langle m\left|\frac{\partial\rho^{(2)}}{\partial\alpha}\right|i\right\rangle &= \frac{\left\langle m\left|\frac{\partial u^{(1)}}{\partial\alpha}\right|i\right\rangle \epsilon_{mi} + \left\langle m\left|\frac{\partial u^{(1)}}{\partial\beta}\right|i\right\rangle i\omega}{\omega^2 - \epsilon_{mi}^2} \\ \left\langle m\left|\frac{\partial\rho^{(2)}}{\partial\beta}\right|i\right\rangle &= \frac{\left\langle m\left|\frac{\partial u^{(1)}}{\partial\beta}\right|i\right\rangle \epsilon_{mi} - \left\langle m\left|\frac{\partial u^{(1)}}{\partial\alpha}\right|i\right\rangle i\omega}{\omega^2 - \epsilon_{mi}^2}\end{aligned} \tag{9.11}$$

From the matrix elements we can construct the density

$$\begin{aligned}\rho_1^{(2)}(\vec{r},\vec{r}';t) &\equiv \langle\vec{r}|\rho_1^{(2)}(t)|\vec{r}'\rangle \\ &= \sum_{mi}\left[\langle\vec{r}|m\rangle\langle m|\rho_1^{(2)}(t)|i\rangle\langle i|\vec{r}'\rangle + \langle\vec{r}|i\rangle\langle i|\rho_1^{(2)}(t)|m\rangle\langle m|\vec{r}'\rangle\right] \\ &= \sum_{mi}\left[C_{mi}(t)\,\varphi_m(\vec{r})\,\varphi_i^*(\vec{r}') + C_{mi}^*(t)\,\varphi_i(\vec{r})\,\varphi_m^*(\vec{r}')\right]\end{aligned} \tag{9.12}$$

Integrating over the two-body interaction, according to Eq. (9.6), we obtain the second approximation $u_1^{(2)}(t)$ to the field $u_1(t)$. Thus we can iterate the process until it converges, provided we have some means of quantizing the frequency ω at each successive stage. For this purpose we need some intermediate self-consistency condition.

The full self-consistency condition

$$\frac{\partial u^{(2)}}{\partial\alpha} = \frac{\partial u^{(1)}}{\partial\alpha}\,, \qquad \frac{\partial u^{(2)}}{\partial\beta} = \frac{\partial u^{(1)}}{\partial\beta}$$

being an equality of two functions over all space, can only be achieved after many iterations. But merely to quantize the frequency we can manage with a far less stringent condition; for example we can require the numerical equality[7]

$$\begin{aligned}\int\frac{\partial\rho^{(1)}}{\partial\alpha}\,\frac{\partial u^{(2)}}{\partial\alpha} &= \int\frac{\partial\rho^{(1)}}{\partial\alpha}\,\frac{\partial u^{(1)}}{\partial\alpha}\quad\left(\equiv\iint d\vec{r}\,d\vec{r}'\,\frac{\partial\rho^{(1)}}{\partial\alpha}(\vec{r},\vec{r}')\,\frac{\partial u^{(1)}}{\partial\alpha}(\vec{r}',\vec{r})\right) \\ \int\frac{\partial\rho^{(1)}}{\partial\beta}\,\frac{\partial u^{(2)}}{\partial\beta} &= \int\frac{\partial\rho^{(1)}}{\partial\beta}\,\frac{\partial u^{(1)}}{\partial\beta}\end{aligned} \tag{9.13}$$

[7] In the limit that

$$\frac{\partial u^{(1)}}{\partial\alpha} = \frac{\partial u}{\partial\beta} \qquad \frac{\partial u^{(1)}}{\partial\alpha} = \frac{\partial u}{\partial\beta}$$

(Eqs. (9.13) should lead to exact frequencies ω, regardless of $\partial\rho^{(1)}/\partial\alpha$ and $\partial\rho^{(1)}/\partial\beta$. This is important because we expect that our guesses $\partial u^{(1)}/\partial\alpha$ and $\partial u^{(1)}/\partial\beta$ for the field will be considerably more realistic than the corresponding guesses $\partial\rho^{(1)}/\partial\alpha$ and $\partial\rho^{(1)}/\partial\beta$ for the density.

Since we calculate $\partial\rho^{(2)}/\partial\alpha$ rather than $\partial u^{(2)}/\partial\alpha$ it is convenient to make use of the identities

$$\mathcal{I}r\left(\frac{\partial\rho^{(1)}}{\partial\alpha}\,\frac{\partial u^{(2)}}{\partial\alpha}\right) = \mathcal{I}r\left(\frac{\partial\rho^{(1)}}{\partial\alpha}\,V\,\frac{\partial\rho^{(2)}}{\partial\alpha}\right) = \mathcal{I}r\left(\frac{\partial u^{(1)}}{\partial\alpha}\,\frac{\partial\rho^{(2)}}{\partial\alpha}\right)$$

$$\mathcal{I}r\left(\frac{\partial\rho^{(1)}}{\partial\beta}\,\frac{\partial u^{(2)}}{\partial\beta}\right) = \mathcal{I}r\left(\frac{\partial\rho^{(1)}}{\partial\beta}\,V\,\frac{\partial\rho^{(2)}}{\partial\beta}\right) = \mathcal{I}r\left(\frac{\partial u^{(1)}}{\partial\beta}\,\frac{\partial\rho^{(2)}}{\partial\beta}\right)$$

Thus we take as the intermediate self-consistency equations

$$\begin{aligned}\mathcal{I}r\left(\frac{\partial u^{(1)}}{\partial\alpha}\,\frac{\partial\rho^{(2)}}{\partial\alpha}\right) &= \int\frac{\partial\rho^{(1)}}{\partial\alpha}\,\frac{\partial u^{(1)}}{\partial\alpha}\\ \mathcal{I}r\left(\frac{\partial u^{(1)}}{\partial\beta}\,\frac{\partial\rho^{(2)}}{\partial\beta}\right) &= \int\frac{\partial\rho^{(1)}}{\partial\beta}\,\frac{\partial u^{(1)}}{\partial\beta}\end{aligned} \qquad (9.14)$$

Inserting the matrix elements of $\partial\rho^{(2)}/\partial\alpha$ and $\partial\rho^{(2)}/\partial\beta$ from Eq. (9.11) into the trace, we finally obtain

$$\sum_{mi}\left\langle i\left|\frac{\partial u^{(1)}}{\partial\alpha}\right|m\right\rangle\left\{\frac{\left\langle m\left|\frac{\partial u^{(1)}}{\partial\alpha}\right|i\right\rangle\epsilon_{mi} + \left\langle m\left|\frac{\partial u^{(1)}}{\partial\beta}\right|i\right\rangle i\omega}{\omega^2-\epsilon_{mi}^2}\right\}+\text{c.c.} = \int\frac{\partial\rho^{(1)}}{\partial\alpha}\,\frac{\partial u^{(1)}}{\partial\alpha} \qquad (9.15)$$

$$\sum_{mi}\left\langle i\left|\frac{\partial u^{(1)}}{\partial\beta}\right|m\right\rangle\left\{\frac{\left\langle m\left|\frac{\partial u^{(1)}}{\partial\beta}\right|i\right\rangle\epsilon_{mi} - \left\langle m\left|\frac{\partial u^{(1)}}{\partial\alpha}\right|i\right\rangle i\omega}{\omega^2-\epsilon_{mi}^2}\right\}+\text{c.c.} = \int\frac{\partial\rho^{(1)}}{\partial\beta}\,\frac{\partial u^{(1)}}{\partial\beta}$$

This is a pair of coupled dispersion equations in ω, which can be solved for any guess $\partial u^{(1)}/\partial\alpha$ and $\partial u^{(1)}/\partial\beta$. The number of solutions will be equal to the number of particle-hole configurations included in the calculation. In iterating, therefore, one must be careful to select consistently the solution corresponding to the same normal mode at each stage.

9.3. The mass parameters

The mass parameter $\mathcal{B}$, associated with a particular normal mode, is given in the TDHF approximation by the energy increment

$$\langle\chi(t)|H|\chi(t)\rangle \equiv \left\langle\chi(t)\left|i\frac{\partial}{\partial t}\right|\chi(t)\right\rangle = E_0 + \tfrac{1}{2}\epsilon^2\omega^2\mathcal{B} \qquad (9.16)$$

which can be evaluated after convergence is achieved. From Eq. (9.8) for $|\chi(t)\rangle$

$$\langle \chi(t) \left| i \frac{\partial}{\partial t} \right| \chi(t) \rangle = E_0 + \sum_{mi} C^*_{mi}\, i \frac{\partial C_{mi}}{\partial t} - \frac{1}{2} \sum_{mi} i \frac{\partial}{\partial t} |C_{mi}|^2$$

$$= E_0 + \frac{1}{2} \sum_{mi} \left[C^*_{mi}\, i \frac{\partial C_{mi}}{\partial t} - i \frac{\partial C^*_{mi}}{\partial t} C_{mi} \right] \tag{9.17}$$

Inserting the expressions for C_{mi} from Eq. (9.9) we obtain

$$\mathscr{B} = \frac{1}{\omega} \sum_{mi} \frac{\left(\langle m \left| \frac{\partial u}{\partial \alpha} \right| i \rangle \omega + \langle m \left| \frac{\partial u}{\partial \beta} \right| i \rangle i\epsilon_{mi} \right) \left(\langle i \left| \frac{\partial u}{\partial \alpha} \right| m \rangle \epsilon_{mi} - \langle i \left| \frac{\partial u}{\partial \beta} \right| m \rangle i\omega \right)}{(\omega^2 - \epsilon^2_{mi})^2}$$

$$+ \text{c.c.} \tag{9.18}$$

10. DERIVATION OF THE UNIFIED MODEL

10.1. The collective model

We have shown that, quite generally, we can define a set of normal co-ordinates $\hat{q}_a$, $\hat{p}_a$ for all excited states $|a\rangle$, and a time-dependent wave function

$$\psi^{(a)}(t) = e^{-iW_0 t} \exp \left[\epsilon \sqrt{\frac{\omega_a \mathscr{B}_a}{2}} \left(O^\dagger_a e^{-i\omega_a t} - O_a e^{-i\omega_a t} \right) \right] |0\rangle \tag{10.1}$$

describing small amplitude harmonic oscillations in these co-ordinates,

$$\langle \psi^{(a)}(t) | \hat{q}_a | \psi^{(a)}(t) \rangle \equiv \alpha = \epsilon \cos \omega_a t$$

$$- \frac{1}{\omega_a \mathscr{B}_a} \langle \psi^{(a)}(t) | \hat{p}_a | \psi^{(a)}(t) \rangle \equiv \beta = \epsilon \sin \omega_a t \tag{10.2}$$

with energy expectation

$$\langle \psi^{(a)}(t) | H | \psi^{(a)}(t) \rangle = W_0 + \tfrac{1}{2} \epsilon^2 \omega_a^2 \mathscr{B}_a$$

$$= W_0 + \tfrac{1}{2} \mathscr{B}_a \dot{\alpha}^2 + \tfrac{1}{2} \mathscr{C}_a \alpha^2 \tag{10.3}$$

Now it is clear that, within the harmonic region of Hilbert space, H can be identified with

$$H_{vib} = W_0 + \sum_a \omega_a O^\dagger_a O_a$$

$$= W_0 - \frac{1}{2} \sum_a \omega_a + \sum_a \left\{ \frac{1}{2 \mathscr{B}_a} \hat{p}^2_a + \frac{1}{2} \mathscr{C}_a \hat{q}^2_a \right\} \tag{10.4}$$

since this Hamiltonian gives correct eigenstates and excitation energies within this region. This gives meaning to the collective model approach, at least for first excited states, even for modes which are not in the least harmonic.

However, to be useful the collective model must specify the normal modes. The guess made for the low-lying collective states is, by analogy with the oscillations of a liquid drop, a pure volume-conserving oscillation. This is a bad guess, as we saw in Chapter 2, because it puts all the collective strength into a single normal mode, whereas we know from experiment that, although one state may contain a large fraction of the strength, it does not contain all of it. But to make a better guess is not easy.

10.2. Collective co-ordinates and collective parameters

The problem with the collective model is that the collective mode is not a normal mode. But since we are interested in the distribution of collective strength, it is convenient to define a collective co-ordinate, even though it is not a normal co-ordinate. One possibility is to define the collective state (which is not an eigenstate) as the state which contains all the multipole strength. Thus if $\hat{\xi}$ is the collective co-ordinate, for a $\lambda, \mu = 0$ mode,

$$\hat{\xi}\,|0\rangle = \sum_{i}^{A} r_i^{\lambda}\, Y_{\lambda 0}\,(\theta_i)\,|0\rangle$$

which can also be written

$$\hat{\xi}\,|0\rangle = \sqrt{\frac{\hbar}{2\omega' \mathscr{B}'}}\,(A^{\dagger} + A)\,|0\rangle$$

such that

$$A\,|0\rangle \equiv 0$$

where ω' and $\mathscr{B}'$ have the dimensions of a frequency and a mass parameter respectively and are included to normalize the 'collective' phonon operators $A^{\dagger}$, A by the pseudo-boson commutators

$$\langle 0|\,A\,A^{\dagger}\,|0\rangle = \langle 0|\,[A,\ A^{\dagger}]\,|0\rangle = 1$$

Let us now expand the collective state in terms of eigenstates

$$A^{\dagger}\,|0\rangle = \sum_{a} b_a\,|a\rangle$$

so that

$$\hat{\xi}\,|0\rangle = \sum_{a} b_a \sqrt{\frac{\hbar}{2\omega' \mathscr{B}'}}\,(O_a^{\dagger} + O_a)\,|0\rangle = \sum_{a} b_a \sqrt{\frac{\omega_a \mathscr{B}_a}{\omega' \mathscr{B}'}}\,\hat{q}_a\,|0\rangle$$

Hence we obtain the transformation between the normal co-ordinates and the collective co-ordinate[8]

$$\hat{\xi} = \sum_a b_a \sqrt{\frac{\omega_a \mathscr{B}_a}{\omega' \mathscr{B}'}}\, \hat{q}_a \equiv \sum_a k_a \hat{q}_a \tag{10.5}$$

Similarly the conjugate momentum co-ordinate $\hat{\xi}$ is expressed

$$\hat{\xi} = \sum_a b_a \sqrt{\frac{\omega' \mathscr{B}'}{\omega_a \mathscr{B}_a}}\, \hat{p}_a \tag{10.6}$$

To span the space, other co-ordinates $\hat{\xi}_2 \ldots \hat{\xi}_\nu \ldots$, $\hat{\xi}_2 \ldots \hat{\xi}_\nu \ldots$ can be defined in any convenient manner.[9] The transformation between this new set of co-ordinates (sometimes referred to generically as collective co-ordinates) and the normal co-ordinates is

$$\hat{\xi}_\nu = \sum_a b_{\nu a} \sqrt{\frac{\omega_a \mathscr{B}_a}{\omega'_\nu \mathscr{B}'_\nu}}\, \hat{q}_a \equiv \sum_a k_{\nu a} \hat{q}_a \tag{10.7}$$

H_{vib} of Eq. (10.4) can be expressed in terms of these collective co-ordinates but, because of the coupling between the different co-ordinates, it becomes rather complicated. It only has the simple decoupled form of Eq. (10.4) when expressed in terms of normal co-ordinates.

For oscillation of the system in a particular normal mode a, described by the wave-function $\psi^{(a)}(t)$ of Eq. (10.1), we can define a collective parameter $\sigma = \sigma(t)$ as the instantaneous mean value of the collective co-ordinate

$$\sigma(t) \equiv \langle \psi^{(a)}(t) | \hat{\xi} | \psi^{(a)}(t) \rangle = k_a \alpha_a = k_a \epsilon \cos \omega_a t \tag{10.8}$$

The energy expectation is

$$\begin{aligned} \langle \psi^{(a)}(t) | H | \psi^{(a)}(t) \rangle &= W_0 + \tfrac{1}{2} \mathscr{B}_a \dot{\alpha}_a^2 + \tfrac{1}{2} \mathscr{C}_a \alpha_a^2 \\ &= W_0 + \tfrac{1}{2} B_a \dot{\sigma}^2 + \tfrac{1}{2} C_a \sigma^2 \end{aligned} \tag{10.9}$$

where B_a and C_a are defined by

$$k_a^2 B_a = \mathscr{B}_a, \qquad k_a^2 C_a = \mathscr{C}_a \tag{10.10}$$

---

[8] Note that for $\hat{\xi}$ to be hermitian the b_n must be real (Eq. (9.5)). This is in fact no restriction since the phase of the wave-function $|a\rangle$ is arbitrary. Note also that, for the transformation to be unitary, we require $\sum_a b_a^2 = 1$, so that $\sum_a k_a^2 \neq 1$.

[9] Note that the above definition of the collective co-ordinate is not at all unique. It is a natural choice, but later we shall find it more useful to choose the collective mode as our guess to a normal mode.

so that

$$\omega_a = \sqrt{\frac{\mathscr{C}_a}{\mathscr{B}_a}} = \sqrt{\frac{C_a}{B_a}} \tag{10.11}$$

Thus the collective parameters B_a and C_a are equally as good as the normal mode parameters $\mathscr{B}_a$ and $\mathscr{C}_a$ for calculating the frequency ω_a. They are even more useful for calculating transition strengths:

$$\langle a | \sum_i r_i^\lambda Y_{\lambda 0}(\theta_i) | 0 \rangle = \langle a | \hat{\xi} | 0 \rangle = k_a \langle a | \hat{q}_a | 0 \rangle$$

$$= k_a \sqrt{\frac{\hbar}{2\omega_a \mathscr{B}_a}}$$

$$= \sqrt{\frac{\hbar}{2\omega_a B_a}} \tag{10.12}$$

10.3. The VPM as a time-dependent shell model

The vibrating potential model (VPM), or unified model approach is to suppose that the vibrating nucleus is describable, at all instants in time, as a system of independent particles moving in an oscillating potential well. This is clearly an approximation to TDHF theory, which represents the best possible description of this kind. The VPM method is to guess the motion of the field corresponding to a normal mode oscillation of the nucleus, and for this guess to derive a dispersion equation for the frequency and a mass parameter. It is, in fact, nothing more than the first iteration of a full TDHF calculation; in other words a time-dependent shell model.[10] Its validity must therefore depend on how good this guess is to the motion of the field. Let us examine therefore what is the best first guess that we can make and whether it can reasonably be expected to give a good result without a second iteration.

From Eq. (9.7) we have the important result that the oscillating field does not have a simple cos ωt time dependence, but also contains powers of sin ωt;

$$u_1(t) = \epsilon \cos \omega t \frac{\partial u}{\partial \alpha} + \epsilon \sin \omega t \frac{\partial u}{\partial \beta} + \ldots \tag{10.13}$$

However, one wonders whether the two first order terms can be united into a single term of the form $\epsilon \cos(\omega t + \delta) \cdot (\partial u / \partial \alpha')$, which would give us one rather than two objects to guess. It appears that, except in the extreme adiabatic limit, this is not generally possible, although one can go a long way in making $\partial u / \partial \beta$ small. What can be done is to make

[10] The relationship of the VPM to TDHF theory is directly equivalent to the relationship between the shell model and static HF theory. In both cases one guesses the field, which is usually taken to be a local potential well, and calculates a wave-function. But no attempt is made to iterate or achieve self-consistency. It is probably more appropriate, therefore, to call the VPM the 'time-dependent shell model'.

$\partial u/\partial\alpha$ positive under time reversal and $\partial u/\partial\beta$ negative.[11] Now if we are considering predominantly S = 0, T = 0 modes, as for example the low-lying 2^+ or 3^- states of even-even nuclei, our first guess will naturally be a purely spatial field. For a spatial field, time reversal is equivalent to complex conjugation which means that $\partial u/\partial\alpha$ must be purely real and $\partial u/\partial\beta$ purely imaginary. The self-consistent field is also hermitian so that

$$\frac{\partial u}{\partial\alpha}(\vec{r}, \vec{r}') = \frac{\partial u^*}{\partial\alpha}(\vec{r}', \vec{r}) = \frac{\partial u}{\partial\alpha}(\vec{r}', \vec{r}) \quad \text{(Real)}$$

$$\frac{\partial u}{\partial\beta}(\vec{r}, \vec{r}') = \frac{\partial u^*}{\partial\beta}(\vec{r}', \vec{r}) = -\frac{\partial u}{\partial\beta}(\vec{r}', \vec{r}) \quad \text{(Imaginary)} \tag{10.14}$$

Whence it follows that the diagonal, or local part of $\partial u/\partial\beta$ must vanish. Now for a local two-body interaction the non-locality of the field is of short range (of the range of the two-body interaction) and comes solely from the exchange terms. We shall therefore neglect $\partial u/\partial\beta$. If we were to neglect exchange completely, as in Hartree rather than HF theory, the field would become local and $\partial u/\partial\beta$ vanish. The neglect of $\partial u/\partial\beta$ is therefore better than the Hartree approximation, since the bulk of the exchange terms are included in $\partial u/\partial\alpha$ which does not vanish in the local limit.

The problem remaining now is what approximation should we make for $\partial u/\partial\alpha$. In deciding this there are two considerations:

(a) Nuclear matter is virtually incompressible. This means that the nucleus exerts a large restoring force against any attempt to compress it. This does not mean that compressional motion cannot occur, but that

---

[11] This is achieved by defining the normal modes in terms of excited states classified according to their time reversal properties rather than their angular momentum properties, i.e. define

$$O^\dagger_{JM+}|0\rangle = \frac{1}{\sqrt{2}}(1+\tau)|JM\rangle$$

$$O^\dagger_{JM-}|0\rangle = \frac{i}{\sqrt{2}}(1-\tau)|JM\rangle$$

where τ is the time reversal operator. With such a classification it follows that

$$\tau|\chi(t)\rangle = \tau e^{-iE_0 t}\exp\left[\epsilon\sqrt{\frac{\omega\mathcal{P}}{2}}(O^\dagger e^{-i\omega t} - Oe^{i\omega t})\right]|\rangle$$

$$= |\chi(-t)\rangle$$

Hence

$$\tau\rho(t) = \rho(-t)$$

and, since the two-body interaction is time reversal invariant,

$$\tau u_1(t) = u_1(-t) = \epsilon\cos\omega t\frac{\partial u}{\partial\alpha} - \epsilon\sin\omega t\frac{\partial u}{\partial\beta}$$

Thus it follows that

$$\tau\frac{\partial u}{\partial\alpha} = \frac{\partial u}{\partial\alpha}, \qquad \tau\frac{\partial u}{\partial\beta} = -\frac{\partial u}{\partial\beta}$$

it will be associated with a large energy increment. Conversely, for a given energy increment the amplitude of compressional motion must be very small and its effect on the field correspondingly small.

(b) As far as calculating a wave-function is concerned, the overall shape of the field, associated with the coherent long-range density oscillations, is likely to be very much more important than details associated with incoherent short-range density fluctuations. This is the impression one gets from shell model calculations, where the deformation field of the Nilsson potential can be of much more significance than, for example, the differences between a harmonic oscillator and a Woods-Saxon potential.

These considerations suggest that, within some sub-space of normal modes, there is one component of each mode which has much more influence on the field than any other. This is the volume-conserving mode, in which the motion of the density has maximum coherence and involves no compressional motion. It is defined as the mode for which the equi-density surfaces all oscillate in phase and enclose volumes independent of deformation. The volume-conserving mode is not a normal mode. It will be appropriate rather to define it as the collection mode according to section 10.2. The VPM approximation is to neglect the effect on the field of all but this collective component of the density motion in any particular normal mode of oscillation of the nucleus.

These remarks can be expressed more precisely. The application of static HF theory (without residual interactions) to excited states implies that no component of the density motion affects the field. This is a bad approximation and, in particular, does not give rise to collective states. In TDHF theory, we admit that the field must reflect the motion of the density and produce a feedback. The magnitude and form of this feedback, for the a'th normal mode, is characterized by $(\omega_a \mathscr{B}_a)^{-\frac{1}{2}} \partial u/\partial \alpha_a$ since $(\omega_a \mathscr{B}_a)^{-\frac{1}{2}}$ is proportional to the RMS amplitude of the motion in, for example, its one-phonon state. Transforming to collective co-ordinates,

$$\frac{1}{\sqrt{\omega_a \mathscr{B}_a}} \frac{\partial u}{\partial \alpha_a} = \frac{1}{\sqrt{\omega_a \mathscr{B}_a}} \left\{ \frac{\partial u}{\partial \sigma} \frac{\partial \sigma}{\partial \alpha_a} + \sum_{\nu \neq 1} \frac{\partial u}{\partial \sigma_\nu} \frac{\partial \sigma_\nu}{\partial \alpha_a} \right\}$$

$$= \frac{1}{\sqrt{\omega_a \mathscr{B}_a}} \left\{ k_a \frac{\partial u}{\partial \sigma} + \sum_{\nu \neq 1} k_{\nu a} \frac{\partial u}{\partial \sigma_\nu} \right\}$$

$$= b_a \frac{1}{\sqrt{\omega' \mathscr{B}'}} \frac{\partial u}{\partial \sigma} + \sum_{\nu \neq 1} b_{\nu a} \frac{1}{\sqrt{\omega'_\nu \mathscr{B}'_\nu}} \frac{\partial u}{\partial \sigma_\nu}$$

The VPM approximation is to neglect the last term on the right, on the grounds that either $\partial u/\partial \sigma_\nu$ has little effect on the wave function, or that its coefficient $(\omega'_\nu \mathscr{B}'_\nu)^{-\frac{1}{2}}$ is small, because this component involves compressional motion, or both. Thus we make the substitution

$$\frac{\partial u}{\partial \alpha_a} \rightarrow k_a \frac{\partial u}{\partial \sigma} \tag{10.15}$$

One might question the validity of this approximation for a normal mode with negligible collective strength when $b_a \to 0$ and the neglected term may well be the larger. However, it is the absolute and not the relative magnitude of terms that is important. In the limit of zero collective strength no term is considered important and the VPM gives the static HF result as expected. Thus the VPM approximation is to admit a feedback via the self-consistent field of just the collective component of the various normal modes of the density. This is not equivalent to guessing the normal mode of the density. To see whether it is a good approximation one must go through the second iteration and see what changes appear. One can nevertheless see immediately why the unified model, as realised in the VPM, is so much superior to the collective model. One also sees why it is possible to consider exactly the same motion of the field for many orthogonal normal modes which can be parametrized in terms of the same collective parameter σ which is not, and is not intended to be, a collective co-ordinate.

Viewing the VPM in this light, as a first approximation to TDHF theory which we fully understand, let us examine the equations that result and their correct interpretation. In particular, let us see how to derive transition probabilities without resorting to semi-classical approximations and without treating the collective parameter σ as a dynamic or a redundant co-ordinate.

10.4. The VPM dispersion equation

For the a'th normal mode, the VPM approximation of not continuing beyond the first iteration is the approximation

$$\frac{\partial u}{\partial \alpha_a} \approx \frac{\partial u^{(1)}}{\partial \alpha_a} \equiv k_a \frac{\partial u}{\partial \sigma}$$
$$\frac{\partial u}{\partial \beta_a} \approx \frac{\partial u^{(1)}}{\partial \beta_a} \equiv 0 \qquad (10.16)$$

In this approximation the coupled TDHF equations (9.15) reduce to a single VPM dispersion equation

$$2 \sum_{mi} \frac{|\langle m|\frac{\partial u}{\partial \sigma}|i\rangle|^2 \epsilon_{mi}}{\epsilon_{mi}^2 - \omega^2} = -\int \frac{\partial \rho}{\partial \sigma} \frac{\partial u}{\partial \sigma} = K \qquad (10.17)$$

The important result is that this equation does not involve the constant k and is therefore the same for all normal modes. Consequently, all solutions of this equation are meaningful, unlike those of the TDHF equations where we must select the particular solution appropriate to the normal mode under consideration.

The parameter σ is a parameter characterizing the instantaneous shape of the nucleus for a volume-conserving deformation. For a harmonic oscillator shell model potential, this could conveniently be taken as the

Nilsson parameter. Generally it can be defined in terms of the deformation parameters $\alpha_{\lambda\mu}$ used in the unified model. For a volume-conserving deformation, equipotential surfaces are given by

$$r_\theta = r\left(1 + \sum_{\lambda\mu} \alpha^*_{\lambda\mu} Y_{\lambda\mu}(\theta)\right) \tag{10.18}$$

to leading order in the deformation parameters $\alpha_{\lambda\mu}$. For a λ-pole mode, we can take

$$\begin{aligned} \sigma &= \frac{1}{\sqrt{2}}(\alpha^*_{\lambda\mu} + \alpha_{\lambda\mu}), && \mu \neq 0 \\ &= \alpha_{\lambda 0}, && \mu = 0 \end{aligned} \tag{10.19}$$

corresponding to modes positive under time reversal. The deformed potential $u_\sigma(r, \theta)$ is related to the undeformed potential by

$$u_\sigma(r_\theta, \theta) = u_0(r)$$

or

$$u_\sigma(r, \theta) = u_0\left(\frac{r}{1 + \frac{\sigma}{\sqrt{2}}(Y_{\lambda\mu}(\theta) + Y^*_{\lambda\mu}(\theta)}\right), \quad \mu \neq 0$$

Thus we obtain

$$\begin{aligned} \left.\frac{\partial u}{\partial \sigma}\right|_{\sigma=0} &= -\frac{\partial u_0}{\partial r} r \frac{Y_{\lambda\mu}(\theta) + Y^*_{\lambda\mu}(\theta)}{\sqrt{2}}, && \mu \neq 0 \\ &= -\frac{\partial u_0}{\partial r} r Y_{\lambda 0}(\theta), && \mu = 0 \end{aligned} \tag{10.20}$$

Similarly $\partial\rho/\partial\sigma$ can be evaluated, giving us all the information required for a solution of Eq. (10.17).

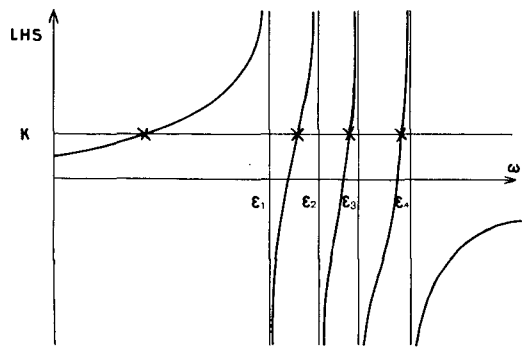

FIG. 18. Graphical solution of the dispersion equation (10.17)

The dispersion Eq. (10.17) is readily solved graphically as illustrated in Fig. 18. It is clear that one solution falls much lower than the rest and, as we shall see, acquires extra collective strength. All of the other solutions remain trapped between the unperturbed energy levels.

10.5. The collective mass parameters

The mass parameter $\mathscr{B}_a$ is given in the TDHF approximation by Eq. (9.18). Making the VPM approximation, Eq. (10.16), this becomes

$$\mathscr{B}_a = 2k_a \sum_{mi} \frac{|\langle m|\frac{\partial u}{\partial \sigma}|i\rangle|^2 \epsilon_{mi}}{(\omega_a^2 - \epsilon_{mi}^2)^2} \tag{10.21}$$

Now we do not know the k_a and so have no direct means of calculating these mass parameters. However, these parameters are in any case of very little practical value. Much more useful are the associated collective parameters defined by Eq. (10.10). Not surprisingly, it is these parameters that emerge naturally in the VPM;

$$B_a = 2 \sum_{mi} \frac{|\langle m|\frac{\partial u}{\partial \sigma}|i\rangle|^2 \epsilon_{mi}}{(\omega_a^2 - \epsilon_{mi}^2)^2} \tag{10.22}$$

The collective strength of a given excited state $|a\rangle$, associated with the a'th normal mode, is given according to Eq. (10.12) by

$$\langle a|\hat{\xi}|0\rangle = \sqrt{\frac{\hbar}{2\omega_a B_a}} \tag{10.23}$$

which we can now evaluate in spite of the fact that the collective co-ordinate $\hat{\xi}$ of the volume-conserving mode has not and will not be defined explicitly. Thus if B_a is small the a'th normal mode has a large collective strength and vice versa. Now it is clear that for the lowest frequency solution, the denominators $(\omega^2 - \epsilon_{mi}^2)^2$, in Eq. (10.22), have on average their maximum value, so that the collective mass parameter B will normally be minimized for this normal mode which will correspondingly have the bulk of the collective strength.

10.6. Excited state wave functions

Since the VPM is a first approximation to TDHF theory and hence of the RPA, we know how excited states are defined. According to Eq. (8.5) we write

$$C_{mi}(a) = N\{Y_{mi}(a)\, e^{-i\omega_a t} + Z_{mi}^*(a)\, e^{i\omega_a t}\}$$

Comparison with Eq. (9.9), and making the VPM approximation, gives

$$Y_{mi}(a) = N \frac{\langle m \left| \frac{\partial u}{\partial \sigma} \right| i \rangle}{\epsilon_{mi} - \omega_a} \quad , \qquad Z_{mi}(a) = N \frac{\langle i \left| \frac{\partial u}{\partial \sigma} \right| M \rangle}{\epsilon_{mi} + \omega_a}$$

The normalization constant N is defined by the condition

$$\sum_{mi} \{ |Y_{mi}(a)|^2 - |Z_{mi}(a)|^2 \} = 1 \tag{10.24}$$

which gives

$$N^2 \sum_{mi} \frac{|\langle m \left| \frac{\partial u}{\partial \sigma} \right| i \rangle| \; 4 \epsilon_{mi} \omega_a}{(\epsilon_{mi}^2 - \omega_a^2)^2} = 2 \omega_a B_a N^2 = 1$$

Thus we have in the VPM approximation

$$Y_{mi}(a) = \frac{1}{\sqrt{2\omega_a B_a}} \frac{\langle m \left| \frac{\partial u}{\partial \sigma} \right| i \rangle}{\epsilon_{mi} - \omega_a} \quad , \quad Z_{mi}(a) = \frac{1}{\sqrt{2\omega_a B_a}} \frac{\langle i \left| \frac{\partial u}{\partial \sigma} \right| m \rangle}{\epsilon_{mi} + \omega_a} \tag{10.25}$$

Excited states are now defined in the usual manner;

$$\left. \begin{aligned} |a\rangle &= O_a^\dagger |0\rangle \\ O_a |0\rangle &\equiv 0 \end{aligned} \right\} \quad \text{all } a \tag{10.26}$$

where

$$O_a^\dagger = \sum_{mi} \{ Y_{mi}(a) a_m^\dagger a_i - Z_{mi}(a) a_i^\dagger a_m \} \tag{10.27}$$

Because of the VPM approximation, it is conceivable that these states will not be orthogonal. Orthogonality is guaranteed, within the approximations of the RPA, by the pseudo-boson commutators

$$\langle | [O_a, O_b^\dagger] | \rangle = \delta_{ab} \tag{10.28}$$

In the VPM approximation

$$\langle | [O_a, O_b^\dagger] | \rangle = \sum_{mi} \{ Y_{mi}^*(a) Y_{mi}(b) - Z_{mi}^*(a) Z_{mi}(b) \}$$

$$= \frac{1}{\sqrt{4\omega_a B_a \omega_b B_b}} \sum_{mi} |\langle m \left| \frac{\partial u}{\partial \sigma} \right| i \rangle|^2 \left\{ \frac{1}{(\epsilon_{mi} - \omega_a)(\epsilon_{mi} - \omega_b)} - \frac{1}{(\epsilon_{mi} + \omega_a)(\epsilon_{mi} + \omega_b)} \right\}$$

$$= \frac{1}{\sqrt{4\omega_a B_a \omega_b B_b}} \frac{1}{(\omega_a - \omega_b)} \sum_{mi} |\langle m \left| \frac{\partial u}{\partial \sigma} \right| i \rangle|^2 \epsilon_{mi} \left\{ \frac{1}{\epsilon_{mi}^2 - \omega_a^2} - \frac{1}{\epsilon_{mi}^2 - \omega_a^2} \right\}$$

Now ω_a and ω_b are both solutions of the dispersion equation (10.17) so that, provided $\omega_a \neq \omega_b$, the right-hand side of this expression vanishes. If a = b then it is normalized to unity by Eq. (10.24). In the case of degenerate solutions it is always possible to orthogonalize the solutions so that Eq. (10.28) is satisfied generally. Thus the VPM wave functions are all orthogonal to within the limitations of the RPA.

It is apparent that the wave functions defined by Eqs. (10.26) and (10.27) will not arise naturally in a phenomenological derivation of the model. However, in practice it is rarely necessary to derive wave functions explicitly, provided we know how to calculate matrix elements. Let us see, therefore, if the phenomenological formulae for matrix elements are confirmed in this microscopic treatment.

10.7. Matrix elements

Matrix elements for a single-particle operator W are given, according to the RPA, by

$$\langle a|W|0\rangle = \sum_{mi} \{Y^*_{mi}(a)\, W_{mi} + Z^*_{mi}(a)\, W_{im}\}$$

$$= \frac{1}{\sqrt{2\omega_a B_a}} \sum_{mi} \left\{ \frac{\langle i|\frac{\partial u}{\partial \sigma}|m\rangle\langle m|W|i\rangle}{\epsilon_{mi} - \omega_a} + \frac{\langle i|W|m\rangle\langle m|\frac{\partial u}{\partial \sigma}|i\rangle}{\epsilon_{mi} + \omega_a} \right. \tag{10.29}$$

The expression reduces to the unified model result in the special case when W is proportional to $\partial u/\partial\sigma$, since

$$\langle a|\frac{\partial u}{\partial \sigma}|0\rangle = \frac{1}{\sqrt{2\omega_a B_a}} \sum_{mi} |\langle m|\frac{\partial u}{\partial \sigma}|i\rangle|^2 \left\{ \frac{1}{\epsilon_{mi} - \omega_a} + \frac{1}{\epsilon_{mi} + \omega_a} \right\}$$

$$= \frac{K}{\sqrt{2\omega_a B_a}} \tag{10.30}$$

This happens, for example, for the quadrupole oscillations of a harmonic oscillator potential; i. e. if

$$u_0(r) = -V_0 + v r^2$$

then from Eq. (10.20)

$$\frac{\partial u}{\partial \sigma} = -\frac{\partial u_0}{\partial r} r Y_{20} = -2v r^2 Y_{20}, \qquad \mu = 0$$

In general this does not happen for any reasonable choice of shell model potential. It is nevertheless possible to derive the unified model expression by making the additional approximation of neglecting all but

the contribution from the collective component to the multipole strength. Making this approximation we obtain

$$\langle \lambda(t) | r^\lambda Y_{\lambda 0} | \lambda(t) \rangle \approx \frac{\lambda+3}{4\pi} \langle | r^\lambda | \rangle \sigma(t) \equiv \frac{\lambda+3}{4\pi} \langle | r^\lambda | \rangle \langle \lambda(t) | \hat{\xi} | \lambda(t) \rangle \tag{10.31}$$

to leading order in the deformation. Hence follows the unified model expression

$$\langle a | r^\lambda Y_{\lambda 0} | 0 \rangle \approx \frac{\lambda+3}{4\pi} \langle | r^\lambda | \rangle \frac{1}{\sqrt{2\omega_a B_a}} \tag{10.32}$$

Since other components of the motion, orthogonal to the collective, may also have some multipole strength, this expression should be a slight underestimate.

10.8. Relationship between the VPM and the schematic model

To simplify the RPA equations it is common to suppose that the anti-symmetrized two-body interaction is separable (section 7.6).

$$V(\vec{r}_1 \vec{r}_2 ; \vec{r}_1' \vec{r}_2') \Rightarrow -\chi \hat{Q}(\vec{r}_1, \vec{r}_1') \hat{Q}(\vec{r}_2, \vec{r}_2') \tag{10.33}$$

For such a separable interaction the RPA equations also reduce to a single dispersion equation

$$2 \sum_{mi} \frac{|\langle m | \hat{Q} | i \rangle|^2 \epsilon_{mi}}{\epsilon_{mi}^2 - \omega^2} = \frac{1}{\chi} \tag{10.34}$$

The similarity between this equation and the VPM equation is remarkable, but is not coincidental. The two approaches are equivalent.

Since TDHF theory and the RPA are equivalent, it is clear that all two-body interactions which generate the same self-consistent field must yield the same RPA solutions. In particular, for some specified normal mode, we can make the substitution

$$V(\vec{r}_1 \vec{r}_2 ; \vec{r}_1' \vec{r}_2') \Rightarrow -\frac{1}{K_\alpha} \frac{\partial u}{\partial \alpha}(\vec{r}_1 \vec{r}_1') \frac{\partial u}{\partial \alpha}(\vec{r}_2 \vec{r}_2') - \frac{1}{K_\beta} \frac{\partial u}{\partial \beta}(\vec{r}_1 \vec{r}_1') \frac{\partial u}{\partial \beta}(\vec{r}_2 \vec{r}_2') \tag{10.35}$$

where

$$K_\alpha = -\int d\vec{r}\, d\vec{r}\,' \frac{\partial \rho}{\partial \alpha}(\vec{r}\,\vec{r}\,') \frac{\partial u}{\partial \alpha}(\vec{r}\,'\vec{r}) \equiv -\int \frac{\partial \rho}{\partial \alpha} \frac{\partial u}{\partial \alpha}$$

Now since $\partial\rho/\partial\alpha$ and $\partial u/\partial\alpha$ are positive under time reversal while $\partial\rho/\partial\beta$ and $\partial u/\partial\beta$ are negative, and since all are hermitian, it follows that

$$\int \frac{\partial \rho}{\partial \alpha} \frac{\partial u}{\partial \beta} = \int \frac{\partial \rho}{\partial \beta} \frac{\partial u}{\partial \alpha} = 0$$

The substitution of Eq. (10.35) will therefore generate the correct field

$$\int V(\vec{r}_1\vec{r}_2;\ \vec{r}_1'\vec{r}_2')\frac{\partial\rho}{\partial\alpha}(\vec{r}_2'\vec{r}_2)\,d\vec{r}_2\,d\vec{r}_2' \Rightarrow -\frac{\partial u}{\partial\alpha}(\vec{r}_1\vec{r}_1')\frac{1}{K_\alpha}\int\frac{\partial u}{\partial\alpha}\frac{\partial\rho}{\partial\alpha}$$

$$= \frac{\partial u}{\partial\alpha}(\vec{r}_1\vec{r}_1') \qquad (10.36)$$

$$\int V(\vec{r}_1\vec{r}_2;\ \vec{r}_1'\vec{r}_2')\frac{\partial\rho}{\partial\beta}(\vec{r}_2'\vec{r}_2)\,d\vec{r}_2\,d\vec{r}_2' \Rightarrow -\frac{\partial u}{\partial\beta}(\vec{r}_1\vec{r}_1')\frac{1}{K_\beta}\int\frac{\partial u}{\partial\beta}\frac{\partial\rho}{\partial\beta}$$

$$= \frac{\partial u}{\partial\beta}(\vec{r}_1\vec{r}_1')$$

Inserting this sum of two separable potentials into the RPA equations, one can also rederive the coupled TDHF dispersion equations (9.15).

Now this interaction must inevitably be different for every normal mode and is therefore of little value. However, if we make the VPM approximation

$$V(\vec{r}_1\vec{r}_2;\ \vec{r}_1'\vec{r}_2') \Rightarrow -\frac{1}{K}\frac{\partial u}{\partial\sigma}(\vec{r}_1\vec{r}_1')\frac{\partial u}{\partial\sigma}(\vec{r}_2\vec{r}_2') \qquad (10.37)$$

we have a single separable interaction, which is the same for a whole class of normal modes. Using this interaction in the RPA gives immediately the VPM dispersion equation (10.17).

The two models are thus equivalent, although the VPM has the advantage of physical argument to support its choice of separable interaction, whereas the schematic model choice is purely one of mathematical convenience. The VPM also specifies the coupling constant.

APPENDIX

THE OCCUPATION NUMBER REPRESENTATION AND SECOND QUANTIZATION

A.1. CREATION AND DESTRUCTION OPERATORS

Suppose we have a complete set of orthonormal single-particle wave functions φ_ν. From these we can construct a set of anti-symmetrized product wave functions, for the A particle system, which form a complete basis for the expansion of any more general wave functions. These A particle basis wave functions are Slater determinants.

Now the determinant is in a sense overdescriptive. It involves putting labels onto the particle co-ordinates, whereas indistinguishable particles cannot, stricly speaking, be labelled. Of course, since we anti-symmetrize, no harm is done. However a more compact description is clearly desirable. Now it is clear that all the information needed to

construct the determinant is given if the single-particle states and their order are specified. Thus we write in occupation number representation

$$|\alpha\ \beta\ \gamma \ldots\rangle = \frac{1}{\sqrt{A}} \begin{vmatrix} \varphi_\alpha(1) & \varphi_\beta(1) & \varphi_\gamma(1) & \cdot & \cdot & \cdot \\ \varphi_\alpha(2) & \varphi_\beta(2) & \varphi_\gamma(2) & \cdot & \cdot & \cdot \\ \cdot & \cdot & \cdot & \cdot & \cdot & \cdot \end{vmatrix} \tag{A.1}$$

In order to manipulate wave functions, evaluate matrix elements, etc., it is necessary to construct an algebra. This is done conveniently in the language of second quantization. First we define the particle creation operator $a_\nu^\dagger$, which creates a particle in the state ν. Thus we equate

$$|\alpha\ \beta\ \gamma \ldots\rangle = a_\alpha^\dagger a_\beta^\dagger a_\gamma^\dagger \ldots |-\rangle \tag{A.2}$$

where $|-\rangle$ is the bare vacuum wave function describing a state of zero particles.

In order that the A particle wave function be anti-symmetric under interchange of particles we must require that

$$a_\alpha^\dagger a_\beta^\dagger a_\gamma^\dagger \ldots |-\rangle = -a_\beta^\dagger a_\alpha^\dagger a_\gamma^\dagger \ldots |-\rangle$$

Furthermore, it is not permitted that two particles should occupy the same state and hence

$$a_\alpha^\dagger a_\alpha^\dagger a_\gamma^\dagger \ldots |-\rangle = 0$$

These two requirements can be simultaneously expressed by the anti-commutation relations

$$\{a_\alpha^\dagger,\ a_\beta^\dagger\} \equiv a_\alpha^\dagger a_\beta^\dagger + a_\beta^\dagger a_\alpha^\dagger = 0 \tag{A.3}$$

If we construct the adjoint equation to (A.2)

$$\langle \alpha\ \ \beta\ \ \gamma \ldots | = \langle -| \ldots a_\gamma a_\beta a_\alpha \tag{A.4}$$

then

$$\langle \alpha\ \ \beta\ \gamma \ldots | \alpha\ \ \beta\ \gamma \ldots \rangle = \langle -| \ldots a_\gamma a_\beta a_\alpha a_\alpha^\dagger a_\beta^\dagger a_\gamma^\dagger \ldots |-\rangle = 1$$

It follows that

$$|-\rangle = a_\alpha a_\alpha^\dagger |-\rangle = a_\beta a_\alpha a_\alpha^\dagger a_\beta^\dagger |-\rangle \quad \text{etc.}$$

and that the hermitian conjugate a_ν of $a_\nu^\dagger$ is an operator which annihilates a particle in the state ν.

We also have

$$a_\beta a_\alpha^\dagger a_\beta^\dagger a_\gamma^\dagger \ldots |-\rangle = -a_\beta a_\beta^\dagger a_\alpha^\dagger a_\gamma^\dagger \ldots |-\rangle = -a_\alpha^\dagger a_\gamma^\dagger \ldots |-\rangle$$
$$= -a_\alpha^\dagger a_\beta a_\beta^\dagger a_\gamma^\dagger \ldots |-\rangle$$

or

$$\{a_\beta, a_\alpha^\dagger\} |\beta\, \gamma \ldots\rangle = 0, \qquad \alpha \neq \beta$$

In this equation the anti-commutator is operating on the most favourable wave function; namely, one with state β occupied and state α unoccupied. Operating on any other wave function, both elements of the anti-commutator must vanish separately. Thus

$$\{a_\beta, a_\alpha\} = 0, \qquad \alpha \neq \beta$$

generally. Now

$$\begin{aligned} a_\alpha a_\alpha^\dagger |\alpha\, \beta\, \gamma \ldots\rangle &= 0 & a_\alpha a_\alpha^\dagger |\beta\, \gamma\, \delta \ldots\rangle &= 1 \\ a_\alpha^\dagger a_\alpha |\alpha\, \beta\, \gamma \ldots\rangle &= 1 & a_\alpha^\dagger a_\alpha |\beta\, \gamma\, \delta \ldots\rangle &= 0 \end{aligned} \tag{A.5}$$

The general anti-commutation relation is therefore

$$\{a_\beta, a_\alpha^\dagger\} = \delta_{\alpha_\beta} \tag{A.6}$$

One can also define operators $a_r^\dagger$, a_r which create and destroy a particle, respectively, at the point r. These operators behave in exactly the same manner as those defined in configuration space. Thus

$$|r\rangle = a_r^\dagger |-\rangle$$
$$\langle r|r'\rangle = \langle -|a_r a_{r'}^\dagger|-\rangle = \delta(r - r')$$
$$\{a_r, a_{r'}^\dagger\} = \delta(r - r')$$

The two sets of operators are related by

$$a_\nu^\dagger = \int d\vec{r}\, \varphi_\nu(\vec{r})\, a_r^\dagger$$

$$a_\nu = \int d\vec{r}\, \varphi_\nu^*(\vec{r})\, a_r$$

A.2. ONE- AND TWO-BODY OPERATORS

We now come to the problem of expressing operators in the language of second quatization. From Eq. (A.5) we have immediately one useful

operator; the operator n_ν which measures the occupancy of the single particle level ν

$$n_\nu = a_\nu^\dagger a_\nu \tag{A.7}$$

The number operator n which measures the total number of particles is therefore

$$n = \sum_\nu a_\nu^\dagger a_\nu \tag{A.8}$$

Consider a general single-particle operator,

$$T = \sum_i^A T(i) \tag{A.9}$$

for example the kinetic energy operator. The expectation of T in some state $|\alpha\,\beta\,\gamma\,\ldots\rangle$ is

$$\langle \alpha\,\beta\,\gamma\,\ldots|T|\alpha\,\beta\,\gamma\,\ldots\rangle = T_{\alpha\alpha} + T_{\beta\beta} + T_{\gamma\gamma} + \ldots$$

The matrix element of T between states differing by the state of only one particle is, for example

$$\langle \alpha\,\beta\,\gamma\,\ldots|T|\alpha\,\beta'\,\gamma\,\ldots\rangle = T_{\beta\beta'}, \qquad \beta \neq \beta'$$

The matrix element between states differing by the state of two or more particles vanishes

$$\langle \alpha\,\beta\,\gamma\,\ldots|T|\alpha'\,\beta'\,\gamma\,\ldots\rangle = 0 \qquad \alpha, \beta \neq \alpha', \beta'$$

It is clear that all these expressions are reproduced by

$$T = \sum_{\nu,\nu'} T_{\nu\nu'} a_\nu^\dagger a_{\nu'} \tag{A.10}$$

Consider a two-particle operator

$$V = \frac{1}{2} \sum_{i,j}^A V(i,j) \tag{A.11}$$

for example the two-body interaction. We define matrix elements of V between anti-symmetrized two-particle states

$$V_{\alpha\beta\alpha'\beta} = \langle \alpha\beta|V|\alpha'\beta'\rangle$$

$$= \iint d\vec{r}\,d\vec{r}'\,\varphi_\alpha^*(\vec{r})\,\varphi_\beta^*(\vec{r}')\,V(r,r')\,\varphi_{\alpha'}(\vec{r})\,\varphi_{\beta'}(\vec{r}') -$$

$$- \iint d\vec{r}\,d\vec{r}'\,\varphi_\alpha^*(\vec{r})\varphi_\beta^*(\vec{r}')\,V(r,r')\,\varphi_{\alpha'}(\vec{r}')\,\varphi_{\beta'}(\vec{r}) \tag{A.12}$$

(Note that this expression is appropriate only to a local interaction but is trivially generalized.)

Since the wave functions are anti-symmetric

$$V_{\alpha\beta\alpha'\beta'} = -V_{\beta\alpha\alpha'\beta'} = -V = V_{\beta\alpha\beta'\alpha'} \tag{A.13}$$

In second quantization, V is expressed

$$V = \frac{1}{4} \sum_{\mu\nu\mu'\nu'} V_{\mu\nu\mu'\nu'}\ a_\nu^\dagger a_\mu^\dagger a_{\mu'} a_{\nu'} \tag{A.14}$$

One can readily ascertain that this expression leads to correct matrix elements in any case of interest; for example

$$\langle \alpha\ \beta\ \gamma\ \delta \ldots | V | \alpha'\ \beta'\ \gamma\ \delta \ldots \rangle$$

$$= \frac{1}{4} \sum_{\mu\nu\mu'\nu'} V_{\mu\nu\mu'\nu'} \quad \langle - | \ldots a_\delta a_\gamma a_\beta a_\alpha a_\nu^\dagger a_\mu^\dagger a_{\mu'} a_{\nu'} a_{\alpha'}^\dagger a_{\beta'}^\dagger a_\gamma^\dagger a_\delta^\dagger \ldots | - \rangle$$

$$= \frac{1}{4} (V_{\beta\alpha\beta'\alpha'} - V_{\beta\alpha\alpha'\beta'} - V_{\alpha\beta\beta'\alpha'} + V_{\alpha\beta\alpha'\beta'})$$

$$= V_{\alpha\beta\alpha'\beta'}$$

which is what we obtain by working with the determinants.

A.3. NORMAL ORDERED PRODUCTS

The normal ordered product, of a set of creation and destruction operators, is the product arranged in the most unfavourable order, with respect to some specified vacuum, multiplied by a factor ± 1 according as the necessary rearrangement requires an even or an odd number of permutations of the operators, respectively. We shall write the normal ordered product of the product of operators ABCD... as $\{ABCD...\}$.

(a) One obvious choice of vacuum is the vacuum of the operators themselves, i.e. the bare vacuum $|-\rangle$. The most unfavourable order is then with all destruction operators on the right and creation operators on the left; e.g.

$$\begin{aligned} \{a_\alpha^\dagger a_\beta\} &= a_\alpha^\dagger a_\beta & \{a_\beta a_\alpha^\dagger\} &= -a_\alpha^\dagger a_\beta \\ \{a_\alpha^\dagger a_\beta^\dagger\} &= a_\alpha^\dagger a_\beta^\dagger = -a_\beta^\dagger a_\alpha^\dagger \\ \{a_\alpha^\dagger a_\beta a_\gamma^\dagger\} &= -a_\alpha^\dagger a_\gamma^\dagger a_\beta = a_\gamma^\dagger a_\alpha^\dagger a_\beta \end{aligned} \tag{A.15}$$

etc.

(b) Another possibility is the HF vacuum $|\rangle$. Throughout this paper we reserve the indices i j k l to label single-particle states occupied

in the HF wave function and m n p q to label unoccupied states (see Fig. 19).

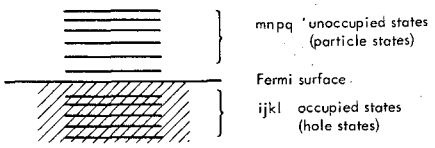

FIG. 19. Labelling of particle and hole states

Thus

$$|\rangle = |ijkl\ldots\rangle$$

and

$$\begin{aligned} a_i^\dagger|\rangle &= 0 \qquad & a_i|\rangle &= |(i)^{-1}\rangle \\ a_m|\rangle &= 0 \qquad & a_m^\dagger|\rangle &= |m\rangle \end{aligned} \tag{A.16}$$

With respect to the HF wave function $|\rangle$ a more natural set of operators might be the quasi-particle operators

$$\begin{aligned} \alpha_m^\dagger &= a_m^\dagger \qquad \text{(creates a particle)} \\ \alpha_i^\dagger &= a_i \qquad \text{(creates a hole)} \end{aligned} \tag{A.17}$$

which have the property

$$\alpha_\nu|\rangle = 0 \qquad \text{all } \nu \tag{A.18}$$

In terms of these quasi-particle operators the normal ordering is as above; destruction operators to the right, creation operators to the left, e.g.

$$\{\alpha_\alpha^\dagger \alpha_\beta \alpha_\gamma^\dagger \alpha_\delta\} = -\alpha_\alpha^\dagger \alpha_\gamma^\dagger \alpha_\beta \alpha_\delta$$

However, it is equally possible to arrange the ordinary particle operators in normal order directly; e.g.

$$\{a_m^\dagger a_i^\dagger a_j a_n\} = \{\alpha_m^\dagger \alpha_i \alpha_j^\dagger \alpha_n\} = -\alpha_m^\dagger \alpha_j^\dagger \alpha_i \alpha_n = -a_m^\dagger a_j a_i^\dagger a_n \tag{A.19}$$

The rule is that the operators must be arranged in the most unfavourable order; any operator which gives zero when operating on the vacuum goes to the right and any operator which does not goes to the left. As a consequence we obtain the significant result that the vacuum expectation of any normal ordered set of operators vanishes

$$\langle\{ABCD\ldots\}\rangle = 0 \tag{A.20}$$

A.4. THE 'WELL-KNOWN' FIELD THEOREM

This theorem is a simple case of a more general theorem known as Wicks' theorem. It states that a set of creation and destruction operators ABCD... can be expressed as a sum of these operators arranged in normal order for all possible contractions.

$$\begin{aligned} ABCD\ldots &= \{ABCD\ldots\} \\ &+ \{\overbrace{A}BCD\ldots\} + \{\overbrace{AB}CD\ldots\} + \ldots + \{A\overbrace{BC}D\ldots\} + \ldots \\ &+ \{\overbrace{A}B\overbrace{C}D\ldots\} + \{\overbrace{A}B\overbrace{CDE}\ldots\} + \ldots + \{\overbrace{A\overbrace{BC}D}\ldots\} + \ldots \\ &+ \ldots \end{aligned} \tag{A.21}$$

A contraction of two operators is defined as the vacuum expectation of these two operators; e.g.

$$\begin{aligned} \{\overbrace{AB}CD\ldots\} &= \langle AB\rangle\{CD\ldots\} \\ \{\overbrace{A\overbrace{BC}D}EF\ldots\} &= -\langle AC\rangle\langle BD\rangle\{EF\ldots\} \end{aligned} \tag{A.22}$$

The theorem is readily proved for two operators. Clearly

$$AB = \{AB\} + C(AB)$$

where C(AB) is a constant depending on whether AB needs rearranging or not, to get it into normal order. Taking the vacuum expectation of both sides of this equation and using Eq. (A.20) gives C(AB) and we obtain

$$AB = \{AB\} + \langle AB\rangle \equiv \{AB\} + \{\overbrace{AB}\} \tag{A.23}$$

The general theorem now follows by induction, from a consideration of

$$\begin{aligned} A\{BCD\ldots\} &= \{ABCD\ldots\} + \{\overbrace{A}BCD\ldots\} + \{\overbrace{AB}CD\ldots\} \\ &\quad + \text{and all possible contractions involving A.} \end{aligned} \tag{A.24}$$

A case of particular interest is the normal ordering of the set of operators ocurring in the two-body interaction:

$$\begin{aligned} a_\nu^\dagger a_\mu^\dagger a_{\mu'} a_{\nu'} &= \{a_\nu^\dagger a_\mu^\dagger a_{\mu'} a_{\nu'}\} \\ &+ \langle a_\nu^\dagger a_{\nu'}\rangle\{a_\mu^\dagger a_{\mu'}\} - \langle a_\nu^\dagger a_{\mu'}\rangle\{a_\mu^\dagger a_{\nu'}\} \\ &+ \langle a_\mu^\dagger a_{\mu'}\rangle\{a_\nu^\dagger a_{\nu'}\} - \langle a_\mu^\dagger a_{\nu'}\rangle\{a_\nu^\dagger a_{\mu'}\} \\ &+ \langle a_\nu^\dagger a_{\nu'}\rangle\langle a_\mu^\dagger a_{\mu'}\rangle - \langle a_\nu^\dagger a_{\mu'}\rangle\langle a_\mu^\dagger a_{\nu'}\rangle \end{aligned} \tag{A.25}$$

Note that the contraction

$$\{\overbrace{a_\nu^\dagger a_\mu^\dagger} a_{\mu'} a_{\nu'}\} \equiv \langle a_\nu^\dagger a_\mu^\dagger\rangle\{a_{\mu'} a_{\nu'}\} \tag{A.26}$$

vanishes. But this is only true if the particular vacuum chosen has a definite particle number, as for example the bare vacuum or the HF vacuum. Later on we shall have cause to introduce more general quasi-particle operators by the transformation

$$\alpha_\nu^\dagger = u_\nu a_\nu^\dagger - v_\nu a_{\bar{\nu}}$$

which do not conserve particle number. The vacuum $|\,\rangle$ of these quasi-particles, defined by

$$\alpha_\nu \,|\,\rangle \equiv 0 \qquad \text{all } \nu$$

does not describe a definite number of physical particles. If we make a normal order expansion of the two-body interaction with respect to this vacuum, contractions of the type of Eq. (A. 26) no longer vanish and must be included.

A. 5. THOULESS' THEOREM

Since the class of anti-symmetrized product wave functions is so important, it is useful to have a simple method of transforming the total wave function under a transformation of the single-particle basis. We now take $|\,\rangle$ to be a general product wave function

$$|\,\rangle = \prod_{i=1}^{A} a_i^\dagger \,|-\rangle \tag{A.27}$$

where i runs over all occupied orbitals.

Thouless' theorem states that any other product wave function $|\,\rangle'$, not actually orthogonal to $|\,\rangle$, can be expressed in unnormalized form

$$|\,\rangle' = \exp\left[\sum_{m=A+1}^{\infty}\sum_{i=1}^{A} C_{mi}\, a_m^\dagger a_i\right]|\,\rangle$$

$$= \left[1 + \sum_{mi} C_{mi} a_m^\dagger a_i + \frac{1}{2}\sum_{mi}\sum_{nj} C_{mi} C_{nj}\, a_m^\dagger a_i a_n^\dagger a_j + \ldots\right]|\,\rangle \tag{A.28}$$

for some particular set of coefficients C_{mi}.

It is apparent that

$$|\,\rangle' = \prod_{i=1}^{A} b_i^\dagger |-\rangle \tag{A.29}$$

where

$$b_i^\dagger = a_i^\dagger + \sum_m C_{mi} a_m^\dagger \tag{A.30}$$

One can also check that

$$b_m |\rangle' = b_i^\dagger |\rangle' = 0$$

where

$$\begin{aligned} b_m &= a_m - \sum_i C_{mi}\, a_i \\ b_m^\dagger &= a_m^\dagger - \sum_i C_{mi}^*\, a_i^\dagger \end{aligned} \tag{A.31}$$

Note that this transformation does not preserve the normalization either of the single-particle wave functions or of $|\rangle'$. We always have the normalization

$$\langle |\rangle' = 1 \tag{A.32}$$

and hence the proviso that $|\rangle'$ must not actually be orthogonal to $|\rangle$.

A.6. GENERALIZED THOULESS' THEOREM

If Thouless' theorem is expressed in terms of the quasi-particle operators, with respect to which $|\rangle$ is the vacuum

$$\alpha_\nu |\rangle = 0 \qquad \text{all } \nu$$

then it takes a much more general form. The vacuum $|\rangle'$ of any other quasi-particles, which is not actually orthogonal to $|\rangle$, can be expressed.

$$\begin{aligned} |\rangle' &= \exp\left[\frac{1}{2}\sum_{\mu\nu} C_{\mu\nu}\, \alpha_\mu^\dagger\, \alpha_\nu^\dagger\right]|\rangle \\ &= \left[1 + \frac{1}{2}\sum_{\mu\nu} C_{\mu\nu}\, \alpha_\mu^\dagger\, \alpha_\nu^\dagger + \frac{1}{8}\sum_{\mu\nu}\sum_{\mu'\nu'} C_{\mu\nu}\, C_{\mu'\nu'}\, \alpha_\mu^\dagger\, \alpha_\nu^\dagger\, \alpha_{\mu'}^\dagger\, \alpha_{\nu'}^\dagger + \ldots\right]|\rangle \end{aligned} \tag{A.33}$$

where we take $C_{\mu\nu}$ to be anti-symmetrized

$$C_{\mu\nu} = -C_{\nu\mu} \tag{A.34}$$

It is readily observed that $|\rangle'$ is the vacuum of the operators

$$\begin{aligned} \beta_\mu^\dagger &= \alpha_\mu^\dagger - \sum_\nu C_{\mu\nu}^*\, \alpha_\nu \\ \beta_\mu &= \alpha_\mu - \sum_\nu C_{\mu\nu}\, \alpha_\nu^\dagger \end{aligned} \tag{A.35}$$

REFERENCES

[1] MOSZKOWSKI, S.A., SCOTT, B.L., Ann. Phys. 11 (1960) 65.
[2] BLOMQUIST, J., WAHLBORN, S., Ark. Fys. 16 (1960) 545, after BROWN, G.E., Unified Theory of Nuclear Models, North-Holland Publishing Co., Amsterdam (1964).
[3] KURATH, D., PICMAN, L., Nucl. Phys. 10 (1959) 313.
[4] PEIERLS, R.E., YOCCOZ, J., Proc. phys. Soc. 70 (1957) 381.
[5] VERHAAR, B.J., Nucl. Phys. 45 (1963) 129;
VERHAAR, B.J., Nucl. Phys. 54 (1964) 641.
[6] PEIERLS, R.E., THOULESS, D.J., Nucl. Phys. 38 (1962) 154.
[7] THOULESS, D.J., Nucl. Phys. 21 (1960) 225;
THOULESS, D.J., VALATIN, J.G., Nucl. Phys. 31 (1962) 211.
[8] VILLARS, F.M.H., Nucl. Phys. 14 (1965) 353.
[9] LANE, A.M., Nuclear Theory, Benjamin, New York (1964).
[10] KISSLINGER, L.S., SORENSEN, R.A., Mat.-fys. Meddr 32 9 (1960).
[11] COHEN, B.L., PRICE, R.E., Phys. Rev. 121 (1961) 1441.
[12] ELLIOTT, J.P., LEA, D.A., Phys. Lett. 19 (1965) 291.
[13] BELYAEV, S.T., Mat.-fys. Meddr 31 11 (1959).
[14] ELLIOTT, J.P., FLOWERS, B.H., Proc. R. Soc. 24 2A (1957) 57.
[15] BROWN, G.E., BOLSTIRLI, M., Phys. Rev. Lett. 3 (1959) 472.
[16] THOULESS, D.J., Nucl. Phys. 22 (1961) 78.
[17] BROWN, G.E., EVANS, J.A., THOULESS, D.J., Nucl. Phys. 24 (1961) 1.
[18] GILLET, V., Nucl. Phys. 51 (1964) 410;
GILLET, V., VINH MAU, N., Nucl. Phys. 54 (1964) 321;
GILLET, V., SANDERSON, E.A., Nucl. Phys. 54 (1964).
[19] GILLET, V., MELKANOFF, M., Phys. Rev. 133 (1964) B1190.

CHAPTER 11

EQUILIBRIUM SHAPES OF LIGHT NUCLEI

G. RIPKA

1. KINETIC AND POTENTIAL ENERGY IN THE INDEPENDENT PARTICLE MODEL

Since we shall be concerned with the independent particle model let us establish a few useful formulae and properties of this model. In the independent particle model the wave function of the nucleus is approximated by a Slater determinant $|\varphi\rangle$ made up of orbits described by the nucleons

$$|\varphi\rangle = b^+_{\lambda_1} b^+_{\lambda_2} \ldots b^+_{\lambda_A} |0\rangle \tag{1.1}$$

b^+_λ is the operator which places a nucleon in the orbit λ.

The orbits $|\lambda\rangle$ are eigenstates of a single particle Hamiltonian h.

$$h|\lambda\rangle = e_\lambda |\lambda\rangle \tag{1.2}$$

$|\lambda\rangle$ is the wavefunction of the orbit λ and e_λ is its energy. When the single particle Hamiltonian is calculated explicitly in terms of the interaction between the nucleons by a variational procedure discussed later, it is called the Hartree-Fock Hamiltonian. Only in this case do the energies e_λ have a physical meaning (Fig. 1).

The Hamiltonian h may be invariant under various symmetry operations which may be reflected by the wavefunction $|\varphi\rangle$. Some of the most frequently met symmetries are:

Time reversal symmetry in even-even nuclei. In a real representation this is equivalent to a rotation of π about the y-axis:

$$[h, e^{i\pi J_y}] = 0 \qquad e^{i\pi J_y} = |\varphi\rangle \tag{1.3}$$

The author is at the Centre d'études nucléaires de Saclay, Commissariat à l'énergie atomique, France.

Proton-neutron exchange symmetry. In nuclei with equal numbers of neutrons and protons, this symmetry is violated by the Coulomb interaction but it remains a good approximation in light nuclei.
Axial symmetry is a frequent occurrence. The Hamiltonian h commutes with J_z:

$$[h, J_z] = 0$$

and the orbits have a definite angular momentum component along the z-axis.

$$h|\lambda\rangle = e_\lambda|\lambda\rangle, \quad J_z|\lambda\rangle = m_\lambda|\lambda\rangle \tag{1.4}$$

Time reversal and proton-neutron exchange symmetry may be combined in even-even N = Z nuclei in which the orbits λ are four-fold degenerate: we may place a neutron and a proton in each orbit $|\lambda\rangle$ and in the time reversed orbit:

$$e^{i\pi J_y}|\lambda\rangle = |-\lambda\rangle$$

The configurations of the ground states of even-even N = Z nuclei are of this type as shown in Fig. 2.

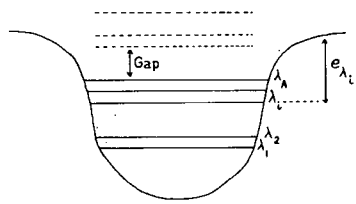

FIG. 1. Energies of single particle orbits in the independent particle model. Full lines represent occupied orbits, dashed lines represent empty orbits. The energies e_λ of the orbits are measured relative to the edge of the potential well and they are equal to the energy required to extract a nucleon in the level λ from the nucleus

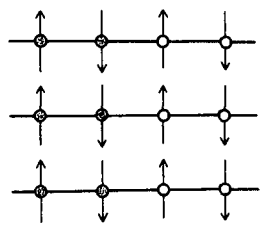

FIG. 2. The four-fold degeneracy of even-even N=Z nuclei. Protons are represented by shaded circles, neutrons by open circles. Upward and downward pointing arrows distinguish orbits $|\lambda\rangle$ from the time reversed orbit $|-\lambda\rangle = \exp i\pi J_y|\rangle$

In the case of axial symmetry where $J_z|\lambda\rangle = m_\lambda|\lambda\rangle$ the orbit $|-\lambda\rangle$ has $J_z|-\lambda\rangle = -m_\lambda|-\lambda\rangle$ and the state $|\varphi\rangle$ has no angular momentum projection along the z-axis

Invariance under rotations. The Hamiltonian h will not in general be invariant under rotations. Closed shells are the only exceptions. But if the Hamiltonian h is spin independent it is invariant under rotations in spin-space only:

$$[h, \vec{S}] = 0 \qquad [h, \vec{L}] \neq 0 \tag{1.5}$$

Such a symmetry is broken by the spin-orbit interaction which does not act very strongly in even-even nuclei up to about A = 28.

Then neglecting the Coulomb interaction the Hamiltonian h in these nuclei also commutes with the isospin operator and the orbits λ factorize into spatial, spin and isospin components:

where
$$|\lambda\rangle = |\lambda_x\rangle\,|\lambda_\sigma\rangle\,|\lambda_\tau\rangle \tag{1.6}$$

λ_x is the wavefunction of the orbit in configuration space (it is a function only of the position $\vec{r}$ of the nucleon with respect to the centre of mass of the nucleus), and λ_σ and λ_τ are spin and isospin functions. Even-even nuclei may then be built up of quartets of nucleons each in a given orbit λ_x and forming a closed shell of spin and isospin. This state may also be represented by Fig. 2 in which the arrows represent the actual spins.

The wavefunction $|\varphi\rangle$ then has spin zero:

$$\vec{S}|\varphi\rangle = 0$$

It is therefore an L-S coupling wavefunction.

This is a special case of four-fold degeneracy. The four-fold degeneracy is more general and does not necessarily imply the factorization of the orbit λ into space and spin parts.

1.1. Kinetic and potential energy

The Hamiltonian h is not the nuclear Hamiltonian. Is it only used to generate the orbits λ and hence the wavefunction $|\varphi\rangle$ which approximates the nuclear wavefunction. The nuclear Hamiltonian is

$$H = \sum_{i=1}^{A} \frac{P_i^2}{2m} + \frac{1}{2}\sum_{i\neq j} v(ij) \tag{1.7}$$

where $P_i^2/2m$ is the kinetic energy of the i^{th} nucleon, and v(ij) is the interaction between the i^{th} and j^{th} nucleons. The nuclear Hamiltonian may be written in second quantization in any representation, in particular in the representation λ of eigenstates of h:

$$H = \sum_{\lambda_1\lambda_2} \langle\lambda_1|\frac{P^2}{2m}|\lambda_2\rangle\, b^+_{\lambda_1} b_{\lambda_2} + \frac{1}{4}\sum_{\lambda_1\lambda_2\lambda_3\lambda_4} \langle\lambda_1\lambda_2|V|\lambda_3\lambda_4\rangle\, b^+_{\lambda_1} b^+_{\lambda_2} b_{\lambda_4} b_{\lambda_3} \tag{1.8}$$

$\langle \lambda_1 | \frac{P^2}{2m} | \lambda_2 \rangle$ is the matrix element of the kinetic energy operator, and $\langle \lambda_1 \lambda_2 | V | \lambda_3 \lambda_4 \rangle = - \langle \lambda_1 \lambda_2 | V | \lambda_4 \lambda_3 \rangle$ is the antisymmetrized matrix element of the nucleon-nucleon interaction.

The binding energy of the nucleus when approximated by the wavefunction $|\varphi\rangle$ is easily found to be:

$$E = \langle \varphi | H | \varphi \rangle = \sum_{\lambda=1}^{A} \langle \lambda | \frac{P^2}{2m} | \lambda \rangle + \frac{1}{2} \sum_{\lambda,\mu=1}^{A} \langle \lambda\mu | v | \lambda\mu \rangle \tag{1.9}$$

The sums over λ are extended over the occupied orbits only. (To derive equation (1.9) use Wick's theorem or any other tedious method!).

Consider the special case of L-S coupling in which the orbits λ factorize into spin and space parts as in Eq.(1.6). Assume the nucleon-nucleon interaction is a central potential with spin and isospin exchange components:

$$v(12) = (\underline{W} + \underline{B}\, P_\sigma - \underline{H}\, P_\tau + \underline{M}\, P_x)\, v(r_{12}) \tag{1.10}$$

where $v(r_{12})$ is a potential depending on the relative co-ordinates $|\vec{r}_1 - \vec{r}_2|$ such as a Gaussian or a Yukawa potential. P_σ and P_τ are the spin and isospin exchange operators

$$P_\sigma = \frac{1 + \vec{\sigma}_1 \cdot \vec{\sigma}_2}{2}, \quad P_\tau = \frac{1 + \vec{\tau}_1 \cdot \vec{\tau}_2}{2} \tag{1.11}$$

whose effect is to exchange the spin and isospin co-ordinates of the nucleons. The space exchange operator P_x when acting on anti-symmetrized wavefunctions equals $P_x = -P_\sigma P_\tau$. P_x exchanges the spatial co-ordinates of the nucleons. $\underline{W}$, $\underline{B}$, $\underline{H}$, and $\underline{M}$ measure the intensity of what are called the Wigner, Bartlett, Heisenberg and Majorana components of the nucleon-nucleon potential. Then the matrix element appearing in Eq.(1.9) becomes:

$$\langle \lambda\mu | V | \lambda\mu \rangle = \langle \lambda_x \lambda_\sigma \lambda_\tau, \mu_x \mu_\sigma \mu_\tau | \underline{W} + \underline{B}\, P_\sigma - \underline{H}\, P_\tau + \underline{M}\, P_x | \lambda_x \lambda_\sigma \lambda_\tau, \mu_x \mu_\sigma \mu_\tau \rangle_D$$
$$- \langle \lambda_x \lambda_\sigma \lambda_\tau, \mu_x \mu_\sigma \mu_\tau | \underline{W} + \underline{B}\, P_\sigma - \underline{H}\, P_\tau + \underline{M}\, P_x | \mu_x \mu_\sigma \mu_\tau, \lambda_x \lambda_\sigma \lambda_\tau \rangle_D$$

We have made explicit the direct and exchange terms. The subscript D in the matrix element

$$\langle \alpha\beta | v(12) | \gamma\delta \rangle_D = \quad \gamma \searrow \cdots \swarrow \delta \quad (\alpha, \beta)$$

means that only the direct term should be taken; the states α and γ refer

to co-ordinates of nucleon 1 and the states β and δ refer to co-ordinates of nucleon 2. The matrix element $\langle\lambda\mu|v|\lambda\mu\rangle$ then becomes

$$\begin{aligned}\langle\lambda\mu|V|\lambda\mu\rangle = {} & \underline{W}\left[\langle\lambda_x\mu_x|v(r)|\lambda_x\mu_x\rangle - \langle\lambda_x\mu_x|v(r)|\mu_x\lambda_x\rangle\delta_{\lambda_\sigma\mu_\sigma}\delta_{\lambda_\tau\mu_\tau}\right] \\ & + \underline{B}\left[\langle\lambda_x\mu_x|v(r)|\lambda_x\mu_x\rangle\delta_{\lambda_\sigma\mu_\sigma} - \langle\lambda_x\mu_x|v(r)|\mu_x\lambda_x\rangle\delta_{\lambda_\tau\mu_\tau}\right] \\ & - \underline{H}\left[\langle\lambda_x\mu_x|v(r)|\lambda_x\mu_x\rangle\delta_{\lambda_\tau\mu_\tau} - \langle\lambda_x\mu_x|v(r)|\mu_x\lambda_x\rangle\delta_{\lambda_\sigma\mu_\sigma}\right] \\ & - \underline{M}\left[\langle\lambda_x\mu_x|v(r)|\lambda_x\mu_x\rangle\delta_{\lambda_\sigma\mu_\sigma}\,\delta_{\lambda_\tau\mu_\tau} - \langle\lambda_x\mu_x|v(r)|\mu_x\,\lambda_x\rangle\right] \qquad (1.12)\end{aligned}$$

The spin and isospin sums are now easily performed in the expression (1.9) for the binding energy which becomes:

$$\begin{aligned}E = {} & 4\sum_{\lambda_x=1}^{n}\langle\lambda_x|\frac{P^2}{2m}|\lambda_x\rangle + 2S\sum_{\lambda_x\mu_x=1}^{n}\langle\lambda_x\mu_x|v(r)|\lambda_x\mu_x\rangle \\ & - 2G\sum_{\lambda_x\mu_x}\langle\lambda_x\mu_x|v(r)|\mu_x\lambda_x\rangle \qquad (1.13)\end{aligned}$$

S and G are the following linear combinations of $\underline{W}$, $\underline{B}$, $\underline{H}$ and $\underline{M}$:

$$S = 4\underline{W} + 2\underline{B} - 2\underline{H} - \underline{M}, \qquad G = \underline{W} + 2\underline{B} - 2\underline{H} - 4\underline{M} \qquad (1.14)$$

We see that when the orbits of an even-even N = Z nucleus factorize into space and spin parts the binding energy given by Eq.(1.13) depends on only two combinations S and G of spin and isospin exchange parameters. An attractive Rosenfeld force for example has S = 0 and G > 0.

Closed shell nuclei ^{4}He, ^{16}O and ^{40}Ca are necessarily of the type considered here even if the orbits λ are eigenfunctions of a Hamiltonian h which contains a spin-orbit interaction. This is because the determinental wavefunction $|\varphi\rangle$ is invariant when an occupied orbit is replaced by any linear combination of other occupied orbits. Thus the wavefunction of ^{16}O is the same whether one considers the filled P-shell to be composed of the orbits

$$\begin{aligned}P^{1/2}_{1/2} &= +\sqrt{\frac{1}{3}}\,P_{0\uparrow} - \sqrt{\frac{2}{3}}\,P_{1\downarrow} \\ P^{3/2}_{1/2} &= +\sqrt{\frac{2}{3}}\,P_{0\uparrow} + \sqrt{\frac{1}{3}}\,P_{1\downarrow} \qquad (1.15) \\ P^{3/2}_{3/2} &= P_{1\uparrow}\end{aligned}$$

TABLE I. BINDING ENERGIES OF EVEN-EVEN N = Z NUCLEI WITH A ≤ 40.

The binding energy of a bound nucleus is defined as negative. E and E/A are the binding energy and binding energy per particle. E_c is the Coulomb potential energy. $E-E_c$ and $E-E_c/A$ are the binding energy and binding energy per particle corrected for the Coulomb energy

Nucleus	E	E/A	E_c	$E-E_c$	$E-E_c/A$
^{4}He	- 28.29	-7.07	0.76	- 29.05	- 7.26
^{8}Be	- 56.54	-7.07	3.95	- 60.49	- 7.56
^{12}C	- 92.16	-7.68	9.22	-101.38	- 8.45
^{16}O	-127.62	-7.98	15.26	-142.88	- 8.83
^{20}Ne	-160.64	-8.03	21.34	-181.98	- 9.10
^{24}Mg	-198.25	-8.26	30.46	-228.71	- 9.53
^{28}Si	-236.53	-8.45	40.73	-277.26	- 9.90
^{32}S	-271.77	-8.49	51.46	-323.23	-10.10
^{36}A	-306.71	-8.52	62.71	-369.42	-10.26
^{40}Ca	-342.05	-8.55	74.92	-416.97	-10.42

or of the linear combination of orbits

$$P_0\uparrow = \sqrt{\frac{1}{3}}\, P^{1/2}_{1/2} + \sqrt{\frac{2}{3}}\, P^{3/2}_{1/2}$$

$$P_1\downarrow = -\sqrt{\frac{2}{3}}\, P^{1/2}_{1/2} + \sqrt{\frac{1}{3}}\, P^{3/2}_{1/2} \qquad (1.16)$$

$$P_1\uparrow = P^{3/2}_{3/2}$$

which factorize into spin and space parts.

For nuclei such as ^{8}Be, ^{12}C, ^{20}Ne, ^{24}Mg and possibly ^{28}Si, it is a good approximation for the energy to assume the orbits factorize into spin and space parts.

The binding energies of even-even N = Z nuclei are known experimentally and they are given in Table I. They contain a Coulomb repulsion which is easily subtracted in the following way.

The Coulomb interaction is very long ranged and it is a good approximation to assume the nucleus is an uniformly charged sphere of radius proportional to $A^{1/3}$. The Coulomb potential energy is then:

$$E_c(Z, A) = \alpha \frac{Z(Z-1)}{A^{1/3}} \qquad (1.17)$$

α is a proportionality constant which can be calculated for each nucleus by comparing the binding energies of the mirror nuclei which have a proton or a neutron less than the even-even N = Z nucleus. The difference between the binding energies of the mirror nuclei is assumed to be due to the Coulomb potential alone. Using this method the binding energies shown in Table I are obtained. We shall discuss later the variation of E/A with A.

How much of the binding energy is kinetic energy, how much is potential energy?

One can only answer this question in the framework of a nuclear model, and let us consider the oscillator model of the spherical nuclei ^{4}He, ^{16}O and ^{40}Ca.

These nuclei are formed by making up quartets of nucleons which respectively fill the 1s, 1p and the 2s - 1d shell orbits of the harmonic oscillator. The kinetic energy of these nuclei is equal to the mean value in the state $|\varphi\rangle$ of the operator

$$T = \sum_{i=1}^{A} \frac{p^2}{2m} - \frac{P^2}{2Am} \qquad (1.18)$$

$\vec{P} = \sum_{i=1}^{A} \vec{P}_i$ is the momentum of the centre of the mass of the nucleus and it is necessary to subtract the centre of mass kinetic energy.

In the present case the centre of mass correction amounts to multiplying the mean value of the kinetic energy operator $\sum_i P_i^2/2m$ by the factor (1-1/A).

In a harmonic oscillator orbit $|\lambda\rangle = |n\ell m\rangle$ the total energy is: $h|n\ell m\rangle = \left(2n+\ell-\frac{1}{2}\right)\hbar\omega|n\ell m\rangle$ and the kinetic energy is $\langle\lambda|\frac{P^2}{2m}|\lambda\rangle = \langle n\ell m|\frac{P^2}{2m}|n\ell m\rangle = \frac{1}{2}\hbar\omega\left(2n+\ell-\frac{1}{2}\right)$.

Summing over all the orbits and correcting for the centre of mass kinetic energy one obtains:

$$\begin{aligned} \text{K.E.} &= 93.46\,\alpha^2 \quad \text{for } {}^4\text{He} \\ &= 716.47\,\alpha^2 \quad \text{for } {}^{16}\text{O} \\ &= 2461\,\alpha^2 \quad \text{for } {}^{40}\text{Ca} \end{aligned} \tag{1.19}$$

where α is the harmonic oscillator constant $\alpha = \sqrt{(m\omega/\hbar)}$

$$\hbar\omega = 41.54\,\alpha^2 \text{ MeV} \quad (\alpha \text{ in fm}^{-1}) \tag{1.20}$$

The values of α are known from the mean square radii of the ^{4}He, ^{16}O and ^{40}Ca nuclei. These have been measured by electron scattering experiments [1]. The root mean square radii of ^{4}He, ^{16}O and ^{40}Ca are measured to be 1.61 fm, 2.64 fm and 3.52 fm, respectively. The values of α which yield these values are:

$$\begin{aligned} \alpha &= 0.756 \quad \text{in } {}^4\text{He} \\ \alpha &= 0.568 \quad \text{in } {}^{16}\text{O} \\ \alpha &= 0.492 \quad \text{in } {}^{40}\text{Ca} \end{aligned} \tag{1.21}$$

Thus we need to know the nuclear radii in order to estimate the kinetic energy in the independent particle model. Substituting the values (1.21) in Eq.(1.19) and using the fact that the total energy given in Table I is the sum of the potential and kinetic energies we obtain the following values of kinetic and potential energy per particle in ^{4}He, ^{16}O and ^{40}Ca (Table IIa).

In nuclear matter using the independent particle model with Fermi momentum $k_f = 1.36$ fm^{-1}, the kinetic energy per particle is 23 MeV and the potential energy per particle is -39 MeV.

1.2. Separation energies and single particle energies

Separation energies and single particle energies are easily calculated in the independent particle model. Let $|\varphi\rangle$ be the wavefunction of an even-even N = Z nucleus (Eq.1.1). One may expect the ground state of the A-1 nucleus with a neutron missing to be well represented by the hole wavefunction:

$$|\varphi_\lambda\rangle = b_\lambda|\varphi\rangle \tag{1.22}$$

where λ is an occupied orbit. The ground state would be the state $|\varphi_\lambda\rangle$ where λ is the highest occupied orbit.

TABLE IIa. KINETIC, POTENTIAL AND TOTAL ENERGY PER PARTICLE IN CLOSED SHELL NUCLEI

Nucleus	K.E./A	$\langle V \rangle$/A	E/A
^{4}He	13.35	-20.61	- 7.26
^{16}O	14.45	-23.38	- 8.93
^{40}Ca	14.89	-25.31	-10.42

TABLE IIb. THE ENERGY OF THE LOWEST EMPTY ORBIT $e_\lambda = E(A+1)-E(A)$, THE ENERGY OF THE HIGHEST FILLED ORBIT $e_\alpha = E(A)-E(A-1)$ AS GIVEN BY THE EXPERIMENTAL VALUES OF THE NEUTRON SEPARATION ENERGY OF THE A+1 AND OF THE A NUCLEUS. THE LAST COLUMN SHOWS THE VALUE OF THE ENERGY GAP $e_\alpha - e_\lambda$ SEPARATING THE LOWEST EMPTY AND HIGHEST FILLED ORBITS.

Nucleus	A	E(A+1)-E(A)	E(A)-E(A-1)	Gap
^{4}He	4	-1.04	-20.58	19.54
^{8}Be	8	-1.66	-18.90	17.24
^{12}C	12	-4.95	-18.72	13.77
^{16}O	16	-4.14	-15.67	11.53
^{20}Ne	20	-6.76	-16.87	10.11
^{24}Mg	24	-7.33	-16.54	9.21
^{28}Si	28	-8.48	-17.17	8.69
^{32}S	32	-8.65	-15.08	6.43
^{36}Ar	36	-8.79	-15.27	6.48
^{40}Ca	40	-8.36	-15.36	7.27
^{44}Ti	44	-9.41	-16.39	6.98

The neutron separation energy is equal to the difference between the binding energies of the A-1 nucleus and of the even-even nucleus. It is equal to the energy required to lift a neutron from the highest occupied orbit out of the potential well. The energy of the orbit is therefore:

$$e_\lambda = \langle \varphi | H | \varphi \rangle - \langle \varphi_\lambda | H | \varphi_\lambda \rangle$$

$$= \langle \lambda | \frac{P^2}{2m} | \lambda \rangle + \sum_{\mu=1}^{A} \langle \lambda\mu | v | \lambda\mu \rangle \qquad (1.23)$$

The expression (1.23) gives the energy of any occupied orbit, although the states of the A-1 nucleus will not all be adequately described by the wavefunction (1.22). We have also tacitly assumed that the wavefunction of the orbits λ have not been changed by the removal of a neutron.

Note also that the value of e_λ, the energy of the single particle orbit λ, given by Eqs.(1.23) and (1.22) are the same only if h is the Hartree-Fock Hamiltonian. If not the expression (1.23) for e_λ is the only one which has physical significance.

When the orbits separate into spin and space parts as in Eq.(1.6) and when the nucleons interact with the central force (1.10) the energy of the orbit is still given in terms of the coefficients S and G (1.14) only:

$$e_\lambda = \langle \lambda_x | t | \lambda_x \rangle + S \sum_{\mu_x=1}^{n} \langle \lambda_x \mu_x | v(r) | \lambda_x \mu_x \rangle$$

$$- G \sum_{\mu_x=1}^{n} \langle \lambda_x \mu_x | v(r) | \mu_x \lambda_x \rangle \qquad (1.24)$$

The separation energy of the A+1 nucleus gives directly the energy of the lowest empty orbit α:

$$e_{\alpha'} = \langle \varphi | b_\alpha H b_\alpha^+ | \varphi \rangle - \langle \varphi | H | \varphi \rangle$$

$$= \langle \alpha | \frac{P^2}{2m} | \alpha \rangle + \sum_{\mu=1}^{A} \langle \alpha\mu | v | \alpha\mu \rangle \qquad (1.25)$$

The energy difference between the lowest empty orbit α and the highest filled orbit λ (often called the Fermi level) is called the energy gap separating the occupied and empty orbits (Fig.1).

The values of e_λ, e_α and of the gap are shown on Table IIb. The Fermi level e_λ remains fairly constant in a major shell. The gap decreases with A.

It should be emphasized that in this chapter the energetics of the independent particle model are presented in their crudest form. We have

completely neglected the question of angular momentum. Independent particle wavefunctions most often do not have a definite angular momentum and this must be allowed for when comparing them with nuclear states which do. We shall see that the orbits of odd-A nuclei are somewhat different from those of an even-even nucleus due to polarization effects. Finally nuclear states are more complicated than suggested by the independent particle model. There is evidence for mixtures of various states $|\varphi\rangle$ even in the nuclear ground states. None the less the independent particle model provides a very useful basis from which to study nuclear states.

1.3. Correlation functions in the independent particle model

It is instructive to express the potential energy (1.13) in terms of the density operator which is defined as

$$\rho(\vec{r}, \vec{r}') = \sum_{\lambda=1}^{A} \varphi_\lambda^*(\vec{r})\, \varphi_\lambda(\vec{r}') \tag{1.26}$$

where $\varphi_\lambda(\vec{r})$ is the spatial part of the orbital wavefunction (1.6). ρ is a density operator because it satisfies the equations

$$\begin{aligned} &\int d\vec{r}\, \rho(\vec{r}_1, \vec{r})\ \rho(\vec{r}, \vec{r}_2) = \rho(\vec{r}_1, \vec{r}_2) && \rho^2 = \rho \\ &\int d\vec{r}\, \rho(\vec{r}, \vec{r}) = n && \mathrm{Tr}\rho = n \end{aligned} \tag{1.27}$$

where $n = A/4$ is the number of different orbits in configuration space occupied by four nucleons. The diagonal element $\rho(\vec{r}, \vec{r})$ is just equal to the density of matter at the point $\vec{r}$. Nucleons are not localized in space and thus the density operator is non-local.

The potential energy (13) may be written thus:

$$\begin{aligned} \langle V\rangle &= 2S \sum_{\lambda_x \mu_x=1}^{n} \langle \lambda_x \mu_x | V(r) | \lambda_x \mu_x \rangle - 2G \sum_{\lambda_x \mu_x=1}^{n} \langle \lambda_x \mu_x | v(r) | \mu_x \lambda_x \rangle \\ &= 2S \int d\vec{r}_1\, d\vec{r}_2\, \rho(\vec{r}_1, \vec{r}_1)\ \rho(\vec{r}_2, \vec{r}_2)\, v(r_{12}) \\ &\quad - 2G \int d\vec{r}_1\, d\vec{r}_2\, |\rho(\vec{r}_1, \vec{r}_2)|^2\, v(r_{12}) \end{aligned} \tag{1.28}$$

where $r_{12} = |\vec{r}_1 - \vec{r}_2|$. Introducing the two correlation functions

$$\nu(\vec{r}) = \int d\vec{R}\, \rho(\vec{r}_1, \vec{r}_1)\ \rho(\vec{r}_2, \vec{r}_2)$$

$$K(\vec{r}) = \int d\vec{R} |\rho(\vec{r}_1, \vec{r}_2)|^2 \tag{1.29}$$

which satisfy the equations

$$\nu(0) = K(0), \qquad \int d\vec{r}\ \nu(\vec{r}) = n^2, \qquad \int d\vec{r}\ K(\vec{r}) = n \tag{1.30}$$

the potential energy (1.28) becomes

$$\langle V \rangle = 2S \int d\vec{r}\ \nu(\vec{r})\ v(r) - 2G \int d\vec{r}\ K(\vec{r})\ v(r) \tag{1.31}$$

The integrals (1.29) should be understood thus: Transform the integrand into a function of relative and centre of mass co-ordinates $\vec{r}$ and $\vec{R}$:

$$\vec{r} = \vec{r}_1 - \vec{r}_2, \qquad \vec{R} = \frac{1}{2}(\vec{r}_1 + \vec{r}_2) \tag{1.32}$$

and integrate over $\vec{R}$.

Let us consider the spherical nuclei ^{4}He, ^{16}O and ^{40}Ca in the oscillator model. For these nuclei it is quite easy to perform the sum (1.26) and the integral (1.29) analytically since harmonic oscillator wavefunctions are well known. We use the index 0, 1 and 2 for the correlation functions ν and K in ^{4}He, ^{16}O and ^{40}Ca, respectively. One finds

$$\nu_0(r) = K_0(r) = \frac{\alpha^3}{\pi^{3/2}}\ \frac{1}{2\sqrt{2}}\ e^{-\alpha^2 r^2/2} \qquad (^4\text{He}) \tag{1.33}$$

$$\left.\begin{aligned} \nu_1(r) &= \frac{\alpha^3}{\pi^{3/2}}\ \frac{1}{8\sqrt{2}}\ \left[31 + 6(\alpha r)^2 + (\alpha r)^4\right] e^{-\alpha^2 r^2/2} \\ K_1(r) &= \frac{\alpha^3}{\pi^{3/2}}\ \frac{1}{8\sqrt{2}}\ \left[31 - 10(\alpha r)^2 + (\alpha r)^4\right] e^{-\alpha^2 r^2/2} \end{aligned}\right\} \qquad (^{16}\text{O}) \tag{1.34}$$

$$\left.\begin{aligned} \nu_2(r) &= \frac{\alpha^3}{\pi^{3/2}}\ \frac{1}{128\sqrt{2}}\ \left[1945 + 540(\alpha r)^2 + 98(\alpha r)^4 + 4(\alpha r)^6 + (\alpha r)^8\right] e^{-\alpha^2 r^2/2} \\ K_2(r) &= \frac{\alpha^3}{\pi^{3/2}}\ \frac{1}{128\sqrt{2}}\ \left[1945 - 1220(\alpha r)^2 + 290(\alpha r)^4 - 28(\alpha r)^6 + (\alpha r)^8\right] e^{-\alpha^2 r^2/2} \end{aligned}\right\}$$

$$(^{40}\text{Ca}) \tag{1.35}$$

In nuclear matter where the orbits are plane waves

$$\varphi_{\vec{k}}(\vec{r}) = \frac{e^{i\vec{k}.\vec{r}}}{\sqrt{\Omega}}$$

the density operator is

$$\rho(\vec{r}_1, \vec{r}_2) = \sum_{k \le k_f} \frac{e^{i\vec{k}(\vec{r}_2 - \vec{r}_1)}}{\Omega} = \frac{3n}{\Omega} \frac{j_1(k_f r)}{k_f r} \tag{1.36}$$

k_f is related to the density by the relation

$$\frac{n}{\Omega} = \frac{k_f^3}{6\pi^2}$$

and $j_1(x)$ is the spherical Bessel function $j_1(x) = \frac{\sin x}{x^2} - \frac{\cos x}{x}$

In nuclear matter the functions ν and K are:

$$\nu_\infty(r) = \frac{nk_f^3}{6\pi^2}, \qquad K_\infty(r) = \frac{3nk_f^3}{2\pi^2} \left(\frac{j_1(k_f r)}{k_f r}\right)^2 \tag{1.37}$$

Figures 3 and 4 show the curves of the functions $4\pi r^2 \nu(r)$ and $4\pi r^2 K(r)$ for ^{4}He, ^{16}O, ^{40}Ca and infinite nuclear matter, divided by the number of particles. The functions are plotted using the values (1.21) of the oscillator constant α which reproduce the observed root mean square radii of each nucleus. It is seen that with an attractive force the potential energy term $2S \int v(r)\, \nu(r)\, d\vec{r}$ will give more and more binding as the nucleus gets heavier. In order to estimate how much of the correlation function the force v(r) will see, a Yukawa force $(\exp -r/\mu)(r/\mu)^{-1}$ with μ equal to the Compton wavelength of the π meson is shown by a dashed line on the figures. Clearly the force only sees the beginning of the function $\nu(r)$. The curve for infinite nuclear matter was drawn using the Fermi momentum $k_f = 1.36$ fm. If this is indeed the correct value to use in infinite nuclear matter it is seen that $\nu(r)$ in ^{40}Ca is still far from reaching its value in nuclear matter even within the range of the force v(r). Finally note that the potential energy term $2S \int v(r)\, \nu(r)\, d\vec{r}$ increases as the nucleus gets heavier. The increase of the binding energy per particle as a nucleus gets larger is interpreted as a surface energy effect, similar to the one encountered in a liquid drop. It appears in the semi-empirical mass formula of Weizsäcker as a repulsive term proportional to the nuclear surface.

The potential energy term $-2G \int K(r)\, v(r)\, d\vec{r}$ on the other hand is very similar in ^{4}He, ^{16}O and ^{40}Ca. This is the exchange term in configuration space. The exchange term appears therefore to contribute less to the surface energy. It is amusing to note that if the ratio k_f/α is chosen in such a way as to make the kinetic energy per particle equal in nuclear matter and in the finite nuclei ^{4}He, ^{16}O and ^{40}Ca then the correlation functions $\nu(r)$ and K(r) are very similar at $r = 0$ and the function K(r) in the

finite nucleus follows very closely its values in infinite nuclear matter, within the range of the force v(r). But with the experimental values (1.21) of α this would mean that $k_f = 1.1$ fm.

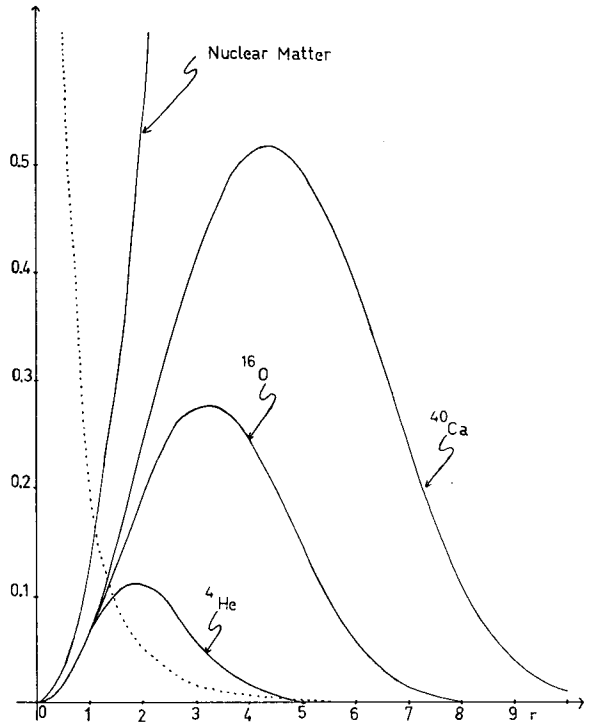

FIG.3. The functions $\nu(r)$ divided by the number of particles in ^{4}He, ^{16}O, ^{40}Ca and nuclear matter plotted against the distance r in fm. The functions are calculated with oscillator constants (1.21) which yield the experimental mean square radii. For infinite nuclear matter the value $k_f = 1.36$ fm is used. The dashed line represents a Yukawa force: $(\exp -r/\mu)\,(r/\mu)^{-1}$ with $\mu = 1.435$ fm dawn on an arbitrary scale

If the nuclear force v(r) has a hard core the potential energy (1.31) will diverge unless the correlation functions $\nu(r)$ and K(r) go to zero at small distances. Equation (1.29) shows that $\nu(0) \geq 0$ and that $\nu(0)$ is zero only when $\rho(\vec{r}, \vec{r}) = 0$ at all points. It is therefore impossible for an independent wavefunction to have a vanishing correlation function at small distances, and it is not possible to use a nuclear Hamiltonian (1.7) with hard cores in the independent particle model. Thus if the nucleon-nucleon interaction has a hard core, the potential v(i, j) in Eq.(1.7) can only be an effective interaction from which the hard core has been removed.

2. THE HARTREE-FOCK THEORY

The purpose of the Hartree-Fock theory is to determine the wavefunction λ of the orbits described by the nucleons in the independent particle model.

This is achieved by requiring that the energy [Eq. (1.9)] of the state $|\varphi\rangle$ be stationary and minimum. The state $|\varphi\rangle$ will then represent the nucleus at equilibrium.

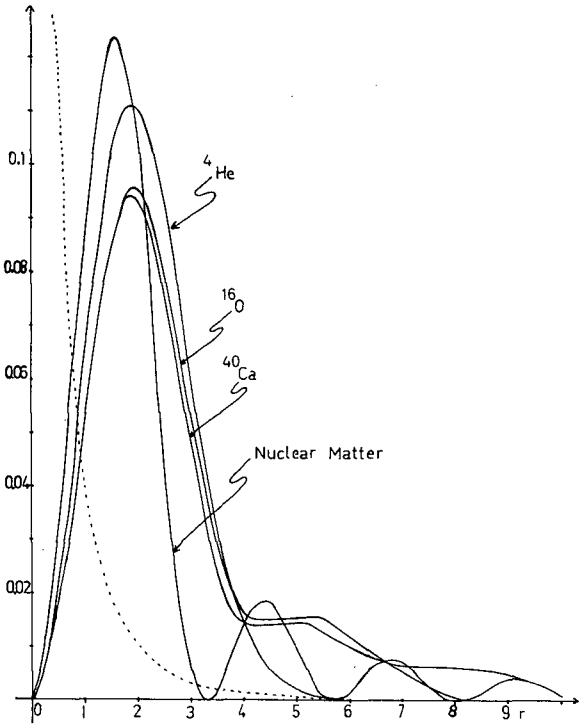

FIG. 4. The functions K(r) divided by the number of particles in ^{4}He, ^{16}O, ^{40}Ca and nuclear matter. The same oscillator constants α and Fermi momentum k_f are used as in Fig. 3. The dashed line is a Yukawa force $(\exp -r/\mu)\ (r/\mu)^{-1}$ with $\mu = 1.435$ fm drawn on an arbitrary scale

A convenient way to obtain the wavefunctions of the orbits is to expand them on a basis of known wavefunctions with which one is able to calculate matrix elements of the nucleon-nucleon interaction.

Harmonic oscillator wavefunctions for example provide a useful basis which has the advantage of making the orbital expansion rapidly converging, as we shall see. Thus we expand:

$$|\lambda\rangle = \sum_{jm} C^{\lambda}_{jm} |jm\rangle \qquad (2.1)$$

where j stands for the three quantum numbers n, ℓ and j. Other expansions may be more convenient. For example it is easier to use the uncoupled $|\ell\, m_\ell m_s\rangle$ representation in the special case where L-S coupling wavefunctions $|\varphi\rangle$ can be used as trial wavefunctions. We shall specialize to the expansion (2.1) because it is trivial to pass from one representation of the orbits to another.

The Slater determinant $|\varphi\rangle$ is now determined by the expansion parameters C^{λ}_{jm} and the energy will be stationary when:

$$\frac{\partial}{\partial C^{\lambda *}_{jm}}\left[\langle\varphi|H|\varphi\rangle - e_{\lambda}\sum_{jm} C^{\lambda *}_{jm}\, C^{\lambda}_{jm}\right] = 0 \tag{2.2}$$

The e_{λ}'s are introduced here as Lagrange multipliers which ensure that the variations made on the wavefunctions λ preserve their norm.

The matrix element $\langle\lambda\mu|v|\lambda\mu\rangle$ appearing in the expression (1.9) for $\langle\varphi|H|\varphi\rangle$ may be expressed in terms of the expansion coefficients C^{λ}_{jm}:

$$\langle\lambda\mu|v|\lambda\mu\rangle = \sum_{\substack{j_1 j_2 j_3 j_4 \\ m_1 m_2 m_3 m_4}} C^{\lambda *}_{j_1 m_1}\, C^{*}_{j_2 m_2} \langle j_1 m_1, j_2 m_2 |v| j_3 m_3, j_4 m_4\rangle C^{\lambda}_{j_3 m_3}\, C^{\mu}_{j_4 m_4} \tag{2.3}$$

Substituting Eqs. (1.9) and (2.2) in expression (2.1) we obtain the following set of coupled equations:

$$\sum_{j_2 m_2} \langle jm|t|j_2 m_2\rangle\, C^{\lambda}_{j_2 m_2} + \sum_{\substack{j_2 j_3 j_4 \\ m_2 m_3 m_4}} C^{\mu *}_{j_2 m_2} \langle jm j_2 m_2 |v| j_3 m_3 j_4 m_4\rangle\, C^{\lambda}_{j_3 m_3}\, C^{\mu}_{j_4 m_4}$$

$$\mu \qquad\qquad = e_{\lambda}\, C^{\lambda}_{jm} \tag{2.4}$$

The equation (2.4) has the form of an eigenvalue problem:

$$h|\lambda\rangle = e_{\lambda}\,|\lambda\rangle \tag{2.5}$$

where h is a one-body operator defined in terms of its matrix elements:

$$\langle j_1 m_1 |h| j_2 m_2\rangle = \langle j_1 m_1 |t| j_2 m_2\rangle + \sum_{\lambda=1}^{A} \langle j_1 m_1, \lambda |v| j_2 m_2, \lambda\rangle \tag{2.6}$$

The sum over λ is limited to the orbits occupied in the state $|\varphi\rangle$ (1.1). The Eqs. (2.5) and (2.6) are the Hartree-Fock equations. h is called the Hartree-Fock Hamiltonian and the e_{λ} are the energies of the orbits in the Hartree-Fock (H-F) field.

The matrix element:

$$\langle j_1 m_1, \lambda |v| j_2 m_2, \lambda\rangle = \sum_{\substack{j_3 j_4 \\ m_3 m_4}} C^{\lambda *}_{j_3 m_3}\, \langle j_1 m_1, j_3 m_3 |v| j_2 m_2, j_4 m_4\rangle\, C^{\lambda}_{j_4 m_4} \tag{2.7}$$

is easily calculated when a convenient basis $|jm\rangle$ is used, such as that provided by harmonic oscillator wavefunctions.

The Hartree-Fock equations are solved by an iteration process consisting of the following steps:
(1) An initial guess at the wavefunctions λ is made. One may choose the leading term in the expansion (2.1). One might also choose the initial set of C^{λ}_{jm} coefficients to be those of Nilsson orbits in a defromed harmonic oscillator well. The initial guess may be quite crucial because different initial guesses may lead to different solutions.
(2) With this set of coefficients C^{λ}_{jm} the matrix element (2.7) is computed and the Hamiltonian h (2.6) is diagonalized in order to satisfy Eq.(2.5). The result of the diagonalization is a set of e_{λ}'s and a new set of C^{λ}_{jm} coefficients.

The second step is repeated until successive sets of C^{λ}_{jm} coefficients are the same. Rapid convergence is usually obtained. The actual calculations are usually performed on a computer. The time involved in solving the Hartree-Fock equations depends on the possibility of storing the matrix elements in the fast memories of the computer. Time is consumed in the actual calculation of a matrix elements, but once they are stored an iteration is a matter of seconds or less on a computer such as the IBM-7090.

2.1. Symmetries of the Hartree-Fock Hamiltonian

We have already mentioned in Section 1 some of the symmetries encountered in the independent particle model. The Hartree-Fock theory allows us to make a systematic analysis of the possible symmetries of the average field and hence of the wavefunction $|\varphi\rangle$. A given symmetry may not be arbitrarily assumed. For example one might limit the expansion (2.1) to states of a given angular momentum in the initial guess of the wavefunctions. But in general the Hartree-Fock Hamiltonian (2.6) will have non-vanishing matrix elements between states of different angular momentum in spite of the initial guess, so that at the next iteration the expansion (2.1) will contain states of various angular momenta. This will occur in all cases except when the occupied orbits happen to form a closed shell. A symmetry which, once assumed at the initial guess of the orbital wavefunctions, is preserved in the successive iterations is called a self-consistent symmetry. Such a symmetry is due to the existence of an operator which commutes with the Hartree-Fock Hamiltonian (2.6).

To investigate which self-consistent symmetries may occur we use the following theorem [2]:

Theorem: Let U be a unitary operator which commutes with the nuclear Hamiltonian H. Then if U leaves the set of A occupied orbits invariant, it commutes with the Hartree-Fock Hamiltonian h.

If U commutes with the nuclear Hamiltonian then

$$H = U^{-1} H\, U = U^{-1} t\, U + U^{-1} v\, U$$

The Hartree-Fock Hamiltonian (2.6) is therefore equal to

$$\langle i|h|j\rangle = \langle i|U^{-1} t\, U|j\rangle + \sum_{\lambda=1}^{A} \langle i\lambda|U^{-1} v\, U|j\lambda\rangle$$

We use the notation i and j to denote all the quantum numbers of any known basis on which we choose to expand the occupied orbit λ. Let us denote by a bar the states $|i\rangle$ which undergo the transformation U:

$$|\bar{i}\rangle = U|i\rangle,$$

(Strictly $\quad |\bar{i}\rangle = U\, a_i^\dagger |0\rangle = (U\, a_i^\dagger\, U^{-1})\, U|0\rangle = a_{\bar{i}}^\dagger |0\rangle$

where $\quad a_i^\dagger = U\, a_{\bar{i}}^\dagger U^{-1}$ and $U|0\rangle = |0\rangle$)

so that:

$$\langle i|h|j\rangle = \langle \bar{i}|t|\bar{j}\rangle + \sum_{\lambda=1}^{A} \langle \bar{i}\,\bar{\lambda}|v|\bar{j}\,\bar{\lambda}\rangle \tag{2.8}$$

Now if U leaves the set of occupied orbits invariant any occupied orbit λ which undergoes the transformation U can be expressed as a linear combination of occupied orbits only:

$$U|\lambda\rangle = \sum_{\mu=1}^{A} X_\mu^\lambda |\mu\rangle$$

where

$$\sum_\mu X_\mu^{\lambda^*} X_\mu^{\lambda'} = \delta_{\lambda\lambda'} \quad \text{and} \quad \sum_\lambda X_\mu^{\lambda^*} X_{\mu'}^{\lambda} = \delta_{\mu\mu'}$$

Thus the interaction term in equation (2.8) becomes

$$\sum_{\lambda=1}^{A} \langle \bar{i}\,\bar{\lambda}|v|\bar{j}\,\bar{\lambda}\rangle = \sum_{\lambda=1}^{A} \sum_{\mu\mu'=1}^{A} X_\mu^{\lambda^*} \langle \bar{i}\mu|v|j\mu'\rangle X_{\mu'}^{\lambda}$$

$$= \sum_{\mu=1}^{A} \langle \bar{i}\mu|v|\bar{j}\mu\rangle$$

Substituting into equation (2.8) we find that

$$\langle i|h|j\rangle = \langle \bar{i}|t|\bar{j}\rangle = \langle \bar{i}|t|\bar{j}\rangle + \sum_{\mu=1}^{A} \langle \bar{i}\mu|v|\bar{j}\mu\rangle = \langle \bar{i}|h|\bar{j}\rangle$$

$$= \langle i|U^{-1}\, hU|j\rangle$$

so that

$$h = U^{-1} h U \tag{2.9}$$

h commutes with U, and the orbits $|\lambda\rangle$ and $|\bar{\lambda}\rangle$ are degenerate.

We can check that the four-fold degeneracy of the orbits which we assumed in section 1 is indeed a self-consistent symmetry of even-even N = Z nuclei.

For if neutrons and protons are equal in number we may place them in the same orbits, because the exchange of a neutron with a proton will then leave the set of occupied orbits invariant. The proton-neutron exchange operator commutes with the Hamiltonian if Coulomb forces are neglected. Furthermore if there is an even number of protons and neutrons, we may place a neutron in the orbit $|\lambda\rangle$ and another in the orbit $|\bar{\lambda}\rangle = (\exp i\pi J_y)|\lambda\rangle$. Then the operator $(\exp i\pi J_y)$ which commutes with the nuclear Hamiltonian will leave the set of occupied orbits invariant.

Axial symmetry is always a self-consistent symmetry. For if we choose the orbits $|\lambda\rangle$ to be eigenstates of j_z, then the unitary operator $(\exp i\pi J_z)$ which commutes with the nuclear Hamiltonian will leave the set of occupied orbits invariant.

This does not imply that the axial symmetry, or any other symmetry will actually occur in nuclei. A better solution of Hartree-Fock equations with a lower energy may be found which does not have the same symmetry. For example ^{24}Mg has a solution which has lower energy than the axially symmetric solution.

In each case the possible symmetries of a nucleus must be investigated separately. Often the spectrum and transition probabilities suggest or eliminate certain symmetries.

2.2. Choice of the expansion of the orbits

In practice the expansion (2.1) is always limited. It is first limited by the symmetries of the solution. In axially symmetric solutions for example, the states $|jm\rangle$ all have the same projection m_λ of angular momentum along the z-axis so that the expansion becomes:

$$|\lambda\rangle = \sum_j C_j^\lambda |jm_\lambda\rangle \tag{2.10}$$

We may also expect the expansion (2.1) to be rapidly converging and, in particular, limit the expansion of each orbit to one major shell since major shells are separated by large energy gaps. Although we shall see that wavefunctions obtained this way do not yield good quadrupole moments and are not a fair estimate of kinetic energy in deformed nuclei we shall investigate this case in some detail because it is simple and most of the features of Hartree-Fock wavefunctions are already apparent there. We shall therefore call a single-major-shell (S.M.S.) Hartree-Fock calculation one in which the expansion (2.1) is such that each orbit belongs to one major shell of a harmonic oscillator.

We shall investigate separately in the next two Sections the single-major-shell Hartree-Fock calculations and those in which major shell mixing is allowed in the expansion of the orbits.

3. SINGLE MAJOR SHELL HARTREE-FOCK CALCULATIONS

In section 1 we already described the spherical nuclei ^{4}He, ^{16}O, ^{40}Ca as closed shell nuclei. We assumed that nucleons in these nuclei described orbits $|jm\rangle$ of a spherical harmonic oscillator well. When extra nucleons are added to these nuclei the Hartree-Fock (H-F) field is no longer spherical. The first effect of the deformation of the Hartree-Fock field will be to mix the degenerate states which belong to a major shell of the oscillator well. In this chapter we consider this mixing only and we neglect entirely the mixing of states $|jm\rangle$ belonging to different major shells of the oscillator. The expansion (2.1) of the orbits will be:

$$|\lambda\rangle = \sum_{jm} C^{\lambda}_{jm} |jm\rangle$$

where

$$\begin{aligned} &j = 1s^{1/2} && \text{for 1s shell orbits} \\ &j = 1p^{3/2} \text{ and } 1p^{1/2} && \text{for 1p shell orbits} \\ &j = 1d^{5/2},\ 2s^{1/2} \text{ and } 1d^{3/2} && \text{for 2s-1d shell orbits} \\ & && \ldots\text{.etc.} \end{aligned} \tag{3.1}$$

When the expansion (3.1) is used, it is better to rewrite the Hartree-Fock Hamiltonian in such a way as to use the closed shell nuclei as a reference. Let us choose ^{16}O as a reference nucleus. In the ground state of ^{16}O the four 1s-shell orbits and all the 12 1p-shell orbits are filled. For another nucleus the filling will be different and we can compare it to the ^{16}O filling by writing the sum appearing in the potential terms of the Hartree-Fock Hamiltonian (2.6) thus:

$$\sum_{\lambda=1}^{A} = \sum_{\lambda \in 1s,1p} + \sum_{\mu=1}^{M} - \sum_{\nu=1}^{N} \tag{3.2}$$

The orbits μ are the orbits which are filled in the nucleus under consideration but empty in ^{16}O. These we call particle orbits. The orbits ν are the orbits which are empty in the nucleus under consideration but which are filled in ^{16}O. These we call hole orbits. In ^{20}Ne for example we add two neutrons and two protons to the ^{16}O closed shell. This nucleus has M = 4 particle orbits μ in the 2s-1d shell but no hole orbits ν. ^{12}C on the other hand can be obtained by removing four nucleons from ^{16}O, so it has N = 4 hole orbits ν but no particle orbits. Negative parity

states of ^{19}F can be formed by placing four nucleons in the 2s-1d shell and leaving a hole in the 1p-shell. These states have M = 4 particle states μ and N = 1 hole states ν.

The Hartree-Fock Hamiltonian (2.6) can be written:

$$\langle j_1 m_1 |h| j_2 m_2\rangle = \langle j_1 m_1 |t| j_2 m_2\rangle + \sum_{\lambda \in 1s,1p} \langle j_1 m_1, \lambda |v| j_2 m_2, \lambda\rangle + \sum_{\mu=1}^{M} \langle j_1 m_1, \mu |v| j_2 m_2, \mu\rangle - \sum_{\nu=1}^{N} \langle j_1 m_1, \nu |v| j_2 m_2, \nu\rangle \qquad (3.3)$$

The first line of equation (3.3) is simply the Hartree-Fock Hamiltonian of ^{16}O which is spherical and therefore diagonal in the $|jm\rangle$ representation:

$$\langle j_1 m_1 |t| j_2 m_2\rangle + \sum_{\lambda \in 1s,1p} \langle j_1 m_1, \lambda |v| j_2 m_2, \lambda\rangle = \epsilon_{j_1} \delta_{j_1 j_2} \delta_{m_1 m_2} \qquad (3.4)$$

ϵ_j are the energies of the orbits in the ^{16}O ground state field. Indeed because the expansion of the orbits is limited to one major shell only, the sum over λ in Eq.(3.4) is independent of the C^{λ}_{jm} coefficients of the 1s and 1p orbits. This simply reflects the fact that the ^{16}O ground state determinant is unaltered when its orbits are replaced by a unitary linear combination of themselves.

With the help of Eqs.(3.3) and (3.4) the Hartree-Fock Hamiltonian becomes:

$$\langle j_1 m_1 |h| j_2 m_2\rangle = \epsilon_{j_1} \delta_{j_1 j_2} \delta_{m_1 m_2} + \sum_{\mu=1}^{M} \langle j_1 m_1, \mu |v| j_2 m_2, \mu\rangle - \sum_{\nu=1}^{N} \langle j_1 m_1, \nu |v| j_2 m_2, \nu\rangle \qquad (3.5)$$

Only the particle and hole orbits appear in this expression and the kinetic energy is replaced by the single particle energies ϵ_j of the spherical ^{16}O field.

By expressing the sums appearing in Eq.(2.9) in terms of sums over particle and hole orbits as in Eq.(3.2) we find the following expressions for the Hartree-Fock energy:

$$E = E_0 + \frac{1}{2} \sum_{\mu\mu'=1}^{M} \langle \mu\mu' |v| \mu\mu'\rangle + \frac{1}{2} \sum_{\nu\nu'=1}^{N} \langle \nu\nu' |v| \nu\nu'\rangle - \sum_{\mu=1}^{M} \sum_{\nu=1}^{N} \langle \mu\nu |v| \mu\nu\rangle + \sum_{\mu} \langle \mu |K| \mu\rangle - \sum_{\lambda} \langle \lambda |K| \lambda\rangle \qquad (3.6)$$

E_0 is the ^{16}O binding energy

$$E_0 = \sum_{\lambda \in 1s,1p} \langle \lambda | t | \lambda \rangle + \frac{1}{2} \sum_{\lambda, \lambda' \in 1s,1p} \langle \lambda\lambda' | v | \lambda\lambda' \rangle \tag{3.7}$$

E_0 is also independent of the C^{λ}_{jm} coefficients of the 1s and 1p shell orbits. When the Hartree-Fock equations are solved the Hartree-Fock energy can be calculated with the following expression:

$$E = E_0 + \frac{1}{2} \sum_{\mu=1}^{M} \left[\langle \mu | K | \mu \rangle + e_\mu \right] - \frac{1}{2} \sum_{\nu=1}^{N} \left[\langle \nu | K | \nu \rangle + e_\nu \right] \tag{3.8}$$

where K is the ^{16}O spherical field operator

$$\langle j_1 m_1 | K | j_2 m_2 \rangle = \epsilon_{j_1} \delta_{j_1 j_2} \delta_{m_1 m_2} \tag{3.9}$$

The Hartree-Fock equations:

$$h|\mu\rangle = e_\mu |\mu\rangle, \qquad h|\nu\rangle = e_\nu |\nu\rangle \tag{3.10}$$

are solved by the iteration procedure described in section 2.

We have now formulated the Hartree-Fock problem with reference to the ^{16}O closed shell. This formulation is suitable to the description of 2s-1d shell nuclei in which A-16 nucleons are in 2s-1d shell orbits and where the ^{16}O core remains inert. This is just the shell model description of these nuclei, in which the nuclear Hamiltonian is diagonalized among the A-16 nucleon configurations in the 2s-1d shell.

Such diagonalizations are very lengthy and the S.M.S. Hartree-Fock theory is an approximation to the exact diagonalization.

3.1. Additional practical details

In order to carry out a Hartree-Fock calculation it is necessary to choose the oscillator constant $\alpha = (m\omega/\hbar)$, the single particle energies ϵ_j and a suitable effective interaction v.

The oscillator constant α may be chosen so as to fit the experimental mean square radius of the nucleus which is known from electron scattering. Since $\langle jm | r^2 | jm \rangle$ is the same for any state $|jm\rangle$ of a given major shell, the mean square radius is independent of the C^{λ}_{jm} coefficients in a single-major-shell calculation. It is easy to check that for a nucleus which has M_p proton particle orbits and N_p proton hole orbits, the mean value of the monopole operator $\sum_{i=1}^{Z} r_p^2$ is:

$$\langle r^2 \rangle = \frac{1}{\alpha^2} \left[18 + \frac{7M_p}{2} - \frac{5N_p}{2} \right] \tag{3.11}$$

and the mean square radius is $R = (\langle r^2 \rangle / Z)^{\frac{1}{2}}$.

TABLE III. MEAN SQUARE RADII AND CORRESPONDING OSCILLATOR CONSTANTS

Nucleus	Mean-square radius (fermi)	α (fermi^{-1})
^{4}He	1.62	0.756
^{12}C	2.37	0.620
^{16}O	2.64	0.568
^{24}Mg	2.98	0.547
^{28}Si	3.04	0.548
^{32}S	3.19	0.531
^{40}Ca	3.52	0.492

The values of α obtained from mean-square radii measured by electron scattering [1] are shown in Table III.

The mean-square radii are expressed in fermis and α in inverse fermis. Each nucleus should be calculated with the appropriate α.

The single particle energies may be obtained from the ^{16}O and ^{17}O neutron separation energies and from the ^{17}O and ^{15}O spectrum. It follows from equation (3.5) that the eigenstates of h for ^{17}O and ^{15}O which are respectively one particle and one hole in ^{16}O are just the $|jm\rangle$ states of the ^{16}O field. We have seen in section 1 that the difference between the ^{16}O and ^{15}O binding energies is the energy ϵ_j of the highest occupied orbit. ^{15}O has a $1/2^-$ ground state. Thus the energy of the $1p^{1/2}$ state will be given by the binding energy equation:

$$\epsilon_{1p_{\frac{1}{2}}} = {}^{16}\text{O}-{}^{15}\text{O} = -15.67 \text{ MeV} \tag{3.12}$$

^{15}O has a $3/2^-$ excited state at 6.16 MeV which is easily seen in an ^{16}O(p, d)^{15}O experiment in which a neutron is picked up from ^{16}O. This state is probably a $1p^{3/2}$ hole state, of energy:

$$\epsilon_{1p_{\frac{1}{2}}} = -15.67-6.16 = -21.83 \text{ MeV}$$

Similarly ^{17}O has 4.14 MeV more binding than ^{16}O. The ^{17}O ground state is $5/2^+$ so that the energy of the $1d^{5/2}$ state is $\epsilon_{1d^{5/2}} = -4.14$ MeV. The excited states $1/2^+$ and $3/2^+$ at 0.871 MeV and 5.08 MeV, respectively, may be considered as the $2s^{1/2}$ and $1d^{3/2}$ particle states so that

$$\begin{aligned} \epsilon_{2s^{1/2}} &= -4.14+0.87 = -3.27 \text{ MeV} \\ \epsilon_{1d^{3/2}} &= -4.14+5.08 = +0.94 \text{ MeV} \end{aligned} \tag{3.13}$$

The energies ϵ_j may be visualized as the energies of the $|jm\rangle$ states relative to the edge of the ^{16}O spherical Hartree-Fock potential. When the energies ϵ_j are taken from experimental binding energies it should not be forgotten that they represent the sum (3.4) calculated with the oscillator constant α which yields the ^{16}O mean square radius. The ϵ_j's will change when a different value of α is used in another nucleus. The variation of ϵ_j with α may be taken into account by considering the ^{40}Ca Hartree-Fock closed shell solution. In ^{40}Ca the Hartree-Fock orbits are also $|jm\rangle$ states and the energy of the orbits in ^{40}Ca are:

$$e_j = \epsilon_j + \sum_{\mu=1}^{24} \langle j,\mu|v|j,\mu\rangle \tag{3.14}$$

since the 24 particle orbits μ of the 2s-1d shell are filled in ^{40}Ca. The energies e_j are known experimentally from pick-up experiments on ^{40}Ca.

$$\left.\begin{aligned} e_{1d^{5/2}} &= -21.73 \text{ MeV} \\ e_{2s^{1/2}} &= -18.20 \text{ MeV} \\ e_{1d^{3/2}} &= -15.73 \text{ MeV} \end{aligned}\right\} \tag{3.15}$$

We can always write the two-body interaction in the form $V_0\, v(12)$ where V_0 measures the strength of the interaction. Then we have the set of four equations:

$$\begin{aligned} e_j &= \epsilon_j + V_0 \sum_{\mu=1}^{24} \langle j,\mu|v|j,\mu\rangle \\ E_{^{40}Ca} - E_{^{16}O} &= 2\sum_j (2j+1)\epsilon_j + \frac{1}{2} V_0 \sum_{\mu\mu'=1}^{24} \langle \mu\mu'|v|\mu\mu'\rangle \end{aligned} \tag{3.16}$$

where $j = 1d^{5/2}$, $2s^{1/2}$ and $1d^{3/2}$.

The unknown quantities in equations (3.16) are V_0 and the three ϵ_j's. The latter represent the expression (3.4) calculated with $\alpha = 0.492$ fm^{-1}, the ^{40}Ca value. The e_j's are given in Eq.(3.15) and the difference $E_{^{40}Ca} - E_{^{16}O}$ between the ^{40}Ca and ^{16}O binding energies is found from Table I:

$$E_{Ca\text{-}40} - E_{O\text{-}16} = -416.97 + 142.88 = -274.09 \text{ MeV}$$

The sums in Eq.(3.16) must be calculated with the interaction chosen and with $\alpha = 0.492$ fm^{-1}. For example if a Rosenfeld force

$$v(12) = V_0\, e^{-(r/\mu)^2} \frac{\vec{\tau}_1 \cdot \vec{\tau}_2}{3} [0.3 + 0.7\, \vec{\sigma}_1 \cdot \vec{\sigma}_2] \tag{3.17}$$

with $\mu = 1.48$ fm is used, the solutions of Eqs.(3.16) will yield a strength

$$V_0 = +70.82 \text{ MeV}$$

and single particle energies ϵ_j to be used in ^{40}Ca:

$$\epsilon_{1d^{5/2}} = -6.19, \qquad \epsilon_{2s^{1/2}} = -3.22, \qquad \epsilon_{1d^{3/2}} = -0.25 \tag{3.18}$$

Since the ϵ_j for $\alpha = 0.492$ in ^{40}Ca are quite similar to the ones for $\alpha = 0.568$ in ^{16}O it may be reasonable to extrapolate them linearly for the values of α in the intermediate nuclei. The results presented in these lectures will have been obtained this way.

This method has the advantage of treating symmetrically ^{16}O and ^{40}Ca nuclei which open and close the 2s-1d shell. The advantage of using experimental values of ϵ_j comes from the fact that the central forces commonly used in shell-model calculations fail to yield the correct ϵ_j's when directly calculated from Eq.(3.4). A central force will yield no spin-orbit splitting for example.

The choice of an effective interaction is more delicate. One might choose an effective interaction derived from realistic potentials which fit scattering data [3]. But if central forces are used the strength is fixed by Eqs.(3.16) and in even-even N = Z nuclei only the components S and G (see Eq.(1.14)) contribute significantly. Large gaps are only obtained with a small value of S compared to G; a Rosenfeld force may then be adequate for most N = Z nuclei of the 2s-1d shell. At the present time a systematic investigation of nuclei with neutron excess is not completed.

3.2. Solutions of the Hartree-Fock equations in even-even N = Z nuclei

Kelson [3] was the first to solve the Hartree-Fock equations for even-even N = Z nuclei of the 2s-1d shell. Results obtained with the Rosenfeld force [17] are shown in Tables IV, V, VI and VII. On Fig. 5 the energies of the Hartree-Fock orbits are plotted, and the eigenvalue of J_z is marked wherever the Hartree-Fock solution has axial symmetry. It is seen that the energy of the highest occupied orbit is remarkably constant, and that the gap is a slowly decreasing function of A. The gap and the binding of the highest occupied orbit are somewhat smaller than the experimental ones shown in Table IIb. They both increase when major shells are allowed to mix. Bar-Touv and Kelson [2] found that ^{24}Mg and ^{32}S have an ellipsoidal solution with a lower energy and a larger gap than the axially symmetric solution. In the ellipsoidal solution the Hartree-Fock Hamiltonian no longer commutes with J_z but it retains the ellipsoidal symmetry of rotation by an angle π about the x, y and z axes:

$$[h, \exp(i\pi J_y)] = [h, \exp(i\pi J_x)] = [h, \exp(i\pi J_z)] = 0 \tag{3.19}$$

TABLE IV. AXIALLY SYMMETRIC SOLUTIONS

The first three lines give the values of the oscillator constant and of the three single particle energies of the $1d^{5/2}$, $2s^{1/2}$ and $1d^{3/2}$ states; the underlined numbers are the energies of the H.F. orbits; the energy of each orbit is followed by its components; the energies of K=1/2 orbits are followed by their components on the $1d^{5/2}_{1/2}$, $2s^{1/2}_{1/2}$ and $1d^{3/2}_{1/2}$ states respectively; the energies of K=3/2 orbits are followed by their components on the $1d^{5/2}_{3/2}$ and $1d^{3/2}_{3/2}$ states; orbits not followed by components are K=5/2 orbits which are pure $1d^{5/2}_{5/2}$ states. The bottom line gives the value of the H.F. energy (3.6). The radial wavefunction of the 2s state is proportional to $(3/2-\alpha^2r^2)\exp(-\alpha^2r^2/2)$.

^{20}Ne	^{24}Mg	^{28}Si oblate	^{28}Si prolate	^{32}S oblate	^{32}S prolate	^{36}At
α = 0.559	α = 0.547	α = 0.548	α = 0.548	α = 0.531	α = 0.531	α = 0.496
$d^{5/2}$= -4.38	$d^{5/2}$= -4.71	$d^{5/2}$= -4.68	$d^{5/2}$= -4.68	$d^{5/2}$= -5.14	$d^{5/2}$= -5.14	$d^{5/2}$= -6.09
$s^{1/2}$= -3.26	$s^{1/2}$= -3.26	$s^{1/2}$= -3.26	$s^{1/2}$= -3.26	$s^{1/2}$= -3.25	$s^{1/2}$= -3.25	$s^{1/2}$= -3.22
$d^{3/2}$= 0.79	$d^{3/2}$= 0.605	$d^{3/2}$= 0.62	$d^{3/2}$= 0.62	$d^{3/2}$= 0.36	$d^{3/2}$= 0.36	$d^{3/2}$= -0.18
814.58 [a]	-16.33 [a]	-18.53 [a]	-19.37 [a]	-18.26 [a]	-19.74 [a]	-20.92 [a]
-0.7576	-0.7895	-17.98 [a]	-0.7763	-0.7475	-0.8846	-19.78 [a]
-0.5273	0.5459	-0.5783	0.6188	-0.5902	0.4641	0.9941
-0.3847	0.2806	-0.7596	0.1203	0.3048	0.0203	0.1084
-6.58	-11.99 [a]	0.2977	-17.97 *	-17.97 [a]	-19.91 [a]	-18.80 [a]
-0.9932	0.9704	-14.99 [a]	-0.9531	-16.44 [a]	-0.9753	0.8054
0.1167	-0.2414	0.6935	0.3027	-0.5632	0.2209	0.5873
-5.19	-9.86	0.7204	-14.68 *	0.8064	-15.51 [a]	0.0801
-0.6357	-0.5443	-8.32	-0.4572	0.1802	-0.2985	-15.82 [a]
-0.7298	-0.4114	0.7204	-0.4212	-15.18 [a]	-0.5350	-0.4393
-0.2516	-0.7311	-0.6935	-0.7833	0.8794	-0.7903	0.6822
-5.14	-7.52	-8.11	-9.28	0.4761	-14.33 [a]	-0.5844
-2.36	-4.91	0.8044	-6.50	-11.31	-10.23	-14.74 [a]
-0.1481	0.2837	-0.4702	0.4340	-0.4761	0.2209	0.1084
0.4351	0.7299	0.3630	0.6630	0.8794	0.9753	-0.9941
-0.8881	-0.6219	-4.10	-0.6099	-9.79	-10.03	-10.14
-0.26	-3.01	0.1358	-4.70	0.3522	0.3559	0.3979
0.1167	0.2414	-0.4494	0.3027	0.0370	0.7060	-0.4355
0.9932	0.9704	-0.8830	0.9531	0.9352	0.6123	-0.8075
-35.78	-73.14	-123.00	-122.01	-169.20	-168.80	-220.48

[a] Occupied orbit

TABLE V. ELLIPSOIDAL SOLUTIONS OF ^{24}Mg AND ^{32}S

Magnesium-24	$\alpha = 0.547$	$d^{5/2} = -4.71$		$s^{1/2} = -3.26$	$d^{3/2} = 0.61$	$E = -76.73$
e_λ	$d^{5/2}_{-3/2}$	$d^{5/2}_{1/2}$	$d^{5/2}_{5/2}$	$2s^{1/2}_{1/2}$	$d^{3/2}_{1/2}$	$d^{3/2}_{-3/2}$
-16.89[a]	-0.2118	-0.7794	0.1213	0.5327	0.1544	-0.1595
-14.48[a]	0.7553	0.1051	0.0870	0.3343	0.5201	0.1690
- 7.90	0.3945	-0.5034	-0.6553	-0.3544	-0.1644	0.0945
- 6.94	-0.3558	0.2971	-0.7253	0.3311	0.3828	-0.0545
- 4.92	-0.2788	-0.1976	0.1486	-0.5581	0.6951	0.2577
- 2.45	-0.1570	-0.0294	-0.0120	0.2403	-0.2212	0.9315
Sulphur-32	$\alpha = 0.531$	$d^{5/2} = -5.14$		$s^{1/2} = -3.24$	$d^{3/2} = 0.35$	$E = -170.64$
-19.99[a]	-0.1048	0.2115	-0.8853	0.3995	-0.0297	-0.0044
-19.19[a]	0.6669	-0.5839	-0.3381	-0.2743	-0.1055	-0.1167
-16.31[a]	0.5865	0.4134	0.2452	0.4427	-0.4771	-0.0367
-15.46[a]	0.1133	0.4510	-0.0696	-0.3552	0.2246	-0.7760
- 9.93	0.1931	0.4858	-0.1752	-0.5901	-0.0246	0.5893
- 8.26	0.3874	0.0624	0.0788	0.3080	0.8422	0.1885

[a] Occupied orbit

TABLE VI. SPHERICAL CLOSED SHELL SOLUTIONS

Energies $e^{5/2}$, $e^{1/2}$ and $e^{3/2}$ of the $1d^{5/2}$, $2s^{1/2}$ and $1d^{3/2}$ orbits in the spherical field of closed shell solutions of various nuclei. The first line indicates the value of the oscillator constant used in each nucleus. The next three lines are the values of the single particle energies ϵ_j used in the Hartree-Fock Eqs. (3.5). The bottom line is the value of the Hartree-Fock energy $E-E_0$ relative to the ^{16}O energy given by Eq. (3.8).

Nucleus	^{16}O[a]	^{28}Si	^{32}S	^{36}A	^{40}Ca[a]
α	0.568	0.548	0.531	0.496	0.492
$\epsilon^{5/2}$	-4.14	-4.68	-5.14	-6.08	-6.19
$\epsilon^{1/2}$	-3.27	-3.26	-3.25	-3.22	-3.22
$\epsilon^{3/2}$	0.93	0.62	0.36	-0.18	-0.25
$e^{5/2}$	-4.14	-14.41[b]	-16.19[b]	-20.34[b]	-21.73[b]
$e^{1/2}$	-3.27	-10.18	-17.08[b]	-11.21	-18.20[b]
$e^{3/2}$	0.93	- 8.96	-11.65	-14.44[b]	-15.73[b]
E	0	-114.57	-168.64	-217.10	-274.09

[a] Closed shell

[b] The single particle energies and the interaction strength are chosen so as to fit the observed single particle energies ϵ_j in ^{16}O and e_j in ^{40}Ca, as well as the ^{40}Ca binding energy.

TABLE VII. CARBON-12 SOLUTIONS

The table of deformed solutions lists the energies e_λ of the Hartree-Fock orbits and their components on the states j of the p-shell and of the 2s-1d shell. The Hartree-Fock energy E is the ^{12}C binding energy relative to the ^{16}O binding energy. The single particle energies ϵ_j used in the Hartree-Fock Hamiltonian were the same for both solutions.

^{12}C deformed solution					$\alpha = 0.620$		E = 41.06		
e_λ	$1p^{3/2}_{1/2}$	$1p^{3/2}_{3/2}$	$1p^{1/2}_{1/2}$	$1d^{5/2}_{1/2}$	$1d^{5/2}_{3/2}$	$1d^{5/2}_{5/2}$	$1s^{1/2}_{1/2}$	$1d^{3/2}_{1/2}$	$1d^{3/2}_{3/2}$
-18.29[a]	0	1	0	0	0	0	0	0	0
-14.79[a]	0.7343	0	0.6789	0	0	0	0	0	0
- 2.71	0	0	0	0	0	1	0	0	0
- 1.84	0.6789	0	-0.7343	0	0	0	0	0	0
- 1.64	0	0	0	-0.2450	0	0	-0.9652	0.0914	0
0.13	0	0	0	0	0.8521	0	0	0	0.5234
3.40	0	0	0	0.9493	0	0	-0.2196	0.2251	0
4.35	0	0	0	0	0.5234	0	0	0	-0.8521
8.01	0	0	0	0.1972	0	0	-0.1419	-0.9700	-

^{12}C spherical solution			$\alpha = 0.620$	E = 48.56	
J	$1p^{3/2}$	$1p^{1/2}$	$1d^{5/2}$	$2s^{1/2}$	$1d^{3/2}$
ϵ_j	-22.01	-15.85	-4.15	-3.28	0.93
e_j	-13.24[a]	- 8.43	+0.83	-1.19	+5.12

[a] Occupied orbit

With these symmetries the expansion of an orbit μ may be limited to the following states:

$$d^{5/2}_{5/2} \quad d^{5/2}_{1/2} \quad d^{5/2}_{-3/2} \quad d^{3/2}_{1/2} \quad d^{3/2}_{-3/2}, \quad \text{and} \quad S^{1/2}_{1/2} \tag{3.20}$$

and to each orbit $|\mu\rangle$ there corresponds another filled orbit $e^{i\pi J_y}|\mu\rangle$ orthogonal to $|\mu\rangle$. This expansion ensures further that the x, y and z-axes are the principal axes of the ellipsoidal field.

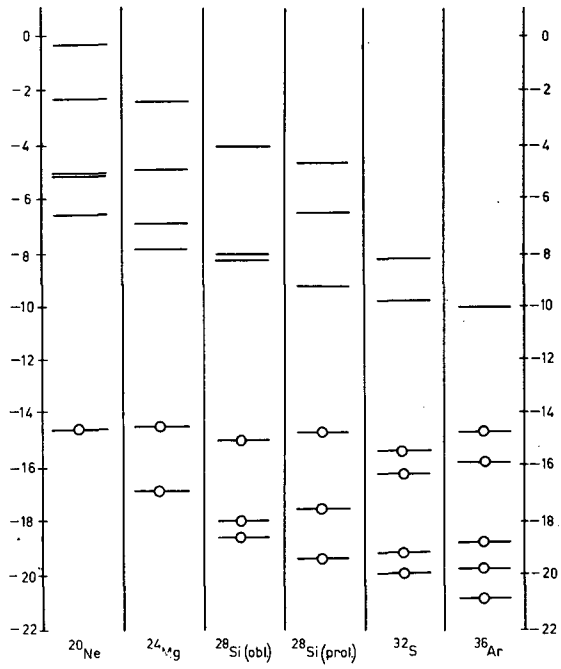

FIG. 5. Energies e_μ of the Hartree-Fock orbits of even-even nuclei of the 2s-1d shell

Compare the orbits and the Hartree-Fock energies of the ellipsoidal and axially symmetric solution of ^{24}Mg. The gap is larger for the ellipsoidal solution suggesting its greater stability.

Spherical minima are only obtained for ^{16}O and ^{40}Ca. Compare the orbits and the Hartree-Fock energies of the spherical and deformed solutions of ^{12}C, ^{28}Si and ^{32}S. In each case a better energy and a reasonable gap is obtained with the deformed solution, although the ^{32}S solutions are very close in energy.

3.3. The effect of spin-orbit splitting

In the absence of spin-orbit splitting the Hartree-Fock solution of even-even N = Z nuclei converges towards the L-S coupling wavefunction discussed in section 1. The orbits factorize into spin and space parts

as in Eq.(1.6). Hartree-Fock solutions with no spin orbit splitting may be obtained by assuming the $\epsilon_{1d^{3/2}}$-$\epsilon_{1d^{5/2}}$ splitting is due to a term of the form $a\vec{\ell}\cdot\vec{S}$ and letting $a \to 0$. The energies $\epsilon_{1d^{3/2}}$ and $\epsilon_{1d^{5/2}}$ then come to a common energy equal to

$$\frac{1}{5}(2\epsilon_{1d^{3/2}} + 3\epsilon_{1d^{5/2}})$$

The ^{20}Ne occupied orbit then becomes:

$$-0.629 d^{5/2}_{1/2} + 0.584 S^{1/2}_{1/2} - 0.513 d^{3/2}_{1/2} = (-0.812 d_0 + 0.584 S_0)\uparrow \qquad (3.21)$$

and the ^{24}Mg occupied orbits become:

$$(0.739 d_0 - 0.653 S_0 - 0.12 d_2 - 0.12 d_{-2})\uparrow$$

$$\frac{1}{\sqrt{2}}(d_1 + d_{-1})\uparrow$$

States in which four nucleons fill each orbit forming closed shells of spin and isospin have a zero expectation value of the spin-orbit splitting $a\vec{\ell}\cdot\vec{S}$. Considered as a perturbation the first order effect of the spin-orbit on the energy is zero. In fact the effect of the spin-orbit splitting on the Hartree-Fock energy of ^{20}Ne and ^{24}Mg is quite small. When the full spin orbit splitting is switched on the wavefunctions of the orbits (which can be read off Table V) are:

in ^{20}Ne:

$$(-0.832 d_0 + 0.527 s_0)\uparrow - 0.179 d_1\downarrow$$

in ^{24}Mg:

$$(-0.70 d_0 + 0.53 s_0 + 0.12 d_2 + 0.05 d_{-2})\uparrow + (-0.26 d_{-1} - 0.37 d_1)\downarrow$$

$$(0.75 d_{-1} + 0.47 d_1)\downarrow + (0.19 d_{-2} + 0.09 d_2 - 0.25 d_0 + 0.33 s_0)\uparrow$$

It is seen that the spin-orbit splitting introduces significant changes in the orbital wavefunctions compared to their L-S limit given by Eqs.(3.21) and (3.22). The energy which is a stationary quantity will not be seriously affected by the change in the wavefunction due to the spin-orbit splitting. Other quantities such as magnetic moments of odd-A nuclei are sensitive to the spin orbit splitting as we shall see. A small change in the energy does not guarantee a small change in all the other properties of a nuclear wavefunction.

The gap separating filled and empty orbits is introduced by the spin-orbit splitting, and it is greatest in the L-S limit of vanishing spin-orbit splitting. The large gap hinders the effect of the spin orbit term $a\vec{\ell}\cdot\vec{S}$ in so far as it makes it difficult to produce particle-hole excitations which are the first order corrections to the L-S wavefunction. But as the

nucleus gets larger, the oscillator constant becomes smaller (see Table IV) and this effectively reduces the interaction v and hence the gap. Distortions due to the spin orbit term which does not decrease become more important and this is particularly true of ^{32}S in which the ellipsoidal, the axially symmetric prolate and oblate and the spherical closed shell solutions are quite close as seen on Fig. 6.

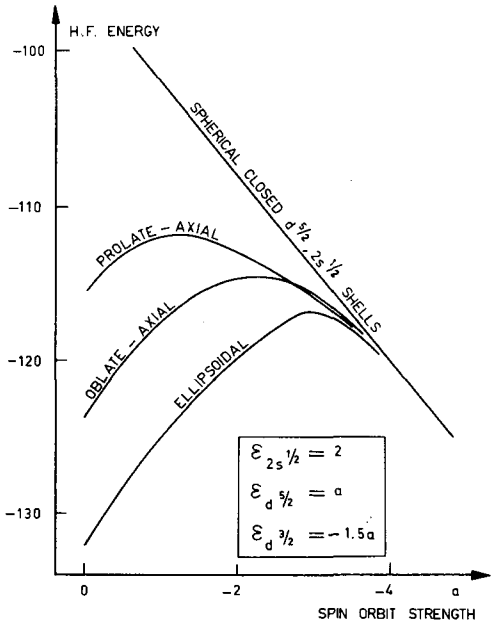

FIG. 6. Energies of the spherical closed shell and various deformed H.F. solutions of ^{32}S plotted against the spin-orbit splitting of the $d^{5/2}$ and $d^{3/2}$ states [6]

Thus in ^{32}S the spin-orbit splitting apparently destroys the stability of the deformed intrinsic state against β and γ vibrations. We shall see evidence for this in the magnetic moment of ^{33}S.

Obviously the spin-orbit splitting is far more effective in lowering the spherical solutions. For example if it is increased so as to lower the energy $\epsilon_{1d\,5/2}$ of the $d^{5/2}$ state by 1 MeV, the spherical solutions of ^{28}Si and ^{32}S, in which twelve particles fill the $d^{5/2}$ shell, are lowered by 12 MeV.

It should be borne in mind that this discussion of spin-orbit effects has been limited to the effects of the spin-orbit splitting occurring in the single particle energies ϵ_j. A better discussion, which has not yet been made, would be obtained with a force v which could reproduce the spin-orbit splitting in the ϵ_j's from Eq. (3.4) and which could hence evaluate the spin-orbit interaction between the nucleons in the 2s-1d shell. The latter interaction has been neglected here.

3.4. Ellipsoidal symmetry and maximum spatial symmetry

We have seen in Eqs. (3.21) and (3.22) that in the absence of spin-orbit splitting the Hartree-Fock solution converges to an L-S solution

in which four nucleons fill the same orbit in configuration space. Eqs.(3.23) show that this remains true to a considerable extent even in the presence of spin-orbit splitting. An L-S solution in which four nucleons occupy the same spatial orbit is a wavefunction with maximum spatial symmetry. Indeed the Hartree-Fock wavefunctions are quite close to the wavefunctions obtained from Elliott's (λ, μ) classification scheme [7], or to Nilsson's asymptotic wavefunctions [8]. Maximum spatial symmetry wavefunctions come close to minimizing the potential energy of a central force. The ellipsoidal solution of ^{24}Mg, which does not have axial symmetry, is nothing but an attempt of the wavefunction to have maximum spatial symmetry [5, 9].

In ^{20}Ne the orbit has both spatial maximum symmetry and axial symmetry. But in ^{24}Mg the only way to obtain axial symmetry with the d_1 and $d_{-1\downarrow}$ orbit would be to fill the $d_{1\uparrow}$ and $d_{-1\downarrow}$ orbits. Then the nucleons with spin up and down are not in the same spatial orbit and the spatial symmetry is partly destroyed. But if the neutrons are placed in the $(d_1 + d_{-1})$ orbit then axial symmetry is destroyed but spatial symmetry is preserved. In fact the Hartree-Fock calculations entirely confirm the symmetries predicted by Elliott's (λ, μ) classification scheme.

3.5. The ^{28}Si degeneracy

^{28}Si has twelve particles in the 2s-1d shell. Exactly half of the 2s-1d shell orbits are occupied in ^{28}Si. There are two near degenerate solutions for this nucleus which has opposite signs for the quadrupole moment [6]. They are both shown in Table IV. One is obtained by filling a $K = 1/2$, $3/2$ and $5/2$ orbit and the other is obtained by filling the remaining two $K = 1/2$ orbits and one $K = 3/2$ orbit. The former solution has a negative quadrupole moment and oblate shape, the latter has a positive quadrupole moment and prolate shape. The two solutions are very orthogonal to one another, and both have a large gap.

The occupied orbits of the oblate solution are not exactly the same as the empty orbits of the prolate solution essentially because of the spin orbit splitting.

The problem of the possible mixing of the Hartree-Fock solutions which differ by the rearrangement of a large number of particles is not yet solved.

4. ROTATIONAL BANDS IN THE 2s-1d SHELL NUCLEI

How do we relate the Hartree-Fock wavefunction $|\varphi\rangle$ to the actual nuclear states of a given angular momentum? There are basically two methods used to obtain the nuclear states which have good angular momentum from Hartree-Fock wavefunctions which do not:

A – The adiabatic approximation

B – Angular momentum projection.

Method A is an approximation of method B.

4.1. Method A: the adiabatic approximation

This method is based on the unified model of Bohr and Mottelson [10] and it is the one used by Nilsson [8]. The Hartree-Fock wavefunction

$|\varphi\rangle$ is assumed to be a state permanently deformed in a frame of reference attached to the nucleus. This state and frame of reference are often called intrinsic to the nucleus. When the intrinsic Hartree-Fock state $|\varphi\rangle$ is expected to be very stable, as the large energy gap suggests, the degrees of freedom which require least energy are expected to be rotations of the intrinsic state. In such a rotation the nucleus behaves like a symmetric top and the rotation will produce states of angular momentum J and projection M on the z-axis of the laboratory frame which are described by the symmetric top wavefunctions $D^{J*}_{MK}(\Omega)$.

The $D^{J}_{MK}(\Omega)$ wavefunction is defined as:

$$D^{J}_{MK}(\Omega) = \langle JM|R(\Omega)|JK\rangle \tag{4.1}$$

where Ω represents three Euler angles (α, β, γ) and R is the rotation operator:

$$R(\Omega) = e^{-i\alpha J_z}\ e^{-i\beta J_y}\ e^{-i\gamma J_z} \tag{4.2}$$

Ω represents the orientation of the nucleus, to which the intrinsic frame of reference is attached, with respect to the laboratory frame, K is the projection of the angular momentum of the Hartree-Fock state $|\varphi_K\rangle$ along the z-axis of the intrinsic frame.

Consider an even-even nucleus with $K = 0$.

If its Hartree-Fock state $|\varphi_0\rangle$ is stable, the motion of the nucleons in the intrinsic frame is assumed to be uncoupled to the rotation. The wavefunction of the nucleus with spin J and projection M will thus factorize:

$$|\Psi^{J}_{M0}\rangle = \sqrt{\frac{2J+1}{8\pi^2}}\, D^{*J}_{M_0}(\Omega)|\varphi_0\rangle \tag{4.3}$$

The co-ordinate Ω and the co-ordinates of the Hartree-Fock wavefunction $|\varphi_0\rangle$ in the intrinsic frame are treated as independent variables. That the wavefunction (4.3) represents a nucleus rotating with angular momentum J is obvious from the relation

$$D^{*J}_{M0}(\alpha, \beta, \gamma) = \sqrt{\frac{4\pi}{2j+1}}\, Y^{J}_{M}(\beta, \alpha) \tag{4.4}$$

where $Y^{J}_{M}(\beta, \alpha)$ is a spherical harmonic.

The wavefunction (4.3) is the eigenfunction of the Hamiltonian

$$H = \frac{\vec{R}^2}{2\theta} + H_0$$

where $\vec{R}$ is the angular momentum operator of the rotating intrinsic frame. It acts only on the variable Ω:

$$\vec{R}^2 D^{J*}_{MK}(\Omega) = J(J+1)\, D^{J*}_{MK}(\Omega) \tag{4.5}$$

H_0 is the Hartree-Fock Hamiltonian describing the independent particle motion in the deformed Hartree-Fock field:

$$H_0 = \sum_{\lambda} e_\lambda b_\lambda^+ b_\lambda \tag{4.6}$$

and it acts only on the intrinsic state $|\varphi_0\rangle$:

$$H_0|\varphi_0\rangle = E_0|\varphi_0\rangle = \left(\sum_{\lambda=1}^{A} e_\lambda\right)|\varphi_0\rangle$$

e_λ are the energies of the Hartree-Fock orbits λ.

Thus the spectrum of the states $|\Psi^J_{M0}\rangle$ generated by the intrinsic state $|\varphi_0\rangle$ is:

$$E_J = \langle\Psi^J_{M0}|H|\Psi^J_{M0}\rangle = E_0 + \frac{1}{2\theta}J(J+1) \tag{4.7}$$

A spectrum of the form (4.7) is called a rotational band, and θ is the moment of inertia of the nucleus.

When a particle or hole is added to an axially symmetric core $|\varphi_0\rangle$ it will go into an orbit λ which has definite angular momentum projection $K = m_\lambda$ along the intrinsic z-axis.

The intrinsic state now has angular momentum K along the z intrinsic axis and instead of the wavefunction (4.3) the following wavefunction must be used to represent the nucleus in a state of spin J.

$$|\Psi^J_{MK}\rangle = \sqrt{\frac{2J+1}{16\pi^2}}\left\{D^{J*}_{MK}(\Omega)|\varphi_K\rangle + (-)^{J+K} D^{J*}_{M-K}(\Omega)|\varphi_{-K}\rangle\right\} \tag{4.8}$$

$|\varphi_K\rangle$ is the particle or hole intrinsic state,

$|\varphi_K\rangle = b^\dagger_\lambda|\varphi_0\rangle$ or $b_\lambda|\varphi_0\rangle$,

$|\varphi_{-K}\rangle = (\exp -i\pi J_y)|\varphi_K\rangle$

K equals m_λ for a particle state and $-m_\lambda$ for a hole state.

The second term in Eq. (4.8) is introduced because of the $\exp(-i\pi J_y)$ symmetry. When K = 0 the wavefunction (4.8) reduces to the wavefunction (4.3) for even values of J and vanishes for odd values of J. Thus the rotational band generated by a K = 0 intrinsic state with the $\exp(-i\pi J_y)$ symmetry will consist of only even values of J.

The Hamiltonian of the odd system is

$$H = \frac{\vec{R}^2}{2\theta} + H_0 = \frac{(\vec{J}-\vec{j})^2}{2\theta} + H_0 \tag{4.9}$$

since the total angular momentum $\vec{J}$ is the sum $\vec{R}+\vec{j}$ of the deformed core and odd particle angular momenta respectively.

The particle operator $\vec{j}$ acts on the intrinsic state $|\varphi_K\rangle$ and $\vec{J}$ acts on the variable Ω. We now have

$$H_0|\varphi_K\rangle = E_0 + e_\lambda \text{ for particle states}$$

$$= E_0 - e_\lambda \text{ for hole states}$$

The cross-term $\vec{J}\cdot\vec{j}$ in the Hamiltonian (4.9) will mix states $|\Psi^J_{MK}\rangle$ with different values of K. Since the orbits e_λ are quite close to one another this mixing is not negligible. The term $\vec{J}\cdot\vec{j}$ is called the Coriolis perturbation. So H must be diagonalized among the possible $|\Psi^J_{MK}\rangle$ configurations. The Coriolis perturbation affects the diagonal energies of K = 1/2 bands, and it is readily shown that the spectrum generated by a R = 1/2 band is

$$E_J = \frac{1}{2\theta}\left[J(J+1)+a(-)^{J+1/2}\delta_{K,1/2}(J+1/2)\right] \tag{4.10}$$

where $a = \sum_j C_j^{\lambda^2}(j+1/2)(-)^{j+1/2}$

This perturbation which is special to K = 1/2 bands is called the decoupling of K = 1/2 bands.

To illustrate how to use the wavefunction (4.6) let us calculate a matrix element of a tensor operator T^k_q of rank k and component q. Any operator may be expressed as a sum of tensor operators.

The matrix element is calculated in the laboratory frame and we must first express T^k_q in the intrinsic frame:

$$T^k_q \rightarrow \sum_\nu D^{k*}_{q\nu}(\Omega)\, T^k_\nu \tag{4.11}$$

The tensor T^k_ν now operates on the intrinsic wavefunction $|\varphi_K\rangle$. Using the relation

$$\int d\Omega\, D^{J_1}_{M_1K_1}(\Omega)\; D^{k*}_{q\nu}(\Omega)\; D^{J_2*}_{M_2K_2}(\Omega) = \frac{8\pi^2}{2J_1+1}\begin{bmatrix} J_2 & k & J_1 \\ M_2 & q & M_1\end{bmatrix}\begin{bmatrix} J_2 & k & J_1 \\ K_2 & \nu & K_1\end{bmatrix} \tag{4.12}$$

the matrix element of T^k_q between wavefunctions (4.6) is:

$$\langle \Psi^{J_1}_{M_1K_1} | T^k_q | \Psi^{J_2}_{M_2K_2}\rangle = \left(\frac{2J_2+1}{2J_1+1}\right)^{\frac{1}{2}}\begin{bmatrix} J_2 & k & J_1 \\ M_2 & q & M_1\end{bmatrix}$$

$$\sum_\nu \begin{bmatrix} J_2 & k & J_1 \\ K_2 & \nu & K_1\end{bmatrix}\langle K_1|T^k_\nu|K_2\rangle + (-)^{J_1+K_1}\begin{bmatrix} J_2 & k & J_1 \\ K_2 & \nu & -K_1\end{bmatrix}\langle -K_1|T^k_\nu|K_2\rangle \tag{4.13}$$

In expression (4.13) $|K\rangle$ and $|-K\rangle$ are the intrinsic states $|\varphi_k\rangle$ and $(\exp -i\pi J_y)\,|\varphi_k\rangle$.

$\begin{bmatrix} j_1 & j_2 & J \\ m_1 & m_2 & M \end{bmatrix}$ are Clebsch-Gordan coefficients (not 3-j symbols). The first Clebsch-Gordan coefficient is a result of the Wigner-Eckart theorem. The second and third Clebsch-Gordan coefficients are a result of our model according to which the states $|\Psi^J_{MK}\rangle$ are generated from an intrinsic state $|\varphi_k\rangle$, they yield the additional selection rule:

$$|K_1 - K_2| \leq k \tag{4.14}$$

4.2. Method B: angular momentum projection

An imperfection of the adiabatic model is apparent when one counts the number of variables of the wavefunction (4.8). The intrinsic state $|\varphi_k\rangle$ is already a function of all the dynamical variables of the system including Ω which was treated as an independent variable. The adiabatic model is none the less very useful because of its simplicity and it is often a very good approximation. We shall see in this section that the method of angular momentum projection produces a wavefunction $|\Psi^J_{MK}\rangle$ with no redundant variables and that the adiabatic model is an approximation of the former. In the angular momentum projection method the wavefunction $|\Psi^J_{MK}\rangle$ is [11]

$$|\Psi^J_{MK}\rangle = \frac{1}{N_{JK}^{1/2}} \frac{2J+1}{8\pi^2} \int d\Omega\, D^{J*}_{MK}(\Omega)\, R(\Omega)\, |\varphi_K\rangle \tag{4.15}$$

The wavefunction (4.15) is normalized when

$$N_{JK} = \frac{2J+1}{8\pi^2} \int d\Omega\, D^{J*}_{KK}(\Omega) \langle \varphi_K | R(\Omega) | \varphi_K \rangle \tag{4.16}$$

For $M = K$ Eq.(4.15) is a projection of $|\varphi_K\rangle$ on the subspace of angular momentum J because it is easily checked that

$$\frac{2J+1}{8\pi^2} \int d\Omega\, D^{J*}_{KK}(\Omega)\, R(\Omega) = \sum_{\alpha} |\alpha JK\rangle \langle \alpha JK| \tag{4.17}$$

where α is any complete set of quantum numbers other than J and K.

Let us calculate a matrix element of tensor operator T^k_q between states (4.15)

$$\langle \Psi^{J_1}_{M_1K_1} | T^k_q | \Psi^{J_2}_{M_2K_2} \rangle = \frac{(2J_1+1)(2J_2+1)}{(8\pi^2)^2 N^{1/2}_{J_1K_1} N^{1/2}_{J_2K_2}}$$

$$\times \int d\Omega_1\, d\Omega_2\, D^{J_1}_{M_1K_1}(\Omega_1)\, D^{J_2*}_{M_2K_2}(\Omega_2) \langle K_1 | R^{-1}(\Omega_1)\, T^k_q\, R(\Omega_2) | K_2 \rangle \tag{4.18}$$

We can reduce expression (4.18) to a single integral. T^k_q being a tensor operator has the following commutation rules with the rotation operator $R(\Omega_2)$:

$$T^k_q R(\Omega_2) = \sum_\nu D^{*k}_{q\nu}(\Omega_2)\, R(\Omega_2)\, T^k_\nu \tag{4.19}$$

Rotations form a group, hence the product $R^{-1}(\Omega_1)\, R(\Omega_2)$ is equal to a single rotation $R(\Omega_3)$:

$$R^{-1}(\Omega_1)\, R(\Omega_2) = R(\Omega_3) \quad \text{or} \quad R(\Omega_1) = R(\Omega_2)\, R^{-1}(\Omega_3) \tag{4.20}$$

Taking matrix elements of (4.20) between states $|J_1 M_1\rangle$ and $|J_1 K_1\rangle$ one obtains

$$D^{J_1}_{M_1 K_1}(\Omega_1) = \sum_\mu D^{J_1}_{M_1 \mu}(\Omega_2)\; D^{J_1 *}_{K_1 \mu}(\Omega_3) \tag{4.21}$$

Equations (4.19), (4.21) and (4.12) yield the desired matrix element:

$$\langle \Psi^{J_1}_{M_1 K_1} | T^k_q | \Psi^{J_2}_{M_2 K_2} \rangle = \frac{(2J_2+1)}{8\pi^2 N^{1/2}_{J_1 K_1} N^{1/2}_{J_2 K_2}} \begin{bmatrix} J_2 & k & J_1 \\ M_2 & q & M_1 \end{bmatrix}$$

$$\times \sum_{\mu\nu} \begin{bmatrix} J_2 & k & J_1 \\ K_2 & \nu & \mu \end{bmatrix} \int d\Omega\; D^{*J_1}_{K_1 \mu}(\Omega) \langle K_1 | R(\Omega) T^k_\nu | K_2 \rangle \tag{4.22}$$

The matrix element (4.22) is similar in structure to the matrix element (4.13) obtained in the adiabatic approximation. Because of axial symmetry the integral over Ω reduces to a single integral: the term (4.16) and the integral (4.22) become:

$$N_{JK} = \frac{2J+1}{2} \int_0^\pi \sin\beta\; d^J_{KK}(\beta) \langle \varphi_K | e^{-i\beta J_y} | \varphi_K \rangle\, d\beta$$

$$\frac{2J_1+1}{8\pi^2} \int d\Omega\; D^{*J_1}_{K_1 \mu}(\Omega) \langle K_1 | R(\Omega)\, T^k_\nu | K_2 \rangle$$

$$= \frac{2J_1+1}{2} \int_0^\pi \sin\beta\; d^J_{K_1 \mu}(\beta) \langle \varphi_{K_1} | e^{-i\beta J_y}\, T^k_\nu | \varphi_{K_2} \rangle\, d\beta \tag{4.23}$$

The adiabatic approximation is obtained by assuming the overlap functions $\langle \varphi_K | e^{-i\beta J_y} | \varphi_K \rangle$ and $\langle \varphi_{K_1} | e^{-i\beta J_y}\, T^k_\nu | \varphi_{K_2} \rangle$ are strongly peaked at

the angles $\beta = 0$ and $\beta = \pi$. One can derive the matrix element (4.13) from the expression (4.20) by keeping only the contribution of these angles to the integral. The K selection rule (4.14) is only strictly true in this approximation.

The energy of the system is a particular case of (4.23) because the Hamiltonian H, given by equation (1.8), is a tensor of rank $k = 0$. Thus the energy E_J of a state of spin J generated by an intrinsic state $|\varphi_K\rangle$ is

$$E_J = \frac{\int_0^\pi \sin\beta \; d^J_{KK}(\beta) \langle \varphi_K | e^{-i\beta J_y} H | \varphi_K \rangle}{\int_0^\pi \sin\beta \; d^J_{KK}(\beta) \langle \varphi_K | e^{-i\beta J_y} | \varphi_K \rangle} \tag{4.24}$$

In order to use expression (4.24) it is necessary to calculate the overlap functions $\langle \varphi_{K_1} | (\exp -i\beta J_y) T^k_\nu | \varphi_{K_2} \rangle$.

Consider the matrix element $\langle \varphi_1 | (\exp -i\beta J_y) | \varphi_2 \rangle$ where $|\varphi_1\rangle$ and $|\varphi_2\rangle$ are two Slater determinants:

$$\begin{aligned} |\varphi_1\rangle &= b^\dagger_{\lambda_1} b^\dagger_{\lambda_2} \ldots b^\dagger_{\lambda_A} |0\rangle \\ |\varphi_2\rangle &= b^\dagger_{\mu_1} b^\dagger_{\mu_2} \ldots b^\dagger_{\mu_A} |0\rangle \end{aligned} \tag{4.25}$$

where:

$$\begin{aligned} |\lambda\rangle &= \sum_j C^\lambda_j |j m_\lambda\rangle \\ |\mu\rangle &= \sum_j C^\mu_j |j m_\mu\rangle \end{aligned} \tag{4.26}$$

Then:

$$e^{-i\beta J_y} |\varphi_2\rangle = b^\dagger_{\mu_1'} b^\dagger_{\mu_2'} \ldots b^\dagger_{\mu_A'} |0\rangle$$

where:

$$b^\dagger_{\mu'} = e^{-i\beta J_y} b^\dagger_\mu e^{i\beta J_y}$$

and

$$|\mu'\rangle = \sum_j C^\mu_j e^{-i\beta J_y} |j m \mu\rangle = \sum_{jm'} C^\mu_j d^j_{m' m_\mu}(\beta) |j m'\rangle \tag{4.27}$$

Thus:

$$\langle\varphi_1|e^{-i\beta J_y}|\varphi_2\rangle = \langle 0|b_{\lambda_A}\ldots b_{\lambda_2} b_{\lambda_1} b^\dagger_{\mu'_1} b^\dagger_{\mu'_2} \ldots b^\dagger_{\mu'_A}|0\rangle$$

$$= \det\,[N_{\lambda\mu'}(\beta)] \tag{4.28}$$

$N_{\lambda\mu}$ is the $A\times A$ matrix of the scalar products $\langle\lambda|\mu'\rangle$ of the orbits λ of $|\varphi_1\rangle$ with the rotated orbits μ' of $|\varphi_2\rangle$. The value of the scalar product is obtained from Eq.(4.27):

$$N_{\lambda\mu} = \sum_j C^\lambda_j C^\mu_j d^j_{m_\lambda m_\mu}(\beta) \tag{4.29}$$

One can evaluate the matrix $N_{\lambda\mu'}$ and the determinant (4.28) numerically. The overlap function $\langle\varphi_K|e^{-i\beta J_y}|\varphi_K\rangle$ is simply obtained from (4.28) by using $|\varphi_1\rangle = |\varphi_2\rangle = |\varphi_K\rangle$.

For the overlap function $\langle\varphi_{K_1}|e^{-i\beta J_y} T^k_\nu|\varphi_{K_2}\rangle$ we use a complete set of intermediate states $|n\rangle$:

$$\langle\varphi_{K_1}|e^{-i\beta J_y} T^k_\nu|\varphi_{K_2}\rangle = \sum_n \langle\varphi_{K_1}|e^{-i\beta J_y}|n\rangle\langle n|T^k_\nu|\varphi_{K_2}\rangle \tag{4.30}$$

The operator $\exp(-i\beta J_y)$ can only change the magnetic quantum number of a state $|jm\rangle$ and cannot move a particle from one shell to another. Thus the set $|n\rangle$ of the intermediate states is limited to states in which all the particles are in the same major-shell as in $|\varphi_1\rangle$. If T^k_ν is a one body operator, a multipole moment for example, the set $|n\rangle$ is further limited to particle hole excitations:

$$|n\rangle = b^\dagger_\nu b_\mu|\varphi_{K_2}\rangle \tag{4.31}$$

where ν and μ are, respectively, empty and filled orbits belonging to the same major shell as the orbits μ.

If T^k_ν is a two-body operator, the set $|n\rangle$ includes in addition to the particle-hole states (4.31) the two particle-two hole states

$$|n\rangle = b^\dagger_{\nu_1} b^\dagger_{\nu_2} b_{\mu_1} b_{\mu_2}|\varphi_K\rangle \tag{4.32}$$

Since each intermediate state $|n\rangle$ is still a Slater determinant the overlap function $\langle\varphi_{K_1}|(\exp-i\beta J_y)|n\rangle$ can be calculated with aid of expression (4.28), and $\langle n|T^k_\nu|\varphi_{K_2}\rangle$ is a simple matrix element of the operator T^k_ν. The limitations of the set $|n\rangle$ make the angular momentum projection method quite feasible on a computer.

4.3. Magnetic moments of odd-A nuclei

As an application of adiabatic model, consider the magnetic moment operator $\vec{\mu}$:

$$\vec{\mu} = \sum_{i=1}^{A} (G_s \vec{S} + G_\ell \vec{\ell}_i) \tag{4.33}$$

G_s and G_ℓ are the gyromagnetic ratios of spin and orbital angular momentum.

$$\begin{aligned} G_\ell &= 1 \quad G_s = 5.58 \quad \text{for protons} \\ G_\ell &= 0 \quad G_s = -3.85 \quad \text{for neutrons} \end{aligned} \tag{4.34}$$

When $\vec{S}$ and $\vec{\ell}$ are expressed in units of $\hbar$, $\vec{\mu}$ is expressed in units of nuclear magnetons $eh/2m_p c$.

We can separate the contributions of the even-even core and of the odd-particle (or hole) in the expression (4.33) by writing

$$\sum_{i \in \text{ core}} (G_s \vec{S}_i + G_e \vec{\ell}_i) = G_R \vec{R} \tag{4.35}$$

where G_R is the gyromagnetic ratio of the core.
Then

$$\vec{\mu} = G_R \vec{R} + G_s \vec{S} + G_e \vec{\ell} \tag{4.36}$$

In Eq. (4.36) $\vec{S}$ and $\vec{\ell}$ are the spin and orbital angular momentum of the odd particle (or hole). The total angular momentum of the system is:

$$\vec{J} = \vec{R} + \vec{\ell} + \vec{S}$$

so that we obtain the final expression for the magnetic moment

$$\vec{\mu} = G_R \vec{J} + (G_s - G_R)\vec{S} + (G_\ell - G_R)\vec{\ell} \tag{4.37}$$

This expression for the magnetic moment in analogous to the expression (4.9) obtained for the Hamiltonian in the adiabatic model. $\vec{J}$ operates on the variable Ω, $\vec{S}$ and $\vec{\ell}$ operate on the intrinsic wavefunction $|\varphi_K\rangle$.

In the absence of spin orbit coupling the even-even core is a closed shell of spin and the spin part of Eq. (4.35) does not contribute. When there is an equal number of protons and neutrons the angular momentum of neutrons is the same as that of the protons since they are in the same orbits, hence $G_R = 0.5$.

TABLE VIII. MAGNETIC MOMENTS OF ODD-A NUCLEI [12]

Nucleus	K	J	Even core	Calculated	Experimental	Schmidt
^{11}B	$3/2^-$	$3/2^-$	^{12}C	2.57	2.69	3.79
^{13}C	$1/2^-$	$1/2^-$		0.86	0.72	0.64
^{19}F	$1/2^+$	$1/2^+$	^{20}Ne	2.82	2.63	2.79
	$1/2^+$	$5/2^+$		3.86	3.5 ± 0.5	4.79
^{21}Ne	$3/2^+$	$3/2^+$		-0.582	-0.66	1.14
^{23}Na	$3/2^+$	$3/2^+$	^{24}Mg	2.44	2.22	0.12
^{25}Mg	$5/2^+$	$5/2^+$		-1.01	-0.85	-1.91
^{27}Al	$5/2^+$	$5/2^+$	^{28}Si	3.78	3.64	4.79
	$1/2^+$	$5/2^+$	^{28}Si oblate	3.81		
^{29}Si	$1/2^+$	$1/2^+$	^{28}Si oblate	-0.47	-0.56	-1.91
			^{28}Si prolate	-1.689		
^{33}S	$3/2^+$	$3/2^+$	^{32}S oblate	0.05	0.64	1.14
			^{32}S prolate	1.22		
^{35}Ci	$3/2^+$	$3/2^+$	^{36}Ar	0.63	0.82	0.12

The magnetic moments of odd nuclei can be calculated using expression (4.13) and the wavefunctions of the orbits given in Table IV. Axially symmetric solutions are used together with the approximation $G_R = 0.5$. The ground states of the nuclei are assumed to be I = K rotational band heads, and Coriolis mixing of the rotational bands is neglected. The results are shown on Table VIII [12].

4.4. Projected Hartree-Fock spectra

As an application of the angular momentum projection method consider the energy E_J given by Eq.(4.24) [13], writing:

$$\langle\varphi_K|e^{-i\beta J_y}H|\varphi_K\rangle = \langle\varphi_K|e^{-i\beta J_y}|\varphi_K\rangle E_{H.F.} + \sum_{n\neq\varphi}\langle\varphi_K|e^{-i\beta J_y}|n\rangle\langle n|H|\varphi_K\rangle \qquad (4.38)$$

where $E_{H.F.} = \langle\varphi_K|H|\varphi_K\rangle$ is the Hartree-Fock energy given by Eq. (3.6) we obtain:

$$E_J = E_{H.F.} + \frac{\sum_n \int_0^\pi \sin\beta\, d^J_{KK}(\beta)\langle\varphi_K|e^{-i\beta J_y}|n\rangle\langle n|H|\varphi_K\rangle}{\int_0^\pi \sin\beta\, d^J_{KK}(\beta)\langle\varphi_K|e^{-i\beta J_y}|\varphi_K\rangle}$$

$$\equiv E_{H.F.} + \Delta_J \qquad (4.39)$$

Δ_J is the shift between the Hartree-Fock energy and the energy of the projected state $|\Psi^J_{MK}\rangle$. In equations (4.38) and (4.39) the states $|n\rangle$ are limited to the two particle two hole configurations (4.32) because the matrix element of the nuclear Hamiltonian between a Hartree-Fock state $|\varphi_K\rangle$ and a particle hole state (4.31) is zero.

$\langle n|H|\varphi_K\rangle$ is a simple matrix element:

$$\langle n|H|\varphi_K\rangle = \langle\varphi_K|b^\dagger_{\mu_2}\, b^\dagger_{\mu_1}\, b_{\nu_2}\, b_{\nu_1}\, H|\varphi_K\rangle = \langle\nu_1\,\nu_2\,|v|\mu_1\mu_2\rangle \qquad (4.40)$$

Figures 7 and 8 show the overlap functions:

$$\langle\varphi_K|e^{-i\beta J_y}|\varphi_K\rangle \text{ and } \sum_n \langle\varphi_K|e^{-i\beta J_y}|n\rangle\langle n|H|\varphi_K\rangle$$

when $|\varphi_K\rangle$ is the solution of ^{20}Ne given in Table IV.

Table IX gives the values of N_{JK} calculated with by equation (4.23) for ^{20}Ne, ^{28}Si and ^{36}A. The values of N_{JK} show how the various angular momenta are distributed in the Hartree-Fock wavefunction. For if we

expand the Hartree-Fock wavefunction in the intrinsic frame on states of good angular momenta we find

$$|\varphi_K\rangle = \sum_J P_{JK} |\varphi_K\rangle = \sum N_{JK} |JK\rangle$$

where P_{JK} is the projection operator given by Eq.(17). N_{JK} is zero for odd values of J because of the $\exp(-i\pi J_y)$ symmetry. N_{JK} is zero for $J > 8$ because the maximum angular momentum of two protons and two neutrons in the 2s-1d shell is $J = 8$. The same holds for ^{36}A because this nucleus is equivalent to four 2s- 1d holes in ^{40}Ca. The rotational bands of ^{20}Ne and ^{36}A are said to have a cut-off above $J = 8$.

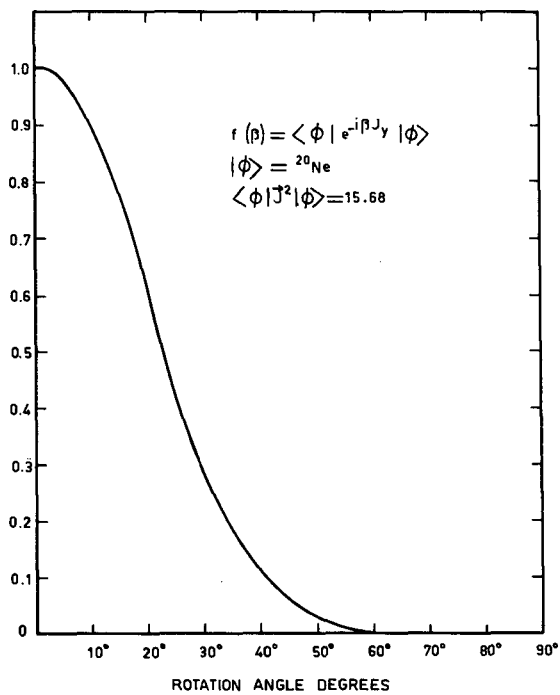

FIG.7. The overlap of the ^{20}Ne H.F. deformed state with the same state rotated by an angle θ about the O_y axis. The curve is symmetrical about 90° [5]

Figure 9 shows the spectra of ^{20}Ne, ^{28}Si and ^{36}A obtained by projecting the ground state intrinsic states given in Table IV. There are some systematic deviations for experiment.

The distances between the 0^+ and the 2^+ states are too small. The ^{28}Si spectrum is altogether too compressed. The reason why is not clear yet. It may be for example that the states of light nuclei are mixtures of various determinants.

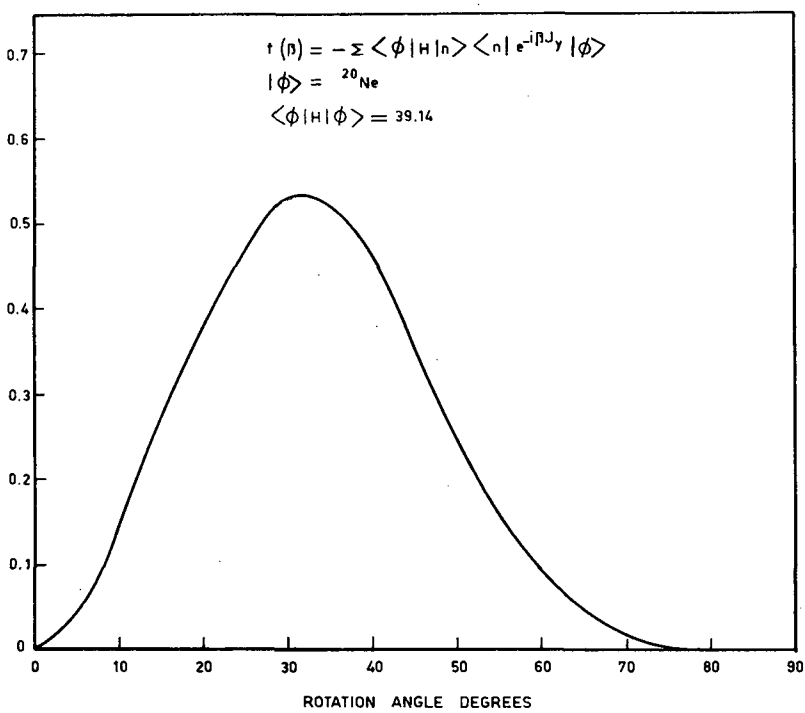

FIG. 8. The overlap function

$$F(\theta) = - \sum_{n=2p2h} \langle \phi | H | n \rangle \langle n | (\exp - i\beta J_y) | \phi \rangle$$

needed to calculate $\langle \phi | HP^J | \phi \rangle$ for ^{20}Ne [5]

TABLE IX. THE DISTRIBUTION N_{JK} OF ANGULAR MOMENTUM IN THE DEFORMED INTRINSIC STATES OF ^{20}Ne, THE OBLATE SOLUTION OF ^{28}Si AND ^{36}A FOR VALUES OF J UP TO 8 WHICH IS THE NATURAL CUT-OFF FOR THE ^{20}Ne AND ^{36}A ROTATIONAL BANDS [5].

J	^{20}Ne	^{28}Si	^{36}Ar
0	0.109	0.079	0.132
2	0.398	0.313	0.440
4	0.336	0.326	0.314
6	0.134	0.194	0.100
8	0.022	0.071	0.013

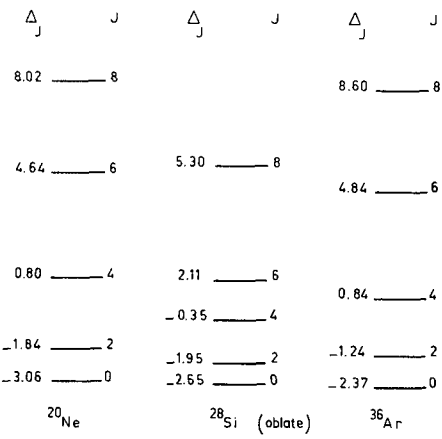

FIG. 9. Projected Hartree-Fock spectra of ^{20}Ne, the oblate solution of ^{28}Si and ^{36}Ar. To the left of each level is the energy Δ_J (Eq. (4.39)), which equals the difference between the energy of the projected Hartree-Fock state and the Hartree-Fock energy of the unprojected state

5. MAJOR SHELL MIXING HARTREE-FOCK CALCULATIONS

It is easy to see the limitations of the Hartree-Fock calculations discussed in section 3, in which the motion of each nucleon was limited to configurations of one major shell of an isotropic harmonic oscillator. From the variational point of view the Hartree-Fock wavefunctions obtained this way are not stable against particle-hole excitations from one major shell to another. It is true, of course, that as long as deformations of even parity are considered a particle has to jump two major shells in order to produce a particle-hole configuration of even parity which can mix to the ground state. But even small admixtures can produce large effects if they are coherent. Any configuration belonging to a given major shell has the same kinetic energy. Hence the trial wavefunctions used in section 3 can at best minimize the potential energy. More energy may be gained by allowing the kinetic energy to reduce and we shall see that this is an important effect.

Large quadrupole deformations are observed in the 2s-1d shell nuclei; they are larger than those expected from 2s-1d shell configurations. ^{17}O has a static charge quadrupole moment equal to -2.6 fm^2 (= -0.026 barns)[1]. The neutron carries no charge and the proton closed shell has zero angular momentum and so it cannot produce a quadrupole moment. The ^{17}O quadrupole moment is understood as a polarization effect of the odd neutron on the closed shell ^{16}O core. If each proton orbit acquires a small extra quadrupole moment due to an external field produced by the neutron these will add up coherently to produce a total quadrupole moment. ^{21}Ne has a charge quadrupole moment equal to 9 fm^2. With single major shell configurations this quadrupole moment can only be produced by the two protons in the 2s-1d shell. The maximum quadrupole moment which two protons can have is the one obtained

[1] fm = fermi = 10^{-13} cm

by placing them both in the $(n_x, n_y, n_z) = (0, 0, 2)$ orbit. The intrinsic quadrupole moment of ^{21}Ne is then:

$$Q_0 = \langle\varphi| \sum_{i=1}^{Z} (2z_i^2 - x_i^2 - y_i^2) |\varphi\rangle = \frac{2\hbar}{m\omega_0} \left[2 \times \frac{5}{2} - 2 \times \frac{1}{2} \right]$$

Table IV shows that in ^{20}Ne $\hbar/m\omega_0 \simeq 1/(0.56)^2$ so that $Q_0 = 25.5$ fm^2.

It can be shown using equation (4.13) that the measured quadrupole moment of a state of spin J generated by an intrinsic state $|\varphi_K\rangle$ is given by

$$Q = \frac{3K^2 - J(J+1)}{(J+1)(2J+3)} Q_0 \tag{5.1}$$

so that $Q = 5.1$ fm^2, which is much less than the experimental value. It is therefore necessary to extend the configuration space beyond the limitations used in section 3. This means that the expansion (3.1) of the orbits is no longer adequate and many of the results which are dependent critically on this expansion cease to be valid.

First the advantage of using ^{16}O and ^{40}Ca as reference nuclei is lost. Although the derivation of Eq.(3.5) is rigorous and does not depend on the expansion (3.1) it is of no particular use since the single particle energies ϵ_j may no longer be obtained from ^{17}O and ^{15}O binding energy data. Indeed the configurations which produce the observed quadrupole moment of the ground state of ^{17}O may well change its energy which will therefore no longer be equal to the energy of a $d_{5/2}$ neutron outside an ^{16}O closed shell given by the expression (3.4). We must therefore solve the Hartree-Fock equations using the expansion (2.6) for the Hartree-Fock Hamiltonian.

We may in fact even question the use of oscillator wavefunctions to describe a spherical nucleus such as ^{16}O or ^{40}Ca. Oscillator wavefunctions certainly have the wrong asymptotic form $r^\ell \exp(-\alpha^2 r^2/2)$. If an orbit λ with angular momentum ℓ is bound and has an energy e_λ, its asymptotic form (or tail) is $r^\ell e^{-\beta r}$ where:

$$\beta = \sqrt{\frac{2m\, e_\lambda}{\hbar^2}}$$

We shall first investigate the validity of the use of oscillator wavefunctions in Hartree-Fock calculations of closed shell nuclei, and then investigate the quadrupole deformations of deformed nuclei.

5.1. Radial Hartree-Fock calculations

In closed shell nuclei such as ^{16}O and ^{40}Ca the orbits have definite parity and angular momentum, and they may be expanded on harmonic

oscillator wavefunctions $|n\ell jm\rangle$ with different principal quantum numbers n:

$$|\lambda\rangle = \sum_n C_n^\lambda |n\ell jm\rangle \tag{5.2}$$

the coefficients C_n^λ measure the components of the orbit λ on various major shells n. The art of a Hartree-Fock calculation in which major shells are mixed is in the choice of the two-body interaction v to be used in the Hartree-Fock Hamiltonian (2.6). We have seen in section 1 that the hard core potentials cannot be used. A proper discussion of the interaction v to be used is outside the scope of these lectures and it is still a subject of debate [14]. There have been attempts to derive the effective force to be used in a Hartree-Fock calculation from forces known to fit the two-nucleon scattering data.

Phenomenological potentials have also been used. A given form is then assumed for the radial dependence of the potential and the various parameters used are chosen so as to fit various data, such as the binding energy per particle, and the equilibrium density of nuclear matter and of the finite nucleus, for example.

Since all the components of the orbit λ in Eq. (5.2) have the same ℓ, j and m, the radial wavefunction remains to be determined. The determination of the coefficients C_j^λ is called a radial Hartree-Fock calculation.

A calculation of this type has been made by Davies, Krieger and Baranger [15]. They used a velocity-dependent interaction of the form

$$v_i = \frac{\hbar^2}{m}\left[-A_i e^{-r^2/\mu_i^2} + B_i P^2 e^{-r^2/\mu_i^2} + B_i e^{-r^2/\mu_i^2} P^2\right] \tag{5.3}$$

where the index i distinguishes the potentials between two nucleons in a singlet and triplet state. The parameters chosen were:

Spin state	A (fm^{-2})	B	μ (fm)
Singlet	0.835	0.5	2
Triplet	2.56	0.7	1.43

This interaction yields a binding energy of -15.48 MeV and an equilibrium Fermi momentum of $k_f = 1.417$ in nuclear matter. It is assumed to act only when two nucleons are in a relative S-state. A velocity-dependent potential of the type (5.3) has a similar effect on the S-wave phase shift as a hard core.

The S-wave phase shift of two nucleons interacting with an attractive long range potential and a short range hard core will reverse its sign at a given energy. In the singlet state the S-wave phase shift reverses sign at 220 MeV, in the triplet state it reverses sign at about 300 MeV.

The factor $P^2 = \hbar^2 \Delta^2/2m$ in the potential (5.3) ensures that the short range repulsion will only be felt when the two nucleons have a large enough relative kinetic energy. Yet no divergence will occur in a Hartree-Fock calculation because the volume integral of the potential, which is equal to the potential energy of two nucleons with zero relative momentum, has no contributions from the repulsive part of the force. The parameters used for the potential (5.3) only give the correct qualitative behaviour of the S-wave phase shift. The parameters were chosen so as to fit nuclear matter rather than scattering data, and a simultaneous fit of both was not possible with the potential (5.3).

The convergence of the expansion (5.2) was investigated up to n = 8 major shells for various nuclei and it was found excellent. The radial wavefunctions of the ^{16}O-occupied orbits when three major shells are included are found to be

$$|\lambda_{1s}\rangle = 0.9842|1s\rangle + 0.1725|2s\rangle + 0.0384|3s\rangle$$
$$|\lambda_{1p}\rangle = 0.9936|1p\rangle + 0.0997|2p\rangle + 0.0526|3p\rangle \qquad (5.4)$$

Thus oscillator wavefunctions appear to be a good approximation to the radial wavefunctions within the nucleus. At larger distances in the surface of the nucleus the exponential tail is only apparent when a large number of radial wavefunctions are used. The equilibrium mean square radius of ^{16}O was found to be 2.91 fm, about 10% larger than the experimental value, and the binding energy per particle was -5.5 MeV. But better agreement was obtained for single particle energies, and these are important in shell-model calculations.

5.2. Quadrupole deformations

Since harmonic oscillator wavefunctions appear to be a good approximation for the orbits of spherical nuclei, it is not unreasonable to consider deformed harmonic oscillator wavefunctions to be a good approximation for the wavefunctions of deformed nuclei, especially since it is known that deformed nuclei have large quadrupole deformations. Let us therefore consider h to be a deformed harmonic oscillator:

$$h = \frac{p^2}{2m} + \frac{1}{2} m\omega_x^2 x^2 + \frac{1}{2} m\omega_y^2 y^2 + \frac{1}{2} m\omega_z^2 z^2 \qquad (5.5)$$

The eigenfunctions of h may be written in the (n_x, n_y, n_z) representation where n_x, n_y and n_z represent the number of quanta in the x, y and z directions. For an isotopic oscillator

$$\omega_x = \omega_y = \omega_z = \omega_0 \qquad (5.6)$$

and the sum $n_x + n_y + n_z$ is constant in any major shell. The 1s shell has $n_x = n_y = n_z = 0$, the three 1p shell orbits have $n_x + n_y + n_z = 1$, the six 2s-1d shell orbits have $n_x + n_y + n_z = 2$ etc. The (n_x, n_y, n_z) representation is

similar to the Nilsson asymptotic representation valid for a vanishing spin-orbit interaction.

When the axes of the oscillator are not equal the orbits (n_x, n_y, n_z) can be expressed as a mixture of orbits belonging to various major shells of an isotropic oscillator. Major shell mixing thus is reproduced by the deformation of the oscillator. Even-even N = Z nuclei may be built by filling each (n_x, n_y, n_z) orbit with four nucleons. ^{4}He will consist of the $(n_x, n_y, n_z) = (0, 0, 0)$ orbit; ^{12}C will consist of the (0, 0, 0), (0, 0, 1), (0, 1, 0) orbits. It does not matter which of the three p-shell orbits are used to make up ^{12}C since the resulting wavefunctions can be obtained one from another by the proper exchange of the x, y and z axes. ^{20}Ne might consist of the (0, 0, 0), (0, 0, 1), (0, 1, 0), (1, 0, 0) and (0, 0, 2) orbits, etc.

Consider an even-even nucleus where n = A/4 orbits of the deformed oscillator (5.5) are filled. We can define the total number of quanta in the x, y and z directions thus:

$$N_x = \sum_{\lambda=1}^{n} \left(n_x + \frac{1}{2}\right) \quad N_y = \sum_{\lambda=1}^{n} \left(n_y + \frac{1}{2}\right) \quad N_z = \sum_{\lambda=1}^{n} \left(n_z + \frac{1}{2}\right) \tag{5.7}$$

The mean values $\langle X^2 \rangle$ and $\langle P_x^2/2m \rangle$ of the operators $\sum_{i=1}^{A} x_i^2$ and $\sum_{i=1}^{A} P_i^2/2m$ are

$$\langle X^2 \rangle = 4\frac{\hbar}{m\omega_x} N_x, \quad \left\langle \frac{P_x^2}{2m} \right\rangle = 4\,\frac{\hbar\omega_x}{2} N_x \tag{5.8}$$

The charge quadrupole moment of the nucleus is

$$Q_0 = \frac{1}{2}\langle 2z^2 - x^2 - y^2 \rangle = \frac{2\hbar}{m}\left[2\,\frac{N_z}{\omega_z} - \frac{N_x}{\omega_x} - \frac{N_y}{\omega_y} \right] \tag{5.9}$$

The charge monopole moment of the nucleus is

$$\langle r^2 \rangle = \frac{1}{2}\,\langle x^2 + y^2 + z^2 \rangle = \frac{2\hbar}{m}\left[\frac{N_x}{\omega_x} + \frac{N_y}{\omega_y} + \frac{N_z}{\omega_z} \right] \tag{5.10}$$

Consider an axially symmetric ellipsoid of uniformly distributed nuclear matter; let a be the major axis along the z-direction and let b be the minor axis. The quadrupole and monopole moments of this ellipsoid are respectively:

$$\left.\begin{aligned} Q_0 &= \frac{2}{5}(a^2 - b^2) \\ \langle r^2 \rangle &= \frac{1}{5}(a^2 + 2b^2) \end{aligned}\right\} \tag{5.11}$$

The volume of the ellipsoid is $4/3\ \pi R^3$ where $R = (ab^2)^{\frac{1}{3}}$ is the equivalent radius of the ellipsoid.

We can vary the ratio a/b of the principal axes of the ellipsoid keeping R constant. In doing this we deform the ellipsoid into prolate shapes ($a > b$, $Q > 0$) or oblate shapes ($a < b$, $Q < 0$) keeping it at constant volume. The monopole and quadrupole moments may be expressed in terms of the ratio a/b and R thus:

$$\langle r^2 \rangle = \frac{R^2}{5}\left[\left(\frac{a}{b}\right)^{4/3} + \left(\frac{b}{a}\right)^{2/3}\right] \tag{5.12}$$

$$Q_0 = \frac{2R^2}{5}\left[\left(\frac{a}{b}\right)^{4/3} - \left(\frac{b}{a}\right)^{2/3}\right] \tag{5.13}$$

We see that at constant volume the monopole moment of the ellipsoid increases with deformation. We shall see that a nucleus behaves very much like an incompressible ellipsoid. Thus if we wish to vary the oscillator parameters ω_x, ω_y and ω_z in such a way as to reproduce the deformations of an incompressible ellipsoid we must keep the product

$$\omega_x \omega_y \omega_z = \omega_0^3 \tag{5.14}$$

constant. It is then convenient to write

$$\omega_x = e^{\alpha}\omega_0, \quad \omega_y = e^{\beta}\omega_0, \quad \omega_z = e^{-(\alpha+\beta)}\omega_0 \tag{5.15}$$

5.3. The model of Mottelson

A simple model has been formulated by Mottelson [16]. The potential seen by the particles in a nucleus is assumed to have the same shape as the mass distribution of the nucleus. The principal axes of the potential of the oscillator (5.5) are proportional to $1/\omega_x$, $1/\omega_y$ and $1/\omega_z$. According to equation (5.8) the principal axes of the mass distribution are proportional to $\langle x^2 \rangle^{\frac{1}{2}}$, $\langle y^2 \rangle^{\frac{1}{2}}$ and $\langle z^2 \rangle^{\frac{1}{2}}$, that is to $(N_x/\omega_x)^{\frac{1}{2}}$, $(N_y/\omega_y)^{\frac{1}{2}}$ and $(N_z/\omega_z)^{\frac{1}{2}}$.

If the ratios of the principal axes are same for the potential and for the mass distribution then

$$N_x \omega_x = N_y \omega_y = N_z \omega_z \tag{5.16}$$

The deformation of the nucleus may be measured by the ratio $Q_0/\langle r^2 \rangle$ of the quadrupole to the monopole moments.

In an isotropic oscillator for which $\omega_x = \omega_y = \omega_z$

$$\left.\begin{aligned} \frac{Q_0}{\langle r^2 \rangle} &= \frac{2N_z - N_x - N_y}{N_x + N_y + N_z} \\ \omega_x &= \omega_y = \omega_z \end{aligned}\right\} \tag{5.17}$$

For a deformed oscillator whose axes obey the relation (5.16) of the Mottelson model:

$$\left.\begin{aligned} \frac{Q_0}{\langle r^2\rangle} &= \frac{2N_z^2 - N_x^2 - N_y^2}{N_x^2 + N_y^2 + N_z^2} \\ N_x\omega_x &= N_y\omega_y = N_z\omega_z \end{aligned}\right\} \qquad (5.18)$$

In ^{20}Ne where the 1s, 1p shell orbits and the (0, 0, 2) orbits in the 2s-1d shell are filled one has $N_x = N_y = 7/2$ and $N_z = 11/2$. According to equation (5.17) the deformation in an isotropic oscillator will then be 0.32, and according to equation (5.18) the deformation in a deformed oscillator will be 0.66, which is twice the value in the isotropic oscillator. A similar result is found for other nuclei. Thus Mottelson's model predicts that quadrupole deformations will double when one passes from an isotropic oscillator (single major shell) configuration to a deformed oscillator (major shell mixing) configuration. The (0, 0, 2) orbit which in the isotropic oscillator has a quadrupole moment of 4 (in units of $\hbar/m\omega_0$) has a quadrupole moment equal to 5.89 in the deformed oscillator. The closed 1s and 1p shells which have zero quadrupole moment in the isotropic oscillator acquire a quadrupole moment of 3 in the deformed oscillator. These increases are a mutual polarization effect of the closed shell core and of the valence particles in the (0, 0, 2) orbits. Polarizations double quadrupole deformations, and this fact is often expressed by saying that neutrons have an effective charge of 1/2e (e is the charge of the electron) and that protons have an effective charge of 1.5e. With these effective charges the 2s-1d shell configurations in an isotropic oscillator have roughly the correct experimental values. But the effective charge is only a name, the polarization is the physical effect which is entirely due to the admixture of configurations outside of the 2s-1d shell.

5.4. The kinetic energy

The relation (5.16) fixing the ratio of the axes of the deformed oscillator (5.5) obtained from the model of Mottelson is exactly the same as that which would be obtained by minimizing the kinetic energy of the nucleus subject to the constant volume condition (5.14).

The kinetic energy of the system is

$$\begin{aligned} T(\alpha,\beta) &= 4\,\frac{\hbar}{2}\{N_x\omega_x + N_y\omega_y + N_z\omega_z\} \\ &= 2\,\hbar\omega_0\{N_x e^{\alpha} + N_y e^{\beta} + N_z e^{-(\alpha+\beta)}\} \end{aligned} \qquad (5.19)$$

The kinetic energy is minimum when:

$$\frac{\partial T}{\partial \alpha} = \frac{\partial T}{\partial \beta} = 0 \qquad (5.20)$$

This immediately yields the relation (5.16). Therefore the deformations obtained with model of Mottelson will be correct if the potential energy calculated with the expression (1.9) using the (n_x, n_y, n_z) wavefunctions for the orbits λ and μ remains constant when α and β are varied. This would be true of a zero range δ-force. There are indications that this would still remain true to a considerable extent with a finite range force. If it is true another interesting feature appears.

At the minimum the kinetic energy of a configuration $\{N_x, N_y, N_z\}$ is

$$T_{min} = 6\,\hbar\omega_0 (N_x N_y N_z)^{\frac{1}{3}} \tag{5.21}$$

This relation tells us which configuration has lowest kinetic energy. Since the potential energy is the same for $\alpha = \beta$ we may use the model of Elliott [7] to choose the configuration which has lowest potential energy. According to this model it is the configuration which maximizes the quantity

$$G = \lambda^2 + \mu\lambda + \mu^2 + 3(\lambda + \mu) \tag{5.22}$$

where $\lambda = N_z - N_y$ and $\mu = N_y - N_x$. Single major-shell Hartree-Fock calculations agree with the ground state assignments of the Elliott model. It is shown on Table X that for all the configurations of 2s-1d shell nuclei in which four particles fill various (n_x, n_y, n_z) orbits the configurations with a lower potential energy also have a lower kinetic energy. Thus kinetic and potential energy are minimized by the same configuration $\{N_x, N_y, N_z\}$, the potential energy is already minimized in the single major-shell calculation, and the mixing of major shells minimizes the kinetic energy.

5.5. Major shell mixing Hartree-Fock calculation

Are the results of the preceding section verified in an actual Hartree-Fock calculation? Volkov has performed calculations in the p-shell in 1964 and calculations in the 2s-1d shell have only recently begun. They have not yet been performed with very satisfying forces so that it is not yet certain to what extent the potential energy remains independent of α and β. The preliminary results indicate that the kinetic energy changes more than the potential energy. The quadrupole deformations are quite well predicted by the Mottelson model.

Let us illustrate this with the results of a major shell mixing calculation using a Volkov force [6]:

$$v = \left[-78.03\, e^{-(r/1.5)^2} + 82.5\, e^{-(r/0.8)^2}\right](0.29 + 0.2P_\sigma - 0.05P_\tau + 0.71P_x) \tag{5.23}$$

The Hartree-Fock Hamiltonian (2.6) was solved; to the kinetic energy operator t a single particle spin-orbit field $a\vec{\ell}\cdot\vec{s}$ was added, and the value of a was chosen as to fit the spin-orbit splitting observed next to the

TABLE X. VARIOUS STATES OF EVEN-EVEN NUCLEI OBTAINED BY FILLING OSCILLATOR ORBITS (n_x, n_y, n_z) BY FOUR NUCLEONS.

The second column indicates which orbits are filled. The third and fourth columns indicate the value of (λ, μ) and the weight G of the state obtained. The states are ordered by decreasing values of the weight. The last column gives the product $N_x N_y N_z$. In the Mottelson model, the kinetic energy at equilibrium is proportional to the cube root of this product.

Nucleus	Filled 2s-1d shell orbits (n_x, n_y, n_z)	(λ, μ)	G $(= \lambda^2 + \mu\lambda + \mu^2 + 3(\lambda+\mu))$	$\{N_x, N_y, N_z\}$
^{20}Ne	002	(8, 0)	88	539/8
	110	(0, 4)	28	567/8
^{24}Mg	002 011	(8, 4)	148	140
	002 020	(0, 8)	88	144
	002 110	(4, 0)	28	150
	101 011	(4, 0)	28	150
^{28}Si	200 020 110	(0, 12)	180	2025/8
	002 011 101	(12, 0)	180	2057/8
	002 101 110	(8, 4)	148	2145/8
	200 020 101	(4, 8)	148	2145/8

TABLE X. (cont.)

Nucleus	Filled 2s-1d shell orbits (n_x, n_y, n_z)	(λ, μ)	G $(= \lambda^2 + \mu\lambda + \mu^2 + 3(\lambda+\mu))$	$\{N_x, N_y, N_z\}$
^{28}Si	002 020 200	(0, 0)	0	2197/8
	110 101 011	(0, 0)	0	2197/8
^{32}S	200 020 101 110	(4, 8)	148	432
	200 110 101 011	(8, 0)	88	441
	200 020 002 110	(0, 4)	28	448
	200 020 011 101	(0, 4)	28	448
^{36}Ar	020 200 110 101 011	(0, 8)	88	5415/8
	002 020 200 101 011	(4, 0)	28	5491/8

closed shell nuclei. Quadrupole deformations are not sensitive to a. The expansion (2.1) of the orbits was limited to the states

$j = 1s^{1/2}, 1d^{5/2}, 2s^{1/2}, 1d^{3/2}, 1g^{9/2}, 2s^{5/2}, 2s^{3/2}, 3s^{1/2}, 1g^{7/2}$ for positive parity orbits and to the states

$$j = 1p^{3/2}, 1p^{1/2}, 1f^{7/2}, 2p^{3/2}, 2p^{1/2}, 1f^{5/2} \qquad (5.24)$$

for negative parity orbits.

With this expansion every orbit which has a main component belonging to a given major shell can admix components belonging to the neighbouring major shells of the same parity. The Hartree-Fock equations were solved for successive values of the oscillator constant α which determines the radial wavefunctions of the components (5.24) until the Hartree-Fock energy was minimum. Quadrupole deformations defined as the ratio of the expectations values in the Hartree-Fock state of the quadrupole moment operator to the monopole moment operator are calculated. Table XI shows the quadrupole deformations obtained from a single major shell calculation and those obtained from a major shell mixing calculation. We see that prolate deformations double as predicted by the Mottelson model. It is also possible to calculate the static quadrupole moments of the odd-A nuclei. These are given by the expression (5.1) in terms of the intrinsic quadrupole moment Q_0. The Volkov force

TABLE XI. EFFECT OF CLOSED SHELL POLARIZATIONS ON QUADRUPOLE DEFORMATIONS

Nucleus	Single major shell	Major shell mixing
^{12}C	-0.3	-0.47
^{20}Ne	0.31	0.59
^{24}Mg	0.30	0.63
^{28}Si oblate	-0.30	-0.49
^{28}Si prolate	0.30	0.75
^{32}S oblate	-0.08	-0.13
^{32}S prolate	0.17	0.35
^{36}Ar	-0.15	-0.24

TABLE XII. QUADRUPOLE MOMENTS

(in units of 10^{-26} cm^2)

Nucleus	K	J	Even core	Single shell	Shell mixing	Experimental
^{11}B	$3/2^-$	$3/2^-$	^{12}C	-1.52	-2.54	±3.1
^{21}Ne	$3/2^+$	$3/2^+$	^{20}Ne	4.83	9.65	9.0
^{23}Na	$3/2^+$	$3/2^+$	^{24}Mg	5.70	12.0	11
^{25}Mg	$5/2^+$	$5/2^+$		11.2	23.2	22
^{27}Al	$5/2^+$	$5/2^+$	^{28}Si oblate	-11.3	-20	15
	$1/2^+$	$5/2^+$		9.15	16.1	
^{33}S	$3/2^+$	$3/2^+$	^{32}S oblate	-2.52	-4.32	-5.5
	$3/2^+$	$3/2^+$	^{32}S prolate	7.6	11.8	
^{35}Cl	$3/2^+$	$3/2^+$	^{36}Ar	-5.84	-9.8	-7.9

TABLE XIII. VALUES OF $\langle r^2 \rangle$, $Q_0/\langle r^2 \rangle$, a/b AND R FOR ^{28}Si

Solution	$\langle r^2 \rangle$	$Q_0/\langle r^2 \rangle$	a/b	R
Single major shell oblate	90.2	-0.30	0.85	12.45
Major shell mixing oblate	99.8	-0.49	0.74	13.00
Major shell mixing prolate	124.7	0.75	1.41	12.8

does not give very good equilibrium radii. In order not to be exposed to errors in the overall size of the nucleus the quadrupole moments were calculated using the deformation obtained from the Hartree-Fock calculation and the experimental monopole moment (derived from the mean square radius). The results are shown in Table XII. The calculation of magnetic and quadrupole moments may help us choose between the two degenerate solutions of ^{28}Si discussed in section 3. Table VIII shows that the magnetic moment of ^{29}Si is only obtained when an oblate ^{28}Si core is assumed. But the case of ^{27}Al requires special attention. ^{27}Al is a proton hole in ^{28}Si. It has spin 5/2 and its quadrupole moment is positive, equal to 15 fm^2.

A natural way to obtain this would be to consider ^{27}Al as a $J = K = 5/2$ hole state in the prolate solution of ^{28}Si. But Hartree-Fock calculations show that unless an unusually strong spin orbit splitting is used, the prolate solution of ^{28}Si is made up of two $K = 1/2$ bands and one $k = 3/2$ band, but no $K = 5/2$ band (see Table IV). The oblate solution of ^{28}Si has a $K = 5/2$ band but the corresponding $J = K = 5/2$ state has a negative quadrupole moment. It is interesting to note that the $K = 1/2$ $J = 5/2$ assignment gives a quadrupole moment of the right sign and magnitude; if one calculated the magnetic moment with this assignment a good value would also be obtained. With this assignment ^{29}Si and ^{27}Al are a particle and a hole in the same oblate ^{28}Si equilibrium shape. We may finally investigate whether the constant volume assumption is verified. We may calculate the major and minor axes of an equivalent ellipsoid by requiring that it should have the same quadrupole and monopole moments. One may then check whether $R=(ab^2)^{\frac{1}{3}}$ constant as one goes from a single major shell to a major shell mixing calculation. The values in Table XIII are obtained for ^{28}Si.

We see that the increase of the monopole moment with deformation is very similar to that of incompressible ellipsoid.

REFERENCES

[1] HOFSTADTER, R., Rev. Mod. Phys. 28 (1956) 214.
[2] BAR-TOUV, KELSON, I., Phys. Rev. 138 (1965).
[3] KELSON, I., Phys. Rev. 132 (1963) 2189.
[4] BASSICHIS, W.H., RIPKA, G., Phys. Lett. 15 4 (1965) 320.

[5] RIPKA, G., "The Hartree-Fock theory and nuclear deformations", Lectures in Theoretical Physics, VIII-C, University of Colorado Press (1965).
[6] RIPKA, G., "Deformations in light nuclei", International Conference on Nuclear Physics, Gatlinbur Tennessee, Sept. 1966.
[7] ELLIOTT, J.P., Selected Topics in Nuclear Theory, IAEA, Vienna (1963) 157.
[8] NILSSON, S.G., Dan. Mat. Fys. Medd. 29 16 (1955).
[9] BAR-TOUV, LEVINSON, C.A., Phys. Rev. 153 (1967) 1099.
[10] BOHR, A., MOTTELSON, R.B., Dan. Mat. Fys. Medd. 27 16 (1953).
[11] PEIERLS, R.E., YOCCOZ, J., Proc. Roy. Soc., Lond. A70 (1957) 381.
[12] ZAMICK, L., RIPKA, G., Phys. Lett. 23 (1966) 347.
[13] BASSICHIS, W.H., GIRARD, B., RIPKA, G., Phys. Rev. Lett. 15 (1965) 980.
[14] BARANGER, M., "Hartree-Fock calculations of finite nuclei";
BETHE, H.A., "The theory of nuclear matter", in Int. Conf. on Nuclear Physics, Gatlinburg, Tennessee, Sept. 1966.
[15] DAVIES, K.T.R., KRIEGER, S.J., BARANGER, M., Nucl. Phys. 84 (1966) 545.
[16] MOTTELSON, B.R., Ecole d'Eté de Physique Théorique, Les Houches, New York, Gordon and Breach (1964).

CHAPTER 12

GROUP THEORY AND NUCLEAR STRUCTURE

M. MOSHINSKY

1. INTRODUCTION

The purpose of this Chapter is to indicate how techniques of group theory can be used in a systematic way in the many-body problems associated with nuclear structure. By this is not meant any of the uses of the properties of the three-dimensional rotation group and its irreducible representations (IR) in the, by now, well-known recoupling techniques. Here we concentrate on the uses of the IR of the unitary and rotation groups of an arbitrary number of dimensions in the classification of n-nucleon states. Once these states are obtained explicitly, we shall indicate how to determine the matrix elements of relevant Hamiltonians with respect to them, showing, in particular, that states associated with irreducible representations of certain chains of groups are eigenstates of physically significant interactions.

The author is at the Instituto de Física, Universidad de México, Mexico City, D.F.
The chapter has been compiled from notes taken by various participants. For details see the Acknowledgements at the end of the chapter. The work was supported by the Comisión Nacional de Energía Nuclear, Mexico City, D.F.

Our discussion of the classifications of states from a group-theoretical standpoint divides naturally into two parts, sections 1 to 3 inclusive forming the first part and sections 4 to 8 inclusive, the second.

In the first part our states are given in the second quantization pictures, so the Pauli principle is satisfied ab initio and it is not necessary to mention the IR of the symmetric group of n-particles S_n explicitly.

In the second part we construct the wave functions of our states separately in the configuration and the spin-isospin spaces and then combine them to satisfy the Pauli principle. This would require that in each space the states lie associated with IR of S_n. Furthermore, in this approach we take for the single-particle states those in a spherically symmetrical harmonic oscillator potential, making full use of the symmetry group of this single-particle Hamiltonian, i.e. the unitary group in three dimensions U_3.

In the first part our main objective is to restate the many-body problem whose Hamiltonian is

$$H = \sum_{i=1}^{n} \left[\frac{p_i^2}{2m} + U_i \right] + \sum_{i<j=1}^{n} V_{ij} \tag{1.1}$$

(where U_i, V_{ij} are single-body and two-body potentials, neither of which is necessarily central) in such a way that its group-theoretical nature becomes explicitly apparent. Before attempting this, we shall briefly discuss an elementary problem of quantum mechanics, the asymmetric top, from a group-theoretical standpoint. We shall later see that this problem has most of the features that we shall encounter in our restatement of problem (1.1).

The Hamiltonian of the asymmetric top can be expressed as

$$H_T = \frac{L_1^2}{2I_1} + \frac{L_2^2}{2I_2} + \frac{L_3^2}{2I_3} \tag{1.2}$$

where L_1, L_2, L_3 are the components of the angular momenta in a system fixed in the body with its co-ordinates taken along the three principal axes, and I_1, I_2, I_3 are the moments of inertia along these axes. The commutation relation between the L's (taking $\hbar = 1$ and remembering that the L's are given in the system fixed in the body) are

$$[L_1, L_2] = -iL_3, \text{ and cyclically.} \tag{1.3}$$

From (1.3) we conclude that L_1, L_2, L_3 are the operators associated with the infinitesimal rotations of the three-dimensional rotation group R_3, and furthermore that the total angular momentum

$$L^2 = L_1^2 + L_2^2 + L_3^2 \tag{1.4}$$

commutes with the L_i's and therefore also with the Hamiltonian (1.2).

Our purpose now should be to find a matrix representation for both H_T and L^2, and by diagonalizing these matrices simultaneously to obtain the energy and angular momentum eigenvalues. This we can achieve

entirely by group-theoretical arguments of a very familiar type. From the commutation relation (1.3) we conclude that the eigenstates $|\ell m\rangle$ of L^2, L_3 have the eigenvalues

$$L^2 |\ell m\rangle = \ell(\ell+1) |\ell m\rangle \tag{1.5a}$$

$$L_3 |\ell m\rangle = m |\ell m\rangle \tag{1.5b}$$

and that the matrix elements of L_1, L_2, L_3 have the form

$$\langle \ell m' | L_1 | \ell m\rangle = \tfrac{1}{2} \{[(\ell - m)(\ell + m + 1)]^{\frac{1}{2}} \delta_{m'm+1} + [(\ell + m)(\ell - m + 1)]^{\frac{1}{2}} \delta_{m'm-1}\} \tag{1.6a}$$

$$\langle \ell m' | L_2 | \ell m\rangle = \frac{i}{2} \{[(\ell - m)(\ell + m + 1)]^{\frac{1}{2}} \delta_{m'm+1} - [(\ell + m)(\ell - m + 1)]^{\frac{1}{2}} \delta_{m'm-1}\} \tag{1.6b}$$

$$\langle \ell m' | L_3 | \ell m\rangle = m \delta_{m'm} \tag{1.6c}$$

The matrix of the Hamiltonian is then given by

$$\begin{aligned} \langle \ell m' | H_T | \ell m\rangle = {} & (\tfrac{1}{8})(I_1^{-1} - I_2^{-1}) \\ & \times \{[(\ell - m - 1)(\ell - m)(\ell + m + 1)(\ell + m + 2)]^{\frac{1}{2}} \\ & \times \delta_{m'm+2} + 2[\ell(\ell+1) - m^2] \delta_{m'm} \\ & + [(\ell + m - 1)(\ell + m)(\ell - m + 1)(\ell - m + 2)]^{\frac{1}{2}} \\ & \times \delta_{m'm-2}\} + [(2I_2)^{-1} \ell(\ell+1) + \tfrac{1}{2}(I_3^{-1} - I_2^{-1}) m^2] \delta_{m'm} \end{aligned} \tag{1.7}$$

and its diagonalization provides the energy levels associated with the angular momentum ℓ.

For the particular case when $I_1 = I_2$, i.e. a symmetric top, the Hamiltonian is clearly diagonal and the energy levels are given by the last bracket of (1.7). This, of course, also happens when either $I_2 = I_3$ or $I_1 = I_3$, but in those cases the bases $|\ell m\rangle$ must be defined by L^2, L_1 or L^2, L_2 instead of L^2, L_3, i.e. we must choose our $|\ell m\rangle$ so that they are not only bases for an irreducible representation of the group R_3, but also that an appropriate two-dimensional rotation sub-group is explicitly reduced.

We shall show in the next section that a second quantized version of the Hamiltonian Eq. (1.1) can be reformulated in such a way that it will have many analogies with the simple problem we have just discussed.

2. THE MANY-BODY PROBLEM

In this section we want to develop a group-theoretical description of the many-nucleon problem. We discuss the Hamiltonian operating on totally anti-symmetric many-particle wave functions so that its description is most naturally given in second quantized formalism.

Let us consider the creation and annihilation operators $b_\rho^\dagger$ and $b^{\rho'}$, satisfying the fermion anti-commutation relations:

$$\left\{ b_\rho^\dagger, b^{\rho'} \right\} = b_\rho^\dagger b^{\rho'} + b^{\rho'} b_\rho^\dagger = \delta_\rho^{\rho'}$$

$$\left\{ b_{\rho'}^\dagger, b_\rho^\dagger \right\} = \left\{ b^{\rho'}, b^{\rho} \right\} = 0 \qquad (2.1)$$

The labels ρ specify the quantum numbers of the states. In general we shall use a classification involving the quantum numbers which characterize the eigenfunctions of a harmonic oscillator, ν, ℓ, m, plus the spin σ and isospin τ where the last two take the values $+\frac{1}{2}$, i.e.

$$\rho \equiv \nu \ell m, \sigma \tau$$

An alternative choice is

$$\rho = \nu \ell j m; \tau$$

where orbital angular momentum and spin are coupled to a total angular momentum j. Wave functions expressed in second quantized form are equivalent to Slater determinants

$$b_{\rho_1}^\dagger b_{\rho_2}^\dagger b_{\rho_3}^\dagger \ldots b_{\rho_n}^\dagger |0\rangle = \sum_P (-)^P P \psi_{\rho_1}(1) \ldots \psi_{\rho_n}(n) \qquad (2.2)$$

where P indicates a permutation of variables 1 ... n, and $(-1)^P$ is +1 or -1 if P is even or odd.

We also need to discuss the one- and two-body operators which occur in the nuclear many-body problem. We have one-body operators such as particle kinetic energy, spin or angular momentum, which we represent by

$$W_1 = \frac{\vec{p}_1^{\,2}}{2m} \quad \text{or} \quad \vec{\ell}_1 \quad \text{or} \quad \vec{s}_1 \qquad (2.3a, b, c)$$

and two-body operators such as a two-body potential

$$V_{12} = V(\vec{r}_{12}) \qquad (2.3d)$$

These become, in the second quantized picture,

$$\mathscr{W} = \sum_{\rho_1 \rho_1'} \langle \rho_1 | W_1 | \rho_1' \rangle b_{\rho_1}^\dagger b^{\rho_1'} \qquad (2.4a)$$

with

$$\langle \rho_1 | W_1 | \rho_1' \rangle = \int \psi_{\rho_1}^*(1) W_1 \psi_{\rho_1'}(1) d\tau_1 \qquad (2.4b)$$

and

$$\mathscr{V} = \frac{1}{2} \sum_{\substack{\rho_1 \rho_2 \\ \rho_1' \rho_2'}} \langle \rho_1 \rho_2 | V_{12} | \rho_1' \rho_2' \rangle \, b^{\dagger}_{\rho_2} \, b^{\dagger}_{\rho_1} \, b^{\rho_1'} \, b^{\rho_2'} \tag{2.5a}$$

with

$$\langle \rho_1 \rho_2 | V_{12} | \rho_1' \rho_2' \rangle = \int \psi^{*}_{\rho_1}(1) \; \psi_{\rho_2}(2) \, V_{12} \times \psi_{\rho_1'}(2) \; \psi_{\rho_2'}(2) \, d\tau_1 d\tau_2 \tag{2.5b}$$

We shall start our discussion by just analysing a general Hamiltonian, independent of spin and isospin, i.e.

$$H = \sum_{i=1}^{n} \left(\frac{p_i^2}{2m} + U(r_i) \right) + \sum_{i<j=1}^{n} V(r_{ij}) \tag{2.6}$$

Our aim now is to express this Hamiltonian in terms of the generators of a certain group and then determine the matrix elements of the Hamiltonian with respect to states characterized by the irreducible representations (IR) of this group and its sub-groups. The diagonalization of this matrix provides us with the energy level of the system and with the eigenstates expressed as a linear combination of Slater determinants of the type (2.2). This procedure would then be entirely analogous to the one followed in section 1 for the asymmetric top, where the group was the familiar rotation group in three dimensions.

We shall achieve our aim by a simple transcription. Let us first divide ρ into two parts

$$\rho \equiv \nu \, \ell \, m, \; \sigma\tau \equiv \mu, s \tag{2.7a, b, c}$$

$\mu \equiv \nu \, \ell \, m$ deals with the orbital part

$s \equiv \sigma\tau$ deals with the spin-isospin co-ordinates.

We also introduce an enumeration procedure for μ and s. For example, for s we define

s	1	2	3	4
$\sigma\tau$	$\frac{1}{2} \; \frac{1}{2}$	$\frac{1}{2} \; -\frac{1}{2}$	$-\frac{1}{2} \; \frac{1}{2}$	$-\frac{1}{2} \; -\frac{1}{2}$

(2.8)

This division is convenient in the case where we deal with operators independent of spin and isospin. In this case we can integrate separately over the orbital and spin variables in (2.4b) and (2.5b), obtaining the

expressions

$$\langle \mu_1 s_1 | W_1 | \mu_1' s_1' \rangle \equiv \langle \mu_1 | W_1 | \mu_1' \rangle \delta_{s_1}^{s_1'} \tag{2.9}$$

$$\langle \mu_1 s_1 \mu_2 s_2 | V_{12} | \mu_1' s_1' \mu_2' s_2' \rangle \equiv \langle \mu_1 \mu_2 | V_{12} | \mu_1' \mu_2' \rangle \delta_{s_1}^{s_1'} \delta_{s_2}^{s_2'} \tag{2.10}$$

Now we can define

$$\mathscr{E}_{\mu}^{\mu'} \equiv \sum_{s} b_{\mu s}^{\dagger} b^{\mu' s} \tag{2.11}$$

With these operators, and making use of the commutation relations (2.1), the one- and two-body operators can be rewritten as

$$\mathscr{W} = \sum_{\mu_1 \mu_1'} \sum_{s_1 s_1'} \langle \mu_1 | W_1 | \mu_1' \rangle \delta_{s_1}^{s_1'} b_{\mu_1 s_1}^{\dagger} b^{\mu_1' s_1'}$$

$$= \sum_{\mu_1 \mu_1'} \langle \mu_1 | W_1 | \mu_1' \rangle \mathscr{E}_{\mu_1}^{\mu_1'} \tag{2.12}$$

$$\mathscr{V} = \frac{1}{2} \sum_{\mu_1 \mu_1'} \sum_{\mu_2 \mu_2'} \langle \mu_1 \mu_2 | V(r_{12}) | \mu_1' \mu_2' \rangle \left(\mathscr{E}_{\mu_1}^{\mu_1'} \mathscr{E}_{\mu_2}^{\mu_2'} - \delta_{\mu_2}^{\mu_1'} \mathscr{E}_{\mu_1}^{\mu_2'} \right) \tag{2.13}$$

So far we have simply rewritten the Hamiltonian in terms of the $\mathscr{E}_{\mu}^{\mu'}$ operators. We want to discuss these operators and their properties and, in fact, to show that they correspond to the generators of a certain group.

(a) How many operators do we have? As μ is a shorthand notation for ν, ℓ, m, if we consider the full problem we see that μ can take an infinite number of values which means that whatever group these operators belong to, it will have an ∞ number of generators and so be intractable. We therefore make the basic assumption that we can limit ourselves to a finite number of single-particle states.

For example, in the discussion of even-parity states of nuclei between ^{16}O–^{40}Ca, it would be reasonable to restrict ourselves to the 2s, 1d shell where

$$\begin{aligned} &2s \quad \nu = 2 \quad \ell = m = 0 \quad \text{has 1 state} \\ &1d \quad \nu = 2 \quad \ell = 2 \quad m = -2, \ldots +2 \quad \text{has 5 states} \end{aligned} \tag{2.14}$$

so in this case we have a total number of $(5+1) = 6$ states in configuration space. Let us assume then that μ has a limited number of values r, and enumerate these in some order, i.e. $\mu = 1, 2 \ldots, r$. Then we see that the number of operators $\mathscr{E}_{\mu}^{\mu'}$ is equal to r^2.

(b) Hermiticity property

$$(\mathscr{E}^{\mu'}_{\mu})^{\dagger} = \sum_{s} b^{\dagger}_{\mu's} b^{\mu s} = \mathscr{E}^{\mu}_{\mu'}$$

(c) Commutation relations of the $\mathscr{E}^{\mu'}_{\mu}$. From the anti-commutation relation of the $b^{\dagger}_{\mu s}$, $b^{\mu' s'}$ operators, and the definition of the $\mathscr{E}^{\mu'}_{\mu}$ we obtain

$$[\mathscr{E}^{\mu'}_{\mu}, \mathscr{E}^{\mu'''}_{\mu''}] = \mathscr{E}^{\mu'''}_{\mu} \delta^{\mu'}_{\mu''} - \mathscr{E}^{\mu'}_{\mu''} \delta^{\mu'''}_{\mu} \qquad (2.15)$$

We shall see in the next section that these commutation relations are those of the generators of a unitary group.

The Hamiltonian now contains a linear and quadratic form of the generators of a unitary group of r dimensions $\mathscr{U}_r$. Thus the formulation of our many-body problem in relation to the generators of $\mathscr{U}_r$ is analogous to that of the asymmetric top in relation to the generators of R_3.

3. THE UNITARY GROUP, IRREDUCIBLE REPRESENTATIONS AND GEL'FAND STATES

In this section we discuss the properties of the unitary groups and in particular determine the generators of the groups. We later discuss the irreducible representations (IR) of these groups and the bases for the IR, i.e. Gel'fand states. We give these bases in terms of many-body states that are linear combinations of the Slater determinants of the previous section, which were expressed in terms of the creation operators.

3.1. Generators of the unitary group

We start by considering a unitary transformation in an r-dimensional space.

$$x'_{\mu'} = \sum_{\mu} U^{\mu}_{\mu'} x_{\mu} \qquad (3.1)$$

For an infinitesimal transformation the operator U can be taken as

$$U = I + i\epsilon B \qquad (3.2)$$

where I is the unit operator and B is an arbitrary hermitian operator divided into a symmetric part S and an anti-symmetric part A, both real, i.e.

$$B = S + iA \qquad (3.3)$$

in which case

$$U^{\dagger}U = (I - i\epsilon B^{\dagger})(I + i\epsilon B) \simeq 1 \qquad (3.4)$$

When the co-ordinates $x_{\mu'}$ transform according to (3.1) a wave function $\Psi(x_{\mu'})$ becomes:

$$\Psi(x'_{\mu'}) = \Psi\left[x_{\mu'} + i\epsilon \sum_{\mu} (S^{\mu}_{\mu'} + iA^{\mu}_{\mu'}) x_{\mu}\right] \tag{3.5}$$

and if it is developed in a Taylor series where the term with $\mu = \mu'$ is written separately, we obtain

$$\Psi(x'_{\mu'}) = \Psi(x_{\mu'}) + i\epsilon \sum_{\mu\mu'} \frac{\partial \Psi}{\partial x^{\mu'}} (S^{\mu}_{\mu'} + iA^{\mu}_{\mu'}) x_{\mu} + \ldots$$

$$= \Psi(x_{\mu'}) + i\epsilon \sum_{\mu} S^{\mu}_{\mu} x_{\mu} \frac{\partial \Psi}{\partial x^{\mu}} + i\epsilon \sum_{\mu < \mu'} S^{\mu'}_{\mu'} \left[\left(x_{\mu} \frac{\partial}{\partial x^{\mu'}} + x_{\mu'} \frac{\partial}{\partial x^{\mu}}\right) \Psi\right]$$

$$+ i\epsilon \sum_{\mu < \mu'} iA^{\mu}_{\mu'} \left[\left(x_{\mu} \frac{\partial}{\partial x^{\mu'}} - x^{\mu'} \frac{\partial}{\partial x^{\mu}}\right) \Psi\right] \quad \text{where } \mu, \mu' = 1, 2 \ldots r \tag{3.6}$$

We then have for the generators of the unitary group $\mathcal{U}_r$, the operators

$$x_{\mu} \frac{\partial}{\partial x^{\mu}}, \quad x_{\mu} \frac{\partial}{\partial x^{\mu'}} + x_{\mu'} \frac{\partial}{\partial x^{\mu}}, \quad i\left(x_{\mu} \frac{\partial}{\partial x^{\mu'}} - x_{\mu'} \frac{\partial}{\partial x^{\mu}}\right) \tag{3.7}$$

or, in analogy with $L_{\pm}$ operators of R_3, we can consider linear combinations of the last two, i.e.

$$\frac{1}{2}\left\{\left[x_{\mu} \frac{\partial}{\partial x^{\mu'}} + x_{\mu'} \frac{\partial}{\partial x^{\mu}}\right] \pm i\left[i\left(x_{\mu} \frac{\partial}{\partial x^{\mu'}} - x_{\mu'} \frac{\partial}{\partial x^{\mu}}\right)\right]\right\} \tag{3.8}$$

from which we obtain the generators

$$x_{\mu} \frac{\partial}{\partial x^{\mu'}} \quad (\mu < \mu') \qquad \text{and} \qquad x_{\mu'} \frac{\partial}{\partial x^{\mu}} \quad (\mu' > \mu) \tag{3.9}$$

so that finally there are r^2 generators denoted by

$$\mathscr{C}^{\mu'}_{\mu} = x_{\mu} \frac{\partial}{\partial x^{\mu'}} \tag{3.10}$$

without any restriction for μ, μ'.

From the definition (3.10) we get the commutation relations

$$[\mathscr{C}^{\mu'}_{\mu}, \mathscr{C}^{\mu'''}_{\mu''}] = \mathscr{C}^{\mu'''}_{\mu} \delta^{\mu'}_{\mu''} - \mathscr{C}^{\mu'}_{\mu''} \delta^{\mu'''}_{\mu} \tag{3.11}$$

which are the same as the relation (2.15). This permits us to identify the operators $\mathscr{C}^{\mu'}_{\mu}$ as the generators of a unitary group. At this point it is

necessary to discuss which unitary groups appear in the many-body problems (MBP). We have defined the operators $b^{\dagger}_{\rho} = b^{\dagger}_{\mu s}$ where $\mu \equiv \nu\, \ell\, m$ and $s = \sigma\tau$. The total number of orthonormal states μs in the Hilbert space is 4r, and as a 'basic symmetry group' for the MBP we shall consider first the $\mathbb{U}_{4r}$ group which conserves the orthonormality properties of the states μs. For example, for the s-d shell we shall start with the group $\mathbb{U}_{24}$. We denote the $\mathbb{U}_{4r}$ generators with

$$\mathbb{C}^{\rho'}_{\rho} = b^{\dagger}_{\rho} b^{\rho'} = b^{\dagger}_{\mu s} b^{\mu' s'} \tag{3.12}$$

whose number is $(4r)^2$. Their commuting relation is similar to that for $\mathscr{C}^{\mu'}_{\mu}$ and $\check{\mathscr{C}}^{\mu'}_{\mu}$. Then we can consider sub-groups of $\mathbb{U}_{4r}$. For example, we can consider unitary transformations that affect the indices μ and s separately and thus we shall deal with the chain $\mathbb{U}_{4r} \supset \mathscr{U}_r \otimes U_4$. The groups $\mathscr{U}_r$ and U_4 have, respectively, r^2 and 16 generators defined as:

$$\mathscr{C}^{\mu'}_{\mu} = \sum_{s=1}^{4} b^{\dagger}_{\mu s} b^{\mu' s} \quad \text{for } \mathscr{U}_r \tag{3.13}$$

$$C^{s'}_{s} = \sum_{\mu=1}^{r} b^{\dagger}_{\mu s} b^{\mu s'} \quad \text{for } U_4 \tag{3.14}$$

respectively, where $C^{s'}_{s}$ satisfy the commutation relations for unitary groups, i.e.

$$[C^{s'}_{s}, C^{s''}_{s'''}] = C^{s''}_{s} \delta^{s'}_{s'''} - C^{s'}_{s'''} \delta^{s''}_{s} \tag{3.15}$$

3.2. Irreducible representations (IR) of the unitary groups. Gel'fand states

Due to the fact that we are dealing with a system of n fermions, the group problem simplifies very much because we have to choose among all the irreducible representations of $\mathbb{U}_{4r}$ only those completely anti-symmetric, which will be characterized by the partition

$$\underbrace{[1, 1, \ldots 1}_{n}, \underbrace{0, \ldots 0]}_{4r-n} \tag{3.16}$$

Then the direct product sub-group $\mathscr{U}_r \otimes U_4$ is associated with the Wigner supermultiplet classification. Further, we shall chose a mathematically natural chain of sub-groups which allows us to label the states completely. This kind of classification scheme was sytematically discussed by Gel'fand and Zetlin (Dokl. Akad. Nauk 71 (1950) 825), and we shall denote the corresponding states as Gel'fand states. Later on we shall pass to chains of sub-groups which have physical meaning.

If we consider the chains of sub-groups

$$\mathscr{U}_r \supset \begin{pmatrix} \mathscr{U}_{r-1} & 0 \\ 0 & 1 \end{pmatrix} \supset \begin{pmatrix} \mathscr{U}_{r-2} & 0 & 0 \\ 0 & 1 & 0 \\ 0 & 0 & 1 \end{pmatrix} \supset \ldots \supset \begin{pmatrix} \mathscr{U}_1 & 0 \ldots 0 \\ 0 & 1 \ldots 0 \\ 0 & 0 \ldots 1 \end{pmatrix} \tag{3.17}$$

and

$$U_4 \supset \begin{pmatrix} U_3 & 0 \\ 0 & 1 \end{pmatrix} \supset \begin{pmatrix} U_2 & 0 & 0 \\ 0 & 1 & 0 \\ 0 & 0 & 1 \end{pmatrix} \supset \begin{pmatrix} U_1 & 0 & 0 & 0 \\ 0 & 1 & 0 & 0 \\ 0 & 0 & 1 & 0 \\ 0 & 0 & 0 & 1 \end{pmatrix} \tag{3.18}$$

and characterize their irreducible representations by the partitions

$$\begin{aligned} &\mathscr{U}_r \rightarrow [h_{1r}, h_{2r}, \ldots\ldots\ldots h_{rr}] \text{ and } U_4 \rightarrow \{v_{14}\ v_{24}\ v_{34}\ v_{44}\} \\ &\mathscr{U}_{r-1} \rightarrow [h_{1r-1}, h_{2r-1}, \ldots h_{r-1,r-1}] \qquad U_3 \rightarrow \{v_{13}\ v_{23}\ v_{33}\} \\ &\vdots \qquad\qquad\qquad\qquad\qquad\qquad\quad U_2 \rightarrow \{v_{12}\ v_{22}\} \\ &\mathscr{U}_1 \rightarrow [h_{11}] \qquad\qquad\qquad\qquad\quad U_1 \rightarrow \{v_{11}\} \end{aligned} \tag{3.19}$$

the Gel'fand states can be noted by

$$\left|\begin{array}{llll} h_{1r}, h_{2r}, \ldots\ldots\ldots h_{rr}, & v_{14} & v_{24} & v_{34} \quad v_{44} \\ h_{1r-1}, \ldots\ldots h_{r-1,r-1} & & v_{13} & v_{23} \quad v_{33} \\ \ldots\ldots\ldots & & & v_{12} \quad v_{22} \\ h_{11} & & & v_{11} \end{array}\right\rangle \tag{3.20}$$

A partition can be represented graphically by a Young diagram, i.e. a tableau of boxes arranged in rows and columns, in which each row (column) is smaller than or equal to the row above (column to the left).

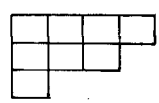

(3.21)

For the partition $[h_{1r}, h_{2r}, \ldots h_{rr}]$ the number of rows is r and the row i has h_{ir} boxes.

The partition $[v_{14}, v_{24}, v_{34}, v_{44}]$ has 4 rows with v_{14}, v_{24}, v_{34}, v_{44} boxes respectively. These two partitions will be shown to be associated, that is, one can be obtained from the other by interchanging the rows and the columns. This property is required by the anti-symmetry of the total function.

The total number of boxes in each of these partitions is equal to n, the number of particles:

$$h_{1r} + h_{2r} + \ldots h_{rr} = v_{14} + v_{24} + v_{34} + v_{44} = n \tag{3.22}$$

The comparison of the chain (3.17) with the chain $R_3 \supset \begin{pmatrix} R_2 & 0 \\ 0 & 1 \end{pmatrix}$ suggests that the relation between the partitions $[h_{1r}, h_{2r}, \ldots h_{rr}]$ and $[h_{1r-1}, h_{2r-1}, \ldots h_{r-1,r-1}]$ is of similar type to the relation between ℓ and m, i.e. it is the problem of reduction of a representation of a group with respect to a sub-group.

Before proceeding, let us, in Table I, briefly review the situation by comparing the corresponding concepts we have introduced in connection with the asymmetric top (AT) and in connection with the many-body problem (MBP). It is important to stress the fact that the Hamiltonian of the asymmetric top is not invariant with respect to the three-dimensional rotation group R_3 associated with a co-ordinate system fixed in the body, because, as can easily be seen $[L_i, H_T] \neq 0$. (The equality $[L_i, H_T] = 0$ for all $i = 1, 2, 3$ takes place only for $I_1 = I_2 = I_3$.)

We are nevertheless able to classify the eigenstates of H_T by the irreducible representations of R_3, because $[H_T, L^2] = 0$, and there thus exists a basis in which H_T and L^2 can be simultaneously diagonalized. (If $I_1 = I_2$, the states can also be classified (labelled) by the irreducible representations of R_2.)

The same type of considerations are valid for the MBP Hamiltonian. The MBP Hamiltonian is <u>not</u> an invariant of the U_{4r} group, but we can label the eigenstates of the MBP Hamiltonian by the irreducible representations of the U_{4r} group. There is, however, only one irreducible representation of U_{4r} of physical interest for a system of n particles, namely $[\underbrace{1\ 1 \ldots 1}_{n}\ \underbrace{0\ 0 \ldots 0}_{4r-n}]$.

3.3. The concept of weight

Let us now consider the problem of the rotation group and some of its characteristics. Let

$$P(x, y, z) \tag{3.23}$$

be a homogeneous polynomial of degree n. Then, by Euler's theorem:

$$\vec{r} \cdot \nabla \cdot P = nP \tag{3.24}$$

so that the homogeneous polynomials of degree n can be characterized as eigenpolynomials of the operator $\vec{r} \cdot \nabla$, belonging to the eigenvalue n.

We shall try to classify the set of homogeneous polynomials of degree n into distinct sub-sets which should constitute bases for the irreducible representations of the R_3 group.

Let L_{+1}, L_0, L_{-1} be the generators of R_3

$$L_{\pm 1} = \mp \frac{1}{\sqrt{2}} [L_x \pm iL_y]$$

$$L_0 = L_3 \tag{3.25}$$

TABLE I. REVIEW OF THE PROBLEMS

	Asymmetric top (AT)	Many-body problem (MBP)
Hamiltonian	$H = \frac{L_1^2}{2I_1} + \frac{L_2^2}{2I_2} + \frac{L_3^2}{2I_3}$	$\mathscr{H} = \mathscr{W} + \mathscr{V}$ where $\mathscr{W} = \sum_{\rho_1 \rho_1'} \langle \rho_1 \vert W_1 \vert \rho_1' \rangle C_{\rho_1}^{\rho_1'}$ is a single-body operator and $\mathscr{V} = \frac{1}{2} \sum_{\substack{\rho_1 \rho_1' \\ \rho_2 \rho_2'}} \langle \rho_1 \rho_2 \vert V_{12} \vert \rho_1' \rho_2' \rangle (C_{\rho_1}^{\rho_1'} C_{\rho_2}^{\rho_2'} - \delta_{\rho_2}^{\rho_1'} C_{\rho_1}^{\rho_2'})$ is a two-body operator
Group used for classification of states	R_3	U_{4r} *
Generators of the group	L_i $i = 1, 2, 3$	$C_\rho^{\rho'} = b_\rho^\dagger b^{\rho'}$ * $\rho, \rho' = 1, 2, \ldots, 4r$
Commutation relations for the generators	$[L_i, L_j] = -i\hbar L_k$ $(i, j, k) = (1, 2, 3)$ and cyclic permutations	$[C_\rho^{\rho'}, C_{\rho''}^{\rho'''}] = C_\rho^{\rho'''} \delta_{\rho''}^{\rho'} - C_{\rho''}^{\rho'} \delta_\rho^{\rho'''}$
States with respect to which matrix elements have to be calculated	The functions $\vert \ell m \rangle$ which correspond to a given irreducible representation ℓ of the group R_3, and are labelled by the irreducible representation m of its sub-group R_2 (transform as IR of R_2)	The "Gel'fand states" $\left\vert \begin{matrix} h_{1r}, h_{2r}, \ldots\ldots, h_{rr}, & v_{14} & v_{24} & v_{34} & v_{44} \\ h_{1,r-1}, \ldots, h_{r-1,r-1} & & v_{13} & v_{23} & v_{33} \\ \vdots & & & v_{12} & v_{22} \\ h_{11} & & & & v_{11} \end{matrix} \right\rangle$ that correspond to the representation $[1\,1\,1 \ldots 1\ \underbrace{0\,0 \ldots 0}_{4r-n}]$ (n ones) of the group U_{4r} and are labelled by the sequences of irreducible representations $[h_{1r}, h_{2r}, \ldots h_{rr}]$, $[h_{1,r-1}, \ldots, h_{r-1,r-1}], \ldots [h_{11}]$ and $\{v_{14}, \ldots v_{44}\}, \ldots \{v_{11}\}$ of its chains of sub-groups $\mathscr{U}_r \supset \begin{pmatrix} \mathscr{U}_{r-1} & 0 \\ 0 & 1 \end{pmatrix} \supset \ldots \supset \begin{pmatrix} \mathscr{U}_1 & 0 \ldots 0 \\ 0 & 1 \\ \vdots & \ddots \\ 0 \ldots\ldots & 1 \end{pmatrix}$ $U_4 \supset \begin{pmatrix} U_3 & 0 \\ 0 & 1 \end{pmatrix} \supset \ldots \supset \begin{pmatrix} U_1 & 0 & 0 & 0 \\ 0 & 1 & 0 & 0 \\ 0 & 0 & 1 & 0 \\ 0 & 0 & 0 & 1 \end{pmatrix}$

* If the one- and two-body potentials $\mathscr{W}$ and $\mathscr{V}$ are independent of spin and isospin, then the starting group used for the classification of the states is $\mathscr{U}_r$ and its generators are $\mathscr{C}_\mu^{\mu'}$

As $\vec{r} \cdot \nabla$ is a scalar, it commutes with $L_{\pm 1}$, L_0

$$[L_q, \vec{r} \cdot \nabla] = 0, \quad q = 1, 0, -1 \tag{3.26}$$

this implies that the homogeneous polynomials of degree n (eigenpolynomials of $\vec{r} \cdot \nabla$) can simultaneously be eigenpolynomials of one of the operators L_q, for example of L_0

$$L_0 P = mP \tag{3.27}$$

We shall call the eigenvalue m of L_0 the weight of the polynomial P.

What happens to the eigenpolynomials of L_0 if we apply to them the operators $L_{\pm 1}$? These operators will not take us out of the given set of eigenpolynomials of $\vec{r} \cdot \nabla$ (because, as we have seen, $L_{\pm 1}$ and $\vec{r} \cdot \nabla$ commute), but they will produce polynomials belonging to another eigenvalue of L_0. It can easily be seen that

$$L_0(L_{\pm 1} P) = (m \pm 1)(L_{\pm 1} P) \tag{3.28}$$

i.e. $L_{\pm 1} P$ corresponds to the eigenvalue $(m \pm 1)$, or $L_{\pm 1} P$ is a polynomial of weight $m \pm 1$.

The operator L_{+1} is thus an operator that raises the weight, while L_{-1} is an operator that lowers the weight.

If we apply successively the raising (step-up) operator L_{+1}, starting from a polynomial P_m of given weight m, we shall get a sequence of polynomials

$$P_{m+1}, P_{m+2}, \ldots \tag{3.29}$$

having the weights

$$m+1, \; m+2, \; \ldots \tag{3.30}$$

This sequence is finite, i.e. we shall reach a polynomial for which

$$L_{+1} P_{m+k} = 0 \tag{3.31}$$

We shall call P_{m+k} a polynomial of highest weight and, for short, denote it by $\mathbf{P}$. In order to see that there exists a value of k for which Eq.(3.31) takes place, let us define

$$\begin{aligned} x_{\pm 1} &= \mp \frac{1}{\sqrt{2}} (x \pm iy) \\ x_0 &= z \end{aligned} \tag{3.32}$$

The most general polynomial of degree n then has the form

$$\sum_{\substack{n_+, n_0, n_- \\ (n_+ + n_0 + n_- = n)}} A_{n_+ n_0 n_-} x_{+1}^{n_+} x_0^{n_0} x_{-1}^{n_-} \tag{3.33}$$

From (3.25) and (3.32) we get

$$L_0 = x_{+1} \frac{\partial}{\partial x_{+1}} - x_{-1} \frac{\partial}{\partial x_{-1}} \tag{3.34}$$

and therefore

$$L_0 (x_{+1}^{n_+} x_0^{n_0} x_{-1}^{n_-}) = (n_+ - n_-) x_{+1}^{n_+} x_0^{n_0} x_{-1}^{n_-} \tag{3.35}$$

i.e. the eigenvalues of L_0 are less than n. We conclude that we cannot raise the weight indefinitely, and that there thus exists a polynomial of highest weight.

From the definition of an n-degree homogeneous polynomial of highest weight as a polynomial that satisfies the three equations:

$$\vec{r} \cdot \nabla \mathbf{P} \equiv \left[x_{+1} \frac{\partial}{\partial x_{+1}} + x_0 \frac{\partial}{\partial x_0} + x_{-1} \frac{\partial}{\partial x_{-1}} \right] \mathbf{P} = n \mathbf{P} \tag{3.36}$$

$$L_0 \mathbf{P} \equiv \left[x_{+1} \frac{\partial}{\partial x_{+1}} - x_{-1} \frac{\partial}{\partial x_{-1}} \right] \mathbf{P} = \ell \mathbf{P} \tag{3.37}$$

$$L_{+1} \mathbf{P} \equiv -\left[x_{+1} \frac{\partial}{\partial x_0} + x_0 \frac{\partial}{\partial x_{-1}} \right] \mathbf{P} = 0 \tag{3.38}$$

we obtain straightforwardly the homogeneous polynomials of degree n and highest weight ℓ

$$P_{n,\ell} \equiv x_1^{\ell} (r^2)^{\frac{n-\ell}{2}} \tag{3.39}$$

with

$$\ell = n, n-2, n-4, \ldots, 1 \text{ or } 0 \tag{3.40}$$

where

$$r^2 \equiv x^2 + y^2 + z^2 = x_0^2 - 2x_1 x_{-1} \tag{3.41}$$

By successively applying the lowering operator L_{-1} to each polynomial $P_{n\ell}$ we get a complete set of linearly independent homogeneous polynomials

$$P_{n,\ell,m} \equiv L_{-1}^{\ell - m} x_{+1}^{\ell} (r^2)^{\frac{n-\ell}{2}}, \quad m = 1, 2, \ldots, 2\ell \tag{3.42}$$

which are nothing but the solid spherical harmonics of order ℓ.

We have thus decomposed the set of all homogeneous polynomials of degree n into sub-sets characterized by the number ℓ, each sub-set constituting a basis for the irreducible representation ℓ of R_3.

Let us now determine the concepts of weight and highest weight for the group $\mathscr{U}_r$.

In order to do that, let us divide the set $\{\mathscr{G}_\mu^{\mu'}\}$ of the generators of the group $\mathscr{U}_r$ into three parts:

(i) containing all generators $\mathscr{G}_\mu^{\mu'}$ with $\mu < \mu'$

(ii) containing all generators $\mathscr{G}_\mu^{\mu}$ $(\mu = 1, 2, \ldots, r)$

(iii) containing all generators $\mathscr{G}_\mu^{\mu'}$ with $\mu > \mu'$.

The states of the MBP will be linear combinations of the n-particle wave functions

$$b_{\rho_1}^\dagger b_{\rho_2}^\dagger \ldots b_{\rho_n}^\dagger |0\rangle \tag{3.43}$$

namely, all linearly independent homogeneous polynomials of degree n in the $b_{\rho_i}^\dagger$, applied to the vacuum state

$$P_n(b_\rho^\dagger)|0\rangle \tag{3.44}$$

We can now ask what are the homogeneous polynomials of degree n that are simultaneously eigenpolynomials of the set of generators

$$\mathscr{G}_1^1, \mathscr{G}_2^2, \ldots, \mathscr{G}_r^r \tag{3.45}$$

To be able to do that we must first verify that all operators (3.43) commute:

$$[\mathscr{G}_\mu^\mu, \mathscr{G}_{\mu'}^{\mu'}] = \mathscr{G}_\mu^{\mu'}\delta_{\mu'}^\mu - \mathscr{G}_{\mu'}^{\mu}\delta_\mu^{\mu'} = 0 \tag{3.46}$$

It is thus possible to find polynomials $P_n|0\rangle$ such that

$$\mathscr{G}_\mu^\mu P_n|0\rangle = w_\mu P_n|0\rangle \quad \text{for all } \mu = 1, 2, \ldots, r \tag{3.47}$$

We shall call the set of eigenvalues

$$(w_1, w_2, \ldots, w_r) \tag{3.48}$$

of the operators (3.45) corresponding to the same eigenpolynomial $P_n|0\rangle$ the weight of the polynomial $P_n|0\rangle$.

The set of r eigenvalues (3.48) constitutes for the $\mathscr{U}_r$ group the equivalent of the m value for the R_3 group.

Let us now introduce an order into the set of sequences (3.48). We shall say that the sequence

$$A \equiv (w_1, w_2, \ldots, w_r) \tag{3.49}$$

is greater than the sequence

$$B \equiv (w_1', w_2', \ldots, w_r') \tag{3.50}$$

$(A > B)$ if in the sequence of differences

$$A - B \equiv (w_1 - w_1', w_2 - w_2', \ldots, w_r - w_r') \tag{3.51}$$

the first non-zero term (when reading from left to right) is positive.

Example: Let

$$A \equiv (4, 3, 2) \quad \text{and}$$
$$B \equiv (4, 2, 3) \tag{3.52}$$

The sequence of differences being

$$A - B \equiv (0, 1, -1) \tag{3.53}$$

we conclude that $A > B$.

3.4. Generators that raise or lower the weight

We should now like to determine generators that correspond, for the group $\mathscr{U}_r$, to the raising and lowering generators L_{+1} and L_{-1}. We shall proceed to show that the generators $\{\mathscr{C}^{\mu'}_{\mu}, \mu < \mu'\}$ are generators that raise the weight (i.e. by applying them to a function of given weight one obtains a function of higher weight) while the generators $\{\mathscr{C}^{\mu'}_{\mu}, \mu > \mu'\}$ lower the weight.

For this purpose, let us first write down the commutation relation between an operator belonging to the set $\{\mathscr{C}^{\mu}_{\mu}\}$ and an operator belonging to one of the other two sets:

$$[\mathscr{C}^{\mu}_{\mu}, \mathscr{C}^{\mu''}_{\mu'}] = \mathscr{C}^{\mu''}_{\mu}\delta^{\mu}_{\mu'} - \mathscr{C}^{\mu}_{\mu'}\delta^{\mu''}_{\mu} = \mathscr{C}^{\mu''}_{\mu'}(\delta^{\mu}_{\mu'} - \delta^{\mu''}_{\mu}) \tag{3.54}$$

Now, let $P|0\rangle$ be a polynomial[1] of weight $(w_1, w_2, \ldots, w_r)$ and let us consider the polynomial

$$P'|0\rangle \equiv \mathscr{C}^{\mu''}_{\mu'} P|0\rangle \tag{3.55}$$

(which is also of degree n as is easily seen). $P'|0\rangle$ is also a polynomial of a given weight which may be determined by using the commutation relation (3.54). We get

$$\mathscr{C}^{\mu}_{\mu}\mathscr{C}^{\mu''}_{\mu'} P|0\rangle = \mathscr{C}^{\mu''}_{\mu'}\mathscr{C}^{\mu}_{\mu} P|0\rangle + \mathscr{C}^{\mu''}_{\mu'}(\delta^{\mu}_{\mu'} - \delta^{\mu''}_{\mu'})P|0\rangle$$
$$= [w_{\mu} + (\delta^{\mu}_{\mu'} - \delta^{\mu''}_{\mu})]\mathscr{C}^{\mu''}_{\mu'} P|0\rangle \tag{3.56}$$

It follows that $P'|0\rangle$ is an eigenfunction of $\mathscr{C}^{\mu}_{\mu}$ corresponding to the eigenvalue $w_{\mu} + (\delta^{\mu}_{\mu'} - \delta^{\mu''}_{\mu})$, so that for $\mu' < \mu''$ the weight of the function

---

[1] We shall speak in the following of the 'polynomials'

$$\sum_{\rho_1 \cdots \rho_n} A_{\rho_1 \rho_2 \cdots \rho_n} b^{+}_{\rho_1} b^{+}_{\rho_2} \cdots b^{+}_{\rho_n} |0\rangle$$

but it should not be forgotten that in fact this function is a linear combination of Slater determinants. Our denomination, although incorrect, is intended to stress the polynomial character of the above expression with respect to the creation operators $b^{+}_{\rho_i}$.

$P'|0\rangle = \mathscr{C}^{\mu''}_{\mu'} P|0\rangle$ is

$$(w_1, \ldots, w_{\mu'} + 1, \ldots, w_{\mu''} - 1, \ldots, w_r) \tag{3.57}$$

while for $\mu' > \mu''$ the weight is

$$(w_1, \ldots, w_{\mu''} - 1, \ldots, w_{\mu'} + 1, \ldots, w_r) \tag{3.58}$$

The raising property of $\mathscr{C}^{\mu''}_{\mu'}$, $\mu' < \mu''$ and the lowering property of $\mathscr{C}^{\mu''}_{\mu'}$, $\mu' > \mu''$ is thus established.

3.5. The polynomial of highest weight

Let us now define, in analogy with the rotation group (for which the highest weight function is defined as the solution of the pair of equations,

$$L_0 \mathbf{P} = \ell \mathbf{P}, \quad L_{+1} \mathbf{P} = 0 \tag{3.59}$$

a highest weight function in the set of homogeneous eigenpolynomials of degree n. This polynomial of highest weight which we shall denote by $\mathbf{P}|0\rangle$ is defined by the set of equations

$$\mathscr{C}^{\mu}_{\mu} \mathbf{P}|0\rangle = h_\mu \mathbf{P}|0\rangle \tag{3.60}$$

$$\mathscr{C}^{\mu'}_{\mu} \mathbf{P}|0\rangle = 0 \quad \text{for all } \mu < \mu' \tag{3.61}$$

The highest weight is in turn denoted by the set of eigenvalues

$$[h_1, h_2, \ldots, h_r] \tag{3.62}$$

As the operator $\mathscr{C}^{\mu}_{\mu}$ counts the number of times that the index μ appears in the polynomial, this must be the same in each monomial $b^\dagger_{\mu_1 s_1} b^\dagger_{\mu_2 s_2} \ldots b^\dagger_{\mu_n s_n}|0\rangle$ and so we conclude (as the polynomial is of degree n) that the number of times any of the indices μ appears is n, namely,

$$h_1 + h_2 + \ldots + h_r = n \tag{3.63}$$

We shall now prove that if $\mu < \mu'$, then $h_\mu \geq h_{\mu'}$. It will then follow that $[h_1, h_2, \ldots, h_r]$ represents a partition of n. Let us first observe that if $\mu < \mu'$ we have

$$\mathscr{C}^{\mu'}_{\mu} \mathbf{P}|0\rangle = 0 \tag{3.64}$$

but that in general,

$$\mathscr{C}^{\mu}_{\mu'} \mathbf{P}|0\rangle \neq 0 \tag{3.65}$$

Let us then take the scalar product of the state $\mathscr{C}^{\mu}_{\mu'} \mathbf{P}|0\rangle$ with itself. As

$$(\mathscr{C}^{\mu}_{\mu'})^\dagger = \mathscr{C}^{\mu'}_{\mu} \tag{3.66}$$

we can write, by also taking into account (3.64)

$$0 \leq \langle 0 | \mathbb{P}^\dagger (\mathscr{C}^{\mu}_{\mu'})^\dagger \mathscr{C}^{\mu}_{\mu'} \mathbb{P} | 0 \rangle = \langle 0 | \mathbb{P}^\dagger \mathscr{C}^{\mu'}_{\mu} \mathscr{C}^{\mu}_{\mu'} \mathbb{P} | 0 \rangle$$

$$= \langle 0 | \mathbb{P}^\dagger [\mathscr{C}^{\mu'}_{\mu}, \mathscr{C}^{\mu}_{\mu'} \mathbb{P}] | 0 \rangle \tag{3.67}$$

But

$$[\mathscr{C}^{\mu'}_{\mu}, \mathscr{C}^{\mu}_{\mu'} \mathbb{P}] = [\mathscr{C}^{\mu'}_{\mu}, \mathscr{C}^{\mu}_{\mu'}] \mathbb{P} + \mathscr{C}^{\mu}_{\mu'} [\mathscr{C}^{\mu'}_{\mu}, \mathbb{P}] \tag{3.68}$$

From (3.64) and $\mathscr{C}^{\mu'}_{\mu} | 0 \rangle = 0$ it follows that $[\mathscr{C}^{\mu'}_{\mu}, \mathbb{P}] | 0 \rangle = 0$ and our inequality becomes

$$\langle 0 | \mathbb{P}^\dagger [\mathscr{C}^{\mu'}_{\mu}, \mathscr{C}^{\mu}_{\mu'}] \mathbb{P} | 0 \rangle \geq 0 \tag{3.69}$$

Taking into account the commutation relation

$$[\mathscr{C}^{\mu'}_{\mu}, \mathscr{C}^{\mu}_{\mu'}] = \mathscr{C}^{\mu}_{\mu} \delta^{\mu'}_{\mu'} - \mathscr{C}^{\mu'}_{\mu'} \delta^{\mu}_{\mu} = \mathscr{C}^{\mu}_{\mu} - \mathscr{C}^{\mu'}_{\mu'} \tag{3.70}$$

it follows that

$$0 \leq \langle 0 | \mathbb{P}^\dagger (\mathscr{C}^{\mu}_{\mu} - \mathscr{C}^{\mu'}_{\mu'}) \mathbb{P} | 0 \rangle = (h_\mu - h_{\mu'}) \langle 0 | \mathbb{P}^\dagger \mathbb{P} | 0 \rangle \tag{3.71}$$

As the highest weight polynomial $\mathbb{P} | 0 \rangle$ is non-vanishing we have

$$\langle 0 | \mathbb{P}^\dagger \mathbb{P} | 0 \rangle > 0 \tag{3.72}$$

and as a result $h_\mu - h_{\mu'} \geq 0$ if $\mu < \mu'$.

We have thus obtained

$$h_1 \geq h_2 \geq \ldots \geq h_r \geq 0 \tag{3.73}$$

so that the set of numbers that gives the highest weight is actually a partition of n.

Let us now consider the U_4 group. The polynomials we have defined till now have a given weight with respect to the $\mathscr{U}_r$ group. Due to the fact that the generators of $\mathscr{U}_r$ (which acts in orbital space) and U_4 (which acts in spin-isospin space) commute

$$[\mathscr{C}^{\mu'}_{\mu}, C^{s'}_{s}] = 0 \tag{3.74}$$

we can define polynomials that are at the same time of highest weight with respect to both $\mathscr{U}_r$ and U_4. For U_4 we can again divide the set of generators into three sub-sets[2]

$$\{C^{s'}_{s},\ s < s'\}, \{C^{s}_{s}\}, \{C^{s'}_{s},\ s > s'\} \tag{3.75}$$

The polynomials of highest weight (with respect to U_4) will be solutions

---

[2] There are $2\binom{4}{2} + 4 = 16$ generators.

of the equations

$$C_s^s \mathbb{P} |0\rangle = v_s \mathbb{P} |0\rangle \tag{3.76}$$

$$C_s^{s'} \mathbb{P} |0\rangle = 0 \quad \text{for all } s < s' \tag{3.77}$$

The highest weight for U_4 will be the vector

$$\{v_1, v_2, v_3, v_4\} \tag{3.78}$$

for which again it may be proved that $v_1 + v_2 + v_3 + v_4 = n$ and that if $s < s'$, $v_s \geq v_{s'}$, i.e. $v_1 \geq v_2 \geq v_3 \geq v_4$. The set of numbers (3.78) also corresponds to a partition of n.

We shall now write down the expression of the polynomial which is of highest weight with respect to both $\mathscr{U}_r$ and U_4. We shall admit without proof that for each partition of n there is only one polynomial of highest weight in $\mathscr{U}_r$ and U_4. This is related to the fact that to a given irreducible representation $[1^n]$ of U_{4r} correspond well-determined irreducible representations of $\mathscr{U}_r$ and U_4, which are associated with each other.

Let us describe the construction of highest weight eigenpolynomials by an example. We shall take n = 8 particles. Now we take a Young tableau of 8 boxes and put in every box one creation operator $b^\dagger_{\mu s}$ in such a manner that the row μ has only μ states and the column s has only s states. Besides this, the partitions formed with respect to both types of states must respect the property that if $\mu < \mu'$ $(s < s')$ then $h_\mu \geq h_{\mu'}$ $(v_s \geq v_{s'})$. Let us take, for example, [3 2 2 1] with respect to μ states and {4 3 1} with respect to s states. Then we will show below that the h.w. state for both $\mathscr{U}_r$ and U_4 is given by

$b^\dagger_{11}$	$b^\dagger_{12}$	$b^\dagger_{13}$
$b^\dagger_{21}$	$b^\dagger_{22}$	
$b^\dagger_{31}$	$b^\dagger_{32}$	
$b^\dagger_{41}$		

(3.79)

This Young tableau represents the state

$$b^\dagger_{11} b^\dagger_{12} b^\dagger_{13} b^\dagger_{21} b^\dagger_{22} b^\dagger_{31} b^\dagger_{32} b^\dagger_{41} |0\rangle \tag{3.80}$$

To demonstrate that (3.80) is a h.w. for both $\mathscr{U}_r$ and U_4 we shall apply to the state either $\mathscr{C}^{\mu'}_{\mu}$ $(\mu < \mu')$ or $C_s^{s'}$ $(s < s')$, and the result will be zero because these operators move the particles in the states which are already occupied or annihilate states which do not exist. ($\mathscr{C}^{\mu'}_{\mu}$ moves the indices on columns and $C_s^{s'}$ the indices on rows.)

Now applying the operators $\mathscr{C}^{\mu}_{\mu}$ and C_s^s we obtain the degree of the monomial (3.80) with respect to indices μ and s. In the index μ $(\mu = 1, 2, \ldots, r)$ the degrees form the partition $[3\ 2\ 2\ 1\ 0\ \ldots\ 0] \equiv [3\ 2\ 2\ 1]$ and in the index s $(s = 1, 2, 3, 4)$ the degrees form the partition $\{4\ 3\ 1\ 0\} \equiv \{4\ 3\ 1\}$.

The procedure of constructing the highest weight state having been indicated, the first question is: to what Gel'fand state does this h.w. state correspond? For this let us look into the generators of $\mathscr{U}_r$ and U_4 and into the generators of the sub-groups which enter into their mathematically natural chains. For the moment let us carry out the analysis for the case of U_4 and put its generators into a square array

$$\begin{array}{|c|c|c|c|} \hline C_1^1 & C_1^2 & C_1^3 & C_1^4 \\ \hline C_2^1 & C_2^2 & C_2^3 & C_2^4 \\ \hline C_3^1 & C_3^2 & C_3^3 & C_3^4 \\ \hline C_4^1 & C_4^2 & C_4^3 & C_4^4 \\ \hline \end{array} \tag{3.81}$$

If we restrict ourselves to the first three indices, that is, take away the row and the column which contain the index 4, we just obtain the generators of U_3. Then if we restrict ourselves to the first two indices, we obtain the generators of U_2 and, at last, restricting ourselves to the first index, we obtain the generators of the chain

$$U_4 \supset \begin{pmatrix} U_3 & 0 \\ 0 & 1 \end{pmatrix} \supset \begin{pmatrix} U_2 & 0 & 0 \\ 0 & 1 & 0 \\ 0 & 0 & 1 \end{pmatrix} \supset \begin{pmatrix} U_1 & 0 & 0 & 0 \\ 0 & 1 & 0 & 0 \\ 0 & 0 & 1 & 0 \\ 0 & 0 & 0 & 1 \end{pmatrix} \tag{3.82}$$

as sub-sets of the generators of the group U_4.

Now if we recall what an h.w. state for U_4 satisfies, i.e.

$$C_s^s \mathbf{P}|0\rangle = v_{s4} \mathbf{P}|0\rangle; \quad C_s^{s'} \mathbf{P}|0\rangle = 0$$
$$\text{for } s < s' \text{ where } s, s' = 1, 2, 3, 4 \tag{3.83}$$

(the index 4 in the first equation specifies that we are dealing with U_4) we observe that $\mathbf{P}|0\rangle$ is at the same time an h.w. state for U_3, U_2 and U_1 because the Eqs.(3.83) contain the equations which give the h.w. states for U_3, U_2 and U_1, as the set of generators of U_4 contains as sub-sets the generators of U_3, U_2 and U_1.

On the other hand, we have seen in this section that the components of the weight belonging to an h.w. state form a partition that characterizes the state. In our case the state $\mathbf{P}|0\rangle$ is an h.w. state of U_4 and thus can be characterized by the partition $[v_{14}, v_{24}, v_{34}, v_{44}]$ formed from the components of its weight. But $\mathbf{P}|0\rangle$ is an h.w. state of U_3 with the weight of components $v_{13} = v_{14}$, $v_{23} = v_{24}$, $v_{33} = v_{34}$ resulting from Eq.(3.83) written for U_3. Then it can also be characterized by the partition $[v_{14}, v_{24}, v_{34}]$. Moreover, being the h.w. state for U_2 and U_1, it can be characterized by the partitions $[v_{14}, v_{24}]$ and $[v_{14}]$ associated with the components of its weight in U_2 and U_1, respectively.

Following the same considerations for $\mathcal{U}_r$ and its natural chain we can characterize an h.w. state of $\mathcal{U}_r$ by a sequence of partitions representing the property that this h.w. state of $\mathcal{U}_r$ is an h.w. state for all groups in the natural chain

$$\mathcal{U}_r \supset \mathcal{U}_{r-1} \supset \ldots \supset \mathcal{U}_2 \supset \mathcal{U}_1 \tag{3.84}$$

Then, an h.w. state of the direct product $\mathcal{U}_r \otimes U_4$, i.e. an h.w. state for both $\mathcal{U}_r$ and U_4, can be written as a definite Gel'fand state

$$\left| \begin{array}{cccccc} h_{1r} & h_{2r} & h_{3r} & \ldots\ldots & h_{rr} & \end{array} \right. \quad \begin{array}{cccc} v_{14} & v_{24} & v_{34} & v_{44} \end{array}$$
$$\begin{array}{cccc} h_{1r} & h_{2r} & h_{3r} \ldots & h_{r-1,r} \end{array} \quad \begin{array}{ccc} v_{14} & v_{24} & v_{34} \end{array}$$
$$\ldots\ldots\ldots \quad \begin{array}{cc} v_{14} & v_{24} \end{array}$$
$$h_{1r} \quad v_{14} \qquad \left. \right\rangle \tag{3.85}$$

Now the question arises of how to construct the most general Gel'fand state. The answer to this question must take into account the following property: If we have an IR of $\mathcal{U}_r$ characterized by the partition $[h_{1r}, h_{2r}, \ldots, h_{r,r}]$ and want to find IR of $\mathcal{U}_{r-1}$, whose partitions $[h_{1r-1}, h_{2,r-1}, \ldots, h_{r-1,r-1}]$ are contained in it, the components $h_{\mu\mu'}$ of these two partitions satisfy the inequality (H. Weyl, The Theory of Groups and Quantum Mechanics, Dover (1931) 391)

$$h_{1r} \geq h_{1r-1} \geq h_{2r} \geq h_{2r-1} \geq \ldots \geq h_{r-1,r-1} \geq h_{rr} \geq 0 \tag{3.86}$$

This is a fundamental relation for the unitary group and it is the equivalent one to the relation $\ell \geq m \geq -\ell$ for the chain $R_3 \supset R_2$ of rotational groups. Keeping this property in mind, we shall try to get a general Gel'fand state starting from the h.w. Gel'fand state.

This problem separates into two parts, one referring to $\mathcal{U}_r$ and the other to U_4. For the moment we restrict ourselves to $\mathcal{U}_r$. Our aim is to get the state

$$\left| \begin{array}{ccccccc} h_{1r} & \ldots\ldots\ldots\ldots\ldots & h_{rr} & \end{array} \right.$$
$$\begin{array}{ccccc} h_{1r-1} & \ldots\ldots\ldots & h_{r-1,r-1} \end{array}$$
$$\ldots\ldots\ldots\ldots$$
$$h_{11} \qquad \left. \right\rangle \tag{3.87}$$

from the h.w. state. The first thing we have to do is to find the components of the weight for such a state. For this purpose let us define the operator

$$\mathcal{N}_r = \sum_{\mu=1}^{r} \mathcal{C}_{\mu}^{\mu} \tag{3.88}$$

This operator represents a contraction of the upper and lower indices of the generator and therefore would be invariant under unitary transformations of the creation and annihilation operators. One therefore expects that $\mathscr{N}_r$ commutes with all the generators, which we proceed to show.

$$\left[\mathscr{C}^{\mu''}_{\mu'}, \sum_{\mu=1}^{r} \mathscr{C}^{\mu}_{\mu} \right] = \sum_{\mu=1}^{r} [\mathscr{C}^{\mu''}_{\mu'}, \mathscr{C}^{\mu}_{\mu}] = \sum_{\mu=1}^{r} (\mathscr{C}^{\mu}_{\mu'} \delta^{\mu''}_{\mu} - \mathscr{C}^{\mu''}_{\mu} \delta^{\mu}_{\mu'})$$

$$= \mathscr{C}^{\mu''}_{\mu'} \sum_{\mu=1}^{r} (\delta^{\mu''}_{\mu} - \delta^{\mu}_{\mu'}) = 0 \tag{3.89}$$

Operators that commute with all the generators will be denoted here as Casimir operators, though the word is usually used in a more restricted sense. The operator $\mathscr{N}_r$, being linear in the $\mathscr{C}^{\mu'}_{\mu}$, will be designated as a Casimir operator of the first order for the group $\mathscr{U}_r$. Obviously, the first order Casimir operator of $\mathscr{U}_{r-1}$ is

$$\mathscr{N}_{r-1} = \sum_{\mu=1}^{r-1} \mathscr{C}^{\mu}_{\mu} \tag{3.90}$$

Now, using the definition and the properties of $\mathscr{N}_r$, we can find the weight of a general Gel'fand state. For the w_r component let us calculate

$$\mathscr{C}^{r}_{r} \left| \begin{matrix} h_{1r} \; h_{2r} \; \ldots\ldots\ldots \; h_{rr} \\ h_{1r-1} \ldots h_{r-1,r-1} \\ \ldots\ldots\ldots \\ h_{11} \end{matrix} \right\rangle = (\mathscr{N}_r - \mathscr{N}_{r-1}) \left| \begin{matrix} h_{1r} \; h_{2r} \; \ldots\ldots\ldots \; h_{rr} \\ h_{1r-1} \ldots h_{r-1,r-1} \\ \ldots\ldots\ldots \\ h_{11} \end{matrix} \right\rangle$$

$$= [(h_{1r}+h_{2r}+\ldots h_{rr})-(h_{1r-1}+h_{2r-1}+\ldots h_{r-1,r-1})] \left| \begin{matrix} h_{1r} \; h_{2r} \; \ldots\ldots\ldots h_{rr} \\ h_{1r-1} \ldots h_{r-1,r-1} \\ \ldots\ldots\ldots \\ h_{11} \end{matrix} \right\rangle \tag{3.91}$$

and obtain

$$w_r = (h_{1r}+h_{2r}+\ldots h_{rr}) - (h_{1r-1}+h_{2r-1}+\ldots h_{r-1,r-1}) \tag{3.92}$$

as the difference between the eigenvalues of $\mathscr{N}_r$ and $\mathscr{N}_{r-1}$. Here the eigenvalues are the same as those for the h.w. state of $\mathscr{U}_r$ and $\mathscr{U}_{r-1}$ because the Casimir operator commutes with the generators of the group and in particular with the lowering generators which pass us from the h.w. state to an arbitrary state.

To obtain the w_{r-1} component we apply to the Gel'fand state the operator $\mathscr{C}^{r-1}_{r-1} = \mathscr{N}_{r-1} - \mathscr{N}_{r-2}$, and so on. Generally, the w_μ component is:

$$w_\mu = (h_{1\mu} + h_{2\mu} + \ldots h_{\mu\mu}) - (h_{1\mu-1} + h_{2\mu-1} + \ldots h_{\mu-1,\mu-1}) \tag{3.93}$$

The set w_μ where $\mu = 1, 2, \ldots r$ gives the weight of a general Gel'fand state of the unitary group in r dimensions and, as one sees from the expression of w_μ, there are in general several Gel'fand states corresponding to a given weight except for the highest weight state which is simple. This result does not occur in R_3 where only one state corresponds to a given weight.

3.6. How to get an arbitrary state for a given irreducible representation from the highest weight state

For the three-dimensional rotation group, the h.w.s corresponding to the irreducible representation ℓ are solutions of the equations

$$L_0 Y_{\ell\ell} = \ell Y_{\ell\ell} \tag{3.94}$$

$$L_+ Y_{\ell\ell} = 0 \tag{3.95}$$

The states of given weight $Y_{\ell m}$ are obtained from $Y_{\ell\ell}$ by applying to it the lowering operator L_-:

$$L_- Y_{\ell\ell} \propto Y_{\ell,\ell-1} \tag{3.96}$$

This suggests that by applying the lowering generators of $\mathscr{U}_r$ to the h.w. states, we should be able to generate all the orbital states of the n particle system. This is in fact true with the observation that by following such a way we shall not succeed in carrying out our step-down procedure via Gel'fand states. This happens because for $\mathscr{U}_r$ there are several ways of going down from a function of highest weight to a function of lower weight, ($\mathscr{U}_r$ has several lowering operators) in contrast with the R_3 group, where the way of obtaining states of lower weight is unique (R_3 has only one step-down operator).

If we are permitted an analogy, the situation for $\mathscr{U}_r$ is somewhat similar to getting down from the peak of a mountain (the h.w. state). There are generally several ways to get down from a peak, but we are interested in a well defined way of getting down, namely, the way that passes only through Gel'fand states. (Actually we have two mountains: $\mathscr{U}_r$ and U_4 !)

We shall carry out the stepping-down analysis for $\mathscr{U}_r$. Let us first consider two particular cases $r = 2$ and $r = 3$. The analysis of the process of stepping down for these cases will enable us to infer the general rule. Let us begin with $r = 2$ whose general Gel'fand state is

$$\left| \begin{matrix} h_{12} & & h_{22} \\ & h_{11} & \end{matrix} \right\rangle \tag{3.97}$$

Its weight is [3]

$$(h_{11},\ h_{12} + h_{22} - h_{11})$$

If we now want to apply the lowering operator $\mathscr{C}_2^1$ to $\left|\begin{matrix} h_{12} & h_{22} \\ & h_{11} \end{matrix}\right\rangle$ we first observe that the numbers h_{12}, h_{22} cannot change because they characterize the irreducible representation of $\mathscr{U}_2$ to which the function $\left|\begin{matrix} h_{12} & h_{22} \\ & h_{11} \end{matrix}\right\rangle$ belongs.[4] So only h_{11} will change and we obtain [5]

$$\mathscr{C}_2^1 \left|\begin{matrix} h_{12} & h_{22} \\ & h_{11} \end{matrix}\right\rangle \propto \left|\begin{matrix} h_{12} & h_{22} \\ & h'_{11} \end{matrix}\right\rangle \tag{3.98}$$

The value of h'_{11} is obtained by observing that,

$$[\mathscr{C}_1^1,\ \mathscr{C}_2^1] = -\mathscr{C}_2^1 \quad \text{i.e.} \quad \mathscr{C}_1^1\mathscr{C}_2^1 = \mathscr{C}_2^1(\mathscr{C}_1^1 - 1) \tag{3.99}$$

whence

$$\mathscr{C}_1^1\mathscr{C}_2^1 \left|\begin{matrix} h_{12} & h_{22} \\ & h_{11} \end{matrix}\right\rangle = (h_{11} - 1)\, \mathscr{C}_2^1 \left|\begin{matrix} h_{12} & h_{22} \\ & h_{11} \end{matrix}\right\rangle \tag{3.100}$$

so that

$$h'_{11} = h_{11} - 1$$

Now, an arbitrary state $\left|\begin{matrix} h_{12} & h_{22} \\ & h_{11} \end{matrix}\right\rangle$ is obtained from the h.w. state, by applying to the h.w. state the operator $(\mathscr{C}_2^1)^{h_{12} - h_{11}}$

$$(\mathscr{C}_2^1)^{h_{12} - h_{11}} \left|\begin{matrix} h_{12} & h_{22} \\ & h_{12} \end{matrix}\right\rangle \propto \left|\begin{matrix} h_{12} & h_{22} \\ & h_{11} \end{matrix}\right\rangle \tag{3.101}$$

---

[3] The state $\left|\begin{matrix} h_{12} & h_{22} \\ & h_{11} \end{matrix}\right\rangle$ satisfies the two eigenvalue equations:

$$\mathscr{C}_1^1 \left|\begin{matrix} h_{12} & h_{22} \\ & h_{11} \end{matrix}\right\rangle = h_{11} \left|\begin{matrix} h_{12} & h_{22} \\ & h_{11} \end{matrix}\right\rangle$$

$$\mathscr{C}_2^2 \left|\begin{matrix} h_{12} & h_{22} \\ & h_{11} \end{matrix}\right\rangle = (h_{12} + h_{22} - h_{11}) \left|\begin{matrix} h_{12} & h_{22} \\ & h_{11} \end{matrix}\right\rangle$$

[4] If we apply the generator of a group to a state belonging to a given irreducible representation of that group, we get a state belonging to the same irreducible representation.

[5] We should get, in fact, a sum over Gel'fand states with the same h_{12} and h_{22} but with different values of h'_{11}, but we shall prove that h'_{11} has a well determined value.

This is analogous to the R_3 relation

$$(L_-)^{\ell-m} \, |\ell\ell\rangle \propto |\ell m\rangle \tag{3.102}$$

It would perhaps be instructive to point out that the correspondence between relations (3.101) and (3.102) is not only an analogy but even a one-to-one correspondence, which can be determined if we observe that the operators

$$L_+, \; L_0, \; L_- \tag{3.103}$$

can be put into correspondence with the operators

$$\mathscr{C}^2_1, \; \tfrac{1}{2}(\mathscr{C}^1_1 - \mathscr{C}^2_2), \; \mathscr{C}^1_2 \tag{3.104}$$

This originates from the fact that the operators (3.104) are obtained from the four generators of the $\mathscr{U}_2$ group by taking the linear combinations $\frac{1}{2}(\mathscr{C}^1_1 + \mathscr{C}^2_2)$, $\frac{1}{2}(\mathscr{C}^1_1 - \mathscr{C}^2_2)$ instead of the operators $\mathscr{C}^1_1$, $\mathscr{C}^2_2$ and by removing the operator $\frac{1}{2}(\mathscr{C}^1_1 + \mathscr{C}^2_2)$ which is just the generator of the unitary transformation

$$U = e^{i\delta} I \cong (1 + i\delta) I, \quad \text{when} \quad \delta \ll 1 \tag{3.105}$$

But, as for a general unitary transformation U, we have $\det U = e^{i\varphi}$, we conclude that by removing transformations of type (3.105) one gets the unitary unimodular group in two dimensions SU_2. This is equivalent to the fact that by removing the generator $\frac{1}{2}(\mathscr{C}^1_1 + \mathscr{C}^2_2)$ from the set $\mathscr{C}^2_1$, $\frac{1}{2}(\mathscr{C}^1_1 + \mathscr{C}^2_2)$, $\frac{1}{2}(\mathscr{C}^1_1 - \mathscr{C}^2_2)$, $\mathscr{C}^1_2$ one gets the generators of the group SU_2, which, as we know, is homomorphic to R_3. The equality between the powers of the lowering operators in (3.101) and (3.102) results, if one observes that $|\ell\ell\rangle$ corresponds to $\left|\begin{matrix} h_{12} & h_{22} \\ & h_{12} \end{matrix}\right\rangle$ and $|\ell m\rangle$ corresponds to $\left|\begin{matrix} h_{12} & h_{22} \\ & h_{11} \end{matrix}\right\rangle$, while the operator L_0 corresponds to $\frac{1}{2}(\mathscr{C}^1_1 - \mathscr{C}^2_2)$. The difference ℓ-m of the eigenvalues of L_0 for the states $|\ell\ell\rangle$ and $|\ell m\rangle$ should correspond to the difference of the eigenvalues of $\frac{1}{2}(\mathscr{C}^1_1 - \mathscr{C}^2_2)$ for the states $\left|\begin{matrix} h_{12} & h_{22} \\ & h_{12} \end{matrix}\right\rangle$ and $\left|\begin{matrix} h_{12} & h_{22} \\ & h_{11} \end{matrix}\right\rangle$. We have

$$\begin{aligned} \tfrac{1}{2}(\mathscr{C}^1_1 - \mathscr{C}^2_2) \left|\begin{matrix} h_{12} & h_{22} \\ & h_{12} \end{matrix}\right\rangle &= \tfrac{1}{2}[h_{12} - (h_{12} + h_{22} - h_{12})] \left|\begin{matrix} h_{12} & h_{22} \\ & h_{12} \end{matrix}\right\rangle \\ &= \tfrac{1}{2}(h_{12} - h_{22}) \left|\begin{matrix} h_{12} & h_{22} \\ & h_{12} \end{matrix}\right\rangle \end{aligned} \tag{3.106}$$

and

$$\tfrac{1}{2}(\mathscr{C}^1_1 - \mathscr{C}^2_2) \left|\begin{matrix} h_{12} & h_{22} \\ & h_{11} \end{matrix}\right\rangle = \tfrac{1}{2}[h_{11} - (h_{12} + h_{22} - h_{11})] \left|\begin{matrix} h_{12} & h_{22} \\ & h_{11} \end{matrix}\right\rangle \tag{3.107}$$

The difference between the two eigenvalues gives the power of the lowering operator and is equal to $h_{12} - h_{11}$, as it should be. The equality (3.101) has been written up to a normalization coefficient, which may be shown to be

$$N \begin{pmatrix} h_{12} & h_{22} \\ & h_{11} \end{pmatrix} = \sqrt{\frac{(h_{11} - h_{22})!}{(h_{12} - h_{11})!\,(h_{12} - h_{22})!}} \tag{3.108}$$

We can thus write

$$\left| \begin{matrix} h_{12} & h_{22} \\ & h_{11} \end{matrix} \right\rangle = N \begin{pmatrix} h_{12} & h_{22} \\ & h_{11} \end{pmatrix} (\mathscr{E}_2^1)^{h_{12} - h_{11}} \left| \begin{matrix} h_{12} & h_{22} \\ & h_{12} \end{matrix} \right\rangle \tag{3.109}$$

Let us now consider an arbitrary Gel'fand state of $\mathscr{U}_3$

$$\left| \begin{matrix} h_{13} & h_{23} & h_{33} \\ & h_{12} & h_{22} \\ & & h_{11} \end{matrix} \right\rangle \tag{3.110}$$

and try to obtain it by a stepping-down procedure from the h.w. state

$$\left| \begin{matrix} h_{13} & h_{23} & h_{33} \\ & h_{13} & h_{23} \\ & & h_{13} \end{matrix} \right\rangle \tag{3.111}$$

As we know how to obtain any U_2 state from the U_2 h.w. state, we shall now only worry about obtaining the state of h.w. in U_2

$$\left| \begin{matrix} h_{13} & h_{23} & h_{33} \\ & h_{12} & h_{22} \\ & & h_{12} \end{matrix} \right\rangle \tag{3.112}$$

from the U_3 h.w. state (3.111). To achieve this, we shall start by examining the effect of the lowering operators $\mathscr{E}_3^2$, $\mathscr{E}_3^1$ upon a given Gel'fand state. The commutation relation

$$[\mathscr{E}_1^1, \mathscr{E}_3^2] = 0 \tag{3.113}$$

tells us that

$$\mathscr{E}_1^1 \mathscr{E}_3^2 \left| \begin{matrix} h_{13} & h_{23} & h_{33} \\ & h_{12} & h_{22} \\ & & h_{12} \end{matrix} \right\rangle = h_{12} \mathscr{E}_3^2 \left| \begin{matrix} h_{13} & h_{23} & h_{33} \\ & h_{12} & h_{22} \\ & & h_{12} \end{matrix} \right\rangle \tag{3.114}$$

From the commutation relations (3.11) we get

$$\mathscr{C}^2_2\mathscr{C}^2_3 = \mathscr{C}^2_3(\mathscr{C}^2_2 - 1), \quad \mathscr{C}^3_3\mathscr{C}^2_3 = \mathscr{C}^2_3(\mathscr{C}^3_3 + 1) \tag{3.115}$$

so that when we replace $\mathscr{C}^1_1$ by $\mathscr{C}^2_2$ or $\mathscr{C}^3_3$ in (3.114), we see that the state

$$\mathscr{C}^2_3 \left| \begin{matrix} h_{13} & h_{23} & h_{33} \\ & h_{12} \quad h_{22} & \\ & h_{12} & \end{matrix} \right\rangle \tag{3.116}$$

has weight

$$(h_{12},\ h_{22}-1,\ h_{13}+h_{23}+h_{33}-h_{12}-h_{22}+1) \tag{3.117}$$

We see furthermore that $\mathscr{C}^2_1$ and $\mathscr{C}^2_3$ commute, so the state (3.116) is of highest weight in the $\mathscr{U}_2$ sub-group. We conclude from (3.117) that

$$\mathscr{C}^2_3 \left| \begin{matrix} h_{13} & h_{23} & h_{33} \\ & h_{12} \quad h_{22} & \\ & h_{12} & \end{matrix} \right\rangle \propto \left| \begin{matrix} h_{13} & h_{23} & h_{33} \\ & h_{12} \quad h_{22}-1 & \\ & h_{12} & \end{matrix} \right\rangle \tag{3.118}$$

Let us now examine the effect that $\mathscr{C}^1_3$ has upon the state $\left| \begin{matrix} h_{13} & h_{23} & h_{33} \\ & h_{12} \quad h_{22} & \\ & h_{12} & \end{matrix} \right\rangle$

The generator $\mathscr{C}^1_3$ has the following commutation relation with the weight generators

$$[\mathscr{C}^1_1,\ \mathscr{C}^1_3] = -\mathscr{C}^1_3;\ [\mathscr{C}^2_2,\ \mathscr{C}^1_3] = 0;\ [\mathscr{C}^3_3,\ \mathscr{C}^1_3] = \mathscr{C}^1_3 \tag{3.119}$$

which tells us that

$$\mathscr{C}^1_3 \left| \begin{matrix} h_{13} & h_{23} & h_{33} \\ & h_{12} \quad h_{22} & \\ & h_{12} & \end{matrix} \right\rangle \tag{3.120}$$

is an eigenfunction of $\mathscr{C}^\mu_\mu$, $\mu = 1, 2, 3$ with eigenvalues

$$(h_{12}-1,\ h_{22},\ h_{13}+h_{23}+h_{33}-h_{12}-h_{22}+1) \tag{3.121}$$

The weight of (3.120) is then given by (3.121).

Let us now consider the operator $\mathscr{C}^1_2\mathscr{C}^2_3$, which has the same commutation relations with the weight operators as $\mathscr{C}^1_3$, namely,

$$[\mathscr{C}^1_1,\ \mathscr{C}^1_2\mathscr{C}^2_3] = -\mathscr{C}^1_2\mathscr{C}^2_3 \tag{3.122}$$

$$[\mathscr{C}^2_2, \mathscr{C}^1_2\mathscr{C}^2_3] = 0 \tag{3.123}$$

$$[\mathscr{C}^3_3,\ \mathscr{C}^1_2\mathscr{C}^2_3] = \mathscr{C}^1_2\mathscr{C}^2_3 \tag{3.124}$$

The identity of the commutation rules of $\mathscr{C}_2^1\mathscr{C}_3^2$ and $\mathscr{C}_3^1$ with the weight operators tells us that the effect of $\mathscr{C}_2^1\mathscr{C}_3^2$ upon the weight of a Gel'fand state will be the same as for $\mathscr{C}_3^1$. We have then the hope that there exists a linear combination of $\mathscr{C}_3^1$ and $\mathscr{C}_2^1\mathscr{C}_3^2$ which, applied to a function of h.w. in $\mathscr{U}_2$, should give us a function of h.w. in $\mathscr{U}_2$. That is, we want to determine a and b such that

$$(a\,\mathscr{C}_3^1 + b\,\mathscr{C}_2^1\mathscr{C}_3^2)\left|\begin{matrix} h_{13} & h_{23} & h_{33} \\ & h_{12} & h_{22} \\ & & h_{12} \end{matrix}\right\rangle \propto \left|\begin{matrix} h_{13} & h_{23} & h_{33} \\ & h_{12}-1 & h_{22} \\ & & h_{12}-1 \end{matrix}\right\rangle \tag{3.125}$$

As the resulting state is of highest weight in $\mathscr{U}_2$, the application of a raising operator in U_2 should give zero. We thus get the following equation for the determination of a and b

$$\mathscr{C}_1^2(a\,\mathscr{C}_3^1 + b\,\mathscr{C}_2^1\mathscr{C}_3^2)\left|\begin{matrix} h_{13} & h_{23} & h_{33} \\ & h_{12} & h_{22} \\ & & h_{12} \end{matrix}\right\rangle = 0 \tag{3.126}$$

As

$$\mathscr{C}_1^2\left|\begin{matrix} h_{13} & h_{23} & h_{33} \\ & h_{12} & h_{22} \\ & & h_{12} \end{matrix}\right\rangle = 0 \tag{3.127}$$

we can write Eq.(3.126) in the form:

$$[\mathscr{C}_1^2, (a\,\mathscr{C}_3^1 + b\,\mathscr{C}_2^1\mathscr{C}_3^2)]\left|\begin{matrix} h_{13} & h_{23} & h_{33} \\ & h_{12} & h_{22} \\ & & h_{12} \end{matrix}\right\rangle = 0 \tag{3.128}$$

But

$$[\mathscr{C}_1^2,\ \mathscr{C}_3^1] = -\mathscr{C}_3^2 \tag{3.129}$$

and

$$[\mathscr{C}_1^2,\ \mathscr{C}_3^2] = 0 \tag{3.130}$$

so Eq.(3.128) becomes

$$0 = [-a\,\mathscr{C}_3^2 + b[\mathscr{C}_1^2, \mathscr{C}_2^1]\mathscr{C}_3^2]\left|\begin{matrix} h_{13} & h_{23} & h_{33} \\ & h_{12} & h_{22} \\ & & h_{12} \end{matrix}\right\rangle \tag{3.131}$$

$$= [-a + b(\mathscr{C}_1^1 - \mathscr{C}_2^2)]\mathscr{C}_3^2 \left| \begin{matrix} h_{13} & h_{23} & h_{33} \\ & h_{12} & h_{22} \\ & & h_{12} \end{matrix} \right\rangle$$

$$\propto [-a + b(\mathscr{C}_1^1 - \mathscr{C}_2^2)] \left| \begin{matrix} h_{13} & h_{23} & h_{33} \\ & h_{12} & h_{22}-1 \\ & & h_{12} \end{matrix} \right\rangle \qquad (3.132)$$

the last equation resulting from (3.118). We finally get

$$[-a + b(h_{12} - h_{22} + 1)] \left| \begin{matrix} h_{13} & h_{23} & h_{33} \\ & h_{12} & h_{22}-1 \\ & & h_{12} \end{matrix} \right\rangle = 0 \qquad (3.133)$$

whence

$$a = b(h_{12} - h_{22} + 1) \qquad (3.134)$$

As we are not interested yet in the normalization problem, we can put $b = 1$ and get

$$a = h_{12} - h_{22} + 1 \qquad (3.135)$$

We have thus succeeded in obtaining the operator which, applied to a Gel'fand state of $\mathscr{U}_3$ of highest weight in the $\mathscr{U}_2$ sub-group, gives us another Gel'fand state of highest weight in $\mathscr{U}_2$:

$$[\mathscr{C}_3^1(h_{12} - h_{22} + 1) + \mathscr{C}_2^1\mathscr{C}_3^2] \left| \begin{matrix} h_{13} & h_{23} & h_{33} \\ & h_{12} & h_{22} \\ & & h_{12} \end{matrix} \right\rangle \propto \left| \begin{matrix} h_{13} & h_{23} & h_{33} \\ & h_{12}-1 & h_{22} \\ & & h_{12}-1 \end{matrix} \right\rangle \qquad (3.136)$$

We shall now introduce the following definitions. We shall call L_2^1 the lowering operator for U_2, whose effect is

$$L_2^1 \left| \begin{matrix} h_{12} & h_{22} \\ & h_{11} \end{matrix} \right\rangle \propto \left| \begin{matrix} h_{12} & h_{22} \\ & h_{11}-1 \end{matrix} \right\rangle \qquad (3.137)$$

As we have already seen,

$$L_2^1 \equiv \mathscr{C}_2^1 \qquad (3.138)$$

and the following are lowering operators for U_3

$$L_2^1 \equiv \mathscr{C}_3^1(\mathscr{C}_1^1 - \mathscr{C}_2^2 + 1) + \mathscr{C}_2^1 \mathscr{C}_3^2 \tag{3.139}$$

$$L_3^2 \equiv \mathscr{C}_3^2 \tag{3.140}$$

where to get (3.139) we replaced in (3.136) the eigenvalue $h_{12} - h_{22} + 1$ by the operator which produces it when acting on the Gel'fand state in (3.136). An arbitrary Gel'fand state may thus be obtained from an h.w. Gel'fand state by the equation

$$\left| \begin{matrix} h_{13} & h_{23} & h_{33} \\ & h_{12} & h_{22} \\ & & h_{11} \end{matrix} \right\rangle = N' \begin{pmatrix} h_{12} & h_{22} \\ & h_{11} \end{pmatrix} N \begin{pmatrix} h_{13} & h_{23} & h_{33} \\ & h_{12} & h_{22} \end{pmatrix} \times (L_2^1)^{h_{12}-h_{11}} (L_3^1)^{h_{13}-h_{12}} (L_3^2)^{h_{23}-h_{22}} \left| \begin{matrix} h_{13} & h_{23} & h_{33} \\ & h_{13} & h_{23} \\ & & h_{13} \end{matrix} \right\rangle \tag{3.141}$$

where N' and N are normalization factors associated, respectively, with the operator $(L_2^1)^{h_{12}-h_{11}}$ that acts in $\mathscr{U}_2$ and to the product of operators $(L_3^1)^{h_{13}-h_{12}}(L_3^2)^{h_{23}-h_{22}}$ that acts in $\mathscr{U}_3$.

Once we know the expressions for the lowering operators, the calculation of matrix elements of a generator $\mathscr{C}_\mu^{\mu'}$ between Gel'fand states of $\mathscr{U}_3$

$$\left\langle \begin{matrix} h_{13} & h_{23} & h_{33} \\ & h'_{12} & h'_{22} \\ & & h'_{11} \end{matrix} \right| \mathscr{C}_\mu^{\mu'} \left| \begin{matrix} h_{13} & h_{23} & h_{33} \\ & h_{12} & h_{22} \\ & & h_{11} \end{matrix} \right\rangle \tag{3.142}$$

is reduced to a calculation of commutation relations between $\mathscr{C}_\mu^{\mu'}$ and the operators L_2^1, L_3^1, L_3^2, and the explicit expressions are given in Ref. [1].

The procedure for determining the lowering operators for $\mathscr{U}_3$ has been generalized to the case $\mathscr{U}_r$ by Nagel and Moshinsky and the explicit expression of the lowering operators for this general case as well as of the normalization coefficients is given in Ref. [2]. Furthermore the matrix elements of the generators of $\mathscr{U}_r$ with respect to Gel'fand states were also obtained by the same procedure as that indicated for $\mathscr{U}_3$ in (3.142) thus giving an independent derivation of the analysis of Gel'fand and Zetlin.

3.7. Definition and eigenvalues of Casimir operators

For the purpose of our analysis we define as a Casimir operator an operator formed from the generators of a group that commutes with all of them.

Examples: For the R_3 group the operator

$$L^2 = L_1^2 + L_2^2 + L_3^2 \tag{3.143}$$

is a Casimir operator as it commutes with L_i $i = 1, 2, 3$.

For the $\mathscr{U}_r$ group

$$\mathscr{N}_r = \sum_{\mu=1}^{r} \mathscr{C}_{\mu}^{\mu} \tag{3.144}$$

is a Casimir operator, as we showed in a previous sub-section that it commuted with all $\mathscr{C}_{\mu'}^{\mu'}$. We could have seen this also from the fact that as $\mathscr{N}_r$ is given by a contraction between a creation and an annihilation operator that transform by conjugate unitary transformations, $\mathscr{N}_r$ is clearly an invariant with respect to $\mathscr{U}_r$, and so we would expect that it commutes with all generators of $\mathscr{U}_r$ that are in fact associated with infinitesimal unitary transformations. This suggests then that invariants under $\mathscr{U}_r$ such as

$$\Gamma_r = \sum_{\mu,\mu'=1}^{r} \mathscr{C}_{\mu}^{\mu'} \mathscr{C}_{\mu'}^{\mu} \tag{3.145}$$

should commute with all the generators of $\mathscr{U}_r$, which we easily check by making use of the commutation relations (3.11). Therefore Γ_r is a Casimir operator of $\mathscr{U}_r$ and we shall refer to it as second order Casimir operator to distinguish it from $\mathscr{N}_r$. We could by a procedure similar to (3.145) discuss Casimir operators of higher order, but as they will be of no special use to us, we restrict ourselves in this section to the analysis of the eigenvalues of Γ_r.

To obtain these eigenvalues we shall apply Γ_r to a Gel'fand state, but before doing this we shall discuss the corresponding problem for R_3.

If we apply L^2 to the state $|\ell m\rangle$ we note from the fact that L_- commutes with $L^2 = L_- L_+ + L_0(L_0+1)$ that we can write

$$\begin{aligned} L^2 |\ell m\rangle &= \left[\frac{(\ell+m)!}{(\ell-m)!\,2\ell!}\right]^{\frac{1}{2}} L_-^{\ell-m} L^2 |\ell\ell\rangle \\ &= \left[\frac{(\ell+m)!}{(\ell-m)!\,2\ell!}\right]^{\frac{1}{2}} L_-^{\ell-m} [L_- L_+ + L_0(L_0+1)] |\ell\ell\rangle \\ &= \ell(\ell+1) |\ell m\rangle \end{aligned} \tag{3.146}$$

where we used the fact that for the highest weight state $L_+ |\ell\ell\rangle = 0$.

The analysis of the previous paragraph, together with a development similar to (3.146) for $\mathscr{U}_r$, suggests that in the search of the eigenvalues of Γ_r we could restrict our discussion to the application of Γ_r to the h.w.

state of $\mathscr{U}_r$ i.e.

$$\Gamma_r \left| \begin{array}{c} h_{1r} \ldots\ldots\ldots h_{rr} \\ h_{1r} \ldots\ldots h_{r-1\,r} \\ \ldots\ldots\ldots \\ h_{1r} \end{array} \right\rangle \equiv \Gamma_r \, \mathbf{P} \, |0\rangle \tag{3.147}$$

We now rewrite Γ_r in the following form:

$$\begin{aligned} \Gamma_r &= \sum_{\mu\mu'=1}^{r} \mathscr{C}^{\mu}_{\mu'} \mathscr{C}^{\mu'}_{\mu} \\ &= \sum_{\mu<\mu'=2}^{r} \mathscr{C}^{\mu}_{\mu'} \mathscr{C}^{\mu'}_{\mu} + \sum_{\mu=1}^{r} (\mathscr{C}^{\mu}_{\mu})^2 + \sum_{\mu>\mu'=1}^{r} \mathscr{C}^{\mu}_{\mu'} \mathscr{C}^{\mu'}_{\mu} \\ &= 2 \sum_{\mu<\mu'=2}^{r} \mathscr{C}^{\mu}_{\mu'} \mathscr{C}^{\mu'}_{\mu} + \sum_{\mu=1}^{r} (\mathscr{C}^{\mu}_{\mu})^2 + \sum_{\mu<\mu'=2}^{r} [\mathscr{C}^{\mu'}_{\mu}, \mathscr{C}^{\mu}_{\mu'}] \\ &= 2 \sum_{\mu<\mu'=2}^{r} \mathscr{C}^{\mu}_{\mu'} \mathscr{C}^{\mu'}_{\mu} + \sum_{\mu=1}^{r} (\mathscr{C}^{\mu}_{\mu})^2 + \sum_{\mu<\mu'=2}^{r} (\mathscr{C}^{\mu}_{\mu} - \mathscr{C}^{\mu'}_{\mu'}) \end{aligned} \tag{3.148}$$

In this last summation the first term acting on the state of highest weight gives zero, due to the effect of the raising generator $\mathscr{C}^{\mu'}_{\mu}$ $\mu<\mu'$. The second term gives $\sum_{\mu=1}^{r} h_\mu h_\mu$, the third $2 \sum_{\mu<\mu'=2}^{r} (h_\mu - h_{\mu'})$. Adding up we get for γ_r in

$$\Gamma_r \, \mathbf{P} \, |0\rangle = \gamma_r \, \mathbf{P} \, |0\rangle \tag{3.149}$$

the value

$$\gamma_r = \sum_{\mu=1}^{r} \{h_\mu (h_\mu - 2\mu)\} + n(r+1)$$

where

$$n \equiv \sum h\mu \tag{3.150}$$

4. THE PROBLEM OF A SINGLE SHELL

4.1. The concept of generalized pairing interaction

We wish to investigate interactions which can be diagonalized in a way similar to the case of the symmetric top. This means we want to express our interactions in terms of Casimir operators of physically meaningful sub-groups. We first consider the case of particles in a single shell specified by ℓ, in which case we have

$$r = 2\ell + 1 \tag{4.1}$$

This means that we restrict our quantum numbers $\rho = \nu\ell m$, $\sigma\tau$ to one fixed value of $\nu\,\ell$; m can take $2\ell+1$ values from $+\ell$ to $-\ell$. So instead of specifying the generators $\mathscr{C}_{\mu}^{\mu'}$ by the set $\mu = \nu\ell m, \mu' = \nu\ell m'$, we can simply use m:

$$\mathscr{C}_{\mu}^{\mu'} \equiv \mathscr{C}_{m}^{m'} \tag{4.2}$$

If we define an order

$$\begin{aligned} &\mu = 1, 2, 3, \ldots\ldots, 2\ell+1 \\ &m = \ell, \ell-1, \ell-2, \ldots, -\ell \end{aligned} \tag{4.3}$$

we only have to notice that increasing μ corresponds to decreasing m so that the rising generators $\mathscr{C}_{m}^{m'}$ correspond to $m > m'$ and the lowering generators to $m < m'$. Let us now look at the Hamiltonian Eq. (2.6)

$$H = \sum_{i} \left(\frac{p_i^2}{2m} + U(r) \right) + \sum_{i<j} V(r_{ij}) \tag{4.4}$$

$$\mathscr{H} = \mathscr{W} + \mathscr{V} \tag{4.5}$$

The states $|\nu\ell m\rangle$ could be chosen to diagonalize the single-particle part of the Hamiltonian

$$W_1 = \frac{p_i^2}{2m} + U(r_1) \tag{4.6}$$

$$\langle \nu\ell m' | W_1 | \nu\ell m \rangle = \delta_{mm'} E_{\nu\ell} \tag{4.7}$$

So the one-body part takes the very simple form

$$\begin{aligned} \mathscr{W} &= \sum_{mm'} \langle \nu\ell m | W_1 | \nu\ell m' \rangle \mathscr{C}_{m}^{m'} \\ &= E_{\nu\ell} \sum_{m} \mathscr{C}_{m}^{m} \\ &= E_{\nu\ell} \mathscr{N} \end{aligned} \tag{4.8}$$

that is, the single-particle energy multiplied by the number operator. The two-body operator

$$\mathscr{V} = \frac{1}{2} \sum_{\substack{m_1 m_1' \\ m_2 m_2'}} \langle \nu\ell m_1', \nu\ell m_2' \,|\, V(r_{12}) \,|\, \nu\ell m_1, \nu\ell m_2 \rangle (\mathscr{C}^{m_1}_{m_1'} \mathscr{C}^{m_2}_{m_2'} - \delta^{m_1}_{m_2'} \mathscr{C}^{m_2}_{m_1'}) \tag{4.9}$$

can be rewritten by introducing the total orbital angular momentum two-particle functions

$$|\nu\ell\, \nu\ell,\, \mathscr{J}\mathscr{M}\rangle = \sum_{m_1 m_2} (\ell\ell m_1 m_2 | \mathscr{J}\mathscr{M}) \,|\nu\ell m_1, \nu\ell m_2\rangle \tag{4.10}$$

Using the properties of the Clebsch-Gordan coefficients

$$\sum_{\mathscr{J}\mathscr{M}} (\ell\ell m_1 m_2 | \mathscr{J}\mathscr{M})(\ell\ell \bar{m}_1 \bar{m}_2 | \mathscr{J}\mathscr{M}) = \delta^{\bar{m}_1}_{m_1}\, \delta^{\bar{m}_2}_{m_2} \tag{4.11}$$

and the fact that $V(r_{12})$ is rotationally invariant and so diagonal with respect to $|\mathscr{J}\mathscr{M}\rangle$, we may write

$$\mathscr{V} = \mathscr{V}' + \mathscr{V}'' \tag{4.12}$$

with $\mathscr{V}'$ being the quadratic and $\mathscr{V}''$ the linear part of (4.9), with the first part given by

$$\mathscr{V}' = \frac{1}{2} \sum_{\mathscr{J}} \frac{1}{(2\ell+1)} \langle \nu\ell, \nu\ell, \mathscr{J} \,|\, V(r_{12}) \,|\, \nu\ell, \nu\ell, \mathscr{J}\rangle \mathscr{P}(\mathscr{J}) \tag{4.13}$$

where

$$\mathscr{P}(\mathscr{J}) = \sum_{\mathscr{M}} \sum_{m_1 m_2} \sum_{m_1' m_2'} (2\ell+1) \langle \ell\ell m_1 m_2 | \mathscr{J}\mathscr{M}\rangle \langle \ell\ell m_1' m_2' | \mathscr{J}\mathscr{M}\rangle \mathscr{C}^{m_1}_{m_1'} \mathscr{C}^{m_2}_{m_2'} \tag{4.14}$$

We call this operator $\mathscr{P}(\mathscr{J})$ the generalized pairing interaction. If V is a central interaction such that its matrix elements for a two-particle system are zero for all $\mathscr{J} \neq J$ this means that the two particles only interact when their angular momenta are coupled to a definite value $\mathscr{J} = J$. For $J = 0$ this definition gives

$$\langle \nu\ell\, \nu\ell\, 0 \,|\, V \,|\, \nu\ell\, \nu\ell\, 0\rangle = 2\ell + 1 \tag{4.15a}$$

$$\langle \nu\ell\, \nu\ell\, \mathscr{J} \,|\, V \,|\, \nu\ell\, \nu\ell\, \mathscr{J}\rangle = 0 \qquad \text{for} \qquad \mathscr{J} \neq 0 \tag{4.15b}$$

The simple attractive pairing interaction $-\mathscr{P}(0)$ is such that for a two-particle system in a single shell ℓ, for which $\mathscr{J} = 0, 1, \ldots, 2\ell$, it will

lower the level with angular momentum $\mathcal{J} = 0$, leaving the others untouched. This is Racah's definition of pairing force and is the reason for the name of generalized pairing force for $\mathcal{P}(\mathcal{J})$. This effect of $\mathcal{P}(0)$ is similar to that of a delta type of interaction which out of $\mathcal{J} = 0, 1, \ldots, 2\ell$ two-particle states will also lower the state with $\mathcal{J} = 0$ much more pronouncedly than the others, though the remaining states $\mathcal{J} = 1, \ldots, 2\ell$ will no longer remain degenerate.

In a similar way one can obtain for $\mathcal{V}''$

$$\mathcal{V}'' = -\frac{1}{2} \left\{ \sum_{\mathcal{J}} (-)^{\mathcal{J}} (2\mathcal{J}+1)(2\ell+1)^{-1} \langle \nu\ell\, \nu\ell\, \mathcal{J} \,|\, V_{12} \,|\, \nu\ell\, \nu\ell\, \mathcal{J} \rangle \right\} \mathcal{N} \tag{4.16}$$

So $\mathcal{V}''$ can be coupled to $\mathcal{W}$ to form a term which just multiplies the $\mathcal{N}$ operator. We then need only to be concerned with the term $\mathcal{V}'$.

Looking at Eq. (4.13) we see that the interaction is separated into two factors, one geometrical and the other dynamical. The $\mathcal{P}(\mathcal{J})$ are geometrical concepts depending only on group-theoretical properties, independent of the dynamics of the system. The coefficients are two-body matrix elements of V_{12} that can be evaluated easily and that are related to the detailed dynamical aspects of the problem.

Let us now discuss the standard pairing interaction in Racah's definition

$$\mathcal{V}' = \mathcal{P}(0) \tag{4.17}$$

$$\mathcal{P}(0) = \sum_{\substack{m_1 m_2 \\ m_1' m_2'}} (2\ell+1)(\ell\ell\, m_1 m_2 \,|\, 00)(\ell\ell\, m_1' m_2' \,|\, 00)\, \mathcal{C}^{\,m_1}_{m_1'}\, \mathcal{C}^{\,m_2}_{m_2'} \tag{4.18}$$

From the particular value of

$$\langle \ell\ell\, m_1 m_2 \,|\, 00 \rangle = (2\ell+1)^{-\frac{1}{2}} (-1)^{m_1} \delta_{m_1, -m_2} \tag{4.19}$$

we get

$$\mathcal{P}(0) = \sum_{mm'} (-1)^{m+m'}\, \mathcal{C}^{\,m}_{m'}\, \mathcal{C}^{\,-m}_{-m'} \tag{4.20}$$

This gives us the pairing interaction in terms of the generators of $\mathcal{U}_{2\ell+1}$. We shall show in the next sub-sections that the pairing interaction can be further expressed in terms of the Casimir operators of the $\mathcal{U}_{2\ell+1}$ group and its orthogonal sub-group $\mathcal{O}_{2\ell+1}$, and that the eigenstates of these interactions are classified by the following chain of sub-groups

$$\mathcal{U}_{2\ell+1} \supset \mathcal{O}_{2\ell+1} \supset \mathcal{D}^{\ell}(R_3) \tag{4.21}$$

where the last is the irreducible representation of R_3 of order ℓ given in terms of $(2\ell+1) \times (2\ell+1)$ orthogonal matrices.

4.2. The chain of groups $\mathscr{U}_{2\ell+1} \supset \mathcal{O}_{2\ell+1}$

We must determine the generators of the group $\mathcal{O}_{2\ell+1}$ of interest to us in terms of linear combinations of the generators $\mathscr{C}_m^{m'}$ of $\mathscr{U}_{2\ell+1}$. For this purpose we shall first discuss the transformation properties under the rotation group of $b^\dagger_{\nu\ell m,\sigma\tau}$ and $b^{\nu\ell m,\sigma\tau}$. For a fixed $\nu\ell$ we could denote the creation and annihilation operators by the short-hand notation $b^\dagger_{ms}$, b^{ms}, $s = \sigma\tau$. As $b^\dagger_{ms}$ transforms under rotation in configuration space in the same way as $Y_{\ell m}(\theta, \varphi)$, then $b^{ms} = (b^\dagger_{ms})^\dagger$ transforms under rotation as

$$[Y_{\ell m}(\theta,\varphi)]^* = (-1)^m Y_{\ell - m}(\theta,\varphi) \tag{4.22}$$

We can therefore express the annihilation operators in the same covariant notation as the creation operators if

$$b_m{}^s = \sum_{m'} g_{mm'} b^{m's} \tag{4.23}$$

where from (4.22) the metric tensor $g_{mm'}$ is given by

$$g_{mm'} = (-1)^m \delta_{m,-m'} \tag{4.24}$$

Making use of the metric tensor (4.24) we can put the generators of $\mathscr{U}_{2\ell+1}$ in the purely covariant form

$$\mathscr{C}_{mm'} = \sum_{m''} g_{m'm''} \mathscr{C}_m^{m''} \tag{4.25}$$

or

$$\mathscr{C}_{mm'} = (-1)^{m'} \mathscr{C}_m{}^{-m'} \tag{4.26}$$

We now define the operators

$$\Lambda_{mm'} = \tfrac{1}{2}(\mathscr{C}_{mm'} - \mathscr{C}_{m'm}) \tag{4.27}$$

and proceed to show that they are the generators of an orthogonal group of $2\ell+1$ dimensions. We note first that the number of independent $\Lambda_{mm'}$ in (4.27) is $\frac{1}{2} r(r-1)$ where $r = 2\ell+1$, which is the number of generators of $\mathcal{O}_{2\ell+1}$. Furthermore, from the commutation relations of the $\mathscr{C}_m^{m'}$ we obtain immediately that

$$[\Lambda_{mm'}, \Lambda_{m''m'''}] = \tfrac{1}{2}(\Lambda_{mm'''} g_{m''m'} + \Lambda_{m'm''} g_{m'''m} + \Lambda_{m'''m} g_{mm''} + \Lambda_{m''m} g_{m'm'''}) \tag{4.28}$$

so that the $\Lambda_{mm'}$ are the generators of a sub-group of $\mathscr{U}_{2\ell+1}$. To show that this sub-group is $\mathcal{O}_{2\ell+1}$, we note that the infinitesimal transformations of this sub-group can be written as

$$O = I + \epsilon A \tag{4.29}$$

where A is a real matrix which, because of the orthogonality property

$$O\tilde{O} = (I+\epsilon A)(I+\epsilon\tilde{A}) = I+\epsilon(A+\tilde{A})+\ldots = I \tag{4.30}$$

has the property that the transposed matrix $\tilde{A}$ equals $-A$ so that A is anti-symmetric.

An infinitesimal transformation on an r-dimensional space

$$x_i' = x_i + \epsilon \sum_{ij} a_{ij} x_j, \quad i, j = 1, \ldots r, \quad a_{ij} = -a_{ji} \tag{4.31}$$

implies

$$\psi(x_i') = \psi(x_i) + \epsilon \sum_{ij} a_{ij} x_j \frac{\partial\psi}{\partial x_i} + \ldots$$

$$= \psi(x_i) + 2\epsilon \sum_{i<j} a_{ij} \left[\frac{1}{2}\left(x_j \frac{\partial}{\partial x_i} - x_i \frac{\partial}{\partial x_j}\right)\psi\right] + \ldots \tag{4.32}$$

This shows that the generators of the orthogonal group are the anti-symmetric combination of the ones of the unitary group

$$\check{\mathscr{C}}_{ij} = x_i \frac{\partial}{\partial x_j} \tag{4.33}$$

$$\check{\Lambda}_{ij} = \tfrac{1}{2}(\check{\mathscr{C}}_{ij} - \check{\mathscr{C}}_{ji}) \tag{4.34}$$

The commutation relations of the Λ_{ij} are identical to those in (4.28), except that $g_{mm'}$ is replaced by $\delta_{ii'}$ which is the metric in this case. As the $\Lambda_{mm'}$ are related to the $\mathscr{C}_{mm'}$ in the same way as $\check{\Lambda}_{ij}$ and $\mathscr{C}_{ij}$, we conclude that $\Lambda_{mm'}$ are generators of the group $\mathcal{O}_{2\ell+1}$.

Using the metric defined above, we can raise one of the indices to write

$$\Lambda_m{}^{m'} = \tfrac{1}{2}(\mathscr{C}_m{}^{m'} - \mathscr{C}^{m'}{}_m) \tag{4.35}$$

$$\mathscr{C}^{m'}{}_m = (-)^{m'+m}\,\mathscr{C}_{-m'}{}^{-m} \tag{4.36}$$

This gives the $\Lambda_m^{m'}$ in a mixed covariant and contravariant way as

$$\Lambda_m{}^{m'} = \tfrac{1}{2}(\mathscr{C}_m{}^{m'} - (-)^{m'+m}\,\mathscr{C}_{-m'}{}^{-m}) \tag{4.37}$$

We can contract indices to define the operator

$$\Phi = \sum_{mm'} \Lambda_m{}^{m'} \Lambda_{m'}{}^{m} \tag{4.38}$$

We can furthermore check, using the commutation relations (4.28), that Φ commutes with all $\Lambda_m^{m'}$ and so is a Casimir operator of $\mathcal{O}_{2\ell+1}$. Explicitly

$$\Phi = \frac{1}{2} \sum_{mm'} (\mathscr{C}_m{}^{m'} \mathscr{C}_{m'}{}^{m} - (-)^{m+m'} \mathscr{C}_m{}^{m'} \mathscr{C}_{-m}{}^{-m'}) \tag{4.39}$$

If we compare with the Casimir operator of $\mathscr{U}_{2\ell+1}$

$$\Gamma = \sum_{mm'} \mathscr{C}_m{}^{m'} \mathscr{C}_{m'}{}^{m} \tag{4.40}$$

we get

$$\sum_{mm'} (-)^{m+m'} \mathscr{C}_m{}^{m'} \mathscr{C}_{-m}{}^{-m'} = \Gamma - 2\Phi \tag{4.41}$$

or

$$\mathscr{P}(0) = \Gamma - 2\Phi \tag{4.42}$$

which is exactly the expansion of the interaction we wanted.

Let us look at some properties of the $\Lambda_m^{m'}$. They can be considered as an element of a $(2\ell+1)\times(2\ell+1)$ matrix, m' specifying columns, m the rows, in a decreasing order $(\ell, \ell-1, \ldots, -\ell)$. The anti-diagonal elements of the matrix

$$\Lambda_m{}^{-m} = (\mathscr{C}_m{}^{-m} - \mathscr{C}_m{}^{-m}) = 0 \tag{4.43}$$

The terms below the anti-diagonal are equivalent to those above

$$\begin{aligned} \Lambda_{-m}{}^{-m'} &= \tfrac{1}{2}(\mathscr{C}_{-m}{}^{-m'} - (-)^{-m'-m} \mathscr{C}_{m'}{}^{m}) \\ &= -(-)^{m+m'} \Lambda_{m'}{}^{m} \end{aligned} \tag{4.44}$$

Above the anti-diagonal we can divide them into 3 sets.

(1) The Λ_m^m that commute among themselves

$$\Lambda_m^m = \tfrac{1}{2}(\mathscr{C}_m^m - \mathscr{C}_{-m}^{-m}) \tag{4.45}$$

Being linear combination of weight generators of $\mathscr{U}_{2\ell+1}$, the eigenvalues of Λ_m^m are half integers or integers

$$\Lambda_m^m P|0\rangle = \tfrac{1}{2}\omega_{\ell-m+1} P|0\rangle \tag{4.46}$$

The set of eigenvalues of $2\Lambda_m^m$, $\ell \geq m \geq 1$ gives the weight

$$(\omega_1, \omega_2 \ldots, \omega_\ell) \tag{4.47}$$

(2) The operators $\Lambda_{m'}^{m''}$, $m' > m'' > -m'$ are a combination of weight-raising generators of $\mathcal{U}_{2\ell+1}$ and from (4.28) can be shown to be weight-raising generators of $\mathcal{O}_{2\ell+1}$.

(3) Similarly, $\Lambda_{m'}^{m''}$, $-m'' < m' < m''$ are combinations of weight-lowering generators of $\mathcal{U}_{2\ell+1}$ and from (4.28) can be shown to be weight-lowering generators of $\mathcal{O}_{2\ell+1}$.

Therefore the generators $\Lambda_m^{m'}$ above the anti-diagonal can be divided into raising, weight and lowering generators as indicated symbolically by the symbols $+, 0, -$ respectively in the matrix

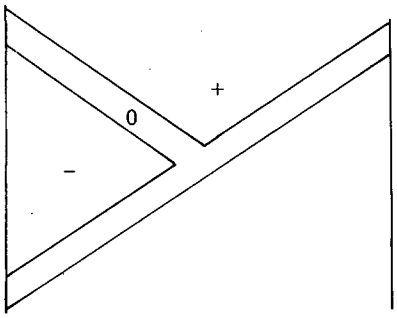

(4.48)

The polynomials of highest weight **P** are determined by the equations

$$\Lambda_m{}^m \mathbf{P}|0\rangle = \tfrac{1}{2}\lambda_{\ell-m+1}\ \mathbf{P}|0\rangle \tag{4.49}$$

$$\Lambda_m{}^{m'} \mathbf{P}|0\rangle = 0, \quad m > m' > -m \tag{4.50}$$

The set $(\lambda_1, \lambda_2, \ldots, \lambda_\ell)$ characterizes the highest weight state. If we have this state of highest weight, we can also obtain the eigenvalue of the Casimir operator $\Phi = \sum_{mm'} \Lambda_m^{m'} \Lambda_{m'}^{m}$ by an analysis entirely similar to the one given for the Casimir operator Γ in section 3.7, obtaining the eigenvalue

$$\varphi = \frac{1}{2} \sum_{\mu=1}^{K} \lambda_\mu (\lambda_\mu + r - 2\mu) \tag{4.51}$$

with $K = \frac{1}{2}(r-1)$ r odd
$K = \frac{1}{2}r$ r even

We have included the r even case because the result is general, but in our problem we only have r odd $(= 2\ell+1)$. Combining φ with γ_r of (3.150) we have determined the eigenvalues for the pairing operator

$$\mathcal{P}(0) = \Gamma - 2\Phi \tag{4.52}$$

and so the energy levels associated with this force are given by

$$E^{h_1 \ldots h_{2\ell+1}}_{h_1 \ldots \lambda_\ell} = \sum_{\mu=1}^{2\ell+1} h_\mu (h_\mu - 2\mu) - \sum_{\mu=1}^{\ell} \lambda_\mu (\lambda_\mu + 2\ell + 1 - 2\mu) + n(2\ell+2) \tag{4.53}$$

How can we determine the states of $\mathscr{P}(0)$? In the case of Gel'fand chains we found an explicit way of obtaining the states. How should we proceed now? We shall indicate one way and illustrate the technique for the case of the p shell, for which $\ell = 1$, $r = 2\ell + 1 = 3$, and so we have the chain $\mathscr{U}_3 \supset \mathcal{O}_3$ and the generators

$$\begin{bmatrix} \Lambda_1^0 & \Lambda_1^0 & 0 \\ \Lambda_0^1 & 0 & \\ 0 & & \end{bmatrix} \tag{4.54}$$

From the discussion in section 3 we can determine the matrix elements of $\mathscr{C}_m^{m'}$, m, m' = 1, 0, -1 with respect to Gel'fand states, for which we use the enumeration convention

μ	1	2	3
m	1	0	-1

(4.55)

In fact, these matrix elements are given explicitly in Ref. [1].

As the generators of $\mathcal{O}_3$ are given by (4.37), we clearly have also the matrix elements

$$\left\langle \begin{matrix} h_{13} & h_{23} & h_{33} \\ & h'_{12} & h'_{22} \\ & & h'_{11} \end{matrix} \middle| \Lambda_m^{m'} \middle| \begin{matrix} h_{13} & h_{23} & h_{33} \\ & h_{12} & h_{22} \\ & & h_{11} \end{matrix} \right\rangle \tag{4.56}$$

From them we can straightforwardly obtain the corresponding matrix elements of the Casimir operator of

$$\Phi = \sum_{mm'} \Lambda_m^{m'} \Lambda_{m'}^{m} = \tfrac{1}{2} \mathscr{L}^2 \tag{4.57}$$

Once we have the matrix elements of Φ we can diagonalize them to obtain the eigenstates corresponding to the eigenvalues (4.51). In the process we determine the transformation brackets which take us from the Gel'fand states into eigenstates of $\mathcal{O}_3$, i.e.

$$\left\langle \begin{matrix} h_{13} & h_{23} & h_{33} \\ & h_{12} & h_{22} \\ & & h_{11} \end{matrix} \middle| \begin{matrix} h_{13} & h_{23} & h_{33} \\ & \Omega LM & \end{matrix} \right\rangle \tag{4.58}$$

where Ω is an additional quantum number necessary to characterize the state in the $\mathscr{U}_3 \supset \mathcal{O}_3$ chain.

In this example we go from states classified by the IR of the chain of groups

$$(\mathcal{U}_3) \supset \begin{pmatrix} \mathcal{U}_2 & 0 \\ 0 & 1 \end{pmatrix} \supset \begin{pmatrix} \mathcal{U}_1 & 0 & 0 \\ 0 & 1 & 0 \\ 0 & 0 & 1 \end{pmatrix} \tag{4.59a}$$

to states classified by the chains of groups

$$\mathcal{U}_3 \supset \mathcal{O}_3 \supset \mathcal{O}_2 \tag{4.59b}$$

The matrix elements of $\mathcal{L}^2$ with respect to the Gel'fand states have been given in another publication (Ref. [1]) and a computer programme has been elaborated to obtain the transformation brackets explicitly. Therefore we can determine any state in the $\mathcal{U}_3 \supset \mathcal{O}_3$ chain as a linear combination of the Gel'fand states, which in turn can be obtained in terms of Slater determinants by the procedures of section 3.

A similar procedure can be followed in the case $\mathcal{U}_{2\ell+1} \supset \mathcal{O}_{2\ell+1}$, though the programmes equivalent to the above are not yet available. Other procedures for determining the states in the chain $\mathcal{U}_{2\ell+1} \supset \mathcal{O}_{2\ell+1}$ have been discussed in previous publications (Refs. [1, 3, 4]).

So far we have only discussed the generators and the states associated with the $\mathcal{O}_{2\ell+1}$ sub-group. We note that with respect to the index m, the $b^{\dagger}_{ms}$, $m = \ell, \ldots, -\ell$ not only form $2\ell+1$ dimensional vectors corresponding to the irreducible representation (IR) [1] of both $\mathcal{U}_{2\ell+1}$ and $\mathcal{O}_{2\ell+1}$, but that the vectors are the basis for an IR of order ℓ of the R_3 group, i.e. that under rotations in physical space they are transformed by the $(2\ell+1)\times(2\ell+1)$ dimensional matrices $\mathcal{D}^{\ell}(R_3)$. These matrices, which constitute an IR of R_3, are clearly a sub-group[6] of $\mathcal{O}_{2\ell+1}$ and therefore of $\mathcal{U}_{2\ell+1}$, so that we would like to determine both the generators of R_3 in terms of those of $\mathcal{O}_{2\ell+1}$ and the states classified by all the groups in the chain (4.21).

The generators of R_3 are clearly the angular momentum operators and we shall proceed to derive them in the next sub-section.

4.3. The angular momentum operator

The operator of angular momentum is a one-body operator acting in configuration space only, so it can be written in terms of the generators $\mathcal{C}_{m}^{m'}$ of $\mathcal{U}_{2\ell+1}$. With Eq. (2.12)

$$\mathcal{L}_q = \sum_{mm'} \langle \nu \ell m | L_q | \nu \ell m' \rangle \, \mathcal{C}_{m}^{m'} \tag{4.60}$$

where $\nu\ell$ are fixed since we are in a single shell. With the Wigner-Eckart theorem, the coefficients can be calculated immediately and we get

$$\mathcal{L}_q = \sum_{mm'} \sqrt{\ell(\ell+1)} \langle \ell 1 \, m' q | \ell m \rangle \mathcal{C}_{m}^{m'} \tag{4.61}$$

[6] Actually the matrices $\mathcal{D}^{\ell}(R_3)$ are unitary but not orthogonal. This is due to the fact that the $b^{\dagger}_{ms}$ transform as the $Y_{\ell m}(\theta, \varphi)$ which are not real. Had we made a choice of real spherical harmonics, the corresponding IR of order ℓ would have been real and so the matrices would have been orthogonal.

We proceed to show that $\mathscr{L}_q$ is actually a linear combination of the generators of the orthogonal group $\mathcal{O}_{2\ell+1}$ which were defined above. Indeed we can write

$$\mathscr{L}_q = \frac{1}{2}\left[\sum_{mm'} \sqrt{\ell(\ell+1)}(\ell 1 m' q \,|\, \ell m)\mathscr{C}_m^{m'} + \sum_{mm'} \sqrt{\ell(\ell+1)}(\ell 1 -m q \,|\, \ell -m')\mathscr{C}_{-m'}^{-m}\right] \tag{4.62}$$

Now

$$\langle \ell 1 -m q \,|\, \ell -m' \rangle = -(-)^{m+m'} \langle \ell 1 m' q \,|\, \ell m \rangle$$

so that

$$\mathscr{L}_q = \sum_{mm'} \sqrt{\ell(\ell+1)}\, \langle \ell 1 m' q \,|\, \ell m \rangle \Lambda_m^{m'} \tag{4.63}$$

From the way they were formed, we know also that $\mathscr{L}_q$ must satisfy the following commutation relations:

$$[\mathscr{L}_0, \mathscr{L}_{\pm 1}] = \pm \mathscr{L}_{\pm 1} \tag{4.64}$$

$$[\mathscr{L}_{-1}, \mathscr{L}_1] = \mathscr{L}_0$$

This can easily be checked by using the commutation relations of either the generators of $\mathscr{U}_{2\ell+1}$ in (4.60), or of $\mathcal{O}_{2\ell+1}$ in (4.63). The operators $\mathscr{L}_q$ are therefore the generators of the sub-group R_3 of $\mathcal{O}_{2\ell+1}$.

We will compare now the generators of the groups $\mathscr{U}_{2\ell+1}$, $\mathcal{O}_{2\ell+1}$, and R_3 with some unit generators considered by Racah. We note that $\mathscr{C}_{mm'}$ has indices m and m' taking values from $-\ell$ to $+\ell$ and with respect to each one of the indices it transforms like a spherical harmonic. We now define the operators

$$u_{kq} \equiv \sum_{mm'} \langle \ell\ell\, mm' \,|\, kq \rangle \mathscr{C}_{mm'} \tag{4.65}$$

These are linear combinations of $\mathscr{C}_{mm'}$ and from the orthogonality properties of the Clebsch-Gordan coefficients it follows that

$$\mathscr{C}_{mm'} = \sum_{kq} \langle \ell\ell\, mm' \,|\, kq \rangle u_{kq} \tag{4.66}$$

so that either $\mathscr{C}_{mm'}$ or u_{kq} can be used as generators of the group.

Interesting properties of u_{kq} are

(a) the possible values of k:

$$k = 0, 1, \ldots, 2\ell$$

(b) from the symmetry properties of the Clebsch-Gordan coefficients:

$$\langle \ell\ell\, m'm \,|\, kq \rangle = (-)^{\ell+\ell-k} \langle \ell\ell\, mm' \,|\, kq \rangle$$

we see that we have 2 classes of operator u_{kq} depending on whether k is even or odd. If k is odd then

$$u_{kq} = \frac{1}{2} \sum_{mm'} [\langle \ell\ell mm' \,|\, kq \rangle \mathscr{C}_{mm'} + \langle \ell\ell\, mm' \,|\, kq \rangle \mathscr{C}_{m'm}]$$

$$= \sum_{mm'} \langle \ell\ell\, mm' \,|\, kq \rangle \Lambda_{mm'} \tag{4.67}$$

so u_{kq} k odd is another way of writing the generators of $\mathcal{O}_{2\ell+1}$. We note also that u_{1q} is proportional to $\mathscr{L}_q$, so that the generators of the different groups in the chain are given below in terms of u_{kq}

$$\begin{array}{ccccc} \mathscr{U}_{2\ell+1} & \supset & \mathcal{O}_{2\ell+1} & \supset & R_3 \\ u_{kq} & & u_{kq} & & u_{kq} \\ k = 0, 1, 2 \ldots \ell & & k = 1, 3, & & k = 1 \\ -k \leq q \leq k & & -k \leq q \leq k & & -1 \leq q \leq 1 \end{array} \tag{4.68}$$

4.4. The eigenstates of the pairing interaction

From (4.42) we saw that the pairing interaction could be expressed in terms of the Casimir operators of $\mathscr{U}_{2\ell+1}$ and $\mathcal{O}_{2\ell+1}$ and so the corresponding eigenstates could be characterized by the IR of these two groups. Since, in addition, we would like to have states with definite total orbital angular momentum, the configuration part of our eigenstates is given by the ket

$$|[h_1 \ldots h_{2\ell+1}] \alpha(\lambda_1 \ldots \lambda_\ell) \Omega LM\rangle$$

$$\begin{array}{ccccc} \mathscr{U}_{2\ell+1} & \supset & \mathcal{O}_{2\ell+1} & \supset & \mathscr{D}^{\ell}(R_3) \\ \mathscr{C}^{m'}_{m} & & \Lambda^{m'}_{m} & & \mathscr{L}_q \end{array}$$

where under the corresponding quantum numbers we have put the groups for which they are IR, as well as the generators of these groups. The symbols α, Ω indicate the extra sets of quantum numbers needed to characterize the states, as the chain of groups is not a canonical one.

4.5. Spin and isospin part of the wave function

This corresponds to the U_4 part of the decomposition $\mathbb{U}_{4r} \supset \mathscr{U}_r \times U_4$ where U_4 has generators $C^{s'}_{s}$. We recall that the s index is the following enumeration of the spin-isospin states:

s	1	2	3	4
$\sigma\tau$	$\frac{1}{2}\ \frac{1}{2}$	$\frac{1}{2}\ -\frac{1}{2}$	$-\frac{1}{2}\ \frac{1}{2}$	$-\frac{1}{2}\ -\frac{1}{2}$

(4.69)

We shall proceed to determine linear combinations of these 16 generators which are physically meaningful. They correspond to the second quantized form of total spin and isospin operators and of the operators appearing in allowed Gamow-Teller (GT) transitions.

Consider the one-body operators S_0

$$S_0 = \sum_{ss'} \langle s | s_0 | s' \rangle C^{s'}_{s}$$

From

$$\langle \sigma\tau | s_0 | \sigma'\tau' \rangle = \delta^{\tau}_{\tau'}\, \sigma\, \delta^{\sigma}_{\sigma'}$$

we have

$$S_0 = \sum_{\sigma\tau\sigma'\tau'} \sigma\, \delta^{\sigma}_{\sigma'}\, \delta^{\tau}_{\tau'}\, C^{\sigma'\tau'}_{\sigma\tau}$$

$$= \sum_{\sigma\tau} \sigma\, C^{\sigma\tau}_{\sigma\tau}$$

$$= \tfrac{1}{2} C^{\frac{1}{2}\frac{1}{2}}_{\frac{1}{2}\frac{1}{2}} + \tfrac{1}{2} C^{\frac{1}{2}-\frac{1}{2}}_{\frac{1}{2}-\frac{1}{2}} - \tfrac{1}{2} C^{-\frac{1}{2}\frac{1}{2}}_{-\frac{1}{2}\frac{1}{2}} - \tfrac{1}{2} C^{-\frac{1}{2}-\frac{1}{2}}_{-\frac{1}{2}-\frac{1}{2}}$$

$$= \tfrac{1}{2}(C^1_1 + C^2_2 - C^3_3 - C^4_4) \qquad (4.70a)$$

In a similar way we calculate

$$S_1 = -\frac{1}{\sqrt{2}}(C^3_1 + C^4_2) \qquad (4.70b)$$

$$S_{-1} = \frac{1}{\sqrt{2}}(C^1_3 + C^2_4) \qquad (4.70c)$$

$$T_1 = -\frac{1}{\sqrt{2}}(C^2_1 + C^4_3) \qquad (4.70d)$$

$$T_0 = \frac{1}{2}(C^1_1 + C^3_3 - C^2_2 - C^4_4) \qquad (4.70e)$$

$$T_{-1} = \frac{1}{\sqrt{2}}(C^1_2 + C^3_4) \qquad (4.70f)$$

So we have found six generators corresponding to the spin generators of the SU_2 group associated with spin and isospin which incidentally satisfy the commutation relations

$$[S_{-1}, S_1] = S_0, \quad [S_0, S_{\pm 1}] = \pm S_{\pm 1}, \quad [T_0, T_{\pm 1}] = \pm T_{\pm 1}, \quad [T_{-1}, T_1] = T_0$$

$$[S_q, T_{\bar{q}}] = 0 \tag{4.71}$$

This implies that the U_4 group has the following physically relevant sub-group:

$$U_4 \supset SU_2^{(\sigma)} \times SU_2^{(\tau)}$$

We still have to find 10 operators independent of S_q, $T_{\bar{q}}$ and of each other, which would constitute, with the generators of $SU_2^{(\sigma)} \times SU_2^{(\tau)}$, a set equivalent to the generators $C_s^{s'}$ of U_4. For this purpose let us define

$$\Theta_{q\bar{q}}^{k\bar{k}} = \sum_{\sigma\tau} \sum_{\sigma'\tau'} \langle \tfrac{1}{2} k \sigma' q | \tfrac{1}{2} \sigma \rangle \langle \tfrac{1}{2} \bar{k} \tau' \bar{q} | \tfrac{1}{2} \tau \rangle \, C_{\sigma\tau}^{\sigma'\tau'} \tag{4.72}$$

where $k = 0, 1$ and similarly for $\bar{k}$, while of course $q = 0$ if $k = 0$ and $q = 1, 0, -1$ if $k = 1$ and similarly for $\bar{k}$, $\bar{q}$. Because of the orthonormality of the Clebsch-Gordan coefficients, the 16 operators $\Theta_{q\bar{q}}^{k\bar{k}}$ are linearly independent, and from the previous discussion in this section we clearly see that

$$\mathcal{N} = \Theta_{00}^{00}, \quad S_q = \sqrt{\frac{3}{4}}\, \Theta_{q0}^{10}, \quad T_{\bar{q}} = \sqrt{\frac{3}{4}}\, \Theta_{0\bar{q}}^{01} \tag{4.73}$$

where $\mathcal{N}$ is the number operator $\sum_s C_s^s$. The remaining $\Theta \to q$ linearly independent operators are given by $\Theta_{q\bar{q}}^{11}$, and, as they can be rewritten in the form

$$\Theta_{q\bar{q}}^{11} = \frac{4}{3} R_{q\bar{q}} \equiv \frac{4}{3} \sum_{\sigma\tau} \langle \sigma \tau | s_q t_{\bar{q}} | \sigma' \tau' \rangle \, C_{\sigma\tau}^{\sigma'\tau'} \tag{4.74}$$

we conclude that they are related to the operators $R_{q\bar{q}}$ associated with allowed GT transitions (Ref. [5]).

4.6. The highest weight state for a physically significant chain of sub-groups

In previous sections we have determined the state of highest weight in $\mathcal{U}_r$ and U_4 and proceed to show that it corresponds to a definite Gel'fand state. In the previous paragraphs of section 4, we discussed chains of groups of physical significance for both the configuration and the spin-isospin part of the state, and if we introduce the classification scheme

that they suggest, our states would be characterized by the ket

$$\begin{array}{l} |[h_1 \ldots h_{2\ell+1}]\alpha(\lambda_1 \ldots \lambda_\ell)\Omega L;\ \{V_1 \ldots V_4\}\beta S T,\ J M\rangle \\ \qquad \mathscr{U}_{2\ell+1}, \quad \mathcal{O}_{2\ell+1}, \quad R_3; \qquad U_4,\ SU_2^{(\sigma)},\ SU_2^{(\tau)},\ \vec{J}=\vec{L}+\vec{S} \end{array} \tag{4.75}$$

where underneath the relevant quantum numbers we have put the groups for which they give IR. As indicated above, α, Ω, β would be extra quantum numbers associated with the fact that our chain of groups is not canonical.

We can now ask the question whether the highest weight state in $\mathscr{U}_r$ and U_4 corresponds to a particular state of the type (4.75). We shall answer the questions for the particular example of highest weight state discussed in section 3, noting before that from Table II all raising and weight generators of the groups involved in (4.75) are given respectively in terms of raising or weight generators of the groups $\mathscr{U}_r$, U_4. The example of highest weight state we will consider is:

$$\begin{array}{|c|c|c|} \hline b_{11}^\dagger & b_{12}^\dagger & b_{13}^\dagger \\ \hline b_{21}^\dagger & b_{22}^\dagger & \\ \cline{1-2} b_{31}^\dagger & b_{32}^\dagger & \\ \cline{1-2} b_{41}^\dagger & & \\ \cline{1-1} \end{array} |0\rangle \tag{4.76}$$

Before proceeding with its analysis we must specify the value of r. For this purpose let us assume that

$$\ell = 2 \qquad r = 2\ell + 1 = 5 \tag{4.77}$$

so the chain of groups we have is

$$\mathscr{U}_5 \supset \mathcal{O}_5 \supset \mathscr{D}^2(R_3); \quad U_4 \supset SU_2^{(\sigma)} \times SU_2^{(\tau)} \tag{4.78}$$

and the state is

$$|[h_1 h_2 h_3 h_4 h_5]\ \alpha(\lambda_1 \lambda_2)\,\Omega\, L;\ \{V_1 V_2 V_3 V_4\}\beta\, S\, T\, M_T\, J\, M\rangle \tag{4.79}$$

Using the weight generators of Table II we show in the next sub-section that the state (4.76) is

$$\begin{array}{l} |[3\ 2\ 2\ 1\ 0]\ (3\ \ 1)\ 7\ \{4\ 3\ 1\ 0\}\ 3\ 1\ 1\ 10\ 10\rangle \\ |[h_1 h_2 h_3 h_4 h_5]\ (\lambda_1 \lambda_2)\, L\ \ \{V_1 V_2 V_3 V_4\}\ S\, T\, M_T\, J\, M\rangle \end{array} \tag{4.80}$$

where we have put underneath each set of numbers the quantum number it belongs to, but have suppressed α, Ω, β as they are redundant, there being only one state of this type.

TABLE II. RAISING GENERATORS AND WEIGHT GENERATORS FOR SOME GROUPS

Groups	Raising generators	Weight generators
$\mathcal{U}_{2\ell+1}$	$\mathscr{C}^{m'}_{m}$ $m > m'$	$\mathscr{C}^{m}_{m}$
$\mathcal{O}_{2\ell+1}$	$\Lambda^{m'}_{m}$ $m > m' > -m$	Λ^{m}_{m}
R_3	$\mathscr{L}_1 = \sum_m \sqrt{\ell(\ell+1)} \langle \ell m-1\ q \mid \ell m \rangle\ \mathscr{C}^{m-1}_{m}$	$\mathscr{L}_0 = \sum_m m \mathscr{C}^{m}_{m}$
U_4	$C^{s'}_{s}$ $s < s'$	C^{s}_{s}
SU_2	$S_{+1} = \frac{-1}{\sqrt{2}} (C^3_1 + C^4_2)$	$S_0 = \frac{1}{2}(C^1_1 + C^2_2 - C^3_3 - C^4_4)$
SU_2	$T_{+1} = \frac{-1}{\sqrt{2}} (C^2_1 + C^4_3)$	$T_0 = \frac{1}{2}(C^1_1 - C^2_2 + C^3_3 - C^4_4)$

4.7. Detailed determination of the quantum numbers for the highest weight state

Let us now show how the particular numbers in (4.80) were obtained. First of all we need an enumeration procedure. Let us take the following:

μ	1	2	3	4	5
m	2	1	0	-1	-2

(4.81)

Now let us consider

(1) $[h_1 h_2 h_3 h_4 h_5]$: By definition, h_j counts the number of squares in the i-th row. So we have [3 2 2 1 0].

(2) $\{V_1 V_2 V_3 V_4\}$: By definition, V_i counts the number of squares in the i-th column. So we get {4 3 1 0}.

(3) $(\lambda_1 \lambda_2)$: We have seen that

$$\Lambda^{m}_{m}\ \mathbf{P} = \tfrac{1}{2} \lambda_{\ell - m + 1}\ \mathbf{P} \tag{4.82}$$

and

$$\Lambda^{m'}_{m} = \tfrac{1}{2}(C^{m'}_{m} - (-)^{m+m'} C^{-m}_{-m'}) \quad \text{for} \quad m > m' > -m \tag{4.83}$$

Using these two relations and the enumeration procedure given above, we get

For λ_1: $\lambda_1 \mathbb{P} = 2\Lambda_2^2 \mathbb{P}$

$$\Lambda_2^2 \mathbb{P} = \tfrac{1}{2}(\mathscr{C}_2^2 - \mathscr{C}_{-2}^{-2})\mathbb{P} = \tfrac{1}{2}(\mathscr{C}_1^1 - \mathscr{C}_5^5)\mathbb{P}$$

$$= \tfrac{1}{2}(3-0)\mathbb{P} = \tfrac{3}{2}\mathbb{P} \qquad (4.84)$$

So $\lambda_1 = 3$

For λ_2: $\lambda_2 \mathbb{P} = 2\Lambda_1^1 \mathbb{P}$

$$\Lambda_1^1 \mathbb{P} = \tfrac{1}{2}(\mathscr{C}_1^1 + \mathscr{C}_{-1}^{-1})\mathbb{P} = \tfrac{1}{2}(\mathscr{C}_2^2 - \mathscr{C}_4^4)\mathbb{P}$$

$$= \tfrac{1}{2}(2-1)\mathbb{P} = \tfrac{1}{2}\mathbb{P} \qquad (4.85)$$

So $\lambda_2 = 1$

(4) L we can get by calculating

$$\mathscr{L}_0 = \sum_m m \mathscr{C}_m^m$$

So

$$\mathscr{L}_0 \mathbb{P}|0\rangle = (2\mathscr{C}_2^2 + 1\mathscr{C}_1^1 + 0\mathscr{C}_0^0 - 1\mathscr{C}_{-1}^{-1} - 2\mathscr{C}_{-2}^{-2})\mathbb{P}|0\rangle$$

$$= (2\mathscr{C}_1^1 + \mathscr{C}_2^2 - \mathscr{C}_4^4 - 2\mathscr{C}_5^5)\mathbb{P}|0\rangle \qquad (4.86)$$

$L = 2\times 3 + 2 - 1$

$L = 7$

(5) S can be calculated by

$$S_0 = \tfrac{1}{2}(C_1^1 + C_2^2 - C_3^3 - C_4^4)$$

$$S_0 \mathbb{P}|0\rangle = \tfrac{1}{2}(4+3-1)\mathbb{P}|0\rangle \qquad (4.87)$$

$$S_0 = 3$$

(6) T: $T_0 = \tfrac{1}{2}(C_1^1 - C_2^2 + C_3^3 - C_4^4)$

So $$T_0 \mathbb{P}|0\rangle = \tfrac{1}{2}(4-3+1)\mathbb{P}|0\rangle \qquad (4.88)$$

$$T_0 = 1$$

(7) M_T: This is the projection of the isospin and, as we are dealing with the state of highest weight, it is equal to the isospin itself.

$$M_T = 1 \qquad (4.89)$$

(8) J: The total angular momentum is given by

$$J_1 = L_1 + S_1$$

$$J_0 = L_0 + S_0 \qquad (4.90)$$

So $$J_0 = 7 + 3$$

$$J_0 = 10$$

(9) M: This is the projection of the total angular momentum, so, in this case,

$$M = 10 \qquad (4.91)$$

We have shown how to determine, in terms of Slater determinants, highest weight states in physically relevant chains of groups. All other states could be obtained from the highest weight state by use of lowering operators associated with the chains of groups in question. Detailed analysis of these techniques, as well as many short cuts in their application, are given in the next section and also in Refs. [1, 3, 4, 6]. A computer programme has been elaborated by Flores to implement these ideas numerically.

5. SYMMETRY OF THE HARMONIC OSCILLATOR AND EIGENSTATES OF THE QUADRUPOLE-QUADRUPOLE INTERACTION. APPLICATIONS TO NUCLEAR STRUCTURE IN THE 2S-1D SHELL

In the previous section we discussed the many-body problem in a single shell of fixed $\nu\ell$. In this section we are going to generalize our results to the many shells of a single level of the harmonic oscillator with the purpose of using the symmetry properties of the latter problem in the analysis of special types of interactions of physical interest.

5.1. Symmetry group of the harmonic oscillator (h. o.)

Let us consider the symmetry properties of a simple harmonic oscillator as a quantum mechanical system. We take units such that

$$\hbar = m = \omega = 1$$

and then the Hamiltonian is given by

$$H_0 = \tfrac{1}{2}(\vec{p}^2 + \vec{x}^2) \qquad (5.1)$$

The transformation in $\vec{x}$ and $\vec{p}$ should leave invariant the Hamiltonian H_0, at the same time retaining the canonically conjugate relation of $\vec{x}$ and $\vec{p}$, i.e. leave invariant the commutation $[x_i, p_j] = i\,\delta_{ij}$ or the corresponding Poisson's bracket in the classical system. The orthogonal transformations in the 6-dimensional space of $\vec{x}$ and $\vec{p}$ leave invariant the Hamiltonian H_0,

but only a sub-group of this O_6 group, the group of unitary transformation in a three-dimensional space (U_3), leaves also invariant the commutation relation between $\vec{x}$ and $\vec{p}$. This can be easily seen through the introduction of creation-annihilation operators for the oscillator quanta

$$\vec{a}^\dagger = \frac{1}{\sqrt{2}}(\vec{x} - i\vec{p}) \tag{5.2}$$

$$\vec{a} = \frac{1}{\sqrt{2}}(\vec{x} + i\vec{p}) \tag{5.3}$$

where the commutation relations satisfied by a and $a^\dagger$ are

$$[a_i, a_j^\dagger] = \delta_{ij} \tag{5.4}$$

$$[a_i, a_j] = 0 = [a_i^\dagger, a_j^\dagger] \tag{5.5}$$

We introduce a unitary transformation U

$$\vec{a}' = U\vec{a}, \quad \vec{a}^{\dagger\prime} = U^* a^\dagger \tag{5.6}$$

and see that the commutation relations (5.4) are maintained, i.e.

$$\begin{aligned}[a_i', a_j^{\dagger\prime}] &= \left[\sum_k U_{ik}\, a_k, \sum_\ell U_{j\ell}^*\, a_\ell^\dagger\right] \\ &= \sum_{k,\ell} U_{ik}\, U_{j\ell}^*\, [a_k, a_\ell^\dagger] \\ &= \sum U_{ik}\, U_{j\ell}^*\, \delta_{k\ell} = \sum U_{ik}\, U_{jk}^* = \delta_{ij}\end{aligned} \tag{5.7}$$

Similarly, one can trivially show that all the other commutation relations are maintained. In addition, H_0 is invariant.

$$H_0 = \vec{a}^\dagger \cdot \vec{a} + \frac{3}{2} = \vec{a}^{\dagger\prime} \cdot \vec{a}' + \frac{3}{2} \tag{5.8}$$

What is the corresponding transformation in the six-dimensional space $(\vec{x}, \vec{p})$? We can write in both systems

$$\vec{x} = \frac{1}{\sqrt{2}}(\vec{a}^\dagger + \vec{a})$$

$$\vec{p} = \frac{i}{\sqrt{2}}(\vec{a}^\dagger - \vec{a})$$

$$\vec{x}' = \frac{1}{\sqrt{2}}(\vec{a}^{\dagger\prime} + \vec{a}')$$

$$\vec{p}' = \frac{i}{\sqrt{2}}(\vec{a}^{\dagger\prime} - \vec{a}')$$

So

$$\left.\begin{aligned}\vec{x}' &= \frac{1}{\sqrt{2}}(U^*\vec{a}^\dagger + U\vec{a}) \\ &= \frac{1}{2}(U+U^*)\vec{x} + \frac{i}{2}(-U^*+U)\vec{p}\end{aligned}\right\} \tag{5.9}$$

$$\left.\begin{aligned}\vec{p}' &= \frac{i}{\sqrt{2}}(U^*\vec{a}^\dagger - U\vec{a}) \\ &= \frac{i}{2}(U^*-U)\vec{x} + \frac{1}{2}(U^*+U)\vec{p}\end{aligned}\right\} \tag{5.10}$$

The six-dimensional matrix

$$\frac{1}{2}\begin{pmatrix} U+U^* & i(-U^*+U) \\ i(U^*-U) & U+U^* \end{pmatrix} \tag{5.11}$$

is an orthogonal matrix, but not the most general one. As a product of matrices of this form has again the same form, the matrices (5.11) are a representation of U_3.

It is convenient to use the spherical form instead of the cartesian system used above. In this form, the spherical tensor property of the operators is explicit. The metric is

$$g_{qq'} = (-1)^q \delta_{q,-q'} \quad ; \quad q = -1, 0, 1$$

$$a_q^\dagger = \frac{1}{\sqrt{2}}(x_q - ip_q) \qquad a^q = \frac{1}{\sqrt{2}}(x^q + ip^q)$$

The commutation relations become

$$[a^q, a_{q'}^\dagger] = \delta_{q'}^q, \quad [a^q, a^{q'}] = 0 = [a_q^\dagger, a_{q'}^\dagger] \tag{5.12}$$

The raising and lowering of indices can be done as follows:

$$a^q = (-)^q a_q, \quad a_q^\dagger = (-)^q a^{\dagger -q} \tag{5.13}$$

The corresponding commutation relations are

$$[a_q^q, a_{q'}^\dagger] = g_{qq'} = (-)^q \delta_{q,-q'} \tag{5.14}$$

Now we introduce the generators of the group U_3, $c_q^{q'} = a_q^\dagger a^{q'}$. They satisfy

$$[c_q^{q'}, c_{q''}^{q'''}] = c_q^{q'''}\delta_{q''}^{q'} - c_{q''}^{q'}\delta_q^{q'''} \tag{5.15}$$

We can form the Racah tensors of orders 2, 1 and 0 which will also span

the total space of nine generators, i.e.

$$Q_m = \sqrt{\frac{5}{3}} \sum_{q'',q'} \langle 1\,2\,q''\,m \,|\, 1\,q' \rangle\, c^{q''}_{q'} \qquad -2 \leqq m \leqq 2 \tag{5.16}$$

$$L_q = \sqrt{2} \sum_{q',q''} \langle 1\,1\,q''\,q \,|\, 1\,q' \rangle\, c^{q''}_{q'} \qquad -1 \leqq q \leqq 1 \tag{5.17}$$

$$H_0 = \sum_q c^q_q + \frac{3}{2} \tag{5.18}$$

We shall drop the constant $3/2$ in H_0 and we note that it is then the Casimir operator of first order of the group U_3. The Casimir operator G of second order is given by

$$G = \sum_{q,q'} c^{q'}_q c^q_{q'}$$

$$= \sum (-)^m Q_m Q_{-m} + \frac{1}{2} \sum (-)^q L_q L_{-q} + \frac{1}{3} (H_0)^2$$

$$= Q^2 + \frac{1}{2} L^2 + \frac{1}{3} H_0^2 \tag{5.19}$$

It can be verified that L_0 are components of the angular momentum operator defined by

$$L_q = (\vec{x} \times \vec{p})_q$$

The form of G then shows immediately that the operator Q^2 would be diagonal in the scheme $U_3 \supset R_3$.

We can also rewrite Q_m as

$$Q_m = \sqrt{\frac{8\pi}{15}}\, (\mathscr{Y}_{2m}(\vec{x}) + \mathscr{Y}_{2m}(\vec{p}) \tag{5.20a}$$

where $\mathscr{Y}_{2m}(\vec{x})$ is the solid spherical harmonic

$$\mathscr{Y}_{2m}(\vec{x}) = r^2 Y_{2m}(\theta, \varphi)$$

As in a single level of the harmonic oscillator $\langle x_i x_j \rangle = \langle p_i p_j \rangle$, we conclude that for states restricted to a single level of the h.o. the Q^2 operator in (5.19) is equivalent to

$$Q^2 = \frac{32\pi}{15} \sum_m (-1)^m \mathscr{Y}_{2m}(\vec{x})\, \mathscr{Y}_{2-m}(\vec{x}) \tag{5.20b}$$

When we extend our analysis from 1 to n particles in the harmonic oscillator potential, the Q^2 operator within a single level becomes the familiar quadrupole-quadrupole force with added self-interaction terms.

A single-particle state in the oscillator potential can be written as

$$|n_1\, n_0\, n_{-1}\rangle = \frac{(a_1^\dagger)^{n_1}\,(a_0^\dagger)^{n_0}\,(a_{-}^\dagger)^{n_{-1}}}{\sqrt{n_1!\; n_0!\; n_{-1}!}}\;|0\rangle \tag{5.21}$$

where $|0\rangle = (1/\pi^{3/2}) \exp -\frac{1}{2}x^2$ is the 1s ground state of the harmonic oscillator. The set of degenerate states ψ satisfying

$$H_0\psi = \nu\psi$$

form a basis for the representation of the group U_3. This is the set of states $|n_1 n_0 n_{-1}\rangle$ such that $n_1 + n_0 + n_{-1} = \nu$. In the Gel'fand scheme the same state can be written as follows:

$$|n_1,\, n_0,\, n_{-1}\rangle = \left|\begin{matrix} \nu, & 0, & 0 \\ \nu - n_{-1}, & 0 & \\ & n_1 & \end{matrix}\right\rangle \tag{5.22}$$

The weight of the state (5.22) is (n_1, n_0, n_{-1}). Instead of using the above Gel'fand classification, we may characterize the single-particle states by quantum numbers of the rotational sub-group. Such states we denote by $|\nu, \ell, m\rangle$. The chains of sub-groups involved in these two classifications are, respectively,

$$\begin{aligned} &U_3 \supset U_2 \supset U_1 \\ \text{and} \qquad &U_3 \supset R_3 \supset \begin{pmatrix} R_2 & 0 \\ 0 & 1 \end{pmatrix} \end{aligned} \tag{5.23}$$

There are many values of ℓ possible, i.e. $\ell = \nu, \nu-2, \ldots, 1$ or 0, the total degeneracy being $(\nu+1)(\nu+2)/2$.

For an arbitrary central potential the degenerate eigenstates constitute a representation of the group R_3. This representation may or may not be irreducible. We have seen that the degenerate states of a harmonic oscillator carry a reducible representation of the group R_3, while the representation of the group U_3 is irreducible, as all states can be written as Gel'fand states associated with the single representation $(\nu\, 0\, 0)$. This is illustrated in Fig. 1.

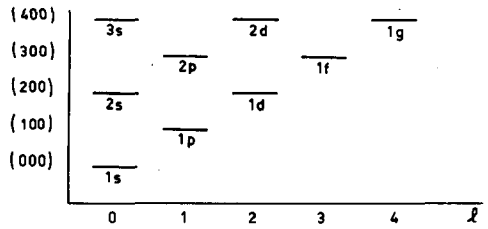

FIG. 1. Classification of simple harmonic oscillator states by U_3 and R_3, showing degeneracy of each oscillator level

The existence of accidental degeneracy of the oscillator is due to the existence of the higher symmetry (U_3) of the oscillator Hamiltonian. A similar degeneracy in the hydrogen spectrum is due to the invariance of the Coulomb Hamiltonian under the group O_4.

5.2. The chain of groups in the 2s-1d shell

The generators $c_q^{q'}$ introduced before are single-particle operators. They could be expressed in the second quantized form by using as a basis the complete set of states $b_\rho^\dagger$, $\rho = \mu s$ where $\mu = (n_1 n_0 n_{-1})$ and s is the spin-isospin index. We shall illustrate this by considering the example of the (2s-1d) shell. We introduce the following enumeration convention

μ	1	2	3	4	5	6
$(n_1 n_0 n_{-1})$	(2 0 0)	(1 1 0)	(1 0 1)	(0 2 0)	(0 1 1)	(0 0 2)

(5.24)

From (2.12) the corresponding second quantized operators are

$$\mathfrak{C}_q^{q'} = \sum_{\mu\mu'} \langle \mu | c_q^{q'} | \mu' \rangle \mathscr{C}_\mu^{\mu'} \tag{5.25}$$

The commutation relations between $\mathfrak{C}_q^{q'}$ are the same as those among $c_q^{q'}$. This is shown as follows:

$$[\mathfrak{C}_q^{q'}, \mathfrak{C}_{\bar{q}}^{\bar{q}'}] = \sum_{\mu\mu'} \sum_{\bar{\mu}\bar{\mu}'} \langle \mu | c_q^{q'} | \mu' \rangle \langle \bar{\mu} | c_{\bar{q}}^{\bar{q}'} | \bar{\mu}' \rangle \mathscr{C}_\mu^{\mu'}, \mathscr{C}_{\bar{\mu}}^{\bar{\mu}'}$$

$$= \sum_{\mu\mu'} \sum_{\bar{\mu}\bar{\mu}'} \langle \mu | c_q^{q'} | \mu' \rangle \langle \bar{\mu} | c_{\bar{q}}^{\bar{q}'} | \bar{\mu}' \rangle [\mathscr{C}_\mu^{\mu'} \delta_{\bar{\mu}}^{\bar{\mu}'} - \mathscr{C}_{\bar{\mu}}^{\bar{\mu}'} \delta_\mu^{\mu'}] \tag{5.26}$$

Now we have to use the fact that the states $|\mu\rangle$ form for operators such as $c_q^{q'}$ a complete basis, i.e.

$$\sum |\mu\rangle\langle\mu'| \delta_\mu^{\mu'} = 1 \tag{5.27}$$

and also that the $c_q^{q'}$ satisfy the commutation relation

$$[c_q^{q'}, c_{\bar{q}}^{\bar{q}'}] = c_q^{\bar{q}'} \delta_{\bar{q}}^{q'} - c_{\bar{q}}^{q'} \delta_q^{\bar{q}'}$$

We then get

$$[\mathfrak{C}_q^{q'}, \mathfrak{C}_{\bar{q}}^{\bar{q}'}] = \mathfrak{C}_q^{\bar{q}'} \delta_{\bar{q}}^{q'} - \mathfrak{C}_{\bar{q}}^{q'} \delta_q^{\bar{q}'} \tag{5.28}$$

The $\mathfrak{C}_q^{q'}$ are linear combinations of the generators $\mathscr{G}_\mu^{\mu'}$ of $\mathscr{U}_6$ (or of the generators of $\mathscr{U}_r$, $r = \frac{1}{2}(\nu+1)(\nu+2)$ if we extend our analysis to an arbitrary level of ν quanta of the h.o.) whose commutators can again be expressed in terms of the $\mathfrak{C}_q^{q'}$. Therefore they are the generators of a sub-group U_3 of $\mathscr{U}_6$. The existence of this sub-group becomes clear when we note that the operators $b^+_{n_1 n_0 n_{-1}, \sigma\tau}$ transform under a unitary transformation of the a_q^+, $q = 1, 0, -1$ in the same way as the states (5.21) with $n_1 + n_0 + n_{-1} = 2$. As the latter states form a basis for an IR of U_3 characterized by (200), which, furthermore, from Fig.1 contains the 2s and 1d states, our chain of groups is clearly

$$\mathscr{U}_6 \supset D^{(200)}(U_3) \supset \begin{pmatrix} \mathscr{D}^{(2)}(R_3) & 0 \\ 0 & \mathscr{D}^{(0)}(R_3) \end{pmatrix} \tag{5.29}$$

In the (2s-1d) shell the total number of states is $6 \times 4 = 24$. The group chain of classification of states is then

$$U_{24} \supset \mathscr{U}_6 \times U_4$$

$$[1^n] \qquad \begin{array}{|c|c|}\hline \multicolumn{2}{|c|}{} \\ \hline \multicolumn{2}{|c|}{} \\ \hline & \\ \hline & \\ \hline \end{array} \qquad \begin{array}{|c|c|}\hline \multicolumn{2}{|c|}{} \\ \hline \multicolumn{2}{|c|}{} \\ \hline & \\ \hline \end{array} \tag{5.30}$$

i.e. the completely antisymmetry state in U_{24} is broken into space and spin-isospin parts with associate representations. The spin-isospin part is further classified by $U_4 \supset SU_2^{(\sigma)} \times SU^{(\tau)}$, while the spatial part of the wave function is classified by the chain of groups (5.29). This classification scheme, however, may not be complete, in which case we need to use additional quantum numbers. Apart from these, the state we have constructed could be written as

$$|[h_1 h_2 h_3 h_4 h_5 h_6]\,(k_1 k_2)L,\ \{V_1 V_2 V_3 V_4\},\ ST, JM\rangle \tag{5.31}$$

where we have coupled the angular momentum L with the total spin S to give the total angular momentum J. The quantum numbers k_1, k_2 are the eigenvalues of the operators

$$\begin{aligned} \mathfrak{C}_1^1 - \mathfrak{C}_{-1}^{-1} &\to k_1 \\ \mathfrak{C}_0^0 - \mathfrak{C}_{-1}^{-1} &\to k_2 \end{aligned} \tag{5.32}$$

These quantum numbers characterize the IR of SU_3 and are related to the (λ, μ) of Elliott (Proc. R. Soc. A 245 (1958) 128) by $\lambda = k_1 - k_2$, $\mu = k_2$.

5.3. Determination of highest weight states of SU_3 and U_4 in the 2s-1d shell

How can we construct explicitly states of the type (5.31)? We shall show that the Slater determinants can be "weighed" according to the SU_3 and U_4 groups and that linear combinations of Slater determinants of the same weight can have maximum weight in these two groups. Once we have

these maximum weight states we can obtain all other states with the help of lowering operators in the appropriate chain of groups.

We shall first illustrate the procedure of the previous paragraph in the elementary case of the R_3 group. Starting from two states of angular momenta ℓ_1, ℓ_2, i.e. $|\ell_1, m_1\rangle, |\ell_2, m_2\rangle$, we would like to construct a state corresponding to a given IR of R_3 and at first of maximum weight, i.e. with $M = L$. We consider a linear combination of all states of two particles with weight $m_1 + m_2 = L$, i.e.

$$|L, L\rangle = \sum_m A_m |\ell_1, m\rangle |\ell_2, L-m\rangle \tag{5.33}$$

To guarantee that this state is of maximum weight, we apply to it the operator L_+ and

$$\begin{aligned} L_+ |L, L\rangle &= (L_+^{(1)} + L_+^{(2)}) |L, L\rangle \\ &= \sum_m \{(A_{m-1} \langle \ell_1, m | L_+^{(1)} | \ell_1, m-1\rangle \\ &\quad + A_m \langle \ell_2, L-m+1 | L_+^{(2)} | \ell_2, L-m\rangle) \\ &\quad |\ell_1, m\rangle |\ell_2, L-m+1\rangle\} = 0 \end{aligned} \tag{5.34}$$

where $L_+^{(1)}$, $L_+^{(2)}$ are the corresponding angular momentum operators of particles 1 and 2. This equation implies a recursion relation for the A_m which in fact determines the Clebsch-Gordan coefficient $\langle \ell_1, \ell_2, m, L-m | L, L\rangle$ up to a normalization coefficient. All other states $|L, M\rangle$ are then obtained from $|L, L\rangle$ by applying $L_-^{\ell - m}$.

We shall follow the same steps for the determination of the state (5.31) which we will illustrate by the detailed discussion of the example

$$|\psi\rangle = |[22](44)L, \{22\}ST, J\rangle \tag{5.35}$$

we denote our creation operators by $b_{\mu s}^\dagger$ where for μ and s we use the enumeration procedure given in (5.24) and (4.69) respectively. As [22] is a partition of 4, the state (5.31) must be a linear combination of Slater determinants of the form

$$b_{\mu_1 s_1}^\dagger b_{\mu_2 s_2}^\dagger b_{\mu_3 s_3}^\dagger b_{\mu_4 s_4}^\dagger |0\rangle \tag{5.36}$$

where the eigenvalues of these states with respect to the weight operators $\{C_1^1, C_2^2, C_3^3, C_4^4\}$ of U_4 and $(\mathfrak{C}_1^1 - \mathfrak{C}_{-1}^{-1}, \mathfrak{C}_0^0 - \mathfrak{C}_{-1}^{-1})$ of SU_3 must be respectively {2200} and (44). From Tables III and IV, in the first of which the $\mathfrak{C}_q^q$ were expressed in terms of $\mathscr{C}_\mu^\mu$ using (5.25), we see that the most general state of the desired weight is

$$|\varphi\rangle = (\alpha b_{11}^\dagger b_{21}^\dagger b_{22}^\dagger b_{42}^\dagger + \beta b_{12}^\dagger b_{21}^\dagger b_{22}^\dagger b_{41}^\dagger + \gamma b_{11}^\dagger b_{12}^\dagger b_{41}^\dagger b_{42}^\dagger) |0\rangle \tag{5.37}$$

Now $|\varphi\rangle$ will be of highest weight in U_4 and SU_3 if, when applying the

TABLE III. WEIGHT AND RAISING GENERATORS OF U_3 IN TERMS OF THE GENERATORS OF $\mathscr{U}_6$ AS GIVEN BY (5.25)

Weight generators	Raising generators
$\mathfrak{C}_1^1 = 2\mathscr{C}_1^1 + \mathscr{C}_2^2 + \mathscr{C}_3^3$	$\mathfrak{C}_1^0 = \sqrt{2}\mathscr{C}_1^2 + \sqrt{2}\mathscr{C}_2^4 + \mathscr{C}_5^5$
$\mathfrak{C}_0^0 = \mathscr{C}_2^2 + 2\mathscr{C}_4^4 + \mathscr{C}_5^5$	$\mathfrak{C}_1^{-1} = \sqrt{2}\mathscr{C}_1^3 + \mathscr{C}_2^5 + \sqrt{2}\mathscr{C}_3^6$
$\mathfrak{C}_{-1}^{-1} = \mathscr{C}_3^3 + \mathscr{C}_5^5 + 2\mathscr{C}_6^6$	$\mathfrak{C}_0^{-1} = \mathscr{C}_2^3 + \sqrt{2}\mathscr{C}_4^5 + \sqrt{2}\mathscr{C}_5^6$

TABLE IV. LINEARLY INDEPENDENT MONOMIALS WHOSE EIGENVALUES WITH RESPECT TO THE SET OF OPERATORS $\{C_1^1, C_2^2, C_3^3, C_4^4\}$ AND $(\mathfrak{C}_1^1 - \mathfrak{C}_{-1}^{-1}, \mathfrak{C}_0^0 - \mathfrak{C}_{-1}^{-1})$ ARE, RESPECTIVELY, {2200}, (44)

$b_{11}^\dagger b_{21}^\dagger b_{22}^\dagger b_{42}^\dagger$	$b_{12}^\dagger b_{21}^\dagger b_{22}^\dagger b_{41}^\dagger$	$b_{11}^\dagger b_{12}^\dagger b_{41}^\dagger b_{42}^\dagger$

raising generators in these two groups, we get zero. As the second index of the $b_{\mu s}^\dagger$ in (5.37) does not exceed 2, we see that C_s^3, $s<3$, C_s^4, $s<4$, when applied to (5.37) give zero, and so we must only worry about C_1^2 which gives

$$C_1^2 = (\alpha+\beta)\, b_{11}^\dagger b_{21}^\dagger b_{22}^\dagger b_{41}^\dagger \,|0\rangle = 0 \tag{5.38}$$

or $\alpha = -\beta$. After imposing this restriction on (5.37) we proceed to discuss the effect of the raising generators of SU_3, $\mathfrak{C}_1^0$, $\mathfrak{C}_1^{-1}$, $\mathfrak{C}_0^{-1}$ on our state. From Table III we see that $\mathfrak{C}_1^{-1}$, $\mathfrak{C}_0^{-1}$ are expressed in terms of generators of $\mathscr{U}_6$ containing upper indices 3, 5, 6 in our enumeration procedure. Since among the indices μ in the $b_{\mu s}^\dagger$ appearing in (5.37) there are no such values, the application of $\mathfrak{C}_1^{-1}$, $\mathfrak{C}_0^{-1}$ to our state automatically gives 0 and so we have only to worry about

$$\mathfrak{C}_1^0 = \sqrt{2}\,\mathscr{C}_1^2 + \sqrt{2}\,\mathscr{C}_2^4 + \mathscr{C}_6^5 \tag{5.39}$$

Applying $\mathfrak{C}_1^0$ to (5.37) with $\beta = -\alpha$ we get

$$\mathfrak{C}_1^0 |\varphi\rangle = (\alpha-\gamma)(b_{11}^\dagger b_{21}^\dagger b_{12}^\dagger b_{42}^\dagger - b_{12}^\dagger b_{11}^\dagger b_{22}^\dagger b_{41}^\dagger)\,|0\rangle = 0 \tag{5.40}$$

i.e. $\alpha = \gamma = -\beta$.

We have now derived the normalized state

$$|[22]\ (44)\ L=4,\ \{22\}\ S=2\quad T=0,\ J=M=6\rangle$$

$$= \frac{1}{\sqrt{3}}\,[b_{11}^\dagger b_{21}^\dagger b_{22}^\dagger b_{42}^\dagger - b_{12}^\dagger b_{21}^\dagger b_{22}^\dagger b_{41}^\dagger + b_{11}^\dagger b_{12}^\dagger b_{41}^\dagger b_{42}^\dagger]\ |0\rangle \tag{5.41}$$

where IR {22} of U_4 and (44) of SU_3 were obtained by construction. The IR [22] of U_6 comes in automatically as it is the associate partition

of {22}. This state, being of highest weight SU_3, is also of highest weight in its sub-group R_3, and, as $\mathscr{L}_0 = \mathfrak{C}^1_1 - \mathfrak{C}^{-1}_{-1}$, the eigenvalue of angular momentum is $L = 4$. It is also of highest weight in the sub-group $SU_2^{(\sigma)} \times SU_2^{(\tau)}$, and looking into the expressions for S_0, T_0 in (4.70) we see that their eigenvalues are $S = 2$, $T = 0$. Finally, as $J_+ = \mathscr{L}_+ + s_+$ applied to the state gives zero, the eigenvalue of $J_0 = \mathscr{L}_0 + s_0$, i.e. $4 + 2 = 6$, gives J and its projection.

We have illustrated by an example how we could get states of highest weight of SU_3 and U_4 which could be considered the equivalent ones in our case of the $|L, L\rangle$ state for R_3. We still have not outlined the procedure for determining the states equivalent to $|L, M\rangle$, i.e. the states (5.35) for any allowed L, S, T, J. We shall discuss this in detail in relation with the eigenvalue L, for which we first rewrite the generators $\mathfrak{C}^{q'}_{q}$ of U_3 in a more convenient way and then determine the lowering operators in the $SU_3 \supset R_3$ chain.

5.4. Lowering operators in the $SU_3 \supset R_3$ chain and the determination of the full set of states

The generators of U_3 in the second quantized picture could be expressed as Racah tensors of order 2, 1, 0 following the same analysis as in (5.16) - (5.18), i.e.

$$\mathscr{Q}_m = \sqrt{\frac{5}{3}} \sum_{q''q'} \langle 1\,2\,q''m \,|\, 1\,q' \rangle \; \mathfrak{C}^{q''}_{q'} \tag{5.42}$$

$$\mathscr{L}_q = \sqrt{2} \sum_{q''q'} \langle 1\,1\,q''q \,|\, 1\,q' \rangle \; \mathfrak{C}^{q''}_{q'} \tag{5.43}$$

$$\mathscr{H} = \sum_{q} \mathfrak{C}^{q}_{q} = \nu \mathscr{N} \tag{5.44}$$

As the operators $\mathscr{Q}_m$, $\mathscr{L}_q$ are generators of SU_3, when applied to states (5.31), they do not affect the IR of $\mathscr{U}_6$, SU_3 or of U_4 and its sub-groups. We could therefore use for these states (before the L, S are coupled to a definite J) the shorthand notation

$$|(k_1 k_2) L\; M_L\rangle \tag{5.45}$$

where there could be more than one state of definite L associated with a given $(k_1 k_2)$, in which case we could distinguish these states by some appropriate quantum number.

Both $\mathscr{Q}_m$ and $|(k_1 k_2) L\, M_L\rangle$ are irreducible tensors with respect to the R_3 group, so it follows from the Wigner-Eckart theorem, and the observations of the previous paragraph, that

$$\sum_{M_L m} \{\langle 2L\, M_L\, m \,|\, L'L'\rangle \; \mathscr{Q}_m \,|(k_1 k_2) L\, M_L\rangle\} \; \alpha \; |(k_1 k_2) L' L'\rangle \tag{5.46}$$

Since we could in turn express the state (5.45) in terms of the state $|(k_1 k_2) L\, L\rangle$ using the lowering operator $\mathscr{L}_-^{L-M_L}$, it follows that the operator

$$\mathscr{M}^{(2)}_{LL'} = \sum_{M_L\, m} \left\{ \langle 2L\, M_L\, m | L'L' \rangle \sqrt{\frac{(L+M_L)!}{(L-M_L)!\,(2L)!}}\, \mathscr{Q}_m (\mathscr{L}_-)^{L-M_L} \right\} \tag{5.47}$$

when acting on a state $|(k_1 k_2) L\, L\rangle$ gives us a state $|(k_1 k_2)\, L'L'\rangle$ with $L' = L \pm 2,\ L \pm 1,\ L$. The index 2 in the operator $\mathscr{M}^{(2)}_{LL'}$ is introduced to indicate that, with respect to the R_3 group, the operator $\mathscr{Q}_m$ appearing in it is a Racah tensor of order 2.

Starting then with the state $|(k_1 k_2)\, L = M = k_1\rangle$ we could apply the operator $\mathscr{M}^{(2)}_{LL'}$ to obtain the states for all compatible L's.

In a similar fashion we could apply the generators $R_{q\bar{q}}$ defined in (4.74) to the U_4 part of the state and obtain an operator that would give us all states of S, T compatible with the IR $\{V_1\, V_2\, V_3\, V_4\}$ of U_4, from the highest weight state for which

$$S_{h.w.} = \tfrac{1}{2}(V_1 + V_2 - V_3 - V_4), \qquad T_{h.w.} = \tfrac{1}{2}(V_1 - V_2 + V_3 - V_4) \tag{5.48}$$

Explicit forms of these operators are given in Ref. [1].

As we could furthermore apply $\mathscr{L}_-$ and S_- to our states, we obtain all projections M_L, M_S in them, which we could finally couple to a definite J.

In this way we get explicitly any state (5.31) as a linear combination of Slater determinants, i.e.

$$|\psi\rangle \equiv |[h_1 \ldots h_6]\, \alpha (k_1 k_2)\, \Omega L,\ \{V_1\, V_2\, V_3\, V_4\}\, \beta\, S\, T\, M_T, J\, M\rangle$$

$$= \sum_{\mu, s} A(\mu_1 \ldots \mu_n,\ s_1 \ldots s_n) b^\dagger_{\mu_1 s_1} \ldots b^\dagger_{\mu_n s_n} |0\rangle \tag{5.49}$$

where α, Ω, β are extra quantum numbers we need to introduce into the chain $\mathscr{U}_6 \supset \mathscr{D}^{(20)}(SU_3)$, $SU_3 \supset R_3$ and $U_4 \supset SU_2^{(\sigma)} \times SU_2^{(\tau)}$ respectively, and the $A(\mu_1 \ldots s_n)$ are appropriate constants.

5.5. The quadrupole-quadrupole and the pairing interactions

We indicated above that $\mathscr{Q}_m$ of (5.42) is the second quantized form of the single-body quadrupole operator Q_m. Therefore the corresponding operator associated with a quadrupole-quadrupole interaction (including self energy terms) is given by

$$\mathscr{Q}^2 = \sum_m (-1)^m \mathscr{Q}_m\, \mathscr{Q}_{-m} \tag{5.50}$$

As the relation between the operators $\mathscr{C}^{q'}_q$, $\mathscr{Q}_m$, $\mathscr{L}_q$, $\mathscr{H} = \nu\mathscr{N}$ are the same as those between $c^{q'}_q$, Q_m, L_q, H_0, we conclude from (5.19) that in the 2s-1d shell

$$\mathscr{Q}^2 = \Gamma_3 - \tfrac{1}{2}\mathscr{L}^2 - \tfrac{1}{3}(2\mathscr{N})^2 \tag{5.51}$$

where

$$\Gamma_3 = \sum_{q,q'} \mathfrak{C}_q^{q'} \mathfrak{C}_{q'}^{q} \tag{5.52}$$

As the operators Γ_3, $\mathscr{L}^2$, $\mathscr{N}$ are diagonal with respect to the states (5.49) characterized by $IR(k_1 k_2)$ of SU_3, L of R_3 and the number n of particles, we conclude from (3.150), (5.32), that the eigenvalues associated with $\mathscr{Q}^2$ have the form

$$E_L^{(k_1 k_2)} = [\tfrac{2}{3}(k_1 + k_2)^2 - 2k_1(k_2 - 1) - \tfrac{1}{2}L(L+1)] \tag{5.53}$$

If we expand an interaction, say of Gaussian form, in inverse powers of its range, we can easily show that for states in a single level of the harmonic oscillator, the first relevant term in this expansion is equivalent to a quadrupole-quadrupole interaction. Therefore the states (5.49), being eigenstates of $\mathscr{Q}^2$, have already correlations associated with long range interactions. If we would like now to see what is the effect of short range correlations, such as those of the pairing interaction, we have to apply them to the states (5.49). For this purpose we need to extend the concept of pairing interaction from one shell to several shells in a single level of the harmonic oscillator. For different ℓ's the only matrix element different from 0 of the pairing interaction is

$$\langle \nu\ell,\ \nu\ell,\ 0 | V | \nu\ell',\ \nu\ell',\ 0 \rangle = \sqrt{(2\ell+1)(2\ell'+1)} \tag{5.54}$$

In the case of a single level, ν is fixed and ℓ changes. This means that we may suppress the index ν in the creation operator, which can now be written as $b^\dagger_{\ell m,s}$. The invariants of an orthogonal sub-group of the $\mathscr{U}_r$ group are then given by

$$\sum_{\ell} \sum_{m} (-1)^m b^\dagger_{\ell m,s} b^\dagger_{\ell -m,s'} \tag{5.55}$$

In the 2s-1d shell we have six states in configuration space, five in the 1d and one in the 2s, so that the above bilinear form is invariant under an orthogonal group of six dimensions. The chain of groups involved is

$$\mathscr{U}_6 \supset \mathcal{O}_6 \supset \begin{pmatrix} \mathcal{O}_5 & 0 \\ 0 & 1 \end{pmatrix} \supset \begin{pmatrix} \mathscr{D}^{(2)}(R_3) & 0 \\ 0 & 1 \end{pmatrix} \tag{5.56}$$

where $\mathcal{O}_5$ is the orthogonal group involved in the 1d shell alone. The corresponding state characterized by the IR of the groups of the chain is

$$|\chi\rangle \equiv |\underset{\mathscr{U}_6}{[h_1 \ldots h_6]}\ \underset{\mathcal{O}_6}{\alpha'(\lambda_1\lambda_2\lambda_3)(\mu_1\mu_2)\Omega' L}\ \underset{\mathcal{O}_5}{\{V_1 V_2 V_3 V_4\}\ \beta S T}\ \underset{R_3}{M_T,\ J M}\rangle \tag{5.57}$$

where under each IR in the orbital part we have put the corresponding

group. We can construct the states $|\chi\rangle$ in terms of Slater determinants by a procedure entirely similar to the one used before for the $|\psi\rangle$ states.

In an earlier section we indicated how one could express a single-shell pairing interaction in terms of Casimir operators of $\mathscr{U}_{2\ell+1}$ and $\mathscr{O}_{2\ell+1}$. A similar analysis holds in the many-shell case. In particular for the 2s-1d shell the pairing interaction $\mathscr{P}$ is given by

$$\mathscr{P} = \Gamma - 2\Phi - \mathscr{N} \tag{5.58}$$

where Γ, Φ are respectively the Casimir operators of $\mathscr{U}_6$ and $\mathscr{O}_6$ and $\mathscr{N}$ is the number operator. From the discussion in sections 3 and 4 we conclude that the states (5.57) are eigenstates of $\mathscr{P}$ with eigenvalues

$$E^{(h_1 \ldots h_6)}_{(\lambda_1\lambda_2\lambda_3)} = \sum_{\mu=1}^{6} [h_\mu(h_\mu - 2\mu - 6) - \lambda_3^2 - \lambda_2(\lambda_2+2) - \lambda_1(\lambda_1+4)] \tag{5.59}$$

If we want to apply the pairing interaction to the states (5.49) of the U_3 chain, we can do this either by applying the pairing operator directly to the states using the computer programmes recently developed by Flores, or we can develop the states $|\psi\rangle$ in terms of the states $|\chi\rangle$ and recall that the latter are eigenstates of $\mathscr{P}$ with eigenvalue (5.59). For the second case we need the transformation brackets $\langle\chi|\psi\rangle$, which for our present problem are equivalent to the transformation brackets $\langle \ell m | \overline{\ell m'} \rangle = \mathscr{D}^{\ell}_{mm'}(0, \frac{\pi}{2}, 0)$ between the chains of R_3

$$R_3 \supset \begin{pmatrix} R_2 & 0 \\ 0 & 1 \end{pmatrix} \qquad R_3 \supset \begin{pmatrix} 1 & 0 \\ 0 & R_2 \end{pmatrix}$$

$$|\ell m\rangle \qquad |\overline{\ell m'}\rangle \tag{5.60}$$

The latter transformation brackets were used to solve the asymmetric top problem from our knowledge of the eigenvalues of the Hamiltonian for two symmetric tops around axes x or z fixed in the body. The former transformation brackets $\langle\chi|\psi\rangle$, which could be written explicitly as

$$\langle\chi|\psi\rangle = \langle [h_1 \ldots h_6]\alpha'(\lambda_1\lambda_2\lambda_3)(\mu_1\mu_2)\Omega' L | [h_1 \ldots h_6]\alpha(k_1k_2)\Omega L\rangle \tag{5.61}$$

as they are clearly independent of the spin-isospin part of the states, could be used to determine the matrix representation of the pairing interaction $\mathscr{P}$ with respect to the states $|\psi\rangle$ in a SU_3 basis. Tables of transformation brackets are given for particular cases in Ref. [4]. They were obtained from scalar products of the corresponding states $|\chi\rangle$, $|\psi\rangle$, of highest weight in U_4, given in terms of Slater determinants.

As the pairing $\mathscr{P}$ and quadrupole-quadrupole $\mathscr{Q}^2$ interactions give rise, respectively, to short and long correlations, we could inquire whether a linear combination

$$-V_0[(1-x)\mathscr{P} + x\mathscr{Q}^2], \quad 0 \leq x \leq 1 \tag{5.62}$$

would be a good model for a central interaction and, if so, how we could

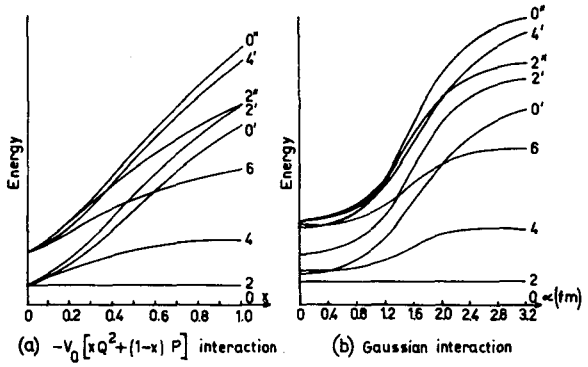

FIG. 2. Energy levels for $P + Q^2$ force as a function of x and for a Gaussian interaction as a function of the range α, for the partition [4]. Only some of the 18 levels have been drawn, in order not to confuse the graph (Ref. [3], courtesy of North-Holland Publishing Co.)

determine its matrix elements with respect to the states $|\psi\rangle$. The latter point has been answered above in terms of either direct application of $\mathscr{D}$ to the eigenstates $|\psi\rangle$ of $\mathscr{Q}^2$, or of the use of transformation brackets $\langle\chi|\psi\rangle$. For the first point we consider simple 2-, 3- and 4-particle problems and compare the interaction (5.62) with a Gaussian interaction. We illustrate the analysis here only for the case of 4 particles with partition [4]. In Figs. 2(a) and (b) we indicate the behaviour of the levels as a function, respectively, of the parameter x or of the range a of the Gaussian. The ground level was taken as base line in both cases and the distance between ground and first excited level was kept fixed, i.e. independent of x or of a. The behaviour of the rest of the levels is clearly similar throughout the range of the respective parameters. This indicates that (5.62) is a good model for a central interaction and that the parameter x plays the role of a range.

5.6. Applications to nuclear structure in the 2s-1d shell

The model interaction (5.62) and a spin orbit coupling term given by the one-body operator

$$W_{s.o.} = \sum_{i=1}^{n} \vec{\ell}_i \cdot \vec{s}_i \qquad (5.63)$$

were used in extensive calculations in the 2s-1d shell. We report here a few illustrative cases. Detailed applications are given in Refs. [3] [4] and [6].

Let us first consider the even parity states of ^{20}Ne. These states can reasonably be represented by four particles in the 2s-1d shell. We would expect the lowest state to come from the most symmetric representation of 4 particles in configuration space, i.e. [4] of $\mathscr{U}_6$, as this would make the most effective use of the atractive interaction. This representation corresponds to {1111} of U_4, which contains only a state $S = 0$, $T = 0$. Therefore the spin orbit coupling has no effect on these

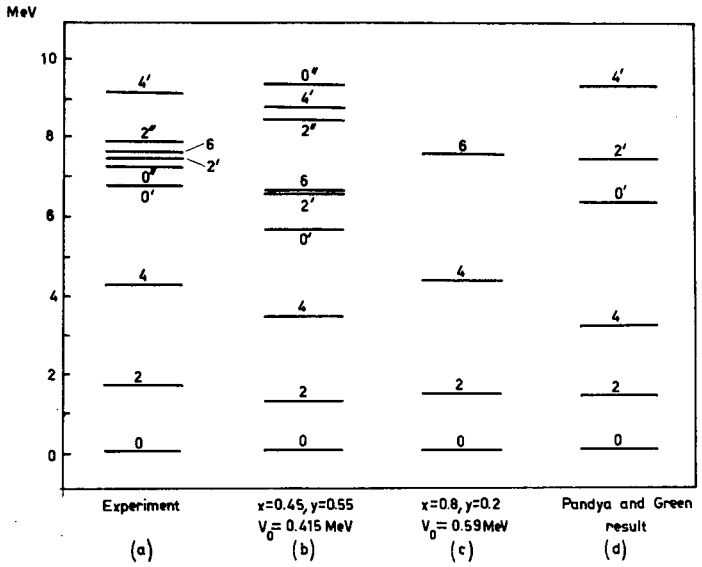

FIG. 3. Experimental and theoretical spectra of ^{20}Ne (Ref. [4], courtesy of North-Holland Publishing Co.)

states (for which L = J) and so we can restrict our analysis to the model interaction (5.62) where the behaviour of the energy levels as a function of x is given in Fig. 2. Comparison with the experimental spectra for values of the parameter x are given in Fig. 3 where $y = 1 - x$. Column c of Fig. 3 indicates comparison of the first band for the value of the parameter, while column d indicates results of Pandya and Green obtained by other methods. Detailed expressions for the wave functions are given in Ref. [4].

As another example let us consider the even parity states of ^{20}O. Again n = 4, but as T = 2 the representation of U_4 containing this T = 2 that is most antisymmetric is {22} (which corresponds to the most symmetric compatible representation [22] of $\mathscr{U}_6$). For T = 2 the only compatible s in the IR {22} of U_4 is s = 0, so we can restrict ourselves, as in the case of ^{20}Ne, only to the model interaction. The behaviour of the energy levels as function of the parameter x is given in Fig. 4 where, on the left-hand side, there are the IR of $\mathscr{O}_6(\lambda_1\lambda_2\lambda_3)$ and their corresponding L values, while on the right-hand side we have the IR of U_3 (not SU_3) given by $(\kappa_1\kappa_2\kappa_3)$ (where $k_1 = \kappa_1 - \kappa_3$, $k_2 = \kappa_2 - \kappa_3$, $n = \frac{1}{2}(\kappa_1 + \kappa_2 + \kappa_3)$) and the L values. The matrix elements were calculated with the help of the transformation brackets given in Ref. [4]. Reasonable agreement with experimental energy levels is obtained for x = 0.15.

Let us now discuss a couple of examples for which $\mathscr{W}_{s.o.}$ (related to $W_{s.o.}$ by (2.12)) is relevant. In the first example we consider ^{20}F where again n = 4 but T = 1. Following the same reasoning as in the previous paragraph, the lowest energy states should be well represented by the partition {211} in U_4 which contains s = 1, 0 associated with T = 1, to which corresponds the partition [31] of $\mathscr{U}_6$. Now the lowest level for a $\mathscr{Q}^2$ interaction would correspond to the highest weight SU_3 state, i.e. $(k_1k_2) = (71)$ in this IR [31] of $\mathscr{U}_6$. We could therefore explore the possibility of restricting our states to these representations $\mathscr{U}_6$ and

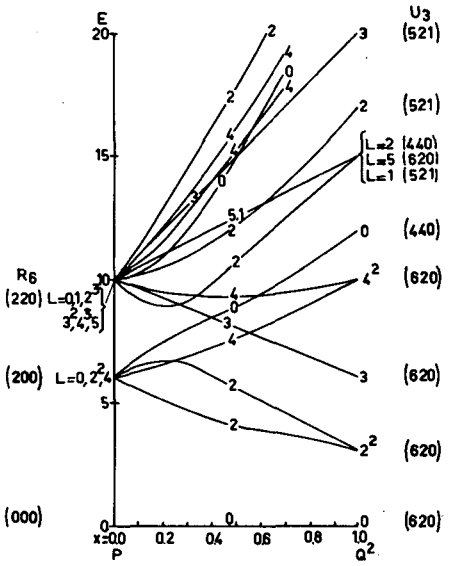

FIG. 4. Theoretical energy levels of ^{20}O (Ref. [4], courtesy of North-Holland Publishing Co.)

SU_3. This has been carried out in Ref. [4], the states associated with these IR being first determined along the lines outlined in this chapter. Then the matrix elements with respect to these states of $\mathcal{Q}^2$ (diagonal and trivial), $\mathcal{P}$ and $\mathcal{W}_{s.o.}$, were explicitly calculated. Finally the matrix of

$$-V_0[x\,\mathcal{Q}^2 + y\,\mathcal{P} + z\,\mathcal{W}_{s.o.}], \qquad x+y+z=1 \tag{5.64}$$

was diagonalized as a function of the parameters. The first energy levels are given in Fig. 5 for some values of the parameters. In columns d and e, the $\mathcal{Q}^2$ force was multiplied by an exchange factor $\mathcal{J}$ of the Rosenfeld type, whose explicit form was discussed in Ref. [7]. The eigenstates for the case d of Fig. 5 are given in Ref. [4]. A good fit to the energy levels can also be obtained with no pairing force, i.e. $y=0$ as seen in Fig. 6 of Ref. [4].

Finally, we discuss the case of ^{22}Na for which the number of particles in the 2s-1d shell is $n=6$ and $T=0$. The most anti-symmetric representation of U_4 that contains $T=0$ is $\{2211\}$ for which s is restricted to the value $s=1$. The corresponding partition for $\mathcal{U}_6$ is [42] and among the IR of SU_3 contained in it, the one that comes lowest in energy is $(k_1 k_2) = (1\,0,2)$. As the analysis of ^{20}F indicated the possibility of neglecting the $\mathcal{P}$ interaction for this odd-odd nucleus, for ^{22}Na we shall explore the effect of an interaction of the type

$$\mathcal{V} = -V_0\left[\frac{1}{10}\,x\,\mathcal{Q}^2 + (1-x)\,\mathcal{W}_{s.o.}\right] \tag{5.65}$$

where the factor 1/10 is introduced to facilitate the graphication. Now $\mathcal{Q}^2$ is clearly diagonal and proportional to $L(L+1)$ for definite IR [42]

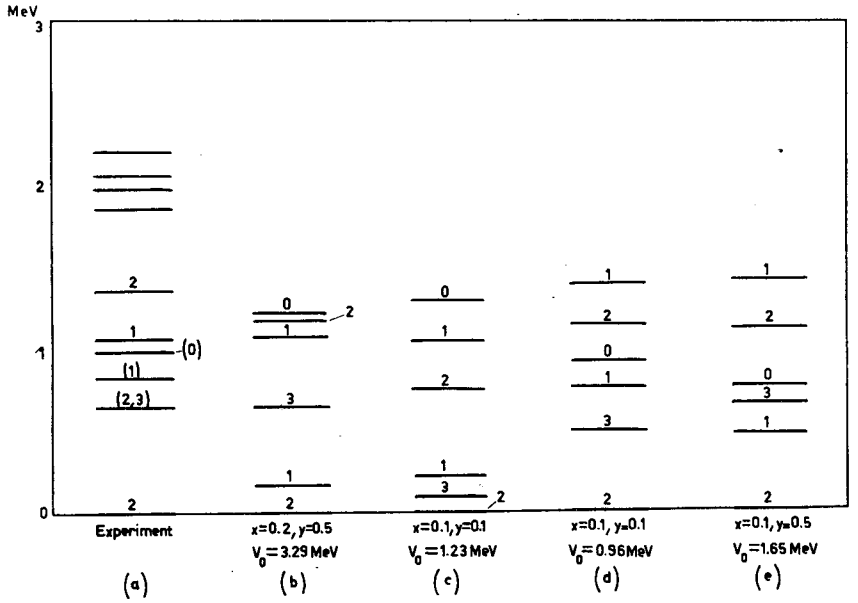

FIG. 5. Experimental and theoretical spectra of ^{20}F. In (b) and (c) exchange forces were not taken into account (Ref. [4], courtesy of North-Holland Publishing Co.)

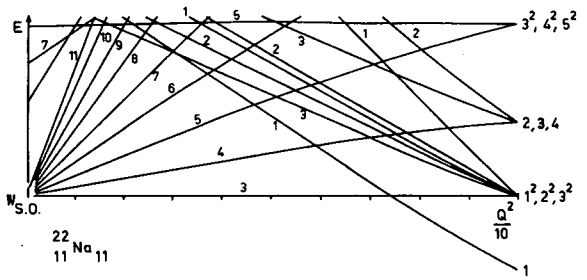

FIG. 6. Energy levels of ^{22}Na for the interaction (5.65). The experimental ground state $J = 3^+$ was taken as base line (from Ref. [6] p.129)

of $\mathscr{U}_6$, (1 0, 2) of SU_3 and L of R_3. The matrix elements of $\mathscr{W}_{s.o.}$ with respect to the states (5.49) can be evaluated using essentially the irreducible tensor character of this interaction with respect to SU_3 and the corresponding Wigner-Eckart theorem, as discussed in detail in Refs. [1] and [6]. In this way we obtain matrices whose diagonalization gives the energy level as functions of χ, as seen in Fig. 6. In this figure the experimental ground state is taken as a base line to see at a glance whether one could obtain the ground state for some value of the parameter χ. It is clear from Fig. 6 that the ground state could be obtained correctly, i.e. $J = 3^+$, for sufficiently strong spin orbit coupling, and that in a limited region the first excited state is $J = 1^+$ in accordance with experiment. The next two (doubtful) experimental levels are not predicted correctly, but here an admixture of a pairing interaction could be helpful. The procedures given in this chapter allow us to obtain also the states associated with these levels.

Discussions similar to the one given here for ^{22}Na have been presented for all odd-odd nuclei in the 2s-1d shell in Ref. [6]. A general computer programme along the lines presented in this section has been developed by Flores and will be applied to all nuclei in the 2s-1d shell.

The present picture can also be extended to negative parity states of nuclei between A = 16 to A = 40 by using particle hole configurations as discussed in Ref. [8].

6. APPLICATION OF GROUP THEORY TO THE FEW-NUCLEON PROBLEM

Up to now we have been discussing the application of group theory to the many-body problem in the formulation of second quantization. In this formulation the Pauli principle was automatically satisfied. Although no explicit mention of the symmetric group has been made, information about the symmetry properties of the orbital and spin-isospin parts has been implicitly taken into account by the irreducible representations of $\mathcal{U}_r$ and U_4 to which our wave functions belong.

We now present another approach based upon the idea of constructing the total wave function by combining products of space and spin-isospin wave functions in such a manner as to satisfy the Pauli principle. We shall consider this old approach to the problem (originating already in Wigner's work on supermultiplet theory) in a new manner, namely, by first restricting ourselves to the problem of n nucleons in a harmonic oscillator potential or interacting via two-body harmonic oscillator forces.

The reason for doing this is the large symmetry of the problem which, as we shall see, is invariant under the U_{3n} group. This group admits a large number of chains of sub-groups and it is possible to show that there exist well defined chains of sub-groups of U_{3n} to which some fundamental concepts of nuclear physics, such as the shell model, the collective model and the cluster model can be related.

We shall start by discussing the problem of translationally invariant states (elimination of centre-of-mass motion) for the general n nucleon problem, and then illustrate our general approach by discussing in detail the four-nucleon case.

6.1. The auxiliary Hamiltonian, its symmetry groups and eigenstates

Let us consider the Hamiltonian $\mathcal{H}'$ of n particles interacting with each other through harmonic oscillator forces:

$$\mathcal{H}' = \sum_{s=1}^{n} \sum_{i=1}^{3} \frac{1}{2m} (p_i^s)^2 + \frac{m\omega^2}{4n} \sum_{s,t=1}^{n} \sum_{i=1}^{3} (x_i^s - x_i^t)^2 \qquad (6.1)$$

By performing a transformation to Jacobi co-ordinates

$$\dot{x}_i^1 = \frac{1}{\sqrt{2}} (x_i^1 - x_i^2)$$

.....

$$\dot{x}_i^s = [s(s+1)]^{-\frac{1}{2}} \sum_{t=1}^{s} x_i^t - s^{\frac{1}{2}}(s+1)^{-\frac{1}{2}} x_i^{s+1} \qquad (6.2)$$

$$\cdots\cdots\cdots\cdots\cdots\cdots$$

$$\dot{x}_i^n = n^{-\frac{1}{2}} \sum_{t=1}^{n} x_i^t$$

and adding a potential energy term $\frac{1}{2} m\omega^2 \sum_{i=1}^{3} (\dot{x}_i^n)^2$ the Hamiltonian (6.1) becomes

$$\mathscr{H}'' = \sum_{s=1}^{n} \sum_{i\ 1}^{3} \frac{1}{2m} (\dot{p}_i^s)^2 + \frac{m\omega^2}{2} \sum_{s=1}^{n} \sum_{i=1}^{3} (\dot{x}_i^s)^2 \qquad (6.3)$$

The purpose of the addition of the potential energy term is to have in $\mathscr{H}''$ a dependence on the centre-of-mass co-ordinate and momenta of the form

$$\frac{1}{2m} \sum_{i\ 1}^{3} (\dot{p}_i^n)^2 + \tfrac{1}{2} m\omega^2 \sum_{i\ 1}^{3} (\dot{x}_i^n)^2 \qquad (6.4)$$

This would allow us to eliminate spurious states associated with centre-of-mass motion by restricting ourselves to eigenstates of (6.3) which have zero quanta for the part (6.4) of this Hamiltonian.

We shall now express our Hamiltonian (6.3) in terms of relative creation and annihilation operators

$$\eta_i^s = \sqrt{\frac{1}{2}} \left(\sqrt{\frac{m\omega}{\hbar}}\, \dot{x}_i^s - i \sqrt{\frac{1}{m\omega\hbar}}\, \dot{p}_i^s \right) \qquad (6.5)$$

$$\xi_i^s = \sqrt{\frac{1}{2}} \left(\sqrt{\frac{m\omega}{\hbar}}\, \dot{x}_i^s + i \sqrt{\frac{1}{m\omega\hbar}}\, \dot{p}_i^s \right) = \eta_i^{s\dagger} \qquad (6.6)$$

which satisfy commutation relations for Bose operators. In terms of these operators a dimensionless $\mathscr{H}$ may be expressed as

$$\mathscr{H} = \frac{1}{\hbar\omega} \mathscr{H}'' - \frac{3n}{2} = \sum_{s=1}^{n} \sum_{i=1}^{3} \eta_i^s \xi_i^s = \sum_{s=1}^{n} \sum_{i=1}^{3} \eta_i^s \eta_i^{s\dagger} \qquad (6.7)$$

We see from (6.7) that $\mathscr{H}$ is invariant under an arbitrary 3n-dimensional unitary transformation $\mathbb{U}_{3n}$ of the η_i^s, i = 1, 2, 3, s = 1 ... n. Furthermore, from the commutation relations of η_i^s, ξ_j^t we note that

$$\mathbb{C}_{ij}^{st} = \eta_i^s \xi_j^t \qquad (6.8)$$

TABLE V. SYMMETRY GROUPS AND THEIR GENERATORS

Symmetry groups	Generators
U_{3n}	$C_{ij}^{st} = \eta_i^s \xi_j^t$
$\mathscr{U}_3 \times U_n$ { $\mathscr{U}_3$; U_n	$\mathscr{C}_{ij} = \sum_{s=1}^{n} C_{ij}^{ss}$; $C^{st} = \sum_{i=1}^{3} C_{ii}^{st}$
$\mathscr{U}_3 \supset \mathscr{U}_2 \supset \mathscr{U}_1$	$\mathscr{C}_{ij}$, $i, j \leq k$, $k = 3, 2, 1$
$U_n \supset U_{n-1} \supset \ldots \supset U_p \supset \ldots \supset U_1$	C^{st}, $s, t \leq p$, $p = n, n-1 \ldots 1$

commute with $\mathscr{H}$ and satisfy commutation relations that indicate they are the generators of U_{3n}. This group contains as a sub-group, the direct product $\mathscr{U}_3 \times U_n$, where $\mathscr{U}_3$ is a unitary transformation in the co-ordinate space (space of the components), while U_n is a unitary transformation in the particle index space. Their generators are obtained by contractions with respect to the upper indices and the lower indices respectively. The situation is summarized in Table V where we also include the generators of the sub-groups of $\mathscr{U}_3$ and U_n for the mathematically natural chain.

Let us now construct the states corresponding to these chains of sub-groups of the U_{3n} groups. The state for a system of n particles corresponding to a definite number N of quanta will be obtained as a homogeneous polynomial of degree N in the creation operators η_i^s applied to the 'vacuum state':

$$P(\eta_i^s)\,|0\rangle \tag{6.9a}$$

where the 'vacuum state' is now the ground state of the 3n-dimensional harmonic oscillator:

$$|0\rangle = \pi^{-\frac{3}{4}n} \exp\left(-\frac{1}{2}\sum_{i,s}\left[(\dot{x}_i^s)^2 \frac{m\omega}{\hbar}\right]\right) \tag{6.9b}$$

Because of the commutation relations we could write

$$\mathscr{H} = \sum_{i,s} \eta_i^s \xi_i^s = \sum_{i,s} \eta_i^s \frac{\partial}{\partial \eta_i^s} \tag{6.10}$$

so it is clear that the effect of $\mathscr{H}$ acting upon a homogeneous polynomial of degree N is to reproduce this polynomial multiplied by its degree N.

The homogeneous polynomials (6.9) are thus eigenstates of $\mathscr{H}$. Furthermore, all the homogeneous polynomials of degree N in η_1^s can be obtained from $(\eta_1^1)^N$ by applying to it the generators $\mathbb{C}_{ij}^{st}$. As we also have

$$\mathbb{C}_{ij}^{st}(\eta_1^1)^N|0\rangle = 0 \text{ for } i<j,\ s<t, \quad \mathbb{C}_{ii}^{ss}(\eta_1^1)^N|0\rangle = N(\eta_1^1)^N|0\rangle\delta_{i1}\delta^{s1} \tag{6.11a, b}$$

we conclude that all the homogeneous polynomials of degree N form a basis for the IR

$$\underbrace{[N, 0, 0, \ldots 0]}_{3n-1} \tag{6.12}$$

of $\mathbb{U}_{3n}$.

What are now the possible IR for the sub-group $\mathscr{U}_3 \times U_n$ and the corresponding basis functions?

It may be proved (see Ref. [9]) that the IR of the groups $\mathscr{U}_3$ and U_n that appear in the reduction of the IR $[N, \underbrace{0, \ldots, 0}_{3n-1}]$ of $\mathbb{U}_{3n}$ are grouped in pairs, namely, if the representation of $\mathscr{U}_3$ is

$$[h_1, h_2, h_3] \text{ with } h_1+h_2+h_3 = N,\ h_1 \geq h_2 \geq h_3 \geq 0 \tag{6.13}$$

then for U_n appears the following 'associate' representation:

$$\underbrace{[h_1, h_2, h_3, 0, 0, \ldots, 0]}_{n-3} \tag{6.14}$$

The basis states corresponding to these representations are the Gel'fand states

$$\begin{array}{c|ccccccccccc|c}
\mathscr{U}_3 & h_1 & & h_2 & & h_3 & & h_1 & h_2 & h_3 & 0 & 0 & U_n \\
\mathscr{U}_2 & & q_1 & & q_2 & & ; & & u_1 & u_2 & u_3 & 0\ldots 0 & U_{n-1} \\
\mathscr{U}_1 & & & r_1 & & & & & & v_1 & v_2 & v_3\ 0\ldots 0 & U_{n-2} \\
 & & & & & & & & & & \cdots\cdots & & \vdots \\
 & & & & & & & & & & & z_1 & U_1
\end{array} \tag{6.15}$$

The highest weight state will be:

$$\left|\begin{array}{ccccccccccccc} h_1 & & h_2 & & h_3 & & h_1 & & h_2 & & h_3 & 0 & 0 \ldots\ldots\ldots 0 \\ & h_1 & & h_2 & ; & & & h_1 & & h_2 & & h_3 & 0 \ldots\ldots\ldots 0 \\ & & h_1 & & & & & & h_1 & & h_2 & & h_3 \quad 0 \ldots 0 \\ & & & & & & & & & \ldots\ldots\ldots\ldots\ldots & & & \\ & & & & & & & & & & h_1 & & h_2 \\ & & & & & & & & & & & h_1 & \end{array}\right\rangle \tag{6.16}$$

This state may be given an explicit expression if we define

$$\Delta^{s_1 \ldots s_p}_{i_1 \ldots i_p} = \sum_{p_s} (-1)^{p_s} p_s \, \eta^{s_1}_{i_1} \eta^{s_2}_{i_2} \ldots \eta^{s_p}_{i_p} \tag{6.17}$$

p_s being a permutation of the s indices. In terms of the functions (6.17), the h.w. state (6.16) up to a normalization constant, has the expression (Ref. [9])

$$(\Delta^1_1)^{h_1 - h_2} (\Delta^{12}_{12})^{h_2 - h_3} (\Delta^{123}_{123})^{h_3} \, |0\rangle \tag{6.18}$$

where

$$h_1 + h_2 + h_3 = N \tag{6.19}$$

It may, in fact, be proved that by applying the raising generators $\mathscr{C}_{ij}$ $(i < j)$ of the group $\mathscr{U}_3$ to the state (6.18) one gets zero. Let us show for instance that $\mathscr{C}_{12} \Delta^{12}_{12} |0\rangle = 0$.

$$\mathscr{C}_{12} \Delta^{12}_{12} |0\rangle = (\eta^1_1 \xi^1_2 + \eta^2_1 \xi^2_2)(\eta^1_1 \eta^2_2 - \eta^2_1 \eta^1_2) |0\rangle = (\eta^1_1 \eta^2_1 - \eta^2_1 \eta^1_1) |0\rangle = 0 \tag{6.20}$$

In a similar manner it may be shown that the application of the raising generators C^{st} $(s < t)$ to (6.18) gives zero. The weight of the state (6.18) is obtained by applying the weight operators $\mathscr{C}_{11}$, $\mathscr{C}_{22}$, $\mathscr{C}_{33}$ for $\mathscr{U}_3$ and C^{11}, C^{22}, ..., C^{nn} for U_n. One obtains the weights $[h_1, h_2, h_3]$ and $[h_1, h_2, h_3, \underbrace{0, \ldots, 0}_{n-3}]$ respectively. The general Gel'fand states are obtained in the usual way by application of products of lowering operators to the h.w. state

6.2. Elimination of spurious states due to the centre-of-mass motion

Let us remember that the creation operators η^s_i have been defined in connection with the Jacobi co-ordinates, so that the index s designates the relative co-ordinate s and not the co-ordinate of particle s. As the n-th Jacobi co-ordinate was associated with the motion of the centre of

mass, it is now simple to construct states with no quanta in the centre-of-mass co-ordinate; this may be realized by requiring that the eigenvalue of the generator C^{nn}, which counts the number of quanta for the centre-of-mass degree of freedom $\dot{x}_i^n$, be zero. But, as C^{nn} applied to a Gel'fand state has the eigenvalue

$$h_1 + h_2 + h_3 - (u_1 + u_2 + u_3) \tag{6.21}$$

and as

$$h_1 \geq u_1 \geq h_2 \geq u_2 \geq h_3 \geq u_3 \tag{6.22}$$

we conclude that the states having zero number of quanta for the centre-of-mass oscillation are characterized by Gel'fand states for which

$$h_1 = u_1, \quad h_2 = u_2, \quad h_3 = u_3 \tag{6.23}$$

The Gel'fand states (6.15) we introduced in connection with problem (6.3) constitute the 'mathematically natural states'.

6.3. Physical chains of sub-groups

Let us discuss now the physical chain of groups and the corresponding basis.

For the unitary transformations in the space of the components the chain is

$$\mathcal{U}_3 \supset \mathcal{O}_3 \supset \mathcal{O}_2 \tag{6.24}$$

and this is a chain we are already familiar with.

Now as far as unitary transformations in particle space U_n are concerned, the first link in our group chain will certainly be

$$U_n \supset U_{n-1} \tag{6.25}$$

which eliminates the centre of mass. Let us remember that U_{n-1} are unitary transformations in the space of $(n-1)$ relative co-ordinates

$$\begin{aligned} \vec{\dot{x}}^1 &= \frac{1}{\sqrt{2}}(\vec{x}^1 - \vec{x}^2) \\ &\cdots\cdots\cdots\cdots\cdots\cdots \\ \vec{\dot{x}}^{n-1} &= \frac{1}{\sqrt{n(n-1)}}[\vec{x}^1 + \vec{x}^2 + \ldots \vec{x}^{n-1} - (n-1)\vec{x}^n] \end{aligned} \tag{6.26}$$

But the U_{n-1} representation in the space of the Jacobi co-ordinates admits as a sub-group the IR

$$D^{(n-1,1)}(S_n) \tag{6.27}$$

of the symmetrical group of n particle S_n. The $(n-1, 1)$ irreducible representation of S_n is given by $(n-1)\times(n-1)$ matrices, as is seen from (6.26) and may also be proved by counting the number of ways the set of

numbers {1, 2, . . . , n} may be arranged into a Young diagram

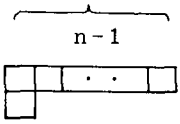

(6.28)

so that they should be situated in increasing order if read from left to right and from top to bottom. It should be stressed that the group S_n refers to the permutations of the n particles, and not to their relative coordinates. It can be easily shown that the $(n-1)\times(n-1)$ matrices in the IR $D^{(n-1,1)}(S_n)$ are orthogonal ones.

We have thus succeeded in getting as a final group of the reduction of $\mathscr{U}_3 \times U_n$, the group $\mathcal{O}_3 \times S_n$, which is physically interesting as it provides orbital wave functions of definite angular momentum and of given symmetry with respect to the permutation of the particles.

Between U_{n-1} and $D^{(n-1,1)}(S_n)$ an O_{n-1} group may be included which has no physical significance, but provides us with labels for classifying the states. The chain of groups in particle space is thus

$$U_n \supset U_{n-1} \supset O_{n-1} \supset D^{(n-1,1)}(S_n) \tag{6.29}$$

We shall illustrate the problem of the construction of wave functions corresponding to the above chains for the particular case $n = 4$.

6.4. The four-particle problem

6.4.1. The orbital part of the state

For the chain of groups (6.24) the basis functions are

$$\left| \begin{matrix} h_1 & h_2 & h_3 \\ \Omega & L & M \end{matrix} \right\rangle \tag{6.30}$$

and we have only to calculate the transformation brackets

$$\left\langle \begin{matrix} h_1 & h_2 & h_3 \\ & q_1 \quad q_2 & \\ & r_1 & \end{matrix} \middle| \begin{matrix} h_1 & h_2 & h_3 \\ \Omega & L & M \end{matrix} \right\rangle \tag{6.31}$$

which is a problem that has already been discussed in section 3. The chain of sub-groups of the U_4 transformations in particle space (6.29) becomes

$$U_4 \supset U_3 \tag{6.32a}$$

$$U_3 \supset O_3 \supset D^{(3,1)}(S_4) \tag{6.32b}$$

It may be shown that the $D^{(3,1)}$ representation of the S_4 group is isomorphic to the tetrahedral group in three dimensions T_d. As we already

know the transformation brackets

$$\left\langle \begin{matrix} h_1 & h_2 & h_3 \\ & v_1 \quad v_2 & \\ & w_1 & \end{matrix} \middle| \begin{matrix} h_1 & h_2 & h_3 \\ \varphi & \lambda & \mu \end{matrix} \right\rangle \tag{6.33}$$

from the mathematically natural chain to the physical chain[7]

$$\begin{matrix} U_3 & \supset & O_3 & \supset & O_2 \\ [h_1 h_2 h_3] & & \lambda & & \mu \end{matrix} \tag{6.34}$$

we have only to worry about the transformation brackets between states corresponding to the chains (6.34) and (6.32b). As in these chains we are dealing with the same U_3 and O_3 groups, we need only the transformation brackets between the states characterized by the IR of the sub-chains

$$O_3 \supset O_2 \quad \text{and} \quad O_3 \supset D^{(3,1)}(S_4) = \mathrm{Td} \tag{6.35a, b}$$

The states associated with (6.35a) can be denoted by the ket $|\lambda\mu\rangle$ with λ, μ being the IR of O_3 and O_2, respectively. The IR of S_4 are characterized by a partition $f \equiv [f_1 f_2 f_3 f_4]$ of 4, and their rows by the Yamanouchi symbol $r \equiv (1 r_2 r_3 r_4)$. The corresponding ket can then be denoted by $|\lambda\chi f r\rangle$, where χ is an extra quantum number that distinguishes between repeated IR of S_4 contained in a given IR of O_3. The transformation bracket we need to determine is then

$$\langle \lambda\mu | \lambda\chi f r \rangle \tag{6.36}$$

As $D^{(3,1)}(S_4) = \mathrm{Td}$, the determination of (6.36) is a problem well known in molecular physics and solid-state theory where it appears in the explicit construction in terms of spherical harmonics of the symmetry-adapted wave functions of the tetrahedral group (see, for example, Jahn, Proc. R. Soc. 168 (1938) 469). A systematic determination of these coefficients has been given by Kramer and Moshinsky in Ref. [10].

Using then (6.31), (6.33) and (6.36) we can pass from the four-particle states of the type (6.15) with zero excitation for the centre-of-mass motion to the states

$$\left| \begin{matrix} h_1 & h_2 & h_3 \\ \omega & L & M \end{matrix} ; \varphi \lambda \chi f r \right\rangle \tag{6.37}$$

where we suppressed the redundant partitions for the $U_4 \supset U_3$ groups in the particle indices. We have therefore an explicit procedure for constructing the orbital part of the four-particle state and, in principle, this could be extended to the n-particle state.

---

[7] We have indicated under the groups in the chain (6.34) their corresponding IR. The quantum number φ plays for (6.34) the same role as Ω for (6.31).

6.4.2. The spin-isospin part of the state

We would like now to introduce the spin-isospin part of the four-particle state so as to be able later to construct the complete anti-symmetric wave function to which we would apply the physical interaction.

The spin-isospin part of the state would be characterized by the total spin (S), isospin (T) and their projections (M_S, M_T) as well as by the IR of S_4 associated with the partition f and the Yamanouchi symbol r, so that it could be denoted by the ket

$$|STM_SM_T, fr\rangle \tag{6.38}$$

The explicit construction of states of this type for an arbitrary number of particles was given in Refs.[11] and [12]. We note only that the procedure followed there was very similar to the one we have given in the previous sub-sections for the explicit determination of the orbital part of the state.

6.4.3. The full anti-symmetric wave function and the matrix elements of the physical Hamiltonian

We could build up the full anti-symmetric wave function by combining the orbital states of partition f and Yamanouchi symbol r with spin-isospin states of the associated partition $\tilde{f}$ and Yamanouchi symbol $\tilde{r}$. We illustrate the relation between the partitions and Yamanouchi symbols and their associates by the example in (6.39)

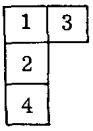

$f = [211]$, $r = (1213)$, 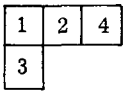 $\tilde{f} = [31]$, $\tilde{r} = (1121)$ (6.39)

Furthermore, we vector couple L, S to a definite J so as to get the anti-symmetric wave function

$$|N\rangle \equiv \left| \begin{matrix} h_1 & h_2 & h_3 \\ \Omega & L & \end{matrix} ; \varphi\lambda\chi f, STM_T, JM \right\rangle$$

$$= \sum_r \frac{(-1)^r}{\sqrt{\ell_f}} \left[\left| \begin{matrix} h_1 & h_2 & h_3 \\ \Omega & L & \end{matrix} ; \varphi\lambda\chi fr \right\rangle |STM_T, \tilde{f}\tilde{r}\rangle \right]_{JM} \tag{6.40}$$

where ℓ_f is the dimension of the IR of S_4 characterized by f, $[\ ]_{JM}$ is the familiar bracket notation for vector coupling of L, S, and $(-1)^r$ is 1 if the Young tableau corresponding to r is obtained from

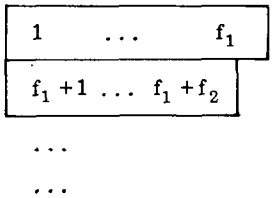

(6.41)

by an even number of successive interchanges of two numbers, and -1 otherwise. When convenient we shall use the shorthand notation $|N\rangle$, where N is the number of quanta, for this state.

We should now like to apply to our state (6.40) an intrinsic physical Hamiltonian H, where the adjective intrinsic means that we remove from this Hamiltonian the kinetic energy associated with the centre-of-mass motions, i.e. for an n-particle system it is given by

$$H = \sum_{s=1}^{n-1} \frac{1}{2m} (\vec{p}^{\,s})^2 + \sum_{s<t=1}^{n} V(s,t) \tag{6.42}$$

where $\vec{p}^{\,s}$ are the momenta associated with the relative Jacobi co-ordinates (6.2) and V(s, t) is a two-body, not necessarily central, interaction between particles s and t.

As the states (6.40) are eigenstates of $\mathscr{H}$, we could express the kinetic energy in (6.42) in terms of $\mathscr{H}$ and the potential energy of the harmonic oscillator interactions. Furthermore, as the states (6.40) are anti-symmetric under interchange of the co-ordinates, spin and isospin of any two particles, we could write, in the shorthand notation introduced for (6.40), that

$$\langle N' | H | N \rangle = \hbar\omega \left[N + \tfrac{3}{2}(n-1)\right] \delta_{N',N}$$
$$+ \tfrac{1}{2} n(n-1) \langle N' | V(1,2) - \frac{m\omega^2}{2n} (\vec{x}^{\,1} - \vec{x}^{\,2})^2 | N \rangle \tag{6.43}$$

where the $\delta_{N',N}$ is 1 only if all the quantum numbers in the states of bra and ket are equal. For our particular problem the number of particles n = 4.

Having then the explicit states (6.40) we must evaluate with respect to them the matrix elements of a two-body interaction associated with particles 1 and 2. This can be achieved in three steps:

(a) We use standard Racah algebra to decompose the matrix elements in (6.43) in terms of a product of the reduced matrix elements of the separate orbital and spin-isospin parts in the interaction.

(b) We determine from the explicit form of the orbital state (6.37) the fractional parentage coefficients (fpc) with whose help we can decompose the state into a part associated with the relative co-ordinate $\vec{x}^{\,1} = \frac{1}{\sqrt{2}} (\vec{x}^{\,1} - \vec{x}^{\,2})$ and a part associated with the other co-ordinates. We then use these fpc in the standard way to determine the orbital reduced matrix element.

(c) We determine from the explicit form of the spin-isospin state (6.38) the fractional parentage coefficient (fpc) with whose help we can decompose the state into a part associated with spin-isospin co-ordinates of particles 1, 2 and a part associated with the other co-ordinates. We then use these fpc in the standard way to determine the spin-isospin reduced matrix element. All these steps have been carried out explicitly by Kramer and Moshinsky (Ref. [12]).

TABLE VI. PARAMETERS AND TALMI INTEGRALS OF THE SERBER FORCE

The Serber Force
$\mathscr{V} = {}^3V^e(r)\left[\frac{1+p^B}{2}\right] + {}^1V^e\left[\frac{1-p^B}{2}\right]$
$V(r) = -V_0(\mu r)^{-1}\exp(-\mu r)$
${}^3V_0^e = 52.13$ MeV $\quad {}^3\mu^e = 0.7261\ f^{-1}$
${}^1V_0^e = 46.87$ MeV $\quad {}^1\mu^e = 0.8547\ f^{-1}$
Talmi integrals $\quad I_p = (2/\Gamma(p+\frac{3}{2}))\int_0^\infty r^{2p+2}e^{-r^2}V(r)\,dr$
${}^3I_0^e = -14.29$ MeV, $\quad {}^3I_1^e = -5.2$ MeV, $\quad {}^3I_2^e = -2.61$ MeV
${}^1I_0^e = -9.4$ MeV, $\quad {}^1I_1^e = -3.2$ MeV, $\quad {}^1I_2^e = -1.62$ MeV
$\hbar\omega = 21.8$ MeV

6.4.4. Energy levels of the four-nucleon system

We have explicitly determined the matrix elements of (6.43) for $n = 4$ and $N, N' = 0, 1, 2$ for a Serber force of a type used recently by de-Shalit and Walecka (Phys. Rev. 147 (1966) 763) in their calculations of one-particle-one-hole excitations for the four-nucleon system. The parameters of this force and the Talmi integrals, for the $\hbar\omega = 21.8$ MeV associated with the mean square radius of the α particle, are given in Table VI.

As the interaction is a Serber force with exchange, we have that L, S are integrals of motion as, of course, will also be J^π and T, where π is the parity. We furthermore give the partition $\{f_1f_2f_3f_4\}$ for each level. This partition is almost a good quantum number since the Bartlet part of the force, when compared with the Wigner part, is relatively weak.

The energy levels for the Serber force are given in Fig. 7. We note that there is only one state of negative energy, i.e. actually bound, as is the case for the α particle. The binding energy of $\simeq 24$ MeV is not far removed from the experimental value of $\simeq 28$ MeV. The ground state is a mixture of the states of $N = 2$ and $N = 0$ quanta with $L = S = 0$ and partition [4], though the ratio of the square of the amplitudes of the states 1:10 indicates that the $N = 2$ admixture is still small. The first excited state is a O^+ state and afterwards follow the negative parity states as experimentally observed. The position of the levels with $T = 1, 2$ vis-à-vis those of $T = 0$ is also in reasonable agreement with experiment.

In Fig. 8 we present the way in which the negative parity states, i.e. those with $N = 1$, are decomposed by a two-particle spin orbit force, for

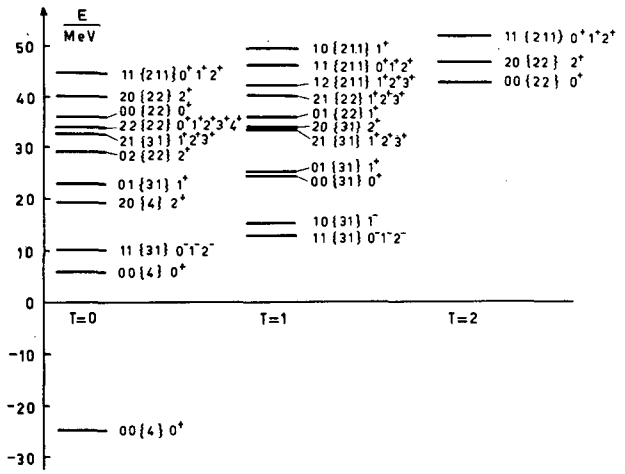

FIG. 7. Energy levels of a Serber force for a four-nucleon system with states up to N = 2 quanta. The quantum numbers indicated correspond to L S $\{f\}$ J^{π} (Ref. [13], courtesy of North-Holland Publishing Co.)

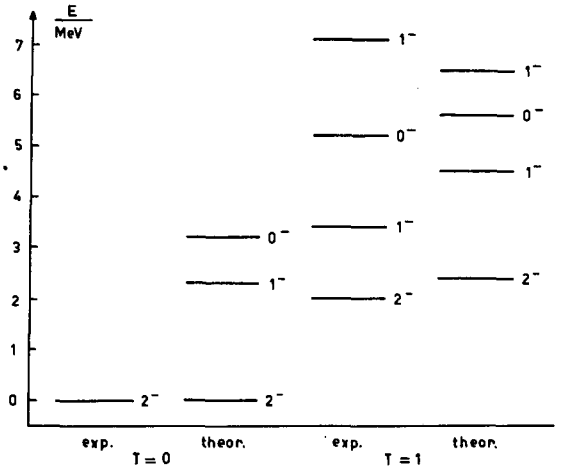

FIG. 8. Effect of a two-body spin orbit interaction on the negative parity states N = 1 (Ref. [13], courtesy of North-Holland Publishing Co.)

which there is only one Talmi integral I_1^{ls}, whose value was taken as -1.1 MeV. These energy levels are compared with experiment, it being assumed that the lowest negative parity level with T = 0, i.e. 2^-, agrees with the experimental one.

The results presented have been taken from a paper by Kramer and Moshinsky given in Ref. [13].

It is clear that in principle the approach presented here could be extended to any number N of quanta and n of particles. It seems that the present approach would have definite advantages over the second quantized one discussed in the previous sections, when n is not too large. The reason is that in this case the summation over the Yamanouchi

symbols r is not too large and so, by including larger values of N, we could go to configurations that would involve many shells for the few-nucleon problem.

7. THE HARMONIC OSCILLATOR (h.o.) AND SHELL MODEL STATES

It is well known that harmonic oscillator states play an important role in the calculations of the nuclear shell model, among other reasons because of the ease with which the matrix elements of two-body interactions can be evaluated by using the transformation brackets to the centre-of-mass and relative co-ordinate system. A detailed exposition of this last point is given in Ref. [14].

In the above calculations, however, the harmonic oscillator is, so to say, grafted into an existing nuclear shell theory formalism. In this section we would like to turn the problem round and see how, in general, a multiple-shell configuration can be associated with a system of n particles in an h.o. potential. The explicit construction of the states associated with this problem allows us to define a generalized concept of fractional parentage coefficients (fpc) for systems of n particles in an h.o. potential. These fpc are basic in any calculation of the matrix elements with respect to these states of one- and two-body operators.

We shall start our analysis by first discussing the symmetry group associated with the problem of n nucleons in an h.o. potential rather than interacting through two-body h.o. forces as in the previous section. The Hamiltonian is now

$$\bar{\mathscr{H}} = \sum_{i,s} \frac{1}{2m} (p_i^s)^2 + \tfrac{1}{2} m\omega^2 \sum_{i,s} (x_i^s)^2 \tag{7.1}$$

and, with the creation and annihilation operators defined as

$$\eta_i^s = \sqrt{\frac{m\omega}{2\hbar}}\, x_i^s - i \frac{1}{\sqrt{2m\hbar\omega}}\, p_i^s ; \quad \xi_i^s = \sqrt{\frac{m\omega}{2\hbar}}\, x_i^s + i \frac{1}{\sqrt{2m\hbar\omega}}\, p_i^s \tag{7.2a, b}$$

the dimensionless Hamiltonian could be written as

$$\mathscr{H} = \frac{1}{\hbar\omega} \bar{\mathscr{H}} - \frac{3}{2} n = \sum_{i,s} \eta_i^s \xi_i^s \tag{7.3}$$

The problem is then identical to the one discussed in the previous section except for the fact that $s = 1, \ldots, n$ stands now for the actual particle index and not for a Jacobi co-ordinate index.

We then restate for $\mathscr{H}$ of (7.3) the results we obtained in the previous section for the $\mathscr{H}$ defined there. The symmetry group is U_{3n} and the states could be further characterized by the $\mathscr{U}_3 \times U_n$ sub-group, with the generators of these groups being given by

$$C_{ij}^{st} = \eta_i^s \xi_j^t, \quad \mathscr{C}_{ij} = \sum_s C_{ij}^{ss}, \quad C^{st} = \sum_i C_{ii}^{st}. \tag{7.4a, b, c}$$

respectively. In the natural chain of sub-groups of $\mathscr{U}_3$ and U_n the states are described by the Gel'fand states of (6.15), which are in turn constructed from the highest weight state (6.16) by applying the usual lowering operators.

The physical chain of sub-groups includes as before

$$\mathscr{U}_3 \supset \mathcal{O}_3 \supset \mathcal{O}_2 \tag{7.5}$$

and the transformation of the states (6.15) to those associated with the chain (7.5) is again done by the transformation brackets (6.31).

The present problem differs from the one we discussed in the previous section only when we consider the physical chain of sub-groups associated with U_n. As the index s is now the particle index itself, the sub-group of U_n, with respect to which we would like to classify our states, is S_n, i.e. our chain has the form:

$$U_n \supset \ldots \supset S_n \tag{7.6}$$

We have not included as yet any definite group between U_n and S_n because we shall try to define this group in a way that its IR give information on the multi-shell structure of the state. We could obviously fit the group O_n between U_n and S_n but while this group provides indices for a classification scheme, it has no particular physical significance.

Before proceeding to derive the appropriate group to be included in the chain (7.6), we shall give a method for actually projecting out of the Gel'fand states (6.15), states that correspond to bases of an IR of the symmetric group S_n.

7.1. States with permutational symmetry

We would like to find linear combinations of the states (6.15), transformed to the $\mathscr{U}_3 \supset \mathcal{O}_3 \supset \mathcal{O}_2$ chain, that are characterized by an IR of S_n associated with the partition $f = [f_1 f_2 \ldots f_n]$ and that correspond to the row of the IR associated with the Yamanouchi symbol $(1 r_2 \ldots r_n)$. Assuming that the IR f of S_n is contained in the IR $[h_1 h_2 h_3 O^{n-3}]$ of U_n (which can be found by standard methods as discussed in detail in references [10] and [12]) we could obtain the states we are interested in by applying to the Gel'fand state

$$\left| \begin{array}{cccccccccc} h_1 & h_2 & h_3 & h_1 & h_2 & h_3 & 0 & \ldots & 0 & \\ \Omega & L & M & u_1 & u_2 & u_3 & 0 & \ldots & 0 & \\ & & & & & \vdots & & & & \\ & & & & & z_1 & & & & \end{array} \right\rangle \tag{7.7}$$

the projection operator

$$\frac{\ell_f}{n!} \sum_{p \in S_n} D^{f*}_{rr}(p) p \tag{7.8}$$

where ℓ_f is the dimension of the IR f of S_n, $D^f_{rr}(p)$ is a known IR of S_n characterized by f and r, and p is an arbitrary element of S_n. The partner functions associated with the same f but other r's could be obtained by an appropriate ladder procedure.

As the permutations p form a sub-group of the group U_n and are independent of the symmetry group $\mathscr{U}_3$ associated with the component index of the vectors, it is clear that we could apply the projection operator (7.8) to (7.7) if we knew the effect of p on a Gel'fand state in U_n, i.e. if we could determine the matrix elements of p in the development

$$p \left| \begin{matrix} h_1 & h_2 & h_3 & 0 & \dots & 0 \\ u_1 & u_2 & u_3 & 0 & \dots & 0 \\ & & \vdots & & & \\ & & z_1 & & & \end{matrix} \right\rangle$$

$$= \sum_{u',v',\dots z'} \left| \begin{matrix} h_1 & h_2 & h_3 & 0 & \dots & 0 \\ u_1' & u_2' & u_3' & 0 & \dots & 0 \\ & & \vdots & & & \\ & & z_1' & & & \end{matrix} \right\rangle \left\langle \begin{matrix} h_1 & h_2 & h_3 & 0 & \dots & 0 \\ u_1' & u_2' & u_3' & 0 & \dots & 0 \\ & & \vdots & & & \\ & & z_1' & & & \end{matrix} \right| p \left| \begin{matrix} h_1 & h_2 & h_3 & 0 & \dots & 0 \\ u_1 & u_2 & u_3 & 0 & \dots & 0 \\ & & \vdots & & & \\ & & z_1 & & & \end{matrix} \right\rangle \tag{7.9}$$

This problem is a particular case of determining the finite irreducible representations of the U_n group. In the same way that in the case of the R_3 group we have the irreducible representations of the infinitesimal transformations of the group, i.e. the matrices

$$\| \langle \ell m' | L_i | \ell m \rangle \| \tag{7.10a}$$

and irreducible representations for finite transformations, i.e.

$$\| \mathscr{D}^{\ell}_{mm'}(\alpha \beta f) \| \tag{7.10b}$$

we have for the unitary groups U_n the corresponding infinitesimal problem

$$\langle h'_{pq} | C^{st} | h_{pq} \rangle \tag{7.11a}$$

completely solved by Gel'fand and Zetlin, and the corresponding finite problem which does not seem to have been fully solved as yet.

It is easy to show, though, (see Ref. [15]) that the finite representations of U_n can be obtained in terms of the familiar finite IR of SU_2, i.e. (7.10b), and the matrix elements with respect to Gel'fand states of the permutations. As the permutations in turn can be decomposed into transpositions of neighbouring number, i.e. $(p-1, p)$, and as these are elements of U_p, it is clear that we could give a full solution to our problem if for any n we could get the matrix element of the transposition

$$\left\langle \begin{matrix} h_1 & h_2 & h_3 & 0 & \dots & 0 \\ u_1' & u_2' & u_3' & 0 & \dots & 0 \\ & & \vdots & & & \\ & & z_1' & & & \end{matrix} \right| (n-1, n) \left| \begin{matrix} h_1 & h_2 & h_3 & 0 & \dots & 0 \\ u_1 & u_2 & u_3 & 0 & \dots & 0 \\ & & \vdots & & & \\ & & z_1 & & & \end{matrix} \right\rangle \tag{7.11b}$$

with respect to Gel'fand states of U_n.

For n = 2 this is trivial, while for n = 3 it already represents a rather complicated problem which was solved in Ref. [15]. The result turns out to be given in terms of a Racah coefficient and it is presented here for the sake of reference:

$$\left\langle \begin{matrix} h_1 & h_2 & h_3 \\ u_1' & u_2' & \\ v_1' & & \end{matrix} \middle| (2,3) \middle| \begin{matrix} h_1 & h_2 & h_3 \\ u_1 & u_2 & \\ v_1 & & \end{matrix} \right\rangle$$

$$= (-1)^{h_3}\, \delta_{v_1' v_1}\, \delta_{u_1' + u_2' - v_1',\ h_1 + h_2 + h_3 - u_1 - u_2}\, [(u_1 - u_2 + 1)(u_1' - u_2' + 1)]^{\frac{1}{2}} \times W(abcd; ef)$$

$$\begin{aligned} a &= \tfrac{1}{2}(h_1 - u_1' + h_2 - u_2') \\ b &= \tfrac{1}{2}(v_1 - u_2 + h_2 - u_2') \\ c &= \tfrac{1}{2}(u_1' - v_1 + u_1 - h_2) \\ d &= \tfrac{1}{2}(u_1' - v_1 + u_2' - h_3) \\ e &= \tfrac{1}{2}(h_1 - u_1' + v_1 - u_2) \\ f &= \tfrac{1}{2}(h_1 - u_1 + v_1 - u_2') \end{aligned} \qquad (7.12)$$

Once the explicit result of the type (7.12) is extended to the general matrix element (7.11b), we are in a position to project states with given permutational symmetry out of Gel'fand states. We would, however, have the problem that as soon as the number of quanta $N = h_1 + h_2 + h_3$ starts to increase, the IR of S_n of definite f in a given IR of U_n repeat themselves, and so we have to find a procedure for distinguishing between them. For this purpose it is important to get an intermediate group between U_n and S_n, whose IR could, at least partially, distinguish between the repeated IR of S_n in U_n. In view of the success of the shell model, we would also like to see if this intermediate group could in some way be related to the shell structure.

7.2. Chain of groups associated with a multi-shell structure

The Gel'fand states (7.7) are eigenstates of the set of generators C^{ss}, $s = 1, \ldots n$ with the set of eigenvalues

$$(w^1, \ldots \ w^n) \qquad (7.13)$$

which constitute precisely the weight of the state in U_n. Each eigenvalue w^s, which is a non-negative integer number, tells us that particle s in the state (7.7) has w^s quanta. Therefore, the weight (7.13) is actually giving us some information on the multi-shell structure of the Gel'fand state. For a given $N = h_1 + h_2 + h_3$ each w^s may take some value in the interval

$$w_s = 0, 1, 2, 3, 4, 5, \ldots N \qquad (7.14)$$

If we count the number of times each value in this interval appears, we would have the number of particles in each energy level of the h.o. for the Gel'fand state in question. For example, if in the same order as in (7.14) we put the number of times the corresponding value of w^s appears as

$$3,\ 1,\ 2,\ 0,\ 1,\ 0,\ \ldots,\ 0 \tag{7.15}$$

then this means that we have 3 particles in the 1s shell, 1 particle in the p shell, 2 particles in the 2s-1d shell, 0 in the 2p-1f shell, 1 in the 3s-2d-1g shell, 0 in the 3p-2f-1h shell, etc.

Clearly the shell structure is related to the eigenvalues of the set of generators $(C^{11}, \ldots, C^{nn})$. This set must correspond to the generators of some sub-group of U_n as the operators C^{ss} are closed under commutation and, in fact, the sub-group must be abelian as the C^{ss} commute. Which sub-group is this?

The question is easily answered by considering the set of all diagonal unitary transformations, i.e.

$$\begin{pmatrix} x_1' \\ x_2' \\ \vdots \\ x_n' \end{pmatrix} = \begin{pmatrix} e^{i\varphi_1} & 0 & \ldots & 0 \\ 0 & e^{i\varphi_2} & \ldots & 0 \\ \vdots & \vdots & & \\ 0 & 0 & \ldots & e^{i\varphi_n} \end{pmatrix} \begin{pmatrix} x_1 \\ x_2 \\ \vdots \\ x_n \end{pmatrix} \tag{7.16}$$

The matrices associated with infinitesimal transformations of this type are of the form

$$\begin{pmatrix} 1+i\varphi_1 & 0 & \ldots & 0 \\ 0 & 1+i\varphi_2 & \ldots & 0 \\ \vdots & \vdots & & \vdots \\ 0 & 0 & & 1+i\varphi_n \end{pmatrix} \tag{7.17}$$

and so if we take all φ's as zero except φ_s, we get the corresponding operator

$$\check{C}^{ss} = x_s \frac{\partial}{\partial x_s} \tag{7.18}$$

as a generator of the group. As these operators are clearly equivalent to our previous C^{ss}, we conclude that the C^{ss}, $s = 1, \ldots, n$ are the generators of the n-dimensional abelian sub-group of U_n, consisting of all diagonal unitary matrices. We shall designate this sub-group as A_n and an arbitrary element of it as a.

Clearly then the sub-group A_n must in some way figure in our chain of groups (7.6) if we want to have a multi-shell structure for our states. We cannot, however, naively introduce A_n between U_n and S_n, as A_n does not contain S_n and in fact has only the unit element in common with it. We note that A_n is actually too restricted to characterize the multi-shell structure of our state as the eigenvalues of the C^{ss} not only tell us how many particles there are in each shell but identify these particles explicit-

ly. This suggests then that we extend the A_n sub-group in such a way that it also includes the permutation group, so that while we could still have information on a definite number of particles in each shell, we no longer identify the particles explicitly.

The extension can be made by considering the semi-direct product

$$A_n \wedge S_n \equiv K_n \tag{7.19}$$

which is then the group whose elements are all of the type

$$a\,p \tag{7.20}$$

where $a \in A_n$ and $p \in S_n$. The first question is to see if this is a group, i.e. if

$$(ap)(a'p') = a''p'' \tag{7.21}$$

This is easily proved by noting that

$$p^{-1}ap = \bar{a} \tag{7.22}$$

where $\bar{a}$ is the diagonal unitary matrix whose elements are permuted by p. For example, if n = 2

$$(1,2)^{-1}\begin{pmatrix} e^{i\varphi_1} & 0 \\ 0 & e^{i\varphi_2} \end{pmatrix}(1,2) = \begin{pmatrix} 0 & 1 \\ 1 & 0 \end{pmatrix}\begin{pmatrix} e^{i\varphi_1} & 0 \\ 0 & e^{i\varphi_2} \end{pmatrix}\begin{pmatrix} 0 & 1 \\ 1 & 0 \end{pmatrix} = \begin{pmatrix} e^{i\varphi_2} & 0 \\ 0 & e^{i\varphi_1} \end{pmatrix} \tag{7.23}$$

We can then write

$$(ap)(a'p') = a(pa'p^{-1})pp' = (a\bar{a}')(pp') \tag{7.24}$$

thus proving that the elements (7.20) form a group, as we could also use (7.24) to find the inverse of any element as well as the unit element.

The group (7.19) is a semi-direct product as from (7.22), A_n is an invariant sub-group of K_n and, as mentioned before, A_n and S_n have only the unit element in common. As K_n contains S_n as a sub-group we clearly can now introduce the chain

$$U_n \supset K_n \supset S_n \tag{7.25}$$

where the presence of A_n in K_n will serve to characterize the states classified by the IR of the groups in the chain (7.25) by their multi-shell structure.

As is well known from the work of many authors and particularly of MacIntosh (J. mol. Spectry. 5 (1960) 269; ibid. 10 (1963) 51) the IR of a semi-direct product can be fully determined from the knowledge of the IR of its component groups. Using these results, Kramer (J. math. Phys., in the press) has fully discussed the IR of K_n and their reduction

under S_n as well as the reduction of the IR of U_n under K_n. An application of this analysis has been given in the previously quoted reference of Kramer and Moshinsky for the 3-particle multi-shell states. Extension of this work to more particles is in progress.

We could say that a definite group-theoretical procedure is available for the construction of n particle h.o. states which have a shell structure and specific permutational symmetry. These states are furthermore classified by the $\mathscr{U}_3$ group in orbital space, so they are eigenfunctions of the quadrupole-quadrupole (Q^2) interaction. When combined with the appropriate spin-isospin wave function (which will have the same structure as in the last section), these states will satisfy the Pauli principle and could serve as starting points of more detailed calculations, having the advantage that they already include the correlations associated with long range, i.e. Q^2 interactions as well as a definite multi-shell structure.

8. THE HARMONIC OSCILLATOR AND CLUSTERING

In the previous section we showed how the states of n particles in an h.o. potential classified by an appropriate chain of sub-groups of the fundamental group U_{3n} exhibit a shell model structure. In this section we shall illustrate, through the analysis of the four-nucleon problem, the possibility of clustering effects in the h.o. states, and some consequences of these properties. A more extensive and detailed discussion of this problem is given in Ref. [12] as well as in papers in preparation.

One great advantage of the harmonic oscillator model is that the co-ordinates could be defined in a variety of ways without changing the form of what we called, in section 6, the auxiliary Hamiltonian. For the four-nucleon problem we could, for example, rather than use the relative co-ordinates $\dot{x}_i^s$ defined there, introduce the co-ordinates

$$\begin{aligned}
\ddot{\vec{x}}^1 &= \frac{1}{\sqrt{2}}(\vec{x}^1 - \vec{x}^2) \\
\ddot{\vec{x}}^2 &= \frac{1}{\sqrt{2}}(\vec{x}^3 - \vec{x}^4) \\
\ddot{\vec{x}}^3 &= \tfrac{1}{2}(\vec{x}^1 + \vec{x}^2 - \vec{x}^3 - \vec{x}^4) \\
\ddot{\vec{x}}^4 &= \tfrac{1}{2}(\vec{x}^1 + \vec{x}^2 + \vec{x}^3 + \vec{x}^4)
\end{aligned} \tag{8.1}$$

Eliminating the spurious states associated with centre-of-mass motion, i.e. limiting ourselves to states of zero quanta in the co-ordinate $\ddot{\vec{x}}^4$, we find that the orbital states characterized by the chain of groups

$$\mathscr{U}_3 \supset \mathcal{O}_3 \supset \mathcal{O}_2, \quad U_4 \supset U_3 \supset U_2 \supset U_1 \tag{8.2}$$

are represented by

$$\left\langle \ddot{\vec{x}}^1 \ddot{\vec{x}}^2 \ddot{\vec{x}}^3 \;\middle|\; \begin{matrix} [h_1\ h_2\ h_3] \\ \Omega\ \ L\ \ M \end{matrix} ; \begin{matrix} h_1 & h_2 & h_3 \\ & u_1 & u_2 \\ & v_1 & \end{matrix} \right\rangle \tag{8.3}$$

where here we use the full Dirac notation and indicate the variables $\vec{\vec{x}}^s$, $s = 1, 2, 3$, because we want to distinguish these states from those in which the variables are $\vec{x}^s$ or $\vec{\vec{x}}^s$. Furthermore, we suppressed the redundant

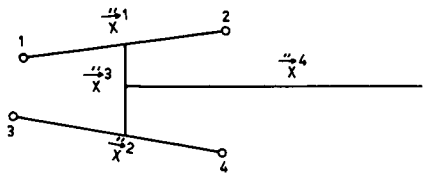

FIG. 9. Dependence of the states (8.3) on the co-ordinates

extra line giving the IR $[h_1 h_2 h_3 0]$ of U_4. The partition $[h_1 h_2 h_3]$ giving the IR of U_3 is a partition of the number of quanta N. The states (8.3) depend on the co-ordinates represented diagrammatically in Fig. 9.

8.1. Definition of clustering

We could, in terms of the co-ordinates in Fig. 9, give the following definition of clustered states: The states (8.3) represent a set of 4 particles clustered in two sets of two particles each, if there is no internal excitation of the clusters, i.e. if the number of quanta associated with co-ordinates $\vec{\vec{x}}^1$ and $\vec{\vec{x}}^2$ is zero. Now, from the properties of Gel'fand states, it is very easy to see that the states (8.3) are clustered according to the above definition only if $v_1 = 0$ and $u_1 + u_2 - v_1 = 0$, but because of the inequality $u_1 \geq v_1 \geq u_2$ this implies $u_1 = u_2 = v_1 = 0$, which in turn leads to $h_2 = h_3 = 0$, $h_1 = N$.

Therefore, from our definition of a two-cluster (of two particles each) state, it is clear that only states

$$\left\langle \vec{\vec{x}}^1 \vec{\vec{x}}^2 \vec{\vec{x}}^3 \left| \begin{matrix} [N] \\ L\,M \end{matrix} ; \begin{matrix} N & 0 & 0 \\ 0 & 0 & \\ & 0 & \end{matrix} \right\rangle \equiv \left| \begin{matrix} [N] \\ L\,M \end{matrix} ; (2)(2) \right\rangle \tag{8.4}$$

have this type of clustering. We use for these states the shorthand notation of the right-hand side where each parenthesis indicates one cluster as well as the number of particles in it.

In section 6 we discussed the complete set of states for a system of four nucleons, in terms of the co-ordinates $\vec{\vec{x}}^s$, $s = 1, 2, 3$ of (6.2), for the chain of groups

$$\mathscr{U}_3 \supset \mathscr{O}_3 \supset \mathscr{O}_2,\ U_4 \supset U_3 \supset O_3 \supset D^{(3,1)}(S_4) \tag{8.5}$$

We showed in Ref. [10] how we can express these states as linear combinations of the corresponding states in terms of the co-ordinates $\vec{\vec{x}}^s$. A complete set of states characterized by the chain (8.5) is then also given by

$$\left\langle \vec{\vec{x}}^1 \vec{\vec{x}}^2 \vec{\vec{x}}^3 \left| \begin{matrix} [h_1 h_2 h_3] \\ \Omega\ L\ M \end{matrix} ; \varphi \lambda \chi \mathrm{fr} \right\rangle \tag{8.6}$$

From the scalar product of (8.6) and (8.4) we could estimate the degree of clustering in these general states. This, however, would be a measure of a kind of naive clustering, as (8.4) actually specifies that particle 1, 2 form one cluster and 3, 4 form another. We would like to be able to analyse the degree of clustering without specification to the particles involved in each cluster.

For this purpose we shall introduce a cluster projection operator defined for the (2)(2) case by

$$\mathscr{P}^{(2)(2)} \equiv \frac{1}{2!\,2!} \sum_{\bar{N}\bar{L}\bar{M}} \sum_{p} p^{-1} \left| \begin{matrix} [\bar{N}] \\ \bar{L}\,\bar{M} \end{matrix} ; (2)(2) \right\rangle \left\langle \begin{matrix} [\bar{N}] \\ \bar{L}\,\bar{M} \end{matrix} ; (2)(2) \right| p \qquad (8.7)$$

where p is an arbitrary permutation of the four particles and the 2! take into account the exchange of particles within the cluster. This operator will project from the states (8.6) (or of any linear combination of them that represents a physical situation as, for example, in the ground state of the α particle discussed in section 6) the part that has two clusters of two particles each, irrespective of the intercluster excitation or of the enumeration of the particles in each cluster.

To see this point more clearly, let us analyse in detail the expectation value of the operator (8.7) with respect to the states (8.6). For this purpose we first note that the application of a permutation p to the state (8.6) gives

$$p \left\langle \vec{x}^{s} \left| \begin{matrix} [h_1 h_2 h_3] \\ \Omega\ L\ M \end{matrix} ; \varphi\lambda\chi f r \right\rangle = \sum_{r'} \left\langle \vec{x}^{s} \left| \begin{matrix} [h_1 h_2 h_3] \\ \Omega\ L\ M \end{matrix} ; \varphi\lambda\chi f r' \right\rangle D^{f}_{r'r}(p) \right. \qquad (8.8)$$

where $D^{f}_{r'r}(p)$ is the IR of S_4 characterized by f. Using the orthonormality properties of these IR, we easily conclude that

$$\left\langle \begin{matrix} [h_1 h_2 h_3] \\ \Omega\ L\ M \end{matrix} ; \varphi\lambda\chi f r \right| \mathscr{P}^{(2)(2)} \left| \begin{matrix} [h_1 h_2 h_3] \\ \Omega\ L\ M \end{matrix} ; \varphi\lambda\chi f r \right\rangle$$

$$= \frac{4!}{2!\,2!} \frac{1}{|f|} \sum_{r'} \sum_{\bar{N}\bar{L}\bar{M}} \left| \left\langle \begin{matrix} [h_1 h_2 h_3] \\ \Omega\ L\ M \end{matrix} ; \varphi\lambda\chi f r' \right| \begin{matrix} [\bar{N}] \\ \bar{L}\,\bar{M} \end{matrix} ; (2)(2) \right\rangle \Bigg|^2 \qquad (8.9)$$

where |f| is the dimension of the IR of S_4. Clearly (8.9) is zero unless $[h_1 h_2 h_3] = [N\,0\,0]$ and in this case, it reduces to

$$\frac{4!}{2!\,2!} \frac{1}{|f|} \sum_{r'} \left| \left\langle \begin{matrix} [N] \\ L\,M \end{matrix} ; \lambda\chi f r' \right| \begin{matrix} [N] \\ L\,M \end{matrix} ; (2)(2) \right\rangle \Bigg|^2 \qquad (8.10)$$

so that, as before, clustering is present only in states of a single row and the degree of clustering for each state of this type is given by the non-negative value (8.10).

As the operator (8.7) is hermitian and its expectation value for any state is non-negative, we can also reach the conclusion that the eigenstate of $\mathscr{P}^{(2)(2)}$ of maximum eigenvalue has the maximum possible clustering. This can be seen as follows: First all eigenvalues of $\mathscr{P}^{(2)(2)}$ are non-negative, because if the state $|\rho\rangle$ corresponds to the eigenvalue ρ then

$$0 \leqslant \langle\rho|\mathscr{P}^{(2)(2)}|\rho\rangle = \rho \tag{8.11}$$

and so ρ is non-negative. Any normalized state $|\psi\rangle$ can be expanded in terms of states $|\rho\rangle$ as

$$|\psi\rangle = \sum_{\rho} |\rho\rangle\langle\rho|\psi\rangle, \quad \text{where} \quad \sum_{\rho} |\langle\rho|\psi\rangle|^2 = 1 \tag{8.12}$$

Then the expectation value

$$\langle\psi|\mathscr{P}^{(2)(2)}|\psi\rangle = \sum_{\rho} \rho|\langle\rho|\psi\rangle|^2$$

$$\leqslant \rho_{\max} \sum_{\rho} |\langle\rho|\psi\rangle|^2 = \rho_{\max} \tag{8.13}$$

thus proving our assertion.

If we have a set of states (8.6), the matrix elements of $\mathscr{P}^{(2)(2)}$ with respect to this set could be obtained in a way very similar to (8.9), so that they would be zero unless $[h_1h_2h_3] = [N\,0\,0]$ and have the same [N], L, M, f, r in bra and ket. The matrix associated with the operator $\mathscr{P}^{(2)(2)}$ breaks into finite blocks of at most $\frac{1}{2}(N+1)(N+2)$ dimensions. The diagonalization of these blocks provides us with the eigenstates of $\mathscr{P}^{(2)(2)}$ associated with definite [N], f, r (they are independent of L, M) among which the one corresponding to the maximum eigenvalue ($\rho_{\max}$) has the largest clustering.

This $\rho_{\max}$ can be easily obtained without even the need of determining explicitly all the matrix elements in the corresponding matrix associated with [N]f, as is shown in Ref. [12]. For f = [4] this $\rho_{\max}$ is given as function of N in Fig. 10. Only for even N it is different from zero and takes the values indicated by the circles. For N = 0 the $\rho_{\max}$ is clearly given by the geometrical factor

$$\frac{4!}{2!\,2!} = \binom{4}{2} = 6 \tag{8.14}$$

concerned with the number of ways we can distribute 4 particles in sets of two, as the number of quanta in the relative motion of any pair of particles is zero. For any other N, the maximum eigenvalue of $\mathscr{P}^{(2)(2)}$ must be lower and, in fact, is given by 2.

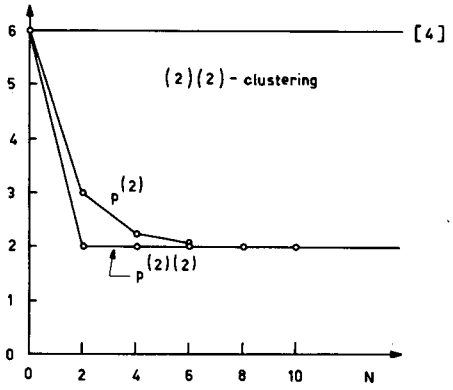

FIG. 10. Maximum eigenvalue of the cluster projection operator $\mathcal{P}^{(2)(2)}$ and of the clustering interaction $\mathcal{P}^{(2)}$ as functions of the number N of quanta for f = [4]

8.2. Clustering interaction

The above definition of clustered state, for a four-nucleon system into sets of two particles each, suggests a two-particle interaction $\mathscr{P}^{(2)}$, which has matrix elements different from zero only when the number of quanta in the relative co-ordinates between the two particles is zero, i.e.

$$\langle \nu' \ell' m' | \mathscr{P}^{(2)} | \nu \ell m \rangle = \delta_{\nu' 0}\, \delta_{\ell' 0}\, \delta_{m' 0}\, \delta_{\nu 0}\, \delta_{\ell 0}\, \delta_{m 0} \tag{8.15}$$

where

$$| \nu \ell m \rangle \equiv \left\langle \frac{1}{\sqrt{2}} (\vec{x}^1 - \vec{x}^2) \right| \nu \ell m \rangle \tag{8.16}$$

The interaction $\mathscr{P}^{(2)}$ is fully defined by (8.15) if we limit its application to harmonic oscillator states.

It is intuitively clear, and has also been checked explicitly for the four-nucleon system, that the eigenstates of $\mathscr{P}^{(2)}$, associated with the maximum eigenvalue of $\mathscr{P}^{(2)}$, show a large amount of clustering. For f = [4] we give (also in Fig. 10), the maximum eigenvalues of $\mathscr{P}^{(2)}$ as function of N. Again only for even N it is different from zero, and it approaches the value 2 for $N \to \infty$, indicating that for well separated clusters it is equal to the number of internal pairs. For even values of N closer to N = 0, the eigenvalue of $\mathscr{P}^{(2)}$ is higher than 2 due to cluster overlap. This is also shown in Fig. 10.

The clustering interaction $\mathscr{P}^{(2)}$ is, from its definition, a short-range interaction that commutes with the long-range quadrupole-quadrupole (Q^2) interaction discussed previously, since the former is clearly associated with the U_n group while the latter is associated with $\mathscr{U}_3$. A linear combination of them can therefore be exactly diagonalized, and was used by Kramer (Ref. [16]) to discuss the binding energies of nuclei in the 1s and 1p shells.

We have tried in this section to give a brief outline of the problem of clustering for harmonic oscillator states, using their group theoretical classification schemes. Even for the four-nucleon problem there are types of clustering we have not discussed here as, for example, $\mathscr{P}^{(3)(1)}$,

in which we have two clusters of 3 and 1 particles, respectively. For this problem, and for the general analysis of clustering in n particle states, as well as for overlap between different types of clustering, etc., we refer the reader to Ref.[12].

9. SUMMARY AND CONCLUSION

In this Chapter we have tried to outline how modern group theoretical methods can be used systematically in the analysis of the n nucleon problems associated with the understanding of nuclear structure. These methods can be implemented both in the second quantized picture and in the ordinary configuration and spin-isospin space of the particles involved. In the first case the Hamiltonian was expressed in terms of the generators of a certain fundamental group, and the states were characterized by the IR of sub-groups of this group. Explicit procedures were given for the determination both of these states, and of the matrix elements of physical interactions with respect to them, leading finally to the determination of energy levels and eigenstates.

In the second case the configuration part of the state was described in terms of h.o. states, to make full use of the symmetry group associated with them. We saw that this allowed us to discuss in detail a few nucleon problems, shell model states and clustering effects.

This Chapter merely constitutes an introduction to the subject. It is the belief of the author that group theoretical methods can be developed much further and that they will play an increasingly important role in our understanding both of nuclear structure and of many other fields of physics.

ACKNOWLEDGEMENTS

This Chapter, compiled from lecture notes, is based for the most part on material published either in journals or review books given in the reference list. Rather than reproduce the published information again, it seemed convenient to present the material from the fresher viewpoint of the note-takers. The lecturer has checked the notes for scientific accuracy and overall coherence, but has not attempted to change the style of the individual note-takers. He would like to express his thanks for their very effective collaboration. The lecture notes were taken by:

J. A. De Raedt (Louvain, Belgium)
M. Iosifescu (Bucharest, Romania)
S. B. Khadkikar (Bombay, India)
A. Maciel (Porto Alegre, Brazil)
F. Stancu (Bucharest, Romania)

Coordinator:

S. Ali (Dacca, Pakistan)

The lecturer would like also to thank Dr. P. Kramer for his collaboration in the development of the material of the last sections.

REFERENCES

The present list of references includes only papers by the lecturer or his collaborators. The reader will find in these references an extensive bibliography on the work of other authors. Some very important or specific references to other work were also given in the text of the Chapter.

[1] MOSHINSKY, M., Group Theory and the Many Body Problems and Other Selected Topics of Theoretical Physics, Lecture notes of the 1965 Latin American School of Physics (MOSHINSKY, M., BRODY, T. A., JACOB, G., Eds) Gordon and Breach, New York (1966) 289-377.
[2] NAGEL, J., MOSHINSKY, M., J. math. Phys. 6 (1965) 682.
[3] FLORES, J., CHACON, E., MELLO, P. A., DE LLANO, M., Nucl. Phys. 72 (1965) 352.
[4] DE LLANO, M., MELLO, P. A., CHACON, E., FLORES, J., Nucl. Phys. 72 (1965) 379.
[5] KUSHNER, M., QUINTANILLA, J., Phys. Lett. 23 (1966) 572.
[6] MOSHINSKY, M., BERRONDO, M., PINEDA, J., Second Symposium on the Structure of Low-Medium Mass Nuclei, published by the University of Kansas (GOLDHAMMER, P., Ed.) 129-94.
[7] CHACON, E., DE LLANO, M., Revta mex. Fís. 13 (1964) 87.
[8] FLORES, J., MOSHINSKY, M., Nucl. Phys. A93 (1967) 81.
[9] MOSHINSKY, M., J. math. Phys. 4 (1963) 1128.
[10] KRAMER, P., MOSHINSKY, M., Nucl. Phys. 82 (1966) 241.
[11] MOSHINSKY, M., J. math. Phys. 7 (1966) 691.
[12] KRAMER, P., MOSHINSKY, M., Group Theory of Harmonic Oscillators and Nuclear Structure in Group Theory and Applications (LOEBL, E.M., Ed.) Academic Press (to appear in 1967).
[13] KRAMER, P., MOSHINSKY, M., Phys. Lett. 23 (1966) 574.
[14] BRODY, T. A., MOSHINSKY, M., Tables of Transformation Brackets, Monografías del Instituto de Física, Universidad de México (1960).
[15] CHACON, E., MOSHINSKY, M., Phys. Lett. 23 (1966) 567.
[16] KRAMER, P., Phys. Lett. 21 (1966) 182.

CHAPTER 13

Selected topics in theoretical nuclear physics

SHELL-MODEL DESCRIPTION OF NUCLEAR REACTIONS

K. DIETRICH

My aim is to give an introduction to the shell-model description of nuclear reactions, i.e. to a formulation of the dynamical theory in which the shell model is explicitly used from the outset, as a lowest order approximation to the scattering.

As a consequence, this theory is restricted to situations in which an independent particle approach makes sense in contrast to the general dynamical theory of reactions as developed by Feshbach [1].

Motivated by the success of the shell model in the theory of nuclear structure, several authors [2-8] incorporated this picture into the formulation of the reaction mechanism. Here the procedure of Weidenmüller [7, 8] is followed. It is based on a method devised by Fano [9] for the case of electron scattering by atoms, and is very similar to the formulation given by C. Bloch and V. Gillet [3].

Firstly, the basic formalism is introduced (section 1) and then, as a simple situation, the case of one doorway state embedded in one continuum is treated (sections 2.1, 2.2). This leads to the discussion of simultaneous occurrence of shell-model resonances and compound nucleus resonances (section 2.2).

In section 2.3 the method of proceeding in a general case is shown.

A generalization of the formalism is made so as to include direct reactions (section 3) and the scattering of light projectiles (section 4). In section 3, one is confronted with the rather cumbersome problem of a diagonalization of the Hamiltonian in the subspace of continuous shell-model states. In section 5, a method which seems to be well suited for a practical solution of this task is discussed.

The work here described is closely related to that of Chapter 9.

The author is at the Institute for Theoretical Physics, University of Heidelberg, Federal Republic of Germany.

1. THE GENERAL FORMALISM

We are to find a stationary scattering solution $\Psi_{\alpha E}$ of the total Hamiltonian H which contains, apart from an ingoing wave in channel α, only outgoing waves in all open channels.

$$H\Psi_{\alpha E} = E\Psi_{\alpha E} \tag{1.1}$$

We write the total Hamiltonian as a sum of a shell-model Hamiltonian H_0

$$H_0 = \sum_{i=1}^{A} T(i) + \sum_{i=1}^{A} U(i) \tag{1.2}$$

and the residual interactions V

$$V = \sum_{i<j}^{A} v(i,j) - \sum_{i=1}^{A} U(i) \tag{1.3}$$

where U(i) represents a finite shell-model potential. Therefore, the Hamiltonian H_0 has discrete and continuous eigenfunctions, ϕ_i and $\phi_{\beta E}$

$$H_0 \phi_i = \epsilon_i \phi_i$$

$$H_0 \phi_{\lambda\epsilon} = (E_\lambda + \epsilon)\, \phi_{\lambda\epsilon} \tag{1.4}$$

For the time being, we restrict ourselves to continuous eigenfunctions with only one nucleon in the continuum. ϵ is the kinetic energy of this nucleon and E_λ the threshold energy which corresponds to the shell-model state. $\phi_{\lambda\epsilon} \cdot \lambda$ is the set of discrete quantum numbers which, apart from the continuous energy ϵ, are necessary to specify a given shell-model state.

It is convenient to choose the energy scale in such a way that the threshold energy E_1 of the elastic channel is zero

$$E_1 = 0 \tag{1.5}$$

We have to define the asymptotic behaviour of the continuous shell-model wave functions. It is convenient to use standing wave boundary conditions:

$$\phi_{\lambda\epsilon} \xrightarrow[r\to\infty]{} Q_\lambda \frac{\sin(k_\lambda r - \frac{l_\lambda \pi}{2} + \delta_\lambda)}{r} \tag{1.6}$$

Here, $k_\lambda^2 = \epsilon$ is the kinetic energy in channel λ, the quantity r is the radial co-ordinate of one of the A nucleons, l_λ and δ_λ are the angular momentum and the potential scattering phase shift in channel λ, and Q_λ is the remainder of the A-particle wave function. It can be shown that with the asymptotic behaviour (1.6) and appropriate phase conventions all matrix elements of the Hamiltonian H (see Ref. [7]) become real. If the shell model is to be a reasonable lowest-order approximation, it

will be convenient to expand the total state $\Psi_{\alpha E}$ in terms of shell-model states

$$\Psi_{\alpha E} = \sum_i \phi_i \, b(i) + \sum_{\lambda'} \int d\epsilon' \, \phi_{\lambda'\epsilon'} a(\lambda'\epsilon') \tag{1.7}$$

and rewrite the Schrödinger equation (1.1) in terms of a set of equations for the coefficients b(i), $a(\lambda'\epsilon')$. These coefficients depend, of course, on the entrance channel α, E: $b_{\alpha E}(i)$, $a_{\alpha E}(\lambda\epsilon)$. We shall, in general, omit these indices in order to keep the notation simple.

The system of equations for the coefficients b(i) and $a(\lambda'\epsilon')$ is easily seen to be of the following form:

$$\sum_i V_{ji} \, b(i) - Eb(j) + \sum_{\lambda'} \int d\epsilon' \, V_{j,\lambda'\epsilon'} \, a(\lambda'\epsilon') = 0 \tag{1.8}$$

$$\sum_i V_{\lambda\epsilon,i} \, b(i) + \sum_{\lambda'} \int d\epsilon' \, V_{\lambda\epsilon,\lambda'\epsilon'} \, a(\lambda'\epsilon') - Ea(\lambda,\epsilon) = 0 \tag{1.9}$$

The matrix elements $V_{\mu\nu}$ are all real and symmetric, as a consequence of our boundary conditions (1.6), and are defined as follows:

$$\begin{aligned} V_{ji} &= \langle \phi_j | H | \phi_i \rangle \\ V_{\lambda\epsilon,i} &= \langle \phi_{\lambda\epsilon} | H | \phi_i \rangle \\ V_{\lambda\epsilon,\lambda'\epsilon'} &= \langle \phi_{\lambda\epsilon} | H | \phi_{\lambda'\epsilon'} \rangle \end{aligned} \tag{1.10}$$

For the sake of simplicity, we shall assume that the Hamiltonian H is diagonal in the subspace of continuous shell-model states:

$$V_{\lambda\epsilon,\lambda'\epsilon'} = V_{\lambda\epsilon\lambda\epsilon} \, \delta_{\lambda\lambda'} \, \delta(\epsilon-\epsilon') = E_{\lambda\epsilon} \, \delta_{\lambda\lambda'} \, \delta(\epsilon-\epsilon') \tag{1.11}$$

Thereby we exclude the possibility of "direct reactions". We shall see later on (section 3) that it requires only a slight formal device to include such transitions.

Furthermore, it elucidates the physical content if we distinguish between two classes of bound shell-model states ϕ_i. States ϕ_i which are directly coupled to continuum states ($V_{i,\lambda\epsilon} \neq 0$) will be called doorway states (DWS)[1]. The other and more complicated shell-model states (MCS) have vanishing transition elements to the continuum: ($V_{i,\lambda\epsilon} = 0$).

Among the N bound shell-model configurations there will be $M \ll N$ such doorway states which we choose to label by i = 1, ..., M. The DWS are embedded in the continuum and the system has to pass through them whenever a compound state is formed. So we expect them to be intimately connected with the occurrence of compound nuclear resonances.

[1] For a detailed discussion of the DWS concept see Ref.[10].

With the assumption (1.11) and the distinction between DWS and MCS, the equations (1.8) and (1.9) will have the form:

$$\sum_{i=1}^{N} V_{ji}\ b(i) - Eb(j) + \sum_{\lambda'} \int d\epsilon'\, V_{j,\lambda'\epsilon'}\, a(\lambda'\epsilon') = 0 \quad (\text{for } j = 1 \ldots M) \tag{1.12}$$

$$\sum_{i=1}^{N} V_{ji}\ b(i) - Eb(j) = 0 \quad (\text{for } j = M+1, \ldots, N) \tag{1.13}$$

$$\sum_{i=1}^{M} V_{\lambda\epsilon, i}\ b(i) + (E_{\lambda\epsilon} - E)\, a(\lambda, \epsilon) = 0 \tag{1.14}$$

We now have to discuss the solution of the set of equations (1.12) to (1.14). If we want to discuss the formation of compound states, it is convenient to first eliminate the coefficients $a(\lambda, \epsilon)$ and then discuss the resulting finite set of equations for b(i): If we eliminate $a(\lambda, \epsilon)$ from (1.14), the division is not defined for $E = E_{\lambda\epsilon}$. We choose to define it by the principal value and retain the full generality by adding an arbitrary function $Z_\lambda(E)$ at $E = E_{\lambda\epsilon}$ (see Refs. [9, 11])

$$a(\lambda, \epsilon) = \left\{ P\left(\frac{1}{E - E_{\lambda\epsilon}}\right) + Z_\lambda(E)\, \delta(E - E_{\lambda\epsilon}) \right\} \cdot \sum_{i=1}^{M} V_{\lambda\epsilon, i}\ b(i) \tag{1.15}$$

We shall see that the functions $Z_\lambda(E)$ are determined by the asymptotic behaviour of $\Psi_{\alpha E}$ and the condition of a non-trivial solution to the equations (1.12) to (1.14).

Substituting (1.15) in (1.12) we obtain a set of N linear homogeneous equations for the coefficients b(i):

$$\sum_{i=1}^{N} v_{ji}\ b(i) = 0 \tag{1.16}$$

with

$$v_{ji} = V_{ji} - \delta_{ji}\, E + \sum_{\lambda'} \left[F_{ji}^{\lambda'} + Z_{\lambda'}(E) G_{ji}^{\lambda'} \right] \tag{1.16a}$$

$$F_{ji}^{\lambda'}(E) = P \int \frac{V_{j,\lambda'\epsilon'}\, V_{\lambda'\epsilon', i}}{E - E_{\lambda'\epsilon'}}\, d\epsilon' \tag{1.17}$$

$$G_{ji}^{\lambda'}(E) = V_{j,\lambda' E}\ V_{i,\lambda' E}\ \theta(E - E_{\lambda'}) \tag{1.18}$$

(E_λ = threshold energy for the shell-model continuum λ). The quantities F^λ_{ji} and G^λ_{ji} are, of course, only $\neq 0$ if $i,j<M$. A non-trivial solution will only be obtained if

$$\det \{ v_{ij} \} = 0 \tag{1.19}$$

which yields a condition for the functions $Z_\lambda(E)$. Our final purpose is to find the S-matrix $S_{\lambda\alpha}$ which is defined as the quotient of the amplitudes of outgoing and incoming waves:

$$S_{\lambda\alpha} = \frac{\text{amplitude of outgoing wave in channel } \lambda}{\text{amplitude of ingoing wave in channel } \alpha} \tag{1.20}$$

In order to obtain the amplitudes of outgoing and incoming waves we have to consider the asymptotic behaviour of $\Psi_{\alpha E}$:

$$\begin{aligned} \Psi_{\alpha E} \xrightarrow[r\to\infty]{} & \int d\epsilon_\alpha \, Q_\alpha \sin\left(k_\alpha r - \frac{\ell_\alpha \pi}{2} + \delta_\alpha\right) a(\alpha, \epsilon_\alpha) \\ & + \sum_{\lambda\neq\alpha} \int d\epsilon_\lambda \, Q_\lambda \sin\left(k_\lambda r - \frac{\ell_\alpha \pi}{2} + \delta_\lambda\right) a(\lambda, \epsilon_\lambda) \end{aligned} \tag{1.21}$$

where ($k^2_\lambda = \epsilon_\lambda$; $k^2_\alpha = \epsilon_\alpha$)

and substitute the solutions $a(\lambda, \epsilon_\lambda)$ obtained from (1.15) and (1.16). By appropriate choice of $Z_\lambda(E)$ there will be only outgoing waves in the channels $\lambda \neq \alpha$ and an additional incoming wave in channel α.

2. DISCUSSION OF SIMPLE MODEL SITUATIONS

2.1. One doorway state, one continuum

The simplest case to be considered is the one of only one DWS ϕ and one shell-model continuum ϕ_ϵ. In this case we can omit the indices i and λ, and Eqs. (1.12) to (1.14) assume the form:

$$(E_\phi - E) b + \int d\epsilon' \, V_{\epsilon'} \, a(\epsilon') = 0 \tag{2.1}$$

$$V_\epsilon b + (E_\epsilon - E) a(\epsilon) = 0 \tag{2.2}$$

where

$$\begin{aligned} E_\phi &= \langle \phi | H | \phi \rangle \\ V_\epsilon &= \langle \phi | H | \phi_\epsilon \rangle \\ \delta(\epsilon - \epsilon') \, E_\epsilon &= \langle \phi_{\epsilon'} | H | \phi_\epsilon \rangle \end{aligned} \tag{2.3}$$

Eliminating $a(\epsilon)$ from Eq. (2.2) we obtain the following equation for b:

$$[E_\phi - E + F(E) + Z(E)\,G(E)]\,b = 0 \tag{2.4}$$

with

$$F(E) = P\int \frac{V_{\epsilon'}^2}{E - E_{\epsilon'}}\,d\epsilon' \qquad G(E) = V_E^2\,\theta(E) = V_E^2 \tag{2.4a}$$

(We choose the energy scale in such a way that the threshold $E_1 = 0$ and put $E = E_\epsilon$ for simplicity.)

A non-trivial solution is obtained if

$$E_\phi - E + F(E) + Z(E)\,V_E^2 = 0$$

or

$$Z(E) = \frac{1}{V_E^2}\left(E - E_\phi - F(E)\right) \tag{2.5}$$

The asymptotic behaviour of Ψ will be

$$\Psi \xrightarrow[r\to\infty]{} Q\int d\epsilon\, \sin(kr - \frac{\ell\pi}{2} + \delta_\ell)\,a(\epsilon) \qquad (k^2 = \epsilon) \tag{2.6}$$

where Q is again the remainder of the wave function ϕ_ϵ. Substituting for $a(\epsilon)$ we obtain

$$\Psi \xrightarrow[r\to\infty]{} bQ\left\{P\int d\epsilon\, \frac{\sin(kr - \frac{\ell\pi}{2} + \delta_\ell)}{E - \epsilon}\,V_\epsilon + Z(E)\,V_E\,\sin(k_0 r - \frac{\ell\pi}{2} + \delta_\ell)\right\}_{(k_0^2 = E)} \tag{2.6a}$$

Because of $r \to \infty$ the $P\int$ gives only a contribution for $\epsilon = E$. A very simple calculation leads to

$$\Psi \xrightarrow[r\to\infty]{} b\,V_E\,\{[Z(E) - i\pi]\,e^{i(k_0 r + \delta)} - [Z(E) + i\pi]\,e^{-i(k_0 r + \delta)}\}$$

where $l = 0$ and $\delta_l = \delta$.
From this we obtain the scattering amplitude

$$S = -e^{2i\delta}\,\frac{Z(E) - i\pi}{Z(E) + i\pi} \tag{2.7}$$

$$S = -e^{2i\delta}\left[1 - \frac{2\pi i}{Z(E) + i\pi}\right] = -e^{2i\delta}\left[1 - i\frac{2\pi V_E^2}{E - E_\phi - F(E) + i\pi V_E^2}\right] \tag{2.8}$$

This formula lends itself to an obvious interpretation: The scattering amplitude S appears as a sum of an amplitude $\exp 2i\delta$ for elastic scattering by the shell-model potential U and an amplitude for resonance scattering. If $V_E \approx$ const in the energy region of interest $E \approx E_\phi$, then $F(E) \approx 0$ and the second term is the usual Breit-Wigner form for an isolated resonance of width $\Gamma = 2\pi V_E^2$:

$$S_{Res} = i e^{2i\delta} \frac{\Gamma}{E - E_\phi + i\frac{\Gamma}{2}} \tag{2.9}$$

From the expression (2.7) we conclude that poles of the S-matrix occur for

$$Z(E) = -i\pi \tag{2.10}$$

If we substitute this value of Z(E) in (2.6a) we see immediately that in this case Ψ contains only outgoing waves, i.e. it is the well-known Gamow state. The complex solutions E_{Res} of (2.10) give the position and width of the resonances. As long as the energy dependence of V_E^2 is small, the resonance energy is given by

$$E_{Res} \approx E + F(E) - i\pi V_E^2 \tag{2.11}$$

i.e. F(E) is the level shift and $2\pi V_E^2$ the width.

If, however, the matrix element V_E is strongly energy-dependent, as is the case in the neighbourhood of a single-particle resonance, the resonance energies are determined as the complex solutions of the equation

$$E - E_\phi - F(E) + i\pi V_E^2 = 0 \tag{2.12}$$

We now turn to that case in more detail.

2.2. Occurrence of shell-model resonances

If the energy E is near to a shell-model resonance

$$E^\alpha = \mathrm{Re}\, E^\alpha + i\, \mathrm{Im} E^\alpha = \mathrm{Re} E^\alpha - i\frac{\Gamma^\alpha}{2} \tag{2.13}$$

it will be possible to write V_E approximately as a sum of an energy-independent and a resonating term. In order to find an adequate form, it is convenient to recur to the usual scattering states $\phi_E^{(+)}$ which are related to ϕ_E by

$$\sqrt{2\pi}\, \phi_E = e^{-i\delta}\, \phi_E^{(+)} \tag{2.14}$$

From unitarity it follows that the amplitude $e^{2i\delta}$ for potential scattering must have the form

$$e^{2i\delta} = e^{2i\xi} \frac{E - E^{\alpha *}}{E - E^\alpha} \tag{2.15}$$

where ξ is a real constant.

The function $\phi_E^{(+)}$ can be analytically continued and acquires a pole at the energy $E = E^\alpha$ in the lower half plane of the second sheet. This will in turn lead to a singularity of the analytic continuation of the matrix element $\langle \phi | V | \phi_E^{(+)} \rangle$. So we have

$$V_E = \frac{1}{\sqrt{2\pi}} e^{-i\delta} \langle \phi | V | \phi_E^{(+)} \rangle = e^{-i\delta} \left[\frac{T - \frac{i}{2}\Gamma^\alpha R}{E - E^\alpha} + R \right] e^{i\xi} \tag{2.16}$$

where the expression $[\,] \cdot \exp i\xi$ is just a convenient form of parameterizing the background and the resonance term. The quantities T and R can be seen to be real from $V_E = V_E^*$ and (2.15). Using (2.16) and (2.15) we obtain

$$V_E^2 = \frac{(T - \mathrm{Re}E^\alpha \cdot R + E \cdot R)^2}{|E - E^\alpha|^2} \tag{2.17}$$

and evaluating the principal value with (2.17) we find for $|\Gamma^\alpha| << \mathrm{Re}E^\alpha$:

$$F(E) - i\pi V_E^2 = \left(\sqrt{\frac{2\pi}{\Gamma}}\, T - i\pi \sqrt{\frac{\Gamma}{2\pi}}\, R \right)^2 \frac{1}{E - E^\alpha} - i\pi R^2 \tag{2.18}$$

Now the resonance condition (2.12) takes the form

$$E - E_\phi - \left(\sqrt{\frac{i\pi}{\Gamma}}\, T - i \sqrt{\frac{\Gamma}{2\pi}}\, R \right)^2 \frac{1}{E - E^\alpha} + i\pi R^2 = 0 \tag{2.19}$$

which can be written in terms of a determinant

$$\begin{vmatrix} E^\alpha - E & \sqrt{\frac{2\pi}{\Gamma}}\, T - i\pi \sqrt{\frac{\Gamma}{2\pi}}\, R \\ \sqrt{\frac{2\pi}{\Gamma}}\, T - i\pi \sqrt{\frac{\Gamma}{2\pi}}\, R & E_\phi - i\pi R^2 - E \end{vmatrix} = 0 \tag{2.19a}$$

This form is interesting since it can be compared with two other situations:

(a) If $\Gamma \to 0$ and $R \to 0$ which can be realized by adding to the single-particle potential a repulsive barrier the height of which tends to infinity, then the single-particle resonance becomes a bound state. A more detailed discussion of this case leads to the result that $\lim_{\text{barrier} \to \infty} \sqrt{\frac{2\pi}{\Gamma}}\, T$ is finite and equal to the matrix element V_{12} between the two bound shell-model states [12]. So the determinant approaches the form

$$\begin{vmatrix} \mathrm{Re}E^\alpha - E & ; & V_{12} \\ V_{12} & ; & E_\phi - E \end{vmatrix} = 0 \tag{2.20}$$

which is well known from the calculation of mixed configurations in an infinite shell-model potential.

So the formalism can be looked upon as a simple generalization of the classical shell-model theory.

(b) If we specialize the general formalism of section 1 to the case of two doorway states and one continuum, we are led to the determinant (see (1.19))

$$\begin{vmatrix} \epsilon_1 + F_{11} - i\pi V_{1E}^2 - E & ; & V_{12} + F_{12} - i\pi V_{1E} V_{2E} \\ V_{12} + F_{12} - i\pi V_{1E} V_{2E} & ; & \epsilon_2 + F_{22} - i\pi V_{2E}^2 - E \end{vmatrix} = 0 \qquad (2.21)$$

where we have put

$$\tilde{\epsilon}_1 = V_{11};\ \tilde{\epsilon}_2 = V_{22}$$

If V_{1E} and V_{2E} are weakly energy-dependent, the principal values $F_{ij}(E)$ are negligibly small and Eq. (2.21) is seen to be identical in form with Eq. (2.19a). Thus we see that one doorway state coupled to a continuum at resonance produces qualitatively the same effect as two doorway states coupled to the continuum far from a single particle resonance.

If, in our formalism, "shell-model resonances" appear in a different way than other resonances, this is only due to our using a shell-model basis. It is satisfactory that in the final S-matrix there is no way of telling the origin of a resonance.

2.3. Case of several doorway states and single-particle continua

Let us return to the general case (section 1):

It is rather obvious how we have to proceed in a general case of several continua and several bound shell-model states.

We have to fulfil the general boundary condition of only outgoing waves in all open channels $\lambda \neq \alpha$ and an additional incoming wave in channel α. This is obtained if we put

$$Z_\lambda(E) = -i\pi \quad \text{for } \lambda \neq \alpha \qquad (2.22)$$

and determine the function $Z_\alpha(E)$ from the condition (1.19) of a non-trivial solution.

We obtain the S-matrix $S_{\beta\alpha}$ for a reaction leading from the entrance channel α to the exit channel β if we consider the asymptotic behaviour of $\Psi_{\alpha E}$

$$\Psi_{\alpha E\, r \to \infty} \Big\{ Q_\alpha [\, Z_\alpha(E) + i\pi]\, e^{-i(k_\alpha r - \ell_\alpha \cdot \frac{\pi}{2} + \delta_\alpha)} \sum_i b_{\alpha E}(i)\, V_{\alpha E,\, i} + \sum_\lambda Q_\lambda [\, Z_\lambda(E) - i\pi]\, e^{+i(k_\lambda r - \ell_\lambda \cdot \frac{\pi}{2} + \delta_\lambda)} \sum_i b_{\alpha E}(i)\, V_{\lambda E,\, i} \Big\} \qquad (2.23)$$

Here we indicated explicitly the dependence of b(i) on the entrance channel αE and otherwise used the definitions of section 1. With

(2.22) the diagonal and non-diagonal part of the S-matrix follows from (2.23)

$$S_{\alpha\alpha} = \frac{Z_\alpha(E) - i\pi}{Z_\alpha(E) + i\pi} e^{2i\delta_\alpha} \tag{2.24}$$

$$S_{\beta\alpha} = \frac{-2\pi i e^{i(\delta_\beta + \delta_\alpha)}}{Z_\alpha(E) + i\pi} \frac{\sum_{i=1}^{M} b_{\alpha E}(i)\, V_{\beta E, i}}{\sum_{i=1}^{M} b_{\alpha E}(i)\, V_{\lambda E, i}} \quad (\text{with } \beta \neq \alpha) \tag{2.25}$$

The coefficients $b_{\alpha E}(i)$ are to be obtained from the set of equations (1.16) where the $Z_\lambda(E)$ are chosen in the above-mentioned way. In this context it is important to note that the matrix $\{\bar{v}_{ij}\}$ which is obtained from $\{v_{ij}\}$ if we put <u>all</u> $Z_\lambda = i\pi$, is a complex symmetric matrix of finite rank. Such a matrix can always be brought into diagonal form by a complex orthogonal transformation O.

$$\sum_{ij} \tilde{O}_{ki}\, \bar{v}_{ij}\, O_{j\ell} = \sum_{ij} O_{ik} \bar{v}_{ij}\, O_{j\ell} = \delta_{k\ell}\mu_k \tag{2.26}$$

By writing the coefficients $b_{\alpha E}(i)$ as a function of this transformation O, it can be shown quite easily [7, 8] that the following form of the S-matrix arises

$$S_{\beta\alpha} = \delta_{\beta\alpha} e^{2i\delta_\alpha} - i \sum_{\ell=1}^{N} \frac{\Gamma_{\ell\beta}^{\frac{1}{2}}\, \Gamma_{\ell\alpha}^{\frac{1}{2}}}{E - \mu_\ell} \tag{2.27}$$

where

$$\Gamma_{\ell\lambda}^{\frac{1}{2}} := \sqrt{2\pi} \sum_{i=1}^{M} O_{\ell i}\, V_{i,\lambda E} \tag{2.28}$$

If the matrix elements $V_{i,\lambda E}$ can be considered as energy-independent, the eigenvalues μ_ℓ of the matrix and the transformation O are also energy-independent and we have obtained the desired decomposition of the S-matrix into resonances and background. Then the complex quantities μ_l describe position and width of the resonances and the quantities $\Gamma_{\ell\lambda}$ are to be interpreted as the partial widths for the decay of the compound system ℓ into channel λ. If, however, the energy-dependence of the coupling elements $V_{i,\lambda E}$ is not negligible, i.e. if single-particle resonances come into play, μ_ℓ as well as $\Gamma_{\ell\lambda}$ depend on the energy E and do not have an obvious physical interpretation.

In this case we may obtain the desired decomposition of the S-matrix by generalizing the procedure which was outlined in section 2.2 [8].

3. INCLUSION OF DIRECT REACTIONS

In our discussion of the basic equations (1.8) and (1.9) we made the assumption (1.11)

$$V_{\lambda\epsilon\,\lambda'\epsilon'} = E_{\lambda\epsilon}\ \delta_{\lambda\lambda'}\ \delta(\epsilon-\epsilon') \tag{1.11}$$

which precluded transitions from continuum to continuum, i.e. the so-called direct reactions. It is formally quite easy to get rid of this restriction. For this we introduce instead of the $\phi_{\lambda\epsilon}$ a new set of continuum functions $\psi_{\alpha\epsilon}$

$$\psi_{\alpha\epsilon} = \sum_{\lambda'} \int d\epsilon'\, \phi_{\lambda'\epsilon'}\, c_{\alpha\epsilon}(\lambda'\epsilon') \tag{3.1}$$

We determine them in such a way that the Hamiltonian H is diagonal in this new basis while the original shell-model functions $\phi_{\lambda\epsilon}$ do not have this property.

$$\langle \psi_{\alpha\epsilon} | H | \psi_{\beta\epsilon'} \rangle = E_{\alpha\epsilon}\, \delta_{\alpha\beta}\, \delta(\epsilon - \epsilon') \tag{3.2}$$

We then use, instead of the continuous shell-model states $\phi_{\lambda\epsilon}$, the functions $\psi_{\lambda\epsilon}$ as basis functions in the expansion of $\Psi_{\alpha E}$ (1.7). All the formal procedures of sections 1 and 2 can now be followed in exactly the same way with the only difference that the matrix elements $V_{i,\lambda\epsilon}$ are now defined with respect to the new basis

$$V_{i,\lambda\epsilon} = \langle \phi_i | H | \psi_{\lambda\epsilon} \rangle \tag{3.3}$$

and that the functions $\psi_{\lambda\epsilon}$ show a more complicated asymptotic behaviour:

$$\psi_{\lambda\epsilon} \xrightarrow[r\to\infty]{} Q_\lambda\, e^{-i\left(k_\lambda r - \frac{\ell_\lambda \pi}{2}\right)} \sum_{\rho} \mathring{S}_{\rho\lambda}\, Q_\rho\, e^{+i\left(k_\rho r - \frac{\ell_\rho \pi}{2}\right)} \tag{3.4}$$

The matrix $\mathring{S}_{\rho\lambda}$ which is determined by the diagonalization (3.1) and (3.2) describes those transitions $\lambda \to \rho$ which do not involve bound shell-model configurations as intermediate states. It is almost obvious that, beside the new definition (3.3) of the matrix elements $V_{i,\lambda E}$, the only change due to the new basis is that in the final expression (2.27) for the S-matrix the amplitude for potential scattering is replaced by the S-matrix $\mathring{S}_{\beta\alpha}$ of direct continuum transitions:

$$S_{\beta\alpha} = \mathring{S}_{\beta\alpha} - i \sum_{\ell=1}^{N} \frac{\Gamma_{\ell\beta}^{\frac{1}{2}}\ \Gamma_{\ell\alpha}^{\frac{1}{2}}}{E - \mu_\ell} \tag{3.5}$$

The matrix $\mathring{S}_{\beta\alpha}$ will in general contain single-particle resonances. Therefore, even in the subspace of continuum states $\phi_{\lambda\epsilon}$, the diagonalization of H cannot be performed in perturbation theory. We shall come back to that problem in section 5.

4. REACTIONS WITH LIGHT-BOUND FRAGMENTS

One expects the shell-model description to be useful also in the case of reactions of light projectiles like d, t, α with a heavy target. In order to extend the shell-model description to these cases [8] we have to include in the expansion (1.7) of $\Psi_{\alpha E}$ shell-model states with more than one nucleon in the continuum. We call $\phi_\alpha^{(n)}$ a state with n nucleons in the continuum. The index α which characterizes the state will now, in general, contain more than one continuous quantum number. If $\tilde{n}$ is the maximum number of nucleons in the continuum, determined by the mass of the heaviest fragment to be described, the expansion of $\Psi_{\alpha E}$ must necessarily be extended up to $n = \tilde{n}$

$$\Psi_{\alpha E} = \sum_i \phi_i^{(0)} b(i) + \sum_{n=1}^{\tilde{n}} \sum \int d\lambda \, \phi_\lambda^{(n)} a(\lambda, n) \tag{4.1}$$

$\phi_\alpha^{(n)}$ represents the independent scattering of n nucleons by the shell-model potential U, the remaining (A-n) nucleons being in a bound shell-model configuration. As all basis functions, the $\phi_\lambda^{(n)}$, too, are fully antisymmetrical. The problem is now to construct linear combinations of shell-model states $\phi_\alpha^{(n)}$ which asymptotically describe bound fragments.

To explain the procedure we propose, it is convenient to decompose the Hamiltonian H into three parts in the following way:

We define operators P_n which project onto the subspace of shell-model states with n nucleons in the continuum:

$$P_n = \sum \int d\alpha \; \phi_\alpha^{(n)} \rangle\langle \phi_\alpha^{(n)} \tag{4.2}$$

Then the total Hamiltonian can be written in the following way:

$$H = \mathscr{H}_0 + \mathscr{H}_{(1)} + \mathscr{H}_{(2)} \tag{4.3}$$

with

$$\begin{aligned} \mathscr{H}_0 &= \sum_{n=0}^{\tilde{n}} P_n \, H P_n \\ \mathscr{H}_{(1)} &= \sum_{\substack{n,m=1 \\ n \neq m}}^{\tilde{n}} P_n \, H P_m \\ \mathscr{H}_{(2)} &= \sum_{n=1}^{\tilde{n}} (P_n \, H P_0 + P_0 \, H P_n) \end{aligned} \tag{4.4}$$

The Hamiltonian $\mathscr{H}_{(1)}$ describes direct transfer reactions, while $\mathscr{H}_{(2)}$ implies the coupling between the continuous and bound states of the shell model and is therefore expected to lead to compound nuclear

reactions. The Hamiltonian $\mathscr{H}_0$ contains that part of the interaction which leads to elastic and inelastic scattering and to break-up of the incoming fragment; at the same time, $\mathscr{H}_0$ produces the binding of the fragments.

Our purpose is now to introduce approximate eigenstates of $\mathscr{H}_0$ and then use this basis in order to treat the Hamiltonian $\mathscr{H}_{(2)}$ according to the Weidenmüller-Fano method and $\mathscr{H}_{(1)}$ with some modified perturbation technique (see section 5).

We neglect break-up channels, i.e. we restrict ourselves to reactions of the type

$$A+X \rightarrow B+Y$$

We know that asymptotically the total scattering wave function $\Psi_{\alpha E}$ must be a superposition of the following states $\pi^{(n)}_{\alpha\epsilon}$

$$\pi^{(n)}_{\alpha\epsilon} = N_\alpha \mathscr{A}\left\{g_\alpha(1,\ldots,n)G_\alpha(n+1,\ldots,A)\frac{j_{L\alpha}(R)}{R}Y_{L_\alpha M_\alpha}(\hat{R})\right\} \quad (4.5)$$

Here g_α is the exact intrinsic wave function of the bound fragment (X or Y), G_α is the target wave function represented as a superposition of bound shell-model states $H\phi^{(0)}_i$, $j_{L_\alpha}(R)$ is the spherical Bessel function, $\hat{R}$ a unit vector connecting the two centres of mass and R their distance, N_α a normalisation factor, and $Y_{L_\alpha M_\alpha}$ the usual spherical harmonic. The operator $\mathscr{A}$ antisymmetrizes between the nucleons in different fragments. ϵ is the kinetic energy of relative motion.

We now project $\pi^{(n)}_{\alpha\epsilon}$ on the subspace of shell-model states $\phi^{(n)}_\alpha$

$$\hat{\pi}^{(n)}_{\alpha\epsilon} = P_n \pi^{(n)}_{\alpha\epsilon} \quad (4.6)$$

and use these states as a basis for the diagonalization of $\mathscr{H}_0$. Another, and maybe more convenient basis is obtained if we replace in (4.5) the Bessel function by the scattering states $\chi_{L_\alpha}(R)$ in a shell-model potential U(R). In any case, the states $\hat{\pi}^{(n)}_{\alpha\epsilon}$ represent a set of linearly independent functions which depend on only one continuous parameter, the kinetic energy ϵ of relative motion. They are orthogonal with respect to all discrete quantum numbers α, but non-orthogonal with respect to the continuous quantum number ϵ. The general form (3.5) of the S-matrix remains the same with the only difference that $\hat{S}$ now describes also direct transfer reactions, and in the matrix elements $V_{i,\lambda\epsilon}$ the continuous shell-model states $\phi_{\lambda\epsilon}$ are to be replaced by the approximate eigenstates of $\mathscr{H}_0$.

For practical calculations it will be usually sufficient to consider the states $\hat{\pi}^{(n)}_{\alpha\epsilon}$ with $j_{L_\alpha}(R)$ replaced by $\chi_{L_\alpha}(R)$ as approximate eigenstates of $\mathscr{H}_0$. Physically this means that we neglect the intrinsic polarization of the fragments.

5. PRACTICAL TREATMENT OF THE CONTINUUM-CONTINUUM INTERACTION

Let us return to the problem of diagonalizing H in the subspace of continuous shell-model states and let us, for the sake of simplicity,

restrict our attention to one-nucleon continua $\phi_{\lambda\epsilon}$. Several methods have been used [3, 4, 6] and unfortunately I cannot discuss them all here. I shall only describe briefly the procedure which was recently chosen by Glöckle, Hüfner and Weidenmüller [13] and which is based on a method of Weinberg [14]. This approach may be of quite general value whenever perturbation theory fails. We consider the general case of an integral equation

$$\Psi = \Phi + \frac{1}{W - h_0} v \Psi = \Phi + K(W)\Psi \tag{5.1}$$

as it occurs in every scattering problem. Here Φ is a known function; h_0 and v are to be the "undisturbed" and the interaction part of a Hamiltonian $h = h_0 + v$. The quantity W is a complex parameter. We ask the question, "How can we obtain the solution Ψ to the equation (5.1) in case v is not small?"

Mathematically, the answer is contained in the two following theorems which can be found in any textbook on integral equations:

Theorem I: Whenever the kernel K(W) is square-integrable (Hilbert-Schmidt kernel), i.e.

$$\mathrm{Tr}\, K^{\dagger} K < \infty \tag{5.2}$$

it can be approximated by a separable kernel of finite rank n

$$K_{sep} = \sum_{\nu=1}^{n} |\Gamma_\nu >< \tilde{\Gamma}_\nu| \tag{5.3}$$

such that the norm of the difference K_1 is smaller than any given number

$$\|K_1\| = \|K - K_{sep}\| < \epsilon \tag{5.4}$$

Theorem II: The Born series

$$\Psi = (1 + K + K^2 + \ldots)\Phi \tag{5.5}$$

converges, if, and only if, all eigenvalues $\eta_\nu(W)$ of the kernel K

$$K|\Psi_\nu(W)> = \eta_\nu(W)|\Psi_\nu(W)> \tag{5.6}$$

lie inside the unit circle

$$|\eta_\nu(W)| < 1 \tag{5.7}$$

(Note: The eigenvalues η_ν are determined by the requirement of a square-integrable solution Ψ_ν.)
Usually this is not the case; but for a square-integrable K, at most a finite number N of eigenvalues $\eta_1, \ldots, \eta_N$ lies outside the unit circle.

For the following remarks it is convenient to introduce the resolvent operator F defined by

$$\Psi = (1 + F)\Phi \tag{5.8}$$

It is easily seen to satisfy the integral equation

$$F = K + KF = K + FK \tag{5.9}$$

Let us now introduce a reduced kernel K_1 as the difference between the original kernel K and a separable one which is used to approximate it:

$$K_1 = K - K_{sep} \tag{5.10}$$

The corresponding resolvent operator F_1 is defined as the solution of the equation

$$F_1 = K_1 + K_1 F_1 = K_1 + F_1 K_1 \tag{5.11}$$

By some simple algebra [14] it can be seen from the definition of K, K_1, F and F_1 that the resolvent F can be expressed as a function of F_1

$$F = \mathscr{F}(F_1) \tag{5.12}$$

the detailed form of which is of no importance at the moment.

Now the idea of Weinberg's method is almost apparent: Choose a separable kernel K_{sep} such that all eigenvalues ϵ_ν of the reduced kernel K_1

$$K_1 \chi_\nu(W) = \epsilon_\nu \chi_\nu(W) \tag{5.13}$$

lie far enough inside the unit circle not only for the Born series for F_1

$$F_1 = K_1 + K_1^2 + \ldots \tag{5.14}$$

to converge, but even for the first Born term K_1 to be a good approximation for F_1

$$F_1 \approx K_1 \tag{5.15}$$

If this is so, the resolvent F and also the solution Ψ of (5.1) are obtained from a known function of K_1

$$F \approx \mathscr{F}(K_1) \tag{5.16}$$

The function $\mathscr{F}$ is in general quite complicated. There exists, however, an "ideal choice" [14] of the separable kernel K_{sep} by which it becomes very simple. This ideal choice consists in constructing $|\Gamma_\nu>$ and $<\tilde{\Gamma}_\nu|$ of (5.3) from the right and left eigenstates of K

$$K|\Psi_\nu(W)> = \eta_\nu(W)\,|\Psi_\nu(W)> \tag{5.17}$$

$$<\Psi_\nu(W^*)|\,v\,K = \eta_\nu(W)<\Psi_\nu(W^*)|\,v$$

in the following way:

$$K_{sep} = \sum_{\nu=1}^{N} K|\Psi_\nu(W)><\Psi_\nu(W^*)|\,v \tag{5.18}$$

From (5.17) it is easily seen that the "Weinberg states" satisfy the orthogonality relations

$$\langle \Psi_\mu (W^*) | v | \Psi_\nu (W) \rangle = \delta_{\mu\nu} \tag{5.19}$$

with an appropriate normalisation.

From (5.19) it is immediately inferred that the reduced kernel K_1 has the following eigenvalues and eigenfunctions:

$$K_1 | \Psi_\nu (W) \rangle = 0 \text{ for } \nu = 1 \ldots N$$

$$K_1 | \Psi_\nu (W) \rangle = K | \Psi_\nu (W) \rangle = \eta_\nu | \Psi_\nu \rangle \text{ for } \nu > N \tag{5.20}$$

Consequently, it is sufficient for the Born series (5.14) to converge if the sum in (5.18) is extended over all eigenstates Ψ_ν whose eigenvalues $|\eta_\nu(W)| > 1$. These eigenvalues are "projected to 0", and all the others remain unchanged.

For this "ideal choice" of the separable kernel, the resolvent operator F has the form

$$F = F_1 + \sum_{\nu=1}^{N} \frac{\eta_\nu (W)}{1 - \eta_\nu (W)} | \Psi_\nu (W) \rangle \langle \Psi_\nu (W^*) | v \tag{5.21}$$

and the T-operator of scattering theory is

$$T = T_1 + \sum_{\nu=1}^{N} v | \Psi_\nu (W) \rangle \frac{1}{1 - \eta_\nu (W)} \langle \Psi_\nu (W^*) | v \tag{5.22}$$

T_1 is defined as solution of

$$T_1 = v_1 + v_1 \frac{1}{W - h_0} T_1 \tag{5.23}$$

with $T_1 \approx v_1$

$$v_1 = v - \sum_{\nu=1}^{N} v | \Psi_\nu (W) \rangle \langle \Psi_\nu (W^*) | v \tag{5.24}$$

The last equation exhibits clearly the physical meaning of this approach: The interaction v is approximated by an optimally chosen sum of separable potentials and the difference is treated as a first-order perturbation. Separable potentials have a long history in nuclear physics. The special merit of the above-mentioned one is probably its dependence on the energy W which is such that the difference v_1 may be small for a wide range of energies W (namely that range for which all eigenvalues of $K_1(W)$ remain inside the unit circle). We can write equation (5.6) in the form

$$\left[h_0 + \frac{v}{\eta_\nu (W)} \right] \Psi_\nu (W) \rangle = W \Psi_\nu (W) \rangle \tag{5.25}$$

and may describe $\eta_\nu(W)$ as that number by which we have to divide the interaction v in order to produce a "bound state" at the energy W [14].

So $\eta_\nu(W)$ may be considered as a generalization of the well-depth parameter of effective range theory. From (5.22) we see that whenever $\eta_\nu(W)$ approaches 1, the scattering amplitude will exhibit a resonance. Furthermore, $\eta_\nu(W) = 1$ for all bound states of the Hamiltonian h. The exact form of the eigenvalues $\eta_\nu(W)$ depends, of course, on h_0 and v. Weinberg [14] discusses the case of potential scattering of a single particle:

$$h_0 = T\,;\ v = U \tag{5.26}$$

Glöckle et al. [13] treat two cases:

(a) Scattering of a particle by a potential U to which they add a small perturbation u.

$$h_0 = T + U\,;\ \ v = u \tag{5.27}$$

(b) Scattering of a particle by a system of A-1 particles confined to bound states of a shell-model potential U. This last case is exactly the problem we were confronted with in section 3.

$$h_0 = \sum_{i=1}^{A} [\,T(i) + U(i)] = H_0 \tag{5.28}$$

$$v = \sum_{i<j}^{A} v(ij) - \sum_{i}^{A} U(i) = V$$

Now the kernel $K = [1/(W-H_0)]\,V$ of the Lippmann-Schwinger equation

$$\Psi = \Phi + \frac{1}{W-H_0}\,V\Psi \tag{5.29}$$

is in general not of the Hilbert-Schmidt type as can easily be seen.

If, however, we confine ourselves to eigenstates of H_0 with at most one nucleon in the continuum, it can be shown [13] that K is a sum K_0 of separable terms plus a non-separable, but square-integrable part K' which contains the continuum-continuum interaction[2]:

$$K = \frac{1}{W-H_0}\,V \longrightarrow \frac{1}{W-H_0}\,(P_0 + P_1)\,V\,(P_0 + P_1)$$

$$K = \frac{1}{W-H_0}\,(P_0\,V\,P_0 + P_0\,V\,P_1 + P_1\,V\,P_0) \tag{5.30}$$

$$+ \frac{1}{W-H_0}\,P_1 V P_1$$

[2] Actually K' is not square-integrable as it stands but can be easily made so [13].

Here, P_0 and P_1 are projection operators defined as in section 4:

$$P_0 = \sum_i \phi_i >< \phi_i$$

$$P_1 = \sum_{\lambda'} \int d\epsilon' \, \phi_{\lambda'\epsilon'} >< \phi_{\lambda'\epsilon'} \tag{5.31}$$

$$K_0 = \frac{1}{W-H_0} (P_0 \, V P_0 + P_0 \, V P_1 + P_1 \, V P_0) \tag{5.32}$$

$$K' = \frac{1}{W-H_0} P_1 \, V P_1$$

Thus the method of Weinberg can be applied in principle. The problem, however, remains to find a good approximation for the Weinberg states $\Psi_\nu(W)$. Analytical forms for these functions of course only exist in very simple cases like potential scattering. Approximate Weinberg states of the kernel K are then obtained by expanding them in terms of a finite number of eigenstates $\Psi_i^{(0)}$ of a simpler kernel, and by diagonalizing $(P_0 + P_1)[H_0 + V/\eta_\nu](P_0 + P_1)$ in this subspace. The simpler states are taken to be the eigenstates of a single-particle shell-model kernel:

$$\Psi_\nu(W) = \sum_i c_{\nu i} \, \Psi_i^{(0)}$$

$$\frac{1}{W-T} U \Psi_i^{(0)} = \eta_i^{(0)}(W) \, \Psi_i^{(0)} \tag{5.33}$$

So, again, the solution of the integral equation is reduced to the solution of a finite set of linear equations (for the coefficients $c_{\nu i}$).

Preliminary results obtained by Glöckle et al. for the case of neutron scattering by ^{15}N agree well with results which Lemmer and Shakin obtained by a different method [6].

Let me conclude these observations by summarizing "virtues and vices" of the shell-model description of nuclear reactions: It is restricted to reactions of nucleons and very light projectiles (like d, t, α) with a heavy target nucleus. If the mass of the target nucleus is not very large, the violation of translational invariance which is inherent in any shell-model treatment will lead to errors.

On the other hand, if it can be applied it provides a simple description which is easily amenable to practical calculations, and it does not suffer complications by retaining full antisymmetry.

REFERENCES

[1] FESHBACH, H., Ann.Phys. (N.Y.) 5 (1958) 357; ibid 19 (1962) 287.
[2] MAC DONALD, W.M., Nucl.Phys. 54 (1963) 393; ibid 56 (1964) 636.
[3] BLOCH, C., GILLET, V., Phys.Lett. 16 (1965) 62; ibid 18 (1965) 58.

[4] BLOCH, C., Introduction to the Many-Body Theory of Nuclear Reactions, Rep.C.E.N. de Saclay.
[5] BALASHOV, W.W. et al., J.nucl.Phys., Moscow 2 (1965) 643.
DANOS, M., GREINER, W., Phys.Rev. 138 (1965) 877B.
[6] LEMMER, R.H., SHAKIN, C.M., Ann.Phys. (N.Y.) 27 (1964) 13.
[7] WEIDENMÜLLER, H.A., Nucl.Phys. 75 (1966) 189.
[8] WEIDENMÜLLER, H.A., DIETRICH, K., Nucl.Phys. 83 (1966) 332.
[9] FANO, U., Phys.Rev. 124 (1961) 1866.
[10] BLOCK, B., FESHBACH, H., Ann.Phys. (N.Y.) 23 (1963) 47;
WEISSKOPF, V.F., Physics Today 14 (1961) 18.
[11] DIRAC, Z.Phys. 44 (1927) 585.
[12] WEIDENMÜLLER, H.A., Ann.Phys.(N.Y.) 29 (1964) 378.
[13] GLÖCKLE, W., HÜFNER, J., WEIDENMÜLLER, H.A., Nucl.Phys. A90 (1967) 481.
[14] WEINBERG, S., Phys.Rev. 133 (1964) B 232.

A COMPARATIVE DISCUSSION OF TWO FORMAL THEORIES OF RESONANCE REACTIONS

L. FONDA

Introductory remarks. 1. The case of two orthogonal channels and bound states embedded in the continuum. 2. The formalism of the two theories. 2. A. Feshbach theory. 2. B. Fonda-Newton theory. 3. Comparative discussion.

INTRODUCTORY REMARKS

My aim here is to make a comparison of two recent formal theories of resonance reactions: that by Feshbach of 1958 [1] and that constructed by Newton and myself early in 1960 [2]. The great merit of Feshbach's work was that he succeeded in writing down a far-reaching theory of nuclear resonance reactions free from the concept of channel radius. Various applications of it have been performed (see Chapter 9). In spite of the great generality of the Feshbach theory, it could not explain however a situation which Newton and myself were confronted with in 1959, i.e. the appearance of a narrow resonance in a many-channel problem in an energy region where certainly the closed channels could not have any bound state. This is the reason why we have been stimulated to seek a new theory. What we have been able to construct is a general compound nucleus resonance theory which coincides with the Feshbach theory when the coupling between open and closed channels is weak. Even though the difference between the two theories from the mathematical point of view may seem to the unwary to be only formal, there is however a radically different way of looking at things, most particularly in the interpretation of the mechanism responsible for the formation of compound nucleus resonances. Feshbach, in fact, makes the bound states of the closed channel submatrix of the total Hamiltonian responsible for the compound nucleus resonances, while in the Fonda-Newton theory these resonances are produced by 'almost' bound states embedded in the continuum of the total Hamiltonian.

1. THE CASE OF TWO ORTHOGONAL CHANNELS AND BOUND STATES EMBEDDED IN THE CONTINUUM

Let us have a particle impinging on a target nucleus which is capable of only two states, the ground and an excited state. The impinging particle is different from those of the target nucleus, and no rearrangement can occur. The channels so obtained are then said to be orthogonal in this case. We define the projection operator on the channel consisting of the considered incident particle and the nucleus in its ground state

$$P_1 = |\varphi_1^{(N)}\rangle\langle\varphi_1^{(N)}| \qquad (1.1)$$

The author is at the Istituto di Fisica teorica dell'Università, Trieste, Italy.

$\varphi_1^{(N)}$ being the ground state of the nucleus:

$$H_N \varphi_1^{(N)} = E_1 \varphi_1^{(N)} \tag{1.2}$$

The total Hamiltonian is

$$H = H_N + T_0 + V_{0N} \tag{1.3}$$

where T_0 is the kinetic energy of the incident particle, whose mass has been replaced by the reduced mass, and V_{0N} the mutual interaction between the nucleus and the impiñging particle.

Defining

$$P_2 \equiv 1 - P_1 = |\varphi_2^{(N)}\rangle\langle\varphi_2^{(N)}| \tag{1.4}$$

where $\varphi_2^{(N)}$ describes the excited state of the nucleus, the stationary Schrödinger equation

$$(E - H)\psi = 0 \tag{1.5}$$

gives rise to the following coupled equations:

$$(E - E_1 - T_0 - V_{11})\, P_1 \psi = V_{12} P_2 \psi \tag{1.6}$$

$$(E - E_2 - T_0 - V_{22})\, P_2 \psi = V_{21} P_1 \psi \tag{1.7}$$

where E_2 is the energy of the excited state of the nucleus and $V_{ij} = P_i V_{0N} P_j$.

To obtain an exactly solvable model so that certain properties of the system of Eqs. (1.6) and (1.7) be explicitly exploited, suppose that the interactions are separable:

$$V_{ij} = - g_i g_j \int\int d^3p\, d^3p'\, f_i(p) f_j(p')\, P_i\, |\vec{p}\,\rangle\langle\vec{p}\,'|\, P_j \tag{1.8}$$

$|\vec{p}\,\rangle$ is an eigenstate of relative momentum $\vec{p}$. $f_i(p)$ is a real function. From the hermiticity of H it follows that either g_1 and g_2 are both real or they are both purely imaginary. Note that g_i^2 positive or negative corresponds to attractive or repulsive V_{ii} respectively. We have therefore either V_{11} and V_{22} both repulsive or both attractive.

The proper values of H are immediately obtained. Expanding $P_i \psi$ as

$$P_i \psi = \int d^3p\, c_i(\vec{p})\, P_i\, |\vec{p}\,\rangle \tag{1.9}$$

we get the following coupled equations for the c_i's

$$\left[\frac{p^2}{2\mu} + E_i - E\right] c_i(\vec{p}) = g_i f_i(p) \left[\sum_{j=1}^{2} \int d^3p'\, c_j(\vec{p}\,') g_j f_j(p')\right]$$

In order that ψ be normalizable, $f_i(p)$ must vanish for $p^2 = 2\mu\,(E_e - E_i)$ when consideration is given to a discrete eigenvalue E_e falling on the continuous spectrum of H. These coupled equations have the solution ($\mathcal{N}$ is a normalization factor independent of the channel index)

$$c_i(\vec{p}) = \mathcal{N} g_i f_i(p) \left[\frac{p^2}{2\mu} + E_i - E \right]^{-1}$$

provided that E satisfies the equation

$$\phi_1(E) = 1 - \phi_2(E) \tag{1.10}$$

with

$$\phi_i(E) = g_i^2 \int d^3p \, \frac{f_i^2(p)}{\frac{p^2}{2\mu} + E_i - E}$$

We are now interested in seeking solutions of (1.10) in the energy interval $E_1 < E < E_2$ when the corresponding problem with $g_1 = 0$ does not exhibit normalizable eigenstates for $E < E_2$; that is, when there are no bound states of the isolated closed channel 2 (coupling $V_{21} = 0$). We choose therefore the case of V_{11} and V_{22} repulsive (g_1^2 and g_2^2, negative). It is immediately seen that, owing to the large arbitrariness left to the parameters appearing in (1.10) we can certainly make a bound state embedded in the continuum to appear at the energy $E = E_e$ falling between the two thresholds. The cut-off function $f_1(p)$ must be chosen such that it vanishes at E_e and such that $\phi_1(E)$ changes its sign in the interval $E_1 < E < E_2$. We have then only to play on the values of g_1 and g_2 to obtain the desired normalizable state. Note the trivial fact that the result is independent of the sign of $g_1 g_2$ and that there are no normalizable states with energy $E < E_1$. The situation is illustrated in Fig. 1.

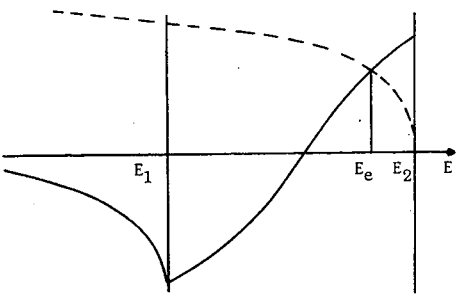

FIG. 1. The solid line represents the function $\phi_1(E)$. The dashed line represents the function $1 - \phi_2(E)$. The intersection at $E = E_e$, accompanied by the vanishing of the cutoff function $f_1(p)$ gives rise to a bound state embedded in the continuum

This example clearly shows that one can reproduce a situation in which, even though channel 2, uncoupled from channel 1, does not exhibit any bound states for $E < E_2$, i.e. the equation

$$(T_0 + E_2 + P_2\, V_{0N}\, P_2)\, \phi_s = \epsilon_s\, \phi_s \tag{1.11}$$

has no normalizable solution, a bound state of the total Hamiltonian can appear embedded in the continuum in the energy interval $E_1 < E < E_2$. By many people it is usually tacitly assumed that in an energy region where some channels are open, H cannot have discrete eigenvalues unless there is no coupling between open and closed channels. The example given above shows that this assumption is incorrect. Moreover, the bound state embedded in the continuum can occur even if the closed channel submatrix H_{22} contains a repulsive interaction. This means that, in this case, the bound state is present in a regime of strong coupling.

2. THE FORMALISM OF THE TWO THEORIES

We shall now summarize the main features of the two theories for the general case when many channels are present. In the general case we define a projection operator P_o whose manifold contains all channels which are open in the energy region of interest [3]. If the open channels belong to different fragmentations, some closed channels will have non-vanishing P_o-projection, but this fact will not matter, as we shall see. We next define the projection operator P_c as

$$P_c \equiv 1 - P_o \qquad (2.1)$$

Then, all the open channels have vanishing P_c-projection, which is all that is necessary in what follows.

We are interested in looking for the resonances which appear in the scattering and reaction processes in the energy region below the closed channel threshold. The T-matrix reads

$$T_{fi} = ((H - E)\varphi_f, \psi) \qquad (2.2)$$

where φ_f describes the relative free motion of the final fragments and their internal (bound) states. ψ is that solution of the Schrödinger equation satisfying outgoing wave boundary conditions with 'incident' wave φ_i. φ_f and φ_i have non-vanishing projection only on the P_o-manifold: $\varphi_{i,f} = P_o\varphi_{i,f}$. ψ satisfies the channel equations

$$(E - H_{oo})\, P_o\psi = H_{oc} P_c \psi \qquad (2.3)$$

$$(E - H_{cc})\, P_c\psi = H_{co} P_o\psi \qquad (2.4)$$

where H_{ij} is given by

$$H_{ij} = P_i\, H\, P_j, \qquad i, j = o \text{ and } c.$$

Let us first see how the Feshbach approach goes.

2.A. Feshbach theory

We obtain the closed channel wave function $P_c\psi$ from (2.4) as

$$P_c\psi = G_c\, H_{co}\, P_o\psi \qquad (2.5)$$

where G_c is defined by

$$(E - H_{cc})\, G_c = P_c \tag{2.6}$$

and outgoing wave boundary conditions. Substitute now (2.5) in (2.3):

$$(E - H_{oo} - H_{oc} G_c H_{co})\, P_o \psi = 0 \tag{2.7}$$

Suppose now that the closed channel Hamiltonian H_{cc} has an isolated bound state

$$H_{cc}\, \phi_s = \epsilon_s\, \phi_s \tag{2.8}$$

where ϕ_s has non-vanishing projection only on the P_c-manifold: $\phi_s = P_c\, \phi_s$. Let us then separate in G_c the contribution from ϕ_s:

$$G_c = \frac{\phi_s \rangle\langle \phi_s}{E - \epsilon_s} + G_c' \tag{2.9}$$

The first term will then be clearly responsible for an isolated resonance.

We now want to separate $P_o\psi$ into a resonant and a non-resonant part. For this purpose write Eq. (2.7) as

$$(E - H')\, P_o \psi = H_{oc} \phi_s\, \frac{(\phi_s, H_{co} P_o \psi)}{E - \epsilon_s} \tag{2.10}$$

where

$$H' = H_{oo} + H_{oc}\, G_c'\, H_{co} \tag{2.11}$$

H' is hermitian in the considered energy region. We now solve Eq. (2.10) formally, obtaining

$$P_o\, \psi = \chi_i^{(+)} + G_{H'}\, H_{oc}\, \phi_s\, \frac{(\phi_s,\, H_{co} P_o\, \psi)}{E - \epsilon_s} \tag{2.12}$$

where

$$(E - H')\, \chi_i^{(+)} = 0 \tag{2.13}$$

$$(E - H')\, G_{H'} = P_o \tag{2.14}$$

$\chi_i^{(+)}$ and $G_{H'}$ are defined with outgoing wave boundary conditions. $\chi_i^{(+)}$ contains as 'incident' wave φ_i.

The quantity $(\phi_s, H_{co} P_o \psi)/(E - \epsilon_s)$ can be evaluated by substituting in it the expression (2.12) for $P_o\psi$. We get

$$\frac{(\phi_s, H_{co} P_o\, \psi)}{E - \epsilon_s} = \frac{(\phi_s,\, H_{co} \chi_i^{(+)})}{E - \epsilon_s - (\phi_s, H_{co} G_{H'}\, H_{oc}\, \phi_s)} \tag{2.15}$$

The splitting of $P_0\psi$ into a resonant and a non-resonant part is completed. We can now write the T-matrix as the sum of two terms, one of which is the contribution of ϕ_s. Writing $\psi = P_0\psi + P_c\psi$ and using Eqs.(2.12), (2.15), (2.5) and the formulas

$$P_0(1 + H_{oc}G'^{\dagger}_c)(H - E)\varphi_f = (H' - E)\varphi_f,$$

$$P_c\left[1 + H_{co}G^{\dagger}_{H'}(1 + H_{oc}G'^{\dagger}_c)\right](H - E)\varphi_f$$

$$= H_{co}\left[1 + G^{\dagger}_{H'}(H' - E)\right]\varphi_f \equiv H_{co}\chi^{(-)}_f,$$

we then get for the T-matrix:

$$T_{fi} = ((H' - E)\varphi_f, \chi^{(+)}_i) + \frac{(\chi^{(-)}_f, H_{oc}\phi_s)(\phi_s, H_{co}\chi^{(+)}_i)}{E - \epsilon_s - (\phi_s, H_{co}G_{H'}H_{oc}\phi_s)}. \tag{2.16}$$

Here $\chi^{(-)}_f$ is the solution of (2.13) satisfying incoming wave boundary conditions with 'incident' wave φ_f. The matrix element appearing in the denominator can be written as:

$$(\phi_s, H_{co}G_{H'}H_{oc}\phi_s) = \Delta_s - i\pi\sum_{\mu}\left|\left(\phi_s, H_{co}\chi^{(\pm)}(E,\mu)\right)\right|^2 \tag{2.17}$$

where Δ_s determines the so-called level shift and is defined by the left hand side of (2.17) with $G^{(P)}_{H'}$ substituted in place of $G_{H'}$. $G^{(P)}_{H'}$ is the standing wave or 'principal value' Green's function. Either the $\chi^{(+)}$ or $\chi^{(-)}$ can be used in (2.17) at will. μ indicates all quantum numbers which together with the energy are necessary to specify $\chi^{(\pm)}$ completely. The second term at the right hand side is the total width of the resonance and it is given as a sum over the partial widths which appear in the numerator of the second term at the right hand side of Eq.(2.16). Eq.(2.16) has therefore the familiar Breit-Wigner form (apart from the energy dependence of the width and shift of the level).

When some bound states of H_{cc} lie close to each other, they give rise to a situation of overlapping resonances. The derivation of an expression for the T-matrix in which the rapidly energy-varying contribution coming from these bound states is separated is more complicated than in the case considered above. We give here only the result of Feshbach (see for details Ref. 1, Section V(b) or Ref. 3 Section IV B)

$$T_{fi} = T''_{Pfi} + \sum_j \frac{(\chi^{(-)}_f, H_{oc}\omega_j)(\omega_j, H_{co}\chi^{(+)}_i)}{E - E_j} \tag{2.18}$$

where $\chi_i^{(+)}$ and $\chi_f^{(-)}$ are the appropriate scattering eigenstates of

$H'' = H_{oo} + H_{oc}[G_c - \sum_s (\phi_s \rangle\langle \phi_s)/(E - \epsilon_s)] H_{co}$

and ω_j is given by

$$\omega_j = \sum_s a_s^{(j)} \phi_s \tag{2.19}$$

$a_s^{(j)}$ being the solutions of the secular equation

$$\sum_r \left[(E_j - \epsilon_s)\delta_{sr} - W_{sr} \right] a_r^{(j)} = 0, \tag{2.20}$$

$$W_{sr} = (\phi_s, H_{co} G_{H''} H_{oc} \phi_r). \tag{2.21}$$

$G_{H''}$ is the outgoing wave Green's function belonging to H''. Note that in this case Im E_j is not given in compact form in terms of a sum over partial widths as in the case of an isolated resonance. There follows that in this case each of the resonance terms in (2.18) is not in the Breit-Wigner form. Only certain sum rules can be given, for example

$$\sum_j \text{Im } E_j = -\pi \sum_s (\phi_s, H_{co}\, \delta(E - H'')\, H_{oc}\, \phi_s). \tag{2.22}$$

Let us see now how the Fonda-Newton approach goes.

2.B. Fonda-Newton theory

We solve now first Eq. (2.3) for the open channel wave function $P_o \psi$:

$$P_o \psi = \phi_{oi}^{(+)} + G_o H_{oc} P_c \psi \tag{2.23}$$

where

$$(E - H_{oo})\, \phi_{oi}^{(+)} = 0 \tag{2.24}$$

$$(E - H_{oo})\, G_o = P_o \tag{2.25}$$

$\phi_{oi}^{(+)}$ and G_o are defined with outgoing wave boundary conditions. $\phi_{oi}^{(+)}$ contains as 'incident' wave φ_i. We substitute now (2.23) into (2.4)

$$(E - H_{cc} - H_{co} G_o H_{oc})\, P_c \psi = H_{co} \phi_{oi}^{(+)} \tag{2.26}$$

and solve for $P_c \psi$

$$P_c \psi = \mathscr{G}_c H_{co} \phi_{oi}^{(+)} \tag{2.27}$$

where $\mathcal{G}_c$ satisfies

$$(E - \mathcal{H}_{cc})\, \mathcal{G}_c = P_c \tag{2.28}$$

and the usual outgoing wave boundary conditions. $\mathcal{H}_{cc}$ is the effective Hamiltonian describing the closed channels. It is non-hermitian. In fact

$$\begin{aligned} \mathcal{H}_{cc} &\equiv H_{cc} + H_{co} G_o H_{oc} \\ &= H_{cc} + H_{co} G_o^{(P)} H_{oc} - i\pi H_{co}\, \delta(E - H_{oo})\, H_{oc} \end{aligned} \tag{2.29}$$

where $G_o^{(P)}$ is the standing wave or 'principal value' Green's function. The eigenvalues of $\mathcal{H}_{cc}$ are then in general complex and, because the operator $H_{co}\delta(E - H_{oo})H_{oc}$ is positive definite, their imaginary part is non-positive. In fact

$$\mathcal{H}_{cc} u_n = A_n u_n \tag{2.30}$$

$$\begin{aligned} \operatorname{Im} A_n &= -\pi (u_n, H_{co}\delta(E - H_{oo}) H_{oc} u_n) \\ &= -\pi \sum_{\mu} \left| (u_n(E), H_{co}\, \phi_o^{(\pm)}(E, \mu)) \right|^2 \le 0 \end{aligned} \tag{2.31}$$

where either $\phi_o^{(+)}$ or $\phi_o^{(-)}$ can be used at will. μ indicates all quantum numbers which together with the energy are necessary to specify $\phi_o^{(\pm)}$ completely. The u_n's are supposed to be normalized. They have, of course, non-vanishing projection only on the P_c-manifold: $u_n = P_c u_n$. Note that the Hamiltonian $\mathcal{H}_{cc}$, as well as its eigenstates u_n and eigenvalues A_n, is energy dependent.

Writing $\psi = P_o\psi + P_c\psi$ and using (2.27), (2.23) and the formula:

$$P_c(1 + H_{co}G_o^{\dagger})(H - E)\varphi_f = H_{co}\left[1 + G_o^{\dagger}(H_{oo} - E)\right]\varphi_f \equiv H_{co}\,\phi_{of}^{(-)}$$

we then get for the T-matrix:

$$T_{fi} = \left((H_{oo} - E)\varphi_f, \phi_{oi}^{(+)}\right) + \left(\phi_{of}^{(-)}, H_{oc}\, \mathcal{G}_c H_{co}\, \phi_{oi}^{(+)}\right) \tag{2.32}$$

$\phi_{of}^{(-)}$ contains as 'incident' wave φ_f. If we introduce the set $\{v_n\}$ biorthogonal to $\{u_n\}$ defined by

$$\mathcal{H}_{cc}^{\dagger} v_n = A_n^{*} v_n \tag{2.33}$$

with v_n normalized, we can write $\mathcal{G}_c$ as

$$\mathcal{G}_c = \sum_n \frac{u_n \rangle\langle v_n}{(v_n, u_n)\,[E - A_n(E)]} + \text{Remainder} \tag{2.34}$$

where the remainder is the contribution from the continuous spectrum of $\mathscr{H}_{cc}$. For the T-matrix we finally get

$$T_{fi} = T_{Pfi} + \sum_r \frac{(\phi_{of}^{(-)}, H_{oc} u_r)(v_r, H_{co}\phi_{oi}^{(+)})}{(v_r, u_r)[E - \mathrm{Re}\, A_r(E) + i\pi \sum_\mu \left|\left(\phi_o^{(-)}(E,\mu), H_{oc} u_r(E)\right)\right|^2]} \tag{2.35}$$

where in the sum over r we have retained only those u_r whose $\mathrm{Re}\, A_r(E) \approx E$ and $\mathrm{Im}\, A_r(E) \approx 0$. All the others, together with the contribution from the continuous states of $\mathscr{H}_{cc}$, have been lumped in T_{Pfi}. In writing (2.35) use has been made of (2.31). Note that for a sharp resonance $(v_r, u_r) \approx 1$ (see for details Ref. 2 Section 4).

If time reversal invariance holds good, the two matrix elements involving $\phi_o^{(-)}$ and $\phi_o^{(+)}$ are connected. In fact, in that case we define

$$\begin{aligned} v_r(s_r, \nu_r) &= (-)^{s_r - \nu_r}\, \theta\, u_r(s_r, -\nu_r) \\ \phi_{oi}^{(+)}(\vec{k}_i, s_i, \nu_i) &= (-)^{s_i - \nu_i}\, \theta\, \phi_{oi}^{(-)}(-\vec{k}_i, s_i, -\nu_i) \end{aligned} \tag{2.36}$$

where θ is the time reversal operator. s and ν are the operators representing the spin and its projection on the z-axis.

If the theory is invariant for time reversal we then have:

$$T_{fi} = T_{Pfi} + \sum_r \eta_r \frac{\gamma_r^{(f)}(\vec{k}_f, \nu_f, \nu_r)\gamma_r^{(i)}(-\vec{k}_i, -\nu_i, -\nu_r)}{E - \mathrm{Re}\, A_r(E) - i\pi \sum_\mu \left|\gamma_r^{(\mu)}(E)\right|^2} \tag{2.37}$$

where

$$\begin{aligned} \gamma_r^{(\alpha)}(\vec{k}_\alpha, \nu_\alpha, \nu_r) &= \left(\phi_{o\alpha}^{(-)}(\vec{k}_\alpha, s_\alpha, \nu_\alpha)\, H_{oc} u_r(s_r, \nu_r)\right) \\ \eta_r &= (-)^{s_i - \nu_i}\left(\theta\, u_r(s_r, -\nu_r), u_r(s, \nu_r)\right)^{-1}. \end{aligned} \tag{2.38}$$

The physics underlying these peculiar states u_r can be understood if instead of playing around with the wave function ψ we take into consideration the complete Green's function $(E + i\epsilon - H)^{-1}$. We have (the limit $\epsilon \to 0^+$ is understood):

$$(E + i\epsilon - H)^{-1} = G + G(H_{oc} + H_{co})(E + i\epsilon - H)^{-1} \tag{2.39}$$

with $G = G_o + G_c$, where G_o and G_c are defined through Eqs. (2.25) and (2.6), respectively. From (2.39) we get

$$P_o(E + i\epsilon - H)^{-1} = G_o + G_o H_{oc} P_c (E + i\epsilon - H)^{-1} \tag{2.40}$$

$$P_c(E + i\epsilon - H)^{-1} = G_c + G_c H_{co} P_o (E + i\epsilon - H)^{-1} \tag{2.41}$$

Substitute (2.40) into (2.41), multiply the resulting equation times $(E - H_{cc})$ and then solve formally for $P_c (E + i\epsilon - H)^{-1}$ using the Green's function $\mathcal{G}_c$ given by (2.28)

$$P_c (E + i\epsilon - H)^{-1} = \mathcal{G}_c (1 + H_{co} G_o) \tag{2.42}$$

We finally get for the complete Green's function (use (2.42) and (2.40))

$$(E + i\epsilon - H)^{-1} = G_o + \left[1 + G_o H_{oc}\right] \mathcal{G}_c \left[H_{co} G_o + 1\right] \tag{2.43}$$

From (2.43) we also have

$$P_c (E + i\epsilon - H)^{-1} P_c = \mathcal{G}_c \tag{2.44}$$

which tells us that if all physical considerations are limited only to the P_c-manifold we can replace the total Hamiltonian H with the effective non-hermitian energy-dependent Hamiltonian $\mathcal{H}_{cc}$ which includes then all relevant couplings to the open channels.

Of course, it is immediately realized that (2.43) leads again to the expression (2.32) for the T-matrix.

Eq. (2.43) gives us the sought-for physical meaning of the u_r's. Suppose in fact that among the discrete eigenvalues of $\mathcal{H}_{cc}$ there is one which at E_e has Re $A_r(E_e) = E_e$ and Im $A_r(E_e) = 0$. In this case $\mathcal{G}_c(E)$ has a pole on the energy axis at $E = E_e$ and from (2.43) so does $(E + i\epsilon - H)^{-1}$. E_e is then an eigenvalue also for the total Hamiltonian H: we have a bound state embedded in the continuous spectrum of H.

It is instructive to see this directly from the Schrödinger equation. In fact Eqs. (2.3) and (2.4) can be put in the form (see Eqs. (2.23) and (2.26)):

$$P_o \psi = \phi_o + G_o H_{oc} P_c \psi \tag{2.45}$$

$$(E - \mathcal{H}_{cc}(E)) P_c \psi = H_{co} \phi_o \tag{2.46}$$

We solve then this set of coupled equations at $E = E_e$, and call the solution ψ_e, by putting $\phi_o \equiv 0$. Considering that $A_r(E_e) = E_e$ we clearly have from (2.46)

$$P_c \psi = u_r(E_e) \tag{2.47}$$

We project Eq. (2.45) on $\phi^{rel}_{\vec{x}_j} \psi_{B1j} \psi_{B2j}$, where $\phi^{rel}_{\vec{x}_j}$ is the relative position eigenvector for the fragments in channel j whose internal (bound) states are described by the vectors ψ_{B1j} and ψ_{B2j}, respectively. For $\vec{x}_j \to \infty$ we get

$$\left(\phi^{rel}_{\vec{x}_j} \psi_{B1j} \psi_{B2j}, P_o \psi_e\right) \underset{\vec{x}_j \to \infty}{\sim} \text{const.} \frac{e^{ik_j x_j}}{x_j} \left(\phi^{(-)}_{oj}(E_e; \vec{k}_j, s_j, \nu_j), H_{oc} u_r(E_e)\right) + O(x_j^{-2}), \tag{2.48}$$

where $\vec{k}_j = k_j \vec{x}_j / x_j$. From (2.31), being Im $A_r(E_e) = 0$, we get for all μ

$$\left(\phi_o^{(-)}(E_e, \mu),\ H_{oc} u_r(E_e)\right) = 0. \tag{2.49}$$

There follows that the vector

$$\psi_e = u_r(E_e) + G_o(E_e) H_{oc} u_r(E_e) \tag{2.50}$$

is normalizable. The vanishing of the matrix element (2.49) makes clearly possible for the level E_e of H to have infinite life time as required. It is characteristic of these states that their eigenfunctions do not vanish exponentially at infinity [4].

Suppose now that the forces which led to the actual bound state of H embedded in the continuum at the energy E_e are slightly altered. As a consequence the bound state will disappear, the level will in fact in general acquire a finite ($\neq 0$) width giving rise to a sharp resonance at $E = E_e$ in the scattering process. The nice point is now that, while H loses its eigenvalue, $\mathscr{H}_{cc}^{(E)}$ retains it, and, moreover, that Re $A_r(E_e) \approx E_e$, Im $A_r(E_e) \approx 0$. The so obtained resonance is then described by the eigenstate u_r of $\mathscr{H}_{cc}$. u_r is now unstable, its time graph exploiting the usual exponential decay law at intermediate times [5].

Vice versa, if there is a sharp resonance due to an eigenvalue of $\mathscr{H}_{cc}$ such that Re $A_r(E_e) \approx E_e$ and Im $A_r(E_e) \approx 0$, then a small perturbation can always shift A_r on the real axis in such a way that Re $A_r(E_e) = E_e$. We have then a bound state embedded in the continuum of H at the energy E_e. The u_r's are then in this approach compound nucleus states. By compound states we mean those states which can be made actually stable (infinite life-time) by a proper small perturbation of the forces. Note that if the coupling between open and closed channels is weak this can be achieved by just turning off this very coupling; if the coupling instead is strong this will be achieved in a more complicated way. It is then clearly emphasized that sharp resonances can appear even when the coupling between the channels is strong [6].

The above discussion pertains to those bound states of H embedded in the continuum which are originated by real eigenvalues of $\mathscr{H}_{cc}$ for which $A_r(E_e) = E_e$. The last point to be discussed is whether to each bound state of H degenerate with the continuum there always corresponds an eigenvalue of $\mathscr{H}_{cc}$ for which $A_r(E_e) = E_e$. But this is certainly true as one can easily see from Eq. (2.43). In fact to a pole of $(E + i\epsilon - H)^{-1}$ there will certainly correspond a pole of $\mathscr{G}_c(E)$ since $G_o(E)$ cannot have a pole, except accidentally, at the same energy where $(E + i\epsilon - H)^{-1}$ does. We must be reminded of the fact that G_o is obtained from $(E + i\epsilon - H)^{-1}$ by turning off the coupling between open and closed channels. We come to the conclusion that the u_r's are then in this scheme the compound nucleus states; in other words, every resonance which can be made infinitely sharp by slightly altering the forces is described by an eigenstate u_r of $\mathscr{H}_{cc}$.

Finally, note that this theory treats on the same footing both the case of isolated and the case of overlapping resonances. Besides, in Eq. (2.35) each resonance term has the familiar Breit-Wigner form (apart from the energy dependence of the γ's). Note also that wide 'single-particle' resonances will be present in the term T_{Pfi} of (2.35).

3. COMPARATIVE DISCUSSION

As follows from the preceding review, the essential difference between the two theories consists in the identification of the compound nucleus states. While in Feshbach's approach they correspond to bound states of the closed channel submatrix H_{cc} of the total Hamiltonian, in the Fonda-Newton approach they are those normalizable eigenstates of the closed channel effective Hamiltonian $\mathscr{H}_{cc} = H_{cc} + H_{co}G_oH_{oc}$ which are near – in the sense of slightly altered forces – bound states embedded in the continuum of the total Hamiltonian.

The following remarks can be made. First of all it is clear that the two theories give the same answers in the limit of weak coupling between open and closed channels. Second, when open and closed channels are strongly coupled, the Fonda-Newton theory reveals resonances which are not given by the Feshbach theory. This is shown by the model example of section 1, where an infinitely sharp resonance has been produced in a case in which H_{cc} has no bound states. Third, Feshbach's level widths and shifts can become so large, when the coupling is strong, that the bound states of H_{cc} which fall in the energy region of interest do not produce any resonance in that region, while in the Fonda-Newton theory no such situation arises.

The last two remarks imply that no correspondence exists between the compound nucleus resonances foreseen by the two theories when the coupling is strong.

The discussion here is formal in the sense that it takes as starting points certain properties of the Hamiltonian matrix (e.g. the weak or strong coupling between open and closed channels) regardless of the actual nuclear situation. The next question is then whether in the actual case the coupling is weak or strong. This question is very difficult to answer. Here we would like only to note that the fact that the compound nucleus resonances are sharp by no means implies that the coupling is weak. Again this is demonstrated by our model example of section 1, in which an infinitely sharp resonance is constructed in a regime of strong coupling.

The applicability of the theories considered is not limited to nuclear reactions. Of course, electron-atom scattering is covered just as well [7], and it is conceivable that certain concepts, like that of bound states embedded in the continuum for the total Hamiltonian, can be extended to the relativistic domain of elementary particle physics [8].

ACKNOWLEDGEMENTS

The author wishes to thank C. Villi for having suggested and stimulated this discussion. Thanks are are also due to K.W. McVoy, A. Rimini, C.A. Engelbrecht, G.C. Ghirardi and T.Weber for various remarks.

REFERENCES

[1] FESHBACH, H., Ann. Phys. 5 (1958) 357.
[2] FONDA, L., NEWTON, R.G., Ann. Phys. 10 (1960) 490.
[3] FESHBACH, H., Ann. Phys. 19 (1962) 287.
[4] See also FONDA, L., GHIRARDI, G.C., Ann. Phys. 26 (1964) 240.

[5] See FONDA, L., Ann. Phys. 29 (1964) 401, where also the optical potential model for the Fonda-Newton theory is derived.

[6] This has been stressed recently also by various other authors. See, for example, OEHME, R., Nuovo Cimento 20 (1961) 334; WEIDENMÜLLER, H. A., Z. für Physik 180 (1964) 425.

[7] FANO, U., COOPER, J. W., Phys. Rev. 137 (1965) A1364. In atomic physics bound states embedded in the continuum of the total Hamiltonian are known to exist; see for example, HOLØIEN, E., MIDTDAL, J., Proc. phys. Soc. A68 (1955) 815.

[8] WEIDENMÜLLER, H. A., see Ref. [6].

TREATMENT OF PAIRING CORRELATIONS WITHOUT VIOLATION OF CONSERVATION LAWS

M. JEAN, X. CAMPI and H. VUCETICH

1. INTRODUCTION

During the past few years methods of approximation originally developed in studies [1-3] of the superconducting state in metals have been applied to nuclear physics by a considerable number of authors. In particular, one of these methods (the B.C.S. theory) has been extensively used [4-7] to study the effect of pairing forces on the structure of single closed-shell nuclei. The state of a nucleus is characterized by the probability amplitudes v_j for occupancy of the pair states (jm, j-m) in the common average potential. The basic approximation of the theory is to describe the properties of a given nucleus as the average of the properties of an ensemble of nuclei. Then the state vector is not an eigenstate of the particle number operator:

$$N = \sum_{jm} C^{\dagger}_{jm} C_{jm} \tag{1}$$

where C_{jm} and C^{+}_{jm} are nucleon annihilation and creation operators. For instance the ground state of an even-even nucleus is represented by the state vector

$$|\tilde{0}\rangle = \prod (u_j + v_j s_{jm} C^{\dagger}_{jm} C^{\dagger}_{j-m}) |0\rangle \tag{2}$$

where s_{jm} is a phase factor equal to $(-)^{j-m}$ and $|0\rangle$ is the vacuum state vector. For the real parameters u and v one has the normalization conditions

$$u_j^2 + v_j^2 = 1 \tag{3}$$

and

$$A = \langle \tilde{0} | N | \tilde{0} \rangle = \sum_j 2\Omega_j v_j^2 \tag{4}$$

The authors are in the Division de Physique Théorique, Institut de Physique Nucléaire, Orsay, France. Mr. Vucetich is also Fellow of Consejo Nacional de Investigaciones Científicas y Técnicas, Argentina.

where $\Omega_j = j+\frac{1}{2}$ is the pair degeneracy of level j, and A the nucleon number. The approximate ground state is identified with what is called the quasi-particle vacuum, the original system of interacting particles being replaced approximately by a system of non-interacting quasi-particles. These quasi-particles, the normal modes of the system, are introduced by a canonical transformation (Bogolubov-Valatin transformation [2, 3])

$$\eta^{\dagger}_{jm} = \alpha_j C^{\dagger}_{jm} - s_{jm} \alpha_j C_{j-m} \tag{5}$$

where η^{+} is the quasi-particle creation operator. By definition the state vector obeys

$$\eta_{jm} |\tilde{0}\rangle = 0 \tag{6}$$

The parameters of transformation (5) are determined by minimizing the quantity

$$H - \lambda N \tag{7}$$

where H is the Hamiltonian of the interacting nucleons and λ is a Lagrange multiplier. Then the approximate ground state energy E_0 of the even-even nucleus is given by

$$E_0 = \langle \tilde{0}|H|\tilde{0}\rangle \tag{8}$$

As explained above the exact Hamiltonian for the interacting nucleons is then replaced, through transformation (5), by the following approximate Hamiltonian:

$$H_{qp} = E_0 + \sum_{jm} E_j \eta^{\dagger}_{jm} \eta_{jm} \tag{9}$$

describing non-interacting quasi-particles (E_j: free quasi-particle energy). In this approximation the lowest state in odd nuclei are described as single quasi-particle excitations, i.e., by the state vectors

$$|\tilde{jm}\rangle = \eta^{\dagger}_{jm} |\tilde{0}\rangle \tag{10}$$

The energy of such a state is $E_0 + E_j$. In the same manner the excited states of even-even nuclei are approximated by exciting two quasi-particles. If the unpaired nucleons are in levels j_1 and j_2 the state vector and energy of such a state are

$$\eta^{\dagger}_{j_1 m_1} \eta^{\dagger}_{j_2 m_2} |\tilde{0}\rangle \quad \text{and} \quad E_0 + E_{j_1} + E_{j_2} \tag{11}$$

The canonical transformation (5) has been generalized by Bogolubov [8] who let the linear combinations of annihilation and creation operators be

a completely arbitrary one. Therefore, we write instead of (5)

$$\eta_\lambda^\dagger = \sum_\ell \alpha_{\ell\lambda} C_\ell^\dagger + \varkappa_{\ell\lambda} C_\ell \tag{12}$$

where we put ℓ for all quantum numbers of a single nucleon state and λ for all quantum numbers of a quasi-particle state. Very little has been done with this formulation, the so-called Hartree-Bogolubov theory. Some attempts have been made to apply it to the description of deformed nuclei [9] and to the treatment of neutron-proton correlations [10-13]. In each case one is led to introduce additional violations of conservation laws besides the non-conservation of particle number. The trial state vector $|\tilde{0}\rangle$ is no longer an eigenvector either of the angular momentum or the isospin or of both operators. Then one meets with the difficult problem of eliminating spurious states.

This is certainly one of the most serious drawbacks of the Hartree-Bogolubov theory. Also there have been numerous efforts to improve on the basic approximation of this theory, especially in connection with the problem of particle number conservation. Without going into details we may mention Nogami's work [14, 15] inspired by Lipkin's idea [16] to use in the B.C.S. theory the operator

$$H - \lambda_1 N - \lambda_2 N^2 \tag{13}$$

instead of (7), the Bayman method [17] which is based on the use of a number-conserving state vector and the projection technique of Kerman-Lawson-MacFarlane [18] in which one employs the projected B.C.S. state vector for the evaluation of all observables.

In this note we present another approximation scheme which formally is quite close to the Hartree-Bogolubov theory but in principle avoids the difficulties associated with the violation of conservation laws. This new method is inspired by Salusti's work [19] in which it has been shown that the use of the trial state vector

$$|A, jm\rangle = \alpha_j C_{jm}^\dagger |A-1, 0\rangle + s_{jm} \varkappa_j C_{j-m} |A+1, 0\rangle \tag{14}$$

instead of (2) led to an approximate treatment of pairing correlations which though conserving the nucleon number is otherwise quite similar to the B.C.S. approximation. In (14) $|A, jm\rangle$ is the state vector of the low-lying states of an odd nucleus and $|A \pm 1, 0\rangle$ the ground state vector of the adjacent even-even nuclei. We have reformulated [20] Salusti's idea in a way which brings it closer to the Hartree-Bogolubov formalism and which is capable of further generalization.

2. GENERAL FORMULATION

We consider a shell model Hamiltonian with a residual interaction

$$H = \sum_\ell \epsilon_\ell C_\ell^\dagger C_\ell + \frac{1}{4} \sum_{\ell mpq} C_\ell^\dagger C_m^\dagger V_{\ell m, pq} C_q C_p \tag{15}$$

The ϵ's are the single-particle energies of the shell model. We take the residual interaction V to be already anti-symmetrized, so that

$$V_{\ell m, pq} = -V_{m\ell, pq} = -V_{\ell m, qp} = V^*_{pq, \ell m} \tag{16}$$

It should be invariant under rotations and time reversal, but we leave all questions of geometry for later.

Let us call $|A, L\rangle$ a complete set of eigenvectors of H belonging to the eigenvalues E^A_L, A being the nucleon number and L denoting the set of quantum numbers characterizing the state:

$$H|A, L\rangle = E^A_L|A, L\rangle \qquad N|A, L\rangle = A|A, L\rangle \tag{17}$$

Some of these quantum numbers can be inferred from the invariance properties of H. We define the following amplitudes [21]:

$$\mathcal{U}^A_\ell(L, M) = \langle A, L|C^\dagger_\ell|A\text{-}1, M\rangle \qquad \mathcal{V}^A_\ell(L, M) = \langle A, L|C_\ell|A+1, M\rangle \tag{18}$$

which can be considered as coefficients of fractional parentage between the nucleus A and the two adjacent nuclei $A \pm 1$. These amplitudes are not all independent since one has

$$\mathcal{U}^{A*}_\ell(L, M) = \mathcal{V}^{A-1}_\ell(M, L) \tag{19}$$

Taking matrix elements, between states of nucleus A, of the anti-commutation relations of the c, s and c^+, s one gets the ortho-normality conditions

$$\delta_{\ell m}\delta_{LM} = \sum_K \{\mathcal{V}^A_\ell(L, K)\mathcal{V}^{A*}_m(M, K) + \mathcal{U}^A_m(L, K)\mathcal{U}^{A*}_\ell(M, K)\} \tag{20}$$

$$0 = \sum_K \{\mathcal{V}^A_\ell(L, K)\mathcal{U}^{A*}_m(M, K) + \mathcal{V}^A_m(L, K)\mathcal{U}^{A*}_\ell(M, K)\} \tag{21}$$

The condition on the nucleon number gives, further,

$$A\delta_{LM} = \sum_{\ell K} \mathcal{U}^A_\ell(L, K)\mathcal{U}^{A*}_\ell(M, K) \tag{22}$$

In order to write the equations of motion of our amplitudes in a compact

form we define the quantities

$$\rho^{A}_{\ell m}(L, M)=\langle A, L|C^{\dagger}_{\ell} C_{m}|A, M\rangle=\sum_{K} \mathscr{U}^{A}_{\ell}(L, K)\mathscr{U}^{A*}_{m}(M, K) \tag{23}$$

$$\kappa^{A}_{\ell m}(L, M) = \langle A-1, L|C_{m} C_{\ell}|A+1, M\rangle=\sum_{K} \mathscr{U}^{A}_{\ell}(K, L)\mathscr{V}^{A*}_{m}(K, M) \tag{24}$$

$$\Delta^{A}_{\ell m}(L, M) =\frac{1}{2}\sum_{pq} V_{\ell m, pq}\, \kappa^{A}_{pq}(L, M) \tag{25a}$$

$$\Gamma_{\ell m} = \sum_{n} V_{\ell n, mn} \tag{25b}$$

By an obvious analogy we call ρ generalized matrix density, κ generalized pairing tensor and Δ generalized pairing potential. One has the following symmetry properties:

$$\rho^{A*}_{\ell m}(L, M) = \rho^{A}_{m\ell}(M, L) \tag{26a}$$

$$\kappa^{A}_{\ell m}(L, M) = -\kappa^{A}_{m\ell}(L, M) \tag{26b}$$

$$\Delta^{A}_{\ell m}(L, M) = -\Delta^{A}_{m\ell}(L, M) \tag{27a}$$

$$\Gamma^{*}_{m\ell}= \Gamma_{\ell m} \tag{27b}$$

The equations we seek will be obtained from the equations of motion of the annihilation and creation operators. The latter can be written

$$[H, C^{\dagger}_{\ell}] = \epsilon_{\ell} C^{\dagger}_{\ell}+\sum_{mn} V^{*}_{\ell n, mn} C^{\dagger}_{m}+\frac{1}{2}\sum_{m, pq} C_{m} V^{*}_{\ell m, pq} C^{\dagger}_{p} C^{\dagger}_{q} \tag{28a}$$

$$[H, C_{\ell}] = -\epsilon_{\ell} C_{\ell}-\frac{1}{2}\sum_{mpq} C^{\dagger}_{m} V_{\ell m, pq} C_{q} C_{p} \tag{28b}$$

Taking matrix elements of the first equation between states $|A, L\rangle$ and $|A-1, M\rangle$ and of the second between states $|A, L\rangle$ and $|A+1, M\rangle$ one gets,

using (17), (18) and (25)

$$0 = (E_L^A - E_M^{A-1} - \epsilon_\ell)\mathcal{U}_\ell^A(L, M) - \sum_m \Gamma_{\ell m}^* \mathcal{U}_m^A(L, M) - \sum_{mK} \Delta_{\ell m}^{A*}(M, K)\mathcal{V}_m^A(L, K) \quad (29a)$$

$$0 = (E_L^A - E_M^{A+1} + \epsilon_\ell)\mathcal{V}_\ell^A(L, M) + \sum_{mK} \Delta_{\ell m}^A(K, M)\mathcal{U}_m^A(L, K) \quad (29b)$$

Those are the equations of motion of our amplitudes, which bear a strong formal resemblance to the Hartree-Bogolubov equations [9]. The energy E_L^A in the state $|A, L\rangle$ can also be expressed in terms of the u and v's amplitude to give

$$E_L^A = \sum_\ell \epsilon_\ell \rho_{\ell\ell}^A(L, L) + \frac{1}{2} \sum_{mK} \Delta_{\ell m}^{A-1}(K, L) \kappa_{\ell m}^{A-1*}(K, L) \quad (30)$$

We have thus obtained a set of coupled non-linear equations which are obeyed by the exact amplitudes. In principle it provides us with a means of solving exactly the problem of A interacting nucleons. This is in general impossible and one must now seek some approximation method to make our equations manageable. In this note we limit ourselves to showing that this can be done in at least one way which leads to an approximation which, though conserving the number of nucleons, is otherwise quite close to the B.C.S. method.

3. GEOMETRY

We have already stated that we assume our Hamiltonian to be invariant under rotations. There is one way, well adapted to the structure of our Eqs.(29), of writing that the residual interaction V possesses this invariance. It is

$$V_{\ell m, pq} = -\frac{1}{2} \sum_{JM} G^J(\ell m, pq) \langle j_\ell j_m m_\ell m_m | JM \rangle \langle j_p j_q m_p m_q | JM \rangle \quad (31)$$

The $\langle | JM \rangle$ are vector coupling coefficients. $G^J(\ell mpq)$ is independent of magnetic quantum numbers. It is real and, except for coefficients, can be regarded as the interaction matrix element between two particles p and q coupled to J, scattering into two particles ℓm, coupled to J.

The rotational invariance implies that among the quantum numbers denoted globally by the index L into the state vector $|A, L\rangle$ we can choose the total angular momentum J and its projection M. Thus from now on we shall write our state vector as

$$|A, JM\alpha\rangle \quad (32)$$

where we put α for all the other quantum numbers needed to completely

specify the state. We can make use of the property of $C^{\dagger}_{a j_a m_a}$ and $(-)^{j-m} C_{a j_a -m_a}$ to transform like irreducible tensor operators of rank j under rotations to define reduced amplitudes independent of the magnetic quantum numbers. In order to simplify the notation we shall make the assumption that giving j, m and parity is enough to single out a single particle state as this is true of most practical shell model calculations. From the Wigner-Eckart theorem it follows that we can write

$$\mathcal{U}^{A}_{jm}(JM\alpha, J'M'\alpha') = (-)^{J-M}\begin{pmatrix} J & j & J' \\ -M & -m & M' \end{pmatrix} \mathcal{U}^{A}_{j}(J\alpha, J'\alpha') \tag{33a}$$

$$\mathcal{V}^{A}_{jm}(JM\alpha, J'M'\alpha') = (-)^{J+j-M+m}\begin{pmatrix} J & j & J' \\ -M & -m & M' \end{pmatrix} \mathcal{V}^{A}_{j}(J\alpha, J'\alpha') \tag{33b}$$

where the $\mathcal{U}$'s and $\mathcal{V}$'s are the reduced amplitudes.

Before going further we can use our assumption of time reversal invariance of the Hamiltonian to prove in the standard way that the $\mathcal{U}$'s and $\mathcal{V}$'s can be taken as real quantities.

Our task is now to rewrite the preceding definitions and equations in terms of the reduced amplitudes. Condition (19) becomes:

$$\mathcal{U}^{A}_{j}(J\alpha, J'\alpha') = (-)^{J'-J+j}\mathcal{V}^{A-1}_{j}(J'\alpha', J\alpha) \tag{34}$$

We find that the orthogonality condition (21) is identically satisfied while (20) gives

$$(2j+1)(2J+1)\delta_{\alpha\alpha'} = \sum_{J''\alpha''} \{\mathcal{V}^{A}_{j}(J\alpha, J''\alpha'')\mathcal{V}^{A}_{j}(J\alpha', J''\alpha'') + \mathcal{U}^{A}_{j}(J\alpha, J''\alpha'')\mathcal{U}^{A}_{j}(J\alpha', J''\alpha'')\} \tag{35}$$

We can write for the matrix elements (22) of the nucleon number operator

$$A(2J+1)\delta_{\alpha\alpha'} = \sum_{jJ''\alpha''} \mathcal{U}^{A}_{j}(J\alpha, J''\alpha'')\mathcal{U}^{A}_{j}(J\alpha', J''\alpha'') \tag{36}$$

In order to rewrite our equations of motion (29) in terms of the reduced amplitudes we have to express the generalized pairing potential in terms of the new amplitudes. First we define a reduced pairing tensor by

$$\chi^{A}_{J_1 M_1 j_1 m_1 j_2 m_2}(JM\alpha, J'M'\alpha') = \langle A-1, JM\alpha | \{ s_{j_2 -m_2} C_{j_2 m_2} \otimes s_{j_1 -m_1} C_{j_1 m_1} \}^{J_1}_{-M_1}$$

$$| A+1, J'M'\alpha' \rangle (-)^{j_1+j_2+m_1+m_2}$$

$$= (-)^{J-M}\begin{pmatrix} J & J_1 & J' \\ -M & -M_1 & M' \end{pmatrix} \chi^{A}_{J_1 j_1 j_2}(J\alpha, J'\alpha')(-)^{j_1+j_2+m_1+m_2} \tag{37}$$

By straightforward calculation, we find that

$$\mathcal{X}^{A}_{J_1 j_1 j_2}(J\alpha, J'\alpha') = \sqrt{2J_1+1} \sum_{J''\alpha''} \mathcal{U}^{A}_{j_2}(J''\alpha'', J\alpha)\mathcal{V}^{A}_{j_1}(J''\alpha'', J'\alpha') \begin{Bmatrix} j_1 j_2 J_1 \\ J' J J'' \end{Bmatrix} (-)^{J_1+J'+J''+j_2} \tag{38}$$

Now we introduce a reduced generalized pairing potential

$$\Delta^{A}_{J_1 j_1 j_2}(J\alpha, J'\alpha') = \frac{1}{4}(-)^{J_1+j_1+J'} \sum_{j_3 j_4 J''} G^{J''}(j_1 j_2 j_3 j_4)\, \mathcal{X}^{A}_{J'' j_3 j_4}(J\alpha, J'\alpha')$$

$$\times \begin{Bmatrix} J'' J J' \\ J_1 j_2 j_1 \end{Bmatrix} \sqrt{2J''+1}\,(-)^{j_3+j_4} \tag{39}$$

and we put

$$\Gamma_j = \frac{1}{2} \sum_{j'J} G^{J}(jj', jj') \frac{2J+1}{2J+1} \tag{40}$$

then we find that Eqs. (29) transform into

$$0 = (E^{A}_{J\alpha} - E^{A-1}_{J'\alpha'} - \epsilon_j + \Gamma_j)\mathcal{U}^{A}_{j}(J\alpha, J'\alpha')$$

$$+ \sum_{j'J''\alpha''} \Delta^{A}_{Jjj'}(J'\alpha', J''\alpha'')\mathcal{V}^{A}_{j'}(J\alpha, J''\alpha'') \tag{41a}$$

$$0 = (E^{A}_{J\alpha} - E^{A+1}_{J'\alpha'} + \epsilon_j)\mathcal{V}^{A}_{j}(J\alpha, J'\alpha')$$

$$+ \sum_{j'J''\alpha''} \Delta^{A}_{Jjj'}(J''\alpha'', J'\alpha')\mathcal{U}^{A}_{j'}(J\alpha, J''\alpha'') \tag{41b}$$

It will be convenient for the following application to introduce the notations

$$\omega^{A}_{J\alpha}(jJ'\alpha') = E^{A}_{J\alpha} + \frac{1}{2}\Gamma_j - \frac{E^{A+1}_{J'\alpha'} + E^{A-1}_{J'\alpha'}}{2} \tag{42}$$

$$\tilde{\epsilon}^{A}(jJ'\alpha') = \epsilon_j - \frac{1}{2}\Gamma_j - \frac{E^{A+1}_{J'\alpha'} - E^{A-1}_{J'\alpha'}}{2} \tag{43}$$

Then Eqs.(41) take the simpler form

$$0 = (\omega^A_{J\alpha}(jJ'\alpha') - \tilde{\epsilon}^A(jJ'\alpha'))\mathcal{U}^A_j(J\alpha, J'\alpha') + \sum_{j'J''\alpha'} \Delta^A_{Jjj'}(J'\alpha', J''\alpha'')\mathcal{V}^A_{j'}(J\alpha, J''\alpha'') \quad (44a)$$

$$0 = \sum_{j'J''\alpha''} \Delta^A_{Jj'j}(J''\alpha'', J'\alpha')\mathcal{U}^A_{j'}(J\alpha, J''\alpha'') + (\omega^A_{J\alpha}(jJ'\alpha') + \tilde{\epsilon}^A(jJ'\alpha')\mathcal{V}^A_{j'}(J\alpha, J''\alpha'') \quad (44b)$$

One may remark the strong formal similarity between these equations and the Hartree-Bogolubov equations.

For the energy of the state $|A, JM\alpha\rangle$ one has from Eq.(30)

$$E^A_{J\alpha} = \frac{1}{2J+1}\Big\{\sum_{jJ'\alpha'} \epsilon_j |\mathcal{U}^A_j(J\alpha, J'\alpha')|^2$$

$$-\frac{1}{8}\sum_{\substack{j_1 j_2 j_3 j_4 \\ J'J''\alpha''}} G^{J'}(j_1 j_2 j_3 j_4)\, \chi^{A-1}_{J'j_1 j_2}(J''\alpha'', J\alpha)\, \chi^{A-1}_{J'j_3 j_4}(J''\alpha'', J\alpha)\Big\} \quad (45)$$

Obviously rotational invariance is not the only symmetry property of the Hamiltonian one can exploit. For instance, one may assume, as is usually done, charge independence of the Hamiltonian. In the same manner as we have done for angular momentum, one can extract from the amplitudes the T_z dependence to get reduced amplitudes $\mathcal{U}$ and $\mathcal{V}$ which depend only on T. One may also consider an invariant Hamiltonian in quasi-spin (seniority) space. Then, use of the Wigner-Eckart theorem gives us immediately the dependence of our amplitudes $\mathcal{U}^A$ and $\mathcal{V}^A$ with respect to the nucleon number A.

4. B.C.S.-LIKE APPROXIMATION

We wish now to show that it is possible to derive, from our general formulation, an approximation scheme which is quite similar to the usual B.C.S. method. As in the B.C.S. theory we shall restrict our discussion to the case of identical particles.

Going back to the introduction it is easy to prove that Eq.(5) and its adjoint can be reversed to give

$$C^\dagger_{jm} = u_j \eta^\dagger_{jm} + s_{jm} v_j \eta_{j-m} \quad (46a)$$

$$C_{jm} = u_j \eta_{jm} + s_{jm} v_j \eta^\dagger_{j-m} \quad (46b)$$

It follows from the anti-commutation relations of the η's and from (6) that the parameters u_j and v_j are related to the approximate ground state $|\tilde{0}\rangle$ of the even-even nuclei and to the approximate low-lying state $|\tilde{jm}\rangle$

of the odd nuclei (cf. Eq.(10)) by

$$u_j = \langle j\tilde{m}|C^{\dagger}_{jm}|\tilde{0}\rangle , \qquad v_j = \langle j\text{-}\tilde{m}|C_{jm}|\tilde{0}\rangle \; s_{j-m} \tag{47}$$

Comparison of this result to the definition (18) of our $\mathcal{U}^A$ and $\mathcal{V}^A$ (A odd) amplitudes suggests strongly that we build our approximation scheme on the assumption that the parentage of the ground state of an even-even nucleus is restricted to the low-lying states of the adjacent odd nucleus. Looking back to Eqs.(33) we notice that jJ' and J obey the law of addition of angular momenta. Taking A an odd number and the ground state of the $A \pm 1$ even-even nuclei having $J' = 0$, our assumption means more precisely that we shall deal only with the reduced amplidudes

$$\mathcal{U}^A_j(j, 0) = \mathcal{U}^A_j \qquad \mathcal{V}^A_j(j, 0) = \mathcal{V}^A_j \tag{48}$$

where we have furthermore assumed that the $|A, jm\rangle$ state is unique. Then the whole set of equations simplify considerably. The equations of motion (44) reduce to

$$0 = (\omega^A_j - \tilde{\epsilon}^A_j)\,\mathcal{U}^A_j + \Delta^A_j \mathcal{V}^A_j \tag{49a}$$

$$0 = \Delta^A_j \mathcal{U}^A_j + (\omega^A_j + \tilde{\epsilon}^A_j)\,\mathcal{V}^A_j \tag{49b}$$

with

$$\omega^A_j = E^A_j + \frac{1}{2}\Gamma_j - \frac{E^{A+1}_0 + E^{A-1}_0}{2} \tag{50}$$

$$\tilde{\epsilon}^A_j = \epsilon_j - \frac{1}{2}\Gamma_j - \frac{E^{A+1}_0 - E^{A-1}_0}{2} \tag{51}$$

$$\Delta^A_j = -\frac{1}{4}\sum_{j'} \frac{G^0(jj, j'j')}{\sqrt{(2j+1)(2j'+1)}}\,\mathcal{U}^A_{j'}\mathcal{V}^A_{j'} \tag{52}$$

$$\Gamma_j = \frac{1}{2(2j+1)}\,G^0(jj, jj) \tag{53}$$

To be consistent with our fundamental assumptions one sees that the condition (36) on the number of nucleons must be written for the (A+1) nucleus. Using (34) one obtains

$$A+1 = \sum_j (\mathcal{V}^A_j)^2 \tag{54}$$

Similarly Eq.(35) gives

$$(2j+1) = (\mathcal{U}^{A+2}_j) + (\mathcal{V}^A_j)^2 \tag{55}$$

Finally the ground state energy of the even-even nucleus (A+1), taken from (45) can be expressed as

$$E_0^{A+1} = \sum_j \{\epsilon_j (\mathcal{V}_j^A)^2 + \frac{1}{2}\Delta_j^A \mathcal{U}_j^A \mathcal{V}_j^A\} \tag{56}$$

At this point it is interesting to notice that the ground state energy of the even-even nucleus (A-1) can also be expressed in terms of the $\mathcal{U}_j^A$'s and $\mathcal{V}_j^A$'s. One has[1]

$$E_0^{A-1} = \sum_j \{(2j+1)(\epsilon_j - \frac{1}{2}\Gamma_j) - (\epsilon_j - \Gamma_j)(\mathcal{U}_j^A)^2 + \frac{1}{2}\Delta_j^A \mathcal{U}_j^A \mathcal{V}_j^A\} \tag{57}$$

Thus, except for (55), our set of Eqs.(49)-(57) is completely expressed in terms of $\mathcal{U}_j^A$ and $\mathcal{V}_j^A$. Were we to ignore the difference between A+2 and A in (55) this set would very much look like the familiar equations of the B.C.S. theory. The resemblance can be made still stronger by introducing the quantities

$$u_j^A = \frac{-1}{\sqrt{2j+1}}\mathcal{U}_j^A, \quad v_j^A = \frac{-1}{\sqrt{2j+1}}\mathcal{V}_j^A \tag{58}$$

as suggested by comparing the definitions (33) of the reduced amplitudes to the expressions (47) for the u_j and v_j parameters of the B.C.S. theory. The re-definition (58) of our amplitudes amounts to using Clebsch-Gordan coefficients in (33) instead of 3-j symbols.

Then, to make our treatment still closer to the B.C.S. one, we shall put

$$G^0(jj, j'j') = 2\sqrt{(2j+1)(2j'+1)}\, G_{jj'} \tag{59}$$

and use (58) so that we have finally to deal with the following set of

---

[1] This expression results from the following one:

$$E_L^{A-1} = \sum_\ell (\epsilon_\ell + \frac{1}{2}\Gamma_{\ell\ell}) - \sum_{\ell K} \epsilon_\ell |\mathcal{V}_\ell^A(K, L)|^2 - \sum_{\ell p K} \Gamma_{\ell p} \mathcal{V}_p^{A*}(K, L)\mathcal{V}_\ell^A(K, L) + \frac{1}{2}\sum_{\ell m K} \Delta_{\ell m}^A(L, K)\kappa_{\ell m}^{A*}(L, K) \tag{57a}$$

which is obtained from the Hamiltonian (15) by reversing the order of the creation and annihilation operators. As an intermediate step between (57) and (57a) one has in terms of the reduced amplitudes

$$E_{J\alpha}^{A-1} = \sum_j (2j+1)(\epsilon_j - \frac{1}{2}\Gamma_j) - \sum_{jJ'\alpha'} \frac{\epsilon_j - \Gamma_j}{2J+1} |\mathcal{U}_j^A(J'\alpha', J\alpha)|^2 - \frac{1}{8}\sum_{\substack{j_1 j_2 j_3 j_4 \\ J'J''\alpha''}} G^{J'}_{(j_1 j_2 j_3 j_4)} \; \mathcal{X}^A_{J' j_1 j_2}(J\alpha, J''\alpha'') \, \mathcal{X}^A_{J' j_3 j_4}(J\alpha, J''\alpha'')$$

equations [22]:

$$0 = (\omega_j^A - \tilde{\epsilon}_j^A)\, u_j^A + \Delta_j^A\, v_j^A$$
$$0 = \Delta_j^A\, u_j^A + (\omega_j^A + \tilde{\epsilon}_j^A)\, v_j^A \tag{60}$$

where

$$\omega_j^A = E_j^A + \frac{1}{2} G_{jj} - \frac{E_0^{A+1} + E_0^{A-1}}{2} \tag{61}$$

$$\Gamma_j = G_{jj}$$

$$\epsilon_j^A = \epsilon_j - \frac{1}{2} G_{jj} - \frac{E_0^{A+1} - E_0^{A-1}}{2} \tag{62}$$

$$\Delta_j^A = -\sum_{j'} G_{jj'}\, \Omega_{j'}\, u_{j'}^A v_{j'}^A \ , \quad \Omega_j = j + \frac{1}{2} \tag{63}$$

To these are added the conditions

$$A+1 = \sum_j 2\Omega_j (v_j^A)^2 \tag{64}$$

$$1 = (u_j^{A+2})^2 + (v_j^A)^2 \tag{65}$$

The energies of the even-even nuclei ($A \pm 1$) are given by

$$E_0^{A+1} = \sum_j 2\Omega_j \{\epsilon_j (v_j^A)^2 + \frac{1}{2} \Delta_j^A u_j^A v_j^A\} \tag{66}$$

and

$$E_0^{A-1} = \sum_j 2\Omega_j \{(\epsilon_j - \frac{1}{2} G_{jj}) - (\epsilon_j - G_{jj})(u_j^A)^2 + \frac{1}{2} \Delta_j^A u_j^A v_j^A\} \tag{67}$$

It is important to remark that as a consequence of our approximation it follows, as in the B.C.S. case, that we are taking into account only the $J = 0$ component (see Eq.(52)) of the expansion (31) of the potential. One may say that we are extracting the pairing part of the nuclear force.

5. METHOD OF SOLUTION AND NUMERICAL RESULTS

In this section we discuss numerical calculations which we have carried out in order to compare our approximation to known exact results

and to the B.C.S. approximation. For this reason we consider the so-called "pairing force". This means that we assume all matrix elements $G_{jj'}$ defined by Eq.(59) to be equal to a constant G

$$G_{jj'} = G \qquad \forall\, j, j' \tag{68}$$

5.1. Degenerate model

First let us discuss the degenerate model, wherein all single-particle energies ϵ_j are equal.

$$\epsilon_j = \epsilon \qquad \forall\, j \tag{69}$$

It is interesting to look at this case since it can be solved exactly very easily and is quite instructive. Furthermore we expect our theory to be exact for it. This is because we know that seniority is a good quantum number for the degenerate model, the ground state of our even-even nucleus having seniority $v = 0$. From the known transformation properties of the single-particle operators C_{jm} and $C^{\dagger}_{jm}$ in quasi-spin space it follows that the only parents of the ground state of an even-even nucleus are the seniority one-states of the adjacent odd nuclei. One shows easily that the pairing potential Δ is diagonal in the seniority representation and, because there is no excited state of seniority zero, our set of equations, in this case, is complete so that we must get the exact solution.

One has

$$\Gamma_j \equiv \Gamma = G, \qquad \Delta_j^A \equiv \Delta = -G \sum_{j'} \Omega_{j'} u_{j'}^A v_{j'}^A \tag{70}$$

and

$$\tilde{\epsilon}_j^A \equiv \tilde{\epsilon}^A = \epsilon - \frac{1}{2} G - \frac{E_0^{A+1} - E_0^{A-1}}{2} \tag{71}$$

From Eq.(60), inserting (70) and (71), we have

$$\omega_j \equiv \omega = \sqrt{(\tilde{\epsilon}^A)^2 + (\Delta^A)^2} \tag{72}$$

Finally it follows that the amplitudes u^A and v^A are independent of j. Putting

$$\sum_j \Omega_j = \Omega \tag{73}$$

we get, both from (64) and (65),

$$(v^A)^2 = \frac{A+1}{2\Omega} \qquad (u^A)^2 = 1 - \frac{A-1}{2\Omega} \tag{74}$$

For the even-even nucleus (A+1) one obtains

$$\Delta^A = -G\Omega\sqrt{\frac{A+1}{2\Omega}\left(1-\frac{A-1}{2\Omega}\right)} \tag{75}$$

and for the ground state energy

$$E_0^{A+1} = 2\Omega\{\epsilon(v^A)^2+\frac{1}{2}\Delta^A u^A v^A\}$$

$$=\left(\epsilon-\frac{G}{2}\right)\left(A+1\right) - \frac{G\Omega}{2}(A+1)\left(1-\frac{A+1}{2\Omega}\right) \tag{76}$$

which is the exact result. We recall the B.C.S. result

$$E_{0,BCS}^{A+1}=\left(\epsilon-\frac{G}{2}\frac{A+1}{2\Omega}\right)\ (A+1) - \frac{G\Omega}{2}(A+1)\left(1-\frac{A+1}{2\Omega}\right) \tag{77}$$

Were we to ignore the difference between u_j^{A+2} and u_j^A and use condition

$$(u_j^A)^2+(v_j^A)^2 = 1 \tag{78}$$

as done in B.C.S. theory (cf. Eq.(3)), instead of the exact one (65), the approximate E_0^{A+1} would be

$$E_{0,app}^{A+1}=\epsilon(A+1) - \frac{G\Omega}{2}(A+1)\left(1-\frac{A+1}{2\Omega}\right) \tag{79}$$

Both approximate results (77) and (79) differ from the exact one by the renormalization of the single-particle energies.

5.2. Non-degenerate model

In this case the ϵ_j take different values and it is no longer possible to get directly the amplitudes u_j and v_j from Eqs.(64) and (65). One has to solve numerically the whole set of equations. One important feature is that because Eq.(65) connects u_j^{A+2} to v_j^A there arises the necessity of treating several A values simultaneously. As we have seen that in order to get the exact solution of the degenerate case one has to use Eq.(65) rather than Eq.(78), we shall insist on retaining this difference from the B.C.S. theory. To circumvent this difficulty we shall use a step-by-step method. We assume that u_j^A is known and we utilize Eqs.(60) and (64) to obtain ω_j^A and v_j^A. Then Eq.(65) allows us to determine u_j^{A+2} and to proceed further for higher A. As we know that

$$u_j^1 = 1 \qquad \forall j \tag{80}$$

we start our step-by-step procedure for A = 1. But before solving Eqs.(60)

TABLE I. VALUES OF THE GROUND STATE ENERGY IN THE MODEL OF REFERENCE[23], BOTH EXACTLY AND IN VARIOUS APPROXIMATION SCHEMES INCLUDING THE PRESENT WORK (P.W.). THE ENERGIES ARE IN UNITS OF THE SINGLE PARTICLE SEPARATIONS

	Exact	B.C.S.	Projected B.C.S.	Nogami-Zucker	P.W.
E_0^6	6.83	8.08	6.85	6.86	7.20

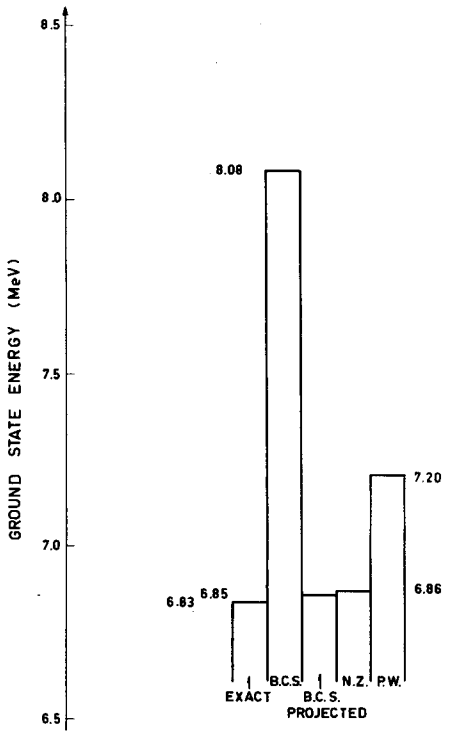

FIG.1. Pawlikowski and Rybarska model where 6 particles interacting through the pairing force (G = 1) are distributed over 5 doubly degenerate levels ($\epsilon_j = 1,2,3,4,5$). Values of the ground state energy obtained in various approximation schemes are compared to the exact one ($\lambda = 2.503$, $(E_6 - E_4)/2 = 2.61$)

and (64) for the unknowns ω_j and $\varkappa_j$ one must realize that we have altogether 2n unknowns (n being the number of j's which enter into our model) for 2n+1 equations. Were our method an exact one, these equations would be compatible, as one can verify in the degenerate model. We do

TABLE II. VALUES OF THE SINGLE PARTICLE LEVEL OCCUPATION PROBABILITIES v_j^2 IN THE MODEL OF REFERENCE [23].

v_j^2	Level				
	1	2	3	4	5
B.C.S.	0.892	0.810	0.649	0.418	0.229
Nogami-Zucker	0.883	0.797	0.641	0.430	0.249
Exact	0.911	0.853	0.716	0.338	0.182
P.W.	0.872	0.822	0.684	0.396	0.226

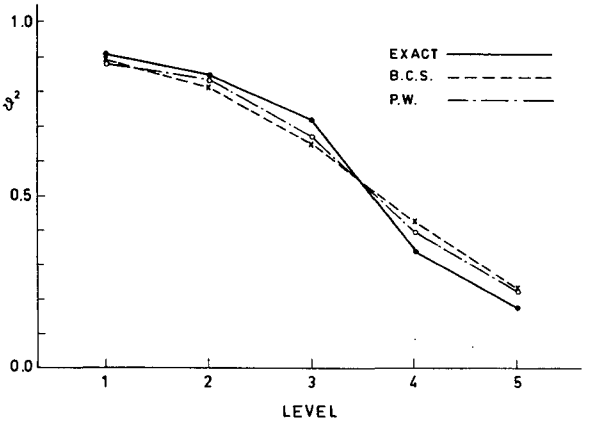

FIG. 2. Density distribution in the ground state in the Pawlikowski and Rybarska model. The exact single particle level occupation probabilities V_j^2 are compare to those obtained in the B.C.S. approximation and in the present work (P.W.) (pairing force G = 1, 5 doubly-degenerate equidistant levels)

not expect this to be the case so that we must in some way relax the self-consistency of our equations. As we believe Eq.(64) is important to normalize our amplitudes to the correct number of particles, we introduce, by analogy with the B.C.S. treatment, a supplementary unknown λ by putting

$$\tilde{\epsilon}_j^A = \epsilon_j - \frac{1}{2}\Gamma - \lambda \tag{81}$$

TABLE III. VALUES OF THE GROUND STATE ENERGY IN THE MODEL OF THE EVEN NICKEL ISOTOPES SOLVED EXACTLY IN REFERENCE[18]. ENERGIES ARE MEASURED IN MeV

E_0^{A+1}	A+1 = 2 ^{58}Ni	4 ^{60}Ni	6 ^{62}Ni	8 ^{64}Ni	10 ^{66}Ni
B.C.S.	-1.13	-1.51	-1.09	-0.22	+2.48
Nogami-Zucker	-1.49	-2.07	-1.72	-0.44	+1.85
Exact	-1.49	-2.11	-1.75	-0.51	+1.70
P.W.	-1.48	-2.07	-1.68	-0.39	+1.83

TABLE IV. VALUES OF THE PARAMETER λ DEFINED BY EQUATION (81) COMPARED TO THE SELF-CONSISTENT VALUE $\lambda' = (E_0^{A+1} - E_0^{A-1})/2$

A	1	3	5	7	9
λ^A	-0.702	-0.264	0.197	0.657	1.145
$\lambda'^A = \frac{E_0^{A+1} - E_0^{A-1}}{2}$	-0.741	-0.295	0.197	0.643	1.109

Thus if our theory were to be completely self-consistent, λ should be equal to

$$\lambda = \frac{E_0^{A+1} - E_0^{A-1}}{2}$$

Hence our procedure to solve the set of non-linear equations is, for a given value of A, to start with the known value of α^A and with a trial value of α^A. Then $\tilde{\epsilon}_j^A$ and Δ^A are given functions of λ which are used

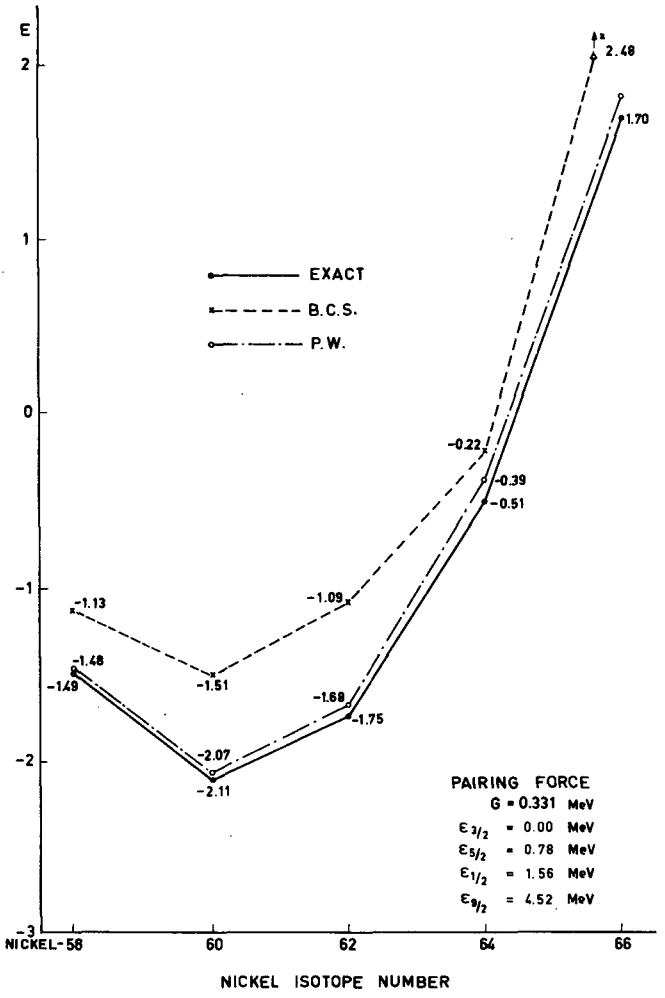

FIG.3. Model of the nickel isotopes solved exactly by Kerman, Lawson and MacFarlane. The exact ground state energy is compared to the values obtained in the B.C.S. approximation and in the present work (P.W.). The value of the coupling constant G and the positions of the single particle levels were as shown in the figure

to obtain

$$\omega_j^A(\lambda) = \sqrt{\tilde{\epsilon}_j^A(\lambda)^2 + (\Delta_j^A(\lambda)^2}$$

$$v_j^A(\lambda) = \frac{-\Delta_j^A(\lambda)}{\tilde{\epsilon}_j^A(\lambda) + \omega_j^A(\lambda)}\, u_j^A \qquad (82)$$

The parameter λ is fixed by imposing condition (64). And we go on by successive iterations. We found that this iterative procedure converges

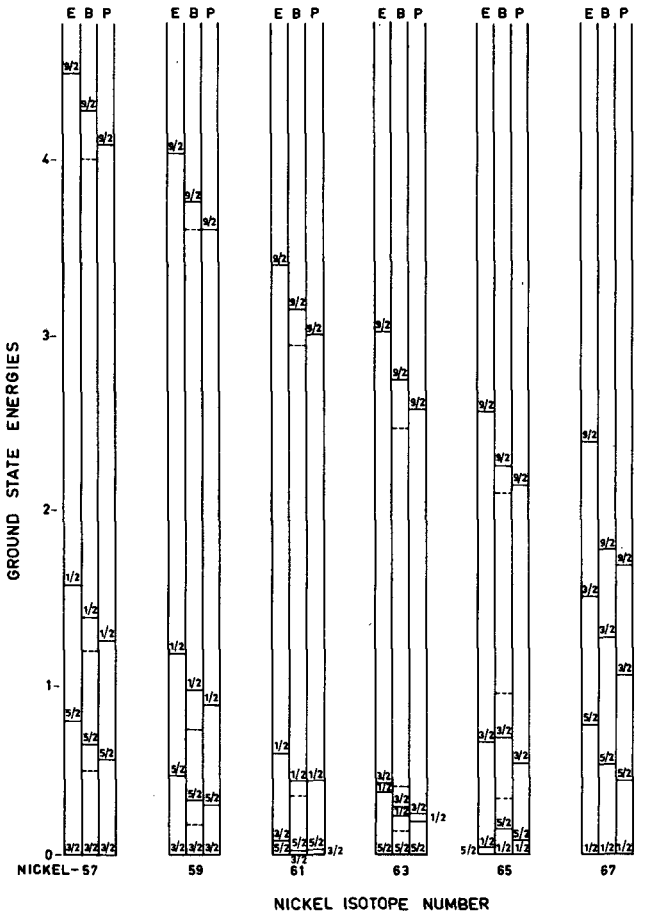

FIG. 4. Low-lying (seniority one) excited states in the odd nickel isotopes. The notations 3/2 etc. represent the spin of the state. The columns labelled E are those obtained from the exact calculations of Kerman, Lawson and MacFarlane, and the entries under B and P are the states determined in the BCS approximation and in the present work. The coupling constant G and the ϵ's are the same as used in Fig. 3

very rapidly. The ground state energy of the (A+1) nucleus is given by (66) and the low-lying levels of the A nucleus by the differences between the ω_j^A's.

We have considered successively two examples[2] for which there are exact calculations: the Pawlikowski-Rybarska [23] model and the model of the nickel isotopes solved exactly by Kerman-Lawson and MacFarlane [18].

5.2.1. Pawlikowski-Rybarska Model

In this model A+1 = 6 identical nucleons are distributed over 5 doubly degenerate equidistant levels ($\epsilon_j = 1, 2, 3, 4, 5$). Numerical values have

[2] These examples have also been discussed by Nogami and Zucker (see Ref. [15]) and by Do Dang and Klein (see Ref. [22]) in a similar context.

been obtained for different values of A and G. In Table I, we compare for G = 1 our value (PW) of the ground state energy of the even-even nucleus A+1 = 6 with the B.C.S., the projected B.C.S., the Nogami-Zucker [14, 15] and the exact result of Pawlikowski-Rybarska. This is illustrated in Fig. 1. In order to get an idea of the non-self-consistency of our solution it is interesting to compare the λ parameter with the calculated value of $\lambda' = (E_0^6 - E_0^4)/2$. We find $\lambda = 2.503$ and $\lambda' = 2.612$. We have observed that λ converges to λ' when G increases. This is to be expected since the differences between the ϵ_j's become negligibly small compared to G and we approach the situation of the degenerate case. Our result represents a considerable improvement over B.C.S., but is inferior to those of the projected B.C.S. and of the Nogami-Zucker method. Table II and Fig. 2 show a comparison of the density distribution ($\varkappa_j^2$) which again favours our ground state wave function against the B.C.S. one.

5.2.2. Nickel isotopes model

Kisslinger and Sorensen [6] have treated the pairing force problem for the nickel isotopes by the B.C.S. method taking

$$G = 0.331 \qquad \epsilon_{3/2} = 0 \qquad \epsilon_{5/2} = 0.78 \qquad \epsilon_{1/2} = 1.56 \qquad \epsilon_{9/2} = 4.52$$

The model has been solved exactly by Kerman-Lawson and MacFarlane. In Table III and Fig. 3 we compare our results for the ground state energies of the even-even isotopes to those of the above authors. Our values are again considerably better than the B.C.S. ones and they are much nearer to the exact energies than in the previous example. Table IV gives the values λ^A and $\lambda'^A = (E_0^{A+1} - E_0^{A-1})/2$. The relative positions of the low-lying excited states of the odd-A nickel isotopes can be obtained from the differences of the ω_j^A. Our results are compared to the exact ones in Fig. 4 where we have also represented the differences between the quasi-particle energies of the B.C.S. theory. The qualitative agreement is satisfactory although the quasi-particle excitations seem to be quantitatively more reliable. However, one should remark that the quasi-particle energies reproduced here are obtained by using condition (4) for an odd number of particles and the same equations as used for even-even nuclei. Should we use the quasi-particle energies corresponding to the following even-even isotopes we would obtain levels which are represented by dotted lines. In that sense we may regard our results as not worse than the B.C.S. ones.

In conclusion we may claim that this new formulation of the treatment of pairing correlations in nuclei leads us to an approximation scheme which, in many respects, is comparable to the B.C.S. theory, the price we have to pay for a particle-number-conserving theory being now a loss of self-consistency. It remains to be seen if the improvements suggested by the general formalism itself can be carried out without a considerable increase in complexity.

REFERENCES

[1] BARDEEN, J., COOPER, L.N., SCHRIEFFER, J.R., Phys. Rev. 108 (1957) 1175.
[2] BOGOLUBOV, N.N., Soviet Phys.-JETP 7 (1958) 41.

[3] VALATIN, J.C., Nuovo Cim. 7 (1958) 843.
[4] BOHR, A., MOTTELSON, B., PINES, D., Phys. Rev. 110 (1958) 936.
[5] BELYAEV, S.T., Kgl. Danske Videnskab. Selskab, Mat. Fys. Medd. 31 11 (1959).
[6] KISSLINGER, L.S., SORENSEN, R.A., Kgl. Danske Videnskab. Selskab, Mat. Fys. Medd. 32 9 (1960).
[7] ARVIEU, R., BARANGER, E.M., GILLET, V., VENERONI, M., Phys. Letters 4 (1963) 407.
[8] BOGOLUBOV, N.N., Soviet Phys.-Usp. 2 (1959) 236.
[9] BARANGER, M., Phys. Rev. 122 (1961) 992.
[10] CAMIZ, P., COVELLO, A., JEAN, M., Nuovo Cim. 36 (1965) 1663, and 42 (1966) 199.
[11] VOGEL, P., Phys. Letters 13 (1964) 144.
[12] PAL, M.K., BANERJEE, M.K., Phys. Letters 13 (1964) 155.
[13] GOSWAMI, A., Nucl. Phys. 60 (1964) 228.
[14] NOGAMI, Y., Phys. Rev. 134 (1964) B313.
[15] NOGAMI, Y., ZUCKER, L.J., Nucl. Phys. 60 (1964) 203.
[16] LIPKIN, H.J., Ann. Phys., N.Y. 9 (1960) 272.
[17] BAYMAN, B.F., Nucl. Phys. 15 (1960) 33.
[18] KERMAN, A.K., LAWSON, R.D., MacFARLANE, M.H., Phys. Rev. 124 (1961) 162.
[19] SALUSTI, E., Nuovo Cim. 37 (1965) 199.
[20] JEAN, M., Nuovo Cim. 40 (1965) 1224.
[21] Such amplitudes have also been considered by:
KERMAN, A., KLEIN, A., Phys. Rev. 132 (1963) 1326.
[22] A similar set of equations for the treatment of the pairing force has also been derived by:
DO DANG, Giu, KLEIN, A., Phys. Rev. 143 (1966) 735.
[23] PAWLIKOVSKI, A., RYBARSKA, W., Soviet Phys.-JETP 16 (1963) 388.

PART III

NEUTRON SPECTROSCOPY

CHAPTER 14

FUNDAMENTAL METHODS IN NEUTRON SPECTROSCOPY

E. R. RAE

1. INTRODUCTION

The neutron is a most important particle in the study of nuclear reactions and of the structure of solids and liquids. Because of the absence of charge, neutrons can be used as bombarding particles at very much lower energies than is possible with charged particles. Measurements of nuclear cross-sections for low energy neutrons, for example, led to the observation of compound nucleus resonances which was of fundamental importance to the development of nuclear theory and there are many other aspects of nuclear structure which have been investigated sucessfully with the use of neutrons. Slow neutrons are also employed in crystallography and in the study of inelastic scattering from solids and liquids. This work too has proved to be basic to the understanding of the structure of bulk matter.

Neutron spectroscopy is the name given to experimental studies in which the energy or wavelength of neutrons is measured, so that our field might include physical phenomena ranging from the study of the interaction of very slow neutrons with bulk matter, through the energy range from a few eV to a few tens of MeV where the interest is in nuclear structure, right up to high energy interactions where the topics studied are the nucleon-nucleon forces or the structure of the nucleons themselves. In this chapter our primary field of interest is that of nuclear structure so that we shall restrict our discussions to methods relevant to that field. Some of the techniques described will, of course, be applicable also to the very low and very high energy studies.

In discussing neutron spectroscopy we shall be mainly interested in studying the interaction of neutrons produced in a 'Neutron Source' with other nuclei chosen by the experimenter. The techniques described, however, can be and are also used to study the energy spectra of neutrons emitted in nuclear reactions.

The author is at the Atomic Energy Research Establishment, Harwell, Didcot, Berks, United Kingdom.

2. NEUTRON SOURCES AND DETECTORS

2.1. Neutron sources

The neutron is a neutral particle of mass comparable to the proton and is a constituent of nuclear matter. It was first observed in 1930 by Bothe and Becker (see, for example, Segré [1]) when they bombarded beryllium with alpha particles, but was not identified as being a neutral heavy particle until 1932 when Chadwick [2] analysed the recoils of protons and other light nuclei following collisions with the new radiation and showed that all of the data were consistent with the existence of this new neutral particle of near protonic mass which he called the neutron. The simplest neutron sources still utilise the (α, n) reaction [3] in light elements and consist of an intimate mixture of an α-emitter such as Ra or Po with a light element such as Be. These sources are small in size and can produce typically 10^6 to 10^8 fast neutrons per second. The neutron spectrum obtained (Fig. 1) is rather ill defined owing to the straggling of the α-particles, the high excitation produced in the compound nucleus which allows the emission of neutrons leaving the residual nucleus in several different states, and the Doppler broadening of any sharp groups which might otherwise be present.

Another type of radioactive source [3] consists of a mixture of an energetic γ-ray emitter with Be or D. Here the γ-rays are homogeneous in energy, and the excitation of the compound nucleus modest, so that a reasonably monoenergetic group of neutrons can be produced. (Energy range ~ 25 keV → MeV).

In this case the source strengths obtained are of the order 10^5 to 10^7 neutrons per second, for a conveniently small source.

For more intense neutron sources, accelerators or reactors must be used. Charged particle reactions with light elements can give intense sources of nearly monochromatic neutrons [4] over a range of energies up to ~ 20 MeV. The reaction $^7\mathrm{Li} + \mathrm{p} \rightarrow {}^7\mathrm{Be} + \mathrm{n} - 1.647$ MeV (endothermic) is an effective neutron source for energies from a few tens of keV up to ~ 600 keV where a second group of neutrons appears (Fig. 2). Above this the reaction $\mathrm{T} + \mathrm{p} \rightarrow {}^3\mathrm{He} + \mathrm{n} - 0.764$ MeV takes over (also endothermic) and is used up to ~ 4 MeV. For higher energy neutrons exothermic reactions such as $\mathrm{D} + \mathrm{D} \rightarrow {}^3\mathrm{He} + \mathrm{n} + 3.27$ MeV and $\mathrm{T} + \mathrm{D} \rightarrow {}^4\mathrm{He} + \mathrm{n} + 17.6$ MeV are used. Very high energy neutrons (50 MeV and higher) are usually obtained by deuteron stripping or by charge exchange collisions with light nuclei (Fig. 3).

White sources of neutrons: for slow neutrons, reactors can give fluxes up to $\sim 10^{15}$ neutrons/cm^2 sec and intense beams can be extracted. Intense pulsed white sources of neutrons for use in time-of-flight neutron spectroscopy are best obtained from accelerators [5] such as electron linacs where (γ, n) and (γ, F) reactions are used, or cyclotrons where heavy element targets are bombarded directly with energetic protons each of which can boil off several neutrons from the compound nucleus. With these machines, the neutron production rate during the pulse can be $\sim 10^{18}$ n/sec.

2. 2. Slowing down of neutrons

Reactor sources of neutrons are normally provided by thermal reactors where the primary fast fission neutrons have been moderated by collisions with light nuclei, principally of deuterium or carbon. In such an environment, and in the absence of capture or escape, a fast neutron loses energy by elastic collisions with the moderator nuclei until finally coming into thermal equilibrium with the moderator atoms. It can easily be shown that in such collisions (before thermal equilibrium has been reached) a neutron has an equal probability of having an energy after the collision lying anywhere between E_0 and $E_0[(A-1)/(A+1)]^2$ where E_0 is its initial energy, and A is the mass of the moderator nucleus. For the case of hydrogen as a moderator, A = 1, and the final energy is equally likely to lie anywhere between E_0 and 0. From this law of energy loss it can be deduced that the spectrum of neutrons

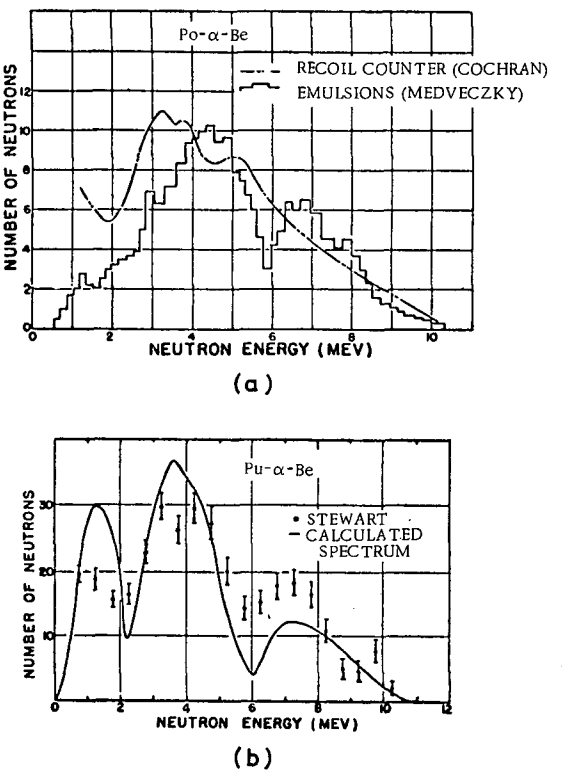

FIG. 1 (a) The neutron energy spectrum from Po-α-Be as measured by Cochran and Henry and by Medveczky

(b) The neutron energy spectrum from Pu-α-Be as measured by Stewart. The solid line is the spectrum calculated by Hess on the assumption that all the reactions proceed to levels in ^{11}C (Ref. [4] p. 10).(Courtesy of Interscience Publishers, New York.)

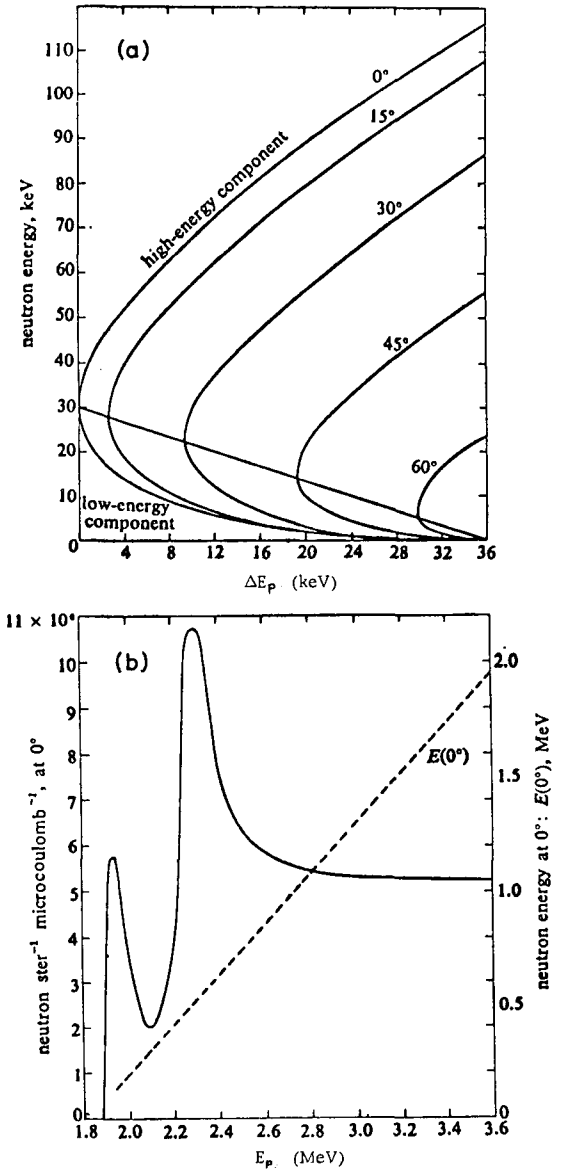

FIG. 2 (a) Neutron energies from a thin lithium target as a function of the difference ΔE_p between the energy of the bombarding proton and the threshold energy, for various angles of emission in the laboratory system

(b) Yield of neutrons at 0° from the Li(p,n) reaction as a function of the proton energy; target thickness 40 keV [Hanson, Taschek and Williams, Rev. mod. Phys. 21 (1949) 435]. (Courtesy of American Institute of Physics)

slowing down in a moderator, in the absence of capture or escape, is given by

$$N_E \, dE \propto \frac{dE}{E} \qquad (2.1)$$

and the slowing down spectrum observed in well moderated reactors follows this law closely.

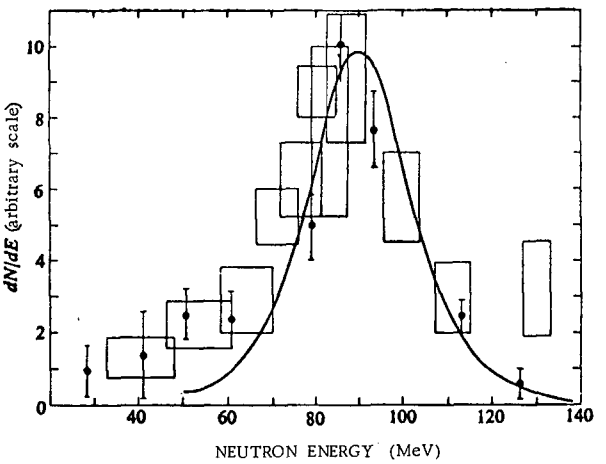

FIG. 3. Energy distribution of neutrons obtained by stripping a 190-MeV deuteron on a 1.27-cm-thick beryllium target. The curve is from the stripping approximation (Ref. [1] p. 533). (Courtesy of W. A. Benjamin Inc.)

When the neutrons reach thermal equilibrium they give rise to the well-known Maxwellian spectrum which is the dominant feature of the spectrum of a well moderated reactor. This comes about since the slowing down process occupies about 10^{-4} sec while the neutrons spend perhaps 10^{-3} sec in thermal equilibrium before being captured or escaping.

Moderators are also used with pulsed accelerator sources in order to degrade the energy of the neutrons produced into the energy range required. In this case however, since time-of-flight velocity measurements are normally involved, it is desirable to obtain the shortest possible pulse and the moderator is normally a sheet of hydrogenous material a few centimetres in thickness placed close to the neutron source. The criteria used in choosing such moderators will be discussed more fully later, but it is clear that escape of the neutrons from such a moderating slab is relatively easy which leads to a much weaker thermal peak, a relatively enhanced slowing down spectrum, and a marked hardening of the latter spectrum.

2.3. Sources of polarized neutrons

Fast neutrons emitted from nuclear reactions such as ^{7}Li(p, n) ^{7}Be are, in general, polarized [6]. High energy polarized neutrons can also be produced by scattering on helium [6] for example, where the

scattering is predominantly of a $p^{3/2}$ nature, i.e. p-wave scattering with the neutron's intrinsic spin parallel to the direction of the orbital angular momentum.

Slow (thermal) neutrons can be polarized by the interaction of the neutron's magnetic moment with the atomic magnetic fields in a ferromagnet [7]. This interaction produces two distinct scattering lengths for interactions in which the neutron's spin is parallel or antiparallel to the magnetic field. Hence transmission of slow neutrons through a saturated ferromagnet produces a polarized beam, and polarizations of up to 50% have been obtained by this method. Reflection from a cobalt mirror where one amplitude is negative, can lead to complete polarization. Polarization of epithermal neutron beams can best be achieved by transmission through a paramagnetic crystal containing water of crystallization in which the protons in the water are aligned at low temperature in a magnetic field and then polarized by means of hyperfine coupling with the paramagnetic ions, using microwave pumping [8] (Fig. 4). The large difference in cross-section between singlet and triplet interactions between the neutrons and protons produces a polarization of the transmitted neutron beam.

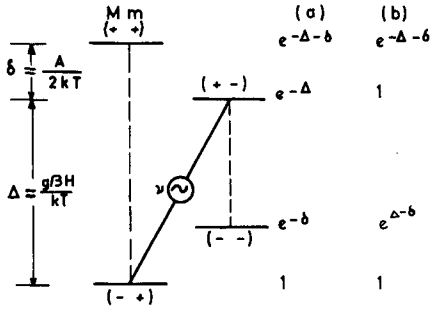

FIG. 4. Dynamic polarization (Ref. [8] p. 5) (Courtesy of Interscience Publishers, New York)

2.4. Neutron detectors

Probably the most common detector of slow neutrons is the BF_3 proportional counter. Here the neutron is detected through the $^{10}B(n,\alpha)^7Li$ reaction, and if boron highly enriched in ^{10}B is used, the efficiency of these detectors can approach unity for thermal neutrons. The collection of charge in a proportional counter is however essentially slow and introduces a considerable time jitter ($\gtrsim$ 0.5 μsec) into the response of these counters, so that they are unsuitable for use in time-of-flight spectroscopy where the timing error from other sources is $\lesssim$ 1 μsec.

A much more efficient and rather faster detector is obtained by the use of a ^{10}B loaded liquid scintillator, or a mixture of ^{10}B with a zinc sulphide scintillator. For fast timing however, two detectors stand out. These are

(1) the ^{10}B-plug with NaI crystal to detect the γ-rays following the emission of α-particles in the $^{10}B(n,\alpha)^7Li$ reaction which leave the ^7Li in an excited state 480 keV above the ground state.

For neutrons of energy less than 100 keV, the probability of the emission of the γ-ray is $\sim 95\%$.

(2) ^{6}Li loaded glass where the charged particles from the ^{6}Li(n, α)T reaction are detected in a scintillating glass.

Both of these detectors are capable of timing jitters of only a few nsec (provided a fast-slow system is used with the NaI detector). The ^{6}Li glass has the higher efficiency below ~ 1 keV, but is more sensitive to γ-rays from the neutron source: the ^{10}B plug can preserve a relatively constant efficiency up to ~ 10 keV. At energies $\gtrsim 100$ keV, proton recoil detectors become attractive, and in the MeV region they are the most common type, generally taking the form of a liquid or plastic organic scintillator. In the case of liquid organic scintillators, the sensitivity to γ-rays can be drastically reduced by the use of pulse shape discrimination (PSD) in addition to pulse-height selection (PHS). Here one takes advantage of the difference in the decay time constants between the light pulses produced in the scintillator by protons and α-particles on the one hand, and electrons on the other.

The properties of a range of neutron detectors are summarized [9] in Table I and Fig. 5.

3. NEUTRON SPECTROMETERS

3.1. General types of spectrometer

Most neutron spectroscopy at low energies ($\lesssim 1$ eV) utilizes neutron diffraction (Bragg condition) either as a monochromator or analyser. At high energies ($\gtrsim 1$ MeV) the observation of the energies of charged reaction products (e.g. ^{3}He(n, p)T) or knock-on elastic collisions with protons can be used to infer the energies of fast neutrons. Experiments can also be carried out with neutrons produced by charged particle reactions such as ^{7}Li(p, n)^{7}Be where the neutron energy is fixed by the reaction.

The only technique, however, which offers a precise determination of neutron energies over the entire range of interest (certainly from 10^{-2} -10^{8} eV) is that of time-of-flight where the neutrons are produced or released in short pulses, and their flight timed over a measured distance. Given sufficient intensity, the precision of these measurements can always be arbitrarily increased by increasing the distance (flight-path) over which the timing is accomplished, and furthermore the use of multi-channel time analysers permits measurements to be made at thousands of different energies simultaneously. We shall therefore devote most of our time in this section to studying the time-of-flight method and the properties of pulsed neutron sources.

3.2. Crystal spectrometer

Figure 6 shows a schematic drawing of the Argonne crystal spectrometer [30]. Neutrons from the reactor are collimated into a parallel beam and strike the crystal. The diffracted beam (again collimated) strikes the detector after passing through the sample being studied (transmission experiment). If the small angles of incidence

TABLE I. PROPERTIES OF SLOW NEUTRON DETECTORS

Detector[a]	Typical thickness		Timing resolution μs	Neutron peak			Discriminat. against gammas[b]	References	
	cm	atom/barn ^{10}Bi or ^{6}Li		Full width at half max.	Eqv. electr. energy (MeV)	Relative pulse height		Specific	General
(1) $^{10}BF_3$ Counter (at 150 cm Hg)	10	0.0004	$\geqslant$ 0.5	~5%	2.3	-	PHS		
(2) ^{10}B-plug and NaI(Tl) cryst.	2(^{10}B) 3(NaI)	0.14	0.05	~10%	0.48	480	PHS	10	
(3) ^{6}LiI(Eu) cryst.	2.5	0.046	~0.1	12%	4.1	1400	PHS	11	12
(4) ^{10}B-loaded liq.scint.	1.0	0.006	~0.4	60%	0.10	10-20	PHS & PSD	13	14,15
(5) ^{10}B-loaded glass	1.0	0.016	0.05	50%	0.18	(10)	PHS	16,17	20
(6) ^{6}Li-loaded glass	3.8	0.045	0.005	25%	1.6	200	PHS	18,19	21,22 23
(7) ^{10}B-ZnS(Ag) mixture	0.05	0.0004	~0.1	No peak			PHD & PSD	24	25,19 26
(8) Proton recoil	3	-	~0.01	No peak			TOF	27,28	
(9) Self-indication	-	-	~0.01	No peak			(PHD)	29	

Notes

[a] Detector compositions in percentage weight:
(4) Toluene (50), Methyl borate (50) + 4 g/l PBD + 0.02 g/l. POPOP (ref.11). For other recipes see ref.56.
(5) Na_2O (14.4), $^{10}B_2O_3$ (47.3), Al_2O_3 (30.7). Ce_2O_3 (7.6) (Ref.13).
(6) $^{6}Li_2O$ (11.7), Al_2O_3 (8.8), Ce_2O_3 (3.8), SiO_2 (75.7) (Ref.62).
(7) ZnS(Ag) (65) + Boron plastic (35), prepared from ethyelene glycol, n-butanol and boric acid in ratio 3.7 : 2.65 : 10 (ref.17).

[b] Method of discrimination against γ-rays.
PHS = Pulse Height Selection (i.e. single channel). PSD = Pulse Shape Discrimination.
PHD = Pulse Height Discrimination. TOF = Time-Of-Flight.

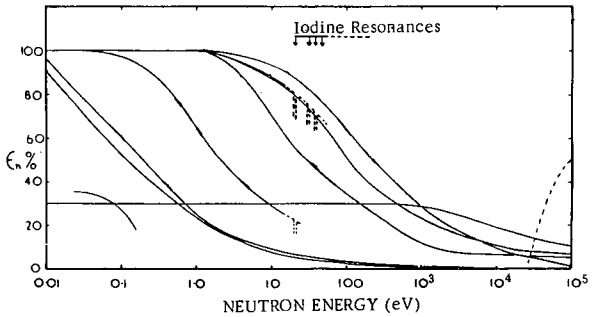

FIG. 5. Neutron detector characteristics for various detectors

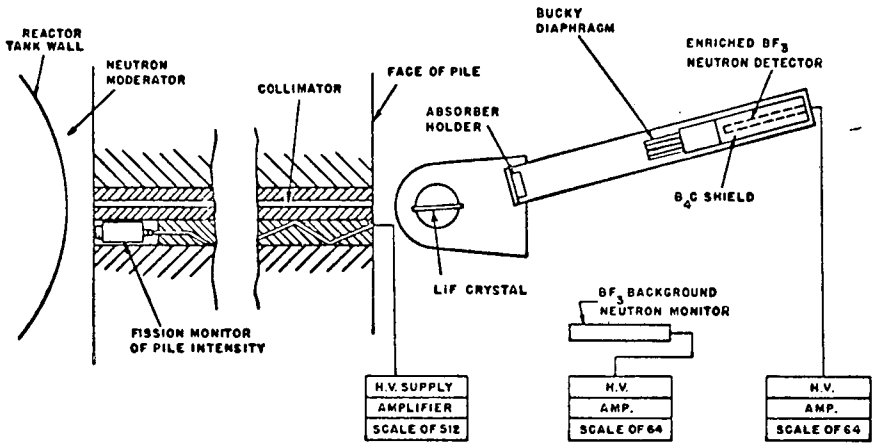

FIG. 6. The principle of the crystal monochromator for production of monoenergetic neutrons; shown here in schematic form is the apparatus at the Argonne heavy water pile (Ref. [7] p. 160). (Reprinted by permission from D.J. Hughes, Pile Neutron Research (1953), Addison-Wesley, Reading, Mass., USA)

and reflection are both equal to θ then the Bragg condition determines the wavelengths for which there is an interference maximum, namely

$$2d \sin \theta = n \lambda \tag{3.1}$$

where d is the spacing of the lattice planes of the crystal (parallel to surface), λ is the neutron wavelength for Bragg reflection, and n is an integer denoting the order of the reflection.

We have also

$$\Delta\lambda = \frac{2d}{n} \cos\theta \ \Delta\theta \tag{3.2}$$

$$\text{i.e.} \ \frac{\Delta\lambda}{\lambda} = \cot\theta \ \ \Delta\theta \tag{3.3}$$

or for small θ,

$$\frac{\Delta\lambda}{\lambda} = \frac{\Delta\theta}{\theta} = \frac{1}{2}\frac{\Delta E}{E} \tag{3.4}$$

Clearly the energy resolution ($\Delta E/E$) becomes worse as λ and θ become small, since $\Delta\theta$ (and so $\Delta\lambda$) is fixed by the collimator design. We have then

$$\frac{\Delta E}{E} = \frac{2\Delta\theta}{\theta} = \frac{2\Delta\lambda}{\lambda} = \text{const. } 2v \tag{3.5}$$

where v is the neutron velocity (non relativistic). This is the same law as will be derived later for time-of-flight spectrometers and the constant, which has the dimensions of an inverse velocity is normally expressed in microseconds or nanoseconds per metre. The factor 2 is inserted for consistency with the time of flight analysis (Eq. (3.7)).

The use of the crystal spectrometer at neutron energies much below thermal is limited by the importance of higher order reflections ($n > 1$) involving the intense Maxwellian peak. This difficulty can be overcome by the use of mechanical monochromators. At higher energies its usefulness is limited by its relatively poor resolution and its falling intensity – the reflectivity of the crystal varies as $1/E$. The usefulness of crystal spectrometers is therefore restricted to neutron energies below about 10 eV.

3.3. Time-of-flight spectrometers

Time-of-flight spectrometers utilize normally a pulsed source which provides neutrons over a wide band of energies. The basic principle of the method is that the time interval between the emission of the pulse of neutrons and the arrival of individual neutrons at a distant detector is a measure of the neutron velocity, and so energy. By connecting the output of the detector to a multi-channel time sorter, the distribution in velocity of the neutrons from the source is obtained directly. Let us suppose that the neutron pulse has duration Δt, that measurements are made over a flight path of length l and that the delay t between the start of the neutron pulse and its detection can be determined exactly. Let us further assume that the physical dimensions of the pulsed source and detector introduce an uncertainty Δl into the flight path length. Then we can write the energy resolution $\Delta E/E$ as:

$$\frac{\Delta E}{E} = \frac{2\Delta v}{v} = \frac{2\sqrt{(\Delta l)^2 + (v\Delta t)^2}}{l} \tag{3.6}$$

Δl and Δt being assumed to have independent gaussian distributions, and v being, as before, the neutron velocity. We observe at once that in the high energy limit, where $(v\Delta t)^2 \gg (\Delta l)^2$, this expression becomes

$$\frac{\Delta E}{E} = 2v\frac{\Delta t}{l} \tag{3.7}$$

where $\Delta t/l$ is the nominal resolution in microseconds or nanoseconds per metre.

It is also clear that in the low energy limit, the resolution is given by $\Delta E/E = 2\Delta l/l$ which is independent of the neutron's velocity and of the pulse length provided the latter satisfies the inequality $(v\Delta t)^2 \ll (\Delta l)^2$. Hence to achieve good resolution at low neutron energies (say $E_n < 100$ eV) the important factors are a long flight path and short detector, while at high energies, say $E_n > 10$ keV, the most important factor apart from the flight path length, is the shortness of the pulse Δt. The timing uncertainty in the moderation process in the case of pulsed accelerators can be shown to be roughly equivalent to an irreducible length uncertainty Δl of the order of a few centimetres (Eq. (3.8)). This fact must be borne in mind in calculating resolution widths.

3.3.1. Mechanical choppers

A chopper consists essentially of a rotor which is opaque to the neutrons being studied, but which has a slit or slits cut across it which come momentarily into line with a collimated neutron beam as the rotor spins, thereby allowing a pulse of neutrons to proceed down a flight path which is either evacuated or filled with a gas of low neutron cross-section. Many different designs of chopper have been made with slit systems designed to give high transmission, good resolution, good stopping power to neutrons and gamma rays between neutron pulses, and also to modify the neutron spectrum transmitted so as to prevent the passage of very slow neutrons whose arrival at the detector might coincide with that of faster neutrons from the next burst. Choppers have also been constructed which employ two or more phased rotating systems to give more control of the neutron spectrum and pulse length and to make these quantities independent of the pulse repetition frequency. A general discussion on neutron chopper spectrometers will be found in Ref. [31].

Although many of the early neutron resonance cross-section measurements were made with choppers, it is now generally recognized that the development of very intense pulsed accelerator neutron sources has restricted the energy region in which choppers are competitive to below about 100 eV. (This limitation is due essentially to the rather long pulse, ~ 1 μsec). We shall not therefore devote too much time to this instrument, but Fig. 7 shows a schematic drawing of the ORNL Fast Chopper (the adjective fast implies that it is for use with epithermal neutrons). This instrument, which in normal use produces a 1 μsec pulse every millisecond, is used with flight paths of up to 100 m, where it achieves a nominal resolution of 10 nsec/m. This should be compared with the corresponding figure of about 100 nsec/m obtainable with crystal spectrometers, and also with figures of better than 0.5 nsec/m obtainable with pulsed accelerators. Choppers, of course, have found other uses in conjunction with pulsed accelerator neutron sources. For example two choppers are used in conjunction with the Nevis Pulsed Cyclotron in order to reduce gamma-flash problems and neutron overlap [32], and choppers are also used to analyse the time dependence of neutron spectra in moderating systems pulsed by accelerators [33].

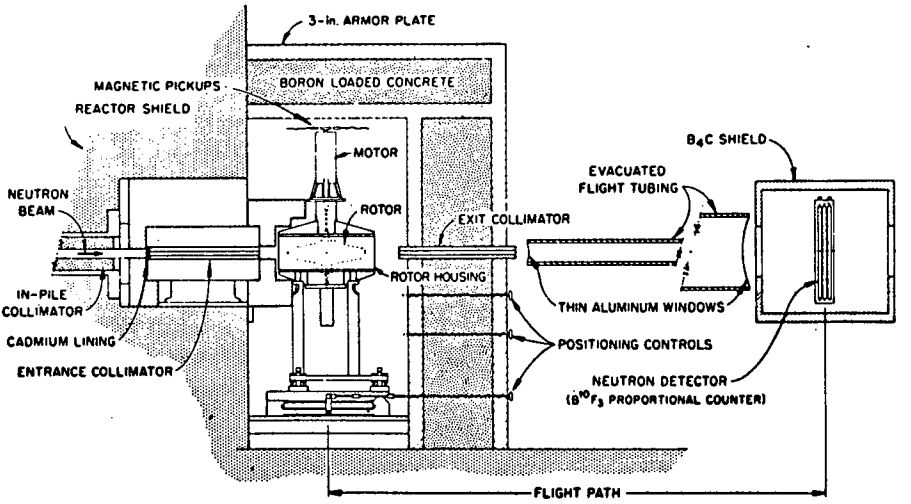

FIG. 7. A schematic section of the ORNL fast chopper time-of-flight neutron spectrometer [Harvey, J. A., Neutron Physics (Yeater, M. L., Ed.) 2 (1962) 65, Academic Press]. (Courtesy of Academic Press, New York)

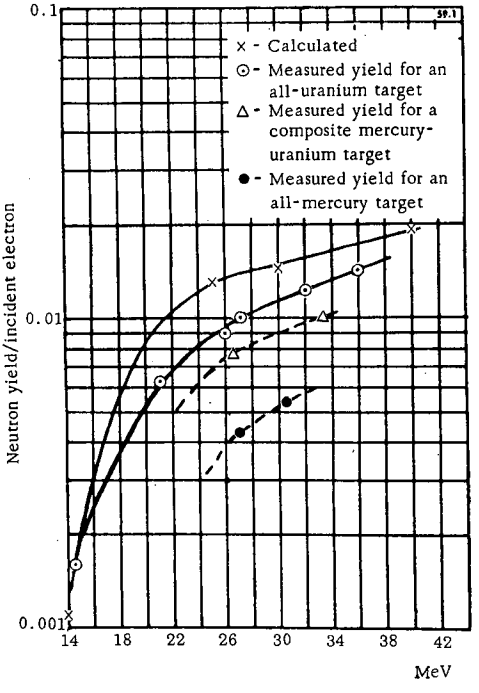

FIG. 8. Variation of neutron yield from uranium with electron energy [34]

3.3.2. Pulsed accelerators

(a) Electron linear accelerator. The commonest type of particle accelerator to be used as an intense pulsed neutron source is the electron linear accelerator. Here a pulsed electron beam, characteristically ~1 A, is produced from an electron gun and accelerated by an electromagnetic wave travelling along the inside of a wave guide. The waveguide is such that the electric field is axial, and is loaded so that the phase velocity of the wave at the input end matches the injection velocity of the electrons from the gun. The phase velocity increases until after a few metres it is indistinguishable from the velocity of light. The electron beam emerges from the end of the waveguide with an energy of at least several tens of MeV and strikes a heavy element target where it produces an extremely intense flash of bremsstrahlung. The photons produced eject photo and fission neutrons from the heavy target and these are moderated in a slab of hydrogeneous material before being allowed to escape down a system of flight tubes. Figure 8 [34] shows the variation in neutron yield with electron energy for several different heavy targets and it will be seen that an electron energy of at least 25 MeV is required for efficient neutron generation. Above that energy the neutron yield increases only slightly faster than the electron energy and depends essentially on the total power in the beam.

The primary neutron spectrum produced is essentially a fission spectrum peaking at an energy ~1 MeV and dropping off fairly rapidly both below and above this energy. The neutron producing target frequently has dimensions of the order of a few mean free paths in order to obtain efficient conversion of the bremsstrahlung beam, so that some degradation of the neutron spectrum occurs owing to inelastic scattering in the heavy target. Hence the effective spectrum tends to peak rather below 1 MeV. This neutron spectrum then interacts with the moderator in order to produce a slowing down spectrum which increases the flux below about 100 keV.

Figure 9 shows a schematic section of the Saclay neutron target which consists of a cylinder of natural uranium 3 cm in diam. by 10 cm long, surrounded by a water jacket and boron absorbers. Outside this assembly are placed the two moderator slabs of polyethylene. The function of the boron absorber is to prevent the passage of slow neutrons between the two moderator slabs which would prolong the neutron pulse. The boron is nevertheless transparent to the primary fast neutrons. Figure 10 shows the Harwell boosted neutron target. Here the electron beam is stopped in a cell containing flowing mercury, while most of the bremsstrahlung produced is absorbed in the ^{235}U sub-critical assembly with which it is surrounded. The neutrons produced are multiplied in the assembly by a factor of 10 giving a peak neutron-emission rate ~10^{18} n/sec. The neutrons then penetrate a boron absorber and are moderated in the water tanks. The relaxation time of the multiplying assembly is ~80 nsec which is the price paid for the multiplication obtained. The relaxation time of the Saclay plain target is of the order of the time taken for a primary neutron to cross it – say ~3 nsec. It is technically possible with an electron linac to achieve neutron emission rates of a few times 10^{18} by making use of the energy stored in the waveguide to accelerate currents of 20 or 30 A of electrons for a period of a few nsec, which is short compared to the filling time of the guide.

This technique is then complementary to the use of a boosted target and allows high instantaneous emission to be obtained in short pulses for use at higher neutron energies.

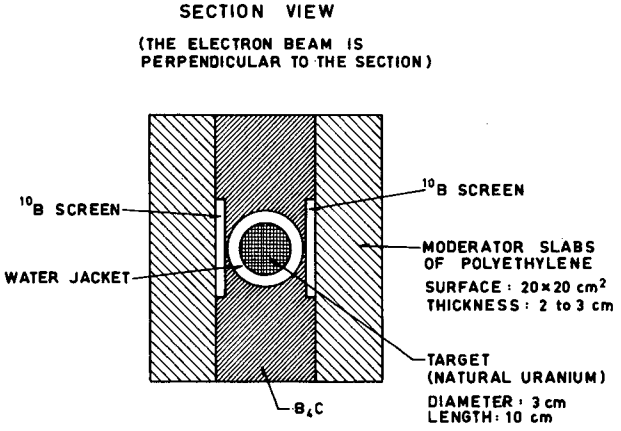

FIG. 9. Schematic section of the Saclay neutron target [36]

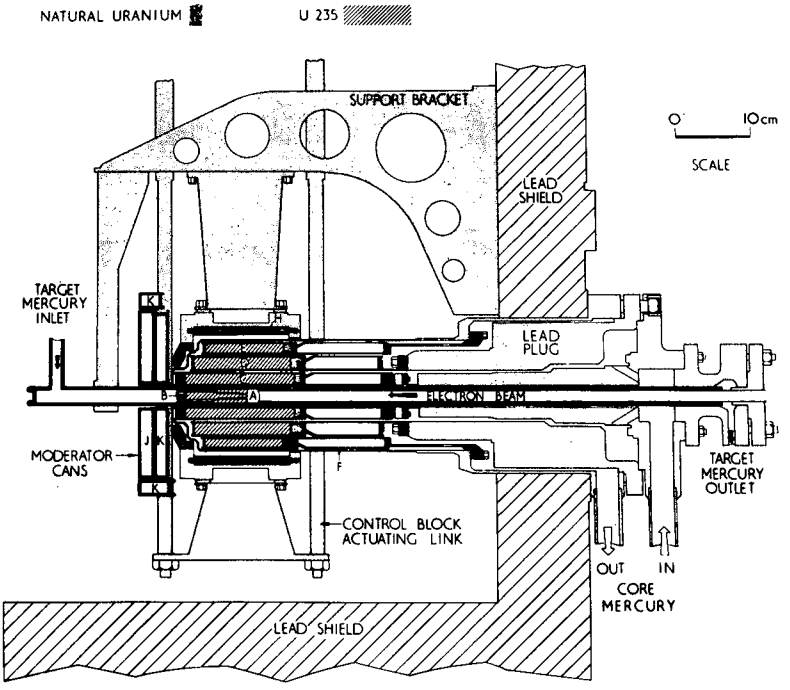

FIG. 10. Neutron target (Harwell Booster) [34]

Figure 11 [35] shows the spectrum from the Harwell boosted neutron source with and without the moderator present. The unmoderated flux for this rather large neutron source (linear dimensions ~ 15 cm) is shown

to peak between 200 and 300 keV, and the moderated flux is greater than the unmoderated flux for energies below about 55 keV, their ratio being about a factor of 100 at 1 keV. We should also note how the presence of the moderator removes some of the structure in the spectrum due to the steel canning of the target, and replaces it with another structure due to the thin aluminium walls of the moderator water tank and, at higher energies, the oxygen in the water (440 and 1000 keV). Before leaving this slide we should observe that the smooth moderated spectrum below about 10 keV has an energy dependence proportional to $E^{-0.78}$ (rather than E^{-1}) due to the large amount of leakage from the system. Above about 10 keV the spectrum decays even more slowly with increasing energy due, in part, to the falling neutron cross-section for hydrogen above this energy[1].

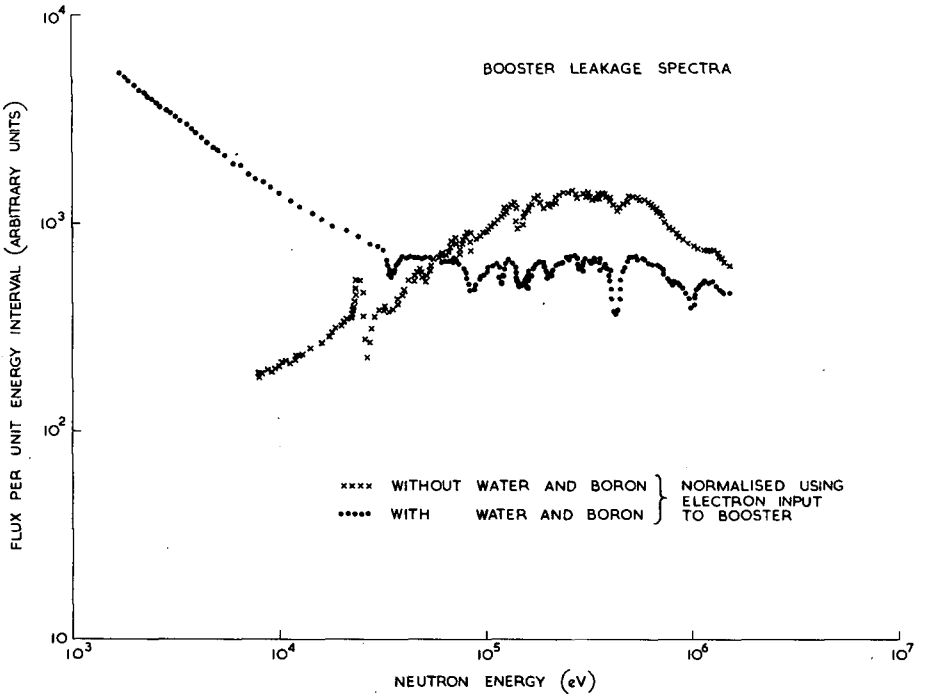

FIG. 11. Neutron booster leakage spectra

Let us now consider the problem of the choice of moderator material and thickness to obtain an optimum system, both as regards flux and timing uncertainties due to the slowing down process. The choice of material is essentially simple since clearly neutrons are moderated more rapidly in hydrogen than in any other material, so our moderator must contain as many hydrogen atoms per unit volume as possible. Michaudon [36] has studied carefully the best choice of material and

[1] The theory of neutron moderation shows that it is the product of the flux and the cross-section of the moderator nuclei which varies as 1/E for an infinite medium in the absence of capture.

concludes that nylon (6.6×10^{22} atoms/cm^3) and polyethylene (7.9×10^{22} atoms/cm^3) are the best practical moderators. Water has a similar hydrogen atom density to nylon but suffers from the disadvantage of having to be contained.

The choice of thickness of moderator is more complex. Michaudon [36, 37] has studied this problem theoretically and carried out Monte Carlo calculations on infinite slabs of moderator (water) of variable thickness, calculating the neutron flux (N), the slowing down time t and the variance σ^2 on the latter quantity as functions of the slab thickness, and of neutron entrance and emission energy and angle. It was found that both t and σ increase with the thickness initially, tending eventually to limiting values which correspond to the conditions in an infinite moderating medium. In Fig. 12 is plotted the quotient N/σ^2 which is taken as a factor of quality of the source[2], for 100 eV neutrons leaving the moderator. We see that the optimum thickness of moderator is a sensitive function of the energy of the primary neutrons, as one might expect, on account of the falling off of the hydrogen cross-section with increasing neutron energy.

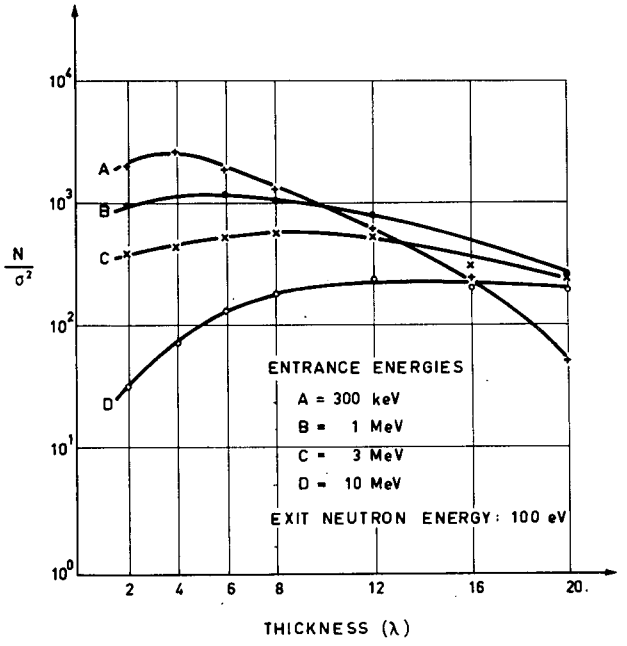

FIG. 12. . N/σ^2 versus λ for various E_e [36]

For a fission source however, the optimum thickness appears to be from 3 to 5 mean free paths according to the hardness of the spectrum. This thickness of moderator then leads to a moderation time jitter equivalent to a rectangular distribution of duration

$$\Delta t_m \approx \frac{2000}{\sqrt{E(eV)}} \text{ nsec}$$

[2] This quantity is proportional to the neutron flux for constant resolution if the neutron burst is of very short duration.

This is equivalent to a length uncertainty in the flight path of the order of 2-3 cm.

Figure 13 [36] shows the calculated spectra of the exit neutrons for various entrance energies and for a moderator of thickness 4λ. The effect of the drop off in the hydrogen cross-section above 10 keV is clearly seen. Finally Fig. 14 shows the variation of N and σ with exit angle and demonstrates that the high energy end of the spectrum becomes rather softer for large angles of emission. It should be mentioned here that the variation of σ with θ_{exit} shown in Fig. 14 takes account only of the variation in effective moderator thickness with angle. Since the moderator slab, in a practical case, is likely to be ~ 20 cm in diameter, the length uncertainty introduced into the flight path by having the finite slab other than normal to the direction of flight, far outweighs the rather small increase due to the change in effective thickness.

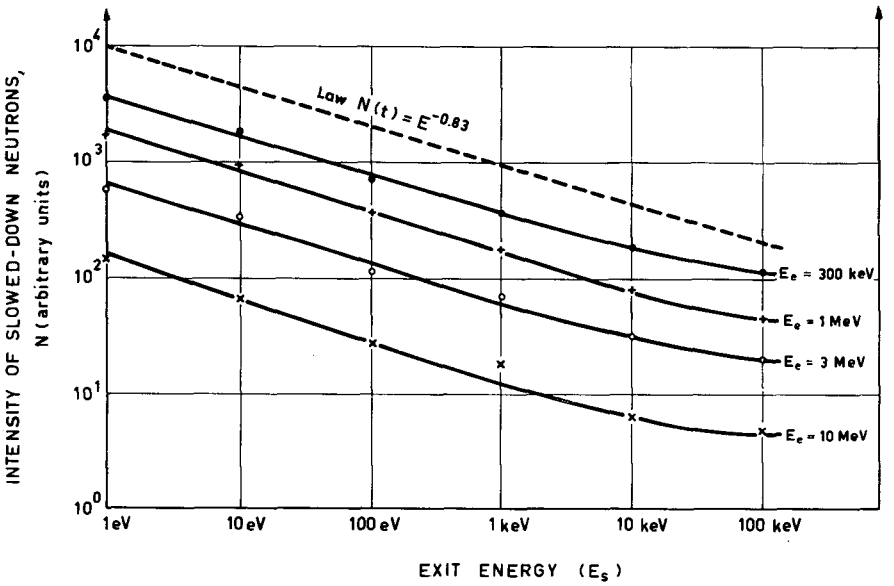

FIG. 13. Energy spectrum of exit neutrons versus thickness of the moderator for different entrance energies E_e [36]

This discussion has shown that the problem of designing an optimum target arrangement for a pulsed accelerator spectrometer is very complex since there are many parameters which can be varied. In practice the pulsed source is normally being used simultaneously by a number of experimenters each of whom has different requirements, so that the final solution is inevitably a compromise. Figure 15, which shows the general layout of the Harwell electron linac spectrometer system shows clearly how many beams can be used from the same pulsed source. These beams are used for time-of-flight experiments covering the energy region from about 10^{-2} to 10^{7} eV. Under these circumstances the shortest pulse compatible with the relaxation time of the boosted target (~ 100 nsec) is normally used, which optimizes

the system somewhere between 10^2 and 10^3 eV which is at about the geometric mean of the whole energy range used[3].

(b) Cyclotron. The use of the cyclotron as a pulsed neutron source has been developed at Columbia University where the Nevis 170-in. Synchrocyclotron has been used for many years in high resolution neutron spectroscopy. The synchrocyclotron accelerates protons to about 400 MeV, these particles forming a very intense bunch in the final orbit. This bunch can then be deflected downwards during one single orbit so that the whole bunch strikes the heavy lead target in a time short compared to the orbiting time. In the case of the Columbia machine, this ultimate burst width is about 20 nsec, and during this burst the instantaneous neutron production rate is $\sim 5 \times 10^{18}$ n/sec,

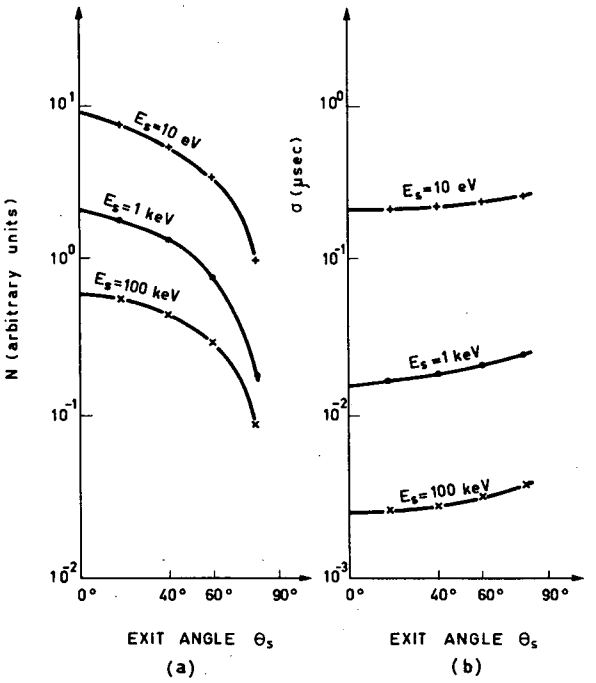

FIG. 14. Variation of N and σ with exit angle [36]

each proton boiling off several neutrons. Figure 16 [32] shows the general layout of the Nevis spectrometer including the two choppers referred to earlier which serve to remove the gamma flash and thermal neutrons from the beam. The discussion above concerning pulsed sources and moderation applies equally well to this accelerator, except the dimensions of the moderator are much greater (~10 cm) because of the higher energy of the incident neutrons. This leads to a slightly greater moderation time jitter than for the linacs, and to a slowing down spectrum which varies as $E^{-0.9}$.

[3] i.e. the accelerator pulse length becomes equal to the moderator time jitter in this energy range.

The 50 MeV sector focused cyclotron at Karlsruhe [38] has recently been used successfully as a neutron time-of-flight spectrometer. This accelerator can provide a high instantaneous neutron production rate ($\sim 10^{18}$) in a 1 nsec pulse and can also provide a very high repetition rate (2×10^4 ppsec) which makes it a very powerful source for fast neutrons. In the resonance region, of course, the very short burst is not helpful because of the moderation time spread, and the high repetition rate cannot be used because of overlap. At 1 keV, for example, the moderation time spread is ~ 50 nsec, so that the effective neutron production rate is $\sim 10^{16}$, and if a 100-m flight path is used to obtain a good resolution of 0.5 nsec/m, then the repetition rate must be reduced to, at most, 10^3 ppsec. Used under these conditions the count rate obtained would be at least an order of magnitude lower than the present Columbia or Harwell capabilities.

The Canadian proposal to build an Intense Neutron Generator (ING)[39], however, promises to provide a neutron time-of-flight system which will give fluxes in the resonance region which are several orders of magnitude higher than are presently available, for comparable energy resolution. This machine, which would provide facilities for a wide range of physics research, might be basically a series of three separated orbit cyclotrons sequentially accelerating protons to 1 GeV. For time-of-flight spectroscopy, it would provide micropulses of 2.3 nsec duration providing a current of ~ 0.5 A of protons on target, at a cyclotron frequency of 50 MHz. Either single micropulses, giving an instantaneous neutron production rate of 3×10^{19} n/sec, or assemblies of a few micropulses, giving 4×10^{18} n/sec, would be used, the repetition rate being adjustable, by the use of pulsed magnets, up to 10^4 pulses per second. Used in this direct way the performance of ING in the resonance region would be only marginally (if any) better than an advanced electron linac. It is proposed, however, that the output of the accelerator might be dumped in a storage ring, to be withdrawn 500 times per second to produce a 150-nsec pulse of staggering power, giving a neutron production rate in the pulse of 10^{23} n/sec. Even allowing for inefficiency of moderation because of the large size of the high power (65 MW) target, such a machine would clearly provide a source for use in the resonance region which exceeds its competitors by several orders of magnitude. In all fairness, however, it must be pointed out that its cost would also exceed that of an electron linac by several orders of magnitude, and that we are talking here about a system which, if built, would be pushing technology to the limit or beyond.

(c) Van de Graaff. The Van de Graaff accelerator is not competitive as a pulsed source of neutrons over a wide energy range with modern developments of pulsed linacs and cyclotrons. It does however have the advantage of comparatively low cost, and is unique in that it can produce very short pulses of neutrons in a narrow energy interval. With the advent of top terminal pulsing and the use of compression magnets, pulses of 10 mA of protons of duration 1 nsec can be produced. With the use of the ^{7}Li(p, n)^{7}Be and T(p, n)^{3}He reactions, these can produce short pulses of essentially monochromatic neutrons which can then be used to study by time-of-flight the spectra of neutrons inelastically scattered from suitable targets. The pulsed Van de Graaff accelerator

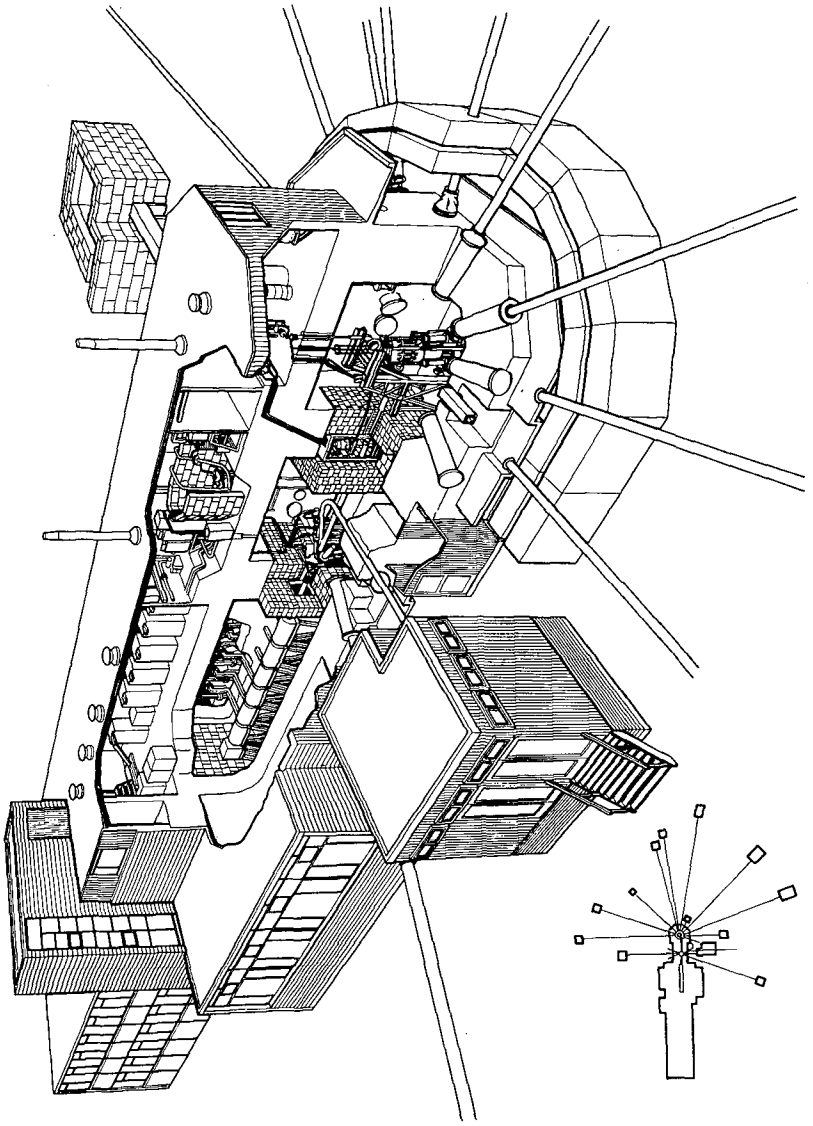

FIG. 15. Experimental layout of Harwell neutron project

can also be used to study directly, by time-of-flight, the spectra of neutrons produced in nuclear reactions such as the (p, n) reaction for a range of target nuclei.

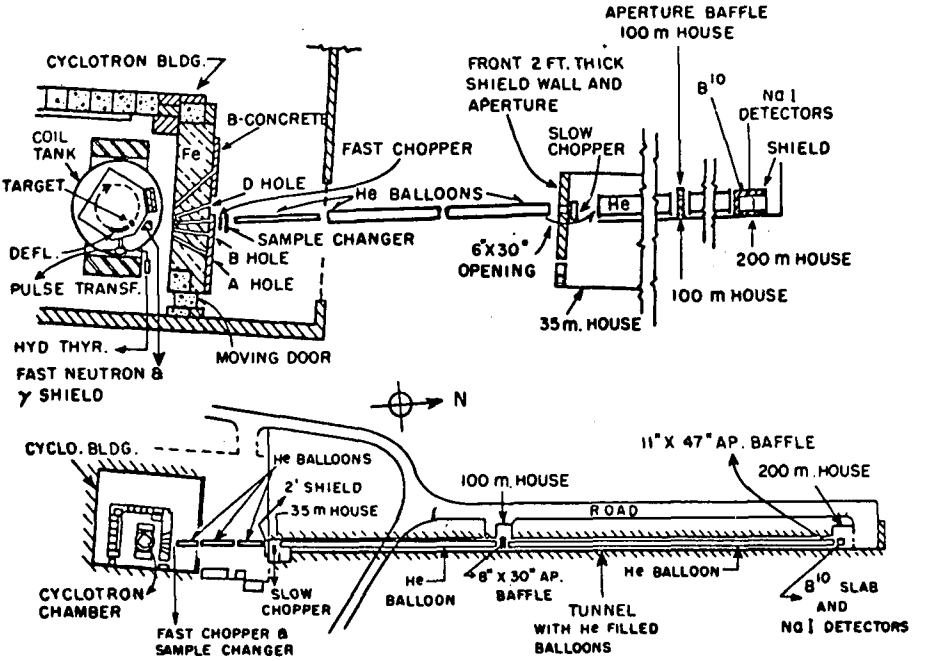

FIG. 16. Plan view of the Nevis neutron time-of-flight system including the synchrocyclotron and the 200 m flight path [32]. (Courtesy of U.S. Atomic Energy Commission)

The Van de Graaff accelerator has, of course, been used for many years as a continuous source of monochromatic neutrons, and this technique has been pushed by Newson close to its limit of resolution. By the use of the ^{7}Li(p, n) Be reaction with conical collimation in a backward direction he is able to achieve a resolution of $\lesssim 1$ keV with counting rates ~ 1000 counts/min. This technique permits total neutron cross-sections to be measured rather rapidly one energy point at a time. The disadvantage is that this resolution is only really competitive with the pulsed accelerators using time-of-flight at energies in excess of 100 keV. This point is shown clearly in Fig. 17 [40] which compares the energy spread ΔE obtained with various neutron spectrometers.

3.3.3. Pulsed reactor

The IBR pulsed reactor at Dubna [41] is another pulsed source which has been extensively used for neutron time-of-flight spectroscopy. This machine is the antithesis of the synchrocyclotron, producing a long intense pulse of duration at least 40 μsec at half height. Here the accelerator pulse length exceeds the irreducible moderation time jitter at all useful energies so that good resolution can only be obtained with the aid of very long flight paths. In fact flight paths of up to 1 km in length are employed.

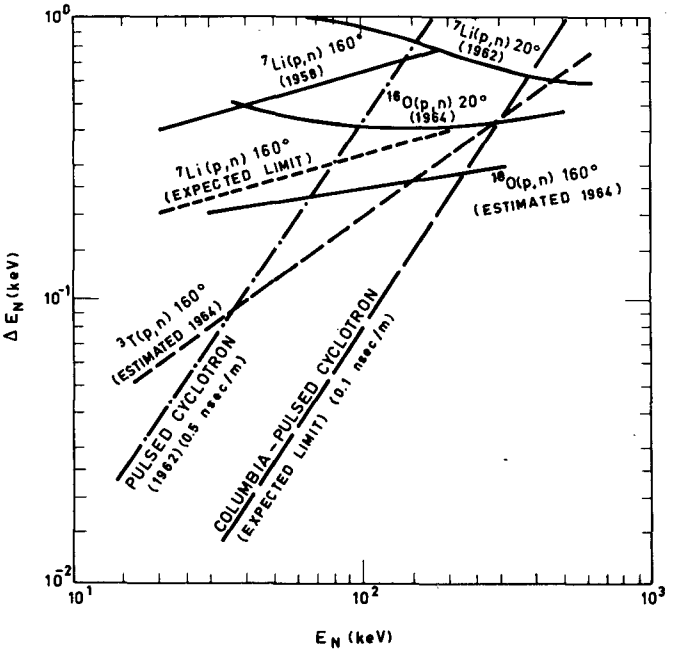

FIG. 17. A summary of neutron energy resolution in the keV region. The Harwell pulsed cyclotron corresponds to the "pulsed cyclotron expected limit curve" above about 200 keV (Ref. [40] p. 209). (Courtesy of North-Holland Publishing Co.)

The reactor core consists of a fixed part (plutonium rods inside a stainless steel shell) and two moving parts consisting of two lumps of ^{235}U fastened to discs rotating about a horizontal axis. The larger of the two ^{235}U lumps is mounted on a 110-cm diam. disc at a distance of 44 cm from its centre. It moves with a peripheral velocity of 276 m/sec when the disc is rotating at its normal rate of 6000 rev/min and passes through the centre of the core with each revolution. A smaller lump of ^{235}U is fastened to a small rotating disc of variable speed and passes with each turn through the edge of the core. When the two uranium lumps pass through the core simultaneously the reactor core becomes super-critical and generates an intense pulse of neutrons 8 times per second, of width ~ 36 μsec at half height. The purpose of the smaller lump of uranium is to enable the neutron pulse repetition rate to be altered without changing the pulse shape.

The larger lump causes a reactivity change of 7.4%; the smaller lump a change of 0.4%. The peak intensity in the pulse is $\sim 3 \times 10^{18}$ n/sec; the mean intensity is 3×10^{14} n/sec. The upper limit to the mean power level is fixed by the cooling problems at about 6 kW.

Used in this way the nominal resolution of the IBR with the 1000-m flight path is at best 40 nsec/m which is very poor except at low neutron energies.

In 1965 however the IBR was successfully operated in a subcritical state (compare Harwell boosted target) being driven by a 30 MeV electron microtron giving a pulse length of 2μsec 50 times per second.

The multiplication of the IBR during the pulse was 200, and out of the pulse was 10. Used in this way the neutron pulse length at half maximum was 4 μsec giving a time-of-flight resolution with the 1000-m flight path of 4 nsec/m which is intermediate between chopper and pulsed accelerator performance. This pulsed source has been used for many measurements including the first experiments with neutrons polarized by a dynamically polarized proton filter [42].

3.3.4. Nuclear explosions

The technique of using nuclear explosions for time-of-flight experiments has been developed at Los Alamos [43]. Here only a single pulse of neutrons is produced, but of such intensity that whole time-of-flight experiments are completed in one cycle, currents from detectors being recorded, rather than single events, as functions of the flight time. The nuclear device is situated at the bottom of a shaft 200 to 300 m deep, which serves as a flight path (it is evacuated), and the experimental equipment is set up in a tower above the shaft (Fig. 18). In the

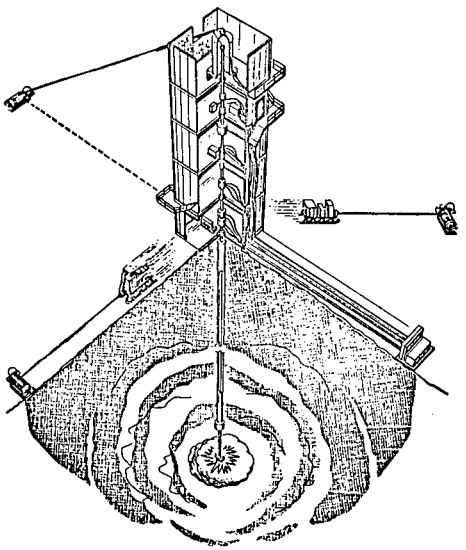

FIG. 18. Layout of a set of experiments using a nuclear explosion as a neutron source. The nuclear device was exploded a few seconds earlier two or three hundred metres underground. The vacuum pipe through which the neutrons travelled extends to the ground surface and on up the tower that houses the experiments. Two sleds containing experimental equipment are being towed to safety by winches while a third winch is pulling a package from the top of the tower. A few minutes later the ground will collapse and the tower will drop into a shallow crater (Ref. [43] p. 443). (Courtesy of North-Holland Publishing Co.)

'Petrel' explosion of June 1965 the moderator consisted of 5 cm of polyethylene with 6 cm of lead on the side towards the source, and 2 cm of lead on the other side of the polyethylene. The nearest lead was 29 cm from the centre of the source, and it served to absorb gamma rays, to keep the moderator cool, and to control the velocity of the moderator. The duration of the primary pulse was less than

100 nsec, and by the time the neutrons were emitted from the moderator its thickness had been reduced to 8 mm, its velocity was 5.5 cm/μsec, and its temperature 25 eV. In the Petrel experiment the lowest neutron velocity observed was 18 eV, corresponding to the velocity of the moderator, and the thermal flux peaked at 60 eV in the laboratory system, corresponding to 25 eV in the moving moderator. The moderator design can be adjusted to place the thermal peak in any desired energy region from a few eV to a few keV.

The production rate of neutrons in the pulse is 10^{31} n/sec, so that 10^{24} neutrons are produced in the 100 nsec pulse. This corresponds to running the present Harwell linac with 100 nsec boosted pulses for at least 10^{10} seconds or about 300 years. Even if one allows say a factor of 10 for the large number of flight paths used with the linac, it still corresponds to 30 years of running, so that clearly a nuclear explosion is a very powerful time-of-flight source. Its most useful feature is the very short duration of the experiment which means that measurements can be made on highly active materials which could not be attempted with more conventional methods. For example it becomes possible to measure very small sub-threshold fission cross-sections of highly active nuclides. The great disadvantage of course, apart from the cost and possible political difficulties, lies in the impossibility of repeating a measurement – and in the vulnerability to electronic failure.

3.3.5. Time-of-flight electronics (data acquisition)

This is a vast subject and is discussed at length in the literature [44]. It will suffice here to mention only the basic principles. A time-of-flight analyser consists essentially of a source of timing (clock) pulses, often locked to the basic cycle of the pulsed source, a scaler, and a memory of some sort. At the moment when the source is pulsed, or at some known time thereafter, the scaler is made to start counting the clock pulses. When the first neutron is detected at the end of the flight path, the scaler is stopped, so that its contents correspond to the time-of-flight of the neutron. The contents of the memory cell whose address corresponds to the contents of the scaler, is then incremented by one. In the case of the simplest (single-shot) type of electronics, the scaler contents are then set to zero and the whole process is repeated on the next cycle of the pulsed source. Thus there is built up in the memory a distribution of numbers corresponding to the time-of-flight spectrum of the neutrons. It is clear, however that if a second neutron is detected during a cycle, its time of arrival is not recorded, so that the single-shot system tends to record too few counts in the later channels. If the count rate is small compared to the repetition rate of the pulsed source (p.r.f.), this effect is small and is easily corrected for. If however the count rate begins to approach the p.r.f. then this simple system is insufficient.

The next stage of development is to add a 'buffer' between the scaler and memory. This is a small fast temporary memory capable of recording only a few words of data. The scaler is then stopped only long enough to transfer its contents to the buffer and is then started again, its contents having been adjusted meantime to allow for the

momentary stop (~ 1 μsec). This process can be repeated several times during a cycle of the pulsed source. Meantime the process of incrementing the cells in the main memory whose addresses correspond to the words in the buffer, goes on at a much slower speed, the transfer time in this case may be as fast as ~ 20 μsec, in which case the buffer is not strictly necessary, or as slow as a few hundred μsec when the need for the fast buffer is obvious. With such a system for restarting the clock and for temporary storage of a few words of data, it is possible to operate at counting rates of a few times the p. r. f. with negligible losses.

The clock pulses will be at the intervals chosen for the time channels, anywhere between a few nsec and a few μsec, and may even be programmed so as to give a certain number of very narrow channels followed by a number of wider channels, and so on, in order to achieve something approaching a constant value of ΔE over the whole energy range studied.

The main memory may be a core store memory with a relatively fast cycle time (a few μ sec) or it may be magnetic tape with a relatively slow writing speed (few hundred μsec). The advantage of the former is fast writing speed, higher permissible count rates with the same buffer, and immediate display of data. The advantage of the latter is relative cheapness, permanence of data, and very much larger number of channels available. Core store memories in excess of 4000 channels become very expensive whereas quite inexpensive magnetic tape systems can give millions of channels if necessary. This is especially important if two-dimensional experiments are involved. The data recorded on magnetic tape are later analysed, in blocks, in a digital computer.

The trend nowadays is towards the use of standard small computer hardware to provide both the core store and magnetic tape systems used for time-of-flight work.

3.4. Slowing down time spectrometer

This instrument [45] does not compete in resolution with modern time-of-flight spectrometers. It consists of a large lead cube into which a pulse of fast (14 MeV) neutrons from the T(d, n) reaction is introduced from a 300 kV Cockcroft Walton set. It utilizes the fact that these fast neutrons slow down by many collisions with lead nuclei so that they remain as a nearly homogenous energy group, allowing the energy at which the neutrons are captured in a small sample placed in the cube to be deduced from the time between the initial pulse and the detection of the prompt capture gamma rays. The thermalization time is 2 msec in lead. This device has good enough resolution to allow some individual resonances in capture cross-sections to be observed, and has mainly been used for measurements of capture cross-sections in the energy range up to 50 keV.

3.5. Other types of spectrometer [46]

Where the neutron source is weak and continuous, poor resolution measurements of fast neutron energy spectra can be obtained from the study of proton recoil tracks in nuclear emulsions, or from pulse

heights caused by suitably collimated recoil protons in proportional counters or scintillators. Another type of fast neutron spectrometer utilizes the exothermic reaction $^3He(n,p)T + 0.76$ MeV. Here the kinetic energy of the neutron is added to the reaction energy and can therefore be deduced from the pulse height obtained in a proportional counter containing the ^3He. This type of reaction spectrometer has the advantage that no knowledge is required of the direction of motion of the incident neutron so that such an instrument is suitable for measuring fast neutron spectra close to a weak source. The resolution obtained here is typically $\gtrsim 10\%$.

4. LOW ENERGY NEUTRON SPECTROSCOPY

4.1. Neutron resonances

By low energy neutron spectroscopy we mean essentially the study of neutron resonance interactions with nuclei, the cross-sections for these reactions, and the products of the reactions. The reactions we refer to consist of scattering and radiative capture which occur for all target nuclei, exothermic reactions such as (n, p) and (n, α) which occur for a few light nuclei like ^3He, ^6Li, and ^{10}B, and fission which occurs in ^{235}U and some heavier nuclei.

The energy region of sharp resonance peaks in the cross-section extends up to many MeV for the light elements, while for heavy fissile nuclei like ^{235}U, all sharp structure is gone from the cross-section above a few keV. Of course we must be careful to distinguish between the absence of structure due to poor resolution, and that due to the genuine overlap of many resonances. Since our purpose in this section is to study resonance cross-sections and reactions, let us begin by considering what a resonance is, what are its measurable features, and how we should determine these with the aid of the spectrometers described in section 3.

We find pronounced resonances, or peaks in the cross-section for nuclear reactions when semi-stationary states exist in the compound nucleus formed in the collision. By semi-stationary states we mean decaying states whose lifetimes are long compared with the periodic time of the compound nucleus -i.e. the time taken for the compound nucleus to return to its configuration at the moment of impact. This implies that the widths (Γ) of the states are small compared with their separation (D). The widths of the states are related to their lifetimes through the uncertainty relationship, and we can write for a resonance, s

$$\Gamma^s \tau^s \sim \hbar \tag{4.1}$$

and the mean separation is related to the periodic time in the same way

$$DT \sim \hbar \tag{4.2}$$

Where the compound nucleus can decay in a number of different ways, the total width Γ^s is the sum of the partial widths Γ_i^s corresponding to the various modes, or channels of decay. Each mode of decay for which the quantum mechanical states of the products are completely

determined, is called a channel. Thus the probability of decay of the compound nucleus per unit time through channel i is given by

$$P_i^s = \frac{\Gamma_i^s}{\hbar} \tag{4.3}$$

In low energy neutron induced reactions, the open channels are those for neutron re-emission, for charged particle emission in the case of a few light elements, for fission in the case of a few heavy elements, and for radiation. There are many channels for radiative decay, because of the large number of states lying below the neutron separation energy, so that very often only the sum of the partial widths of the radiation channels

$$\Gamma_\gamma^s = \sum_{i'} \Gamma_{\gamma i'}^s, \tag{4.4}$$

is observed. It might easily be imagined that the fission mode of decay would also occur through many channels, corresponding to the multitude of possible quantum states of the fragments. Experiment has shown, however, that the low energy neutron induced fission process corresponds to only a small number of open channels, which implies that the fission channels correspond not to the many possible final products, but to the small number of quantum states in which the compound nucleus can exist at the so-called saddle point. This interesting topic is discussed in detail in the companion lecture course of J. E. Lynn (not published in these proceedings).

The effect of the existence of a well isolated semi-stationary state on the cross-section for a low energy (s-wave) neutron interaction is expressed in the Breit-Wigner single level formulae [47]. Since we are now speaking about a single level, we shall drop the superscript s and write for a reaction channel r,

$$\sigma_{n,r}(E) = \pi \lambda\!\!\!^{-2} g(J) \frac{\Gamma_n \Gamma_r}{(E-E_R)^2 + (\frac{1}{2}\Gamma)^2} \tag{4.5}$$

where $\lambda\!\!\!^{-}$ is the de Broglie wavelength of the relative motion of neutron and target (divided by 2π), Γ_n is the neutron width, Γ the total width of the resonance, E is the neutron energy and E_R the resonance energy, and g(J) a statistical spin factor depending on the total angular momentum J of the compound nucleus state associated with the resonance: $g(J) = (2J+1)/2(2I+1)$. Γ_r is the width associated with the reaction being considered and may correspond to one or more channels.

The total width

$$\Gamma = \Gamma_n + \sum_r \Gamma_r \tag{4.6}$$

The reason why we have grouped the partial widths in this way is that for neutron interactions, the neutron width Γ_n, corresponds to the entrance channel (we assume here low energy s-wave neutrons involved, and that only one neutron channel is open). The re-emission

of a neutron through the entrance channel (elastic scattering) leads to a different behaviour of the cross-section because of interference between the resonance scattered wave and the wave corresponding to hard sphere, or potential scattering. The Breit-Wigner single level formula for s-wave scattering is therefore

$$\sigma_{n,n}(E) = \pi \lambda^2 g(J) \frac{\Gamma_n^2}{(E-E_R)^2 + (\frac{1}{2}\Gamma)^2} + \frac{4\pi \lambda g(J)\Gamma_n (\sigma_p/4\pi)^{\frac{1}{2}} (E-E_R)}{(E-E_R)^2 + (\frac{1}{2}\Gamma)^2} + \sigma_p \qquad (4.7)$$

where σ_p is the cross-section for potential scattering. The second term is the one describing the interference between the resonance and potential scattered waves.

These formulae contain implicitly the assumption that $kR \ll 1$ where k is the neutron number outside the nucleus ($k = 2\pi/\lambda$), and R is the nuclear radius. In this simple form, however, they represent a very good approximation to the behaviour of the cross-section up to an energy of several keV. We note that while the reaction widths in general change only very slowly with E, the s-wave neutron width Γ_n, varies as $\sqrt{E}$. It is clear from the Breit-Wigner formulae that the total width of a well-isolated resonance is indeed closely related to the width of the cross-section peak as observed on an energy scale. In the absence of resolution or other broadening of the curve it would be equal to the full width at half height of the peak in the cross-section curve. These simple formulae can be generalized to allow for finite values of kR and $1 > 0$, or the much more elaborate multilevel formalism can be invoked to deal with the situation where Γ is not small compared with D. Nevertheless the majority of the level parameters obtained from low energy neutron cross-section measurements have been deduced with the use of the single level formulae only and we shall make use of them in the interpretation of the cross-section curves, wherever possible. From an analysis of the cross-sections for low energy neutron induced reactions, we can hope to derive values of the potential scattering cross-sections, σ_p, the neutron and radiation widths of resonances in a wide variety of nuclei, and the fission widths in very heavy nuclei. We can also observe the resonance spacings D, and in favourable cases, the angular momenta J, of the resonances. The spectra of gamma rays following neutron capture into definite resonance levels can be studied, and also in certain cases, the mass distribution of the fragments released in the fission of heavy nuclei.

Since all of these quantities relate to highly excited semi-stationary states above the neutron separation energy, i.e. at excitations of 5-10 MeV, we cannot hope in general to interpret these quantities individually in terms of nuclear theory. We can, however, hope to interpret the mean values of the widths and spacings and the ratios of these quantities. In particular we would wish to observe the variation of these mean values with nuclear mass and charge and hope to interpret the variations in terms of nuclear structure. In addition to the mean values of widths and spacings, we also obtain the statistical distributions of these quantities, and the dependence, if any, of the mean values and distributions on angular momentum.

In the case of radiative capture, the study of resonance capture gamma-ray spectra helps to explain the behaviour of the total radiation

width Γ_γ with nuclear mass and charge. It also throws light on the nature of low lying states in the compound nucleus, which are the final states reached in transitions from the capturing state. Here we obtain information about low lying states which can be fitted into detailed level schemes which depend strongly on the structure of the compound nucleus. Similarly in the study of fission cross-sections, we also obtain useful information concerning the low lying states of the highly deformed fissioning compound nuclei at the saddle point.

4.2. The transmission experiment

This is the most fundamental method of deriving a cross-section, in that it provides an absolute measurement of the total cross-section through the defining equation

$$T = N/N_0 = \exp(-n\sigma_{nT}) \qquad (4.8)$$

where N_0 is the number of neutrons of fixed energy incident normally per unit time on a uniform slab sample of the pure nuclide under study, having a superficial atomic density of n atoms per barn (10^{-24} cm^2) and a total cross-section of σ_{nT} barns, N is the number transmitted per unit time without interaction, and $T = N/N_0$ is called the transmission of the sample. Note that this equation follows immediately from the concept of the total cross-section as the effective cross-section area of the nucleus for incident point particles.

Hence a measurement of T, with n known, defines σ_{nT} absolutely. Note that in such a measurement the efficiency of the neutron detector used need not be known, so long as it is constant, since the same efficiency factor ϵ will appear in both N and N_0 and will cancel. The measurement must, of course, be done in good geometry, that is, the neutron source and detector must be well separated, so that the neutron flux is nearly normal to the sample, and the sample must be far from both the source and detector. If the sample is close to the detector or the source, there will be a considerable probability of neutrons scattered in the sample reaching the detector, so that the apparent total cross-section measured will be too low. The sample must be far enough from both source and detector that the solid angle (divided by 4π) subtended by either at the sample, is very much smaller than the uncertainty aimed at in the cross-section measurement.

Again in a real experiment, one must distinguish carefully between those events observed in the detector which are due to the arrival of neutrons in the narrow energy interval being studied, and those events which are due to other causes (background). Merely to block the beam, or switch off the neutron source, is not normally a useful way of determining the background count rate, since part or even most of the background is usually associated with the neutron beam itself. In the case of the crystal spectrometer, it may be due to higher order Bragg reflections which introduce neutrons of energy different from the primary beam. In the case of monochromatic neutrons from nuclear reactions, there is the possibility of neutrons being thermalized and counted with high efficiency, and in the time-of-flight spectrometers, there is normally a very intense flux of gamma rays and fast neutrons through the detector early in the cycle, which may cause delayed events

in the detector which are indistinguishable from slower neutrons. Furthermore the background counting rate is generally dependent on the thickness of the transmission sample being studied, since most of the background events are due to neutrons or gamma rays which have in fact passed through the sample.

The normal means of determining the true background is by the use of resonance filters in which filters of materials having very strong resonances are inserted in the beam. Close to those resonances the value of $n\,\sigma_{nT}$ for the filter is very large so that the transmission T of the filter at resonance is arbitrarily close to zero. This then gives a spot measurement of the background at the energy of the filter resonance, and the effect of the thickness of the sample and the filter itself on the background must be studied and corrected for. When a number of background points have been established in this way, and their dependence on sample thickness understood, the background can then be calculated for a given experiment. The resonance filter technique, of course, can only be applied where the spectrometer resolution is reasonably good, i.e. $\Delta E \ll D$.

Let us suppose then that we have a time-of-flight spectrometer with a multichannel time analyser so that we can make transmission measurements at many energy points simultaneously over a range of energy up to a few keV. We shall assume that our transmission measurement is done in good geometry, that we have eliminated the very slow neutrons from previous cycles of the pulsed source by use of a suitably chosen boron filter, and we have studied carefully the background conditions so as to ensure that the background count rate is small ($\lesssim 10\%$ of wanted counts) and known. We are then ready to make transmission measurements as a function of neutron time-of-flight, moving the transmission sample into and out of the neutron beam every few minutes with some automatic device, in order to minimize normalization errors between N and N_0. We then obtain a transmission curve such as is shown in Fig. 19, or possibly a series of such curves, for different sample thicknesses. In order to analyse these curves, let us rewrite the single level Breit-Wigner formula for the total cross-section ($\sigma_{nn} + \sigma_{nr}$) in the following simple way

$$\sigma_{nT} = \frac{\sigma_0}{1+x^2} + \frac{2\sigma_0 a}{\lambda\!\!\!^{-}} \cdot \frac{x}{1+x^2} + 4\pi a^2 \qquad (4.9)$$

where

$$\sigma_0 = \sigma_{nT}(E_R) = 4\pi\,\lambda\!\!\!^{-2}\; g\Gamma_n/\Gamma$$

$$x = (E-E_R)/(\tfrac{1}{2}\Gamma)$$

and

$$\sigma_p = 4\pi a^2$$

where a is the scattering length. We note that Eq. (4.9) like (4.5) and (4.7) refers to centre of mass energies and wavelengths. The same forms of the equations hold also for laboratory co-ordinates, which are

the ones used in practice, except that in this case it is understood that the target nuclei are at rest. The target nuclei, however, have thermal motions and so the formulae for laboratory co-ordinates must take into account these thermal motions (Doppler broadening) and we must write

$$\sigma_{\Delta nT} = \sigma_0 \psi(\beta, x) + \frac{2a\,\sigma_0}{\chi} \phi(\beta, x) + 4\pi a^2 \qquad (4.10)$$

where

$$\beta = \frac{2\Delta}{\Gamma}, \qquad \Delta = 2\left(kT_{eff}\ E_0 \frac{m}{M}\right)^{\frac{1}{2}}$$

k is Boltzmann's constant, m and M are the masses of the neutron and target nucleus respectively, and T_{eff} is an effective temperature which depends on the Debye temperature of the target crystal

$$\psi(\beta, x) = \frac{1}{\beta\sqrt{\pi}} \int_{-\infty}^{\infty} \frac{1}{1+y^2} \exp\left\{\frac{-(x-y)^2}{\beta^2}\right\} dy$$

and

$$\phi(\beta, x) = \frac{1}{\beta\sqrt{\pi}} \int_{-\infty}^{\infty} \frac{y}{1+y^2} \exp\left\{\frac{-(x-y)^2}{\beta^2}\right\} dy$$

The expression for the transmission can then be written as

$$T(E) = \int_{-\infty}^{\infty} \exp\left[-n\sigma_{\Delta nT}(E')\right] R(E'-E)dE' \qquad (4.11)$$

where R(E) is the resolution function of the spectrometer, which in general is a complicated skew function.

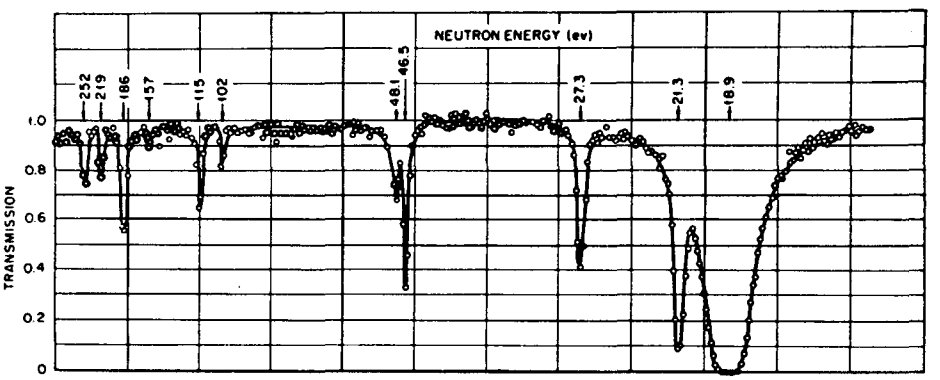

FIG. 19. Transmission measurements on W [from Harvey, J. A., Neutron Physics, (Yeater, M. L., Ed.) (1962) 84]. (Courtesy of Academic Press, New York)

The most obvious way to determine the parameters of the resonances in our measured transmission curves is then to attempt to fit them with the above formula (4.11). In this case we must know the resolution function R(E) of the spectrometer (seldom easy to achieve). The shape analysis programme of Harvey and Atta [49] does exactly this for well isolated resonances using the IBM 7090 computer, provided that the resolution function can be represented by a gaussian function, and that the resolution and Doppler widths are small, compared with the natural width of the resonance. The programme starts from a first estimate of E_R, Γ and $g\Gamma_n$, and derives by a least squares technique a best set of parameters. It then starts from this new set and re-iterates until a convergence criterion is satisfied. The cost on the 7090 computer of fitting a single resonance in a single sample (say 2 iterations) was estimated at about $2. The programme can handle up to 6 resonances at one time.

More sophisticated shape analysis programmes are now in use, for example at Saclay [50] where the programme can handle multiple resonances and multiple samples simultaneously, where the resolution function can be given arbitrary shape, where first order multilevel interference effects are included in the addition of the 'tails' of resonances, and where also the change in the potential scattering phase shift with increasing energy is taken into account.

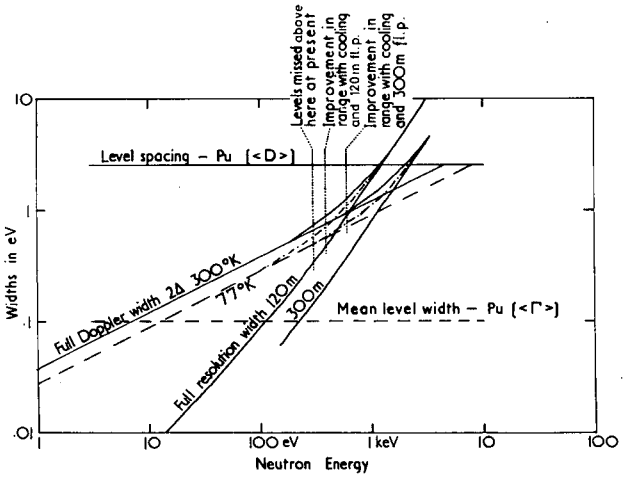

FIG. 20. 2Δ and R as functions of E for two flight paths on Harwell Linac, with and without cooling

All shape analysis programmes, however, rapidly lose their usefulness when Δ or R become comparable with Γ. Since, however, Γ is normally much less than D, the level spacing, there is still a wide energy region where Δ and R are small compared with D, so that sharp dips are still observed in the transmission curve, even although their widths bear little relation to the resonance widths (Fig. 20). This is the energy region where area analysis is useful. Provided the resolution function does not have long tails associated with it, the area above a dip in the transmission curve is independent of the resolution function, depending only on the level widths and Δ. Indeed for very thin samples,

the limiting area is also independent of Δ being given by [51]: $A_E = \pi n\sigma_0\Gamma/2$ ($n\sigma_0 \ll 1$) where A_E is the area (in energy units) above the transmission dip when plotted on an energy scale. For thicker samples, the Doppler broadening becomes important, and for very thick samples the resonance area is dominated by the interference term $\phi(\beta, x)$ in (4.10). This is an odd term which leads to the well-known interference minimum in the cross-section at an energy just below the resonance. For thick samples the increased transmission at this low cross-section point gives rise to a positive hump in the transmission curve (Fig. 21), and when the sample is thick enough this hump has a

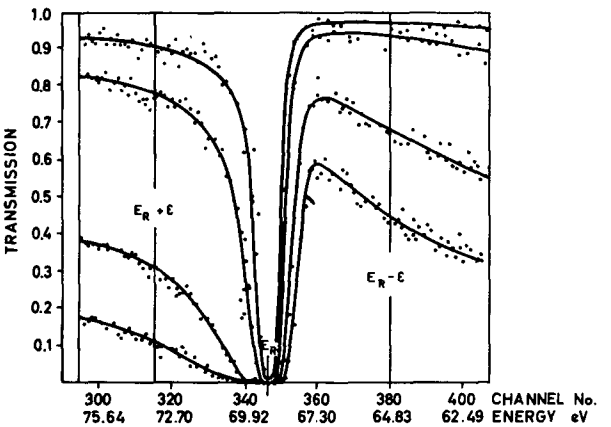

FIG. 21. The transmission of four samples of thorium over the 69 eV resonance (Ref. [86], p. 204). (Courtesy of North-Holland Publishing Co.)

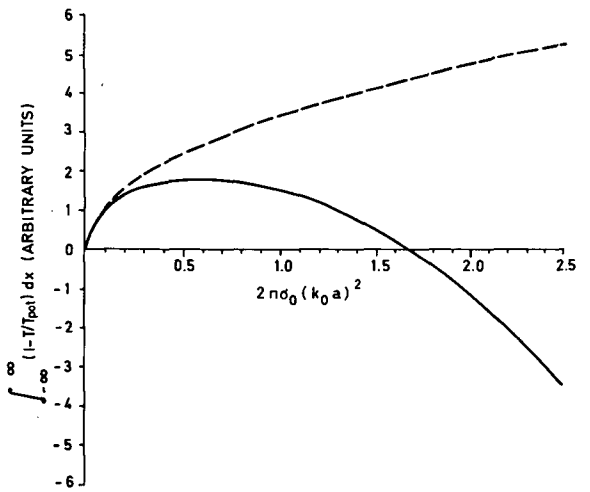

FIG. 22. Transmission area versus sample thickness. (Lynn, J. E., Nucl. Phys. 7 (1958) 605, Fig. 5). (Courtesy of North-Holland Publishing Co.)

larger area than the resonance dip, leading to negative resonance areas (Fig. 22). In the method of analysis due to Lynn [52], the experimental resonance area measurement is used to obtain values of the quantity $\sigma_0 a^2/\lambda^2$ (barns) corresponding to a series of values of $\Gamma\lambda/a$ (eV). Several such curves are obtained from area measurements on the same resonance but with different sample thicknesses, and the convergence of these curves yields values of σ_0 and Γ or $g\Gamma_n$ and Γ, the best fit being obtained by a least squares procedure using tangents to the curves close to the region of convergence (Fig. 23).

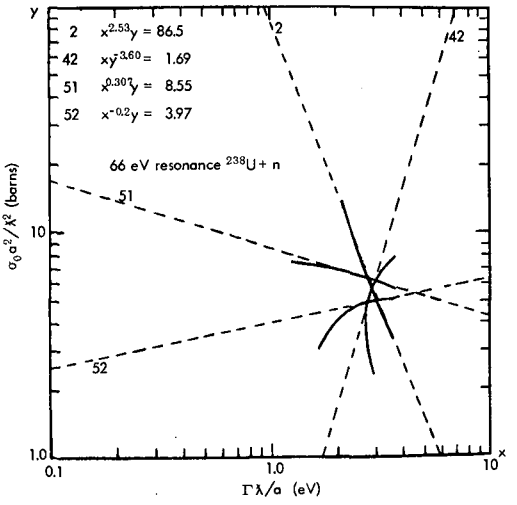

FIG. 23. Resonance analysis with thick samples (Ref. [52], p. 315). (Courtesy of North-Holland Publishing Co.)

Harvey and Atta [49] have also written a computer programme which fits resonance areas to up to 20 resonances at a time for a single sample thickness. This programme outputs the value of $g\Gamma_n$ corresponding to a given value of Γ so that if this is done for number of values of Γ and for several different samples, in principle Γ and $g\Gamma_n$ can again be determined for each level. The cost here of the computing time was quoted as ~$10 for one sample and one value of Γ.

A further variation on the area method of analysis is the use of the self-indication area as used by the Columbia team [32]. Here the detector consists of a foil of the material under study surrounded by an array of γ-ray detectors. The spectrum observed with no transmission sample in the beam is thus a series of peaks corresponding to the resonances, and the effect of the transmission sample is to reduce the intensity of these peaks (Fig. 24). The advantage of this method is that the background level is obtained at once, but the interpretation of the data is less straightforward than for a 'flat detector' and the method has not been adopted by other experimenters.

Although the majority of tabulated values of $g\Gamma_n$ and Γ have been obtained from area analyses, nevertheless shape analysis makes much better use of the available data; where for example two resonance curves overlap due to rather poor resolution, it is necessary to use a combination of shape

and area analysis in order to obtain values of $g\Gamma_n$ for each of the two levels. Of course in such a case the shape analysis cannot give the values of Γ with any precision, since we postulated poor resolution. To obtain the full widths it is necessary to use this type of fitting on the transmission curves for a number of very different sample thicknesses.

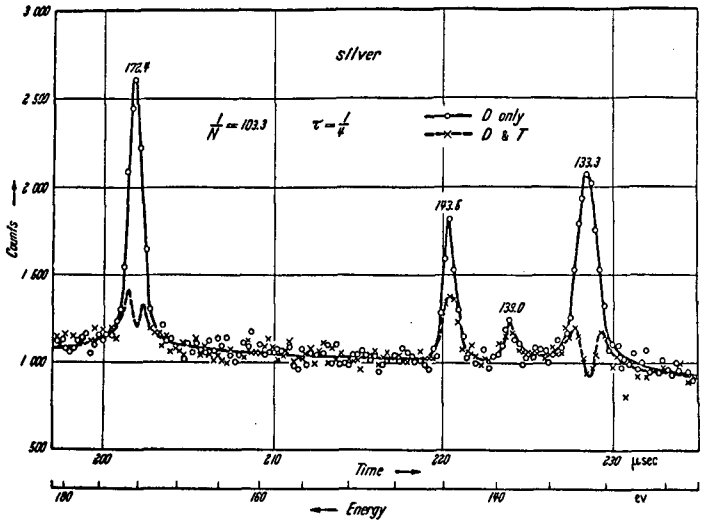

FIG. 24. Old (1956) self-indication curve for natural Ag showing resonant peaks at 133 to 172 eV, with and without an Ag transmission sample (Ref. [32], p. 395). (Courtesy of U.S. Atomic Energy Commission)

Another useful feature of shape analysis is that the study of the cross-section between levels can reveal small resonance – resonance interference effects which can lead to spin assignments of resonances once the spin of one resonance is known [55]. It must also be noted that such a careful analysis of the shape of the transmission curves is necessary to extract the potential scattering cross-section σ_p .

For several nuclei in the region $A \approx 50\text{-}60$ the level spacing is rather wide (a few keV), but the s-wave strength function $\langle \Gamma_n^0 \rangle / \langle D \rangle$ is large which leads to strong overlapping of the resonances (Fig. 25) [56]. In this region the single level Breit-Wigner formula is not capable of providing a fit to the shape of the cross-section curve, although rough values of the parameters of the resonances can be extracted.

Since for these nuclei $\Gamma_n \gg \Gamma_\gamma$, the value of J can also be obtained by inspection of the resonance peak cross-sections which have the value $4\pi\lambda^2 g(J)$. In order to fit the cross-section (or transmission) curves however, and to obtain σ_p , a multi-level cross-section formula must be used.

The method used to fit the data on Fig. 25 is described in Ref. [57]. It is based on the R-matrix formalism of Wigner and Eisenbud [53], but makes use of a modification due to Thomas [58]. This reduces the complicated R-matrix to a relatively simple function in the case where the reaction partial width for each channel, except the entrance channel, is much less than the level spacing. This condition holds for the predominantly scattering cross-section of the nuclei in the mass region 50-60, and in

this case the reduced R-function (for total angular momentum J) can be written

$$R_J(E) = \sum_{\lambda} \frac{\gamma^2_{\lambda Jn}}{E_{\lambda J} - E - \frac{1}{2} i \Gamma_{\lambda Jp}} \qquad (4.12)$$

where the sum is over all levels λ of angular momentum J with eigenvalues $E_{\lambda J}$ and reduced neutron widths $\gamma^2_{\lambda Jn}$. The width $\Gamma_{\lambda Jr}$ is the total reaction width of the level λ. The neutron width (for s-wave neutrons) is given by

$$\Gamma_{\lambda Jn} = 2ka\,\gamma^2_{\lambda Jn} \qquad (4.13)$$

where k is the neutron wave-number and a is the arbitrary radius for the entrance channel.

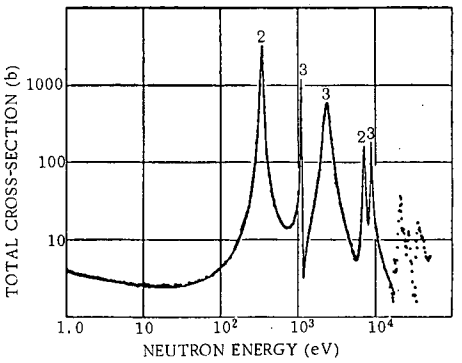

FIG. 25. The observed total neutron cross-section of manganese [56]. (Courtesy of American Institute of Physics)

The collision function $U_J(E)$ which is the amplitude of the outgoing wave in the entrance channel resulting from the scattering of a unit plane wave is, for s-waves,

$$U_J(E) = \exp(-2ika)\,\frac{1 + ika\,R_J(E)}{1 - ika\,R_J(E)} \qquad (4.14)$$

and from this the total cross-section is given by

$$\sigma_{nT}(E) = \frac{2\pi}{k^2} \sum_{J=\left|I-\frac{1}{2}\right|}^{I+\frac{1}{2}} g_J\,(1 - \mathrm{Re}\,U_J(E)) \qquad (4.15)$$

where Re signifies the real part of the complex $U_J(E)$.

In the application of these equations to fitting the cross-section curve, the R function is split up into 2 components

$$R_J(E) = R_J^{\text{local}} + R_J^{\text{residual}} \qquad (4.16)$$

The first term is calculated from the parameters of the levels in the energy range under study, and is responsible for the main features in the observed curve. The second term, $R_J^{residual}$ is responsible for slow 'background' variations in the cross-section and can be further split into a small real constant part R_J^{∞} which is due to the effects of large numbers of distant levels, and a power series in terms of $(E - E_{\frac{1}{2}})$ where $E_{\frac{1}{2}}$ is the energy corresponding to the centre of the observed region. In principle there are two such series involving real and imaginary coefficients, but in practice the imaginary coefficients, which correspond to the reaction cross-section, can be neglected and only the first (linear) term in $(E - E_{\frac{1}{2}})$ is necessary in the real series. We can therefore write

$$R_J^{residual} = A_J + B_J (E - E_{\frac{1}{2}}).$$

The object of the fitting procedure is thus to optimize the values of the parameters for the observed resonances, together with R_J^{∞} and the coefficients of the energy dependent terms due to neighbouring unknown resonances.

One interesting result of a fit of this nature is that the determination of $R^{residual}$ leads to a determination of the s-wave strength function $\langle \Gamma_n^0 \rangle / \langle D \rangle$. The slope B_J of the residual R function is directly related to the strength function for levels of spin J, and if the data are good, the values of the strength functions for both spin values can be extracted from the fit. These values are based on the effect of many levels close to the experimentally observed region, and in the case of the fit to the data on vanadium [57], the inclusion of the data from $R^{residual}$ with that from the local resonances led to a much better value of $\langle \Gamma_n^0 \rangle / \langle D \rangle$ than could be obtained from the local measurements alone. The analysis of the residual R-function led to the conclusion that there was, in this case, no J-dependence of the strength function (contrary to the analysis of the local results) but that the potential scattering length was J-dependent.

If we then summarize the information obtained from transmission measurements in the resonance region, we can say that we obtain in general values of $g\Gamma_n$ and Γ from both shape and area analyses. From the shape analysis we get in addition σ_p and sometimes also g, either from the value of peak cross-section when $\Gamma_n \gg \Gamma_\gamma$, or from the study of level-level interference.

From both types of analysis we obtain values of Γ_γ when $\Gamma_n \ll \Gamma_\gamma$ by putting $g = \frac{1}{2}$, or in the case of fissile targets we obtain $\Gamma_\gamma + \Gamma_F$. To separate these two, and to obtain, in general, values of g and Γ_γ, requires the measurement of at least one partial cross-section in addition. Of course the use of the single level formalism to analyse the cross-sections of fissile nuclei is not justified since here D is small (~ 1 eV) and the fission widths are frequently comparable with the spacings. The use of the multi-level formalism is, however, much less satisfactory in this case than it is for scattering, since several channels other than the entrance channel, have widths comparable with the spacings, and the signs of the reduced widths are arbitrary. Hence such fitting procedures are tedious, since matrix methods must be employed, and furthermore the fits obtained are not unique. A more fundamental objection to these methods has been made by Lynn [59] who suggests that where really strong interference occurs in the fission channels, it is impossible to determine

from the cross-section curves even the approximate position of the R-matrix levels. It is probably true then that the analysis of the cross-section curves for fissile nuclei can only be done with any confidence for those cases where Γ is considerably less than D. In this context ^{239}Pu is reasonably well behaved, but even here the use of multi-level formalism is only justified insofar as it permits unique determination of the level spins.

Because of the strong interference effects in the cross-sections of the fissile nuclei, it is not possible to deduce with any certainty either the level parameters or the s-wave potential scattering and strength function from a detailed analysis of the resonances. The latter two quantities can, however, be deduced from measurements of the average total cross-section. Indeed these nuclei are particularly suited for such measurements since their high value of Γ/D minimizes the effect of resonance self-shielding which is normally a source of difficulty in average cross-section measurements.

The use of average cross-section measurements to obtain potential scattering and strength function parameters has been most rigorously developed by Uttley [60] whose analysis is based on the formalism of Lane and Thomas [61]. Uttley's measurements utilize two ^{10}B plug detectors in a flight path of total length 300 m. The first detector, at 120 m, provides on overlap filter for the longer 300-m flight path, so that he records the transmission of a sample over the energy range from 100 eV to 10 MeV. The shorter flight path covers 70 eV to 100 keV, and the longer 10 keV to 10 MeV, giving a useful region of overlap. In measurements of this type great care must be taken to avoid systematic error. Firstly resonance self screening effects must be avoided as these lead to systematically low values for the average cross-section. This is achieved by the use of very thin samples and checked by the comparison of measurements with samples of different thickness, and with different effective values of the resolution width. Secondly with the use of thin samples, and hence nearly equal values for N and N_0 (4.8) automatic sample changers are essential, and the usual care must be taken with background measurements. Finally, although this is seldom a worry in time-of-flight measurements, the geometry of the experiment must be above reproach – there must be no in-scattering of neutrons by the sample.

The analysis of the measurements is based on the expression for the average total cross-section $\langle \sigma_{nT}(\ell) \rangle$ in terms of the average collision function $\langle U(\ell) \rangle$ over many levels:

$$\langle \sigma_{nT}(\ell) \rangle = 2(2\ell+1)\pi\lambda\!\!\!^{-2}\left(1-\mathrm{Re}\langle U(\ell)\rangle\right) \qquad (4.17)$$

where

$$\langle U(\ell)\rangle = e^{-2i\varphi_\ell}\,\frac{1-\hat{L}_\ell^{*}R_\ell}{1-\hat{L}_\ell R_\ell} \qquad (4.18)$$

where φ_ℓ is the scattering phase shift from a hard sphere of radius R, $\hat{L} = L + 1$ where L is the logarithmic derivative of the outgoing wave at radius R, and is related to the modified shift factor $\hat{S}_\ell = S_\ell + 1$ and the

penetration factor P_ℓ according to $L_\ell = S_\ell + iP_\ell$. $R_\ell = R_\ell^\infty + i\pi S_\ell$ is the R-function in which R_ℓ^∞ is the overall effect of very distant levels, and S_ℓ is the strength function.

For each partial wave ℓ, only two parameters enter the total cross-section, R_ℓ^∞ and S_ℓ. The total cross-section can further be split into shape elastic and compound nucleus terms

$$\sigma_{SE}(\ell) = (2\ell+1)\pi\lambda\!\!\!^{-2}\left|1 - \langle U(\ell)\rangle\right|^2 \tag{4.19}$$

and

$$\sigma_{CN}(\ell) = (2\ell+1)\pi\lambda\!\!\!^{-2}\left(1 - \left|\langle U(\ell)\rangle\right|^2\right) \tag{4.20}$$

We note that for s-wave neutrons and $kR \ll 1$, we can deduce from the general equations that

$$\sigma_p = 4\pi R^2 (1 - R_0^\infty)^2 = 4\pi R'^2 \tag{4.21}$$

Figure 26 shows the fit to the average total cross-section of ^{235}U using the above expressions and a value of the nuclear radius R of $1.35A^{\frac{1}{3}}$ fm. Here we have large Γ/D, hence rather small fluctuations at low energies and the values of R_0^∞ and S_0 were obtained from fitting to the cross-section curve below 20 keV. The contribution of the higher ℓ-values was then obtained assuming $S_3 = S_1$, $R_2^\infty = R_3^\infty = 0$. Thus the free parameters were R_1^∞, S_1 and S_2 and these were fitted to the whole curve to 1 MeV as shown.

Figure 27 shows the fit to the average cross-section of ^{93}Nb over the energy range 10 keV to 2 MeV. This time Γ/D is small so that average cross-section measurements below a few keV are unreliable. In this case S_0 was obtained from published parameters [62, 63] and R_0^∞ obtained from shape fitting to the region between resonances, allowance being made for the tails of levels contributing significantly to the cross-section according to the expression

$$R' = R(1 - R_0^\infty) = R_{\text{effective}} - \frac{\lambda\!\!\!^{-}_0}{2}\sum_r \frac{\Gamma_{nr}^0}{E - E_R} \tag{4.22}$$

The parameters for $\ell = 1, 2$ and 3 were fitted as before.

Measurements and analyses of this type provide the most convincing measurements of the higher ℓ value parameters, particularly S_1 and R_1^∞. Other measurements of S_1 have been made by identifying p-wave resonances at low neutron energy by shape analysis (no interference with s-wave background) and from anomalous distributions of neutron widths which also seem to be reliable, but many early values of S_1 based on average capture cross-section measurements in particular, have now been discredited due to their dependence on assumptions about level densities and radiation widths.

This is probably the point at which we should stop for a moment and look at the data which have been obtained over the years from trans-

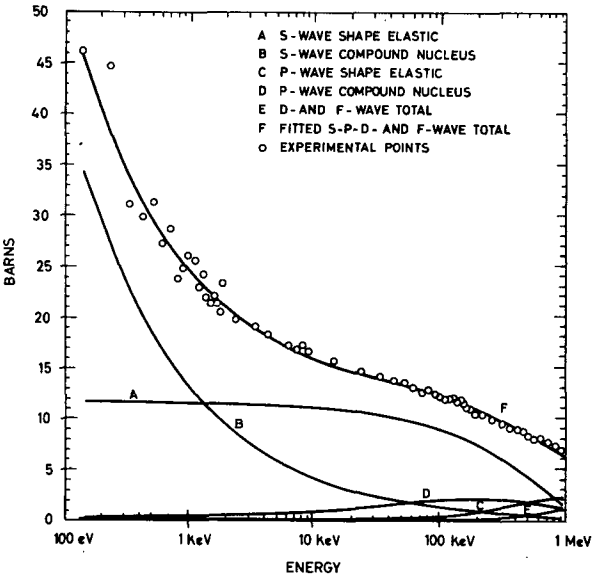

FIG. 26. Least squares fit to uranium 235 [60]

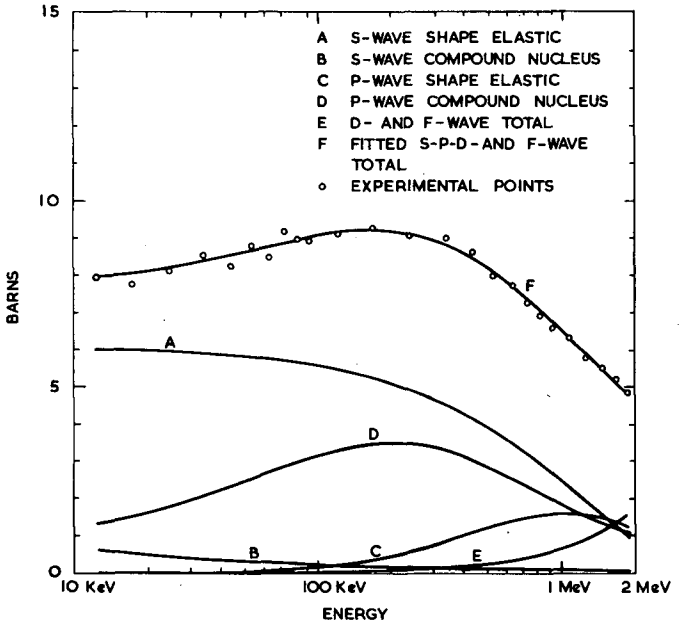

FIG. 27. Least squares fit to niobium 93 [60]

mission measurements of one sort or another. Perhaps the simplest measurements, since no resonance analysis is concerned, is that of level spacing or level density. Figure 28 shows a plot of all level densities

obtained from neutron resonance studies. These have been corrected for variations in the binding energies and normalised to 6.5 MeV according to the Fermi gas model ($\rho \propto \exp\sqrt{aE}$). They have also been corrected for the $(2J+1)$ factor, and normalized to the values corresponding to $J = 0$. The most prominent feature of the plot is the large dip in the level density near the doubly magic ^{208}Pb nucleus. Subsidiary dips are also seen at other closed shells confirming the importance of shell structure in determining the level density.

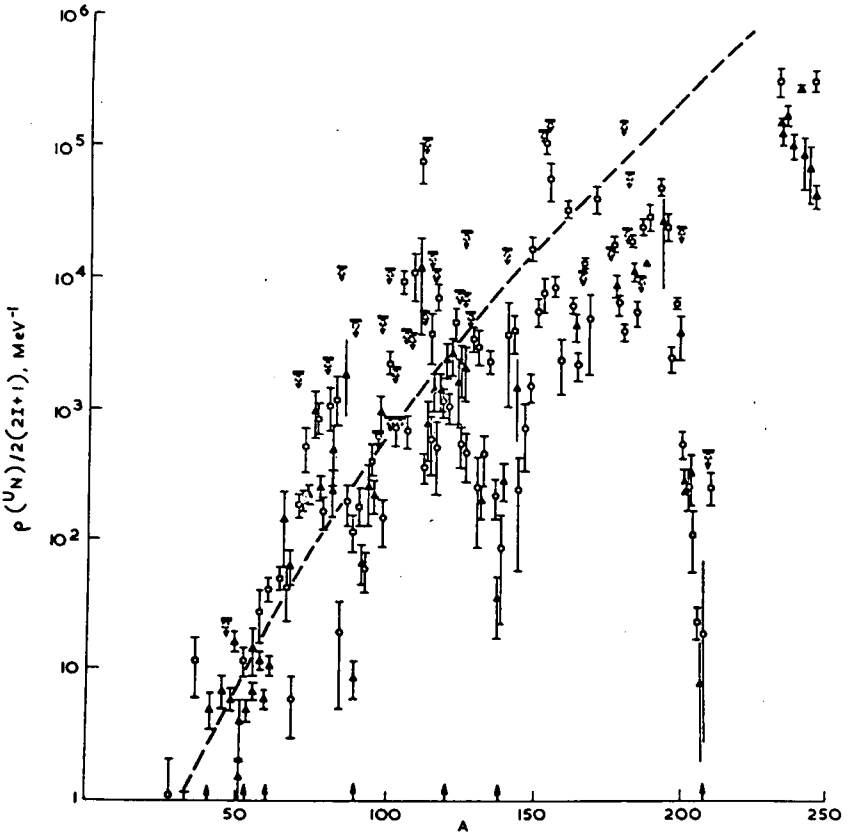

FIG. 28. Corrected level density as a function of atomic number (from Lynn, J. E., unpublished lecture notes)

Figure 29 shows some rather old Harwell data [64] on ^{238}U which still serves to illustrate several points. The top part of the slide shows the usual 'staircase' plot of the number of levels below the energy E, as a function of E. Where only s-wave neutrons are involved, this plot should be linear over the rather small energy range considered (2 keV). A drop off from linearity at the higher energies indicates that levels are being missed due to poor resolution, while a steeper rise might indicate the inclusion of levels accessible to p-wave neutrons, since the neutron widths of these levels increase as $E^{\frac{3}{2}}$ compared with $E^{\frac{1}{2}}$ of s-levels.

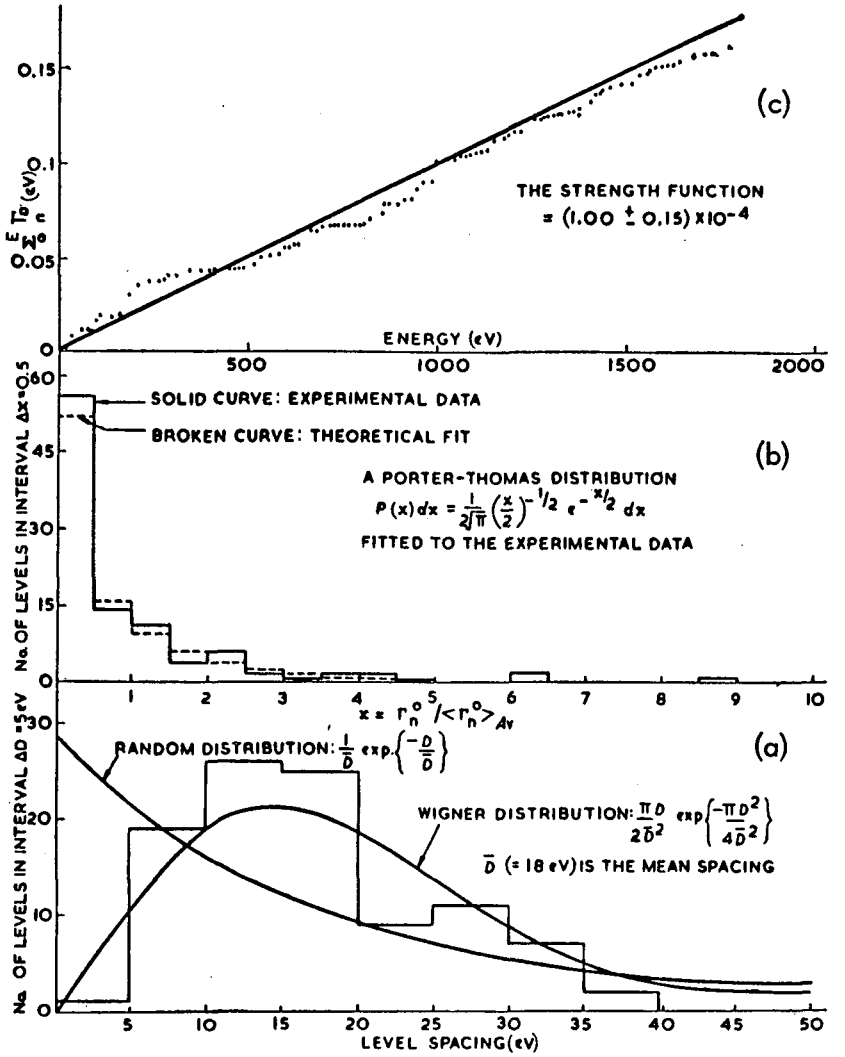

FIG. 29(a) A histogram of the level spacings observed in Lynn and Moxon's series of measurements compared with the exponential and Wigner forms

(b) A histogram of the reduced neutron widths of the first 100 resonances of the ^{238}U neutron cross-section. A theoretical histogram based on the Porter-Thomas distribution is shown for comparison

(c) The sum of reduced neutron widths from zero neutron energy to energy E as a function of E. The slope of this function is the neutron strength function Γ_n^0/D (Ref. [64], p. 425). (Courtesy of North-Holland Publishing Co.)

The second part of the slide is a plot of the distribution of the reduced neutron widths of the s-wave resonances and shows this compared with the theoretical Porter-Thomas distribution. The third part of the figure shows the distribution of the level spacings (^{238}U being even-even, only levels of spin 1/2 are involved) and this is compared to the Wigner one population distribution.

More recent work has, of course, confirmed the Porter-Thomas distribution, but some doubt was thrown on the validity of the Wigner distribution for cases where more than one population was present, particularly in measurements on odd nuclei at Columbia, where the results showed consistently a lack of small level spacings. A careful measurement on gold at Saclay [55], however, showed good agreement with a Wigner two population distribution and recent Russian measurements on separated isotopes of silver also confirm the Wigner law [65]. Experimental distributions for next nearest neighbour spacings also agree with theoretical predictions [55].

Perhaps the most important quantity determined from the study of neutron resonances is the s-wave strength function $\langle \Gamma_n^0 \rangle / \langle D \rangle$. The observed variation of this quantity with mass number A was one of the foundation stones of the optical model. Figure 30 shows a plot of Lynn's compilation of strength functions for separated isotopes, and the main optical model peaks are clearly seen, being distorted because of the presence of nuclear deformations. There are still some discrepancies between experiment and theory, but the strength function plot is a powerful tool for examining the average interaction of neutrons with the nuclei and in determining the conditions at the nuclear surface. There is some evidence of a J dependence of the s-wave strength functions [55] but this is very difficult to establish with any certainty.

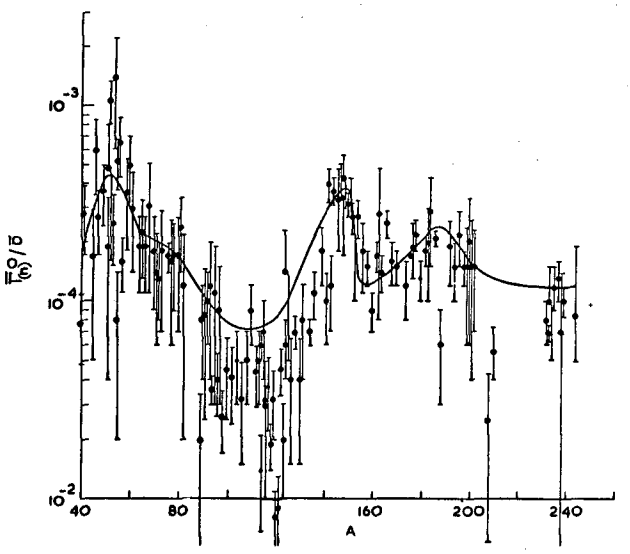

FIG. 30. Data on the s-wave neutron strength function compared with the model (solid curve) of a diffuse complex potential coupled to vibrational and rotational motion (from Lynn, J.E., unpublished lecture notes)

Figure 31 shows a plot of the s-wave potential scattering length [denoted by a or $R' = R(1 - R_0^{\infty})$] as a function of mass number A. We observe that, superposed on the smooth $A^{\frac{1}{3}}$ curve, are quite violent oscillations which involve a very rapid increase at the values of A corresponding to the peaks in the s-wave strength function curve. This is easily

understandable in a qualitative way, as being due to the variation in R_0^∞ which is due predominantly to the coherent effect of the tails of the distant levels. For values of A below a maximum in the strength function, the s-wave giant resonance lies above the neutron separation energy, and the tails of the strong resonances interfere destructively with the potential scattering, leading to a reduction in R' (R_0^∞ is positive). For values of A just above the peak in the strength function curve, the giant resonance lies below the neutron separation energy, and the interference is constructive (R_0^∞ is negative). Half way between the peaks the effect vanishes and $R' = R = 1.35A^{\frac{1}{3}}$.

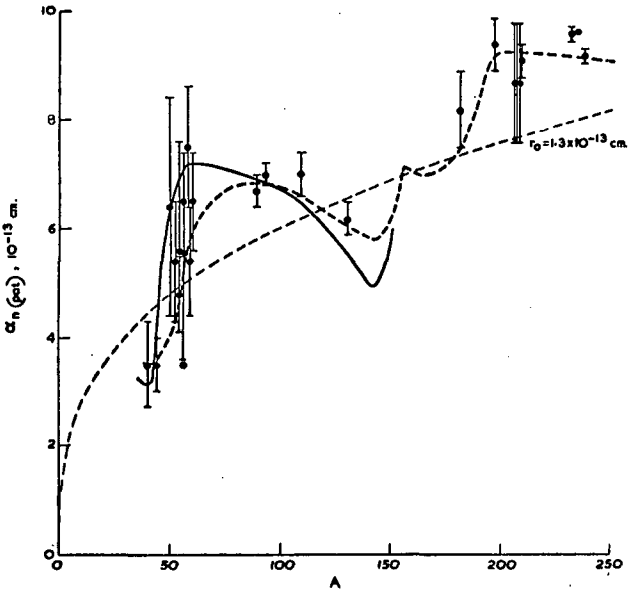

FIG. 31. Potential scattering length data and comparison with models. The full curve is calculated from a spherical complex potential (Moldauer, 1963). The broken curve is for a complex potential with vibrational and rotational coupling, calculated by Jain (1964) (from Lynn, J.E., unpublished lecture notes)

Figure 32 is a plot of the radiation widths obtained from neutron resonances, again as a function of A and once again the effect of the double shell closure at ^{208}Pb is the most prominent feature. This corresponds basically to the increase in the level spacing in this region due to the restriction in the number of energetically possible particle transitions, the total strength being therefore shared among fewer states.

Finally Fig. 33 shows the p-wave strength functions as compiled by Newson [67]. There is still some scarcity of p-wave data, but hopefully with time this curve will be completed and also possibly one for d-waves together with their complementary curves for R_ℓ^∞. Uttley's measurements of R_1^∞ bear out the behaviour of the s-wave parameter, R_1^∞ being positive below the strength function peak at A = 100, and negative above this peak.

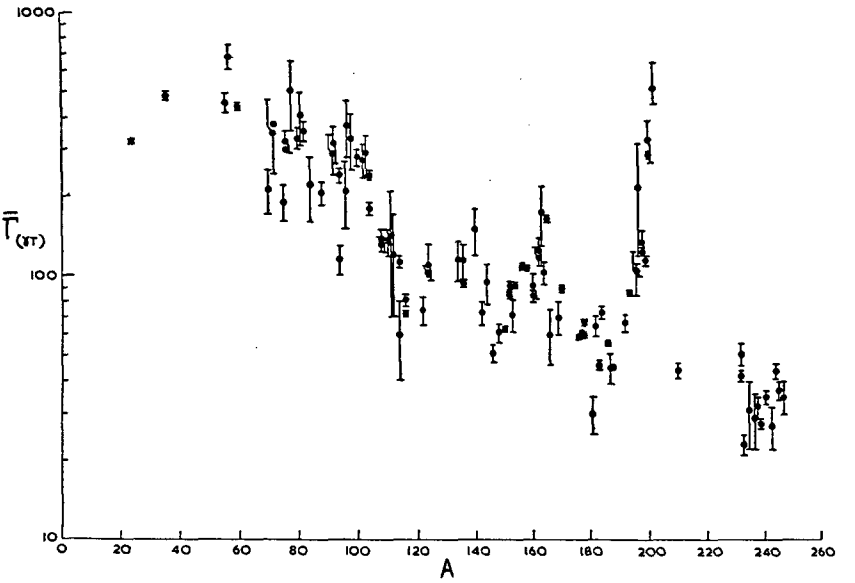

FIG. 32. Radiation width as a function of atomic number (from Lynn, J.E., unpublished lecture notes)

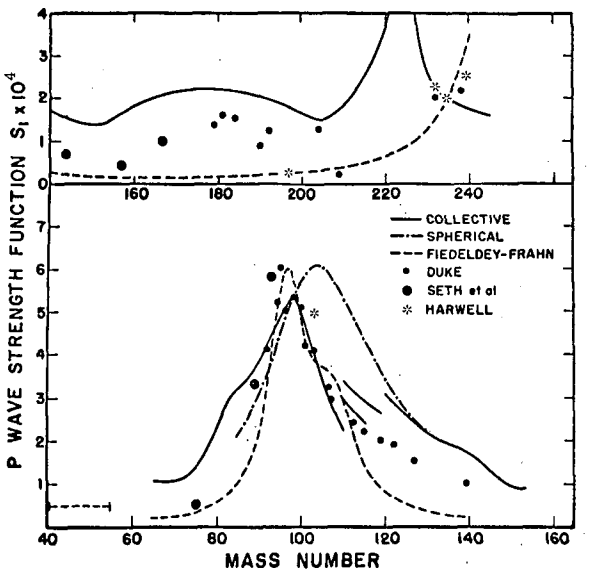

FIG. 33. A plot of p-wave strength functions. The measurements were repeated where in-scattering was too important for accurate correction [67]. (Courtesy of U.S. Atomic Energy Commission)

4.3. Elastic scattering

Measurements of the elastic scattering cross-section are most valuable in the case of low-lying resonances in medium weight and heavy

nuclei, where the level spacing is small so that $\Gamma_n < \Gamma_\gamma$ and scattering is weak compared with capture. For the lighter nuclei where scattering predominates, there is little point in attempting these measurements, since they are equivalent to transmission measurements, but very much more difficult to carry out.

In order to understand the function of the scattering measurement in determining the resonance parameters, let us recall that the transmission measurement, when shape fitting is possible, yields $g\Gamma_n$ and Γ and that area analysis with several sample thicknesses leads to the same parameters. Area analysis with a single sample gives $g\Gamma_n$ as a function of Γ, in a relationship of the form $g\Gamma_n \Gamma^p = \text{const.}$, where $0 \leqslant p \leqslant 1$.

In a scattering measurement in the immediate vicinity of a resonance, we measure a cross-section which is given by $\sigma_{nn} = \sigma_{nT} \Gamma_n/\Gamma$. In particular the peak scattering cross-section $\sigma_{0n} = \sigma_0 \Gamma_n/\Gamma$ or $4\pi\lambda\!\!\!^{-2} g\Gamma_n^2/\Gamma^2$, and the area under the peak in the scattering yield curve (i.e., plot of fraction of incident neutrons scattered as a function of E_n) in the thin sample limit is given by:

$$\begin{aligned} A_{E(\text{scat})} &= \pi n \sigma_0 \Gamma_n / 2 \\ &= 2\pi^2 g n \lambda\!\!\!^{-2} \Gamma_n^2/\Gamma \end{aligned} \tag{4.23}$$

A measurement of either the peak scattering cross-section, or the thin sample scattering area, then gives a new relationship between g, Γ_n and Γ so that in principle we can solve for all three parameters. If of course $\Gamma_n \gg \Gamma_\gamma$, so that $\Gamma_n \approx \Gamma$, then as pointed out before, g is obtained from a measure of the peak total cross-section. In this case however, Γ_γ is not determined and a measurement of the peak capture cross-section or the thin sample capture area is necessary for a complete solution since this yields $\sigma_{0\gamma} = \sigma_0 \Gamma_\gamma/\Gamma$ or

$$A_{E(\text{capt})} = \pi n \sigma_0 \Gamma_\gamma / 2 = 2\pi^2 g n \lambda\!\!\!^{-2} \Gamma_n \Gamma_\gamma / \Gamma \tag{4.24}$$

To return to the elastic scattering, then, we see that a scattering measurement, where $\Gamma_n \ll \Gamma$, i.e., for low-lying resonances in medium and heavy nuclei, allows us to solve for g, Γ_n and Γ, and hence Γ_γ in the absence of other reactions. In the case of fissile nuclei, apart from the difficulty of the form of the cross-section curve, it is clear that a second partial cross-section measurement (either $\sigma_{n\gamma}$ or σ_{nF}) is required in order to divide up the total reaction width $(\Gamma - \Gamma_n)$ into Γ_γ and Γ_F.

In practice, of course, the equations obtained from the various measurements are only approximate and the data are obtained in the form of a few calculated values of $g\Gamma_n$ as a function of Γ. In this case the best method of solution is by graphical display and least squares fitting, which can be applied to all the available data. Figure 34 shows the data for probably the first resonance to be analysed in this way, the 5 eV resonance in silver [68]. As you will see, the curves in the (Γ_n, Γ) plane corresponding to all the data are nearly concurrent for J = 1 (g = 3/4) and definitely not so for J = 0. In this case least squares fitting is scarcely

necessary to obtain the parameters, but it is still needed to estimate the errors on the parameters and to justify the choice of J. Figure 35 shows much later data for the 35 and 93 eV resonances in Ho [69]. In the case of the 35 eV resonance, the choice of J is not so obvious, but is obtained with high probability from a least squares fit.

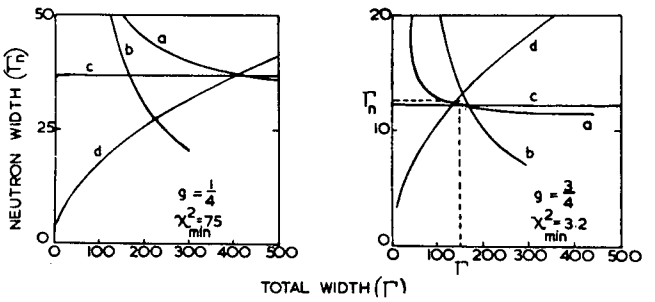

FIG. 34. Combination of the experimental data to determine Γ_n and Γ for the 5.2 eV resonance in ^{110}Ag and the appropriate statistical weight factor, g. Ordinate and abscissa scales are in milli-electron-volts. Curves show the variation of Γ_n with Γ as determined by: (a) radiative capture in a thin sample; (b) thick sample transmission; (c) thin sample transmission; (d) elastic scattering (Ref. [68], p. 104) (Courtesy of North-Holland Publishing Co.)

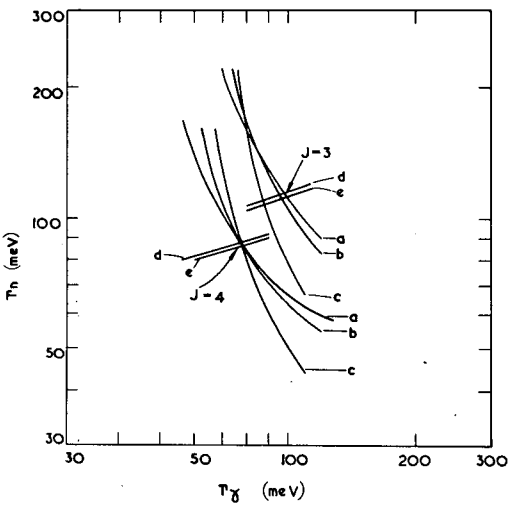

FIG. 35. Area analysis of resonances in holmium

Since this section follows on from the analysis of transmission data, we have reversed our usual order here and considered how the elastic scattering data are analysed before describing how they are obtained. In general one can make scattering measurements in one of two basic ways. In the first, or conventional method, the velocity or energy of the neutrons before striking the sample is determined, say by time-of-flight. In this case the sample is placed at the end of a flight path and the scattered neutrons are observed in some detector suitably screened from the direct beam.

In the second method the energy of the neutrons is determined after scattering. In this case (the bright-line method) the sample is placed close to the neutron source, and the scattered neutrons are allowed to fly down the flight path to the detector.

The advantage of the second method is that gamma rays and fast neutrons from the neutron source, together with possible fission neutrons and capture gamma rays from the sample, all reach the detector very early in the time of flight cycle, and so do not confuse the interpretation of the scattering yield. This method has been used very effectively by Sauter and Bowman [70] at Livermore in the study of resonance scattering from fissile samples. The great disadvantage of the method is that in the interests of intensity and signal to background ratio, the sample is normally surrounded by the neutron source (a reactor in the case of the first experiments by Borst [71] and Wood [72], and a moderating shell in Bowman's case). Thus neutrons strike it from all directions, so that the neutrons scattered from a sharp resonance at E_R can have any energy from E_R down to $E_R[(A-1)/(A+1)]^2$ corresponding to a total energy spread of $4E_R/A$. In the case of plutonium, this represents a spread of ~ 2 eV at 100 eV, which is equal to the mean level spacing. Since the energy spread is inversely proportional to A, the effect is still serious for lighter nuclei, despite the increased level spacing.

Hence, if full use is to be made of the resolution obtainable from the time-of-flight method, the conventional method with the detectors close to the target is the most generally useful. Ideally the detector should have 4π geometry in order to nullify the effect of the centre of mass motion. Both sample and detector should also be physically small in order to minimize the difference in total flight path length between neutrons scattered at 90° and those scattered at small and large angles. There is also the very serious problem of multiple scattering. If Γ_n/Γ_γ is small, which is the case of most interest, then a scattered neutron which makes a second collision is likely to be lost. This of course is most likely for those neutrons scattered close to 90° in a foil normal to the beam. It would seem then that the best geometrical form for the scattering detector is in two rings, one in front of, and one behind the sample so that the neutrons observed are emitted at reasonably large angles to the surface of the sample, while the two detectors still tend to offset the effect of the centre of mass motion for lighter targets.

The detector chosen for a neutron scattering measurement should have low sensitivity to gamma rays, especially since we study just those cases where capture predominates over scattering. It should also have good efficiency, and for a time-of-flight experiment, have good timing properties; these various requirements are to some extent mutually exclusive. Early resonance scattering measurements such as those described in Ref. [68] made use of BF_3 counters. In those days the rather long pulses obtained from pulsed sources, or the DC beams from crystal spectrometers made few demands on the detector speed, and the rather narrow energy range which could be studied with reasonable resolution meant that the efficiency of high pressure $^{10}BF_3$ counters was acceptable. The detector used by Collins [68] and later by Fraser and Schwartz [73] to study scattering from ^{239}Pu consisted of an annulus of $^{10}BF_3$ counters giving nearly 4π geometry. The former took care of multiple scattering

corrections empirically by using a series of samples of different thickness and plotting the observed areas divided by sample thickness as a function of sample thickness. They then extrapolated to zero thickness, being guided in the extrapolation by a Monte Carlo calculation which was made for the 5 eV resonance (in silver). In the Fraser and Schwartz experiment on ^{239}Pu, only a single very thin foil was used having $n\sigma_{0\Delta}$ everywhere < 0.1 and the multiple scattering correction was calculated. In the case of ^{239}Pu the ratio of Γ_n to Γ is very small, for the lower energy resonances $\sim 1\%$, so that the correction for the detection of γ-rays and fission neutrons could not be ignored, even though the $^{10}BF_3$ proportional counters were insensitive to both fast neutrons and γ-rays. Hence the effect of the slow scattered neutrons was determined by taking the difference between the observed counts with and without a sleeve of B_4C placed between the sample and detector.

In all cases the fractional scattered yield was obtained by comparing the observed counting rate due to scattering from the sample, with that obtained with a thin sheet of lead replacing the sample. The scattering cross-section of lead is known accurately from transmission measurement ($\sigma_{n\gamma} \ll \sigma_{nn}$) so the only remaining correction is that for the change in efficiency of the detector for neutrons scattered from the sample, and from lead, owing to the different energy shift in the two cases. I have described the early Harwell scattering measurements, partly because I am familiar with them, and partly because they were the first to produce enough spin measurements to make possible a confirmation of the $2J+1$ factor in the level density for slow neutron resonances. Several other measurements have since been made with BF_3 and other detectors using choppers and crystal spectrometers.

In order to improve the technique however, and to take advantage of the fast pulses obtained from electron linacs and cyclotrons to push upwards the energy range accessible to scattering measurements, it has become necessary to use a much faster detector.

Such an improvement was achieved by Asghar and Brooks [75] when they utilized lithium loaded glass detectors. They eliminated the gamma-ray sensitivity of the glass detectors by using two otherwise identical detectors, one loaded with lithium highly enriched in ^6Li, the other with the natural element. The gamma ray background was then removed by subtraction. Figure 36 shows part of the scattering yield from ^{238}U (capture counts having been subtracted) and the low background is evidenced by the appearance of interference effects. Since the response time of the glass is a few nanoseconds, the limitation on resolution really lies with the geometry of the experiment. Those measurements were made on a 60-m flight path with length uncertainties of 5-10 cm, so that the geometrical part of the resolution $\Delta E/E$ is a few parts per thousand in energy. This same technique has been employed by Asghar to measure the spins of 40 levels in the case of the fissile target ^{239}Pu [76], the fission neutron sensitivity of the glass (which is very small) being removed by subtraction of a constant times the yield of a small stilbene crystal used with pulse shape discrimination to remove the gamma-ray sensitivity of the stilbene. The relative efficiencies of the glass detector and the stilbene for fission events was obtained by the use of a ^{240}Pu spontaneous fission source. As was stated earlier, these measurements are not so elegant as those made by Sauter and Bowman with the bright-

line method, but the fact that the geometrical part of the energy resolution is an order of magnitude smaller allows the conventional measurements to be pushed to much higher energies. It should be mentioned that while scattering measurements become more difficult at higher energies because of Doppler broadening and poorer resolution, it is also true that multiple scattering corrections become much smaller because the energy lost in scattering becomes large compared to the level width so that the scattered neutrons easily escape from the sample. Hence while full Monte Carlo calculations are frequently necessary at low energies, first order corrections suffice at higher energies. Scattering measurements have by now established the spins of a few hundred neutron induced resonances, and have contributed to the measurement of radiation widths of heavy nuclei such as uranium and thorium.

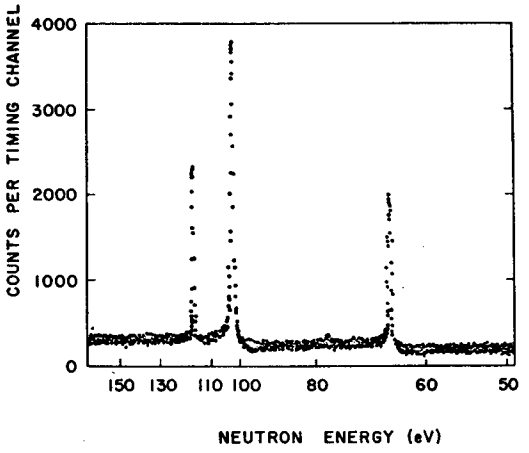

FIG. 36. Neutron scattering from ^{238}U (Ref. [106], p. 1048). (Courtesy of U.S. Atomic Energy Commission)

4.4. Capture measurements

Radiative capture measurements are most useful when $\Gamma_n \gg \Gamma_\gamma$. They are therefore useful in determining Γ_γ and J for higher energy resonances in medium and heavy nuclei, and are essential in the determination of Γ_γ for lighter nuclei.

Where a monochromatic beam of neutrons is available, capture cross-sections can be obtained by measuring the activity produced on irradiating a sample. This method, however, is only useful where the product nucleus is radioactive and has a suitable lifetime[4]. These methods have been used extensively to measure thermal capture cross-sections and the activation method is useful in the measurement of high energy cross-sections with Van de Graaff accelerators. Activation is the only method suitable for measuring very small (μb) cross-sections, but is not suitable for work in the resonance region.

[4] If no activity is produced, a mass spectrometer study is necessary to determine the number of nuclei which have captured neutrons.

Time-of-flight methods of measuring capture cross-sections invariably make use of the detection of the prompt gamma rays emitted as the compound nucleus decays to its ground state. The detector used in such a measurement should have a low sensitivity to scattered neutrons and an efficiency which depends only on the number of capture events, and the total energy released, but not on the detailed cascade by which the compound nucleus decayed.

Two basic types of detectors are available with essentially these characteristics: the first, which achieves nearly constant efficiency by making this efficiency approach 100%, is the large liquid scintillator tank [77–79]; the second is the Moxon-Rae type of detector [80] which achieves independence of the cascade by making the efficiency for detecting a photon proportional to its energy. The Moxon-Rae detector is intrinsically insensitive to slow neutrons, although in its original form it becomes sensitive to neutrons of energy greater than a few hundred keV; the large tank can be made insensitive to slow neutrons by loading it with boron and biassing above the energy of the boron pulses.

The large tank has the great advantage that at high neutron energies, the pulses caused by proton recoils in the scintillator are still small compared with the capture γ-ray pulses and can be removed by suitable biassing, so that these devices can be used up to a neutron energy of several MeV. Against this must be weighed their high natural background because of their great size (1–2 m in diam.), their relatively slow response ($\sim$ 20 nsec) if very fast timing is to be used, and the fact that for practical dimensions, their sensitivity is by no means independent of the cascade, if appreciable high-energy components exist in the spectrum. For example, for a 1-m diam. tank, the probability of escape of a 6 MeV photon is 40%. The high mean efficiency of such a tank ($\sim$90%) depends on the emission of a large number of rather soft quanta, under which conditions the large tank is an excellent detector. For certain heavy nuclei however, which have anomalously intense high-energy transitions, one must be careful before accepting the constancy of the tank efficiency.

In the Moxon-Rae detector, the electrons produced from the surface of a thick graphite cylinder surrounding the capturing sample, are detected in thin plastic scintillators. The efficiency of this system is only a few per cent for detecting capture events, but because of the linearity with energy of the efficiency for detecting individual photons, the efficiency for detecting capture events does not drop off appreciably for single high-energy photon events. Calculations by Macklin for a 1-inch converter show a 35% drop off at 6 MeV, similar to the behaviour of the scintillation tank, but his experimental results suggest that the figure is closer to a 10% drop from the mean efficiency. The drop off with the thicker ($1\frac{1}{4}$ in.) converter used at Harwell is probably rather less and no such effect has been observed there experimentally so that the Moxon-Rae detector is distinctly less sensitive in practice to variations in the cascade than is the large tank[5]. The speed is also much higher (3 nsec) which, together with the small size, has made this detector particularly useful with a short flight path on a Van de Graaff neutron source [81]. Both detectors have excellent discrimination against neutron detection $\epsilon_n/\epsilon_\gamma < 10^{-4}$.

[5] Macklin has also shown that the energy dependence of the efficiency can be improved by the addition of a small amount of high Z material, such as bismuth, to the convertor.

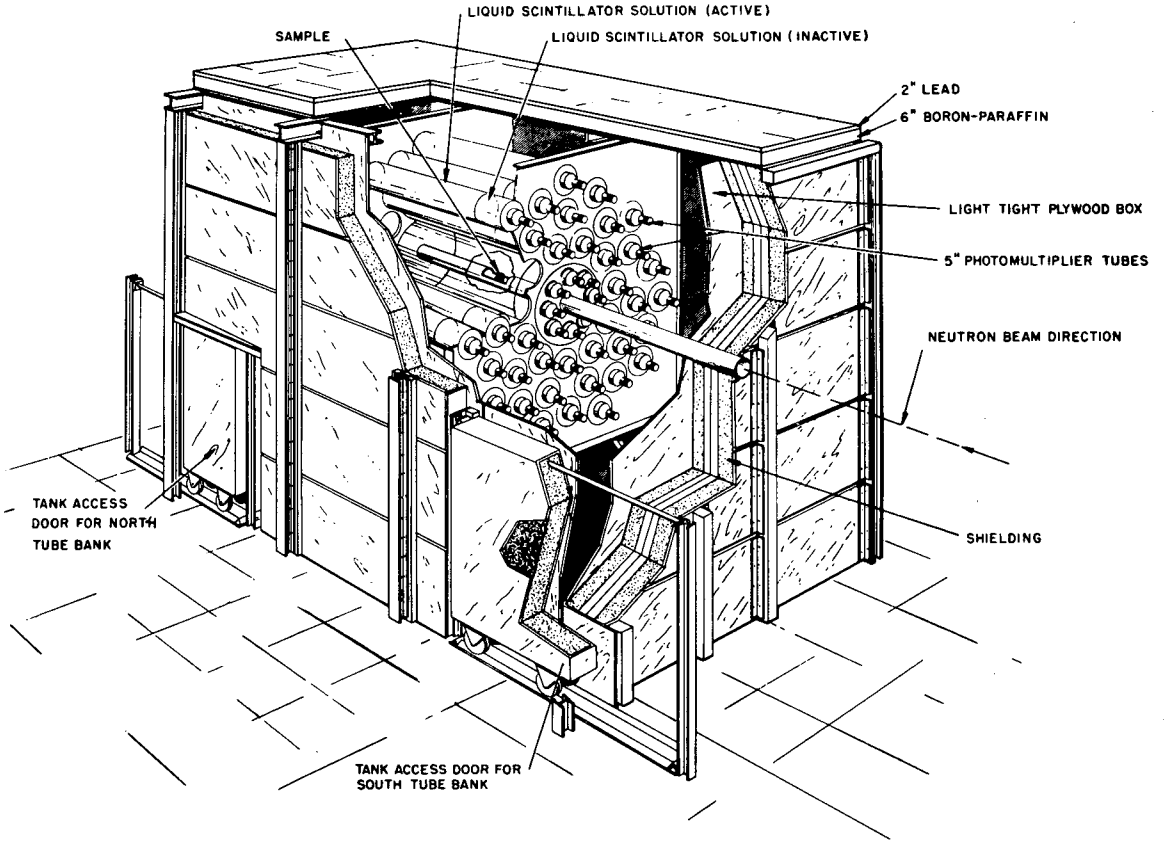

FIG. 37. Large liquid scintillator (Ref. [84], p. 6). (Courtesy of General Atomics)

Up till very recently, high backgrounds in large tanks prevented them from being used in practice in time-of-flight measurements above a few tens of keV while the Moxon-Rae detector, with its low background, could be used up to the onset of proton recoil detection – say 200 keV. Recently however, Block at RPI has improved the shielding and collimation of his tank system. He has also reduced the gamma ray and fast neutron flash by rearrangement of the neutron target geometry so that only back-scattered particles go down the flight path. Under these conditions the background in his experiments has been so reduced that he can now make measurements certainly up to 1 MeV [82]. For the Moxon-Rae detector it can also be said that developments which involve coincidence measurements between pairs of phototubes have been under consideration for some time in Geel [83] and these promise to remove the recoil proton restriction and increase the efficiency to maybe 10%. A version of this detector in which the plastic scintillator is replaced by a solid state electron detector has also been used to make capture cross-section measurements with highly active samples using a nuclear explosion [43]. Here too the measurements can be taken to high neutron energies, since the detector contains no hydrogen. Thus both detectors and their uses are under active development.

Figure 37 shows what is perhaps the largest tank of all, that of Haddad at General Atomics [84]. This one is made of a series of 'logs', each with its own phototubes which can be separately adjusted for gain to attain optimum pulse-height distributions. Figure 38 shows such distributions for resonances in the two isotopes of erbium, the difference in binding energy being obvious. We should observe the high value of bias used, which permits the removal of counts due to activity in the sample (note that this cannot be done with the Moxon-Rae detector).

From a time-of-flight experiment with a capture detector, one obtains a curve of counts per channel against time-of-flight. In this case the raw data cannot readily be converted to a fractional yield curve by comparison with some standard, as in the case of scattering. The most suitable standard is the $^{10}B(n, \alpha\gamma)$ cross-section, but the γ-ray energy emitted (480 keV) is too low for this to be used directly in a large tank. Normalization is therefore performed in two stages: firstly a ^{10}B yield curve is taken, perhaps with an ion chamber, and the capture curve is divided by the ^{10}B yield curve and multiplied by the $^{10}B(n, \alpha)$ cross-section, channel by channel. The second stage is to convert this relative yield curve to a fractional yield, which is done by observing the yield from saturated low-energy resonances in heavy nuclei where $\Gamma_n \ll \Gamma_\gamma$. The fractional yield here is close to unity, and the thin sample curve can be normalized to this. For a thin sample ($n\sigma_{nT} \ll 1$) the fractional yield is $(1-T)\sigma_{n\gamma}/\sigma_{nT} \approx n\sigma_{n\gamma}$. Hence $\sigma_{n\gamma}(E)$ is obtained.

Figure 39 shows such a curve for In (Haddad). Note the general $1/\sqrt{E}$ decay of the cross-section in this energy range where $\Gamma_n \ll \Gamma_\gamma$.

Figure 40 shows the capture cross-section of Co as measured with the Moxon-Rae detector at Harwell. Note that for this much lighter nucleus, the cross-section is not so well behaved. Note also the absence of interference in the capture cross-section, despite the strong overlapping of levels.

Measurements such as this [85] and those of Block [82] and Macklin [81] are slowly providing measurements of Γ_γ for the lighter nuclei, but these are difficult experiments in view of the huge neutron

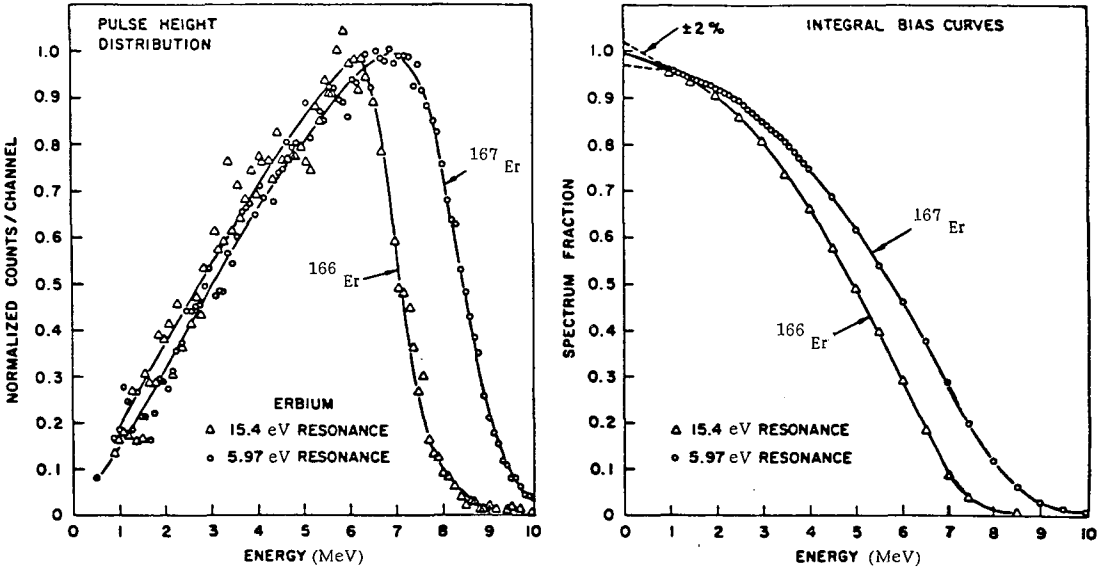

FIG. 38. Liquid scintillator pulse height distributions. Left-hand graph: sum spectra from the 5.97-eV ^{167}Er (n,γ) resonance and the 15.4-eV ^{166}Er (n,γ) resonance. Right-hand graph: curves of the spectrum fractions for the 5.97-eV and 15.4-eV erbium resonances. The data have been corrected for ambient and accelerator-associated backgrounds (Ref. [84], p. 10). (Courtesy of General Atomics)

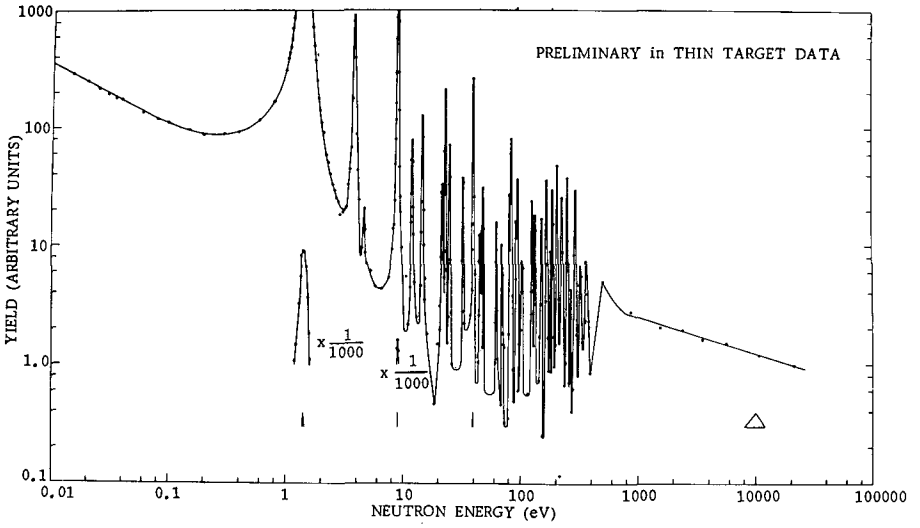

FIG. 39. Capture cross-section of indium (Ref. [84], p. 12)

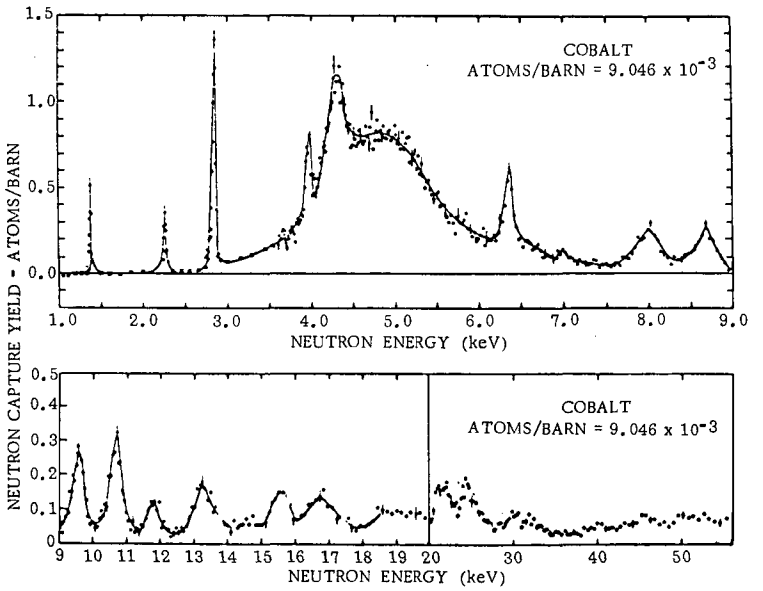

FIG. 40. Neutron capture cross-section of cobalt [85]. (Courtesy of North-Holland Publishing Co.)

widths of the levels concerned, and the need for accurate multiple scattering corrections. Even so Moxon [85] was able to deduce that the mean radiation width for ^{59}Co was 447 ± 69 MeV with a natural spread of 185 meV. This spread is consistent with a number of channels for radiative decay corresponding to the number of strong transitions observed in the thermal neutron capture spectrum (assuming Porter-Thomas

distributions for the partial widths). Determinations of radiation width distributions are now becoming possible even for heavy nuclei where both capture and scattering cross-sections are measured [86], and once again they are consistent with known features of the capture gamma-ray decay spectra.

So far we have omitted all mention of radiative capture measurements on fissile nuclei. These measurements are extremely difficult since fission events produce more total energy in the form of gamma radiation than do capture events in the same nuclei, so that the capture detector measures a yield proportional to $\sigma_{n\gamma} + K\sigma_{nF}$ where $K > 1$. These measurements are however of considerable technological importance. Measurements of $\sigma_{n\gamma}$ for fissile materials often employ an anti-coincidence technique to remove some or most of the fission events, or else a separate measurement is made of σ_{nF} under identical conditions of resolution, and a suitable normalization and subtraction is performed. An example of the anti-coincidence technique is the work of Weston, de Saussure and Gwin [87], who used a fission chamber inside a large scintillator tank. Van Shi-di et al. [88] used a cadmium loaded liquid scintillator and distinguished fission from capture events by the presence in the former case of a delayed coincidence due to the eventual capture of a moderated fission neutron. Since, however, the efficiency of their detector for fissions was only 50%, this experiment was in reality an example of the subtraction technique, with the coefficient K reduced by a factor of 2 by the delayed coincidence system, thereby reducing the error involved in subtraction. The advantage of the subtraction technique is that there is more freedom of choice for the fission detector – it can be a recoil proton detector for the fission neutrons, in which case α-particle activity in the sample causes no problems and quite thick foils can be used. The advantage in statistical accuracy obtained in this way can outweigh the disadvantage of the large correction factor K.

4.5. Capture gamma-ray spectra

The study of the spectra of gamma rays following neutron capture is an old subject, but one which has been greatly stimulated by the development of the lithium drifted germanium detector. This device, which is in effect a solid state ion chamber which requires only 3 eV of particle energy to produce an electron-hole pair, is inferior in resolution to the bent quartz crystal diffraction spectrometer below a few hundred keV, but at energies above 1 MeV it is superior. At higher energies it is at least as good as the best Compton spectrometers, so that it has a highly competitive resolution over a wide energy range combined with good efficiency and the capability of recording the whole spectrum of capture gamma rays from a few hundred keV to say 10 MeV, simultaneously. These desirable features were rapidly exploited in the study of thermal capture spectra, where the high efficiency of the germanium spectrometers permits the study of small samples of separated isotopes, even in cases where the capture cross-section is low. This has led to an extension of the available data to nuclides not previously studied, and to much more detailed spectra owing to the removal of superposed spectra from other isotopes in natural element samples. These improved measurements are yielding a mass of data on the positions of levels in the compound

nuclei formed, and in the transition probabilities between them, which lead to assignment of level parameters and to their interpretation in terms of nuclear models. In particular the information obtained from (n, γ) work is complementary to that obtained from stripping reaction studies, and the combination of data from the two experiments can lead to very complete specification of the level schemes [89].

The study of resonance capture spectra gives information about the transitions from the capturing states to the lower lying states. In thermal capture these transition strengths are arbitrary, and indeed it is dangerous to make any inference about the nature of lower lying states from these strengths. In resonance capture measurements, one obtains sets of transition strengths from a variety of capturing states, and so mean values of the reduced strengths are obtained which have definite physical meanings. The distribution of these strengths is also obtained and can be compared with theory (Porter-Thomas). A further practical advantage in making resonance capture studies is that the spectra from individual isotopes are easily obtained, by selecting appropriate resonances for study, without the need for separated isotope samples, and many spectra can be obtained simultaneously, thereby eliminating effects of drifts.

In this field the advent of the lithium drifted germanium detector has caused a revolution since previously intensity considerations had restricted such work to the use of sodium iodide crystals which gave, at best, a resolution of around 200 keV [90].

Thus for heavy nuclei only transitions to a few levels could be observed even under favourable circumstances. With germanium detectors, in principle, the resolution available in the resonance work is comparable to that obtained in thermal studies: in practice it has been slightly worse because of experimental effects associated with the use of time-of-flight spectrometers. This means that the resolution available at 5-10 MeV is in the 10-20 keV range, rather than the 5-10 keV range reached in thermal studies. Such a resolution is still more than an order of magnitude better than was available with sodium iodide spectrometers, and is adequate for the analysis of most spectra.

In the study of resonance capture spectra by the time-of-flight method, it is essential to minimize the 'gamma-flash' from the neutron source and to use the shortest possible time constants in the amplification system in order to minimize the effect of fluctuations in the tails of the gamma flash pulse on the amplitude of the signal pulses. These considerations lead to a compromise in amplifier band width since too wide a band width causes a low signal-to-noise ratio which adversely affects the resolution, while too small a band width causes a degradation in resolution due to the effect of pile-up of tails of pulses. With a suitable compromise, resolutions of 10-20 keV can be achieved.

Figure 41 shows the spectra obtained with such a system for capture by ^{199}Hg of thermal neutrons, and resonance neutrons of energy 34 eV, 130 eV and 175 eV [91]. These spectra which run from 4 MeV upwards, are essentially the spectra of transitions from the capturing states to a series of bound states of energy up to 4 MeV, and the fluctuations in the strengths of the transitions are obvious. The statistical behaviour of the transition strengths can be analysed on the assumption that all the observed transitions are of E1 character (this is known to be true for all the strong transitions observed in thermal capture in ^{199}Hg [92]. The

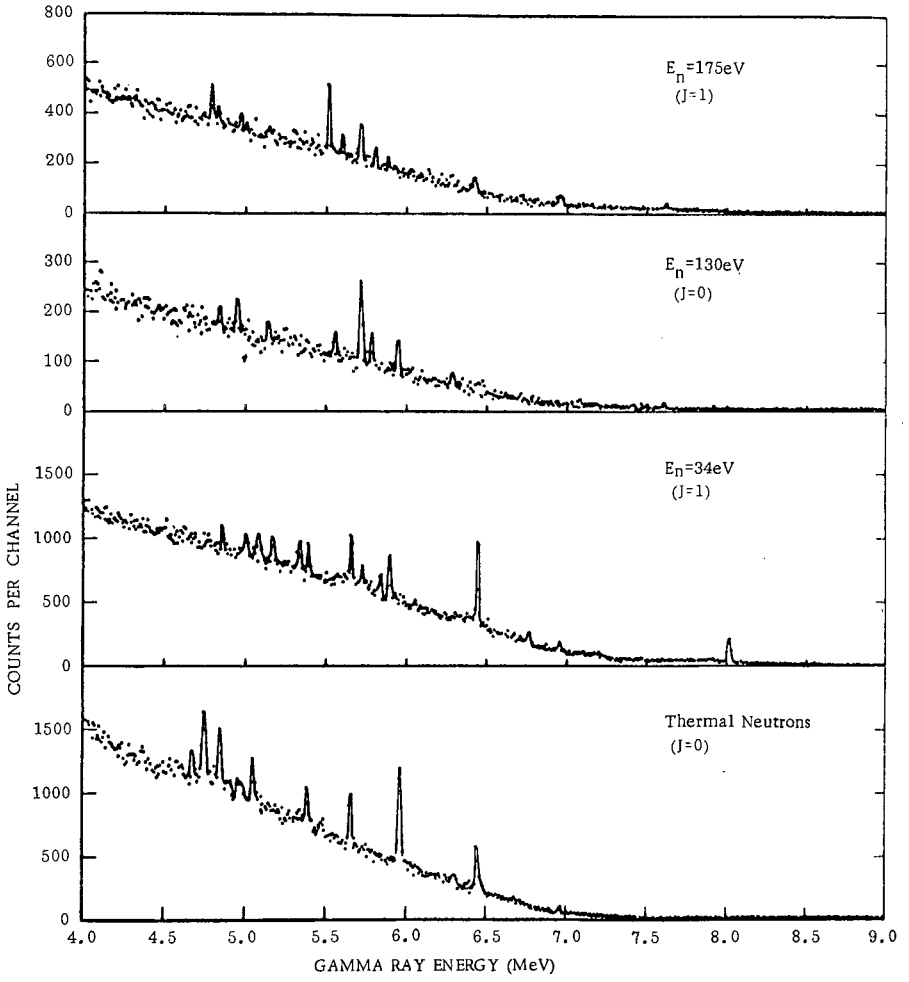

FIG. 41. Gamma ray spectra for reaction $^{199}Hg(n,\gamma)^{200}Hg$ [91]. (Courtesy of American Institute of Physics)

distribution of the reduced strengths (S^1/E_γ^3) for 88 E1 transitions obtained from the mercury data (corrected for variation of detector efficiency with energy), is shown in Fig. 42. Corrections have also been applied for missed weak transitions, for overlap of lines and for the inclusion of M1 transitions on the assumption that the mean E1 strength is 10 times the mean M1 strength. The theoretical curve shown for comparison is the Porter-Thomas distribution and the agreement is clearly good. Figure 43 shows the result of a least squares fit of the data to the chi-squared family of curves, which provides a more quantitative comparison with the theory. The result of this comparison is that the best fit is to a curve whose number of degrees of freedom (channels) $\nu = 0.96^{+0.24}_{-0.17}$. This confirms

that the Porter-Thomas distribution holds for the E1 strengths and confirms the essentially real nature of the wave functions of the states involved. Another experiment which provides a more rigorous proof of the Porter-Thomas distribution for E1 transition strengths is that of Jackson et al. [93] in which they examined transitions in the compound nucleus ^{196}Pt. They determined the strengths of transitions to the ground state and first two excited states in ^{196}Pt, all of which are E1 transitions from the 1^- levels in ^{195}Pt + n, and they did this for 22 resonances of this nature, giving 66 transitions in all. This is a smaller number of

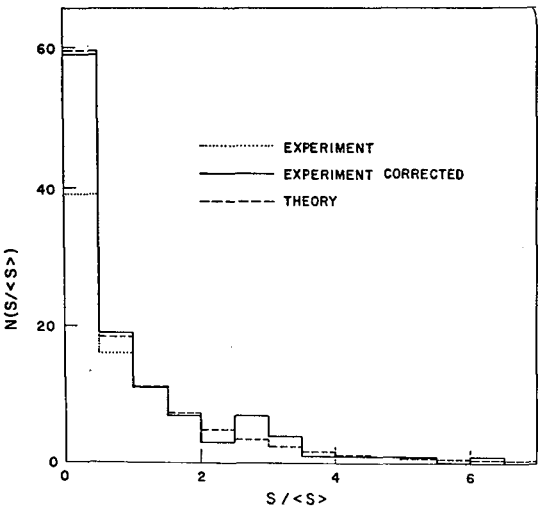

FIG. 42. Corrected experimental histogram showing distribution of reduced strengths for 88 E1 transitions in ^{200}Hg. The Porter Thomas distribution is shown for comparison [91]. (Courtesy of American Institute of Physics)

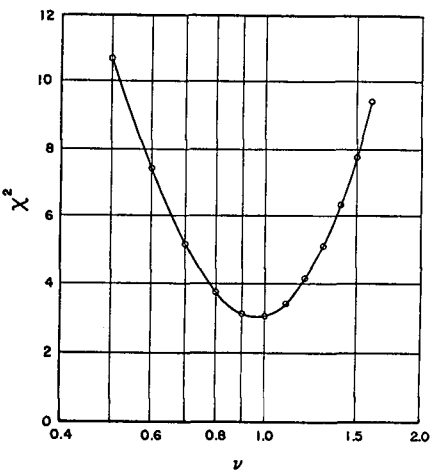

FIG. 43. Least squares fit to experimental distribution of E1 strengths [91]. (Courtesy of American Institute of Physics)

transitions than was observed by Rae et al., but the experiment is better because (1) all transitions were positively assigned as E1, (2) the energy range of the transitions was only from 7231 to 7920 keV so that corrections for variation in detector efficiency with energy were small, and any energy variation in the reduced matrix elements was minimized, (3) the probability of missing levels was negligible.

The result of this work was to establish the observed distribution of the reduced strengths as a chi-squared function with a number of degrees of freedom $\nu = 1.23 \pm 0.19$ again confirming the Porter-Thomas distribution and implying real wave functions. They also observed the distribution of the sum of the strengths to the three levels, over the 22 resonances as corresponding to a chi-squared function with $\nu = 3.57 \pm 1.00$, again confirming the Porter-Thomas distribution.

These two experiments are important in that previous experiments and their interpretation had led to some considerable doubt [55] as to whether ν had the value 1 or 2.

Considerations of the reduced strengths of transitions to low-lying bound states averaged over several capturing states show significant differences for bound states of different character: for example in the case of the compound nucleus ^{200}Hg, the mean reduced strength of transitions from the 1^- capturing states to the 1^+ states above 1255 keV is 43.9 ± 8.8 μeV while the mean reduced strength to the low-lying collective states is 7.1 ± 3.6 μeV. Similar effects are also observed in other nuclei.

A further type of comparison, not yet made with germanium detectors, is to compare mean reduced strengths to the same levels or bands for s-wave and p-wave neutron capture. Measurements of this type can establish the parities of the level or band concerned [94]. The use of high resolution germanium detectors should permit such parity assignments to be made to a large number of levels not previously resolved. Angular correlation measurements and polarization correlation measurements between primary and secondary transition gamma rays following neutron capture can determine both spin and parity of the intermediate state [92].

Thus a study of the detailed spectra and correlations for the gamma rays emitted following neutron capture is in principle capable of providing very complete information about spin, parity and character of states in the compound nucleus.

We have not so far mentioned the possible use of the capture gamma-ray spectra to infer the spin of the capturing state. Certainly this can be obtained in principle in the case of the ^{200}Hg compound nucleus, for example by observing the strength of the transitions from the capturing states to the two 0^+ states at low energy. These are E1 transitions for 1^- capturing states, and are absolutely forbidden for 0^- states. Such measurements however are unreliable owing to the Porter-Thomas distribution in reduced strengths which gives a high probability of very weak (unobservable) transitions. The spin of the capturing state will however affect the multiplicity of the decay cascade in the case of high spin capturing states in even-even compound nuclei, since the decay will proceed preferentially by E1 or M1 transitions. Thus if one observes two-photon decay to the ground state, for example, this will be more probable for the lower possible spin in s-wave capture, than for the higher value. A recent measurement of this type observing the ratio of coincidences to single events (where the higher

multiplicity of the gamma rays from the higher spin state augments the coincidence count rate) was carried out by Coceva et al. [95] at Ispra. The compound nucleus was ^{106}Pd and 17 spin assignments were made.

4.6. Fission cross-sections

The fission cross-sections of heavy nuclei are perhaps the most interesting of all. The behaviour of neutron capture, scattering and total cross-sections can be explained very well in terms of simple concepts like the scattering of an attenuated neutron wave from a semi-transparent sphere (optical model) coupled with the concept of compound nucleus resonances which periodically produce zeros in the logarithmic derivative of the channel wave function. On the basis of these ideas we can explain all of the phenomena of neutron scattering. There is some difficulty in the case of capture in that the observed radiation widths, although varying qualitatively with A, N and Z in the manner expected, are larger than would be expected theoretically on the basis of existing level density theory. This however is a single systematic effect presumably requiring a more sophisticated treatment of the level density theory.

In the case of fission, however, these simple ideas cannot be applied directly. For example, up to the mid 1950's fission was thought, like capture, to be a multichannel mode of decay, and fission widths, like radiation widths, were expected to be nearly constant.

Of course the fission of heavy nuclei was understood crudely in terms of the liquid drop model. A simple classical analogy shows that as one progressively deforms such a charged spherical drop towards a prolate shape, work must be done initially against the surface tension forces. However the charge then tends to migrate to the ends of the drop, and eventually the deformation continues spontaneously, due to electrostatic repulsion and the weakening of the surface tension force, and the drop flies apart. A simple calculation shows that such a spherical charged drop will split spontaneously in two if the ratio of its electrostatic energy to surface energy exceeds a critical value, i.e., if Z^2/A exceeds a critical value. These simple considerations show that only the heaviest nuclei are unstable against spontaneous fission. Figure 44 shows the general nature of the potential barrier against fission, i.e. the energy which must be used to deform it to the 'saddle point' at which fission will occur. For nuclei of charge 92 and greater, the height of this barrier becomes comparable with the binding energy of a neutron, so that if a slow neutron is added, for example to ^{235}U, there is a finite probability that all of the excitation energy in the ^{236}U will be concentrated in deforming the compound nucleus, and fission will result. The potential barrier is a quantum mechanical one however, so there is no sharp energy at which fission suddenly occurs, rather there is an increase in the probability of fission as the barrier is approached, and this probability, expressed as a mean fission width, is given in the well-known penetration formula of Hill and Wheeler [96]

$$\frac{2\pi\langle\Gamma_F\rangle}{D} = \frac{1}{1+\exp\{2\pi\,(E_F - E)/\hbar\,\omega\}} \qquad (4.25)$$

where D, as usual, is the level density in the compound nucleus, E is the excitation energy, E_F is the height of the fission barrier and Γ is a measure of the barrier thickness, $\hbar\omega \lesssim 1$ MeV. We see at once in resonance fission, where the measurements extend at most over a few hundreds of eV, that $\langle \Gamma_F \rangle / D$ is expected to be essentially constant, with a value of $\langle \Gamma_F \rangle$ which depends on the value of E_F as compared with the neutron separation energy. A more detailed study of the conditions at the fission saddle point[6] [97, 98] shows that the distorted nucleus at that point has a ground state and a series of excited states in the same way as any other [Fig. 44) each with definite values of angular momentum and parity, and each corresponding to a definite value of E_F. A more correct expression for the mean fission width is therefore given by

$$\frac{2\pi \langle \Gamma_F^{J\pi} \rangle}{D} = \sum_{\mu} \frac{1}{1+\exp\{2\pi (E_{F\mu}^{J\pi} - E)/\hbar\omega\}} \qquad (4.26)$$

where the sum is over all saddle point states μ of the appropriate spin and parity. Each such saddle point state represents a fission channel, and on this channel theory of fission it is clear that $\langle \Gamma_F^{J\pi} \rangle$ can be considerably larger than $D/2\pi$ if several channels are open, i.e. if several of the $E_{F\mu}^{J\pi}$ lie close to or below the neutron separation energy for the compound nucleus.

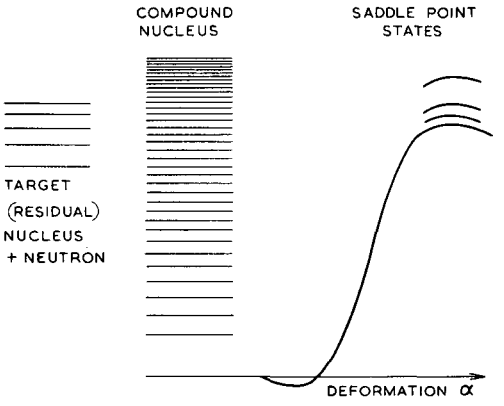

FIG. 44. Energy diagram for fission (Ref. [109], p. 182)

Now for slow neutron induced fission, we know that the difference between E_F and the neutron binding energy is small, hence only a few channels at most can be open, and it is this concept which gives rise to the idea of there being only a few definite quantum mechanical channels for decay of the compound nucleus by fission, and hence to the fluctuations in the fission width, the interference effects in fission cross-sections, and variation in mean fission wdith and in fission mass distributions with the

[6] The term 'saddle point' arises from a plot of the potential energy surface as a function of α_2 and α_3, the coefficients of P_2 and P_3 in a crude description of the shape of the fissioning nucleus.

spin of the resonant state involved. Now the average fission cross-section is given approximately by $\langle \sigma_{nF} \rangle = \langle \sigma_{CN} \rangle \langle \Gamma_F / (\Gamma_F + \Gamma_n + \Gamma_\gamma) \rangle$ where σ_{CN} is the compound nucleus formation cross-section. Hence for those compound nuclei for which the fission barrier energies exceed the neutron separation energy, and indeed correspond to a neutron bombarding energy for which $kR \gtrsim 1$ ($\sim$250 keV for a heavy nucleus) we expect to see a series of rising steps in the fission cross-section as channels open and $\langle \Gamma_F \rangle$ increases stepwise, accompanied by a series of drops as inelastic neutron channels open and $\langle \Gamma_n \rangle$ increases suddenly. At higher energies, the fission cross-section is determined by the relative number of fission and neutron channels which are open, i.e. by the level densities in the compound nucleus at the saddle point, and in the target nucleus.

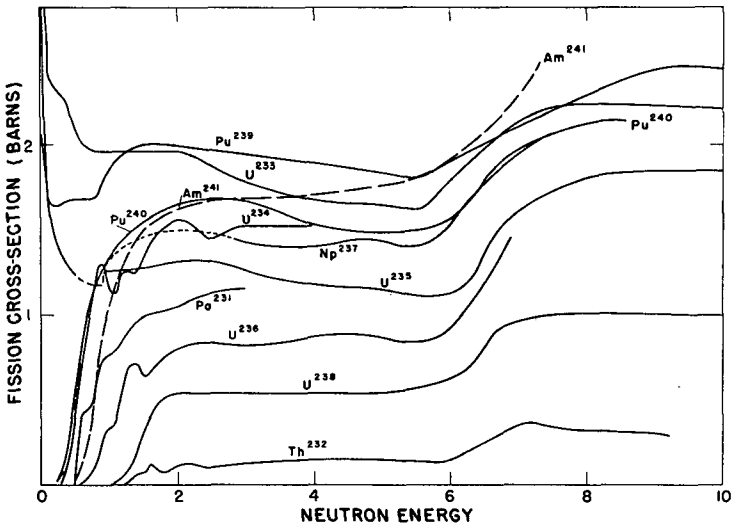

FIG. 45. Compilation of fission cross-section curves for 11 nuclei (Ref. [109], p. 192)

Figure 45 [99] shows a compilation of fission cross-section curves for nuclei having $Z > 90$. We note immediately that three of the curves, for ^{233}U, ^{235}U and ^{239}Pu show a rise at low neutron energies where $kR < 1$ showing that their fission thresholds lie below the neutron separation energies. These are all targets with an odd number of neutrons and the apparently low thresholds are due to the increased binding energy of a neutron due to the pairing force. Since in this mass region the neutron binding energy and the fission barrier are of the same order, the pairing energy is critical in determining the behaviour with slow neutrons. At slightly higher energies the rises in cross-section corresponding to opening fission channels are clearly seen and also some drops in cross-section which may be due to inelastic scattering competition. This is usually followed by a relatively flat region in which the level densities in the target nucleus and the fissioning nucleus are increasing in a similar manner. At around 6 MeV a second strong rise in the cross-section curves takes place due to the possibility of neutron emission followed by fission of the residual (target) nucleus. This converts part of the neutron width

into a fission width and allows a rise in the cross-section. Similar steps are observed at higher energies as fission can follow the emission of 2, 3 or more neutrons. These then are the main features of the fission cross-section. As we noted earlier, the appearance of interference effects in the resonance fission cross-sections of the odd-N nuclei, and the fluctuations in fission widths obtained, were evidence for the Bohr channel theory. For the even-even target nuclei which showed threshold behaviour, the channel theory predicted that the compound nuclei, at the saddle point, would once again be in states of very low intrinsic excitation which would correspond, because of their large prolate distortions, to a rotational band of low K where K is the projection of the total angular momentum on the symmetry axis. Examination of the angular distribution of the fragments for neutron bombardment of even-even targets at threshold showed the expected forward-backward peaking, typical of $K = \frac{1}{2}$ close to threshold, thereby again confirming the channel theory of fission [100].

Returning to the resonance cross-sections of the thermally fissile nuclei, it is possible to find the position of the fission thresholds for these nuclei, even though they occur at negative neutron energies by means of the (d, pF) reaction. From such measurements Northrop et al. [101] showed that for ^{233}U, ^{235}U and ^{239}Pu, these thresholds lie between 1 and 2 MeV below the neutron binding energy. The positions of these thresholds suggest values of $2\pi\langle\Gamma_F\rangle/D$ of 1 or 2 (see Eq. (4.26)). Observed values, however, lie considerably lower, the value for ^{235}U, for example, being 0.22 ± 0.04 (Lynn's tabulation). Such discrepancies have caused considerable theoretical interest in the fission cross-sections (see Lynn's lectures) to be added to the already strong practical interest from the point of view of reactor technology.

The measurement of fission cross-sections also raises some technical problems. Scattering cross-sections, you will remember, could easily be made relative to some standard, like lead or carbon, where the cross-section was almost entirely due to scattering, was independent of E up to several keV at least, and so could be easily determined absolutely in an accurate transmission experiment. In the case of capture, normalization was a little more difficult, since in the nature of the capture process, no such convenient constant cross-section exists. A few light nuclei, however, like ^{10}B, show (n, α) cross-sections which vary essentially as $1/\sqrt{E}$, and since ^{10}B also emits a 480 keV γ-ray, and the (n, $\alpha\gamma$) cross-section also varies as $1/\sqrt{E}$ up to 100 keV, this reaction can be used to determine the shape of the neutron spectrum (N(E)dE) and only the ratio of efficiencies of the detectors for capture events in the sample, and in ^{10}B, need be determined. This is done with the use of convenient low energy resonances where $\Gamma_\gamma \approx \Gamma$, so that with multiple scattering in a thick sample ($n\sigma_0 \gg 1$), all the neutrons in the beam are captured at resonance, and the required absolute calibration of the system is achieved.

For fission, however, there is no cross-section which may be obtained by transmission, neither are there any resonances for which $\Gamma_F \approx \Gamma$ so that all the resonance neutrons would produce fission. We are therefore forced, in the case of fission, to that most undesirable of experiments, the absolute measurement of a cross-section. This means essentially the absolute measurement of a neutron flux, and the calculation of the absolute efficiency of the fission detector.

The absolute measurement of neutron fluxes has been the subject of much study, both for thermal neutrons and for fast neutrons produced by Van de Graaff accelerators. In the case of thermal neutrons, or rather mono-kinetic neutrons in the thermal energy range, the flux can be obtained with high accuracy by the measurement of the activation of foils of materials with large thermal capture cross-sections, such as gold, where the capture cross-section can be determined accurately from a transmission measurement ($\sigma_{n\gamma} \approx \sigma_{nT}$), and where the decay scheme is well known. Alternatively ^{10}B ion chambers with accurately known performance can be used. This involves an accurate knowledge of the quantity of ^{10}B in the chamber, and of the corrections for lost counts due to absorption in the foil and wall effects. A similar problem presents itself for determining the absolute efficiency of the fission chamber, usually an ion chamber in the case of thermal fission. Even so, with very accurate work, such measurements can be made to an accuracy approaching 1% [102].

A novel scheme for the absolute measurement of the thermal fission cross-section of ^{235}U was that adopted by Sapakoglu [103]. This involved a measurement of the neutron flux with a ^{10}B chamber whose efficiency was determined by a coincidence measurement in which the α-particle was detected in the chamber and the associated γ-ray was detected in a sodium iodide detector. The efficiency of the fission detector was likewise determined absolutely by another coincidence measurement with a liquid scintillator detector for the fast neutrons. In this way the efficiency of the fast neutron detector for fission events was also determined. The ion chamber was then replaced by a ^{235}U foil whose mass was obtainable by weighing (it is done by α-particle counting for the very thin ion chamber foils), and in principle the apparatus could then measure σ_{nF} for ^{235}U to 1%. Unfortunately the authors did not take account of the spatial correlation between the direction of emission of the fission fragments and the fission neutrons, due to the fact that the neutrons are emitted from the moving fragments. This effect introduced a bias into the measurement of the efficiency of the fast neutron detector, since the ion chamber efficiency for fragments emitted close to the plane of the foil was low. Hence there was a systematic error in the measurement of several percent which was not explained until several years later when careful measurements of the same nature by Maslin [104] at Aldermaston, with a variety of detector geometries, revealed the effect. Another method of obtaining an accurate measurement of the thermal neutron fission cross-sections, is to determine the ratio α of capture to fission by a mass spectrometer analysis of a sample both before and after a long irradiation in the thermal flux of a reactor. Since the fission cross-section is the dominant one, and since the total absorption cross-section is available to high accuracy from transmission measurements, a measurement of α to, say, 5%, is enough to yield σ_{nF} to an accuracy close to 1%.

The absolute determination of fast neutron fission cross-sections is more difficult. The problem of determining the efficiency of the chamber is here made more difficult by correlations between the fragment emission direction and that of the incident neutron, and the neutron flux measurement represents a formidable problem involving the thermalization of the fast neutrons and their detection then with high efficiency. We shall not pursue this subject, but note that in the past the discrepancies between

measurements have far exceeded their claimed accuracies which were of the order of 3%.

To return to measurements in the resonance region, we must first consider the choice of detector. The fission fragment detector should have a sensitive thickness of the order of the range of the fragments so as to maximize the discrimination against the α-particles which are inevitably emitted by the fission foil. Several types of detector have been used successfully for this purpose including ion chambers, gas scintillation detectors, surface barrier semiconductor detectors and spark chambers. The ion chambers, although the easiest to use, have rather a slow response which makes them unsuitable for use with extremely active foils. The spark chambers at the other extreme, are claimed to be incapable of being triggered at all by α-particles.

Having measured a fission yield curve as a function of neutron energy, the technique for obtaining the cross-section is to remove the effect of the neutron spectrum and then to normalize the curve at thermal energy, where, as we have said, the cross-sections are known to ~1% for the common fissile nuclides. Figure 46 shows the fission cross-section of ^{241}Pu [105] across the resonance region. As in the case of the capture cross-section of In, the $1/\sqrt{E}$ variation of the average cross-section is clear, indicating that $\Gamma_n < \Gamma_\gamma + \Gamma_F$ over the energy range studied.

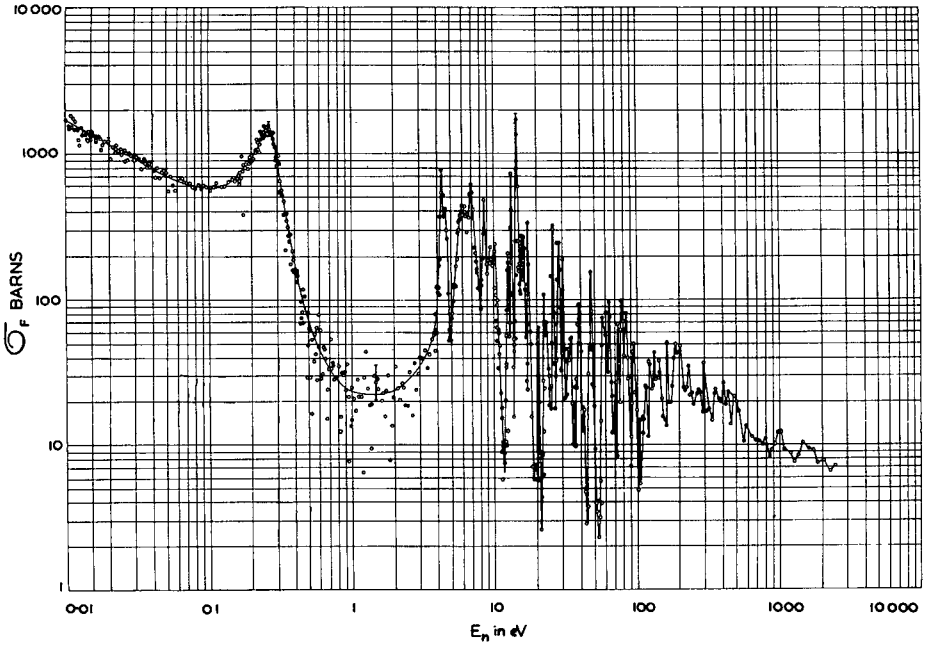

FIG. 46. ^{241}Pu fission cross-section from 0.01 eV to 3 keV [105]

Because of the great interest in the cross-sections of the fissile nuclei, both for their technological importance and for their intrinsic significance in connection with the channel theory of fission, it is very desirable to make these measurements with the highest possible resolution in order

to have an accurate record of the shape of the cross-section curves over the widest possible energy range. In transmission measurements on fissile targets it is relatively easy to achieve nominal resolutions of better than 1 nsec/m. In fission cross-section measurements with fragment detection, however, particularly if the material is very active and only small amounts can be used, it is difficult if not impossible to approach this resolution. Because of the great intensity of neutrons available from a nuclear explosion, it is in principle quite possible to achieve very high resolution with this technique [106] (and various measurements have recently been made in this way), but for work with accelerators, the obvious way to improve the resolution on fission cross-section measurements is to abondon fragment detection and detect the fission events through the fast fission neutrons. In this way the α-particles from the foil are no longer troublesome and the foil need no longer be extremely thin to allow the escape of the fragments, so that larger samples can be used. Such measurements have now been made on the Harwell linac [107] using a flight path of 100 m, which with a 100-nsec pulse gives a nominal resolution $\sim$1 nsec/m.

When really thick samples are used in an experiment of this sort ($n\sigma \gg 1$) and are combined with a transmission measurement carried out under identical conditions of resolution, the result is that a quantity is measured which is proportional to $\eta = \overline{\nu}\sigma_{nF}/\sigma_{nA}$. If the transmission is really zero, and if we ignore for the moment the loss of energy on scattering, it is clear that all the incident neutrons are absorbed in the sample, and must either be captured or produce fission events. If our detector utilizes a liquid scintillator with pulse shape discrimination, it is sensitive to the fission neutrons, but not to the capture γ-rays, and so it is clear that it records a quantity proportional to $\overline{\nu}\sigma_{nF}/\sigma_{nA}$, or η. In a real case, corrections are made for the finite transmission of the sample, for energy loss of the neutrons on scattering, and for the probability of their escape from the foil, and η is obtained, for those energy regions where the sample has $n\sigma \gg 1$. This is done then for a range of sample thicknesses: where $n\sigma \ll 1$, σ_{nF} is obtained, where $n\sigma \gg 1$, η is obtained, and of course from the transmission part of the experiment σ_{nT} is obtained. From all these data one can extract both σ_{nF} and $\sigma_{n\gamma}$ (always assuming $\overline{\nu}(E)$ to be constant), provided σ_{nn} can be calculated or measured. In fact the scattering has a negligible effect on the resonances being only important in regions of low cross-section. $\sigma_{n\gamma}$ is therefore not obtained with any accuracy in regions of low cross-section. Figure 47 shows a measurement of σ_{nF} for ^{239}Pu [108] obtained by this method. We note that this method also produces a determination of $\sigma_{n\gamma}$, at least at low neutron energies.

Much more could be said about the subject of neutron induced fission in the resonance region, such as the anomalously low values of the fission widths for many nuclei showing threshold fission at relatively low neutron energies [109] and the relationship of this to the channel theory, and the study of fission mass distributions as a function of J and π [110]. Unfortunately time does not permit this, but these topics may be covered by Mr. Lynn in his theoretical course (not published). For a general review of fission physics, the reader is referred to Physics and Chemistry of Fission, published by the IAEA (1965).

5. INTERMEDIATE ENERGY NEUTRON SPECTROSCOPY

On the basis that neutron spectroscopy is the study of sharp nuclear states through neutron energy and intensity measurements, this brief section does not consider measurements of neutron cross-sections at higher energies, where we are dealing with a continuum. Rather, we shall look at the study of the energy and intensity distributions of fast neutrons emitted in nuclear reactions where these distributions involve sharp groups corresponding to quantum mechanical states in the compound or residual nucleus.

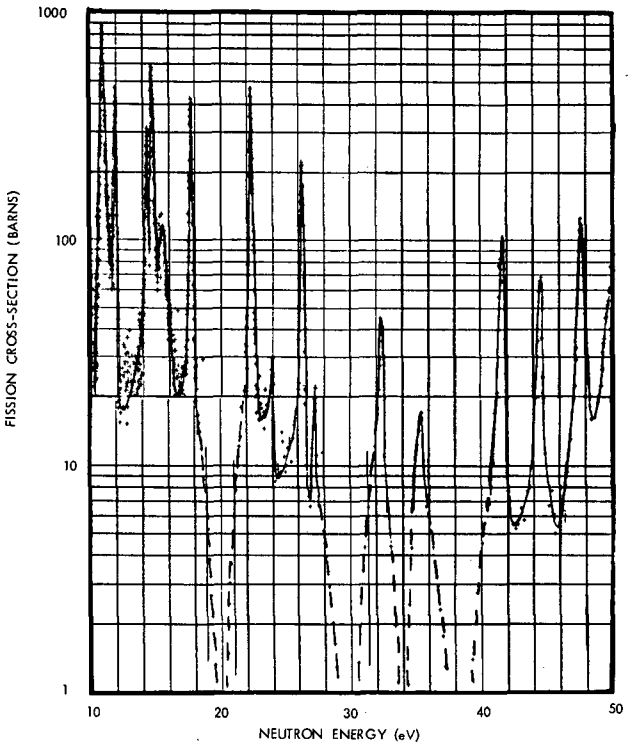

FIG. 47. Fission cross-section of ^{239}Pu. The dotted lines indicate regions where the cross-section is too low to be measured [108]

In this category are the photoneutron production cross-sections which have been studied most effectively by time-of-flight techniques [111]. Here the principal object of study is the photonuclear giant dipole resonance. The simple liquid drop model which predicted easily the simplest basic facts about the fission process is also able to predict the existence of a photonuclear dipole resonance in which the protons in the nucleus are set vibrating relative to the neutrons. Such a model predicts the existence of a resonance in the photon absorption cross-section at an energy of about 20 MeV for nuclei in the calcium region, dropping off in energy with mass number as the size of the resonator increases. This observation is in qualitative agreement with experiment. The simple hydromechanical

model can also account qualitatively for such effects as the increased width of the giant resonance for very highly deformed nuclei in the rare earth region. The observation, however, of fine structure in the photonuclear cross-sections of light nuclei, and the failure in these cases of the simple relationship between the resonance energy and the nuclear radius, require the introduction of a more sophisticated model. In this case the electromagnetic waves interact with the nucleons rather than with the nucleus as a whole, and the interaction is rather of the nature of raising individual neutrons and protons to higher energy states. Such a description, in terms of shell model states, and taking into account the residual particle-hole interaction, is capable of explaining rather well the general behaviour of the photonuclear cross-sections in light nuclei, particularly if these have a rather simple structure like the doubly closed shell nucleus ^{16}O. In this case, for example, the theory predicts four main peaks in the cross-section curve corresponding to definite nucleon transitions. This means that if the nucleus is irradiated with a white spectrum of photons covering the energy region of the giant resonance, a series of peaks is seen in the spectrum of particles emitted (neutrons or protons are energetically possible). The neutrons, of course, are much easier to observe than the protons, since they escape easily from the target, and their energy and intensity distribution can be examined by the time-of-flight technique.

The experimental arrangement for these studies is to produce a bremsstrahlung pulse of a few nanoseconds' duration using an electron linac. This means causing the electron beam to strike a thin heavy (tantalum or tungsten) target, removing the transmitted electrons with a magnetic field or light absorber, and allowing the transmitted bremsstrahlung beam to irradiate the target to be studied. The photoneutrons produced are allowed to fly down a long flight path set preferably at a backward angle to minimize γ-ray scattering effects, and the time spectrum of the neutrons is measured in the usual way with a multi-channel analyser. In the Harwell system the pulse length is 10 nsec and the flight path length 100 m giving a nominal resolution of 0.1 nsec/m. By adjusting the energy of the electron beam, and so the energy of the tip of the bremsstrahlung beam, it is possible to infer which of the neutron groups observed leave the daughter nucleus in its ground state. The energy of these neutrons is then uniquely related to the energy of the photon causing the reaction, and the yield curve can be plotted as a function of photon energy. Before looking at the experimental results, let us consider for a moment, the energy resolution available in such an experiment with a nominal resolution of 0.1 nsec/m. In the case of ^{16}O for example, as target, the binding energy of a neutron is about 16 MeV, and the giant resonance extends at least to 26 or 27 MeV. Hence the neutrons emitted cover an energy range up to the order of 10 MeV. Now the detector used in such an experiment is of the proton recoil type, a plastic scintillator, of thickness, say, 3-5 cm, to achieve good efficiency. Likewise the water photonuclear target used has a thickness of $\sim$3 cm. Hence there is a length uncertainty of say 5 cm altogether in the flight path, and so the energy resolution ($\Delta E/E$), given by Eq. (3.6) is $2\times 5/10^4$ for low-energy neutrons ($v\Delta t \ll \Delta \ell$) going to $2v\,\Delta t/\ell$ where $v\Delta t \gg \Delta \ell$. This latter reduces to a

numerical value of $E^{\frac{1}{2}}/360$ where E is the energy in MeV. Hence the resolution width ΔE for a range of neutron energies is as tabulated below

E (keV)	10	10^2	10^3	10^4
ΔE (keV)	0.01	0.13	2.9	88

These figures can be compared with the curves in Fig. 20, and we observe that they are more pessimistic at the lower energy end in that they take into account the dimensions of source and target. They are probably over-pessimistic in that at these lower energies, the rise in the hydrogen cross-section reduces the effective thickness of the detector. In any case they indicate clearly that over the energy range studied the resolution is always better than 100 keV, and that in the range below 1 MeV it is extremely good, bearing in mind that this technique is used to study light elements where the level spacing is wide.

Let us then return to the experimental data, and look at the neutron energy spectra observed when a light element is irradiated with a bremsstrahlung beam. Two such curves, corresponding to different bremsstrahlung end points, are shown in Fig. 48 for an oxygen (water) target [112].

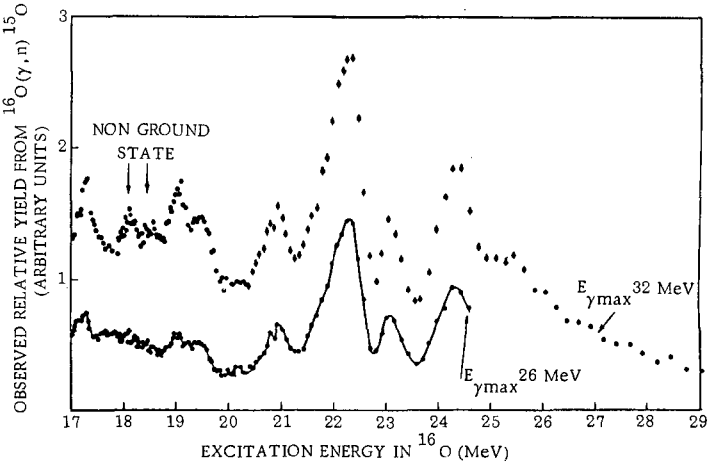

FIG. 48. The observed relative yield of photoneutrons from the reaction $^{16}O(\gamma,n)^{15}O$ assuming ground state transitions only. The bremsstrahlung energies are 26 and 32 MeV. No corrections have been made for background effects. The time-of-flight resolution is 0.5 nsec · m^{-1} [112]. (Courtesy of North-Holland Publishing Co.)

The structure, corresponding to the 'giant dipole resonance' in oxygen is clearly seen. An interesting feature is that the shell model calculations with particle-hole interactions predict 4 main peaks, all of which are observed in the experiment. The experiment data, however, contain much more structure, showing more than 10 states. These are presumably due to coupling with the shell model states of more complicated states due possibly to collective motions of the highly excited and therefore no longer spherical nucleus. Similar studies of other light nuclei show much more complex structure.

Another application of the fast neutron time-of-flight technique is the study of neutron inelastic scattering [113]. This is very useful in investigating low-lying levels particularly in heavy nuclei, where charged particles of very high energy would be required to excite the same states on account of the Coulomb barrier. This use of pulsed neutron sources has been made attractive by the development of very intense pulsed Van de Graaff accelerators, utilizing post acceleration bunching. Such acclerators give proton pulses with duration <1 nsec and pulse currents in excess of 10 mA. Another factor in the development of the work is the improvement in proton recoil detectors due to the use of photo-tubes in coincidence to reduce the noise, and so to lower the neutron threshold for their use, and the reduction of γ-ray sensitivity by the use of pulse-shape discrimination.

The technique here is to produce a primary pulse of highly monoenergetic neutrons by means of a suitable reaction, and then to look at the inelastically scattered neutrons by time-of-flight, in 'bright-line' geometry over a short flight path of a metre or two. The geometry of such an experiment is shown schematically in Fig. 49 which illustrates the Ibis 3 MeV pulsed Van de Graaff accelerator at Harwell. The post acceleration bunching magnet is shown, and the neutron source, scattering target and detector are all mounted high above the floor to avoid back scattering. The heavy shielding which protects the detector against neutrons coming from sources other than the scattering sample, is clearly seen. The nominal resolution here is $\sim$0.5 nsec/m and the low energy limit of $\Delta E/E$ is $\sim$2%. Hence over the energy range 10 keV to 1 MeV, the resolution width goes from 0.2 keV to about 25 keV.

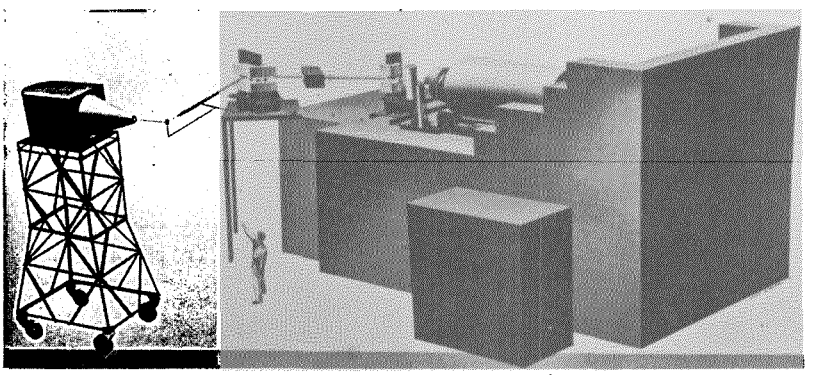

FIG. 49. Ibis neutron time-of-flight facility [113]. (Courtesy of North-Holland Publishing Co.)

Figure 50 shows the yield curve of neutrons scattered from a target of ^{238}U. The large elastic scattering peak has been drawn on a smaller scale, but many peaks are seen due to inelastically scattered neutrons which leave the ^{238}U in states other than the ground state. Figure 51 shows the interpretation of the experiment in terms of a level scheme for ^{238}U. This is compared with a similar scheme obtained by Coulomb excitation using charged particles with energies of the order of 12 MeV. It will be observed that states of very high angular momentum are more easily excited by Coulomb excitation as might be expected, but on the other hand several states of higher energy (which are presumably not of

a collective nature) are excited by the neutrons but not by the charged particles.

Our final topic is the use of fast neutron time-of-flight spectroscopy to study the neutrons emitted from nuclear reactions initiated by charged particles [114]. Here the use of a time-of-flight spectrometer for the neutrons is the analogue of a magnetic spectrometer for charged reaction products, only a simple neutron time-of-flight system is much less expensive than its charged particle counterpart. The main use of such a system is in the study of direct reactions of the type (p, n), (d, n), (^{3}He, n), etc. The (p, n) reaction is of course the simplest reaction in which isospin analogue states were first studied (see chapter 3). Typically in the

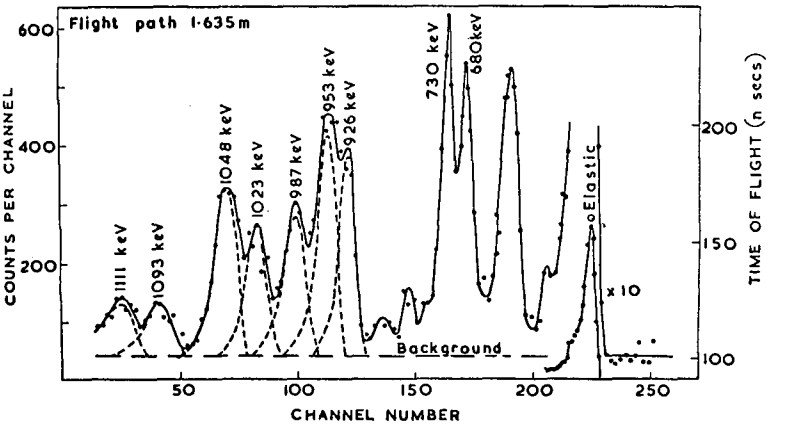

FIG. 50. Time-of-flight spectrum of scattered neutrons. Incident energy, 1305 keV [113]. (Courtesy of North-Holland Publishing Co.)

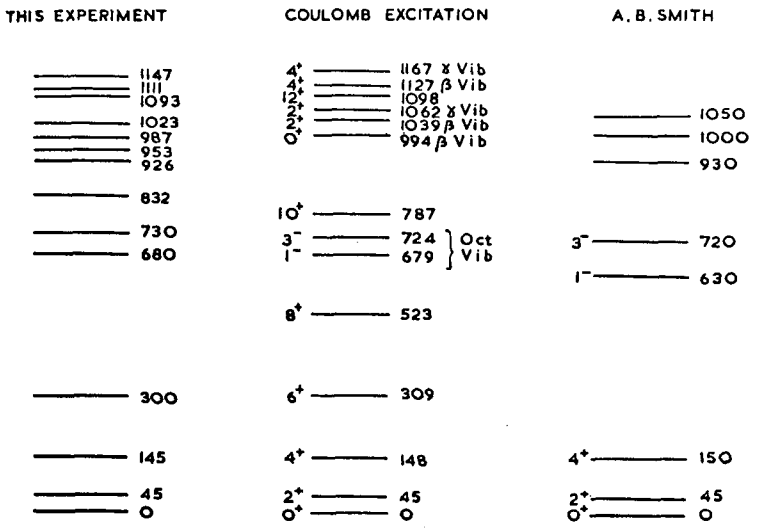

FIG. 51. Energy level diagram for uranium-238 [113]. (Courtesy of North-Holland Publishing Co.)

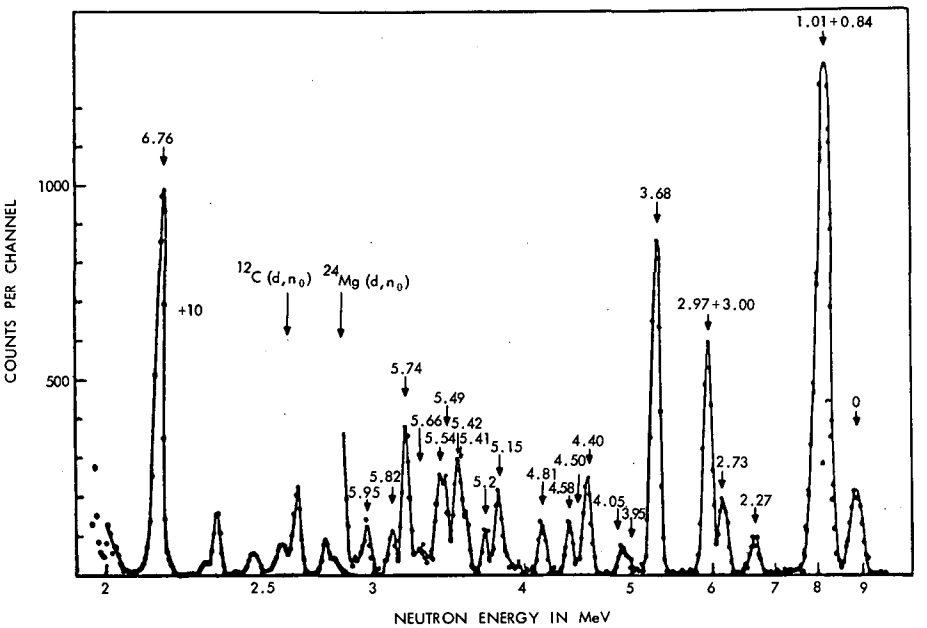

FIG. 52. Pulse-height spectrum for the reaction ^{26}Mg(d,n)^{27}Al. Of particular interest is the strength of the transition to the 6.76 MeV level (Ref. [114], p. 47). (Courtesy of North-Holland Publishing Co.)

spectrum of emitted neutrons one sees high energy groups going to the low-lying states in the daughter nucleus, and then, at much lower neutron energy, a further series of prominent states which are the analogues of states in the target nucleus, and which are states in the daughter nucleus having the same T assignments as the ground state and first few states in the target nucleus [115]. The study of (p, n) reactions must, of course, be undertaken with energetic protons since the Q values are always negative and may be large. Hence to be able to excite many states in the final nucleus, a tandem Van de Graaff accelerator is required. Where more modest energy is available, the positive Q reactions involving heavier projectiles are used and the (d, n) reaction has also been used extensively in a search for isobaric analogue states in light nuclei. Our final Figure 52 shows the neutron spectrum from the reaction ^{26}Mg(d, n)^{27}Al obtained with deuterons of only 3 MeV energy, displaying a large number of excited states in ^{27}Al up to 7 MeV. Of interest is the very strongly excited state at 6.76 MeV (note yield is divided by 10) which is the isobaric analogue of the ground state of ^{27}Mg. These few illustrative examples should serve to indicate the great power of neutron spectroscopy when applied at intermediate energies to the study of nuclear structure.

REFERENCES

[1] SEGRE, E., Nuclei and Particles, Benjamin, New York, 1965.
[2] CHADWICK, J., Proc.R.Soc. A136 (1932) 692.

[3] HANSON, A.O., Fast Neutron Physics, Pt.I (MARION, J.B., FOWLER, J.L., Eds), Interscience, New York (1960) 3-48.
[4] BROLLEY, J.E., FOWLER, J.L., Fast Neutron Physics, Pt.I (MARION, J.B., FOWLER, J.L., Eds), Interscience, New York (1960) 49-72.
[5] Proc.Seminar on Intense Neutron Sources, Santa Fé, 1966.
[6] HAEBERLI, W., Fast Neutron Physics, Pt.II (MARION, J.B., FOWLER, J.L., Eds), Interscience, New York (1960) 1379.
[7] HUGHES, D.J., Pile Neutron Research, Addison Wesley, Reading, Mass. (1953).
[8] JEFFRIES, C.D., Dynamic Nuclear Polarization, Interscience, New York (1963).
[9] BROOKS, F.D., Neutron Time of Flight Methods (SPAEPEN, J., Ed.), EANDC, Brussels (1961) 389.
[10] RAE, E.R., BOWEY, E.M., Proc.phys.Soc. A66 (1953) 1073.
[11] NICHOLSON, K.P., SNELLING, G.F., AERE EL/R (1954) 1350.
[12] SCHENK, J., HEATH, R.L., Phys.Rev. 85 (1952) 923.
[13] BOLLINGER, L.M., THOMAS, G.E., R.S.I. (1961).
[14] MUELHOUSE, C.O., THOMAS, G.E., Phys.Rev. 85 (1952) 926.
[15] FURST, M., KALLMANN, H., BROWN, F.H., Nucleonics 13 (1955) 58.
[16] BOLLINGER, L.M., THOMAS, G.E., GINTHER, R.G., R.S.I. 30(1959) 1135.
[17] BISHAY, A.M., J.Am.Ceram.Soc. 231 (May 1961).
[18] FIRK, F.W.K., SLAUGHTER, G.G., GINTHER, R.J., Nucl.Instrum. 13 (1961) 313.
[19] COCEVA, C., Nucl.Instrum. 21 (1963) 93.
[20] EGELSTAFF, P.A., Nucl.Instrum. 1 (1957) 197.
[21] GINTHER, R.J., SCHULMAN, J.H., I.R.E. Trans.on Nucl.Sci. N55 3 (1960) 321.
[22] VOITOVETSKII, V.K., TOLMACHEVA, N.S., Atomn.Energ. 6 (1960) 472.
[23] GINTHER, R.J., I.R.E. Trans.on Nucl.Sci. NS-7 2-3 (1960) 28.
[24] HARRIS, D.H.C., AERE-R3688 (1961).
[25] SUN, K.H., MALMBERG, P.R., PECJAK, F.A., Nucleonics 14 (1956) 46.
[26] RAFFLE, J.F., HALL, J.W., AERE-M461 (1959).
[27] CRANBERG, L. et al., ORNL-2309 (1956) 148.
[28] CRANBERG, L., BEAUCHAMP, R.K., LEVIN, J.S., R.S.I. 28 (1957) 89.
[29] RAINWATER, J., HAVENS, W.W.,Jr., DESJARDINS, J.S., ROSEN, J.L., R.S.I. 31 (1960) 481.
[30] HUGHES, D.J., Pile Neutron Research, Addison Wesley, Cambridge, Mass. (1953) 160.
[31] EGELSTAFF, P.A., Neutron Time of Flight Methods (SPAEPEN, J., Ed.), EANDC, Brussels (1961) 261.
[32] RAINWATER, J., Proc.Conf.on Neutron Cross Section Technology, Washington (1966) 381.
[33] NICHOLSON, K.P., POOLE, M.J., Automatic Acquisition and Reduction of Nuclear Data (BECKURTS, K. et al., Eds), EANDC, Karlsruhe (1964) 96.
[34] POOLE, M.J., WIBLIN, E.R., Proc.2nd UN Int.Conf.PUAE 14 (1958) 266.
[35] COATES, M., GAYTHER, D.B., private communication (1966).
[36] MICHAUDON, A., CEA-R2552.
[37] RIBON, P., MICHAUDON, A., Neutron Time of Flight Methods (SPAEPEN, J., Ed.), EANDC, Brussels (1961) 357.
[38] CIERJACKS, S. et al., Proc.Santa Fé Seminar on Intense Neutron Sources, 1966.
[39] Intense Neutron Generator, AECL-2600 (1966).
[40] NEWSON, H., Nuclear Structure with Neutrons (NEVE,M. et al., Eds), North-Holland Publishing Co., Amsterdam (1966) 195.
[41] BLOKHIN, G.E. et al., Physics of Fast and Intermediate Reactors III, IAEA Vienna (1962) 399; also MALYSHEV, A.V., Nuclear Structure Study with Neutrons (NEVE,M. et al., Eds), North-Holland Publishing Co., Amsterdam (1966) 236.
[42] SHAPIRO, F.L., Nuclear Structure Study with Neutrons (NEVE, M.et al., Eds), North-Holland Publishing Co., Amsterdam (1966) 223.
[43] DIVEN, B., Nuclear Structure Study with Neutrons (NEVE, M. et al., Eds), North-Holland Publishing Co., Amsterdam (1966) 441.
[44] Proc.Int.Conf.on Automatic Acquisition and Reduction of Nuclear Data (BECKURTS, K. et al., Eds), EANDC, Karlsruhe (1964).
[45] BERGMAN, A.A. et al., Proc.UN Int.Conf.PUAE 4 (1958) 135.
[46] MARION, J.B., FOWLER, J.L. (Eds), Fast Neutron Physics, Pt.I,Interscience, New York (1960).
[47] BLATT, J.M., WEISKOPF, V.F., Theoretical Nuclear Physics, John Wiley Sons, New York (1952).
[48] LAMB, W.E., Phys.Rev. 55 (1939) 190.

[49] HARVEY, J.A., ATTA, S.E., Neutron Time of Flight Methods (SPAEPEN, J., Ed.), EANDC, Brussels (1961) 555.
[50] RIBON, P. et al., private communication (1965).
[51] MELKONIAN, E., HAVENS, W.W., RAINWATER, L.J., Phys.Rev. 92 (1953) 702.
[52] LYNN, J.E., Nucl.Instrum.Meth. 91 (1960) 315.
[53] WIGNER, E.P., EISENBUD, L., Phys.Rev. 72 (1947) 29.
[54] HUMBLET, J., ROSENFELD, L., Nucl.Phys. 26 (1961) 529.
[55] JULIEN, J., Nuclear Structure Study with Neutrons (NEVE, M., et al., Eds), North-Holland Publishing Co., Amsterdam (1966) 162.
[56] COTE, R.E., BOLLINGER, L.M., THOMAS, G.E., Phys.Rev. 134B (1964) 1047.
[57] FIRK, F.W.K., LYNN, J.E., MOXON, M.C., Proc.phys.Soc. 82 (1963) 477.
[58] THOMAS, R.G., Phys.Rev. 97 (1955) 224.
[59] LYNN, J.E., Nuclear Structure Study with Neutrons (NEVE, M., et al., Eds), North-Holland Publishing Co., Amsterdam (1966) 125.
[60] UTTLEY, C.A., NEWSTEAD, C.M., DIMENT, K.M., Proc.Paris Conf.on Nuclear Data, 1966, Paper No. CN-23/36.
[61] LANE, A.M., THOMAS, R.G., Rev.mod.Phys. 30 (1958) 257.
[62] Le POITTEVIN, G. et al., Nucl.Phys. 70 (1965) 497.
[63] RIBON, P., LOTTIN, A., MICHAUDON, A., TROCHON, J., Proc.Antwerp Conf. on Study of Nuclear Structure with Neutrons, 1965, Paper No.165.
[64] FIRK, F.W.K., LYNN, J.E., MOXON, M.C., Nucl.Phys. 41 (1963) 614.
[65] MURADYAN, G.V., ADAMCHOUK, Yu.V., Proc.Paris Conf. on Nuclear Data, 1966, Paper No. CN-23/107.
[66] LYNN, J.E., private communications (1966).
[67] NEWSON, H., Proc.Washington Conf.on Nuclear Cross Sections (1966) 562.
[68] RAE, E.R., COLLINS, E.R., KINSEY, B.B., LYNN, J.E., WIBLIN, E.R., Nucl.Phys. 5 (1958) 89.
[69] ASGHAR, M., MOXON, M.C., CHAFFEY, C.M., to be published (1967).
[70] SAUTER, G.T., BOWMAN, C.D., Phys.Rev.Lett. 15 (1965) 761.
[71] BORST, L.B., Phys.Rev. 90 (1953) 859.
[72] WOOD, R.E., Phys.Rev. 104 (1956) 1425.
[73] FRASER, J.S., SCHWARTZ, R.B., Nucl.Phys. 30 (1962) 269.
[74] MOORE, M.S., SIMPSON, F.B., Nucl.Sci.Engng 13 (1962) 18; SINGH, P.P., Chalk River preprint (1964); POORTMANS, F., CEULEMANS, H., NEVE, M., Proc.Washington Conf. on Nuclear Cross Sections (1966) 755.
[75] ASGHAR, M., BROOKS, F.D., Nucl.Instrum., to be published.
[76] ASGHAR, M., Proc.Paris Conference on Nuclear Data (1966), to be published in Nuclear Physics (1967).
[77] DIVEN, B.C., TERRELL, J., HEMMENDINGER, A., Phys.Rev. 120 (1960) 556.
[78] GIBBONS, J.H., MACKLIN, P.L., MILLER, P.D., NEILER, J.H., Phys.Rev. 122 (1961) 182.
[79] BLOCK, R.C., SLAUGHTER, G.G., WESTON, L.W., VONDERLAGE, F.C., Neutron Time of Flight Methods (SPAEPEN, J., Ed.), EANDC, Brussels (1961) 203.
[80] MOXON, M.C., RAE, E.R., Nucl.Instrum. 24 (1963) 445.
[81] MACKLIN, R.L., GIBBONS, J.H., INADA, T., Nucl.Phys. 43 (1963) 353.
[82] BLOCK, R.C., private communications (1966); and Proc.Paris Conf.on Nuclear Data, 1966, Paper No. CN-23/126.
[83] WEIGMANN, H., CARRARO, G., BÖCKHOFF, K.H., submitted to Nucl.Instrum.Meth.
[84] HADDAD, E., FRÖHNER, F.H., LOPEZ, W.M., FRIESENHAHN, S.J., General Atomics Report G-A-6919 (1966).
[85] MOXON, M.C., Proc.Antwerp Conf.on Nuclear Structure Study with Neutrons, 1965, Paper 88.
[86] ASGHAR, M., et al., Nucl.Phys. 76 (1966) 196.
[87] WESTON, L.W., de SAUSSURE, G., GWIN, R., Nucl.Sci.Engng 20 (1964) 80; and Proc.Paris Conf. on Nuclear Data, 1966.
[88] SHI-DI, Van, YUN-CHAN, Van, DERMENDZHIEV, E., RYABOV, Yu.V., Physics and Chemistry of Fission 1 IAEA, Vienna (1965) 287.
[89] VERRIER, J., Nuclear Structure Study with Neutrons (NEVE, M., et al., Eds), North-Holland Publishing Co., Amsterdam (1966) 94.

[90] BOLLINGER, L.M., COTE, R.E., CARPENTER, R.T., MARION, J.P., Phys.Rev. 132 (1963) 1640.
[91] RAE, E.R., MOYER, W., FULLWOOD, R.R., ANDREWS, J.L., to be published in Phys.Rev. (1967).
[92] BARTHOLOMEW, G.A., EARLE, E.D., GUNYE, M.R., Proc.Antwerp Conf.on Nuclear Structure Study with Neutrons (1965) Paper No.43.
[93] JACKSON, H.E. et al., private communication (1966), to be published.
[94] STARFELT, N., Nuclear Structure Study with Neutrons (NEVE, M. et al., Eds), North-Holland Publishing Co., Amsterdam (1966) 317.
[95] COCEVA, C., CORVI, F., GIACOBBE, P., STEFANO, M., Phys.Lett. 16(1965) 159.
[96] HILL, D.L., WHEELER, J.A., Phys.Rev. 89 (1953) 1102.
[97] BOHR, A., UN Int.Conf.PUAE 2 (1956) 151.
[98] WHEELER, J.A., Fast Neutron Physics II (MARION, J.B., FOWLER, J.L., Eds), Interscience, New York 1963, p.2051.
[99] HENKEL, R.L., Fast Neutron Physics II (MARION, J.B., FOWLER, J.L., Eds), Interscience, New York 1963, p.2001.
[100] LAMPHERE, R.W., Physics and Chemistry of Fission I IAEA, Vienna (1965) 63.
[101] NORTHROP, J.A., STOKES, R.H., BOYER, K., Phys. Rev. 115 (1959) 1277.
[102] BNL-325 3rd ed., 1966.
[103] SAPAKOGLU, A., Proc. 2nd UN Int.Conf.PUAE 16 (1958) 103.
[104] MASLIN, E., Phys.Rev. 139 (1965) B852.
[105] JAMES, G.D., Physics and Chemistry of Fission I IAEA, Vienna (1965) 235.
[106] See various contributions to Pt. 2 of Proc.Washington Conference on Neutron Cross Section; Technology AEC Report CONF-660303 (1966).
[107] PATRICK, B., SCHOMBERG, M.G., SOWERBY, M.G., Proc.Paris Conf. on Nuclear Data, 1966, Paper No. CN-23/30.
[108] PATRICK, B.N. et al., Proc.Paris Conf.on Nuclear Data, 1966, Paper No. CN-23/30.
[109] RAE, E.R., Physics and Chemistry of Fission I IAEA, Vienna (1965) 187.
[110] COWAN, G. et al., Physics and Chemistry of Fission I IAEA, Vienna (1965) 347; also CUNNINGHAME, J.G., FRITZE, K., LYNN, J.E., WEBSTER, C.B., Nucl.Phys. 84 (1966) 49.
[111] FULLER, E.G., Nuclear Structure Study with Neutrons (NEVE, M. et al., Ed.), North-Holland Publishing Co., Amsterdam (1966) 359.
[112] FIRK, F.W.K., Nucl.Phys. 52 (1964) 437.
[113] FERGUSON, A.T.G., Nuclear Structure Study with Neutrons (NEVE, M. et al., Eds), North-Holland Publishing Co., Amsterdam (1966) 63.
[114] WEINBERG, R.B., Nuclear Structure Study with Neutrons (NEVE, M. et al., Eds), North-Holland Publishing Co., Amsterdam (1966) 37.
[115] SAJI, Y. et al., Proc.Antwerp Conf.on Nuclear Structure Studies with Neutrons (1965) Paper No.20.

INTERNATIONAL COURSE ON NUCLEAR PHYSICS HELD IN TRIESTE, 3 OCTOBER - 16 NOVEMBER 1966

FACULTY AND PARTICIPANTS

DIRECTORS

A. de-Shalit	Weizmann Institute of Science, Dept of Nuclear Physics, Rehovoth	Israel
C. Villi	Università degli Studi di Padova, Istituto di Fisica Galileo Galilei, Padova	Italy

LECTURERS

W.E. Frahn	Dept of Physics, University of Cape Town, Rodenbosch, C.P.	South Africa
J. Humblet	Université de Liège, Physique Nucléaire Théorique, Liège	Belgium
R.H. Lemmer	Massachusetts Institute of Technology, Dept of Physics, Cambridge, Mass.	United States of America
J.E. Lynn	Atomic Energy Research Establishment, Nuclear Physics Division, Harwell, Berks	United Kingdom
G.S. Mani	Dept of Physics, University of Manchester, Manchester, Lancs, United Kingdom	India
K.W. McVoy	Dept of Physics, University of Wisconsin, Madison, Wis.	United States of America
M. Moshinsky	Universidad Nacional Autónoma de Mexico, Mexico 20, D.F.	Mexico
E.R. Rae	Atomic Energy Research Establishment, Harwell, Berks	United Kingdom
G. Ripka	Centre d'Etudes Nucléaires de Saclay, Gif-sur-Yvette (S. & O.)	France
D.J. Rowe	Atomic Energy Research Establishment, Harwell, Berks	United Kingdom
G.M. Temmer	Rutgers - The State University, Dept of Physics, New Brunswick, N.J.	United States of America
F. Villars	Massachusetts Institute of Technology, Cambridge, Mass.	United States of America

SEMINAR LECTURERS

G. Alaga	Institut R. Bošković, Zagreb	Yugoslavia
V. Benzi	Centro di Calcolo del C.N.E.N., Bologna	Italy
L. Biasini	Centro di Calcolo del C.N.E.N., Bologna	Italy
F. Calogero	Istituto di Fisica, Roma	Italy
K. Dietrich	Institut für theoretische Physik, Heidelberg	Federal Republic of Germany
A. Faessler	University of Freiburg, Freiburg/Breisgau	Federal Republic of Germany
L. Fonda	University of Trieste, Dept of Physics, Trieste	Italy
M.E. Haglund	Institut de Physique Nucléaire, Division de Physique Théorique, Orsay	France
F. Janouch	Czechoslovak Academy of Sciences, Prague	Czechoslovak Socialist Republic
M. Jean*	Institut de Physique Nucléaire, Orsay	France
P. Kramer	Institut für theoretische Physik der Universität Tübingen, Tübingen	Federal Republic of Germany
W. Laskar	Faculté des Sciences, Université de Nantes, Nantes	France
C. Lolli	Centro di Calcolo del C.N.E.N., Bologna	Italy
C. Noack	Institut für theoretische Physik, Heidelberg	Federal Republic of Germany
R. Ricci	Istituto di Fisica dell'Università, Firenze	Italy
M. Riou	Institut de Physique Nucléaire, Orsay	France
M. Schneider-Ludovici	I.B.M., Roma	Italy
P. Tomás	Institut R. Bošković, Zagreb	Yugoslavia
L. Trlifaj	Nuclear Research Institute, Řež near Prague	Czechoslovak Socialist Republic
V.G. Soloviev	Joint Institute for Nuclear Research, Dubna	Union of Soviet Socialist Republics

EDITOR

A.M. Hamende	International Centre for Theoretical Physics, Trieste	Italy

* For Mr. Jean's contribution, part of Chapter 13, there are two co-authors, X. Campi and H. Vucetich, both of the Institut de Physique Nucléaire, Orsay, France.

PARTICIPANTS

Afzal, S.A.	Atomic Energy Centre, Dacca	Pakistan
Ahmed, N.	Atomic Energy Centre, Dacca	Pakistan
Alberi, G.	Dept of Theoretical Physics, Trieste University	Italy
Ali, Saqeba	Atomic Energy Centre, Dacca	Pakistan
Ali, Shamsher	Atomic Energy Centre, Dacca	Pakistan
Alzetta, R.	Dept of Theoretical Physics, Trieste University	Italy
Assimakopoulos, P.A.	N.R.C. Democritus, Athens	Greece
Baba, C.V.K.	Tata Institute of Fundamental Research, Bombay	India
Bergère, R.	Section des Mesures Neutroniques Fondamentales, Saclay	France
Berthier, J.	Centre d'Etudes nucléaires de Grenoble	France
Bertrand, F.J.	Commissariat à l'Energie Atomique, Paris	France
Bijedić, N.	Institute Boris Kidrič, Belgrade	Yugoslavia
Bisiacchi, G.	Dept of Theoretical Physics, Trieste University	Italy
Blasi, P.	*Istituto di Fisica, Firenze*	*Italy*
Bogdan, D.	Institute for Atomic Physics, Bucharest	Romania
Cabe, J.F.	Commissariat à l'Energie Atomique, Paris	France
Coceva, C.	Gruppo Misure Sezioni d'Urto, Ispra	Italy
Cuttler, J.M.	Dept of Nuclear Science, Technion, Israel	Canada
Cvelear, F.	Nuklearni Institut J. Stefan, Ljubljana	Yugoslavia
Darling, T.B.	Dept de Physique Université Laval, Quebec P.Q.	Canada
Dechargé, J.	Commissariat à l'Energie Atomique, Paris	France
De Guarrini, F.	Dept of Theoretical Physics, Trieste University	Italy
De Raedt, J.A.	Centre de Physique Nucleaire, Université de Louvain	Belgium/United Kingdom

Derrien, H.	Section des Mesures Neutroniques Fondamentales, Saclay	France
Donà dalle Rose, L.F.	Istituto di Fisica, Padova	Italy
Drigo, L.M.	Istituto di Fisica, Padova	Italy
Engelbrecht, C.A.	Atomic Energy Board, Pretoria	South Africa
Erkelenz, K.	Institut für theoretische Kernphysik, University of Bonn	Federal Republic of Germany
Fenin, Yu.I.	Joint Institute for Nuclear Research, Dubna	Union of Soviet Socialist Republics
Fort, E.M.	Section des Mesures Neutroniques Fondamentales, Saclay	France
Friedrich, A.	Institut für theoretische Kernphysik, University of Bonn	Federal Republic of Germany
Frullani, S.	Laboratori Fisica Istituto Superiore Sanità, Roma	Italy
Gabrielli, I.G.	Istituto di Fisica Sperimentale, Trieste University	Italy
Geramb, H.	Reaktorzentrum, Seibersdorf	Austria
Giacobbe, P.	Gruppo Misure Sezioni d'Urto, Ispra	Italy
Giacomich, R.	Dept of Theoretical Physics, Trieste University	Italy
Gmitro, M.	Nuclear Research Institute of Czechoslovak Academy of Sciences, Prague	Czechoslovak Socialist Republic
Goudergues, J.	Commissariat à l'Energie Atomique, Paris	France
Gratton, J.	Facultad de Ciencias Exactas y Naturales, Universidad de Buenos Aires	Argentina
Grypeos, M.*	University of Oxford, Dept of Theoretical Physics, Oxford	Greece
Haberler, P.*	Dept of Physics, University of Vienna	Austria
Hendeković, J.	Nuclear Institute R. Bošković, Zagreb	Yugoslavia
Hudoklin, A.	Nuklearni Institut J. Stefan, Ljubljana	Yugoslavia
Huq, A.	Atomic Energy Centre, Dacca	Pakistan
Hussain, M.A.M.	Atomic Energy Centre, Dacca	Pakistan

* Also held a seminar

Iosifescu, M.	Institute for Atomic Physics, Bucharest	Romania
Justin, D.	Institute J. Stefan, Ljubljana	Yugoslavia
Khadkikar, S.	Tata Institute of Fundamental Research, Bombay	India
Kok, L.P.	Institute for Theoretical Physics, Groningen	Netherlands
Koltay, B.	ATOMKI, Debrecen	Hungary
Koneska, S.	Faculty of Science, University of Skopje	Yugoslavia
Kriechbaum, M.	Reaktorzentrum, Seibersdorf	Austria
Leonardi, R.	Istituto di Fisica, Bologna	Italy
Le Rigoleur, C.	Section des Mesures Neutroniques Fondamentales, Saclay	France
Lipnik, P.	Centre de Physique Nucléaire, Université de Hérvelé-Louvain	Belgium
Maciel, A.	Instituto de Fisica da UFRGS, Porto Alegre, Rio Grande do Sul	Brazil
Maqueda, E.	University of Sussex, Physics Laboratory, Brighton, Sussex	Argentina
Marangoni, M.	Centro di Calcolo del C.N.E.N., Bologna	Italy
Marseguerra, M.	Centro di Calcolo del C.N.E.N., Bologna	Italy
Maurenzig, P.R.	Istituto di Fisica, Firenze	Italy
Mayer, B.	Commissariat à l'Energie Atomique, Paris	France
Migneco, E.	EURATOM, Geel	Italy
Mihailović, M.V.*	Nuklearni Institut J. Stefan, Ljubljana	Yugoslavia
Minelli, T.A.	Istituto di Fisica, Padova	Italy
Mouilhayrat, G.G.	Centre d'Etudes Nucléaires de Saclay	France
Nadjakov, E.G.	Institute of Physics, Bulgarian Academy of Sciences, Sofia	Bulgaria
Naqvi, J.H.	Department of Physics, Aligarh Muslim University, Aligarh	India
Nunberg, P.	Centro Studi Nucleari della Casaccia, Laboratorio Fisica Nucleare Applicata, Roma	Italy

* Also held a seminar

Pacati, F.	Istituto Fisica Teorica, Pavia	Italy
Pascolini, A.	Istituto di Fisica, Padova	Italy
Passatore, G.	Istituto di Fisica, Genova,	Italy
Pauli, G.	Dept of Theoretical Physics, Trieste University	Italy
Paya, D.	Commissariat à l'Energie Atomique, Paris	France
Perillo, A.E.	Istituto di Fisica Superiore, Napoli	Italy
Perrin, A.E.	Commissariat à l'Energie Atomique, Paris	France
Pietarinen, E.U.	Institute for Theoretical Physics, Helsinki	Finland
Pisent, G.	Istituto di Fisica, Padova	Italy
Pittel, S.	University of Minnesota, Dept of Physics, Minneapolis, Minn.	United States of America
Pluhar, Z.	Dept of Theoretical Physics, Faculty of Technical and Nuclear Physics, Prague	Czechoslovak Socialist Republic
Poiani, G.	Dept of Theoretical Physics, Trieste University	Italy
Porceddu, C.	Centro di Calcolo del C.N.E.N., Bologna	Italy
Potokar, M.	Nuklearni Institut J. Stefan, Ljubljana	Yugoslavia
Rahman, M.	Atomic Energy Centre, Dacca	Pakistan
Rendić, D.	Institute R. Bošković, Zagreb	Yugoslavia
Ribon, P.	Commissariat à l'Energie Atomique, Paris	France
Rimini, A.	Dept of Theoretical Physics, Trieste University	Italy
Rolard, J.	Commissariat à l'Energie Atomique, Paris	France
Rosina, M.	Nuklearni Institut J. Stefan, Ljubljana	Yugoslavia
Sambo, P.O.	Istituto di Fisica, Padova	Italy
Saruis, A.M.	Centro di Calcolo del C.N.E.N., Bologna	Italy
Seligmann, T.H.	University of Basel	Switzerland
Shah, K.T.	Istituto di Fisica, Bologna	Pakistan
Shelest, V.P.	Institute of Theoretical Physics, Academy of Sciences, Kiev	Union of Soviet Socialist Republics

Sobiczewski, A.	Institute for Nuclear Research, Warsaw	Poland
Sona, P.	Istituto di Fisica, Firenze	Italy
Sotona, M.	Nuclear Research Institute of Czechoslovak Academy of Sciences, Prague	Czechoslovak Socialist Republic
Stancu, F.	Institute for Atomic Physics, Bucharest	Romania
Strnad, J.	Nuklearni Institut J. Stefan, Ljubljana	Yugoslavia
Uguzzoni, A.	Istituto di Fisica A. Righi, Bologna	Italy
Vanzani, V.G.	Istituto di Fisica, Padova	Italy
Viennet, R.	Institut de Physique, Neuchâtel	Switzerland
Weber, T.	Dept of Theoretical Physics, Trieste University	Italy
Weigmann, H.	EURATOM, Geel	Federal Republic of Germany
Zardi, F.	Istituto di Fisica, Padova	Italy
Zuffi, L.	Centro di Calcolo del C.N.E.N., Bologna	Italy

IAEA SALES AGENTS

Orders for Agency publications can be placed with your bookseller or any of our sales agents listed below:

ARGENTINA
Comisión Nacional de
Energía Atómica
Avenida del Libertador
General San Martin 8250
Buenos Aires - Suc. 29

AUSTRALIA
Hunter Publications,
23 McKillop Street
Melbourne, C.1

AUSTRIA
Georg Fromme & Co.
Spengergasse 39
A-1050, Vienna V

BELGIUM
Office international de librairie
30, avenue Marnix
Brussels 5

BRAZIL
Livraria Kosmos Editora
Rua do Rosario, 135-137
Rio de Janeiro

Agencia Expoente Oscar M. Silva
Rua Xavier de Toledo, 140-1° Andar
(Caixa Postal No. 5.614)
São Paulo

BYELORUSSIAN SOVIET SOCIALIST REPUBLIC
See under USSR

CANADA
The Queen's Printer
Ottawa, Ontario

CHINA (Taiwan)
Books and Scientific Supplies
Service, Ltd.,
P.O. Box 83
Taipei

CZECHOSLOVAK SOCIALIST REPUBLIC
S.N.T.L.
Spolena 51
Nové Mĕsto
Prague 1

DENMARK
Ejnar Munksgaard Ltd.
6 Nörregade
Copenhagen K

FINLAND
Akateeminen Kirjakauppa
Keskuskatu 2
Helsinki

FRANCE
Office international de
documentation et librairie
48, rue Gay-Lussac
F-75, Paris 5e

GERMANY, Federal Republic of
R. Oldenbourg
Rosenheimer Strasse 145
8 Munich 8

HUNGARY
Kultura
Hungarian Trading Co. for Books
and Newspapers
P.O.B. 149
Budapest 62

ISRAEL
Heiliger and Co.
3 Nathan Strauss Street
Jerusalem

ITALY
Agenzia Editoriale Internazionale
Organizzazioni Universali (A.E.I.O.U.)
Via Meravigli 16
Milan

JAPAN
Maruzen Company Ltd.
6, Tori Nichome
Nihonbashi
(P.O. Box 605)
Tokyo Central

MEXICO
Librería Internacional
Av. Sonora 206
Mexico 11, D.F.

NETHERLANDS
N.V. Martinus Nijhoff
Lange Voorhout 9
The Hague

NEW ZEALAND
Whitcombe & Tombs, Ltd.
G.P.O. Box 1894
Wellington, C.1

NORWAY
Johan Grundt Tanum
Karl Johans gate 43
Oslo

PAKISTAN
Karachi Education Society
Haroon Chambers
South Napier Road
(P.O. Box No. 4866)
Karachi 2

POLAND
Ośrodek Rozpowszechniana
Wydawnictw Naukowych
Polska Akademia Nauk
Pałac Kultury i Nauki
Warsaw

ROMANIA
Cartimex
Rue A. Briand 14-18
Bucarest

SOUTH AFRICA
Van Schaik's Bookstore (Pty) Ltd.
Libri Building
Church Street
(P.O. Box 724)
Pretoria

SPAIN
Librería Bosch
Ronda de la Universidad 11
Barcelona

SWEDEN
C.E. Fritzes Kungl. Hovbokhandel
Fredsgatan 2
Stockholm 16

SWITZERLAND
Librairie Payot
Rue Grenus 6
1211 Geneva 11

TURKEY
Librairie Hachette
469, Istiklâl Caddesi
Beyoğlu, Istanbul

UKRAINIAN SOVIET SOCIALIST REPUBLIC
See under USSR

UNION OF SOVIET SOCIALIST REPUBLICS
Mezhdunarodnaya Kniga
Smolenskaya-Sennaya 32-34
Moscow G-200

UNITED KINGDOM OF GREAT BRITAIN AND NORTHERN IRELAND
Her Majesty's Stationery Office
P.O. Box 569
London, S.E.1

UNITED STATES OF AMERICA
National Agency for
International Publications, Inc.
317 East 34th Street
New York, N.Y. 10016

VENEZUELA
Sr. Braulio Gabriel Chacares
Gobernador a Candilito 37
Santa Rosalía
(Apartado Postal 8092)
Caracas D.F.

YUGOSLAVIA
Jugoslovenska Knjiga
Terazije 27
Belgrade

IAEA publications can also be purchased retail at the United Nations Bookshop at United Nations Headquarters, New York, at the news-stand at the Agency's Headquarters, Vienna, and at most conferences, symposia and seminars organized by the Agency.

In order to facilitate the distribution of its publications, the Agency is prepared to accept payment in UNESCO coupons or in local currencies.

Orders and inquiries from countries where sales agents have not yet been appointed may be sent to:

Distribution and Sales Group, International Atomic Energy Agency,
Kärntner Ring 11, A-1010, Vienna I, Austria

INTERNATIONAL
ATOMIC ENERGY AGENCY
VIENNA, 1967

PRICE: US $16.00
Austrian Schillings 414,-
(£5.13.0; F.Fr. 78,40; DM 64,-)